

# **NEHRP Recommended Provisions: Design Examples**

FEMA 451 - August 2006





### **GENERAL DISCLAIMER**

This document may have problems that one or more of the following disclaimer statements refer to:

- This document has been reproduced from the best copy furnished by the sponsoring agency. It is being released in the interest of making available as much information as possible.
- This document may contain data which exceeds the sheet parameters. It was furnished in this condition by the sponsoring agency and is the best copy available.
- This document may contain tone-on-tone or color graphs, charts and/or pictures which have been reproduced in black and white.
- ✤ This document is paginated as submitted by the original source.
- Portions of this document are not fully legible due to the historical nature of some of the material. However, it is the best reproduction available from the original submission.



of the National Institute of Building Sciences

# **NEHRP Recommended Provisions: Design Examples**

### FEMA 451 - August 2006

Prepared by the Building Seismic Safety Council for the Federal Emergency Management Agency of the Department of Homeland Security

> National Institute of Building Sciences Washington, D.C.

NOTICE: Any opinions, findings, conclusions, or recommendations expressed in this publication do not necessarily reflect the views of the Federal Emergency Management Agency. Additionally, neither FEMA nor any of its employees make any warranty, expressed or implied, nor assume any legal liability or responsibility for the accuracy, completeness, or usefulness of any information, product, or process included in this publication.

The opinions expressed herein regarding the requirements of the *International Residential Code* do not necessarily reflect the official opinion of the International Code Council. The building official in a jurisdiction has the authority to render interpretation of the code.

This report was prepared under Contract EMW-1998-CO-0419 between the Federal Emergency Management Agency and the National Institute of Building Sciences.

For further information on the Building Seismic Safety Council, see the Council's website --<u>www.bssconline.org</u> -- or contact the Building Seismic Safety Council, 1090 Vermont, Avenue, N.W., Suite 700, Washington, D.C. 20005; phone 202-289-7800; fax 202-289-1092; e-mail bssc@nibs.org.

### FOREWORD

One of the goals of the Department of Homeland Security's Federal Emergency Management Agency (FEMA) and the National Earthquake Hazards Reduction Program (NEHRP) is to encourage design and building practices that address the earthquake hazard and minimize the resulting risk of damage and injury. The 2003 edition of the *NEHRP Recommended Provisions for Seismic Regulation of New Buildings and Other Structures* and its *Commentary* affirmed FEMA's ongoing support to improve the seismic safety of construction in this country. The *NEHRP Recommended Provisions* serves as the basis for the seismic requirements in the ASCE *7 Standard Minimum Design Loads for Buildings and Other Structures* as well as both the *International Building Code* and *NFPA 5000 Building Construction Safety Code*. FEMA welcomes the opportunity to provide this material and to work with these codes and standards organizations.

This product provides a series of design examples that will assist the user of the *NEHRP Recommended Provisions*. This material will also be of assistance to those using the ASCE 7 standard and the models codes that reference the standard.

FEMA wishes to express its gratitude to the authors listed elsewhere for their significant efforts in preparing this material and to the BSSC Board of Direction and staff who made this possible. Their hard work has resulted in a guidance product that will be of significant assistance for a significant number of users of the nation's seismic building codes and their reference documents.

Department of Homeland Security/ Federal Emergency Management Agency

## PREFACE

This volume of design examples is intended for those experienced structural designers who are relatively new to the field of earthquake-resistant design and to application of seismic requirements of the *NEHRP* (*National Earthquake Hazards Reduction Program*) *Recommended Provisions for Seismic Regulations for New Buildings and Other Structures* and, by extension, the model codes and standards because the *Provisions* are the source of seismic design requirements in most of those documents including ASCE 7, *Standard Minimum Design Loads for Buildings and Other Structures*; the *International Building Code*; and the *NFPA 5000 Building Construction and Safety Code*.

This compilation of design examples is an expanded version of an earlier document (entitled *Guide to Application of the NEHRP Recommended Provisions*, FEMA 140) and reflects the expansion in coverage of the *Provisions* and the expanding application of the *Provisions* concepts in codes and standards. The widespread use of the *NEHRP Recommended Provisions* signals the success of the Federal Emergency Management Agency and Building Seismic Safety Council efforts to ensure that the nation's building codes and standards reflect the state of the art of earthquake-resistant design.

In developing this set of design examples, the BSSC first decided on the types of structures, types of construction and materials, and specific structural elements that needed to be included to provide the reader with at least a beginning grasp of the impact the *NEHRP Recommended Provisions* has on frequently encountered design problems. Some of the examples draw heavily on a BSSC trial design project conducted prior to the publication of the first edition of the *NEHRP Recommended Provisions* in 1985 but most were created by the authors to illustrate issues not covered in the trial design program. Further, the authors have made adjustments to those examples drawn from the trial design program as necessary to reflect the 2000 Edition of the *NEHRP Recommended Provisions*. Finally, because it obviously is not possible to present in a volume of this type complete building designs for all the situations and features that were selected, only portions of designs have been used.

The BSSC is grateful to all those individuals and organizations whose assistance made this set of design examples a reality:

- James Robert Harris, J. R. Harris and Company, Denver, Colorado, who served as the project manager, and Michael T. Valley, Magnusson Klemencic Associates, Seattle, Washington, who served as the technical editor of this volume
- The chapter authors Robert Bachman, Finley A. Charney, Richard Drake, Charles A. Kircher, Teymour Manzouri, Frederick R. Rutz, Peter W. Somers, Harold O. Sprague, Jr., and Gene R. Stevens – for there unstinting efforts

- Greg Deierlein, J. Daniel Dolan, S. K. Ghosh, Robert D. Hanson, Neil Hawkins, and Thomas Murray for their insightful reviews
- William Edmands and Cambria Lambertson for their hard work behind the scenes preparing figures

Special thanks go to Mike Valley and Peter Somers for their work annotating the design examples to reflect the 2003 edition of the *Provisions* and updated versions of other standards referenced in the 2003 version. The BSSC Board is also grateful to FEMA Project Officer Michael Mahoney for his support and guidance and to Claret Heider and Carita Tanner of the BSSC staff for their efforts preparing this volume for publication and issuance as a CD-ROM.

Jim. W. Sealy, Chairman, BSSC Board of Direction

## **TABLE OF CONTENTS**

1. FUNDAMENTALS by James Robert Harris, P.E., Ph.D.1-11.1 Earthquake Phenomena1-21.2 Structural Response to Ground Shaking1-31.3 Engineering Philosophy1-131.4 Structural Analysis1-131.5 Nonstructural Elements of Buildings1-151.6 Quality Assurance1-16
2. GUIDE TO USE OF THE <i>PROVISIONS</i> by Michael Valley, P.E
3 STRUCTURAL ANALYSIS by Finley A. Charney, Ph.D., P.E.3-13.1 Irregular 12-Story Steel Frame Building, Stockton, California3-33.1.1 Introduction3-33.1.2 Description of Structure3-33.1.3 Provisions Analysis Parameters3-63.1.4 Dynamic Properties3-73.1.5 Equivalent Lateral Force Analysis3-113.1.6 Modal-Response-Spectrum Analysis3-253.1.7 Modal-Time-History Analysis3-353.1.8 Comparison of Results from Various Methods of Analysis3-433.2 Six-Story Steel Frame Building, Seattle, Washington3-513.2.1 Description of Structure3-513.2.2 Loads3-513.2.3 Preliminaries to Main Structural Analysis3-653.2.4 Description of Model Used for Detailed Structural Analysis3-653.2.5 Static Pushover Analysis3-613.2.7 Summary and Conclusions3-143
4. FOUNDATION ANALYSIS AND DESIGN by Michael Valley, P.E.4-14.1 Shallow Foundations for a Seven -Story Office Building, Los Angeles, California4-44.1.1 Basic Information4-44.1.2 Design for Gravity Loads4-84.1.3 Design for Moment-Resisting Frame System4-114.1.4 Design for Concentrically Braced Frame System4-174.1.5 Cost Comparison4-244.2 Deep Foundations for a 12-Story Building, Seismic Design Category D4-264.2.1 Basic Information4-264.2.2 Pile Analysis, Design, and Detailing4-344.2.3 Other Considerations4-47

5.	TRUCTURAL STEEL DESIGN by James R. Harris, P.E., Ph.D.,	
	Frederick R. Rutz, P.E., Ph.D., and Teymour Manzouri, P.E., Ph.D.	. 5-1
	.1 Industrial High-Clearance Building, Astoria, Oregon	. 5-3
	5.1.1 Building Description	. 5-3
	5.1.2 Design Parameters	
	5.1.3 Structural Design Criteria	
	5.1.4 Analysis	
	5.1.5 Proportioning and Details	
	2.2 Seven-Story Office Building, Los Angeles, California	
	5.2.1 Building Description	
	5.2.2 Basic Requirements	
	5.2.3 Structural Design Criteria	
	5.2.4 Analysis	
	5.2.5 Cost Comparison	
	3.3 Two-Story Building, Oakland, California	
	5.3.1 Building Description	
	5.3.2 Method	
	5.3.3 Analysis	5-77
	5.3.4 Design of Eccentric Bracing	5-78
6.	REINFORCED CONCRETE by Finley A. Charney, Ph.D., P.E	. 6-1
	6.1 Development of Seismic Loads and Design Requirements	. 6-6
	6.1.1 Seismicity	. 6-6
	6.1.2 Structural Design Requirements	
	6.1.3 Structural Configuration	
	6.2 Determination of Seismic Forces	
	6.2.1 Approximate Period of Vibration	
	6.2.2 Building Mass	
	6.2.3 Structural Analysis	
	6.2.4 Accurate Periods from Finite Element Analysis	
	6.2.5 Seismic Design Base Shear	
	6.2.6 Development of Equivalent Lateral Forces	
	6.3 Drift and P-delta Effects	
	6.3.1 Direct Drift and P-delta Check for the Berkeley Building	
	6.3.2 Test for Torsional Irregularity for Berkeley Building	
	6.3.3 Direct Drift and P-delta Check for the Honolulu Building	6-24
	6.3.4 Test for Torsional Irregularity for the Honolulu Building	6-28
	6.4 Structural Design of the Berkeley Building	6-28
	6.4.1 Material Properties	6-28
	6.4.2 Combination of Load Effects	
	6.4.3 Comments on the Structure's Behavior Under E-W Loading	
	6.4.4 Analysis of Frame-Only Structure for 25 Percent of Lateral Load	
	6.4.5 Design of Frame Members for the Berkeley Building	
	6.5 Structural Design of the Honolulu Building	
	6.5.1 Material Properties	
	6.5.2 Combination of Load Effects	
	6.5.3 Accidental Torsion and Orthogonal Loading (Seismic Versus Wind)	
	6.5.4 Design and Detailing of Members of Frame 1	6-80

	6.5.5 Design of Members of Frame 3	6-92
7.	PRECAST CONCRETE DESIGN by Gene R. Stevens, P.E. and James Robert Harris, P.E., Ph.D.	7-1
	7.1 Horizontal Diaphragms	7-5
	7.1.1 Untopped Precast Concrete Units for Five-Story Masonry Buildings Located in Birmingham, Alabama, and New York, New York	7-5
	7.1.2 Topped Precast Concrete Units for Five-Story Masonry Building, Los Angeles, Califorr	
		7-22
	7.2 Three-Story Office Building With Precast Concrete Shear Walls	7-30
		7-30
		7-31
	7.2.3 Load Combinations	
	7.2.4 Seismic Force Analysis	
	7.2.5 Proportioning and Detailing	
	7.3 One-Story Precast Shear Wall Building	
	7.3.1 Building Description	
	7.3.2 Design Requirements	
		7-53
		7-54
	7.3.5 Proportioning and Detailing	
	Frederick R. Rutz, P.E., Ph.D.8.1 Building Description8.2 Summary of Design Procedure for Composite Partially Restrained	
	Moment Frame System	8-6
	8.3 Design Requirements	8-7
	8.3.1 <i>Provisions</i> Parameters	8-7
	8.3.2 Structural Design Considerations Per the <i>Provisions</i>	
	8.3.3 Building Weight and Base Shear Summary	
	8.4 Details of the PRC Connection and System	
	8.4.1 Connection <i>M-q</i> Relationships	
	8.4.2 Connection Design and Connection Stiffness Analysis	
	8.5 Analysis	
	8.5.1 Load Combinations	
	8.5.2 Drift and P-delta	
	8.5.3 Required and Provided Strength	
	8.6 Details of the Design	
	8.6.1 Overview	
	8.6.2 Width-Thickness Ratios	
	8.6.3 Column Axial Strength	
	8.6.4 Details of the Joint	8-25
9	MASONRY by James Robert Harris, P.E., Ph.D., Frederick R. Rutz, P.E., Ph.D. and	
	Teymour Manzouri, P.E., Ph.D.	9-1
	9.1 Warehouse with Masonry Walls and Wood Roof, Los Angeles, California	
	9.1.1 Building Description	9-3
	9.1.2 Design Requirements	9-4

9.1.3 Load Combinations	9-6
9.1.4 Seismic Forces	9-9
9.1.5 Longitudinal Walls	. 9-10
9.1.6 Transverse Walls	. 9-25
9.1.7 Bond Beam	. 9-40
9.1.8 In-Plane Deflection	
9.2 Five-story Masonry Residential Buildings in Birmingham, Alabama; New York, New York;	
and Los Angeles, California	
9.2.1 Building Description	
9.2.2 Design Requirements	
9.2.3 Load Combinations	
9.2.4 Seismic Design for Birmingham 1	
9.2.5 Seismic Design for New York City	
9.2.6 Birmingham 2 Seismic Design	
9.2.7 Seismic Design for Los Angeles	
9.3.1 Building Description	
9.3.2 Design Requirements	
9.3.3 Seismic Force Analysis	
9.3.4 Deflections	
9.3.5 Out-of-Plane Forces	
9.3.6 Orthogonal Effects	
9.3.7 Anchorage	
9.3.8 Diaphragm Strength	
,	/
10 WOOD DESIGN by Peter W. Somers, P.E. and Michael Valley, P.E.	. 10-1
10.1 Three-story Wood Apartment Building; Seattle, Washington	
10.1.1 Building Description	
10.1.2 Basic Requirements	
10.1.3 Seismic Force Analysis	
10.1.4 Basic Proportioning	
10.2 Warehouse with Masonry Walls and Wood Roof, Los Angeles, California	
10.2.1 Building Description	
10.2.2 Basic Requirements	
10.2.3 Seismic Force Analysis	
10.2.4 Basic Proportioning of Diaphragm Elements	
	10
11 SEISMICALLY ISOLATED STRUCTURES by Charles A. Kircher, P.E., Ph.D.	. 11-1
11.1 Background and Basic Concepts	
11.1.1 Types of Isolation Systems	
11.1.2 Definition of Elements of an Isolated Structure	
11.1.3 Design Approach	
11.1.4 Effective Stiffness and Effective Damping	
11.2 Criteria Selection	
11.3 Equivalent Lateral Force Procedure	
11.3.1 Isolation System Displacement	
11.3.2 Design Forces	
11.4 Dynamic Lateral Response Procedure	
11.4.1 Minimum Design Criteria	
	11-13

	11.4.2 Modeling Requirements	11-14
	11.4.3 Response Spectrum Analysis	
	11.4.4 Time History Analysis	
11.5	Emergency Operations Center Using Elastomeric Bearings, San Francisco, California	
	11.5.1 System Description	
	11.5.2 Basic Requirements	
	11.5.3 Seismic Force Analysis	
	11.5.4 Preliminary Design Based on the ELF Procedure	
	11.5.5 Design Verification Using Nonlinear Time History Analysis	
	11.5.6 Design and Testing Criteria for Isolator Units	11-45
12 NO	NBUILDING STRUCTURE DESIGN by Harold O. Sprague Jr., P.E.	12-1
	Nonbuilding Structures Versus Nonstructural Components	
	12.1.1 Nonbuilding Structure	
	12.1.2 Nonstructural Component	
12.2	Pipe Rack, Oxford, Mississippi	
	12.2.1 Description	
	12.2.2 Provisions Parameters	
	12.2.3 Design in the Transverse Direction	
	12.2.4 Design in the Longitudinal Direction	
12.3	Steel Storage Rack, Oxford, Mississippi	
1210	12.3.1 Description	
	12.3.2 <i>Provisions</i> Parameters	
	12.3.3 Design of the System	
12.4	Electric Generating Power Plant, Merna, Wyoming	
12.1	12.4.1 Description	
	12.4.2 <i>Provisions</i> Parameters	
	12.4.3 Design in the North-South Direction	
	12.4.4 Design in the East-West Direction	
12.5	Pier/Wharf Design, Long Beach, California	
12.0	12.5.1 Description	
	12.5.2 <i>Provisions</i> Parameters	
	12.5.3 Design of the System	
12.6	Tanks and Vessels, Everett, Washington	
12.0	12.6.1 Flat-Bottom Water Storage Tank	
	12.6.2 Flat-bottom Gasoline Tank	
12.7	Emergency Electric Power Substation Structure, Ashport, Tennessee	
12.7	12.7.1 Description	
	12.7.2 <i>Provisions</i> Parameters	
	12.7.3 Design of the System	
		12-30
13 DES	SIGN FOR NONSTRUCTURAL COMPONENTS by Robert Bachman, P.E., and	
	ard Drake, P.E.	13-1
	Development and Background of the Provisions for Nonstructural Components	
13.1	13.1.1 Approach to Nonstructural Components	
	13.1.2 Force Equations	
	13.1.3 Load Combinations and Acceptance Criteria	
	13.1.4 Component Amplification Factor	
		13-4

	13.1.5 Seismic Coefficient at Grade	13-5
	13.1.6 Relative Location Factor	13-5
	13.1.7 Component Response Modification Factor	13-5
	13.1.8 Component Importance Factor	
	13.1.9 Accommodation of Seismic Relative Displacements	
	13.1.10 Component Anchorage Factors and Acceptance Criteria	
	13.1.11 Construction Documents	
13.2	Architectural Concrete Wall Panel	13-7
	13.2.1 Example Description	
	13.2.2 Design Requirements	
	13.2.3 Spandrel Panel	
	13.2.4 Column Cover	
	13.2.5 Additional Design Considerations	
13.3	HVAC Fan Unit Support	
	13.3.1 Example Description	
	13.3.2 Design Requirements	
	13.3.3 Direct Attachment to Structure	
	13.3.4 Support on Vibration Isolation Springs	13-24
	13.3.5 Additional Considerations for Support on Vibration Isolators	13-29
13.4	Analysis of Piping Systems	13-30
	13.4.1 ASME Code Allowable Stress Approach	13-30
	13.4.2 Allowable Stress Load Combinations	13-32
	13.4.3 Application of the <i>Provisions</i>	13-33
Append	lix A THE BUILDING SEISMIC SAFETY COUNCIL	. A-1

#### LIST OF CHARTS, FIGURES, AND TABLES

Earthquake ground acceleration in epicentral regions 1-4
Holiday Inn ground and building roof motion during the M6.4 1971 San Fernando
earthquake 1-5
Response spectrum of North-South ground acceleration recorded at the Holiday Inn,
approximately 5 miles from the causative fault in the 1971 San Fernando earthquake . 1-6
Averaged spectrum 1-7
Force controlled resistance versus displacement controlled resistance 1-9
Initial yield load and failure load for a ductile portal frame 1-10
Overall Summary of Flow
Scope of Coverage
Application to Existing Structures 2-5
Basic Requirements
Structural Design
Equivalent Lateral Force
Soil-Structure Interaction
Modal Analysis
Response History Analysis 2-11
Seismically Isolated Structures

Chart 2.11	Strength Requirements	2-13
Chart 2.12	Deformation Requirements	
Chart 2.13	Design and Detailing Requirements	
Chart 2.14	Steel Structures	
Chart 2.15	Concrete Structures	2-17
Chart 2.16	Precast Concrete Structures	2-18
Chart 2.17	Composite Steel and Concrete Structures	2-19
Chart 2.18	Masonry Structures	
Chart 2.19	Wood Structures	
Chart 2.20	Nonbuilding Structures	2-22
Chart 2.21	Foundations	2-23
Chart 2.22	Architectural, Mechanical, and Electrical Components	2-24
Chart 2.23	Quality Assurance	2-25
Table 2-1	Navigating Among the 2000 and 2003 NEHRP Recommended Provisions	
	and ASCE 7	2-26
Figure 3.1-1	Various floor plans of 12-story Stockton building	. 3-4
Figure 3.1-2	Sections through Stockton building	. 3-5
Figure 3.1-3	Three-dimensional wire-frame model of Stockton building	. 3-6
Table 3.1-1	Area Masses on Floor Diaphragms	. 3-8
Table 3.1-2	Line Masses on Floor Diaphragms	. 3-9
Figure 3.1-4	Key Diagram for Computation of Floor Mass	
Table 3.1-3	Floor Mass, Mass Moment of Inertia, and Center Mass Locations	
Figure 3.1-5	Computed ELF total acceleration response system spectrum	
Figure 3.1-6	Computed ELF relative displacement response spectrum	
Table 3.1-4	Equivalent Lateral Forces for Building Responses in X and Y Directions	
Figure 3.1-7	Amplification of accidental torsion	3-15
Table 3.1-5	Computation for Torsional Irregularity with ELF Loads Acting in X Direction	3-16
Table 3.1-6	Computation for Torsional Irregularity with ELF Loads Acting in Y Direction	3-16
Table 3.1-7	ELF Drift for Building Responding in X Direction	3-17
Table 3.1-8	ELF Drift for Building Responding in Y Direction	3-18
Table 3.1-9	Rayleigh Analysis for X-Direction Period of Vibration	3-19
Table 3.1-10	Rayleigh Analysis for Y-Direction Period of Vibration	3-20
Table 3.1-11	Computation of P-delta Effects for X-Direction Response	3-21
Figure 3.1-8	Basic load causes used in ELF analysis	
Table 3.1-12	Seismic and Gravity Load Combinations as Run on SAP 2000	3-25
Figure 3.1-9	Seismic shears in girders (kips) as computed using ELF analysis	3-26
Figure 3.1-10	Mode shapes as computed using SAP2000	
Table 3.1-13	Computed Periods and Directions Factors	3-29
Table 3.1-14	Computed Periods and Effective Mass Factors	3-29
Table 3.1-15	Response Structure Coordinates	3-30
Table 3.1-16	Story Shears from Modal-Response-Spectrum Analysis	3-32
Table 3.1-17	Response Spectrum Drift for Building Responding in X Direction	3-33
Table 3.1-18	Spectrum Response Drift for Building Responding in Y Direction	3-33
Table 3.1-19	Computation of P-delta Effects for X-Direction Response	3-34
Figure 3.1-12	Load combinations from response-spectrum analysis	3-35
Figure 3.1-13	Seismic shears in girders (kips) as computed using response-spectrum analysis	3-36
Table 3.1-20	Seattle Ground Motion Parameters	3-37

Figure 3.1-15       Ratio average scaled SRSS spectrum to <i>Provisions</i> spectrum       3-49         Table 3.1-21       Result Maxima from Time-History Analysis       3-40         Table 3.1-22       Result Maxima from Time-History Analysis       3-40         Table 3.1-23       Time-History Drift for Building Responding in X Direction to Motion       3-42         Table 3.1-24       Scaled Inertial Force and Story Shear Envelopes from Analysis AdoX       3-42         Table 3.1-25       Computation of P-delta Effects for X-Direction Response       3-42         Figure 3.1-16       Combinations, Iaa M 2, beam shears (kips) as computed using time history analysis       3-44         Table 3.1-26       Summary of Results from Various Methods of Analysis: Story Shear       3-45         Table 3.1-26       Summary of Results from Various Methods of Analysis: Story Drift       3-46         Table 3.1-27       Summary of Results from Various Methods of Analysis: Beam Shear       3-47         Figure 3.2-1       Plan of structural system       3-53         Table 3.2-2       Gravity Loads on Seattle Building       3-53         Table 3.2-3       Elevention analysis       3-60         Table 3.2-4       Simple wire frame model used for preliminary analysis       3-62         Table 3.2-3       Equivalent Lateral Forces for Seattle Building Responding in N-S Directions       3-58 <th>Figure 3.1-14</th> <th>Unscaled SRSS of spectra of ground motion pairs</th> <th>3-38</th>	Figure 3.1-14	Unscaled SRSS of spectra of ground motion pairs	3-38
Table 3.1-21       Result Maxima from Time-History Analysis       3-40         Table 3.1-22       Result Maxima from Time-History Analysis       3-40         Table 3.1-23       Time-History Drift for Building Responding in X Direction to Motion       3-42         Table 3.1-24       Scaled Inertial Force and Story Shear Envelopes from Analysis A00X       3-42         Figure 3.1-15       Combinations 1 and 2, beam shears (kips) as computed using time-history analysis       3-43         Figure 3.1-16       Summary of Results from Various Methods of Analysis: Story Drift       3-44         Table 3.1-26       Summary of Results from Various Methods of Analysis: Story Drift       3-46         Table 3.1-27       Summary of Results from Various Methods of Analysis: Story Drift       3-46         Table 3.1-28       Summary of Results from Various Methods of Analysis: Story Drift       3-46         Table 3.2-2       Elevation of structural system       3-53         Figure 3.2-3       Gravity Loads on Seattle Building       3-53         Figure 3.2-3       Element loads used in analysis       3-60         Table 3.2-4       Results of Preliminary Analysis Using P-delta Effects       3-62         Table 3.2-5       Results of Preliminary Analysis Using P-delta Effects       3-62         Table 3.2-6       Periods of Varation From Preliminiary Analysis with P-delta effects included <td>Figure 3.1-15</td> <td></td> <td></td>	Figure 3.1-15		
Table 3.1-23       Time-History Drift for Building Responding in X Direction to Motion       3-42         Table 3.1-24       Scaled Inertial Force and Stroy Shear Envelopes from Analysis A00X       3-42         Figure 3.1-16       Combination of P-delta Effects for X-Direction Response       3-43         Figure 3.1-16       Combinations of and 2, beam shears (kips) as computed using time history analysis       3-43         Figure 3.1-17       All combinations, beam shears (kips) as computed using time history analysis       3-44         Table 3.1-26       Summary of Results from Various Methods of Analysis: Story Drift       3-46         Table 3.1-27       Summary of Results from Various Methods of Analysis: Story Drift       3-46         Table 3.2-1       Plan of structural system       3-53         Figure 3.2-2       Elevation of structural system       3-53         Table 3.2-3       Gravity Loads on Seattle Building       3-53         Figure 3.2-4       Simple wire frame model used for preliminary analysis       3-60         Table 3.2-3       Elemviator Lateral Forces for Scattle Building Responding in N-S Directions       3-58         Figure 3.2-4       Results of Preliminary Analysis Using P-delta Effects       3-62         Table 3.2-6       Results of Preliminary Analysis Using P-delta Effects       3-62         Table 3.2-6       Periods of Vibration From Prelim	Table 3.1-21		
Table 3.1-23       Time-History Drift for Building Responding in X Direction to Motion       3-42         Table 3.1-24       Scaled Inertial Force and Stroy Shear Envelopes from Analysis A00X       3-42         Figure 3.1-16       Combination of P-delta Effects for X-Direction Response       3-43         Figure 3.1-16       Combinations of and 2, beam shears (kips) as computed using time history analysis       3-43         Figure 3.1-17       All combinations, beam shears (kips) as computed using time history analysis       3-44         Table 3.1-26       Summary of Results from Various Methods of Analysis: Story Drift       3-46         Table 3.1-27       Summary of Results from Various Methods of Analysis: Story Drift       3-46         Table 3.2-1       Plan of structural system       3-53         Figure 3.2-2       Elevation of structural system       3-53         Table 3.2-3       Gravity Loads on Seattle Building       3-53         Figure 3.2-4       Simple wire frame model used for preliminary analysis       3-60         Table 3.2-3       Elemviator Lateral Forces for Scattle Building Responding in N-S Directions       3-58         Figure 3.2-4       Results of Preliminary Analysis Using P-delta Effects       3-62         Table 3.2-6       Results of Preliminary Analysis Using P-delta Effects       3-62         Table 3.2-6       Periods of Vibration From Prelim	Table 3.1-22	Result Maxima from Time-History Analysis	3-40
Table 3.1-24       Scaled Inertial Force and Story Shear Envelopes from Analysis A00X       3-42         Table 3.1-25       Computation of P-delta Effects for X-Direction Response       3-43         Figure 3.1-16       Combinations I and 2, beam shears (kips) as computed using time-history analysis       3-44         Table 3.1-26       Summary of Results from Various Methods of Analysis: Story Shear       3-45         Table 3.1-27       Summary of Results from Various Methods of Analysis: Story Drift       3-46         Table 3.1-28       Summary of Results from Various Methods of Analysis: Beam Shear       3-47         Figure 3.2-1       Plan of structural system       3-53         Table 3.2-2       Elevation of structural system       3-53         Table 3.2-3       Element loads used in analysis       3-56         Figure 3.2-4       Edivialent Lateral Forces for Seattle Building Responding in N-S Directions       3-58         Figure 3.2-5       Edivialent Lateral Forces for Seattle Building Responding in N-S Directions       3-58         Figure 3.2-6       Periods of Vibration From Preliminary Analysis Using P-delta Effects       3-62         Table 3.2-7       Results of Preliminary Analysis Including P-delta Effects       3-62         Table 3.2-6       Periods of Vibration From Preliminary Analysis with P-delta effects included 3       363         Table 3.2-7	Table 3.1-23	Time-History Drift for Building Responding in X Direction to Motion	3-42
Table 3.1-25       Computation of P-delta Effects for X-Direction Response       3-42         Figure 3.1-16       Combinations, leam shears (kips) as computed using time history analysis       3-44         Table 3.1-26       Summary of Results from Various Methods of Analysis: Story Drift       3-44         Table 3.1-27       Summary of Results from Various Methods of Analysis: Story Drift       3-45         Table 3.1-28       Summary of Results from Various Methods of Analysis: Beam Shear       3-47         Figure 3.2-1       Plan of structural system       3-52         Figure 3.2-2       Elevation of structural system       3-53         Table 3.2-3       Member Sizes Used in N-S Moment Frames       3-53         Table 3.2-3       Element loads used in analysis       3-56         Figure 3.2-4       Simple wire frame model used for preliminary analysis       3-60         Table 3.2-3       Results of Preliminary Analysis Using P-delta Effects       3-62         Table 3.2-4       Results of Preliminary Analysis       3-62         Figure 3.2-5       Demand-to-capacity ratios for elements from analysis with P-delta effects included       3-63         Table 3.2-6       Plastic mechanism for computing lateral strength       3-65         Figure 3.2-7       Detailed analytical model of story frame       3-67         Figure 3.2-10       <	Table 3.1-24		
Figure 3.1-16       Combinations 1 and 2, beam shears (kips) as computed using time-history analysis       3-43         Figure 3.1-17       All combinations, beam shears (kips) as computed using time history analysis       3-44         Table 3.1-26       Summary of Results from Various Methods of Analysis: Story Drift       3-45         Table 3.1-27       Summary of Results from Various Methods of Analysis: Beam Shear       3-47         Figure 3.2-1       Plan of structural system       3-53         Table 3.2-2       Elevation of structural system       3-53         Table 3.2-2       Gravity Loads on Seattle Building       3-53         Figure 3.2-3       Element loads used in analysis       3-56         Figure 3.2-4       Simple wire frame model used for preliminary analysis       3-60         Table 3.2-5       Equivalent Lateral Forces for Seattle Building Responding in N-S Directions       3-58         Figure 3.2-4       Results of Preliminary Analysis Using P-delta Effects       3-62         Table 3.2-6       Periods of Vibration From Preliminary analysis       3-62         Figure 3.2-7       Demand-to-capacity ratios for elements from analysis with P-delta effects included       3-63         Table 3.2-6       Pariods of Vibration From Preliminary Analysis       3-65         Figure 3.2-7       Detailed analytical model of 6-story frame       3-67	Table 3.1-25		
Figure 3.1-17       All combinations, beam shears (kips) as computed using time history analysis       3-44         Table 3.1-26       Summary of Results from Various Methods of Analysis: Story Drift       3-46         Table 3.1-27       Summary of Results from Various Methods of Analysis: Story Drift       3-46         Table 3.1-28       Summary of Results from Various Methods of Analysis: Story Drift       3-46         Figure 3.2-1       Plan of structural system       3-53         Table 3.2-2       Elevation of structural system       3-53         Table 3.2-3       Gravity Loads on Seattle Building       3-53         Figure 3.2-4       Simple wire frame model used for preliminary analysis       3-56         Figure 3.2-5       Results of Preliminary Analysis Including P-delta Effects       3-62         Table 3.2-4       Results of Preliminary Analysis Including P-delta Effects       3-62         Table 3.2-5       Results of Preliminary Analysis Including P-delta Effects       3-62         Figure 3.2-6       Periods of Vibration From Preliminary Analysis with P-delta effects included       3-65         Figure 3.2-7       Lateral Strength on Basis of Rigid-Plastic Mechanism       3-65         Figure 3.2-7       Lateral Strength on Basis of Rigid-Plastic Mechanism       3-65         Figure 3.2-10       Koramine and panel zone resistance       3-71 <td>Figure 3.1-16</td> <td></td> <td></td>	Figure 3.1-16		
Table 3.1-26Summary of Results from Various Methods of Analysis: Story Dirft.3-45Table 3.1-27Summary of Results from Various Methods of Analysis: Story Dirft.3-46Figure 3.2-1Plan of structural system3-52Figure 3.2-2Elevation of structural system3-53Table 3.2-3Member Sizes Used in N-S Moment Frames3-53Table 3.2-1Gravity Loads on Seattle Building3-53Figure 3.2-3Element loads used in analysis3-56Figure 3.2-4Simple wire frame model used for preliminary analysis3-60Table 3.2-5Results of Preliminary Analysis Including P-delta Effects3-62Table 3.2-6Periods of Vibration From Preliminary Analysis3-62Table 3.2-7Lateral Strength on Basis of Rigid-Plastic Mechanism3-65Figure 3.2-6Demand-to-capacity ratios for elements from analysis with P-delta effects included3-63Table 3.2-7Lateral Strength on Basis of Rigid-Plastic Mechanism3-65Figure 3.2-7Detaite denalytical model of 6-fory frame3-67Figure 3.2-7Detaite danalytical model of of story frame3-67Figure 3.2-10Krawinkler beam-column joint model3-68Figure 3.2-11Column flange component of panel zone resistance3-71Figure 3.2-12Column need component of panel zone resistance3-72Figure 3.2-13Force-deformation behavior of panel zone resistance3-72Figure 3.2-14Transforming shear deformation to rotational deformation in the Krawinkler model3-74Table 3.8-8	Figure 3.1-17		
Table 3.1-27Summary of Results from Various Methods of Analysis: Story Drift3-46Table 3.1-28Summary of Results from Various Methods of Analysis: Beam Shear3-47Figure 3.2-1Plan of structural system3-52Figure 3.2-2Elevation of structural system3-53Table 3.2-1Member Sizes Used in N-S Moment Frames3-53Table 3.2-2Gravity Loads on Seattle Building3-53Figure 3.2-3Element loads used in analysis3-56Table 3.2-3Element loads used in analysis3-56Table 3.2-4Results of Preliminary Analysis Using P-delta Effects3-62Table 3.2-5Results of Preliminary Analysis Including P-delta Effects3-62Table 3.2-6Periods of Vibration From Preliminary Analysis3-62Figure 3.2-7Demand-to-capacity ratios for elements from analysis with P-delta effects included3-63Table 3.2-7Lateral Strength on Basis of Rigid-Plastic Mechanism3-65Figure 3.2-6Plastic mechanism for computing lateral strength3-66Figure 3.2-7A compound node and attached spring3-68Figure 3.2-10Column Hange component of panel zone resistance3-72Figure 3.2-11Column Hange component of panel zone resistance3-72Figure 3.2-12Column web component of panel zone resistance3-72Figure 3.2-13A component of panel zone resistance3-72Figure 3.2-14Transforming shear deformation to rotational deformation in the Krawinkler model3-74Table 3.8-8Properties for the Krawinkler B	Table 3.1-26	Summary of Results from Various Methods of Analysis: Story Shear	3-45
Table 3.1-28Summary of Results from Various Methods of Analysis: Beam Shear3-47Figure 3.2-1Plan of structural system3-53Figure 3.2-2Elevation of structural system3-53Table 3.2-1Member Sizes Used in N-S Moment Frames3-53Table 3.2-2Gravity Loads on Seattle Building3-53Figure 3.2-3Element loads used in analysis3-56Table 3.2-3Equivalent Lateral Forces for Seattle Building Responding in N-S Directions3-58Figure 3.2-4Simple wire frame model used for preliminary analysis3-60Table 3.2-5Results of Preliminary Analysis Using P-delta Effects3-62Table 3.2-6Periods of Vibration From Preliminary Analysis3-62Figure 3.2-5Demand-to-capacity ratios for elements from analysis with P-delta effects included3-63Table 3.2-7Lateral Strength on Basis of Rigid-Plastic Mechanism3-66Figure 3.2-6Plastic mechanism for computing lateral strength3-66Figure 3.2-7Detailed analytical model of 6-story frame3-67Figure 3.2-10Krawinkler beam-column joint model3-68Figure 3.2-11Column flange component of panel zone resistance3-71Figure 3.2-12Column flange component of panel zone resistance3-73Figure 3.2-13Force-efformation to rotational deformation in the Krawinkler model3-74Figure 3.2-12Column flange deformation to rotational deformation in the Krawinkler model3-74Figure 3.2-13Force-efformation behavior of panel zone resistance3-73<	Table 3.1-27	• • •	
Figure 3.2-1Plan of structural system3-52Figure 3.2-2Elevation of structural system3-53Table 3.2-1Member Sizes Used in N-S Moment Frames3-53Table 3.2-3Gravity Loads on Seattle Building3-53Figure 3.2-3Element loads used in analysis3-56Figure 3.2-4Equivalent Lateral Forces for Seattle Building Responding in N-S Directions3-58Figure 3.2-4Simple wire frame model used for preliminary analysis3-60Table 3.2-5Results of Preliminary Analysis Using P-delta Effects3-62Table 3.2-5Demand-to-capacity ratios for elements from analysis with P-delta effects included3-63Table 3.2-7Lateral Strength on Basis of Rigid-Plastic Mechanism3-65Figure 3.2-6Plastic mechanism for computing lateral strength3-66Figure 3.2-7Detailed analytical model of 6-story frame3-67Figure 3.2-9A compound node and attached spring3-68Figure 3.2-10Krawinkler beam-column joint model3-69Figure 3.2-11Column web component of panel zone resistance3-71Figure 3.2-12Column web component of panel zone region3-73Figure 3.2-14Transforming shear deformation to rotational deformation in the Krawinkler model3-74Figure 3.2-15Assumed stress-strain curve for modeling girder3-88Figure 3.2-16Moment curvature diagram for W27x94 girder3-78Figure 3.2-17Developing moment-deflection of moment-deflection curves3-82Figure 3.2-16Moment curvature diagram	Table 3.1-28	• • •	
Figure 3.2-2Elevation of structural system3-53Table 3.2-1Member Sizes Used in N-S Moment Frames3-53Table 3.2-2Gravity Loads on Seattle Building3-53Figure 3.2-3Element loads used in analysis3-56Table 3.2-3Equivalent Lateral Forces for Seattle Building Responding in N-S Directions3-58Figure 3.2-4Simple wire frame model used for preliminary analysis3-60Table 3.2-5Results of Preliminary Analysis Using P-delta Effects3-62Table 3.2-6Periods of Vibration From Preliminary Analysis3-62Figure 3.2-7Demand-to-capacity ratios for elements from analysis with P-delta effects included3-63Figure 3.2-6Plastic mechanism for computing lateral strength3-65Figure 3.2-7Detailed analytical model of 6-story frame3-66Figure 3.2-7Detailed analytical model of 6-story frame3-67Figure 3.2-10Krawinkler beam-column joint model3-68Figure 3.2-11Column flange component of panel zone resistance3-71Figure 3.2-12Column web component of panel zone resistance3-72Figure 3.2-13Force-deformation tor totational deformation in the Krawinkler model3-74Table 3.8-8Properties for the Krawinkler Beam-Column Joint Model3-75Figure 3.2-13Boveloping moment-deflection diagrams for a typical girder3-78Figure 3.2-14Transforming shear deformation to rotational deformation in the Krawinkler model3-74Table 3.8-8Properties for the Krawinkler Beam-Column Joint Model3-	Figure 3.2-1	•	
Table 3.2-1Member Sizes Used in N-S Moment Frames3-53Table 3.2-2Gravity Loads on Seattle Building3-53Figure 3.2-3Element loads used in analysis3-56Figure 3.2-4Simple wire frame model used for preliminary analysis3-56Table 3.2-3Equivalent Lateral Forces for Seattle Building Responding in N-S Directions3-58Figure 3.2-4Results of Preliminary Analysis Using P-delta Effects3-62Table 3.2-5Results of Preliminary Analysis Including P-delta Effects3-62Table 3.2-6Periods of Vibration From Preliminary Analysis3-62Figure 3.2-5Demand-to-capacity ratios for elements from analysis with P-delta effects included3-63Table 3.2-7Lateral Strength on Basis of Rigid-Plastic Mechanism3-66Figure 3.2-7Detatiled analytical model of 6-story frame3-67Figure 3.2-8Model of girder and panel zone region3-67Figure 3.2-9A compound node and attached spring3-68Figure 3.2-11Column flange component of panel zone resistance3-72Figure 3.2-12Column web component of panel zone resistance3-71Figure 3.2-13Force-deformation behavior of panel zone region3-73Figure 3.2-14Moment curvature diagram for W27x94 girder3-78Figure 3.2-15Assumed stress-strain curve for modeling girders3-78Figure 3.2-16Moment curvature diagram for W27x94 girder3-80Figure 3.2-17Developiment of equations for deflection of moment-deflection curves3-82Table 3.2-9 <td>•</td> <td>•</td> <td></td>	•	•	
Table 3.2-2Gravity Loads on Seattle Building3-53Figure 3.2-3Element loads used in analysis3-56Table 3.2-3Equivalent Lateral Forces for Seattle Building Responding in N-S Directions3-58Figure 3.2-4Simple wire frame model used for preliminary analysis3-60Table 3.2-4Results of Preliminary Analysis Using P-delta Effects3-62Table 3.2-5Results of Preliminary Analysis Including P-delta Effects3-62Table 3.2-6Periods of Vibration From Preliminary Analysis3-62Figure 3.2-5Demand-to-capacity ratios for elements from analysis with P-delta effects included3-63Table 3.2-7Lateral Strength on Basis of Rigid-Plastic Mechanism3-65Figure 3.2-6Plastic mechanism for computing lateral strength3-66Figure 3.2-7Detailed analytical model of 6-story frame3-67Figure 3.2-8Model of girder and panel zone region3-67Figure 3.2-9A compound node and attached spring3-68Figure 3.2-10Krawinkler beam-column joint model3-69Figure 3.2-11Column web component of panel zone resistance3-71Figure 3.2-12Column web component of panel zone region3-73Figure 3.2-13Force-deformation to rotational deformation in the Krawinkler model3-74Table 3.8-8Properties for the Krawinkler Beam-Column Joint Model3-75Figure 3.2-17Developing moment-deflection diagrams for a typical girder3-80Figure 3.2-17Developing moment-deflection diagrams for a typical girder3-82	Table 3.2-1	•	
Figure 3.2-3Element loads used in analysis3-56Table 3.2-3Equivalent Lateral Forces for Seattle Building Responding in N-S Directions3-58Figure 3.2-4Simple wire frame model used for preliminary analysis3-60Table 3.2-4Results of Preliminary Analysis Using P-delta Effects3-62Table 3.2-5Results of Preliminary Analysis Including P-delta Effects3-62Table 3.2-6Periods of Vibration From Preliminary Analysis3-62Table 3.2-7Demand-to-capacity ratios for elements from analysis with P-delta effects included3-63Table 3.2-7Lateral Strength on Basis of Rigid-Plastic Mechanism3-65Figure 3.2-7Detailed analytical model of 6-story frame3-66Figure 3.2-8Model of girder and panel zone region3-67Figure 3.2-9A compound node and attached spring3-68Figure 3.2-10Krawinkler beam-column joint model3-69Figure 3.2-12Column flange component of panel zone resistance3-71Figure 3.2-13Force-deformation to rotational deformation in the Krawinkler model3-74Table 3.8-8Properties for the Krawinkler Beam-Column Joint Model3-75Figure 3.2-15Assumed stress-strain curve for word/x94 girder3-80Figure 3.2-16Moment curvature diagram for W27x94 girder3-80Figure 3.2-17Development of equations for deflection of moment-deflection curves3-82Table 3.2-9Girder Properties as Modeled in DRAIN3-84Figure 3.2-14Moment-deflection curve for W27x94 girder3-80<	Table 3.2-2		
Table 3.2-3Equivalent Lateral Forces for Seattle Building Responding in N-S Directions3-58Figure 3.2-4Simple wire frame model used for preliminary analysis3-60Table 3.2-4Results of Preliminary Analysis Using P-delta Effects3-62Table 3.2-5Results of Preliminary Analysis Including P-delta Effects3-62Table 3.2-6Periods of Vibration From Preliminary Analysis3-62Figure 3.2-5Demand-to-capacity ratios for elements from analysis with P-delta effects included3-63Table 3.2-7Lateral Strength on Basis of Rigid-Plastic Mechanism3-65Figure 3.2-6Plastic mechanism for computing lateral strength3-66Figure 3.2-7Detailed analytical model of 6-story frame3-67Figure 3.2-8Model of girder and panel zone region3-67Figure 3.2-9A compound node and attached spring3-68Figure 3.2-10Krawinkler beam-column joint model3-69Figure 3.2-11Column flange component of panel zone resistance3-72Figure 3.2-12Column flange component of panel zone region3-73Figure 3.2-13Force-deformation to rotational deformation in the Krawinkler model3-74Table 3.8-8Properties for the Krawinkler Beam-Column Joint Model3-75Figure 3.2-15Moment curvature diagram for W27x94 girder3-70Figure 3.2-17Developing moment-deflection diagrams for a typical girder3-80Figure 3.2-18Developing noment-deflection diagrams for a typical girder3-82Figure 3.2-19Diveloping noment-deflection of mom	Figure 3.2-3		
Figure 3.2-4Simple wire frame model used for preliminary analysis3-60Table 3.2-4Results of Preliminary Analysis Using P-delta Effects3-62Table 3.2-5Results of Preliminary Analysis Including P-delta Effects3-62Table 3.2-6Periods of Vibration From Preliminary Analysis3-62Figure 3.2-7Demand-to-capacity ratios for elements from analysis with P-delta effects included3-63Table 3.2-7Lateral Strength on Basis of Rigid-Plastic Mechanism3-65Figure 3.2-6Plastic mechanism for computing lateral strength3-66Figure 3.2-7Detailed analytical model of 6-story frame3-67Figure 3.2-8Model of girder and panel zone region3-67Figure 3.2-9A compound node and attached spring3-68Figure 3.2-10Krawinkler beam-column joint model3-69Figure 3.2-11Column flange component of panel zone resistance3-72Figure 3.2-12Column web component of panel zone region3-73Figure 3.2-13Force-deformation to rotational deformation in the Krawinkler model3-74Table 3.8-8Properties for the Krawinkler Beam-Column Joint Model3-75Figure 3.2-15Assumed stress-strain curve for modeling girders3-78Figure 3.2-19Developing moment-deflection diagrams for a typical girder3-80Figure 3.2-19Developing moment-deflection dimgrams for a typical girder3-82Table 3.2-9Girder Properties as Modeled in DRAIN3-84Figure 3.2-10Lateral Load Patterns Used in Nonlinear Static Pushover Analysis<	Table 3.2-3		
Table 3.2-4Results of Preliminary Analysis Using P-delta Effects3-62Table 3.2-5Results of Preliminary Analysis Including P-delta Effects3-62Table 3.2-6Periods of Vibration From Preliminary Analysis3-62Figure 3.2-5Demand-to-capacity ratios for elements from analysis with P-delta effects included3-63Table 3.2-7Lateral Strength on Basis of Rigid-Plastic Mechanism3-65Figure 3.2-8Model of girder and panel zone region3-66Figure 3.2-9A compound node and attached spring3-66Figure 3.2-9A compound node and attached spring3-66Figure 3.2-10Column flange component of panel zone resistance3-71Figure 3.2-11Column flange component of panel zone region3-73Figure 3.2-12Column web component of panel zone region3-73Figure 3.2-13Force-deformation behavior of panel zone region3-73Figure 3.2-14Transforming shear deformation to rotational deformation in the Krawinkler model3-74Table 3.2-7Assumed stress-strain curve for modeling girders3-78Figure 3.2-16Moment curvature diagram for W27x94 girder3-80Figure 3.2-17Developing moment-deflection diagrams for a typical girder3-83Figure 3.2-18Development of panel role W27x94 girder3-85Figure 3.2-19Moment-deflection curve for W27x94 girder3-85Figure 3.2-20Development of panel solutions for deflection curves3-82Figure 3.2-218Development of panel model in DRAIN3-84Figure 3.2-			
Table 3.2-5Results of Preliminary Analysis Including P-delta Effects3-62Table 3.2-6Periods of Vibration From Preliminary Analysis3-62Figure 3.2-5Demand-to-capacity ratios for elements from analysis with P-delta effects included3-63Table 3.2-7Lateral Strength on Basis of Rigid-Plastic Mechanism3-65Figure 3.2-6Plastic mechanism for computing lateral strength3-66Figure 3.2-7Detailed analytical model of 6-story frame3-67Figure 3.2-8Model of girder and panel zone region3-67Figure 3.2-9A compound node and attached spring3-68Figure 3.2-10Krawinkler beam-column joint model3-69Figure 3.2-11Column flange component of panel zone resistance3-71Figure 3.2-12Column web component of panel zone region3-73Figure 3.2-13Force-deformation behavior of panel zone region3-73Figure 3.2-14Transforming shear deformation to rotational deformation in the Krawinkler model3-74Table 3.8-8Properties for the Krawinkler Beam-Column Joint Model3-75Figure 3.2-15Assumed stress-strain curve for modeling girders3-78Figure 3.2-17Developing moment-deflection diagrams for a typical girder3-80Figure 3.2-18Development of equations for deflection of moment-deflection curves3-82Figure 3.2-19Moment-deflection curve for W27x94 girder3-84Figure 3.2-19Development of plastic hinge properties for the W27x97 girder3-86Figure 3.2-20Development of plastic hinge properti	<b>U</b>		
Table 3.2-6Periods of Vibration From Preliminary Analysis3-62Figure 3.2-5Demand-to-capacity ratios for elements from analysis with P-delta effects included3-63Table 3.2-7Lateral Strength on Basis of Rigid-Plastic Mechanism3-65Figure 3.2-6Plastic mechanism for computing lateral strength3-66Figure 3.2-7Detailed analytical model of 6-story frame3-67Figure 3.2-8Model of girder and panel zone region3-67Figure 3.2-9A compound node and attached spring3-68Figure 3.2-10Krawinkler beam-column joint model3-69Figure 3.2-11Column flange component of panel zone resistance3-71Figure 3.2-12Column web component of panel zone region3-73Figure 3.2-13Force-deformation behavior of panel zone region3-73Figure 3.2-14Transforming shear deformation to rotational deformation in the Krawinkler model3-74Table 3.8-8Properties for the Krawinkler Beam-Column Joint Model3-75Figure 3.2-15Assumed stress-strain curve for modeling girders3-78Figure 3.2-16Moment curvature diagram for W27x94 girder3-80Figure 3.2-17Developing moment-deflection of moment-deflection curves3-82Figure 3.2-19Girder Properties as Modeled in DRAIN3-84Figure 3.2-10Lateral Load Patterns Used in Nonlinear Static Pushover Analysis3-89Figure 3.2-21Yield surface used for modeling columns3-87Figure 3.2-22Two base shear components of pushover response3-90Figu			
Figure 3.2-5Demand-to-capacity ratios for elements from analysis with P-delta effects included3-63Table 3.2-7Lateral Strength on Basis of Rigid-Plastic Mechanism3-65Figure 3.2-6Plastic mechanism for computing lateral strength3-66Figure 3.2-7Detailed analytical model of 6-story frame3-67Figure 3.2-8Model of girder and panel zone region3-67Figure 3.2-9A compound node and attached spring3-66Figure 3.2-10Krawinkler beam-column joint model3-69Figure 3.2-11Column flange component of panel zone resistance3-71Figure 3.2-12Column web component of panel zone region3-73Figure 3.2-13Force-deformation behavior of panel zone region3-73Figure 3.2-14Transforming shear deformation to rotational deformation in the Krawinkler model3-74Table 3.8-8Properties for the Krawinkler Beam-Column Joint Model3-75Figure 3.2-15Assumed stress-strain curve for modeling girders3-78Figure 3.2-16Moment curvature diagram for W27x94 girder3-80Figure 3.2-17Developing moment-deflection of moment-deflection curves3-82Table 3.2-9Girder Properties as Modeled in DRAIN3-84Figure 3.2-10Lateral Load Patterns Used in Nonlinear Static Pushover Analysis3-87Figure 3.2-20Development of plastic hinge properties for the W27x97 girder3-86Figure 3.2-20Tivel as the components of pushover response3-90Figure 3.2-21Vield surface used for modeling columns3-87 <td></td> <td></td> <td></td>			
Table 3.2-7Lateral Strength on Basis of Rigid-Plastic Mechanism3-65Figure 3.2-6Plastic mechanism for computing lateral strength3-66Figure 3.2-7Detailed analytical model of 6-story frame3-67Figure 3.2-8Model of girder and panel zone region3-67Figure 3.2-9A compound node and attached spring3-68Figure 3.2-10Krawinkler beam-column joint model3-69Figure 3.2-11Column flange component of panel zone resistance3-71Figure 3.2-12Column web component of panel zone resistance3-72Figure 3.2-13Force-deformation behavior of panel zone region3-73Figure 3.2-14Transforming shear deformation to rotational deformation in the Krawinkler model3-74Table 3.8-8Properties for the Krawinkler Beam-Column Joint Model3-75Figure 3.2-15Assumed stress-strain curve for modeling girders3-78Figure 3.2-16Moment curvature diagram for W27x94 girder3-80Figure 3.2-17Developing moment-deflection diagrams for a typical girder3-82Table 3.2-9Girder Properties as Modeled in DRAIN3-84Figure 3.2-19Development of plastic hinge properties for the W27x97 girder3-86Figure 3.2-20Development of plastic hinge properties for the W27x97 girder3-86Figure 3.2-20Development of plastic hinge properties for the W27x97 girder3-86Figure 3.2-21Yield surface used for modeling columns3-87Table 3.2-10Lateral Load Patterns Used in Nonlinear Static Pushover Analysis3-89 </td <td></td> <td></td> <td></td>			
Figure 3.2-6Plastic mechanism for computing lateral strength3-66Figure 3.2-7Detailed analytical model of 6-story frame3-67Figure 3.2-8Model of girder and panel zone region3-67Figure 3.2-9A compound node and attached spring3-68Figure 3.2-10Krawinkler beam-column joint model3-69Figure 3.2-11Column flange component of panel zone resistance3-71Figure 3.2-12Column web component of panel zone resistance3-72Figure 3.2-13Force-deformation behavior of panel zone region3-73Figure 3.2-14Transforming shear deformation to rotational deformation in the Krawinkler model3-74Table 3.8-8Properties for the Krawinkler Beam-Column Joint Model3-75Figure 3.2-16Moment curvature diagram for W27x94 girder3-78Figure 3.2-17Developing moment-deflection diagrams for a typical girder3-80Figure 3.2-18Development of plastic hinge properties for the W27x97 girder3-84Figure 3.2-20Development of plastic hinge properties for the W27x97 girder3-86Figure 3.2-21Tustface used for modeling columns3-87Table 3.2-21Development of plastic hinge properties for the W27x97 girder3-86Figure 3.2-21Two base shear components of pushover response3-80Figure 3.2-21Two base shear components of pushover response3-80Figure 3.2-22Two base shear components of pushover response3-89Figure 3.2-23Response of strong panel model to three load pattern, excluding P-delta effects	<b>U</b>		
Figure 3.2-7Detailed analytical model of 6-story frame3-67Figure 3.2-8Model of girder and panel zone region3-67Figure 3.2-9A compound node and attached spring3-68Figure 3.2-10Krawinkler beam-column joint model3-69Figure 3.2-11Column flange component of panel zone resistance3-71Figure 3.2-12Column web component of panel zone resistance3-72Figure 3.2-13Force-deformation behavior of panel zone region3-73Figure 3.2-14Transforming shear deformation to rotational deformation in the Krawinkler model3-74Table 3.8-8Properties for the Krawinkler Beam-Column Joint Model3-75Figure 3.2-16Moment curvature diagram for W27x94 girder3-78Figure 3.2-17Developing moment-deflection diagrams for a typical girder3-80Figure 3.2-18Development of Plastic hinge properties for the W27x97 girder3-84Figure 3.2-19Moment-deflection curve for W27x94 girder3-85Figure 3.2-20Development of plastic hinge properties for the W27x97 girder3-86Figure 3.2-21Yield surface used for modeling columns3-87Table 3.2-10Lateral Load Patterns Used in Nonlinear Static Pushover Analysis3-87Figure 3.2-23Response of strong panel model to three load pattern, excluding P-delta effects3-90Figure 3.2-24Response of strong panel model to three load pattern, excluding P-delta effects3-91Figure 3.2-25Response of strong panel model to three loading patters, including P-delta effects3-92Fi			
Figure 3.2-8Model of girder and panel zone region3-67Figure 3.2-9A compound node and attached spring3-68Figure 3.2-10Krawinkler beam-column joint model3-69Figure 3.2-11Column flange component of panel zone resistance3-71Figure 3.2-12Column web component of panel zone resistance3-72Figure 3.2-13Force-deformation behavior of panel zone region3-73Figure 3.2-14Transforming shear deformation to rotational deformation in the Krawinkler model3-74Table 3.8-8Properties for the Krawinkler Beam-Column Joint Model3-75Figure 3.2-15Assumed stress-strain curve for modeling girders3-78Figure 3.2-16Moment curvature diagram for W27x94 girder3-79Figure 3.2-17Developing moment-deflection diagrams for a typical girder3-80Figure 3.2-18Development of equations for deflection of moment-deflection curves3-82Table 3.2-9Girder Properties as Modeled in DRAIN3-84Figure 3.2-19Moment-deflection curve for W27x94 girder3-85Figure 3.2-20Development of plastic hinge properties for the W27x97 girder3-86Figure 3.2-21Yield surface used for modeling columns3-87Table 3.2-10Lateral Load Patterns Used in Nonlinear Static Pushover Analysis3-89Figure 3.2-23Response of strong panel model to three load pattern, excluding P-delta effects3-91Figure 3.2-24Response of strong panel model to three loading patters, including P-delta effects3-92Figure 3.2-25Response of	•		
Figure 3.2-9A compound node and attached spring3-68Figure 3.2-10Krawinkler beam-column joint model3-69Figure 3.2-11Column flange component of panel zone resistance3-71Figure 3.2-12Column web component of panel zone resistance3-72Figure 3.2-13Force-deformation behavior of panel zone region3-73Figure 3.2-14Transforming shear deformation to rotational deformation in the Krawinkler model3-74Table 3.8-8Properties for the Krawinkler Beam-Column Joint Model3-75Figure 3.2-15Assumed stress-strain curve for modeling girders3-78Figure 3.2-16Moment curvature diagram for W27x94 girder3-79Figure 3.2-17Developing moment-deflection diagrams for a typical girder3-80Figure 3.2-18Development of equations for deflection of moment-deflection curves3-82Table 3.2-9Girder Properties as Modeled in DRAIN3-84Figure 3.2-19Moment-deflection curve for W27x94 girder3-85Figure 3.2-10Lateral Load Patterns Used in Nonlinear Static Pushover Analysis3-89Figure 3.2-21Yield surface used for modeling columns3-89Figure 3.2-23Response of strong panel model to three load pattern, excluding P-delta effects3-90Figure 3.2-24Response of strong panel model to three loading patters, including P-delta effects3-92Figure 3.2-25Response of strong panel model to three loading patters, including P-delta effects3-92	-	• •	
Figure 3.2-10Krawinkler beam-column joint model3-69Figure 3.2-11Column flange component of panel zone resistance3-71Figure 3.2-12Column web component of panel zone resistance3-72Figure 3.2-13Force-deformation behavior of panel zone region3-73Figure 3.4-14Transforming shear deformation to rotational deformation in the Krawinkler model3-74Table 3.8-8Properties for the Krawinkler Beam-Column Joint Model3-75Figure 3.2-15Assumed stress-strain curve for modeling girders3-78Figure 3.2-16Moment curvature diagram for W27x94 girder3-79Figure 3.2-17Developing moment-deflection diagrams for a typical girder3-80Figure 3.2-18Development of equations for deflection of moment-deflection curves3-82Table 3.2-9Girder Properties as Modeled in DRAIN3-84Figure 3.2-10Development of plastic hinge properties for the W27x97 girder3-86Figure 3.2-210Lateral Load Patterns Used in Nonlinear Static Pushover Analysis3-89Figure 3.2-22Two base shear components of pushover response3-90Figure 3.2-23Response of strong panel model to three load pattern, excluding P-delta effects3-91Figure 3.2-24Response of strong panel model to ML loads, with and without P-delta effects3-92	<b>U</b>		
Figure 3.2-11Column flange component of panel zone resistance3-71Figure 3.2-12Column web component of panel zone resistance3-72Figure 3.2-13Force-deformation behavior of panel zone region3-73Figure 3.4-14Transforming shear deformation to rotational deformation in the Krawinkler model3-74Table 3.8-8Properties for the Krawinkler Beam-Column Joint Model3-75Figure 3.2-15Assumed stress-strain curve for modeling girders3-78Figure 3.2-16Moment curvature diagram for W27x94 girder3-79Figure 3.2-17Developing moment-deflection diagrams for a typical girder3-80Figure 3.2-18Development of equations for deflection of moment-deflection curves3-82Table 3.2-9Girder Properties as Modeled in DRAIN3-84Figure 3.2-10Development of plastic hinge properties for the W27x97 girder3-86Figure 3.2-21Yield surface used for modeling columns3-87Table 3.2-22Two base shear components of pushover response3-90Figure 3.2-23Response of strong panel model to three load pattern, excluding P-delta effects3-91Figure 3.2-24Response of strong panel model to three loading patters, including P-delta effects3-92Figure 3.2-25Response of strong panel model to ML loads, with and without P-delta effects3-92	<b>U</b>	· · ·	
Figure 3.2-12Column web component of panel zone resistance3-72Figure 3.2-13Force-deformation behavior of panel zone region3-73Figure 3.2-13Force-deformation behavior of panel zone region3-73Figure 3.4-14Transforming shear deformation to rotational deformation in the Krawinkler model3-74Table 3.8-8Properties for the Krawinkler Beam-Column Joint Model3-75Figure 3.2-15Assumed stress-strain curve for modeling girders3-78Figure 3.2-16Moment curvature diagram for W27x94 girder3-79Figure 3.2-17Developing moment-deflection diagrams for a typical girder3-80Figure 3.2-18Development of equations for deflection of moment-deflection curves3-82Table 3.2-9Girder Properties as Modeled in DRAIN3-84Figure 3.2-19Moment-deflection curve for W27x94 girder3-85Figure 3.2-20Development of plastic hinge properties for the W27x97 girder3-86Figure 3.2-21Yield surface used for modeling columns3-87Table 3.2-10Lateral Load Patterns Used in Nonlinear Static Pushover Analysis3-89Figure 3.2-23Response of strong panel model to three load pattern, excluding P-delta effects3-91Figure 3.2-24Response of strong panel model to three loading patters, including P-delta effects3-92Figure 3.2-25Response of strong panel model to ML loads, with and without P-delta effects3-92			
Figure 3.2-13Force-deformation behavior of panel zone region3-73Figure 3.4-14Transforming shear deformation to rotational deformation in the Krawinkler model3-74Table 3.8-8Properties for the Krawinkler Beam-Column Joint Model3-75Figure 3.2-15Assumed stress-strain curve for modeling girders3-78Figure 3.2-16Moment curvature diagram for W27x94 girder3-79Figure 3.2-17Developing moment-deflection diagrams for a typical girder3-80Figure 3.2-18Development of equations for deflection of moment-deflection curves3-82Table 3.2-9Girder Properties as Modeled in DRAIN3-84Figure 3.2-10Development of plastic hinge properties for the W27x97 girder3-86Figure 3.2-20Development of plastic hinge properties for the W27x97 girder3-87Table 3.2-10Lateral Load Patterns Used in Nonlinear Static Pushover Analysis3-89Figure 3.2-23Response of strong panel model to three load pattern, excluding P-delta effects3-91Figure 3.2-24Response of strong panel model to ML loads, with and without P-delta effects3-92			
Figure 3.4-14Transforming shear deformation to rotational deformation in the Krawinkler model .3-74Table 3.8-8Properties for the Krawinkler Beam-Column Joint Model .3-75Figure 3.2-15Assumed stress-strain curve for modeling girders .3-78Figure 3.2-16Moment curvature diagram for W27x94 girder .3-79Figure 3.2-17Developing moment-deflection diagrams for a typical girder .3-80Figure 3.2-18Development of equations for deflection of moment-deflection curves .3-82Table 3.2-9Girder Properties as Modeled in DRAIN .3-84Figure 3.2-19Moment-deflection curve for W27x94 girder .3-85Figure 3.2-20Development of plastic hinge properties for the W27x97 girder .3-86Figure 3.2-21Yield surface used for modeling columns .3-87Figure 3.2-22Two base shear components of pushover response .3-90Figure 3.2-23Response of strong panel model to three load pattern, excluding P-delta effects .3-91Figure 3.2-24Response of strong panel model to ML loads, with and without P-delta effects .3-92	<b>U</b>		
Table 3.8-8Properties for the Krawinkler Beam-Column Joint Model3-75Figure 3.2-15Assumed stress-strain curve for modeling girders3-78Figure 3.2-16Moment curvature diagram for W27x94 girder3-79Figure 3.2-17Developing moment-deflection diagrams for a typical girder3-80Figure 3.2-18Development of equations for deflection of moment-deflection curves3-82Table 3.2-9Girder Properties as Modeled in DRAIN3-84Figure 3.2-19Moment-deflection curve for W27x94 girder3-85Figure 3.2-20Development of plastic hinge properties for the W27x97 girder3-86Figure 3.2-21Yield surface used for modeling columns3-87Table 3.2-10Lateral Load Patterns Used in Nonlinear Static Pushover Analysis3-89Figure 3.2-22Two base shear components of pushover response3-90Figure 3.2-23Response of strong panel model to three load pattern, excluding P-delta effects3-91Figure 3.2-24Response of strong panel model to ML loads, with and without P-delta effects3-92	<b>U</b>		
Figure 3.2-15Assumed stress-strain curve for modeling girders3-78Figure 3.2-16Moment curvature diagram for W27x94 girder3-79Figure 3.2-17Developing moment-deflection diagrams for a typical girder3-80Figure 3.2-18Development of equations for deflection of moment-deflection curves3-82Table 3.2-9Girder Properties as Modeled in DRAIN3-84Figure 3.2-19Moment-deflection curve for W27x94 girder3-85Figure 3.2-20Development of plastic hinge properties for the W27x97 girder3-86Figure 3.2-21Yield surface used for modeling columns3-87Table 3.2-10Lateral Load Patterns Used in Nonlinear Static Pushover Analysis3-89Figure 3.2-23Response of strong panel model to three load pattern, excluding P-delta effects3-91Figure 3.2-24Response of strong panel model to ML loads, with and without P-delta effects3-92	Table 3.8-8		
Figure 3.2-16Moment curvature diagram for W27x94 girder3-79Figure 3.2-17Developing moment-deflection diagrams for a typical girder3-80Figure 3.2-18Development of equations for deflection of moment-deflection curves3-82Table 3.2-9Girder Properties as Modeled in DRAIN3-84Figure 3.2-19Moment-deflection curve for W27x94 girder3-85Figure 3.2-20Development of plastic hinge properties for the W27x97 girder3-86Figure 3.2-21Yield surface used for modeling columns3-87Table 3.2-10Lateral Load Patterns Used in Nonlinear Static Pushover Analysis3-89Figure 3.2-23Response of strong panel model to three load pattern, excluding P-delta effects3-91Figure 3.2-24Response of strong panel model to ML loads, with and without P-delta effects3-92	Figure 3.2-15		
Figure 3.2-17Developing moment-deflection diagrams for a typical girder3-80Figure 3.2-18Development of equations for deflection of moment-deflection curves3-82Table 3.2-9Girder Properties as Modeled in DRAIN3-84Figure 3.2-19Moment-deflection curve for W27x94 girder3-85Figure 3.2-20Development of plastic hinge properties for the W27x97 girder3-86Figure 3.2-21Yield surface used for modeling columns3-87Table 3.2-10Lateral Load Patterns Used in Nonlinear Static Pushover Analysis3-89Figure 3.2-23Response of strong panel model to three load pattern, excluding P-delta effects3-91Figure 3.2-24Response of strong panel model to ML loads, with and without P-delta effects3-92	<b>U</b>		
Figure 3.2-18Development of equations for deflection of moment-deflection curves3-82Table 3.2-9Girder Properties as Modeled in DRAIN3-84Figure 3.2-19Moment-deflection curve for W27x94 girder3-85Figure 3.2-20Development of plastic hinge properties for the W27x97 girder3-86Figure 3.2-21Yield surface used for modeling columns3-87Table 3.2-10Lateral Load Patterns Used in Nonlinear Static Pushover Analysis3-89Figure 3.2-22Two base shear components of pushover response3-90Figure 3.2-23Response of strong panel model to three load pattern, excluding P-delta effects3-91Figure 3.2-24Response of strong panel model to ML loads, with and without P-delta effects3-92	U		
Table 3.2-9Girder Properties as Modeled in DRAIN3-84Figure 3.2-19Moment-deflection curve for W27x94 girder3-85Figure 3.2-20Development of plastic hinge properties for the W27x97 girder3-86Figure 3.2-21Yield surface used for modeling columns3-87Table 3.2-10Lateral Load Patterns Used in Nonlinear Static Pushover Analysis3-89Figure 3.2-22Two base shear components of pushover response3-90Figure 3.2-23Response of strong panel model to three load pattern, excluding P-delta effects3-91Figure 3.2-24Response of strong panel model to three loading patters, including P-delta effects3-92Figure 3.2-25Response of strong panel model to ML loads, with and without P-delta effects3-92	<b>U</b>		
Figure 3.2-19Moment-deflection curve for W27x94 girder3-85Figure 3.2-20Development of plastic hinge properties for the W27x97 girder3-86Figure 3.2-21Yield surface used for modeling columns3-87Table 3.2-10Lateral Load Patterns Used in Nonlinear Static Pushover Analysis3-89Figure 3.2-22Two base shear components of pushover response3-90Figure 3.2-23Response of strong panel model to three load pattern, excluding P-delta effects3-91Figure 3.2-24Response of strong panel model to three loading patters, including P-delta effects3-92Figure 3.2-25Response of strong panel model to ML loads, with and without P-delta effects3-92	-		
Figure 3.2-20Development of plastic hinge properties for the W27x97 girder3-86Figure 3.2-21Yield surface used for modeling columns3-87Table 3.2-10Lateral Load Patterns Used in Nonlinear Static Pushover Analysis3-89Figure 3.2-22Two base shear components of pushover response3-90Figure 3.2-23Response of strong panel model to three load pattern, excluding P-delta effects3-91Figure 3.2-24Response of strong panel model to three loading patters, including P-delta effects3-92Figure 3.2-25Response of strong panel model to ML loads, with and without P-delta effects3-92			
Figure 3.2-21Yield surface used for modeling columns3-87Table 3.2-10Lateral Load Patterns Used in Nonlinear Static Pushover Analysis3-89Figure 3.2-22Two base shear components of pushover response3-90Figure 3.2-23Response of strong panel model to three load pattern, excluding P-delta effects3-91Figure 3.2-24Response of strong panel model to three loading patters, including P-delta effects3-92Figure 3.2-25Response of strong panel model to ML loads, with and without P-delta effects3-92	<b>U</b>		
Table 3.2-10Lateral Load Patterns Used in Nonlinear Static Pushover Analysis3-89Figure 3.2-22Two base shear components of pushover response3-90Figure 3.2-23Response of strong panel model to three load pattern, excluding P-delta effects3-91Figure 3.2-24Response of strong panel model to three loading patters, including P-delta effects3-92Figure 3.2-25Response of strong panel model to ML loads, with and without P-delta effects3-92	<b>U</b>		
Figure 3.2-22Two base shear components of pushover response3-90Figure 3.2-23Response of strong panel model to three load pattern, excluding P-delta effects3-91Figure 3.2-24Response of strong panel model to three loading patters, including P-delta effects3-92Figure 3.2-25Response of strong panel model to ML loads, with and without P-delta effects3-92	<b>U</b>		
Figure 3.2-23Response of strong panel model to three load pattern, excluding P-delta effects3-91Figure 3.2-24Response of strong panel model to three loading patters, including P-delta effects3-92Figure 3.2-25Response of strong panel model to ML loads, with and without P-delta effects3-92		•	
Figure 3.2-24Response of strong panel model to three loading patters, including P-delta effects3-92Figure 3.2-25Response of strong panel model to ML loads, with and without P-delta effects3-92	<b>U</b>		
Figure 3.2-25 Response of strong panel model to ML loads, with and without P-delta effects 3-92	Figure 3.2-24		
Figure 3.2-26 Tangent stiffness history for structure under ML loads, with and without	Figure 3.2-26	Tangent stiffness history for structure under ML loads, with and without	

	P-delta effects	3-93
Figure 3.2-27	Patterns of plastic hinge formation: SP model under ML load, including	
C	P-delta effects	3-95
Table 3.2-11	Strength Comparisons: Pushover vs. Rigid Plastic	3-96
Figure 3.2-28	Weak panel zone model under ML load	
Figure 3.2-29	Comparison of weak panel zone model with strong panel zone model,	
1.8010 0.12 25	excluding P-delta effects	3-97
Figure 3.2-30	Comparison of weak panel zone model with strong panel zone model,	5 71
1 iguie 5.2 50	including P-delta effects	3-98
Figure 3.2-31	Tangent stiffness history for structure under ML loads, strong versus	5 70
1 iguie 5.2 51	weak panels, including P-delta effects	3-98
Figure 3.2-32	Patterns of plastic hinge formation: weak panel zone model under ML load, includin	
Tiguie 5.2-52	delta effects	
Table 3.2-12	Modal Properties and Expected Inelastic Displacements for the	5-99
Table 3.2-12	Strong and Weak Panel Models Subjected to the Modal Load Pattern	3 100
Eiguro 2 2 22 A		
-	A simple capacity spectrum	
Figure 3.2-34	A simple demand spectrum	
Figure 3.2-35	Capacity and demand spectra plotted together	
Figure 3.2-36	Capacity spectrum showing control points	
Table 3.2-13	Damping Modification Factors	
Figure 3.2-37	Damping modification factors	
Figure 3.2-38	Capacity spectrum used in iterative solution	
Table 3.2-14	Results of Iteration for Maximum Expected Displacement	
Table 3.2-15	Points on Capacity Spectrum Corresponding to Chosen Damping Values	3-110
Figure 3.2-39	Capacity spectrum with equivalent viscous damping points and	
	secant stiffnesses	
Figure 3.2-40	Demand spectra for several equivalent viscous damping values	
Figure 3.2-41	Capacity and demand spectra on single plot	
Figure 3.2-42	Close-up view of portion of capacity and demand spectra	
Table 3.2-16	Summary of Results from Pushover Analysis	
Table 3.2-17	Structural Frequencies and Damping Factors Used in Time-History Analysis	
Table 3.2-18	Seattle Ground Motion Parameters	
Figure 3.2-43	Time histories and response spectra for Record A	3-119
Figure 3.2-44	Time histories and response for Record B	3-120
Figure 3.2-45	Time histories and response spectra for Record C	3-121
Figure 3.2-46	Ground motion scaling parameters	3-123
Table 3.2-19	Maximum Base Shear in Frame Analyzed with 5 Percent Damping,	
	Strong Panels, Excluding P-delta Effects	3-124
Table 3.2-20	Maximum Story Drifts from Time-History Analysis with 5 Percent Damping, Strong	5
	Panels, Excluding P-delta Effects	
Table 3.2-21	Maximum Base Shear in Frame analyzed with 5 Percent Damping,	
	Strong Panels, Excluding P-delta Effects	3-124
Table 3.2-22	Maximum Story Drifts from Time-History Analysis with 5 Percent Damping, Strong	g
	Panels, Including P-delta Effects	
Figure 3.2-47	Time history of roof and first-story displacement, ground Motion A00,	
0	excluding P-delta effects	3-126
Figure 3.2-48	Time history of total base shear, Ground Motion A00, excluding P-delta effects	
Figure 3.2-49	Energy time history, Ground Motion A00, excluding P-delta effects	3-127
0		

Figure 3.2-50 Figure 3.2-51	Time history of roof and first story displacement	3-127
Figure 5.2-51	excluding P-delta effects	3-128
Figure 3.2-52	Energy time history, Ground Motion B00, excluding P-delta effects	3-128
Figure 3.2-53	Time history of roof and first-story displacement, Ground Motion C00,	5 120
1 iguie 5.2 55	excluding P-delta effects	3-129
Figure 3.2-54	Time history of total base shear, Ground Motion C00,	5 12)
119010 512 51	excluding P-delta effects	3-129
Figure 3.2-55	Energy time history, Ground Motion C00, excluding P-delta effects	3-130
Figure 3.2-56	Time history of roof and first-story displacement, Ground motion A00,	5 150
118010 012 00	including P-delta effects	3-130
Figure 3.2-57	Time history of total base shear, Ground Motion A00,	
118010 012 07	including P-delta effects	3-131
Figure 3.2-58	Energy time history, Ground Motion A00, including P-delta effects	
Figure 3.2-59	Time history of roof and first-story displacement, Ground Motion B00,	
0	including P-delta effects	3-132
Figure 3.2-60	Time history of total base shear, Ground motion B00,	
U	including P-delta effects	3-132
Figure 3.2-61	Energy time history, Ground Motion B00, including P-delta effects	
Figure 3.2-62	Time history of roof and first-story displacement, Ground Motion C00,	
U	including P-delta effects	3-133
Figure 3.2-63	Time history of total base shear, Ground Motion C00,	
C	including P-delta effects	3-134
Figure 3.2-64	Energy time history, Ground Motion C00, including P-delta effects	
Figure 3.2-65	Time-history of roof displacement, Ground Motion A00,	
C	with and without P-delta effect	3-135
Figure 3.2-66	Time history of base shear, Ground Motion A00, 135	
C	with and without P-delta effects	3-135
Figure 3.2-67	Yielding locations for structure with strong panels subjected to Ground Motion A00	,
-	including P-delta effects	3-136
Table 3.2-23	Summary of All Analyses for Strong Panel Structure,	
	Including P-delta Effects	3-137
Figure 3.2-68	Comparison of inertial force patterns	3-138
Table 3.2-24	Maximum Base Shear (kips) in Frame Analyzed Ground Motion A00,	
	Strong Panels, Including P-delta Effects	3-138
Table 3.2-25	Maximum Story Drifts (in.) from Time-History Analysis Ground Motion A00, Stron	ıg
	Panels, Including P-delta Effects	3-139
Figure 3.2-69	Modeling a simple damper	3-140
Figure 3.2-70	Response of structure with discrete dampers and with	
	equivalent viscous damping	3-141
Figure 3.2-71	Base shear time histories obtained from column forces	3-141
Figure 3.2-72	Base shear time histories as obtained from inertial forces	
Figure 3.2-73	Energy time-history for structure with discrete added damping	3-143
Figure 4.1-1	Typical framing plan	. 4-4
Table 4.1-1	Geotechnical Parameters	
Figure 4.1-2	Critical sections for isolated footings	
Figure 4.1-3	Soil pressure distributions	. 4-7

Table 4.1-2	Footing Design for Gravity Loads	4-10
Figure 4.1-4	Foundation plan for gravity-load-resisting system	
Figure 4.1-5	Framing plan for moment resisting frame system	
Table 4.1-3	Demands for Moment-Resisting Frame System	
Figure 4.1-6	Foundation plan for moment-resisting frame system	
Figure 4.1-7	Framing plan for concentrically braced frame system	
Figure 4.1-8	Soil Pressures for controlling bidirectional case	
Figure 4.1-9	Foundation plan for concentrically braced frame system	
Table 4.1-4	Mat Foundation Section Capacities	
Figure 4.1-10	Envelope of mat foundation flexural demands	4-21
Figure 4.1-11	Mat foundation flexural reinforcement.	
Figure 4.1-12	Section of mat foundation	4-23
Figure 4.1-13	Critical sections for shear and envelope of mat foundation shear demands	4-24
Table 4.1-5	Summary of Material Quantities and Cost Comparison	
Figure 4.2-1	Design condition	
Table 4.2-1	Geotechnical Parameters	4-27
Table 4.2-2	Gravity and Seismic Demands	4-28
Figure 4.2-2	Schematic model of deep foundation system	4-29
Figure 4.2-3	Pile cap free body diagram curves	
Figure 4.2-4	Representative <i>p</i> - <i>y</i> curves	
Figure 4.2-5	Passive pressure mobilization curve	
Figure 4.2-6	Calculated group effect factors	
Figure 4.2-7	Results of pile analysis – sheer versus depth	4-35
Figure 4.2-8	Results of pile analysis – moment versus depth	
Figure 4.2-9	Results of pile analysis – displacement versus depth	
Figure 4.2-10	Results of pile analysis – applied lateral load versus head moment	
Figure 4.2-11	Results of pile – head displacement versus applied lateral load	4-36
Figure 4.2-12	P-M interaction diagram for Site Class C	4-38
Figure 4.2-13	P-M interaction diagram for Site Class E	4-39
Figure 4.2-14	Pile axial capacity as a function of length for Site Class C	4-41
Figure 4.2-15	Pile axial capacity as a function of length for Site Class E	4-42
Table 4.2-3	Pile Lengths Required for Axial Loads	4-42
Table 4.2-4	Summary of Pile Size, Length, and Longitudinal Reinforcement	4-43
Figure 4.2-16	Pile detailing for Site Class C	4-44
Figure 4.2-17	Pile detailing for Site Class E	4-45
Figure 4.2-18	Foundation tie section	4-47
Figure 5.1-1	Framing elevation and sections	. 5-4
Figure 5.1-2	Roof framing and mezzanine framing plan	
Figure 5.1-3	Foundation plan	. 5-5
Table 5.1-1	ELF Vertical Distribution for N-S Analysis	5-11
Table 5.1-2	ELF Analysis in N-S Direction	
Figure 5.1-4	Design response spectrum	
Table 5.1-3	Design Response Spectra	
Table 5.1-4	Moments in Gable Frame Members	5-16
Table 5.1-5	Axial Forces in Gable Frames Members	5-16
Figure 5.1-5	Moment diagram for seismic load combinations	5-16
Figure 5.1-6	Gable frame schematic	5-17

Table 5.1-6	Comparison of Standards	5-18
Figure 5.1-7	Arrangement at knee	5-19
Figure 5.1-8	Bolted stiffened connection at knee	5-20
Figure 5.2-9	End plate connection at ridge	5-24
Figure 5.1-10	Mezzanine framing	5-26
Figure 5.2-11	Shear force in roof deck diagram	5-28
Figure 5.2-1	Typical floor framing plan and building section	5-30
Figure 5.2-2	Framing plan for special moment frame	
Figure 5.2-3	Concentrically braced frame elevations	5-31
Figure 5.2-4	Approximate effect of accidental of torsion	5-35
Table 5.2-1	Alternative A, Moment Frame Seismic Forces and Moments by Level	5-41
Table 5.2-2	Alternative B, Braced Frame Seismic Forces and Moments by Level	5-41
Table 5.2-3	Alternative C, Dual System Seismic Forces and Moments by Level	5-42
Figure 5.2-5	SMRF frame in E-W direction	5-44
Figure 5.2-6	SMRF frame in N-S direction	5-45
Table 5.2-4	Alternative A (Moment Frame) Story Drifts under Seismic Loads	5-45
Table 5.2-5	Alternative A Torsional Analysis	5-46
Figure 5.2-7	Projection of expected moment strength of beam	5-47
Figure 5.2-8	Story height and clear height	5-48
Figure 5.2-9	Free body diagram bounded by plastic hinges	
Table 5.2-4	Column-Beam Moment Ratios for Seven-Bay Frame	
Table 5.2-5	Column-Beam Moment Ratios for Five-Bay Frame	
Figure 5.2-10	Illustration of AISC Seismic vs. FEMA 350 Methods for panel zone shear	
Figure 5.2-11	Column shears for E-W direction	
Figure 5.2-12	Column shears for N-S direction	5-54
Figure 5.2-13	Forces at beam/column connection	5-55
Figure 5.2-14	WUF-W connection, Second level, NS-direction	5-56
Figure 5.2-15	WUF-W weld detail	5-57
Figure 5.2-16	Braced frame in E-W direction	5-59
Figure 5.2-17	Braced frame in N-S direction	5-59
Table 5.2-6	Alternative B Amplification of Accidental Torison	5-61
Table 5.2-7	Alternative B Story Drifts under Seismic Load	5-62
Figure 5.2-18	Lateral force component in braces for N-S direction	5-63
Figure 5.2-19	Bracing connection detail	5-64
Figure 5.2-20	Whitmore section	5-65
Figure 5.2-21	Brace-to-brace connection	5-68
Figure 5.2-22	Moment frame of dual system in E-W direction	5-69
Figure 5.2-23	Moment frame of dual system in N-S direction	5-70
Table 5.2-8	Alternative C Amplification of Accidental Torsion	5-71
Figure 5.2-24	Braced frame of dual system in E-W-direction	5-72
Figure 5.2-25	Braced frame of dual system in N-S direction	5-72
Table 5.2-9	Alternative C Story Drifts under Seismic Load	5-73
Figure 5.3-1	Main floor framing plan	5-75
Figure 5.3-2	Section on Grid F	5-76
Table 5.3-1	Summary of Critical Member Design Forces	5-77
Figure 5.3-3	Diagram of eccentric braced bream	
Figure 5.3-4	Typical eccentric braced frame	
Figure 5.3-5	Link and upper brace connection	5-85

Figure 5.3-6	Lower brace connections	5-86
Figure 6-1	Typical floor plan of the Berkeley building	6-2
Figure 6-2	typical elevations of the Berkeley building	6-3
Table 6-1	Response Modification, Overstrength, and Deflection Amplification	
	Coefficients for Structural Systems Used	6-7
Table 6-2	Story Weights, Masses, and Moments of Inertia	6-11
Table 6-3	Periods and Modal Response Characteristics for the Berkeley building	6-13
Table 6-4	Periods and Modal Response for the Honolulu Building	6-13
Table 6-5	Comparison of Approximate and "Exact" Periods	6-13
Table 6-6	Comparison of Periods, Seismic Shears Coefficients, and Base Shears for the Berkeley	
	and Honolulu buildings	
Table 6-7a	Vertical Distribution of N-S Seismic Forces for the Berkeley Building	
Table 6-7b	Vertical Distribution of E-W Seismic Forces for the Berkeley Building	6-16
Table 6-8	Vertical Distribution of N-S and E-W Seismic Forces	
	for the Honolulu Building	
Figure 6-3	Comparison of wind and seismic story shears for the Berkeley building	
Figure 6-4		
Figure 6-5	Drift profile for Berkeley building	
Table 6-9a	Drift Computations for the Berkeley Building Loaded in the N-S Direction	
Table 6-9b	1 5 6	
Table 6-10a	P-delta Computations for the Berkeley Building Loaded in the N-S Direction	
Table 6-10b	P-delta Computations for the Berkeley Building Loaded in the E-W Direction	
Figure 6-6	Drift profile for the Honolulu building	
Table 6-11a	Drift Computations for the Honolulu Building Loaded in the N-S Direction	
Table 6-11b	1 6	6-26
Table 6-12a		6-27
Table 6-12b	1 0	6-28
Figure 6-7	Story forces in the E-W direction	
Figure 6-8	Story shears in the E-W direction	
Figure 6-9	Story overturning moments in the E-W direction	
Figure 6-10	25 percent story shears, Frame 1 E-W direction	
Figure 6-11	25 percent story shears, Frame 2 E-W direction	
Figure 6-12	25 percent story shear, Frame 3 E-W direction	6-36
Figure 6-13	Layout for beam reinforcement	6-37
Table 6-13	Tension Development Length Requirements for Hooked Bars and	
	Straight Bars in 4,000 psi LW Concrete	6-38
Figure 6-14	Bending moments Frame 1	6-40
Figure 6-15	Preliminary rebar layout for Frame 1	
Table 6-14	Design and Maximum Probable Flexural Strength for Beams in Frame 1	6-43
Figure 6-16	Diagram for computing column shears	6-45
Figure 6-17	Computing joint shear stress	6-46
Figure 6-18	Loading for determination of rebar cutoffs	6-48
Figure 6-19		6-48
Figure 6-20	Development length for top bars	6-49
Figure 6-21		
Table 6-15	Design and Maximum Probable Flexural Strength For Beams in Frame 1	6-50
Figure 6-22	Shears forces for transverse reinforcement	6-52

Figure 6-23 Detailed shear force envelope in Span B-C	
Figure 6-24 Layout and loads on column of Frame A	0-33
Figure 6-25 Design interaction diagram for column on Gridline A	
Figure 6-26 Details of reinforcement for column	
Figure 6-27 Design forces and detailing of haunched girder	
Figure 6-28 Computing shear in haunched girder	
Table 6-16Design of Shear Reinforcement for Haunched Girder	
Figure 6-29 Computation of column shears for use in joint	
Figure 6-30 Computing joint shear force	
Figure 6-31 Column loading	
Figure 6-32 Interaction diagram and column design forces	
Figure 6-32 Column detail	
Table 6-17     Design Forces for Structural Wall	
Table 6-18     Design forces for structural Wall for Shear	
•	
Figure 6-34 Interaction diagram for structural wall	
Figure 6-35 Variation of neutral axis depth with compressive force	
Figure 6-36 Details of structural wall boundary element	
Figure 6-37 Overall details of structural wall	
Figure 6-38    With loading requirements from ASCE 7	
Figure 6-39Wind vs. seismic shears in exterior bay of Frame 1	
Figure 6-40Bending moment envelopes at Level 5 of Frame 1	
Figure 6-41Preliminary reinforcement layout for Level 5 of Frame 1	
Figure 6-42Shear strength envelopes for Span A-B of Frame 1	
Figure 6-43 Isolated view of Column A	
Figure 6-44Interaction diagram for column	6-89
Figure 6-45Column reinforcement	6-91
Figure 6-46 Loads, moments, and reinforcement for haunched girder	6-92
Figure 6-47Shear force envelope for haunched girder	6-95
Figure 6-48 Loading for Column A, Frame 3	6-97
Figure 6-49 Interaction diagram for Column A	6-98
Figure 6-50 Details for Column A, Frame 3	6-99
Table 7.1-1Design Parameters from Example 9.2	
Table 7.2-2Shear Wall Overstrength	
Table 7.1-3Birmingham 1 $F_{px}$ Calculations	7-9
Figure 7.1-1 Diagram force distribution and analytical model	7-11
Figure 7.1-2 Diagram plan and critical design regions	7-12
Figure 7.1-3 Joint 3 chord reinforcement at the exterior edge	7-15
Figure 7.1-4 Interior joint reinforcement at the ends of plank and the collector	
reinforcement	
Figure 7.1-5 Anchorage region of shear reinforcement and collector reinforcement	7-17
Figure 7.1-6 Joint 2 transverse wall joint reinforcement	7-19
Figure 7.1-7 Joint 4 exterior longitudinal walls to diaphragm reinforcement and out-of-plane	anchorage
Figure 7.1-8 Wall-to-diaphragm reinforcement along interior longitudinal walls	7-21
Table 7.1-4Design Parameters form Sec. 9.2	7-22
Table 7.1-5 $F_{px}$ Calculations from Sec. 9.2	
Figure 7.1-9 Diaphragm plan and section cuts	
Figure 7.1-10 Boundary member and chord and collector reinforcement	

Figure 7.1-11	Collector reinforcement at the end of the interior longitudinal walls	7-26
Figure 7.1-12	Wall-to-wall diaphragm reinforcement along interior longitudinal walls	7-27
Figure 7.1-13	Exterior longitudinal wall-to-diaphragm reinforcement and out-of-plane	
	anchorage	7-28
Figure 7.2-1	Three-story building plan	7-30
Table 7.2-1	Design Parameters	
Figure 7.2-2	Forces on the longitudinal walls	
Figure 7.2-3	Forces on the transverse walls	7-36
Figure 7.2-4	Free-body diaphragm for longitudinal walls	7-37
Figure 7.2-5	Free-body diaphragm of the transverse walls	7-39
Figure 7.2-6	Overturning connection detail at the base of the walls	7-41
Figure 7.2-7	Shear connection at base	7-42
Figure 7.2-8	Shear connections on each side of the wall at the second and third floors	7-46
Figure 7.3-1	Single-story industrial warehouse building plan	7-49
Table 7.3-1	Design Parameters	7-50
Figure 7.3-2	Free-body diagram of a panel in the longitudinal direction	
Figure 7.3-3	Free-body diagram of a panel in the transverse direction	
Figure 7.3-4	Cross section of the DT dry-packed at the footing	
Figure 7.3-5	Cross section of one DT leg showing the location of the bonded prestressing tendons	
	strand	7-58
Figure 7.3-6	Free-body of the angle and the fillet weld connecting the embedded	
	plates in the DT and the footing	7-60
Figure 7.3-7	Free-body of angle with welds, top view, showing only shear forces and	
	resisting moments	7-62
Figure 7.3-8	Section at the connection of the precast/prestressed shear wall panel and the footing	7-64
Figure 7.3-9	Details of the embedded plate in the DT at the base	7-66
Figure 7.3-11	Sketch of connection of load-bearing DT wall panel at the roof	7-66
Figure 7.3-10	Sketch of connection of non-load-bearing DT wall panel at the roof	7-67
Figure 8-1	Typical floor plan	8-3
Figure 8-2	Building and elevation	
Figure 8-3	Building side elevation	
Figure 8-4	Typical composite connection	
Table 8-1	Design Parameters	
Figure 8-5	$M-\theta$ Curve for W18x35 connection with 6-#5	
Figure 8-6	$M$ - $\theta$ Curve for W21x44 connection with 8-#5	
Table 8-2	Partially Restrained Composite Connection Design	
Figure 8-7	Analysis of seat-angle for tension	8-15
Figure 8-8	Moment diagram for typical beam	
Figure 8-10	elevation of typical connection	8-19
Figure 8-11	Illustration of input for load combination for $1.2D + 0.5L + 1.0Q_E + 0.2S_{DS}D$	
Figure 8-12	Illustration of input for load combination for $0.9D + 1.0Q_E + 0.2S_{DS}D^{-1}$	8-20
Table 8-3	Story Drift (in.) and P-delta Analysis $\dots \dots \dots$	8-21
Table 8-3	Maximum Connection Moments and Capacities	
Table 8-4 Table 8-5	Column Strength Check, for W10x77	8-22 8-23
	0	
Figure 8-13	Detail at column	8-25
Figure 8-14	Detail at spandrel	8-26
Figure 8-15	Detail at building corner	8-26

Figure 8-16	Force transfer from deck to column	8-27
Figure 9.1-1	Roof plan	9-3
Figure 9.1-2	End wall elevation	
Table 9.1-1	Comparison of $E_m$	
Figure 9.1-3	Trial design for 8-inthick CMU wall	
Figure 9.1-4	Investigation of-out-plane ductility for the 8-inthick CMU side wall	
Table 9.1-2	Comparison of Variables	
Figure 9.1-6	Basis for interpolation of modulus of rupture, $f_x$	
Figure 9.1-7	Cracked moment of inertia $(I_{cr})$ for 8-inthick CMU side walls	
Figure 9.1-8	Out-of-plane strength for 8-inthick CMU walls	
Figure 9.1-9	In-plane ductility check for side walls	
Figure 9.1-10	Grout cells solid within 10 ft of each end of side walls	
Table 9.1-3	Combined Loads for Shear in Side Wall	
Figure 9.1-11	Trial design for piers on end walls	
Figure 9.1-12	In-plane loads on end walls	
Figure 9.1-13	Out-of-plane load diagram and resultant of lateral loads	
Figure 9.1-14	Investigation for out-of-plane ductility for end walls	
Figure 9.1-15	Cracked moment of inertia for end walls	
Figure 9.1-16	Out-of-plane seismic strength of pier on end wall	
Figure 9.1-17	Input loads for in-plane and end wall analysis	
Figure 9.1-18	In-plane design condition for 8-ftwide pier	
Figure 9.1-19	In-plane ductility check for 8-ftwide pier	
Figure 9.1-20	In-plane seismic strength of pier	
Figure 9.1-21	In-plane $\Phi P_{11} - \Phi M_{11}$ diagram for pier	
Table 9.1-4	Combined Loads for Flexure in End Pier	
Figure 9.1-22	In-plane shear on end wall and pier	
Table 9.1-5	Combined Loads for Shear in End Wall	
Figure 9.1-23	In-plane deflection of end wall	
Figure 9.2-1	Typical floor plan	
Figure 9.2-2	Building elevation	
Figure 9.2-3	Plan of walls	9-44
Table 9.2-1	Design Parameters	9-45
Table 9.2-2	Birmingham 1 Seismic Forces and moments by Level	9-51
Figure 9.2-4	Location of moments due to story shears	9-51
Table 9.2-3	Shear Strength Calculations for Birmingham 1 Wall D	9-54
Table 9.2-4	Demands for Birmingham 1 Wall D	9-54
Figure 9.2-5	Strength of Birmingham 1 Wall D	9-57
Figure 9.2-6	$\Phi P_{11} - \Phi M_{11}$ diagram for Birmingham 1 Wall D	9-60
Figure 9.2-7	Ductility check for Birmingham 1 Wall D	9-61
Table 9.2-5	Birmingham 1 Cracked Wall Determination	9-63
Figure 9.2-8	Shear wall deflections	9-63
Table 9.2-6	Deflections, Birmingham 1	9-64
Table 9.2-7	New York City Seismic Forces and Moments by Level	9-66
Table 9.2-8	New York City Shear Strength	9-69
Table 9.2-9	Demands for New York City Wall D	9-69
Figure 9.2-9	Strength of New York City and Birmingham 2 Wall D	9-70
Figure 9.2-10	$\Phi P_{II} - \Phi M_{II}$ Diagram for New York City and Birmingham 2 Wall D	9-72

Figure 9.2-11	Ductility check for New York City and Birmingham 2 Wall D	9-74
Table 9.2-10	New York City Cracked Wall Determination	9-75
Table 9.2-11	New York City Deflections	9-76
Table 9.2-12	Birmington 2 Periods, Mass Participation Factors, and Modal Base Shears	9-79
Table 9.2-13	Birmingham 2 Seismic Forces and Moments by Level	
Table 9.2-14	Birmingham Periods, Mass Participation Factors, and Modal Base	
Table 9.2-15	Shear Strength Calculations for Wall D, Birmingham 2	
Table 9.2-16	Birmingham 2 Demands for Wall D	
Figure 9.2-12	Typical wall section fro the Los Angeles location	
Table 9.2-17	Los Angeles Seismic Forces and Moments by Level	
Table 9.2-18	Los Angeles Shear Strength Calculations for Wall D	
Table 9.2-19	Los Angeles Load Combinations for Wall D	
Figure 9.2-13	Los Angeles: Strength of wall D	
Figure 9.2-14	$\Phi P_{11} - \Phi M_{11}$ diagram for Los Angeles Wall D	9-91
Figure 9.2-15	Ductility check for Los Angeles Wall D	9-92
Table 9.2-20	Los Angeles Cracked Wall Determination	
Table 9.2-21	Los Angeles Deflections	
Table 9.2-22	Variation in Reinforcement and Grout by Location	
Figure 9.3-1	Floor plan	
Figure 9.3-2	Elevation	
Table 9.3-1	Design Parameters	9-98
Table 9.3-2	Periods, Mass Particiaptions Ratios, and Modal Base Shears	
Table 9.3-3	Seismic Forces and Moments by Level	
Table 9.3-4	Relative Rigidities	
Figure 9.3-3	Wall dimensions	
Table 9.3-5	Shear for Wall D	9-108
Table 9.3-6	Periods, Mass Participations Ratios, and Modal Base Shears	
Table 9.3-7	Load Combinations for Wall D	
Figure 9.3-4	Bulb reinforcement at lower levels	9-111
Figure 9.3-5	Strength of Wall D, Level 1	9-112
Figure 9.3-6	$\Phi P_{11} - \Phi M_{11}$ Diagram for Level 1	9-115
Figure 9.3-7	Ductility check for Wall D, Level 1	
Figure 9.3-8	Bulb reinforcement at upper levels	
Figure 9.3-9	Strength of Wall D at Level 7	
Figure 9.3-10	$\Phi P_{11} - \Phi M_{11}$ Diagram for Level 7	
Figure 9.3-11	Ductility check for Wall D, Level 7	
Table 9.3-8	Shear Strength for Wall D	
Table 9.3-9	Cracked Wall Determination	
Table 9.3-10	Deflection for ELF Analysis	9-129
Table 9.3-11	Displacements from Modal Analysis	
Figure 9.3-12	Floor anchorage to wall	
Table 9.3-12	Diaphragm Seismic Forces	
Figure 9.3-13	Shears and moments for diaphragm	
Figure 10.1-1	Typical floor plan	10-4
Figure 10.1-2	Longitudinal section and elevation	
Figure 10.1-3	Foundation plan	
Figure 10.1-4	Load path and shear walls	
0	r ···· r	

Figure 10.1-5	Vertical shear distribution	10-11
Table 10.1-1	Seismic Coefficients, Forces, and Moments	10-12
Figure 10.1-6	Transverse section: end wall	
Table 10.1-2	Fastener slip equations	
Table 10.1-3	Wall Deflection	
Figure 10.1-7	Force distribution for flexural deflections	
Table 10.1-4	Wall Deflection (per story) Due to Bending and Anchorage Slip	
Table 10.1-5	Total Elastic Deflection and Drift of End Wall	10-22
Figure 10.1-8	Shear wall tie down at suspended floor framing	10-25
Figure 10.1-9	Transverse wall: overturning	10-28
Figure10.1-10	Bearing wall	
Figure10.1-11	Nonbearing wall	
Figure10.1-12	Foundation wall detail	
Figure10.1-12	Diaphragm chord splice	
Table 10.1-6a	Total Deflection and Drift	
Table 10.1-6a	Total Deflection and Drift (Structural I Plywood Shear Walls)	
Table 10.1-00 Table 10.1-7	P-delta Stability Coefficient	10-30
	Perforated shear wall at exterior	10-37
Figure 10.1-14		10-39
Figure 10.1-15	Perforated shear wall detail at foundation	
Figure10.1-16	Perforated shear wall detail at floor framing	10-43
Figure 10.2-1	Building plan	10-44
Table 10.2-1	Roof Diaphragm Framing and Nailing Requirements	
Figure 10.2-2	Diaphragm framing and nailing layout	
Figure 10.2-3	Plywood layout	
Figure 10.2-4	Chord splice detail	
Figure 10.2-5	Adjustment for non-uniform nail spacing	
Figure 10.2-6	Diaphragm at roof opening	
Figure 10.2-7	Chord forces and Element 1 free-body diagram	
Figure 10.2-8	Free-body diagram for Element 2	
Figure 10.2-9	Anchorage of masonry wall perpendicular to joists	
Figure10.2-10	Chord tie at roof opening	10-59
Figure10.2-11	Cross tie plan layout and subdiaphragm free-body diagram for side walls	10-60
Figure10.2-12	Anchorage of masonry wall parallel to joists	10-61
Figure10.2-13	Cross tie plan layout and subdiaphragm free-body diagram for end walls	10-62
Figure 11.1-1	Isolation system terminology	. 11-6
Figure 11.1-2	Effective stiffness and effective damping	. 11-8
Table 11.2-1	Acceptable Methods of Analysis	11-8
Figure 11.3-1	Isolation system capacity and earthquake demand	11-10
Figure 11.3-2	Design, maximum, and total maximum displacement	11-11
Figure 11.3-3	Isolation system displacement and shear force as function of period	11-13
Table 11.4-1	Summary of Minimum Design Criteria for Dynamic Analysis	11-14
Figure 11.4-1	Moments due to horizontal shear and P-delta effects	11-15
Figure 11.4-2	Bilinear idealization of isolator unit behavior	11-16
Figure 11.5-1	Three-dimensional model of the structural system	11-17
Figure 11.5-2	Typical floor framing plan	11-18
Figure 11.5-3	Penthouse roof framing plan	11-18
Figure 11.5-4	Longitudinal bracing elevation	11-19
<u> </u>		

Figure 11.5-5	Transverse bracing elevations	11-19
Table 11.5-1	Gravity Loads on Isolator Units	
Figure 11.5-6	Example design spectra	
Table 11.5-2	Earthquake Time History Records and Scaling Factors	11-24
Figures11.5-7	Comparison of design earthquake spectra	
Table 11.5-3	Vertical Distribution of Reduced Design Earthquake Forces	
Table 11.5-4	Vertical Distribution of Unreduced DE and MCE Forces	11-32
Table 11.5-5	Maximum Downward Force for Isolator Design	11-33
Table 11.5-6	Minimum Downward Force for Isolator Design	11-33
Table 11.5-7	Maximum Downward Force on Isolator Units	11-34
Table 11.5-8	Maximum Uplift Displacement of Isolator Units	11-34
Figure 11.5-8	Elevation of framing on Column Line 2	
Figure 11.5-9	Elevation of framing on Column Line B	11-36
Figure11.5-10	First floor framing plan	11-36
Table 11.5-9	Summary of Key Design Parameters	11-38
Figure11.5-11	Typical detail of the isolation system at columns	11-39
Figure11.5-12	Stiffness and damping properties of EOC isolator units	11-42
Figure11.5-13	Comparison of modeled isolator properties to test data	11-43
Table 11.5-10	Design Earthquake Response Parameters	11-44
Table 11.5-11	Maximum Considered Earthquake Response Parameters	11-44
Table 11.5-12	Maximum Downward Force (kips) on Isolator Units	11-45
Table 11.5-13	Maximum Uplift Displacement (in.) Of Isolator Units	11-45
Figure11.5-14	Isolator dimensions	11-46
Table 11.5-14	Prototype Test Requirements	11-47
Table 12-1	Applicability of the Chapters of the <i>Provisions</i>	
Figure 12-1	Combustion turbine building	
Figure 12-2	Pipe rack	
Figure 12-3	Steel storage rack	
Table 12.3-1	Seismic Forces, Shears and Overturning Moments	
Figure 12-4	Boiler building	
Figure 12-5	Pier plan and elevation	
Figure 12-6	Storage tank section	
Figure 12-7	Platform for elevated transformer	12-29
Figure 12.2.1	Five-story building evaluation showing panel location	12.0
Figure 13.2-1 Figure 13.2-2	Detailed building elevation	
Figure 13.2-2 Figure 13.2-3	Spandrel panel connection payout from interior	
Figure 13.2-3 Figure 13.2-4	Spandrel panel moments	
Figure 13.2-4 Figure 13.2-5	Spandrel panel connections forces	
Figure 13.2-5 Figure 13.2-6	Column cover connection layout	
<b>U</b>	·	
Figure 13.3-1 Figure 13.3-2	Air handling fan unit Free-body diagram for seismic force analysis	
Figure 13.3-2 Figure 13.3-3	Anchor for direct attachment to structure	13-22
Figure 13.3-4	ASHRAE diagonal seismic force analysis for vibration isolation springs	
Figure 13.3-4 Figure 13.3-5	Another and snubber loads for support on vibration isolation springs	
Figure 13.3-6	Lateral restraint required to resist seismic forces	
1 19010 19.9-0	Lateral restaunt required to resist beisine refees	15 4)

1

### FUNDAMENTALS

### James Robert Harris, P.E., Ph.D.

In introducing their well-known text, *Fundamentals of Earthquake Engineering*, Newmark and Rosenblueth (1971) comment:

In dealing with earthquakes, we must contend with appreciable probabilities that failure will occur in the near future. Otherwise, all the wealth of the world would prove insufficient to fill our needs: the most modest structures would be fortresses. We must also face uncertainty on a large scale, for it is our task to design engineering systems – about whose pertinent properties we know little – to resist future earthquakes and tidal waves – about whose characteristics we know even less. . . In a way, earthquake engineering is a cartoon. . . . Earthquake effects on structures systematically bring out the mistakes made in design and construction, even the minutest mistakes.

Several points essential to an understanding of the theories and practices of earthquake-resistant design bear restating:

- 1. Ordinarily, a large earthquake produces the most severe loading that a building is expected to survive. The probability that *failure* will occur is very real and is greater than for other loading phenomena. Also, in the case of earthquakes, the definition of *failure* is altered to permit certain types of behavior and damage that are considered unacceptable in relation to the effects of other phenomena.
- 2. The levels of uncertainty are much greater than those encountered in the design of structures to resist other phenomena. This applies both to knowledge of the loading function and to the resistance properties of the materials, members, and systems.
- 3. The details of construction are very important because flaws of no apparent consequence often will cause systematic and unacceptable damage simply because the earthquake loading is so severe and an extended range of behavior is permitted.

The remainder of this chapter is devoted to a very abbreviated discussion of fundamentals that reflect the concepts on which earthquake-resistant design are based. When appropriate, important aspects of the *NEHRP Recommended Provisions for Seismic Regulations for New Buildings and Other Structures* are mentioned and reference is made to particularly relevant portions of the document. Note that through 2000, the *NEHRP Recommended Provisions* has been composed of two volumes of text and a separate set of maps. Part 1 (referred to herein as the *Provisions*) contains the actual requirements and Part 2 (referred to herein as the *Commentary*) provides a discussion of various aspects of the requirements.

Although the set of design examples is based on the 2000 *Provisions*, it is annotated to reflect changes made to the 2003 *Provisions*. Annotations within brackets, [], indicate both organizational changes (as a result of a reformat of all of the chapters of the 2003 *Provisions*) and substantive technical changes to the 2003 *Provisions* and its primary reference documents. While the general concepts of the changes are

described, the design examples and calculations in this book have not been revised to reflect the changes to the 2003 *Provisions*. Where related to the discussion in this chapter, significant changes to the 2003 *Provisions* and primary reference documents are noted. However, some minor changes to the 2003 *Provisions* and the reference documents may not be noted.

#### **1.1 EARTHQUAKE PHENOMENA**

According to the most widely held scientific belief, most earthquakes occur when two segments of the earth's crust suddenly move in relation to one another. The surface along which movement occurs is known as a fault. The sudden movement releases strain energy and causes seismic waves to propagate through the crust surrounding the fault. These waves cause the surface of the ground to shake violently, and it is this ground shaking that is the principal concern of structural engineering to resist earthquakes.

Earthquakes have many effects in addition to ground shaking. For various reasons, the other effects generally are not major considerations in the design of buildings and similar structures. For example, seismic sea waves or tsunamis can cause very forceful flood waves in coastal regions, and seiches (long-period sloshing) in lakes and inland seas can have similar effects along shorelines. These are outside the scope of the *Provisions*. This is not to say, however, that they should not be considered during site exploration and analysis. Designing structures to resist such hydrodynamic forces is a very specialized topic, and it is common to avoid constructing buildings and similar structures where such phenomena are likely to occur. Long-period sloshing of the liquid contents of tanks is addressed by the *Provisions*.

Abrupt ground displacements occur where a fault intersects the ground surface. (This commonly occurs in California earthquakes but apparently did not occur in the historic Charleston, South Carolina, earthquake or the very large New Madrid, Missouri, earthquakes of the nineteenth century.) Mass soil failures such as landslides, liquefaction, and gross settlement are the result of ground shaking on susceptible soil formations. Once again, design for such events is specialized, and it is common to locate structures so that mass soil failures and fault breakage are of no major consequence to their performance. Modification of soil properties to protect against liquefaction is one important exception; large portions of a few metropolitan areas with the potential for significant ground shaking are susceptible to liquefaction. Lifelines that cross faults require special design beyond the scope of the *Provisions*. The structural loads specified in the *Provisions* are based solely on ground shaking; they do not provide for ground failure. The *Commentary* includes a method for prediction of susceptibility to liquefaction as well as general guidelines for locating potential fault rupture zones.

Nearly all large earthquakes are *tectonic* in origin – that is, they are associated with movements of and strains in large segments of the earth's crust, called *plates*, and virtually all such earthquakes occur at or near the boundaries of these plates. This is the case with earthquakes in the far western portion of the United States where two very large plates, the North American continent and the Pacific basin, come together. In the central and eastern United States, however, earthquakes are not associated with such a plate boundary and their causes are not as completely understood. This factor, combined with the smaller amount of data about central and eastern earthquakes (because of their infrequency), means that the uncertainty associated with earthquake loadings is higher in the central and eastern portions of the nation than in the West. Even in the West, the uncertainty (when considered as a fraction of the predicted level) about the hazard level is probably greater in areas where the mapped hazard is low than in areas where the mapped hazard is high.

The amplitude of earthquake ground shaking diminishes with distance from the source, and the rate of attenuation is less for lower frequencies of motion than for higher frequencies. This effect is captured, to an extent, by the fact that the *Provisions* uses two sets of maps define the hazard of seismic ground shaking – one is pertinent for higher frequency motion (the  $S_s$  maps) and the other for lower frequencies (the  $S_1$  maps). There is evidence that extreme motions near the fault in certain types of large earthquakes

are not captured by the maps, but interim adjustments to design requirements for such a possibility are included in the *Provisions*.

Two basic data sources are used in establishing the likelihood of earthquake ground shaking, or seismicity, at a given location. The first is the historical record of earthquake effects and the second is the geological record of earthquake effects. Given the infrequency of major earthquakes, there is no place in the United States where the historical record is long enough to be used as a reliable basis for earthquake prediction – certainly not as reliable as with other phenomena such as wind and snow. Even on the eastern seaboard, the historical record is too short to justify sole reliance on the historical record. Thus, the geological record is essential. Such data require very careful interpretation, but they are used widely to improve knowledge of seismicity. Geological data have been developed for many locations as part of the nuclear power plant design process. On the whole, there are more geological data available for the far western United States than for other regions of the country. Both sets of data have been taken into account in the *Provisions* seismic hazard maps. Ground shaking, however, is known to vary considerably over small distances and the *Provisions* maps do not attempt to capture all such local variations (commonly called *microzoning*).

The *Commentary* provides a more thorough discussion of the development of the maps, their probabilistic basis, the necessarily crude lumping of parameters, and other related issues. In particular, note the description of the newest generation of maps introduced in 1997 and their close relationship to the development of a new design criterion. There are extended discussions of these issues in the appendices to the *Commentary*. Prior to its 1997 edition, the basis of the *Provisions* was to "provide *life safety* at the design earthquake motion," which was defined as having a 10 percent probability of being exceeded in a 50-year reference period. As of the 1997 edition, the basis became to "avoid *structural collapse* at the maximum considered earthquake (MCE) ground motion," which is defined as having a 2 percent probability of being exceeded in a 50-year reference period. In the long term, the change from life safety to structural collapse prevention as the limit state will create significant changes in procedures for design analysis. In the present interim, the ground motions for use with present design procedures are simply taken as being two-thirds of the MCE ground motions.

#### **1.2 STRUCTURAL RESPONSE TO GROUND SHAKING**

The first important difference between structural response to an earthquake and response to most other loadings is that the earthquake response is *dynamic*, not *static*. For most structures, even the response to wind is essentially static. Forces within the structure are due almost entirely to the pressure loading rather than the acceleration of the mass of the structure. But with earthquake ground shaking, the aboveground portion of a structure is not subjected to any applied force. The stresses and strains within the superstructure are created entirely by its dynamic response to the movement of its base, the ground. Even though the most used design procedure resorts to the use of a concept called the equivalent static force for actual calculations, some knowledge of the theory of vibrations of structures is essential.

#### 1.2.1 Response Spectra

Figure 1.2-1 shows accelerograms, records of the acceleration at one point along one axis, for several representative earthquakes. Note the erratic nature of the ground shaking and the different characteristics of the different accelerograms. Precise analysis of the elastic response of an ideal structure to such a pattern of ground motion is possible; however, it is not commonly done for ordinary structures. The increasing power and declining cost of computational aids are making such analyses more common but, at this time, only a small minority of structures are analyzed for specific response to a specific ground motion.

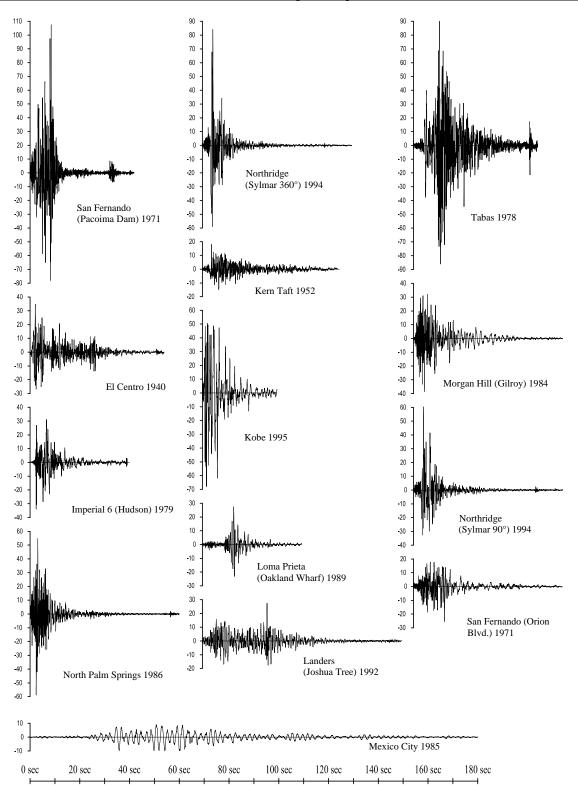
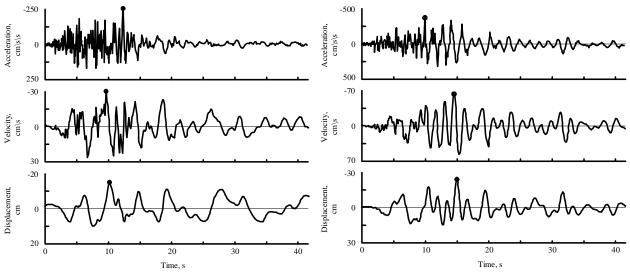


**Figure 1.2-1** Earthquake ground acceleration in epicentral regions (all accelerograms are plotted to the same scale for time and acceleration). Great earthquakes extend for much longer periods of time.

Figure 1.2-2 shows further detail developed from an accelerogram. Part (a) shows the ground acceleration along with the ground velocity and ground displacement derived from it. Part (b) shows the

acceleration, velocity, and displacement for the same event at the roof of the building located where the ground motion was recorded. Note that the peak values are larger in the diagrams of Figure 1.2-2(b) (the vertical scales are different). This increase in response of the structure at the roof level over the motion of the ground itself is known as dynamic amplification. It depends very much on the vibrational characteristics of the structure and the characteristic frequencies of the ground shaking at the site.

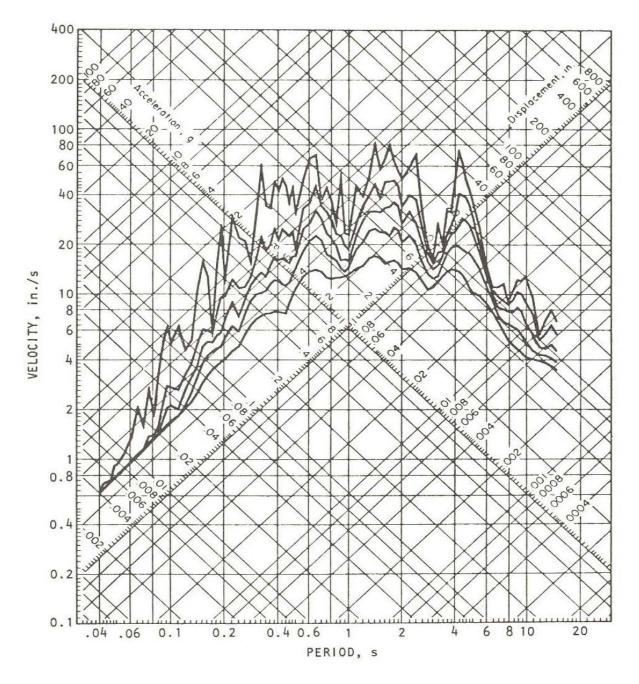


(a) Ground acceleration, velocity, and displacement (b) Roof acceleration, velocity, and displacement

Figure 1.2-2 Holiday Inn ground and building roof motion during the M6.4 1971 San Fernando earthquake: (a) north-south ground acceleration, velocity, and displacement and (b) north-south roof acceleration, velocity, and displacement (Housner and Jennings 1982). Note that the vertical scale of (b) is different from (a). The Holiday Inn, a 7-story, reinforced concrete frame building, was approximately 5 miles from the closest portion of the causative fault. The recorded building motions enabled an analysis to be made of the stresses and strains in the structure during the earthquake.

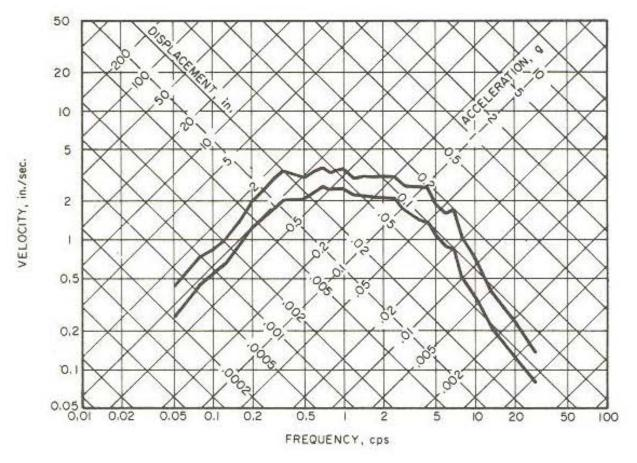
In design, the response of a specific structure to an earthquake is ordinarily predicted from a design response spectrum such as is specified in the *Provisions*. The first step in creating a design response spectrum is to determine the maximum response of a given structure to a specific ground motion (see Figure 1.2-2). The underlying theory is based entirely on the response of a single-degree-of-freedom oscillator such as a simple one-story frame with the mass concentrated at the roof. The vibrational characteristics of such a simple oscillator may be reduced to two: the natural frequency and the amount of damping. By recalculating the record of response versus time to a specific ground motion for a wide range of natural frequencies and for each of a set of common amounts of damping, the family of response spectra for one ground motion may be determined. It is simply the plot of the maximum value of response for each combination of frequency and damping.

Figure 1.2-3 shows such a result for the ground motion of Figure 1.2-2(a) and illustrates that the erratic nature of ground shaking leads to a response that is very erratic in that a slight change in the natural period of vibration brings about a very large change in response. Different earthquake ground motions lead to response spectra with peaks and valleys at different points with respect to the natural frequency. Thus, computing response spectra for several different ground motions and then averaging them, based on some normalization for different amplitudes of shaking, will lead to a smoother set of spectra. Such smoothed spectra are an important step in developing a design spectrum.



**Figure 1.2-3** Response spectrum of north-south ground acceleration (0, 0.02, 0.05, 0.10, 0.20 of critical damping) recorded at the Holiday Inn, approximately 5 miles from the causative fault in the 1971 San Fernando earthquake (Housner and Jennings 1982).

Figure 1.2-4 is an example of an averaged spectrum. Note that the horizontal axes of Figures 1.2-3 and 1.2-4 are different, one being for the known frequency (period) while the other is for the cyclic frequency. Cyclic frequency is the inverse of period; therefore, Figure 1.2-4 should be rotated about the line f = 1 to compare it with Figure 1.2-3. Note that acceleration, velocity, or displacement may be obtained from Figure 1.2-3 or 1.2-4 for a structure with known frequency (period) and damping.



**Figure 1.2-4** Averaged spectrum (Newmark, Blume, and Kapur 1973). Mean and mean plus one standard deviation acceleration, horizontal components (2.0 percent of critical damping). Reprinted with permission from the American Society of Civil Engineers.

Prior to the 1997 editions of the *Provisions*, the maps that characterized the ground shaking hazard were plotted in terms of peak ground acceleration, and design response spectra were created using expressions that amplified (or de-amplified) the ground acceleration as a function of period and damping. With the introduction of the MCE ground motions, this procedure changed. Now the maps present spectral response accelerations at two periods of vibration, 0.2 and 1.0 second, and the design response spectrum is computed more directly. This has removed a portion of the uncertainty in predicting response accelerations.

Few structures are so simple as to actually vibrate as a single-degree-of-freedom system. The principles of dynamic modal analysis, however, allow a reasonable approximation of the maximum response of a multi-degree-of-freedom oscillator, such as a multistory building, if many specific conditions are met. The procedure involves dividing the total response into a number of natural modes, modeling each mode as an equivalent single-degree-of-freedom oscillator, determining the maximum response for each mode from a single-degree-of-freedom response spectrum, and then estimating the maximum total response by statistically summing the responses of the individual modes. The *Provisions* does not require consideration of all possible modes of vibration for most buildings because the contribution of the higher modes (higher frequencies) to the total response is relatively minor.

The soil at a site has a significant effect on the characteristics of the ground motion and, therefore, on the structure's response. Especially at low amplitudes of motion and at longer periods of vibration, soft soils amplify the motion at the surface with respect to bedrock motions. This amplification is diminished somewhat, especially at shorter periods as the amplitude of basic ground motion increases, due to yielding in the soil. The *Provisions* accounts for this effect by providing amplifiers that are to be applied to the 0.2 and 1.0 second spectral accelerations for various classes of soils. (The MCE ground motion maps are drawn for sites on rock.) Thus, very different design response spectra are specified depending on the type of soil(s) beneath the structure. The *Commentary* contains a thorough explanation of this feature.

#### **1.2.2 Inelastic Response**

The preceding discussion assumes elastic behavior of the structure. The principal extension beyond ordinary behavior referenced at the beginning of this chapter is that structures are permitted to strain beyond the elastic limit in responding to earthquake ground shaking. This is dramatically different from the case of design for other types of loads in which stresses, and therefore strains, are not permitted to approach the elastic limit. The reason is economic. Figure 1.2-3 shows a peak acceleration response of about 1.0 g (the acceleration due to gravity) for a structure with moderately low damping – for only a moderately large earthquake! Even structures that are resisting lateral forces well will have a static lateral strength of only 20 to 40 percent of gravity.

The dynamic nature of earthquake ground shaking means that a large portion of the shaking energy can be dissipated by inelastic deformations if some damage to the structure is accepted. Figure 1.2-5 illustrates the large amount of strain energy that may be stored by a ductile system in a displacement-controlled event such as an earthquake. The two graphs are plotted with the independent variables on the horizontal axis and the dependent response on the vertical axis. Thus, part (b) of the figure is characteristic of the response to forces such as gravity weight or wind pressure, while part (c) is characteristic of induced displacements such as foundation settlement or earthquake ground shaking. The figures should not be interpreted as a horizontal beam and a vertical column. Figure 1.2-5(a) would represent a beam if the load W were small and a column if W were large. The point being made with the figures is that ductile structures have the ability to resist displacements much larger than those that first cause yield.

The degree to which a member or structure may deform beyond the elastic limit is referred to as ductility. Different materials and different arrangements of structural members lead to different ductilities. Response spectra may be calculated for oscillators with different levels of ductility. At the risk of gross oversimplification, the following conclusions may be drawn:

- 1. For structures with very low natural frequencies, the acceleration response is reduced by a factor equivalent to the ductility ratio (the ratio of maximum usable displacement to effective yield displacement note that this is displacement and not strain).
- 2. For structures with very high natural frequencies, the acceleration response of the ductile structure is essentially the same as that of the elastic structure, but the displacement is increased.
- 3. For intermediate frequencies (which applies to nearly all buildings), the acceleration response is reduced, but the displacement response is generally about the same for the ductile structure as for the elastic structure strong enough to respond without yielding.

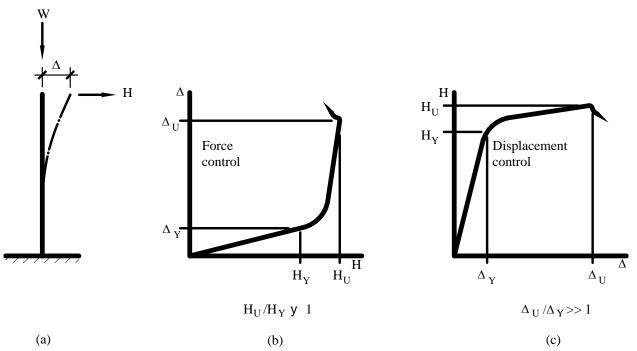


**Figure 1.2-5** Force controlled resistance versus displacement controlled resistance (after Housner and Jennings 1982). In part (b) the force *H* is the independent variable. As *H* is increased, the displacement increases until the yield point stress is reached. If *H* is given an additional increment (about 15 percent), a plastic hinge forms giving large displacements. For this kind of system, the force producing the yield point stress is close to the force producing collapse. The ductility does not produce a large increase in load capacity. In part (c) the displacement is the independent variable. As the displacement is increased, the base moment ( $F\ell$ ) increases until the yield point is reached. As the displacement can be increased 10 to 20 times the yield point displacement before the system collapses under the weight *W*. (As *W* increases, this ductility is decreased dramatically.) During an earthquake, the oscillator is excited into vibrations by the ground motion and it behaves essentially as a displacement-controlled system and can survive displacements much beyond the yield point. This explains why ductile structures can survive ground shaking that produces displacements much greater than yield point displacement.

Inelastic response is quite complex. Earthquake ground motions involve a significant number of reversals and repetitions of the strains. Therefore, observation of the inelastic properties of a material, member, or system under a monotonically increasing load until failure can be very misleading. Cycling the deformation can cause degradation of strength, stiffness, or both. Systems that have a proven capacity to maintain a stable resistance to a large number of cycles of inelastic deformation are allowed to exercise a greater portion of their ultimate ductility in designing for earthquake resistance. This property is often referred to as toughness, but this is not the same as the classic definition used in mechanics of materials.

Most structures are designed for seismic response using a linear elastic analysis with the strength of the structure limited by the strength at its critical location. Most structures possess enough complexity so that the peak strength of a ductile structure is not accurately captured by such an analysis. Figure 1.2-6 shows the load versus displacement relation for a simple frame. Yield must develop at four locations before the peak resistance is achieved. The margin from the first yield to the peak strength is referred to as overstrength and it plays a significant role in resisting strong ground motion. Note that a few key design standards (for example, ACI 318 for the design of concrete structures) do allow for some redistribution of internal forces from the critical locations based upon ductility; however, the redistributions allowed therein are minor compared to what occurs in response to strong ground motion.

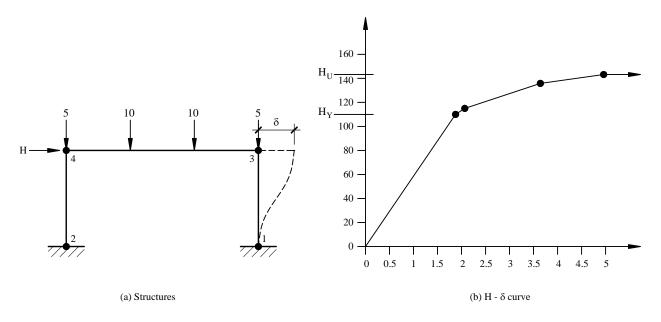


**Figure 1.2-6** Initial yield load and failure load for a ductile portal frame. The margin from initial yield to failure (mechanism in this case) is known as overstrength.

To summarize, the characteristics important in determining a building's seismic response are natural frequency, damping, ductility, stability of resistance under repeated reversals of inelastic deformation, and overstrength. The natural frequency is dependent on the mass and stiffness of the building. Using the *Provisions*, the designer calculates, or at least approximates, the natural period of vibration (the inverse of natural frequency). Damping, ductility, toughness, and overstrength depend primarily on the type of building system, but not the building's size or shape. Three coefficients – *R*, *C*<sub>d</sub>, and  $\Omega_0$  – are provided to encompass damping, ductility, stability of resistance, and overstrength. *R* is intended to be a conservatively low estimate of the reduction of acceleration response in a ductile system from that for an elastic oscillator with a certain level of damping. It is used to compute a required strength. Computations of displacement based upon ground motion reduced by the factor *R* will underestimate the actual displacements. *C*<sub>d</sub> is intended to be a reasonable mean for the amplification necessary to convert the elastic displacement response computed for the reduced ground motion to actual displacements.  $\Omega_0$  is intended to deliver a reasonably high estimate of the peak force that would develop in the structure. Sets of *R*, *C*<sub>d</sub>, and  $\Omega_0$  are specified in the *Provisions* for the most common structural materials and systems.

### **1.2.3 Building Materials**

The following brief comments about building materials and systems are included as general guidelines only, not for specific application.

### 1.2.3.1 Wood

Timber structures nearly always resist earthquakes very well, even though wood is a brittle material as far as tension and flexure are concerned. It has some ductility in compression (generally monotonic), and its strength increases significantly for brief loadings, such as earthquake. Conventional timber structures (plywood or board sheathing on wood framing) possess much more ductility than the basic material primarily because the nails and other steel connection devices yield and the wood compresses against the connector. These structures also possess a much higher degree of damping than the damping that is assumed in developing the basic design spectrum. Much of this damping is caused by slip at the connections. The increased strength, connection ductility, and high damping combine to give timber

structures a large reduction from elastic response to design level. This large reduction should not be used if the strength of the structure is actually controlled by bending or tension of the gross timber cross sections. The large reduction in acceleration combined with the light weight timber structures make them very efficient with regard to earthquake ground shaking when they are properly connected. This is confirmed by their generally good performance in earthquakes.

### 1.2.3.2 Steel

Steel is the most ductile of the common building materials. The moderate-to-large reduction from elastic response to design response allowed for steel structures is primarily a reflection of this ductility and the stability of the resistance of steel. Members subject to buckling (such as bracing) and connections subject to brittle fracture (such as partial penetration welds under tension) are much less ductile and are addressed in the *Provisions* in various ways. Other defects, such as stress concentrations and flaws in welds, also affect earthquake resistance as demonstrated in the Northridge earthquake. The basic and applied research program that grew out of that demonstration has greatly increased knowledge of how to avoid low ductility details in steel construction.

#### 1.2.3.3 Reinforced Concrete

Reinforced concrete achieves ductility through careful limits on steel in tension and concrete in compression. Reinforced concrete beams with common proportions can possess ductility under monotonic loading even greater than common steel beams, in which local buckling is usually a limiting factor. Providing stability of the resistance to reversed inelastic strains, however, requires special detailing. Thus, there is a wide range of reduction factors from elastic response to design response depending on the detailing for stable and assured resistance. The *Commentary* and the commentary with the ACI 318 standard for design of structural concrete explain how controlling premature shear failures in members and joints, buckling of compression bars, concrete compression failures (through confinement with transverse reinforcement), the sequence of plastification, and other factors lead to larger reductions from the elastic response.

### 1.2.3.4 Masonry

Masonry is a more diverse material than those mentioned above, but less is known about its inelastic response characteristics. For certain types of members (such as pure cantilever shear walls), reinforced masonry behaves in a fashion similar to reinforced concrete. The nature of the masonry construction, however, makes it difficult, if not impossible, to take some of the steps (e.g., confinement of compression members) used with reinforced concrete to increase ductility and stability. Further, the discrete differences between mortar and the masonry unit create additional failure phenomena. Thus, the reduction factors for reinforced masonry are not quite as large as those for reinforced concrete. Unreinforced masonry possesses little ductility or stability, except for rocking of masonry piers on a firm base, and very little reduction from the elastic response is permitted.

### 1.2.3.5 Precast Concrete

Precast concrete obviously can behave quite similarly to reinforced concrete, but it also can behave quite differently. The connections between pieces of precast concrete commonly are not as strong as the members being connected. Clever arrangements of connections can create systems in which yielding under earthquake motions occurs away from the connections, in which case the similarity to reinforced concrete is very real. Some carefully detailed connections also can mimic the behavior of reinforced concrete. Many common connection schemes, however, will not do so. Successful performance of such systems requires that the connections perform in a ductile manner. This requires some extra effort in design, but it can deliver successful performance. As a point of reference, the most common wood

seismic resisting systems perform well yet have connections (nails) that are significantly weaker than the connected elements (structural wood panels). The *Provisions* includes guidance, some only for trial use and comment, for seismic design of precast structures.

### 1.2.3.6 Composite Steel and Concrete

Reinforced concrete is a composite material. In the context of the *Provisions*, *composite* is a term reserved for structures with elements consisting of structural steel and reinforced concrete acting in a composite manner. These structures generally are an attempt to combine the most beneficial aspects of each material.

### 1.2.4 Building Systems

Three basic lateral-load-resisting elements – walls, braced frames, and unbraced frames (moment resisting frames) – are used to build a classification of structural types in the *Provisions*. Unbraced frames generally are allowed greater reductions from elastic response than walls and braced frames. In part, this is because frames are more redundant, having several different locations with approximately the same stress levels, and common beam-column joints frequently exhibit an ability to maintain a stable response through many cycles of reversed inelastic deformations. Systems using connection details that have not exhibited good ductility and toughness, such as unconfined concrete and the welded steel joint used before the Northridge earthquake, are penalized with small reduction factors.

Connection details often make development of ductility difficult in braced frames, and buckling of compression members also limits their inelastic response. Eccentrically braced steel frames and new proportioning and detailing rules for concentrically braced frames have been developed to overcome these shortcomings. [The 2003 *Provisions* include proportioning and detailing rules for buckling-restrained braced frames. This new system has the advantages of a special steel concentrically braced frame, but with performance that is superior as brace buckling is prevented. Design provisions appear in 2003 *Provisions* Sec. 8.6.] Walls that are not load bearing are allowed a greater reduction than walls that are load bearing. Redundancy is one reason; another is that axial compression generally reduces the flexural ductility of concrete and masonry elements (although small amounts of axial compression usually improve the performance of materials weak in tension, such as masonry and concrete). Systems that combine different types of elements are generally allowed greater reductions from elastic response because of redundancy.

Redundancy is frequently cited as a desirable attribute for seismic resistance. A quantitative measure of redundance has been introduced in recent editions of the *Provisions* in an attempt to prevent use of large reductions from elastic response in structures that actually possess very little redundancy. As with many new empirical measures, it is not universally accepted and is likely to change in the future. [In the 2003 *Provisions*, a radical change was made to the requirements related to redundancy. Only two values of the redundancy factor,  $\rho$ , are defined: 1.0 and 1.3. Assignment of a value for  $\rho$  is based on explicit consideration of the consequence of failure of a single element of the seismic-force-resisting system. A simple, deemed-to-comply exception is provided for certain structures.]

### **1.3 ENGINEERING PHILOSOPHY**

The *Provisions*, under "Purpose," states:

The design earthquake ground motion levels specified herein could result in both structural and nonstructural damage. For most structures designed and constructed according to the *Provisions*, structural damage from the design earthquake ground motion would be repairable although perhaps not economically so. For essential facilities, it is expected that the damage from the design earthquake ground motion would not be so severe as to preclude continued occupancy and function of the facility... For ground motions larger than the design levels, the intent of the *Provisions* is that there be low likelihood of structural collapse.

The two points to be emphasized are that damage is to be expected when an earthquake (equivalent to the design earthquake) occurs and that the probability of collapse is not zero. The design earthquake ground motion level mentioned is two-thirds of the MCE ground motion.

The basic structural criteria are strength, stability, and distortion. The yield-level strength provided must be at least that required by the design spectrum (which is reduced from the elastic spectrum as described previously). Structural elements that cannot be expected to perform in a ductile manner are to have strengths greater than those required by the  $\Omega_0$  amplifier on the design spectral response. The stability criterion is imposed by amplifying the effects of lateral forces for the destabilizing effect of lateral translation of the gravity weight (the P-delta effect). The distortion criterion as a limit on story drift and is calculated by amplifying the linear response to the (reduced) design spectrum by the factor  $C_d$  to account for inelastic behavior.

Yield-level strengths for steel and concrete structures are easily obtained from common design standards. The most common design standards for timber and masonry are based on allowable stress concepts that are not consistent with the basis of the reduced design spectrum. Although strength-based standards for both materials have been introduced in recent years, the engineering profession has not yet embraced these new methods. In the past, the *Provisions* stipulated adjustments to common reference standards for timber and masonry to arrive at a strength level equivalent to yield and compatible with the basis of the design spectrum. Most of these adjustments were simple factors to be applied to conventional allowable stresses. With the deletion of these methods from the *Provisions*, methods have been introduced into model building codes and the ASCE standard *Minimum Design Loads for Buildings and Other Structures* to factor downward the seismic load effects based on the *Provisions* for use with allowable stress design methods.

The *Provisions* recognizes that the risk presented by a particular building is a combination of the seismic hazard at the site and the consequence of failure, due to any cause, of the building. Thus, a classification system is established based on the use and size of the building. This classification is called the Seismic Use Group (SUG). A combined classification called the Seismic Design Category (SDC) incorporates both the seismic hazard and the SUG. The SDC is used throughout the *Provisions* for decisions regarding the application of various specific requirements. The flow charts in Chapter 2 illustrate how these classifications are used to control application of various portions of the *Provisions*.

### **1.4 STRUCTURAL ANALYSIS**

The *Provisions* sets forth several procedures for determining the force effect of ground shaking. Analytical procedures are classified by two facets: linear versus nonlinear and dynamic versus equivalent static. The two most fully constrained and frequently used are both linear methods: an equivalent static force procedure and a dynamic modal response spectrum analysis procedure. A third linear method, a full history of dynamic response (often referred to as a time-history or response-history analysis), and a nonlinear method are also permitted, subject to certain limitations. These methods use real or synthetic ground motion histories as input but require them to be scaled to the basic response spectrum at the site for the range of periods of interest for the structure in question. Nonlinear analyses are very sensitive to assumptions made in the analysis and a peer review is required. A nonlinear static method, also know as a pushover analysis, is described in an appendix for trial use and comment. [In the 2003 *Provisions*, substantial changes were made to the appendix for the nonlinear static procedure based, in part, on the results of the Applied Technology Council's Project 55.]

The two most common linear methods make use of the same design spectrum. The entire reduction from the elastic spectrum to design spectrum is accomplished by dividing the elastic spectrum by the coefficient R, which ranges from 1-1/4 to 8. The specified elastic spectrum is based on a damping level at 5 percent of critical damping, and a part of the R factor accomplishes adjustments in the damping level. The *Provisions* define the total effect of earthquake actions as a combination of the response to horizontal motions (or forces for the equivalent static force method) with response to vertical ground acceleration. The resulting internal forces are combined with the effects of gravity loads and then compared to the full strength of the members, which are not reduced by a factor of safety.

With the equivalent static force procedure, the level of the design spectrum is set by determining the appropriate values of basic seismic acceleration, the appropriate soil profile type, and the value for R. The particular acceleration for the building is determined from this spectrum by selecting a value for the natural period of vibration. Equations that require only the height and type of structural system are given to approximate the natural period for various building types. (The area and length of shear walls come into play with an optional set of equations.) Calculation of a period based on an analytical model of the structure is encouraged, but limits are placed on the results of such calculations. These limits prevent the use of a very flexible model in order to obtain a large period and correspondingly low acceleration. Once the overall response acceleration is found, the base shear is obtained by multiplying it by the total effective mass of the building, which is generally the total permanent load.

Once the total lateral force is determined, the equivalent static force procedure specifies how this force is to be distributed along the height of the building. This distribution is based on the results of dynamic studies of relatively uniform buildings and is intended to give an envelope of shear force at each level that is consistent with these studies. This set of forces will produce, particularly in tall buildings, an envelope of gross overturning moment that is larger than the dynamic studies indicate is necessary. Dynamic analysis is encouraged, and the modal procedure is required for structures with large periods (essentially this means tall structures) in the higher seismic design categories.

With one exception, the remainder of the equivalent static force analysis is basically a standard structural analysis. That exception accounts for uncertainties in the location of the center of mass, uncertainties in the strength and stiffness of the structural elements, and rotational components in the basic ground shaking. This concept is referred to as horizontal torsion. The *Provisions* requires that the center of force be displaced from the calculated center of mass by an arbitrary amount in either direction (this torsion is referred to as accidental torsion). The twist produced by real and accidental torsion is then compared to a threshold, and if the threshold is exceeded, the torsion must be amplified.

In many respects, the modal analysis procedure is very similar to the equivalent static force procedure. The primary difference is that the natural period and corresponding deflected shape must be known for several of the natural modes of vibration. These are calculated from a mathematical model of the structure. The procedure requires inclusion of enough modes so that the dynamic model represents at least 90 percent of the mass in the structure that can vibrate. The base shear for each mode is determined from a design spectrum that is essentially the same as that for the static procedure. The distribution of forces, and the resulting story shears and overturning moments, are determined for each mode directly from the procedure. Total values for subsequent analysis and design are determined by taking the square root of the sum of the squares for each mode. This summation gives a statistical estimate of maximum response when the participation of the various modes is random. If two or more of the modes have very

similar periods, more advanced techniques for summing the values are required; these procedures must account for coupling in the response of close modes. The sum of the absolute values for each mode is always conservative.

A lower limit to the base shear determined from the modal analysis procedure is specified based on the static procedure and the approximate periods specified in the static procedure. When this limit is violated, which is common, all results are scaled up in direct proportion. The consideration of horizontal torsion is the same as for the static procedure. Because the forces applied at each story, the story shears, and the overturning moments are separately obtained from the summing procedure, the results are not statically compatible (that is, the moment calculated from the story forces will not match the moment from the summation). Early recognition of this will avoid considerable problems in later analysis and checking.

For structures that are very uniform in a vertical sense, the two procedures give very similar results. The modal analysis method is better for buildings having unequal story heights, stiffnesses, or masses. The modal procedure is required for such structures in higher seismic design categories. Both methods are based on purely elastic behavior and, thus, neither will give a particularly accurate picture of behavior in an earthquake approaching the design event. Yielding of one component leads to redistribution of the forces within the structural system. This may be very significant; yet, none of the linear methods can account for it.

Both of the common methods require consideration of the stability of the building as a whole. The technique is based on elastic amplification of horizontal displacements created by the action of gravity on the displaced masses. A simple factor is calculated and the amplification is provided for in designing member strengths when the amplification exceeds about 10 percent. The technique is referred to as the P-delta analysis and is only an approximation of stability at inelastic response levels.

### **1.5 NONSTRUCTURAL ELEMENTS OF BUILDINGS**

Severe ground shaking often results in considerable damage to the nonstructural elements of buildings. Damage to nonstructural elements can pose a hazard to life in and of itself, as in the case of heavy partitions or facades, or it can create a hazard if the nonstructural element ceases to function, as in the case of a fire suppression system. Some buildings, such as hospitals and fire stations, need to be functional immediately following an earthquake; therefore, many of their nonstructural elements must remain undamaged.

The *Provisions* treats damage to and from nonstructural elements in three ways. First, indirect protection is provided by an overall limit on structural distortion; the limits specified, however, may not offer enough protection to brittle elements that are rigidly bound by the structure. More restrictive limits are placed upon those SUGs for which better performance is desired given the occurrence of strong ground shaking. Second, many components must be anchored for an equivalent static force. Third, the explicit design of some elements (the elements themselves, not just their anchorage) to accommodate specific structural deformations or seismic forces is required.

The dynamic response of the structure provides the dynamic input to the nonstructural component. Some components are rigid with respect to the structure (light weights and small dimensions often lead to fundamental periods of vibration that are very short). Application of the response spectrum concept would indicate that the time history of motion of a building roof to which mechanical equipment is attached looks like a ground motion to the equipment. The response of the component is often amplified above the response of the supporting structure. Response spectra developed from the history of motion of a point on a structure undergoing ground shaking are called floor spectra and are a useful in understanding the demands upon nonstructural components.

The *Provisions* simplifies the concept greatly. The force for which components are checked depends on:

- 1. The component mass;
- 2. An estimate of component acceleration that depends on the structural response acceleration for short period structures, the relative height of the component within the structure, and a crude approximation of the flexibility of the component or its anchorage;
- 3. The available ductility of the component or its anchorage; and
- 4. The function or importance of the component or the building.

Also included in the *Provisions* is a quantitative measure for the deformation imposed upon nonstructural components. The inertial force demands tend to control the seismic design for isolated or heavy components whereas the imposed deformations are important for the seismic design for elements that are continuous through multiple levels of a structure or across expansion joints between adjacent structures, such as cladding or piping.

### **1.6 QUALITY ASSURANCE**

Since strong ground shaking has tended to reveal hidden flaws or *weak links* in buildings, detailed requirements for assuring quality during construction are contained in the *Provisions*. Loads experienced during construction provide a significant test of the likely performance of ordinary buildings under gravity loads. Tragically, mistakes occasionally will pass this test only to cause failure later, but it is fairly rare. No comparable proof test exists for horizontal loads, and experience has shown that flaws in construction show up in a disappointingly large number of buildings as distress and failure due to earthquakes. This is coupled with the fact that the design is based on excursions into inelastic straining, which is not the case for response to other loads.

The quality assurance provisions require a systematic approach with an emphasis on documentation and communication. The designer who conceives the systems to resist the effects of earthquake forces must identify the elements that are critical for successful performance as well as specify the testing and inspection necessary to ensure that those elements are actually built to perform as intended. Minimum levels of testing and inspection are specified in the *Provisions* for various types of systems and components.

The *Provisions* also requires that the contractor and building official be aware of the requirements specified by the designer. Furthermore, those individuals who carry out the necessary inspection and testing must be technically qualified and must communicate the results of their work to all concerned parties. In the final analysis, there is no substitute for a sound design, soundly executed.

2

# GUIDE TO USE OF THE PROVISIONS

### Michael Valley, P.E.

The flow charts and table that follow are provided to assist the user of the *NEHRP Recommended Provisions* and, by extension, the seismic provisions of ASCE 7, *Minimum Design Loads for Buildings and Other Structures*, the *International Building Code*, and *NFPA 5000*. The flow charts provide an overview of the complete process for satisfying the *Provisions*, including the content of all technical chapters. The table that concludes this chapter provides cross references for ASCE 7 and the 2000 and 2000 editions of the *NEHRP Recommended Provisions*.

The flow charts are expected to be of most use to those who are unfamiliar with the scope of the *NEHRP Recommended Provisions*, but they cannot substitute for a careful reading of the *Provisions*. Notes indicate discrepancies and errors in the *Provisions*. Both editions of the *Provisions* can be obtained free from the FEMA Publications Distribution Center by calling 1-800-480-2520. Order by FEMA Publication number; the 2003 *Provisions* is available as FEMA 450 in CD form (only a limited number of paper copies are available) and the 2000 *Provisions* are available as FEMA 368 and 369 (2 volumes and maps).

Although the examples in this volume are based on the 2000 *Provisions*, they have been annotated to reflect changes made to the 2003 *Provisions*. Annotations within brackets, [], indicate both organizational changes (as a result of a reformat of all of the chapters of the 2003 *Provisions*) and substantive technical changes to the 2003 *Provisions* and its primary reference documents. For those readers coming from ASCE 7-05, see the cross reference table at the end of this chapter.

The level of detail shown varies, being greater where questions of applicability of the *Provisions* are pertinent and less where a standard process of structural analysis or detailing is all that is required. The details contained in the many standards referenced in the *Provisions* are not included; therefore, the actual flow of information when proportioning structural members for the seismic load effects specified in the *Provisions* will be considerably more complex.

On each chart the flow generally is from a heavy-weight box at the top-left to a medium-weight box at the bottom-right. User decisions are identified by six-sided cells. Optional items and modified flow are indicated by dashed lines.

Chart 2.1 provides an overall summary of the process which begins with consideration of the Scope of Coverage and ends with Quality Assurance Requirements. All of the specific provisions pertaining to nonbuilding structures are collected together on one page (Chart 2.20); application for nonbuilding structures requires the use of various portions of the *Provisions* with appropriate modification.

Additions to, changes of use in, and alterations of existing structures are covered by the *NEHRP Recommended Provisions* (see Chart 2.3), but evaluation and rehabilitation of existing structures is not.

In recent years FEMA has sponsored several coordinated efforts dealing with seismic safety in existing buildings. A *Handbook for Seismic Evaluation of Buildings* (FEMA 310) was developed as an update to the original FEMA 178, although this document has since been replaced by the ASCE 31 Standard (*Seismic Evaluation of Existing Buildings*). *Guidelines for the Seismic Rehabilitation of Buildings* (FEMA 273) and a corresponding *Commentary* (FEMA 274) have also been developed. A prestandard (FEMA 356, *Prestandard and Commentary for the Seismic Rehabilitation of Buildings*) based on FEMA 273 has been developed and is in balloting as ASCE 41. In addition, specific recommendations have been developed for the evaluation, repair, and rehabilitation of earthquake-damaged concrete and masonry wall buildings (FEMA 306, 307, and 308) and for the evaluation, rehabilitation, post-earthquake assessment, and repair of steel moment frame structures (FEMA 351 and 352).

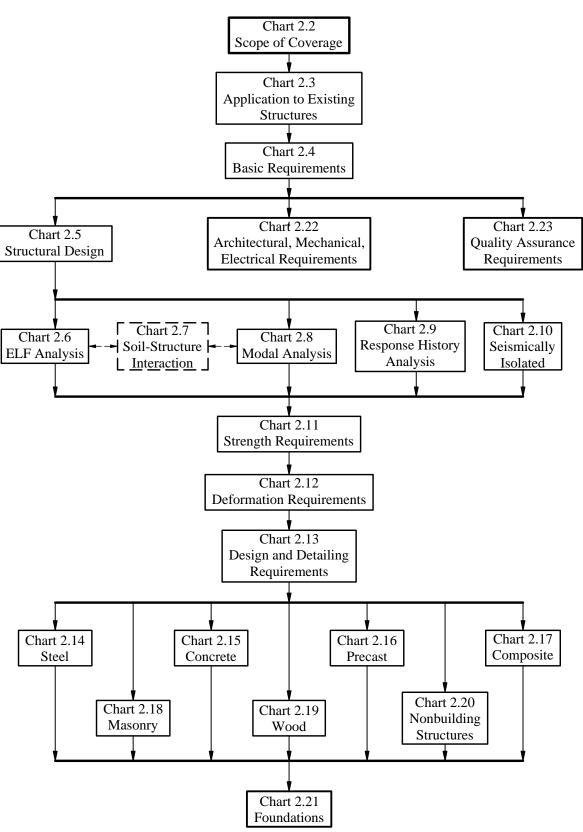
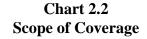
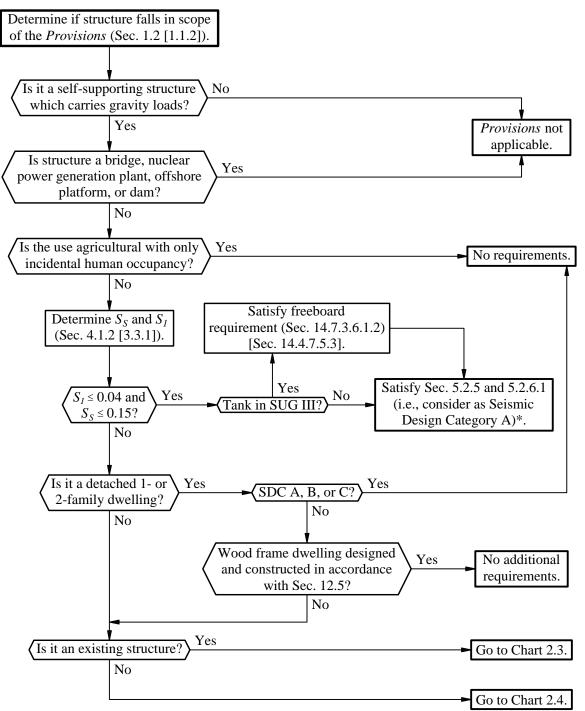


Chart 2.1 Overall Summary of Flow





\*The *Provisions* has never defined clearly the scope of application for structures assigned to Seismic Design Category A. Although the framers of the *Provisions* intended application of only a few simple requirements in Seismic Design Category A, a strict reading of the 2000 *Provisions* would lead to a substantial list of items that remain within the scope. [As a result of the complete re-write of the *Provisions* at the beginning of the 2003 update cycle, this situation is improved considerably as the requirements for Seismic Design Category A all appear in Sec. 1.5.]

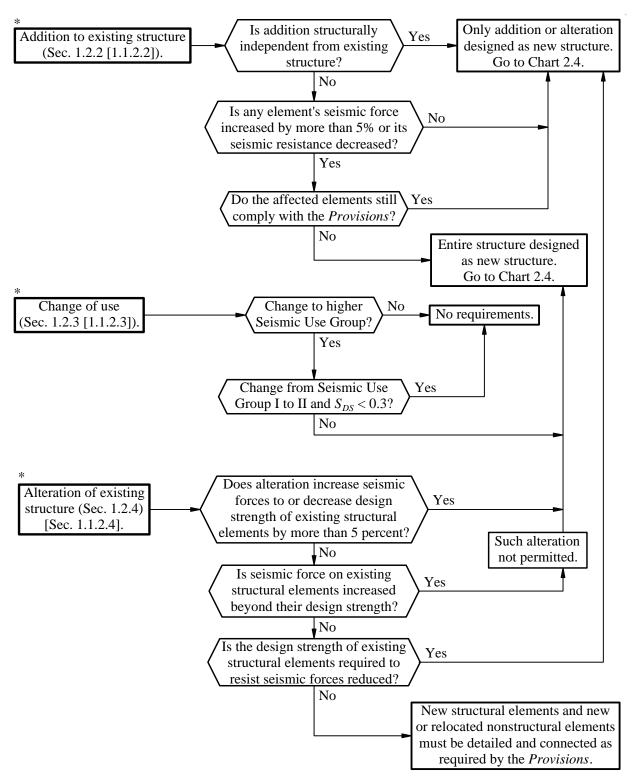


Chart 2.3 Application to Existing Structures

\* The *Provisions* applies to existing structures only in the cases of additions to, changes of use in, and alterations of such structures.

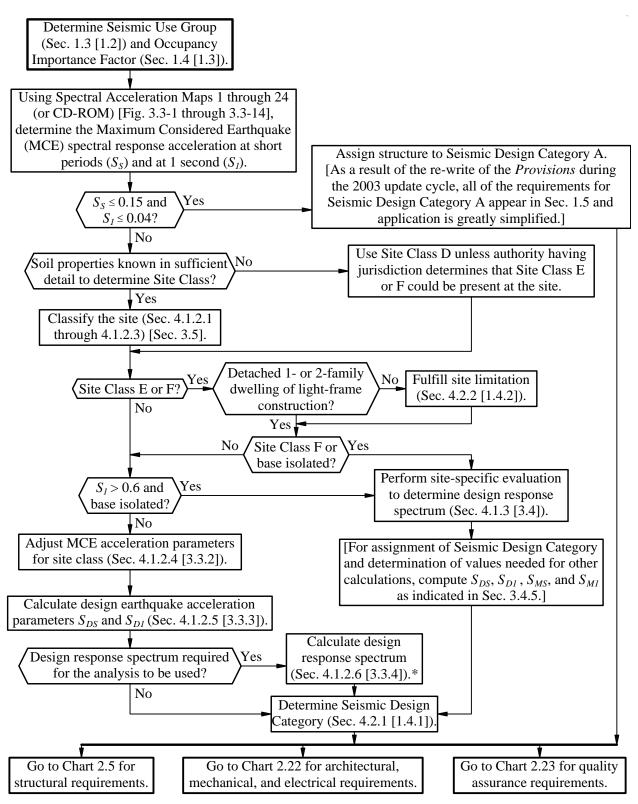
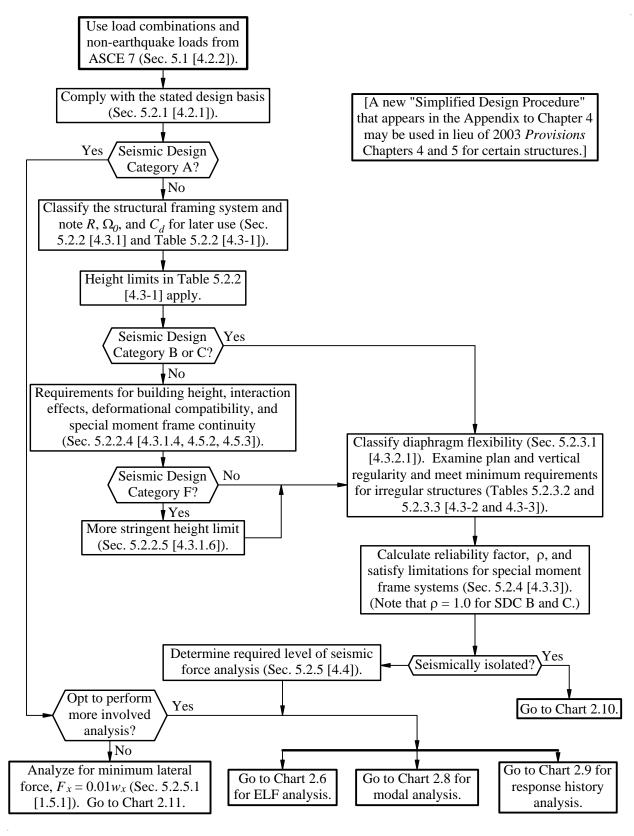
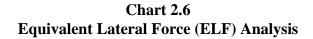


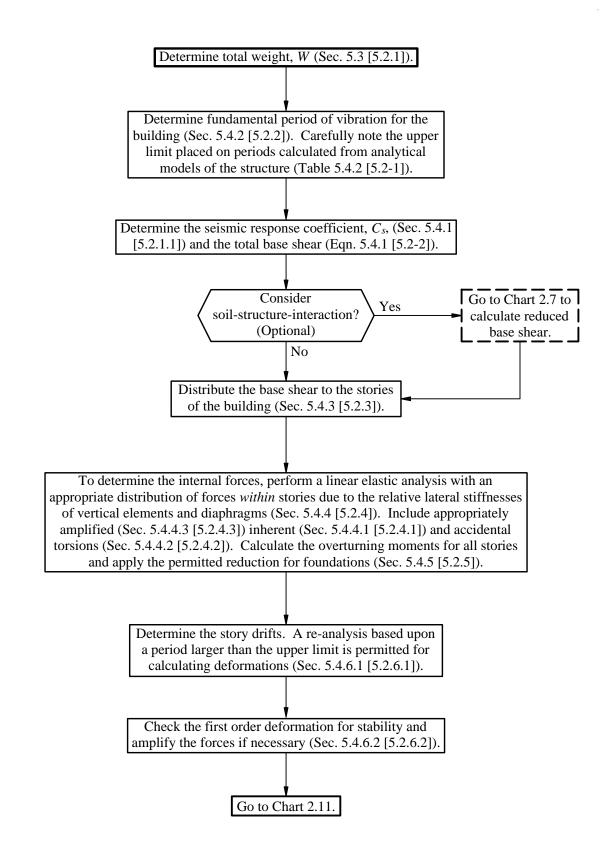
Chart 2.4 Basic Requirements

\* [Sec. 3.3.4 of the 2003 *Provisions* defines reduced spectral ordinates for periods greater than  $T_L$ .]



### Chart 2.5 Structural Design





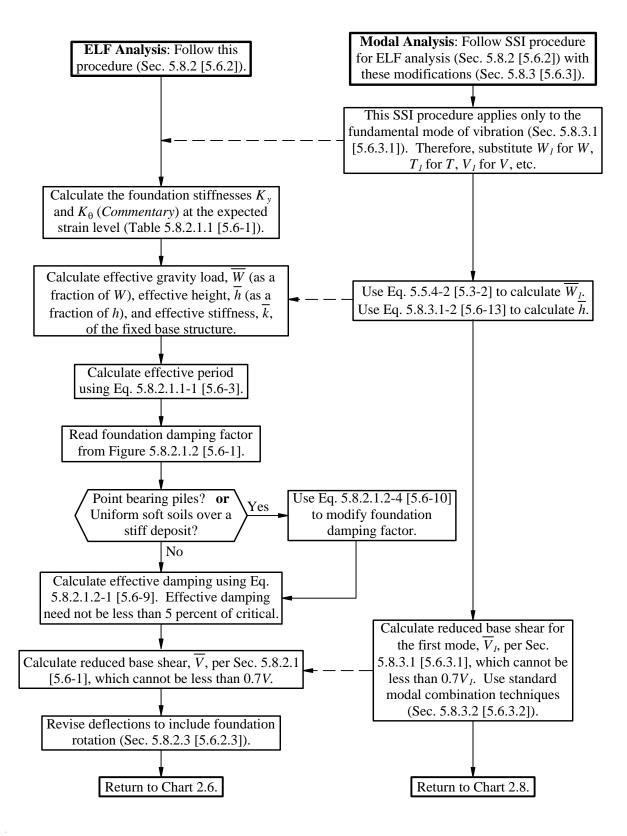
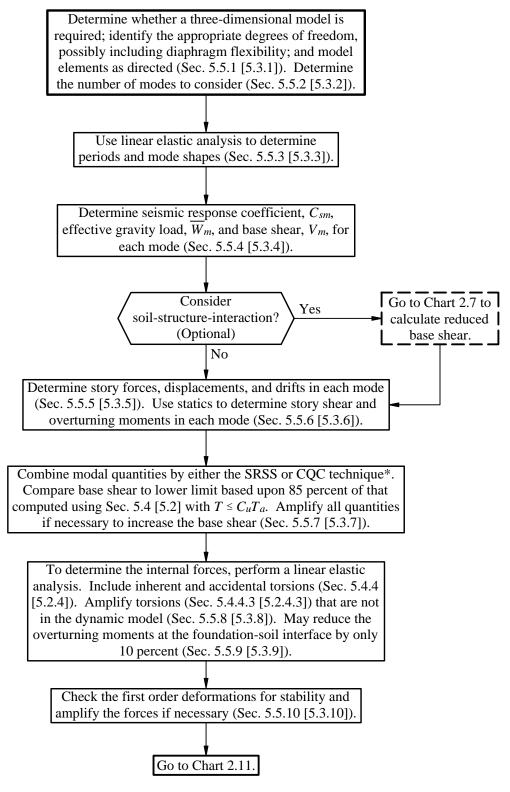
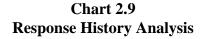


Chart 2.7 Soil-Structure Interaction (SSI)

Chart 2.8 Modal Analysis



\*As indicated in the text, use of the CQC technique is required where closely spaced periods in the translational and torsional modes will result in cross-correlation of the modes.



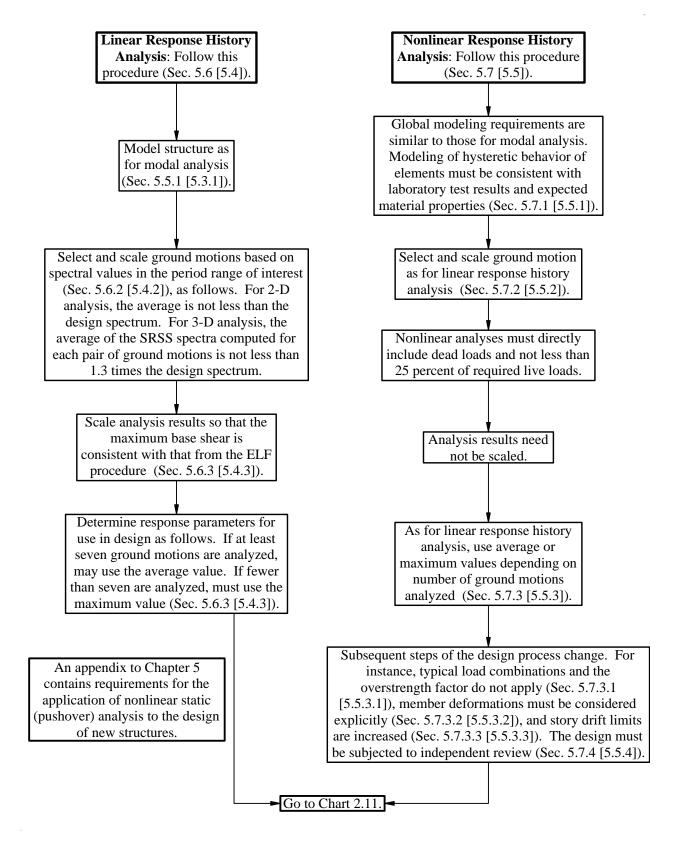
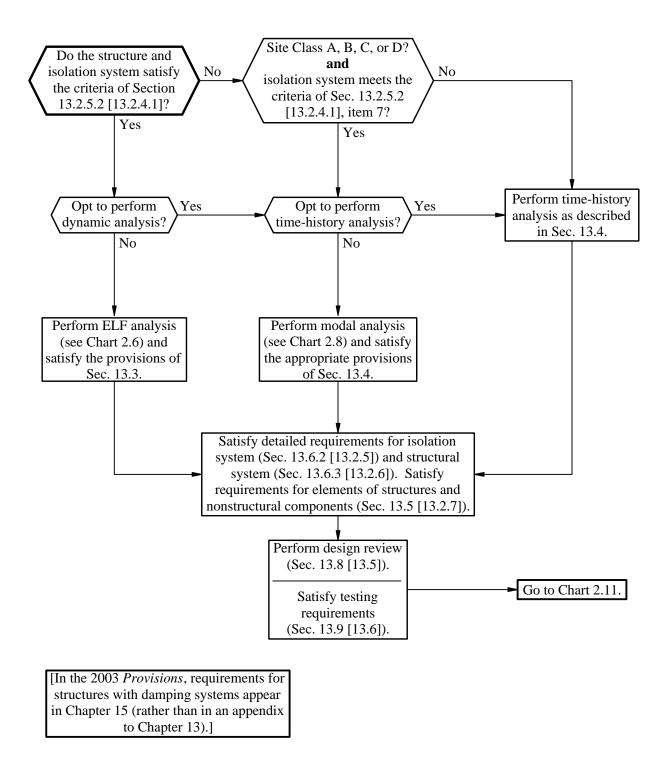
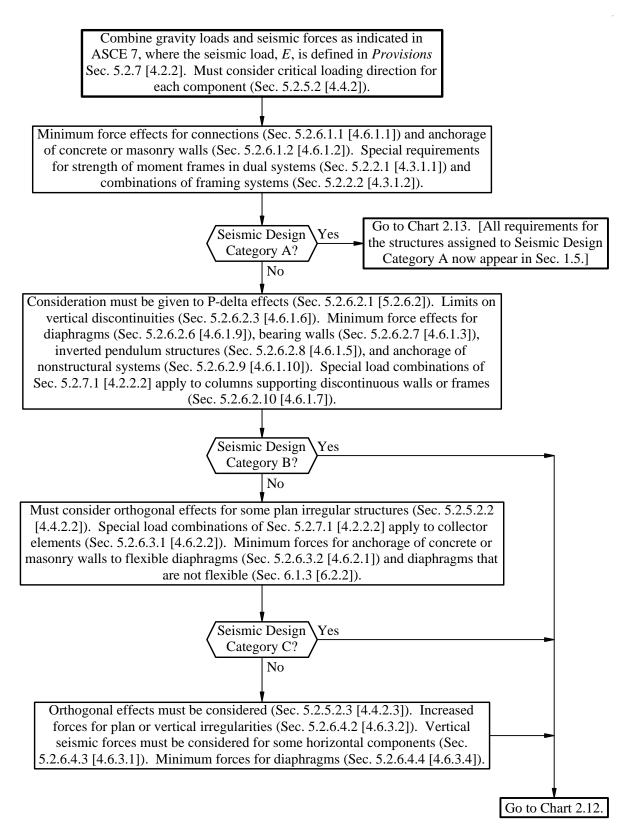


Chart 2.10 Seismically Isolated Structures



### Chart 2.11 Strength Requirements



### Chart 2.12 Deformation Requirements

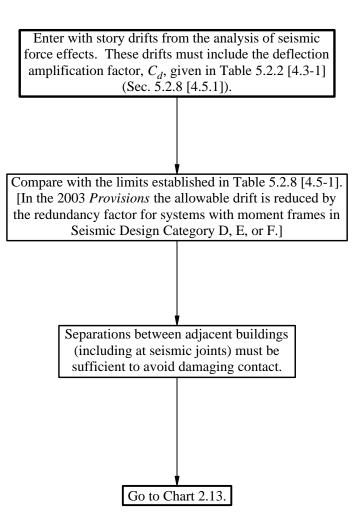


Chart 2.13 Design and Detailing Requirements

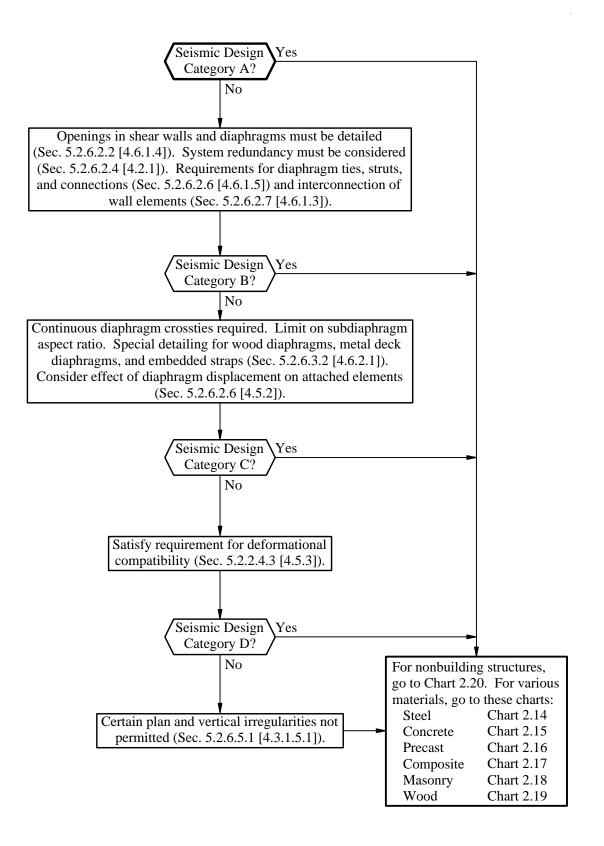


Chart 2.14 Steel Structures

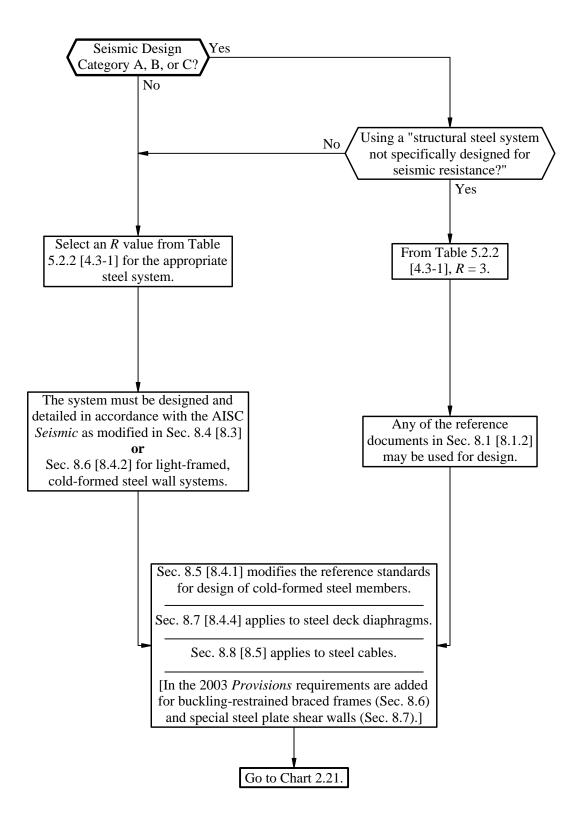


Chart 2.15 Concrete Structures

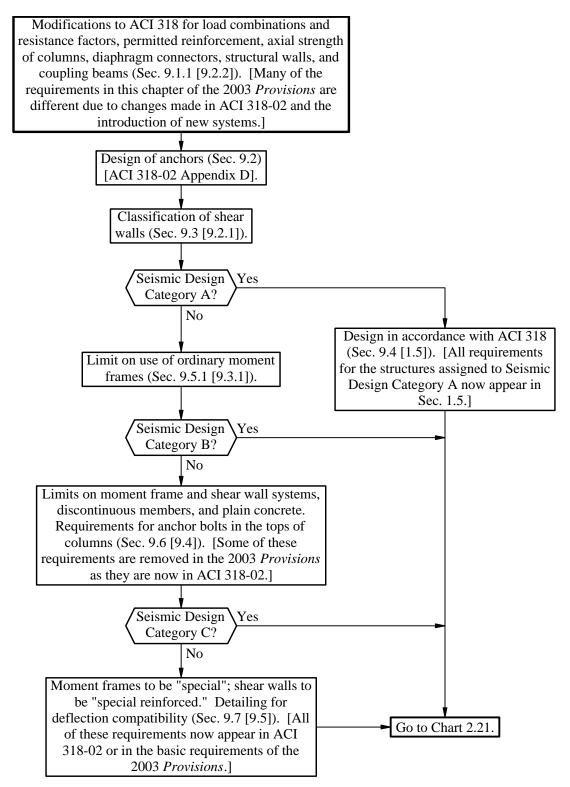


Chart 2.16 Precast Concrete Structures

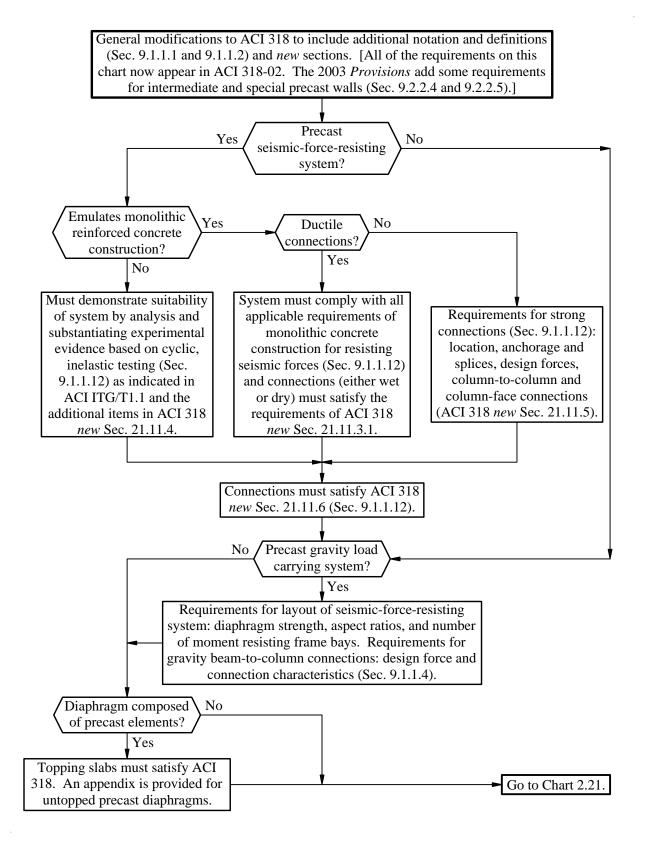
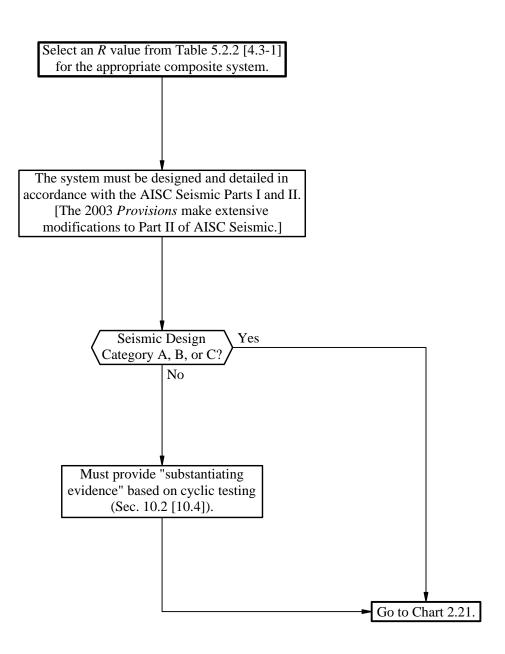


Chart 2.17 Composite Steel and Concrete Structures



### Chart 2.18 Masonry Structures

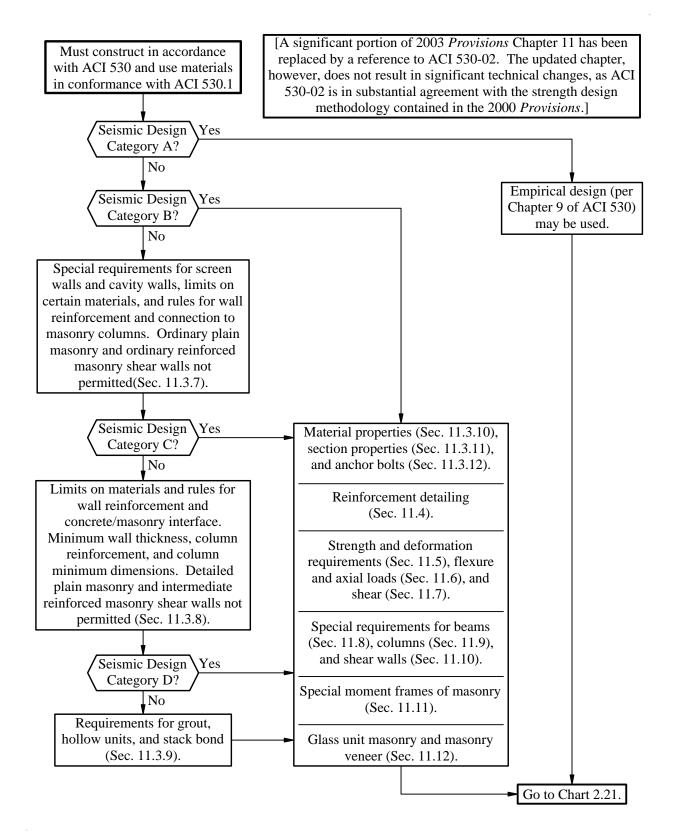
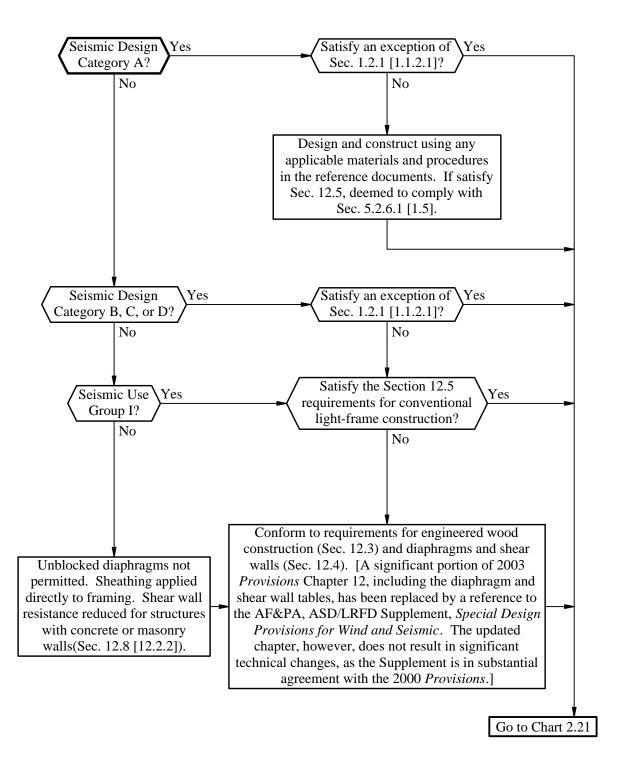


Chart 2.19 Wood Structures



### Chart 2.20 Nonbuilding Structures

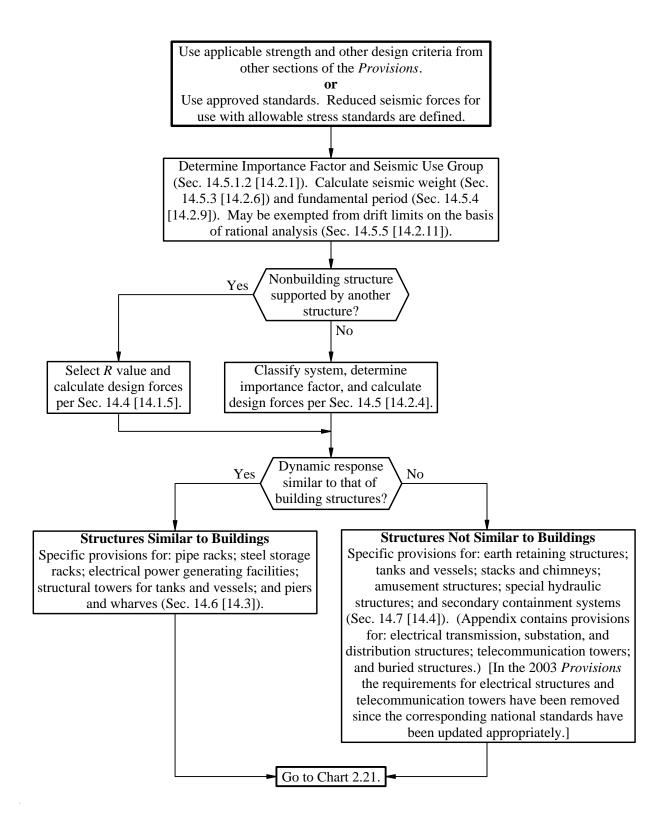
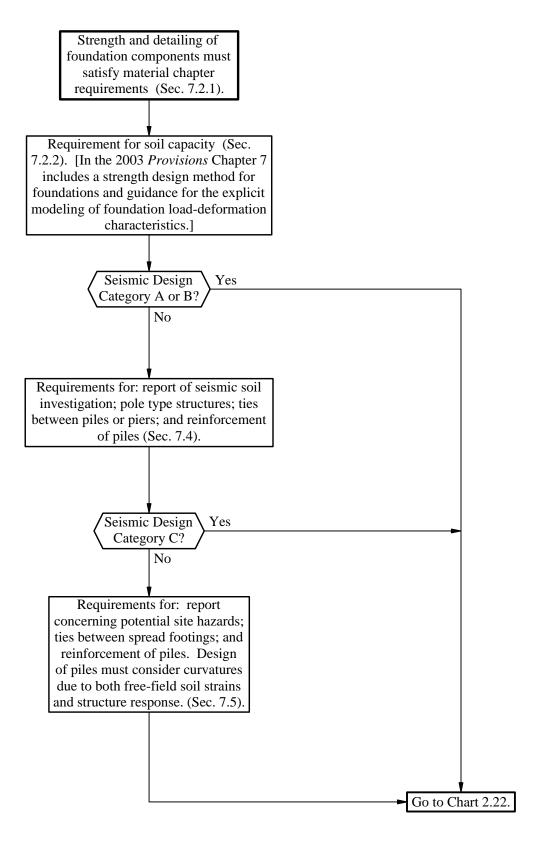


Chart 2.21 Foundations



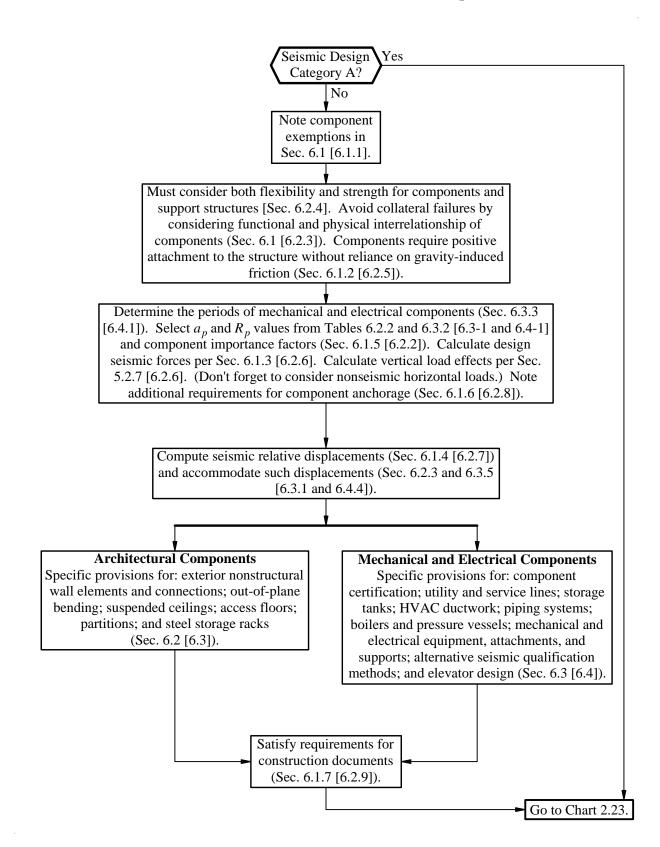
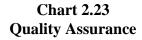
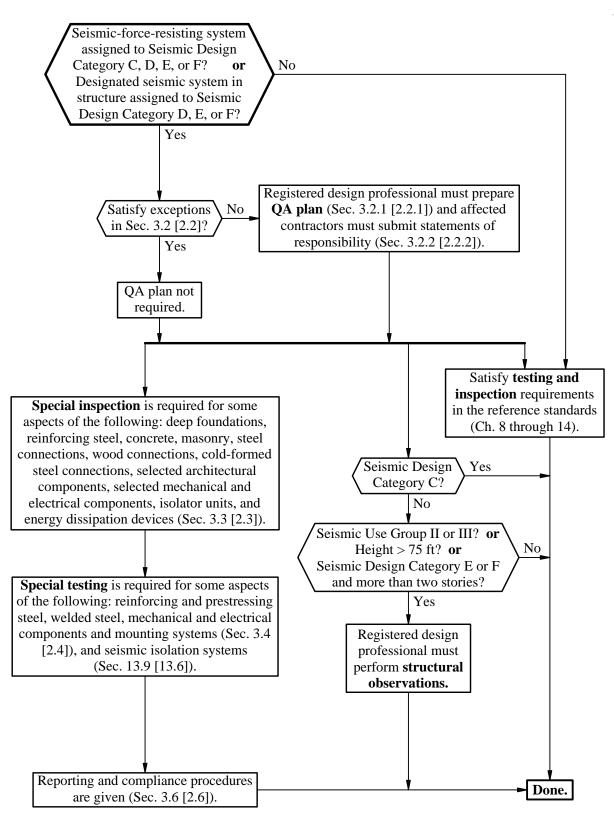


Chart 2.22 Architectural, Mechanical, and Electrical Components





ASCE 7	<b>NEHRP 2000</b>	<b>NEHRP 2003</b>	
Section	Section	Section	Торіс
Beetion	Section	Beetion	
Chapter 11			SEISMIC DESIGN CRITERIA
11.1	1.1, 1.2	1.1	General
11.2	2.1	1.1.4	Definitions
11.2	2.2	1.1.5	Notation
11.5	4.1	3.3	Seismic Ground Motion Values
11.4	1.3, 1.4	1.2, 1.3	Importance Factor and Occupancy Category
11.5	4.2	1.2, 1.3	Seismic Design Category
11.7	5.2.6.1	1.4	Design Requirements for Seismic Design Category A
11.7	4.2, 7.4, 7.5	1.4.2, 7.4, 7.5	Geologic hazards and Geotechnical Investigation
11.0	4.2, 7.4, 7.3	1.4.2, 7.4, 7.3	Geologic nazarus and Geolechinicai investigation
Chapter 12	5	4, 5	SEISMIC DESIGN REQUIREMENTS FOR BUILDING
Chapter 12	5	4, 5	STRUCTURES
12.1	5.2	4.2.1	
<u>12.1</u> 12.2	5.2.2	4.2.1 4.3.1	Structural Design Basis Structural System Selection
12.2			
12.3	5.2.3, 5.2.6,	4.3.2	Diaphragm Flexibility, Configuration Irregularities and
10.4	5.2.4	4.2.2	Redundancy
12.4	5.2.7, 5.2.6	4.2.2	Seismic Load Effects and Combinations
12.5	5.2.5	4.4.2	Direction of Loading
12.6	5.2.5	4.4.1	Analysis Procedure Selection
12.7	5.2, 5.6.2		Modeling Criteria
12.8	5.5	5.2	Equivalent Lateral Force Procedures
12.9	5.6	5.3	Modal Response Spectrum Analysis
12.10	5.2.6	4.6	Diaphragms, Chords and Collectors
12.11	5.2.6	4.6	Structural Walls and Their Anchorage
12.12	5.2.8	4.5	Drift and Deformation
12.13	7	7	Foundation Design
12.14	5.4	4 Alt.	Simplified Alternative Structural Design Criteria for
			Simple Bearing Wall of Building Frame System
Chapter 13			SEISMIC REQUIREMENTS FOR NONSTRUCTURAL
			COMPONENTS
13.1	6.1	6.1	General
13.2	6.1	6.2	General Design Requirements
13.3	6.1.3, 6.1.4	6.2	Seismic Demands on Nonstructural Components
13.4	6.1.2	6.2	Nonstructural Component Anchorage
13.5	6.2	6.3	Architectural Components
13.6	6.3	6.4	Mechanical and Electrical Components
Chapter 14			MATERIAL SPECIFIC SEISMIC DESIGN AND
			DETAILING REQUIREMENTS
14			Scope
14.1	8	8	Steel
14.2	9	9	Concrete
14.3	10	10	Composite Steel and Concrete Structures
14.4	11	11	Masonry
14.5	12	12	Wood

# Table 2-1 Navigating Among the 2000 and 2003 NEHRP Recommended Provisionsand ASCE 7

Chapter 15	14	14	SEISMIC DESIGN DEOLIDEMENTS EOD
Chapter 15	14	14	SEISMIC DESIGN REQUIREMENTS FOR NONBUILDING STRUCTURES
15.1	14.1	14.1	General
15.2	14.2,14.3	14.1.2	Reference Documents
15.3	14.4	14.1.5	Nonbuilding Structures Supported by Other Structures
15.4	14.5	14.2	Structural Design Requirements
15.5	14.6	14.3	Nonbuilding Structures Similar to Buildings
15.6	14.7	14.3	General Requirements for Nonbuilding Structures Not
15.0	14./	14.4	Similar to Buildings
15.7	14.7.3	14.4.7	Tanks and Vessels
13.7	14.7.3	14.4.7	
Chapter 16			SEISMIC RESPONSE HISTORY PROCEDURES
16.1	5.7	5.4	Linear Response History Analysis
16.2	5.8	5.5	Nonlinear Response History Procedure
10.2	5.0	5.5	
Chapter 17	13	13	SEISMIC DESDIGN REQUIREMENTS FOR
Chapter 17	15	15	SEISMICALLY ISOLATED STRUCTURES
17.1	13.1	13.1	General
17.2	13.5, 13.6	13.2	General design Requirements
17.2	13.4.4	13.2.3	Ground Motion for Isolated Systems
17.3	13.2.5		Analysis Procedure Selection
		13.2.4	ž – ž
17.5	13.3	13.3	Equivalent Lateral Force Procedure
17.6	13.4	13.4	Dynamic Analysis Procedures
17.7	13.8	13.5	Design Review
17.8	13.9	13.6	Testing
Chantan 19	124	15	CEICMIC DECICN DECLIDEMENTS EOD
Chapter 18	13A	15	SEISMIC DESIGN REQUIREMENTS FOR
10.1	10 4 1	15 1	STRUCTURES WITH DAMPING SYSTEMS
18.1	13A.1	15.1	General
18.2	13A.2, 13A.8	15.2	General Design Requirements
18.3	13A.6	15.3	Nonlinear Procedures
18.4	13A.5	15.4	Response Spectrum Procedure
18.5	13A.4	15.5	Equivalent Lateral Force Procedure
18.6	13A.3	15.6	Damped Response Modification
18.7	13A.7	15.7	Seismic Load Conditions and Acceptance
18.8	13A.9	15.8	Design Review
18.9	13A.10	15.9	Testing
Chapter 19			SOIL STRUCTURE INTERACTION FOR SEISMIC
•			DESIGN
19.1	5.8.1	5.6.1	General
19.2	5.8.2	5.6.2	Equivalent Lateral Force Procedure
19.3	5.8.3	5.6.3	Modal Analysis Procedure
Chapter 20			SITE CLASSIFICATION PROCEDURE FOR SEISMIC
-			DESIGN
20.1	4.1	3.5	Site Classification
20.2	4.1	3.5	Site Response Analysis for Site Class F Soil
20.3	4.1	3.5	Site Class Definitions
20.4	4.1	3.5	Definitions of Site Class Parameters
	•		

Chapter 21			SITE-SPECIFIC GROUND MOTION PROCEDURES
Ĩ			FOR SEISMIC DESIGN
21.1	4.1	3.4	Site Response Analysis
21.2	4.1	3.4	Ground Motion Hazard Analysis
21.3	4.1	3.4	Design Response Spectrum
21.4	4.1	3.4	Design Acceleration Parameters
Chapter 22	4.1	3.3	SEISMIC GROUND MOTION AND LONG PERIOD TRANSITION MAPS
Chapter 23			SEISMIC DESIGN REFERENCE DOCUMENTS
23.1			Consensus Standards and Other Reference Documents
11A	3	2	QUALITY ASSURANCE PROVISIONS
11A.1	3.1, 3.2, 3.3	2.1, 2.2, 2.3	Quality Assurance
11A.2	3.4	2.4	Testing
11A.3	3.5	2.5	Structural Observations
11A.4	3.6	2.6	Reporting and Compliance Procedures
11B			EXISTING BUILDING PROVISIONS
11B.1	1.2.1	1.1.2	Scope
11B.2	1.2.2.1	1.1.2.2	Structurally Independent Additions
11B.3	1.2.2.2	1.1.2.2	Structurally Dependent Additions
11B.4	1.2.4	1.1.2.4	Alterations
11B.5	1.2.3	1.1.2.3	Change of Use

3

## STRUCTURAL ANALYSIS

### Finley A. Charney, Ph.D., P.E.

This chapter presents two examples that focus on the dynamic analysis of steel frame structures:

- 1. A 12-story steel frame building in Stockton, California The highly irregular structure is analyzed using three techniques: equivalent lateral force (ELF) analysis, modal-response-spectrum analysis, and modal time-history analysis. In each case, the structure is modeled in three dimensions, and only linear elastic response is considered. The results from each of the analyses are compared, and the accuracy and relative merits of the different analytical approaches are discussed.
- 2. A six-story steel frame building in Seattle, Washington. This regular structure is analyzed using both linear and nonlinear techniques. Due to limitations of available software, the analyses are performed for only two dimensions. For the nonlinear analysis, two approaches are used: static pushover analysis in association with the capacity-demand spectrum method and direct time-history analysis. In the nonlinear analysis, special attention is paid to the modeling of the beam-column joint regions of the structure. The relative merits of pushover analysis versus time-history analysis are discussed.

Although the Seattle building, as originally designed, responds reasonably well under the design ground motions, a second set of time-history analyses is presented for the structure augmented with added viscous fluid damping devices. As shown, the devices have the desired effect of reducing the deformation demands in the critical regions of the structure.

Although this volume of design examples is based on the 2000 *Provisions*, it has been annotated to reflect changes made to the 2003 *Provisions*. Annotations within brackets, [], indicate both organizational changes (as a result of a reformat of all of the chapters of the 2003 *Provisions*) and substantive technical changes to the 2003 *Provisions* and its primary reference documents. While the general concepts of the changes are described, the design examples and calculations have not been revised to reflect the changes to the 2003 *Provisions*.

A number of noteworthy changes were made to the analysis requirements of the 2003 *Provisions*. These include elimination of the minimum base shear equation in areas without near-source effects, a change in the treatment of P-delta effects, revision of the redundancy factor, and refinement of the pushover analysis procedure. In addition to changes in analysis requirements, the basic earthquake hazard maps were updated and an approach to defining long-period ordinates for the design response spectrum was developed. Where they affect the design examples in this chapter, significant changes to the 2003 *Provisions* and primary reference documents are noted. However, some minor changes to the 2003 *Provisions* and the reference documents may not be noted.

In addition to the 2000 *NEHRP Recommended Provisions* (herein, the *Provisions*), the following documents are referenced:

AISC Seismic	American Institute of Steel Construction. 1997 [2002]. Seismic Provisions for Structural Steel Buildings.
ATC-40	Applied Technology Council. 1996. Seismic Evaluation and Retrofit of Concrete Buildings.
Bertero	Bertero, R. D., and V.V. Bertero. 2002. "Performance Based Seismic Engineering: The Need for a Reliable Comprehensive Approach," <i>Earthquake Engineering and</i> <i>Structural Dynamics</i> 31, 3 (March).
Chopra 1999	Chopra, A. K., and R. K. Goel. 1999. <i>Capacity-Demand-Diagram Methods for</i> <i>Estimating Seismic Deformation of Inelastic Structures: SDF Systems.</i> PEER-1999/02. Berkeley, California: Pacific Engineering Research Center, College on Engineering, University of California, Berkeley.
Chopra 2001	Chopra, A. K., and R. K. Goel. 2001. A Modal Pushover Procedure to Estimate Seismic Demands for Buildings: Theory and Preliminary Evaluation, PEER-2001/03. Berkeley, California: Pacific Engineering Research Center, College on Engineering, University of California, Berkeley.
FEMA 356	American Society of Civil Engineers. 2000. Prestandard and Commentary for the Seismic Rehabilitation of Buildings.
Krawinkler	Krawinkler, Helmut. 1978. "Shear in Beam-Column Joints in Seismic Design of Frames," <i>Engineering Journal</i> , Third Quarter.

# 3.1 IRREGULAR 12-STORY STEEL FRAME BUILDING, STOCKTON, CALIFORNIA

# 3.1.1 Introduction

This example presents the analysis of a 12-story steel frame building under seismic effects acting alone. Gravity forces due to live and dead load are not computed. For this reason, member stress checks, member design, and detailing are not discussed. For detailed examples of the seismic-resistant design of structural steel buildings, see Chapter 5 of this volume of design examples.

The analysis of the structure, shown in Figures 3.1-1 through 3.1-3, is performed using three methods:

- 1. Equivalent lateral force (ELF) procedure based on the requirements of Provisions Chapter 5,
- 2. Three-dimensional, modal-response-spectrum analysis based on the requirements of *Provisions* Chapter 5, and
- 3. Three-dimensional, modal time-history analysis using a suite of three different recorded ground motions based on the requirements of *Provisions* Chapter 5.

In each case, special attention is given to applying the *Provisions* rules for orthogonal loading and accidental torsion. All analyses were performed using the finite element analysis program SAP2000 (developed by Computers and Structures, Inc., Berkeley, California).

## 3.1.2 Description of Structure

The structure is a 12-story special moment frame of structural steel. The building is laid out on a rectangular grid with a maximum of seven 30-ft-wide bays in the X direction, and seven 25-ft bays in the Y direction. Both the plan and elevation of the structure are irregular with setbacks occurring at Levels 5 and 9. All stories have a height of 12.5 ft except for the first story which is 18 ft high. The structure has a full one-story basement that extends 18.0 ft below grade. Reinforced 1-ft-thick concrete walls form the perimeter of the basement. The total height of the building above grade is 155.5 ft.

Gravity loads are resisted by composite beams and girders that support a normal weight concrete slab on metal deck. The slab has an average thickness of 4.0 in. at all levels except Levels G, 5, and 9. The slabs on Levels 5 and 9 have an average thickness of 6.0 in. for more effective shear transfer through the diaphragm. The slab at Level G is 6.0 in. thick to minimize pedestrian-induced vibrations, and to support heavy floor loads. The low roofs at Levels 5 and 9 are used as outdoor patios, and support heavier live loads than do the upper roofs or typical floors.

At the perimeter of the base of the building, the columns are embedded into pilasters cast into the basement walls, with the walls supported on reinforced concrete tie beams over piles. Interior columns are supported by concrete caps over piles. All tie beams and pile caps are connected by a grid of reinforced concrete grade beams.

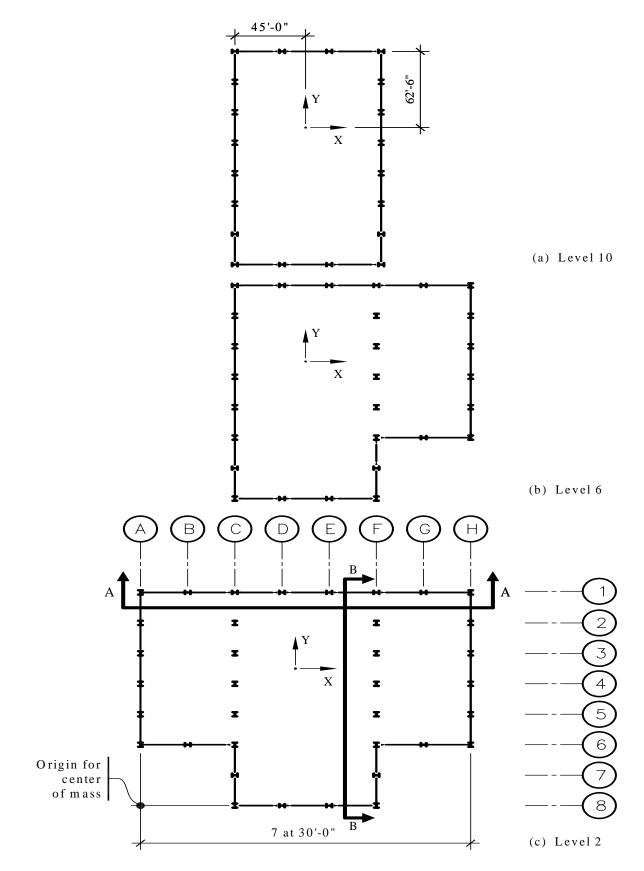


**Figure 3.1-1** Various floor plans of 12-story Stockton building (1.0 ft = 0.3048 m).

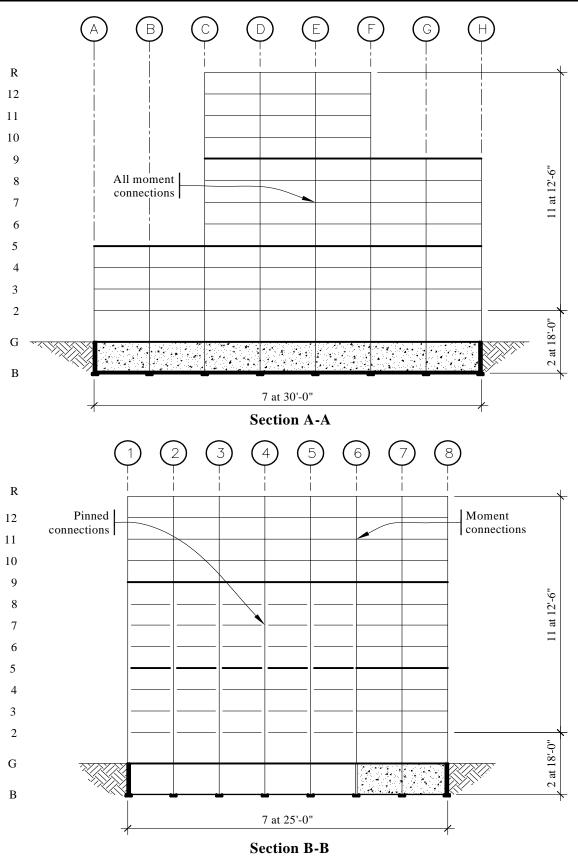


**Figure 3.1-2** Sections through Stockton building (1.0 ft. = 0.3048 m).

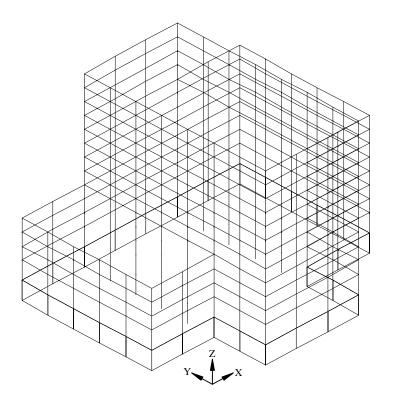


Figure 3.1-3 Three-dimensional wire-frame model of Stockton building.

The lateral-load-resisting system consists of special moment frames at the perimeter of the building and along Grids C and F. For the frames on Grids C and F, the columns extend down to the foundation, but the lateral-load-resisting girders terminate at Level 5 for Grid C and Level 9 for Grid F. Girders below these levels are simply connected. Due to the fact that the moment-resisting girders terminate in Frames C and F, much of the Y-direction seismic shears below Level 9 are transferred through the diaphragms to the frames on Grids A and H. Overturning moments developed in the upper levels of these frames are transferred down to the foundation by outriggering action provided by the columns. Columns in the moment-resisting frame range in size from W24x146 at the roof to W24x229 at Level G. Girders in the moment frames vary from W30x108 at the roof to W30x132 at Level G. Members of the moment resisting frames have a yield strength of 36 ksi, and floor members and interior columns that are sized strictly for gravity forces are 50 ksi.

## 3.1.3 Provisions Analysis Parameters

Stockton, California, is in San Joaquin County approximately 60 miles east of Oakland. According to *Provisions* Maps 7 and 8, the short-period and 1-second mapped spectral acceleration parameters are:

 $S_s = 1.25$  $S_1 = 0.40$ 

[The 2003 *Provisions* have adopted the 2002 USGS probabilistic seismic hazard maps, and the maps have been added to the body of the 2003 *Provisions* as figures in Chapter 3 (instead of being issued in a separate map package).]

Assuming Site Class C, the adjusted maximum considered 5-percent-damped spectral accelerations are obtained from *Provisions* Eq. 4.1.2.4-1 and Eq. 4.1.2.4-2 [3.3-1 and 3.3-2]:

 $S_{MS} = F_a S_s = 1.0(1.25) = 1.25$  $S_{MI} = F_v S_I = 1.4(0.4) = 0.56$ 

where the coefficients  $F_a = 1.0$  and  $F_v = 1.4$  come from *Provisions* Tables 4.1.2.4(a) and 4.1.2.4(b) [3.3-1 and 3.3-2], respectively.

According to *Provisions* Eq. 4.1.2.5-1 and 4.1.2.5-2 [3.3-3 and 3.3-4], the design level spectral acceleration parameters are 2/3 of the above values:

$$S_{DS} = \frac{2}{3}S_{MS} = \frac{2}{3}(1.25) = 0.833$$

$$S_{DI} = \frac{2}{3}S_{MI} = \frac{2}{3}(0.56) = 0.373$$

As the primary occupancy of the building is business offices, the Seismic Use Group (SUG) is I and, according to *Provisions* Table 1.4 [1.3-1], the importance factor (*I*) is 1. According to *Provisions* Tables 4.2.1(a) and 4.2.1(b) [1.4-1 and 1.4-2], the Seismic Design Category (SDC) for this building is D.

The lateral-load-resisting system of the building is a special moment-resisting frame of structural steel. For this type of system, *Provisions* Table 5.2.2 [4.3-1] gives a response modification coefficient (R) of 8 and a deflection amplification coefficient ( $C_d$ ) of 5.5. Note that there is no height limit placed on special moment frames.

According to *Provisions* Table 5.2.5.1 [4.4-1] if the building has certain types of irregularities or if the computed building period exceeds 3.5 seconds where  $T_s = S_{DI}/S_{DS} = 0.45$  seconds, the minimum level of analysis required for this structure is modal-response-spectrum analysis. This requirement is based on apparent plan and vertical irregularities as described in *Provisions* Tables 5.2.3.2 and 5.2.3.3 [4.3-2 and 4.3-3]. The ELF procedure would not be allowed for a final design but, as explained later, certain aspects of an ELF analysis are needed in the modal-response-spectrum analysis. For this reason, and for comparison purposes, a complete ELF analysis is carried out and described herein.

## 3.1.4 Dynamic Properties

Before any analysis can be carried out, it is necessary to determine the dynamic properties of the structure. These properties include mass, periods of vibration and their associated mode shapes, and damping.

## 3.1.4.1 Mass

For two-dimensional analysis, only the translational mass is required. To perform a three-dimensional modal or time-history analysis, it is necessary to compute the mass moment of inertia for floor plates rotating about the vertical axis and to find the location of the center of mass of each level of the structure. This may be done two different ways:

1. The mass moments of inertia may be computed "automatically" by SAP2000 by modeling the floor diaphragms as shell elements and entering the proper mass density of the elements. Line masses, such as window walls and exterior cladding, may be modeled as point masses. The floor diaphragms

may be modeled as rigid in-plane by imposing displacement constraints or as flexible in-plane by allowing the shell elements to deform in their own plane. Modeling the diaphragms as flexible is not necessary in most cases and may have the disadvantage of increasing solution time because of the additional number of degrees of freedom required to model the diaphragm.

2. The floor is assumed to be rigid in-plane but is modeled without explicit diaphragm elements. Displacement constraints are used to represent the in-plane rigidity of the diaphragm. In this case, floor masses are computed by hand (or an auxiliary program) and entered at the "master node" location of each floor diaphragm. The location of the master node should coincide with the center of mass of the floor plate. (Note that this is the approach traditionally used in programs such as ETABS which, by default, assumed rigid in-plane diaphragms and modeled the diaphragms using constraints.)

In the analysis performed herein, both approaches are illustrated. Final analysis used Approach 1, but the frequencies and mode shapes obtained from Approach 1 were verified with a separate model using Approach 2. The computation of the floor masses using Approach 2 is described below.

Due to the various sizes and shapes of the floor plates and to the different dead weights associated with areas within the same floor plate, the computation of mass properties is not easily carried out by hand. For this reason, a special purpose computer program was used. The basic input for the program consists of the shape of the floor plate, its mass density, and definitions of auxiliary masses such as line, rectangular, and concentrated mass.

The uniform area and line masses associated with the various floor plates are given in Tables 3.1-1 and 3.1-2. The line masses are based on a cladding weight of 15.0 psf, story heights of 12.5 or 18.0 ft, and parapets 4.0 ft high bordering each roof region. Figure 3.1-4 shows where each mass type occurs. The total computed floor mass, mass moment of inertia, and locations of center of mass are shown in Table 3.1-3. The reference point for center of mass location is the intersection of Grids A and 8. Note that the dimensional units of mass moment of inertia (in.-kip-sec<sup>2</sup>/radian), when multiplied by angular acceleration (radians/sec<sup>2</sup>), must yield units of torsional moment (in.-kips).

Table 3.1-3 includes a mass computed for Level G of the building. This mass is associated with an extremely stiff story (the basement level) and is not dynamically excited by the earthquake. As shown later, this mass is not included in equivalent lateral force computations.

	Area Mass Designation						
Mass Type —	А	В	С	D	Е		
Slab and Deck (psf)	50	75	50	75	75		
Structure (psf)	20	20	20	20	50		
Ceiling and Mechanical (psf)	15	15	15	15	15		
Partition (psf)	10	10	0	0	10		
Roofing (psf)	0	0	15	15	0		
Special (psf)	0	0	0	60	25		
TOTAL (psf)	95	120	100	185	175		

 Table 3.1-1
 Area Masses on Floor Diaphragms

See Figure 3.1-4 for mass location.

 $1.0 \text{ psf} = 47.9 \text{ N/m}^2$ .

	<b>5.1-2</b> Line M	asses on Floc	or Diaphragin	8		
	Line Mass Designation					
Mass Type	1	2	3	4	5	
From Story Above (plf) From Story Below (plf)	60.0 <u>93.8</u>	93.8 93.8	93.8 <u>0.0</u>	93.8 <u>135.0</u>	135.0 <u>1350.0</u>	
TOTAL (plf)	153.8	187.6	93.8	228.8	1485.0	

Table 3.1-2 Line Masses on Floor Diaphragms

See Figure 3.1-4 for mass location.

1.0 plf = 14.6 N/m.

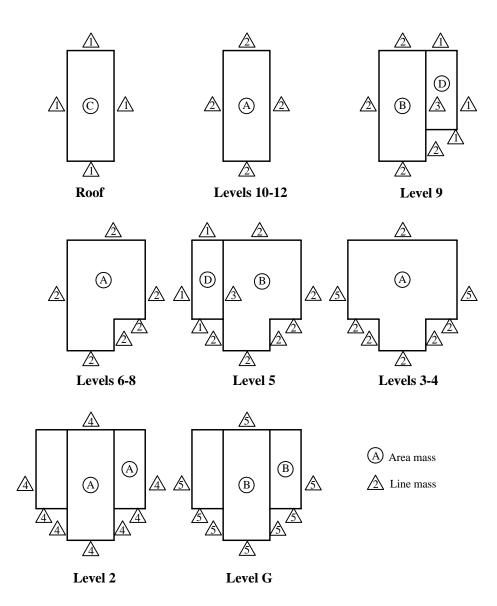


Figure 3.1-4 Key diagram for computation of floor mass.

Level	Weight (kips)	Mass (kip-sec <sup>2/</sup> in.)	Mass Moment of Inertia (inkip- sec <sup>2/</sup> /radian)	X Distance to C.M. (in.)	Y Distance to C.M. (in.)
R	1656.5	4.287	$2.072 \times 10^{6}$	1260	1050
12	1595.8	4.130	$2.017 \times 10^{6}$	1260	1050
11	1595.8	4.130	$2.017 \times 10^{6}$	1260	1050
10	1595.8	4.130	$2.017 \times 10^{6}$	1260	1050
9	3403.0	8.807	5.309x10 <sup>6</sup>	1637	1175
8	2330.8	6.032	$3.703 \times 10^{6}$	1551	1145
7	2330.8	6.032	$3.703 \times 10^{6}$	1551	1145
6	2330.8	6.032	$3.703 \times 10^{6}$	1551	1145
5	4323.8	11.190	$9.091 \times 10^{6}$	1159	1212
4	3066.1	7.935	6.356x10 <sup>6</sup>	1260	1194
3	3066.1	7.935	6.356x10 <sup>6</sup>	1260	1194
2	3097.0	8.015	$6.437 \times 10^{6}$	1260	1193
G	6526.3	16.890	$1.503 \times 10^{7}$	1260	1187
Σ	36918.6				

 Table 3.1-3
 Floor Mass, Mass Moment of Inertia, and Center of Mass Locations

1.0 in. = 25.4 mm, 1.0 kip = 4.45 kN.

### 3.1.4.2 Period of Vibration

#### 3.1.4.2.1 Approximate Period of Vibration

The formula in *Provisions* Eq. 5.4.2.1-1 [5.2-6] is used to estimate the building period:

 $T_a = C_r h_n^x$ 

where  $C_r = 0.028$  and x = 0.8 for a steel moment frame from *Provisions* Table 5.4.2.1 [5.2-2]. Using  $h_n =$  the total building height (above grade) = 155.5 ft,  $T_a = 0.028(155.5)^{0.8} = 1.59$  sec.

When the period is computed from a properly substantiated analysis, the *Provisions* requires that the computed period not exceed  $C_u T_a$  where  $C_u = 1.4$  (from *Provisions* Table 5.4.2 [5.2-1] using  $S_{DI} = 0.373$ g). For the structure under consideration,  $C_u T_a = 1.4(1.59) = 2.23$  seconds. When a modal-response spectrum is used, *Provisions* Sec. 5.5.7 [5.3.7] requires that the displacements, drift, and member design forces be scaled to a value consistent with 85 percent of the equivalent lateral force base shear computed using the period  $C_u T_a = 2.23$  sec. *Provisions* Sec. 5.6.3 [5.4.3] requires that time-history analysis results be scaled up to an ELF shear consistent with  $T = C_u T_a$  (without the 0.85 factor).<sup>1</sup>

Note that when the accurately computed period (such as from a Rayleigh analysis) is less than the approximate value shown above, the computed period should be used. In no case, however, must a period less than  $T_a = 1.59$  seconds be used. The use of the Rayleigh method and the eigenvalue method of determining accurate periods of vibration are illustrated in a later part of this example.

<sup>&</sup>lt;sup>1</sup>This requirements seems odd to the writer since the *Commentary* to the *Provisions* states that time-history analysis is superior to response-spectrum analysis. Nevertheless, the time-history analysis performed later will be scaled as required by the *Provisions*.

### 3.1.4.3 Damping

When a modal-response-spectrum analysis is performed, the structure's damping is included in the response spectrum. A damping ratio of 0.05 (5 percent of critical) is appropriate for steel structures. This is consistent with the level of damping assumed in the development of the mapped spectral acceleration values.

When recombining the individual modal responses, the square root of the sum of the squares (SRSS) technique has generally been replaced in practice by the complete quadratic combination (CQC) approach. Indeed, *Provisions* Sec. 5.5.7 [5.3.7] requires that the CQC approach be used when the modes are closely spaced. When using CQC, the analyst must correctly specify a damping factor. This factor must match that used in developing the response spectrum. It should be noted that if zero damping is used in CQC, the results are the same as those for SRSS.

For time-history analysis, SAP2000 allows an explicit damping ratio to be used in each mode. For this structure, a damping of 5 percent of critical was specified in each mode.

## 3.1.5 Equivalent Lateral Force Analysis

Prior to performing modal or time-history analysis, it is often necessary to perform an equivalent lateral force (ELF) analysis of the structure. This analysis typically is used for preliminary design and for assessing the three-dimensional response characteristics of the structure. ELF analysis is also useful for investigating the behavior of drift-controlled structures, particularly when a virtual force analysis is used for determining member displacement participation factors.<sup>2</sup> The virtual force techniques cannot be used for modal-response-spectrum analysis because signs are lost in the CQC combinations.

In anticipation of the "true" computed period of the building being greater than 2.23 seconds, the ELF analysis is based on a period of vibration equal to  $C_u T_a = 2.23$  seconds. For the ELF analysis, it is assumed that the structure is "fixed" at grade level. Hence, the total effective weight of the structure (see Table 3.1-3) is the total weight minus the grade level weight, or 36918.6 - 6526.3 = 30392.3 kips.

### 3.1.5.1 Base Shear and Vertical Distribution of Force

Using Provisions Eq. 5.4.1 [5.2-1], the total seismic shear is:

$$V = C_S W$$

where *W* is the total weight of the structure. From *Provisions* Eq. 5.4.1.1-1 [5.2-2], the maximum (constant acceleration region) spectral acceleration is:

$$C_{S_{max}} = \frac{S_{DS}}{(R/I)} = \frac{0.833}{(8/1)} = 0.104$$

<sup>&</sup>lt;sup>2</sup>For an explanation of the use of the virtual force technique, see "Economy of Steel Framed Structures Through Identification of Structural Behavior" by F. Charney, *Proceedings of the 1993 AISC Steel Construction Conference*, Orlando, Florida, 1993.

Provisions Eq. 5.4.1.1-2 [5.2-3] controls in the constant velocity region:

$$C_{S} = \frac{S_{DI}}{T(R/I)} = \frac{0.373}{2.23(8/1)} = 0.021$$

However, the acceleration must not be less than that given by *Provisions* Eq. 5.4.1.1-3 [replaced by 0.010 in the 2003 *Provisions*]:

$$C_{S_{min}} = 0.044 IS_{DS} = 0.044(1)(0.833) = 0.037$$

[With the change of this base shear equation, the result of Eq. 5.2-3 would control, reducing the design base shear significantly. This change would also result in removal of the horizontal line in Figure 3.1-5 and the corresponding segment of Figure 3.1-6.]

The value from Eq. 5.4.1.1-3 [not applicable in the 2003 *Provisions*] controls for this building. Using W = 30,392 kips, V = 0.037(30,392) = 1,124 kips. The acceleration response spectrum given by the above equations is plotted in Figure 3.1-5.

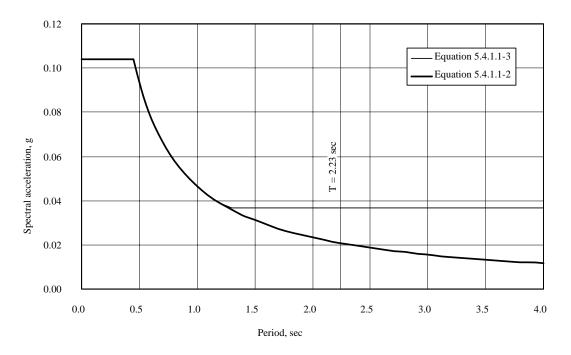


Figure 3.1-5 Computed ELF total acceleration response spectrum.

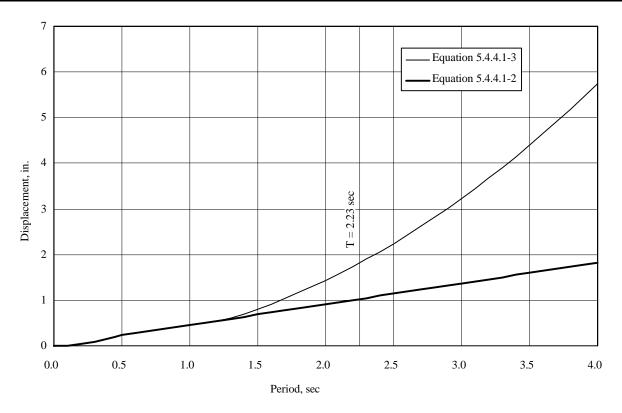


Figure 3.1-6 Computed ELF relative displacement response spectrum (1.0 in. = 25.4 mm).

While it is certainly reasonable to enforce a minimum base shear, *Provisions* Sec. 5.4.6.1 has correctly recognized that displacements predicted using Eq. 5.4.1.1-3 are not reasonable. Therefore, it is very important to note that *Provisions* Eq. 5.4.1.1-3, when it controls, should be used for determining member forces, but should not be used for computing drift. For drift calculations, forces computed according to Eq. 5.4.1.1-2 [5.2-3]should be used. The effect of using Eq. 5.4.1.1-3 for drift is shown in Figure 3.1-6, where it can be seen that the fine line, representing Eq. 5.4.1.1-3, will predict significantly larger displacements than Eq. 5.4.1.1-2 [5.2-3].

[The minimum base shear is 1% of the weight in the 2003 *Provisions* ( $C_s = 0.01$ ). For this combination of  $S_{DI}$  and R, the new minimum controls for periods larger than 4.66 second. The minimum base shear equation for near-source sites (now triggered in the *Provisions* by  $S_I$  greater than or equal to 0.6) has been retained.]

In this example, all ELF analysis is performed using the forces obtained from Eq. 5.4.1.1-3, but for the purposes of computing drift, the story deflections computed using the forces from Eq. 5.4.1.1-3 are multiplied by the ratio (0.021/0.037 = 0.568).

The base shear computed according to *Provisions* Eq. 5.4.1.1-3 is distributed along the height of the building using *Provisions* Eq. 5.4.3.1 and 5.4.3.2 [5.2-10 and 5.2-11]:

$$F_r = C_{vr}V$$

and

$$C_{vx} = \frac{w_x h^k}{\sum\limits_{i=1}^n w_i h_i^k}$$

where k = 0.75 + 0.5T = 0.75 + 0.5(2.23) = 1.86. The story forces, story shears, and story overturning moments are summarized in Table 3.1-4.

Level	<i>W</i> <sub>x</sub>	$h_x$	$w_x h_x^{\ k}$	C	$F_{x}$	$V_x$	$M_{x}$
Х	(kips)	(ft)	$w_x n_x$	$C_{vx}$	(kips)	(kips)	(ft-kips)
R	1656.5	155.5	20266027	0.1662	186.9	186.9	2336
12	1595.8	143.0	16698604	0.1370	154.0	340.9	6597
11	1595.8	130.5	14079657	0.1155	129.9	470.8	12482
10	1595.8	118.0	11669128	0.0957	107.6	578.4	19712
9	3403.0	105.5	20194253	0.1656	186.3	764.7	29271
8	2330.8	93.0	10932657	0.0897	100.8	865.5	40090
7	2330.8	80.5	8352458	0.0685	77.0	942.5	51871
6	2330.8	68.0	6097272	0.0500	56.2	998.8	64356
5	4323.8	55.5	7744119	0.0635	71.4	1070.2	77733
4	3066.1	43.0	3411968	0.0280	31.5	1101.7	91505
3	3066.1	30.5	1798066	0.0147	16.6	1118.2	103372
2	3097.0	18.0	679242	0.0056	6.3	1124.5	120694
Σ	30392.3	-	121923430	1.00	1124.5		

 Table 3.1-4
 Equivalent Lateral Forces for Building Responding in X and Y Directions

1.0 ft = 0.3048 m, 1.0 kip = 4.45 kN.

### 3.1.5.2 Accidental Torsion and Orthogonal Loading Effects

When using the ELF method as the basis for structural design, two effects must be added to the direct lateral forces shown in Table 3.1-4. The first of these effects accounts for the fact that the earthquake can produce inertial forces that act in any direction. For SDC D, E, and F buildings, *Provisions* Sec. 5.2.5.2.3 [4.4.2.3] requires that the structure be investigated for forces that act in the direction that causes the "critical load effect." Since this direction is not easily defined, the *Provisions* allows the analyst to load the structure with 100 percent of the seismic force in one direction (along the X axis, for example) simultaneous with the application of 30 percent of the force acting in the orthogonal direction (the Y axis).

The other requirement is that the structure be modeled with additional forces to account for uncertainties in the location of center of mass and center of rigidity, uneven yielding of vertical systems, and the possibility of torsional components of ground motion. This requirement, given in *Provisions* Sec. 5.4.4.2 [5.2.4.2], can be satisfied for torsionally regular buildings by applying the equivalent lateral force at an eccentricity, where the eccentricity is equal to 5 percent of the overall dimension of the structure in the direction perpendicular to the line of the application of force.

For structures in SDC C, D, E, or F, these accidental eccentricities (and inherent torsion) must be amplified if the structure is classified as torsionally irregular. According to *Provisions* Table 5.2.3.2, a torsional irregularity exists if:

$$\frac{\delta_{max}}{\delta_{avg}} \ge 1.2$$

where, as shown in Figure 3.1-7,  $\delta_{max}$  is the maximum displacement at the edge of the floor diaphragm, and  $\delta_{avg}$  is the average displacement of the diaphragm. If the ratio of displacements is greater than 1.4, the torsional irregularity is referred to as "extreme." In computing the displacements, the structure must be loaded with the basic equivalent lateral forces applied at a 5 percent eccentricity.

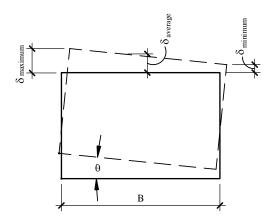


**Figure 3.1-7** Amplification of accidental torsion.

The analysis of the structure for accidental torsion was performed on SAP2000. The same model was used for ELF, modal-response-spectrum, and modal-time-history analysis. The following approach was used for the mathematical model of the structure:

- 1. The floor diaphragm was modeled as infinitely rigid in-plane and infinitely flexible out-of-plane. Shell elements were used to represent the diaphragm mass. Additional point masses were used to represent cladding and other concentrated masses.
- 2. Flexural, shear, axial, and torsional deformations were included in all columns. Flexural, shear, and torsional deformations were included in the beams. Due to the rigid diaphragm assumption, axial deformation in beams was neglected.
- 3. Beam-column joints were modeled using centerline dimensions. This approximately accounts for deformations in the panel zone.
- 4. Section properties for the girders were based on bare steel, ignoring composite action. This is a reasonable assumption in light of the fact that most of the girders are on the perimeter of the building and are under reverse curvature.
- 5. Except for those lateral-load-resisting columns that terminate at Levels 5 and 9, all columns were assumed to be fixed at their base.

The results of the accidental torsion analysis are shown in Tables 3.1-5 and 3.1-6. As may be observed, the largest ratio of maximum to average floor displacements is 1.16 at Level 5 of the building under Y direction loading. Hence, this structure is not torsionally irregular and the story torsions do not need to be amplified.

1 au	e 5.1-5 Compt	itation for fors	ioliai illegulaiti	y with ELF Loat	is Actilig III A	Direction
Level	$\delta_{I}$ (in.)	$\delta_2$ (in.)	$\delta_{avo}(in.)$	$\delta_{max}$ (in.)	$\delta_{max}/\delta_{avg}$	Irregularity
R	6.04	7.43	6.74	7.43	1.10	none
12	5.75	7.10	6.43	7.10	1.11	none
11	5.33	6.61	5.97	6.61	1.11	none
10	4.82	6.01	5.42	6.01	1.11	none
9	4.26	5.34	4.80	5.34	1.11	none
8	3.74	4.67	4.21	4.67	1.11	none
7	3.17	3.96	3.57	3.96	1.11	none
6	2.60	3.23	2.92	3.23	1.11	none
5	2.04	2.52	2.28	2.52	1.11	none
4	1.56	1.91	1.74	1.91	1.10	none
3	1.07	1.30	1.19	1.30	1.10	none
2	0.59	0.71	0.65	0.71	1.09	none

Table 3.1-5 Computation for Torsional Irregularity with ELF Loads A	Acting in X Direction
---	-----------------------

Tabulated displacements are <u>not</u> amplified by  $C_d$ . Analysis includes accidental torsion. 1.0 in. = 25.4 mm.

1 a DI	e 3.1-0 Compt	itation for fors	ional irregularit	y with ELF Load	is Acting in 1	Direction
Level	$\delta_{I}$ (in.)	$\delta_2$ (in.)	$\delta_{avg}(in.)$	$\delta_{max}$ (in)	$\delta_{max}/\delta_{avg}$	Irregularity
R	5.88	5.96	5.92	5.96	1.01	none
12	5.68	5.73	5.71	5.73	1.00	none
11	5.34	5.35	5.35	5.35	1.00	none
10	4.92	4.87	4.90	4.92	1.01	none
9	4.39	4.29	4.34	4.39	1.01	none
8	3.83	3.88	3.86	3.88	1.01	none
7	3.19	3.40	3.30	3.40	1.03	none
6	2.54	2.91	2.73	2.91	1.07	none
5	1.72	2.83	2.05	2.38	1.16	none
4	1.34	1.83	1.59	1.83	1.15	none
3	0.93	1.27	1.10	1.27	1.15	none
2	0.52	0.71	0.62	0.71	1.15	none

Table 3.1-6 Computation for Torsional Irregularity with ELF Loads Acting in Y Direction

Tabulated displacements are <u>not</u> amplified by  $C_d$ . Analysis includes accidental torsion. 1.0 in. = 25.4 mm.

## 3.1.5.3 Drift and P-Delta Effects

Using the basic structural configuration shown in Figure 3.1-1 and the equivalent lateral forces shown in Table 3.1-4, the total story deflections were computed as shown in the previous section. In this section, story drifts are computed and compared to the allowable drifts specified by the *Provisions*.

The results of the analysis are shown in Tables 3.1-7 and 3.1-8. The tabulated drift values are somewhat different from those shown in Table 3.1-5 because the analysis for drift did not include accidental torsion, whereas the analysis for torsional irregularity did. In Tables 3.1-7 and 3.1-8, the values in the first numbered column are the *average* story displacements computed by the SAP2000 program using the lateral forces of Table 3.1-4. Average story drifts are used here instead of maximum story drifts because this structure does not have a "significant torsional response." If the torsional effect were significant, the maximum drifts at the extreme edge of the diaphragm would need to be checked.

The values in column 2 of Tables 3.1-7 and 3.1-8 are the story drifts as reported by SAP2000. These drift values, however, are much less than those that will actually occur because the structure will respond inelastically to the earthquake. The true inelastic story drift, which by assumption is equal to  $C_d = 5.5$ 

times the SAP2000 drift, is shown in Column 3. As discussed above in Sec. 3.1.5.1, the values in column 4 are multiplied by 0.568 to scale the results to the base shear calculated ignoring *Provisions* Eq. 5.4.1.1-3 since that limit does not apply to drift checks. [Recall that the minimum base shear is different in the 2003 *Provisions*.] The allowable story drift of 2.0 percent of the story height per *Provisions* Table 5.2-8 is shown in column 5. (Recall that this building is assigned to Seismic Use Group I.) It is clear from Tables 3.1-7 and 3.1-8 that the allowable drift is not exceeded at any level.

			υī	0	
	1	2	3	4	5
Level	Total Drift	Story Drift from	Inelastic Story	Inelastic Drift	
Level	from SAP2000	SAP2000	Drift	Times 0.568	Allowable Drift
	(in.)	(in.)	(in.)	(in.)	(in.)
R	6.71	0.32	1.73	0.982	3.00
12	6.40	0.45	2.48	1.41	3.00
11	5.95	0.56	3.08	1.75	3.00
10	5.39	5.39	3.38	1.92	3.00
9	4.77	0.59	3.22	1.83	3.00
8	4.19	0.64	3.52	2.00	3.00
7	3.55	0.65	3.58	2.03	3.00
6	2.90	0.63	3.44	1.95	3.00
5	2.27	0.55	3.00	1.70	3.00
4	1.73	0.55	3.00	1.70	3.00
3	1.18	0.54	2.94	1.67	3.00
2	0.65	0.65	3.55	2.02	4.32
<u>a</u> 1 1		<b>E E I I I B (B I</b> )		1 50 1	11.02

**Table 3.1-7** ELF Drift for Building Responding in X Direction

Column 4 adjusts for *Provisions* Eq. 5.4.1.1-2 (for drift) vs 5.4.1.1-3 (for strength). [Such a modification is not necessary when using the 2003 *Provisions* because the minimum base shear is different. Instead, the design forces applied to the model, which produce the drifts in Columns 1 and 2, would be lower by a factor of 0.568.] 1.0 in. = 25.4 mm.

	1	2	3	4	5
Level	Total Drift	Story Drift from	Inelastic Story	Inelastic Drift	
Level	from SAP2000	SAP2000	Drift	Times 0.568	Allowable Drift
	(in.)	(in.)	(in.)	(in.)	(in.)
R	6.01	0.22	1.21	0.687	3.00
12	5.79	0.36	1.98	1.12	3.00
11	5.43	0.45	2.48	1.41	3.00
10	4.98	0.67	3.66	2.08	3.00
9	4.32	0.49	2.70	1.53	3.00
8	3.83	0.57	3.11	1.77	3.00
7	3.26	0.58	3.19	1.81	3.00
6	2.68	0.64	3.49	1.98	3.00
5	2.05	0.46	2.53	1.43	3.00
4	1.59	0.49	2.67	1.52	3.00
3	1.10	0.49	2.70	1.53	3.00
2	0.61	0.61	3.36	1.91	4.32

**TIL 210 FLED '6 6** 

Column 4 adjusts for Provisions Eq. 5.4.1.1-2 (for drift) vs 5.4.1.1-3 (for strength). [Such a modification is not necessary when using the 2003 Provisions because the minimum base shear is different. Instead, the design forces applied to the model, which produce the drifts in Columns 1 and 2, would be lower by a factor of 0.568.] 1.0 in. = 25.4 mm.

#### 3.1.5.3.1 Using ELF Forces and Drift to Compute Accurate Period

Before continuing with the example, it is helpful to use the computed drifts to more accurately estimate the fundamental periods of vibration of the building. This will serve as a check on the "exact" periods computed by eigenvalue extraction in SAP2000. A Rayleigh analysis will be used to estimate the periods. This procedure, which is usually very accurate, is derived as follows:

The exact frequency of vibration  $\omega$  (a scalar), in units of radians/second, is found from the following eigenvalue equation:

 $K\phi = \omega^2 M\phi$ 

where K is the structure stiffness matrix, M is the (diagonal) mass matrix, and  $\phi$ , is a vector containing the components of the mode shape associated with  $\omega$ .

If an approximate mode shape  $\delta$  is used instead of  $\phi$ , where  $\delta$  is the deflected shape under the equivalent lateral forces F, the frequency  $\omega$  can be closely approximated. Making the substitution of  $\delta$  for  $\phi$ , premultiplying both sides of the above equation by  $\delta^T$  (the transpose of the displacement vector), noting that  $F = K\delta$ , and M = (1/g)W, the following is obtained:

$$\delta^T F = \omega^2 \delta^T M \delta = \frac{\omega^2}{g} \delta^T W \delta$$

where W is a vector containing the story weights and g is the acceleration due to gravity (a scalar). After rearranging terms, this gives:

$$\omega = \sqrt{g \frac{\delta^T F}{\delta^T W \delta}}$$

Using the relationship between period and frequency,  $T = \frac{2\pi}{\omega}$ .

Using *F* from Table 3.1-4 and  $\delta$  from Column 1 of Tables 3.1-7 and 3.1-8, the periods of vibration are computed as shown in Tables 3.1-9 and 3.1-10 for the structure loaded in the X and Y directions, respectively. As may be seen from the tables, the X-direction period of 2.87 seconds and the Y-direction period of 2.73 seconds are much greater than the approximate period of  $T_a = 1.59$  seconds and also exceed the upper limit on period of  $C_u T_a = 2.23$  seconds.

Level	Drift, δ (in.)	Force, F (kips)	Weight, W (kips)	$\delta F$ (inkips)	$\delta^2 W/g$
					(inkips-sec <sup>2</sup> )
R	6.71	186.9	1656	1259.71	194.69
12	6.40	154.0	1598	990.22	170.99
11	5.95	129.9	1598	775.50	147.40
10	5.39	107.6	1598	583.19	121.49
9	4.77	186.3	3403	894.24	202.91
8	4.19	100.8	2330	424.37	106.88
7	3.55	77.0	2330	274.89	76.85
6	2.90	56.2	2330	164.10	51.41
5	2.27	71.4	4323	162.79	58.16
4	1.73	31.5	3066	54.81	24.02
3	1.18	16.6	3066	19.75	11.24
2	0.65	6.3	3097	4.10	3.39
				5607.64	1169.42

Table 3.1-9 Rayleigh Analysis for X-Direction Period of Vibration

 $\omega = (5607/1169)^{0.5} = 2.19$  rad/sec.  $T = 2\pi/\omega = 2.87$  sec. 1.0 in. = 25.4 mm, 1.0 kip = 4.45 kN.

Level	Drift, δ (in.)	Force, F (kips)	Weight, W (kips)	$\delta F$	$\delta^2 W/g$
R	6.01	186.9	1656	1123.27	154.80
12	5.79	154.0	1598	891.66	138.64
11	5.43	129.9	1598	705.36	121.94
10	4.98	107.6	1598	535.85	102.56
9	4.32	186.3	3403	804.82	164.36
8	3.83	100.8	2330	386.06	88.45
7	3.26	77.0	2330	251.02	64.08
6	2.68	56.2	2330	150.62	43.31
5	2.05	71.4	4323	146.37	47.02
4	1.59	31.5	3066	50.09	20.06
3	1.10	16.6	3066	18.26	9.60
2	0.61	6.3	3097	3.84	2.98
			_	5067.21	957.81

 $\omega = (5067/9589)^{0.5} = 2.30 \text{ rad/sec.}$   $T = 2\pi/\omega = 2.73 \text{ sec.}$  1.0 in. = 25.4 mm, 1.0 kip = 4.45 kN.

### 3.1.5.3.2 P-Delta Effects

P-delta effects are computed for the X-direction response in Table 3.1-11. The last column of the table shows the story stability ratio computed according to *Provisions* Eq. 5.4.6.2-1 [5.2-16]:

$$\theta = \frac{P_x \Delta}{V_x h_{sx} C_d}$$

[In the 2003 *Provisions*, the equation for the story stability ratio was changed by introducing the importance factor (*I*) to the numerator. As previously formulated, larger axial loads ( $P_x$ ) would be permitted where the design shears ( $V_x$ ) included an importance factor greater than 1.0; that effect was unintended.]

*Provisions* Eq. 5.4.6.2-2 places an upper limit on  $\theta$ :

$$\theta_{max} = \frac{0.5}{\beta C_d}$$

where  $\beta$  is the ratio of shear demand to shear capacity for the story. Conservatively taking  $\beta = 1.0$  and using  $C_d = 5.5$ ,  $\theta_{max} = 0.091$ . [In the 2003 *Provisions*, this upper limit equation has been eliminated. Instead, the *Provisions* require that where  $\theta > 0.10$  a special analysis be performed in accordance with Sec. A5.2.3. This example constitutes a borderline case as the maximum stability ratio (at Level 3, as shown in Table 3.1-11) is 0.103.]

The  $\Delta$  terms in Table 3.1-11 below are taken from Column 3 of Table 3.1-7 because these are consistent with the ELF story shears of Table 3.1-4 and thereby represent the true lateral stiffness of the system. (If 0.568 times the story drifts were used, then 0.568 times the story shears also would need to be used. Hence, the 0.568 factor would cancel out as it would appear in both the numerator and denominator.)

	Table 3.1-11 Computation of F-Dena Effects for X-Direction Response										
Level	$h_{sx}$ (in.)	⊿ (in.)	$P_D$ (kips)	$P_L$ (kips)	$P_T$ (kips)	$P_X$ (kips)	$V_X$ (kips)	$\Theta_X$			
R	150	1.73	1656.5	315.0	1971.5	1971.5	186.9	0.022			
12	150	2.48	1595.8	315.0	1910.8	3882.3	340.9	0.034			
11	150	3.08	1595.8	315.0	1910.8	5793.1	470.8	0.046			
10	150	3.38	1595.8	315.0	1910.8	7703.9	578.4	0.055			
9	150	3.22	3403.0	465.0	3868.0	11571.9	764.7	0.059			
8	150	3.52	2330.8	465.0	2795.8	14367.7	865.8	0.071			
7	150	3.58	2330.8	465.0	2795.8	17163.5	942.5	0.079			
6	150	3.44	2330.8	465.0	2795.8	19959.3	998.8	0.083			
5	150	3.00	4323.8	615.0	4938.8	24898.1	1070.2	0.085			
4	150	3.00	3066.1	615.0	3681.1	28579.2	1101.7	0.094			
3	150	2.94	3066.1	615.0	3681.1	32260.3	1118.2	0.103			
2	216	3.55	3097.0	615.0	3712.0	35972.3	1124.5	0.096			

Table 3.1-11         Computation of P-Delta Effects for X-Direction Resp.
---

1.0 in. = 25.4 mm, 1.0 kip = 4.45 kN.

The gravity force terms include a 20 psf uniform live load over 100 percent of the floor and roof area. The stability ratio just exceeds 0.091 at Levels 2 through 4. However,  $\beta$  was very conservatively taken as 1.0. Because a more refined analysis would most likely show a lower value of  $\beta$ , we will proceed assuming that P-delta effects are not a problem for this structure. Calculations for the Y direction produced similar results, but are not included herein.

### 3.1.5.4 Computation of Member Forces

Before member forces may be computed, the proper load cases and combinations of load must be identified such that all critical seismic effects are captured in the analysis.

### 3.1.5.4.1 Orthogonal Loading Effects and Accidental Torsion

For a nonsymmetric structure such as the one being analyzed, four directions of seismic force (+X, -X, +Y, -Y) must be considered and, for each direction of force, there are two possible directions for which the accidental eccentricity can apply (causing positive or negative torsion). This requires a total of eight possible combinations of direct force plus accidental torsion. When the 30 percent orthogonal loading rule is applied, the number of load combinations increases to 16 because, for each direct application of load, a positive or negative orthogonal loading can exist. Orthogonal loads are applied without accidental eccentricity.

Figure 3.1-8 illustrates the basic possibilities of application of load. Although this figure shows 16 different load combinations, it may be observed that eight of these combinations -7, 8, 5, 6, 15, 16, 13, and 14 – are negatives of one of Combinations 1, 2, 3, 4, 9, 10, 11, and 12, respectively.

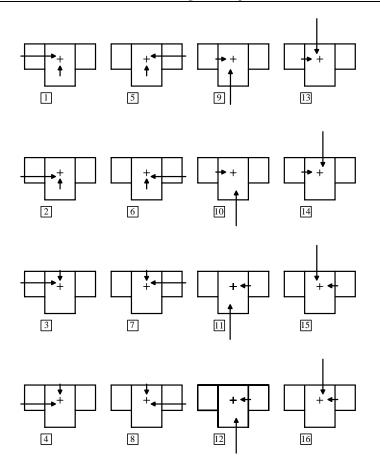


Figure 3.1-8 Basic load cases used in ELF analysis.

#### 3.1.5.4.2 Load Combinations

The basic load combinations for this structure come from ASCE 7 with the earthquake loadings modified according to *Provisions* Sec. 5.2.7 [4.2.2.1].

The basic ASCE 7 load conditions that include earthquake are:

1.4D + 1.2L + E + 0.2S

and

0.9D + E

From Provisions Eq. 5.2.7-1 and Eq. 5.2.7-2 [4.2-1 and 4.2-2]:

$$E = \rho Q_E + 0.2 S_{DS} Q_D$$

and

 $E = \rho Q_E - 0.2 S_{DS} Q_D$ 

where  $\rho$  is a redundancy factor (explained later),  $Q_E$  is the earthquake load effect,  $Q_D$  is the dead load effect, and  $S_{DS}$  is the short period spectral design acceleration.

Using  $S_{DS} = 0.833$  and assuming the snow load is negligible in Stockton, California, the basic load combinations become:

$$1.37D + 0.5L + \rho E$$

and

 $0.73D + \rho E$ 

[The redundancy requirements have been changed substantially in the 2003 *Provisions*. Instead of performing the calculations that follow, 2003 *Provisions* Sec. 4.3.3.2 would require that an analysis determine the most severe effect on story strength and torsional response of loss of moment resistance at the beam-to-column connections at both ends of any single beam. Where the calculated effects fall within permitted limits, or the system is configured so as to satisfy prescriptive requirements in the exception, the redundancy factor is 1.0. Otherwise,  $\rho = 1.3$ . Although consideration of all possible single beam failures would require substantial effort, in most cases an experienced analyst would be able to identify a few critical elements that would be likely to produce the maximum effects and then explicitly consider only those conditions.]

Based on *Provisions* Eq. 5.2.4.2, the redundancy factor ( $\rho$ ) is the largest value of  $\rho_x$  computed for each story:

$$\rho_x = 2 - \frac{20}{r_{max_x}\sqrt{A_x}}$$

In this equation,  $r_{max_x}$  is a ratio of element shear to story shear, and  $A_x$  is the area of the floor diaphragm immediately above the story under consideration;  $\rho_x$  need not be taken greater than 1.5, but it may not be less than 1.0. [In the 2003 *Provisions*,  $\rho$  is either 1.0 or 1.3.]

For this structure, the check is illustrated for the lower level only where the area of the diaphragm is  $30,750 \text{ ft}^2$ . Figure 3.1-1 shows that the structure has 18 columns resisting load in the X direction and 18 columns resisting load in the Y direction. If it is assumed that each of these columns equally resists base shear and the check, as specified by the *Provisions*, is made for any two adjacent columns:

$$r_{max_x} = 2/18 = 0.111$$
 and  $\rho_x = 2 - \frac{20}{0.11\sqrt{30750}} = 0.963$ .

Checks for upper levels will produce an even lower value of  $\rho_x$ ; therefore,  $\rho_x$  may be taken a 1.0 for this structure. Hence, the final load conditions to be used for design are:

$$1.37D + 0.5L + E$$

and

0.73D + E

The first load condition will produce the maximum negative moments (tension on the top) at the face of the supports in the girders and maximum compressive forces in columns. The second load condition will produce the maximum positive moments (or minimum negative moment) at the face of the supports of the girders and maximum tension (or minimum compression) in the columns. In addition to the above load condition, the gravity-only load combinations as specified in ASCE 7 also must be checked. Due to the relatively short spans in the moment frames, however, it is not expected that the non-seismic load combinations will control.

### 3.1.5.4.3 Setting up the Load Combinations in SAP2000

The load combinations required for the analysis are shown in Table 3.1-12.

It should be noted that 32 different load combinations are required only if one wants to maintain the signs in the member force output, thereby providing complete design envelopes for all members. As mentioned later, these signs are lost in response-spectrum analysis and, as a result, it is possible to capture the effects of dead load plus live load plus-or-minus earthquake load in a single SAP2000 run containing only four load combinations.

D		Late	ral*	Gra	vity
Run	Combination	Α	В	1 (Dead)	2 (Live)
One	1	[1]		1.37	0.5
	2	[1]		0.73	0.0
	2 3	[-1]		1.37	0.5
	4	[-1]		0.73	0.0
	5		[2]	1.37	0.5
	6		[2]	0.73	0.0
	7		[-2]	1.37	0.5
	8		[-2]	0.73	0.0
Two	1	[3]		1.37	0.5
	2	[3]		0.73	0.0
	3		[4]	1.37	0.5
	4		[4]	0.73	0.0
	5	[-3]		1.37	0.5
	6	[-3]		0.73	0.0
	7		[-4]	1.37	0.5
	8		[-4]	0.73	0.0
Three	1	[9]		1.37	0.5
	2	[9]		0.73	0.0
	3 4		[10]	1.37	0.5
	4		[10]	0.73	0.0
	5	[-9]		1.37	0.5
	6	[-9]		0.73	0.0
	7		[-10]	1.37	0.5
	8		[-10]	0.73	0.0
Four	1	[11]		1.37	0.5
	2	[11]		0.73	0.0
	3		[12]	1.37	0.5
	4		[12]	0.73	0.0
	5	[-11]		1.37	0.5
	6	[-11]		0.73	0.0
	7		[-12]	1.37	0.5
	8		[-12]	0.73	0.0

 Table 3.1-12
 Seismic and Gravity Load Combinations as Run on SAP 2000

\* Numbers in brackets [#] represent load conditions shown in Figure 3.1-8. A negative sign [-#] indicates that all lateral load effects act in the direction opposite that shown in the figure.

### 3.1.5.4.4 Member Forces

For this portion of the analysis, the earthquake shears in the girders along Gridline 1 are computed. This analysis considers only 100 percent of the X-direction forces applied in combination with 30 percent of the (positive or negative) Y-direction forces. The X-direction forces are applied with a 5 percent accidental eccentricity to produces a clockwise rotation of the floor plates. The Y-direction forces are applied without eccentricity.

The results of the member force analysis are shown in Figure 3.1-9. In a later part of this example, the girder shears are compared to those obtained from modal-response-spectrum and modal-time-history analyses.

			8.31	9.54	9.07		
R-12			16.1	17.6	17.1		
12-11			25.8	26.3	26.9		
11-10			31.2	31.0	32.9		
10-9			32.7	32.7	30.4	28.9	12.5
9-8			34.5	34.1	32.3	36.0	22.4
8-7			39.1	38.1	36.5	39.2	24.2
7-6			40.4	38.4	37.2	39.6	24.8
6-5	13.1	30.0	31.7	34.3	33.1	34.9	22.2
5-4	22.1	33.6	29.1	31.0	30.1	31.6	20.4
4-3	22.0	33.0	30.5	31.7	31.1	32.2	21.4
3-2	20.9	33.0	30.9	31.8	31.1	32.4	20.4
2-G							

**Figure 3.1-9** Seismic shears in girders (kips) as computed using ELF analysis. Analysis includes orthogonal loading and accidental torsion. (1.0 kip = 4.45 kn)

### 3.1.6 Modal-Response-Spectrum Analysis

The first step in the modal-response-spectrum analysis is the computation of the structural mode shapes and associated periods of vibration. Using the Table 3.1-4 structural masses and the same mathematical model as used for the ELF and the Rayleigh analyses, the mode shapes and frequencies are automatically computed by SAP2000.

The computed periods of vibration for the first 10 modes are summarized in Table 3.1-13, which also shows values called the modal direction factor for each mode. Note that the longest period, 2.867 seconds, is significantly greater than  $C_u T_a = 2.23$  seconds. Therefore, displacements, drift, and member forces as computed from the true modal properties may have to be scaled up to a value consistent with 85 percent of the ELF base shear using  $T = C_u T_a$ . The smallest period shown in Table 3.1-13 is 0.427 seconds.

The modal direction factors shown in Table 3.1-13 are indices that quantify the direction of the mode. A direction factor of 100.0 in any particular direction would indicate that this mode responds entirely along one of the orthogonal (X, Y or  $\theta_z$  axes) of the structure.<sup>3</sup> As Table 3.1-13 shows, the first mode is predominantly X translation, the second mode is primarily Y translation, and the third mode is largely

<sup>&</sup>lt;sup>3</sup>It should be emphasized that, in general, the principal direction of structural response will not coincide with one of the axes used to describe the structure in three-dimensional space.

torsional. Modes 4 and 5 also are nearly unidirectional, but Modes 6 through 10 have significant lateral-torsional coupling. Plots showing the first eight mode shapes are given in Figure 3.1-10.

It is interesting to note that the X-direction Rayleigh period (2.87 seconds) is virtually identical to the first mode predominately X-direction period (2.867 seconds) computed from the eigenvalue analysis. Similarly, the Y-direction Rayleigh period (2.73 seconds) is very close to second mode predominantly Y-direction period (2.744 seconds) from the eigenvalue analysis. The closeness of the Rayleigh and eigenvalue periods of this building arises from the fact that the first and seconds modes of vibration act primarily along the orthogonal axes. Had the first and second modes not acted along the orthogonal axes, the Rayleigh periods (based on loads and displacements in the X and Y directions) would have been somewhat less accurate.

In Table 3.1-14, the effective mass in Modes 1 through 10 is given as a percentage of total mass. The values shown in parentheses in Table 3.1-14 are the accumulated effective masses and should total 100 percent of the total mass when all modes are considered. By Mode 10, the accumulated effective mass value is approximately 80 percent of the total mass for the translational modes and 72 percent of the total mass for the torsional mode. *Provisions* Sec. 5.5.2 [5.3.2] requires that a sufficient number of modes be represented to capture at least 90 percent of the total mass of the structure. On first glance, it would seem that the use of 10 modes as shown in Table 3.1-14 violates this rule. However, approximately 18 percent of the total mass for this structure is located at grade level and, as this level is extremely stiff, this mass does not show up as an effective mass until Modes 37, 38, and 39 are considered. In the case of the building modeled as a 13-story building with a very stiff first story, the accumulated 80 percent of effective translational mass in Mode 10 actually represents almost 100 percent of the dynamically excitable mass. In this sense, the *Provisions* requirements are clearly met when using only the first 10 modes in the response spectrum or time-history analysis. For good measure, 14 modes were used in the actual analysis.

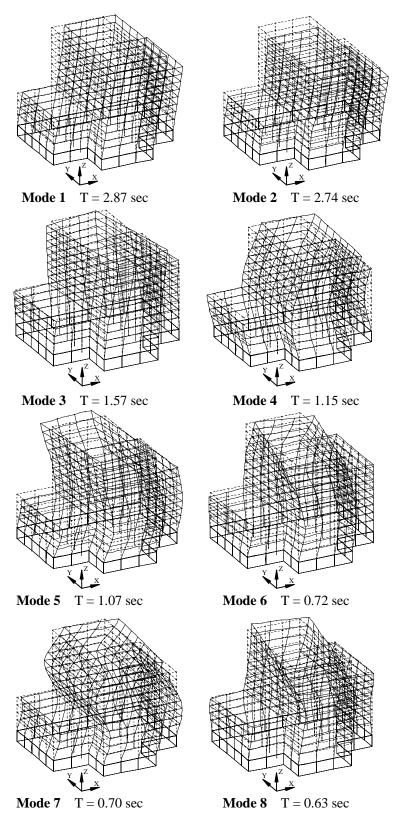


Figure 3.1-10 Mode shapes as computed using SAP2000.

N 1	Period		or	
Mode	(seconds)	X Translation	Y Translation	Z Torsion
1	2.867	99.2	0.7	0.1
2	2.745	0.8	99.0	0.2
3	1.565	1.7	9.6	88.7
4	1.149	98.2	0.8	1.0
5	1.074	0.4	92.1	7.5
6	0.724	7.9	44.4	47.7
7	0.697	91.7	5.23	3.12
8	0.631	0.3	50.0	49.7
9	0.434	30.0	5.7	64.3
10	0.427	70.3	2.0	27.7

 Table 3.1-13
 Computed Periods and Direction Factors

**Table 3.1-14** Computed Periods and Effective Mass Factors

Mada	Period		or	
Mode	(seconds)	X Translation	Y Translation	Z Torsion
1	2.867	64.04 (64.0)	0.46 (0.5)	0.04 (0.0)
2	2.744	0.51 (64.6)	64.25 (64.7)	0.02 (0.1)
3	1.565	0.34 (64.9)	0.93 (65.6)	51.06 (51.1)
4	1.149	10.78 (75.7)	0.07 (65.7)	0.46 (51.6)
5	1.074	0.04 (75.7)	10.64 (76.3)	5.30 (56.9)
6	0.724	0.23 (75.9)	1.08 (77.4)	2.96 (59.8)
7	0.697	2.94 (78.9)	0.15 (77.6)	0.03 (59.9)
8	0.631	0.01 (78.9)	1.43 (79.0)	8.93 (68.8)
9	0.434	0.38 (79.3)	0.00 (79.0)	3.32 (71.1)
10	0.427	1.37 (80.6)	0.01 (79.0)	1.15 (72.3)

#### 3.1.6.1 Response Spectrum Coordinates and Computation of Modal Forces

The coordinates of the response spectrum are based on *Provisions* Eq. 4.1.2.6-1 and 4.1.2.6-2 [3.3-5 and 3.3-6]. [In the 2003 *Provisions*, the design response spectrum has reduced ordinates at very long periods as indicated in Sec. 3.3.4. The new portion of the spectrum reflects a constant ground displacement at periods greater than  $T_L$ , the value of which is based on the magnitude of the source earthquake that dominates the probabilistic ground motion at the site.]

For periods less than  $T_0$ :

$$S_a = 0.6 \frac{S_{DS}}{T_0} T + 0.4 S_{DS}$$

and for periods greater than  $T_s$ :

$$S_a = \frac{S_{D1}}{T}$$

where  $T_0 = 0.2S_{DS} / S_{DI}$  and  $T_S = S_{DI} / S_{DS}$ .

Using  $S_{DS} = 0.833$  and  $S_{DI} = 0.373$ ,  $T_0 = 0.089$  seconds and  $T_S = 0.448$  seconds. The computed responsespectrum coordinates for several period values are shown in Table 3.1-15 and the response spectrum, shown with and without the I/R = 1/8 modification, is plotted in Figure 3.1-11. The spectrum does not include the high period limit on  $C_s$  ( $C_{s, min} = 0.044IS_{DS}$ ), which controlled the ELF base shear for this structure and which ultimately will control the scaling of the results from the response-spectrum analysis. (Recall that if the computed base shear falls below 85 percent of the ELF base shear, the computed response must be scaled up such that the computed base shear equals 85 percent of the ELF base shear.)

Table 3.1-15	Response Spectr	um Coordinates
$T_m$ (seconds)	$C_{sm}$	$C_{sm}(I/R)$
0.000	0.333	0.0416
$0.089(T_o)$	0.833	0.104
$0.448(T_s)$	0.833	0.104
1.000	0.373	0.0446
1.500	0.249	0.0311
2.000	0.186	0.0235
2.500	0.149	0.0186
3.000	0.124	0.0155
I = 1, R = 8.7.		

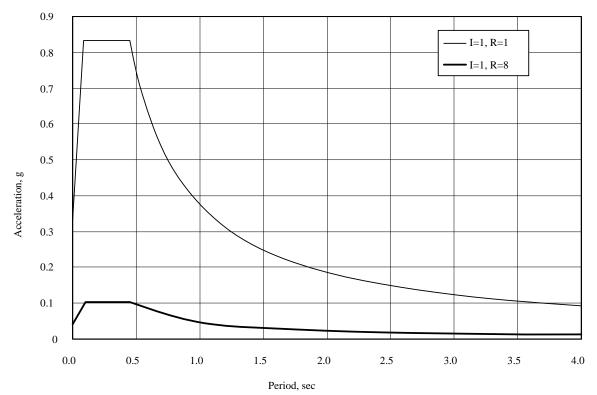


Figure 3.1-11 Total acceleration response spectrum used in analysis.

Using the response spectrum coordinates of Table 3.1-15, the response-spectrum analysis was carried out using SAP2000. As mentioned above, the first 14 modes of response were computed and superimposed using complete quadratic combination (CQC). A modal damping ratio of 5 percent of critical was used in the CQC calculations.

Two analyses were carried out. The first directed the seismic motion along the X axis of the structure, and the second directed the motion along the Y axis. Combinations of these two loadings plus accidental torsion are discussed later. The response spectrum used in the analysis did include I/R.

### 3.1.6.1.1 Dynamic Base Shear

After specifying member "groups," SAP2000 automatically computes and prints the CQC story shears. Groups were defined such that total shears would be printed for each story of the structure. The base shears were printed as follows:

X-direction base shear = 437.7 kips Y-direction base shear = 454.6 kips

These values are much lower that the ELF base shear of 1124 kips. Recall that the ELF base shear was controlled by *Provisions* Eq. 5.4.1.1-3. The modal-response-spectrum shears are less than the ELF shears because the fundamental period of the structure used in the response-spectrum analysis is 2.87 seconds (vs 2.23) and because the response spectrum of Figure 3.1-11 does not include the minimum base shear limit imposed by *Provisions* Eq. 5.4.1.1-3. [Recall that the equation for minimum base shear coefficient does not appear in the 2003 *Provisions*.]

According to *Provisions* Sec. 5.5.7 [5.3.7], the base shears from the modal-response-spectrum analysis must not be less than 85 percent of that computed from the ELF analysis. If the response spectrum shears are lower than the ELF shear, then the computed shears and displacements must be scaled up such that the response spectrum base shear is 85 percent of that computed from the ELF analysis.

Hence, the required scale factors are:

X-direction scale factor = 0.85(1124)/437.7 = 2.18Y-direction scale factor = 0.85(1124)/454.6 = 2.10

The computed and scaled story shears are as shown in Table 3.1-16. Since the base shears for the ELF and the modal analysis are different (due to the 0.85 factor), direct comparisons cannot be made between Table 3.1-11 and Table 3.1-4. However, it is clear that the vertical distribution of forces is somewhat similar when computed by ELF and modal-response spectrum.

	X Direction	(SF = 2.18)	Y Direction (SF = $2.10$ )		
Story	Unscaled Shear (kips)	Scaled Shear (kips)	Unscaled Shear (kips)	Scaled Shear (kips)	
R-12	82.5	180	79.2	167	
12-11	131.0	286	127.6	268	
11-10	163.7	358	163.5	344	
10-9	191.1	417	195.0	410	
9-8	239.6	523	247.6	521	
8-7	268.4	586	277.2	583	
7-6	292.5	638	302.1	635	
6-5	315.2	688	326.0	686	
5-4	358.6	783	371.8	782	
4-3	383.9	838	400.5	843	
3-2	409.4	894	426.2	897	
2-G	437.7	956	454.6	956	

 Table 3.1-16
 Story Shears from Modal-Response-Spectrum Analysis

1.0 kip = 4.45 kN.

### 3.1.6.2 Drift and P-Delta Effects

According to *Provisions* Sec. 5.5.7 [5.3.7], the computed displacements and drift (as based on the response spectrum of Figure 3.1-11) must also be scaled by the base shear factors (SF) of 2.18 and 2.10 for the structure loaded in the X and Y directions, respectively.

In Tables 3.1-17 and 3.1-18, the story displacement from the response-spectrum analysis, the scaled story displacement, the scaled story drift, the amplified story drift (as multiplied by  $C_d = 5.5$ ), and the allowable story drift are listed. As may be observed from the tables, the allowable drift is not exceeded at any level.

P-delta effects are computed for the X-direction response as shown in Table 3.1-19. Note that the scaled story shears from Table 3.1-16 are used in association with the scaled story drifts (including  $C_d$ ) from Table 3.1-17. The story stability factors are above the limit ( $\theta_{max} = 0.091$ ) only at the bottom two levels of the structure and are only marginally above the limit. As the  $\beta$  factor was conservatively set at 1.0 in computing the limit, it is likely that a refined analysis for  $\beta$  would indicate that P-delta effects are not of particular concern for this structure.

	1	2	3	4	5
Level	Total Drift from R.S. Analysis (in.)	Scaled Total Drift [Col-1 × 2.18] (in.)	Scaled Drift (in.)	Scaled Story Drift $\times C_d$ (in.)	Allowable Story Drift (in.)
R	1.96	4.28	0.18	0.99	3.00
12	1.88	4.10	0.26	1.43	3.00
11	1.76	3.84	0.30	1.65	3.00
10	1.62	3.54	0.33	1.82	3.00
9	1.47	3.21	0.34	1.87	3.00
8	1.32	2.87	0.36	1.98	3.00
7	1.15	2.51	0.40	2.20	3.00
6	0.968	2.11	0.39	2.14	3.00
5	0.789	1.72	0.38	2.09	3.00
4	0.615	1.34	0.38	2.09	3.00
3	0.439	0.958	0.42	2.31	3.00
2	0.245	0.534	0.53	2.91	4.32

**TIL 31 15 D** a 1. · VD· . . . .

1.0 in. = 25.4 mm.

 Table 3.1-18
 Spectrum Response Drift for Building Responding in Y Direction

	1	2	3	4	5
Level	Total Drift from R.S. Analysis (in.)	Scaled Total Drift [Col-1 × 2.18] (in.)	Scaled Drift (in.)	Scaled Story Drift $\times C_d$ (in.)	Allowable Story Drift (in.)
R	1.84	3.87	0.12	0.66	3.00
12	1.79	3.75	0.20	1.10	3.00
11	1.69	3.55	0.24	1.32	3.00
10	1.58	3.31	0.37	2.04	3.00
9	1.40	2.94	0.29	1.60	3.00
8	1.26	2.65	0.33	1.82	3.00
7	1.10	2.32	0.35	1.93	3.00
6	0.938	1.97	0.38	2.09	3.00
5	0.757	1.59	0.32	1.76	3.00
4	0.605	1.27	0.36	2.00	3.00
3	0.432	0.908	0.39	2.14	3.00
2	0.247	0.518	0.52	2.86	4.32

1.0 in. = 25.4 mm.

	Table 5.1-19 Computation of P-Dena Effects for X-Direction Response										
Level	$h_{sx}$ (in.)	⊿ (in.)	$P_D$ (kips)	$P_L$ (kips)	$P_T$ (kips)	$P_X$ (kips)	$V_X$ (kips)	$\theta_{X}$			
R	150	0.99	1656.5	315.0	1971.5	1971.5	180	0.013			
12	150	1.43	1595.8	315.0	1910.8	3882.3	286	0.024			
11	150	1.65	1595.8	315.0	1910.8	5793.1	358	0.032			
10	150	1.82	1595.8	315.0	1910.8	7703.9	417	0.041			
9	150	1.87	3403.0	465.0	3868.0	11571.9	523	0.050			
8	150	1.98	2330.8	465.0	2795.8	14367.7	586	0.059			
7	150	2.20	2330.8	465.0	2795.8	17163.5	638	0.072			
6	150	2.14	2330.8	465.0	2795.8	19959.3	688	0.075			
5	150	2.09	4323.8	615.0	4938.8	24898.1	783	0.081			
4	150	2.09	3066.1	615.0	3681.1	28579.2	838	0.086			
3	150	2.31	3066.1	615.0	3681.1	32260.3	894	0.101			
2	216	2.91	3097.0	615.0	3712.0	35972.3	956	0.092			

Table 3.1-19 Computation of P-Delta Effects for X-Direction Response

1.0 in. = 25.4 mm, 1.0 kip = 4.45 kN.

### 3.1.6.3 Torsion, Orthogonal Loading, and Load Combinations

To determine member design forces, it is necessary to add the effects of accidental torsion and orthogonal loading into the analysis. When including accidental torsion in modal-response-spectrum analysis, there are generally two approaches that can be taken:

- 1. Displace the center of mass of the floor plate plus or minus 5 percent of the plate dimension perpendicular to the direction of the applied response spectrum. As there are four possible mass locations, this will require four separate modal analyses for torsion with each analysis using a different set of mode shapes and frequencies.
- 2. Compute the effects of accidental torsion by creating a load condition with the story torques applied as static forces. Member forces created by the accidental torsion are then added directly to the results of the response-spectrum analysis. Since the sign of member forces in the response-spectrum analysis is lost as a result of SRSS or CQC combinations, the absolute value of the member forces resulting from accidental torsion should be used. As with the displaced mass method, there are four possible ways to apply the accidental torsion: plus and minus torsion for primary loads in the X or Y directions. Because of the required scaling, the static torsional forces should be based on 85 percent of the ELF forces.

Each of the above approaches has advantages and disadvantages. The primary disadvantage of the first approach is a practical one: most computer programs do not allow for the extraction of member force maxima from more than one run when the different runs incorporate a different set of mode shapes and frequencies. For structures that are torsionally regular and will not require amplification of torsion, the second approach is preferred. For torsionally flexible structures, the first approach may be preferred because the dynamic analysis will automatically amplify the torsional effects. In the analysis that follows, the second approach has been used because the structure has essentially rigid diaphragms and high torsional rigidity and amplification of accidental torsion is not required.

There are three possible methods for applying the orthogonal loading rule:

- 1. Run the response-spectrum analysis with 100 percent of the scaled X spectrum acting in one direction, concurrent with the application of 30 percent of the scaled Y spectrum acting in the orthogonal direction. Use CQC for combining modal maxima. Perform a similar analysis for the larger seismic forces acting in the Y direction.
- 2. Run two separate response-spectrum analyses, one in the X direction and one in the Y direction, with CQC being used for modal combinations in each analysis. Using a direct sum, combine 100 percent of the scaled X-direction results with 30 percent of the scaled Y-direction results. Perform a similar analysis for the larger loads acting in the Y direction.
- 3. Run two separate response-spectrum analyses, one in the X direction and one in the Y-direction, with CQC being used for modal combinations in each analysis. Using SRSS, combine 100 percent of the scaled X-direction results with 100 percent of the scaled Y-direction results.<sup>4</sup>

All seismic effects can be considered in only two load cases by using Approach 2 for accidental torsion and Approach 2 for orthogonal loading. These are shown in Figure 3.1-12. When the load combinations required by *Provisions* Sec. 5.2.7 [4.2.2.1] are included, the total number of load combinations will double to four.

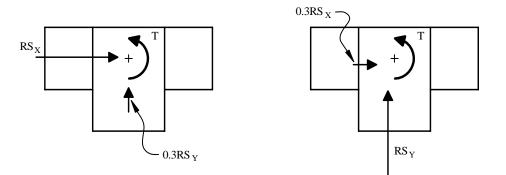


Figure 3.1-12 Load combinations from response-spectrum analysis.

### **3.1.6.4 Member Design Forces**

Earthquake shear forces in the beams of Frame 1 are given in Figure 3.1-13 for the X direction of response. These forces include 100 percent of the scaled X-direction spectrum added to the 30 percent of the scaled Y-direction spectrum. Accidental torsion is then added to the combined spectral loading. The design force for the Level 12 beam in Bay 3 (shown in bold type in Figure 3.1-13) was computed as follows:

<sup>&</sup>lt;sup>4</sup>This method has been forwarded in the unpublished paper *A Seismic Analysis Method Which Satisfies the 1988 UBC Lateral Force Requirements*, written in 1989 by Wilson, Suharwardy, and Habibullah. The paper also suggests the use of a single scale factor, where the scale factor is based on the total base shear developed along the principal axes of the structure. As stated in the paper, the major advantage of the method is that one set of dynamic design forces, including the effect of accidental torsion, is produced in one computer run. In addition, the resulting structural design has equal resistance to seismic motions in all possible directions.

Force from 100 percent X-direction spectrum = 6.94 kips (as based on CQC combination for structure loaded with X spectrum only).

Force from 100 percent Y-direction spectrum = 1.26 kips (as based on CQC combination for structure loaded with Y spectrum only).

Force from accidental torsion = 1.25 kips. Scale factor for X-direction response = 2.18. Scale factor for Y-direction response = 2.10.

Earthquake shear force =  $(2.18 \times 6.94) + (2.10 \times 0.30 \times 1.26) + (0.85 \times 1.25) = 17.0$  kips

			9.4	9.7	9.9		
R-12			17.0	17.7	17.8		
12-11			25.0	24.9	26.0		
11-10			28.2	27.7	29.8		
10-9			26.6	26.5	24.8	22.9	10.2
9-8			27.2	26.7	25.5	28.0	18.0
8-7			30.9	28.8	28.8	30.5	19.4
7-6			32.3	30.4	29.8	31.1	20.1
6-5	11.1	24.4	26.0	27.7	27.1	27.9	18.6
5-4	19.0	28.8	25.7	27.0	26.6	27.1	18.6
4-3	20.1	29.7	28.0	28.8	28.4	29.0	20.2
3-2	20.0	31.5	30.1	30.6	30.4	31.1	20.1
2-G							

**Figure 3.1-13** Seismic shears in girders (kips) as computed using response-spectrum analysis. Analysis includes orthogonal loading and accidental torsion (1.0 kip = 4.45 kN).

## 3.1.7 Modal-Time-History Analysis

In modal-time-history analysis, the response in each mode is computed using step-by-step integration of the equations of motion, the modal responses are transformed to the structural coordinate system, linearly superimposed, and then used to compute structural displacements and member forces. The displacement and member forces for each time step in the analysis or minimum and maximum quantities (response envelopes) may be printed.

Requirements for time-history analysis are provided in *Provisions* Sec. 5.6 [5.4]. The same mathematical model of the structure used for the ELF and response-spectrum analysis is used for the time-history analysis.

As allowed by *Provisions* Sec. 5.6.2 [5.4.2], the structure will be analyzed using three different pairs of ground motion time-histories. The development of a proper suite of ground motions is one of the most critical and difficult aspects of time-history approaches. The motions should be characteristic of the site and should be from real (or simulated) ground motions that have a magnitude, distance, and source mechanism consistent with those that control the maximum considered earthquake.

For the purposes of this example, however, the emphasis is on the *implementation* of the time-history approach rather than on selection of realistic ground motions. For this reason, the motion suite developed for Example 3.2 is also used for the present example.<sup>5</sup> The structure for Example 3.2 is situated in Seattle, Washington, and uses three pairs of motions developed specifically for the site. The use of the Seattle motions for a Stockton building analysis is, of course, not strictly consistent with the requirements of the *Provisions*. However, a realistic comparison may still be made between the ELF, response spectrum, and time-history approaches.

### 3.1.7.1 The Seattle Ground Motion Suite

It is beneficial to provide some basic information on the Seattle motion suites in Table 3.1-20 below. Refer to Figures 3.2-40 through 3.2-42 for additional information, including plots of the ground motion time histories and 5-percent-damped response spectra for each motion.

Table 3.1-20     Seattle Ground Motion Parameters (Unscaled)				
Record Name	Orientation	Number of Points and Time Increment	Peak Ground Acceleration (g)	Source Motion
Record A00	N-S	8192 @ 0.005 seconds	0.443	Lucern (Landers)
Record A90	E-W	8192 @ 0.005 seconds	0.454	Lucern (Landers)
Record B00	N-S	4096 @ 0.005 seconds	0.460	USC Lick (Loma Prieta)
Record B90	E-W	4096 @ 0.005 seconds	0.435	USC Lick (Loma Prieta)
Record C00	N-S	1024 @ 0.02 seconds	0.460	Dayhook (Tabas, Iran)
Record C90	E-W	1024 @ 0.02 seconds	0.407	Dayhook (Tabas, Iran)

 Table 3.1-20
 Seattle Ground Motion Parameters (Unscaled)

Before the ground motions may be used in the time-history analysis, they must be scaled using the procedure described in *Provisions* Sec. 5.6.2.2 [5.4.2.2]. One scale factor will be determined for each pair of ground motions. The scale factors for record sets A, B, and C will be called  $S_A$ ,  $S_B$ , and  $S_C$ , respectively.

The scaling process proceeds as follows:

- 1. For each pair of motions (A, B, and C):
  - a Assume an initial scale factor  $(S_A, S_B, S_C)$ ,
  - b. Compute the 5-percent-damped elastic response spectrum for each component in the pair,
  - c. Compute the SRSS of the spectra for the two components, and
  - d. Scale the SRSS using the factor from (a) above.
- 2. Adjust scale factors ( $S_A$ ,  $S_B$ , and  $S_C$ ) such that the average of the three scaled SRSS spectra over the period range  $0.2T_1$  to  $1.5 T_1$  is not less than 1.3 times the 5-percent-damped spectrum determined in accordance with *Provisions* Sec. 4.1.2.6 [3.3.4].  $T_1$  is the fundamental mode period of vibration of

<sup>&</sup>lt;sup>5</sup>See Sec. 3.2.6.2 of this volume of design examples for a detailed discussion of the selected ground motions.

the structure. (The factor of 1.3 more than compensates for the fact that taking the SRSS of the two

components of a ground motion effectively increases their magnitude by a factor of 1.414.) Note that the scale factors so determined are not unique. An infinite number of different scale factors will satisfy the above requirements, and it is up to the engineer to make sure that the selected scale factors are reasonable.<sup>6</sup> Because the original ground motions are similar in terms of peak ground acceleration, the same scale factor will be used for each motion; hence,  $S_A = S_B = S_C$ . This equality in scale factors would not necessarily be appropriate for other suites of motions.

Given the 5-percent-damped spectra of the ground motions, this process is best carried out using an Excel spreadsheet. The spectra themselves were computed using the program *NONLIN*.<sup>7</sup> The results of the analysis are shown in Figures 3.1-14 and 3.1-15. Figure 3.1-14 shows the average of the SRSS of the *unscaled* spectra together with the *Provisions* response spectrum using  $S_{DS} = 0.833$ g (322 in./sec<sup>2</sup>) and  $S_{DI} = 0.373$ g (144 in./sec<sup>2</sup>). Figure 3.1-15 shows the ratio of the average SRSS spectrum to the *Provisions* spectrum over the period range 0.573 seconds to 4.30 seconds, where a scale factor  $S_A = S_B = S_C = 0.922$  has been applied to each original spectrum. As can be seen, the minimum ratio of 1.3 occurs at a period of approximately 3.8 seconds.

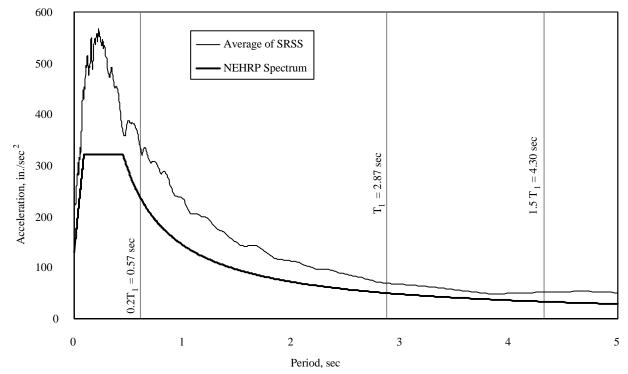


**Figure 3.1-14** Unscaled SRSS of spectra of ground motion pairs together with *Provisions* spectrum (1.0 in. = 25.4 mm).

At all other periods, the effect of using the 0.922 scale factor to provide a minimum ratio of 1.3 over the target period range is to have a relatively higher scale factor at all other periods if those periods significantly contribute to the response. For example, at the structure's fundamental mode, with T = 2.867 sec, the ratio of the scaled average SRSS to the *Provisions* spectrum is 1.38, not 1.30. At the higher modes, the effect is even more pronounced. For example, at the second translational X mode, T = 1.149

<sup>&</sup>lt;sup>6</sup>The "degree of freedom" in selecting the scaling factors may be used to reduce the effect of a particularly demanding motion.

<sup>&</sup>lt;sup>7</sup>NONLIN, developed by Finley Charney, may be downloaded at no cost at <u>www.fema.gov/emi.</u> To find the latest version, do a search for *NONLIN*.

seconds and the computed ratio is 1.62. This, of course, is an inherent difficulty of using a single scale factor to scale ground motion spectra to a target code spectrum.

When performing linear-time-history analysis, the ground motions also should be scaled by the factor I/R. In this case, I = 1 and R = 8, so the actual scale factor applied to each ground motion will be 0.922(1/8) = 0.115.

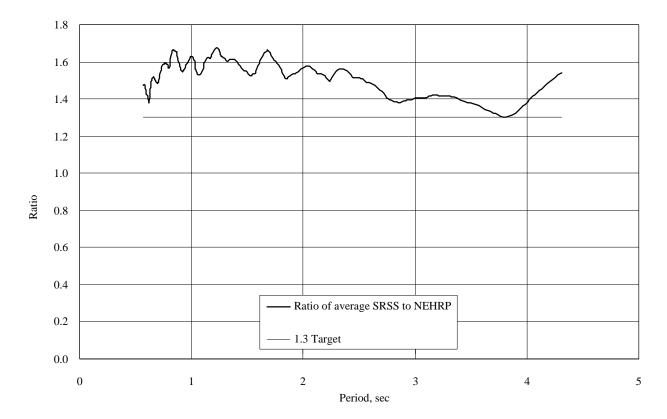


Figure 3.1-15 Ratio of average scaled SRSS spectrum to Provisions spectrum.

If the maximum base shear from any of the analyses is less than that computed from *Provisions* Eq. 5.4.1.1-3 ( $C_s = 0.044IS_{DS}$ ), all forces and displacements<sup>8</sup> computed from the time-history analysis must again be scaled such that peak base shear from the time-history analysis is equal to the minimum shear computed from Eq. 5.4.1.1-3. This is stated in *Provisions* Sec. 5.6.3 [5.4.3]. Recall that the base shear controlled by Eq. 5.4.1.1-3 is 1124 kips in each direction. [In the 2003 *Provisions* base shear scaling is still required, but recall that the minimum base shear has been revised.]

The second paragraph of *Provisions* Sec. 5.6.3 [5.4.3] states that if fewer than seven ground motion pairs are used in the analysis, the design of the structure should be based on the maximum scaled quantity among all analyses.

The *Provisions* is not particularly clear regarding the scaling of displacements in time-history analysis. The first paragraph of Sec. 5.6.3 states that member forces should be scaled, but displacements are not mentioned. The second paragraph states that member forces and displacements should be scaled. In this example, the displacements will be scaled, mainly to be consistent with the response spectrum procedure which, in *Provisions* Sec. 5.5.7, explicitly states that forces and displacements should be scaled. See Sec. 3.1.8 of this volume of design examples for more discussion of this apparent inconsistency in the *Provisions*.

Twelve individual time-history analyses were carried out using SAP2000: one for each N-S ground motion acting in the X direction, one for each N-S motion acting in the Y direction, one for each E-W motion acting in the X direction, and one for each E-W motion acting in the Y direction. As with the response-spectrum analysis, 14 modes were used in the analysis. Five percent of critical damping was used in each mode. The integration time-step used in all analyses was 0.005 seconds. The results from the analyses are summarized Tables 3.1-21 and 3.1-22.

As may be observed from Table 3.1-21, the maximum scaled base shears computed from the time-history analysis are significantly less than the ELF minimum of 1124 kips. This is expected because the ELF base shear was controlled by *Provisions* Eq. 5.4.1.1-3. Hence, each of the analyses will need to be scaled up. The required scale factors are shown in Table 3.1-22. Also shown in that table are the scaled maximum deflections with and without  $C_d = 5.5$ .

	Table 3.1-21         Result Maxima from Time-History Analysis (Unscaled)						
	Maximum Base		Maximum Roof	Time of			
Analysis	Shear	Time of Maximum	Displacement	Maximum			
Allalysis	(S.F. = 0.115)	Shear	(S.F. = 0.115)	Displacement			
	(kips)	(sec)	(in.)	(sec)			
A00-X	394.5	12.73	2.28	11.39			
A00-Y	398.2	11.84	2.11	11.36			
A90-X	473.8	15.42	2.13	12.77			
A90-Y	523.9	15.12	1.91	10.90			
B00-X	393.5	15.35	2.11	14.17			
B00-Y	475.1	14.29	1.91	19.43			
B90-X	399.6	13.31	1.77	16.27			
B90-Y	454.2	12.83	1.68	12.80			
C00-X	403.1	6.96	1.86	7.02			
C00-Y	519.2	6.96	1.70	7.02			
C90-X	381.5	19.40	1.95	19.38			
C90-Y	388.5	19.38	1.85	19.30			

1.0 in. = 25.4 mm, 1.0 kip = 4.45 kN.

 Table 3.1-22
 Result Maxima from Time-History Analysis (Scaled)

	Table 5.1-22 Rest	int Maxima from Time-His	story Analysis (Scale	u)
	Maximum Base	Required Additional	Adjusted	Adjusted Max
Analysis	Shear	Scale Factor for	Maximum Roof	Roof Disp. $\times C_d$
Analysis	(SF = 0.115)	V = 1124 kips	Displacement	(in.)
	(kips)		(in.)	
A00-X	394.5	2.85	6.51	35.7
A00-Y	398.2	2.82	5.95	32.7
A90-X	473.8	2.37	5.05	27.8
A90-Y	523.9	2.15	4.11	22.6
B00-X	393.5	2.86	6.03	33.2
B00-Y	475.1	2.37	4.53	24.9
B90-X	399.6	2.81	4.97	27.4
B90-Y	454.2	2.48	4.17	22.9
C00-X	403.1	2.79	5.19	28.5
C00-Y	519.2	2.16	3.67	20.2
C90-X	381.5	2.95	5.75	31.6
C90-Y	388.5	2.89	5.35	29.4

Scaled base shear = 1124 kips for all cases. 1.0 in. = 25.4 mm, 1.0 kip = 4.45 kN.

# **3.1.7.2 Drift and P-Delta Effects**

In this section, drift and P-delta effects are checked only for the structure subjected to Motion A00 acting in the X direction of the building. As can be seen from Table 3.1-22, this analysis produced the largest roof displacement, but not necessarily the maximum story drift. To be sure that the maximum drift has been determined, it would be necessary to compute the scaled drifts histories from each analysis and then find the maximum drift among all analyses.

As may be observed from Table 3.1-23, the allowable drift has been exceeded at several levels. For example, at Level 11, the computed drift is 4.14 in. compared to the limit of 3.00 inches.

Before computing P-delta effects, it is necessary to determine the story shears that exist at the time of maximum displacement. These shears, together with the inertial story forces, are shown in the first two columns of Table 3.1-24. The maximum base shear at the time of maximum displacement is only 668.9 kips, significantly less that the peak base shear of 1124 kips. For comparison purposes, Table 3.1-24 also shows the story shears and inertial forces that occur at the time of peak base shear.

As may be seen from Table 3.1-25, the P-delta effects are marginally exceeded at the lower three levels of the structure, as the maximum allowable stability ratio for the structure is 0.091 (see Sec. 3.1.5.3 of this example). As mentioned earlier, the fact that the limit has been exceeded is probably of no concern because the factor  $\beta$  was conservatively taken as 1.0.

		-		
Level	1 Elastic Total Drift (in.)	2 Elastic Story Drift (in.)	3 Inelastic Story Drift (in.)	4 Allowable Drift (in.)
R	6.51	0.47	2.57	3.00
12	6.05	0.66	3.63	3.00
11	5.39	0.75	4.14	3.00
10	4.63	0.75	4.12	3.00
9	3.88	0.62	3.40	3.00
8	3.27	0.61	3.34	3.00
7	2.66	0.58	3.20	3.00
6	2.08	0.54	2.95	3.00
5	1.54	0.42	2.32	3.00
4	1.12	0.39	2.12	3.00
3	0.74	0.34	1.89	3.00
2	0.39	0.39	2.13	4.32

**Table 3.1-23** Time-History Drift for Building Responding in X Direction to Motion A00X

Computations are at time of maximum roof displacement from analysis A00X. 1.0 in. = 25.4 mm.

Level	At Time of Maximum Roof Displacement (T = 11.39  sec)		At Time of Maximum Base Shear $(T = 12.73 \text{ sec})$	
	$\frac{(I = 1)}{\text{Story Shear}}$ (kips)	Inertial Force (kips)	Story Shear (kips)	Inertial Force (kips)
R	307.4	307.4	40.2	40.2
12	529.7	222.3	44.3	4.1
11	664.9	135.2	45.7	1.4
10	730.5	65.6	95.6	49.9
9	787.9	57.4	319.0	223.4
8	817.5	29.6	468.1	149.1
7	843.8	26.3	559.2	91.1
6	855.0	11.2	596.5	37.3
5	828.7	-26.3	662.7	66.2
4	778.7	-50.0	785.5	122.8
3	716.1	-62.6	971.7	186.2
2	668.9	-47.2	1124.0	148.3

Table 3.1-24 Scaled Inertial Force and Story Shear Envelopes from Analysis A00X

1.0 kip = 4.45 kN.

Table 3.1-25 Computation of P-Delta Effects for X-Direction Response

Level	$h_{\rm sr}$ (in.)	⊿ (in.)	$P_D$ (kips)	$P_L$ (kips)	$P_T$ (kips)	$P_{\chi}$ (kips)	$V_{\chi}$ (kips)	$\theta_{X}$
R	150	2.57	1656.5	315.0	1971.5	1971.5	307.4	0.020
12	150	3.63	1595.8	315.0	1910.8	3882.3	529.7	0.032
11	150	4.14	1595.8	315.0	1910.8	5793.1	664.9	0.044
10	150	4.12	1595.8	315.0	1910.8	7703.9	730.5	0.053
9	150	3.40	3403.0	465.0	3868.0	11571.9	787.9	0.061
8	150	3.34	2330.8	465.0	2795.8	14367.7	817.5	0.071
7	150	3.20	2330.8	465.0	2795.8	17163.5	843.8	0.079
6	150	2.95	2330.8	465.0	2795.8	19959.3	855.0	0.083
5	150	2.32	4323.8	615.0	4938.8	24898.1	828.7	0.084
4	150	2.12	3066.1	615.0	3681.1	28579.2	778.7	0.094
3	150	1.89	3066.1	615.0	3681.1	32260.3	716.1	0.103
2	216	2.13	3097.0	615.0	3712.0	35972.3	668.9	0.096

Computations are at time of maximum roof displacement from analysis A00X. 1.0 in. = 25.4 mm, 1.0 kip = 4.45 kN.

### 3.1.7.3 Torsion, Orthogonal Loading, and Load Combinations

As with ELF or response-spectrum analysis, it is necessary to add the effects of accidental torsion and orthogonal loading into the analysis. Accidental torsion is applied in exactly the same manner as done for the response spectrum approach, except that the factor 0.85 is not used. Orthogonal loading is automatically accounted for by concurrently running one ground motion in one principal direction with

30 percent of the companion motion being applied in the orthogonal direction. Because the signs of the ground motions are arbitrary, it is appropriate to add the absolute values of the responses from the two directions. Six dynamic load combinations result:

Combination 1:	A00X + 0.3 A90Y + Torsion
Combination 2:	A90X + 0.3 A00Y + Torsion
Combination 3:	B00X + 0.3 B90Y + Torsion
Combination 4:	B90X + 0.3 B00Y + Torsion
Combination 5:	C00X + 0.3 C90Y + Torsion
Combination 6:	C90X + 0.3 C00Y + Torsion

### 3.1.7.4 Member Design Forces

Using the method outlined above, the individual beam shear maxima developed in Fame 1 were computed for each load combination. The envelope values from only the first two combinations are shown in Figure 3.1-16. Envelope values from all combinations are shown in Figure 3.1-17. Note that some of the other combinations (Combinations 3 through 8) control the member shears at the lower levels of the building. These forces are compared to the forces obtained using ELF and modal-response-spectrum analysis in the following discussion.

			16.2	17.5	17.6		
R-12			30.4	32.3	32.3		
12-11			45.5	45.6	47.6		
11-10			50.0	49.3	52.8		
10-9			43.9	44.4	40.9	37.8	16.3
9-8			42.0	41.9	39.6	44.4	28.4
8-7			44.9	44.3	42.1	45.4	28.9
7-6			43.4	42.0	40.2	43.7	27.9
6-5	13.7	30.3	32.3	34.2	33.5	34.9	23.0
5-4	23.2	35.6	31.1	32.9	32.4	33.2	22.8
4-3	23.7	35.6	32.6	34.0	33.6	34.4	24.0
3-2	23.1	36.2	35.1	35.3	35.4	35.8	23.4
2-G							

**Figure 3.1-16** For Combinations 1 and 2, beam shears (kips) as computed using time-history analysis; analysis includes orthogonal loading and accidental torsion (1.0 kip = 4.45 kN).

			16.2	17.5	17.6		
R-12			30.4	32.3	32.3		
12-11			45.5	45.6	47.6		
11-10			50.0	49.3	52.8		
10-9			44.7	44.5	41.7	38.5	17.3
9-8			43.9	43.5	41.3	45.8	29.6
8-7			46.6	45.4	43.6	46.7	29.6
7-6			45.2	42.9	41.8	44.1	28.5
6-5	14.9	32.4	34.4	36.4	35.6	36.7	24.2
5-4	24.9	37.9	33.5	35.3	34.8	35.6	24.2
4-3	25.3	37.1	35.6	36.1	36.0	36.2	25.3
3-2	24.6	38.2	36.9	37.3	37.3	37.8	24.6
2-G							
l							

Figure 3.1-17 For all combinations, beam shears (kips) as computed using time-history analysis; analysis includes orthogonal loading and accidental torsion (1.0 kip = 4.45 kN).

# 3.1.8 Comparison of Results from Various Methods of Analysis

A summary of the results from all of the analyses is provided in Tables 3.1-26 through 3.1-28.

# 3.1.8.1 Comparison of Base Shear and Story Shear

The maximum story shears are shown In Table 3.1-26. For the time-history analysis, the shears computed at the time of maximum displacement and time of maximum base shear (from analysis A00X only) are provided. Also shown from the time-history analysis is the envelope of story shears computed among all analyses. As may be observed, the shears from ELF and response-spectrum analysis seem to differ primarily on the basis of the factor 0.85 used in scaling the response spectrum results. ELF does, however, produce relatively larger forces at Levels 6 through 10.

The difference between ELF shears and time-history envelope shears is much more pronounced, particularly at the upper levels where time-history analysis gives larger forces. One reason for the difference is that the scaling of the ground motions has greatly increased the contribution of the higher modes of response.

The time-history analysis also gives shears larger than those computed using the response spectrum procedure, particularly for the upper levels.

# 3.1.8.2 Comparison of Drift

Table 3.1-27 summarizes the drifts computed from each of the analyses. The time-history drifts are from a single analysis, A00X; envelope values would be somewhat greater. As with shear, the ELF and modal-response-spectrum approaches appear to produce similar results, but the drifts from time-history analysis are significantly greater. Aside from the fact that the 0.85 factor is not applied to time-history response, it is not clear why the time-history drifts are as high as they are. One possible explanation is that the drifts are dominated by one particular pulse in one particular ground motion. As mentioned above, it is also possible that the effect of scaling has been to artificially enhance the higher mode response.

# 3.1.8.3 Comparison Member Forces

The shears developed in Bay D-E of Frame 1 are compared in Table 3.1-28. The shears from the timehistory (TH) analysis are envelope values among all analyses, including torsion and orthogonal load effects. The time-history approach produced larger beam shears than the ELF and response spectrum (RS) approaches, particularly in the upper levels of the building. The effect of higher modes on the response is again the likely explanation for the noted differences.

	Story Shear (kips)				
Level	ELF	RS	TH at Time of Maximum Displacement	TH at Time of Maximum Base Shear	TH. at Envelope
R	187	180	307	40.2	325
12	341	286	530	44.3	551
11	471	358	664	45.7	683
10	578	417	731	95.6	743
9	765	523	788	319	930
8	866	586	818	468	975
7	943	638	844	559	964
6	999	688	856	596	957
5	1070	783	829	663	1083
4	1102	838	779	786	1091
3	1118	894	718	972	1045
2	1124	956	669	1124	1124

Table 3.1-26 Summary of Results from Various Methods of Analysis: Story Shear

1.0 kip = 4.45 kN.

Level	X-Direction Drift (in.)				
Level	ELF	RS	TH		
R	0.982	0.99	2.57		
12	1.41	1.43	3.63		
11	1.75	1.65	4.14		
10	1.92	1.82	4.12		
9	1.83	1.87	3.40		
8	2.00	1.98	3.34		
7	2.03	2.20	3.20		
6	1.95	2.14	2.95		
5	1.70	2.09	2.32		
4	1.70	2.09	2.12		
3	1.67	2.31	1.89		
2	2.02	2.91	2.13		

Table 3.1-27 Summary of Results from Various Methods of Analysis: Story Drift

1.0 in. = 25.4 mm.

Table 3.1-28 Summary of Results from Various Methods of Analysis: Beam Shear

T1	Beam Shear	Beam Shear Force in Bay D-E of Frame 1 (kips)				
Level	ELF	RS	TH			
R	9.54	9.70	17.5			
12	17.6	17.7	32.3			
11	26.3	24.9	45.6			
10	31.0	27.7	49.3			
9	32.7	26.5	44.5			
8	34.1	26.7	43.5			
7	38.1	28.8	45.4			
6	38.4	30.4	42.9			
5	34.3	27.7	36.4			
4	31.0	27.0	35.3			
3	31.7	28.8	36.1			
2	31.8	30.6	37.3			

1.0 kip = 4.45 kN.

# 3.1.8.4 A Commentary on the Provisions Requirements for Analysis

From the writer's perspective, there are two principal inconsistencies between the requirements for ELF, modal-response-spectrum, and modal-time-history analyses:

1. In ELF analysis, the *Provisions* allows displacements to be computed using base shears consistent with Eq. 5.4.1.4-2 [5.2-3] ( $C_s = S_{DI}/T(R/I)$  when Eq. 5.4.1.4-3 ( $C_s = 0.044IS_{DS}$ ) controls for strength. For both modal-response-spectrum analysis and modal time-history analysis, however, the computed

shears and displacements must be scaled if the computed base shear falls below the ELF shear computed using Eq. 5.1.1.1-3. [Because the minimum base shear has been revised in the 2003 *Provisions*, this inconsistency would not affect this example.]

2. The factor of 0.85 is allowed when scaling modal-response-spectrum analysis, but not when scaling time-history results. This penalty for time-history analysis is in addition to the penalty imposed by selecting a scale factor that is controlled by the response at one particular period (and thus exceeding the target at other periods). [In the 2003 *Provisions* these inconsistencies are partially resolved. The minimum base shear has been revised, but time-history analysis results are still scaled to a higher base shear than are modal response spectrum analysis results.]

The effect of these inconsistencies is evident in the results shown in Tables 3.1-26 through 3.1-28 and should be addressed prior to finalizing the 2003 edition of the *Provisions*.

# 3.1.8.5 Which Method Is Best?

In this example, an analysis of an irregular steel moment frame was performed using three different techniques: equivalent-lateral-force, modal-response-spectrum, and modal-time-history analyses. Each analysis was performed using a linear elastic model of the structure even though it is recognized that the structure will repeatedly yield during the earthquake. Hence, each analysis has significant shortcomings with respect to providing a reliable prediction of the actual response of the structure during an earthquake.

The purpose of analysis, however, is not to predict response but rather to provide information that an engineer can use to proportion members and to estimate whether or not the structure has sufficient stiffness to limit deformations and avoid overall instability. In short, the analysis only has to be "good enough for design." If, on the basis of any of the above analyses, the elements are properly designed for strength, the stiffness requirements are met and the elements and connections of the structure are detailed for inelastic response according to the requirements of the *Provisions*, the structure will likely survive an earthquake consistent with the maximum considered ground motion. The exception would be if a highly irregular structure were analyzed using the ELF procedure. Fortunately, the *Provisions* safeguards against this by requiring three-dimensional dynamic analysis for highly irregular structures.

For the structure analyzed in this example, the irregularities were probably not so extreme such that the ELF procedure would produce a "bad design." However, when computer programs (e.g., SAP2000 and ETABS) that can perform modal-response-spectrum analysis with only marginally increased effort over that required for ELF are available, the modal analysis should always be used for final design in lieu of ELF (even if ELF is allowed by the *Provisions*). As mentioned in the example, this does not negate the need or importance of ELF analysis because such an analysis is useful for preliminary design and components of the ELF analysis are necessary for application of accidental torsion.

The use of time-history analysis is limited when applied to a linear elastic model of the structure. The amount of additional effort required to select and scale the ground motions, perform the time-history analysis, scale the results, and determine envelope values for use in design is simply not warranted when compared to the effort required for modal-response-spectrum analysis. This might change in the future when "standard" suites of ground motions are developed and are made available to the earthquake engineering community. Also, significant improvement is

needed in the software available for the preprocessing and particularly, for the post-processing of the huge amounts of information that arise from the analysis.

Scaling ground motions used for time-history analysis is also an issue. The *Provisions* requires that the selected motions be consistent with the magnitude, distance, and source mechanism of a maximum considered earthquake expected at the site. If the ground motions satisfy this criteria, then why scale at all? Distant earthquakes may have a lower peak acceleration but contain a frequency content that is more significant. Near-source earthquakes may display single damaging pulses. Scaling these two earthquakes to the *Provisions* spectrum seems to eliminate some of the most important characteristics of the ground motions. The fact that there is a degree of freedom in the *Provisions* scaling requirements compensates for this effect, but only for very knowledgeable users.

The main benefit of time-history analysis is in the nonlinear dynamic analysis of structures or in the analysis of non-proportionally damped linear systems. This type of analysis is the subject of Example 3.2.

# 3.2 SIX-STORY STEEL FRAME BUILDING, SEATTLE, WASHINGTON

In this example, the behavior of a simple, six-story structural steel moment-resisting frame is investigated using a variety of analytical techniques. The structure was initially proportioned using a preliminary analysis, and it is this preliminary design that is investigated. The analysis will show that the structure falls short of several performance expectations. In an attempt to improve performance, viscous fluid dampers are considered for use in the structural system. Analysis associated with the added dampers is performed in a very preliminary manner.

The following analytical techniques are employed:

- 1. Linear static analysis,
- 2. Plastic strength analysis (using virtual work),
- 3. Nonlinear static (pushover) analysis,
- 4. Linear dynamic analysis, and
- 5. Nonlinear dynamic analysis.

The primary purpose of this example is to highlight some of the more advanced analytical techniques; hence, more detail is provided on the last three analytical techniques. The *Provisions* provides some guidance and requirements for the advanced analysis techniques. Nonlinear static analysis is covered in the Appendix to Chapter 5, nonlinear dynamic analysis is covered in Sec. 5.7 [5.5], and analysis of structures with added damping is prescribed in the Appendix to Chapter 13 [new Chapter 15].

### 3.2.1 Description of Structure

The structure analyzed for this example is a 6-story office building in Seattle, Washington. According to the descriptions in *Provisions* Sec. 1.3 [1.2], the building is assigned to Seismic Use Group I. From *Provisions* Table 1.4 [1.3-1], the occupancy importance factor (*I*) is 1.0. A plan and elevation of the building are shown in Figures 3.2-1 and 3.2-2, respectively. The lateral-load-resisting system consists of steel moment-resisting frames on the perimeter of the building. There are five bays at 28 ft on center in the N-S direction and six bays at 30 ft on center in the E-W direction. The typical story height is 12 ft-6 in. with the exception of the first story, which has a height of 15 ft. There are a 5-ft-tall perimeter parapet at the roof and one basement level that extends 15 ft below grade. For this example, it is assumed that the columns of the moment-resisting frames are embedded into pilasters formed into the basement wall.

For the moment-resisting frames in the N-S direction (Frames A and G), all of the columns bend about their strong axes, and the girders are attached with fully welded moment-resisting connections. It is assumed that these and all other fully welded connections are constructed and inspected according to post-Northridge protocol. Only the demand side of the required behavior of these connections is addressed in this example.

For the frames in the E-W direction (Frames 1 and 6), moment-resisting connections are used only at the interior columns. At the exterior bays, the E-W girders are connected to the weak axis of the exterior (corner) columns using non-moment-resisting connections.

All interior columns are gravity columns and are not intended to resist lateral loads. A few of these

columns, however, would be engaged as part of the added damping system described in the last part of this example. With minor exceptions, all of the analyses in this example will be for lateral loads acting in the N-S direction. Analysis for lateral loads acting in the E-W direction would be performed in a similar manner.

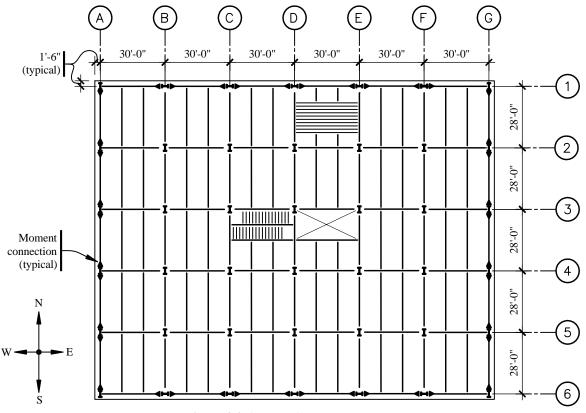


Figure 3.2-1 Plan of structural system.

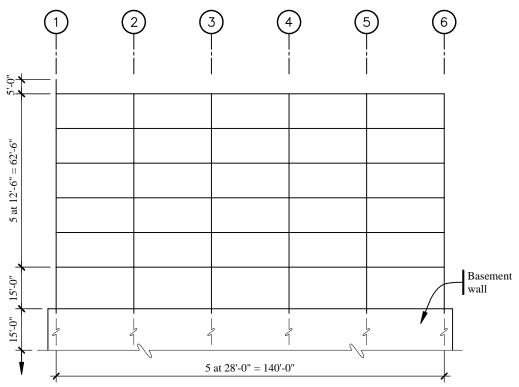


Figure 3.2-2 Elevation of structural system.

Prior to analyzing the structure, a preliminary design was performed in accordance with the AISC Seismic. All members, including miscellaneous plates, were designed using steel with a nominal yield stress of 50 ksi. Detailed calculations for the design are beyond the scope of this example. Table 3.2-1 summarizes the members selected for the preliminary design.<sup>1</sup>

Table 3	Table 3.2-1         Member Sizes Used in N-S Moment Frames					
Member Supporting	Column	Girder	Doubler Plate Thickness			
Level			(in.)			
R	W21x122	W24x84	1.00			
6	W21x122	W24x84	1.00			
5	W21x147	W27x94	1.00			
4	W21x147	W27x94	1.00			
3	W21x201	W27x94	0.875			
2	W21x201	W27x94	0.875			

<sup>&</sup>lt;sup>1</sup>The term *Level* is used in this example to designate a horizontal plane at the same elevation as the centerline of a girder. The top level, Level R, is at the roof elevation; Level 2 is the first level above grade; and Level 1 is at grade. A *Story* represents the distance between adjacent levels. The story designation is the same as the designation of the level at the bottom of the story. Hence, Story 1 is the lowest story (between Levels 2 and 1) and Story 6 is the uppermost story between Levels R and 6.

The sections shown in Table 3.2-1 meet the width-to-thickness requirements for special moment frames, and the size of the column relative to the girders should ensure that plastic hinges will form in the girders. Doubler plates 0.875 in. thick are used at each of the interior columns at Levels 2 and 3, and 1.00 in. thick plates are used at the interior columns at Levels 4, 5, 6, and R. Doubler plates were not used in the exterior columns.

### **3.2.2** Loads

### 3.2.2.1 Gravity Loads

It is assumed that the floor system of the building consists of a normal weight composite concrete slab on formed metal deck. The slab is supported by floor beams that span in the N-S direction. These floor beams have a span of 28 ft and are spaced 10 ft on center.

The dead weight of the structural floor system is estimated at 70 psf. Adding 15 psf for ceiling and mechanical, 10 psf for partitions at Levels 2 through 6, and 10 psf for roofing at Level R, the total dead load at each level is 95 psf. The cladding system is assumed to weigh 15 psf. A basic live load of 50 psf is used over the full floor. Twenty-five percent of this load, or 12.5 psf, is assumed to act concurrent with seismic forces. A similar reduced live load is used for the roof.

Based on these loads, the total dead load, live load, and dead plus live load applied to each level are given in Table 3.2-2. The slight difference in loads at Levels R and 2 is due to the parapet and the tall first story, respectively.

Tributary areas for columns and girders as well as individual element gravity loads used in the analysis are illustrated in Figure 3.2-3. These are based on a total dead load of 95 psf, a cladding weight of 15 psf, and a live load of 0.25(50) = 12.5 psf.

					-0	
	Dead	Load (kips)	Reduced L	Reduced Live Load (kips)		Load (kips)
Level	Story	Accumulated	Story	Accumulated	Story	Accumulated
R	2,549	2,549	321	321	2,870	2,870
6	2,561	5,110	321	642	2,882	5,752
5	2,561	7,671	321	963	2,882	8,634
4	2,561	10,232	321	1,284	2,882	11,516
3	2,561	12,792	321	1,605	2,882	14,398
2	2,573	15,366	321	1,926	2,894	17,292

Table 3.2-2 Gravity Loads on Seattle Building

### **3.2.2.2 Earthquake Loads**

Although the main analysis in this example is nonlinear, equivalent static forces are computed in accordance with the *Provisions*. These forces are used in a preliminary static analysis to determine whether the structure, as designed, conforms to the drift requirements of the *Provisions*.

The structure is situated in Seattle, Washington. The short period and the 1-second mapped spectral

acceleration parameters for the site are:

$$S_s = 1.63$$
$$S_I = 0.57$$

The structure is situated on Site Class C materials. From *Provisions* Tables 4.1.2.4(a) and 4.1.2.4(b) [Tables 3.3-1 and 3.3-2]:

$$F_a = 1.00$$
  
 $F_v = 1.30$ 

From *Provisions* Eq. 4.1.2.4-1 and 4.1.2.4-2 [3.3-1 and 3.3-2], the maximum considered spectral acceleration parameters are:

$$S_{MS} = F_a S_s = 1.00(1.63)$$
  
= 1.63  
$$S_{MI} = F_v S_I = 1.30(0.57)$$
  
= 0.741

And from *Provisions* Eq. 4.1.2.5-1 and Eq. 4.1.2.5-2 [3.3-3 and 3.3-4], the design acceleration parameters are:

$$S_{DS} = (2/3)S_{MI} = (2/3)1.63$$
  
= 1.09  
$$S_{DI} = (2/3)S_{MI} = (2/3)0.741$$
  
= 0.494

Based on the above coefficients and on *Provisions* Tables 4.2.1a and 4.2.1b [1.4-1 and 1.4-2], the structure is assigned to Seismic Design Category D. For the purpose of analysis, it is assumed that the structure complies with the requirements for a special moment frame, which, according to *Provisions* Table 5.2.2 [4.3-1], has R = 8,  $C_d = 5.5$ , and  $\Omega_0 = 3.0$ .

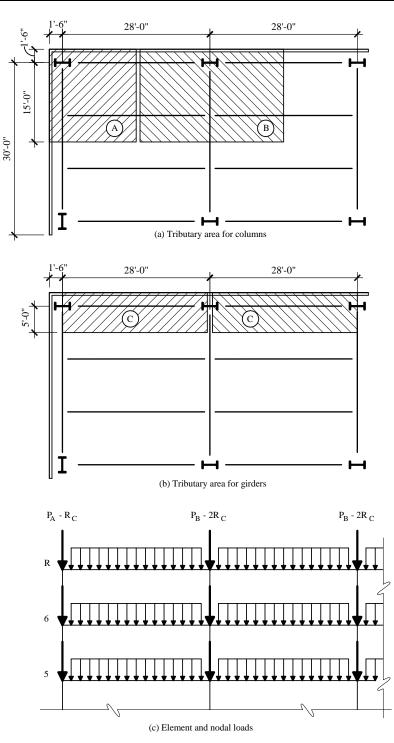


Figure 3.2-3 Element loads used in analysis.

#### 3.2.2.2.1 Approximate Period of Vibration

Provisions Eq. 5.4.2.1-1 [5.2-6] is used to estimate the building period:

$$T_a = C_r h_n^{\lambda}$$

where, from *Provisions* Table 5.4.2.1 [5.5-2],  $C_r = 0.028$  and x = 0.8 for a steel moment frame. Using  $h_n$  (the total building height above grade) = 77.5 ft,  $T_a = 0.028(77.5)^{0.8} = 0.91$  sec.

When the period is determined from a properly substantiated analysis, the *Provisions* requires that the period used for computing base shear not exceed  $C_u T_a$  where, from *Provisions* Table 5.4.2 [5.2-1] (using  $S_{DI} = 0.494$ ),  $C_u = 1.4$ . For the structure under consideration,  $C_u T_a = 1.4(0.91) = 1.27$  sec.

#### 3.2.2.2.2 Computation of Base Shear

Using *Provisions* Eq. 5.4.1 [5.2-1], the total seismic shear is:

$$V = C_S W$$

where *W* is the total weight of the structure. From *Provisions* Eq. 5.4.1.1-1 [5.2-2], the maximum (constant acceleration region) seismic response coefficient is:

$$C_{S_{max}} = \frac{S_{DS}}{(R/I)} = \frac{1.09}{(8/1)} = 0.136$$

Provisions Eq. 5.4.1.1-2 [5.2-3] controls in the constant velocity region:

$$C_S = \frac{S_{DI}}{T(R/I)} = \frac{0.494}{1.27(8/1)} = 0.0485$$

The seismic response coefficient, however, must not be less than that given by Eq. 5.4.1.1-3 [revised for the 2003 *Provisions*]:

$$C_{S_{min}} = 0.044 I S_{DS} = 0.044(1)(1.09) = 0.0480$$
.

[In the 2003 *Provisions*, this equation for minimum base shear coefficient has been revised. The results of this example problem would not be affected by the change.]

Thus, the value from Eq. 5.4.1.1-2 [5.2-3] controls for this building. Using W = 15,366 kips, V = 0.0485(15,366) = 745 kips.

### 3.2.2.3 Vertical Distribution of Forces

The *Provisions* Eq. 5.4.1.1-2 [5.2-3] base shear is distributed along the height of the building using *Provisions* Eq. 5.4.3.1 and 5.4.3.2 [5.2-10 and 5.2-11]:

$$F_x = C_{vx}V$$

and

$$C_{vx} = \frac{w_x h^k}{\sum\limits_{i=1}^n w_i h_i^k}$$

where k = 0.75 + 0.5T = 0.75 + 0.5(1.27) = 1.385. The lateral forces acting at each level and the story shears and story overturning moments acting at the bottom of the story below the indicated level are summarized in Table 3.2-3. These are the forces acting on the whole building. For analysis of a single frame, one-half of the tabulated values are used.

 Table 3.2-3
 Equivalent Lateral Forces for Seattle Building Responding in N-S Direction

Level <i>x</i>	W <sub>x</sub>	$h_x$	$w_{x}h_{x}^{k}$	C	$F_{x}$	$V_x$	$M_{x}$
Levelx	(kips)	(ft)	$W_{\chi}H_{\chi}$	$C_{vx}$	(kips)	(kips)	(ft-kips)
R	2,549	77.5	1,060,663	0.321	239.2	239.2	2,990
6	2,561	65.0	835,094	0.253	188.3	427.5	8,334
5	2,561	52.5	621,077	0.188	140.1	567.6	15,429
4	2,561	40.0	426,009	0.129	96.1	663.7	23,725
3	2,561	27.5	253,408	0.077	57.1	720.8	32,735
2	2,561	15.0	109,882	<u>0.033</u>	24.8	745.6	43,919
Σ	15,366		3,306,133	1.000	745.6		

# 3.2.3 Preliminaries to Main Structural Analysis

Performing a nonlinear analysis of a structure is an incremental process. The analyst should first perform a linear analysis to obtain some basic information on expected behavior and to serve later as a form of verification for the more advanced analysis. Once the linear behavior is understood (and extrapolated to expected nonlinear behavior), the anticipated nonlinearities are introduced. If more than one type of nonlinear behavior is expected to be of significance, it is advisable to perform a preliminary analysis with each nonlinearity considered separately and then to perform the final analysis with all nonlinearities considered. This is the approach employed in this example.

# 3.2.3.1 The Computer Program DRAIN-2Dx

The computer program DRAIN-2Dx (henceforth called DRAIN) was used for all of the analyses described in this example. DRAIN allows linear and nonlinear static and dynamic analysis of two-dimensional (planar) structures only.

As with any finite element analysis program, DRAIN models the structure as an assembly of nodes and elements. While a variety of element types is available, only three element types were used:

Type 1, inelastic bar (truss) element Type 2, beam-column element Type 4, connection element

Two models of the structure were prepared for DRAIN. The first model, used for preliminary analysis and for verification of the second (more advanced) model, consisted only of Type 2 elements for the main structure and Type 1 elements for modeling P-delta effects. All analyses carried out using this model were linear.

For the second more detailed model, Type 1 elements were used for modeling *P*-delta effects, the braces in the damped system, and the dampers in the damped system. It was assumed that these elements would remain linear elastic throughout the response. Type 2 elements were used to model the beams and columns as well as the rigid links associated with the panel zones. Plastic hinges were allowed to form in all columns. The column hinges form through the mechanism provided in DRAIN's Type 2 element. Plastic behavior in girders and in the panel zone region of the structure was considered through the use of Type 4 connection elements. Girder yielding was forced to occur in the Type 4 elements (in lieu of the main span represented by the Type 2 elements) to provide more control in hinge location and modeling. A complete description of the implementation of these elements is provided later.

# 3.2.3.2 Description of Preliminary Model and Summary of Preliminary Results

The preliminary DRAIN model is shown in Figure 3.2-4. Important characteristics of the model are as follows:

- 1. Only a single frame was modeled. Hence one-half of the loads shown in Tables 3.2-2 and 3.2-3 were applied.
- 2. Columns were fixed at their base.
- 3. Each beam or column element was modeled using a Type 2 element. For the columns, axial, flexural, and shear deformations were included. For the girders, flexural and shear deformations were included but, because of diaphragm slaving, axial deformation was not included. Composite action in the floor slab was ignored for all analysis.
- 4. Members were modeled using centerline dimensions without rigid end offsets. This allows, in an approximate but reasonably accurate manner, deformations to occur in the beam-column joint region. Note that this model does not provide any increase in beam-column joint stiffness due to the presence of doubler plates.
- 5. P-delta effects were modeled using the leaner column shown in Figure 3.2-4 at the right of the main frame. This column was modeled with an axially rigid Type 1 (truss) element. *P*-delta effects were activated for this column only (P-delta effects were turned off for the columns of the main frame). The lateral degree of freedom at each level of the P-delta column was slaved to the floor diaphragm at

the matching elevation. When P-delta effects were included in the analysis, a special initial load case was created and executed. This special load case consisted of a vertical force equal to one-half of the total story weight (dead load plus fully reduced live load) applied to the appropriate node of the P-delta column. P-delta effects were modeled in this manner to avoid the inconsistency of needing true column axial forces for assessing strength and requiring total story forces for assessing stability.

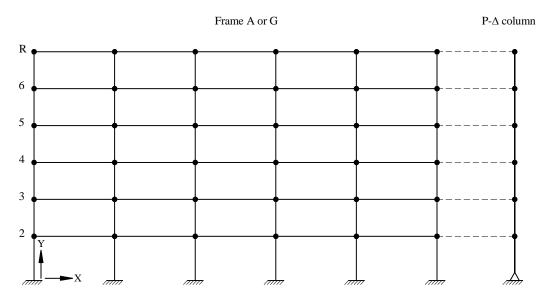


Figure 3.2-4 Simple wire frame model used for preliminary analysis.

# 3.2.3.2.1 Results of Preliminary Analysis: Drift and Period of Vibration

The results of the preliminary analysis for drift are shown in Tables 3.2-4 and 3.2-5 for the computations excluding and including P-delta effects, respectively. In each table, the deflection amplification factor  $(C_d)$  equals 5.5, and the acceptable story drift (story drift limit) is taken as 1.25 times the limit provided by *Provisions* Table 5.2.8. This is in accordance with *Provisions* Sec. 5.7.3.3 [5.5.3.3] which allows such an increase in drift when a nonlinear analysis is performed. This increased limit is used here for consistency with the results from the following nonlinear time-history analysis.

When P-delta effects are not included, the computed story drift is less than the allowable story drift at each level of the structure. The largest magnified story drift, including  $C_d = 5.5$ , is 3.45 in. in Story 2. If the 1.25 multiplier were not used, the allowable story drift would reduce to 3.00 in., and the computed story drift at Levels 3 and 4 would exceed the limit.

As a preliminary estimate of the importance of P-delta effects, story stability coefficients ( $\theta$ ) were computed in accordance with *Provisions* Sec. 5.4.6.2 [5.2.6.2]. At Story 2, the stability coefficient is 0.0839. *Provisions* Sec. 5.4.6.2 [5.2.6.2] allows P-delta effects to be ignored when the stability coefficient is less than 0.10. For this example, however, analyses are performed with and without P-delta effects. [In the 2003 *Provisions*, the stability coefficient equation has been revised to include the importance factor in the numerator and the calculated result is used simply to determine whether a special

analysis (in accordance with Sec. A5.2.3) is required.]

When P-delta effects are included, the drifts at the lower stories increase by about 10 percent as expected from the previously computed stability ratios. (Hence, the stability ratios provide a useful check.<sup>2</sup>) Recall that this analysis ignored the stiffening effect of doubler plates.

	1 able 3.2-4 K	esuits of Themin	haly Analysis Exclud	ing I -uena En	eets
Story	Total Drift	Story Drift	Magnified	Drift Limit	Story Stability
Story	(in.)	(in.)	Story Drift (in.)	(in.)	Ratio
6	3.14	0.33	1.82	3.75	0.0264
5	2.81	0.50	2.75	3.75	0.0448
4	2.31	0.54	2.97	3.75	0.0548
3	1.77	0.61	3.36	3.75	0.0706
2	1.16	0.63	3.45	3.75	0.0839
1	0.53	0.53	2.91	4.50	0.0683

 Table 3.2-4
 Results of Preliminary Analysis Excluding P-delta Effects

<b>Table 3.2-5</b>	Results of	Preliminary	/ Analy	ysis Inc	luding I	P-delta Effects	
							_

Story	Total Drift	Story Drift	Magnified	Drift Limit
Story	(in.)	(in.)	Story Drift (in.)	(in.)
6	3.35	0.34	1.87	3.75
5	3.01	0.53	2.91	3.75
4	2.48	0.57	3.15	3.75
3	1.91	0.66	3.63	3.75
2	1.25	0.68	3.74	3.75
1	0.57	0.57	3.14	4.50

The computed periods for the first three natural modes of vibration are shown in Table 3.2-6. As expected, the period including P-delta effects is slightly larger than that produced by the analysis without such effects. More significant is the fact that the first mode period is considerably longer than that predicted from *Provisions* Eq. 5.4.2.1-1 [5.2-6]. Recall from previous calculations that this period ( $T_a$ ) is 0.91 seconds, and the upper limit on computed period  $C_u T_a$  is 1.4(0.91) = 1.27 seconds. When doubler plate effects are included in the analysis, the period will decrease slightly, but it remains obvious that the structure is quite flexible.

<sup>&</sup>lt;sup>2</sup>The story drifts including P-delta effects can be estimated as the drifts without P-delta times the quantity  $1/(1-\theta)$ , where  $\theta$  is the stability coefficient for the story.

Table 3.2-6 Period	ls of Vibration From Prelim	inary Analysis (sec)
Mode	P-delta Excluded	P-delta Included
1	1.985	2.055
2	0.664	0.679
3	0.361	0.367

FEMA 451, NEHRP Recommended Provisions: Design Examples

### 3.2.3.2.2 Results of Preliminary Analysis: Demand-to-Capacity Ratios

To determine the likelihood of and possible order of yielding, demand-to-capacity ratios were computed for each element. The results are shown in Figure 3.2-5. For this analysis, the structure was subjected to full dead load plus 25 percent of live load followed by the equivalent lateral forces of Table 3.2-3. P-delta effects were included.

For girders, the demand-to-capacity ratio is simply the maximum moment in the member divided by the member's plastic moment capacity where the plastic capacity is  $Z_{girder}F_y$ . For columns, the ratio is similar except that the plastic flexural capacity is estimated to be  $Z_{col}(F_y - P_u/A_{col})$  where  $P_u$  is the total axial force in the column. The ratios were computed at the end of the member, not at the face of the column or girder. This results in slightly conservative ratios, particularly for the columns, because the columns have a smaller ratio of clear span to total span than do the girders.

Level R	0.176	0.177	0.169	0.172	0.164	-
	0.066				0.170	0.135
Level 6	0.282	0.281	0.277	0.282	0.280	4
	0.148		0.255	0.255	0.253	0.189
Level 5	0.344	0.333	0.333	0.333	0.354	
	0.133				0.269	0.175
Level 4	0.407	0.394	0.394	0.394	0.420	
	0.165	0.314	0.308	0.308	0.309	0.211
Level 3	0.452	0.435	0.435	0.434	0.470	
	0.162				0.340	0.223
Level 2	0.451	0.425	0.430	0.424	0.474	
	0.413	0.492	0.485	0.485	0.487	0.492

Figure 3.2-5 Demand-to-capacity ratios for elements from analysis with P-delta effects included.

It is very important to note that the ratios shown in Figure 3.2-5 are based on the inelastic seismic forces (using R = 8). Hence, a ratio of 1.0 means that the element is just at yield, a value less than 1.0 means the element is still elastic, and a ratio greater than 1.0 indicates yielding.<sup>3</sup>

Several observations are made regarding the likely inelastic behavior of the frame:

- 1. The structure has considerable overstrength, particularly at the upper levels.
- 2. The sequence of yielding will progress from the lower level girders to the upper level girders. Because of the uniform demand-to-capacity ratios in the girders of each level, all the hinges in the girders in a level will form almost simultaneously.
- 3. With the possible exception of the first level, the girders should yield before the columns. While not shown in the table, it should be noted that the demand-to-capacity ratios for the lower story columns were controlled by the moment at the base of the column. It is usually very difficult to prevent yielding of the base of the first story columns in moment frames, and this frame is no exception. The column on the leeward (right) side of the building will yield first because of the additional axial compressive force arising from the seismic effects.

#### 3.2.3.2.3 Results of Preliminary Analysis: Overall System Strength

The last step in the preliminary analysis was to estimate the total lateral strength (collapse load) of the frame using virtual work. In the analysis, it is assumed that plastic hinges are perfectly plastic. Girders hinge at a value  $Z_{girder}F_y$  and the hinges form 5.0 in. from the face of the column. Columns hinge only at the base, and the plastic moment capacity is assumed to be  $Z_{col}(F_y - P_u/A_{col})$ . The fully plastic mechanism for the system is illustrated in Figure 3.2-6. The inset to the figure shows how the angle modification term  $\sigma$  was computed. The strength (V) for the total structure is computed from the following relationships (see Figure 3.2-6 for nomenclature):

Internal Work = External Work

Internal Work =  $2[20\sigma\theta M_{PA} + 40\sigma\theta M_{PB} + \theta(M_{PC} + 4M_{PD} + M_{PE})]$ 

External Work = 
$$V\theta \left[\sum_{i=1}^{nLevels} F_i H_i\right]$$
 where  $\sum_{i=1}^{nLevels} F_i = 1.0$ 

Three lateral force patterns were used: uniform, upper triangular, and *Provisions* where the *Provisions* pattern is consistent with the vertical force distribution of Table 3.2-3 in this volume of design examples. The results of the analysis are shown in Table 3.2-7. As expected, the strength under uniform load is significantly greater than under triangular or *Provisions* load. The closeness of the *Provisions* and triangular load strengths is due to the fact that the vertical-load-distributing parameter (*k*) was 1.385, which is close to 1.0. The difference between the uniform and the triangular or *Provisions* patterns is an

<sup>&</sup>lt;sup>3</sup>To determine the demand-to-capacity ratio on the basis of an elastic analysis, multiply all the values listed in Table 3.2-6 by R = 8. With this modification, the ratios are an approximation of the ductility demand for the individual elements.

indicator that the results of a capacity-spectrum analysis of the system will be quite sensitive to the lateral force pattern applied to the structure when performing the pushover analysis.

The equivalent-lateral-force (ELF) base shear, 746 kips (see Table 3.2-3), when divided by the *Provisions* pattern capacity, 2886 kips, is 0.26. This is reasonably consistent with the demand to capacity ratios shown in Figure 3.2-5.

Before proceeding, three important points should be made:

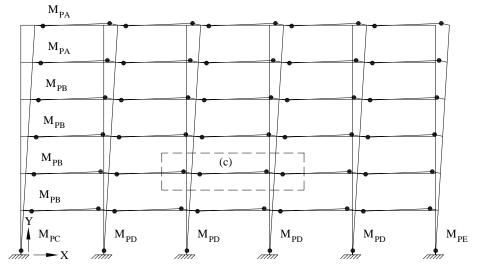
- 1. The rigid-plastic analysis did not include strain hardening, which is an additional source of overstrength.
- 2. The rigid-plastic analysis did not consider the true behavior of the panel zone region of the beam-column joint. Yielding in this area can have a significant effect on system strength.
- 3. Slightly more than 10 percent of the system strength comes from plastic hinges that form in the columns. If the strength of the column is taken simply as  $M_p$  (without the influence of axial force), the "error" in total strength is less than 1 percent.

Table 3.2-7 Lateral Strength on Basis of Rigid-Plastic Mechanism					
Lataral Load Dattarn	Lateral Strength (kips)	Lateral Strength (kips)			
Lateral Load Pattern	Entire Structure	Single Frame			
Uniform	3,850	1,925			
Upper Triangular	3,046	1,523			
Provisions	2,886	1,443			

# 3.2.4 Description of Model Used for Detailed Structural Analysis

Nonlinear-static and -dynamic analyses require a much more detailed model than was used in the linear analysis. The primary reason for the difference is the need to explicitly represent yielding in the girders, columns, and panel zone region of the beam-column joints.

The DRAIN model used for the nonlinear analysis is shown in Figure 3.2-7. A detail of a girder and its connection to two interior columns is shown in Figure 3.2-8. The detail illustrates the two main features of the model: an explicit representation of the panel zone region and the use of concentrated (Type 4 element) plastic hinges in the girders.





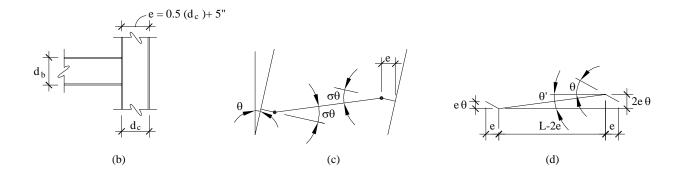


Figure 3.2-6 Plastic mechanism for computing lateral strength.

In Figure 3.2-7, the column shown to the right of the structure is used to represent P-delta effects. See Sec. 3.2.3.2 of this example for details.

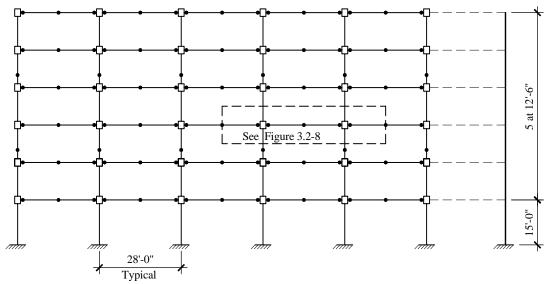


Figure 3.2-7 Detailed analytical model of 6-story frame.

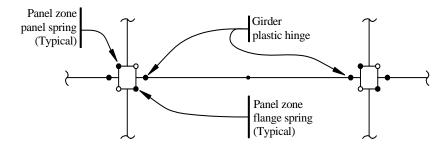


Figure 3.2-8 Model of girder and panel zone region.

The development of the numerical properties used for panel zone and girder hinge modeling is not straightforward. For this reason, the following theoretical development is provided before proceeding with the example.

# 3.2.4.1 Plastic Hinge Modeling and Compound Nodes

In the analysis described below, much use is made of compound nodes. These nodes are used to model plastic hinges in girders and, through a simple transformation process, deformations in the panel zone region of beam-column joints.

A compound node typically consists of a pair of single nodes with each node sharing the same point in space. The X and Y degrees of freedom of the first node of the pair (the slave node) are constrained to be equal to the X and Y degrees of freedom of the second node of the pair (the master node), respectively. Hence, the compound node has four degrees of freedom: an X displacement, a Y displacement, and two independent rotations.

In most cases, one or more rotational spring connection elements (DRAIN element Type 4) are placed between the two single nodes of the compound node, and these springs develop bending moment in resistance to the relative rotation between the two single nodes. If no spring elements are placed between the two single nodes, the compound node acts as a moment-free hinge. A typical compound node with a single rotational spring is shown in Figure 3.2-9. The figure also shows the assumed bilinear, inelastic moment-rotation behavior for the spring.

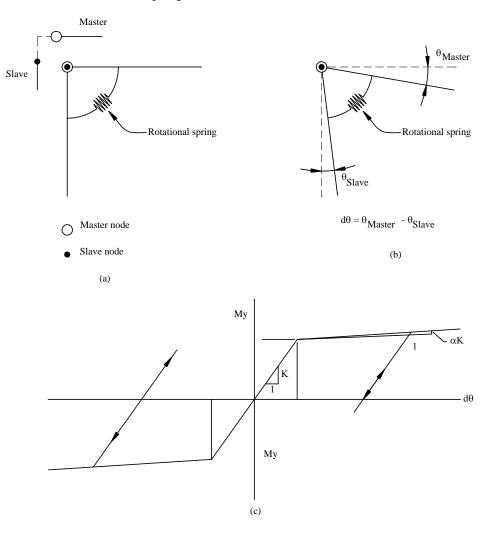


Figure 3.2-9 A compound node and attached spring.

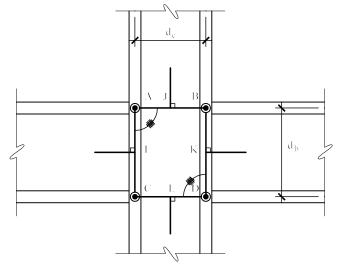


Figure 3.2-10 Krawinkler beam-column joint model.

# 3.2.4.2 Modeling of Beam-Column Joint Regions

A very significant portion of the total story drift of a moment-resisting frame may be due to deformations that occur in the panel zone region of the beam-column joint. In this example, panel zones are modeled using an approach developed by Krawinkler (1978). This model, illustrated in Figure 3.2-10, has the advantage of being conceptually simple, yet robust. The disadvantage of the approach is that the number of degrees of freedom required to model a structure is significantly increased.

A simpler model, often referred to as the scissors model, also has been developed to represent panel zone behavior. The scissors model has the advantage of using fewer degrees of freedom. However, due to its simplicity, it is generally considered to inadequately represent the kinematics of the problem.<sup>4</sup> For this reason, the scissors model is not used here.

The Krawinkler model assumes that the panel zone area has two resistance mechanisms acting in parallel:

- 1. Shear resistance of the web of the column, including doubler plates and
- 2. Flexural resistance of the flanges of the column.

These two resistance mechanisms are apparent in AISC Seismic Eq. (9-1), which is used for determining panel zone shear strength:

<sup>&</sup>lt;sup>4</sup>The author of this example is completing research at Virginia Tech to determine whether the scissors model is adequate to model steel moment frames. Preliminary results indicate that the kinematics error is not significant and that very good results may be obtained by a properly formulated scissors model.

$$R_{v} = 0.6F_{y}d_{c}t_{p}\left[1 + \frac{3b_{cf}t_{cf}^{2}}{d_{b}d_{c}t_{p}}\right]$$

The equation can be rewritten as:

$$R_{v} = 0.6F_{y}d_{c}t_{p} + 1.8\frac{F_{y}b_{cf}t_{cf}^{2}}{d_{b}} \equiv V_{Panel} + 1.8V_{Flanges}$$

where the first term is the panel shear resistance and the second term is the plastic flexural resistance of the column flange. The terms in the equations are defined as follows:

- $F_y$  = yield strength of the column and the doubler plate,  $d_c$  = total depth of column,
- $t_p$  = thickness of panel zone region = column web thickness plus doubler plate thickness,  $b_{cf}$  = width of column flange,
- $t_{cf}$  = thickness of column flange, and  $d_b$  = total depth of girder.

Additional terms used in the subsequent discussion are:

- $t_{bf}$  = girder flange thickness and G = shear modulus of steel.

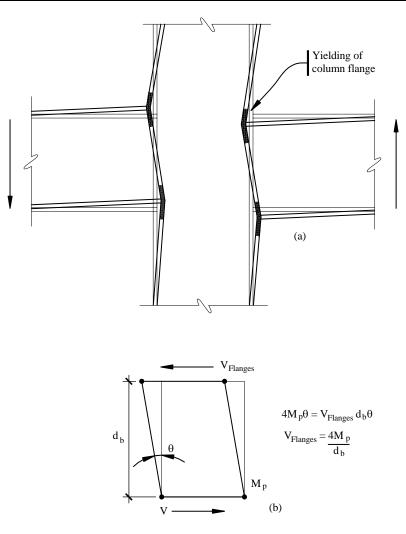


Figure 3.2-11 Column flange component of panel zone resistance.

The panel zone shear resistance  $(V_{Panel})$  is simply the effective shear area of the panel  $d_c t_p$  multiplied by the yield stress in shear, assumed as  $0.6F_y$ . (The 0.6 factor is a simplification of the Von Mises yield criterion that gives the yield stress in shear as  $1/\sqrt{3} = 0.577$  times the strength in tension.)

The second term,  $1.8V_{Flanges}$ , is based on experimental observation. Testing of simple beam-column subassemblies show that a "kink" forms in the column flanges as shown in Figure 3.2-11(a). If it can be assumed that the kink is represented by a plastic hinge with a plastic moment capacity of  $M_p = F_y Z = F_y b_{cf} t_{cf}^2/4$ , it follows from virtual work (see Figure 3.2-11b) that the equivalent shear strength of the column flanges is:

$$V_{Flanges} = \frac{4M_p}{d_b}$$

and by simple substitution for  $M_p$ :

$$V_{Flanges} = \frac{F_y b_{cf} t_{cf}^2}{d_b}$$

This value does not include the 1.8 multiplier that appears in the AISC equation. This multiplier is based on experimental results. It should be noted that the flange component of strength is small compared to the panel component unless the column has very thick flanges.

The shear stiffness of the panel is derived as shown in Figure 3.2-12:

$$K_{Panel,\gamma} = \frac{V_{Panel}}{\gamma} = \frac{V_{Panel}}{\delta/d_b}$$

noting that the displacement  $\delta$  can be written as:

$$\delta = \frac{V_{Panel}d_b}{Gt_pd_c},$$

$$K_{Panel,\gamma} = \frac{V_{Panel}}{\left(\frac{V_{Panel}d_b}{Gt_pd_c}\right)\frac{1}{d_b}} = Gt_pd_c$$

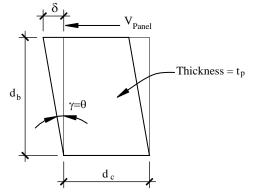


Figure 3.2-12 Column web component of panel zone resistance.

Krawinkler assumes that the column flange component yields at four times the yield deformation of the panel component, where the panel yield deformation is:

$$\gamma_y = \frac{V_{Panel}}{K_{Panel,\gamma}} = \frac{0.6F_y d_c t_p}{G d_c t_p} = \frac{0.6F_y}{G} \,.$$

At this deformation, the panel zone strength is  $V_{Panel} + 0.25_{Vflanges}$ ; at four times this deformation, the strength is  $V_{Panel} + V_{Flanges}$ . The inelastic force-deformation behavior of the panel is illustrated in Figure 3.2-13. This figure is applicable also to exterior joints (girder on one side only), roof joints (girders on both sides, column below only), and corner joints (girder on one side only, column below only).

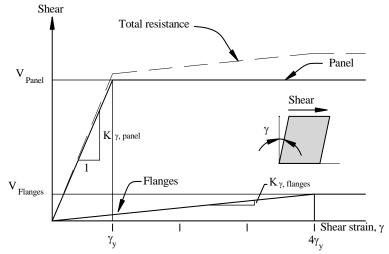


Figure 3.2-13 Force-deformation behavior of panel zone region.

The actual Krawinkler model is shown in Figure 3.2-10. This model consists of four rigid links, connected at the corners by compound nodes. The columns and girders frame into the links at right angles at Points I through L. These are moment-resisting connections. Rotational springs are used at the upper left (point A) and lower right (point D) compound nodes. These springs are used to represent the panel resistance mechanisms described earlier. The upper right and lower left corners (points B and C) do not have rotational springs and thereby act as real hinges.

The finite element model of the joint requires 12 individual nodes: one node each at Points I through L, and two nodes (compound node pairs) at Points A through D. It is left to the reader to verify that the total number of degrees of freedom in the model is 28 (if the only constraints are associated with the corner compound nodes).

The rotational spring properties are related to the panel shear resistance mechanisms by a simple transformation, as shown in Figure 3.2-14. From the figure it may be seen that the moment in the rotational spring is equal to the applied shear times the beam depth. Using this transformation, the properties of the rotational spring representing the panel shear component of resistance are:

 $M_{Panel} = V_{Panel}d_b = 0.6F_yd_cd_bt_p$ 

 $K_{Panel,\theta} = K_{Panel,\gamma}d_b = Gd_cd_bt_p$ 

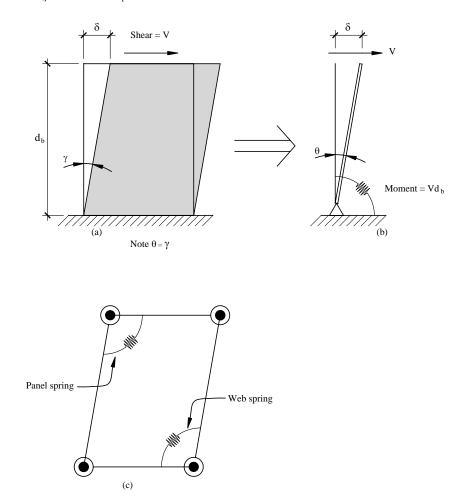


**Figure 3.2-14** Transforming shear deformation to rotational deformation in the Krawinkler model.

It is interesting to note that the shear strength in terms of the rotation spring is simply  $0.6F_y$  times the volume of the panel, and the shear stiffness in terms of the rotational spring is equal to *G* times the panel volume.

The flange component of strength in terms of the rotational spring is determined in a similar manner:

~

$$M_{Flanges} = 1.8V_{Flanges}d_b = 1.8F_y b_{cf}t_{cf}^2$$

Because of the equivalence of rotation and shear deformation, the yield rotation of the panel is the same as the yield strain in shear:

$$\theta_{y} = \gamma_{y} = \frac{M_{Panel}}{K_{Panel,\theta}} = \frac{0.6F_{y}}{G} \, .$$

To determine the initial stiffness of the flange spring, it is assumed that this spring yields at four times the yield deformation of the panel spring. Hence,

$$K_{Flanges,\theta} = \frac{M_{Flanges}}{4\theta_{y}} = 0.75Gb_{cf}t_{cf}^2$$
.

The complete resistance mechanism, in terms of rotational spring properties, is shown in Figure 3.2-13. This trilinear behavior is represented by two elastic-perfectly plastic springs at the opposing corners of the joint assemblage.

If desired, strain-hardening may be added to the system. Krawinkler suggests using a strain-hardening stiffness equal to 3 percent of the initial stiffness of the joint. In this analysis, the strain- hardening component was simply added to both the panel and the flange components:

$$K_{SH,\theta} = 0.03(K_{Panel,\theta} + K_{Flanges,\theta}) \,. \label{eq:K_share}$$

Before continuing, one minor adjustment is made to the above derivations. Instead of using the nominal total beam and girder depths in the calculations, the distance between the center of the flanges was used as the effective depth. Hence:

$$d_c \equiv d_{c,nom} - t_{cf}$$

where the *nom* part of the subscript indicates the property listed as the total depth in the AISC Manual of Steel Construction.

The Krawinkler properties are now computed for a typical interior subassembly of the 6-story frame. A summary of the properties used for all connections is shown in Table 3.2-8.

	Table 3.2-8         Properties for the Krawinkler Beam-Column Joint Model						
Connection	Girder	Column	Doubler Plate (in.)	$M_{_{panel, heta}}\ ( ext{ink})$	$K_{panel, heta}$ (ink/rad)	$M_{flanges,  heta}$ (ink/rad)	$K_{flanges,q}$ (ink/rad)
А	W24x84	W21x122	_	8,701	3,480,000	1,028	102,800
В	W24x84	W21x122	1.00	23,203	9,281,000	1,028	102,800
С	W27x94	W21x147	_	11,822	4,729,000	1,489	148,900
D	W27x94	W21x147	1.00	28,248	11,298,000	1,489	148,900
E	W27x94	W21x201	_	15,292	6,117,000	3,006	300,600
F	W27x94	W21x201	0.875	29,900	11,998,000	3,006	300,600

Example calculations shown for row in **bold** type.

The sample calculations below are for Connection D in Table 3.2-8.

Material Properties:

 $F_y = 50.0$  ksi (girder, column, and doubler plate) G = 12,000 ksi

Girder:

W27x94	
$d_{b,nom}$	26.92 in.
$t_f$	0.745 in.
$d_b$	26.18 in.

#### Column:

W21x147	
$d_{c,nom}$	22.06 in.
$t_w$	0.72 in.
$t_{cf}$	1.150 in.
$d_c$	20.91 in.
$b_{cf}$	12.51 in.

Doubler plate: 1.00 in.

Total panel zone thickness =  $t_p = 0.72 + 1.00 = 1.72$  in.

$$V_{Panel} = 0.6F_y d_c t_p = 0.6(50)(20.91)(1.72) = 1,079$$
 kips

$$V_{Flanges} = 1.8 \frac{F_y b_{cf} t_{cf}^2}{d_b} = 1.8 \frac{50(12.51)(1.15^2)}{26.18} = 56.9$$
 kips

 $K_{Panel,\gamma} = Gt_p d_c = 12,000(1.72)(20.91) = 431,582$  kips/unit shear strain

$$\gamma_y = \theta_y = \frac{0.6F_y}{G} = \frac{0.6(50,000)}{12,000} = 0.0025$$

 $M_{Panel} = V_{Panel} d_b = 1,079(26.18) = 28,248$  in.-kips

$$K_{Panel,\theta} = K_{Panel,\gamma} d_b = 431,582(26.18) = 11,298,000$$
 in.-kips/radian

 $M_{Flanges} = V_{Flanges} d_b = 56.9(26.18) = 1,489$  in.-kips

$$K_{Flanges,\theta} = \frac{M_{Flanges}}{4\gamma_v} = \frac{1,489}{4(0.0025)} = 148,900$$
 in.-kips/radian

#### 3.2.4.3 Modeling Girders

Because this structure is designed in accordance with the strong-column/weak-beam principle, it is anticipated that the girders will yield in flexure. Although DRAIN provides special yielding beam elements (Type 2 elements), more control over behavior is obtained through the use of the Type 4 connection element.

The modeling of a typical girder is shown in Figure 3.2-8. This figure shows an interior girder, together with the panel zones at the ends. The portion of the girder between the panel zones is modeled as four segments with one simple node at mid span and one compound node near each end. The mid-span node is used to enhance the deflected shape of the structure.<sup>5</sup> The compound nodes are used to represent inelastic behavior in the hinging region.

The following information is required to model each plastic hinge:

- 1. The initial stiffness (moment per unit rotation),
- 2. The effective yield moment,
- 3. The secondary stiffness, and
- 4. The location of the hinge with respect to the face of the column.

Determination of the above properties, particularly the location of the hinge, is complicated by the fact that the plastic hinge grows in length during increasing story drift. Unfortunately, there is no effective way to represent a changing hinge length in DRAIN, so one must make do with a fixed hinge length and location. Fortunately, the behavior of the structure is relatively insensitive to the location of the hinges.

<sup>&</sup>lt;sup>5</sup>A graphic post-processor was used to display the deflected shape of the structure. The program represents each element as a straight line. Although the computational results are unaffected, a better graphical representation is obtained by subdividing the member.

To determine the hinge properties, it is necessary to perform a moment-curvature analysis of the cross section, and this, in turn, is a function of the stress-strain curve of the material. In this example, a relatively simple stress-strain curve is used to represent the 50 ksi steel in the girders. This curve does not display a yield plateau, which is consistent with the assumption that the section has yielded in previous cycles, with the Baushinger effect erasing any trace of the yield plateau. The idealized stress-strain curve is shown in Figure 3.2-15.

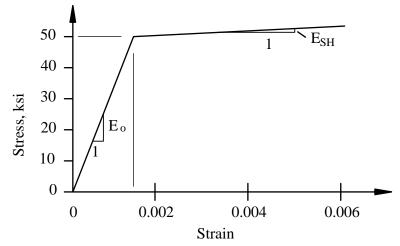


Figure 3.2-15 Assumed stress-strain curve for modeling girders.

To compute the moment-curvature relationship, the girder cross section was divided into 50 horizontal slices, with 10 slices in each flange and 30 slices in the web. The girder cross section was then subjected to gradually increasing rotation. For each value of rotation, strain compatibility (plane sections remain plane) was used to determine fiber strain. Fiber stress was obtained from the stress-strain law and stresses were multiplied by fiber area to determine fiber force. The forces were then multiplied by the distance to the neutral axis to determine that fiber's contribution to the section's resisting moment. The fiber contributions were summed to determine the total resisting moment. Analysis was performed using a Microsoft Excel worksheet. Curves were computed for an assumed strain hardening ratio of 1, 3, and 5 percent of the initial stiffness. The resulting moment-curvature relationship is shown for the W27x94 girder in Figure 3.2-16. Because of the assumed bilinear stress-strain curve, the moment-curvature relationships are essentially bilinear. Residual stresses due to section rolling were ignored, and it was assumed that local buckling of the flanges or the web would not occur.

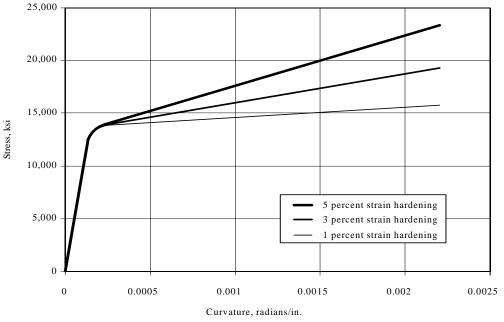
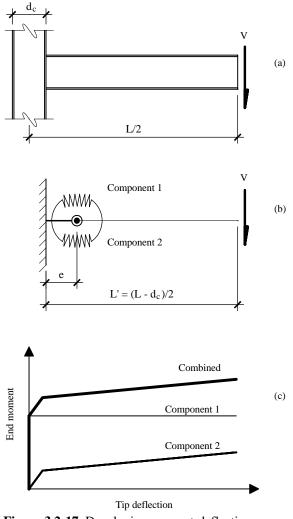


Figure 3.2-16 Moment curvature diagram for W27x94 girder.

To determine the parameters for the plastic hinge in the DRAIN model, a separate analysis was performed on the structure shown in Figure 3.2-17(a). This structure represents half of the clear span of the girder supported as a cantilever. The purpose of the special analysis was to determine a moment-deflection relationship for the cantilever loaded at the tip with a vertical force V. A similar moment-deflection relationship was determined for the structure shown in Figure 3.2-17(b), which consists of a cantilever with a compound node used to represent the inelastic rotation in the plastic hinge. Two Type-4 DRAIN elements were used at each compound node. The first of these is rigid-perfectly plastic and the second is bilinear. The resulting behavior is illustrated in Figure 3.2-17(c).

If the moment-curvature relationship is idealized as bilinear, it is a straightforward matter to compute the deflections of the structure of Figure 3.2-17(a). The method is developed in Figure 3.2-18. Figure 3.2-18(a) is a bilinear moment-curvature diagram. The girder is loaded to some moment M, which is greater than the yield moment. The moment diagram for the member is shown in Figure 3.2-18(b). At some distance x the moment is equal to the yield moment:

$$x = \frac{M_y L}{M}$$



**Figure 3.2-17** Developing moment-deflection diagrams for a typical girder.

The curvature along the length of the member is shown in Figure 3.2-18(c). At the distance *x*, the curvature is the yield curvature ( $\phi_y$ ), and at the support, the curvature ( $\phi_M$ ) is the curvature corresponding to the Point M on the moment-curvature diagram. The deflection is computed using the moment-area method, and consists of three parts:

$$\Delta_{1} = \frac{\phi_{y}x}{2} \cdot \frac{2x}{3} = \frac{\phi_{y}x^{2}}{3}$$
$$\Delta_{2} = \phi_{y}(L'-x)\frac{L'+x}{2} = \frac{\phi_{y}(L'-x)(L'+x)}{2}$$

$$\Delta_{3} = \frac{(\phi_{M} - \phi_{y})(L' - x)}{2} \cdot \left[x + \frac{2(L' - x)}{3}\right]$$
$$= \frac{(\phi_{M} - \phi_{y})(L' - x)(2L' + x)}{6}$$

The first two parts of the deflection are for elastic response and the third is for inelastic response. The elastic part of the deflection is handled by the Type-2 elements in Figure 3.2-17(b). The inelastic part is represented by the two Type-4 elements at the compound node of the structure.

The development of the moment-deflection relationship for the W27x94 girder is illustrated in Figure 3.2-19. Part (a) of the figure is the idealized bilinear moment-curvature relationship for 3 percent strain hardening. Displacements were computed for 11 points on the structure. The resulting moment-deflection diagram is shown in Figure 3.2-19(b), where the total deflection  $(\varDelta_1 + \varDelta_2 + \varDelta_3)$  is indicated. The inelastic part of the deflection  $(\varDelta_3 \text{ only})$  is shown separately in Figure 3.2-19(c), where the moment axis has been truncated below 12,000 in.-kips.

Finally, the simple DRAIN cantilever model of Figure 3.2-17(b) is analyzed. The compound node has arbitrarily been placed a distance e = 5 in. from the face of the support. (The analysis is relatively insensitive to the assumed hinge location.)

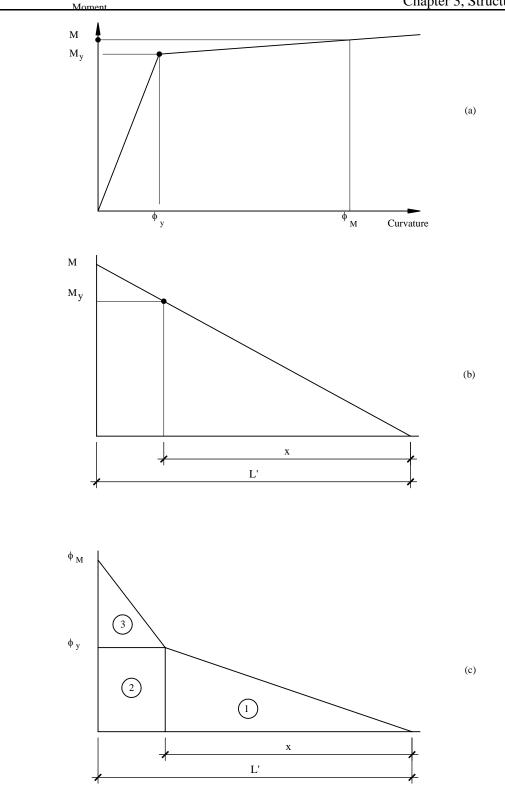


Figure 3.2-18 Development of equations for deflection of moment-deflection curves.

The moment diagram is shown in Figure 3.2-20(a) for the model subjected to a load producing a support moment,  $M_s$ , greater than the yield moment. The corresponding curvature diagram is shown in Figure 3.2-20(b). At the location of the plastic hinge, the moment is:

$$M_H = M_S \frac{(L'-e)}{L'}$$

and all inelastic curvature is concentrated into a plastic hinge with rotation  $\theta_{H}$ . The tip deflection of the structure of Figure 3.2-20(c) consists of two parts:

$$\Delta_E = \frac{M_{Support} L'^2}{3EI}$$

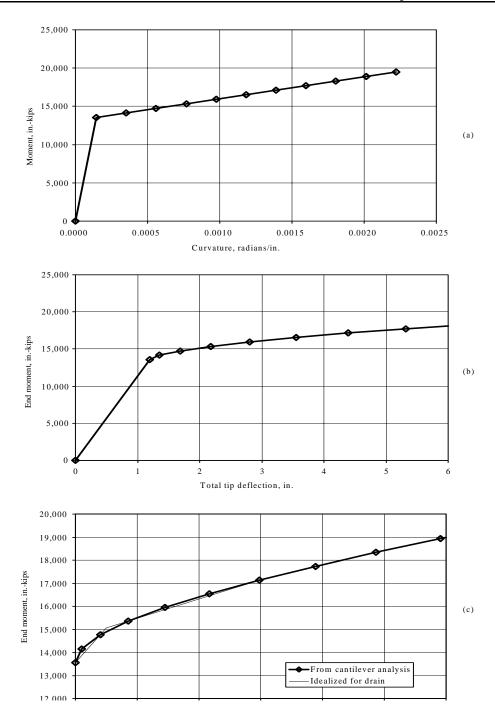


**Figure 3.2-19** Moment-deflection curve for W27x94 girder with 3 percent strain hardening.

 $\Delta_I = \theta_H (L' - e) \,.$ 

The first part is the elastic deflection and the second part is the inelastic deflection. Note that  $\Delta_E$  and  $(\Delta_1 + \Delta_2)$  are not quite equal because the shapes of the curvature diagram used to generate the deflections are not the same. For the small values of strain hardening assumed in this analysis, however, there is little error in assuming that the two deflections are equal. As  $\Delta_E$  is simply the elastic displacement of a simple cantilever beam, it is possible to model the main portion of the girder using its nominal moment of inertia. The challenge is to determine the properties of the two Type-4 elements such that the deflections predicted using  $\Delta_I$  are close to those produced using  $\Delta_3$ . This is a trial-and-error procedure, which is difficult to reproduce in this example. However, the development of the hinge properties is greatly facilitated by the fact that one component of the hinge must be rigid-plastic, with the second component being bilinear. The resulting "fit" for the W27x94 girder is shown in Figure 3.2-19. The resulting properties for the model are shown in Table 3.2-9. The properties for the W24x84 girder are also shown in the table. Note that the first yield of the model will be the yield moment from Component 1, and that this moment is roughly equal to the fully plastic moment of the section.

	Table 3.2-9         Girder Properties as Mode		o <b>n</b>	
Property —		Section		
	· r · · · ·	W24x84	W27x94	
Elastic Properties	Moment of Inertia (in. <sup>4</sup> )	2,370	3,270	
	Shear Area (in. <sup>2</sup> )	11.3	13.2	
Inelastic Component 1 (see note below)	Yield Moment (inkip)	11,025	13,538	
	Initial Stiffness (inkip/radian)	10E10	10E10	
Inelastic Component 2	S.H. Ratio	0.0	0.0	
	Yield Moment (inkip)	1,196	1,494	
	Initial Stiffness (inkip/radian)	326,000	450,192	
Comparative Property	S.H. Ratio	0.284	0.295	
	Yield Moment = $S_x F_y$	9,800	12,150	
	Plastic Moment = $Z_x F_y$	11,200	13,900	

In some versions of DRAIN the strain hardening stiffness of the Type-4 springs is set to some small value (e.g. 0.001) if a zero value is entered in the appropriate data field. This may cause very large artificial strain hardening moments to develop in the hinge after it yields. It is recommended, therefore, to input a strain hardening value of  $10^{-20}$  to prevent this from happening.

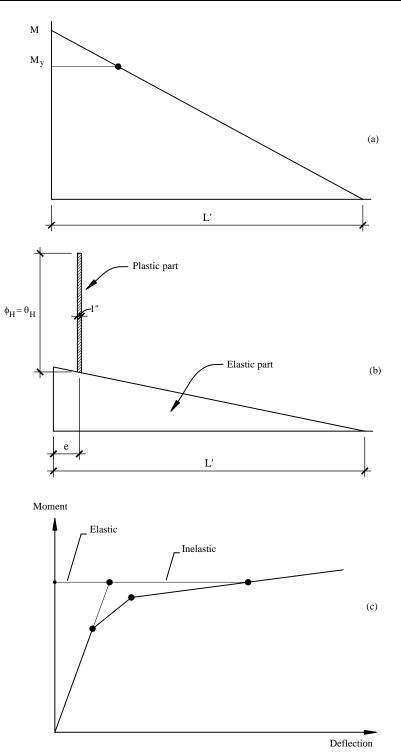


**Figure 3.2-20** Development of plastic hinge properties for the W27x97 girder.

## 3.2.4.4 Modeling Columns

All columns in the analysis were modeled as Type-2 elements. Preliminary analysis indicated that columns should not yield, except at the base of the first story. Subsequent analysis showed that the columns will yield in the upper portion of the structure as well. For this reason, column yielding had to be activated in all of the Type-2 column elements. The columns were modeled using the built-in yielding functionality of the DRAIN program, wherein the yield moment is a function of the axial force in the column. The yield surface used by DRAIN is shown in Figure 3.2-21.

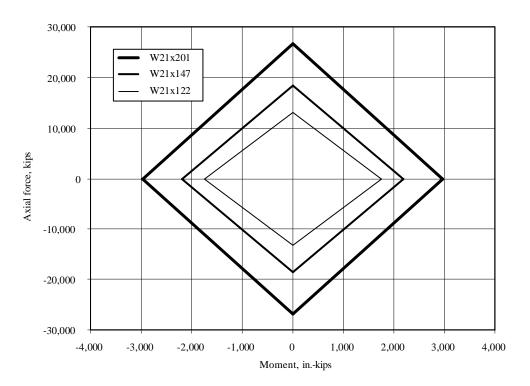


Figure 3.2-21 Yield surface used for modeling columns.

The rules employed by DRAIN to model column yielding are adequate for event-to-event nonlinear static pushover analysis, but leave much to be desired when dynamic analysis is performed. The greatest difficulty in the dynamic analysis is adequate treatment of the column when unloading and reloading. An assessment of the effect of these potential problems is beyond the scope of this example.

### 3.2.5 Static Pushover Analysis

Nonlinear static analysis is covered for the first time in the Appendix to Chapter 5 of the 2000 *Provisions*. Inclusion of these requirements in an appendix rather than the main body indicates that pushover analysis is in the developmental stage and may not be "ready for prime time." For this reason, some liberties are taken in this example; however, for the most part, the example follows the appendix. [In the 2003

*Provisions*, a number of substantive technical changes have been made to the appendix, largely as a result of work performed by the Applied Technology Council in Project 55, Evaluation and Improvement of Inelastic Seismic Analysis Procedures).]

Nonlinear static pushover analysis, in itself, provides the location and sequence of expected yielding in a structure. Additional analysis is required to estimate the amount of inelastic deformation that may occur during an earthquake. These inelastic deformations may then be compared to the deformations that have been deemed acceptable under the ground motion parameters that have been selected. *Provisions* Sec. 5A.1.3 [Appendix to Chapter 5] provides a simple methodology for estimating the inelastic deformations but does not provide specific acceptance criteria.

Another well-known method for determining maximum inelastic displacement is based on the capacity spectrum approach. This method is described in some detail in ATC 40 (Applied Technology Council, 1996). The capacity spectrum method is somewhat controversial and, in some cases may produce unreliable results (Chopra and Goel, 1999). However, as the method is still very popular and is incorporated in several commercial computer programs, it will be utilized here, and the results obtained will be compared to those computed using the simple approach.

*Provisions* Sec. 5A1.1 [A5.2.1] discusses modeling requirements for the pushover analysis in relatively vague terms, possibly reflecting the newness of the approach. However, it is felt that the model of the structure described earlier in this example is consistent with the spirit of the *Provisions*.<sup>6</sup>

The pushover curve obtained from a nonlinear static analysis is a function of the way the structure is both modeled and loaded. In the analysis reported herein, the structure was first subjected to the full dead load plus reduced live load followed by the lateral loads. The *Provisions* states that the lateral load pattern should follow the shape of the first mode. In this example, four different load patterns were initially considered:

- UL = uniform load (equal force at each level)
- TL = triangular (loads proportional to height)
- ML = modal load (lateral loads proportional to first mode shape)
- BL = *Provisions* load distribution (using the forces indicated in Table 3.2-3)

Relative values of these load patterns are summarized in Table 3.2-10. The loads have been normalized to a value of 15 kips at Level 2. Because of the similarity between the TL and ML distributions, the results from the TL distribution are not presented.

DRAIN analyses were run with P-delta effects included and, for comparison purposes, with such effects excluded. The *Provisions* requires "the influence of axial loads" to be considered when the axial load in the column exceeds 15 percent of the buckling load but presents no guidance on exactly how the buckling load is to be determined nor on what is meant by "influence." In this analysis the influence was taken as inclusion of the story-level P-delta effect. This effect may be easily represented through linearized geometric stiffness, which is the basis of the outrigger column shown in Figure 3.2-4. Consistent

<sup>&</sup>lt;sup>6</sup>The mathematical model does not represent strength loss due to premature fracture of welded connections. If such fracture is likely, the mathematical model must be adjusted accordingly.

geometric stiffness, which may be used to represent the influence of axial forces on the flexural flexibility of individual columns, may not be used directly in DRAIN. Such effects may be approximated in DRAIN by subdividing columns into several segments and activating the linearized geometric stiffness on a column-by-column basis. That approach was not used here.

Level	Uniform Load UL (kips)	Triangular Load TL (kips)	Modal Load ML (kips)	BSSC Load BL (kips)
R	15.0	77.5	88.4	150.0
6	15.0	65.0	80.4	118.0
5	15.0	52.5	67.8	88.0
4	15.0	40.0	50.3	60.0
3	15.0	27.5	32.0	36.0
2	15.0	15.0	15.0	15.0

 Table 3.2-10
 Lateral Load Patterns Used in Nonlinear Static Pushover Analysis

As described later, the pushover analysis indicated all yielding in the structure occurred in the clear span of the girders and columns. Panel zone hinging did not occur. For this reason, the ML analysis was repeated for a structure with thinner doubler plates and without doubler plates. Because the behavior of the structure with thin doubler plates was not significantly different from the behavior with the thicker plates, the only comparison made here will be between the structures with and without doubler plates. These structures are referred to as the strong panel (SP) and weak panel (WP) structures, respectively.

The analyses were carried out using the DRAIN-2Dx computer program. Using DRAIN, an analysis may be performed under "load control" or under "displacement control." Under load control, the structure is subjected to gradually increasing lateral loads. If, at any load step, the tangent stiffness matrix of the structure has a negative on the diagonal, the analysis is terminated. Consequently, loss of strength due to P-delta effects cannot be tracked. Using displacement control, one particular point of the structure (the control point) is forced to undergo a monotonically increasing lateral displacement and the lateral forces are constrained to follow the desired pattern. In this type of analysis, the structure can display loss of strength because the displacement control algorithm adds artificial stiffness along the diagonal to overcome the stability problem. Of course, the computed response of the structure after strength loss is completely fictitious in the context of a static loading environment. Under a dynamic loading, however, structures can display strength loss and be incrementally stable. It is for this reason that the post-strength-loss realm of the pushover response is of interest.

When performing a displacement controlled pushover analysis in DRAIN with *P*-Delta effects included, one must be careful to recover the base-shear forces properly.<sup>7</sup> At any displacement step in the analysis, the true base shear in the system consists of two parts:

<sup>&</sup>lt;sup>7</sup>If P-delta effects have been included, this procedure needs to be used when recovering base shear from column shear forces. This is true for displacement controlled static analysis, force controlled static analysis, and dynamic time-history analysis.

$$V = \sum_{i=1}^{n} V_{C,i} - \frac{P_1 \Delta_1}{h_1}$$

where the first term represents the sum of all the column shears in the first story and the second term represents the destabilizing P-delta shear in the first story. The P-delta effects for this structure were included through the use of the outrigger column shown at the right of Figure 3.2-4. Figure 3.2-22 plots two base shear components of the pushover response for the SP structure subjected to the ML loading. Also shown is the total response. The kink in the line representing P-delta forces results because these forces are based on first-story displacement, which, for an inelastic system, will not generally be proportional to the roof displacement.

For all of the pushover analyses reported for this example, the maximum displacement at the roof is 42.0 in. This value is slightly greater than 1.5 times the total drift limit for the structure where the total drift limit is taken as 1.25 times 2 percent of the total height. The drift limit is taken from *Provisions* Table 5.2.8 [4.5-1] and the 1.25 factor is taken from *Provisions* Sec. 5A.1.4.3. [In the 2003 *Provisions*, Sec. A5.2.6 requires multiplication by  $0.85R/C_d$  rather than by 1.25.] As discussed below in Sec. 3.2.5.3, the Appendix to Chapter 5 of the *Provisions* requires only that the pushover analysis be run to a maximum displacement of 1.5 times the expected inelastic displacement. If this limit were used, the pushover analysis of this structure would only be run to a total displacement of about 13.5 in.

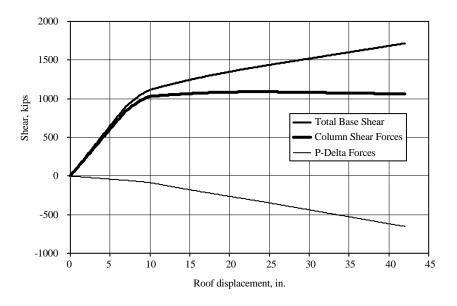
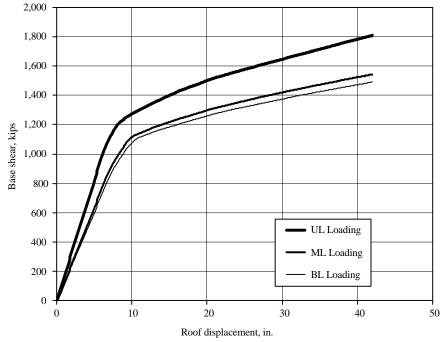


Figure 3.2-22 Two base shear components of pushover response.

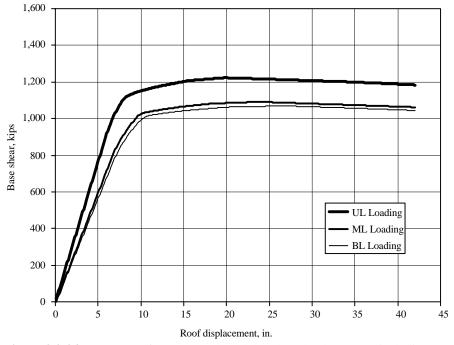
### 3.2.5.1 Pushover Response of Strong Panel Structure

Figure 3.2-23 shows the pushover response of the SP structure to all three lateral load patterns when P-delta effects are excluded. In each case, gravity loads were applied first and then the lateral loads were applied using the displacement control algorithm. Figure 3.2-24 shows the response curves if P-delta effects are included. In Figure 3.2-25, the response of the structure under ML loading with and without

P-delta effects is illustrated. Clearly, P-delta effects are an extremely important aspect of the response of this structure, and the influence grows in significance after yielding. This is particularly interesting in the light of the *Provisions*, which ignore P-delta effects in elastic analysis if the maximum stability ratio is less than 0.10 (see *Provisions* Sec. 5.4.6.2 [5.2.6.2]). For this structure, the maximum computed stability ratio was 0.0839 (see Table 3.2-4), which is less than 0.10 and is also less than the upper limit of 0.0901. The upper limit is computed according to *Provisions* Eq. 5.4.6.2-2 and is based on the very conservative assumption that  $\beta = 1.0$ . While the *Provisions* allow the analyst to exclude P-delta effects in an elastic analysis, this clearly should not be done in the pushover analysis (or in time-history analysis). [In the 2003 *Provisions*, the upper limit for the stability ratio is eliminated. Where the calculated  $\theta$  is greater than 0.10 a special analysis must be performed in accordance with Sec. A5.2.3. Sec. A5.2.1 requires that P-delta effects be considered for all pushover analyses.]



**Figure 3.2-23** Response of strong panel model to three load pattern, excluding P-delta effects.



**Figure 3.2-24** Response of strong panel model to three load patterns, including P-delta effects.

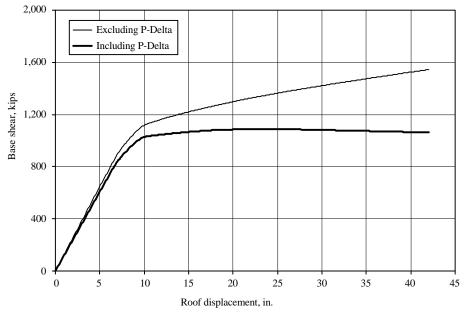
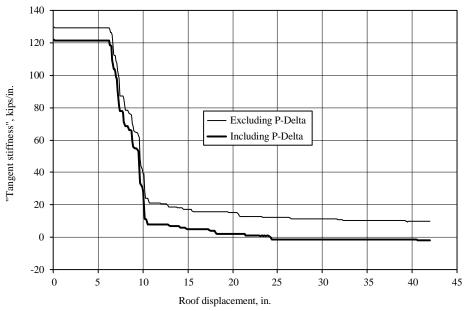


Figure 3.2-25 Response of strong panel model to ML loads, with and wthout P-delta effects.

In Figure 3.2-26, a plot of the tangent stiffness versus roof displacement is shown for the SP structure with ML loading, and with P-delta effects excluded or included. This plot, which represents the slope of the pushover curve at each displacement value, is more effective than the pushover plot in determining when yielding occurs. As Figure 3.2-26 illustrates, the first significant yield occurs at a roof displacement of approximately 6.5 in. and that most of the structure's original stiffness is exhausted by the time the roof drift reaches 10 in.



**Figure 3.2-26** Tangent stiffness history for structure under ML loads, with and without *P*-delta effects.

For the case with P-delta effects excluded, the final stiffness shown in Figure 3.2-26 is approximately 10 kips/in., compared to an original value of 133 kips/in. Hence, the strain-hardening stiffness of the structure is 0.075 times the initial stiffness. This is somewhat greater than the 0.03 (3.0 percent) strain hardening ratio used in the development of the model because the entire structure does not yield simultaneously.

When P-delta effects are included, the final stiffness is -1.6 kips per in. The structure attains this negative residual stiffness at a displacement of approximately 23 in.

### 3.2.5.1.1 Sequence and Pattern of Plastic Hinging

The sequence of yielding in the structure with ML loading and with P-delta effects included is shown in Figure 3.2-27. Part (a) of the figure shows an elevation of the structure with numbers that indicate the sequence of plastic hinge formation. For example, the numeral "1" indicates that this was the first hinge to form. Part (b) of the figure shows a pushover curve with several hinge formation events indicated. These events correspond to numbers shown in part (a) of the figure. The pushover curve only shows selected events because an illustration showing all events would be difficult to read.

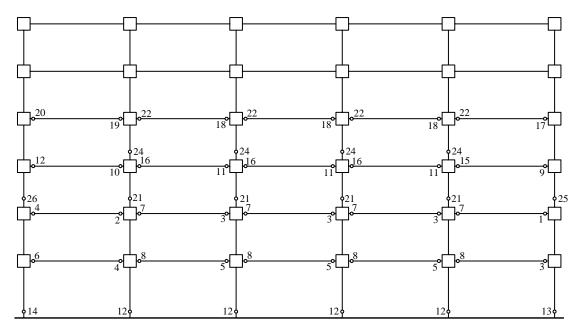
Several important observations are made from Figure 3.2-27:

- 1. There was no hinging in Levels 6 and R,
- 2. There was no hinging in any of the panel zones,
- 3. Hinges formed at the base of all the first-story columns,
- 4. All columns on Story 3 and all the interior columns on Story 4 formed plastic hinges, and
- 5. Both ends of all the girders at Levels 2 through 5 yielded.

It appears the structure is somewhat weak in the middle two stories and is too strong at the upper stories. The doubler plates added to the interior columns prevented panel zone yielding (even at the extreme roof displacement of 42 in.).

The presence of column hinging at Levels 3 and 4 is a bit troublesome because the structure was designed as a strong-column/weak-beam system. This design philosophy, however, is intended to prevent the formation of complete story mechanisms, not to prevent individual column hinging. While hinges did form at the bottom of each column in the third story, hinges did not form at the top of these columns, and a complete story mechanism was avoided.

Even though the pattern of hinging is interesting and useful as an evaluation tool, the performance of the structure in the context of various acceptance criteria cannot be assessed until the expected inelastic displacement can be determined. This is done below in Sec. 3.2.5.3.



(a)

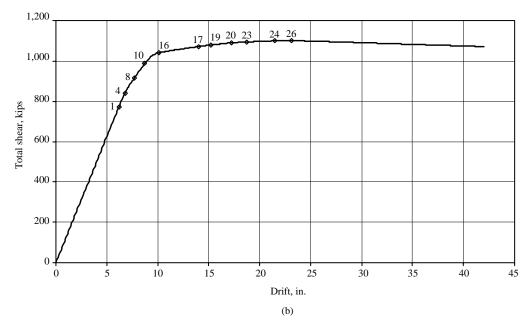


Figure 3.2-27 Patterns of plastic hinge formation: SP model under ML load, including P-delta effects.

## 3.2.5.1.2 Comparison with Strength from Plastic Analysis

It is interesting to compare the strength of the structure from pushover analysis with that obtained from the rigid-collapse analysis performed using virtual work. These values are summarized in Table 3.2-11. The strength from the case with P-delta excluded was estimated from the curves shown in Figure 3.2-23 and is taken as the strength at the principal bend in the curve (the estimated yield from a bilinear representation of the pushover curve). Consistent with the upper bound theorem of plastic analysis, the strength from virtual work is significantly greater than that from pushover analysis. The reason for the difference in predicted strengths is related to the pattern of yielding that actually formed in the structure, compared to that assumed in the rigid-plastic analysis.

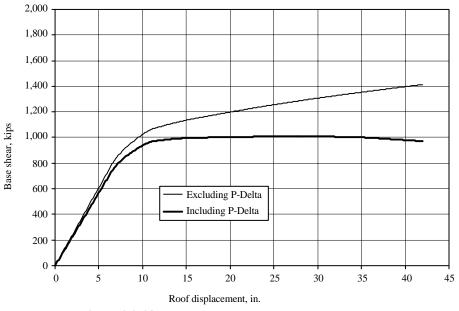
Table 3.2-11         Strength Comparisons: Pushover vs Rigid Plastic				
Pattern	Lateral Strength (kips)			
1 attern	P-delta Excluded	P-delta Included	Rigid-Plastic	
Uniform	1220	1223	1925	
Modal (Triangular)	1137	1101	1523	
BSSC	1108	1069	1443	

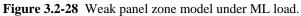
### 3.2.5.2 Pushover Response of Weak Panel Structure

Before continuing, the structure should be re-analyzed without panel zone reinforcing and the behavior compared with that determined from the analysis described above. For this exercise, only the modal load pattern d is considered but the analysis is performed with and without P-delta effects.

The pushover curves for the structure under modal loading and with weak panels are shown in Figure 3.2-28. Curves for the analyses run with and without P-delta effects are included. Figures 3.2-29 and 3.2-30 are more informative because they compare the response of the structures with and without panel zone reinforcement. Figure 3.2-31 shows the tangent stiffness history comparison for the structures with and without doubler plates. In both cases P-delta effects have been included.

From Figures 3.2-28 through 3.2-31 it may be seen that the doubler plates, which represent approximately 2.0 percent of the volume of the structure, increase the strength by approximately 12 percent and increase the initial stiffness by about 10 percent.





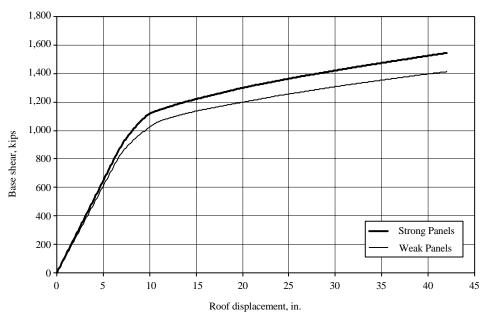


Figure 3.2-29 Comparison of weak panel zone model with strong panel zone model, excluding P-delta effects.

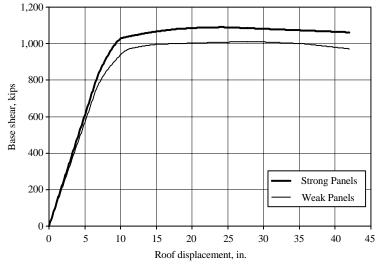


Figure 3.2-30 Comparison of weak panel zone model with strong panel zone model, including P-delta effects.

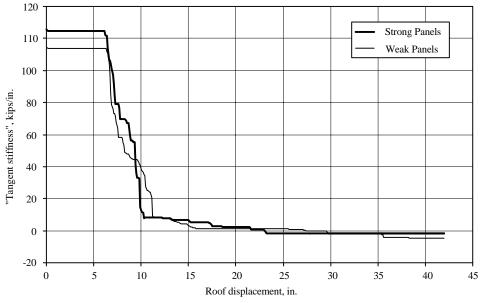
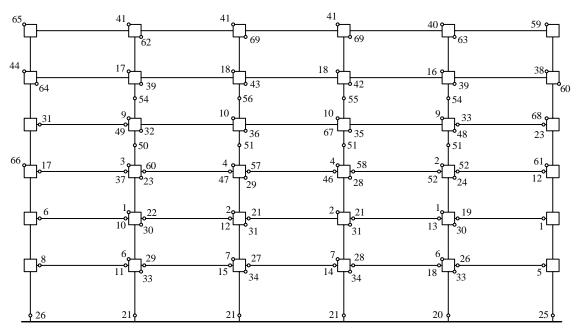
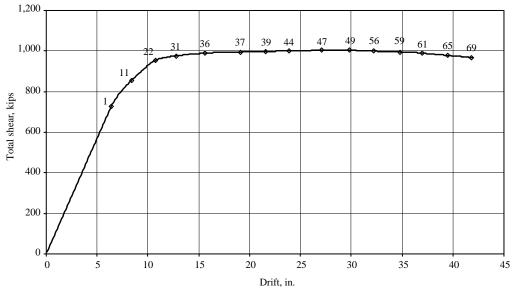


Figure 3.2-31 Tangent stiffness history for structure under ML loads, strong versus weak panels, including P-delta effects.







(b)

**Figure 3.2-32** Patterns of plastic hinge formation: weak panel zone model under ML load, including P-delta effects.

The difference between the behavior of the structures with and without doubler plates is attributed to the yielding of the panel zones in the structure without panel zone reinforcement. The sequence of hinging is illustrated in Figure 3.2-32. Part (a) of this figure indicates that panel zone yielding occurs early. (Panel zone yielding is indicated by a numeric sequence label in the corner of the panel zone.) In fact, the first yielding in the structure is due to yielding of a panel zone at the second level of the structure.

It should be noted that under very large displacements, the flange component of the panel zone yields. Girder and column hinging also occurs, but the column hinging appears relatively late in the response. It is also significant that the upper two levels of the structure display yielding in several of the panel zones.

Aside from the relatively marginal loss in stiffness and strength due to removal of the doubler plates, it appears that the structure without panel zone reinforcement is behaving adequately. Of course, actual performance cannot be evaluated without predicting the maximum inelastic panel shear strain and assessing the stability of the panel zones under these strains.

# 3.2.5.3 Predictions of Total Displacement and Story Drift from Pushover Analysis

In the following discussion, the only loading pattern considered is the modal load pattern discussed earlier. This is consistent with the requirements of *Provisions* Sec. 5A.1.2 [A5.2.2]. The structure with both strong and weak panel zones is analyzed, and separate analyses are performed including and excluding P-delta effects.

# 3.2.5.3.1 Expected Inelastic Displacements Computed According to the Provisions

The expected inelastic displacement was computed using the procedures of *Provisions* Sec. 5.5 [5.3]. In the *Provisions*, the displacement is computed using response-spectrum analysis with only the first mode included. The expected roof displacement will be equal to the displacement computed from the 5-percent-damped response spectrum multiplied by the modal participation factor which is multiplied by the first mode displacement at the roof level of the structure. In the present analysis, the roof level first mode displacement is 1.0.

Details of the calculations are not provided herein. The relevant modal quantities and the expected inelastic displacements are provided in Table 3.2-12. Note that only those values associated with the ML lateral load pattern were used.

Computed Quantity	Strong Panel w/o P-Delta	Strong Panel with P-Delta	Weak Panel w/o P-Delta	Weak Panel with P-Delta
Period (seconds)	1.950	2.015	2.028	2.102
Modal Participation Factor	1.308	1.305	1.315	1.311
Effective Modal Mass (%)	82.6	82.8	82.1	82.2
Expected Inelastic Disp. (in.)	12.31	12.70	12.78	13.33
Base Shear Demand (kips)	1168	1051	1099	987
6 <sup>th</sup> Story Drift (in.)	1.09	1.02	1.12	1.11
5 <sup>th</sup> Story Drift (in.)	1.74	1.77	1.84	1.88
4 <sup>th</sup> Story Drift (in.)	2.28	2.34	2.44	2.53
3 <sup>rd</sup> Story Drift (in.)	2.10	2.73	2.74	2.90
2 <sup>nd</sup> Story Drift (in.)	2.54	2.73	2.56	2.71
1 <sup>st</sup> Story Drift (in.)	2.18	2.23	2.09	2.18

 Table 3.2-12
 Modal Properties and Expected Inelastic Displacements for the Strong and Weak Panel

 Models Subjected to the Modal Load Pattern

As the table indicates, the modal quantities are only slightly influenced by P-delta effects and the inclusion or exclusion of doubler plates. The maximum inelastic displacements are in the range of 12.2 to 13.3 in. The information provided in Figures 3.2-23 through 3.2-32 indicates that at a target displacement of, for example, 13.0 in., some yielding has occurred but the displacements are not of such a magnitude that the slope of the pushover curve is negative when P-delta effects are included.

It should be noted that FEMA 356, *Prestandard and Commentary for the Seismic Rehabilitation of Buildings*, provides a simplified methodology for computing the target displacement that is similar to but somewhat more detailed than the approach illustrated above. See Sec. 3.3.3.2 of FEMA 356 for details.

# 3.2.5.3.2 Inelastic Displacements Computed According to the Capacity Spectrum Method

In the capacity spectrum method, the pushover curve is transformed to a capacity curve that represents the first mode inelastic response of the full structure. Figure 3.2-33 shows a bilinear capacity curve. The horizontal axis of the capacity curve measures the first mode displacement of the simplified system. The vertical axis is a measure of simplified system strength to system weight. When multiplied by the acceleration due to gravity (g), the vertical axis represents the acceleration of the mass of the simple system.

Point E on the horizontal axis is the value of interest, the expected inelastic displacement of the simplified system. This displacement is often called the target displacement. The point on the capacity curve directly above Point E is marked with a small circle, and the line passing from the origin through this point represents the secant stiffness of the simplified system. If the values on the vertical axis are multiplied by the acceleration due to gravity, the slope of the line passing through the small circle is equal to the acceleration divided by the displacement. This value is the same as the square of the circular frequency of the simplified system. Thus, the sloped line is also a measure of the secant period of the simplified structure. As will be shown later, an equivalent viscous damping value ( $\xi_E$ ) can be computed for the simple structure deformed to Point E.

Figure 3.2-34 shows a response spectrum with the vertical axis representing spectral acceleration as a ratio of the acceleration due to gravity and the horizontal axis representing displacement. This spectrum, called a demand spectrum, is somewhat different from the traditional spectrum that uses period of vibration as the horizontal axis. The demand spectrum is drawn for a particular damping value ( $\zeta$ ). Using the demand spectrum, the displacement of a SDOF system may be determined if its period of vibration is known and the system's damping matches the damping used in the development of the demand spectrum. If the system's damping is equal to  $\zeta_E$ , and its stiffness is the same as that represented by the sloped line in Figure 3.2-33, the displacement computed from the demand spectrum will be the same as the expected inelastic displacement shown in Figure 3.2-33.

The capacity spectrum and demand spectrum are shown together in Figure 3.2-35. The demand spectrum is drawn for a damping value exactly equal to  $\xi_E$ , but  $\xi_E$  is not known *a priori* and must be determined by the analyst. There are several ways to determine  $\xi_E$ . In this example, two different methods will be demonstrated: an iterative approach and a semigraphical approach.

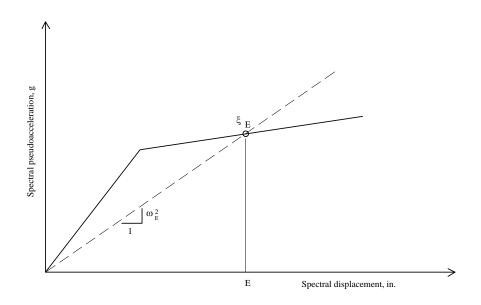


Figure 3.2-33 A simple capacity spectrum.

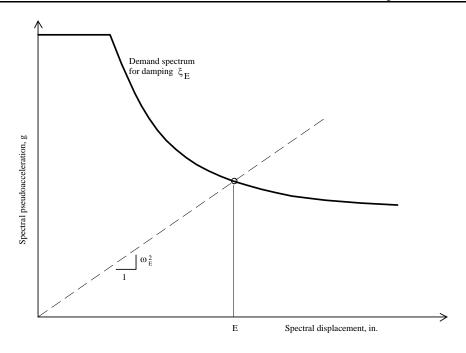


Figure 3.2-34 A simple demand spectrum.

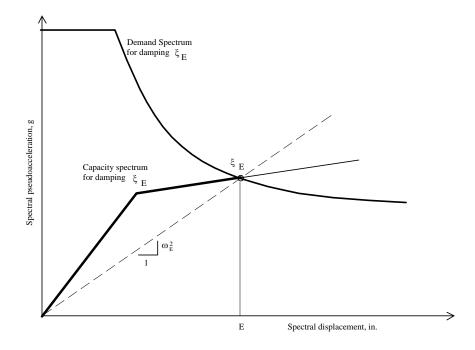


Figure 3.2-35 Capacity and demand spectra plotted together.

The first step in either approach is to convert the pushover curve into a capacity spectrum curve. This is done using the following two transformations:<sup>8</sup>

1. To obtain spectral displacement, multiply each displacement value in the original pushover curve by the quantity:

 $\frac{1}{PF_1\phi_{Roof,1}}$ 

where  $PF_1$  is the modal participation factor for the fundamental mode and  $\phi_{Roof,1}$  is the value of the first mode shape at the top level of the structure. The modal participation factor and the modal displacement must be computed using a consistent normalization of the mode shapes. One must be particularly careful when using DRAIN because the printed mode shapes and the printed modal participation factors use inconsistent normalizations – the mode shapes are normalized to a maximum value of 1.0 and the modal participation factors are based on a normalization that produces a unit generalized mass matrix. For most frame-type structures, the first mode participation factor will be in the range of 1.3 to 1.4 if the mode shapes are normalized for a maximum value of 1.0.

2. To obtain spectral pseudoacceleration, divide each force value in the pushover curve by the total weight of the structure, and then multiply by the quantity:

$$\frac{1}{\alpha_1}$$

where  $\alpha_1$  is the ratio of the effective mass in the first mode to the total mass in the structure. For frame structures,  $\alpha_1$  will be in the range of 0.8 to 0.85. Note that  $\alpha_1$  is not a function of mode shape normalization.

After performing the transformation, convert the smooth capacity curve into a simple bilinear capacity curve. This step is somewhat subjective in terms of defining the effective yield point, but the results are typically insensitive to different values that could be assumed for the yield point. Figure 3.2-36 shows a typical capacity spectrum in which the yield point is represented by points  $a_Y$  and  $d_Y$ . The displacement and acceleration at the expected inelastic displacement are  $d_E$  and  $a_E$ , respectively. The two slopes of the demand spectrum are  $K_I$  and  $K_2$ , and the intercept on the vertical axis is  $a_I$ .

<sup>&</sup>lt;sup>8</sup>Expressions in this section are taken from ATC40 but have been modified to conform to the nomenclature used herein.

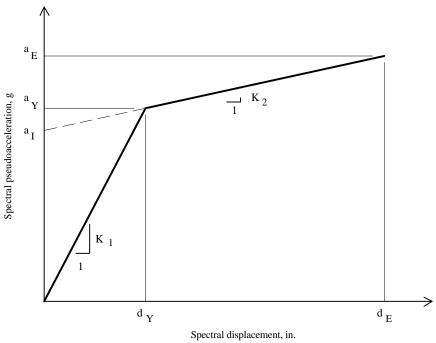


Figure 3.2-36 Capacity spectrum showing control points.

At this point the iterative method and the direct method diverge somewhat. The iterative method will be presented first, followed by the direct method.

Given the capacity spectrum, the iterative approach is as follows:

- I-1. Guess the expected inelastic displacement  $d_E$ . The displacement computed from the simplified procedure of the *Provisions* is a good starting point.
- I-2. Compute the equivalent viscous damping value at the above displacement. This damping value, in terms of percent critical, may be estimated as:

$$\xi_E = 5 + \frac{63.7(a_Y d_E - d_Y a_E)}{a_E d_E}$$

I-3. Compute the secant period of vibration:

$$T_E = \frac{2\pi}{\sqrt{\frac{g \times a_E}{d_E}}}$$

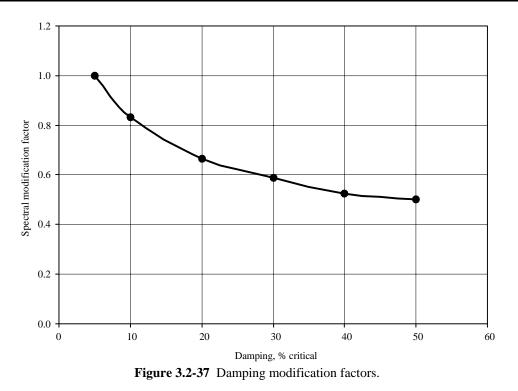
where g is the acceleration due to gravity.

I-4. An estimated displacement must now be determined from the demand spectrum. A damping value of  $\xi_E$  will be assumed in the development of the spectrum. The demand spectrum at this damping value is adapted from the response spectrum given by *Provisions* Sec. 4.1.2.6 [3.3.4]. This spectrum is based on 5 percent of critical damping; therefore, it must be modified for the higher equivalent damping represented by  $\xi_E$ . For the example presented here, the modification factors for systems with higher damping values are obtained from *Provisions* Table 13.3.3.1 [13.3-1], which is reproduced in a somewhat different form as Table 3.2-13 below. In Table 3.2-13, the modification factors are shown as multiplying factors instead of dividing factors as is done in the *Provisions*. The use of the table can be explained by a simple example: the spectral ordinate for a system with 10 percent of critical damping is obtained by multiplying the 5-percent-damped value by 0.833.

The values in Table 3.2-13 are intended for use only for ductile systems without significant strength loss. They are also to be used only in the longer period constant velocity region of the response spectrum. This will be adequate for our needs because the initial period of vibration of our structure is in the neighborhood of 2.0 seconds. See ATC 40 for conditions where the structure does have strength loss or where the period of vibration is such that the constant acceleration region of the spectrum controls. During iteration it may be more convenient to use the information from Table 3.2-13 in graphic form as shown in Figure 3.2-37.

Table 3.2-13 Damping Modification Factors				
Effective Damping (% critical)	Damping Modification Factor			
5	1.000			
10	0.833			
20	0.667			
30	0.588			
40	0.526			
50 or greater	0.500			

 Table 3.2-13
 Damping Modification Factors



I-5. Using the period of vibration computed in Step 3 and the damping computed in Step 4, compute the updated estimate of spectral acceleration  $a_E^{new}$  and convert to displacement using the following expression:

$$d_E^{new} = \frac{g \times a_E^{new}}{\left[2\pi / T_E\right]^2}$$

If this displacement is the same as that estimated in Step 1, the iteration is complete. If not, set the displacement in Step 1 to  $d_E^{new}$  and perform another cycle. Continue iterating until the desired level of accuracy is achieved.

I-6. Convert the displacement for the simple system to the expected inelastic displacement for the complete structure by multiplying by the product of the modal participation factor and the first mode roof displacement.

The procedure will now be demonstrated for the strong panel structure subjected to the ML load pattern. P-delta effects are *excluded*.

For this structure, the modal participation factor and effective modal mass factor for the first mode are:

 $\phi_1 = 1.308$  and  $\alpha_1 = 0.826$ 

The original pushover curve is shown in Figure 3.2-23. The capacity spectrum version of the curve is shown in Figure 3.2-38 as is a bilinear representation of the capacity curve.

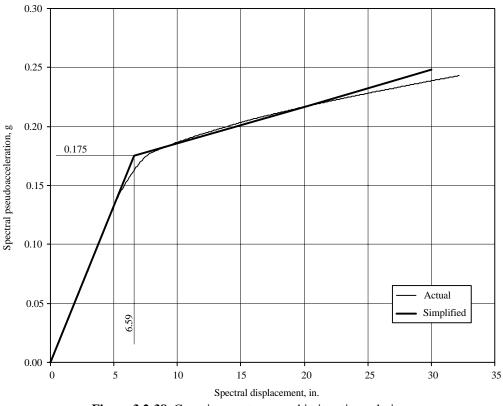


Figure 3.2-38 Capacity spectrum used in iterative solution.

The control values for the bilinear curve are:

 $d_Y = 6.592$  in.  $a_Y = 0.1750$  g  $a_1 = 0.1544$  g  $K_1 = 0.0265$  g/in.  $K_2 = 0.00311$  g/in.

The initial period of the structure (from DRAIN) is 1.95 sec. The same period may be recovered from the demand curve as follows:

$$T = \frac{2\pi}{\sqrt{\frac{g \times a_Y}{d_Y}}} = \frac{2\pi}{\sqrt{\frac{386.1 \times 0.175}{6.659}}} \approx 1.95 \text{ sec.}$$

The 5-percent-damped demand spectrum for this example is based on *Provisions* Figure 4.1.2.6 [3.3-15]. Since the initial period is nearly 2.0 seconds, the only pertinent part of the spectrum is the part that is inversely proportional to period. Using a value of  $S_{DI}$  of 0.494 (see Sec. 3.2.2.2), the spectral acceleration as a function of period *T* is a = 0.494/T where *a* is in terms of the acceleration due to gravity. For higher damping values, the acceleration will be multiplied by the appropriate value from Table 3.2-13 of this example.

At this point the iteration may commence. Assume an initial displacement  $d_E$  of 8.5 in. This is the value computed earlier (see Table 3.2-12) from the simplified procedure in the *Provisions*. At this displacement, the acceleration  $a_E$  is:

$$a_E = a_I + K_2 d_E = 0.1544 + 0.00311(8.5) = 0.1808 \text{ g}$$

At this acceleration and displacement, the equivalent damping is:

$$\xi_E = 5 + \frac{63.7(a_Y d_E - d_Y a_E)}{a_E d_E} = 5 + \frac{63.7(0.175 \times 8.5 - 6.592 \times 0.1808)}{0.1808 \times 8.5} = 17.2\% \text{ critical}.$$

The updated secant period of vibration is:

$$T = \frac{2\pi}{\sqrt{\frac{g \times a_E}{d_E}}} = \frac{2\pi}{\sqrt{\frac{386.4 \times 0.1808}{8.5}}} = 2.19 \,\mathrm{sec}\,.$$

From Table 3.2-13 (or Figure 3.2-37), the damping modification factor for  $\xi_E = 17.2$  percent is 0.71. Therefore, the updated acceleration is:

$$a_E^{new} = 0.71(0.494) / 2.19 = 0.160 \text{ g}.$$

Using this acceleration, the updated displacement for the next iteration is:

$$d_E^{new} = \frac{g \times a_E^{new}}{\left[2\pi / T_E\right]^2} = \frac{386.4 \times 0.160}{\left[2\pi / 2.19\right]^2} = 7.52 \text{ in.}$$

The complete iteration is summarized in Table 3.2-14, where the final displacement from the iteration is 7.82 in. This must be multiplied by the modal participation factor, 1.308, to obtain the actual roof displacement. This value is 7.82(1.308) = 10.2 in. and is somewhat greater than the value of 8.5 in. predicted from the simplified method of the *Provisions*.

This example converged even though some of the accelerations from the demand spectrum were less than the yield value in the development of the capacity spectrum (e.g., 0.161 in iteration 1 is less than 0.175). This particular example predicts displacements very close to the yield displacement  $d_y$ ; consequently, there may be some influence of the choice of  $a_y$  and  $d_y$  on the computed displacement.

Iteration	a* (g)	$d_E$ (in.)	$a_E$ (g)	Damping (%)	Damping Mod. Factor	$T_E$ (sec.)
		8.50	0.181	17.2	0.71	2.19
1	0.161	7.52	0.178	11.8	0.80	2.08
2	0.189	8.01	0.179	14.7	0.75	2.14
3	0.173	7.70	0.179	12.9	0.78	2.10
4	0.183	7.88	0.179	14.0	0.76	2.12
5	0.176	7.77	0.179	13.4	0.77	2.12
6	0.180	7.84	0.179	13.7	0.76	2.12
7	0.178	7.80	0.179	13.5	0.77	2.11
8	0.179	7.82	0.179	13.6	0.76	2.11
9	0.178	7.81	0.179	13.6	0.76	2.11
10	0.179	7.82	0.179	13.6	0.76	2.11

 Table 3.2-14
 Results of Iteration for Maximum Expected Displacement

Note: a\* is from demand spectrum at period  $T_E$ .

In the direct approach, a family of demand spectra are plotted together with the capacity spectrum and the desired displacement is found graphically. The steps in the procedure are as follows:

- D-1. Develop a bilinear capacity spectrum for the structure.
- D-2. Find the points on the capacity spectrum that represent 5, 10, 15, 20, 25, and 30 percent damping.
- D-3. Draw a series of secant stiffness lines, one for each damping value listed above.
- D-4. Develop demand spectra for damping values of 5, 10, 15, 20, 25, and 30 percent of critical.
- D-5. Draw the demand spectra on the same plot as the capacity spectrum.
- D-6. Find the points where the secant stiffness lines (from Step 3) for each damping value cross the demand spectrum line for the same damping value.
- D-7. Draw a curve connecting the points found in Step 6.
- D-8. Find the point where the curve from Step 7 intersects the capacity spectrum. This is the target displacement, but it is still in SDOF spectrum space.
- D-9. Convert the target displacement to structural space.

This procedure is now illustrated for the strong panel structure subjected to the modal load pattern. For this example, P-delta effects are excluded.

- 1. The original pushover curve for this structure is shown in Figure 3.2-23. The effective mass in the first mode is 0.826 times the total mass, and the first mode participation factor is 1.308. The first mode displacement at the roof of the building is 1.0. Half of the dead weight of the structure was used in the conversion because the pushover curve represents the response of one of the two frames. The resulting capacity curve and its bilinear equivalent are shown in Figure 3.2-38. For this example, the yield displacement  $(d_y)$  is taken as 6.59 in. and the corresponding yield strength  $(a_y)$  is 0.175g. The secant stiffness through the yield point is 0.0263g/in. or 10.2 (rad/sec)<sup>2</sup>. Note that the secant stiffness through this point is mathematically equivalent to the circular frequency squared of the structure; therefore, the frequency is 3.19 rad/sec and the period is 1.96 seconds. This period, as required, is the same as that obtained from DRAIN. (The main purpose of computing the period from the initial stiffness of the capacity spectrum is to perform an intermediate check on the analysis.)
- 2-3. The points on the capacity curve representing  $\beta_{eff}$  values of 5, 10, 15, 20, 25, and 30 percent critical damping are shown in Table 3.2-15. The points are also shown as small diamonds on the capacity spectrum of Figure 3.2-39. The secant lines through the points are also shown.

Effective Damping	Displacement $d_{pi}$	Spectral Acceleration $a_{pi}$
(% critical)	(in.)	(g)
5	6.59	0.175
10	7.25	0.177
15	8.07	0.180
20	9.15	0.183
25	10.7	0.188
30	13.1	0.195

**Table 3.2-15** Points on Capacity Spectrum Corresponding to Chosen Damping Values

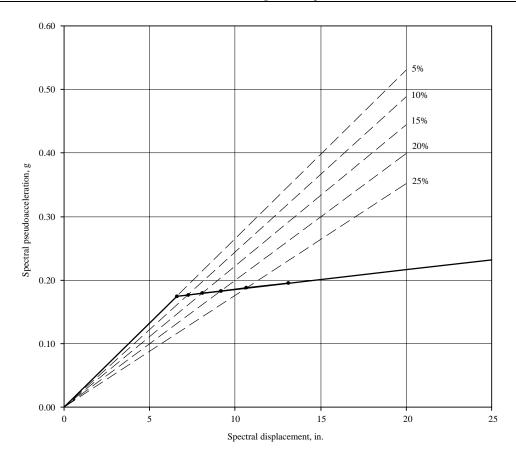


Figure 3.2-39 Capacity spectrum with equivalent viscous damping points and secant stiffnesses.

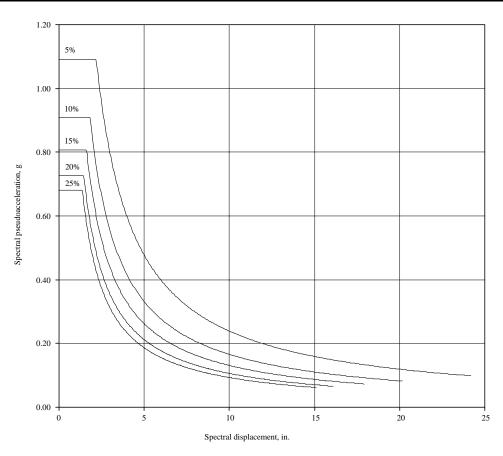
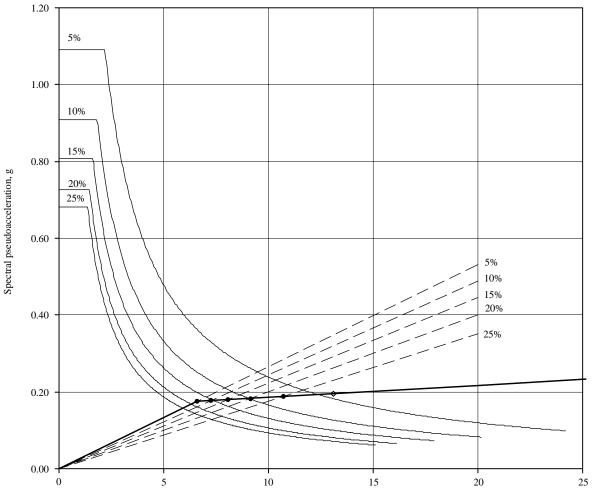


Figure 3.2-40 Demand spectra for several equivalent viscous damping values.

- 4-5. The demand spectra are based on the short period and 1-second period accelerations obtained in Sec. 3.2.2.2e. These values are  $S_{DS} = 1.09$  and  $S_{DI} = 0.494$ . Plots for these spectra are shown individually in Figure 3.2-37. The damping modification factors used to obtain the curves were taken directly or by interpolation from Table 3.2-13. The demand spectra are shown on the same plot as the capacity spectrum in Figure 3.2-41.
- 6-8. The final steps of the analysis are facilitated by Figure 3.2-42, which is a close-up of the relevant portion of Figure 3.2-41. The expected inelastic roof displacement, still in spectral space, is approximately 7.8 in. This is the same as that found from the iterative solution.
- 9. The expected inelastic roof displacement for the actual structure is 1.308(7.8) or 10.2 in. This is 20 percent greater than the value of 8.5 in. obtained from the first mode elastic response-spectrum analysis.



Spectral displacement, in.

Figure 3.2-41 Capacity and demand spectra on single plot.

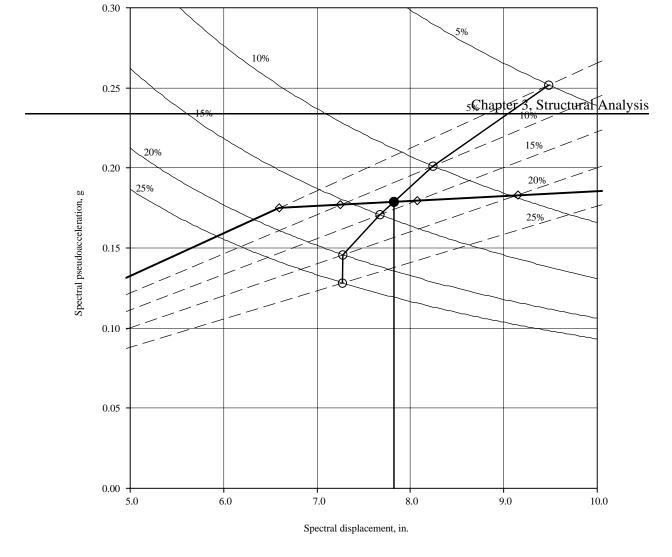


Figure 3.2-42 Close-up view of portion of capacity and demand spectra.

Results for all the strong and weak panel structures under modal load are summarized in Table 3.2-16. All drifts and rotations are consistent with the expected inelastic roof displacement shown at the top of the table.

Computed Quantity	Strong Panel w/o P-Delta	Strong Panel with P-Delta	Weak Panel w/o P-Delta	Weak Panel with P-Delta
Expected Inelastic Disp. (in.)	10.2	10.3	10.2	10.4
Base Shear Demand (kips)	1125	1031	1033	953
6 <sup>th</sup> Story Drift (in.)	0.81	0.78	0.87	0.84
5 <sup>th</sup> Story Drift (in.)	1.35	1.31	1.55	1.45
4 <sup>th</sup> Story Drift (in.)	1.82	1.81	1.96	2.00
3 <sup>rd</sup> Story Drift (in.)	2.19	2.23	2.21	2.29
2 <sup>nd</sup> Story Drift (in.)	2.20	2.27	2.06	2.14
1 <sup>st</sup> Story Drift (in.)	1.83	1.90	1.64	1.68
Max beam plastic hinge rot. (rad)	0.00522	0.00564	0.00511	0.00524
Max column plastic hinge rot. (rad)	0.0	0.0	0.0	0.0
Max panel zone hinge rot. (rad)	0.0	0.0	0.00421	0.00437

#### 3.2.5.4 Summary and Observations from Pushover Analysis

- 1. The simplified approach from the *Provisions* predicts maximum expected displacements about 8 to 10 percent lower than the much more complicated capacity spectrum method. Conclusions cannot be drawn from this comparison, however, as only one structure has been analyzed.
- 2. P-delta effects had a small but significant effect on the response of the system. In particular, base shears for the structure with P-delta effects included were about 8 percent lower than for the structure without P-delta effects. If the maximum expected displacement was larger, the differences between response with and without P-delta effects would have been much more significant.
- 3. The inelastic deformation demands in the hinging regions of the beams and in the panel zones of the beam-column joints were small and are certainly within acceptable limits. The small inelastic deformations are attributed to the considerable overstrength provided when preliminary member sizes were adjusted to satisfy story drift limits.
- 4. The structure without panel zone reinforcement appears to perform as well as the structure with such reinforcement. This is again attributed to the overstrength provided.

## **3.2.6 Time-History Analysis**

Because of the many assumptions and uncertainties inherent in the capacity spectrum method, it is reasonable to consider the use of time-history analysis for the computation of global and local deformation demands. A time-history analysis, while by no means perfect, does eliminate two of the main problems with static pushover analysis: selection of the appropriate lateral load pattern and use of equivalent linear

viscous damping in the demand spectrum to represent inelastic hysteretic energy dissipation. However, time-history analysis does introduce its own problems, most particularly selection and scaling of ground motions, choice of hysteretic model, and inclusion of inherent (viscous) damping.

The time-history analysis of Example 2 is used to estimate the deformation demands for the structure shown in Figures 3.2-1 and 3.2-2. The analysis, conducted only for the structure with panel zone reinforcement, is carried out for a suite of three ground motions specifically prepared for the site. Analyses included and excluded P-delta effects.

#### 3.2.6.1 Modeling and Analysis Procedure

The DRAIN-2Dx program was used for each of the time-history analyses. The structural model was identical to that used in the static pushover analysis. Second order effects were included through the use of the outrigger element shown to the right of the actual frame in Figure 3.2-4.

Inelastic hysteretic behavior was represented through the use of a bilinear model. This model exhibits neither a loss of stiffness nor a loss of strength and, for this reason, it will generally have the effect of overestimating the hysteretic energy dissipation in the yielding elements. Fortunately, the error produced by such a model will not be of great concern for this structure because the hysteretic behavior of panel zones and flexural plastic hinges should be very robust for this structure when inelastic rotations are less than about 0.02 radians. (Previous analysis has indicated a low likelihood of rotations significantly greater than 0.02 radians.) At inelastic rotations greater than 0.02 radians it is possible for local inelastic buckling to reduce the apparent strength and stiffness.

Rayleigh proportional damping was used to represent viscous energy dissipation in the structure. The mass and stiffness proportional damping factors were set to produce 5 percent damping in the first and third modes. This was done primarily for consistency with the pushover analysis, which use a baseline damping of 5 percent of critical. Some analysts would use a lower damping, say 2.5 percent, to compensate for the fact that bilinear hysteretic models tend to overestimate energy dissipation in plastic hinges.

In Rayleigh proportional damping, the damping matrix (D) is a linear combination of the mass matrix M and the initial stiffness matrix K:

 $D = \alpha M + \beta K$ 

where  $\alpha$  and  $\beta$  are mass and stiffness proportionality factors, respectively. If the first and third mode frequencies,  $\omega_1$  and  $\omega_3$ , are known, the proportionality factors may be computed from the following expression:<sup>9</sup>

$$\begin{cases} \alpha \\ \beta \end{cases} = \frac{2\xi}{\omega_1 + \omega_3} \begin{cases} \omega_1 \omega_3 \\ 1 \end{cases}$$

<sup>&</sup>lt;sup>9</sup>See Ray W. Clough and Joseph Penzien, *Dynamics of Structures*, 2<sup>nd</sup> Edition.

Note that  $\alpha$  and  $\beta$  are directly proportional to  $\xi$ . To increase  $\xi$  from 5 percent to 10 percent of critical requires only that  $\alpha$  and  $\beta$  be increased by a factor of 2.0. The structural frequencies and damping proportionality factors are shown in Table 3.2-17 for the models analyzed by the time-history method.

(Damping Factors that Froduce 5 Fercent Damping in Wodes F and 5)						
Model/Damping Parameters	$\omega_1$ (Hz.)	ω <sub>3</sub> (Hz.)	α	β		
Strong Panel with P-Delta Strong Panel without P-Delta	3.118 3.223	18.65 18.92	0.267 0.275	0.00459 0.00451		

**Table 3.2-17** Structural Frequencies and Damping Factors Used in Time-History Analysis.(Damping Factors that Produce 5 Percent Damping in Modes 1 and 3)

It is very important to note that the stiffness proportional damping factor must *not* be included in the Type-4 elements used to represent rotational plastic hinges in the structure. These hinges, particularly those in the girders, have a very high initial stiffness. Before the hinge yields there is virtually no rotational velocity in the hinge. After yielding, the rotational velocity is significant. If a stiffness proportional damping factor is used for the hinge, a viscous moment will develop in the hinge. This artificial viscous moment – the product of the rotational velocity, the initial rotational stiffness of the hinge, and the stiffness proportional damping factor – can be quite large. In fact, the viscous moment may even exceed the intended plastic capacity of the hinge. These viscous moments occur in phase with the plastic rotation; hence, the plastic moment and the viscous moments are additive. These large moments transfer to the rest of the structure, effecting the sequence of hinging in the rest of the structure, and produce artificially high base shears. The use of stiffness proportional damping in discrete plastic hinges can produce a totally inaccurate analysis result.

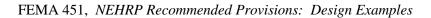
The structure was subjected to dead load and full reduced live load, followed by ground acceleration. The incremental differential equations of motion were solved in a step-by-step manner using the Newmark constant average acceleration approach. Time steps and other integration parameters were carefully controlled to minimize errors. The minium time step used for analysis was 0.00025 seconds. Later analyses used time steps as large as 0.001 seconds.

#### 3.2.6.2 Development of Ground Motion Records

The ground motion time histories used in the analysis were developed specifically for the site. Basic information for the records was shown previously in Table 3.1-20 and is repeated as Table 3.2-18.

	Table 3.2-18         Seattle Ground Motion Parameters (Unscaled)					
Record Name	Orientation	Number of Points and	Peak Ground	Source Motion		
Record Marile	Onentation	Time Increment	Acceleration (g)	Source Motion		
Record A00	N-S	8192 @ 0.005 seconds	0.443	Lucern (Landers)		
Record A90	E-W	8192 @ 0.005 seconds	0.454	Lucern (Landers)		
Record B00	N-S	4096 @ 0.005 seconds	0.460	USC Lick (Loma Prieta)		
Record B90	E-W	4096 @ 0.005 seconds	0.435	USC Lick (Loma Prieta)		
Record C00	N-S	1024 @ 0.02 seconds	0.460	Dayhook (Tabas, Iran)		
Record C90	E-W	1024 @ 0.02 seconds	0.407	Dayhook (Tabas, Iran)		

Time histories and 5-percent-damped response spectra for each of the motions are shown in Figures 3.2-43 through 3.2-45.



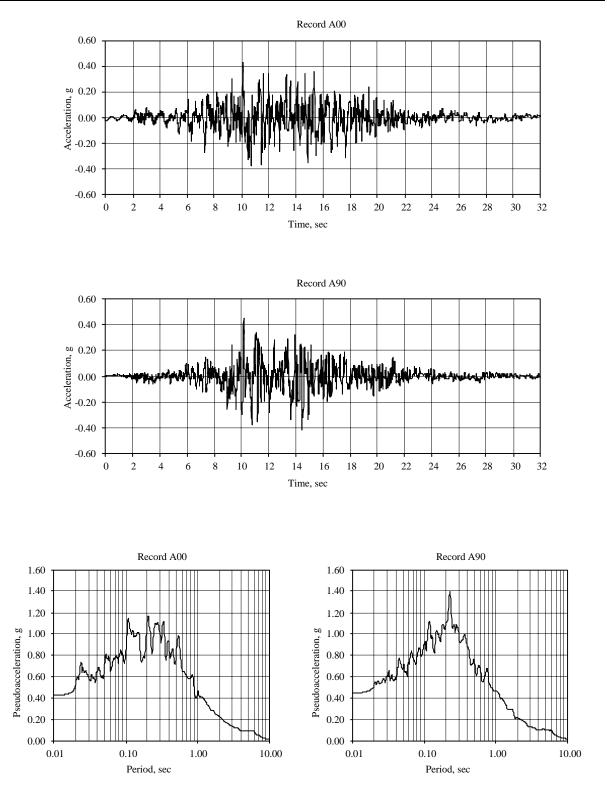
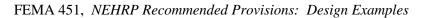


Figure 3.2-43 Time histories and response spectra for Record A.



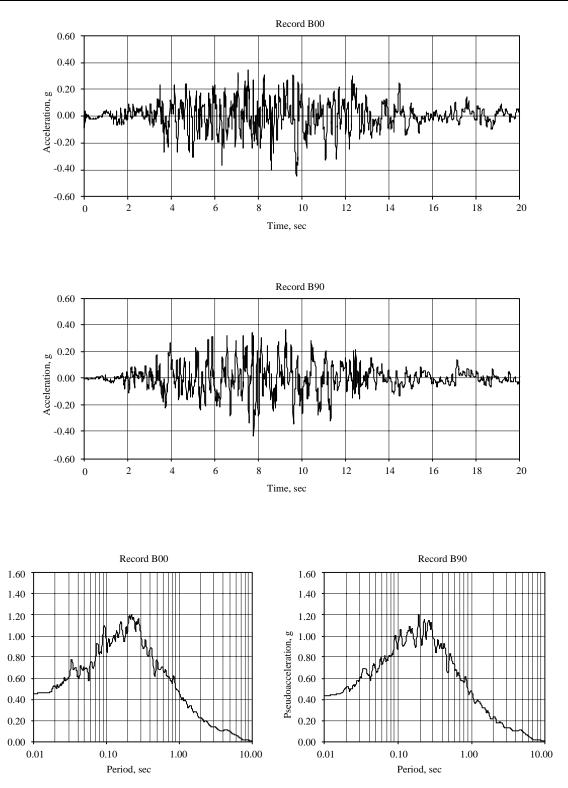


Figure 3.2-44 Time histories and response spectra for Record B.

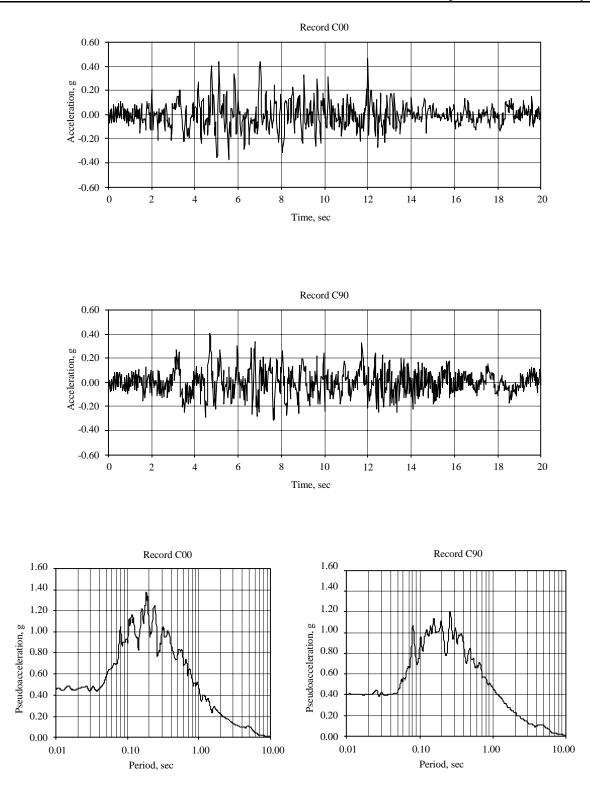


Figure 3.2-45 Time histories and response spectra for Record C.

Because only a two-dimensional analysis of the structure is performed using DRAIN, only a single component of ground motion is applied at one time. For the analyses reported herein, only the N-S (00) records of each ground motion were utilized. A complete analysis would require consideration of both sets of ground motions.

When analyzing structures in two dimensions, *Provisions* Sec. 5.6.2.1 [5.4.2.1] gives the following instructions for scaling:

- 1. For each pair of motions:
  - a. Assume an initial scale factor for each motion pair (for example,  $S_A$  for ground motion A00).
  - b. Compute the 5-percent-damped elastic response spectrum for each component in the pair.
- 2. Adjust scale factors  $S_A$ ,  $S_B$ , and  $S_C$  such that the average of the scaled response spectra over the period range  $0.2T_1$  to  $1.5 T_1$  is not less than the 5-percent-damped spectrum determined in accordance with *Provisions* Sec. 4.1.3.  $T_1$  is the fundamental mode period of vibration of the structure.

As with the three-dimensional time-history analysis for the first example in this chapter, it will be assumed that the scale factors for the three earthquakes are to be the same. If a scale factor of 1.51 is used, Figure 3.2-46 indicates that the criteria specified by the *Provisions* have been met for all periods in the range 0.2(2.00) = 0.40 sec to 1.5(2.00) = 3.0 seconds.<sup>10</sup> The scale factor of 1.51 is probably conservative because it is controlled by the period at 0.47 seconds, which will clearly be in the higher modes of response of the structure. If the *Provisions* had called for a cutoff of 0.25T instead of the (somewhat arbitrary) value of 0.2T, the required scale factor would be reduced to 1.26.

#### 3.2.6.3 Results of Time-History Analysis

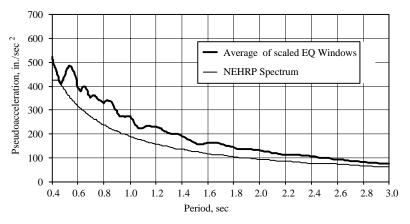
Time-history analyses were performed for the structure subjected to the first 20 seconds of the three different ground motions described earlier. The 20-second cutoff was based on a series of preliminary analyses that used the full duration.

The following parameters were varied to determine the sensitivity of the response to the particular variation:

- 1. Analysis was run with and without P-delta effects for all three ground motions.
- 2. Analysis was run with 2.5, 5, 10, and 20 percent damping (Ground Motion A00, including P-delta effects). These analyses were performed to assess the potential benefit of added viscous fluid damping devices.
- 3.2.6.3.1 Response of Structure with 5 Percent of Critical Damping

 $<sup>^{10}</sup>$ 2.00 seconds is approximately the average of the period of the strong panel model with and without P-delta effects. See Table 3.2-12.

The results from the first series of analyses, all run with 5 percent of critical damping, are summarized in Tables 3.2-19 through 3.2-22. Selected time-history traces are shown in Figures 3.2-47 through 3.2-64. Energy time histories are included for each analysis.



(a) Comparison of Average of Scaled Spectra and NEHRP Spectrum (S.F.=1.51)

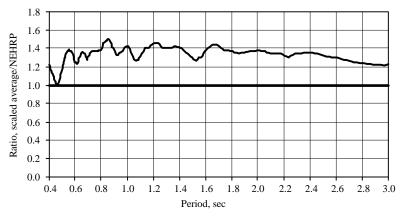




Figure 3.2-46 Ground motion scaling parameters.

The tabulated shears in Tables 3.2-19 and 3.2-21 are for the single frame analyzed and should be doubled to obtain the total shear in the structure. The tables of story shear also provide two values for each ground motion. The first value is the maximum total elastic column story shear, including P-delta effects if applicable. The second value represents the maximum total inertial force for the structure. The inertial base shear, which is not necessarily concurrent with the column shears, was obtained as sum of the products of the total horizontal accelerations and nodal mass of each joint. For a system with no damping, the story shears obtained from the two methods should be identical. For a system with damping, the base shear obtained from column forces generally will be less than the shear from inertial forces because the

viscous component of column shear is not included. Additionally, the force absorbed by the mass proportional component of damping will be lost (as this is not directly recoverable in DRAIN).

The total roof drift and the peak story drifts listed in Tables 3.2-20 and 3.2-22 are peak (envelope) values at each story and are not necessarily concurrent.

Tables 3.2-19 and 3.2-20 summarize the global response of the structure with *excluding* P-delta effects. Time-history traces are shown in Figures 3.2-47 through 3.2-55. Significant yielding occurred in the girders, columns, and panel zone regions for each of the ground motions. Local quantification of such effects is provided later for the structure responding to Ground Motion A00.

Table 3.2-19         Maximum Base Shear (kips) in Frame Analyzed with 5 Percent	
Damping, Strong Panels, Excluding P-Delta Effects	

Level	Motion A00	Motion B00	Motion C00
Column Forces	1559	1567	1636
Inertial Forces	1307	1370	1464

**Table 3.2-20** Maximum Story Drifts (in.) from Time-History Analysis with 5 percent Damping,<br/>Strong Panels, Excluding P-Delta Effects

Level	Motion A00	Motion B00	Motion C00	Limit
Total Roof	16.7	13.0	11.4	NA
R-6	1.78	1.60	1.82	3.75
6-5	3.15	2.52	2.63	3.75
5-4	3.41	2.67	2.65	3.75
4-3	3.37	2.75	2.33	3.75
3-2	3.98	2.88	2.51	3.75
2-G	4.81	3.04	3.13	4.50

 Table 3.2-21
 Maximum Base Shear (kips) in Frame Analyzed with 5 Percent

 Damping, Strong Panels, Including P-Delta Effects

Level	Motion A00	Motion B00	Motion C00
Column Forces	1426	1449	1474
Inertial Forces	1282	1354	1441

		~,8		
Level	Motion A00	Motion B00	Motion C00	Limit
Total Roof	17.4	14.2	10.9	NA
R-6	1.90	1.59	1.78	3.75
6-5	3.31	2.48	2.61	3.75
5-4	3.48	2.66	2.47	3.75
4-3	3.60	2.89	2.31	3.75
3-2	4.08	3.08	2.78	3.75
2-G	4.84	3.11	3.75	4.50

 
 Table 3.2-22
 Maximum Story Drifts (in.) from Time-History Analysis with 5 Percent Damping, Strong Panels, Including P-Delta Effects

The peak base shears (for a single frame), taken from the sum of column forces, are very similar for each of the ground motions and range from 1307 kips to 1464 kips. There is, however, a pronounced difference in the recorded peak displacements. For Ground Motion A00 the roof displacement reached a maximum value of 16.7 in., while the peak roof displacement from Ground Motion C00 was only 11.4 in. Similar differences occurred for the first-story displacement. For Ground Motion A00, the maximum story drift was 4.81 in. for Level 1 and 3.98 in. for Levels 2 through 6. The first-story drift of 4.81 in. exceeds the allowable drift of 4.50 in. Recall that the allowable drift includes a factor of 1.25 that is permitted when nonlinear analysis is performed.

As shown in Figure 3.2-47, the larger displacements observed in Ground Motion A00 are due to a permanent inelastic displacement offset that occurs at about 10.5 seconds into the earthquake. The sharp increase in energy at this time is evident in Figure 3.2-49. Responses for the other two ground motions shown in Figures 3.2-50 and 3.2-53 do not have a significant residual displacement. The reason for the differences in response to the three ground motions is not evident from their ground acceleration time-history traces (see Figures 3.2-43 through 3.2-45).

The response of the structure *including* P-delta effects is summarized in Tables 3.2-21 and 3.2-22. Timehistory traces are shown in Figures 3.2-56 through 3.2-64. P-delta effects have a significant influence on the response of the structure to each of the ground motions. This is illustrated in Figures 3.2-65 and 3.2-66, which are history traces of roof displacement and base shear, respectively, in response to Ground Motion A00. Responses for analysis with and without P-delta effects are shown in the same figure. The P-delta effect is most evident after the structure has yielded.

Table 3.2-21 summarizes the base shear response and indicates that the maximum base shear from the column forces, 1441 kips, occurs during Ground Motion C00. This shear is somewhat less than the shear of 1464 kips which occurs under the same ground motion when P-delta effects are excluded. A reduction in base shear is to be expected for yielding structures when P-delta effects are included.

Table 3.2-22 shows that inclusion of P-delta effects led to a general increase in displacements with the peak roof displacement of 17.4 in. occurring during ground motion A00. The story drift at the lower level of the structure is 4.84 in. when P-delta effects are included and this exceeds the limit of 4.5 in. The larger drifts recorded during Ground Motion A00 are again associated with residual inelastic deformations. This may be seen clearly in the time-history trace of roof and first-story displacement shown in Figure 3.2-56.

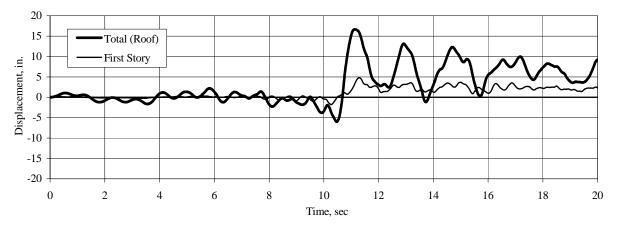


**Figure 3.2-47** Time history of roof and first-story displacement, Ground Motion A00, excluding P-delta effects.

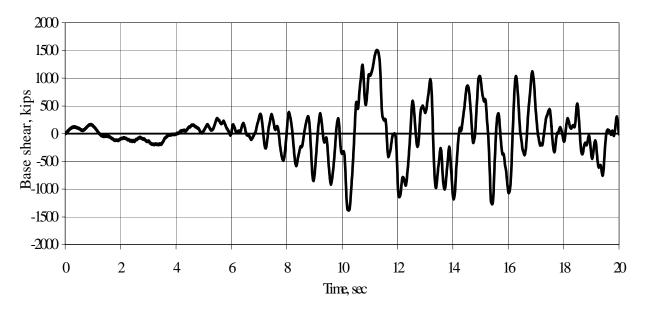


Figure 3.2-48 Time history of total base shear, Ground Motion A00, excluding P-delta effects.

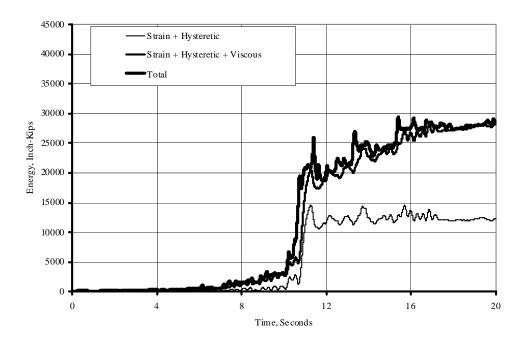
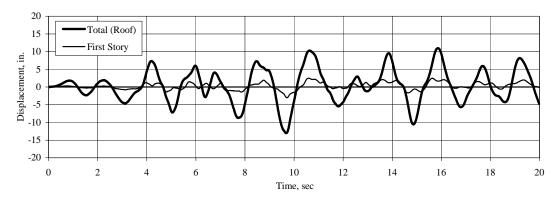


Figure 3.2-49 Energy time history, Ground MotionA00, excluding P-delta effects.



**Figure 3.2-50** Time history of roof and first-story displacement. Ground Motion B00, excluding P-delta effects.



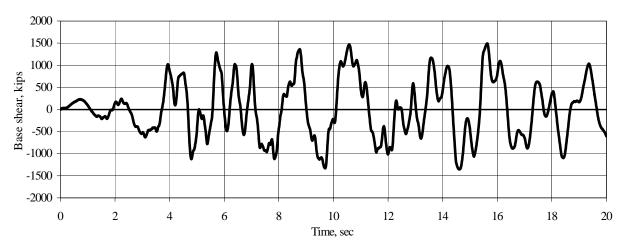


Figure 3.2-51 Time history of total base shear, Ground Motion B00, excluding P-delta effects.

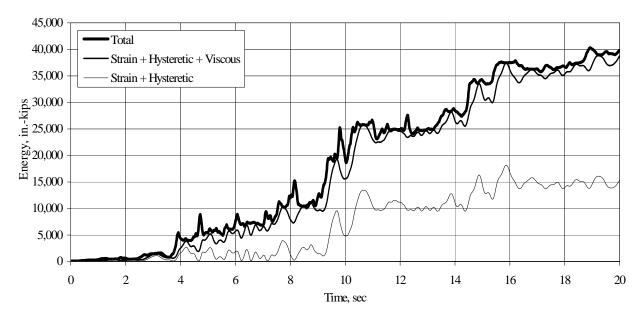


Figure 3.2-52 Energy time history, Ground Motion B00, excluding P-delta effects.

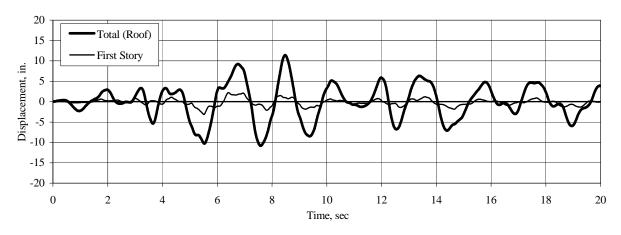


Figure 3.2-53 Time history of roof and first-story displacement, Ground Motion C00, excluding P-delta effects.

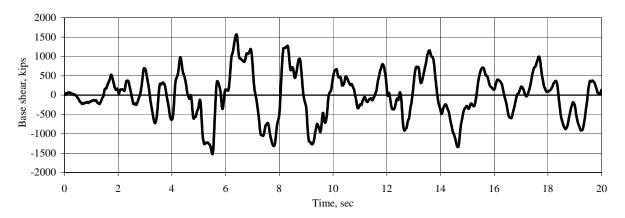


Figure 3.2-54 Time history of total base shear, Ground Motion C00, excluding P-delta effects.

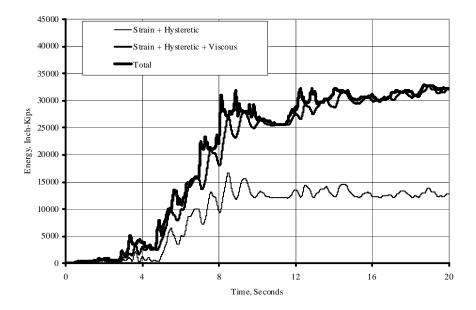


Figure 3.2-55 Energy time history, Ground Motion C00, excluding P-delta effects.

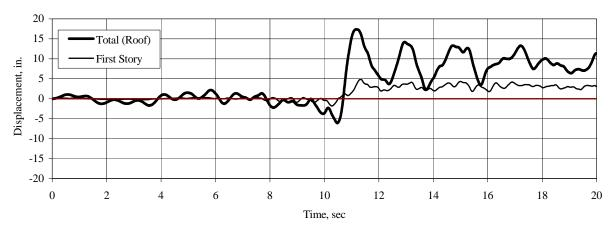


Figure 3.2-56 Time history of roof and first-story displacement, Ground Motion A00, including P-delta effects.

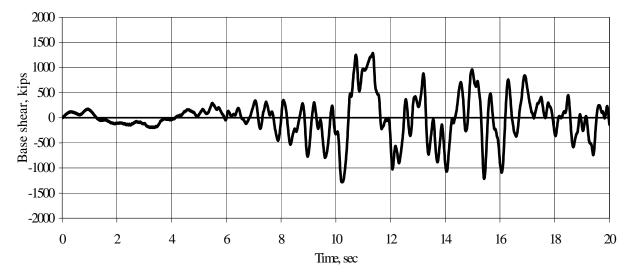


Figure 3.2-57 Time history of total base shear, Ground Motion A00, including P-delta effects.

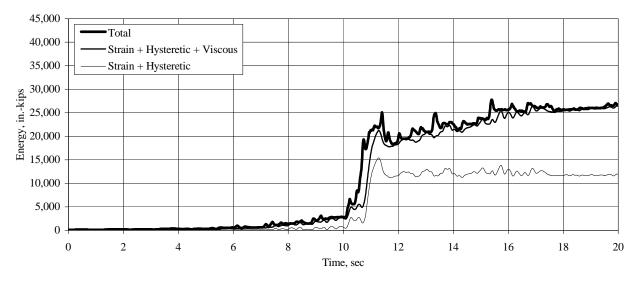


Figure 3.2-58 Energy time history, Ground Motion A00, including P-delta effects.

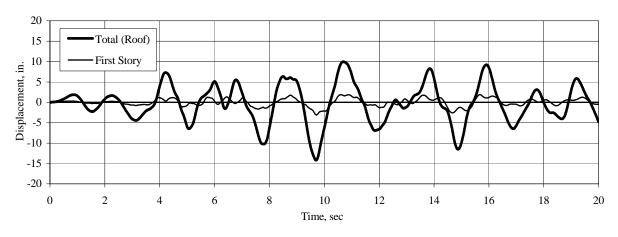


Figure 3.2-59 Time history of roof and first-story displacement, Ground Motion B00, including P-delta effects.

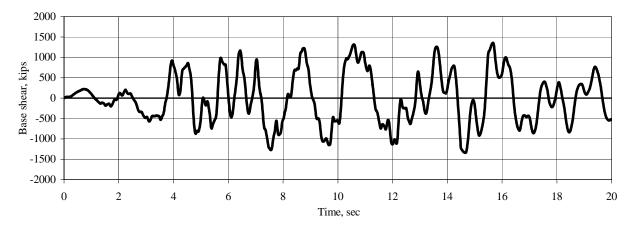


Figure 3.2-60 Time history of total base shear, Ground Motion B00, including P-delta effects.

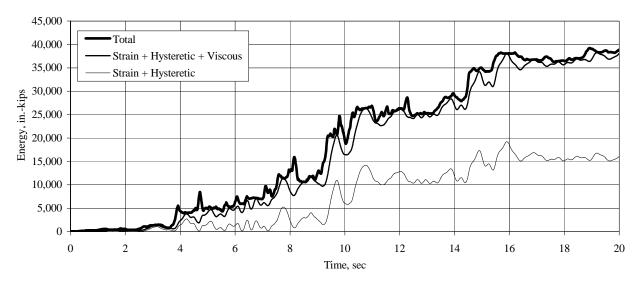
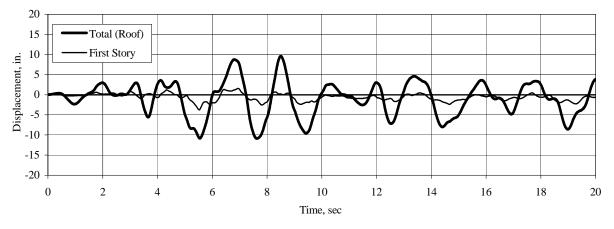


Figure 3.2-61 Energy time history, Ground Motion B00, including P-delta effects.



**Figure 3.2-62** Time history of roof and first-story displacement, Ground Motion C00, including P-delta effects.



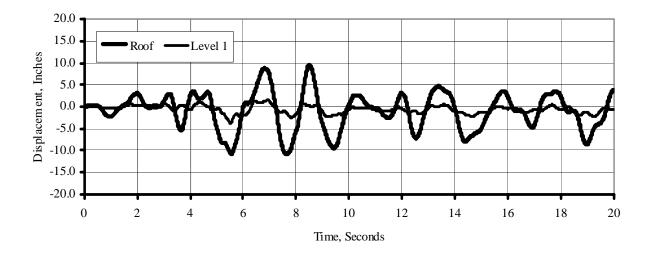


Figure 3.2-63 Time history of total base shear, Ground Motion C00, including P-delta effects.

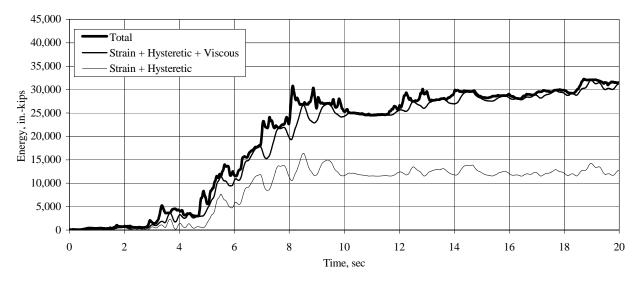


Figure 3.2-64 Energy time history, Ground Motion C00, including P-delta effects.

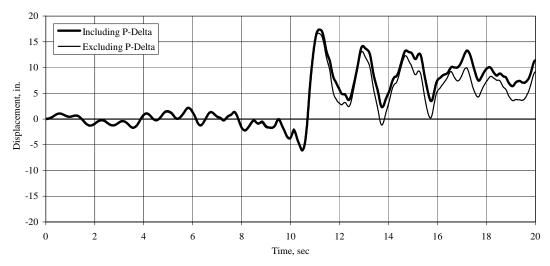


Figure 3.2-65 Time-history of roof displacement, Ground Motion A00, with and without P-delta effect.

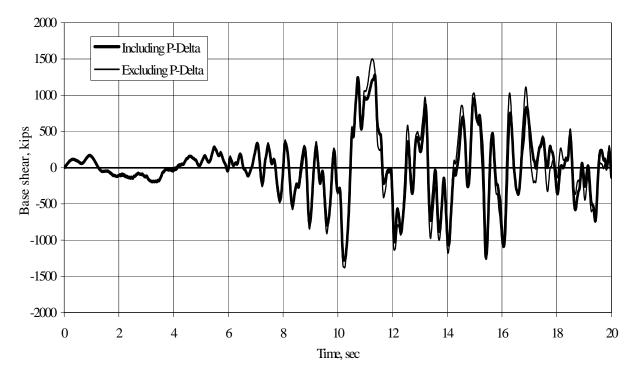
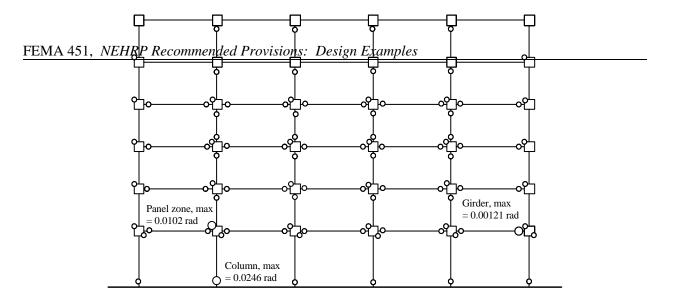


Figure 3.2-66 Time history of base shear, Ground Motion A00, with and without P-delta effects.



**Figure 3.2-67** Yielding locations for structure with strong panels subjected to Ground Motion A00, including P-delta effects.

Figure 3.2-67 shows the pattern of yielding in the structure subjected to Gound Motion A00 including P-delta effects. Recall that the model analyzed incorporated panel zone reinforcement at the interior beam-column joints. Yielding patterns for the other ground motions and for analyses run with and without P-delta effects were similar but are not shown here. The circles on the figure represent yielding at any time during the response; consequently, yielding does not necessarily occur at all locations simultaneously. Circles shown at the upper left corner of the beam-column joint region indicate yielding in the rotational spring that represents the web component of panel zone behavior. Circles at the lower right corner of the panel zone represent yielding of the flange component.

Figure 3.2-67 shows that yielding occurred at both ends of each of the girders at Levels 2, 3, 4, 5, and 6, and in the columns at Stories 1 and 5. The panels zones at the exterior joints of Levels 2 and 6 also yielded. The maximum plastic hinge rotations are shown at the locations they occur for the columns, girders, and panel zones. Tabulated values are shown in Table 3.2-23. The maximum plastic shear strain in the web of the panel zone is identical to the computed hinge rotation in the panel zone spring.

#### 3.2.6.3.2 Comparison with Results from Other Analyses

Table 3.2-23 compares the results obtained from the time-history analysis with those obtained from the ELF and the nonlinear static pushover analyses. Recall that the base shears in the table represent half of the total shear in the building. The differences shown in the results are quite striking:

- 1. The base shear from nonlinear dynamic analysis is more than four times the value computed from the ELF analysis, but the predicted displacements and story drifts are similar. Due to the highly empirical nature of the ELF approach, it is difficult to explain these differences. The ELF method also has no mechanism to include the overstrength that will occur in the structure although it is represented explicitly in the static and dynamic nonlinear analyses.
- 2. The nonlinear static pushover analysis predicts base shears and story displacements that are significantly less than those obtained from time-history analysis. It is also very interesting to note that

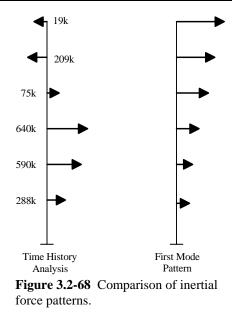
the pushover analysis indicates no yielding in the panel zones, even at an applied roof displacement of 42 in.

While part of the difference in the pushover and time-history response is due to the scale factor of 1.51 that was required for the time-history analysis, the most significant reason for the difference is the use of the first-mode lateral loading pattern in the nonlinear static pushover response. Figure 3.2-68 illustrates this by plotting the inertial forces that occur in the structure at the time of peak base shear and comparing this pattern to the force system applied for nonlinear static analysis. The differences are quite remarkable. The higher mode effects shown in the Figure 3.2-68 are the likely cause of the different hinging patterns and are certainly the reason for the very high base shear developed in the time-history analysis. (If the inertial forces were constrained to follow the first mode response, the maximum base shear that could be developed in the system would be in the range of 1100 kips. See, for example, Figure 3.2-24.)

	Analysis Method				
Response Quantity	Equivalent Lateral Forces	Static Pushover Provisions Method	Static Pushover Capacity- Spectrum	Nonlinear Dynamic	
Base Shear (kips)	373	1051	1031	1474	
Roof Disp. (in.)	18.4	12.7	10.3	17.4	
Drift R-6 (in.)	1.87	1.02	0.78	1.90	
Drift 6-5 (in.)	2.91	1.77	1.31	3.31	
Drift 5-4 (in.)	3.15	2.34	1.81	3.48	
Drift 4-3 (in.)	3.63	2.73	2.23	3.60	
Drift 3-2 (in.)	3.74	2.73	2.27	4.08	
Drift 2-1 (in.)	3.14	2.23	1.90	4.84	
Girder Hinge Rot. (rad)	NA	0.0065	0.00732	0.0140	
Column Hinge Rot. (rad)	NA	0.00130	0.00131	0.0192	
Panel Hinge Rot. (rad)	NA	No Yielding	No Yielding	0.00624	
Panel Plastic Shear Strain	NA	No Yielding	No Yielding	0.00624	

 Table 3.2-23
 Summary of All Analyses for Strong Panel Structure, Including P-Delta Effects

Note: Shears are for half of total structure.



### 3.2.6.3.3 Effect of Increased Damping on Response

The time-history analysis of the structure with panel zone reinforcement indicates that excessive drift may occur in the first story. The most cost effective measure to enhance the performance of the structure would probably be to provide additional strength and/or stiffness at this story. However, added damping is also a viable approach.

To determine the effect of added damping on the behavior of the structure, preliminary analysis was performed by simply increasing the damping ratio from 5 percent to 20 percent of critical in 5-percent increments. For comparison purposes, an additional analysis was performed for a system with only 2.5 percent damping. In each case, the structure was subjected to Ground Motion A00, the panel zones were reinforced, and P-delta effects were included. A summary of the results is shown in Tables 3.2-24 and 3.2-25. As may be seen, an increase in damping from 5 to 10 percent of critical eliminates the drift problem. Even greater improvement is obtained by increasing damping to 20 percent of critical. In is interesting to note, however, that an increase in damping had little effect on the inertial base shear, which is the true shear in the system.

Item		Dampir	ng Ratio		
Item	2.5%	5%	10%	20%	28%
Column Forces	1354	1284	1250	1150	1132
Inertial Forces	1440	1426	1520	1421	1872

 Table 3.2-24
 Maximum Base Shear (kips) in Frame Analyzed Ground Motion A00, Strong Panels, Including P-Delta Effects

1		Dampir	ng Ratio		
Level	2.5%	5%	10%	20%	28%
Total Roof	18.1	17.4	15.8	12.9	11.4
R-6	1.81	1.90	1.74	1.43	1.21
6-5	3.72	3.31	2.71	2.08	1.79
5-4	3.87	3.48	3.00	2.42	2.13
4-3	3.70	3.60	3.33	2.77	2.40
3-2	4.11	4.08	3.69	2.86	2.37
2-G	4.93	4.84	4.21	2.90	2.18

 Table 3.2-25
 Maximum Story Drifts (in.) from Time-History Analysis Ground Motion A00, Strong Panels, Including P-Delta Effects

If added damping were a viable option, additional analysis that treats the individual dampers explicitly would be required. This is easily accomplished in DRAIN by use of the stiffness proportional component of Rayleigh damping; however, only linear damping is possible in DRAIN. In practice, added damping systems usually employ devices with a "softening" nonlinear relationship between the deformational velocity in the device and the force in the device.

If a linear viscous fluid damping device (Figure 3.2-69) were to be used in a particular story, it could be modeled through the use of a Type-1 (truss bar) element. If a damping constant  $C_{device}$  were required, it would be obtained as follows:

Let the length of the Type-1 damper element be  $L_{device}$ , the cross sectional area  $A_{device}$ , and modulus of elasticity  $E_{device}$ .

The elastic stiffness of the damper element is simply:

$$k_{device} = \frac{A_{device}E_{device}}{L_{device}}$$

As stiffness proportional damping is used, the damping constant for the element is:

$$C_{device} = \beta_{device} k_{device}$$

The damper elastic stiffness should be negligible so set  $k_D = 0.001$  kips/in. Thus:

$$\beta_{device} = \frac{C_{device}}{0.001} = 1000 \ C_{device}$$

When modeling added dampers in this manner, the author typically sets  $E_{device} = 0.001$  and  $A_{device} =$  the damper length  $L_{device}$ .

This value of  $\beta_{device}$  is for the added damper element *only*. Different dampers may require different values. Also, a different (global) value of  $\beta$  will be required to model the stiffness proportional component of damping in the remaining nondamper elements.

Modeling the dynamic response using Type-1 elements is *exact* within the typical limitations of finite element analysis. Using the modal strain energy approach, DRAIN will report a damping value in each mode. These modal damping values are approximate and may be poor estimates of actual modal damping, particularly when there is excessive flexibility in the mechanism that connects the damper to the structure.

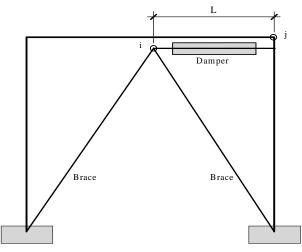


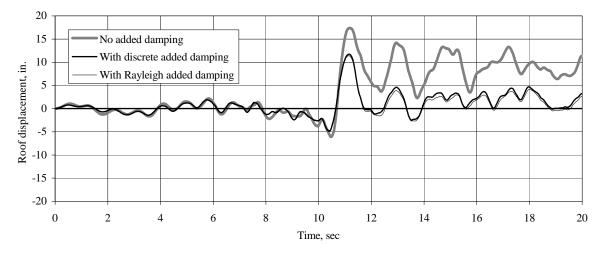
Figure 3.2-69 Modeling a simple damper.

In order to compare the response of the structure with fictitiously high Rayleigh damping to the response with actual discrete dampers, dampers were added in a chevron configuration along column lines C and D, between Bays 3 and 4 (see Figure 3.2-1). As before, the structure is subjected to Ground Motion A00, has strong panels, and has P-delta effects included.

Devices with a damping constant (*C*) of 80 kip-sec/in. were added in Stories 1 and 2, devices with C = 70 kip-sec/in. were added in Stories 3 and 4, and dampers with C = 60 kip-sec/in. were added at Stories 5 and 6. The chevron braces used to connect the devices to the main structure had sufficient stiffness to eliminate any loss of efficiency of the devices. Using these devices, an equivalent viscous damping of approximately 28 percent of critical was obtained in the first mode, 55 percent of critical damping was obtained in the second mode, and in excess of 70 percent of critical damping was obtained in modes three through six..

The analysis was repeated using Rayleigh damping wherein the above stated modal damping ratios were approximately obtained. The peak shears and displacements obtained from the analysis with Rayleigh damping are shown at the extreme right of Tables 3.2-24 and 3.2-25. As may be observed, the trend of decreased displacements and increased inertial shears with higher damping is continued.

Figure 3.2-70 shows the time history of roof displacements for the structure without added damping, with true viscous dampers, and with equivalent Rayleigh damping. As may be seen, there is a dramatic



decrease in roof displacement. It is also clear that the discrete dampers and the equivalent Rayleigh damping produce very similar results.

**Figure 3.2-70** Response of structure with discrete dampers and with equivalent viscous damping (1.0 in. = 25.4 mm).

Figure 3.2-71 shows the time history of base shears for the structure without added damping, with discrete dampers, and with equivalent viscous damping. These base shears were obtained from the summation of column forces, including P-delta effects. For the discrete damper case, the base shears include the horizontal component of the forces in the chevron braces. The base shears for the discretely damped system are greater than the shears for the system without added damping. The peak base shear for the system with equivalent viscous damping is less than the shear in the system without added damping.

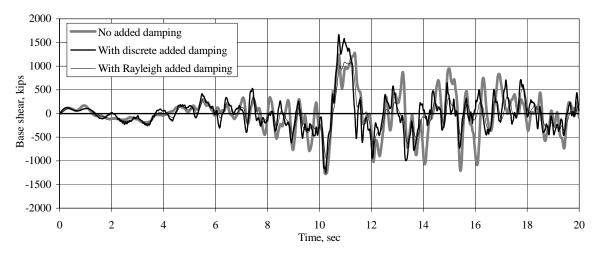


Figure 1Figure 3.2-71 Base shear time histories obtained from column forces (1.0 kip = 4.45 kN).

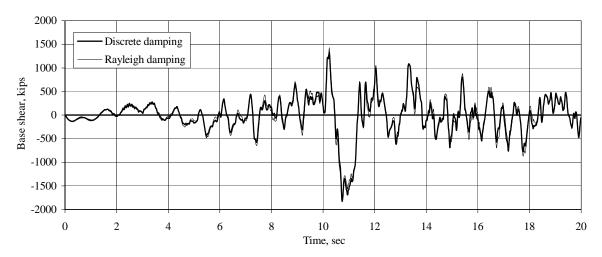


Figure 3.2-72 Base shear time histories as obtained from inertial forces (1.0 kip = 4.45 kN).

The inertial base shears in the system with discrete damping and with equivalent viscous damping are shown in Figure 3.2-72. As may be observed, the responses are almost identical. The inertial forces represent the true base shear in the structure, and should always be used in lieu of the sum of column forces.

As might be expected, the use of added discrete damping reduces the hysteretic energy demand on the structure. This effect is shown in Figure 3.2-73, which is an energy time history for the structure with added discrete damping (which yields equivalent viscous damping of 28 percent of critical). This figure should be compared to Figure 3.2-58, which is the energy history for the structure without added damping. The reduction in hysteretic energy demand for the system with added damping will reduce the damage in the structure.

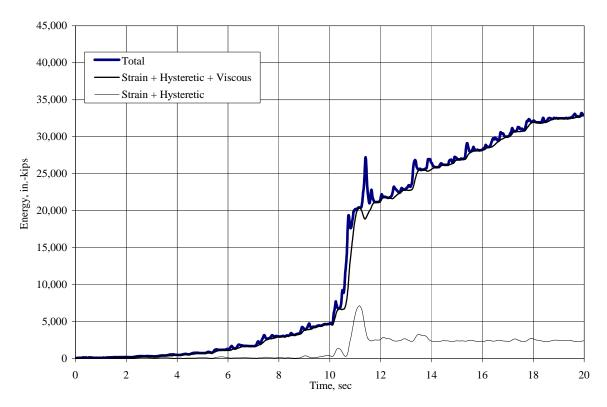


Figure 3.2-73 Energy time-history for structure with discrete added damping (1.0 in.-kip = 0.113 kN-m).

#### 3.2.7 Summary and Conclusions

In this example, five different analytical approaches were used to estimate the deformation demands in a simple unbraced steel frame structure:

- 1. Linear static analysis (the equivalent lateral force method)
- 2. Plastic strength analysis (using virtual work)
- 3. Nonlinear static pushover analysis
- 4. Linear dynamic analysis
- 5. Nonlinear dynamic time-history analysis

Approaches 1, 3, and 5 were carried to a point that allowed comparison of results. In modeling the structure, particular attention was paid to representing possible inelastic behavior in the panel-zone regions of the beam-column joints.

The results obtained from the three different analytical approaches were quite dissimilar. Because of the influence of the higher mode effects on the response, pushover analysis, when used alone, is inadequate.<sup>11</sup> [In the 2003 *Provisions*, a number of substantive technical changes have been made to the appendix,

<sup>&</sup>lt;sup>11</sup>Improved methods are becoming available for pushover analysis (see, for example, Chopra and Goel 2001).

largely as a result of work performed in the development of ATC 55. That report outlines numerous other technical modifications that could be considered in application of nonlinear static analysis methods.] Except for preliminary design, the ELF approach should not be used in explicit performance evaluation as it has no mechanism for determining location and extent of yielding in the structure.

This leaves time-history analysis as the most viable approach. Given the speed and memory capacity of personal computers, it is expected that time-history analysis will eventually play a more dominant role in the seismic analysis of buildings. However, significant shortcomings, limitations, and uncertainties in time-history analysis still exist.

Among the most pressing problems is the need for a suitable suite of ground motions. All ground motions must adequately reflect site conditions and, where applicable, the suite must include near-field effects. Through future research and the efforts of code writing bodies, it may be possible to develop standard suites of ground motions that could be published together with tools and scaling methodologies to make the motions represent the site. The scaling techniques that are currently recommended in the *Provisions* are a start but need improving.

Systematic methods need to be developed for identifying uncertainties in the modeling of the structure and for quantifying the effect of such uncertainties on the response. While probabilistic methods for dealing with such uncertainties seem like a natural extension of the analytical approach, the author believes that deterministic methods should not be abandoned entirely.

In the context of performance-based design, improved methods for assessing the effect of inelastic response and acceptance criteria based on such measures need to be developed. Methods based on explicit quantification of damage should be seriously considered.

The ideas presented above are certainly not original. They have been presented by many academics and practicing engineers. What is still lacking is a comprehensive approach for seismic-resistant design based on these principles. Bertero and Bertero (2002) have presented valuable discussions in these regards.

4

# FOUNDATION ANALYSIS AND DESIGN

# Michael Valley, P.E.

This chapter illustrates application of the 2000 Edition of the *NEHRP Recommended Provisions* to the design of foundation elements. Example 4.1 completes the analysis and design of shallow foundations for two of the alternate framing arrangements considered for the building featured in Example 5.2. Example 4.2 illustrates the analysis and design of deep foundations for a building similar to the one highlighted in Chapter 6 of this volume of design examples. In both cases, only those portions of the designs necessary to illustrate specific points are included.

The force-displacement response of soil to loading is highly nonlinear and strongly time dependent. Control of settlement is generally the most important aspect of soil response to gravity loads. However, the strength of the soil may control foundation design where large amplitude transient loads, such as those occurring during an earthquake, are anticipated.

Foundation elements are most commonly constructed of reinforced concrete. As compared to design of concrete elements that form the superstructure of a building, additional consideration must be given to concrete foundation elements due to permanent exposure to potentially deleterious materials, less precise construction tolerances, and even the possibility of unintentional mixing with soil.

Although the application of advanced analysis techniques to foundation design is becoming increasingly common (and is illustrated in this chapter), analysis should not be the primary focus of foundation design. Good foundation design for seismic resistance requires familiarity with basic soil behavior and common geotechnical parameters, the ability to proportion concrete elements correctly, an understanding of how such elements should be detailed to produce ductile response, and careful attention to practical considerations of construction.

Although this chapter is based on the 2000 *Provisions*, it has been annotated to reflect changes made to the 2003 *Provisions*. Annotations within brackets, [], indicate both organizational changes (as a result of a reformat of all of the chapters of the 2003 *Provisions*) and substantive technical changes to the 2003 *Provisions* and its primary reference documents. While the general concepts of the changes are described, the design examples and calculations have not been revised to reflect the changes to the 2003 *Provisions*. The most significant change to the foundation chapter in the 2003 *Provisions* is the addition of a strength design method for foundations. Another change was made to introduce guidance for the explicit modeling of foundation load-deformation characteristics. Where they affect the design examples in this chapter, other significant changes to the 2003 *Provisions* and primary reference documents are noted. However, some minor changes to the 2003 *Provisions* and the reference documents may not be noted.

In addition to the 2000 *NEHRP Recommended Provisions* and *Commentary* (referred to herein as *Provisions* and *Commentary*), the following documents are either referenced directly or provide useful information for the analysis and design of foundations for seismic resistance:

ACI 318	American Concrete Institute. 1999 [2002]. Building Code Requirements and Commentary for Structural Concrete.
ASCE 7	American Society of Civil Engineers. 1998 [2002]. Minimum Design Loads for Buildings and Other Structures.
Bowles	Bowles, J. E. 1988. Foundation Analysis and Design. McGraw-Hill.
Brown 1987	Brown, D. A., L. C. Reese, and M. W. O'Neill. 1987. "Cyclic Lateral Loading of a Large-Scale Pile Group," <i>Journal of Geotechnical Engineering</i> , Vol. 113, No. 11 (November). ASCE.
Brown 1988	Brown, D. A., C. Morrison, and L. C. Reese. 1988. "Lateral Load Behavior of Pile Group in Sand." <i>Journal of Geotechnical Engineering</i> , Vol 114, No. 11, (November). ASCE.
CRSI	Concrete Reinforcing Steel Institute. 1996. CRSI Design Handbook. Concrete Reinforcing Steel Institute.
FEMA 356	ASCE. 2000. <i>Prestandard and Commentary for the Seismic Rehabilitation of Buildings</i> , FEMA 356, prepared by the American Society of Civil Engineers for the Federal Emergency Management Agency.
GROUP	Reese, L. C., and S. T. Wang. 1996. <i>Manual for GROUP 4.0 for Windows</i> . Ensoft.
Kramer	Kramer, S. L. 1996. Geotechnical Earthquake Engineering. Prentice Hall.
LPILE	Reese, L. C., and S. T. Wang. 1997. <i>Technical Manual for LPILE Plus 3.0 for Windows</i> . Ensoft.
Martin	Martin, G. R., and I. PoLam. 1995. "Seismic Design of Pile Foundations: Structural and Geotechnical Issues." <i>Proceedings: Third International</i> <i>Conference on Recent Advances in Geotechnical Earthquake Engineering and</i> <i>Soil Dynamics.</i>
Pender	Pender, M. J. 1993. "Aseismic Pile Foundation Design Analysis." <i>Bulletin of the New Zealand National Society for Earthquake Engineering</i> , Vol. 26, No. 1 (March).
PoLam	PoLam, I., M. Kapuskar, and D. Chaudhuri. 1998. <i>Modeling of Pile Footings and Drilled Shafts for Seismic Design</i> , MCEER-98-0018. Multidisciplinary Center for Earthquake Engineering Research.
Wang & Salmon	Wang, CK., and C. G. Salmon. 1992. <i>Reinforced Concrete Design</i> . HarperCollins.

Youd Youd, T. L., Idriss, I. M., and et al. 2001. "Liquefaction Resistance of Soils: Summary Report from the 1996 NCEER and 1998 NCEER/NSF Workshops on Evaluation of Liquefaction Resistance of Soils." *Journal of Geotechnical and Geoenvironmental Engineering* (October). ASCE.

Several commercially available programs were used to perform the calculations described in this chapter. RISA: 3D is used to determine the shears and moments in a concrete mat foundation; LPILE, in the analysis of laterally loaded single piles; and PCACOL, to determine concrete pile section capacities.

# 4.1 SHALLOW FOUNDATIONS FOR A SEVEN-STORY OFFICE BUILDING, LOS ANGELES, CALIFORNIA

This example features the analysis and design of shallow foundations for two of the three framing arrangements for the seven-story steel office building described in Sec. 5.2 of this volume of design examples. Refer to that example for more detailed building information and for the design of the superstructure; because Chapter 4 was completed after Chapter 5, some values may differ slightly between the two chapters.

# 4.1.1 Basic Information

#### 4.1.1.1 Description

The framing plan in Figure 4.1-1 shows the gravity-load-resisting system for a representative level of the building. The site soils, consisting of medium dense sands, are suitable for shallow foundations. Table 4.1-1 shows the design parameters provided by a geotechnical consultant. Note the distinction made between *bearing pressure* and *bearing capacity*. If the long-term, service-level loads applied to foundations do not exceed the noted bearing pressure, differential and total settlements are expected to be within acceptable limits. Settlements are more pronounced where large areas are loaded, so the bearing pressure limits are a function of the size of the loaded area. The values identified as bearing capacity are related to gross failure of the soil mass in the vicinity of loading. Where loads are applied over smaller areas, punching into the soil is more likely.

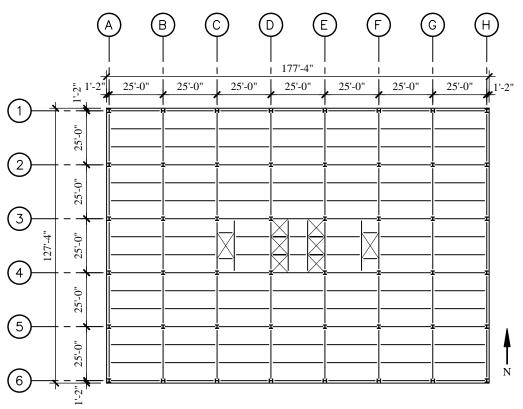


Figure 4.1-1 Typical framing plan.

Because bearing capacities are generally expressed as a function of the minimum dimension of the loaded area and are applied as limits on the maximum pressure, foundations with significantly non-square loaded areas (tending toward strip footings) and those with significant differences between average pressure and maximum pressure (as for eccentrically loaded footings) have higher calculated bearing capacities. The recommended values are consistent with these expectations.

[The 2003 *Provisions* discuss the settlement and strength limit states in Sec. 7.2.2.2 using slightly different nomenclature.]

Parameter	Value		
Basic soil properties	Medium dense sand (SPT) $N = 20$ $\gamma = 125$ pcf angle of internal friction = 33 deg		
Net bearing pressure (to control settlement due to sustained loads)	$\leq$ 4000 psf for $B \leq$ 20 ft $\leq$ 2000 psf for $B \geq$ 40 ft (may interpolate for intermediate dimensions)		
Bearing capacity (for plastic equilibrium strength checks with factored loads)	2000 <i>B</i> psf for concentrically loaded square footings 3000 <i>B</i> ' psf for eccentrically loaded footings where <i>B</i> and <i>B</i> ' are in feet, <i>B</i> is the footing width and <i>B</i> ' is an average width for the compressed area. Resistance factor, $\phi = 0.6$ [In the 2003 <i>Provisions</i> , the $\phi$ factor for cohesionless soil is explicitly defined; the value is set at 0.7 for vertical, lateral, and rocking resistance.]		
Lateral properties	Earth pressure coefficients Active, $K_A = 0.3$ At-rest, $K_0 = 0.46$ Passive, $K_P = 3.3$ "Ultimate" friction coefficient at base of footing = 0.65 Resistance factor, $\phi = 0.8$ [In the 2003 <i>Provisions</i> , the $\phi$ factor for cohesionless soil is explicitly defined; the value is set at 0.7 for vertical, lateral, and rocking resistance.]		

 Table 4.1-1
 Geotechnical Parameters

The structural material properties assumed for this example are:

 $f'_c = 4,000 \text{ psi}$  $f_y = 60,000 \text{ psi}$ 

### 4.1.1.2 Provisions Parameters

The complete set of parameters used in applying the *Provisions* to design of the superstructure is described in Sec. 5.2.2.1 of this volume of design examples. The following parameters, which are used during foundation design, are duplicated here.

Site Class = D  $S_{DS} = 1.0$  Seismic Design Category = D

## 4.1.1.3 Design Approach

#### 4.1.1.3.1 Selecting Footing Size and Reinforcement

Most foundation failures are related to excessive movement rather than loss of load-carrying capacity. Settlement control should be addressed first. In recognition of this fact, settlement control should be the first issue addressed. Once service loads have been calculated, foundation plan dimensions should be selected to limit bearing pressures to those that are expected to provide adequate settlement performance. Maintaining a reasonably consistent level of service load bearing pressures for all of the individual footings is encouraged as it will tend to reduce differential settlements, which are usually of more concern than are total settlements.

When a preliminary footing size that satisfies serviceability criteria has been selected, bearing capacity can be checked. It would be rare for bearing capacity to govern the size of footings subjected to sustained loads. However, where large transient loads are anticipated, consideration of bearing capacity may become important.

The thickness of footings is selected for ease of construction and to provide adequate shear capacity for the concrete section. The common design approach is to increase footing thickness as necessary to avoid the need for shear reinforcement, which is uncommon in shallow foundations.

Design requirements for concrete footings are found in Chapters 15 and 21 of ACI 318. Chapter 15 provides direction for the calculation of demands and includes detailing requirements. Section capacities are calculated in accordance with Chapters 10 (for flexure) and 11 (for shear). Figure 4.1-2 illustrates the critical sections (dashed lines) and areas (hatched) over which loads are tributary to the critical sections. For elements that are very thick with respect to the plan dimensions (as at the pile caps), these critical section definitions become less meaningful and other approaches (e.g., strut-and-tie modeling) should be employed. Chapter 21 provides the minimum requirements for concrete foundations in Seismic Design Categories D, E, and F, which are similar to those provided in prior editions of the *Provisions*.

For shallow foundations, reinforcement is designed to satisfy flexural demands. ACI 318 Sec. 15.4 defines how flexural reinforcement is to be distributed for footings of various shapes.

Sec. 10.5 of ACI 318 prescribes the minimum reinforcement for flexural members where tensile reinforcement is required by analysis. Provision of the minimum reinforcement assures that the strength of the cracked section is not less than that of the corresponding unreinforced concrete section, thus preventing sudden, brittle failures. Less reinforcement may be used as long as "the area of tensile reinforcement provided is at least one-third greater than that required by analysis." Sec. 10.5.4 relaxes the minimum reinforcement requirement for footings of uniform thickness. Such elements need only satisfy the shrinkage reinforcement requirements of Sec. 7.12. Sec. 10.5.4 also imposes limits on the maximum spacing of bars.

### 4.1.1.3.2 Additional Considerations for Eccentric Loads

The design of eccentrically loaded footings follows the approach outlined above with one significant addition – consideration of overturning stability. Stability calculations are sensitive to the characterization of soil behavior. For sustained eccentric loads a linear distribution of elastic soil stresses is generally assumed and uplift is usually avoided. If the structure is expected to remain elastic when subjected to short-term eccentric loads (as for wind loading), uplift over a portion of the footing is acceptable to most designers. Where foundations will be subjected to short-term loads and inelastic

response is acceptable (as for earthquake loading), plastic soil stresses may be considered. It is most common to consider stability effects on the basis of statically applied loads even where the loading is actually dynamic; that approach simplifies the calculations at the expense of increased conservatism. Figure 4.1-3 illustrates the distribution of soil stresses for the various assumptions. Most textbooks on foundation design provide simple equations to describe the conditions shown in parts b, c, and d of the figure; finite element models of those conditions are easy to develop. Simple hand calculations can be performed for the case shown in part f. Practical consideration of the case shown in part e would require modeling with inelastic elements, but offers no advantage over direct consideration of the plastic limit. (All of the discussion in this section focuses on the common case in which foundation elements may be assumed to be rigid with respect to the supporting soil. For the interested reader, Chapter 4 of FEMA 356 provides a useful discussion of foundation compliance, rocking, and other advanced considerations.)

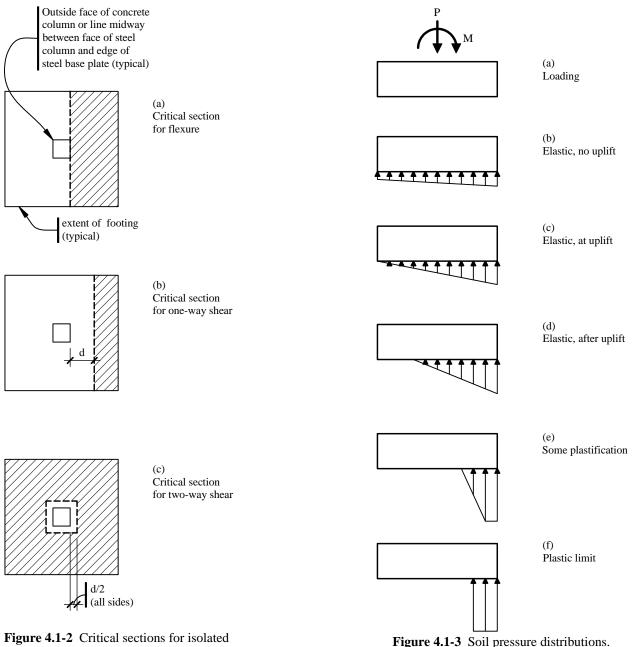


Figure 4.1-2 Critical sections for isolated footings.

# 4.1.2 Design for Gravity Loads

Although most of the examples in the volume do not provide detailed design for gravity loads, it is provided in this section for two reasons. First, most of the calculation procedures used in designing shallow foundations for seismic loads are identical to those used for gravity design. Second, a complete gravity design is needed to make the cost comparisons shown in Sec. 4.1.5 below meaningful.

Detailed calculations are shown for a typical interior footing. The results for all three footing types are summarized in Sec. 4.1.2.5.

# 4.1.2.1 Demands

Dead and live load reactions are determined as part of the three-dimensional analysis described in Sec. 5.2 of this volume of design examples. Although there are slight variations in the calculated reactions, the foundations are lumped into three groups (interior, perimeter, and corner) for gravity load design and the maximum computed reactions are applied to all members of the group, as follows:

Interior: D = 387 kips L = 98 kips Perimeter: D = 206 kips L = 45 kips Corner: D = 104 kips L = 23 kips

The service load combination for consideration of settlement is D + L. Considering the load combinations for strength design defined in Sec. 2.3.2 of ASCE 7, the controlling gravity load combination is 1.2D + 1.6L. Because ASCE 7 load combinations are employed, the alternate strength reduction factors found in ACI 318 Appendix C must be used. [The 2003 *Provisions* refer to ACI 318-02, in which the basic resistance factors have been revised to be consistent with the load combinations in ASCE 7. These new resistance factors (not those found in the ACI 318 Appendix) are used for seismic design. This change would affect slightly the results of the example calculations in this chapter .]

### 4.1.2.2 Footing Size

The preliminary size of the footing is determined considering settlement. The service load on a typical interior footing is calculated as:

P = D + L = 387 kips + 98 kips = 485 kips.

Since the footing dimensions will be less than 20 ft, the allowable bearing pressure (see Table 4.1-1) is 4000 psf. Therefore, the required footing area is 487,000 lb/4000 psf = 121.25 ft<sup>2</sup>.

Check a footing that is 11'-0" by 11'-0":

$$P_{allow} = 11 \text{ ft}(11 \text{ ft})(4000 \text{ psf}) = 484,000 \text{ lb} = 484 \text{ kips} \approx 485 \text{ kips} \text{ (demand)}.$$
 OK

The strength demand is:

 $P_{\mu} = 1.2(387 \text{ kips}) + 1.6(98 \text{ kips}) = 621 \text{ kips}.$ 

As indicated in Table 4.1-1, the bearing capacity  $(q_c)$  is  $2000 B = 2000 \times 11 = 22000 \text{ psf} = 22 \text{ ksf}$ .

The design capacity for the foundation is:

$$\phi P_n = \phi q_c B^2 = 0.6(22 \text{ ksf})(11 \text{ ft})^2 = 1597 \text{ kips} \gg 621 \text{ kips}.$$
 OK

For use in subsequent calculations, the factored bearing pressure  $q_u = 621 \text{ kips}/(11 \text{ ft})^2 = 5.13 \text{ ksf.}$ 

#### 4.1.2.3 Footing Thickness

Once the plan dimensions of the footing are selected, the thickness is determined such that the section satisfies the one-way and two-way shear demands without the addition of shear reinforcement. Because the demands are calculated at critical sections (see Figure 4.1-2) that depend on the footing thickness, iteration is required.

Check a footing that is 26 in. thick:

For the W14 columns used in this building, the side dimensions of the loaded area (taken halfway between the face of the column and the edge of the base plate) are about 16 in. Accounting for cover and expected bar sizes, d = 26 - (3 + 1.5(1)) = 21.5 in.

One-way shear:

$$V_{u} = 11 \left( \frac{11 - \frac{16}{12}}{2} - \frac{21.5}{12} \right) (5.13) = 172 \text{ kips }.$$
  
$$\phi V_{n} = \phi V_{c} = (0.75) 2\sqrt{4000} (11 \times 12) (21.5) \left( \frac{1}{1000} \right) = 269 \text{ kips } > 172 \text{ kips.}$$
OK

Two-way shear:

$$V_u = 621 - \left(\frac{16+21.5}{12}\right)^2 (5.13) = 571 \text{ kips}.$$
  

$$\phi V_n = \phi V_c = (0.75) 4\sqrt{4000} \left[ 4 \times (16+21.5) \right] (21.5) \left(\frac{1}{1000}\right) = 612 \text{ kips} > 571 \text{ kips}.$$
 OK

#### 4.1.2.4 Footing Reinforcement

Footing reinforcement is selected considering both flexural demands and minimum reinforcement requirements. The following calculations treat flexure first because it usually controls:

$$M_u = \frac{1}{2} (11) \left( \frac{11 - \frac{16}{12}}{2} \right)^2 (5.13) = 659 \text{ ft-kips}.$$

Try 10 #8 bars each way. The distance from the extreme compression fiber to the center of the top layer of reinforcement, d = t - cover - 1.5 $d_b = 26$  - 3 - 1.5(1) = 21.5 in.

$$T = A_s f_v = 10(0.79)(60) = 474$$
 kips.

Noting that C = T and solving the expression  $C = 0.85 f'_c b a$  for a produces a = 1.06 in.

$$\phi M_n = \phi T \left( d - \frac{a}{2} \right) = 0.80 \left( 474 \right) \left( 21.5 - \frac{1.06}{2} \right) \left( \frac{1}{12} \right) = 663 \, \text{ft-kips} > 659 \, \text{ft-kips}.$$
 OK

The ratio of reinforcement provided  $\rho = 10(0.79)/[(11)(12)(21.5)] = 0.00278$ . The distance between bars spaced uniformly across the width of the footing s = [(11)(12)-2(3+0.5)]/(10-1) = 13.9 in.

According to ACI 318 Sec. 7.12, the minimum reinforcement ratio = 0.0018 < 0.00278. OK

OK

and the maximum spacing is the lesser of  $3 \times 26$  in. or 18 = 18 in. > 13.9 in.

#### 4.1.2.5 Design Results

The calculations performed in Sec. 4.1.2.2 through 4.1.2.4 are repeated for typical perimeter and corner footings. The footing design for gravity loads is summarized in Table 4.1-2; Figure 4.1-4 depicts the resulting foundation plan.

Location	Loads	Footing Size and Reinforcement; Soil Capacity	Critical Section Demands and Design Strengths		
Interior	<i>D</i> = 387 kip	$11'-0" \times 11'-0" \times 2'-2"$ deep	One-way shear:	$V_{\mu} = 172 \text{ kip}$	
	<i>L</i> = 98 kip	10-#8 bars each way	•	$\phi V_n = 269 \text{ kip}$	
	_		Two-way shear:	$V_{u} = 571 \text{ kip}$	
	<i>P</i> = 485 kip	$P_{allow} = 484 \text{ kip}$		$\phi V_n = 612 \text{ kip}$	
	$P_{u} = 621 \text{ kip}$	$\phi P_n = 1597 \text{ kip}$	Flexure:	$M_{u} = 659 \text{ ft-kip}$	
				$\phi M_n = 663$ ft-kip	
Perimeter	<i>D</i> = 206 kip	8'-0" × 8'-0" × 1'-6" deep	One-way shear:	$V_{u} = 88.1 \text{ kip}$	
	$L = 45 \text{ kip}^{-1}$	10-#6 bars each way		$\phi V_n = 123 \text{ kip}$	
			Two-way shear:	$V_{u} = 289 \text{ kip}$	
	<i>P</i> = 251 kip	$P_{allow} = 256 \text{ kip}$		$\phi V_n = 302 \text{ kip}$	
	$P_{u} = 319 \text{ kip}$	$\phi P_n = 614 \text{ kip}$	Flexure:	$M_{u} = 222 \text{ ft-kip}$	
				$\phi M_n = 230$ ft-kip	
Corner	<i>D</i> = 104 kip	6'-0" × 6'-0" × 1'-2" deep	One-way shear:	$V_{u} = 41.5 \text{ kip}$	
	$L = 23 \text{ kip}^{-1}$	7-#5 bars each way	-	$\phi V_n = 64.9 \text{ kip}$	
			Two-way shear:	$V_u = 141 \text{ kip}$	
	<i>P</i> = 127 kip	$P_{allow} = 144 \text{ kip}$		$\phi V_n = 184 \text{ kip}$	
	$P_{u} = 162 \text{ kip}$	$\phi P_n = 259 \text{ kip}$	Flexure:	$M_u = 73.3 \text{ ft-kip}$	
				$\phi M_n = 80.2$ ft-kip	

**Table 4.1-2** Footing Design for Gravity Loads

[Use of the new resistance factors in ACI 318-02 would change these results.]

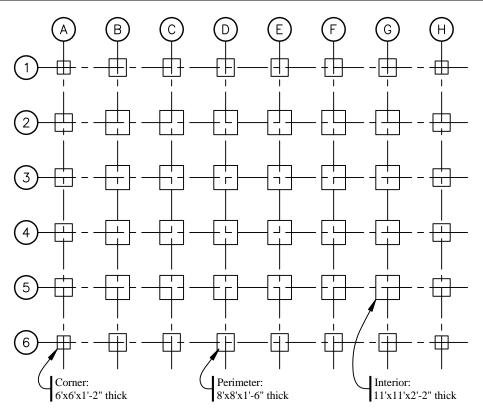


Figure 4.1-4 Foundation plan for gravity-load-resisting system.

# 4.1.3 Design for Moment-Resisting Frame System

Framing Alternate A in Sec. 5.2 of this volume of design examples includes a perimeter moment resisting frame as the seismic-force-resisting system. A framing plan for the system is shown in Figure 4.1-5. Detailed calculations are provided in this section for a combined footing at the corner and focus on overturning and sliding checks for the eccentrically loaded footing; settlement checks and design of concrete sections would be similar to the calculations shown in Sec. 4.1.2. The results for all footing types are summarized in Sec. 4.1.3.4.

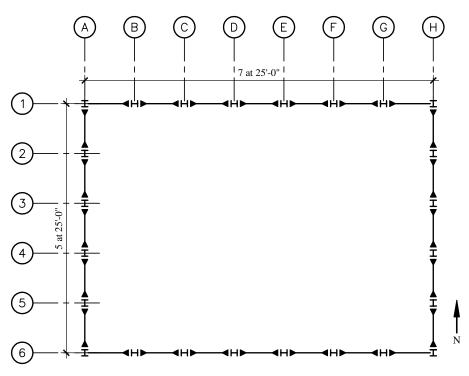


Figure 4.1-5 Framing plan for moment resisting frame system.

#### 4.1.3.1 Demands

A three-dimensional analysis of the superstructure, in accordance with the requirements for the equivalent lateral force (ELF) procedure, is performed using the RAMFRAME program. Foundation reactions at selected grids are reported in Table 4.1-3.

Table 4.1-3         Demands from Moment-Resisting Frame System						
Location	Load	Rx	Ry	Rz	Mxx	Муу
A-5	D			-203.8		
	L			-43.8		
	Ex	-13.8	4.6	3.8	53.6	-243.1
	Ey	0.5	-85.1	-21.3	-1011.5	8.1
A-6	D			-103.5		
	L			-22.3		
	Ex	-14.1	3.7	51.8	47.7	-246.9
	Ey	0.8	-68.2	281.0	-891.0	13.4

Table 4.1-3 Demands from Moment-Resisting Frame System

Note: Units are kips and feet. Load *Ex* is for loads applied toward the east, including appropriately amplified counter-clockwise accidental torsion. Load *Ey* is for loads applied toward the north, including appropriately amplified clockwise accidental torsion.

Sec. 5.2.3.5 of this volume of design examples outlines the design load combinations, which include the redundancy factor as appropriate. Considering two senses of accidental torsion for loading in each direction and including orthogonal effects results in a large number of load cases. The detailed calculations presented here are limited to two primary conditions, both for a combined foundation for columns at Grids A-5 and A-6: the downward case (1.4D + 0.5L + 0.32Ex + 1.11Ey) and the upward case

(0.7D + 0.32Ex + 1.11Ey). [Because the redundancy factor is changed substantially in the 2003 *Provisions*, the factors in these load combinations would change.]

Before loads can be computed, attention must be given to *Provisions* Sec. 5.4.5 [5.2.5]. That section permits "foundations of structures . . . to be designed for three-fourths of the foundation overturning design moment,  $M_{f}$ ." Because the overturning moment in question is the global overturning moment for the *system*, judgment must be used in determining which design actions may be reduced. If the seismic-force-resisting system consists of isolated shear walls, the shear wall overturning moment at the base best fits that description. For a perimeter moment-resisting frame, most of the global overturning resistance is related to axial loads in columns. Therefore, in this example column axial loads (*Rz*) from load cases *Ex* and *Ey* will be multiplied by 0.75 and all other load effects will remain unreduced.

### 4.1.3.2 Downward Case (1.4D + 0.5L + 0.32Ex + 1.11Ey)

In order to perform the overturning checks a footing size must be assumed. Preliminary checks (not shown here) confirmed that isolated footings under single columns were untenable. Check overturning for a footing that is 10 ft wide by 40 ft long by 5 ft thick. Further, assume that the top of the footing is 2 ft below grade (the overlying soil contributes to the resisting moment). (In these calculations the  $0.2S_{DS}D$  modifier for vertical accelerations is used for the dead loads *applied to* the foundation but not for the weight of the foundation and soil. This is the author's interpretation of the *Provisions*. The footing and soil overburden are not subject to the same potential for dynamic amplification as the dead load of the superstructure, and it is not common practice to include the vertical acceleration on the weight of the foundation. Furthermore, for footings that resist significant overturning, this issue makes a significant difference in design.) Combining the loads from columns at Grids A-5 and A-6 and including the weight of the foundation and overlying soil produces the following loads at the foundation-soil interface:

P = applied loads + weight of foundation and soil= 1.4(-203.8 - 103.5) + 0.5(-43.8 - 22.3) + 0.75[0.32(3.8 + 51.8) + 1.11(-21.3 + 281)]- 1.2[10(40)(5)(0.15) + 10(40)(2)(0.125)]= -714 kips.

$$\begin{split} M_{xx} &= \text{direct moments} + \text{moment due to eccentricity of applied axial loads} \\ &= 0.32(53.6 + 47.7) + 1.11(-1011.5 - 891.0) \\ &+ [1.4(-203.8) + 0.5(-43.8) + 0.75(0.32)(3.8) + 0.75(1.11)(-21.3)](12.5) \\ &+ [1.4(-103.5) + 0.5(-22.3) + 0.75(0.32)(51.8) + 0.75(1.11)(281)](-12.5) \\ &= -7258 \text{ ft-kips.} \end{split}$$

 $M_{yy} = 0.32(-243.1 - 246.9) + 1.11(8.1 + 13.4)$ = -133 ft-kips. (The resulting eccentricity is small enough to neglect here, which simplifies the problem considerably.)

$$V_x = 0.32(-13.8 - 14.1) + 1.11(0.5 + 0.8)$$
  
= -7.49 kips.

$$V_y = 0.32(4.6 + 3.7) + 1.11(-85.1 - 68.2)$$
  
= -167.5 kips.

Note that the above load combination does not yield the maximum downward load. Reversing the direction of the seismic load results in P = -1173 kips and  $M_{xx} = 3490$  ft-kips. This larger axial load does not control the design because the moment is so much less that the resultant is within the kern and no uplift occurs.

The soil calculations that follow use a different sign convention than that in the analysis results noted above; compression is positive for the soil calculations. The eccentricity is:

$$e = |M/P| = 7258/714 = 10.17$$
 ft.

Where *e* is less than L/2, a solution to the overturning problem exists; however, as *e* approaches L/2, the bearing pressures increase without bound. Since *e* is greater than L/6 = 40/6 = 6.67 ft, uplift occurs and the maximum bearing pressure is:

$$q_{\text{max}} = \frac{2P}{3B\left(\frac{L}{2} - e\right)} = \frac{2(714)}{3(10)\left(\frac{40}{2} - 10.17\right)} = 4.84 \,\text{ksf}$$

and the length of the footing in contact with the soil is:

$$L' = 3\left(\frac{L}{2} - e\right) = 3\left(\frac{40}{2} - 10.17\right) = 29.5 \,\mathrm{ft}$$

The bearing capacity  $q_c = 3000 B' = 3000 \times \min(B, L'/2) = 3000 \times \min(10, 29.5/2) = 30,000 \text{ psf} = 30 \text{ ksf.}$ (L'/2 is used as an adjustment to account for the gradient in the bearing pressure in that dimension.)

The design bearing capacity  $\phi q_c = 0.6(30 \text{ ksf}) = 18 \text{ ksf} > 4.84 \text{ ksf}.$  OK

The foundation satisfies overturning and bearing capacity checks. The upward case, which follows, will control the sliding check.

#### 4.1.3.3 Upward Case (0.7D + 0.32Ex + 1.11Ey)

For the upward case the loads are:

P = -346 kips  $M_{xx} = -6240 \text{ ft-kips}$   $M_{yy} = -133 \text{ ft-kips (negligible)}$   $V_x = -7.5 \text{ kips}$  $V_y = -167 \text{ kips}$ 

The eccentricity is:

e = |M/P| = 6240/346 = 18.0 ft.

Again, e is greater than L/6, so uplift occurs and the maximum bearing pressure is:

$$q_{\text{max}} = \frac{2(346)}{3(10)\left(\frac{40}{2} - 18.0\right)} = 11.5 \,\text{ksf}$$

and the length of the footing in contact with the soil is:

$$L' = 3\left(\frac{40}{2} - 18.0\right) = 6.0\,\mathrm{ft}$$

The bearing capacity  $q_c = 3000 \times \min(10, 6/2) = 9,000 \text{ psf} = 9.0 \text{ ksf}.$ 

The design bearing capacity  $\phi q_c = 0.6(9.0 \text{ ksf}) = 5.4 \text{ ksf} < 11.5 \text{ ksf}.$  NG

Using an elastic distribution of soil pressures, the foundation fails the bearing capacity check (although stability is satisfied). Try the plastic distribution. Using this approach, the bearing pressure over the entire contact area is assumed to be equal to the design bearing capacity. In order to satisfy vertical equilibrium, the contact area times the design bearing capacity must equal the applied vertical load P. Because the bearing capacity used in this example is a function of the contact area and the value of P changes with the size, the most convenient calculation is iterative.

By iteration, the length of contact area L' = 4.39 ft.

The bearing capacity  $q_c = 3000 \times \min(10, 4.39) = 13,170 \text{ psf} = 13.2 \text{ ksf.}$  (No adjustment to L' is needed as the pressure is uniform.)

The design bearing capacity  $\phi q_c = 0.6(13.2 \text{ ksf}) = 7.92 \text{ ksf}.$ 

(7.92)(4.39)(10) = 348 kips  $\approx 346$  kips, so equilibrium is satisfied; the difference is rounded off.

The resisting moment,  $M_R = P (L/2-L'/2) = 346 (40/2 - 4.39/2) = 6160$  ft-kip  $\approx 6240$  ft-kip. OK

Therefore, using a plastic distribution of soil pressures, the foundation satisfies overturning and bearing capacity checks.

The calculation of demands on concrete sections for strength checks should use the same soil stress distribution as the overturning check. Using a plastic distribution of soil stresses defines the upper limit of static loads for which the foundation remains stable, but the extreme concentration of soil bearing tends to drive up shear and flexural demands on the concrete section. It should be noted that the foundation may remain stable for larger loads if they are applied dynamically; even in that case, the strength demands on the concrete section will not exceed those computed on the basis of the plastic distribution.

For the sliding check, initially consider base traction only. The sliding demand is:

$$V = \sqrt{V_x^2 + V_y^2} = \sqrt{(-7.49)^2 + (-167)^2} = 167.2 \,\text{kips}$$

As calculated previously, the total compression force at the bottom of the foundation is 346 kips. The design sliding resistance is:

$$\phi V_c = \phi \times \text{friction coefficient} \times P = 0.8(0.65)(346 \text{ kips}) = 180 \text{ kips} > 167.2 \text{ kips}.$$
 OK

If base traction alone had been insufficient, resistance due to passive pressure on the leading face could be included. Sec. 4.2.2.2 below illustrates passive pressure calculations for a pile cap.

#### 4.1.3.4 Design Results

The calculations performed in Sec. 4.1.3.2 and 4.1.3.3 are repeated for combined footings at middle and side locations. Figure 4.1-6 shows the results.

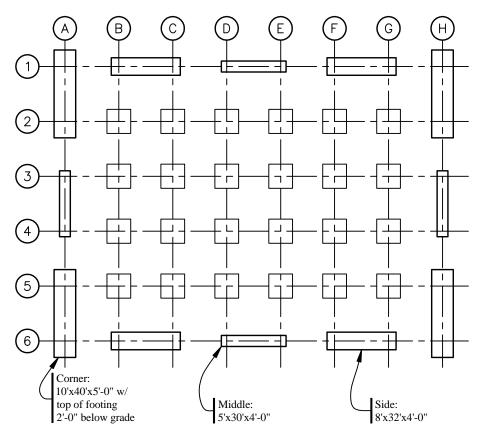
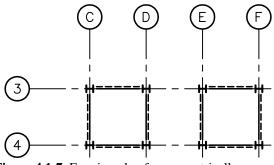


Figure 4.1-6 Foundation plan for moment-resisting frame system.



**Figure 4.1-7** Framing plan for concentrically braced frame system.

One last check of interest is to compare the flexural stiffness of the footing with that of the steel column, which is needed because the steel frame design was based upon flexural restraint at the base of the columns. Using an effective moment of inertia of 50 percent of the gross moment of inertia and also using the distance between columns as the effective span, the ratio of EI/L for the smallest of the combined footings is more than five times the EI/h for the steel column. This is satisfactory for the design assumption.

### 4.1.4 Design for Concentrically Braced Frame System

Framing Alternate B in Sec. 5.2 of this volume of design examples employs a concentrically braced frame system at a central core to provide resistance to seismic loads. A framing plan for the system is shown in Figure 4.1-7.

# 4.1.4.1 Check Mat Size for Overturning

Uplift demands at individual columns are so large that the only practical shallow foundation is one that ties together the entire core. The controlling load combination for overturning has minimum vertical loads (which help to resist overturning), primary overturning effects  $(M_{xx})$  due to loads applied parallel to the short side of the core, and smaller moments about a perpendicular axis  $(M_{yy})$  due to orthogonal effects. Assume mat dimensions of 45 ft by 95 ft by 7 ft thick with the top of the mat 3'-6" below grade. Combining the factored loads applied to the mat by all eight columns and including the weight of the foundation and overlying soil produces the following loads at the foundation-soil interface:

P = -7,849 kips  $M_{xx} = -148,439$  ft-kips  $M_{yy} = -42,544$  ft-kips  $V_x = -765$  kips  $V_y = -2,670$  kips

Figure 4.1-8 shows the soil pressures that result from application in this controlling case, depending on the soil distribution assumed. In both cases the computed uplift is significant. In Part a of the figure the contact area is shaded. The elastic solution shown in Part b was computed by modeling the mat in RISA 3D with compression only soil springs (with the stiffness of edge springs doubled as recommended by Bowles). For the elastic solution the average width of the contact area is 11.1 ft and the maximum soil pressure is 16.9 ksf.

The bearing capacity  $q_c = 3000 \times \min(95, 11.1/2) = 16,650 \text{ psf} = 16.7 \text{ ksf}$ .

The design bearing capacity  $\phi q_c = 0.6(16.7 \text{ ksf}) = 10.0 \text{ ksf} < 16.9 \text{ ksf}.$ 

NG

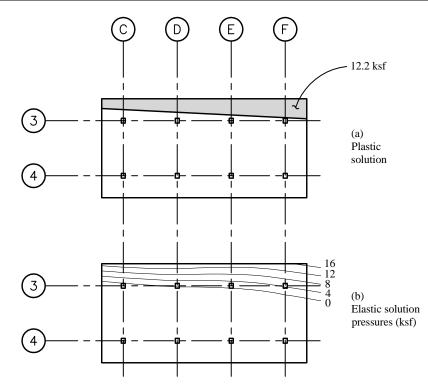


Figure 4.1-8 Soil pressures for controlling bidirectional case.

As was done in Sec. 4.1.3.3 above, try the plastic distribution. The present solution has an additional complication as the off-axis moment is not negligible. The bearing pressure over the entire contact area is assumed to be equal to the design bearing capacity. In order to satisfy vertical equilibrium, the contact area times the design bearing capacity must equal the applied vertical load P. The shape of the contact area is determined by satisfying equilibrium for the off-axis moment. Again the calculations are iterative.

Given the above constraints, the contact area shown in Figure 4.1-8 is determined. The length of the contact area is 4.46 ft at the left side and 9.10 ft at the right side. The average contact length, for use in determining the bearing capacity, is (4.46 + 9.10)/2 = 6.78 ft. The distances from the center of the mat to the centroid of the contact area are

 $\overline{x} = 5.42$  ft  $\overline{y} = 18.98$  ft

The bearing capacity  $q_c = 3000 \times \min(95, 6.78) = 20,340 \text{ psf} = 20.3 \text{ ksf}.$ 

The design bearing capacity  $\phi q_c = 0.6(20.3 \text{ ksf}) = 12.2 \text{ ksf}.$ 

(12.2)(6.78)(95) = 7,858 kips  $\approx 7,849$  kips, confirming equilibrium for vertical loads. (7,849)(5.42) = 42,542 ft-kips  $\approx 42,544$  ft-kips, confirming equilibrium for off-axis moment.

The resisting moment,  $M_{R,xx} = P \overline{y} = 7849(18.98) = 148,974 \text{ ft-kips} > 148,439 \text{ ft-kips}.$  OK

So, the checks of stability and bearing capacity are satisfied. The mat dimensions are shown in Figure 4.1-9.

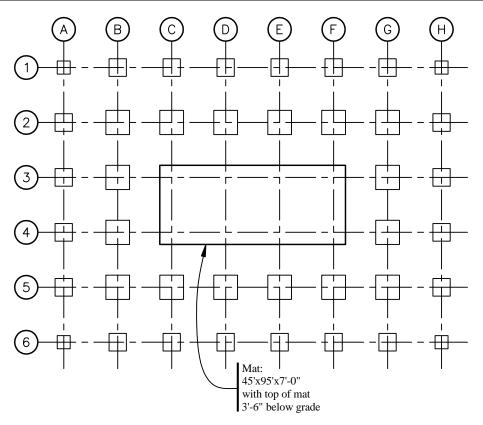


Figure 4.1-9 Foundation plan for concentrically braced frame system.

### 4.1.4.2 Design Mat for Strength Demands

As was previously discussed, the computation of strength demands for the concrete section should use the same soil pressure distribution as was used to satisfy stability and bearing capacity. Because dozens of load combinations were considered and "hand calculations" were used for the plastic distribution checks, the effort required would be considerable. The same analysis used to determine elastic bearing pressures yields the corresponding section demands directly. One approach to this dilemma would be to compute an additional factor that must be applied to selected elastic cases to produce section demands that are consistent with the plastic solution. Rather than provide such calculations here, design of the concrete section will proceed using the results of the elastic analysis. This is conservative for the demand on the concrete for the same reason that it was unsatisfactory for the soil: the edge soil pressures are high (that is, we are designing the concrete for a peak soil pressure of 16.9 ksf, even though the plastic solution gives 12.2 ksf).

[Note that Sec. 7.2.3 of the 2003 *Provisions* requires consideration of parametric variation for soil properties where foundations are modeled explicitly. This example does not illustrate such calculations.]

Concrete mats often have multiple layers of reinforcement in each direction at the top and bottom of their thickness. Use of a uniform spacing for the reinforcement provided in a given direction greatly increases the ease of construction. The minimum reinforcement requirements defined in Sec. 10.5 of ACI 318 were discussed in Sec. 4.1.1.3 above. Although all of the reinforcement provided to satisfy Sec. 7.12 of ACI 318 may be provided near one face, for thick mats it is best to compute and provide the amount of required reinforcement separately for the top and bottom halves of the section. Using a bar spacing of 10 in. for this 7-ft-thick mat and assuming one or two layers of bars, the section capacities indicate in Table 4.1-4 (presented in order of decreasing strength) may be precomputed for use in design. The amount of

reinforcement provided for marks B, C, and D are less than the basic minimum for flexural members, so the demands should not exceed three-quarters of the design strength where those reinforcement patterns are used. The amount of steel provided for Mark D is the minimum that satisfies ACI 318 Sec. 7.12.

			I I I I I I I I I I I I I I I I I I I	
Mark	Reinforcement	$A_s$ (in. <sup>2</sup> per ft)	$\phi M_n$ (ft-kip/ft)	$3/4\phi M_n$ (ft-kip/ft)
А	2 layers of #10 bars at 10 in. o.c.	3.05	899	not used
В	2 layers of #9 bars at 10 in. o.c.	2.40	not used	534
С	2 layers of #8 bars at 10 in. o.c.	1.90	not used	424
D	#8 bars at 10 in. o.c.	0.95	not used	215

**Table 4.1-4** Mat Foundation Section Capacities

Note: Where the area of steel provided is less than the minimum reinforcement for flexural members as indicated in ACI 318 Sec. 10.5.1, demands are compared to 3/4 of  $\phi M_n$  as permitted in Sec. 10.5.3.

To facilitate rapid design the analysis results are processed in two additional ways. First, the flexural and shear demands computed for the various load combinations are enveloped. Then the enveloped results are presented (see Figure 4.1-10) using contours that correspond to the capacities shown for the reinforcement patterns noted in Table 4.1-4.

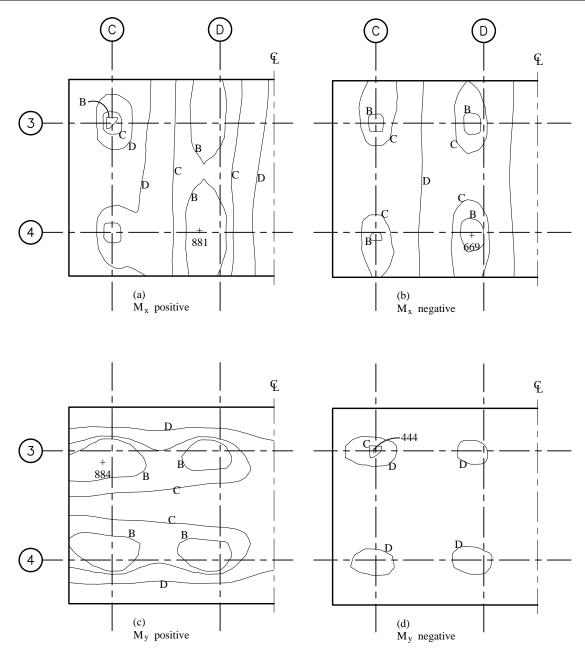


Figure 4.1-10 Envelope of mat foundation flexural demands.

Using the noted contours permits direct selection of reinforcement. The reinforcement provided within a contour for a given mark must be that indicated for the next higher mark. For instance, all areas within Contour B must have two layers of #10 bars. Note that the reinforcement provided will be symmetric about the centerline of the mat in both directions. Where the results of finite element analysis are used in the design of reinforced concrete elements, averaging of demands over short areas is appropriate. In Figure 4.1-11, the selected reinforcement is superimposed on the demand contours. Figure 4.1-12 shows a section of the mat along Gridline C.

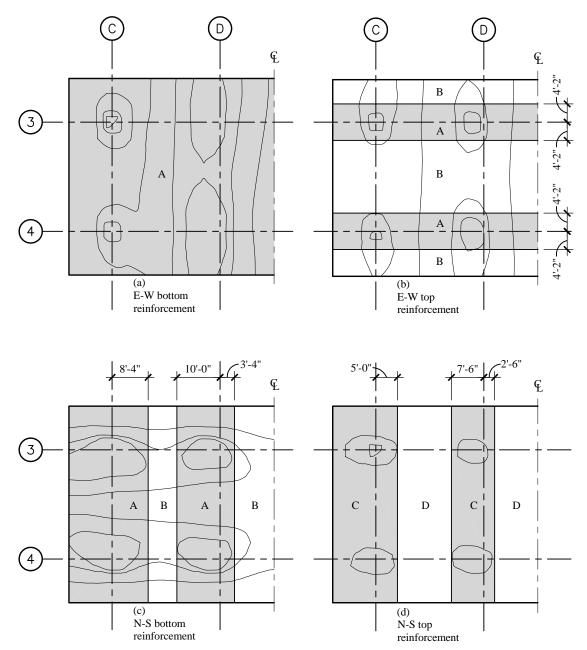


Figure 4.1-11 Mat foundation flexural reinforcement.

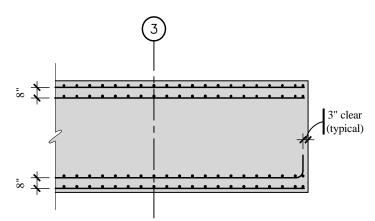


Figure 4.1-12 Section of mat foundation.

Figure 4.1-13 presents the envelope of shear demands. The contours used correspond to the design strengths computed assuming  $V_s = 0$  for one-way and two-way shear. In the hatched areas the shear stress exceeds  $\phi 4\sqrt{f_c'}$  and in the shaded areas it exceeds  $\phi 2\sqrt{f_c'}$ . The critical sections for two-way shear (as discussed in Sec. 4.1.1.3 also are shown. The only areas that need more careful attention (to determine whether they require shear reinforcement) are those where the hatched or shaded areas are outside the critical sections. At the columns on Gridline D, the hatched area falls outside the critical section, so closer inspection is needed. Because the perimeter of the hatched area is substantially smaller than the perimeter of the critical section for punching shear, the design requirements of ACI 318 are satisfied.

One-way shears at the edges of the mat exceed the  $\phi 2\sqrt{f'_c}$  criterion. Note that the high shear stresses are not produced by loads that create high bearing pressures at the edge. Rather they are produced by loads that created large bending stresses parallel to the edge. The distribution of bending moments and shears is not uniform across the width (or breadth) of the mat, primarily due to the torsion in the seismic loads and the orthogonal combination. It is also influenced by the doubled spring stiffnesses used to model the soil condition. However, when the shears are averaged over a width equal to the effective depth (*d*), the demands are less than the design strength.

In this design, reinforcement for punching or beam shear is not required. If shear reinforcement cannot be avoided, bars may be used both to chair the upper decks of reinforcement and provide resistance to shear in which case they may be bent thus:  $\int_{-\infty}^{\infty} dx$ 

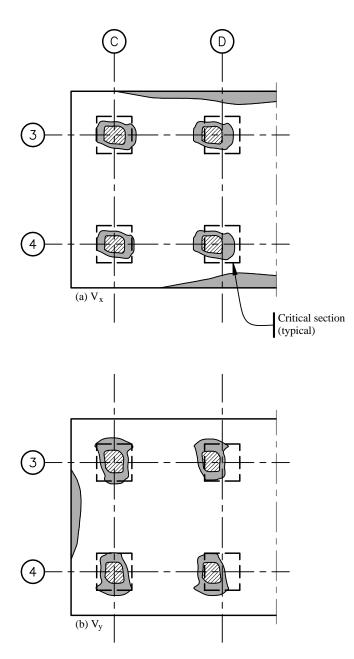


Figure 4.1-13 Critical sections for shear and envelope of mat foundation shear demands.

# 4.1.5 COST COMPARISON

Table 4.1-5 provides a summary of the material quantities used for all of the foundations required for the various conditions considered. Corresponding preliminary costs are assigned. The gravity-only condition does not represent a realistic case because design for wind loads would require changes to the foundations; it is provided here for discussion. It is obvious that design for lateral loads adds cost as compared to a design that neglects such loads. However, it is also worth noting that braced frame systems usually have substantially more expensive foundation systems than do moment frame systems. This condition occurs for two reasons. First, braced frame systems are stiffer, which produces shorter periods and higher design forces. Second, braced frame systems tend to concentrate spatially the demands on the

foundations. In this case the added cost amounts to about  $0.80/ft^2$ , which is an increase of perhaps 4 or 5 percent to the cost of the structural system.

Design Condition	Concrete at Gravity Foundations	Concrete at Lateral Foundations	Total Excavation	Total Cost
Gravity only (see Figure 4.1-4)	310 cy at \$150/cy = \$46,500		310 cy at \$15/cy = \$4,650	\$ 51,150
Moment frame	233 cy at \$150/cy	537 cy at \$180/cy	800 cy at \$15/cy	\$143,610
(see Figure 4.1-6)	= \$34,950	= \$96,660	= \$12,000	
Braced frame	233 cy at \$150/cy	1108 cy at \$180/cy	1895 cy at \$15/cy	\$262,815
(see Figure 4.1-9)	= \$34,950	= \$199,440	= \$28,425	

 Table 4.1-5
 Summary of Material Quantities and Cost Comparison

# **4.2 DEEP FOUNDATIONS FOR A 12-STORY BUILDING, SEISMIC DESIGN CATEGORY D**

This example features the analysis and design of deep foundations for a 12-tory reinforced concrete moment-resisting frame building similar to that described in Chapter 6 of this volume of design examples.

# **4.2.1 Basic Information**

### 4.2.1.1 Description

Figure 4.2-1 shows the basic design condition considered in this example. A  $2\times2$  pile group is designed for four conditions: for loads delivered by a corner and a side column of a moment-resisting frame system for Site Classes C and E. Geotechnical parameters for the two sites are given in Table 4.2-1.

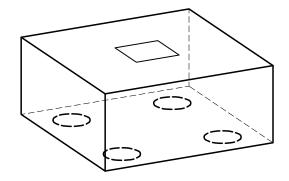


**Figure 4.2-1** Design condition: column of concrete moment resisting frame supported by pile cap and cast-in-place piles.

Depth	Class E Site	Class C Site
0 to 3 ft	Loose sand/fill	Loose sand/fill
	$\gamma = 110 \text{ pcf}$ angle of internal friction = 28 deg soil modulus parameter, $k = 25 \text{ pci}$	$\gamma = 110 \text{ pcf}$ angle of internal friction = 30 deg soil modulus parameter, $k = 50 \text{ pci}$
	neglect skin friction neglect end bearing	neglect skin friction neglect end bearing
3 to 30 ft	Soft clay	Dense sand (one layer: 3 to 100 ft depth)
	$\gamma = 110 \text{ pcf}$ undrained shear strength = 430 psf soil modulus parameter, $k = 25 \text{ pci}$ strain at 50 percent of maximum stress, $\varepsilon_{50} = 0.01$ skin friction (ksf) = 0.3	$\gamma$ = 130 pcf angle of internal friction = 42 deg soil modulus parameter, <i>k</i> = 125 pci
	neglect end bearing	
30 to 100 ft	Medium dense sand $\gamma = 120 \text{ pcf}$ angle of internal friction = 36 deg soil modulus parameter, $k = 50 \text{ pci}$ skin friction (ksf)* = 0.9 + 0.025/ft $\leq 2$	skin friction (ksf)* = $0.3 + 0.03/ft \le 2$ end bearing (ksf)* = $65 + 0.6/ft \le 150$
Dila con	end bearing $(ksf)^* = 40 + 0.5/ft \le 100$	575 por ultimate possive processo
Pile cap resistance	300 pcf, ultimate passive pressure	575 pcf, ultimate passive pressure
Resistance factor for capacity checks ( $\phi$ ) = 0.75. Safety factor for settlement checks = 2.5.		[In the 2003 <i>Provisions</i> , $\phi$ factors for cohesive and cohesionless soils are explicitly defined; for vertical, lateral and rocking resistance, the values would be 0.8 for the clay layer and 0.7 for the sand layers.]

\*Skin friction and end bearing values increase (up to the maximum value noted) for each additional foot of depth below the top of the layer. (The values noted assume a minimum pile length of 20 ft.)

The structural material properties assumed for this example are as follows:

 $f'_c = 3,000 \text{ psi}$  $f_v = 60,000 \text{ psi}$ 

#### 4.2.1.2 Provisions Parameters

Site Class = C and E (both conditions considered in this example)  $S_{DS} = 0.9$ Seismic Design Category = D (for both conditions)

#### 4.2.1.3 Demands

Table 4.2-2         Gravity and Seismic Demands						
Location	Load	Rx	Ry	Rz	Mxx	Муу
Corner	D			-351.0		
	L			-36.0		
	Vx	40.7	0.6	142.5	4.8	439.0
	Vy	0.8	46.9	305.6	489.0	7.0
	ATx	1.2	2.6	12.0	27.4	12.9
	ATy	3.1	6.7	31.9	70.2	33.0
Side	D			-702.0		
	L			-72.0		
	Vx	29.1	0.5	163.4	3.5	276.6
	Vy	0.8	59.3	18.9	567.4	6.5
	ATx	0.1	3.3	8.7	31.6	1.3
	ATy	0.4	8.4	22.2	80.8	3.4

The unfactored demands from the moment frame system are shown in Table 4.2-2.

Note: Units are kips and feet. Load Vx is for loads applied toward the east. ATx is the corresponding accidental torsion case. Load Vy is for loads applied toward the north. ATy is the corresponding accidental torsion case.

Using ASCE 7 Load Combinations 5 and 7, *E* as defined in *Provisions* Sec. 5.2.7 [4.2.2] (with  $0.2S_{DS}D = 0.18D$  and taking  $\rho = 1.0$ ), considering orthogonal effects as required for Seismic Design Category D, and including accidental torsion, the following 32 load conditions must be considered. [Although the redundancy factor is changed substantially in the 2003 *Provisions*, it is expected that this system would still satisfy the conditions needed for  $\rho = 1.0$ , so these load combinations would not change.]

 $\begin{array}{l} 1.38D + 0.5L \pm 1.0Vx \pm 0.3Vy \pm \max(1.0ATx, 0.3ATy) \\ 1.38D + 0.5L \pm 0.3Vx \pm 1.0Vy \pm \max(0.3ATx, 1.0ATy) \\ 0.72D \pm 1.0Vx \pm 0.3Vy \pm \max(1.0ATx, 0.3ATy) \\ 0.72D \pm 0.3Vx \pm 1.0Vy \pm \max(0.3ATx, 1.0ATy) \end{array}$ 

### 4.2.1.4 Design Approach

For typical deep foundation systems resistance to lateral loads is provided by both piles and pile cap. Figure 4.2-2 shows a simple idealization of this condition. The relative contributions of these piles and pile cap depend on the particular design conditions, but often both effects are significant. Resistance to vertical loads is assumed to be provided by the piles alone regardless of whether their axial capacity is primarily due to end bearing, skin friction, or both. Although the behavior of foundation and superstructure are closely related, they typically are modeled independently. Earthquake loads are applied to a model of the superstructure, which is assumed to have fixed supports. Then the support reactions are seen as demands on the foundation system. A similar substructure technique is usually applied to the foundation system itself, whereby the behavior of pile cap and piles are considered separately. This section describes that typical approach.

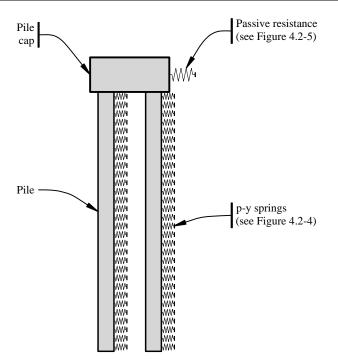


Figure 4.2-2 Schematic model of deep foundation system.

#### 4.2.1.4.1 Pile Group Mechanics

With reference to the free body diagram (of a  $2 \times 2$  pile group) shown in Figure 4.2-3, demands on individual piles as a result of loads applied to the group may be determined as follows:

 $V = \frac{V_{group} - V_{passive}}{4}$  and  $M = V \times \ell$ , where  $\ell$  is a characteristic length determined from analysis of a

laterally loaded single pile.

 $P_{ot} = \frac{V_{group}h + M_{group} + 4M - h_p V_{passive}}{2s}$ , where *s* is the pile spacing, *h* is the height of the pile cap, and  $h_p$  is the height of  $V_{passive}$  above Point O.

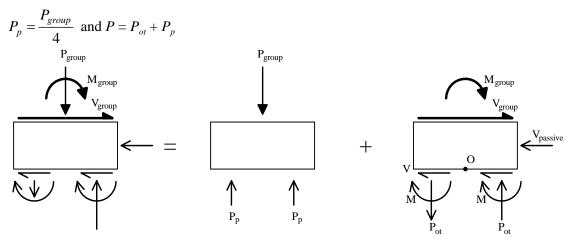
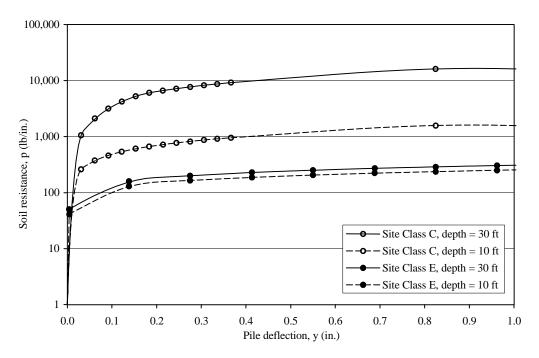


Figure 4.2-3 Pile cap free body diagram.

# 4.2.1.4.2 Contribution of Piles

The response of individual piles to lateral loads is highly nonlinear. In recent years it has become increasingly common to consider that nonlinearity directly. Based on extensive testing of full-scale specimens and small-scale models for a wide variety of soil conditions, researchers have developed empirical relationships for the nonlinear p-y response of piles that are suitable for use in design. Representative p-y curves (computed for a 22 in. diameter pile) are shown in Figure 4.2-4. The stiffness of the soil changes by an order of magnitude for the expected range of displacements (the vertical axis uses a logarithmic scale). The p-y response is sensitive to pile size (an effect not apparent is the figure which is based on a single pile size); soil type and properties; and, in the case of sands, vertical stress, which increases with depth. Pile response to lateral loads, like the p-y curves on which the calculations are based, is usually computed using computer programs like LPILE.



**Figure 4.2-4** Representative *p*-*y* curves (note that a logarithmic scale is used on the vertical axis).

# 4.2.1.4.3 Contribution of Pile Cap

Pile caps contribute to the lateral resistance of a pile group in two important ways: directly as a result of passive pressure on the face of the cap that is being pushed into the soil mass and indirectly by producing a fixed head condition for the piles, which can significantly reduce displacements for a given applied lateral load. Like the p-y response of piles, the passive pressure resistance of the cap is nonlinear. Figure 4.2-5 shows how the passive pressure resistance (expressed as a fraction of the ultimate passive pressure) is related to the imposed displacement (expressed as a fraction of the minimum dimension of the face being pushed into the soil mass).

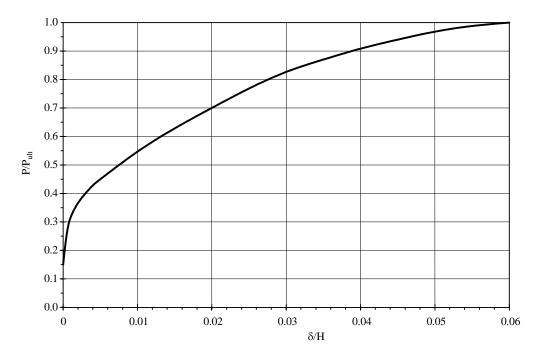


Figure 4.2-5 Passive pressure mobilization curve (after FEMA 356).

#### 4.2.1.4.4 Group Effect Factors

The response of a group of piles to lateral loading will differ from that of a single pile due to pile-soil-pile interaction. (Group effect factors for axial loading of very closely spaced piles may also be developed, but are beyond the scope of the present discussion.) A useful discussion of this "group effect" may be found in PoLam Sec. 2.6.4, from which the following observations are taken:

The pile group effect has been a popular research topic within the geotechnical community for almost 50 years. At present, there is no common consensus on the approach for group effects. Full-size and model tests by a number of authors show that in general, the lateral capacity of a pile in a pile group versus that of a single pile (termed "efficiency") is reduced as the pile spacing is reduced...

[The experimental research reported in Brown 1987, Brown 1988, and other publications] . . . yielded information that largely corroborated each other on the following aspects:

(1) Most of these experiments first used the single pile data to verify the validity of the widely used Reese's and Matlock's benchmark p-y criteria and all concluded that the Reese and Matlock p-y criteria provide reasonable solutions.

(2) The observed group effects appeared to be associated with shadowing effects and the various researchers found relatively consistent pile group behavior in that the leading piles would be loaded more heavily than the trailing piles when all piles are loaded to the same deflection. ... All referenced researchers recommended to modify the single pile p-y curves by adjusting the resistance value on the single pile p-y curves (i.e. p-multiplier). . . .

The experiments reported by McVay also included data for pile center-to-center spacing of 5D which showed p-multipliers of 1.0, 0.85, and 0.7 for the front, middle and back row piles, respectively. For such multipliers, the group stiffness efficiency would be about 95% and group effects would be practically negligible.

The basis of the calculation procedure for group effect factors that is shown below is described in Chapter 6 of GROUP. In these expressions, *D* is the pile diameter and *s* is the center-to-center spacing between the piles in question. In the equation for each efficiency factor, where s/D equals or exceeds the noted upper limit, the corresponding value of  $\beta$  is 1.0.

For piles that are side by side with respect to the applied load, a factor to reflect the reduction in efficiency,  $\beta_{a}$ , may be calculated as:

$$\beta_a = 0.5292 \left(\frac{s}{D}\right)^{0.5659}$$
 for  $1 \le \frac{s}{D} < 3.28$ .

For piles that are in-line with respect to the applied load, a factor to reflect the reduction in efficiency ( $\beta_b$ ) may be calculated as follows:

Leading piles: 
$$\beta_{bL} = 0.7309 \left(\frac{s}{D}\right)^{0.2579}$$
 for  $1 \le \frac{s}{D} < 3.37$ .

Trailing piles: 
$$\beta_{bT} = 0.5791 \left(\frac{s}{D}\right)^{0.3251}$$
 for  $1 \le \frac{s}{D} < 5.37$ .

For piles that are skewed (neither in line nor side by side) with respect to the applied load, a factor to reflect the reduction in efficiency ( $\beta_s$ ) may be calculated as:

$$\beta_s = \sqrt{\beta_a^2 \cos^2 \theta + \beta_b^2 \sin^2 \theta}$$

where  $\beta_a$  and  $\beta_b$  are calculated as defined above using *s* equal to the center-to-center distance along the skew and setting  $\theta$  equal to the angle between the direction of loading and a line connecting the two piles.

If a group contains more than two piles, the effect of each pile on each other pile must be considered. If the effect of pile *j* on pile *i* is called  $\beta_{ji}$  and it is noted that  $\beta_{ji} = 1.0$  when j = i (as this is a single pile condition), the *p*-reduction factor for any given pile *i* is

$$f_{mi} = \prod_{j=1}^n \beta_{ji} \; .$$

Because the direction of loading varies during an earthquake and the overall efficiency of the group is the primary point of interest, the average efficiency factor is commonly used for all members of a group in the analysis of any given member. In that case, the average *p*-reduction factor is:

$$\overline{f}_m = \frac{1}{n} \sum_{i=1}^n \prod_{j=1}^n \beta_{ji} \; .$$

For a 2×2 pile group thus 3 1 2 2 with s = 3D, the group effect factor is calculated as:

$$\beta_{11} = 1.0,$$

$$\beta_{21} = \beta_a \beta_b = 0.5292 \left(\frac{3}{1}\right)^{0.5659} \times 1.0 = 0.985$$
,

$$\beta_{31} = \beta_a \beta_b = 1.0 \times 0.7309 \left(\frac{3}{1}\right)^{0.2579} = 0.970$$
, and

$$\beta_{41} = \beta_a \beta_b = (1.0)(1.0) = 1.0$$
 (because  $s/D = 4.24$ ).

Thus, 
$$f_{m1} = \beta_{11} \times \beta_{21} \times \beta_{31} \times \beta_{41} = (1.00)(0.985)(0.970)(1.00) = 0.955 \approx 0.96.$$

By similar calculations,  $f_{m2} = 0.96$ ,  $f_{m3} = 0.79$ , and  $f_{m4} = 0.79$ .

And finally, 
$$\overline{f}_m = \frac{0.96 + 0.96 + 0.79 + 0.79}{4} = 0.87$$
.

Figure 4.2-6 shows the group effect factors that are calculated for square pile groups of various sizes with piles at several different spacings.

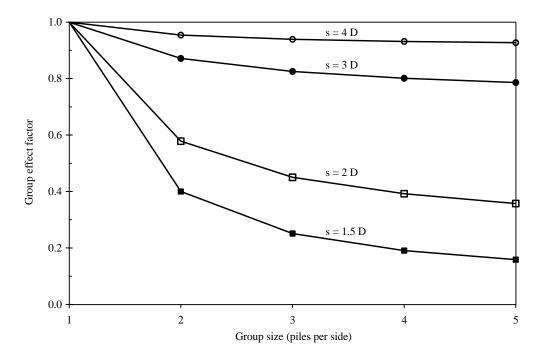


Figure 4.2-6 Calculated group effect factors.

### 4.2.2 Pile Analysis, Design, and Detailing

#### 4.2.2.1 Pile Analysis

For this design example it is assumed that all piles will be fixed-head, 22-in.-diameter, cast-in-place piles arranged in  $2 \times 2$  pile groups with piles spaced at 66 inches center-to-center. The computer program LPILE Plus 3.0 is used to analyze single piles for both soil conditions shown in Table 4.2-1 assuming a

length of 50 ft. Pile flexural stiffness is modeled using one-half of the gross moment of inertia because of expected flexural cracking. The response to lateral loads is affected to some degree by the coincident axial load. The full range of expected axial loads was considered in developing this example, but in this case the lateral displacements, moments, and shears were not strongly affected; the plots in this section are for zero axial load. A *p*-multiplier of 0.87 for group effects (as computed at the end of Sec. 4.2.1.4) is used in all cases. Figures 4.2-7, 4.2-8, and 4.2-9 show the variation of shear, moment, and displacement with depth (within the top 30 ft) for an applied lateral load of 15 kips on a single pile with the group reduction factor. It is apparent that the extension of piles to depths beyond 30 ft for the Class E site (or about 25 ft for the Class C site) does not provide additional resistance to lateral loading; piles shorter than those lengths would have reduced lateral resistance. The trends in the figures are those that should be expected. The shear and displacement are maxima at the pile head. Because a fixed-head condition is assumed, moments are also largest at the top of the pile. Moments and displacements are larger for the soft soil condition than for the firm soil condition.

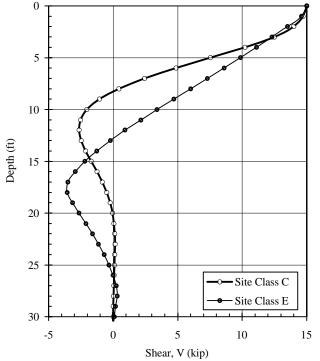


**Figure 4.2-7** Results of pile analysis – shear versus depth (applied lateral load is 15 kips).

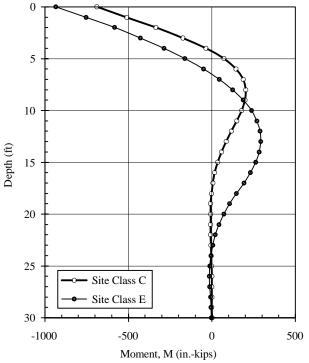


**Figure 4.2-8** Results of pile analysis – moment versus depth (applied lateral load is 15 kips).

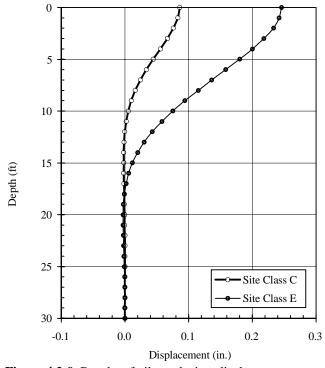
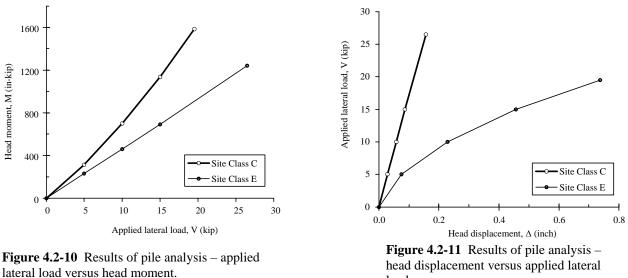


**Figure 4.2-9** Results of pile analysis – displacement versus depth (applied lateral load is 15 kips)

The analyses performed to develop Figures 4.2-7 through 4.2-9 are repeated for different levels of applied lateral load. Figures 4.2-10 and 4.2-11 show how the moment and displacement at the head of the pile are related to the applied lateral load. It may be seen from Figure 4.2-10 that the head moment is related to the applied lateral load in a nearly linear manner; this is a key observation. Based on the results shown, the slope of the line may be taken as a characteristic length that relates head moment to applied load. Doing so produces the following:

l = 46 in. for the Class C site l = 70 in. for the Class E site



head displacement versus applied lateral load.

A similar examination of Figure 4.2-11 leads to another meaningful insight. The load-displacement response of the pile in Site Class C soil is essentially linear. The response of the pile in Site Class E soil is somewhat nonlinear, but for most of the range of response a linear approximation is reasonable (and useful). Thus, the effective stiffness of each individual pile is:

k = 175 kip/in. for the Class C site

k = 40 kip/in. for the Class E site

### 4.2.2.2 Pile Group Analysis

The combined response of the piles and pile cap and the resulting strength demands for piles are computed using the procedure outlined in Sec. 4.2.1.4 for each of the 32 load combinations discussed in Sec. 4.2.1.3. Assume that each  $2 \times 2$  pile group has a 9'-2"  $\times$  9'-2"  $\times$  4'-0" thick pile cap that is placed 1'-6" below grade.

#### Check the Maximum Compression Case under a Side Column in Site Class C

Using the sign convention shown in Figure 4.2-3, the demands on the group are:

P = 1097 kip  $M_{yy} = 93$  ft-kips  $V_{x} = 10$  kips  $M_{yy} = 659$  ft-kips  $V_{\rm v} = 69$  kips

From preliminary checks, assume that the displacements in the x and y directions are sufficient to mobilize 15 percent and 30 percent, respectively, of the ultimate passive pressure:

$$V_{passive,x} = 0.15(575) \left(\frac{18}{12} + \frac{48}{2(12)}\right) \left(\frac{48}{12}\right) \left(\frac{110}{12}\right) \left(\frac{1}{1000}\right) = 11.0 \text{ kips}$$

and

$$V_{passive, y} = 0.30(575) \left( \frac{18}{12} + \frac{48}{2(12)} \right) \left( \frac{48}{12} \right) \left( \frac{110}{12} \right) \left( \frac{1}{1000} \right) = 22.1 \text{ kips}$$

and conservatively take  $h_p = h/3 = 16$  in.

Since  $V_{passive,x} > V_x$ , passive resistance alone is sufficient for this case in the x direction. However, in order to illustrate the full complexity of the calculations, reduce  $V_{passive,x}$  to 4 kips and assign a shear of 1.5 kips to each pile in the x direction. In the y direction the shear in each pile is:

$$V = \frac{69 - 22.1}{4} = 11.7 \,\mathrm{kips}$$

The corresponding pile moments are:

M = 1.5(46) = 69 in.-kips for x-direction loading

and

M = 11.7(46) = 538 in.-kips for y-direction loading.

The maximum axial load due to overturning for x-direction loading is:

$$P_{ot} = \frac{10(48) + 93(12) + 4(69) - 16(4)}{2(66)} = 13.7 \,\text{kips}$$

and for y-direction loading (determined similarly)  $P_{ot} = 98.6$  kips.

The axial load due to direct loading is  $P_p = 1097/4 = 274$  kips.

Therefore the maximum load effects on the most heavily loaded pile are:

$$P_{\mu} = 13.7 + 98.6 + 274 = 386$$
 kips

$$M_u = \sqrt{(69)^2 + (538)^2} = 542$$
 in.-kips.

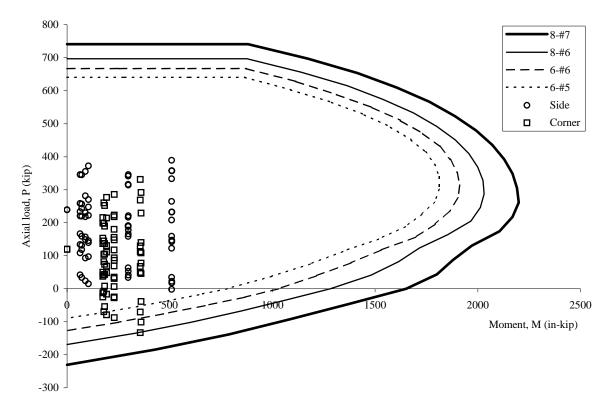
The expected displacement in the y direction is computed as:

 $\delta = V/k = 11.7/175 = 0.067$  in., which is 0.14% of the pile cap height (*h*).

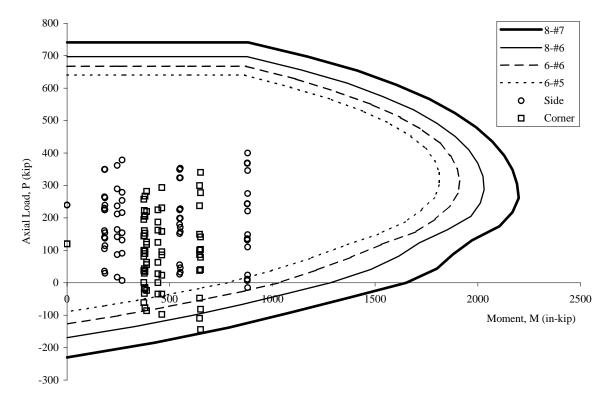
Reading Figure 4.2-5 with  $\delta H = 0.0014$ ,  $P/P_{ult} \approx 0.34$ , so the assumption that 30 percent of  $P_{ult}$  would be mobilized was reasonable.

#### 4.2.2.3 Design of Pile Section

The calculations shown in Sec. 4.2.2.2 are repeated for each of the 32 load combinations under each of the four design conditions. The results are shown in Figures 4.2-12 and 4.2-13. In these figures, circles indicate demands on piles under side columns and squares indicate demands on piles under corner columns. Also plotted are the  $\phi P - \phi M$  design strengths for the 22-in.-diameter pile sections with various amounts of reinforcement (as noted in the legends). The appropriate reinforcement pattern for each design condition may be selected by noting the innermost capacity curve that envelops the corresponding demand points. The required reinforcement is summarized in Table 4.2-4, following calculation of the required pile length.









#### 4.2.2.4 Pile Length for Axial Loads

For the calculations that follow, recall that skin friction and end bearing are neglected for the top three feet in this example. (In these calculations, the pile cap depth is ignored – effectively assuming that piles begin at the ground surface. Because the soil capacity increases with depth and the resulting pile lengths are applied below the bottom of the pile cap, the results are slightly conservative.)

#### 4.2.2.4.1 Length for Settlement

Service loads per pile are calculated as  $P = (P_D + P_L)/4$ .

Check pile group under side column in Site Class C, assuming L = 47 ft:

P = (702 + 72)/4 = 194 kips.

 $P_{skin}$  = average friction capacity × pile perimeter × pile length for friction = 0.5[0.3 + 0.3 + 44(0.03)] $\pi$ (22/12)(44) = 243 kips.

 $P_{end}$  = end bearing capacity at depth × end bearing area =  $[65 + 44(0.6)](\pi/4)(22/12)^2 = 241$  kips.

$$P_{allow} = (P_{skin} + P_{end})/S.F. = (243 + 241)/2.5 = 194 \text{ kips} = 194 \text{ kips} (demand).$$
 OK

Check pile group under corner column in Site Class E, assuming L = 43 ft:

P = (351 + 36)/4 = 97 kips.

 $P_{skin} = [friction capacity in first layer + average friction capacity in second layer] \times pile perimeter = [27(0.3) + (13/2)(0.9 + 0.9 + 13[0.025])]\pi(22/12) = 126 \text{ kips.}$ 

$$P_{end} = [40 + 13(0.5)](\pi/4)(22/12)^2 = 123$$
 kips.

$$P_{allow} = (126 + 123)/2.5 = 100 \text{ kips} > 97 \text{ kips}.$$

4.2.2.4.2 Length for Compression Capacity

All of the strength-level load combinations (discussed in Sec. 4.2.1.3) must be considered.

Check pile group under side column in Site Class C, assuming L = 50 ft:

As seen in Figure 4.1-12, the maximum compression demand for this condition is  $P_u = 390$  kips.

$$P_{skin} = 0.5[0.3 + 0.3 + 47(0.03)]\pi(22/12)(47) = 272$$
 kips.

 $P_{end} = [65 + 47(0.6)](\pi/4)(22/12)^2 = 246$  kips.

$$\phi P_n = \phi (P_{skin} + P_{end}) = 0.75(272 + 246) = 389 \text{ kips} \approx 390 \text{ kips}.$$
 OK

Check pile group under corner column in Site Class E, assuming L = 64 ft:

As seen in Figure 4.2-13, the maximum compression demand for this condition is  $P_u = 340$  kips.

OK

$$P_{skin} = [27(0.3) + (34/2)(0.9 + 0.9 + 34[0.025])]\pi(22/12) = 306$$
 kips.

$$P_{end} = [40 + 34(0.5)](\pi/4)(22/12)^2 = 150$$
 kips.

$$\phi P_n = \phi (P_{skin} + P_{end}) = 0.75(306 + 150) = 342 \text{ kips} > 340 \text{ kips}.$$
 OK

#### 4.2.2.4.3 Length for Uplift Capacity

Again, all of the strength-level load combinations (discussed in Sec. 4.2.1.3) must be considered.

Check pile group under side column in Site Class C, assuming L = 5 ft:

As seen in Figure 4.2-12, the maximum tension demand for this condition is  $P_u = -1.9$  kips.

$$P_{skin} = 0.5[0.3 + 0.3 + 2(0.03)]\pi(22/12)(2) = 3.8 \text{ kips.}$$
  
$$\phi P_n = \phi(P_{skin}) = 0.75(3.8) = 2.9 \text{ kips} > 1.9 \text{ kips.}$$
 OK

Check pile group under corner column in Site Class E, assuming L = 52 ft.

As seen in Figure 4.2-13, the maximum tension demand for this condition is  $P_u = -144$  kips.

$$P_{skin} = [27(0.3) + (22/2)(0.9 + 0.9 + 22[0.025])]\pi(22/12) = 196 \text{ kips.}$$
  
$$\phi P_n = \phi(P_{skin}) = 0.75(196) = 147 \text{ kips} > 144 \text{ kips.}$$
 OK

#### 4.2.2.4.4 Graphical Method of Selecting Pile Length

In the calculations shown above, the adequacy of the soil-pile interface to resist applied loads is checked once a pile length is assumed. It would be possible to generate mathematical expressions of pile capacity as a function of pile length and then solve such expressions for the demand conditions. However, a more practical design approach is to precalculate the capacity for piles for the full range of practical lengths and then select the length needed to satisfy the demands. This method lends itself to graphical expression as shown in Figures 4.2-14 and 4.2-15.

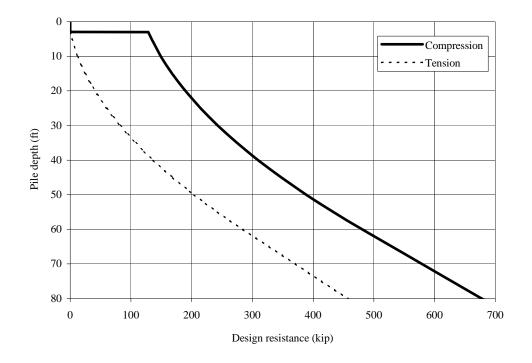


Figure 4.2-14 Pile axial capacity as a function of length for Site Class C.

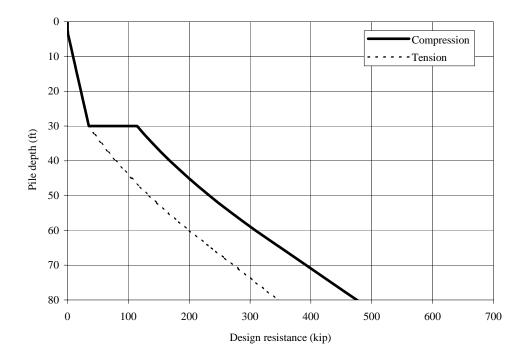
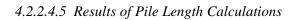


Figure 4.2-15 Pile axial capacity as a function of length for Site Class E.



Detailed calculations for the required pile lengths are provided above for two of the design conditions. Table 4.2-3 summarizes the lengths required to satisfy strength and serviceability requirements for all four design conditions.

			e Zenguis reequi	eu for Final Boue		
	Piles Under Corner Column		Piles Under Side Column		Column	
	Condition	Load	Min Length	Condition	Load	Min Length
	Compression	331 kip	43 ft	Compression	390 kip	50 ft
Site Class C	Uplift	133 kip	40 ft	Uplift	1.9 kip	5 ft
	Settlement	97 kip	19 ft	Settlement	194 kip	47 ft
	Compression	340 kip	64 ft	Compression	400 kip	71 ft
Site Class E	Uplift	144 kip	52 ft	Uplift	14.7 kip	14 ft
	Settlement	97 kip	43 ft	Settlement	194 kip	67 ft

 Table 4.2-3
 Pile Lengths Required for Axial Loads

#### 4.2.2.5 Design Results

The design results for all four pile conditions are shown in Table 4.2-4. The amount of longitudinal reinforcement indicated in the table is that required at the pile-pile cap interface and may be reduced at depth as discussed in the following section.

<b>Table 4.2-4</b>	Summary of Pile Size.	Length, and Lor	ngitudinal Reinforcement

	Piles Under Corner Column	Piles Under Side Column	
Cite Class C	22 in. diameter by 43 ft long	22 in. diameter by 50 ft long	
Site Class C	8-#6 bars	6-#5 bars	
	22 in. diameter by 64 ft long	22 in. diameter by 71 ft long	
Site Class E	8-#7 bars	6-#6 bars	

#### 4.2.2.6 Pile Detailing

*Provisions* Sec. 7.4.4 and 7.5.4, respectively, contain special pile requirements for structures assigned to Seismic Design Category C or higher and D or higher. In this section, those general requirements and the specific requirements for uncased concrete piles that apply to this example are discussed. Although the specifics are affected by the soil properties and assigned site class, the detailing of the piles designed in this example focuses on consideration of the following fundamental items:

- 1. All pile reinforcement must be developed in the pile cap (Provisions Sec. 7.4.4).
- 2. In areas of the pile where yielding might be expected or demands are large, longitudinal and transverse reinforcement must satisfy specific requirements related to minimum amount and maximum spacing.
- 3. Continuous longitudinal reinforcement must be provided over the entire length resisting design tension forces (ACI 318 Sec. 21.8.4.2 [21.10.4.2]).

The discussion that follows refers to the detailing shown in Figures 4.2-16 and 4.2-17.

#### 4.2.2.6.1 Development at the Pile Cap

Where neither uplift nor flexural restraint are required, the development length is the full development length for compression (*Provisions* Sec. 7.4.4). Where the design relies on head fixity or where resistance to uplift forces is required (both of which are true in this example), pile reinforcement must be fully developed in tension unless the section satisfies the overstrength load condition or demands are limited by the uplift capacity of the soil-pile interface (*Provisions* Sec. 7.5.4). For both site classes considered in this example, the pile longitudinal reinforcement is extended straight into the pile cap a distance that is sufficient to fully develop the tensile capacity of the bars. In addition to satisfying the requirements of the *Provisions*, this approach offers two advantages. By avoiding lap splices to field-placed dowels where yielding is expected near the pile head (although such would be permitted by *Provisions* Sec. 7.4.4), more desirable inelastic performance would be expected. Straight development, while it may require a thicker pile cap, permits easier placement of the pile cap's bottom reinforcement followed by the addition of the spiral reinforcement within the pile cap. Note that embedment of the entire pile in the pile cap facilitates direct transfer of shear from pile cap to pile, but is not a requirement of the *Provisions*.

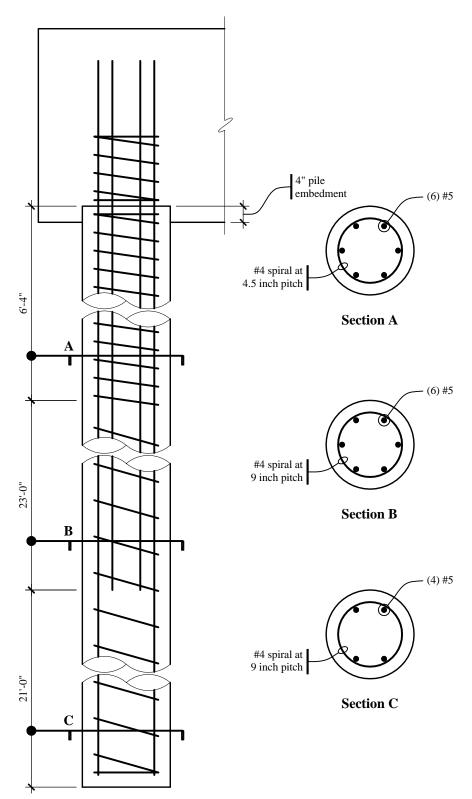


Figure 4.2-16 Pile detailing for Site Class C (under side column).

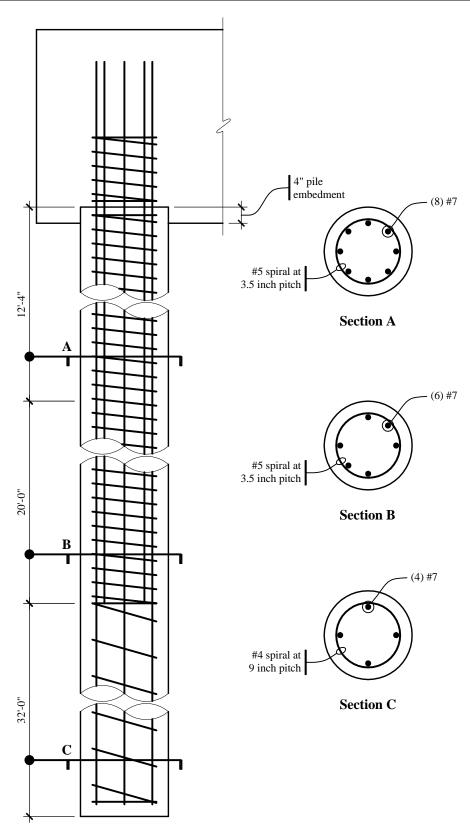


Figure 4.2-17 Pile detailing for Site Class E (under corner column).

## 4.2.2.6.2 Longitudinal and Transverse Reinforcement Where Demands Are Large

Requirements for longitudinal and transverse reinforcement apply over the entire length of pile where demands are large. For uncased concrete piles in Seismic Design Category D at least four longitudinal bars (with a minimum reinforcement ratio of 0.005) must be provided over the largest region defined as follows: the top one-half of the pile length, the top 10 ft below the ground, or the flexural length of the pile. The flexural length is taken as the length of pile from the cap to the lowest point where 0.4 times the concrete section cracking moment (see ACI 318 Sec. 9.5.2.3) exceeds the calculated flexural demand at that point. [A change made in Sec. 7.4.4.1 of the 2003 Provisions makes it clear that the longitudinal reinforcement must be developed beyond this point.] For the piles used in this example, one-half of the pile length governs. (Note that "providing" a given reinforcement ratio means that the reinforcement in question must be developed at that point. Bar development and cutoff are discussed in more detail in Chapter 6 of this volume of design examples.) Transverse reinforcement must be provided over the same length for which minimum longitudinal reinforcement requirements apply. Because the piles designed in this example are larger than 20 in. in diameter, the transverse reinforcement may not be smaller than 0.5 in. diameter. For the piles shown in Figures 4.2-16 and 4.2-17 the spacing of the transverse reinforcement in the top half of the pile length may not exceed the least of:  $12d_b$  (7.5 in. for #5 longitudinal bars and 10.5 in. for #7 longitudinal bars), 22/2 = 11 in., or 12 in.

Where yielding may be expected, even more stringent detailing is required. For the Class C site, yielding can be expected within three diameters of the bottom of the pile cap  $(3D = 3 \times 22 = 66 \text{ in.})$ . Spiral reinforcement in that region must not be less than one-half of that required in ASCE 318 Sec. 21.4.4.1(a) of ACI 318 (since the site is not Class E, F, or liquefiable) and the requirements of Sec. 21.4.4.2 and 21.4.4.3 must be satisfied. Note that Sec. 21.4.4.1(a) refers to Eq. (10-6) [10-5], which often will govern. In this case, the minimum volumetric ratio of spiral reinforcement is one-half that determined using ACI 318 Eq. (10-6) [10-5]. In order to provide a reinforcement ratio of 0.01 for this pile section, a #4 spiral must have a pitch of no more than 4.8 in., but the maximum spacing permitted by Sec. 21.4.4.2 is 22/4 = 5.5 in. or  $6d_b = 3.75$  in., so a #4 spiral at 3.75 in. pitch is used.

For the Class E site, the more stringent detailing must be provided "within seven diameters of the pile cap and of the interfaces between strata that are hard or stiff and strata that are liquefiable or are composed of soft to medium-stiff clay" (*Provisions* Sec. 7.5.4). The author interprets "within seven diameters of . . . the interface" as applying in the direction into the softer material, which is consistent with the expected location of yielding. Using that interpretation, the *Provisions* does not indicate the extent of such detailing into the firmer material. Taking into account the soil layering shown in Table 4.2-1 and the pile cap depth and thickness, the tightly spaced transverse reinforcement shown in Figure 4.2-17 is provided within 7D of the bottom of pile cap and top of firm soil and is extended a little more than 3D into the firm soil. Because the site is Class E, the full amount of reinforcement indicated in ACI 318 Sec. 21.4.4.1 must be provided. In order to provide a reinforcement ratio of 0.02 for this pile section, a #5 spiral must have a pitch of no more than 3.7 in. The maximum spacing permitted by Sec. 21.4.4.2 is 22/4 = 5.5 in. or  $6d_b = 5.25$  in., so a #5 spiral at 3.5 in. pitch is used.

#### 4.2.2.6.3 Continuous Longitudinal Reinforcement for Tension

Table 4.2-3 shows the pile lengths required for resistance to uplift demands. For the Site Class E condition under a corner column (Figure 4.2-17), longitudinal reinforcement must resist tension for at least the top 52 ft (being developed at that point). Extending four longitudinal bars for the full length and providing widely spaced spirals at such bars reflect the designer's judgment (not specific requirements of the *Provisions*). For the Site Class C condition under a side column (Figure 4.2-16), design tension due to uplift extends only about 5 ft below the bottom of the pile cap. Therefore, a design with Section C of Figure 4.2-16 being unreinforced would satisfy the *Provisions* requirements, but the author has decided to extend very light longitudinal and nominal transverse reinforcement for the full length of the pile.

# 4.2.3 Other Considerations

## 4.2.3.1 Foundation Tie Design and Detailing

*Provisions* Sec. 7.4.3 requires that individual pile caps be connected by ties. Such ties are often grade beams, but the *Provisions* would permit use of a slab (thickened or not) or calculations that demonstrate that the site soils (assigned to Site Class A, B, or C) provide equivalent restraint. For this example, a tie beam between the pile caps under a corner column and a side column will be designed. The resulting section is shown in Figure 4.2-18.

For pile caps with an assumed center-to-center spacing of 32 ft in each direction, and given  $P_{group} = 1121$  kips under a side column and  $P_{group} = 812$  kips under a corner column, the tie is designed as follows.

As indicated in *Provisions* Sec. 7.4.3, the minimum tie force in tension or compression equals the product of the larger column load times  $S_{DS}$  divided by 10 = 1121(0.90)/10 = 101 kips.

The design strength for five # 6 bars is  $\phi A_s f_y = 0.8(5)(0.44)(60) = 106$  kips > 101 kips. OK

According to ACI 318 Sec. 21.8.3.2 [21.10.3.2], the smallest cross-sectional dimension of the tie beam must not be less than the clear spacing between pile caps divided by 20 = (32'-0" - 9'-2")/20 = 13.7 in. Use a tie beam that is 14 in. wide and 16 in. deep. ACI 318 Sec. 21.8.3.2 [21.10.3.2] further indicates that closed ties must be provided at a spacing of not more than one-half the minimum dimension = 14/2 = 7 in.

Assuming that the surrounding soil provides restraint against buckling, the design strength of the tie beam concentrically loaded in compression is:

 $\phi P_n = 0.8 \phi [0.85f'_c(A_g - A_{st}) + f_y A_{st}]$ = 0.8(0.65)[0.85(3)(16)(14) + 60(5)(0.44)] = 366 kips > 101 kips. OK

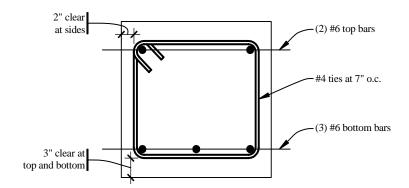


Figure 4.2-18 Foundation tie section.

# 4.2.3.2 Liquefaction

For Seismic Design Categories C, D, E and F, *Provisions* Sec. 7.4.1 requires that the geotechnical report address potential hazards due to liquefaction. For Seismic Design Categories D, E and F, *Provisions* Sec. 7.5.1 and 7.5.3 [7.5.1 and 7.5.2] further require that the geotechnical report describe the likelihood and potential consequences of liquefaction and soil strength loss (including estimates of differential settlement, lateral movement, and reduction in foundation soil-bearing capacity) and discuss mitigation measures. [In the 2003 *Provisions*, Sec. 7.5.2 also requires that the geotechnical report describe lateral loads on foundations, increases in lateral pressures on retaining walls, and flotation of embedded

structures.] During the design of the structure, such measures (which can include ground stabilization, selection of appropriate foundation type and depths, and selection of appropriate structural systems to accommodate anticipated displacements [and forces in the 2003 *Provisions*]) must be considered. *Commentary* Section 7.4.1 contains a calculation procedure that can be used to evaluate the liquefaction hazard, but readers should refer to Youd for an update of the methods described in the *Commentary*. [Sec. 7.4.1 of the 2003 *Commentary* has been updated to reflect Youd and other recent references.]

#### 4.2.3.3 Kinematic Interaction

Piles are subjected to curvature demands as a result of two different types of behavior: inertial interaction and kinematic interaction. The term *inertial interaction* is used to describe the coupled response of the soil-foundation-structure system that arises as a consequence of the mass properties of those components of the overall system. The structural engineer's consideration of inertial interaction is usually focused on how the structure *loads* the foundation and how such loads are transmitted to the soil (as shown in the pile design calculations that are the subject of most of this example) but also includes assessment of the resulting foundation movement. The term *kinematic interaction* is used to describe the manner in which the stiffness of the foundation system impedes development of free-field ground motion. Consideration of kinematic interaction by the structural engineer is usually focused on assessing the strength and ductility demands imposed directly on piles by movement of the soil. Although it is rarely done in practice, the first two sentences of *Provisions* Sec. 7.5.4 require consideration of kinematic interaction for foundations of structures assigned to Seismic Design Category D, E, or F. Kramer discusses kinematic and inertial interaction and the methods of analysis employed in consideration of those effects, and demonstrates "that the solution to the entire soil-structure interaction problem is equal to the sum of the solutions of the kinematic and inertial interaction analyses."

One approach that would satisfy the requirements of the *Provisions* would be as follows:

- 1. The geotechnical consultant performs appropriate kinematic interaction analyses considering free-field ground motions and the stiffness of the piles to be used in design.
- 2. The resulting pile demands, which generally are greatest at the interface between stiff and soft strata, are reported to the structural engineer.
- 3. The structural engineer designs piles for the sum of the demands imposed by the vibrating superstructure and the demands imposed by soil movement.

A more practical, but less rigorous, approach would be to provide appropriate detailing in regions of the pile where curvature demands imposed directly by earthquake ground motions are expected to be significant. Where such a judgment-based approach is used, one must decide whether to provide only additional transverse reinforcement in areas of concern to improve ductility or whether additional longitudinal reinforcement should also be provided to increase strength. The third sentence of *Provisions* Sec. 7.5.4, which defines a specific instance in which this second method is to be employed to define areas requiring additional transverse reinforcement, helps to make an argument for general application of this practical approach.

#### 4.2.3.4 Design of Pile Cap

Design of pile caps for large pile loads is a very specialized topic for which detailed treatment is beyond the scope of this volume of design examples. CRSI notes that "most pile caps are designed in practice by various short-cut rule-of-thumb procedures using what are hoped to be conservative allowable stresses." Wang & Salmon indicates that "pile caps frequently must be designed for shear considering the member as a deep beam. In other words, when piles are located inside the critical sections *d* (for one-way action)

or d/2 (for two-way action) from the face of column, the shear cannot be neglected." They go on to note that "there is no agreement about the proper procedure to use." Direct application of the special provisions for deep flexural members as found in ACI 318 is not possible as the design conditions are somewhat different. CRSI provides a detailed outline of a design procedure and tabulated solutions, but the procedure is developed for pile caps subjected to concentric vertical loads only (without applied overturning moments or pile head moments). Strut-and-tie models (as described in Appendix A of the 2002 edition of ACI 318) may be employed, but their application to elements with important three-dimensional characteristics (such as pile caps for groups larger than  $2 \times 1$ ) is so involved as to preclude hand calculations.

#### 4.2.3.5 Foundation Flexibility and Its Impact on Performance

#### 4.2.3.5.1 Discussion

Most engineers routinely use fixed-base models. Nothing in the *Provisions* prohibits that common practice; the consideration of soil-structure interaction effects (*Provisions* Sec. 5.8 [5.6]) is "permitted" but not required. Such fixed-base models can lead to erroneous results, but engineers have long assumed that the errors are usually conservative. There are two obvious exceptions to that assumption: soft soil site-resonance conditions (e.g., as in the 1985 Mexico City earthquake) and excessive damage or even instability due to increased displacement response.

Site resonance can result in significant amplification of ground motion in the period range of interest. For sites with a fairly long predominant period, the result is spectral accelerations that increase as the structural period approaches the site period. However, the shape of the general design spectrum used in the *Provisions* does not capture that effect; for periods larger than  $T_0$ , accelerations remain the same or decrease with increasing period. Therefore, increased system period (as a result of foundation flexibility) always leads to lower design forces where the general design spectrum is used. Site-specific spectra may reflect long-period site-resonance effects, but the use of such spectra is required only for Class F sites.

Clearly, an increase in displacements, caused by foundation flexibility, does change the performance of a structure and its contents – raising concerns regarding both stability and damage. Earthquake-induced instability of buildings has been exceedingly rare. The analysis and acceptance criteria in the Provisions are not adequate to the task of predicting real stability problems; calculations based on linear, static behavior cannot be used to predict instability of an inelastic system subjected to dynamic loading. While Commentary Sec. 5.2.8 [4.5.1] indicates that structural stability was considered in arriving at the "consensus judgment" reflected in the drift limits, such considerations were qualitative. In point of fact, the values selected for the drift limits were selected considering damage to nonstructural systems (and, perhaps in some cases, control of structural ductility demands). For most buildings, application of the Provisions is intended to satisfy performance objectives related to life safety and collapse prevention, not damage control or post-earthquake occupancy. Larger design forces and more stringent drift limits are applied to structures assigned to Seismic Use Group II or III in the hope that those measures will improve performance without requiring explicit consideration of such performance. Although foundation flexibility can affect structural performance significantly, the fact that all consideration of performance in the context of the *Provisions* is approximate and judgment-based has made it difficult to define how such changes in performance should be characterized. Explicit consideration of performance measures also tends to increase engineering effort substantially, so mandatory performance checks are often resisted by the user community.

The engineering framework established in FEMA 356 is more conducive to explicit use of performance measures. In that document (Sec. 4.4.3.2.1 and 4.4.3.3.1), the use of fixed-based structural models is prohibited for "buildings being rehabilitated for the Immediate Occupancy Performance Level that are

sensitive to base rotations or other types of foundation movement." In this case the focus is on damage control rather than structural stability.

## 4.2.3.5.2 Example Calculations

To assess the significance of foundation flexibility, one may compare the dynamic characteristics of a fixed-base model to those of a model in which foundation effects are included. The effects of foundation flexibility become more pronounced as foundation period and structural period approach the same value. For this portion of the example, use the Site Class E pile design results from Sec. 4.2.2.1 and consider the north-south response of the concrete moment frame building located in Berkeley (Sec. 6.2) as representative for this building.

<u>Stiffness of the Structure</u>. Calculations of the effect of foundation flexibility on the dynamic response of a structure should reflect the overall stiffness of the structure (e.g., that associated with the fundamental mode of vibration), rather than the stiffness of any particular story. Table 6-2 shows that the total weight of the structure is 36,462 kips. Table 6-5 shows that the calculated period of the fixed-base structure is 2.50 seconds, and Table 6-4 indicates that 80.2 percent of the mass participates in that mode. Using the equation for the undamped period of vibration of a single-degree-of-freedom oscillator, the effective stiffness of the structure is:

$$K = \frac{4\pi^2 M}{T^2} = \frac{4\pi^2 ((0.802)36, 462/386.1)}{2.50^2} = 478 \text{ kip/in.}$$

<u>Foundation Stiffness</u>. As seen in Figure 6-1 there are 36 moment frame columns. Assume that a  $2\times 2$  pile group supports each column. As shown in Sec. 4.2.2.1, the stiffness of each pile is 40 kip/in. Neglecting both the stiffness contribution from passive pressure resistance and the flexibility of the beam-slab system that ties the pile caps, the stiffness of each pile group is  $4 \times 40 = 160$  kip/in. and the stiffness of the entire foundation system is  $36 \times 160 = 5760$  kip/in.

<u>Effect of Foundation Flexibility</u>. Because the foundation stiffness is more than 10 times the structural stiffness, period elongation is expected to be minimal. To confirm this expectation the period of the combined system is computed. The total stiffness for the system (springs in series) is:

$$K_{combined} = \frac{1}{\frac{1}{K_{structure}} + \frac{1}{K_{fdn}}} = \frac{1}{\frac{1}{478} + \frac{1}{5760}} = 441 \text{ kip/in.}$$

Assume that the weight of the foundation system is 4000 kips and that 100 percent of the corresponding mass participates in the new fundamental mode of vibration. The period of the combined system is

$$T = 2\pi \sqrt{\frac{M}{K}} = 2\pi \sqrt{\frac{\left[(0.802)(36,462) + (1.0)(4000)\right]/386.1}{441}} = 2.78 \text{ sec}$$

which is an 11 percent increase over that predicted by the fixed-base model. For systems responding in the constant-velocity portion of the spectrum, accelerations (and thus forces) are a function of 1/T and relative displacements are a function of T. Therefore, with respect to the fixed-based model, the combined system would have forces that are 10 percent smaller and displacements that are 11 percent larger. In the context of earthquake engineering, those differences are not significant.

5

# STRUCTURAL STEEL DESIGN

# James R. Harris, P.E., Ph.D., Frederick R. Rutz, P.E., Ph.D., and Teymour Manzouri, P.E., Ph.D.

This chapter illustrates how the 2000 *NEHRP Recommended Provisions* (hereafter the *Provisions*) is applied to the design of steel framed buildings. The three examples include:

- 1. An industrial warehouse structure in Astoria, Oregon;
- 2. A multistory office building in Los Angeles, California; and
- 3. A low-rise hospital facility in the San Francisco Bay area of California.

The discussion examines the following types of structural framing for resisting horizontal forces:

- 1. Concentrically braced frames,
- 2. Intermediate moment frames,
- 3. Special moment frames,
- 4. A dual system consisting of moment frames and concentrically braced frames, and
- 5. Eccentrically braced frames.

For determining the strength of steel members and connections, the 1993 [1999] *Load and Resistance Factor Design Specification for Structural Steel Buildings*, published by the American Institute of Steel Construction, is used throughout. In addition, the requirements of the 1997 [2002] *AISC Seismic Provisions for Structural Steel Buildings* are followed where applicable.

The examples only cover design for seismic forces in combination with gravity, and they are presented to illustrate only specific aspects of seismic analysis and design such as, lateral force analysis, design of concentric and eccentric bracing, design of moment resisting frames, drift calculations, member proportioning, and detailing.

All structures are analyzed using three-dimensional static or dynamic methods. The SAP2000 Building Analysis Program (Computers & Structures, Inc., Berkeley, California, v.6.11, 1997) is used in Example 5.1, and the RAMFRAME Analysis Program (RAM International, Carlsbad, California, v. 5.04, 1997) is used in Examples 5.2 and 5.3.

In addition to the 2000 NEHRP Recommended Provisions, the following documents are referenced:

AISC LRFD American Institute of Steel Construction. 1999. Load and Resistance Factor Design Specification for Structural Steel Buildings.

AISC Manual	American Institute of Steel Construction. 2001. Manual of Steel Construction, Load and Resistance Factor Design, 3rd Edition.
AISC Seismic	American Institute of Steel Construction. 2000. [2002] Seismic Provisions for Structural Steel Buildings, 1997, including Supplement No. 2.
IBC	International Code Council, Inc. 2000. 2000 International Building Code.
FEMA 350	SAC Joint Venture. 2000. <i>Recommended Seismic Design Criteria for New Steel Moment-Frame Buildings</i> .
AISC SDGS-4	AISC Steel Design Guide Series 4. 1990. Extended End-Plate Moment Connections, 1990.
SDI	Luttrell, Larry D. 1981. Steel Deck Institute Diaphragm Design Manual. Steel Deck Institute.

The symbols used in this chapter are from Chapter 2 of the *Provisions*, the above referenced documents, or are as defined in the text. Customary U.S. units are used.

Although the these design examples are based on the 2000 *Provisions*, it is annotated to reflect changes made to the 2003 *Provisions*. Annotations within brackets, [], indicate both organizational changes (as a result of a reformat of all of the chapters of the 2003 *Provisions*) and substantive technical changes to the 2003 *Provisions* and its primary reference documents. While the general concepts of the changes are described, the design examples and calculations have not been revised to reflect the changes to the 2003 *Provisions*.

The most significant change to the steel chapter in the 2003 *Provisions* is the addition of two new lateral systems, buckling restrained braced frames and steel plate shear walls, neither of which are covered in this set of design examples. Other changes are generally related to maintaining compatibility between the *Provisions* and the 2002 edition of AISC Seismic. Updates to the reference documents, in particular AISC Seismic, have some effects on the calculations illustrated herein.

Some general technical changes in the 2003 *Provisions* that relate to the calculations and/or design in this chapter include updated seismic hazard maps, changes to Seismic Design Category classification for short period structures and revisions to the redundancy requirements, new Simplified Design Procedure would not be applicable to the examples in this chapter.

Where they affect the design examples in this chapter, other significant changes to the 2003 *Provisions* and primary reference documents are noted. However, some minor changes to the 2003 *Provisions* and the reference documents may not be noted.

It is worth noting that the 2002 edition of AISC Seismic has incorporated many of the design provisions for steel moment frames contained in FEMA 350. The design provisions incorporated into AISC Seismic are similar in substance to FEMA 350, but the organization and format are significantly different. Therefore, due to the difficulty in cross-referencing, the references to FEMA 350 sections, tables, and equations in this chapter have not been annotated. The design professional is encouraged to review AISC Seismic for updated moment frame design provisions related to the examples in this chapter.

# 5.1 INDUSTRIAL HIGH-CLEARANCE BUILDING, ASTORIA, OREGON

This example features a transverse steel moment frame and a longitudinal steel braced frame. The following features of seismic design of steel buildings are illustrated:

- 1. Seismic design parameters,
- 2. Equivalent lateral force analysis,
- 3. Three-dimension (3-D) modal analysis,
- 4. Drift check,
- 5. Check of compactness and brace spacing for moment frame,
- 6. Moment frame connection design, and
- 7. Proportioning of concentric diagonal bracing.

# 5.1.1 Building Description

This industrial building has plan dimensions of 180 ft by 90 ft and a clear height of approximately 30 ft. It includes a 12-ft-high, 40-ft-wide mezzanine area at the east end of the building. The structure consists of 10 gable frames spanning 90 ft in the transverse (N-S) direction. Spaced at 20 ft o.c., these frames are braced in the longitudinal (EW) direction in two bays at the east end. The building is enclosed by nonstructural insulated concrete wall panels and is roofed with steel decking covered with insulation and roofing. Columns are supported on spread footings.

The elevation and transverse sections of the structure are shown in Figure 5.1-1. Longitudinal struts at the eaves and the mezzanine level run the full length of the building and, therefore, act as collectors for the distribution of forces resisted by the diagonally braced bays and as weak-axis stability bracing for the moment frame columns.

The roof and mezzanine framing plans are shown in Figure 5.1-2. The framing consists of a steel roof deck supported by joists between transverse gable frames. Because the frames resist lateral loading at each frame position, the steel deck functions as a diaphragm for distribution of the effects of eccentric loading caused by the mezzanine floor when the building is subjected to loads acting in the transverse direction.

The mezzanine floor at the east end of the building is designed to accommodate a live load of 125 psf. Its structural system is composed of a concrete slab over steel decking supported by floor beams spaced 10 ft o.c. The floor beams are supported on girders continuous over two intermediate columns spaced approximately 30 ft apart and are attached to the gable frames at each end.

The member sizes in the main frame are controlled by serviceability considerations. Vertical deflections due to snow were limited to 3.5 in. and lateral sway due to wind was limited to 2 in. (which did not control). These serviceability limits are not considered to control any aspect of the seismic-resistant design. However, many aspects of seismic design are driven by actual capacities so, in that sense, the serviceability limits do affect the seismic design.

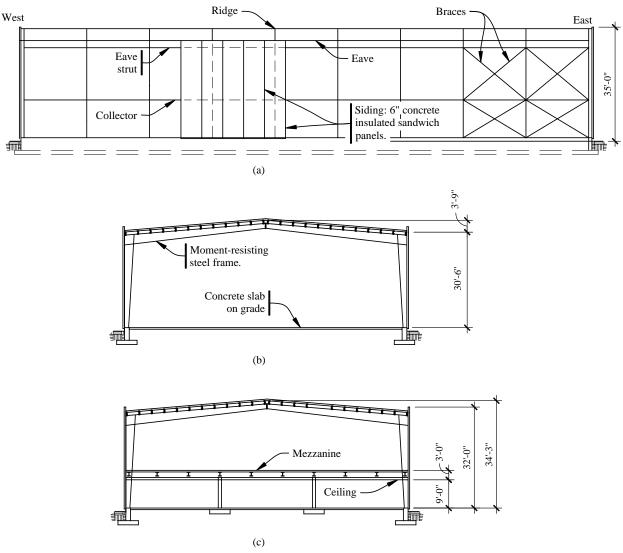


Figure 5.1-1 Framing elevation and sections (1.0 in. = 25.4 mm, 1.0 ft = 0.3048 m).

Earthquake rather than wind governs the lateral design due to the mass of the insulated concrete panels. The panels are attached with long pins perpendicular to the concrete surface. These slender, flexible pins avoid shear resistance by the panels. (This building arrangement has been intentionally contrived to illustrate what can happen to a tapered-moment frame building if high seismic demands are placed on it. More likely, if this were a real building, the concrete panels would be connected directly to the steel frame, and the building would tend to act as a shear wall building. But for this example, the connections have been arranged to permit the steel frame to move at the point of attachment in the in-plane direction of the concrete panels. This was done to cause the steel frame to resist lateral forces and, thus, shear-wall action of the panels does not influence the frames.)

The building is supported on spread footings based on moderately deep alluvial deposits (i.e., medium dense sands). The foundation plan is shown in Figure 5.1-3. Transverse ties are placed between the footings of the two columns of each moment frame to provide restraint against horizontal thrust from the moment frames. Grade beams carrying the enclosing panels serve as ties in the longitudinal direction as well as across the end walls. The design of footings and columns in the braced bays requires consideration of combined seismic loadings. The design of foundations is not included here.

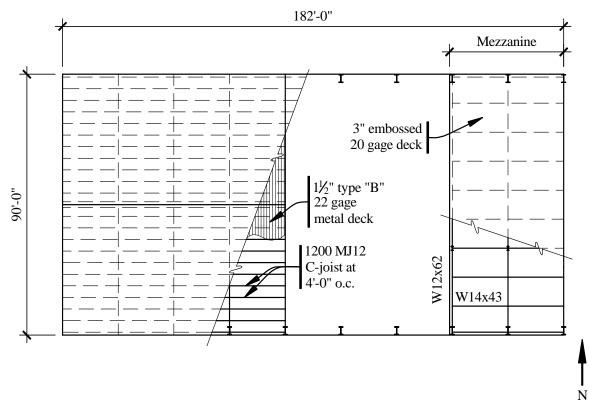
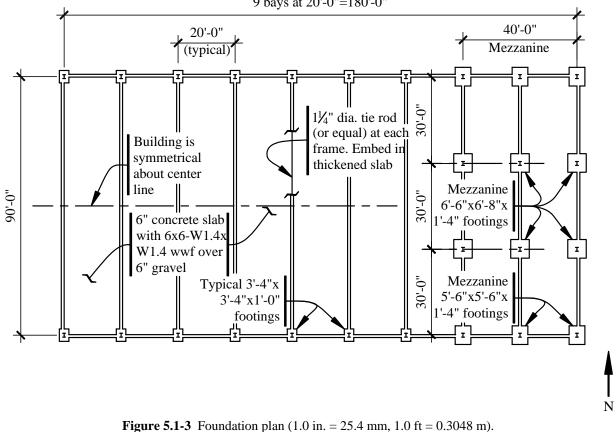


Figure 5.1-2 Roof framing and mezzanine framing plan (1.0 in. = 25.4 mm, 1.0 ft = 0.3048 m).



9 bays at 20'-0"=180'-0"

# 5.1.2 Design Parameters

## 5.1.2.1 Provisions Parameters

Site Class	= D ( <i>Provisions</i> Sec. 4.1.2.1[3.5])
$S_{S}$	= 1.5 ( <i>Provisions</i> Map 9 [Figure 3.3-1])
$S_{I}$	= 0.6 ( <i>Provisions</i> Map 10 [Figure 3.3-2])
$F_a$	= 1.0 ( <i>Provisions</i> Table 4.1.2.4a [3.3-1])
$F_{v}$	= 1.5 ( <i>Provisions</i> Table 4.1.2.4b [3.3-2])
$S_{MS} = F_a S_S$	= 1.5 ( <i>Provisions</i> Eq. 4.1.2.4-1 [3.3-1])
$S_{MI} = F_{v}S_{I}$	= 0.9 ( <i>Provisions</i> Eq. 4.1.2.4-2 [3.3-2])
$S_{DS} = 2/3 S_{MS}$	= 1.0 ( <i>Provisions</i> Eq. 4.1.2.5-1 [3.3-3])
$S_{DI} = 2/3 S_{MI}$	= 0.6 ( <i>Provisions</i> Eq. 4.1.2.5-2 [3.3-4])
Seismic Use Group	= I ( <i>Provisions</i> Sec. 1.3 [1.2])
Seismic Design Category	= D ( <i>Provisions</i> Sec. 4.2.1 [1.4])

[The 2003 *Provisions* have adopted the 2002 USGS probabilistic seismic hazard maps, and the maps have been added to the body of the 2003 *Provisions* as figures in Chapter 3 (instead of the previously used separate map package).]

Note that *Provisions* Table 5.2.2 [4.3-1] permits an ordinary moment-resisting steel frame for buildings that do not exceed one story and 60 feet tall with a roof dead load not exceeding 15 psf. This building would fall within that restriction, but the intermediate steel moment frame with stiffened bolted end plates is chosen to illustrate the connection design issues.

[The height and tributary weight limitations for ordinary moment-resisting frames have been revised in the 2003 *Provisions*. In Seismic Design Category D, these frames are permitted only in single-story structures up to 65 feet in height, with field-bolted end plate moment connections, and roof dead load not exceeding 20 psf. Refer to 2003 *Provisions* Table 4.3-1, footnote h. The building in this example seems to fit these criteria, but the presence of the mezzanine could be questionable. Similarly, the limitations on intermediate moment-resisting frames in Seismic Design Category D have been revised. The same single-story height and weight limits apply, but the type of connection is not limited.]

N-S direction:

Moment-resisting frame system	= intermediate steel moment frame
R	= 4.5 ( <i>Provisions</i> Table 5.2.2 [4.3-1])
$arOmega_0$	= 3 ( <i>Provisions</i> Table 5.2.2 [4.3-1])
$C_d$	= 4 ( <i>Provisions</i> Table 5.2.2 [4.3-1])

E-W direction:

Braced frame system	= ordinary steel concentrically braced frame
	(Provisions Table 5.2.2 [4.3-1])
R	$= 5 (Provisions Table 5.2.2 [4.3-1])^{1}$
$arOmega_0$	= 2 ( <i>Provisions</i> Table 5.2.2 [4.3-1])
$C_d$	= 4.5 ( <i>Provisions</i> Table 5.2.2 [4.3-1])

 $<sup>{}^{1}</sup>R$  must be taken as 4.5 in this direction, due to *Provisions* Sec. 5.2.2.2.1 [4.3.1.2], which states that if the value of *R* in either direction is less than 5, the smaller value of *R* must be used in both directions. If the ordinary steel moment frame were chosen for the N-S direction, this *R* factor would change to 3.5.

## 5.1.2.2 Loads

Roof live load ( <i>L</i> ), snow	= 25 psf
Roof dead load (D)	= 15 psf
Mezzanine live load, storage	= 125  psf
Mezzanine slab and deck dead load	= 69 psf
Weight of wall panels	= 75 psf

Roof dead load includes roofing, insulation, metal roof deck, purlins, mechanical and electrical equipment, and that portion of the main frames that is tributary to the roof under lateral load. For determination of the seismic weights, the weight of the mezzanine will include the dead load plus 25 percent of the storage load (125 psf) in accordance with *Provisions* Sec. 5.3 [5.2.1].) Therefore, the mezzanine seismic weight is 69 + 0.25(125) = 100 psf.

## 5.1.2.3 Materials

Concrete for footings	$f_c' = 2.5 \text{ ksi}$
Slabs-on-grade	$f_c' = 4.5 \text{ ksi}$
Mezzanine concreteon metal deck	$f_c' = 3.0 \text{ ksi}$
Reinforcing bars	ASTM A615, Grade 60
Structural steel (wide flange sections)	ASTM A992, Grade 50
Plates	ASTM A36
Bolts	ASTM A325

## 5.1.3 Structural Design Criteria

#### 5.1.3.1 Building Configuration

Because there is a mezzanine at one end, the building might be considered vertically irregular (*Provisions* Sec. 5.2.3.3 [4.3.2.3]). However, the upper level is a roof, and the *Provisions* exempts roofs from weight irregularities. There also are plan irregularities in this building in the transverse direction, again because of the mezzanine (*Provisions* Sec. 5.2.3.2 [4.3.2.2]).

#### 5.1.3.2 Redundancy

For a structure in Seismic Design Category D, *Provisions* Eq. 5.2.4.2 [not applicable in the 2003 *Provisions*] defines the reliability factor ( $\rho$ ) as:

$$\rho = 2 - \frac{20}{r_{max_x}\sqrt{A_x}}$$

where the roof area  $(A_x) = 16,200$  sq ft.

To checking  $\rho$  in an approximate manner. In the N-S (transverse) direction, there are (2 adjacent columns)/(2 x 9 bays) so:

 $r_{max_{x}} = 0.11$  and  $\rho = 0.57 < 1.00$ .

Therefore, use  $\rho = 1.00$ .

In the E-W (longitudinal) direction, the braces are equally loaded (ignoring accidental torsion), so there is (1 brace)/(4 braces) so

 $r_{max} = 0.25 \text{ and } \rho = 1.37$ .

Thus, the reliability multiplier is 1.00 in the transverse direction and 1.37 in the longitudinal direction. The reliability factor applies only to the determination of forces, not to deflection calculations.

[The redundancy requirements have been substantially changed in the 2003 *Provisions*. For a building assigned to Seismic Design Category D,  $\rho = 1.0$  as long as it can be shown that failure of beam-to-column connections at both ends of a single beam (moment frame system) or failure of an individual brace (braced frame system) would not result in more than a 33 percent reduction in story strength or create an extreme torsional irregularity. Therefore, the redundancy factor would have to be investigated in both directions based on the new criteria in the 2003 *Provisions*.]

#### 5.1.3.3 Orthogonal Load Effects

A combination of 100 percent seismic forces in one direction plus 30 percent seismic forces in the orthogonal direction must be applied to the structures in Seismic Design Category D (*Provisions* Sec. 5.2.5.2.3 and 5.2.5.2.2 [4.4.2.3 and 4.4.2.2, respectively]).

#### 5.1.3.4 Structural Component Load Effects

The effect of seismic load (Provisions Eq. 5.2.7-1 and 5.2.7-2 [4.2-1 and 4.2-2, respectively]) is:

$$E = \rho Q_E \pm 0.2 S_{DS} D.$$

Recall that  $S_{DS} = 1.0$  for this example. The seismic load is combined with the gravity loads as follows:

 $1.2D + 1.0L + 0.2S + E = 1.2D + 1.0L + \rho Q_E + 0.2D = 1.4D + 1.0L + 0.2S + \rho Q_E$ 

Note 1.0*L* is for the storage load on the mezzanine; the coefficient on *L* is 0.5 for many common live loads:

 $0.9D + E = 0.9D + \rho Q_E - 0.2D = 0.7D + \rho Q_E$ 

#### 5.1.3.5 Drift Limits

For a building in Seismic Use Group I, the allowable story drift (Provisions 5.2.8 [4.5-1]) is:

 $\Delta_a = 0.025 h_{\rm sr}$ .

At the roof ridge,  $h_{sx} = 34$  ft-3 in. and  $\Delta_{\alpha} = 10.28$  in.

At the hip (column-roof intersection),  $h_{sx} = 30$  ft-6 in. and  $\Delta_a = 9.15$  in.

At the mezzanine floor,  $h_{sx} = 12$  ft and  $\Delta_a = 3.60$  in.

Footnote b in *Provisions* Table 5.2.8 [4.5-1, footnote c] permits unlimited drift for single-story buildings with interior walls, partitions, etc., that have been designed to accommodate the story drifts. See Sec. 5.1.4.3 for further discussion. The main frame of the building can be considered to be a one-story

building for this purpose, given that there are no interior partitions except below the mezzanine. (The definition of a story in building codes generally does not require that a mezzanine be considered a story unless its area exceeds one-third the area of the room or space in which it is placed; this mezzanine is less than one-third the footprint of the building.)

#### 5.1.3.6 Seismic Weight

The weights that contribute to seismic forces are:

	E-W direction	N-S direction
Roof D and $L = (0.015)(90)(180) =$	243 kips	243 kips
Panels at sides = $(2)(0.075)(32)(180)/2 =$	0 kips	437 kips
Panels at ends = $(2)(0.075)(35)(90)/2 =$	224 kips	0 kips
Mezzanine slab = $(0.100)(90)(40) =$	360 kips	360 kips
Mezzanine framing =	35 kips	35 kips
Main frames =	<u>27 kips</u>	<u>27 kips</u>
Seismic weight =	889 kips	1,102 kips
	·	

The weight associated with the main frames accounts for only the main columns, because the weight associated with the remainder of the main frames is included in roof dead load above. The computed seismic weight is based on the assumption that the wall panels offer no shear resistance for the structure but are self-supporting when the load is parallel to the wall of which the panels are a part.

# 5.1.4 Analysis

Base shear will be determined using an equivalent lateral force (ELF) analysis; a modal analysis then will examine the torsional irregularity of the building. The base shear as computed by the ELF analysis will be needed later when evaluating the base shear as computed by the modal analysis (see *Provisions* Sec. 5.5.7 [5.3.7]).

#### 5.1.4.1 Equivalent Lateral Force Procedure

In the longitudinal direction where stiffness is provided only by the diagonal bracing, the approximate period is computed using *Provisions* Eq. 5.4.2.1-1 [5.2-6]:

$$T_a = C_r h_n^x = (0.02)(34.25^{0.75}) = 0.28 \text{ sec}$$

In accordance with Provisions Sec. 5.4.2 [5.2.2], the computed period of the structure must not exceed:

 $T_{max} = C_u T_a = (1.4)(0.28) = 0.39$  sec.

The subsequent 3-D modal analysis finds the computed period to be 0.54 seconds.

In the transverse direction where stiffness is provided by moment-resisting frames (*Provisions* Eq. 5.4.2.1-1 [5.2-6]):

 $T_a = C_r h_n^x = (0.028)(34.25^{0.8}) = 0.47$  sec

and

$$T_{max} = C_u T_a = (1.4)(0.47) = 0.66$$
 sec.

Also note that the dynamic analysis found a computed period of 1.03 seconds.

The seismic response coefficient ( $C_s$ ) is computed in accordance with *Provisions* Sec. 5.4.1.1 [5.2.1.1]. In the longitudinal direction:

$$C_s = \frac{S_{DS}}{R/I} = \frac{1.0}{4.5/1} = 0.222$$

but need not exceed

$$C_s = \frac{S_{DI}}{T(R/I)} = \frac{0.6}{(0.39)(4.5/1)} = 0.342$$

Therefore, use  $C_s = 0.222$  for the longitudinal direction.

In the transverse direction (Provisions Eq. 5.4.1.1-1 and 5.4.1.1-2 [5.2-2 and 5.2-3, respectively]):

$$C_s = \frac{S_{DS}}{R/I} = \frac{1.0}{4.5/1} = 0.222$$

but need not exceed

$$C_s = \frac{S_{DI}}{T(R/I)} = \frac{0.6}{(0.66)(4.5/1)} = 0.202$$

Therefore, use  $C_s = 0.202$  for the transverse direction.

In both directions the value of  $C_s$  exceeds the minimum value (*Provisions* Eq. 5.4.1.1-3 [not applicable in the 2003 *Provisions*]) computed as:

$$C_s = 0.044I S_{DS} = (0.044)(1)(1.0) = 0.044$$

[This minimum  $C_s$  value has been removed in the 2003 *Provisions*. In its place is a minimum  $C_s$  value for long-period structures, which is not applicable to this example.]

The seismic base shear in the longitudinal direction (Provisions Eq. 5.4.1 [5.2-1]) is:

$$V = C_s W = (0.222)889$$
 kips) = 197 kips.

The seismic base shear in the transverse direction is:

 $V = C_s W = (0.202)(1,102 \text{ kips}) = 223 \text{ kips}.$ 

The seismic force must be increased by the reliability factor as indicated previously. Although this is not applicable to the determination of deflections, it is applicable in the determination of required strengths. The reliability multiplier ( $\rho$ ) will enter the calculation later as the modal analysis is developed. If the ELF method was used exclusively, the seismic base shear in the longitudinal direction would be increased by  $\rho$  now:

$$V = \rho$$
 (197)  
 $V = (1.37)(197) = 270$  kips

[See Sec. 5.1.3.2 for discussion of the changes to the redundancy requirements in the 2003 Provisions.]

*Provisions* Sec. 5.4.3 [5.2.3] prescribes the vertical distribution of lateral force in a multilevel structure. Even though the building is considered to be one story for some purposes, it is clearly a two-level structure. Using the data in Sec. 5.1.3.6 of this example and interpolating the exponent k as 1.08 for the period of 0.66 sec, the distribution of forces for the N-S analysis is shown in Table 5.1-1.

18	IDIE 5.1-1 ELF V	ertical Distribu	tion for N-S	Analysis	
Level	Weight $(w_x)$	Height $(h_x)$	$w_x h_x^{\ k}$	$C_{vx}$	$F_x$
Roof	707 kips	30.5 ft.	28340	0.83	185 kips
Mezzanine	395 kips	12 ft.	5780	0.17	38 kips
Total	1102 kips		34120		223 kips

**Table 5.1-1** ELF Vertical Distribution for N-S Analysis

It is not immediately clear as to whether the roof (a 22-gauge steel deck with conventional roofing over it) will behave as a flexible or rigid diaphragm. If one were to assume that the roof were a flexible diaphragm while the mezzanine were rigid, the following forces would be applied to the frames:

Typical frame at roof (tributary basis) = 185 kips / 9 bays = 20.6 kipsEnd frame at roof = 20.6/2 = 10.3 kipsMezzanine frame at mezzanine = 38 kips/3 frames = 12.7 kips

If one were to assume the roof were rigid, it would be necessary to compute the stiffness for each of the two types of frames and for the braced frames. For this example, a 3-D model was created in SAP 2000.

#### 5.1.4.2 Three-Dimension Static and Modal Response Spectrum Analyses

The 3-D analysis is performed for this example to account for:

- 1. The significance of differing stiffness of the gable frames with and without the mezzanine level,
- 2. The significance of the different centers of mass for the roof and the mezzanine,
- 3. The relative stiffness of the roof deck with respect to the gable frames, and
- 4. The significance of braced frames in controlling torsion due to N-S ground motions.

The gabled moment frames, the tension bracing, the moment frames supporting the mezzanine, and the diaphragm chord members are explicitly modeled using 3-D beam-column elements. The collector at the hip level is included as are those at the mezzanine level in the two east bays. The mezzanine diaphragm is modeled using planar shell elements with their in-plane rigidity being based on actual properties and dimensions of the slab. The roof diaphragm also is modeled using planar shell elements, but their in-plane rigidity is based on a reduced thickness that accounts for compression buckling phenomena and for the fact that the edges of the roof diaphragm panels are not connected to the wall panels. SDI's *Diaphragm Design Manual* is used for guidance in assessing the stiffness of the roof deck. The analytical model includes elements with one-tenth the stiffness of a plane plate of 22 gauge steel.

The ELF analysis of the 3-D model in the transverse direction yields two important results: the roof diaphragm behaves as a rigid diaphragm and the displacements result in the building being classified as torsionally irregular. The forces at the roof are distributed to each frame line in a fashion that offsets the center of force 5 percent of 180 ft (9 ft) to the west of the center of the roof. The forces at the mezzanine are similarly distributed to offset the center of the mezzanine force 5 percent of 40 ft to the west of the

center of the mezzanine. Using grid locations numbered from west to east, the applied forces and the resulting displacements are shown in Table 5.1-2.

		5		
Grid	Roof Force, kips	Mezzanine Force, kips	Roof Displace- ment, in.	
1	13.19		4.56	
2	25.35		4.45	
3	23.98		4.29	
4	22.61		4.08	
5	21.24		3.82	
6	19.87		3.53	
7	18.50		3.21	
8	17.13	14.57	2.86	
9	15.76	12.67	2.60	
10	7.36	10.77	2.42	
Totals	184.99	38.01		

 Table 5.1-2
 ELF Analysis in N-S Direction

The average of the extreme displacements is 3.49 in. The displacement at the centroid of the roof is 3.67 in. Thus, the deviation of the diaphragm from a straight line is 0.18 in. whereas the average frame displacement is about 20 times that. Clearly then, the behavior is as a rigid diaphragm. The ratio of maximum to average displacement is 1.31, which exceeds the 1.2 limit given in *Provisions* Table 5.2.3.2 [4.3-2] and places the structure in the category "torsionally irregular." *Provisions* Table 5.2.5.1 [4.4-1] then requires that the seismic force analysis be any one of several types of dynamic analysis. The simplest of these is the modal response spectrum (MRS) analysis.

The MRS is an easy next step once the 3-D model has been assembled. A 3-D dynamic design response spectrum analysis is performed per *Provisions* Sec. 5.5 [5.3] using the SAP 2000 program. The design response spectrum is based on *Provisions* Sec. 4.1.2.6 [3.3.4] and is shown in Figure 5.1-4. [Although it has no affect on this example, the design response spectrum has been changed for long periods in the 2003 *Provisions*. See the discussion in Chapter 3 of this volume of design examples.]

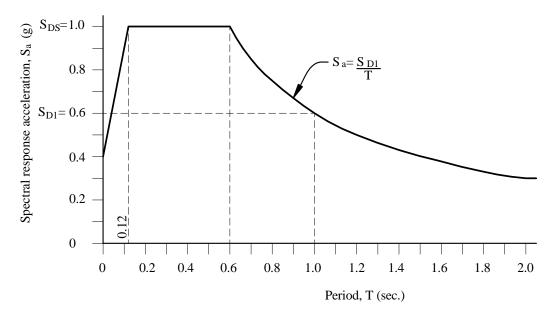


Figure 5.1-4 Design response spectrum.

The modal seismic response coefficient (*Provisions* Eq. 5.5.4-3 [5.3-3]) is  $C_{sm} = \frac{S_{am}}{R/I}$ . The design response spectra expressed in units of g and ft/sec<sup>2</sup> are shown in Table 5.1-3.

T (sec)	$S_{a}(g)$ $S_{am} = S_{a}(g)$	$C_{sm} = \frac{S_{am}}{(R/I)}$ $R = 4.5$	$C_{sm}$ (ft/sec <sup>2</sup> )
0.0	0.4	0.089	2.862
0.12	0.9	0.222	7.155
0.6	1.0	0.222	7.155
0.7	0.857	0.190	6.132
0.8	0.750	0.167	5.367
0.9	0.666	0.148	4.766
1.0	0.600	0.133	4.293
1.1	0.545	0.121	3.900
1.2	0.500	0.111	3.578
1.3	0.461	0.102	3.299
1.4	0.429	0.095	3.070

Table 5.1-3 Design Response Spectra

1.0 ft = 0.3048 m.

With this model, the first 24 periods of vibration and mode shapes of the structure were computed using the SAP2000 program. The first mode had a period of vibration of 1.03 seconds with predominantly transverse participation. The third mode period was 0.54 seconds with a predominantly longitudinal participation. The first 24 modes accounted for approximately 98 percent of the total mass of the

structure in the transverse direction and approximately 93 percent in the longitudinal direction, both of which are is greater than the 90 percent requirement of *Provisions* Sec. 5.5.2 [5.3.2].

The design value for modal base shear  $(V_t)$  is determined by combining the modal values for base shear. The SAP 2000 program uses the complete quadratic combination (CQC) of the modal values, which accounts for coupling of closely spaced modes. In the absence of damping, the CQC is simply the square root of the sum of the squares (SRSS) of each modal value. Base shears thus obtained are:

Longitudinal  $V_t = 159.5$  kips Transverse  $V_t = 137.2$  kips

In accordance with *Provisions* Sec. 5.5.7 [5.3.7], compare the design values of modal base shear to the base shear determined by the ELF method. If the design value for modal base shear is less than 85 percent of the ELF base shear calculated using a period of  $C_uT_a$ , a factor to bring the modal base shear up to this comparison ELF value must be applied to the modal story shears, moments, drifts, and floor deflections. According to *Provisions* Eq. 5.5.7.1 [5.3-10]:

Modification factor =  $0.85 (V/V_t)$ 

E-W modification factor =  $0.85(V/V_t) = (0.85)(197 \text{ kips}/159.5 \text{ kips}) = 1.05$ N-S modification factor =  $0.85(V/V_t) = (0.85)(223 \text{ kips}/137.2 \text{ kips}) = 1.38$ 

The response spectra for the 3-D modal analysis is then revised by the above modification factors:

E-W (1.0)(1.05)(x-direction spectrum) N-S (1.0)(1.38)(y-direction spectrum)

The model is then run again.

The maximum lateral displacements at the ridge due to seismic loads (i.e., design response spectra as increased by the modification factors above) from the second analysis are:

E-W deflection  $\delta_{xe} = 0.84$  in. N-S deflection  $\delta_{ye} = 2.99$  in. at the first frame in from the west end

where  $\delta_{xe}$  and  $\delta_{ye}$  are deflections determined by the elastic modal analysis. Those frames closer to the mezzanine had smaller N-S lateral deflections in much the same fashion as was shown for the ELF analysis. Before going further, the deflections should be checked as discussed in Sec. 5.1.4.3 below.

The response spectra for the 3-D modal analysis are combined to meet the orthogonality requirement of *Provisions* Sec. 5.2.5.2.2a [4.4.2.3]:

E-W (1.0)(E-W direction spectrum) + (0.3)(N-S direction spectrum) N-S (0.3)(E-W direction spectrum) + (1.0)(N-S direction spectrum)

Finally, the design response spectra for the 3-D modal analysis is again revised by increasing the E-W direction response by the reliability factor,  $\rho = 1.37$ . Note that  $\rho$  is equal to unity in the N-S direction. Thus, the factors on the basic spectrum for the load combinations become:

E-W	(1.0)(1.05)(1.37)(E-W direction spectrum) + $(0.3)(1.38)(1.00)$ (N-S direction spectrum)
N-S	(0.3)(1.05)(1.37)(E-W direction spectrum) + $(1.0)(1.38)(1.00)$ (N-S direction spectrum)

and the model is run once again to obtain the final result for design forces, shears, and moments. From this third analysis, the final design base shears are obtained. Applying the  $\rho$  factor (1.37) is equivalent to increasing the E-W base shear from (0.85 x 197 kips) = 167.5 kips to 230 kips.

# 5.1.4.3 Drift

The lateral deflection cited previously must be multiplied by  $C_d = 4$  to find the transverse drift:

$$\delta_x = \frac{C_d \delta_{xe}}{I} = \frac{4.0(2.99)}{1.0} = 12.0$$
 in.

This exceeds the limit of 10.28 in. computed previously. However, there is no story drift limit for singlestory structures with interior wall, partitions, ceilings, and exterior wall systems that have been designed to accommodate the story drifts. (The heavy wall panels were selected to make an interesting example problem, and the high transverse drift is a consequence of this. Some real buildings, such as refrigerated warehouses, have heavy wall panels and would be expected to have high seismic drifts. Special attention to detailing the connections of such features is necessary.)

In the longitudinal direction, the lateral deflection was much smaller and obviously is within the limits. Recall that the deflection computations do not consider the reliability factor. This value must be multiplied by a  $C_d$  factor to find the transverse drift. The tabulated value of  $C_d$  is 4.5, but this is for use when design is based upon R = 5. The *Provisions* does not give guidance for  $C_d$  when the system R factor is overridden by the limitation of *Provisions* Sec. 5.2.2.1 [4.3.1.2]. The authors suggest adjusting by a ratio of R factors.

## 5.1.4.4 P-delta

The AISC LRFD Specification requires P-delta analyses for frames. This was investigated by a 3-D Pdelta analysis, which determined that secondary P-delta effect on the frame in the transverse direction was less than 1 percent of the primary demand. As such, for this example, P-delta was considered to be insignificant and was not investigated further. (P-delta may be significant for a different structure, say one with higher mass at the roof. P-delta should always be investigated for unbraced frames.)

#### 5.1.4.5 Force Summary

The maximum moments and axial forces caused by dead, live, and earthquake loads on the gable frames are listed in Tables 5.1-2 and 5.1-3. The frames are symmetrical about their ridge and the loads are either symmetrical or can be applied on either side on the frame because the forces are given for only half of the frame extending from the ridge to the ground. The moments are given in Table 5.1-4 and the axial forces are given in Table 5.1-5. The moment diagram for the combined load condition is shown in Figure 5.1-5. The load combination is  $1.4D + L + 0.2S + \rho Q_E$ , which is used throughout the remainder of calculations in this section, unless specifically noted otherwise.

The size of the members is controlled by gravity loads, not seismic loads. The design of connections will be controlled by the seismic loads.

Forces in and design of the braces are discussed in Sec. 5.1.5.5 of this chapter.

Location	D (ft-kips)	L (ft-kips)	S (ft-kips)	$Q_E$ (ft-kips)	Combined* (ft-kips)
1- Ridge	61	0	128	0	112 (279)
2- Knee	161	0	333	162	447 (726)
3- Mezzanine	95	83	92	137	79
4- Base	0	0	0	0	0

 Table 5.1-4
 Moments in Gable Frame Members

\* Combined Load =  $1.4D + L + 0.2S + \rho Q_E$  (or 1.2D + 1.6S). Individual maximums are not necessarily on the same frame; combined load values are maximum for any frame. 1.0 ft = 0.3048 m, 1.0 kip = 1.36 kN-m.

Location D L S Combined\*  $\rho Q_E$ (ft-kips) (ft-kips) (ft-kips) (ft-kips) (ft-kips) 1-Ridge 14 3.5 25 0.8 39 2- Knee 16 4.5 27 7.0 37 3- Mezzanine 39 39 23 26 127 39 39 23 4-Base 26 127

 Table 5.1-5
 Axial Forces in Gable Frames Members

\* Combined Load =  $1.4D + L + 0.2S + \rho Q_E$ . Individual maximums are not necessarily on the same frame; combined load values are maximum for any frame. 1.0 ft = 0.3048 m, 1.0 kip = 1.36 kN-m.

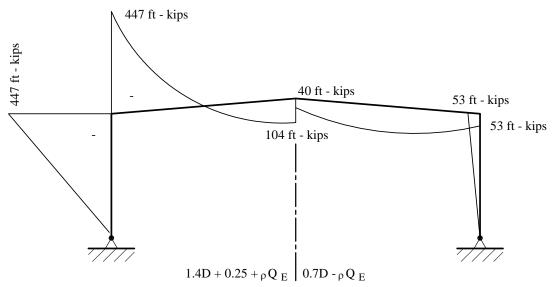
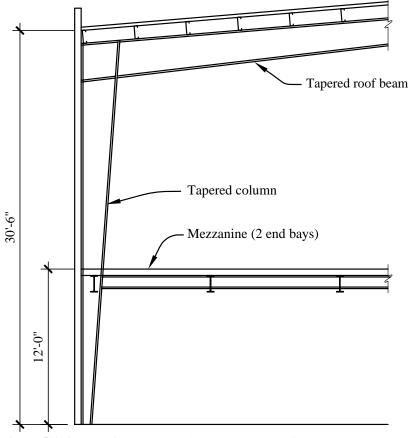


Figure 5.1-5 Moment diagram for seismic load combinations (1.0 ft-kip = 1.36 kN-m).

#### 5.1.5 Proportioning and Details

The gable frame is shown schematically in Figure 5.1-6. Using load combinations presented in Sec. 5.1.3.4 and the loads from Tables 5.1-2 and 5.1-3, the proportions of the frame are checked at the roof beams and the variable-depth columns (at the knee). The mezzanine framing, also shown in Figure 5.1-1, was proportioned similarly. The diagonal bracing, shown in Figure 5.1-1 at the east end of the building, is proportioned using tension forces determined from the 3-D modal analysis.



**Figure 5.1-6** Gable frame schematic: Column tapers from 12 in. at base to 36 in. at knee; roof beam tapers from 36 in. at knee to 18 in. at ridge; plate sizes are given in Figure 5.1-8 (1.0 in. = 25.4 + mm).

#### 5.1.5.1 Frame Compactness and Brace Spacing

According to *Provisions* Sec. 8.4 [8.2.2], steel structures assigned to Seismic Design Categories D, E, and F must be designed and detailed (with a few exceptions) per AISC Seismic. For an intermediate moment frame (IMF), AISC Seismic Part I, Section 1, "Scope," stipulates that those requirements are to be applied in conjunction with AISC LRFD. Part I, Section 10 of AISC Seismic itemizes a few exceptions from AISC LRFD for intermediate moment frames, but otherwise the intermediate moment frames are to be designed per the AISC LRFD Specification.

Terminology for moment-resisting frames varies among the several standards; Table 5.1-6 is intended to assist the reader in keeping track of the terminology.

Total Rotation (story drift angle)	Plastic Rotation	AISC Seismic (1997)	FEMA 350	AISC Seismic (Supplement No. 2)	Provisions
0.04	0.03	SMF	SMF	SMF	SMF
0.03	0.02	IMF	Not used	Not used	Not used
0.02	0.01*	OMF	OMF	IMF	IMF
Not defined	Minimal	Not used	Not used	OMF	OMF

Table 5.1-6         Comparison of Standards	<b>Table 5.1-6</b>	Comparison	of Standards
---	--------------------	------------	--------------

\*This is called "limited inelastic deformations" in AISC Seismic.

SMF = special moment frame.

IMF = intermediate moment frame.

OMF = ordinary moment frame.

For this example, IMF per the Provisions corresponds to IMF per AISC Seismic.

[The terminology in the 2002 edition of AISC Seismic is the same as Supplement No. 2 to the 1997 edition as listed in Table 5.1-6. Therefore, the terminology is unchanged from the 2000 *Provisions*.]

Because AISC Seismic does not impose more restrictive width-thickness ratios for IMF, the width-thickness ratios of AISC LRFD, Table B5.1, will be used for our IMF example. (If the frame were an SMF, then AISC Seismic would impose more restrictive requirements.)

The tapered members are approximated as short prismatic segments; thus, the adjustments of AISC LRFD Specification for web-tapered members will not affect the results of the 3-D SAP 2000 analysis.

All width-thickness ratios are less than the limiting  $\lambda_p$  from AISC LRFD Table B5.1. All P-M ratios (combined compression and flexure) were less than 1.00. This is based on proper spacing of lateral bracing.

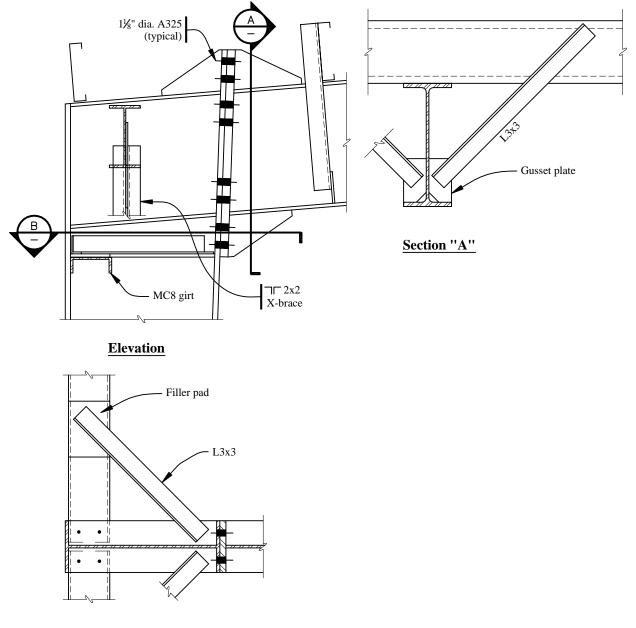
Lateral bracing is provided by the roof joists and wall girts. The spacing of lateral bracing is illustrated for the high moment area of the tapered beam near the knee. The maximum moment at the face of the column under factored load combinations is less than the plastic moment, but under the design seismic ground motion the plastic moment will be reached. At that point the moment gradient will be higher than under the design load combinations (the shear will be higher), so the moment gradient at design conditions will be used to compute the maximum spacing of bracing. The moment at the face of the column is 659 ft.-kip, and 4.0 ft away the moment is 427 ft.-kip. The member is in single curvature here, so the sign on the ratio in the design equation is negative (AISC LRFD Eq. F1-17):

$$L_{pd} = \left[ 0.12 + 0.076 \left( \frac{M_1}{M_2} \right) \right] \left( \frac{E}{F_y} \right) r_y$$
$$L_{pd} \left[ 0.12 + 0.076 \left( \frac{-488}{659} \right) \right] \left( \frac{29,000}{50} \right) (1.35) = 49.9 \text{ in.} > 48 \text{ in.}$$
OK

Also, per AISC LRFD Eq. F1-4:

$$L_p = 300r_y / \sqrt{F_{yf}}$$
  
 $L_p = (300)(1.35) / \sqrt{50} = 57 \text{ in.} > 48 \text{ in.}$  OK

At the negative moment regions near the knee, lateral bracing is necessary on the bottom flange of the beams and inside the flanges of the columns (Figure 5.1-7).



Section "B"

**Figure 5.1-7** Arrangement at knee (1.0 in. = 25.4 mm).

## 5.1.5.2 Knee of the Frame

The knee detail is shown in Figures 5.1-7 and 5.1-8. The vertical plate shown near the upper left corner in Figure 5.1-7 is a gusset providing connection for X-bracing in the longitudinal direction. The beam to column connection requires special consideration. The method of FEMA 350 for bolted, stiffened end plate connections is used for a design guide here. (FEMA 350 has design criteria for specific connection details. The connection for our moment frame, which has a tapered column and a tapered beam is not one of the specific details per FEMA 350. However, FEMA 350 is used as a guide for this example because it is the closest design method developed to date for such a connection.) Refer to Figure 5.1-8 for configuration. Highlights from this method are shown for this portion of the example Refer to FEMA 350 for a discussion of the entire procedure. AISC SDGS-4 is also useful.

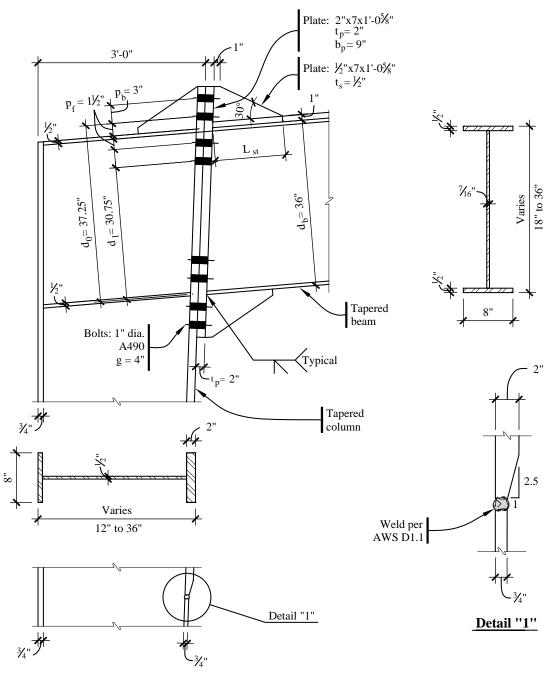


Figure 5.1-8 Bolted stiffened connection at knee (1.0 in. = 25.4 mm, 1.0 ft = 0.3048 m).

The FEMA 350 method for bolted stiffened end plate connection requires the determination of the maximum moment that can be developed by the beam. The steps in FEMA 350 for bolted stiffened end plates follow:

Step 1. The location of the plastic hinge is distance *x* from the face of the column. The end plate stiffeners at the top and bottom flanges increase the local moment of inertia of the beam, forcing the plastic hinge to occur away from the welds at the end of beam/face of column. The stiffeners should be long enough to force the plastic hinge to at least d/2 away from the end of the beam. With the taper of the section, the depth will be slightly less than 36 inches at the location of the hinge, but that reduction will be ignored here. The probable maximum moment ( $M_{pr}$ ) at the plastic hinge is computed (FEMA 350 Eq. 3-1) as follows:

$$M_{pr} = C_{pr}R_{y}Z_{e}F_{y}.$$

Per FEMA 350 Eq. 3-2:

$$C_{pr} = \frac{F_y + F_u}{2F_u} = \frac{(50 + 65)}{(2)(50)} = 1.15$$

AISC Seismic Table I-6-1 indicates:

$$R_y = 1.1$$
  
 $Z_e = 267$  in.<sup>3</sup> at d/2 from the end plate (the plastic hinge location)  
 $F_y = 50$  ksi

Therefore,  $M_{pr} = (1.15)(1.1)(267)(50) = 16,888$  in.-kips. = 1,407 ft-kips.

The moment at the column flange,  $M_f$ , which drives the connection design, is determined from FEMA 350 Figure 3-4 as:

 $M_f = M_{pr} + V_p x$ 

where

 $V_p$  = Shear at location of plastic hinge, assuming the frame has formed two hinges, one near each column.

$$V_p = w_g \frac{l}{2} + \frac{M_{pr1} + M_{pr2}}{l} = (0.52 \text{ klf}) \left(\frac{81 \text{ ft}}{2}\right) + \frac{1407 + 1407 \text{ ft-k}}{81 \text{ ft}} = 55.8 \text{ kips}$$

l = 81 ft comes from the 90 ft out-to-out dimension of the frame, less the column depth and distance to the hinge at each end. Where the gravity moments are a large fraction of the section capacity, the second hinge to form, which will be in positive moment, may be away from the column face, which will reduce *l* and usually increase  $V_p$ . That is not the circumstance for this frame.

$$x = d_h/2 = 18$$
 in. = 1.5 ft

Thus,  $M_f = 1407 + (55.8)(1.5) = 1491$  ft-kips

In a like manner, the moment at the column centerline is found:

$$M_c = M_{pr} + V_p \left( x + \frac{d_c}{2} \right) = 1407 + 55.8(1.5 + 1.5) = 1574$$
 ft-kips

Step 2. Find bolt size for end plates. For a connection with two rows of two bolts inside and outside the flange, FEMA 350 Eq. 3-31 indicates:

$$\begin{split} M_f &< 3.4 \ T_{ub}(d_o + d_i) \\ (1491)(12) &< 3.4 \ T_{ub}(37.25 \ \text{in.} + 30.75 \ \text{in.}) \\ 77.38 &< T_{ub} \\ 77.38 &< 113 \ A_b \ (\text{for A490 bolts}) \\ 0.685 \ \text{in.}^2 &< A_b \end{split}$$

Use 1 in. Diameter A490 bolts.

Now confirm that  $T_{ub}$  satisfies FEMA 350 Eq. 3-32:

$$T_{ub} \ge \frac{0.00002305 \, p_f^{-0.591} F_{fu}^{-2.583}}{t_p^{-0.895} d_{bt}^{-1.909} t_s^{-0.327} b_p^{-0.965}} + T_b$$

where:

 $p_f$  = dimension from top of flange to top of first bolt = 1.5 in.  $t_p$  = end plate thickness = 2 in. (Trial  $t_p$ )  $d_{bt}$  = bolt diameter = 1 in.  $t_s$  = thickness of stiffener plate = 0.44 in.  $b_p$  = width of end plate = 9 in.  $T_b$  = bolt pretension per AISC LRFD Table J3.1  $T_{ub}$  = 113  $A_b$  = (113)(0.785) = 88.7 kips

$$T_{ub} \ge \frac{(0.00002305)(1.5)^{0.591}(504)^{2.583}}{(2)^{0.895}(1)^{1.909}(0.44)^{0.327}(9)^{0.965}} + 64$$

 $T_{ub} = 88.7 \text{ kips} > 87.5 \text{ kips}$ 

OK

Therefore, a 2-in.-thick end plate is acceptable.

- Step 3. Check the bolt size to preclude shear failure. This step is skipped here because 16 bolts will obviously carry the shear for our example.
- Step 4. Determine the minimum end plate thickness necessary to preclude flexural yielding by comparing the thickness determined above against FEMA 350 Eq. 3-34:

$$t_{p} \geq \frac{0.00609 p_{f}^{0.9} g^{0.6} F_{fu}^{0.9}}{d_{bt}^{0.9} t_{s}^{0.1} b_{p}^{0.7}}$$
$$t_{p} \geq \frac{(0.00609)(1.5)^{0.9}(4)^{0.6}(504)^{0.9}}{(1)^{0.9}(0.44)^{0.1}(9)^{0.7}}$$
$$2 \text{ in.} > 1.27 \text{ in.}$$

OK

and against FEMA 350 Eq. 3-35:

$$t_{p} \geq \frac{0.00413 p_{f}^{0.25} g^{0.15} F_{fu}}{d_{bt}^{0.7} t_{s}^{0.15} b_{p}^{0.3}}$$
$$t_{p} \geq \frac{(0.00413)(1.5)^{0.25}(4)^{0.15}(504)}{(1)^{0.7}(0.44)^{0.15}(9)^{0.3}}$$

2 in. > 1.66 in.

OK

Therefore, use a 2-in.-thick end plate.

Step 5. Determine the minimum column flange thickness required to resist beam flange tension using FEMA 350 Eq. 3-37:

$$t_{cf} > \sqrt{\frac{\alpha_m F_{fu} C_3}{0.9 F_{yc} (3.5 p_b + c)}}$$

where

$$C_3 = \frac{g}{2} - d_{bt} - k_1 = \frac{4}{2} - \frac{1}{4} - 0.75 = 1.00$$
 in.

(For purposes of this example,  $k_1$  is taken to be the thickness of the column web, 0.5 in. and an assumed 0.25 in. fillet weld for a total of 0.75 in.).

Using FEMA 350 Eq. 3-38:

$$\alpha_m = C_a \left(\frac{A_f}{A_w}\right)^{\frac{1}{3}} \frac{C_3}{\left(d_{bt}\right)^{\frac{1}{4}}} = (1.48) \left(\frac{(2)(8)(0.5)}{(35)(0.44)}\right)^{\frac{1}{3}} \frac{1}{(1)^{0.25}} = 1.19$$

$$t_{cf} > \sqrt{\frac{(1.19)(504)(1.00)}{(0.9)(50)[(3.5)(3) + (3.5)]}} = 0.95 \text{ in.}$$

Minimum  $t_{cf} = 0.95$  in. but this will be revised in Step 7.

Step 6. Check column web thickness for adequacy for beam flange compression. This is a check on web crippling using FEMA 350 Eq. 3-40:

$$t_{wc} = \frac{M_f}{(d_b - t_{fb})(6k + 2t_p + t_{fb})F_{yc}} = \frac{(1491)(12)}{(36 - 0.5)[(6)(0.75) + (2)(2) + (0.5)](50)} = 1.44 \text{ in.}$$

 $t_{wc \ read} = 1.44$  in. > 0.5 in. =  $t_{wc}$ 

Therefore, a continuity plate is needed at the compression flange. See FEMA 350 Sec. 3.3.3.1 for continuity plate sizing. For one-sided connections, the necessary thickness of the continuity plate is  $0.5(t_{bf} + t_{bf}) = 0.5$  in.

Step 7. Because continuity plates are required,  $t_{cf}$  must be at least as thick as the end plate thickness  $t_p$ . Therefore,  $t_{cf} = 2$  in. For this column, the 2-in.-thick flange does not need to be full height but must continue well away from the region of beam flange compression and the high moment

OK

portion of the column knee area. Some judgment is necessary here. For this case, the 2-in. flange is continued 36 in. down from the bottom of the beam, where it is welded to the 0.75-in.- thick flange. This weld needs to be carefully detailed.

Step 8. Check the panel zone shear in accordance with FEMA 350, Sec. 3.3.3.2. For purposes of this check, use  $d_b = 35.5 + 1.5 + 3 + 1.5 = 41.5$  in. Per FEMA 350 Eq. 3-7:

$$t \ge \frac{C_y M_c \left(\frac{h-d_b}{h}\right)}{(0.9)(0.6F_y) R_{yc} d_c (d_b - t_{fb})}$$

where, according to FEMA 350 Eq. 3-4:

$$C_y = \frac{1}{C_{pr} \frac{Z_{be}}{S_b}} = \frac{1}{1.15 \left(\frac{267}{218}\right)} = 0.71$$

$$t_{cw} \ge \frac{(0.71)(1574 \text{ x } 12) \left(\frac{366 - 41.5}{366}\right)}{(0.9)(0.6)(50)(1.1)(36)(36 - 0.5)} = 0.31 \text{ in.}$$

 $t_{cw \ required} = 0.31 \text{ in.} < 0.50 \text{ in.} = t_{cw}$ 

OK

### 5.1.5.3 Frame at the Ridge

The ridge joint detail is shown in Figure 5.1-9. An unstiffened bolted connection plate is selected.

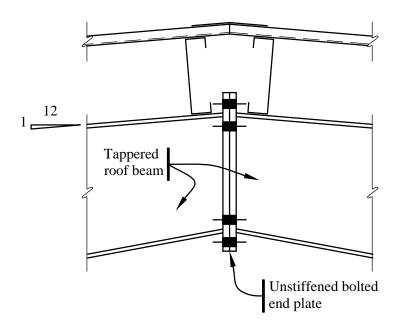


Figure 5.1-9 End plate connection at ridge.

This is an AISC LRFD designed connection, not a FEMA 350 designed connection because there should not be a plastic hinge forming in this vicinity. Lateral seismic force produces no moment at the ridge until yielding takes place at one of the knees. Vertical accelerations on the dead load do produce a

moment at this point; however, the value is small compared to all other moments and does not appear to be a concern. Once lateral seismic loads produce yielding at one knee, further lateral displacement produces some positive moment at the ridge. Under the condition on which the FEMA 350 design is based (a full plastic moment is produced at each knee), the moment at the ridge will simply be the static moment from the gravity loads less the horizontal thrust times the rise from knee to ridge. If one uses 1.2D + 0.2S as the load for this scenario, the static moment is 406 ft-kip and the reduction for the thrust is 128 ft-kip, leaving a net positive moment of 278 ft-kip, coincidentally close to the design moment for the factored gravity loads.

#### 5.1.5.4 Design of Mezzanine Framing

The design of the framing for the mezzanine floor at the east end of the building is controlled by gravity loads. The concrete filled 3-in., 20-gauge steel deck of the mezzanine floor is supported on steel beams spaced at 10 ft and spanning 20 ft (Figure 5.1-2). The steel beams rest on three-span girders connected at each end to the portal frames and supported on two intermediate columns (Figure 5.1-1). The girder spans are approximately 30 ft each. The design of the mezzanine framing is largely conventional as seismic loads do not predominate. Those lateral forces that are received by the mezzanine are distributed to the frames and diagonal bracing via the floor diaphragm. A typical beam-column connection at the mezzanine level is provided in Figure 5.1-10. The design of the end plate connection is similar to that at the knee, but simpler because the beam is horizontal and not tapered.

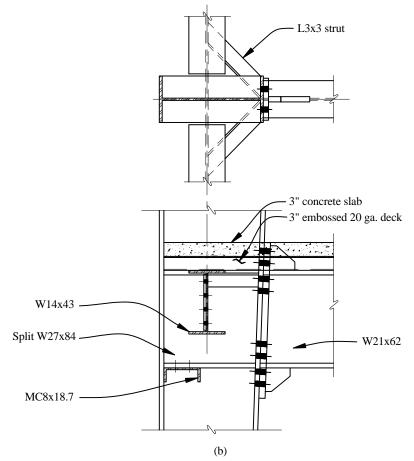


**Figure 5.1-10** Mezzanine framing (1.0 in. = 25.4 mm).

#### 5.1.5.5 Braced Frame Diagonal Bracing

Although the force in the diagonal X braces can be either tension or compression, only the tensile value is considered because it is assumed that the diagonal braces are capable of resisting only tensile forces.

See AISC Seismic Sec. 14.2 (November 2000 Supplement) for requirements on braces for OCBFs. The strength of the members and connections, including the columns in this area but excluding the brace connections, shall be based on AISC Seismic Eq. 4-1.

$$1.2D + 0.5L + 0.2S + \Omega_0 Q_E$$

Recall that a 1.0 factor is applied to *L* when the live load is greater than 100 psf (AISC Seismic Sec. 4.1). For the case discussed here, the "tension only" brace does not carry any live load so the load factor does not matter. For the braced design,  $\Omega_0 = 2$ .

However, *Provisions* Sec. 5.2.7.1, Eq. 5.2.7.1-1 and -2 [4.2-3 and 4.2-4, respectively] requires that the design seismic force on components sensitive to overstrength shall be defined by:

$$E = \Omega_0 Q_E \pm 0.2 S_{DS} D$$

Given that the *Provisions* is being following, the AISC Seismic equation will be used but E will be substituted for  $Q_E$ . Thus, the load combination for design of the brace members reduces to:

$$1.4D + 0.5L + 0.2S + \Omega_0 Q_E$$

[The special load combinations have been removed from the 2002 edition of AISC Seismic to eliminate inconsistencies with other building codes and standards but the design of ordinary braced frames is not really changed because there is a reference to the load combinations including "simplified seismic loads." Therefore, 2003 *Provisions* Eq. 4.2-3 and 4.2-4 should be used in conjunction with the load combinations in ASCE 7 as is done here.]

From analysis using this load combination, the maximum axial force in the X brace located at the east end of the building is 66 kips computed from the combined orthogonal earthquake loads (longitudinal direction predominates). With the  $\Omega_0$  factor, the required strength becomes 132 kips. All braces will have the same design. Using A36 steel for angles:

$$T_n = \phi F_y A_g$$
  
 $A_g = \frac{P_n}{\phi F_y} = \frac{132}{(0.9)(36)} = 4.07 \text{ in.}^2$ 

Try (2) L4  $\times$ 3  $\times$  3/8:

$$A_{a} = (2)(2.49) = 4.98 \text{ in.}^{2} > 4.07 \text{ in.}^{2}$$
 OK

AISC Seismic Sec. 14.2 requires the design strength of the brace connections to be based on the expected tensile strength:

$$R_v F_v A_\rho = (1.5)(36 \text{ ksi})(4.98 \text{ in.}^2) = 269 \text{ kips.}$$

Also be sure to check the eave strut at the roof. The eave strut, part of the braced frame, has to carry compression and that compression is determined using the overstrength factor.

The kl/r requirement of AISC Seismic Sec. 14.2 does not apply because this is not a V or an inverted V

configuration.

# 5.1.5.6 Roof Deck Diaphragm

Figure 5.1-11 shows the in-plane shear force in the roof deck diaphragm for both seismic loading conditions. There are deviations from simple approximations in both directions. In the E-W direction, the base shear is 230 kips (Sec. 5.1.4.2) with 83 percent or 191 kips at the roof. Torsion is not significant so a simple approximation is to take half the force to each side and divide by the length of the building, which yields (191,000/2)/180 ft. = 530 plf. The plot shows that the shear in the edge of the diaphragm is significantly higher in the two braced bays. This is a shear lag effect; the eave strut in the 3-D model is a HSS 6x6x1/4. In the N-S direction, the shear is generally highest in the bay between the mezzanine frame and the first frame without the mezzanine. This might be expected given the significant change in stiffness. There does not appear to be any particularly good simple approximation to estimate the shear here without a 3-D model. The shear is also high at the longitudinal braced bays because they tend to resist the horizontal torsion. The shear at the braced bays is lower than observed for the E-W motion, however.

# FEMA 451, NEHRP Recommended Provisions: Design Examples

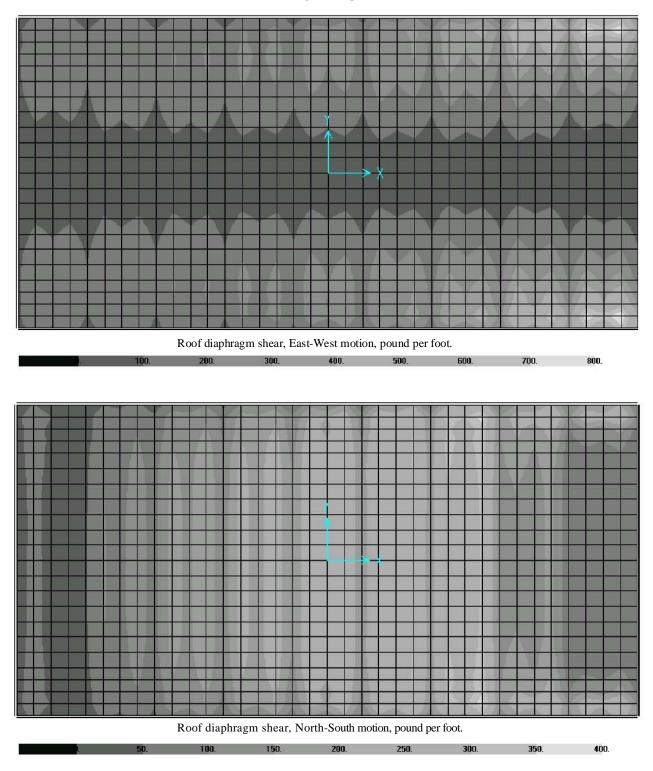


**Figure 5.1-11** Shear force in roof deck diaphragm; upper diagram is for E-W motion and lower is for N-S motion (1.0 lb. /ft. = 14.59 N/M).

# 5.2 SEVEN-STORY OFFICE BUILDING, LOS ANGELES, CALIFORNIA

Three alternative framing arrangements for a seven-story office building are illustrated.

# 5.2.1 Building Description

# 5.2.1.1 General Description

This seven-story office building of rectangular plan configuration is 177 ft, 4 in. long in the E-W direction and 127 ft, 4 in. wide in the N-S direction (Figure 5.2-1). The building has a penthouse. It extends a total of 118 ft, 4 in. above grade. It is framed in structural steel with 25-ft bays in each direction. The story height is 13 ft, 4 in. except for the first story which is 22 ft, 4 in. high. The penthouse extends 16 ft above the roof level of the building and covers the area bounded by gridlines C, F, 2, and 5 in Figure 5.2-1. Floors consist of 3-1/4 in. lightweight concrete placed on composite metal deck. The elevators and stairs are located in the central three bays. The building is planned for heavy filing systems (350 psf) covering approximately four bays on each floor.

# 5.2.1.2 Alternatives

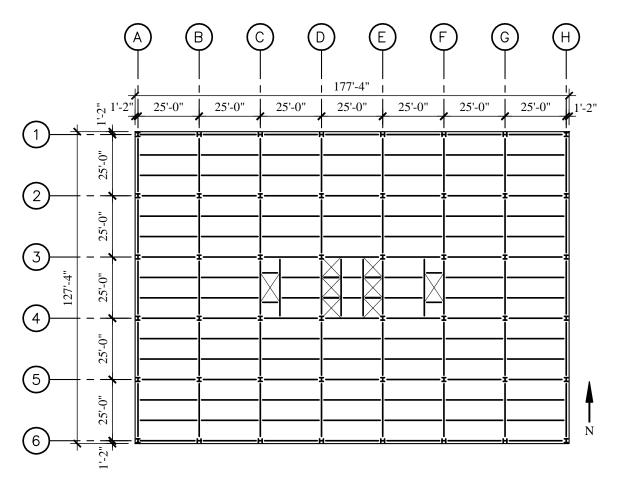
This example features three alternatives -a steel moment-resisting frame, concentrically braced frame, and a dual system with a moment-resisting frame at the perimeter and a concentrically braced frame at the core area -as follows:

- 1. Alternative A Seismic force resistance is provided by special moment frames located on the perimeter of the building (on lines A, H, 1, and 6 in Figure 5.2-1, also illustrated in Figure 5.2-2).
- 2. Alternative B Seismic force resistance is provided by four special concentrically braced frames in each direction. They are located in the elevator core walls between columns 3C and 3D, 3E and 3F, 4C and 4D, and 4E and 4F in the E-W direction and between columns 3C and 4C, 3-D and 4D, 3E and 4E, and 3F and 4F in the N-S direction (Figure 5.2-1). The braced frames in an X configuration are designed for both diagonals being effective in tension and compression. The braced frames are not identical, but are arranged to accommodate elevator door openings. Braced frame elevations are shown in Figure 5.2-3.
- 3. Alternative C Seismic force resistance is provided by a dual system with the special moment frames at the perimeter of the building and a special concentrically braced frames at the core. The moment frames are shown in Figure 5.2-2 and the braced frames are shown in Figure 5.2-3.

# 5.2.1.3 Scope

The example covers:

- 1. Seismic design parameters
- 2. Analysis of perimeter moment frames
- 3. Beam and column proportioning
- 4. Analysis of concentrically braced frames
- 5. Proportioning of braces
- 6. Analysis and proportioning of the dual system



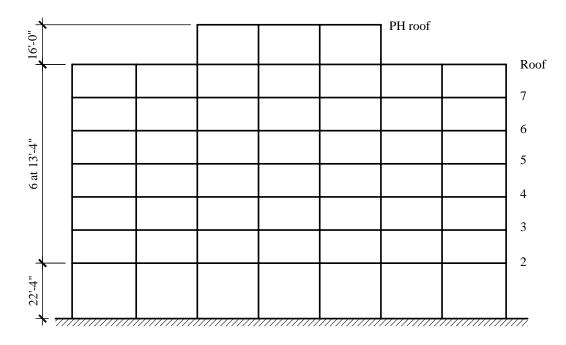


**Figure 5.2-1** Typical floor framing plan and building section (1.0 in. = 25.4 mm, 1.0 ft = 0.3048 m).

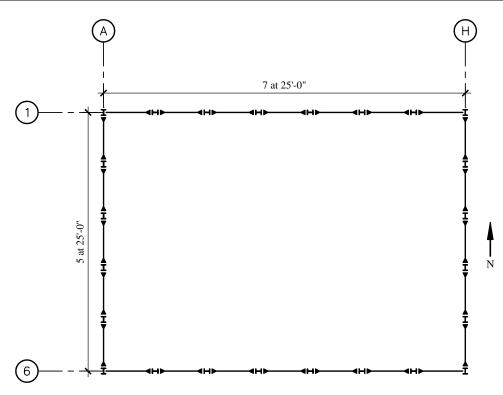


**Figure 5.2-2** Framing plan for special moment frame (1.0 in. = 25.4 mm, 1.0 ft = 0.3048 m).

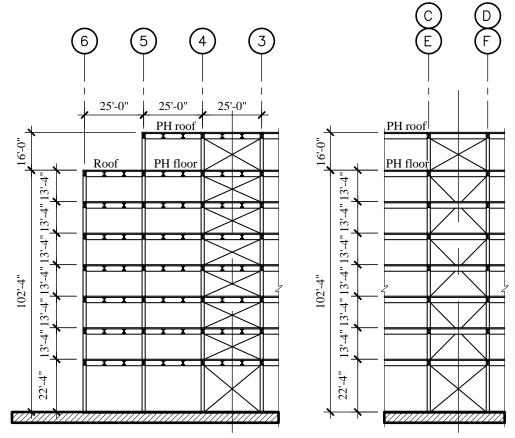


Figure 5.2-3 Concentrically braced frame elevations (1.0 in. = 25.4 mm, 1.0 ft = 0.3048 m).

# 5.2.2 Basic Requirements

# 5.2.2.1 Provisions Parameters

Site $Class = D$	(Provisions Sec. 4.1.2.1 [3.5])
$S_{s} = 1.5$	(Provisions Map 9 [Figure 3.3-3])
$S_1 = 0.6$	(Provisions Map 10 [Figure 3.3-4])
$F_{a} = 1.0$	(Provisions Table 4.1.2.4a [3.3-1])
$F_{v} = 1.5$	(Provisions Table 4.1.2.4b [3.3-2])
$S_{MS} = F_a S_S = 1.5$	(Provisions Eq. 4.1.2.4-1 [3.3-1])
$S_{MI} = F_{v}S_{I} = 0.9$	(Provisions Eq. 4.1.2.4-2 [3.3-2])
$S_{DS} = 2/3 \ S_{MS} = 1.0$	(Provisions Eq. 4.1.2.5-1 [3.3-3])
$S_{DI} = 2/3 \ S_{MI} = 0.6$	(Provisions Eq. 4.1.2.5-2 [3.3-4])
Seismic Use Group = I	(Provisions Sec. 1.3 [1.2])
Seismic Design Category = D	(Provisions Sec. 4.2.1 [1.4])

Alternative A, Special Steel Moment Frame (Provisions Table 5.2.2 [4.3-1])

 $egin{array}{rcl} R &= 8 \ \Omega_0 &= 3 \ C_d &= 5.5 \end{array}$ 

Alternative B, Special Steel Concentrically Braced Frame (Provisions Table 5.2.2 [4.3-1])

 $\begin{array}{ll} R &= 6 \\ \Omega_0 &= 2 \\ C_d &= 5 \end{array}$ 

Alternative C, Dual System of Special Steel Moment Frame Combined with Special Steel Concentrically Braced Frame (*Provisions* Table 5.2.2 [4.3-1])

 $egin{array}{rcl} R &= 8 \ arOmega_0 &= 2.5 \ C_d &= 6.5 \end{array}$ 

# 5.2.2.2 Loads

Roof live load ( <i>L</i> )	= 25 psf
Penthouse roof dead load (D)	= 25  psf
Exterior walls of penthouse	= 25  psf of wall
Roof DL (roofing, insulation, deck beams,	
girders, fireproofing, ceiling, M&E)	= 55 psf
Exterior wall cladding	= 25 psf of wall
Penthouse floor D	= 65 psf
Floor L	= 50 psf
Floor D (deck, beams, girders,	
fireproofing, ceiling, M&E, partitions)	= 62.5 psf
Floor <i>L</i> reductions per the IBC	

# 5.2.2.3 Materials

Concrete for drilled piers	$f_c' = 5$ ksi, normal weight (NW)
Concrete for floors	$f_c' = 3$ ksi, lightweight (LW)

All other concrete	$f_c' = 4 \text{ ksi, NW}$
Structural steel	
Wide flange sections	ASTM A992, Grade 50
HSS	ASTM A500, Grade B
Plates	ASTM A36
Wide flange sections HSS	ASTM A500, Grade B

## 5.2.3 Structural Design Criteria

#### 5.2.3.1 Building Configuration

The building is considered vertically regular despite the relatively tall height of the first story. The exception of *Provisions* Sec. 5.2.3.3 [4.3.2.3] is taken in which the drift ratio of adjacent stories are compared rather than the stiffness of the stories. In the 3-D analysis, it will be shown that the first story drift ratio is less than 130 percent of the story above. Because the building is symmetrical in plan, plan irregularities would not be expected. Analysis reveals that Alternatives B and C are torsionally irregular, which is not uncommon for core-braced buildings.

### 5.2.3.2 Redundancy

According to *Provisions* Sec. 5.2.4.2 [not applicable in the 2003 *Provisions*], the reliability factor, ( $\rho$ ) for a Seismic Design Category D structure is:

$$\rho = 2 - \frac{20}{r_{\max_x} \sqrt{A_x}}$$

In a typical story, the floor area,  $A_x = 22,579$  ft.<sup>2</sup>

The ratio of the design story shear resisted by the single element carrying the most shear force in the story to the total story shear is  $r_{max}$ , as defined in *Provisions* Sec. 5.2.4.2.

Preliminary  $\rho$  factors will be determined for use as multipliers on design force effects. These preliminary  $\rho$  factors will be verified by subsequent analyses.

[The redundancy requirements have been substantially changed in the 2003 *Provisions*. For a building assigned to Seismic Design Category D,  $\rho = 1.0$  as long as it can be shown that failure of beam-to-column connections at both ends of a single beam (moment frame system) or failure of an individual brace (braced frame system) would not result in more than a 33 percent reduction in story strength or create an extreme torsional irregularity. Alternatively, if the structure is regular in plan and there are at least two bays of perimeter framing on each side of the structure in each orthogonal direction, it is permitted to use  $\rho = 1.0$ . Per 2003 *Provisions* Sec. 4.3.1.4.3, special moment frames in Seismic Design Category D must be configured such that the structure satisfies the criteria for  $\rho = 1.0$ . There are no reductions in the redundancy factor for dual systems. Based on the preliminary design,  $\rho = 1.0$  for Alternative A because it has a perimeter moment frame and is regular. The determination of  $\rho$  for Alternatives B and C (which are torsionally irregular) requires the evaluation of connection and brace failures per 2003 *Provisions* Sec. 4.3.3.2.]

### 5.2.3.2.1 Alternative A (moment frame)

For a moment-resisting frame,  $r_{max_x}$  is taken as the maximum of the sum of the shears in any two adjacent columns divided by the total story shear. The final calculation of  $\rho$  will be deferred until the building

frame analysis, which will include the effects of accidental torsion, is completed. At that point, we will know the total shear in each story and the shear being carried by each column at every story. See Sec. 5.2.4.3.1.

*Provisions* Sec. 5.2.4.2 requires that the configuration be such that  $\rho$  shall not exceed 1.25 for special moment frames. [1.0 in the 2003 *Provisions*] (There is no limit for other structures, although  $\rho$  need not be taken larger than 1.50 in the design.) Therefore, it is a good idea to make a preliminary estimate of  $\rho$ , which was done here. In this case,  $\rho$  was found to be 1.11 and 1.08 in the N-S and E-W directions, respectively. A method for a preliminary estimate is explained in Alternative B.

Note that  $\rho$  is a multiplier that applies only to the force effects (strength of the members and connections), not to displacements. As will be seen for this moment-resisting frame, drift, and not strength, will govern the design.

# 5.2.3.2.2 Alternative B (concentrically braced frame)

Again, the following preliminary analysis must be refined by the final calculation. For the braced frame system, there are four braced-bay braces subject to shear at each story, so the direct shear on each line of braces is equal to  $V_x/4$ . The effects of accidental torsion will be estimated as:

The torsional moment  $M_{ta} = (0.05)(175)(V_x) = 8.75V_x$ . The torsional force applied to either grid line C or F is  $V_t = M_{ta}Kd / \Sigma Kd^2$ .

Assuming all frame rigidity factors (*K*) are equal:

$$V_t = \frac{M_{ta}(37.5)}{\left[(2)(37.5)^2 + (6)(12.5)^2\right]} = 0.01M_{ta}$$

 $V_t = (0.01)(8.75 V_x) = 0.0875 V_x$ 

The amplification of torsional shear  $(A_x)$  must be considered in accordance with *Provisions* Sec. 5.4.4.1.3 [5.2.4.3]. Without dynamic amplification of torsion, the direct shear applied to each line of braces is  $V_x/4$  and the torsional shear,  $V_i = 0.0875 V_x$ . Thus, the combined shear at Grid C is  $0.25V_x - 0.0875V_x = 0.1625V_x$ , and the combined shear at Grid F is  $0.25V_x + 0.0875V_x = 0.3375V_x$ . As the torsional deflections will be proportional to the shears and extrapolating to Grids A and H, the deflection at A can be seen to be proportional to  $0.250V_x + (0.0875V_x)(87.5/37.5) = 0.454V_x$ . Likewise, the deflection at H is proportional to  $0.250V_x - (0.0875V_x)(87.5/37.5) = 0.046V_x$ . The average deflection is thus proportional to  $[(0.454 + 0.046)/2]V_x = 0.250V_x$ . These torsional effects are illustrated in Figure 5.2-4.

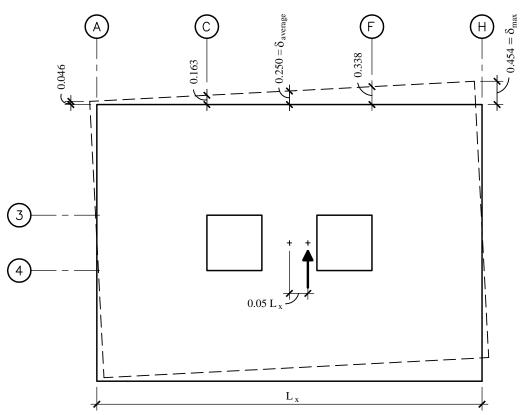


Figure 5.2-4 Approximate effect of accidental of torsion (1.0 in. = 25.4 mm).

From the above estimation of deflections, the torsional amplification can be determined per *Provisions* Eq. 5.4.4.1.3.1 [5.2-13] as:

$$A_{x} = \left(\frac{\delta_{max}}{1.2 \ \delta_{avg}}\right)^{2} = \left(\frac{0.454}{(1.2)(0.250)}\right)^{2} = 2.29$$

The total shear in the N-S direction on Gridlines C or F is the direct shear plus the amplified torsional shear equal to:

$$V_x/4 + A_xV_t = [0.250 + (2.29)(0.0875)]V_x = 0.450V_x$$

As there are two braces in each braced bay (one in tension and the other in compression):

$$r_{max_x} = \frac{0.450}{2} = 0.225$$

and

$$\rho = 2 - \frac{20}{r_{max}\sqrt{A_x}} = 2 - \frac{20}{(0.225)\sqrt{22,579}} = 1.41$$

Therefore, use  $\rho = 1.41$  for the N-S direction. In a like manner, the  $\rho$  factor for the E-W direction is determined to be  $\rho = 1.05$ . These preliminary values will be verified by the final calculations. *5.2.3.2.3 Alternative C (dual system)* 

For the dual system, the preliminary value for  $\rho$  is taken as 1.0. The reason for this decision is that, with the dual system, the moment frame will substantially reduce the torsion at any story, so torsional amplification will be low. The combined redundancy of the braced frame combined with the moment frame (despite the fact that the moment frame is more flexible) will reduce  $\rho$  from either single system. Finally, *Provisions* Sec. 5.2.4.2 [not applicable in the 2003 *Provisions*] calls for taking only 80 percent of the calculated  $\rho$  value when a dual system is used. Thus, we expect the final value to fall below 1.0, for which we will take  $\rho = 1.0$ . This will be verified by analysis later.

# 5.2.3.3 Orthogonal Load Effects

A combination of 100 percent of the seismic forces in one direction with 30 percent seismic forces in orthogonal direction is required for structures in Seismic Design Category D (*Provisions* Sec. 5.2.5.2.3 and 5.2.5.2.2 [4.4.2.2]).

### 5.2.3.4 Structural Component Load Effects

The effect of seismic load is be defined by *Provisions* Eq, 5.2.7-1 [4.2-1] as:

$$E = \rho Q_{E} + 0.2 S_{DS} D$$

Recall that  $S_{DS} = 1.0$ . As stated above,  $\rho$  values are preliminary estimates to be checked and, if necessary, refined later.

For Alternative A

N-S direction	$E = (1.11)Q_E \pm (0.2)D$
E-W direction	$E = (1.08)Q_E \pm (0.2)D$

Alternative B

N-S direction	$E = (1.41)Q_E \pm (0.2)D$
E-W direction	$E = (1.05)Q_E \pm (0.2)D$

Alternative. C

N-S direction  $E = (1.00)Q_E \pm (0.2)D$ E-W direction  $E = (1.00)Q_E \pm (0.2)D$ 

### 5.2.3.5 Load Combinations

Load combinations from ASCE 7 are:

$$1.2D + 1.0E + 0.5L + 0.2S$$

and

0.9D + 1.0E + 1.6H

To each of these load combinations, substitute E as determined above, showing the maximum additive and minimum negative. Recall that  $Q_E$  acts both east and west (or north and south):

### Alternative A

N-S	$1.4D + 1.11Q_E + 0.5L$ and $0.7D + 1.11Q_E$
E-W	$1.4D + 1.08Q_E + 0.5L$ and $0.7D + 1.08Q_E$

## Alternative B

N-S	$1.4D + 1.41Q_E + 0.5L$ and $0.7D + 1.41Q_E$
E-W	$1.4D + 1.05Q_{E} + 0.5L$ and $0.7D + 1.05Q_{E}$

Alternative C

N-S	$1.4D + Q_E + 0.5L$ and $0.7D + Q_E$
E-W	$1.4D + Q_E + 0.5L$ and $0.7D + Q_E$

### 5.2.3.6 Drift Limits

The allowable story drift per *Provisions* Sec. 5.2.8 [4.5-1] is  $\Delta_a = 0.02h_{sx}$ .

The allowable story drift for the first floor is  $\Delta_a = (0.02)(22.33 \text{ ft})(12 \text{ in./ft}) = 5.36 \text{ in.}$ The allowable story drift for a typical story is  $\Delta_a = (0.02)(13.33 \text{ ft})(12 \text{ in./ft}) = 3.20 \text{ in.}$ 

Remember to adjust calculated story drifts by the appropriate  $C_d$  factor from Sec. 5.2.2.1.

Consider that the maximum story drifts summed to the roof of the seven-story building, (102 ft-4 in. main roof/penthouse floor) is 24.56 in.

# 5.2.3.7 Basic Gravity Loads

### Penthouse roof

Roof slab = $(0.025)(75)(75)$	=	141 kips
Walls = (0.025)(8)(300)	=	60 kips
Columns = (0.110)(8)(16)	=	<u>14 kips</u>
Total	=	215 kips

Lower roof

Roof slab = $(0.055)[(127.33)(177.33) - (75)^2]$	=	932 kips
Penthouse floor = $(0.065)(75)(75)$	=	366 kips
Walls = 60 + (0.025)(609)(6.67)	=	162 kips
Columns = 14 + (0.170)(6.67)(48)	=	68 kips
Equipment (allowance for mechanical		
equipment in penthouse)	=_	217 kips
Total	= 1	,745 kips

## Typical floor

Floor = $(0.0625)(127.33)(177.33)$	= 1,412 kips
Walls = $(0.025)(609)(13.33)$	= 203 kips
Columns = $(0.285)(13.33)(48)$	= 182 kips
Heavy storage = $(0.50)(4)(25 \ge 25)(350)$	= <u>438 kips</u>
Total	= 2,235 kips
Total weight of building = $215 + 1,745 + 6(2,235)$	= 15,370 kips

Note that this office building has heavy storage in the central bays of 280 psf over five bays. Use 50 percent of this weight as effective seismic mass. (This was done to add seismic mass to this example thereby making it more interesting. It is not meant to imply that the authors believe such a step is necessary for ordinary office buildings.)

# 5.2.4 Analysis

# 5.2.4.1 Equivalent Lateral Force Analysis

The equivalent lateral force (ELF) procedure will be used for each alternative building system. The seismic base shear will be determined for each alternative in the following sections.

5.2.4.1.1 ELF Analysis for Alternative A, Moment Frame

First determine the building period (T) per Provisions Eq. 5.4.2.1-1 [5.2-6]:

$$T_a = C_r h_n^x = (0.028)(102.3)^{0.8} = 1.14 \text{ sec}$$

where  $h_n$ , the height to the main roof, is conservatively taken as 102.3 ft. The height of the penthouse (the penthouse having a smaller contribution to seismic mass than the main roof or the floors) will be neglected.

The seismic response coefficient  $(C_s)$  is determined from *Provisions* Eq. 5.4.1.1-1 [5.2-2] as:

$$C_s = \frac{S_{DS}}{R/I} = \frac{1}{(8/1)} = 0.125$$

However, *Provisions* Eq. 5.4.1.1-2 [5.2-3] indicates that the value for  $C_s$  need not exceed:

$$C_s = \frac{S_{D1}}{T(R/I)} = \frac{0.6}{1.14(8/1)} = 0.066$$

and the minimum value for  $C_s$  per *Provisions* Eq. 5.4.1.1-3 [not applicable in the 2003 *Provisions*] is:

$$C_s = 0.044 IS_{DS} = (0.044)(1)(1) = 0.044$$

Therefore, use  $C_s = 0.066$ .

Seismic base shear is computed per Provisions Eq. 5.4.1 [5.2-1] as:

 $V = C_s W = (0.066)(15,370) = 1014$  kips

5.2.4.1.2 ELF Analysis for Alternative B, Braced Frame

As above, first find the building period (T) using Provisions Eq. 5.4.2.1-1 [5.2-6]:

$$T_a = C_r h_n^x = (0.02)(102.3)^{0.75} = 0.64 \text{ sec}$$

The seismic response coefficient  $(C_s)$  is determined from *Provisions* Eq. 5.4.1.1-1 [5.2-2] as:

$$C_s = \frac{S_{DS}}{R/I} = \frac{1}{(6/1)} = 0.167$$

However, *Provisions* Eq. 5.4.1.1-2 [5.2-3] indicates that the value for  $C_s$  need not exceed:

$$C_s = \frac{S_{D1}}{T(R/I)} = \frac{0.6}{(0.64)(6/1)} = 0.156$$

and the minimum value for  $C_s$  per Provisions Eq. 5.4.1.1-3 [not applicable in 2003 Provisions] is:

$$C_s = 0.044 IS_{DS} = (0.044)(1)(1) = 0.044$$

Use  $C_s = 0.156$ .

Seismic base shear is computed using Provisions Eq. 5.4.1 [5.2-1] as:

$$V = C_S W = (0.156)(15,370) = 2,398$$
 kips

#### 5.2.4.1.3 ELF Analysis for Alternative C, Dual System

The building period (*T*) is the same as for the braced frame (*Provisions* Eq. 5.4.2.1-1 [5.2-6]):

$$T_a = C_r h_n^x = (0.02)(102.3)^{0.75} = 0.64$$
 sec

The seismic response coefficient ( $C_s$ ) is determined as (*Provisions* Eq. 5.4.1.1-1 [5.2-2]):

$$C_s = \frac{S_{DS}}{R/I} = \frac{1}{(8/1)} = 0.125$$

However, the value for  $C_s$  need not exceed (*Provisions* Eq. 5.4.1.1-2 [5.2-3]):

$$C_s = \frac{S_{D1}}{T(R/I)} = \frac{0.6}{(0.64)(8/1)} = 0.117$$

and the minimum value for  $C_s$  is (*Provisions* Eq. 5.4.1.1-3 [not applicable in the 2003 *Provisions*]):

 $C_s = 0.044 IS_{DS} = (0.044)(1)(1) = 0.044$ Therefore, use  $C_s = 0.117$ . Seismic base shear is computed as (Provisions Eq. 5.4.1 [5.2-1]):

 $V = C_s W = (0.117)(15,370) = 1,798$  kips

## 5.2.4.2 Vertical Distribution of Seismic Forces

*Provisions* Sec. 5.4.3 [5.2.3] provides the procedure for determining the portion of the total seismic load that goes to each floor level. The floor force  $F_x$  is calculated using *Provisions* Eq. 5.4.3-1 [5.2-10] as:

 $F_x = C_{yx}V$ 

where (Provisions Eq. 5.4.3-2 [5.2-11])

$$C_{vx} = \frac{w_x h_x^k}{\sum_{i=1}^n w_i h_i^k}$$

For Alternative A

T = 1.14 secs, thus k = 1.32

For Alternatives B and C

T = 0.64 sec, thus k = 1.07

Using Provisions Eq. 5.4.4 [5.2-12], the seismic design shear in any story is computed as:

$$V_x = \sum_{i=x}^n F_i$$

The story overturning moment is computed from *Provisions* Eq. 5.4.5 [5.2-14]:

$$M_x = \sum_{i=x}^n F_i(h_i - h_x)$$

The application of these equations for the three alternative building frames is shown in Tables 5.2-1, 5.2-2, and 5.1-3.

Level (x)	$W_x$ (kips )	$h_x$ (ft)	$W_x h_x^k$ (ft-kips)	$C_{vx}$	$F_x$ (kips)	$V_x$ (kips)	$M_x$ (ft-kips)
PH Roof	215	118.33	117,200	0.03	32	32	514
Main roof	1,745	102.33	785,200	0.21	215	247	3,810
Story 7	2,235	89.00	836,500	0.23	229	476	10,160
Story 6	2,235	75.67	675,200	0.18	185	661	18,980
Story 5	2,235	62.33	522,700	0.14	143	805	29,710
Story 4	2,235	49.00	380,500	0.10	104	909	41,830
Story 3	2,235	35.67	250,200	0.07	69	977	54,870
Story 2	2,235	22.33	134,800	0.04	37	1,014	77,520
Σ	15,370		3,702,500	1.00	1,014		

 Table 5.2-1
 Alternative A, Moment Frame Seismic Forces and Moments by Level

1.0 kip = 4.45 kN, 1.0 ft = 0.3048 m.

Level (x)	$W_x$ (kips )	$h_x$ (ft)	$W_x h_x^k$ (ft-kips)	$C_{vx}$	$F_x$ (kips)	$V_x$ (kips)	$M_x$ (ft-kips)
PH Roof	215	118.33	35,500	0.03	67	67	1,070
Main roof	1,745	102.33	246,900	0.19	463	530	8,130
Story 7	2,235	89.00	272,300	0.21	511	1,041	22,010
Story 6	2,235	75.67	228,900	0.18	430	1,470	41,620
Story 5	2,235	62.33	186,000	0.15	349	1,819	65,870
Story 4	2,235	49.00	143,800	0.11	270	2,089	93,720
Story 3	2,235	35.67	102,400	0.08	192	2,281	124,160
Story 2	2,235	22.33	62,000	<u>0.05</u>	116	2,398	177,720
Σ	15,370		1,278,000	1.00	2,398		

1.0 kip = 4.45 kN, 1.0 ft = 0.3048 m.

	$W_x$ $h_x$ $W_x h_x^k$ $C_{yx}$ $F_x$ $V_x$ $M_x$									
Level (x)	(kips)	$n_x$ (ft)	(ft-kips)	$C_{vx}$	$I_x$ (kips)	(kips)	(ft-kips)			
PH Roof	215	118.33	35,500	0.03	50	50	800			
Main roof	1,745	102.33	246,900	0.19	347	397	6,100			
Story 7	2,235	89.00	272,350	0.21	383	781	16,500			
Story 6	2,235	75.67	228,900	0.18	322	1,103	31,220			
Story 5	2,235	62.33	186,000	0.15	262	1,365	49,400			
Story 4	2,235	49.00	143,800	0.11	202	1,567	70,290			
Story 3	2,235	35.67	102,386	0.08	144	1,711	93,120			
Story 2	2,235	22.33	62,000	<u>0.05</u>	87	1,798	133,270			
Σ	15,370		1,278,000	1.00	1,798					

**Table 5.2-3** Alternative C, Dual System Seismic Forces and Moments by Level

1.0 kip = 4.45 kN, 1.0 ft = 0.3048 m.

Be sure to note that the seismic mass at any given level, which includes the lower half of the wall above that level and the upper half of the wall below that level, produces the shear applied at that level and that shear produces the moment which is applied at the top of the next level down. Resisting the overturning moment is the weight of the building above that level combined with the moment resistance of the framing at that level. Note that the story overturning moment is applied to the level below the level that receives the story shear. (This is illustrated in Figure 9.2-4 in the masonry examples.)

# 5.2.4.3 Size Members

At this point we are ready to select the sizes of the framing members. The method for each alternative is summarized below.

Alternative A, Special Moment Frame:

1.	Select preliminary member sizes	
2.	Check deflection and drift	(Provisions Sec. 5.2.8 [5.4.1])
3.	Check torsional amplification	(Provisions Sec. 5.4.4.1.3 [5.2.4.3])
4.	Check the column-beam moment ratio rule	(AISC Seismic Sec. 9.6)
5.	Check shear requirement at panel-zone	(AISC Seismic Sec. 9.3; FEMA 350
		Sec. 3.3.3.2)
6.	Check redundancy	(Provisions Sec. 5.2.4.2 [5.3.3])
7.	Check strength	

Reproportion member sizes as necessary after each check. The most significant criteria for the design are drift limits, relative strengths of columns and beams, and the panel-zone shear.

Alternative B, Special Concentrically Braced Frame:

- 1. Select preliminary member sizes
- 2. Check strength
- 3. Check drift
- 4. Check torsional amplification
- 5. Check redundancy

(*Provisions* Sec. 5.2.8 [4.5.1]) (*Provisions* Sec. 5.4.4.1 [5.2.4.3]) (*Provisions* Sec. 5.2.4.2 [4.3.3])

Reproportion member sizes as necessary after each check. The most significant criteria for this design is torsional amplification.

Alternative C, Dual System:

Select preliminary member sizes
 Check strength of moment frame for 25 percent of story shear (*Provisions* Sec. 5.2.2.1 [4.3.1.1])
 Check strength of braced frames
 Check drift for total building (*Provisions* Sec. 5.2.8 [4.5.1])
 Check torsional amplification (*Provisions* Sec. 5.2.4.1 [5.2.4.3])
 Check redundancy (*Provisions* Sec. 5.2.4.2 [4.3.3])

Reproportion member sizes as necessary after each check.

# 5.2.4.3.1 Size Members for Alternative A, Moment Frame

1. Select Preliminary Member Sizes – The preliminary member sizes are shown for the moment frame in the X-direction (7 bays) in Figure 5.2-5 and in the Y direction (5 bays) in Figure 5.2-6.

Check Local Stability – Check beam flange stability in accordance with AISC Seismic Table I-9-1 [I-8-1] (same as FEMA 350 Sec. 3.3.1.1) and beam web stability in accordance with AISC Seismic Table I-9-1 [I-8-1]. (FEMA 350 Sec.3.3.1.2.is more restrictive for cases with low  $P_u/\phi_b P_y$ , such as in this example.) Beam flange slenderness ratios are limited to  $52/\sqrt{F_y}$  and beam web height-to-thickness ratios are limited to  $418/\sqrt{F_y}$ .

[The terminology for local stability has been revised in the 2002 edition of AISC Seismic. The limiting slenderness ratios in AISC Seismic use the notation  $\lambda_{ps}$  ("seismically compact") to differentiate them from  $\lambda_p$  in AISC LRFD. In addition, the formulas appear different because the elastic modulus,  $E_s$ , has been added as a variable. Both of these changes are essentially editorial, but Table I-8-1 in the 2002 edition of AISC Seismic has also been expanded to include more elements than in the 1997 edition.]

Be careful because certain shapes found in the AISC Manual will not be permitted for Grade 50 steel (but may have been permitted for Grade 36 steel) because of these restrictions. For Grade 50, b/t is limited to 7.35.

Further note that for columns in special steel moment frames such as this example, AISC Seismic 9.4b [I-8-1] requires that when the column moment strength to beam moment strength ratio is less than or equal to 2.0, the more stringent  $\lambda_p$  requirements apply for b/t, and when  $P_u/\phi_b P_y$  is less than or equal to 0.125, the more stringent h/t requirements apply.

								H
ן   	• W21x44	W21x44	W21x44	W21x44	W21x44	W21x44	W21x44	   
W14x145	M54x65 M54x65 M54x145	M54x65 M54x145	M54x65 M54x145	M54x95 M54x145	M54x65 M54x145	M54x65 M54x145	W24x62 W24x62 W24x62	
	≥ W27x94	≥ - W27x94 -	≥ - W27x94 -	≥ - W27x94 -	≥ W27x94	≽ - W27x94 -	≥ - W27x94 -	
W14x233	• W27x102 14x233	M52333 6x233	M52333 6x233	W27x102 41 W27x102 41	M52x105 84 8x233	M52333 6x233	W27x102 F1	
-	≥ W30x108	≥ - W30x108	≥ - W30x108	≥ W30x108	≥ - W30x108	≥ - W30x108	≥ - W30x108 -	
W14x283	• W30x108 W	14x257 M30x108	M30x108 M30x10	M30x108 M3057	M30x108 M30x10	M30x108 M30x10	w30x108	
-	© W33x141	≥ - W33x141 -	≥ - W33x141 -	≥ - W33x141	≥ W33x141 -	≥ - W33x141 -	≥ W33x141	Ì
W14x398	W14x370	W14x370	W14x370	W14x370	W14x370	W14x370	W14x398	

Figure 5.2-5 SMRF frame in E-W direction (penthouse not shown).

2. Check Drift – Check drift in accordance with *Provisions* Sec. 5.2.8 [4.5.1]. The building was modeled in 3-D using RAMFRAME. Displacements at the building centroid are used here because the building is not torsionally irregular (see the next paragraph regarding torsional amplification). Calculated story drifts and  $C_d$  amplification factors are summarized in Table 5.2-4. P-delta effects are included.

All story drifts are within the allowable story drift limit of  $0.020h_{sx}$  per *Provisions* Sec. 5.2.8 [4.5.1] and Sec. 5.2.3.6 of this chapter.

As indicated below, the first story drift ratio is less than 130 percent of the story above (*Provisions* Sec. 5.2.3.3 [4.3.2.3]):

$$\frac{C_{d\Delta_{x \text{ story 2}}}}{C_{d\Delta_{x \text{ story 3}}}} = \frac{\left(\frac{5.17 \text{ in.}}{268 \text{ in.}}\right)}{\left(\frac{3.14 \text{ in.}}{160 \text{ in.}}\right)} = 0.98 < 1.30$$

Therefore, there is no vertical irregularity.

Œ	5)	(5	$\mathbf{D}$	(	1)	Ċ	3)		2)	
	W21x44		W21x44		W21x44		W21x44		W21x44	
W14x145	W24x76	W14x145	W24x76	W14x145	W24x76	W14x145	W24x76	W14x145	W24x76	W14x145
_	- W27x94	-	- W27x94	_	- W27x94	_	- W27x94	1	- W27x94	
W14x233	W30x108	W14x233	W30x108	W14x233	W30x108	W14x233	W30x108	W14x233	W30x108	W14x233
_		_		-		-		-		
W14x283	W30x116	W14x283	W30x116	W14x283	W30x116	W14x283	W30x116	W14x283	W30x116	W14x283
-		_		_		_		_	- W33x141	
W14x398		W14x398		W14x398		W14x398		W14x398		W14x398
M		M		M		M		M		×

Figure 5.2-6 SMRF frame in N-S direction (penthouse not shown).

	Total Displacement at Building Centroid (86.5, 62.5)		Story Drift from 3-D Elastic Analysis at Building Centroid		$C_d$	( <i>C</i> <sub>d</sub> (Elastic S	) x tory Drift)	Allowable Story Drift
	∂E-W (in.)	∂N-S (in.)	⊿E-W (in.)	⊿N-S (in.)	5.5	⊿E-W (in.)	⊿N-S (in.)	⊿ (in.)
Roof	4.24	4.24	0.48	0.47	5.5	2.64	2.59	3.20
Floor 7	3.76	3.77	0.57	0.58	5.5	3.14	3.19	3.20
Floor 6	3.19	3.19	0.54	0.53	5.5	2.97	2.92	3.20
Floor 5	2.65	2.66	0.57	0.58	5.5	3.14	3.19	3.20
Floor 4	2.08	2.08	0.57	0.58	5.5	3.14	3.19	3.20
Floor 3	1.51	1.50	0.57	0.57	5.5	3.14	3.14	3.20
Floor 2	0.94	0.93	0.94	0.93	5.5	5.17	5.12	5.36

Table 5.2-4 Alternative A (Moment Frame) Story Drifts under Seismic Loads

1.0 in. = 25.4 mm.

3. Check Torsional Amplification – The torsional amplification factor per *Provisions* Eq. 5.4.4.1.3-1 [5.2-13] is:

$$A_{x} = \left(\frac{\delta_{max}}{1.2\delta_{avg}}\right)^{2}$$

If  $A_x < 1.0$ , then torsional amplification need not be considered. It is readily seen that if the ratio of  $\delta_{max}/\delta_{avg}$  is less that 1.2, then torsional amplification will not be necessary.

The 3-D analysis provided the story deflections listed in Table 5.2-5. Because none of the ratios for  $\delta_{max}/\delta_{avg}$  exceed 1.2, torsional amplification of forces is not necessary for the moment frame alternative.

	Torsion Checks							
	$\delta_{EW_{max}}( ext{in.})$ (175,0)	$\delta_{NS_{max}}$ (in.) (125,0)	$\delta_{\rm EW_{max}}/\delta_{\rm EW_{avg}}$	$\delta_{_{N\!S_{max}}}/\delta_{_{N\!S_{arg}}}$				
Roof	4.39	4.54	1.04	1.07				
Story 7	3.89	4.04	1.04	1.07				
Story 6	3.30	3.42	1.04	1.07				
Story 5	2.75	2.85	1.03	1.07				
Story 4	2.16	2.23	1.04	1.07				
Story 3	1.57	1.62	1.04	1.08				
Story 2	0.98	1.00	1.04	1.08				

Table 5.2-5 Alternative A Torsional Analysis

1.0 in. = 25.4 mm.

Member Design Considerations – Because  $P_u/\phi P_n$  is typically less than 0.4 for the columns (re: AISC Seismic Sec. 8.2 [8.3]), combinations involving  $\Omega_0$  factors do not come into play for the special steel moment frames. In sizing columns (and beams) for strength we will satisfy the most severe value from interaction equations. However, this frame is controlled by drift. So, with both strength and drift requirements satisfied, we will check the column-beam moment ratio and the panel zone shear.

4. Check the Column-Beam Moment Ratio – Check the column-beam moment ratio per AISC Seismic Sec. 9.6. For purposes of this check, the plastic hinge was taken to occur at  $0.5d_b$  from the face or the column in accordance with FEMA 350 for WUF-W connections (see below for description of these connections). The expected moment strength of the beams were projected from the plastic hinge location to the column centerline per the requirements of AISC Seismic Sec. 9.6. This is illustrated in Figure 5.2-7. For the columns, the moments at the location of the beam flanges is projected to the column-beam intersection as shown in Figure 5.2-8.

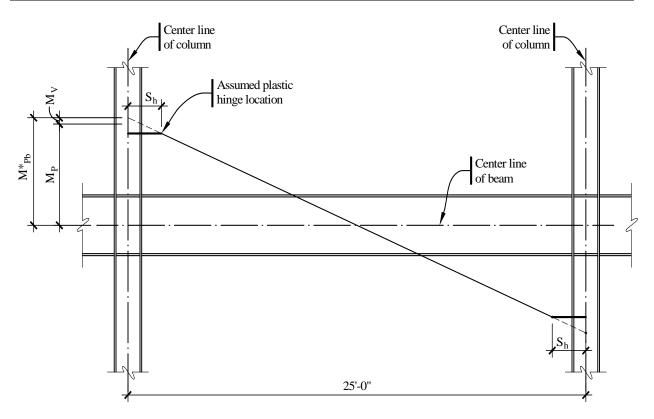


Figure 5.2-7 Projection of expected moment strength of beam (1.0 in = 25.4 mm, 1.0 ft = 0.3048 m).

The column-beam strength ratio calculation is illustrated for the lower level in the E-W direction, Level 2, at gridline G (W14 $\times$ 370 column and W33 $\times$ 141 beam). For the columns:

$$\Sigma M_{pc}^* = \Sigma Z_c \left( F_{yc} - \frac{P_{uc}}{A_g} \right)$$
  
$$\Sigma M_{pc}^* = 2 \left[ 736 \text{ in.}^3 \left( 50 \text{ ksi} - \frac{500 \text{ kips}}{109 \text{ in.}^2} \right) \right] = 66,850 \text{ ft-kips}$$

Adjust this by the ratio of average story height to average clear height between beams, or (268 + 160)/(251.35 + 128.44) = 1.13. Therefore,  $\Sigma M_{pc}^* = (1.13)(66,850) = 75,300$  ft-kips. For the beams,

$$\Sigma M_{pb}^* = \Sigma (1.1 R_y M_p + M_v)$$

where

 $R_y = 1.1$  for Grade 50 steel  $M_p = F_y Z = (50) (514) = 25,700$  in.-kips  $M_v = V_p S_h$   $S_h =$  Distance from column centerline to plastic hinge  $= d_c/2 + d_b/2 = 25.61$  in.  $V_p =$  Shear at plastic hinge location

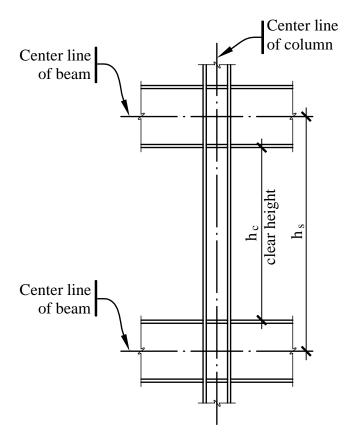


Figure 5.2-8 Story height and clear height.

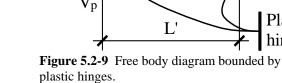
Μ

The shear at the plastic hinge (Figure 5.2-9) is computed as:

$$V_n = [2M_n + (wL'^2/2)]/L'$$

where

L' = Distance between plastic hinges = 248.8 in. w = Factored uniform gravity load along beam w = 1.4D + 0.5L = 1.4(0.0625 ksf)(12.5 ft) + 0.5(0.050 ksf)(12.5 ft) = 1.406 klf



W

M<sub>p</sub>

Plastic

hinges

Therefore,

$$V_{p} = \frac{2M_{p} + \frac{wL'^{2}}{2}}{L'} = \frac{(2)(25,700) + \left(\frac{(1.406)}{12}\frac{(248.8)^{2}}{2}\right)}{248.8} = 221.2 \text{ kips}$$

and

$$M_v = V_p S_h = (221.2)(25.61) = 5,665$$
 in.-kips

Finally,  $\Sigma M_{pb}^* = \Sigma (1.1R_y M_p + M_y) = 2[(1.1)(1.1)(25,700) + 5,665] = 73,500$  in.-kips.

The ratio of column moment strengths to beam moment strengths is computed as:

Ratio = 
$$\frac{\Sigma M_{pc}^*}{\Sigma M_{pb}^*} = \frac{76,900}{73,500} = 1.05 > 1.0$$
 OK

The column-beam strength ratio for all the other stories is determined in a similar manner. They are summarized in Table 5.2-4 for the E-W direction (seven-bay) frame and in Table 5.2-5 for the N-S direction (five-bay) frame. All cases are acceptable because the column-beam moment ratios are all greater than 1.00.

Story		Member	$\Sigma M^*_{pc}$ (inkips)	$\Sigma M^*_{pb}$ (inkips)	Column- Beam Ratio
7	column beam	W14×145 W24×62	29,000	21,300	1.36
5	column beam	W14×233 W27×102	40,000	42,600	1.15
3	column beam	W14×257 W30×108	53,900	48,800	1.11
2	column beam	W14×370 W33×141	75,300	73,500	1.02

 Table 5.2-4
 Column-Beam Moment Ratios for Seven-Bay Frame (N-S Direction)

For levels with the same size column, the one with the larger beam size will govern; only these are shown. 1.0 in.-kip = 0.113 kN-m.

Story		Member	$\Sigma M^*_{pc}$ (inkips)	$\frac{\Sigma M^*_{pb}}{\text{(inkips)}}$	Column- Beam Ratio
7	column beam	W14×145 W24×76	29,400	27,700	1.06
5	column beam	W14×233 W30×108	50,700	48,700	1.04
3	column beam	W14×283 W30×116	63,100	53,900	1.17
2	column beam	W14×398 W33×141	85,900	74,100	1.16

 Table 5.2-5
 Column-Beam Moment Ratios for Five-Bay Frame (N-S Direction)

For levels with the same size column, the one with the larger beam size will govern; only these are shown. 1.0 in.-kip = 0.113 kN-m.

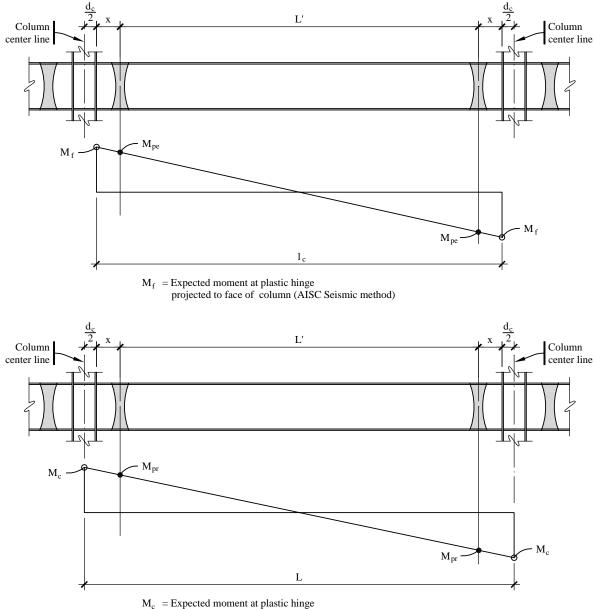
5. Check Panel Zone – The *Provisions* defers to AISC Seismic for the panel zone shear calculation. Because the two methods for calculating panel zone shear (AISC Seismic and FEMA 350) differ, both are illustrated below.

# AISC Seismic Method

Check the shear requirement at the panel zone in accordance with AISC Seismic Sec. 9.3. The factored shear  $R_u$  is determined from the flexural strength of the beams connected to the column. This depends on the style of connection. In its simplest form, the shear in the panel zone  $(R_u)$  is

$$R_u = \Sigma \frac{M_f}{d_b - t_{fb}}$$

 $M_f$  is the moment at the column face determined by projecting the expected moment at the plastic hinge points to the column faces (see Figure 5.2-10).



projected to column centerline (FEMA 350 method)

Figure 5.2-10 Illustration of AISC Seismic vs. FEMA 350 methods for panel zone shear.

For a column with equal beams of equal spans framing into opposite faces (such as on Grids C, D, E, F, 2, 3, 4, and 5), the effect of gravity loads offset, and

$$\Sigma M_f = 2R_y F_y Z_x \left[ \frac{l_c}{l_c - 2x} \right]$$

where  $l_c$  = the clear span and x = distance from column face to plastic hinge location.

For Grids 1 and 6, only one beam frames into the column; at Grids B and G, the distance *x* is different on one side; at Grids A and H, there is no moment because the beams are pin-connected to the corner columns. For all these cases, the above relationship needs to be modified accordingly.

For W33×141 beams framing into each side of a W14×370 column (such as Level 2 at Grid F):

$$\Sigma M_f = (2)(1.1)(50)(514) \left[ \frac{282.1}{282.1 - (2)(16.55)} \right] = 64,056 \text{ in.-kips}$$
$$R_u = \frac{64,056}{1000} = 1,981 \text{ kips}$$

$$R_u = \frac{1}{33.30 - 0.96} = 1,981 \text{ kip}$$

The shear transmitted to the joint from the story above opposes the direction of  $R_u$  and may be used to reduce the demand. From analysis, this is 98 kips at this location. Thus the frame  $R_u = 1,981 - 98 = 1,883$  kips.

The panel zone shear calculation for Story 2 of the frame in the E-W direction at Grid F (column:  $W14 \times 370$ ; beam:  $W33 \times 141$ ) is from AISC Seismic Eq. 9-1:

$$R_{v} = 0.6F_{y}d_{c}t_{p}\left[1 + \frac{3b_{cf}t_{cf}^{2}}{d_{b}d_{c}t_{p}}\right]$$

$$R_{v} = (0.6)(50)(17.92)(t_{p})\left[1 + \frac{(3)(16.475)(2.660)^{2}}{(33.30)(17.92)(t_{p})}\right]$$

$$R_{v} = 537.6t_{p}\left[1 + \frac{0.586}{t_{p}}\right]$$

$$R_{v} = 537.6t_{p} + 315$$

The required total (web plus doubler plate) thickness is determined by:

$$R_v = \phi R_u$$

Therefore,  $537.6t_p + 315 = (1.0)(1883)$  and  $t_p = 2.91$  in.

Because the column web thickness is 1.655 in., the required doubler plate thickness is 1.26 in. Use a plate thickness of 1-1/4 in.

Both the column web thickness and the doubler plate thickness are checked for shear buckling during inelastic deformations by AISC Seismic Eq. 9-2. If necessary, the doubler plate may be plug-welded to the column web as indicated by AISC Seismic Commentary Figure C-9.2. For this case, the minimum individual thickness as limited by local buckling is:

$$t \ge (d_z + w_z)/90$$
  
 $t \ge \frac{(31.38 + 12.6)}{90} = 0.49$  in.

Because both the column web thickness and the doubler plate thicknesses are greater than 0.49 in., plug welding of the doubler plate to the column web is not necessary.

In the case of thick doubler plates, to avoid thick welds, two doubler plates (each of half the required thickness) may be used, one on each side of the column web. For such cases, buckling also must be checked using AISC Seismic Eq. 9-2 as doubler plate buckling would be a greater concern. Also, the detailing of connections that may be attached to the (thinner) doubler plate on the side of the weld needs to be carefully reviewed for secondary effects such as undesirable out-of-plane bending or prying.

# FEMA 350 Method

For the FEMA 350 method, see FEMA 350 Sec. 3.3.3.2, "Panel Zone Strength," to determine the required total panel zone thickness (*t*):

$$t = \sum \frac{C_{y}M_{c} \left[\frac{h - d_{b}}{h}\right]}{(0.9)(0.6)F_{yc}R_{yc}d_{c}(d_{b} - t_{fb})}$$

(Please note the  $\Sigma$ ; its omission from FEMA 350 Eq. 3-7 is an inadvertent typographical error.)

The term  $M_c$  refers to the expected beam moment projected to the centerline of the column; whereas AISC Seismic uses the expected beam moment projected to the face of the column flange. (This difference is illustrated in Figure 5.2-10.) The term  $\left[\frac{h-d_b}{h}\right]$  is an adjustment similar to reducing  $R_u$  by the direct shear in the column, where *h* is the average story height.  $C_v$  is a factor that adjusts the

force on the panel down to the level at which the beam begins to yield in flexure (see FEMA 350 Sec. 3.2.7) and is computed from FEMA 350 Eq. 3-4:

$$C_{y} = \frac{1}{C_{pr} \frac{Z_{be}}{S_{b}}}$$

 $C_{pr}$ , a factor accounting for the peak connection strength, includes the effects of strain hardening and local restraint, among others (see FEMA 350 Sec. 3.2.4) and is computed from FEMA 350 Eq. 3-2:

$$C_{pr} = \frac{(F_y + F_u)}{2F_y}$$

For the case of a  $W33 \times 141$  beam and  $W14 \times 370$  column (same as used for the above AISC Seismic method), values for the variables are:

Distance from column centerline to plastic hinge,  $S_h = d_c/2 + d_b/2 = 17.92/2 + 33.30/2 = 25.61$  in.

Span between plastic hinges, L' = 25 ft - 2(25.61 in.)/12 = 20.73 ft

$$M_{pr} = C_{pr}R_{y}Z_{e}F_{y}$$
 (FEMA 350 Figure 3-4)  
 $M_{pr} = (1.2)(1.1)(514)(50) = 33,924$  in.-kips (FEMA 350, Figure 3-4)

$$V_{p} = \frac{\left[2M_{pr} + \left(\frac{wL'^{2}}{2}\right)\right]}{L'}$$

$$V_p = \frac{\left[(2)(33,924) + \left(\frac{(1.266)(20.73)^2}{(12)(2)}\right)\right]}{(20.73)(12)} = 273 \text{ kips}$$

 $M_c = M_{pr} + V_p(x + d_c/2)$  (FEMA 350 Figure 3-4)

 $M_c = 33,924 + (273)(17.92/2 + 25.61/2) = 40,916$  in.-kips

$$C_{y} = \frac{1}{C_{pr} \frac{Z_{be}}{S_{b}}} = \frac{1}{(1.2) \frac{514}{448}} = 0.73$$

Therefore,

$$t = 2 \left[ \frac{(0.73)(40,916) \left[ \frac{(214) - (33.30)}{(214)} \right]}{(0.9)(0.6)(50)(1.1)(17.92)(33.30 - 0.96)} \right] = 2.93 \text{ in.}$$

The required doubler plate thickness is equal to  $t - t_{cw} = 2.93$  in. - 1.655 in. = 1.27 in. Thus, the doubler plate thickness for 1.27 in. by FEMA 350 is close to the thickness of 1.26 by AISC Seismic.

6. Check Redundancy – Return to the calculation of  $r_x$  for the moment frame. In accordance with *Provisions* Sec. 5.2.4.2 [not applicable in the 2003 *Provisions*],  $r_{max_x}$  is taken as the maximum of the sum of the shears in any two adjacent columns in the plane of a moment frame divided by the story shear. For columns common to two bays with moment resisting connections on opposite sides of the column at the level under consideration, 70 percent of the shear in that column may be used in the column shear summation (Figures 5.2-11 and 5.2-12).

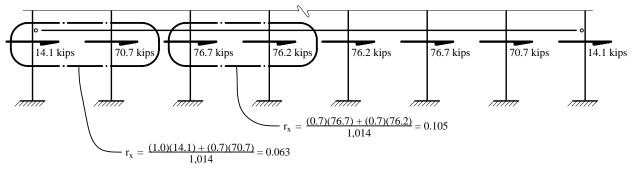


Figure 5.2-11 Column shears for E-W direction (partial elevation, Level 2) (1.0 kip = 4.45 kN).

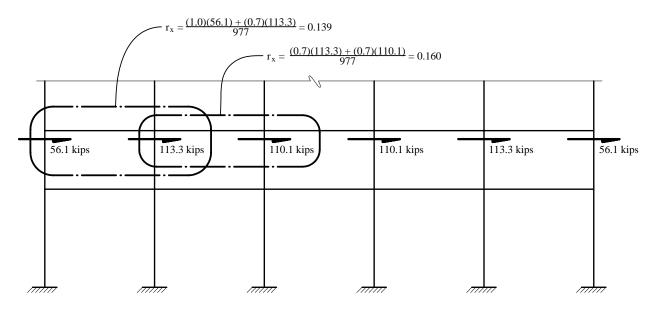


Figure 5.2-12 Column shears for N-S direction (partial elevation, Level 3) (1.0 kip = 4.45 kN).

For this example,  $r_x$  was computed for every column pair at every level in both directions. The shear carried by each column comes from the RAMFRAME analysis, which includes the effect of accidental torsion. Selected results are illustrated in the figures. The maximum value of  $r_{max_x}$  in the N-S direction is 0.160, and  $\rho$  is now determined using *Provisions* Eq.5.2.4.2 [not applicable in the 2003 *Provisions*]:

$$\rho = 2 - \frac{20}{r_{max_x}\sqrt{A_x}}$$

$$\rho = 2 - \frac{20}{0.160\sqrt{21.875 \text{ ft}^2}} = 1.15$$

Because 1.15 is less than the limit of 1.25 for special moment frames per the exception in the *Provisions* Sec. 5.2.4.2 [not applicable in the 2003 *Provisions*], use  $\rho = 1.15$ . (If  $\rho > 1.25$ , then the framing would have to be reconfigured until  $\rho < 1.25$ .)

In the E-W direction,  $r_{max_x} = 0.105$  and  $\rho = 0.71$ , which is less than 1.00, so use  $\rho = 1.00$ . All design force effects (axial force, shear, moment) obtained from analysis must be increased by the  $\rho$  factors. (However, drift controls the design in this example. Drift and deflections are not subject to the  $\rho$  factor.)

7. Connection Design – One beam-to-column connection for the moment-resisting frame is now designed to illustrate the FEMA 350 method for a prequalified connection. The welded unreinforced flanges-welded web (WUF-W) connection is selected because it is prequalified for special moment frames with members of the size used in this example. FEMA 350 Sec. 3.5.2 notes that the WUF-W connection can perform reliably provided all the limitations are met and the quality assurance requirements are satisfied. While the discussion of the design procedure below considers design requirements, remember that the quality assurance requirements are a vital part of the total requirements and must be enforced.

Figure 5.2-13 illustrates the forces at the beam-to-column connection.

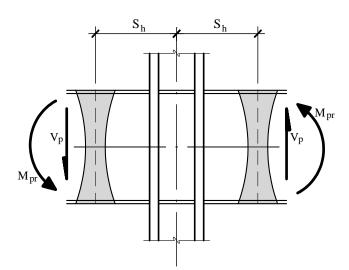


Figure 5.2-13 Forces at beam/column connection.

First review FEMA 350 Table 3-3 for prequalification data. Our case of a W36×135 beam connected to a W14×398 column meets all of these. (Of course, here the panel zone strength requirement is from FEMA 350, not the AISC Seismic method.)

The connection, shown in Figure 5.2-14, is based on the general design shown in FEMA 350 Figure 3-8. The design procedure outlined in FEMA 350 Sec. 3.5.2.1 for this application is reviewed below. All other beam-to-column connections in the moment frame will be similar.

The procedure outlined above for the FEMA 350 method for panel zone shear is repeated here to determine  $S_{lv}$ ,  $M_{pr}$ ,  $V_{p}$ ,  $M_c$ ,  $C_v$  and the required panel zone thickness.

Continuity plates are required in accordance with FEMA 350 Sec. 3.3.3.1:

$$t_{cf} < 0.4 \sqrt{1.8 b_f t_f \frac{F_{yb} R_{yb}}{F_{yc} R_{yc}}}$$

$$t_{cf} < 0.4 \sqrt{(1.8)(11.950)(0.790)\frac{(50)(1.1)}{(50)(1.1)}} = 1.65$$
 in. required  
 $t_{cf} = 2.845$  in. > actual OK

Therefore, continuity plates are not necessary at this connection because the column flange is so thick. But we will provide them anyway to illustrate continuity plates in the example. At a minimum, continuity plates should be at least as thick as the beam flanges. Provide continuity plates of 7/8 in. thickness, which is thicker than the beam flange of 0.79 in.

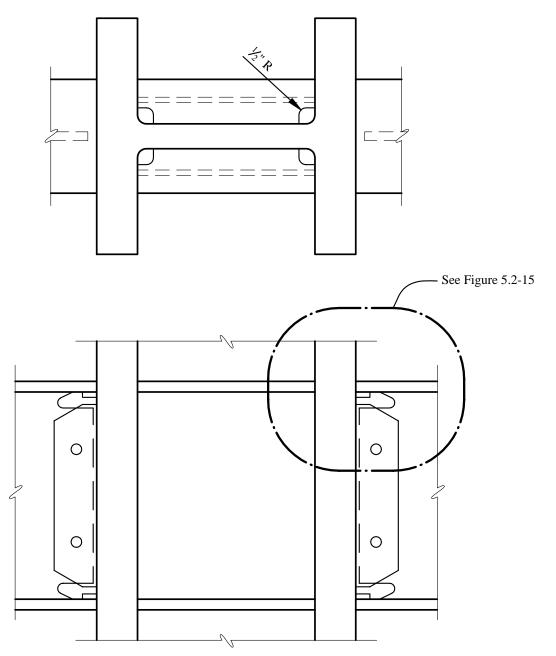


Figure 5.2-14 WUF-W connection, Second level, NS-direction (1.0 in. = 25.4 mm).

Check AISC LRFD K1.9:

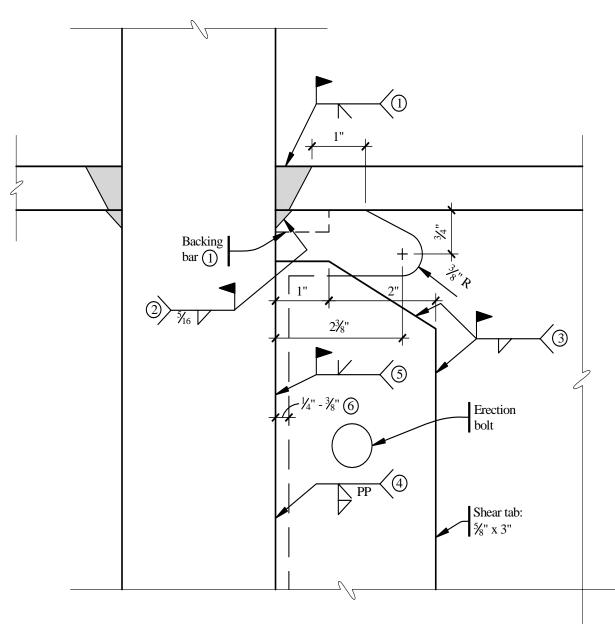
Width of stiffener 
$$+\frac{t_{cw}}{2} \ge \frac{b_{bf}}{3}$$
  
 $\left(5 + \frac{1.77}{2}\right) = 5.88 \text{ in.} > 3.98 \text{ in.} = \frac{11.950}{3}$ 

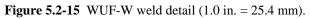
$$t_{stiffener} \ge \frac{b_f}{2}$$

0.875 in. > 0.395 in. = 
$$\frac{0.79}{2}$$
  
 $t_{stiffener} > w_{stiffener} \frac{\sqrt{F_y}}{95}$ 

OK

OK





$$0.875 \text{ in.} > 0.37 \text{ in.} = (5) \left(\frac{\sqrt{50}}{95}\right)$$
 OK

The details shown in Figures 5.2-14 and 5.2-15 conform to the requirements of FEMA 350 for a WUF-W connection in a special moment frame.

Notes for Figure 5.2-15 (indicated by circles in the figure) are:

- 1. CJP groove weld at top and bottom flanges, made with backing bar.
- 2. Remove backing bar, backgouge, and add fillet weld.
- 3. Fillet weld shear tab to beam web. Weld size shall be equal to thickness of shear tab minus 1/16 in. Weld shall extend over the top and bottom third of the shear tab height and extend across the top and bottom of the shear tab.
- 4. Full depth partial penetration weld from far side. Then fillet weld from near side. These are shop welds of shear tab to column.
- 5. CJP groove weld full length between weld access holes. Provide non-fusible weld tabs, which shall be removed after welding. Grind end of weld smooth at weld access holes.
- 6. Root opening between beam web and column prior to starting weld 5.

See also FEMA 350 Figure 3-8 for more elaboration on the welds.

### 5.2.4.3.2 Size Members for Alternative B, Braced Frame

- 1. Select Preliminary Member Sizes The preliminary member sizes are shown for the braced frame in the E-W direction (seven bays) in Figure 5.2-16 and in the N-S direction (five bays) in Figure 5.2-17. The arrangement is dictated by architectural considerations regarding doorways into the stairwells.
- Check Strength First, check slenderness and width-to-thickness ratios the geometrical requirements for local stability. In accordance with AISC Seismic Sec. 13.2, bracing members must satisfy

$$\frac{kl}{r} \le \frac{1000}{\sqrt{F_y}} = \frac{1000}{\sqrt{50}} = 141$$

The columns are all relatively heavy shapes, so kl/r is assumed to be acceptable and is not examined in this example.

Wide flange members and channels must comply with the width-to-thickness ratios contained in AISC Seismic Table I-9-1 [I-8-1]. Flanges must satisfy:

$$\frac{b}{2t} \le \frac{52}{\sqrt{F_y}} = \frac{52}{\sqrt{50}} = 7.35$$

Webs in combined flexural and axial compression (where  $P_u/\phi_b P_y < 0.125$ , which is the case in this example) must satisfy:

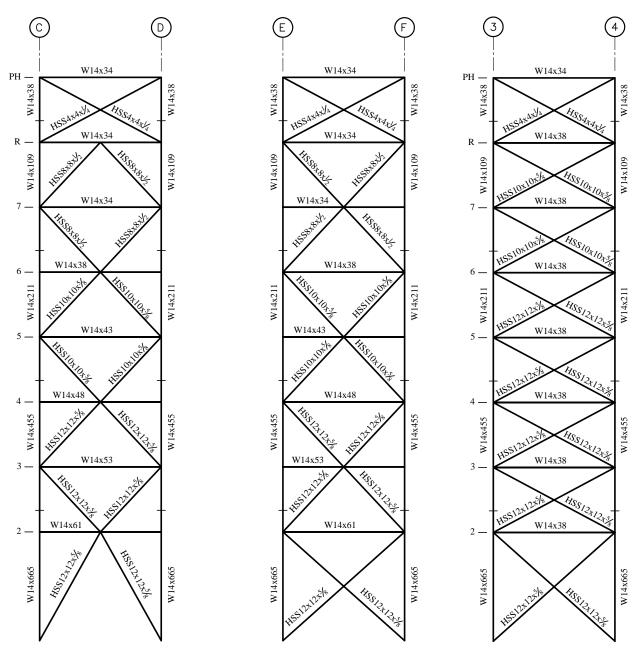
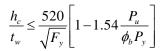
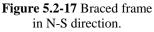


Figure 5.2-16 Braced frame in E-W direction.



Rectangular HSS members must satisfy:

$$\frac{b}{t} \le \frac{110}{\sqrt{F_y}} = \frac{110}{\sqrt{46}} = 16.2$$



Selected members are checked below:

W14×38: 
$$b/2t = 6.6 < 7.35$$
 OK

W14×34: b/2t = 7.4 > 7.35, but is acceptable for this example. Note that the W14×34 is at the penthouse roof, which is barely significant for this braced frame.

HSS12×12×5/8: 
$$\frac{kl}{r} = \frac{(1)\left(\frac{28.33\times12}{2}\right)}{4.62} = 36.8 < 141$$
 OK

$$\frac{b}{t} = \frac{9.4}{0.581} = 16.17 < 16.2$$
 OK

Also note that t for the HSS is actual, not nominal. The corner radius of HSS varies somewhat, which affects the dimension b. The value of b used here, 9.40 in., depends on a corner radius slightly larger than 2t, and it would have to be specified for this tube to meet the b/t limit.

3. Check Drift – Check drift in accordance with *Provisions* Sec. 5.2.8 [4.5]. The building was modeled in 3-D using RAMFRAME. Maximum displacements at the building corners are used here because the building is torsionally irregular. Displacements at the building centroid are also calculated because these will be the average between the maximum at one corner and the minimum at the diagonally opposite corner. Use of the displacements at the centroid as the average displacements is valid for a symmetrical building. Calculated story displacements are used to determine  $A_x$ , the torsional amplification factor. This is summarized in Table 5.2-6. P-delta effects are included.

	Average l Displacer Displacer Building (in.)	ment = nent at	Maximum Elastic Displacement at Building Corner* (in.)		t at $\frac{-max}{\delta}$		Torsional Amplification Factor = $A_{x} = \left(\frac{\delta_{max}}{1.2\delta_{avg}}\right)^{2}$		Amplified Eccentricity = $A_x(0.05 L)^{***}$ ( <i>ft</i> )	
	E-W	N-S	E-W	N-S	E-W	N-S	E-W	N-S	E-W	N-S
R	2.38	2.08	3.03	3.37	1.28	1.62	1.13	1.82	7.08	15.95
7	2.04	1.79	2.62	2.93	1.29	1.64	1.15	1.88	7.20	16.41
6	1.65	1.47	2.15	2.44	1.30	1.67	1.18	1.93	7.37	16.86
5	1.30	1.16	1.70	1.96	1.32	1.69	1.2	1.99	7.52	17.41
4	0.95	0.86	1.27	1.48	1.33	1.72	1.23	2.06	7.71	17.99
3	0.66	0.59	0.89	1.03	1.34	1.75	1.25	2.14	7.80	18.70
2	0.39	0.34	0.53	0.60	1.35	1.79	1.26	2.23	7.89	19.57

 Table 5.2-6 Alternative B Amplification of Accidental Torsion

\* These values are taken directly from the analysis. Accidental torsion is not amplified here.

\*\* Amplification of accidental torsion is required because this term is greater than 1.2 (*Provisions* Table 5.2.3.2 Item 1a [4.3-2, Item 1a]). The building is *torsionally irregular* in plan. *Provisions* Table 5.2.5.1 [4.4-1] indicates that an ELF analysis is "not permitted" for torsionally irregular structures. However, given rigid diaphragms and symmetry about both axes, a modal analysis will not give any difference in results than an ELF analysis insofar as accidental torsion is concerned unless one arbitrarily offsets the center of mass. The *Provisions* does not require an arbitrary offset for center of mass in dynamic analysis nor is it common practice to do so. One reason for this is that the computed period of vibration would lengthen, which, in turn, would reduce the overall seismic demand. See Sec. 9.2 and 9.3 of this volume of design examples for a more detailed examination of this issue. \*\*\* The initial eccentricities of 0.05 in the E-W and N-S directions are multiplied by  $A_x$  to determine the amplified eccentricities. These will be used in the next round of analysis. 1.0 in. = 25.4 mm, 1.0 ft = 0.3048 m.

4. Check Torsional Amplification – A second RAMFRAME 3-D analysis was made, using the amplified eccentricity for accidental torsion instead of merely 0.05L for accidental torsion. The results are summarized in Table 5.2-7.

	Max. Elastic Displacement at Building Corners (in.)		Elastic Story Drift at Location of Max. Displacement (at corners) (in.)		$C_d$	$(C_d) \times (\text{El}$ Story Driv		Allowable Story Drift (in.)
	E-W	N-S	⊿E-W	⊿N-S		⊿E-W	⊿N-S	Δ
R	3.14	4.50	0.42	0.55	5	2.10	2.75	3.20
7	2.72	3.95	0.49	0.64	5	2.46	3.19	3.20
6	2.23	3.32	0.45	0.63	5	2.27	3.16	3.20
5	1.77	2.68	0.45	0.64	5	2.25	3.18	3.20
4	1.32	2.05	0.40	0.61	5	1.98	3.07	3.20
3	0.93	1.43	0.38	0.59	5	1.89	2.93	3.20
2	0.55	0.85	0.55	0.85	5	2.75	4.24	5.36

**Table 5.2-7** Alternative B Story Drifts under Seismic Load

1.0 in. = 25.4 mm

All story drifts are within the allowable story drift limit of  $0.020h_{sx}$  in accordance with *Provisions* Sec. 5.2.8 [4.5-1] and the allowable deflections for this building from Sec. 5.2.3.6 above. This a good point to reflect on the impact of accidental torsion and its amplification on the design of this corebraced structure. The sizes of members were increased substantially to bring the drift within the limits (note how close the N-S direction drifts are). For the final structure, the elastic displacements at the main roof are:

At the centroid	= 2.08 in.
At the corner with accidental torsion	= 3.37 in.
At the corner with amplified accidental torsion	= 4.50 in.

The two effects of torsional irregularity (in this case, it would more properly be called torsional flexibility) of amplifying the accidental torsion and checking the drift limits at the corners combine to create a demand for substantially more stiffness in the structure. Even though many braced frames are controlled by strength, this is an example of how the *Provisions* places significant stiffness demands on some braced structures.

5. Check Redundancy – Now return to the calculation of  $r_x$  for the braced frame. Per *Provisions* Sec. 5.2.4.2 [not applicable in the 2003 *Provisions*],  $r_{max_x}$  for braced frames is taken as the lateral force component in the most heavily loaded brace element divided by the story shear (Figure 5.2-18).

A value for  $r_x$  was determined for every brace element at every level in both directions. The lateral component carried by each brace element comes from the RAMFRAME analysis, which includes the effect of amplified accidental torsion. Selected results are illustrated in the figures. The maximum  $r_x$  was found to be 0.223 below Level 7 in the NS-direction. The reliability factor ( $\rho$ ) is now determined using *Provisions* Eq. 5.2.4.2 [not applicable in the 2003 *Provisions*]:

$$\rho = 2 - \frac{20}{r_{max_x}\sqrt{A_x}} = 2 - \frac{20}{0.223\sqrt{21,875 \text{ ft}^2}} = 1.39$$

In the N-S direction, all design force effects (axial forces, shears, moments) obtained from analysis must be increased by the  $\rho$  factor of 1.39. Similarly, for the E-W-direction,  $r_{max_x}$  and  $\rho$  are found to be 0.192 and 1.26, respectively. (However drift controls the design for this problem. Drift and deflection are not subject to the  $\rho$  factor.)

[See Sec. 5.2.3.2 for a discussion of the significant changes to the redundancy requirements in the 2003 *Provisions*.]

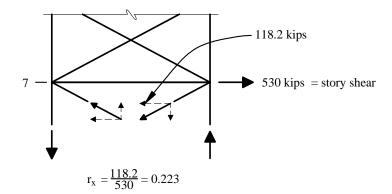


**Figure 5.2-18** Lateral force component in braces for N-S direction – partial elevation, Level 7 (1.0 kip = 4.45 kN).

6. Braced Frame Member Design Considerations – The design of members in the special concentrically braced frame (SCBF) needs to satisfy AISC Seismic Sec. 13 and columns also need to satisfy AISC Seismic Sec. 8. When  $P_u/\phi P_n$  is greater than 0.4, as is the predominant case here, the required axial strength needs to be determined from AISC Seismic Eq. 4-1 and 4-2 [*Provisions* Eq. 4.2-3 and 4.2-4]. These equations are for load combinations that include the  $\Omega_0$ , or overstrength, factors. Moments are generally small for the braced frame so load combinations with  $\Omega_0$  can control column size for strength considerations but, for this building, drift controls because of amplified accidental torsion. Note that  $\rho$  is not used where  $\Omega_0$  is used (see *Provisions* Sec. 5.2.7 [4.2.2.2]).

Bracing members have special requirements as well, although  $\Omega_0$  factors do not apply to braces in a SCBF. Note in particular AISC Seismic Sec. 13.2c, which requires that both the compression brace and the tension brace share the force at each level (as opposed to the "tension only" braces of Example 5.1). AISC Seismic Sec. 13.2 also stipulates a kl/r limitation and local buckling (width-thickness) ratio limits.

Beams in many configurations of braced frames have small moments and forces, which is the case here. V and inverted V (chevron) configurations are an exception to this. There is a panel of chevron bracing at the top story of one of the braced frames (Figure 5.2-16). The requirements of AISC Seismic Sec. 13.4 should be checked although, in this case, certain limitations of AISC Seismic do not apply because the beam is at the top story of a building. (The level above in Figure 5.2-16 is a minor penthouse that is not considered to be a story.) If the chevron bay were not at the top story, the size of the braces must be known in order to design the beam. The load combination for the beam is modified using a  $Q_b$  factor defined in AISC Seismic Sec. 13.4a. Basically, the beam must be able to carry a concentrated load equal to the difference in vertical force between the post-buckling strength of the compression brace and the yield strength of the tension brace (i.e., the compression brace has buckled, but the tension brace has not yet yielded). The prescribed load effect is to use  $0.3\phi_c P_n$  for the compression brace and  $P_y$  for the tension brace in order to determine a design vertical force to be applied to the beam.

 Connection Design – Figure 5.2-19 illustrates a typical connection design at a column per AISC Seismic Sec. 13. First, check the slenderness and width-to-thickness ratios (see above). The bracing members satisfy these checks.

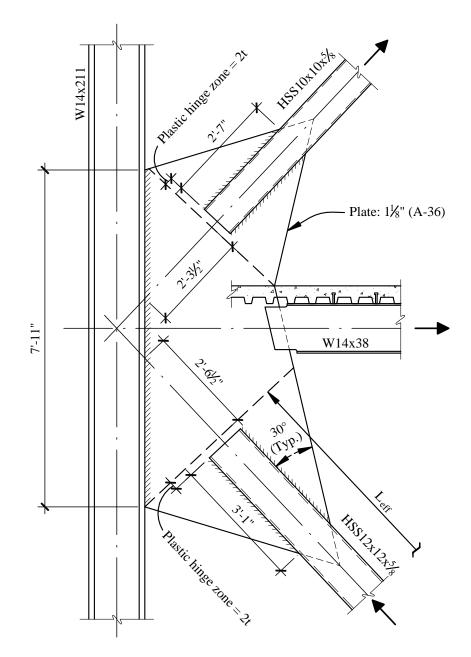


**Figure 5.2-19** Bracing connection detail (1.0 in. = 25.4 mm, 1.0 ft = 0.3048 m).

Next, design the connections. The required strength of the connection is to be the nominal axial tensile strength of the bracing member. For an  $HSS12 \times 12 \times 5/8$ , the nominal axial tensile strength is computed using AISC Seismic Sec. 13.3a:

$$P_n = R_y F_y A_g = (1.3)(46 \text{ ksi})(27.4 \text{ in.}^2) = 1,639 \text{ kips}$$

The area of the gusset is determined using the plate thickness and the Whitmore section for effective width. See Figure 5.2-20 for the determination of this dimension.

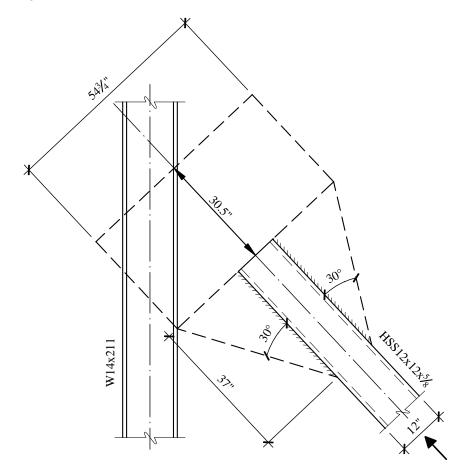


Figure 5.2-20 Whitmore section (1.0 in. = 25.4 mm, 1.0 ft = 0.3048 m).

For tension yielding of the gusset plate:

$$\phi T_n = \phi F_y A_g = (0.90)(36 \text{ ksi})(1.125 \text{ in.} \times 54.7 \text{ in.}) = 1,993 \text{ kips} > 1,639 \text{ kips}$$
 OK

For fracture in the net section:

$$\phi T_n = \phi F_u A_n = (0.75)(58 \text{ ksi})(1.125 \text{ in.} \times 54.7 \text{ in.}) = 2,677 \text{ kips} > 1,639 \text{ kips}$$
 OK

Since 1,933 kips is less than 2,677 kips, yielding (ductile behavior) governs over fracture.

For a tube slotted to fit over a connection plate, there will be four welds. The demand in each weld will be 1,639 kips/4 = 410 kips. The design strength for a fillet weld per AISC LRFD Table J2.5 is:

$$\phi F_w = \phi(0.6F_{exx}) = (0.75)(0.6)(70 \text{ ksi}) = 31.5 \text{ ksi}$$

For a 1/2 in. fillet weld, the required length of weld is determined to be:

$$L_w = \frac{410 \text{ kips}}{(0.707)(0.5 \text{ in.})(31.5 \text{ ksi})} = 37 \text{ in}$$

In accordance with the exception of AISC Seismic Sec. 13.3c, the design of brace connections need not consider flexure if the connections meet the following criteria:

- a. Inelastic rotation associated with brace post-buckling deformations: The gusset plate is detailed such that it can form a plastic hinge over a distance of 2t (where t = thickness of the gusset plate) from the end of the brace. The gusset plate must be permitted to flex about this hinge, unrestrained by any other structural member. See also AISC Seismic C13.3c. With such a plastic hinge, the compression brace may buckle out-of-plane when the tension braces are loaded. Remember that during the earthquake, there will be alternating cycles of compression to tension in a single bracing member and its connections. Proper detailing is imperative so that tears or fractures in the steel do not initiate during the cyclic loading.
- b. The connection design strength must be at least equal to the nominal compressive strength of the brace.

Therefore, the connection will be designed in accordance with these criteria. First, determine the nominal compressive strength of the brace member. The effective brace length  $(L_{eff})$  is the distance between the plastic hinges on the gusset plates at each end of the brace member. For the brace being considered,  $L_{eff} = 169$  in. and the nominal compressive strength is determined using AISC LRFD Eq. E2-4:

$$\lambda_c = \frac{kl}{r\pi} \sqrt{\frac{F_y}{E}} = \frac{(1)(169)}{(4.60)\pi} \sqrt{\frac{46}{29,000}} = 0.466$$

Since  $\lambda_c < 1.5$ , use AISC LRFD Eq. E2-2:

$$F_{cr} = (0.658^{\lambda_c^2})F_y = (0.658^{0.217})(46) = 42.0$$
 ksi

$$P_{cr} = A_g F_{cr} = (27.4)(42.0) = 1,151$$
 kips

Now, using a design compressive load from the brace of 1,151 kips, determine the buckling capacity of the gusset plate using the Whitmore section method. By this method, illustrated by Figure 5.2-20, the compressive force per unit length of gusset plate is (1,151 kips/54.7 in.) = 21.04 kips/in.

Try a plate thickness of 1.125 in.

 $f_a = P/A = 21.04 \text{ kips}/(1 \text{ in.} \times 1.25 \text{ in.}) = 18.7 \text{ ksi}$ 

The gusset plate is modeled as a 1 in. wide by 1.125 in. deep rectangular section, pinned at one end (the plastic hinge) and fixed at the other end where welded to column (see Whitmore section diagram). The effective length factor (k) for this "column" is 0.8.

Per AISC LRFD Eq. E2-4:

$$\lambda_c = \frac{kl}{r\pi} \sqrt{\frac{F_y}{E}} = \frac{(0.8)(30.5)}{(0.54)\pi} \sqrt{\frac{36}{29,000}} = 0.51$$

Since  $\lambda_c < 1.5$ , use AISC LRFD Eq. E2-2:

$$F_{cr} = (0.658^{\lambda_c^2})F_y = (0.658^{0.257})(36) = 32.3$$
 ksi

$$\phi F_{cr} = (0.85)(32.3) = 27.4$$
 ksi

$$\phi F_{cr} = 27.4 \text{ ksi} > 18.7 \text{ ksi}$$

Now consider the brace-to-brace connection shown in Figure 5.2-21. The gusset plate will experience the same tension force as the plate above, and the Whitmore section is the same. However, the compression length is much less, so a thinner plate may be adequate.

Try a 15/16 in. plate. Again, the effective width is shown in Figure 5.2-20. For tension yielding of the gusset plate:

$$\phi T_n = \phi F_y A_g = (0.90)(36 \text{ ksi})(0.9375 \text{ in.} \times 54.7 \text{ in.}) = 1,662 \text{ kips} > 1,639 \text{ kips}$$
 OK

For fracture in the net section:

$$\phi T_n = \phi F_y A_g = (0.75)(58 \text{ ksi})(0.9375 \text{ in.} \times 54.7 \text{ in.}) = 2,231 \text{ kips} > 1,639 \text{ kips}$$
 OK

Since 1,662 kips is less than 2,231 kips, yielding (ductile behavior) governs over fracture.

For compression loads, the plate must be detailed to develop a plastic hinge over a distance of 2t from the end of the brace. The effective length for buckling of this plate will be k[12" + (2)(2t + weld length)]. For this case, the effective length is  $0.65[12 + (2)(2 \times 15/16 + 5/16)] = 9.2$  in. Compression in the plate over this effective length is acceptable by inspection and will not be computed here.

Next, check the reduced section of the-tube, which has a 1 1/4 in. wide slot for the gusset plate (at the column). The reduction in HSS12×12×5/8 section due to the slot is  $(0.581 \times 1.25 \times 2) = 1.45 \text{ in.}^2$ , and the net section,  $A_{net} = (25.7 - 1.45) = 24.25 \text{ in.}^2$ 

Compare yield in the gross section with fracture in the net section:

Yield = 
$$F_y A_g = (46 \text{ ksi})(25.7 \text{ in.}^2) = 1,182 \text{ kips}$$
 OK

Fracture =  $F_{\mu}A_{\mu}$  =(58 ksi)(24.25 in.<sup>2</sup>) = 1,406 kips

AISC Seismic 13.3b could be used to require design fracture strength ( $0.75 \times 1,406 = 1,055$  kips) to exceed probable tensile yield (1,639 kips), but this is clearly impossible, even if the net area equaled the gross area. This design is considered satisfactory.

OK

OK

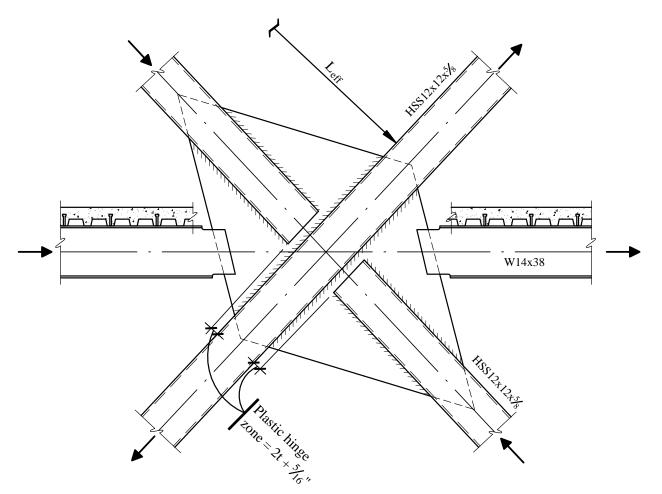


Figure 5.2-21 Brace-to-brace connection (1.0 in. = 25.4 mm).

#### 5.2.4.3.3 Size Members for Alternative C, Dual System

- 1. Select Preliminary Member Sizes A dual system is a combination of a moment-resisting frame with either a shear wall or a braced frame. In accordance with the building systems listed in *Provisions* Table 5.2.2 [4.3-1], a dual system consisting of special moment frames at the perimeter and special concentrically braced frames at the core will be used.
- 2. Check Strength of Moment Frame The moment frame is required to have sufficient strength to resist 25 percent of the design forces by itself (*Provisions* Sec. 5.2.2.1 [4.3.1]). This is a good place to start a design. Preliminary sizes for the perimeter moment frames are shown in Figures 5.2-22 and 5.2-23. It is designed for strength using 25 percent of the design lateral forces. All the design requirements for special moment frames still apply (flange and web width-to-thickness ratios, column-beam moment ratio, panel zone shear, drift, and redundancy) and all must be checked; however, it may be prudent to defer some of the checks until the design has progressed a bit further. The methodology for the analysis and these checks is covered in Sec. 5.2.4.3.1, so they will not be repeated here.

For some buildings this may present an opportunity to design the columns without doubler plates because the strength requirement is only 25 percent of the total. However, for the members used in this example, doubler plates will still be necessary. The increase in column size to avoid doubler plates is substantial, but feasible. The sequence of column sizes that is shown is W  $14 \times 132 - 82 - 68$  -

53 and would become W14×257 - 233 - 211 - 176 to avoid doubler plates. The beams in Figures 5.2-22 and 5.2-23 are controlled by strength because drift is not a criterion.

Note that  $P_u/\phi P_n > 0.4$  for a few of the columns when analyzed without the braced frame so the overstrength requirements of AISC Seismic Sec. 8.2 [8.3] apply to these columns. Because the check using  $\Omega_0 E$  is for axial capacity only and the moment frame columns are dominated by bending moment, the sizes are not controlled by the check using  $\Omega_0 E$ .

3. Check the Strength of the Braced Frames – The next step is to select the member sizes for the braced frame. Because of the presence of the moment frame, the accidental torsion on the building will be reduced as compared to a building with only a braced core. In combination with the larger *R* factor (smaller design forces), this should help to realize significant savings in the braced frame member sizes. A trial design is selected, followed by analysis of the entire dual system. All members need to be checked for width-thickness ratios and the braces need to be checked for slenderness. Note that columns in the braced frame will need to satisfy the overstrength requirements of AISC Seismic Sec. 8.2 [8.3] because  $P_u/\phi P_n > 0.4$ . This last requirement causes a significant increase in column sizes, except in the upper few stories.

¢							
	W16x31	W16x31	W16x31	W16x31	W16x31	W16x31	W16x31
W14x53	M19x31 14x53	M19x31 14x53	M19x31 14x53	M19x31 14x53	M19x31 14x53	M19x31 14x53	W16x31 <sup>5</sup> W16x31 <sup>5</sup>
-	W	w	w	w	w	w	M
-	W16x31	W16x31	W16x31	W16x31	W16x31	W16x31	W16x31
W14x68	W18x35 <sup>89</sup> W18x35 <sup>89</sup>	W18x35 ¥I	W18x35 4	W18x35 ¥1	W18x35 4	W18x35 41	W18x35 <u>4</u>
,	W	w	w	w	w	W	M
_	W18x40	W18x40	W18x40	W18x40	W18x40	W18x40	W18x40
W14x82	W21x44 <sup>4</sup> C <sup>*</sup>	W21x44 <sup>4</sup> Lx44	W21x44 <sup>4</sup> C <sup>x</sup> 41	W21x44 <sup>4</sup> L <sup>x</sup> 41	W21x44 <sup>4</sup> C <sup>x</sup> 41	W21x44 <sup>4</sup> Cx41	W21x44 <sup>7</sup>
	w	W	W	W	W	W	Ň
_	W21x50	W21x50	W21x50	W21x50	W21x50	- W21x50 -	W21x50
W14x132	W14x132	W14x132	W14x132	W14x132	W14x132	W14x132	W14x132

Figure 5.2-22 Moment frame of dual system in E-W direction.

Œ		(5	)	Ć	<b>+</b> )		$\mathbf{b}$		2)		)
	W16x31		W16x31		W16x31	   	W16x31		W16x31		
W14x53	W16x31	W14x53	W16x31	W14x53	W16x31	W14x53	W16x31	W14x53	W16x31	W14x53	
_	- W18x40	-	W18x40	-	W18x40	-	- W18x40	-	- W18x40		
W14x68	W21x44	W14x68	W21x44	W14x68	W21x44	W14x68	W21x44	W14x68	W21x44	W14x68	
_	- W21x50	_	W21x50	1	- W21x50	_	- W21x50	1	- W21x50	-	
W14x82	W21x50	W14x82	W21x50	W14x82	W21x50	W14x82	W21x50	W14x82	W21x50	W14x82	
_	- W24x55	-	W24x55	1	- W24x55	-	- W24x55	-	- W24x55		
W14x132		W14x132		W14x132		W14x132		W14x132		W14x132	

Figure 5.2-23 Moment frame of dual system in N-S direction.

- 4. Check Drift Check drift in accordance with *Provisions* Sec. 5.2.8 [4.5]. The building was modeled in three dimensions using RAMFRAME. Maximum displacements at the building corners are used here because the building is torsionally irregular. Displacements at the building centroid are also calculated because these will be the average between the maximum at one corner and the minimum at the diagonally opposite corner. Use of the displacements at the centroid as the average displacements is valid for a symmetrical building.
- 5. Check Torsional Amplification Calculated story drifts are used to determine  $A_x$ , the torsional amplification factor (Table 5.2-8). P-delta effects are included.

	Displac Displace Buil	e Elastic ement = ement at ding id (in.)	Maximum Elastic Displacement at Building Corner* (in.)		stic $\frac{\delta}{\delta avg}$ ding		Torsional Amplification Factor = $A_x = \left(\frac{\delta_{\text{max}}}{1.2\delta_{\text{avg}}}\right)^2$		Amplified Eccentricity = $A_x(0.05 L)^{***}$ (ft.)	
	E-W	N-S	E-W	N-S	E-W	N-S	E-W	N-S	E-W	N-S
R	2.77	2.69	3.57	3.37	1.29	1.25	1.15	1.09	7.19	9.54
7	2.45	2.34	3.15	3.00	1.28	1.28	1.14	1.14	7.14	10.01
6	2.05	1.91	2.63	2.50	1.28	1.31	1.13	1.20	7.07	10.46
5	1.64	1.51	2.10	2.01	1.28	1.33	1.13	1.23	7.08	10.8
4	1.22	1.11	1.56	1.50	1.28	1.35	1.14	1.27	7.13	11.15
3	0.81	0.75	1.05	1.03	1.29	1.38	1.16	1.31	7.25	11.50
2	0.43	0.41	0.57	0.57	1.32	1.40	1.20	1.37	7.52	11.98

Table 5.2-8 Alternative C Amplification of Accidental Torsion

\* These values are directly from the analysis. Accidental torsion is not amplified here.

\*\* Amplification of accidental torsion is required because this term is greater than 1.2 (*Provisions* Table 5.2.3.2, Item 1a [4.3-2, Item 1a). The building is *torsionally irregular* in plan. See discussion in footnote \*\* of Table 5.2.6.

\*\*\* The initial eccentricities of 0.05L in the E-W and N-S directions are multiplied by  $A_x$  to determine the amplified eccentricities. These will be used in the next round of analysis.

1.0 in. = 25.4 mm, 1.0 ft = 0.3048 m.

The design that yielded the displacements shown in Table 5.2-8 does not quite satisfy the drift limits, even without amplifying the accidental torsion. That design was revised by increasing various brace and column sizes and then re-analyzing using the amplified eccentricity instead of merely 0.05L for accidental torsion. After a few iterations, a design that satisfied the drift limits was achieved. These member sizes are shown in Figures 5.2-24 and 5.2-25. That structure was then checked for its response using the standard 0.05L accidental eccentricity in order to validate the amplifiers used in design. The amplifier increased for the E-W direction but decreased for the N-S direction, which was the controlling direction for torsion. The results are summarized in Table 5.2-9.

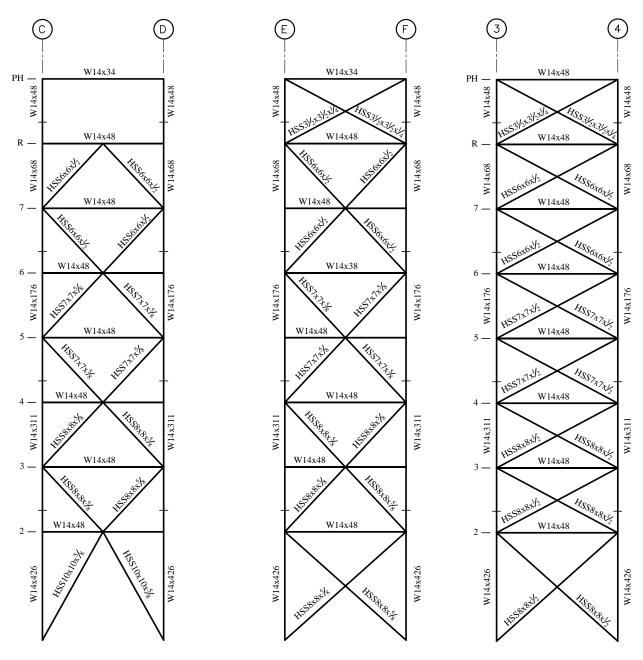
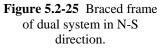


Figure 5.2-24 Braced frame of dual system in E-W-direction.



	Max. Elastic Displacement at Building Corners (in.)		Elastic Story Drift at Location of Max. Displacement (at corners) (in.)		$C_d$	Dr	$(C_d)$ x (Elastic Story Drift) (in.)	
	E-W	N-S	⊿E-W	⊿N-S		⊿E-W	⊿N-S	Δ
R	3.06	3.42	0.37	0.37	6.5	2.43	2.42	3.20
7	2.69	3.05	0.45	0.47	6.5	2.94	3.05	3.20
6	2.24	2.58	0.45	0.49	6.5	2.89	3.17	3.20
5	1.79	2.09	0.45	0.51	6.5	2.93	3.30	3.20
4	1.34	1.58	0.41	0.48	6.5	2.66	3.09	3.20
3	0.93	1.11	0.39	0.46	6.5	2.55	3.01	3.20
2	0.54	0.64	0.54	0.64	6.5	3.52	4.17	5.36

**Table 5.2-9** Alternative C Story Drifts under Seismic Load

1.0 in. = 25.4 mm

The story drifts are within the allowable story drift limit of  $0.020h_{sx}$  as per *Provisions* Sec. 5.2.8 [4.5.1]. Level 5 has a drift of 3.30 in. > 3.20 in. but the difference of only 0.1 in. is considered close enough for this example.

6. Check Redundancy – Now return to the calculation of  $r_x$  for the braced frame. In accordance with *Provisions* Sec. 5.2.4.2 [not applicable in the 2003 *Provisions*],  $r_{\max_x}$  for braced frames is taken as the lateral force component in the most heavily loaded brace element divided by the story shear. This is illustrated in Figure 5.2-18 for Alternative B.

For this design,  $r_x$  was determined for every brace element at every level in both directions. The lateral component carried by each brace element comes from the RAMFRAME analysis, which includes the effect of amplified accidental torsion. The maximum value was found to be 0.1762 at the base level in the N-S direction. Thus,  $\rho$  is now determined to be (see Sec. 5.2.4.2):

$$\rho = 0.8 \left[ 2 - \frac{20}{r_{\max_x} \sqrt{A_x}} \right] = 0.8 \left[ 2 - \frac{20}{0.1762 \sqrt{21,875 \text{ ft.}^2}} \right] = 0.986$$

The 0.8 factor comes from *Provisions* Sec. 5.2.4.2 [not applicable in the 2003 *Provisions*]. As  $\rho$  is less than 1.0,  $\rho = 1.0$  for this example.

In the E-W direction,  $r_{max}$  is less; therefore,  $\rho$  will be less, so use  $\rho = 1.0$  for both directions.

[See Sec. 5.2.3.2 for a discussion of the significant changes to the redundancy requirements in the 2003 *Provisions*.]

7. Connection Design – Connections for both the moment frame and braced frames may be designed in accordance with the methods illustrated in Sec. 5.2.4.3.1 and 5.2.4.3.2.

# 5.2.5 Cost Comparison

Material takeoffs were made for the three alternatives. In each case, the total structural steel was estimated. The takeoffs are based on all members, but do not include an allowance for plates and bolts at connections. The result of the material takeoffs are:

Alternative A, Special Steel Moment Resisting Frame	593 tons
Alternative B, Special Steel Concentrically Braced Frame	640 tons
Alternative C, Dual System	668 tons

The higher weight of the systems with bracing is primarily due to the placement of the bracing in the core, where resistance to torsion is poor. Torsional amplification and drift limitations both increased the weight of steel in the bracing. The weight of the moment-resisting frame is controlled by drift and the strong column rule.

# 5.3 TWO-STORY BUILDING, OAKLAND, CALIFORNIA

This example features an eccentrically braced frame (EBF) building. The following items of seismic design of steel-framed buildings are illustrated:

- 1. Analysis of eccentrically braced frames
- 2. Design of bracing members
- 3. Brace connections

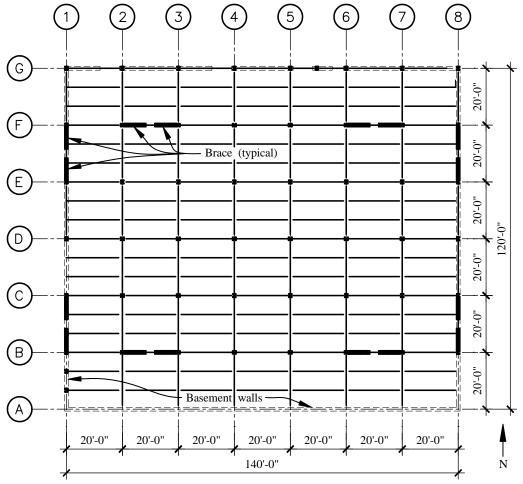
### **5.3.1 Building Description**

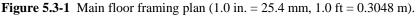
This two-story hospital, 120 ft by 140 ft in plan, is shown in Figure 5.3-1. The building has a basement and two floors. It has an unusually high roof load because of a plaza with heavy planters on the roof.

The vertical-load-carrying system consists of concrete fill on steel deck floors supported by steel beams and girders that span to steel columns and to the perimeter basement walls. The bay spacing is 20 ft each way. Floor beams are spaced three to a bay. The beams and girders on the column lines are tied to the slabs with stud connectors.

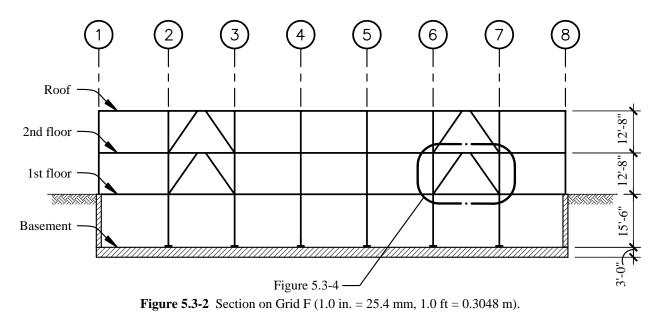
The building is founded on a thick mat. The foundation soils are deep stable deposits of sands, gravels, and stiff clays overlying rock.

The lateral-force-resisting system for Stories 1 and 2 consists of EBFs on Gridlines 1, 8, B, and F as





shown in Figure 5.3-1. A typical bracing elevation is shown in Figure 5.3-2. These EBFs transfer lateral loads to the main floor diaphragm. The braced frames are designed for 100 percent of lateral load and their share of vertical loads. EBFs have been selected for this building because they provide high stiffness and a high degree of ductility while permitting limited story-to-story height.



The structure illustrates a common situation for low-rise buildings with basements. The combination of the basement walls and the first floor diaphragm is so much stiffer that the superstructure that the *base* (see *Provisions* Chapter 2 [4.1.3] for definition) of the building is the first floor, not the foundation. Therefore, the diagonal braces do not extend into the basement because the horizontal force is in the basement walls (both in shear parallel to the motion considered and in direct pressure on perpendicular walls). This has a similarity to the irregularity Type 4 "out-of-plane offsets" defined in *Provisions* Table 5.2.3.2 [4.3-2], but because it is below the base that classification does not apply. However, the columns in the basement that are part of the EBFs must be designed and detailed as being the extension of the EBF that they are. This affects width-thickness ratios, overstrength checks, splice requirements, and so on. Column design for an EBF is illustrated later in this example.

# 5.3.2 Method

The method for determining basic parameters is similar to that for other examples. It will not be repeated here; rather the focus will be on the design of a specific example of an EBF starting with the forces in the frame as obtained from a linear analysis. Keep in mind that the load path is from the floor diaphragm to the beam to the braces. The fundamental concept behind the eccentric braced frame is that seismic energy is absorbed by yielding of the link. Yielding in shear is more efficient than yielding in flexure, although either is permitted. A summary of the method is as follows:

- 1. Select member preliminary sizes.
- 2. Perform an elastic analysis of the building frame. Compute elastic drift ( $\delta_e$ ) and forces in the members.
- 3. Compute the inelastic displacement as the product of  $C_d$  times  $\delta_e$ . The inelastic displacement must be within the allowable story drift from *Provisions* Table 5.2.8 [4.5-1].

- 4. Compute the link rotation angle ( $\alpha$ ) and verify that it is less than 0.08 radians for yielding dominated by shear in the link or 0.02 radians for yielding dominated by flexure in the link. (See Figure 5.3-4 for illustration of  $\alpha$ ). The criteria is based on the relationship between  $M_p$  and  $V_p$  as related to the length of the link.
- 5. To meet the link rotation angle requirement, it may be necessary to modify member sizes, but the more efficient approach is to increase the link length. (The trade-off to increasing the link length is that the moment in the link will increase. Should the moment become high enough to govern over shear yielding, then  $\alpha$  will have to be limited to 0.02 radians instead of 0.08 radians.)
- 6. The braces and building columns are to remain elastic. The portions of the beam outside the link are to remain elastic; only the link portion of the beam yields.
- 7. For this case, there are moment-resisting connections at the columns. Therefore from *Provisions* Table 5.2.2 [4.3-1], R = 8,  $C_d = 4$ , and  $\Omega_0 = 2$ . (Neither the *Provisions* nor AISC Seismic offer very much detailed information about requirements for moment-resisting connections for the beam to column connection in an EBF. There are explicit requirements for the connection from a link to a column. The EBF system will not impose large rotational demands on a beam to column connection; the inelastic deformations are confined to the link. Therefore, without further detail, it is the authors' interpretation that an ordinary moment resisting frame connection will be adequate).

# 5.3.3 Analysis

Because the determination of basic provisions and analysis are so similar to those of other examples, they will not be presented here. An ELF analysis was used.

# 5.3.3.1 Member Design Forces

The critical forces for the design of individual structural elements, determined from computer analysis, are summarized in Table 5.3-1.

Member	Force Designation	Magnitude
Link	<b>P</b> <sub>link</sub>	5.7 kips
	$V_{link}$	85.2 kips
	$M_{left}$	127.9 ft-kips
	$M_{right}$	121.3 ft-kips
Brace	P <sub>brace</sub>	120.0 kips
	$M_{top}$	15.5 ft-kips
	$M_{bot}$	9.5 ft-kips

 Table 5.3-1
 Summary of Critical Member Design Forces

1.0 kip = 4.45 kN, 1.0 ft-kip = 1.36 kN-m.

The axial load in the link at Level 2 may be computed directly from the second-floor forces. The force from the braces coming down from the roof level has a direct pass to the braces below without affecting the link. The axial forces in the link and brace may be determined as follows:

Total second-story shear (determined elsewhere) = 535.6 kips

Second-story shear per braced line = 535.6/2 = 267.8 kips Second-story shear per individual EBF = 267.8/2 = 133.9 kips Second-story shear per brace = 133.9/2 = 66.95 kips Axial force per brace = 66.95 (15.25 ft/8.5 ft) = 120.0 kips

Second-story shear per braced line = 267.8 kips Second-story shear per linear foot = 267.8 kips/140 ft = 1.91 klf Axial force in link = (1.91 klf)(3 ft) = 5.7 kips

# 5.3.3.2 Drift

From the linear computer analysis, the elastic drift was determined to be 0.247 inches. The total inelastic drift is computed as:

 $C_d \delta_c = (4)(0.247) = 0.99$  in.

The link rotation angle is computed for a span length, L = 20 ft, and a link length, e = 3 ft as follows:

$$\alpha = \left(\frac{L}{e}\right)\theta = \left(\frac{20 \text{ ft}}{3 \text{ ft}}\right)\left(\frac{0.99 \text{ in.}}{(12.67 \text{ ft})(12)}\right) = 0.043 \text{ radians}$$

The design is satisfactory if we assume that shear yielding governs because the maximum permissible rotation is 0.08 radians (AISC Seismic Sec. 15.2g [15.2]). For now, we will assume that shear yielding of the link governs and will verify this later.

#### 5.3.4 Design of Eccentric Bracing

Eccentric bracing adds two elements to the frame: braces and links. As can be seen in Figure 5.3-3, two eccentric braces located in one story of the same bay intersect the upper beam a short distance apart, thus creating a link subject to high shear. In a severe earthquake, energy is dissipated through shear yielding of the links while diagonal braces and columns remain essentially elastic.

The criteria for the design of eccentric bracing are given in AISC Seismic Sec. 15. All section sizes and connection details are made similar for all braced bays. The following sections have been selected as a preliminary design:

Typical girders	W16×57
Typical columns	W14×132
Typical braces	HSS 8×8×5/8

Since all members of the braced frames are to be essentially the same, further calculations deal with the braced frames on Line F, shown in Figures 5.3-3 and 5.3-4.

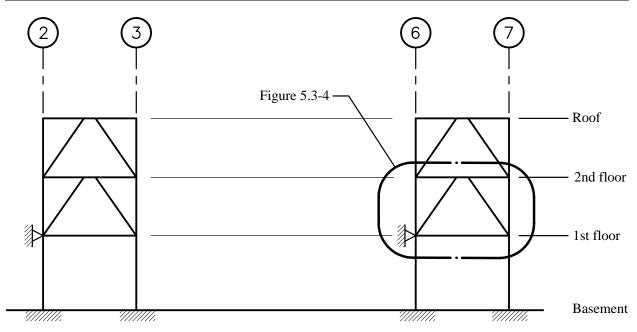
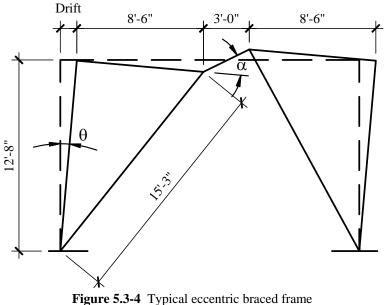


Figure 5.3-3 Diagram of eccentric braced frames on Grid F.



(1.0 in. = 25.4 mm, 1.0 ft = 0.3048 m).

#### 5.3.4.1 Link Design

The first-story eccentric braced frame (identified in Figure 5.3-2) is examined first. The shear force and end moments in the link (W16x57 beam section) are listed in Table 5.3-1 and repeated below:

 $P_{link} = 5.7 \text{ kips}$   $V_{link} = 85.2 \text{ kips}$   $M_{left} = 127.9 \text{ ft-kips}$  $M_{right} = 121.3 \text{ ft-kips}$ 

#### 5.3.4.1.1 Width-Thickness Ratio

The links are first verified to conform to AISC Seismic Sec. 15.2a [15.2], which refers to AISC Seismic Table I-9-1 [I-8-1].

First, check the beam flange width-thickness ratio. For the selected section, b/t = 4.98, which is less than the permitted b/t ratio of :

$$\frac{52}{\sqrt{F_y}} = \frac{52}{\sqrt{50}} = 7.35$$
 OK

The permitted web slenderness is dependent on the level of axial stress. The level of axial stress is determined as:

$$\frac{P_u}{\phi_b P_y} = \frac{5.8}{(0.9)(16.8 \times 50)} = 0.008$$

It is less than 0.125; therefore, the ratio  $t_w/h_c = 33.0$  for the selected section is less than the limiting width-to-thickness ratio computed as:

$$\frac{253}{\sqrt{F_y}} = \frac{253}{\sqrt{50}} = 35.7$$
 OK

#### 5.3.4.1.2 Link Shear Strength

The forces  $V_{link}$ ,  $M_{left}$ , and  $M_{right}$  must not exceed member strength computed from AISC Seismic Sec. 15.2d [15.2]. That section specifies that the required shear strength of the link ( $V_u$ ) must not exceed the design shear strength  $\phi V_n$  where  $V_u = V_{link} = 85.2$  kips and  $V_n$  is the nominal shear strength of link. The nominal shear strength of the link is defined as the lesser of:

$$V_p = (0.60F_y)(d-2t_f)t_w$$

and

$$\frac{2M_p}{e}$$

For the W16×57 section selected for the preliminary design:

$$V_p = (0.60)(50)[16.43 - (2)(0.715)](0.430) = 193.5$$
 kips

and

$$M_p = \phi M_n = 0.9F_y Z_x = (0.9)(50)(105) = 4725 \text{ in.-kips}$$
$$\frac{2M_p}{e} = \frac{(2)(4725)}{(3 \times 12)} = 262.5 \text{ kips}$$

Therefore,

 $V_n = 193.5$  kips  $\phi V_n = (0.9)(193.5) = 174.2$  ft-kips > 85.2 kips

#### 5.3.4.1.3 Link Axial Strength

In accordance with AISC Seismic Sec. 15.2e [15.2], the link axial strength is examined:

 $P_y$  of the link =  $F_y A_g = (50 \text{ ksi})(16.8 \text{ in}) = 840 \text{ kips}$ 

 $0.15P_{v}$  of the link = (0.15)(840) = 126 kips

Since the axial demand of 5.7 kips is less than 126 kips, the effect of axial force on the link design shear strength need not be considered. Further, because  $P_u < P_y$ , the additional requirements of AISC Seismic Sec. 15.f [15.2] do not need to be invoked.

#### 5.3.4.1.4 Link Rotation Angle

In accordance with AISC Seismic Sec. 15.2g [15.2], the link rotation angle is not permitted to exceed 0.08 radians for links  $1.6M_p/V_p$  long or less. Therefore, the maximum link length is determined as:

$$1.6M_p/V_p = (1.6)(4725)/(193.5) = 39.1$$
 in

Since the link length (e) of 36 in. is less than  $1.6M_p/V_p$ , the link rotation angle is permitted up to 0.08 radians. From Sec. 5.3.3.2, the link rotation angle,  $\alpha$ , was determined to be 0.043 radians, which is acceptable.

#### 5.3.4.1.5 Link Stiffeners

AISC Seismic Sec. 15.3a [15.3] requires full-depth web stiffeners on both sides of the link web at the diagonal brace ends of the link. These serve to transfer the link shear forces to the reacting elements (the braces) as well as restrain the link web against buckling.

Because the link length (*e*) is less than  $1.6M_p/V_p$ , intermediate stiffeners are necessary in accordance with AISC Seismic Sec. 15.3b [15.3]. Interpolation of the stiffener spacing based on the two equations presented in AISC Seismic Sec. 15.3b.1 [15.3] will be necessary. For a link rotation angle of 0.08 radians:

Spacing =  $(30t_w - d/5) = (30 \times 0.430 - 16.43/5) = 9.6$  in.

For link rotation angle of 0.02 radians:

Spacing =  $(52t_w - d/5) = (52 \times 0.430 - 16.43/5) = 19.1$  in.

For our case the link rotation angle is 0.043 radians, and interpolation results in a spacing requirement of 15.4 in. Therefore, use a stiffener spacing of 12 in. because it conforms to the 15.4 in. requirement and also fits nicely within the link length of 36 in.

In accordance with AISC Seismic Sec. 15.3a [5.3], full depth stiffeners must be provided on both sides of the link, and the stiffeners must be sized as follows:

OK

Combined width at least  $(b_f - 2t_w) = (7.120 - 2 \times 0.430) = 6.26$  in. Use 3.25 in. each. Thickness at least  $0.75t_w$  or 3/8 in. Use 3/8 in.

#### 5.3.4.1.6 Lateral Support of Link

The spacing of the lateral bracing of the link must not exceed the requirement of AISC LRFD Eq. F1-17, which specifies a maximum unbraced length of:

$$L_{pd} = \frac{[3,600 + 2,200(M_1/M_2)]r_y}{F_y} = \frac{[3,600 + 2,200(121.3/127.9)](1.60)}{50} = 182 \text{ in.}$$

Accordingly, lateral bracing of beams with one brace at each end of the link (which is required for the link design per AISC Seismic Sec. 15.5) is sufficient.

In accordance with AISC Seismic Sec. 15.5, the end lateral supports must have a design strength computed as:

$$0.06R_yF_yb_ft_f = (0.06)(1.1)(50)(7.120)(0.715) = 16.8$$
 kips

While shear studs on the top flange are expected to accommodate the transfer of this load into the concrete deck, the brace at the bottom flange will need to be designed for this condition. Figure 5.3-5 shows angle braces attached to the lower flange of the link. Such angles will need to be designed for 16.8 kips tension or compression.

#### 5.3.4.2 Brace Design

For the design equations used below, see Chapter E. of the AISC LRFD Specification. The braces, determined to be  $8\times8\times5/8$  in. tubes with  $F_y = 46$  ksi in the preliminary design, are subjected to a calculated axial seismic load of 120 kips (from elastic analysis in Table 5.3-1). Taking the length of the brace conservatively as the distance between panel points, the length is 15.26 feet. The slenderness ratio is

$$\frac{kl}{r} = \frac{(1)(15.26)(12)}{2.96} = 61.9$$

(k has been conservatively taken as 1.0, but is actually lower because of restraint at the ends.)

Using AISC LRFD E2-4 for  $F_y = 46$  ksi:

$$\lambda_{c} = \frac{kl}{r\pi} \sqrt{\frac{F_{y}}{E}} = \frac{(1)(15.26 \times 12)}{2.96\pi} \sqrt{\frac{50}{29,000}} = 0.817$$
$$F_{cr} = (0.658^{\lambda_{c}^{2}})F_{y} = (0.658^{0.817^{2}})(46) = 34.8 \text{ ksi}$$

 $P_{br} = \phi_c A_g F_{cr} = (0.85)(17.4)(34.8) = 514$  kips

AISC Seismic Sec. 15.6a [15.6] requires that the design axial and flexural strength of the braces be those resulting from the expected nominal shear strength of the link  $(V_n)$  increased by  $R_v$  and a factor of 1.25.

Thus, the factored  $V_n$  is equal to (193.5 kips)(1.1)(1.25) = 266 kips. The shear in the link, determined from elastic analysis, is 85.2 kips. Thus, the increase is 266/85.2 = 3.12. Let us now determine the design values for brace axial force and moments by increasing the values determined from the elastic analysis by the same factor:

Design  $P_{brace} = (3.12)(120) = 374$  kips Design  $M_{top} = (3.12)(15.5) = 48.4$  ft-kips Design  $M_{bot} = (3.12)(9.5) = 29.6$  ft-kips

The design strength of the brace, 514 kips, exceeds the design demand of 374 kips, so the brace is adequate for axial loading. However, the brace must also be checked for combined axial and flexure using AISC LRFD Chapter H. For axial demand-to-capacity ratio greater than 0.20, axial and flexure interaction is governed by AISC LRFD H1-1a:

$$\frac{P_u}{\phi P_n} + \frac{8}{9} \left( \frac{M_u}{\phi_b M_n} \right) \le 1.0$$

where

$$P_u = 374$$
 kips  
 $P_n = 514$  kips  
 $M_n = ZF_y = (105)(50) = 5250$  in.-kips

The flexural demand,  $M_u$ , is computed in accordance with AISC LRFD Chapter C and must account for second order effects. For a braced frame only two stories high and having several bays, the required flexural strength in the brace to resist lateral translation of the frame only  $(M_u)$  is negligible. Therefore, the required flexural strength is computed from AISC LRFD C1-1 as:

$$M_{\mu} = B_{\mu}M_{\mu t}$$

 $\boldsymbol{C}$ 

where  $M_{nt} = 48.4$  ft-kips as determined above and, per AISC LRFD C1-2:

$$B_{1} = \frac{C_{m}}{1 - P_{u}/P_{e}} \ge 1.0$$

$$P_{e} = \frac{A_{g}F_{y}}{\lambda_{c}^{2}} = \frac{(17.4)(46)}{(0.817)^{2}} = 1,199 \text{ kips}$$

$$Cm = 0.6 - 0.4 \left(\frac{M_{1}}{M_{2}}\right) = 0.6 - 0.4 \left(\frac{29.6}{48.4}\right) = 0.36$$

Therefore,

$$M_u = B_1 M_{nu} = \frac{C_m M_{nu}}{1 - \frac{P_u}{P_e}} = \frac{(0.36)(48.4)}{1 - \frac{374}{1,199}} = (0.52)(48.4) = 25.3 \text{ ft-kips}$$

and

$$\frac{P_u}{\phi P_n} + \frac{8}{9} \left( \frac{M_u}{\phi_b M_n} \right) = \frac{374}{(0.85)(514)} + \frac{8}{9} \left( \frac{(25.3)(12)}{(0.9)(4,830)} \right) = 0.92 < 1.00$$
 OK

The design of the brace is satisfactory.

#### **5.3.4.3 Brace Connections at Top of Brace**

AISC Seismic Sec. 15.6 requires that, like the brace itself, the connection of the brace to the girder be designed to remain elastic at yield of the link. The required strength of the brace-to-beam connection must be at least as much as the required strength of the brace. Because there is a moment at the top of the brace, the connections must also be designed as a fully restrained moment connection. The beam, link, and brace centerlines intersect at a common work point, and no part of this connection shall extend over the link length.

The tube may be attached to the girder with a gusset plate welded to the bottom flange of the girder and to the tube with fillet welds. The design of the gusset and connecting welds is conventional except that cutting the gusset short of the link may require adding a flange. (Such a flange is shown ine Figure 5.3-5.) Adding a similar flange on the other side of the brace will keep the joint compact. In such a case, it may be required, or at least desirable, to add another stiffener to the beam opposite the flange on the gusset. It also should be remembered that the axial force in the brace may be either tension or compression reflecting the reversal in seismic motions.

In addition to the design of the gusset and the connecting welds, a check should be made of stiffener requirements on the beam web opposite the gusset flanges (if any) and the panel zone in the beam web above the connection. All of these calculations are conventional and need no explanation here. Details of the link and adjacent upper brace connection are shown in Figure 5.3-5.

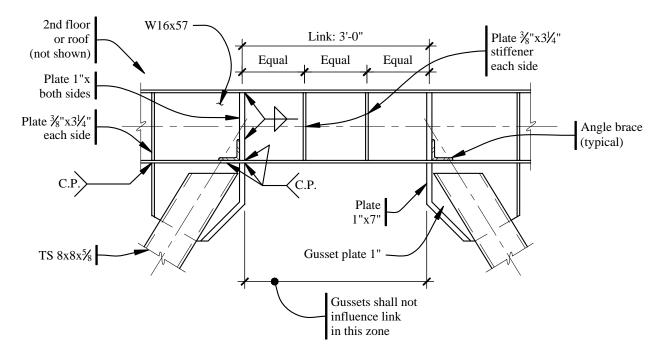
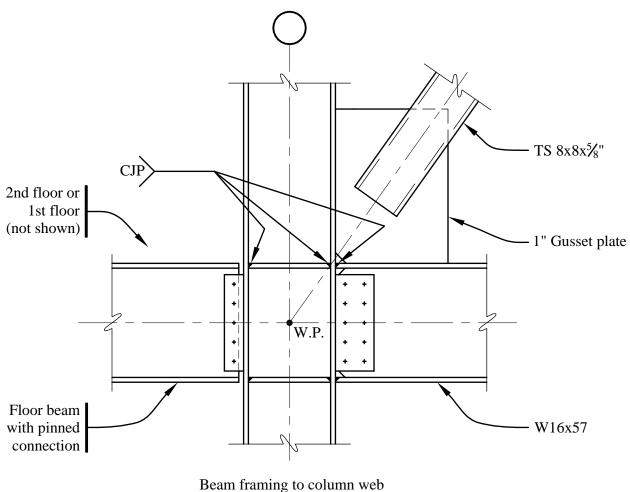


Figure 5.3-5 Link and upper brace connection (1.0 in. = 25.4 mm, 1.0 ft = 0.3048 m).

#### 5.3.4.4 Brace Connections at Bottom of Brace

These braces are concentric at their lower end, framing into the column-girder intersection in a conventional manner.

The design of the gusset plate and welds is conventional. Details of a lower brace connection are shown in Figure 5.3-6. In order to be able to use R = 8, moment connections are required at the ends of the link beams (at the roof and second floor levels). Moment connections could be used, but are not required, outside of the EBF (e.g., the left beam in Figure 5.3-6) or at the bottom of the brace at the first floor (e.g., the right beam in Figure 5.3-6 if it is at the first floor level). The beam on the left in Figure 5.3-6 could be a collector. If so, the connection must carry the axial load (force from floor deck to collector) that is being transferred through the beam to column connection to the link beam on the right side, as well as beam vertical loads.



(not shown)

Figure 5.3-6 Lower brace connections (1.0 in. = 25.4 mm).

#### 5.3.4.5 Beam and Column Design

Refer to AISC Seismic Sec. 15.6 for design of the beam outside the link and AISC Seismic Sec. 15.8 for design of the columns. The philosophy is very similar to that illustrated for the brace: the demand becomes the forces associated with expected yield of the link. Although the moment and shear are less in the beam than in the link, the axial load is substantially higher.

6

# **REINFORCED CONCRETE**

# Finley A. Charney, Ph.D., P.E.

In this chapter, a 12-story reinforced concrete office building with some retail shops on the first floor is designed for both high and moderate seismic loadings. For the more extreme loading, it is assumed that the structure will be located in Berkeley, California, and for the moderate loading, in Honolulu, Hawaii.

Figure 6-1 shows the basic structural configuration for each location in plan view and Figure 6-2, in section. The building, to be constructed primarily from sand-lightweight (LW) aggregate concrete, has 12 stories above grade and one basement level. The typical bays are 30 ft long in the north-south (N-S) direction and either 40 ft or 20 ft long in the east-west (E-W) direction. The main gravity framing system consists of seven continuous 30-ft spans of pan joists. These joists are spaced 36 in. on center and have an average web thickness of 6 in. and a depth below slab of 16 in. Due to fire code requirements, a 4-in.-thick floor slab is used, giving the joists a total depth of 20 in.

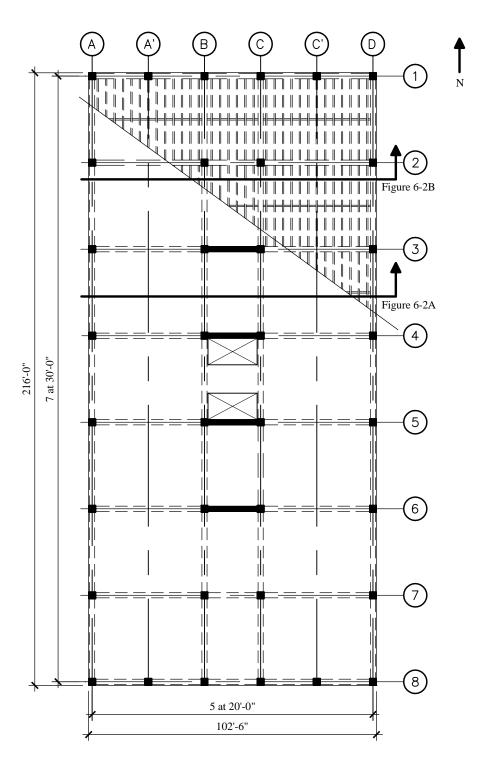
The joists along Gridlines 2 through 7 are supported by variable depth "haunched" girders spanning 40 ft in the exterior bays and 20 ft in the interior bays. The girders are haunched to accommodate mechanical-electrical systems. The girders are not haunched on exterior Gridlines 1 and 8, and the 40-ft spans have been divided into two equal parts forming a total of five spans of 20 ft. The girders along all spans of Gridlines A and D are of constant depth, but along Gridlines B and C, the depth of the end bay girders has been reduced to allow for the passage of mechanical systems.

Normal weight (NW) concrete walls are located around the entire perimeter of the basement level. NW concrete also is used for the first (ground) floor framing and, as described later, for the lower levels of the structural walls in the Berkeley building.

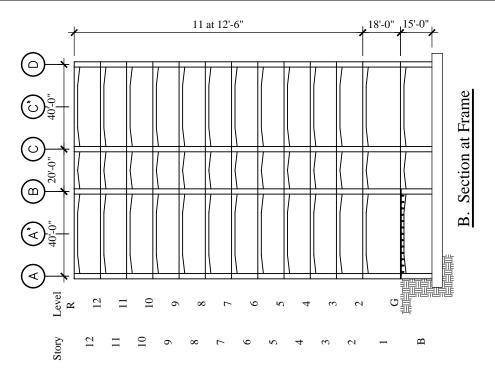
For both locations, the seismic-force-resisting system in the N-S direction consists of four 7-bay momentresisting frames. The interior frames differ from the exterior frames only in the end bays where the girders are of reduced depth. At the Berkeley location, these frames are detailed as special momentresisting frames. Due to the lower seismicity and lower demand for system ductility, the frames of the Honolulu building are detailed as intermediate moment-resisting frames.

In the E-W direction, the seismic-force-resisting system for the Berkeley building is a dual system composed of a combination of frames and frame-walls (walls integrated into a moment-resisting frame). Along Gridlines 1 and 8, the frames have five 20-ft bays with constant depth girders. Along Gridlines 2 and 7, the frames consist of two exterior 40-ft bays and one 20-ft interior bay. The girders in each span are of variable depth as described earlier. At Gridlines 3, 4, 5 and 6, the interior bay has been filled with a shear panel and the exterior bays consist of 40-ft-long haunched girders. For the Honolulu building, the structural walls are not necessary so E-W seismic resistance is supplied by the moment frames along Gridlines 1 through 8. The frames on Gridlines 1 and 8 are five-bay frames and those on Gridlines 2 through 7 are three-bay frames with the exterior bays having a 40-ft span and the interior bay having a 20-ft span. Hereafter, frames are referred to by their gridline designation (e.g., Frame 1 is located on

Gridline 1). It is assumed that the structure for both the Berkeley and Honolulu locations is founded on very dense soil (shear wave velocity of approximately 2000 ft/sec).



**Figure 6-1** Typical floor plan of the Berkeley building. The Honolulu building is similar but without structural walls (1.0 ft = 0.3048 m).



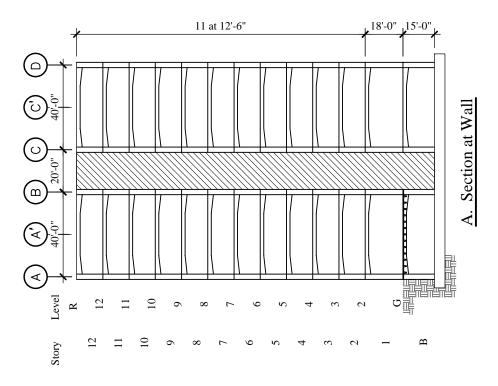


**Figure 6-2** Typical elevations of the Berkeley building; the Honolulu building is similar but without structural walls (1.0 ft = 0.3048 m).

The calculations herein are intended to provide a reference for the direct application of the design requirements presented in the 2000 *NEHRP Recommended Provisions* (hereafter, the *Provisions*) and to assist the reader in developing a better understanding of the principles behind the *Provisions*.

Because a single building configuration is designed for both high and moderate levels of seismicity, two different sets of calculations are required. Instead of providing one full set of calculations for the Berkeley building and then another for the Honolulu building, portions of the calculations are presented in parallel. For example, the development of seismic forces for the Berkeley and Honolulu buildings are presented before structural design is considered for either building. The full design then is given for the Berkeley building followed by the design of the Honolulu building. Each major section (development of forces, structural design, etc.) is followed by discussion. In this context, the following portions of the design process are presented in varying amounts of detail for each structure:

- 1. Development and computation of seismic forces;
- 2. Structural analysis and interpretation of structural behavior;
- 3. Design of structural members including typical girder in Frame 1, typical interior column in Frame 1, typical beam-column joint in Frame 1, typical girder in Frame 3, typical exterior column in Frame 3, typical beam-column joint in Frame 3, boundary elements of structural wall (Berkeley building only) and panel of structural wall (Berkeley building only).

The design presented represents the first cycle of an iterative design process based on the equivalent lateral force (ELF) procedure according to *Provisions* Chapter 5. For final design, the *Provisions* may require that a modal response spectrum analysis or time history analysis be used. The decision to use more advanced analysis can not be made a priori because several calculations are required that cannot be completed without a preliminary design. Hence, the preliminary design based on an ELF analysis is a natural place to start. The ELF analysis is useful even if the final design is based on a more sophisticated analysis (e.g., forces from an ELF analysis are used to apply accidental torsion and to scale the results from the more advanced analysis and are useful as a check on a modal response spectrum or time-history analysis).

In addition to the *Provisions*, ACI 318 is the other main reference in this example. Except for very minor exceptions, the seismic-force-resisting system design requirements of ACI 318 have been adopted in their entirety by the *Provisions*. Cases where requirements of the *Provisions* and ACI 318 differ are pointed out as they occur. ASCE 7 is cited when discussions involve live load reduction, wind load, and load combinations.

Other recent works related to earthquake resistant design of reinforced concrete buildings include:

ACI 318	American Concrete Institute. 1999 [2002]. Building Code Requirements and Commentary for Structural Concrete.
ASCE 7	American Society of Civil Engineers. 1998 [2002]. <i>Minimum Design Loads for Buildings and Other Structures</i> .
Fanella	Fanella, D.A., and M. Munshi. 1997. <i>Design of Low-Rise Concrete Buildings for Earthquake Forces</i> , 2nd Edition. Portland Cement Association, Skokie, Illinois.
ACI 318 Notes	Fanella, D.A., J. A. Munshi, and B. G. Rabbat, Editors. 1999. <i>Notes on ACI 318-99 Building Code Requirements for Structural Concrete with Design Applications</i> . Portland Cement Association, Skokie, Illinois.

ACI SP127	Ghosh, S. K., Editor. 1991. Earthquake-Resistant Concrete Structures Inelastic Response and Design, ACI SP127. American Concrete Institute, Detroit, Michigan.
Ghosh	Ghosh, S. K., A. W. Domel, and D. A. Fanella. 1995. <i>Design of Concrete Buildings for Earthquake and Wind Forces</i> , 2 <sup>nd</sup> Edition. Portland Cement Association, Skokie, Illinois.
Paulay	Paulay, T., and M. J. N. Priestley. 1992. Seismic Design of Reinforced Concrete and Masonry Buildings. John Wiley & Sons, New York.

- --

The Portland Cement Association's notes on ACI 318 contain an excellent discussion of the principles behind the ACI 318 design requirements and an example of the design and detailing of a frame-wall structure. The notes are based on the requirements of the 1997 *Uniform Building Code* (International Conference of Building Officials) instead of the *Provisions*. The other publications cited above provide additional background for the design of earthquake-resistant reinforced concrete structures.

Most of the large-scale structural analysis for this chapter was carried out using the ETABS Building Analysis Program developed by Computers and Structures, Inc., Berkeley, California. Smaller portions of the structure were modeled using the SAP2000 Finite Element Analysis Program, also developed by Computers and Structures. Column capacity and design curves were computed using Microsoft Excel, with some verification using the PCACOL program created and developed by the Portland Cement Association.

Although this volume of design examples is based on the 2000 *Provisions*, it has been annotated to reflect changes made to the 2003 *Provisions*. Annotations within brackets, [], indicate both organizational changes (as a result of a reformat of all of the chapters of the 2003 *Provisions*) and substantive technical changes to the 2003 *Provisions* and its primary reference documents. While the general concepts of the changes are described, the design examples and calculations have not been revised to reflect the changes to the 2003 *Provisions*.

The changes related to reinforced concrete in Chapter 9 of the 2003 *Provisions* are generally intended to maintaining compatibility between the *Provisions* and the ACI 318-02. Portions of the 2000 *Provisions* have been removed because they were incorporated into ACI 318-02. Other chances to Chapter 9 are related to precast concrete (as discussed in Chapter 7 of this volume of design examples).

Some general technical changes in the 2003 *Provisions* that relate to the calculations and/or design in this chapter include updated seismic hazard maps, revisions to the redundancy requirements, revisions to the minimum base shear equation, and revisions several of the system factors (R,  $\Omega_0$ ,  $C_d$ ) for dual systems.

Where they affect the design examples in this chapter, other significant changes to the 2003 *Provisions* and primary reference documents are noted. However, some minor changes to the 2003 *Provisions* and the reference documents may not be noted.

Note that these examples illustrate comparisons between seismic and wind loading for illustrative purposes. Wind load calculations are based on ASCE 7-98 as referenced in the 2000 *Provisions*, and there have not been any comparisons or annotations related to ASCE 7-02.

# 6.1 DEVELOPMENT OF SEISMIC LOADS AND DESIGN REQUIREMENTS

# 6.1.1 Seismicity

Using *Provisions* Maps 7 and 8 [Figures 3.3-3 and 3.3-4] for Berkeley, California, the short period and one-second period spectral response acceleration parameters  $S_s$  and  $S_1$  are 1.65 and 0.68, respectively. [The 2003 *Provisions* have adopted the 2002 USGS probabilistic seismic hazard maps, and the maps have been added to the body of the 2003 *Provisions* as figures in Chapter 3 (instead of the previously used separate map package.] For the very dense soil conditions, Site Class C is appropriate as described in *Provisions* Sec. 4.1.2.1 [3.5.1]. Using  $S_s = 1.65$  and Site Class C, *Provisions* Table 4.1.2.4a [3.3-1] lists a short period site coefficient  $F_a$  of 1.0. For  $S_1 > 0.5$  and Site Class C, *Provisions* Table 4.1.2.4b [3.3-2] gives a velocity based site coefficient  $F_v$  of 1.3. Using *Provisions* Eq. 4.1.2.4-1 and 4.1.2.4-2 [3.3-1 and 3.3-2], the maximum considered spectral response acceleration parameters for the Berkeley building are:

 $S_{MS} = F_a S_s = 1.0 \text{ x } 1.65 = 1.65$  $S_{MI} = F_v S_I = 1.3 \text{ x } 0.68 = 0.884$ 

The design spectral response acceleration parameters are given by *Provisions* Eq. 4.1.2.5-1 and 4.1.2.5-2 [3.3-3 and 3.3-4]:

 $S_{DS} = (2/3) S_{MS} = (2/3) 1.65 = 1.10$  $S_{DI} = (2/3) S_{MI} = (2/3) 0.884 = 0.589$ 

The transition period  $(T_s)$  for the Berkeley response spectrum is:

$$T_s = \frac{S_{DI}}{S_{DS}} = \frac{0.589}{1.10} = 0.535 \text{ sec}$$

 $T_s$  is the period where the horizontal (constant acceleration) portion of the design response spectrum intersects the descending (constant velocity or acceleration inversely proportional to *T*) portion of the spectrum. It is used later in this example as a parameter in determining the type of analysis that is required for final design.

For Honolulu, *Provisions* Maps 19 and 20 [Figure 3.3-10] give the short-period and 1-sec period spectral response acceleration parameters of 0.61 and 0.178, respectively. For the very dense soil/firm rock site condition, the site is classified as Site Class C. Interpolating from *Provisions* Table 4.1.4.2a [3.3-1], the short-period site coefficient ( $F_a$ ) is 1.16 and, from *Provisions* Table 4.1.2.4b [3.3-2], the interpolated long-period site coefficient ( $F_v$ ) is 1.62. The maximum considered spectral response acceleration parameters for the Honolulu building are:

 $S_{MS} = F_a S_s = 1.16 \ge 0.61 = 0.708$  $S_{MI} = F_v S_I = 1.62 \ge 0.178 = 0.288$ 

and the design spectral response acceleration parameters are:

 $S_{DS} = (2/3) S_{MS} = (2/3) 0.708 = 0.472$  $S_{DI} = (2/3) S_{MI} = (2/3) 0.288 = 0.192$ 

The transition period  $(T_s)$  for the Honolulu response spectrum is:

 $T_s = \frac{S_{DI}}{S_{DS}} = \frac{0.192}{0.472} = 0.407$  sec

# 6.1.2 Structural Design Requirements

According to *Provisions* Sec. 1.3 [1.2], both the Berkeley and the Honolulu buildings are classified as Seismic Use Group I. *Provisions* Table 1.4 [1.3] assigns an occupancy importance factor (*I*) of 1.0 to all Seismic Use Group I buildings.

According to *Provisions* Tables 4.2.1a and 4.2.1b [Tables 1.4-1 and 1.4-2], the Berkeley building is classified as Seismic Design Category D. The Honolulu building is classified as Seismic Design Category C because of the lower intensity ground motion.

The seismic-force-resisting systems for both the Berkeley and the Honolulu buildings consist of momentresisting frames in the N-S direction. E-W loading is resisted by a dual frame-wall system in the Berkeley building and by a set of moment-resisting frames in the Honolulu building. For the Berkeley building, assigned to Seismic Design Category D, *Provisions* Sec. 9.1.1.3 [9.2.2.1.3] (which modifies language in the ACI 318 to conform to the *Provisions*) requires that all moment-resisting frames be designed and detailed as special moment frames. Similarly, *Provisions* Sec. 9.1.1.3 [9.2.2.1.3] requires the structural walls to be detailed as special reinforced concrete shear walls. For the Honolulu building assigned to Seismic Design Category C, *Provisions* Sec. 9.1.1.3 [9.2.2.1.3] allows the use of intermediate moment frames. According to *Provisions* Table 5.2.2 [4.3-1], neither of these structures violate height restrictions.

*Provisions* Table 5.2.2 [4.3-1] provides values for the response modification coefficient (R), the system over strength factor ( $\Omega_0$ ), and the deflection amplification factor ( $C_d$ ) for each structural system type. The values determined for the Berkeley and Honolulu buildings are summarized in Table 6-1.

		for Structural Systems Osed			
Location	Response Direction	Building Frame Type	R	$arOmega_{0}$	$C_d$
Berkeley	N-S	Special moment frame	8	3	5.5
	E-W	Dual system incorporating special moment frame and structural wall	8	2.5	6.5
Honolulu	N-S	Intermediate moment frame	5	3	4.5
	E-W	Intermediate moment frame	5	3	4.5

Table 6-1         Response Modification, Overstrength, and Deflection Amplification Coefficients				
for Structural Systems Used				

[For a dual system consisting of a special moment frame and special reinforced concrete shear walls, R = 7,  $\Omega_0 = 2.5$ , and  $C_d = 5.5$  in 2003 *Provisions* Table 4.3-1.]

For the Berkeley building dual system, the *Provisions* requires that the frame portion of the system be able to carry 25 percent of the total seismic force. As discussed below, this requires that a separate analysis of a frame-only system be carried out for loading in the E-W direction.

With regard to the response modification coefficients for the special and intermediate moment frames, it is important to note that R = 5.0 for the intermediate frame is 0.625 times the value for the special frame. This indicates that intermediate frames can be expected to deliver lower ductility than that supplied by the more stringently detailed special moment frames.

For the Berkeley system, the response modification coefficients are the same (R = 8) for the frame and frame-wall systems but are higher than the coefficient applicable to a special reinforced concrete structural wall system (R = 6). This provides an incentive for the engineer to opt for a frame-wall system under conditions where a frame acting alone may be too flexible or a wall acting alone cannot be proportioned due to excessively high overturning moments.

# 6.1.3 Structural Configuration

Based on the plan view of the building shown in Figure 6-1, the only possibility of a plan irregularity is a torsional irregularity (*Provisions* Table 5.2.3.2 [4.3-2]) of Type 1a or 1b. While the actual presence of such an irregularity cannot be determined without analysis, it appears unlikely for both the Berkeley and the Honolulu buildings because the lateral-force-resisting elements of both buildings are distributed evenly over the floor. For the purpose of this example, it is assumed (but verified later) that torsional irregularities do not exist.

As for the vertical irregularities listed in *Provisions* Table 5.2.3.3 [4.3-3], the presence of a soft or weak story cannot be determined without calculations based on an existing design. In this case, however, the first story is suspect, because its height of 18 ft is well in excess of the 12.5-ft height of the story above. As with the torsional irregularity, it is assumed (but verified later) that a vertical irregularity does not exist.

# 6.2 DETERMINATION OF SEISMIC FORCES

The determination of seismic forces requires knowledge of the magnitude and distribution of structural mass, the short period and long period response accelerations, the dynamic properties of the system, and the system response modification factor (R). Using *Provisions* Eq. 5.4.1 [5.2-1], the design base shear for the structure is:

$$V = C_S W$$

where W is the total (seismic) weight of the building and  $C_s$  is the seismic response coefficient. The upper limit on  $C_s$  is given by *Provisions* Eq. 5.4.1.1-1 [5.2-2]:

$$C_S = \frac{S_{DS}}{R/I}$$

For intermediate response periods, Eq. 5.4.1.1-2 [5.2-3] controls:

$$C_{S} = \frac{S_{DI}}{T(R/I)}$$

However, the response coefficient must not be less than that given by Eq. 5.4.1.1-3 [changed in the 2003 *Provisions*]:

$$C_{S} = 0.044 S_{DS} I$$

Note that the above limit will apply when the structural period is greater than  $S_{Dl}/0.044RS_{DS}$ . This limit is  $(0.589)/(0.044 \ge 8 \ge 1.1) = 1.52$  sec for the Berkeley building and  $(0.192)/(0.044 \ge 5 \ge 0.472) = 1.85$  sec for the Honolulu building. [The minimum  $C_s$  value is simply 0.01 in the 2003 *Provisions*, which would not be applicable to this example as discussed below.]

In each of the above equations, the importance factor (I) is taken as 1.0. With the exception of the period of vibration (T), all of the other terms in previous equations have been defined and/or computed earlier in this chapter.

# 6.2.1 Approximate Period of Vibration

Requirements for the computation of building period are given in *Provisions* Sec. 5.4.2 [5.2.2]. For the preliminary design using the ELF procedure, the approximate period ( $T_a$ ) computed in accordance with *Provisions* Eq. 5.4.2.1-1 [5.2-6] could be used:

$$T_a = C_r h_n^x$$

Because this formula is based on lower bound regression analysis of measured building response in California, it will generally result in periods that are lower (hence, more conservative for use in predicting base shear) than those computed from a more rigorous mathematical model. This is particularly true for buildings located in regions of lower seismicity. If a more rigorous analysis is carried out (using a computer), the resulting period may be too high due to a variety of possible modeling errors. Consequently, the *Provisions* places an upper limit on the period that can be used for design. The upper limit is  $T = C_u T_a$  where  $C_u$  is provided in *Provisions* Table 5.4.2 [5.2-1].

For the N-S direction of the Berkeley building, the structure is a reinforced concrete moment-resisting frame and the approximate period is calculated according to *Provisions* Eq. 5.4.2.1-1 [5.2-6]. Using *Provisions* Table 5.4.2.1 [5.2-2],  $C_r = 0.016$  and x = 0.9. With  $h_n = 155.5$  ft,  $T_a = 1.50$  sec. With  $S_{DI} > 0.40$  for the Berkeley building,  $C_u = 1.4$  and the upper limit on the analytical period is T = 1.4(1.5) = 2.1 sec.

For E-W seismic activity in Berkeley, the structure is a frame-wall system with  $C_r = 0.020$  and x = 0.75. Substituting the appropriate values in *Provisions* Eq. 5.4.2.1-1 [5.2-6], the E-W period  $T_a = 0.88$  sec. The upper limit on the analytical period is (1.4)0.88 = 1.23 sec.

For the Honolulu building, the  $T_a = 1.5$  sec period computed above for concrete moment frames is applicable in both the N-S and E-W direction. For Honolulu,  $S_{DI}$  is 0.192g and, from *Provisions* Table 5.4.2 [5.2-1],  $C_u$  can be taken as 1.52. The upper limit on the analytical period is T = 1.52(1.5) = 2.28 sec.

The period to be used in the ELF analysis will be in the range of  $T_a$  to  $C_u T_a$ . If an accurate analysis provides periods greater than  $C_u T_a$ ,  $C_u T_a$  should be used. If the accurate analysis produces periods less than  $C_u T_a$  but greater than  $T_a$ , the period from the analysis should be used. Finally, if the accurate analysis produces periods less than  $T_a$ ,  $T_a$  may be used.

Later in this chapter, the more accurate periods will be computed using a finite element analysis program. Before this can be done, however, the building mass must be determined.

# 6.2.2 Building Mass

Before the building mass can be determined, the approximate size of the different members of the seismic-force-resisting system must be established. For special moment frames, limitations on beam-column joint shear and reinforcement development length usually control. This is particularly true when lightweight (LW) concrete is used. An additional consideration is the amount of vertical reinforcement in the columns. ACI 318 Sec. 21.4.3.1 limits the vertical steel reinforcing ratio to 6 percent for special moment frame columns; however, 4 percent vertical steel is a more practical limit.

Based on a series of preliminary calculations (not shown here), it is assumed that all columns and structural wall boundary elements are 30 in. by 30 in., girders are 22.5 in. wide by 32 in. deep, and the panel of the structural wall is 16 in. thick. It has already been established that pan joists are spaced 36 in. o.c., have an average web thickness of 6 in., and, including a 4-in.-thick slab, are 20 in. deep. For the Berkeley building, these member sizes probably are close to the final sizes. For the Honolulu building (which has no structural wall and ultimately ends up with slightly smaller elements), the masses computed from the above member sizes are on the conservative (heavy) side.

In addition to the building structural weight, the following superimposed dead loads (DL) were assumed:

Partition DL (and roofing)	=	10 psf
Ceiling and mechanical DL	=	15 psf
Curtain wall cladding DL	=	10 psf

Based on the member sizes given above and on the other dead load, the individual story weights, masses, and mass moments of inertia are listed in Table 6-2. These masses were used for both the Berkeley and the Honolulu buildings.

As discussed below, the mass and mass moments of inertia are required for the determination of modal properties using the ETABS program. Note from Table 6-2 that the roof and lowest floor have masses slightly different from the typical floors. It is also interesting to note that the average density of this building is 11.2 pcf. A normal weight (NW) concrete building of the same configuration would have a density of approximately 14.0 pcf.

The use of LW instead of NW concrete reduces the total building mass by more than 20 percent and certainly satisfies the minimize mass rule of earthquake-resistant design. However, there are some disadvantages to the use of LW concrete. In general, LW aggregate reinforced concrete has a lower toughness or ductility than NW reinforced concrete and the higher the strength, the larger the reduction in available ductility. For this reason and also the absence of pertinent test results, ACI 318 Sec. 21.2.4.2 allows a maximum compressive strength of 4,000 psi for LW concrete in areas of high seismicity. [Note that in ACI 318-02 Sec. 21.2.4.2, the maximum compressive strength for LW concrete has been increased to 5,000 psi.] A further penalty placed on LW concrete is the reduction of shear strength. This primarily affects the sizing of beam-column joints (ACI 318 Sec. 21.5.3.2) but also has an effect on the amount of shear reinforcement required in the panels of structural walls.<sup>1</sup> For girders, the reduction in shear strength of LW aggregate concrete usually is of no concern because ACI 318 disallows the use of the concrete in determining the shear resistance of members with significant earthquake shear (ACI 318 Sec. 21.4.5.2). Finally, the required tension development lengths for bars embedded in LW concrete are significantly greater than those required for NW concrete.

Table 6-2         Story Weights, Masses, and Moments of Inertia					
		Mass	Mass Moment of Inertia		
Story Level	Weight (kips)	(kips-sec <sup>2</sup> /in.)	(inkip-sec <sup>2</sup> /rad)		

<sup>&</sup>lt;sup>1</sup>ACI 318 Sec. 21.6.4 [21.7.4] gives equations for the shear strength of the panels of structural walls. In the equations, the term  $\sqrt{f'_c}$  appears, but there is no explicit requirement to reduce the shear strength of the concrete when LW aggregate is used. However, ACI 318 Sec. 11.2 states that wherever the term  $\sqrt{f'_c}$  appears in association with shear strength, it should be multiplied by 0.75 when all-LW concrete is used and by 0.85 when sand-LW concrete is used. In this example, which utilizes

sand-LW concrete, the shear strength of the concrete will be multiplied by 0.85 as specified in ACI 318 Chapter 11.

Roof	2,783	7.202	4,675,000
12	3,051	7.896	5,126,000
11	3,051	7.896	5,126,000
10	3,051	7.896	5,126,000
9	3,051	7.896	5,126,000
8	3,051	7.876	5,126,000
7	3,051	7.896	5,126,000
6	3,051	7.896	5,126,000
5	3,051	7.896	5,126,000
4	3,051	7.896	5,126,000
3	3,051	7.896	5,126,000
2	3,169	8.201	5,324,000
Total	36,462		

1.0 kip = 4.45 kN, 1.0 in. = 25.4 mm.

### 6.2.3 Structural Analysis

Structural analysis is used primarily to determine the forces in the elements for design purposes, compute story drift, and assess the significance of P-delta effects. The structural analysis also provides other useful information (e.g., accurate periods of vibration and computational checks on plan and vertical irregularities). The computed periods of vibration are addressed in this section and the other results are presented and discussed later.

The ETABS program was used for the analysis of both the Berkeley and Honolulu buildings. Those aspects of the model that should be noted are:

- 1. The structure was modeled with 12 levels above grade and one level below grade. The perimeter basement walls were modeled as shear panels as were the main structural walls. It was assumed that the walls were "fixed" at their base.
- 2. As automatically provided by the ETABS program, all floor diaphragms were assumed to be infinitely rigid in plane and infinitely flexible out-of-plane.
- 3. Beams, columns, and structural wall boundary members were represented by two-dimensional frame elements. Each member was assumed to be uncracked, and properties were based on gross area for the columns and boundary elements and on effective T-beam shapes for the girders. (The effect of cracking is considered in a simplified manner.) The width of the flanges for the T-beams is based on the definition of T-beams in ACI 318 Sec. 8.10. Except for the slab portion of the joists which contributed to T-beam stiffness of the girders, the flexural stiffness of the joists was ignored. For the haunched girders, an equivalent depth of stem was used. The equivalent depth was computed to provide a prismatic member with a stiffness under equal end rotation identical to that of the nonprismatic haunched member. Axial, flexural, and shear deformations were included for all members.
- 4. The structural walls of the Berkeley building are modeled as a combination of boundary elements and shear panels.
- 5. Beam-column joints are modeled as 50 percent rigid. This provides effective stiffness for beam-column joints halfway between a model with fully rigid joints (clear span analysis) and fully flexible joints (centerline analysis).

6. P-delta effects are ignored. An evaluation of the accuracy of this assumption is provided later in this example.

## 6.2.4 Accurate Periods from Finite Element Analysis

The computed periods of vibration and a description of the associated modes of vibration are given for the first 11 modes of the Berkeley building in Table 6-3. With 11 modes, the accumulated modal mass in each direction is more than 90 percent of the total mass. *Provisions* Sec. 5.5.2 [5.3.2] requires that a dynamic analysis must include at least 90 percent of the actual mass in each of the two orthogonal directions. Table 6-4 provides the computed modal properties for the Honolulu building. In this case, 90 percent of the total mass was developed in just eight modes.

For the Berkeley building, the computed N-S period of vibration is 1.77 sec. This is between the approximate period,  $T_a = 1.5$  sec, and  $C_u T_a = 2.1$  sec. In the E-W direction, the computed period is 1.40 sec, which is greater than both  $T_a = 0.88$  sec and  $C_u T_a = 1.23$  sec.

If cracked section properties were used, the computed period values for the Berkeley building would be somewhat greater. For preliminary design, it is reasonable to assume that each member has a cracked moment of inertia equal to one-half of the gross uncracked moment of inertia. Based on this assumption, and the assumption that flexural behavior dominates, the cracked periods would be approximately 1.414 (the square root of 2.0) times the uncracked periods. Hence, for Berkeley, the cracked N-S and E-W periods are 1.414(1.77) = 2.50 sec, and 1.414(1.4) = 1.98 sec, respectively. Both of these cracked periods are greater than  $C_u T_a$ , so  $C_u T_a$  can be used in the ELF analysis.

For the Honolulu building, the uncracked periods in the N-S and E-W directions are 1.78 and 1.87 sec, respectively. The N-S period is virtually the same as for the Berkeley building because there are no walls in the N-S direction of either building. In the E-W direction, the increase in period from 1.4 sec to 1.87 sec indicates a significant reduction in stiffness due to the loss of the walls in the Honolulu building. For both the E-W and the N-S directions, the approximate period ( $T_a$ ) for the Honolulu building is 1.5 sec, and  $C_u T_a$  is 2.28 sec. Both of the computed periods fall within these bounds. However, if cracked section properties were used, the computed periods would be 2.52 sec in the N-S direction and 2.64 sec in the E-W direction. For the purpose of computing ELF forces, therefore, a period of 2.28 sec can be used for both the N-S and E-W directions in Honolulu.

A summary of the approximate and computed periods is given in Table 6-5.

	Period <sup>*</sup>	% of Effective Mass	% of Effective Mass Represented by Mode**		
Mode	(sec)	N-S	N-S E-W		
1	1.77	80.23 (80.2)	00.00 (0.00)	First Mode N-S	
2	1.40	0.0 (80.2)	71.48 (71.5)	First Mode E-W	
3	1.27	0.0 (80.2)	0.00 (71.5)	First Mode Torsion	
4	0.581	8.04 (88.3)	0.00 (71.5)	Second Mode N-S	
5	0.394	0.00 (88.3)	0.00 (71.5)	Second Mode Torsion	
6	0.365	0.00 (88.3)	14.17 (85.6)	Second Mode E-W	
7	0.336	2.24 (90.5)	0.00 (85.6)	Third Mode N-S	
8	0.230	0.88 (91.4)	0.00 (85.6)	Fourth Mode N-S	
9	0.210	0.00 (91.4)	0.00 (85.6)	Third Mode Torsion	
10	0.171	0.40 (91.8)	0.00 (85.6)	Fifth Mode N-S	
11	0.135	0.00 (91.8)	4.95 (90.6)	Third Mode E-W	

\* Based on gross section properties. \*\* Accumulated mass in parentheses.

 Table 6-4
 Periods and Modal Response Characteristics for the Honolulu Building

	Period <sup>*</sup>	% of Effective Mass	% of Effective Mass Represented by Mode**		
Mode	(sec)	N-S E-W		Description	
1	1.87	79.7 (79.7)	0.00 (0.00)	First Mode E-W	
2	1.78	0.00 (79.7)	80.25 (80.2)	First Mode N-S	
3	1.38	0.00 (79.7)	0.00 (80.2)	First Mode Torsion	
4	0.610	8.79 (88.5)	0.00 (80.2)	Second Mode E-W	
5	0.584	0.00 (88.5)	8.04 (88.3)	Second Mode N-S	
6	0.452	0.00 (88.5)	0.00 (88.3)	Second Mode Torsion	
7	0.345	2.27 (90.7)	0.00 (88.3)	Third Mode E-W	
8	0.337	0.00 (90.7)	2.23 (90.5)	Third Mode N-S	
9	0.260	0.00 (90.7)	0.00 (90.5)	Third Mode Torsion	
10	0.235	0.89 (91.6)	0.00 (90.5)	Fourth Mode E-W	
11	0.231	0.00 (91.6)	0.87 (91.4)	Fourth Mode N-S	

<sup>8</sup> Based on gross section properties.

\*\* Accumulated mass in parentheses.

	Berl	keley	Honolulu		
Method of Period Computation	N-S	E-W	N-S	E-W	
Approximate $T_a$	1.50	0.88	1.50	1.50	
Approximate $\times C_u$	$2.10^{*}$	1.23	2.28	2.28	
ETABS (gross)	1.77	1.40	1.78	1.87	
ETABS (cracked)	2.50	1.98	2.52	2.64	

 Table 6-5
 Comparison of Approximate and "Exact" Periods (in seconds)

\* Values in italics should be used in the ELF analysis.

### 6.2.5 Seismic Design Base Shear

The seismic design base shear for the Berkeley is computed below.

In the N-S direction with W = 36,462 kips (see Table 6-2),  $S_{DS} = 1.10$ ,  $S_{DI} = 0.589$ , R = 8, I = 1, and T = 2.10 sec:

$$C_{S,max} = \frac{S_{DS}}{R/I} = \frac{1.10}{8/1} = 0.1375$$

$$C_{S} = \frac{S_{DI}}{T(R/I)} = \frac{0.589}{2.10(8/1)} = 0.0351$$

 $C_{S,min} = 0.044 S_{DS} I = 0.044(1.1)(1) = 0.0484$ 

[As noted previously in Sec. 6.2, the minimum  $C_s$  value is 0.01 in the 2003 *Provisions*.]

 $C_{s,min} = 0.0484$  controls, and the design base shear in the N-S direction is V = 0.0484 (36,462) = 1,765 kips.

In the stiffer E-W direction,  $C_{S,max}$  and  $C_{S,min}$  are as before, T = 1.23 sec, and

$$C_{S} = \frac{S_{DI}}{T(R/I)} = \frac{0.589}{1.23(8/1)} = 0.0598$$

In this case,  $C_s = 0.0598$  controls and V = 0.0598 (36,462) = 2,180 kips

For the Honolulu building, base shears are computed in a similar manner and are the same for the N-S and the E-W directions. With W = 36,462 kips,  $S_{DS} = 0.474$ ,  $S_{DI} = 0.192$ , R = 5, I = 1, and T = 2.28 sec:

$$C_{S,max} = \frac{S_{DS}}{R/I} = \frac{0.472}{5/1} = 0.0944$$
$$C_S = \frac{S_{DI}}{T(R/I)} = \frac{0.192}{2.28(5/1)} = 0.0168$$
$$C_{S,min} = 0.044S_{DS}I = 0.044(0.472)(1.0) = 0.0207$$

 $C_s = 0.0207$  controls and V = 0.0207 (36,462) = 755 kips

A summary of the Berkeley and Honolulu seismic design parameters are provided in Table 6-6.

Note that *Provisions* Sec. 5.4.6 [5.2.6.1] states that for the purpose of computing drift, a base shear computed according to *Provisions* Eq. 5.4.1.1-2 [5.2-3] (used to compute  $C_s$  above) may be used in lieu of the shear computed using *Provisions* Eq. 5.4.1.1-3 [5.2-4] (used to compute  $C_{s,min}$  above).

Table 6-6	Comparison of Periods, Seismic Shears Coefficients, and Base Shears
	for the Berkeley and Honolulu Buildings

	Response		Т		V
Location	Direction	Building Frame Type	(sec)	$C_s$	(kips)

			Chapter	6, Reinforce	d Concrete
Berkeley	N-S	Special moment frame	2.10	0.0485	1,765
	E-W	Dual system incorporating special moment frame and structural wall	1.23	0.0598	2,180
Honolulu	N-S	Intermediate moment frame	2.28	0.0207	755
	E-W	Intermediate moment frame	2.28	0.0207	755

1.0 kip = 4.45 kN.

#### 6.2.6 Development of Equivalent Lateral Forces

The vertical distribution of lateral forces is computed from *Provisions* Eq. 5.4.3-1 and 5.4.3-2 [5.2-10 and 5.2-11]:

 $F_x = C_{vx}V$ 

$$C_{vx} = \frac{w_x h_x^k}{\sum_{i=1}^n w_i h_i^k}$$

where

k = 1.0 for T < 0.5 sec k = 2.0 for T > 2.5 sec k = 0.75 + 0.5T for 1.0 < T < 2.5 sec

Based on the equations above, the seismic story forces, shears, and overturning moments are easily computed using an Excel spreadsheet. The results of these computations are shown in Tables 6-7a and 6-7b for the Berkeley buildings and in Table 6-8 for the Honolulu building. A note at the bottom of each table gives the calculated vertical force distribution factor (k). The tables are presented with as many significant digits to the left of the decimal as the spreadsheet generates but that should not be interpreted as real accuracy; it is just the simplest approach. Also, some of the sums are not exact due to truncation error.

Level	Height <i>h</i> (ft)	Weight W (kips)	$Wh^k$	$Wh^k/\Sigma$	Force $F_x$ (kips)	Story Shear $V_x$ (kips)	Overturning Moment $M_x$ (ft-k)
R	155.5	2,783	24,526,067	0.187	330.9	330.9	4,136
12	143.0	3,051	23,123,154	0.177	311.9	642.8	12,170
11	130.5	3,051	19,612,869	0.150	264.6	907.4	23,512
10	118.0	3,051	16,361,753	0.125	220.7	1,128.1	37,613
9	105.5	3,051	13,375,088	0.102	180.4	1,308.5	53,970
8	93.0	3,051	10,658,879	0.081	143.8	1,452.3	72,123
7	80.5	3,051	8,220,056	0.063	110.9	1,563.2	91,663
6	68.0	3,051	6,066,780	0.046	81.8	1,645.0	112,226
5	55.5	3,051	4,208,909	0.032	56.8	1,701.8	133,498
4	43.0	3,051	2,658,799	0.020	35.9	1,737.7	155,219
3	30.5	3,051	1,432,788	0.011	19.3	1,757.0	177,181
2	18.0	3,169	575,987	0.004	7.8	1,764.8	208,947
Total		36,462	130,821,129	0.998	1764.8		

 Table 6-7a
 Vertical Distribution of N-S Seismic Forces for the Berkeley Building\*

\* Table based on T = 2.1 sec and k = 1.8.

1.0 ft = 0.3048 m, 1.0 kip = 4.45 kN, 1.0 ft-kip = 1.36 kN-m.

 Table 6-7b
 Vertical Distribution of E-W Seismic Forces for the Berkeley Building\*

Level	Height <i>h</i> (ft)	Weight W (kips)	$Wh^k$	$Wh^k/\Sigma$	Force $F_x$ (kips)	Story Shear $V_x$ (kips)	Overturning Moment $M_x$ (ft-k)
R	155.5	2,783	2,730,393	0.161	350.6	351	4,382
12	143.0	3,051	2,669,783	0.157	342.8	693	13,049
11	130.5	3,051	2,356,408	0.139	302.5	996	25,497
10	118.0	3,051	2,053,814	0.121	263.7	1,260	41,242
9	105.5	3,051	1,762,714	0.104	226.3	1,486	59,816
8	93.0	3,051	1,483,957	0.087	190.5	1,676	80,771
7	80.5	3,051	1,218,579	0.072	156.5	1,833	103,682
6	68.0	3,051	967,870	0.057	124.3	1,957	128,146
5	55.5	3,051	733,503	0.043	94.2	2,051	153,788
4	43.0	3,051	517,758	0.030	66.5	2,118	180,260
3	30.5	3,051	323,975	0.019	41.6	2,159	207,253
2	18.0	3,169	163,821	0.010	21.0	2,180	246,500
Total		36,462	16,982,575	1.000	2180.5		

\* Table based on T = 1.23 sec and k = 1.365.

1.0 ft = 0.3048 m, 1.0 kip = 4.45 kN, 1.0 ft-kip = 1.36 kN-m.

14	ible 0-8 vert		I OI IN-5 allu E-W	Seisine 10	ices for the i		unung
Level	Height <i>h</i> (ft)	Weight W (kips)	$Wh^k$	$Wh^k/\Sigma$	Force $F_x$ (kips)	Story Shear $V_x$ (kips)	Overturning Moment $M_x$ (ft-k)
R	155.5	2,783	38,626,348	0.193	145.6	145.6	1,820
12	143.0	3,051	36,143,260	0.181	136.2	281.9	5,343
11	130.5	3,051	30,405,075	0.152	114.6	396.5	10,299
10	118.0	3,051	25,136,176	0.126	94.8	491.2	16,440
9	105.5	3,051	20,341,799	0.102	76.7	567.9	23,539
8	93.0	3,051	16,027,839	0.080	60.4	628.3	31,393
7	80.5	3,051	12,210,028	0.061	46.0	674.3	39,822
6	68.0	3,051	8,869,192	0.044	33.4	707.8	48,669
5	55.5	3,051	6,041,655	0.030	22.8	730.5	57,801
4	43.0	3,051	3,729,903	0.019	14.1	744.6	67,108
3	30.5	3,051	1,948,807	0.010	7.3	751.9	76,508
2	18.0	3,169	747,115	0.004	2.8	754.8	90,093
Total		36,462	200,218,197	1.002	754.7		

Table 6-8 Vertical Distribution of N-S and E-W Seismic Forces for the Honolulu Building\*

\* Table based on T = 2.28 sec and k = 1.89.

1.0 ft = 0.3048 m, 1.0 kip = 4.45 kN, 1.0 ft-kip = 1.36 kN-m

The computed seismic story shears for the Berkeley and Honolulu buildings are shown graphically in Figures 6-3 and 6-4, respectively. Also shown in the figures are the story shears produced by ASCE 7 wind loads. For Berkeley, a 3-sec gust of 85 mph was used and, for Honolulu, a 3-sec gust of 105 mph. In each case, an Exposure B classification was assumed. The wind shears have been factored by a value of 1.36 (load factor of 1.6 times directionality factor 0.85) to bring them up to the ultimate seismic loading limit state represented by the *Provisions*.

As can be seen from the figures, the seismic shears for the Berkeley building are well in excess of the wind shears and will easily control the design of the members of the frames and walls. For the Honolulu building, the N-S seismic shears are significantly greater than the corresponding wind shears, but the E-W seismic and wind shears are closer. In the lower stories of the building, wind controls the strength demands and, in the upper levels, seismic forces control the strength demands. (A somewhat more detailed comparison is given later when the Honolulu building is designed.) With regards to detailing the Honolulu building, *all* of the elements must be detailed for inelastic deformation capacity as required by ACI 318 rules for intermediate moment frames.

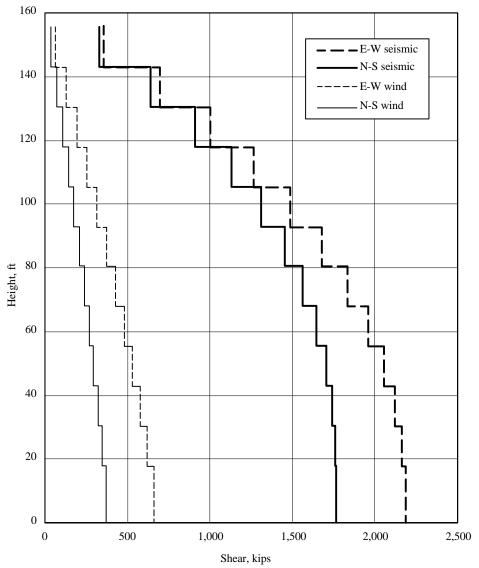


**Figure 6-3** Comparison of wind and seismic story shears for the Berkeley building (1.0 ft = 0.3048 m, 1.0 kip = 4.45 kN).

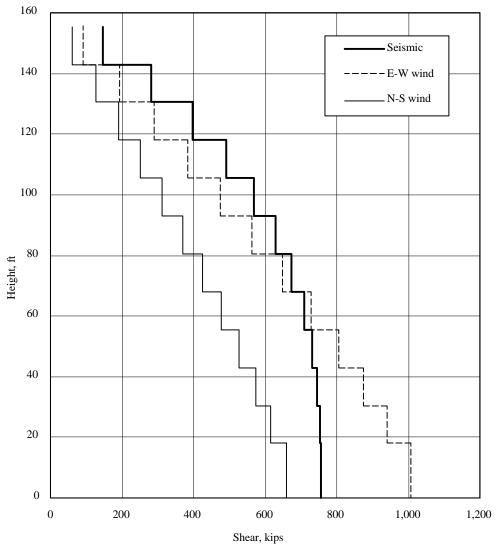


**Figure 6-4** Comparison of wind and seismic story shears for the Honolulu building (1.0 ft = 0.3048 m, 1.0 kip = 4.45 kN).

#### 6.3 DRIFT AND P-DELTA EFFECTS

#### 6.3.1 Direct Drift and P-Delta Check for the Berkeley Building

Drift and P-delta effects are checked according to *Provisions* Sec. 5.2.8 [5.2.6.1] and 5.4.6 [5.2.6.2], respectively. According to *Provisions* Table 5.2.8 [4.5-1], the story drift limit for this Seismic Use Group I building is  $0.020h_{sx}$  where  $h_{sx}$  is the height of story *x*. This limit may be thought of as 2 percent of the story height. Quantitative results of the drift analysis for the N-S and E-W directions are shown in Tables 6-9a and 6-9b, respectively.

With regards to the values shown in Table 6-9a, it must be noted that cracked section properties were used in the structural analysis and that 0.0351/0.0484=0.725 times the story forces shown in Table 6-7a were applied. This adjusts for the use of *Provisions* Eq. 5.4.1.1-3 [not applicable in the 2003 *Provisions*], which governed for base shear, was not used in computing drift. In Table 6-9b, cracked section

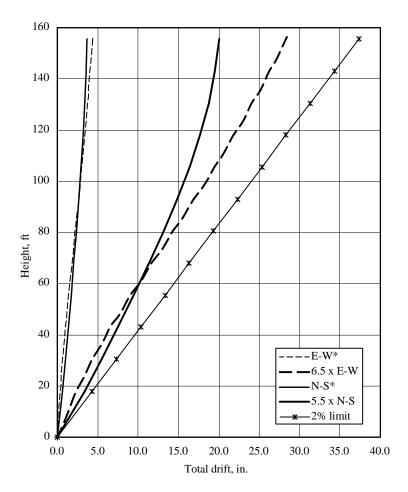
properties were also used, but the modifying factor does not apply because *Provisions* Eq. 5.4.1.1-2 [5.2-3] controlled in this direction.

In neither case does the computed drift ratio (magnified story drift/ $h_{sx}$ ) exceed 2 percent of the story height. Therefore, the story drift requirement is satisfied. A plot of the total drift resulting from both the N-S and E-W equivalent lateral seismic forces is shown in Figure 6-5.

An example calculation for drift in Story 5 loaded in the E-W direction is given below. Note that the relevant row is highlighted in Table 6-9b.

OK

Deflection at top of story =  $\delta_{5e}$  = 1.812 in. Deflection at bottom of story =  $\delta_{4e}$  = 1.410 in. Story drift =  $\Delta_{5e} = \delta_{5e} - \delta_{4e} = 1.812 - 1.410 = 0.402$  in. Deflection amplification factor,  $C_d = 6.5$ Importance factor, I = 1.0Magnified story drift =  $\Delta_5 = C_d \Delta_{5e}/I = 6.5(0.402)/1.0 = 2.613$  in. Magnified drift ratio =  $\Delta_5/h_5 = (2.613/150) = 0.01742 = 1.742\% < 2.0\%$ 



\* Elasticlly computed under code-prescribed seismic forces

**Figure 6-5** Drift profile for Berkeley building (1.0 ft = 0.3048 m, 1.0 in. = 25.4 mm).

Story	Total Deflection (in.)	Story Drift (in.)	Story Drift × $C_d^*$ (in.)	Drift Ratio (%)
12	3.640	0.087	0.478	0.319
11	3.533	0.145	0.798	0.532
10	3.408	0.203	1.117	0.744
9	3.205	0.232	1.276	0.851
8	2.973	0.276	1.515	1.010
7	2.697	0.305	1.675	1.117
6	2.393	0.334	1.834	1.223
5	2.059	0.348	1.914	1.276
4	1.711	0.348	1.914	1.276
3	1.363	0.364	2.002	1.334
2	0.999	0.381	2.097	1.398
1	0.618	0.618	3.397	1.573

 Table 6-9a
 Drift Computations for the Berkeley Building Loaded in the N-S Direction

<sup>\*</sup>  $C_d = 5.5$  for loading in this direction; total drift is at top of story, story height = 150 in. for Levels 3 through roof and 216 in. for Level 2.

1.0 in. = 25.4 mm.

Table 6-9b	<b>Drift Computations</b>	for the Berkeley	Building Loaded in	the E-W Direction

Story	Total Drift (in.)	Story Drift (in.)	Story Drift $\times C_d^*$ (in.)	Drift Ratio (%)
12	4.360	0.300	1.950	1.300
11	4.060	0.340	2.210	1.473
10	3.720	0.340	2.210	1.473
9	3.380	0.360	2.340	1.560
8	3.020	0.400	2.600	1.733
7	2.620	0.400	2.600	1.733
6	2.220	0.408	2.652	1.768
5	1.812	0.402	2.613	1.742
4	1.410	0.386	2.509	1.673
3	1.024	0.354	2.301	1.534
2	0.670	0.308	2.002	1.335
1	0.362	0.362	2.353	1.089

\*  $C_d = 6.5$  for loading in this direction; total drift is at top of story, story height = 150 in. for Levels 3 through roof and 216 in. for Level 2.

1.0 in. = 25.4 mm.

When a soft story exists in a Seismic Design Category D building, *Provisions* Table 5.2.5.1 [4.4-1] requires that a modal analysis be used. However, *Provisions* Sec. 5.2.3.3 [4.3.2.3] lists an exception:

Structural irregularities of Types 1a, 1b, or 2 in Table 5.2.3.3 [4.3-2] do not apply where no story drift ratio under design lateral load is less than or equal to 130 percent of the story drift ratio of the next story above. . . . The story drift ratios of the top two stories of the structure are not required to be evaluated.

For the building responding in the N-S direction, the ratio of first story to second story drift ratios is 1.573/1.398 = 1.13, which is less than 1.3. For E-W response, the ratio is 1.089/1.335 = 0.82, which also is less than 1.3. Therefore, a modal analysis is not required and the equivalent static forces from Tables 6-7a and 6-7b may be used for design.

The P-delta analysis for each direction of loading is shown in Tables 6-10a and 6-10b. The upper limit on the allowable story stability ratio is given by *Provisions* Eq. 5.4.6.2-2 [changed in the 2003 *Provisions*] as:

$$\theta_{max} = \frac{0.5}{\beta C_d} \le 0.50$$

Taking  $\beta$  as 1.0 (see *Provisions* Sec. 5.4.6.2 [not applicable in the 2003 *Provisions*]), the stability ratio limit for the N-S direction is 0.5/(1.0)5.5 = 0.091, and for the E-W direction the limit is 0.5/(1.0)6.5 = 0.077.

[In the 2003 *Provisions*, the maximum limit on the stability coefficient has been replaced by a requirement that the stability coefficient is permitted to exceed 0.10 if and only "if the resistance to lateral forces is determined to increase in a monotonic nonlinear static (pushover) analysis to the target displacement as determined in Sec. A5.2.3. P-delta effects shall be included in the analysis." Therefore, in this example, the stability coefficient should be evaluated directly using 2003 *Provisions* Eq. 5.2.-16.]

For this P-delta analysis a (reduced) story live load of 20 psf was included in the total story weight calculations. Deflections are based on cracked sections, and story shears are adjusted as necessary for use of *Provisions* Eq. 5.4.1.1-3 [5.2-3]. As can be seen in the last column of each table, the stability ratio ( $\theta$ ) does not exceed the maximum allowable value computed above. Moreover, since the values are less than 0.10 at all levels, P-delta effects can be neglected for both drift and strength computed limits according to *Provisions* Sec. 5.4.6.2 [5.2.6.2].

An example P-delta calculation for the Level 5 under E-W loading is shown below. Note that the relevant row is highlighted in Table 6-10b.

Magnified story drift =  $\Delta_5$  = 2.613 in. Story shear =  $V_5$  = 1,957 kips Accumulated story weight  $P_5$  = 27,500 kips Story height =  $h_{s5}$ = 150 in.  $C_d$  = 6.5  $\theta = (P_5 (\Delta_5/C_d)) / (V_5 h_{s5}) = 27,500(2.613/6.5) / (1957.1)(150) = 0.0377 < 0.077$  OK

[Note that the equation to determine the stability coefficient has been changed in the 2003 *Provisions*. The importance factor, *I*, has been added to 2003 *Provisions* Eq. 5.2-16. However, this does not affect this example because I = 1.0.]

Level	Story Drift (in.)	Story Shear * (kips)	Story Dead Load (kips)	Story Live Load (kips)	Total Story Load (kips)	Accum. Story Load (kips)	Stability Ratio θ
12	0.478	239.9	2783	420	3203	3203	0.0077
11	0.798	466.0	3051	420	3471	6674	0.0138
10	1.117	657.8	3051	420	3471	10145	0.0209
9	1.276	817.9	3051	420	3471	13616	0.0257
8	1.515	948.7	3051	420	3471	17087	0.0331
7	1.675	1052.9	3051	420	3471	20558	0.0396
6	1.834	1133.3	3051	420	3471	24029	0.0471
5	1.914	1192.6	3051	420	3471	27500	0.0535
4	1.914	1233.8	3051	420	3471	30971	0.0582
3	2.002	1259.8	3051	420	3471	34442	0.0663
2	2.097	1273.8	3051	420	3471	37913	0.0757
1	3.397	1279.5	3169	420	3589	41502	0.0928

 Table 6-10a
 P-Delta Computations for the Berkeley Building Loaded in the N-S Direction

\* Story shears in Table 6-7a factored by 0.725. See Sec. 6.3.1.

1.0 in. = 25.4 mm, 1.0 kip = 4.45 kN.

Table 6-10b P-Delta Computations for the Berkeley Building Loaded in the E-W Direction

Level	Story Drift (in.)	Story Shear (kips)	Story Dead Load (kips)	Story Live Load (kips)	Total Story Load (kips)	Accum. Story Load (kips)	Stability Ratio θ
12	1.950	350.6	2783	420	3203	3203	0.0183
11	2.210	693.3	3051	420	3471	6674	0.0218
10	2.210	995.9	3051	420	3471	10145	0.0231
9	2.340	1259.6	3051	420	3471	13616	0.0259
8	2.600	1485.9	3051	420	3471	17087	0.0307
7	2.600	1676.4	3051	420	3471	20558	0.0327
6	2.652	1832.9	3051	420	3471	24029	0.0357
5	2.613	1957.1	3051	420	3471	27500	0.0377
4	2.509	2051.3	3051	420	3471	30971	0.0389
3	2.301	2117.8	3051	420	3471	34442	0.0384
2	2.002	2159.4	3051	420	3471	37913	0.0361
1	2.353	2180.4	3169	420	3589	41502	0.0319

1.0 in. = 25.4 mm, 1.0 kip = 4.45 kN.

### 6.3.2 Test for Torsional Irregularity for Berkeley Building

In Sec. 6.1.3 it was mentioned that torsional irregularities are unlikely for the Berkeley building because the elements of the seismic-force-resisting system were well distributed over the floor area. This will now be verified by applying the story forces of Table 6-3a at an eccentricity equal to 5 percent of the building dimension perpendicular to the direction of force (accidental torsion requirement of *Provisions* Sec. 5.4.4.2 [5.2.4.2]). This test is required per *Provisions* Sec. 5.2.3.2 [4.3.2.2]. Analysis was performed using the ETABS program.

The eccentricity is 0.05(102.5) = 5.125 ft for forces in the N-S direction and 0.05(216) = 10.8 ft in the E-W direction.

For forces acting in the N-S direction:

Total displacement at center of mass =  $\delta_{avg}$  = 3.640 in. (see Table 6-9a) Rotation at center of mass = 0.000189 radians Maximum displacement at corner of floor plate =  $d_{max}$  = 3.640 + 0.000189(102.5)(12)/2 = 3.756 in. Ratio  $\delta_{max}/\delta_{avg}$  = 3.756/3.640 = 1.03 < 1.20, so no torsional irregularity exists.

For forces acting in the E-W direction:

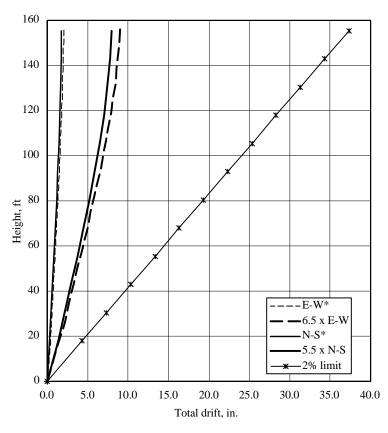
Total displacement at center of mass =  $\delta_{avg}$  = 4.360 in. (see Table 6-9b) Rotation at center of mass = 0.000648 radians Maximum displacement at corner of floor plate =  $d_{max}$  = 4.360 + 0.000648(216)(12)/2 = 5.200 in. Ratio  $d_{max}/d_{avg}$  = 5.200/4.360 = 1.19 < 1.20, so no torsional irregularity exists.

It is interesting that this building, when loaded in the E-W direction, is very close to being torsionally irregular (irregularity Type 1a of *Provisions* Table 5.2.3.2 [4.3-2]), even though the building is extremely regular in plan. The torsional flexibility of the building arises from the fact that the walls exist only on interior Gridlines 3, 4, 5, and 6.

## 6.3.3 Direct Drift and P-Delta Check for the Honolulu Building

The interstory drift computations for the Honolulu building deforming under the N-S and E-W equivalent static forces are shown in Tables 6-11a and 6-11b. As with the Berkeley building, the analysis used cracked section properties. The applied seismic forces, shown previously in Table 6-3b were multiplied by the ratio 0.0168/0.0207 = 0.808 to adjust for the use of *Provisions* Eq. 5.4.1.1-3. [As noted previously in Sec. 6.2, the minimum Cs value has been removed in the 2003 *Provisions*.]

These tables, as well as Figure 6-6, show that the story drift at each level is less than the allowable interstory drift of  $0.020h_{sx}$  (*Provisions* Table 5.2.8 [4.5-1]). Even though it is not pertinent for Seismic Design Category C buildings, a soft first story does not exist for the Honolulu building because the ratio of first story to second story drift does not exceed 1.3.



\* Elasticlly computed under code-prescribed seismic forces

**Figure 6-6** Drift profile for the Honolulu building (1.0 ft = 0.3048 m, 1.0 in. = 25.4 mm).

	1		υ	
Story	Total Drift (in.)	Story Drift (in.)	Story Drift $\times C_d^*$ (in.)	Drift Ratio (%)
12	1.766	0.040	0.182	0.121
11	1.726	0.069	0.313	0.208
10	1.656	0.097	0.436	0.291
9	1.559	0.118	0.531	0.354
8	1.441	0.136	0.611	0.407
7	1.306	0.149	0.669	0.446
6	1.157	0.160	0.720	0.480
5	0.997	0.168	0.756	0.504
4	0.829	0.171	0.771	0.514
3	0.658	0.176	0.793	0.528
2	0.482	0.184	0.829	0.553
1	0.297	0.297	1.338	0.619

Table 6-11a	Drift	Computations	for the	e Honolulu	Building	Loaded in the	N-S Direction

<sup>\*</sup>  $C_d = 4.5$  for loading in this direction; total drift is at top of story, story height = 150 in. for Levels 3 through roof and 216 in. for Level 2.

1.0 in. = 25.4 mm.

Story	Total Drift (in.)	Story Drift (in.)	Story Drift × $C_d^*$ (in.)	Drift Ratio (%)
12	2.002	0.061	0.276	0.184
11	1.941	0.090	0.407	0.271
10	1.850	0.116	0.524	0.349
9	1.734	0.137	0.618	0.412
8	1.597	0.157	0.705	0.470
7	1.440	0.171	0.772	0.514
6	1.269	0.179	0.807	0.538
5	1.089	0.186	0.836	0.558
4	0.903	0.191	0.858	0.572
3	0.713	0.191	0.858	0.572
2	0.522	0.197	0.887	0.591
1	0.325	0.325	1.462	0.677

Table 6-11b Drift Computations for the Honolulu Building Loaded in the E-W Direction

<sup>\*</sup>  $C_d = 4.5$  for loading in this direction; total drift is at top of story, story height = 150 in. for Levels 3 through roof and 216 in. for Level 2.

1.0 in. = 25.4 mm.

A sample calculation for Level 5 of Table 6-11b (highlighted in the table) is as follows:

Deflection at top of story =  $\delta_{5e}$  =1.089 in. Deflection at bottom of story =  $\delta_{4e}$  = 0.903 in. Story drift =  $\Delta_{5e} = \delta_{5e} - \delta_{4e} = 1.089 - 0.0903 = 0.186$  in. Deflection amplification factor,  $C_d = 4.5$ Importance factor, I = 1.0Magnified story drift =  $\Delta_5 = C_d \Delta_{5e}/I = 4.5(0.186)/1.0 = 0.836$  in. Magnified drift ratio =  $\Delta_5 / h_5 = (0.836/150) = 0.00558 = 0.558\% < 2.0\%$  Therefore, story drift satisfies the drift requirements.

Calculations for P-delta effects are shown in Tables 6-12a and 6-12b for N-S and E-W loading, respectively. The stability ratio at the 5th story from Table 6-12b is computed:

Magnified story drift =  $\Delta_5 = 0.836$  in. Story shear =  $V_5 = 571.9 =$  kips Accumulated story weight  $P_5 = 27500$  kips Story height =  $h_{s5} = 150$  in.  $C_d = 4.5$  $\theta = [P_5 (\Delta_5/C_d)]/(V_5h_{s5}) = 27500(0.836/4.5)/(571.9)(150) = 0.0596$ 

[Note that the equation to determine the stability coefficient has been changed in the 2003 *Provisions*. The importance factor, *I*, has been added to 2003 *Provisions* Eq. 5.2-16. However, this does not affect this example because I = 1.0.]

The requirements for maximum stability ratio  $(0.5/C_d = 0.5/4.5 = 0.111)$  are satisfied. Because the stability ratio is less than 0.10 at all floors, P-delta effects need not be considered (*Provisions* Sec. 5.4.6.2 [5.2.6.2]). (The value of 0.1023 in the first story for the E-W direction is considered by the author to be close enough to the criterion.)

Level	Story Drift (in.)	Story Shear * (kips)	Story Dead Load (kips)	Story Live Load (kips)	Total Story Load (kips)	Accum. Story Load (kips)	Stability Ratio θ
12	0.182	117.7	2783	420	3203	3203	0.0073
11	0.313	227.7	3051	420	3471	6674	0.0136
10	0.436	320.4	3051	420	3471	10145	0.0205
9	0.531	396.9	3051	420	3471	13616	0.0270
8	0.611	458.9	3051	420	3471	17087	0.0337
7	0.669	507.7	3051	420	3471	20558	0.0401
6	0.720	544.9	3051	420	3471	24029	0.0470
5	0.756	571.9	3051	420	3471	27500	0.0539
4	0.771	590.3	3051	420	3471	30971	0.0599
3	0.793	601.6	3051	420	3471	34442	0.0672
2	0.829	607.6	3051	420	3471	37913	0.0766
1	1.338	609.8	3169	420	3589	41502	0.0937

Table 6-12a P-Delta Computations for the Honolulu Building Loaded in the N-S Direction

\* Story shears in Table 6-8 factored by 0.808. See Sec. 6.3.3.

1.0 in. = 25.4 mm, 1.0 kip = 4.45 kN.

Level	Story Drift (in.)	Story Shear * (kips)	Story Dead Load (kips)	Story Live Load (kips)	Total Story Load (kips)	Accum. Story Load (kips)	Stability Ratio θ
12	0.276	117.7	2783	420	3203	3203	0.0111
11	0.407	227.7	3051	420	3471	6674	0.0177
10	0.524	320.4	3051	420	3471	10145	0.0246
9	0.618	396.9	3051	420	3471	13616	0.0314
8	0.705	458.9	3051	420	3471	17087	0.0389
7	0.772	507.7	3051	420	3471	20558	0.0463
6	0.807	544.9	3051	420	3471	24029	0.0527
5	0.836	571.9	3051	420	3471	27500	0.0596
4	0.858	590.3	3051	420	3471	30971	0.0667
3	0.858	601.6	3051	420	3471	34442	0.0728
2	0.887	607.6	3051	420	3471	37913	0.0820
1	1.462	609.8	3169	420	3589	41502	0.1023

Table 6-12b P-Delta Computations for the Honolulu Building Loaded in the E-W Direction

\* Story shears in Table 6-8 factored by 0.808. See Sec. 6.3.3.

1.0 in. = 25.4 mm, 1.0 kip = 4.45 kN.

## 6.3.4 Test for Torsional Irregularity for the Honolulu Building

A test for torsional irregularity for the Honolulu building can be performed in a manner similar to that for the Berkeley building. However, it is clear that a torsional irregularity will not occur for the Honolulu building if the Berkeley building is not irregular. This will be the case because the walls, which draw the torsional resistance towards the center of the Berkeley building, do not exist in the Honolulu building.

# 6.4 STRUCTURAL DESIGN OF THE BERKELEY BUILDING

# 6.4.1 Material Properties

For the Berkeley building, sand-LW aggregate concrete of 4,000 psi strength is used everywhere except for the lower two stories of the structural walls where 6,000 psi NW concrete is used. All reinforcement has a specified yield strength of 60 ksi, except for the panel of the structural walls which contains 40 ksi reinforcement. This reinforcement must conform to ASTM A706. According to ACI 318 Sec. 21.2.5, however, ASTM A615 reinforcement may be used if the actual yield strength of the steel does not exceed the specified strength by more than 18 ksi and the ratio of actual ultimate tensile stress to actual tensile yield stress is greater than 1.25.

# 6.4.2 Combination of Load Effects

Using the ETABS program, the structure was analyzed for the equivalent lateral loads shown in Tables 6-7a and 6-7b. For strength analysis, the loads were applied at a 5 percent eccentricity as required for accidental torsion by *Provisions* Sec. 5.4.4.2 [5.2.4.2]. Where applicable, orthogonal loading effects were included per *Provisions* Sec. 5.2.5.2.3 [4.4.2.3]. The torsional magnification factor ( $A_x$ ) given by *Provisions* Eq. 5.4.4.3-1 [5.2-13] was not used because the building has no significant plan irregularities.

*Provisions* Sec. 5.2.7 [4.2.2.1] and Eq. 5.2.7-1 and 5.2.7-2 [4.2-1 and 4.2-2] require combination of load effects be developed on the basis of ASCE 7, except that the earthquake load effect, *E*, be defined as:

 $E = \rho Q_E + 0.2 S_{DS} D$ 

when gravity and seismic load effects are additive and

$$E = \rho Q_E - 0.2 S_{DS} D$$

when the effects of seismic load counteract gravity.

The special load combinations given by *Provisions* Eq. 5.2.7-1 and 5.2.7-2 [4.2-3 and 4.2-4] do not apply to the Berkeley building because there are no discontinuous elements supporting stiffer elements above them. (See *Provisions* Sec. 9.6.2 [9.4.1].)

The reliability factor ( $\rho$ ) in Eq. 5.2.7-1 and 5.2.7-2 [not applicable in the 2003 *Provisions*] should be taken as the maximum value of  $\rho_x$  defined by *Provisions* Eq. 5.2.4.2:

$$\rho_x = 2 - \frac{20}{r_{max_x}\sqrt{A_x}}$$

where  $A_x$  is the area of the floor or roof diaphragm above the story under consideration and  $r_{max_x}$  is the

largest ratio of the design story shear resisted by a single element divided by the total story shear for a given loading. The computed value for  $\rho$  must be greater than or equal to 1.0, but need not exceed 1.5. Special moment frames in Seismic Design Category D are an exception and must be proportioned such that  $\rho$  is not greater than 1.25.

For the structure loaded in the N-S direction, the structural system consists of special moment frames, and  $r_{ix}$  is taken as the maximum of the shears in any two adjacent columns in the plane of a moment frame divided by the story shear. For interior columns that have girders framing into both sides, only 70 percent of the individual column shear need be included in this sum. In the N-S direction, there are four identical frames. Each of these frames has eight columns. Using the portal frame idealization, the shear in an interior column will be  $V_{interior} = 0.25$  (2/14) V = 0.0357V.

Similarly, the shear in an exterior column will be  $V_{exterior} = 0.25 (1/14) V = 0.0179V$ .

For two adjacent interior columns:

$$r_{ix} = \frac{0.7(V_{int} + V_{int})}{V} = \frac{0.7(0.0375V + 0.0375V)}{V} = 0.0525$$

For one interior and one exterior column:

$$r_{ix} = \frac{(0.7V_{int} + V_{ext})}{V} = \frac{0.7(0.0375V) + 0.0179V)}{V} = 0.0441$$

The larger of these values will produce the largest value of  $\rho_x$ . Hence, for a floor diaphragm area  $A_x$  equal to  $102.5 \times 216 = 22,140$  square ft:

$$\rho_x = 2 - \frac{20}{0.0525\sqrt{22,140}} = -0.56$$

As this value is less than 1.0,  $\rho$  will be taken as 1.0 in the N-S direction.

For seismic forces acting in the E-W direction, the walls carry significant shear, and for the purposes of computing  $\rho$ , it will be assumed that they take all the shear. According to the *Provisions*,  $r_{ix}$  for walls is taken as the shear in the wall multiplied by  $10/l_w$  and divided by the story shear. The term  $l_w$  represents the plan length of the wall in feet. Thus, for one wall:

$$r_{max_x} = r_{ix} = \frac{0.25V(10/20)}{V} = 0.125$$

Only 80 percent of the  $\rho$  value based on the above computations need be used because the walls are part of a dual system. Hence, in the E-W direction

$$\rho_x = 0.8 \left( 2 - \frac{20}{0.125\sqrt{22,140}} \right) = 0.740$$

and as with the N-S direction,  $\rho$  may be taken as 1.0. Note that  $\rho$  need not be computed for the columns of the frames in the dual system, as this will clearly not control.

[The redundancy requirements have been substantially changed in the 2003 *Provisions*. For a building assigned to Seismic Design Category D,  $\rho = 1.0$  as long as it can be shown that failure beam-to-column connections at both ends of a single beam (moment frame system) or failure of a single shear wall with aspect ratio greater than 1.0 (shear wall system) would not result in more than a 33 percent reduction in story strength or create an extreme torsional irregularity. Alternatively, if the structure is regular in plan and there are at least 2 bays of perimeter framing on each side of the structure in each orthogonal direction, it is permitted to use,  $\rho = 1.0$ . Per 2003 *Provisions* Sec. 4.3.1.4.3 special moment frames in Seismic Design Category D must be configured such that the structure satisfies the criteria for  $\rho = 1.0$ . There are no reductions in the redundancy factor for dual systems. Based on the preliminary design,  $\rho = 1.0$  for because the structure has a perimeter moment frame and is regular.]

For the Berkeley structure, the basic ASCE 7 load combinations that must be considered are:

 $\begin{array}{l} 1.2D + 1.6L \\ 1.2D + 0.5L \pm 1.0E \\ 0.9D \pm 1.0E \end{array}$ 

The ASCE 7 load combination including only 1.4 times dead load will not control for any condition in this building.

Substituting *E* from the *Provisions*, with  $\rho$  taken as 1.0, the following load combinations must be used for earthquake:

 $(1.2 + 0.2S_{DS})D + 0.5L + E$ (1.2 + 0.2S\_{DS})D + 0.5L - E (0.9 - 0.2 S\_{DS})D + E (0.9 - 0.2S\_{DS})D - E

Finally, substituting 1.10 for  $S_{DS}$ , the following load combinations must be used for earthquake:

```
\begin{array}{l} 1.42D + 0.5L + E \\ 1.42D + 0.5L - E \end{array}
```

0.68D + E0.68D - E

It is very important to note that use of the ASCE 7 load combinations in lieu of the combinations given in ACI Chapter 9 requires use of the alternate strength reduction factors given in ACI 318 Appendix C:

Flexure without axial load  $\phi = 0.80$ Axial compression, using tied columns  $\phi = 0.65$  (transitions to 0.8 at low axial loads) Shear if shear strength is based on nominal axial-flexural capacity  $\phi = 0.75$ Shear if shear strength is <u>not</u> based on nominal axial-flexural capacity  $\phi = 0.55$ Shear in beam-column joints  $\phi = 0.80$ 

[The strength reduction factors in ACI 318-02 have been revised to be consistent with the ASCE 7 load combinations. Thus, the factors that were in Appendix C of ACI 318-99 are now in Chapter 9 of ACI 318-02, with some modification. The strength reduction factors relevant to this example as contained in ACI 318-02 Sec. 9.3 are:

Flexure without axial load  $\varphi = 0.9$  (tension-controlled sections) Axial compression, using tied columns  $\varphi = 0.65$  (transitions to 0.9 at low axial loads) Shear if shear strength is based o nominal axial-flexural capacity  $\varphi = 0.75$ Shear if shear strength is *not* based o nominal axial-flexural capacity  $\varphi = 0.60$ Shear in beam-column joints  $\varphi = 0.85$ ]

### 6.4.3 Comments on the Structure's Behavior Under E-W Loading

Frame-wall interaction plays an important role in the behavior of the structure loaded in the E-W direction. This behavior is beneficial to the design of the structure because:

- 1. For frames without walls (Frames 1, 2, 7, and 8), the shears developed in the girders (except for the first story) do not differ greatly from story to story. This allows for a uniformity in the design of the girders.
- 2. For frames containing structural walls (Frames 3 through 6), the overturning moments in the structural walls are reduced significantly as a result of interaction with the remaining frames (Frames 1, 2, 7, and 8).
- 3. For the frames containing structural walls, the 40-ft-long girders act as outriggers further reducing the overturning moment resisted by the structural walls.

The actual distribution of story forces developed in the different frames of the structure is shown in Figure 6-7.<sup>2</sup> This figure shows the response of Frames 1, 2, and 3 only. By symmetry, Frame 8 is similar to Frame 1, Frame 7 is similar to Frame 2, and Frame 6 is similar to Frame 3. Frames 4 and 5 have a response that is virtually identical to that of Frames 3 and 6.

As may be observed from Figure 6-7, a large reverse force acts at the top of Frame 3 which contains a structural wall. This happens because the structural wall pulls back on (supports) the top of Frame 1. The deflected shape of the structure loaded in the E-W direction (see Figure 6-5) also shows the effect of frame-wall interaction because the shape is neither a cantilever mode (wall alone) nor a shear mode

<sup>&</sup>lt;sup>2</sup>The analysis used to create Figures 6-7 and 6-8 did not include the 5 percent torsional eccentricity or the 30 percent orthogonal loading rules specified by the *Provisions*. The eccentricity and orthogonal load were included in the analysis carried out for member design.

(frame alone). It is the "straightening out" of the deflected shape of the structure that causes the story shears in the frames without walls to be relatively equal.

A plot of the story shears in Frames 1, 2, and 3 is shown in Figure 6-8. The distribution of overturning moments is shown in Figure 6-9 and indicates that the relatively stiff Frames 1 and 3 resist the largest portion of the total overturning moment. The reversal of moment at the top of Frame 3 is a typical response characteristic of frame-wall interaction.

## 6.4.4 Analysis of Frame-Only Structure for 25 Percent of Lateral Load

When designing a dual system, *Provisions* Sec. 5.2.2.1 [4.3.1.1] requires the frames (without walls) to resist at least 25 percent of the total base shear. This provision ensures that the dual system has sufficient redundancy to justify the increase from R = 6 for a special reinforced concrete structural wall to R = 8 for a dual system (see *Provisions* Table 5.2.2 [4.3-1]). [Note that R = 7 per 2003 *Provisions* Table 4.3-1.] The 25 percent analysis was carried out using the ETABS program with the mathematical model of the building being identical to the previous version except that the panels of the structural wall were removed. The boundary elements of the walls were retained in the model so that behavior of the interior frames (Frames 3, 4, 5, and 6) would be analyzed in a rational way.

The results of the analysis are shown in Figures 6-10, 6-11, and 6-12. In these figures, the original analysis (structural wall included) is shown by a solid line and the 25 percent (backup frame) analysis (structural wall removed) is shown by a dashed line. As can be seen, the 25 percent rule controls only at the lower level of the building.

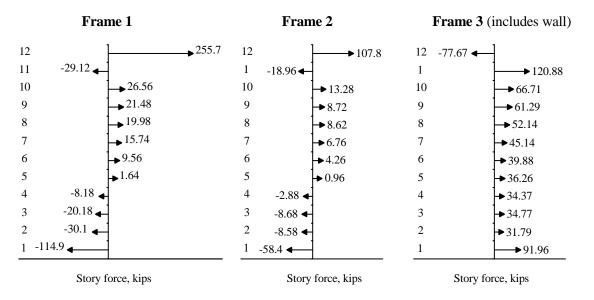


**Figure 6-7** Story forces in the E-W direction (1.0 kip = 4.45 kN).

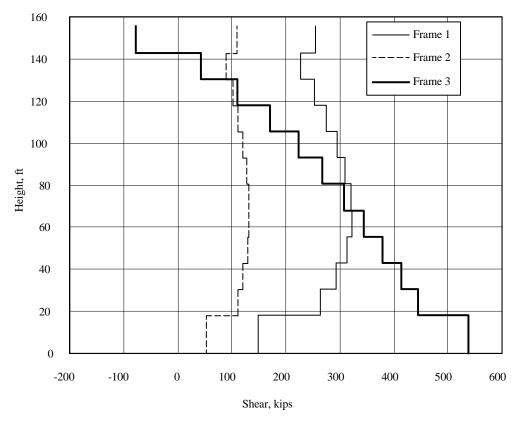
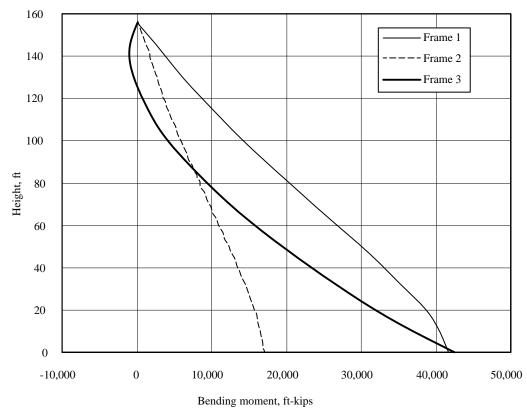
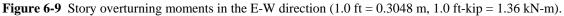
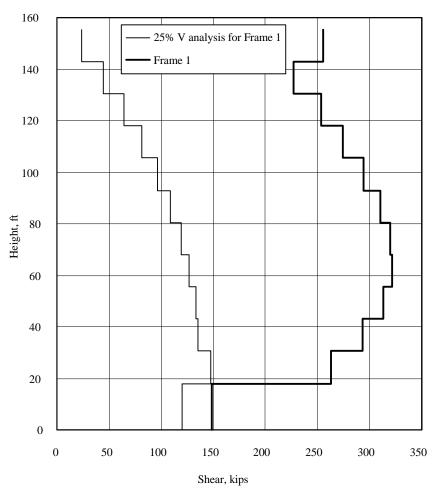


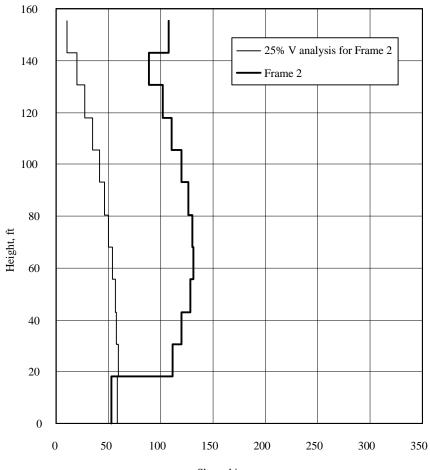
Figure 6-8 Story shears in the E-W direction (1.0 ft = 0.3048 m, 1.0 kip = 4.45 kN).







**Figure 6-10** 25 percent story shears, Frame 1 E-W direction (1.0 ft = 0.3048 m, 1.0 kip = 4.45 kN).



Shear, kips

**Figure 6-11** 25 percent story shears, Frame 2 E-W direction (1.0 ft = 0.3048 m, 1.0 kip = 4.45 kN).

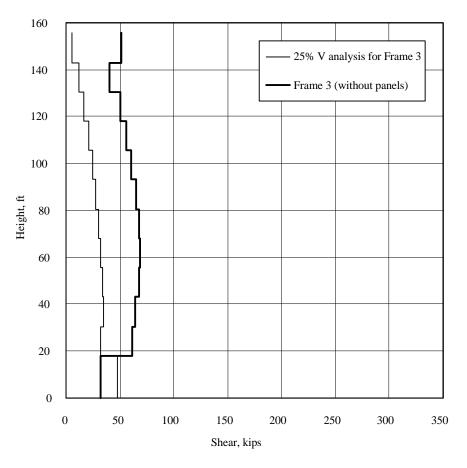


**Figure 6-12** 25 percent story shear, Frame 3 E-W direction (1.0 ft = 0.3048 m, 1.0 kip = 4.45 kN)..

## 6.4.5 Design of Frame Members for the Berkeley Building

A sign convention for bending moments is required in flexural design. In this example, when the steel at the top of a beam section is in tension, the moment is designated as a negative moment. When the steel at the bottom is in tension, the moment is designated as a positive moment. All moment diagrams are drawn using the reinforced concrete or tension-side convention. For beams, this means negative moments are plotted on the top and positive moments are plotted on the bottom. For columns, moments are drawn on the tension side of the member.

#### 6.4.5.1 Initial Calculations

Before the quantity and placement of reinforcement is determined, it is useful to establish, in an overall sense, how the reinforcement will be distributed. The preliminary design established that beams would have a maximum depth of 32 in. and columns would be 30 in. by 30 in. In order to consider the beam-column joints "confined" per ACI 318 Sec. 21.5, it was necessary to set the beam width to 22.5 in., which is 75 percent of the column width.

In order to determine the effective depth used for the design of the beams, it is necessary to estimate the size and placement of the reinforcement that will be used. In establishing this depth, it is assumed that #8 bars will be used for longitudinal reinforcement and that hoops and stirrups will be constructed from #3 deformed bars. In all cases, clear cover of 1.5 in. is assumed. Since this structure has beams spanning in

two orthogonal directions, it is necessary to layer the flexural reinforcement as shown in Figure 6-13. The reinforcement for the E-W spanning beams was placed in the upper and lower layers because the strength demand for these members is somewhat greater than that for the N-S beams.

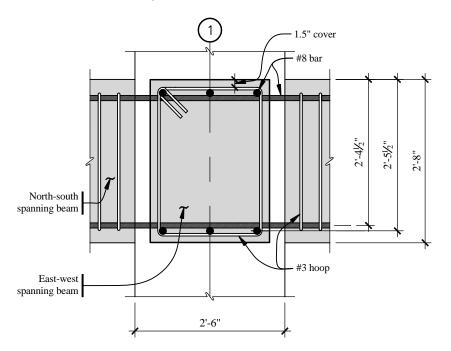


**Figure 6-13** Layout for beam reinforcement (1.0 ft = 0.3048 m, 1.0 in = 25.4 mm).

Given Figure 6-13, compute the effective depth for both positive and negative moment as:

Beams spanning in the E-W direction, d = 32 - 1.5 - 0.375 - 1.00/2 = 29.6 in. Beams spanning in the N-S direction, d = 32 - 1.5 - 0.375 - 1.0 - 1.00/2 = 28.6 in.

For negative moment bending, the effective width is 22.5 in. for all beams. For positive moment, the slab is in compression and the effective T-beam width varies according to ACI 318 Sec. 8.10. The effective widths for positive moment are as follows (with the parameter controlling effective width shown in parentheses):

20-ft beams in Frames 1 and 8	b = 22.5 + 20(12)/12 = 42.5 in. (span length)
Haunched beams	b = 22.5 + 2[8(4)] = 86.5 in. (slab thickness)
30-ft beams in Frames A, B, C, and D	b = 22.5 + [6(4)] = 46.5 in. (slab thickness)

ACI 318 Sec. 21.3.2 controls the longitudinal reinforcement requirements for beams. The minimum reinforcement to be provided at the top and bottom of any section is:

$$A_{s,min} = \frac{200b_w d}{f_v} = \frac{200(22.5)29.6}{60,000} = 2.22 \text{ in.}^2$$

This amount of reinforcement can be supplied by three #8 bars with  $A_s = 2.37$  in.<sup>2</sup> Since the three #8 bars will be provided continuously top and bottom, reinforcement required for strength will include these #8 bars.

Before getting too far into member design, it is useful to check the required tension development length for hooked bars since the required length may control the dimensions of the columns and the boundary elements of the structural walls.

From Eq. 21-6 of ACI 318 Sec. 21.5.4.1, the required development length is:

$$l_{dh} = \frac{f_y d_b}{65\sqrt{f_c'}}$$

For NW concrete, the computed length should not be less than 6 in. or  $8d_b$ . For LW concrete, the minimum length is the larger of 1.25 times that given by ACI 318 Eq. 21-6, 7.5 in., or  $10d_b$ . For  $f_c' = 4,000$  psi LW concrete, ACI 318 Eq. 21-6 controls for #3 through #11 bars.

For straight "top" bars,  $l_d = 3.5l_{dh}$  and for straight bottom bars,  $l_d = 2.5l_{dh}$ . These values are applicable only when the bars are anchored in well confined concrete (e.g., column cores and plastic hinge regions with confining reinforcement). The development length for the portion of the bar extending into unconfined concrete must be increased by a factor of 1.6. Development length requirements for hooked and straight bars are summarized in Table 6-13.

Where hooked bars are used, the hook must be 90 degrees and be located within the confined core of the column or boundary element. For bars hooked into 30-in.-square columns with 1.5 in. of cover and #4 ties, the available development length is 30 - 1.50 - 0.5 = 28.0 in. With this amount of available length, there will be no problem developing hooked bars in the columns. As required by ACI 318 Sec. 12.5, hooked bars have a  $12d_b$  extension beyond the bend. ACI 318 Sec. 7.2 requires that #3 through #8 bars have a  $6d_b$  bend diameter and #9 through #11 bars have a  $8d_b$  diameter.

Table 6-13 is applicable to bars anchored in joint regions only. For development of bars outside of joint regions, ACI 318 Chapter 12 should be used.

and Straight Bars in 4,000 psi Lw Concrete						
Bar Size	$d_b$ (in.)	$l_{dh}$ hook (in.)	$l_d$ top (in.)	$l_d$ bottom (in.)		
#4	0.500	9.1	31.9	22.8		
#5	0.625	11.4	39.9	28.5		
#6	0.750	13.7	48.0	34.3		
#7	0.875	16.0	56.0	40.0		
#8	1.000	18.2	63.7	45.5		
#9	1.128	20.6	72.1	51.5		
#10	1.270	23.2	81.2	58.0		
#11	1.410	25.7	90.0	64.2		

 
 Table 6-13
 Tension Development Length Requirements for Hooked Bars and Straight Bars in 4,000 psi LW Concrete

1.0 in. = 25.4 mm.

## 6.4.5.2 Design of Members of Frame 1 for E-W Loading

For the design of the members of Frame 1, the equivalent lateral forces of Table 6-7b were applied at an eccentricity of 10.5 ft together with 30 percent of the forces of Table 6-7a applied at an eccentricity of 5.0 ft. The eccentricities were applied in such a manner as to maximize torsional response and produce the largest shears in Frame 1.

For this part of the example, the design and detailing of all five beams and one interior column of Level 5 are presented in varying amounts of detail. The beams are designed first because the flexural capacity of the as-designed beams is a factor in the design and detailing of the column and the beam-column joint. The design of a corner column will be presented later.

Before continuing with the example, it should be mentioned that the design of ductile reinforced concrete moment frame members is dominated by the flexural reinforcement in the beams. The percentage and placement of beam flexural reinforcement governs the flexural rebar cutoff locations, the size and spacing of beam shear reinforcement, the cross-sectional characteristics of the column, the column flexural reinforcement, and the column shear reinforcement. The beam reinforcement is critical because the basic concept of ductile frame design is to force most of the energy-absorbing deformation to occur through inelastic rotation in plastic hinges at the ends of the beams.

In carrying out the design calculations, three different flexural strengths were used for the beams. These capacities were based on:

Design strength	$\phi = 0.8$ , tensile stress in reinforcement at $1.00 f_y$
Nominal strength	$\phi = 1.0$ , tensile stress in reinforcement at $1.00 f_y$
Probable strength	$\phi = 1.0$ , tensile stress in reinforcement at 1.25 $f_y$

Various aspects of the design of the beams and other members depend on the above capacities as follows:

Beam rebar cutoffs	Design strength
Beam shear reinforcement	Probable strength of beam
Beam-column joint strength	Probable strength of beam
Column flexural strength	$6/5 \times \text{nominal strength of beam}$
Column shear strength	Probable strength of column

In addition, beams in ductile frames will always have top and bottom longitudinal reinforcement throughout their length. In computing flexural capacities, only the tension steel will be considered. This is a valid design assumption because reinforcement ratios are quite low, yielding a depth to the neutral axis similar to the depth of the compression reinforcement (d'/d is about 0.08, while the neutral axis depth at ultimate ranges from 0.07 to 0.15 times the depth).<sup>3</sup>

The preliminary design of the girders of Frame 1 was based on members with a depth of 32 in. and a width of 22.5 in. The effective depth for positive and negative bending is 29.6 in. and the effective widths for positive and negative bending are 42.5 and 22.5 in., respectively. This assumes the stress block in compression is less than the 4.0-inch flange thickness.

The layout of the geometry and gravity loading on the three eastern-most spans of Level 5 of Frame 1 as well as the unfactored gravity and seismic moments are illustrated in Figure 6-14. The seismic moments are taken directly from the ETABS program output and the gravity moments were computed by hand

<sup>&</sup>lt;sup>3</sup>See Chapter 1 of the 2<sup>nd</sup> Edition of the *Handbook of Concrete Engineering* edited by Mark Fintel (New York: Van Nostrand Reinhold Company, 1984).

using the coefficient method of ACI 318 Chapter 8. Note that all moments (except for midspan positive moment) are given at the face of the column and that seismic moments are considerably greater than those due to gravity.

Factored bending moment envelopes for all five spans are shown in Figure 6-14. Negative moment at the supports is controlled by the 1.42D + 0.5L + 1.0E load combination, and positive moment at the support is controlled by 0.68D - 1.0E. Midspan positive moments are based on the load combination 1.2D + 1.6L. The design process is illustrated below starting with Span B-C.

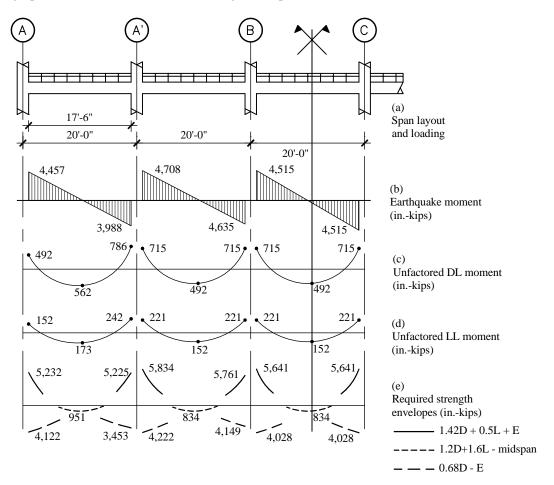


Figure 6-14 Bending moments for Frame 1 (1.0 ft = 0.3048 m, 1.0 in.-kip = 0.113 kN-m).

#### 6.4.5.2.1 Span B-C

1. Design for Negative Moment at the Face of the Support

 $M_u = 1.42(-715) + 0.5(-221) + 1.0(-4515) = -5,641$  in.-kips

Try two #9 bars in addition to the three #8 bars required for minimum steel:

 $A_s = 2(1.0) + 3(0.79) = 4.37 \text{ in.}^2$  $f_c' = 4,000 \text{ psi}$  $f_y = 60 \text{ ksi}$ 

OK

Width *b* for negative moment = 22.5 in. d = 29.6 in. Depth of compression block,  $a = A_s f_y / .85 f_c' b$  a = 4.37 (60)/[0.85 (4) 22.5] = 3.43 in. Design strength,  $\phi M_n = \phi A_s f_y (d - a/2)$  $\phi M_n = 0.8(4.37)60(29.6 - 3.43/2) = 5,849$  in.-kips > 5,641 in.-kips

2. Design for Positive Moment at Face of Support

 $M_{\mu} = [-0.68(715)] + [1.0(4,515)] = 4,028$  in.-kips

Try two #7 bars in addition to the three #8 bars already provided as minimum steel:

 $A_{s} = [2(0.60)] + [3(0.79)] = 3.57 \text{ in.}^{2}$ Width *b* for positive moment = 42.5 in. d = 29.6 in.a = [3.57(60)]/[0.85(4)42.5] = 1.48 in. $\phi M_{n} = 0.8(3.57) \ 60(29.6 - 1.48/2) = 4.945 \text{ in.-kips} > 4.028 \text{ in.-kips}$ OK

3. Positive Moment at Midspan

$$M_{\mu} = [1.2(492)] + [1.6(152)] = 833.6$$
 in.-kips

Minimum reinforcement (three #8 bars) controls by inspection. This positive moment reinforcement will also work for Spans A'-B and A-A'.

6.4.5.2.2 Span A'-B

1. Design for Negative Moment at the Face of Support A'

 $M_{\mu} = [1.42(-715)] + [0.5(-221)] + [1.0(-4,708)] = -5,834$  in.-kips

Three #8 bars plus two #9 bars (capacity = 5,849 in.-kips) will work as shown for Span B-C.

2. Design for Negative Moment at the Face of Support B

 $M_{u} = [1.42(-715)] + [0.5(-221)] + [1.0(-4,635)] = -5,761$  in.-kips

As before, use three #8 bars plus two #9 bars.

3. Design for Positive Moment at Face of Support A'

 $M_u = [-0.68(715)] + [1.0(4708)] = 4,222$  in.-kips

Three #8 bars plus two #7 bars (capacity = 4,945 in.-kips) works as shown for Span B-C.

4. Design for Positive Moment at Face of Support B'

 $M_u = [-0.68(715)] + [1.0(4,635)] = 4,149$  in.-kips

As before, use three #8 bars plus two #7 bars.

#### 6.4.5.2.3 Span A-A'

1. Design for Negative Moment at the Face of Support A

 $M_u = [1.42(-492)] + [0.5(-152)] + [1.0(-4,457)] = -5,232$  in.-kips

Try three #8 bars plus two #8 bars:

 $A_s = 5 \times 0.79 = 3.95 \text{ in.}^2$ Width *b* for negative moment = 22.5 in. d = 29.6 in.a = [3.95(60)/[0.85(4)22.5] = 3.10 in. $\phi M_n = [0.8(3.95)60]$  (29.6 - 3.10/2) = 5,318 in.-kips > 5,232 in.-kips

2. Design for Negative Moment at the Face of Support A'

 $M_{\mu} = [1.42(-786)] + [0.5(-242)] + [1.0(-3,988)] = -5,225$  in.-kips

Use three #8 bars plus two #9 bars as required for Support B of Span A'-B.

OK

3. Design for Positive Moment at Face of Support A

 $M_u = [-0.68(492)] + [1.0(4,457)] = 4,122$  in.-kips

Three #8 bars plus two #7 bars will be sufficient.

4. Design for Positive Moment at Face of Support A'

 $M_{\mu} = [-0.68(786)] + [1.0(3,988)] = 3,453$  in.-kips

As before, use three #8 bars plus two #7 bars.

6.4.5.2.4 Spans C-C' and C'-D

Reinforcement requirements for Spans C-C' and C'-D are mirror images of those computed for Spans A'-B and A-A', respectively.

In addition to the computed strength requirements and minimum reinforcement ratios cited above, the final layout of reinforcing steel also must satisfy the following from ACI 318 Sec. 21.3.2:

Minimum of two bars continuous top and bottom	OK (three #8 bars continuous top and bottom)
Positive moment strength greater than 50 percent negative moment strength at a joint	OK (at all joints)
Minimum strength along member greater than 0.25 maximum strength	OK ( $A_s$ provided = three #8 bars is more than 25 percent of reinforcement provided at joints)

The preliminary layout of reinforcement is shown in Figure 6-15. The arrangement of bars actually provided is based on the above computations with the exception of Span B-C where a total of six #8 top bars were used instead of the three #8 bars plus two #9 bars combination. Similarly, six #8 bars are used at the bottom of Span B-C. The use of six #8 bars is somewhat awkward for placing steel, but it allows

for the use of three #8 continuous top and bottom at all spans. An alternate choice would have been to use two #9 continuous across the top of Span B-C instead of the three of the #8 bars. However, the use of two #9 bars ( $\rho = 0.00303$ ) does not meet the minimum reinforcement requirement  $\rho_{min} = 0.0033$ .

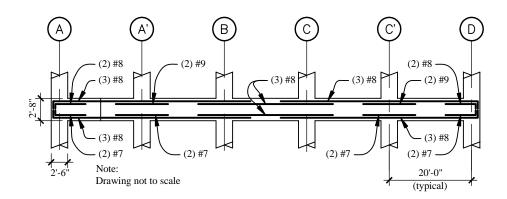


Figure 6-15 Preliminary rebar layout for Frame 1 (1.0 ft = 03.048 m).

As mentioned above, later phases of the frame design will require computation of the design strength and the maximum probable strength at each support. The results of these calculations are shown in Table 6-14.

		Location					
Item		А	A'	В	С	C'	D
Negative Moment	Reinforcement	five #8	three #8 + two #9	six #8	six #8	three #8 + two #9	five #8
	Design Strength (inkips)	5,318	5,849	6,311	7,100	5,849	5,318
	Probable Strength (inkips)	8,195	8,999	9,697	9,697	8,999	8,195
Positive Moment	Reinforcement	three #8 + two #7	three #8 + two #7	six #8	six #8	three #8 + two #7	three #8 + two #7
	Design Strength (inkips)	4,945	4,945	6,510	6,510	4,945	4,945
	Probable Strength (inkips)	7,677	7,677	10,085	10,085	7,655	7,677

 Table 6-14
 Design and Maximum Probable Flexural Strength For Beams in Frame 1

1.0 in.-kip = 0.113 kN-m.

As an example of computation of probable strength, consider the case of six #8 top bars:

 $A_s = 6(0.79) = 4.74 \text{ in.}^2$ Width *b* for negative moment = 22.5 in. d = 29.6 in. Depth of compression block,  $a = A_s(1.25f_y)/0.85f_c'b$ a = 4.74(1.25)60/[0.85(4)22.5] = 4.65 in.  $M_{pr} = 1.0A_s(1.25f_y)(d - a/2)$   $M_{pr} = 1.0(4.74)1.25(60)(29.6 - 4.65/2) = 9,697$  in.-kips

For the case of six #8 bottom bars:

 $A_s = 6(0.79) = 4.74 \text{ in.}^2$ Width *b* for positive moment = 42.5 in. d = 29.6 in.  $a = 4.74(1.25)60/(0.85 \times 4 \times 42.5) = 2.46$  in.  $M_{pr} = 1.0(4.74)1.25(60)(29.6 - 2.46/2) = 10,085$  in.-kips

#### 6.4.5.2.5 Adequacy of Flexural Reinforcement in Relation to the Design of the Beam-Column Joint

Prior to this point in the design process, the layout of reinforcement has been considered preliminary because the quantity of reinforcement placed in the girders has a direct bearing on the magnitude of the stresses developed in the beam-column joint. If the computed joint stresses are too high, the only remedies are increasing the concrete strength, increasing the column area, changing the reinforcement layout, or increasing the beam depth. The option of increasing concrete strength is not viable for this example because it is already at the maximum (4,000 psi) allowed for LW concrete. If absolutely necessary, however, NW concrete with a strength greater than 4,000 psi may be used for the columns and beam-column joint region while the LW concrete is used for the joists and beams.

The design of the beam-column joint is based on the requirements of ACI 318 Sec. 21.5.3. The determination of the forces in the joint of the column on Gridline C of Frame 1 is based on Figure 6-16a, which shows how plastic moments are developed in the various spans for equivalent lateral forces acting to the east. An isolated subassemblage from the frame is shown in Figure 6-16b. The beam shears shown in Figure 6-16c are based on the probable moment strengths shown in Table 6-14.

For forces acting from west to east, compute the earthquake shear in Span B-C:

 $V_E = (M_{pr} + M_{pr})/l_{clear} = (9,697 + 10,085)/(240 - 30) = 94.2$  kips

For Span C-C':

 $V_E = (10,085 + 8,999)/(240 - 30) = 90.9$  kips

With the earthquake shear of 94.2 and 90.9 kips being developed in the beams, the largest shear that theoretically can be developed in the column above Level 5 is 150.5 kips. This is computed from equilibrium as shown at the bottom of Figure 6-16:

 $94.2(9.83) + 90.9(10.50) = 2V_c(12.5/2)$  $V_c = 150.4$  kips

With equal spans, gravity loads do not produce significant column shears, except at the end column, where the seismic shear is much less. Therefore, gravity loads are not included in this computation.

The forces in the beam reinforcement for negative moment are based on six #8 bars at  $1.25 f_y$ :

T = C = 1.25(60)[(6(0.79)] = 355.5 kips

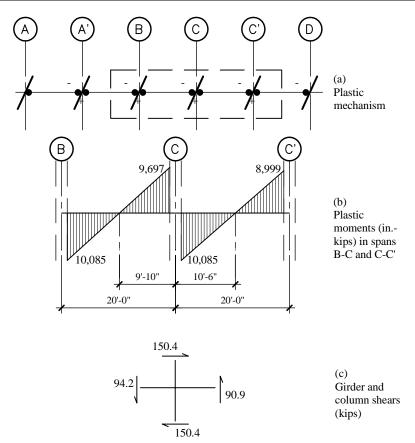


**Figure 6-16** Diagram for computing column shears (1.0 ft = 0.3048 m, 1.0 kip = 4.45 kN, 1.0 in.-kip = 0.113 kN-m).

For positive moment, six #8 bars also are used, assuming C = T, C = 355.5 kips.

As illustrated in Figure 6-17, the joint shear force  $V_i$  is computed as:

$$V_j = T + C - V_E$$
  
= 355.5 + 355.5 - 150.4  
= 560.6 kips

The joint shear stress is:

$$v_j = \frac{V_j}{d_c^2} = \frac{560.5}{30^2} = 623 \text{ psi}$$

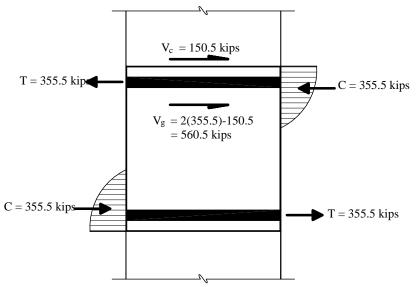


Figure 6-17 Computing joint shear stress (1.0 kip = 4.45kN).

For joints confined on three faces or on two opposite faces, the allowable shear stress for LW concrete is based on ACI 318 Sec. 21.5.3. Using  $\phi = 0.80$  for joints (from ACI Appendix C) and a factor of 0.75 as a modifier for LW concrete:

 $v_{i \text{ allowable}} = 0.80(0.75)(15\sqrt{4,000}) = 569 \text{ psi}$ 

[Note that for joints,  $\varphi = 0.85$  per ACI 318-02 Sec 9.3 as referenced by the 2003 *Provisions*. See Sec 6.4.2 for discussion.]

Since the actual joint stress (623 psi) exceeds the allowable stress (569 psi), the joint is overstressed. One remedy to the situation would be to reduce the quantity of positive moment reinforcement. The six #8 bottom bars at Columns B and C could be reduced to three #8 bars plus two #7 bars. This would require a somewhat different arrangement of bars than shown in Figure 6-15. It is left to the reader to verify that the joint shear stress would be acceptable under these circumstances. Another remedy would be to increase the size of the column. If the column is increased in size to 32 in. by 32 in., the new joint shear stress is:

$$v_j = \frac{V_j}{d_c^2} = \frac{560.5}{32^2} = 547 \text{psi} < 569 \text{ psi}$$

which is also acceptable. For now we will proceed with the larger column, but as discussed later, the final solution will be to rearrange the bars to three #8 plus two #7.

Joint stresses would be checked for the other columns in a similar manner. Because the combined area of top and bottom reinforcement used at Columns A, A', C', and D is less than that for Columns B and C, these joints will not be overstressed.

Given that the joint stress is acceptable, ACI 318 Sec. 21.5.2.3 controls the amount of reinforcement required in the joint. Since the joint is not confined on all four sides by a beam, the total amount of transverse reinforcement required by ACI 318 Sec. 21.4.4 will be placed within the depth of the joint. As shown later, this reinforcement consists of four-leg #4 hoops at 4 in. on center.

Because the arrangement of steel is acceptable from a joint strength perspective, the cutoff locations of the various bars may be determined (see Figure 6-15 for a schematic of the arrangement of reinforcement). The three #8 bars (top and bottom) required for minimum reinforcement are supplied in one length that runs continuously across the two end spans and are cut off in the center span. An additional three #8 bars are placed top and bottom in the center span; these bars are cut off in Spans A'-B and C-C'. At Supports A, A', C' and D, shorter bars are used to make up the additional reinforcement required for strength.

To determine where bars should be cut off in each span, it is assumed that theoretical cutoff locations correspond to the point where the continuous top and bottom bars develop their design flexural strength. Cutoff locations are based on the members developing their design flexural capacities ( $f_y = 60$  ksi and  $\phi = 0.8$ ). Using calculations similar to those above, it has been determined that the design flexural strength supplied by a section with only three #8 bars is 3,311 in.-kips for positive moment and 3,261 in.-kips for negative moment.

Sample cutoff calculations are given first for Span B-C. To determine the cutoff location for negative moment, it is assumed that the member is subjected to earthquake plus 0.68 times the dead load forces. For positive moment cutoffs, the loading is taken as earthquake plus 1.42 times dead load plus 0.5 times live load. Loading diagrams for determining cut off locations are shown in Figure 6-18.

For negative moment cutoff locations, refer to Figure 6-19a, which is a free body diagram of the west end of the member. Since the goal is to develop a negative moment capacity of 3,261 in.-kips in the continuous #8 bars summing moments about Point A in Figure 6-19a:

$$6,311 + \frac{0.121x^2}{2} - 73.7x = 3,261$$

In the above equation, 6,311 (in.-kips) is the negative moment capacity for the section with six #8 bars, 0.121 (kips/in.) is 0.68 times the uniform dead load, 73.3 kips is the end shear, and 3,261 in.-kips is the design strength of the section with three #8 bars. Solving the quadratic equation results in x = 42.9 in. ACI 318 Sec. 12.10.3 requires an additional length equal to the effective depth of the member or 12 bar diameters (whichever is larger). Consequently, the total length of the bar beyond the face of the support is 42.9 + 29.6 = 72.5 in. and a 6 ft-1 in. extension beyond the face of the column could be used.

For positive moment cutoff, see Figure 6-14 and Figure 6-19b. The free body diagram produces an equilibrium equation as:

$$6,510 - \frac{0.281x^2}{2} - 31.6x = 3,311$$

where the distance x is computed to be 75.7 in. Adding the 29.6 in. effective depth, the required extension beyond the face of the support is 76.0 + 29.6 = 105.3 in, or 8 ft-9 in. Note that this is exactly at the midspan of the member.

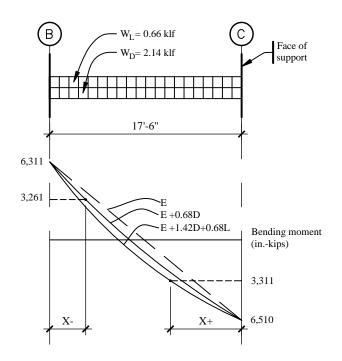
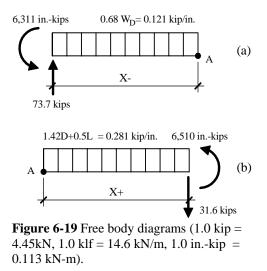


**Figure 6-18** Loading for determination of rebar cutoffs (1.0 ft = 0.3048 m, 1.0 klf = 14.6 kN/m, 1.0 in.-kip = 0.113 kN-m).



Clearly, the short bottom bars shown in Figure 6-15 are impractical. Instead, the bottom steel will be rearranged to consist of three #8 plus two #7 bars continuous. Recall that this arrangement of reinforcement will satisfy joint shear requirements, and the columns may remain at 30 in. by 30 in.

As shown in Figure 6-20, another requirement in setting cutoff length is that the bar being cut off must have sufficient length to develop the strength required in the adjacent span. From Table 6-13, the required development length of the #9 top bars in tension is 72.1 in. if the bar is anchored in a confined joint region. The confined length in which the bar is developed is shown in Figure 6-20 and consists of

the column depth plus twice the depth of the girder. This length is 30 + 32 + 32 = 94 in., which is greater than the 72.1 in. required. The column and girder are considered confined because of the presence of closed hoop reinforcement as required by ACI 318 Sec. 21.3.3 and 21.4.4.

The bottom bars are spliced at the center of Spans A'-B and C-C' as shown in Figure 6-21. The splice length is taken as the bottom bar Class B splice length for #8 bars. According to ACI 318 Sec. 12.15, the splice length is 1.3 times the development length. From ACI 318 Sec. 12.2.2, the development length ( $l_d$ ) is computed from:

$$\frac{l_d}{d_b} = \frac{3}{40} \frac{f_y}{\sqrt{f_c'}} \frac{\alpha \beta \gamma \lambda}{\left(\frac{c + K_{tr}}{d_b}\right)}$$

using  $\alpha = 1.0$  (bottom bar),  $\beta = 1.0$  (uncoated),  $\gamma = 1.0$  (#9 bar),  $\lambda = 1.3$  (LW concrete), taking *c* as the cover (1.5 in.) plus the tie dimension (0.5 in.) plus 1/2 bar diameter (0.50 in.) = 2.50 in., and using  $K_{tr} = 0$ , the development length for one #9 bar is:

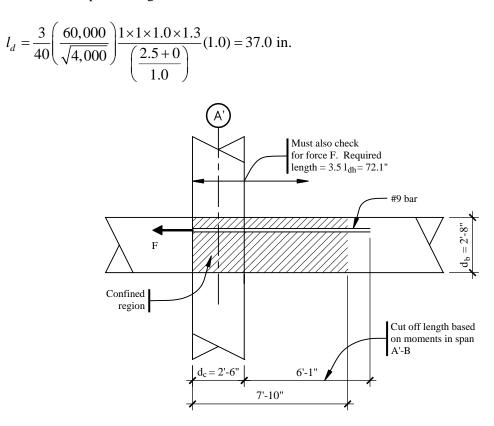


Figure 6-20 Development length for top bars (1.0 ft = 0.3048 m, 1.0 in = 25.4 mm).

The splice length =  $1.3 \times 37.0 = 48.1$  in. Therefore, use a 48-in. contact splice. According to ACI 318 Sec. 21.3.2.3, the entire region of the splice must be confined by closed hoops spaced no closer than d/4 or 4 in.

The final bar placement and cutoff locations for all five spans are shown in Figure 6-21. Due to the different arrangement of bottom steel, the strength at the supports must be recomputed. The results are shown in Table 6-15.

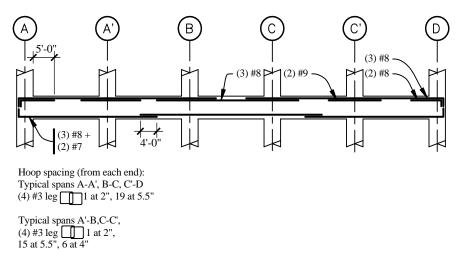


Figure 6-21 Final bar arrangement (1.0 ft = 0.3048 m, 1.0 in = 25.4 mm).

 Table 6-15
 Design and Maximum Probable Flexural Strength For Beams in Frame 1 (Revised)

		Location					
Item		А	A'	В	С	C'	D
Negative Moment	Reinforcement	five #8	three #8 + two #9	six #8	six #8	three #8 + two #9	five #8
	Design Moment (inkips)	5,318	5,849	6,311	6,311	5,849	5,318
	Probable moment (inkips)	8,195	8,999	9,696	9,696	8,999	8,195
Positive Moment	Reinforcement	three #8 + two #7	three #8 + two #7	three #8 + two #7	three #8 + two #7	three #8 + two #7	three #8 + two #7
	Design Moment (inkips)	4,944	4,944	4,944	4,944	4,944	4,944
	Probable moment (inkips)	7,677	7,677	7,677	7,677	7,677	7,677

1.0 in.-kip = 0.113 kN-m.

#### 6.4.5.2.6 Transverse Reinforcement

Transverse reinforcement requirements are covered in ACI 318 Sec. 21.3.3 (minimum reinforcement) and 21.3.4 (shear strength).

To avoid nonductile shear failures, the shear strength demand is computed as the sum of the factored gravity shear plus the maximum probable earthquake shear. The maximum probable earthquake shear is based on the assumption that  $\phi = 1.0$  and the flexural reinforcement reaches a tensile stress of  $1.25f_y$ . The probable moment strength at each support is shown in Table 6-15.

Figure 6-22 illustrates the development of the design shear strength envelopes for Spans A-A', A'-B, and B-C. In Figure 6-22a, the maximum probable earthquake moments are shown for seismic forces acting to the east (solid lines) and to the west (dashed lines). The moments shown occur at the face of the supports.

The earthquake shears produced by the maximum probable moments are shown in Figure 6-22b. For Span A-B, the values shown in the figure are:

$$V_E = \frac{M_{pr}^- + M_{pr}^+}{l_{clear}}$$

where  $l_{clear} = 17$  ft-6 in. = 210 in.

Note that the earthquake shears act in different directions depending on the direction of load.

For forces acting to the east,  $V_E = (9696 + 7677) / 210 = 82.7$  kips. For forces acting to the west,  $V_E = (8999 + 7677) / 210 = 79.4$  kips.

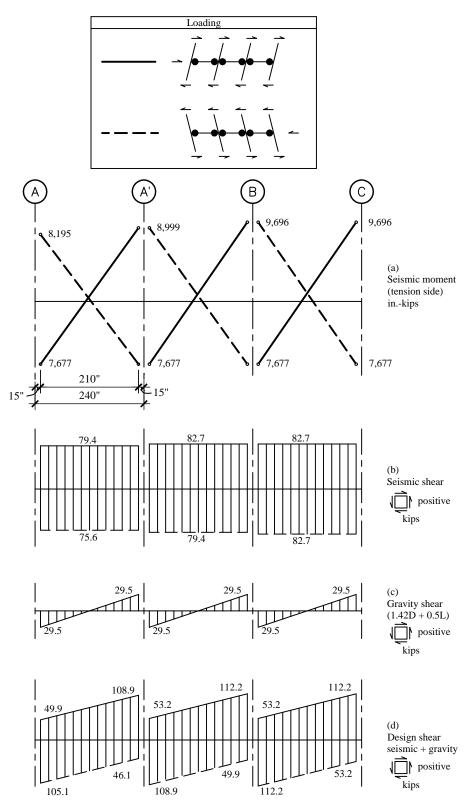


**Figure 6-22** Shear forces for transverse reinforcement (1.0 in = 25.4 mm, 1.0 kip = 4.45kN, 1.0 in.-kip = 0.113 kN-m).

The gravity shears shown in Figure 6-22c are:

Factored gravity shear =  $V_G = 1.42V_{dead} + 0.5V_{live}$  $V_{dead} = 2.14 \times 17.5/2 = 18.7$  kips  $V_{live} = 0.66 \times 17.5/2 = 5.8$  kips  $V_G = 1.42(18.7) + 0.5(5.8) = 29.5$  kips

Total design shears for each span are shown in Figure 6-22d. The strength envelope for Span B-C is shown in detail in Figure 6-23, which indicates that the maximum design shears is 82.7 + 29.5 = 112.2 kips. While this shear acts at one end, a shear of 82.7 - 29.5 = 53.2 kips acts at the opposite end of the member.

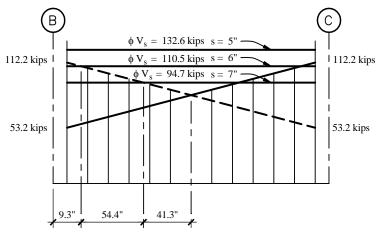


**Figure 6-23** Detailed shear force envelope in Span B-C (1.0 in = 25.4 mm, 1.0 kip = 4.45 kN).

In designing shear reinforcement, the shear strength can consist of contributions from concrete and from steel hoops or stirrups. However, according to ACI 318 Sec. 21.3.4.2, the design shear strength of the concrete must be taken as zero when the axial force is small  $(P_u/A_g f'_c < 0.05)$  and the ratio  $V_E/V_u$  is greater than 0.5. From Figure 6-22, this ratio is  $V_E/V_u = 82.7/112.2 = 0.73$ , so concrete shear strength must be taken as zero. Using the ASCE 7 compatible  $\phi$  for shear = 0.75, the spacing of reinforcement required is computed as described below. [Note that this is the basic strength reduction factor for shear per ACI 318-02 Sec 9.3. See Sec 6.4.2 for discussion.]

Compute the shear at d = 29.6 in. from the face of the support:

$$V_u = \phi V_s = 112.2 - (29.6/210)(112.2 - 53.2) = 103.9$$
 kips  
 $V_s = A_v f_v d/s$ 

Assuming four #3 vertical legs ( $A_v = 0.44 \text{ in.}^2$ ),  $f_v = 60 \text{ ksi}$  and d = 29.6 in., compute the required spacing:

$$s = \phi A_{y} f_{y} d/V_{u} = 0.75[4(0.11)](60)(29.6/103.9) = 5.65$$
 in., say 5.5 in.

At midspan, the design shear  $V_u = (112.2 + 53.2)/2 = 82.7$  kips. Compute the required spacing:

s = 0.75[4(0.11)](60)(29.6/82.7) = 7.08 in., say 7.0 in.

Check maximum spacing per ACI 318 Sec. 21.3.3.2:

d/4 = 29.6/4 = 7.4 in.  $8d_b = 8(1.0) = 8.0$  in.  $24d_h = 24(3/8) = 9.0$  in.

The spacing must vary between 5.5 in. at the support and 7.0 in. at midspan. Due to the relatively flat shear force gradient, a spacing of 5.5 in. will be used for the full length of the beam. The first hoop must be placed 2 in. from the face of the support. This arrangement of hoops will be used for Spans A-A', B-C, and C'-D. In Spans A'-B and C-C', the bottom flexural reinforcement is spliced and hoops must be placed over the splice region at d/4 or a maximum of 4 in. on center.

ACI 318 Sec. 21.3.3.1 states that closed hoops are required over a distance of twice the member depth from the face of the support. From that point on, stirrups may be used. For the girders of Frame 1, however, stirrups will not be used, and the hoops will be used along the entire member length. This is being done because the earthquake shear is a large portion of the total shear, the girder is relatively short, and the economic premium is negligible.

Where hoops are required (first 64 in. from face of support), longitudinal reinforcing bars should be supported as specified in ACI 318 Sec. 7.10.5.3. Hoops should be arranged such that every corner and alternate longitudinal bar is supported by a corner of the hoop assembly and no bar should be more than 6 in. clear from such a supported bar. Details of the transverse reinforcement layout for all spans of Level 5 of Frame 1 are shown in Figure 6-21.

# 6.4.5.3 Design of a Typical Interior Column of Frame 1

This section illustrates the design of a typical interior column on Gridline A'. The column, which supports Level 5 of Frame 1, is 30 in. square and is constructed from 4,000 psi LW concrete, 60 ksi longitudinal reinforcement, and 60 ksi transverse reinforcement. An isolated view of the column is shown in Figure 6-24. The flexural reinforcement in the beams framing into the column is shown in Figure 6-21. Using simple tributary area calculations (not shown), the column supports an unfactored axial dead load of 528 kips and an unfactored axial live load of 54 kips. The ETABS analysis indicates that the maximum axial earthquake force is 84 kips, tension or compression. The load combination used to compute this force consists of full earthquake force in the E-W direction, 30 percent of the N-S force, and accidental torsion. Because no beams frame into this column along Gridline A', the column bending moment for N-S forces can be neglected. Hence, the column is designed for axial force plus uniaxial bending.

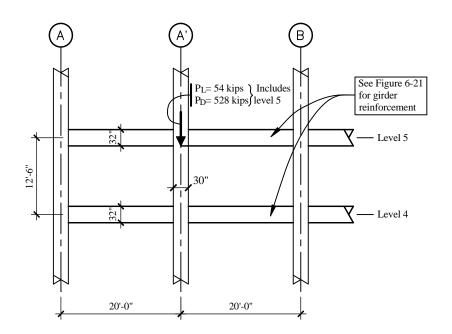


**Figure 6-24** Layout and loads on column of Frame A (1.0 ft = 0.3048 m, 1.0 in = 25.4 mm, 1.0 kip = 4.45 kN).

#### 6.4.5.3.1 Longitudinal Reinforcement

To determine the axial design loads, use the basic load combinations:

1.42D + 0.5L + 1.0E0.68D - 1.0E.

The combination that results in maximum compression is:

 $P_{\mu} = 1.42(528) + 0.5(54) + 1.0(84) = 861$  kips (compression)

The combination for minimum compression (or tension) is:

 $P_u = 0.68(528) - 1.0(84) = 275$  kips (compression)

The maximum axial compression force of 861 kips is greater than  $0.1f_c'A_g = 0.1(4)(30^2) = 360$  kips. Thus, according to ACI 318 Sec. 21.4.2, the nominal column flexural strength must be at least 6/5 of the nominal flexural strength of the beams framing into the column. Beam moments at the face of the support are used for this computation. These capacities are provided in Table 6-15.

Nominal (negative) moment strength at end A' of Span A-A' = 5,849/0.8 = 7,311 in.-kips Nominal (positive) moment strength at end A' of Span A' B = 4,945/0.8 = 6,181 in.-kips Average nominal moment framing into joint = 6,746 in.-kips Nominal column design moment =  $6/5 \times 6746 = 8,095$  in.-kips.

Knowing the factored axial load and the required design flexural strength, a column with adequate capacity must be selected. Figure 6-25 gives design curves for 30 in. by 30 in. columns of 4,000 psi concrete and reinforcement consisting of 12 #8, #9, or #10 bars. These curves, computed with a

Microsoft Excel spreadsheet, are based on a  $\phi$  factor of 1.0 as required for nominal strength. At axial forces of 275 kips and 861 kips, solid horizontal lines are drawn. The dots on the lines represent the required nominal flexural strength (8095 in.-kips) at each axial load level. These dots must lie to the left of the curve representing the design columns. For both the minimum and maximum axial forces, a column with 12 #8 bars (with  $A_s = 9.48$  in.<sup>2</sup> and 1.05 percent of steel) is clearly adequate.

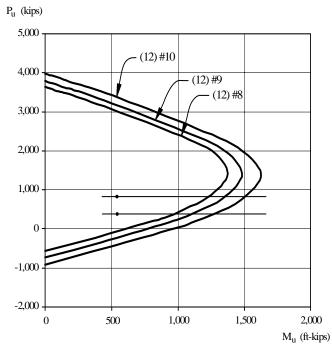


**Figure 6-25** Design interaction diagram for column on Gridline A' (1.0 kip = 4.45 kN, 1.0 ft-kip = 1.36 kN-m).

#### 6.4.5.3.2 Transverse Reinforcement

ACI 318 Sec. 21.4.4 gives the requirements for minimum transverse reinforcement. For rectangular sections with hoops, ACI 318 Eq. 21-3 and 21-4 are applicable:

$$A_{sh} = 0.3 \left( \frac{sh_c f_c'}{f_{yh}} \right) \left( \frac{A_g}{A_{ch}} - 1 \right)$$
$$A_{sh} = 0.09 sh_c \frac{f_c'}{f_{yh}}$$

The first of these equations controls when  $A_e/A_{ch} > 1.3$ . For the 30-in.-by-30-in. columns:

$$A_{ch} = (30 - 1.5 - 1.5)^2 = 729 \text{ in.}^2$$
  
 $A_g = 30 (30) = 900 \text{ in.}^2$   
 $A_g/A_{ch} = 900/729 = 1.24$ 

ACI 318 Eq. 21-4 therefore controls.

For LW concrete, try hoops with four #4 legs and  $f_c' = 4,000$  psi:

 $h_c = 30 - 1.5 - 1.5 - 0.25 - 0.25 = 26.5$  in. s = [4 (0.2) 60,000]/[0.09 (26.5) 4000] = 5.03 in.

However, the maximum spacing of transverse reinforcement is the lesser of one-fourth the maximum column dimension (30/4=7.5 in.), six bar diameters ( $6 \times 1.0 = 6.0$  in.), or the dimension  $s_x$  where:

$$s_x = 4 + \frac{14 - h_x}{3}$$

and where  $h_x$  is the maximum horizontal spacing of hoops or cross ties. For the column with twelve #8 bars and #4 hoops and cross ties,  $h_x = 8.833$  in. and  $s_x = 5.72$  in. The 5.03-in. spacing required by ACI Eq. 21-4 controls, so a spacing of 5 in. will be used. This transverse reinforcement must be spaced over a distance  $l_o = 30$  in. at each end of the member and, according to ACI 318 Sec. 21.5.2, must extend through the joint at (at most) the same spacing.

ACI 318 Sec. 21.4.4.6 requires a maximum spacing of transverse reinforcement in the region of the column not covered by Sec. 21.4.4.4. The maximum spacing is the smaller of 6.0 in. or  $6d_b$ , which for #8 bars is also 6 in. ACI 318 requires transverse steel at this spacing, but it does not specify what the details of reinforcement should be. In this example, hoops and crossties with the same details as those placed in the critical regions of the column are used.

#### 6.4.5.3.3 Transverse Reinforcement Required for Shear

The amount of transverse reinforcement computed above is the minimum required. The column also must be checked for shear with the column shears being based on the maximum probable moments in the beams that frame into the column. The average probable moment is roughly 1.25/0.8 ( $\phi = 0.8$ ) times the average design moment = (1.25/0.8)(5397) = 8,433 in.-kips. With a clear height of 118 in., the column shear can be estimated at 8433/(0.5x118) = 143 kips. This shear will be compared to the capacity provided by the 4-leg #4 hoops spaced at 6 in. on center. If this capacity is well in excess of the demand, the columns will be acceptable for shear.

For the design of column shear capacity, the concrete contribution to shear strength may be considered because  $P_u > A_g f'_c/20$ . Using a shear strength reduction factor of 0.85 for sand-LW concrete (ACI 318 Sec. 11.2.1.2) in addition to the capacity reduction factor for shear, the design shear strength contributed by concrete is:

$$\phi V_c = \phi 0.75 \sqrt{f'_c} b_c d_c = 0.75 (0.85) (\sqrt{4,000}(30)(27.5) = 33.2 \text{ kips}$$
  
$$\phi V_s = \phi A_v f_y d / s = 0.75 (4) (0.2) (60) (27.5) / 6 = 165 \text{ kips}$$
  
$$\phi V_n = \phi V_c + \phi V_s = 33.2 + 165 = 198.2 \text{ kips} > 143 \text{ kips}$$
 OK

The column with the minimum transverse steel is therefore adequate for shear. The final column detail with both longitudinal and transverse reinforcement is given in Figure 6-26. The spacing of reinforcement through the joint has been reduced to 4 in. on center. This is done for practical reasons only. Column bar splices, where required, should be located in the center half of the of the column and must be proportioned as (Class B) tension splices.

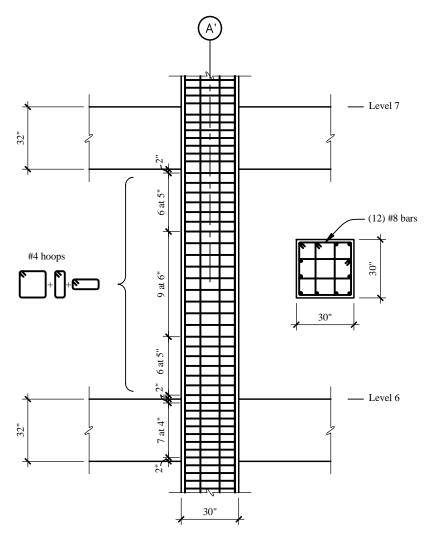


**Figure 6-26** Details of reinforcement for column (1.0 in = 25.4 mm).

### 6.4.5.4 Design of Haunched Girder

The design of a typical haunched girder of Level 5 of Frame 3 is now illustrated. This girder is of variable depth with a maximum depth of 32 in. at the support and a minimum depth of 20 in. for the middle half of the span. The length of the haunch at each end (as measured from the face of the support) is 8 ft-9 in. The width of the web of girder is 22.5 in. throughout.

Based on a tributary gravity load analysis, this girder supports an average of 3.375 kips/ft of dead load and 0.90 kips/ft of reduced live load. For the purpose of estimating gravity moments, a separate analysis of the girder was carried out using the SAP2000 program. End A of the girder was supported with half-height columns pinned at midstory and End B, which is supported by a shear wall, was modeled as fixed. Each haunch was divided into four segments with nonprismatic section properties used for each segment. The loading and geometry of the girder is shown in Figure 6-27a.

For determining earthquake forces, the entire structure was analyzed using the ETABS program. This analysis included 100 percent of the earthquake forces in the E-W direction and 30 percent of the

earthquake force in the N-S direction, and accidental torsion. Each of these systems of lateral forces was placed at a 5 percent eccentricity with the direction of the eccentricity set to produce the maximum seismic shear in the member.

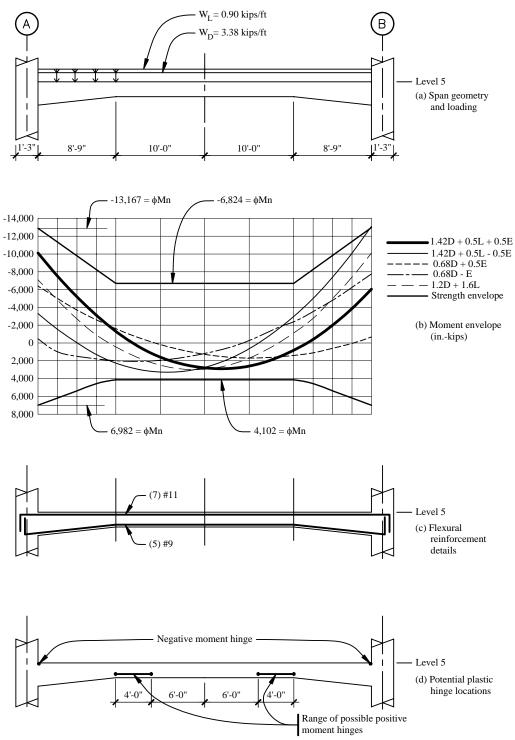


**Figure 6-27** Design forces and detailing of haunched girder (1.0 ft = 0.3048 m, 1.0 k/ft = 14.6 kN/m, 1.0 in.-kip = 0.113 kN-m).

### 6.4.5.4.1 Design and Detailing of Longitudinal Reinforcement

The results of the analysis for five different load combinations are shown in Figure 6-27b. Envelopes of maximum positive and negative moment are shown on the figure indicate that  $1.42D + 0.5L \pm E$  controls negative moment at the support,  $0.68D \pm E$  controls positive moment at the support, and 1.2D + 1.6L controls positive moment at midspan. The maximum positive moment at the support is less than 50 percent of the maximum negative moment; therefore, the design for negative moment controls the amount of reinforcement required at all sections per ACI 318 Sec. 21.3.2.2.

For a factored negative moment of 12,600 in.-kips at Support B, try seven #11 bars, and assuming #3 hoops:

 $\begin{array}{l} A_s = 7 \times 1.54 = 10.92 \text{ in.}^2 \\ d = 32 - 1.5 - 3/8 - 1.41/2 = 29.4 \text{ in.} \\ \rho = 10.92/(29.4 \times 22.5) = 0.0165 < 0.025, \text{ O.K.} \\ b = 22.5 \text{ in.} \\ \end{array}$ Depth of compression block,  $a = [10.92 \ (60)]/[0.85 \ (4) \ 22.5] = 8.56 \text{ in.} \\ \end{array}$ Design strength,  $\phi M_n = [0.8 \ (10.92) \ 60](29.4 - 8.56/2) = 13,167 \text{ in.-kips} > 12,600 \text{ in.-kips}$  OK

For positive moment at the support, try five #9 bars, which supplies about half the negative moment reinforcement:

 $\begin{array}{l} A_s = 5 \ (1.0) = 5.00 \ \text{in.}^2 \\ d = 32 - 1.5 - 3/8 - 1.128/2 = 29.6 \ \text{in.} \\ \rho = 5.00/(29.6 \times 22.5) = 0.0075 > 0.033, \text{ O.K.} \\ b = 86.5 \ \text{in.} \ (\text{assuming stress block in flange}) \\ a = [5.00 \ (60)]/(0.85 \ (4) \ 86.5] = 1.02 \ \text{in.} \\ \phi M_n = [0.8 \ (5.00) \ 60] \ (29.6 - 1.02/2) = 6,982 \ \text{in.-kips.} \end{array}$ 

This moment is larger than the design moment and, as required by ACI 318 Sec. 21.3.2.2, is greater than 50 percent of the negative moment capacity at the face of the support.

For positive moment at midspan the same five #9 bars used for positive moment at the support will be tried:

$$\begin{split} A_s &= 5 \ (1.0) = 5.00 \ \text{in.}^2 \\ d &= 20 - 1.5 - 3/8 - 1.128/2 = 17.6 \ \text{in.} \\ \rho &= 5.00/(17.6 \times 22.5) = 0.0126 \\ b &= 86.5 \ \text{in.} \\ a &= [5.00 \ (60)]/[0.85 \ (4) \ 86.5] = 1.02 \ \text{in.} \\ \phi M_n &= [0.8 \ (5.00) \ 60] \ (17.6 - 1.02/2) = 4,102 \ \text{in.-kips} > 3,282 \ \text{in.-kips.} \end{split}$$

The five #9 bottom bars are adequate for strength and satisfy ACI 318 Sec. 21.3.2.2, which requires that the positive moment capacity be not less than 25 percent of the negative moment capacity at the face of the support.

OK

For negative moment in the 20-ft span between the haunches, four #11 bars ( $\rho = 0.016$ ) could be used at the top. These bars provide a strength greater than 25 percent of the negative moment capacity at the support. Using four bars across the top also eliminates the possibility that a negative moment hinge will form at the end of the haunch (8 ft-9 in. from the face of the support) when the 0.68D - E load combination is applied. These four top bars are part of the negative moment reinforcement already sized

for negative moment at the support. The other three bars extending from the support are not needed for negative moment in the constant depth region and would be cut off approximately 6 ft beyond the haunch; however, this detail results in a possible bar cutoff in a plastic hinge region (see below) that is not desirable. Another alternative would be to extend all seven #11 bars across the top and thereby avoid the bar cutoff in a possible plastic hinge region; however, seven #11 bars in 20-in. deep portion of the girder provide  $\rho = 0.028$ , which is a violation of ACI 21.3.2.1 ( $\rho_{max} = 0.025$ ). The violation is minor and will be accepted in lieu of cutting off the bars in a potential plastic hinge region. Note that these bars provide a negative design moment capacity of 6,824 in.-kips in the constant depth region of the girder.

The layout of longitudinal reinforcement used for the haunched girder is shown in Figure 6-27c, and the flexural strength envelope provided by the reinforcement is shown in Figure 6-27b. As noted in Table 6-13, the hooked #11 bars can be developed in the confined core of the columns. Finally, where seven #11 top bars are used, the spacing between bars is approximately 1.4 in., which is greater than the diameter of a #11 bar and is therefore acceptable. This spacing should accommodate the vertical column reinforcement.

Under combined gravity and earthquake load, a negative moment plastic hinge will form at the support and, based on the moment envelopes from the loading (Figure 6-27b), the corresponding positive moment hinge will form in the constant depth portion of the girder. As discussed in the following sections, the exact location of plastic hinges must be determined in order to design the transverse reinforcement.

#### 6.4.5.4.2 Design and Detailing of Transverse Reinforcement

The design for shear of the haunched girder is complicated by its variable depth; therefore, a tabular approach is taken for the calculations. Before the table may be set up, however, the maximum probable strength must be determined for negative moment at the support and for positive moment in the constant depth region,

For negative moment at the face of the support and using seven #11 bars:

 $\begin{aligned} A_s &= 7 \ (1.56) = 10.92 \ \text{in.}^2 \\ d &= 32 - 1.5 - 3/8 - 1.41/2 = 29.4 \ \text{in.} \\ b &= 22.5 \ \text{in.} \\ a &= [10.92 \ (1.25) \ 60]/[0.85 \ (4) \ 22.5] = 10.71 \ \text{in.} \\ M_{pr} &= 1.0(10.92)(1.25)(60)(29.4 - 10.71/2) = 19,693 \ \text{in.-kips.} \end{aligned}$ 

For positive moment in the constant depth region and using five #9 bars:

 $A_s = 5 (1.0) = 5.00 \text{ in.}^2$  d = 20 - 1.5 - 3/8 - 1.128/2 = 17.6 in. b = 86.5 in. a = [5.00 (1.25) 60]/[0.85 (4) 86.5] = 1.28 in. $M_{pr} = [1.0 (5.00) 1.25 (60)] (17.6 - 1.28/2) = 6,360 \text{ in.-kips}$ 

Before the earthquake shear may be determined, the location of the positive moment hinge that will form in the constant depth portion of the girder must be identified. To do so, consider the free-body diagram of Figure 6-28a. Summing moments (clockwise positive) about point B gives:

$$M_{pr}^{+} + M_{pr}^{-} + Rx - \frac{wx^2}{2} = 0$$

At the positive moment hinge the shear must be zero, thus R - wx = 0

By combining the above equations:

$$x = \sqrt{\frac{2(M_{pr}^+ + M_{pr}^-)}{w}}$$

Using the above equation with  $M_{pr}$  as computed and w = 1.42(3.38) + 0.5(0.90) = 5.25 k/ft = 0.437 k/in., x = 345 in., which is located exactly at the point where the right haunch begins.<sup>4</sup>

The reaction is computed as R = 345 (0.437) = 150.8 kips.

The earthquake shear is computed as  $V_E = R = wL/2 = 150.8 \cdot (0.437)(450)/2 = 52.5$  kips

This earthquake shear is *smaller* than would have been determined if the positive moment hinge had formed at the face of support.

The earthquake shear is constant along the span but changes sign with the direction of the earthquake. In Figure 6-28a, this shear is shown for the equivalent lateral seismic forces acting to the west. The factored gravity load shear  $(1.42V_D + 0.5V_L)$  varies along the length of the span as shown in Figure 6-28b. At Support A, the earthquake shear and factored gravity shear are additive, producing a design ultimate shear of 150.8 kips. At midspan, the shear is equal to the earthquake shear acting alone and, at Support C, the ultimate design shear is -45.8 kips. Earthquake, gravity, and combined shears are shown in Figures 6-28a through 6-28c and are tabulated for the first half of the span in Table 6-16. For earthquake forces acting to the east, the design shears are of the opposite sign of those shown in Figure 6-28.

According to ACI 318 Sec. 21.3.4.2, the contribution of concrete to member shear strength must be taken as zero when  $V_E/V_U$  is greater than 0.5 and  $P_u/A_g f'_c$  is less than 0.05. As shown in Table 6-16, the  $V_E/V_U$ ratio is less than 0.5 within the first three-fourths of the haunch length but is greater than 0.50 beyond this point. In this example, it is assumed that if  $V_E/V_U$  is less than 0.5 at the support, the concrete strength can be used along the entire length of the member.

The concrete contribution to the design shear strength is computed as:

$$\phi V_c = \phi(0.85) 2 \sqrt{f_c} b_w d$$

where the ASCE 7 compatible  $\phi = 0.75$  for shear, and the 0.85 term is the shear strength reduction factor for sand-LW concrete. [Note that this is the basic strength reduction factor for shear per ACI 318-02 Sec 9.3. See Sec 6.4.2 for discussion.] The remaining shear,  $\phi V_s = V_u - \phi V_c$ , must be resisted by closed hoops within a distance 2*d* from the face of the support and by stirrups with the larger of 6*d<sub>h</sub>* or 3.0 in. hook extensions elsewhere. The 6*d<sub>h</sub>* or 3.0 in. "seismic hook" extension is required by ACI 318 Sec. 21.3.3.3.

<sup>&</sup>lt;sup>4</sup>The equation for the location of the plastic hinge is only applicable if the hinge forms in the constant depth region of the girder. If the computed distance x is greater than 28 ft - 9 in. (345 in.), the result is erroneous and a trial and error approach is required to find the actual hinge location.

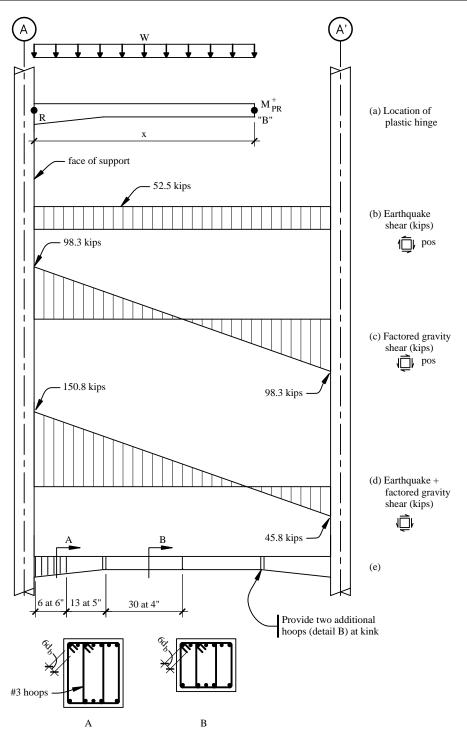


Figure 6-28 Computing shear in haunched girder (1.0 in = 25.4 mm, 1.0 kip = 4.45 kN).

Table 0-10 Design of Shear Reinforcement for Haunched Girder								
<b>T</b> .	Distance from Center of Support (in.)						** •	
Item	15	42.25	67.5	93.75	120	180	240	Units
$V_{e}$	52.5	52.5	52.5	52.5	52.5	52.5	52.5	
$1.42V_D + 0.5V_L$	98.3	86.4	75.4	63.9	52.4	26.2	0.0	kips
$V_{u}$	150.8	139.2	127.9	116.6	104.9	78.7	52.5	
$V_{\scriptscriptstyle E}\!/V_{\scriptscriptstyle U}$	0.35	0.38	0.41	0.45	0.50	0.67	1.00	
d	29.4	26.5	23.5	20.5	17.6	17.6	17.6	in.
$\phi V_C$	53.3	48.1	42.6	37.2	0.0	0.0	0.0	1-1
$\phi V_S$	97.5	91.2	85.3	79.4	104.9	78.7	52.5	kips
S	5.97	5.78	5.46	5.12	3.32	4.43	6.64	
d/4	7.35	6.63	5.88	5.13	4.40	4.40	4.40	in.
Spacing	#3 at 6	#3 at 5	#3 at 5	#3 at 5	#3 at 4	#3 at 4	#3 at 4	

**Table 6-16** Design of Shear Reinforcement for Haunched Girder

1.0 in. = 25.4 mm, 1.0 kip = 4.45 kN.

In Table 6-16, spacings are computed for four #3 vertical leg hoops or stirrups. As an example, consider four #3 vertical legs at the section at the face of the support:

$$\phi V_c = \phi(0.85) 2 \sqrt{f'_c} db = 0.75(0.85) 2(4000)^{0.5} 29.4(22.5) = 53,300 \text{ lb} = 53.3 \text{ kips}$$
  
 $\phi V_s = V_u - \phi V_c = 150.8 - 53.3 = 97.5 \text{ kips}$   
 $\phi V_s = \phi A_s f_s d/s = 97.5 \text{ kips}$   
 $s = [0.75(4)0.11(60)29.4]/97.5 = 5.97 \text{ in}.$ 

The maximum spacing allowed by ACI 318 is shown in Table 6-16. These spacings govern only in the center portion of the beam. In the last line of the table, the hoop and stirrup spacing as actually used is shown. This spacing, together with hoop and stirrup details, is illustrated in Figure 6-28d. The double U-shaped stirrups (and cap ties) in the central portion of the beam work well with the #11 top bars and with the #9 bottom bars.

### 6.4.5.4.3 Design of Beam-Column Joint

The design of the beam-column joint at Support A of the haunched girder is controlled by seismic forces acting to the west, which produces negative moment at Support A. ACI 318 Sec. 21.5 provides requirements for the proportioning and detailing of the joint.

A plastic mechanism of the beam is shown in Figure 6-29a. Plastic hinges have formed at the support and at the location of the far haunch transition. With a total shear at the face of the support of 150.8 kips, the moment at the centerline of the column may be estimated as

 $M_{CL} = M_{pr} + 15(150.6) = 19,693 + 15(150.6) = 21,955$  in.-kips.

The total shear in the columns above and below the joint is estimated as 21,955/(150) = 146.3 kips.

The stresses in the joint are computed from equilibrium considering the reinforcement in the girder to be stressed at  $1.25f_{v}$ . A detail of the joint is shown in Figure 6-30. Compute the joint shear  $V_{i}$ :

Force in the top reinforcement =  $1.25A_x f_y = 1.25(7)1.56(60) = 819$  kips Joint shear =  $V_i = 819.0 - 146.3 = 672.7$  kips

The joint shear stress  $v_i = V_i/d_c^2 = 672.7/[30 (30)] = 0.819$  ksi

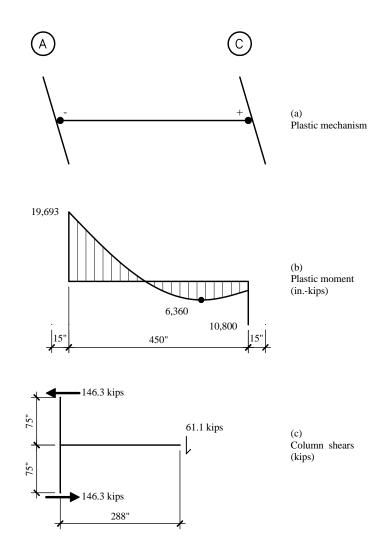


**Figure 6-29** Computation of column shears for use in joint design (1.0 in = 25.4 mm, 1.0 kip = 4.45 kN).

In the case being considered, all girders framing into the joint have a width equal to 0.75 times the column dimension so confinement is provided on three faces of the joint. According to ACI 318 Sec. 21.5.3, the allowable joint shear stress =  $0.75 \phi(15) 2\sqrt{f_c}$ . The 0.75 term is the strength reduction factor for LW concrete. Compute the allowable joint shear stress:

 $v_{j,allowable} = 0.75(0.80)15(4,000)^{0.5}$ = 569 psi = 0.569 ksi This allowable stress is significantly less than the applied joint shear stress. There are several ways to remedy the situation:

- 1. Increase the column size to approximately  $35 \times 35$  (not recommended)
- 2. Increase the depth of the haunch so that the area of reinforcement is reduced to seven #10 bars. This will reduce the joint shear stress to a value very close to the allowable stress.
- 2. Use 5000 psi NW concrete for the column. This eliminates the 0.75 reduction factor on allowable joint stress, and raises the allowable stress to 848 psi.

For the remainder of this example, it is assumed that the lower story columns will be constructed from 5000 psi NW concrete.

Because this joint is confined on three faces, the reinforcement within the joint must consist of the same amount and spacing of transverse reinforcement in the critical region of the column below the joint. This reinforcement is detailed in the following section.

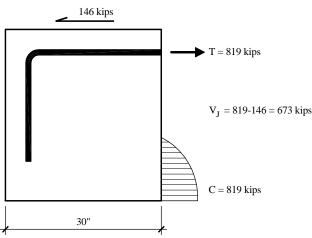


**Figure 6-30** Computing joint shear force (1.0 kip = 4.45 kN).

### 6.4.5.5 Design and Detailing of Typical Interior Column of Frame 3

The column supporting the west end of the haunched girder between Gridlines A and B is shown in Figure 6-31. This column supports a total unfactored dead load of 804 kips and a total unfactored live load of 78 kips. From the ETABS analysis, the axial force on the column from seismic forces is  $\pm 129$  kips. The design axial force and bending moment in the column are based on one or more of the load combinations presented below.

Earthquake forces acting to the west are:

$$P_u = 1.42(804) + 0.5(78) + 1.0(129)$$
  
= 1310 kips (compression)

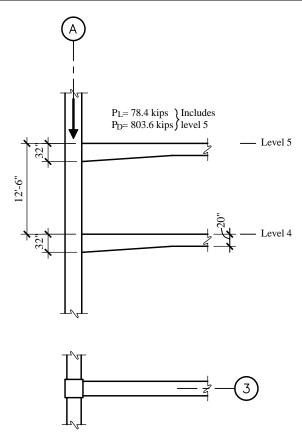


**Figure 6-31** Column loading (1.0 ft = 0.3048 m, 1.0 in = 25.4 mm, 1.0 kip = 4.45kN).

This axial force is greater than  $0.1f_c'A_g = 360$  kips; therefore, according to ACI 318 Sec. 21.4.2.1, the column flexural strength must be at least 6/5 of the nominal strength (using  $\phi = 1.0$  and  $1.0 f_y$ ) of the beam framing into the column. The nominal beam moment capacity at the face of the column is 16,458 in.-kips. The column must be designed for six-fifths of this moment, or 19,750 in-kips. Assuming a midheight inflection point for the column above and below the beam, the column moment at the centerline of the beam is 19,750/2 = 9,875 in.-kips, and the column moment corrected to the face of the beam is 7,768 in.-kips.

Earthquake forces acting to the east are:

 $P_u = 0.68(804) - 1.0(129) = 424$  kips (compression)

This axial force is greater than  $0.1f_c'A_g = 360$  kips. For this loading, the end of the beam supported by the column is under positive moment, with the nominal beam moment at the face of the column being 8,715 in.-kips. Because  $P_u > 0.1f_c'A_g$ , the column must be designed for 6/5 of this moment, or 10,458 in.-kips. Assuming midheight inflection points in the column, the column moment at the centerline and the face of the beam is 5,229 and 4,113 in.-kips, respectively.

Axial force for gravity alone is:

 $P_u = 1.6(804) + 1.2(78) = 1,380$  kips (compression)

This is approximately the same axial force as designed for earthquake forces to the west, but as can be observed from Figure 6-25, the design moment is significantly less. Hence, this loading will not control.

### 6.4.5.5.1 Design of Longitudinal Reinforcement

Figure 6-32 shows an axial force-bending moment interaction diagram for a 30 in. by 30 in. column with 12 bars ranging in size from #8 to #10. A horizontal line is drawn at each of the axial load levels computed above, and the required flexural capacity is shown by a solid dot on the appropriate line. The column with twelve #8 bars provides more than enough strength for all loading combinations.

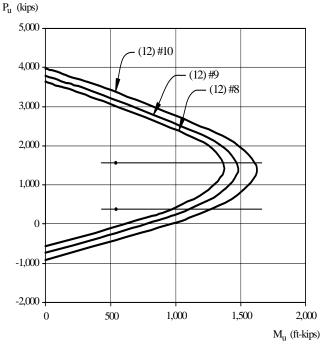


**Figure 6-32** Interaction diagram and column design forces (1.0 kip = 4.45 kN, 1.0 ft-kip = 1.36 kN-m).

# 6.4.5.5.2 Design of Transverse Reinforcement

In Sec. 6.4.5.3, an interior column supporting Level 5 of Frame 1 was designed. This column has a shear strength of 198.2 kips, which is significantly greater than the imposed seismic plus gravity shear of 146.3 kips. For details on the computation of the required transverse reinforcement for this column, see the "Transverse Reinforcement" and "Transverse Reinforcement Required for Shear" subsections in Sec. 6.4.5.3. A detail of the reinforcement of the column supporting Level 5 of Frame 3 is shown in Figure 6-33. The section of the column through the beams shows that the reinforcement in the beam-column joint region is relatively uncongested.

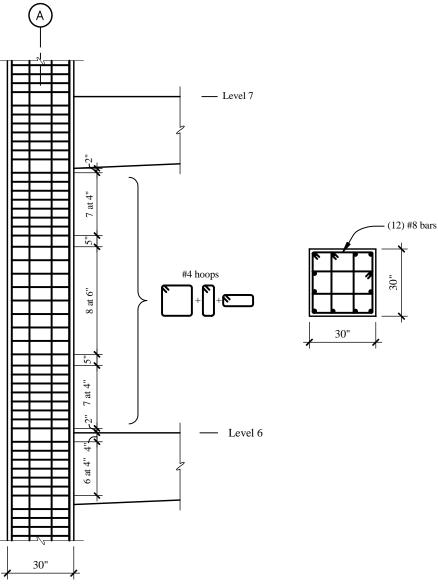


Figure 6-33 Column detail (1.0 in = 25.4 mm).

### 6.4.5.6 Design of Structural Wall of Frame 3

The factored forces acting on the structural wall of Frame 3 are summarized in Table 6-17. The axial compressive forces are based on a tributary area of 1,800 square ft for the entire wall, an unfactored dead load of 160 psf, and an unfactored (reduced) live load of 20 psf. For the purposes of this example it is assumed that these loads act at each level, including the roof. The total axial force for a typical floor is:

 $P_u = 1.42D + 0.5L = 1,800((1.42 \times 0.16) + 0.50 \times 0.02)) = 427$  kips for maximum compression  $P_u = 0.68D = 1,800(0.68 \times 0.16) = 196$  kips for minimum compression

The bending moments come from the ETABS analysis. Note the reversal in the moment sign due to the effects of frame-wall interaction. Each moment contains two parts: the moment in the shear panel and the couple resulting from axial forces in the boundary elements. For example, at the base of Level 2:

ETABS panel moment =162,283 in.-kips ETABS column force = 461.5 kips Total moment,  $M_u$  = 162,283 + 240(461.5) = 273,043 in.-kips

The shears in Table 6-17 also consist of two parts, the shear in the panel and the shear in the column. Using Level 2 as an example:

ETABS panel shear = 527 kips ETABS column shear = 5.90 kips Total shear,  $V_u = 527 + 2(5.90) = 539$  kips

As with the moment, note the reversal in wall shear, not only at the top of the wall but also at Level 1 where the first floor slab acts as a support. If there is some in-plane flexibility in the first floor slab, or if some crushing were to occur adjacent to the wall, the shear reversal would be less significant, or might even disappear. For this reason, the shear force of 539 kips at Level 2 will be used for the design of Level 1 as well.

Recall from Sec. 6.2.2 that the structural wall boundary elements are 30 in. by 30 in. in size. The basic philosophy of this design will be to use these elements as "special" boundary elements where a close spacing of transverse reinforcement is used to provide extra confinement. This avoids the need for confining reinforcement in the wall panel. Note, however, that there is no code restriction on extending the special boundary elements into the panel of the wall.

It should also be noted that preliminary calculations (not shown) indicate that a 12-in. thickness of the wall panel is adequate for this structure. This is in lieu of the 18-in. thickness assumed when computing structural mass.

Compositions	A mial Communication	Ecros D (line)		Sheen V
Supporting Level	Axial Compressive Force $P_u$ (kips)		Moment $M_u$	Shear $V_u$
	1.42D + 0.5L	0.68D	(inkips)	(kips)
R	427	196	-30,054	-145
12	854	392	-39,725	-4
11	1,281	588	-49,954	62
10	1,708	783	-51,838	118
9	2,135	979	-45,929	163
8	2,562	1,175	-33,817	203
7	2,989	1,371	17,847	240
6	3,416	1,567	45,444	274
5	3,843	1,763	78,419	308
4	4,270	1,958	117,975	348
3	4,697	2,154	165,073	390
2	5,124	2,350	273,043	539
1	5,550	2,546	268,187	-376 (use 539)

 Table 6-17 Design Forces for Structural Wall

1.0 kip = 4.45 kN, 1.0 in.-kip = 0.113 kN-m.

#### 6.4.5.6.1 Design of Panel Shear Reinforcement

First determine the required shear reinforcement in the panel and then design the wall for combined bending and axial force. The nominal shear strength of the wall is given by ACI 318 Eq. 21-7:

$$V_n = A_{cv} (\alpha_c \sqrt{f_c'} + \rho_n f_y)$$

where  $\alpha_c = 2.0$  because  $h_w/l_w = 155.5/22.5 = 6.91 > 2.0$ . Note that the length of the wall was taken as the length between boundary element centerlines (20 ft) plus one-half the boundary element length (2.5 ft) at each end of the wall.

Using  $f_c' = 4000$  psi,  $f_y = 40$  ksi,  $A_{cv} = (270)(12) = 3240$  in.<sup>2</sup>, and taking  $\phi$  for shear = 0.55, the ratio of horizontal reinforcement is computed:

$$V_u = \phi V_n$$

$$\rho_n = \frac{\left(\frac{539.000}{0.55}\right) - (0.85 \times 2\sqrt{4,000})3,240}{3,240(40,000)} = 0.0049$$

Note that the factor of 0.85 on concrete strength accounts for the use of LW concrete. Reinforcement ratios for the other stories are given in Table 6-18. This table gives requirements using  $f_c' = 4,000$  psi, as well as 6,000 psi NW concrete. As shown later, the higher strength NW concrete is required to manage the size of the boundary elements of the wall. Also shown in the table is the required spacing of horizontal reinforcement assuming that two curtains of #4 bars will be used. If the required steel ratio is less than 0.0025, a ratio of 0.0025 is used to determine bar spacing.

Level	$f_c' = 4,000 \text{ psi}$	(lightweight)	$f_c' = 6,000$ psi (normal weight)		
	Reinforcement ratio	Spacing <sup>1</sup> (in.)	Reinforcement ratio	Spacing * (in.)	
R	0.00250	13.33 (12.0)	0.00250	13.33 (12.0)	
12	0.00250	13.33 (12.0)	0.00250	13.33 (12.0)	
11	0.00250	13.33 (12.0)	0.00250	13.33 (12.0)	
10	0.00250	13.33 (12.0)	0.00250	13.33 (12.0)	
9	0.00250	13.33 (12.0)	0.00250	13.33 (12.0)	
8	0.00250	13.33 (12.0)	0.00250	13.33 (12.0)	
7	0.00250	13.33 (12.0)	0.00250	13.33 (12.0)	
6	0.00250	13.33 (12.0)	0.00250	13.33 (12.0)	
5	0.00250	13.33 (12.0)	0.00250	13.33 (12.0)	
4	0.00250	13.33 (12.0)	0.00250	13.33 (12.0)	
3	0.00278	12.00 (6.0)	0.00250	13.33 (9.0)	
2	0.00487	6.84 (6.0)	0.00369	9.03 (9.0)	
1	0.00487	6.84 (6.0)	0.00369	9.03 (9.0)	

 Table 6-18
 Design of Structural Wall for Shear

\* Values in parentheses are actual spacing used.

1.0 in. = 25.4 mm.

For LW concrete, the required spacing is 6.84 in. at Levels 1 and 2. Minimum reinforcement requirements control all other levels. For the final design, it is recommended to use a 6-in. spacing at

Levels 1, 2, and 3 and a 12-in. spacing at all levels above. The 6-in. spacing is extended one level higher that required because it is anticipated that an axial-flexural plastic hinge could propagate this far.

For the NW concrete, the required spacing is 9.03 in. at Levels 1 and 2 and minimum reinforcement requirements control elsewhere. For the final design, a 9-in. spacing would be used at Levels 1, 2, and 3 with a 12-in. spacing at the remaining levels.

ACI 318 Sec. 21.6.4.3 [21.7.4.3] requires the vertical steel ratio to be greater than or equal to the horizontal steel ratio if  $h_w l/lw$  is less than 2.0. As this is not the case for this wall, the minimum vertical reinforcement ratio of 0.0025 is appropriate. Vertical steel consisting of two curtains of #4 bars at 12 in. on center provides a reinforcement ratio of 0.0028, which ill be used at all levels.

### 6.4.5.6.2 Design for Flexure and Axial Force

The primary consideration in the axial-flexural design of the wall is determining whether or not special boundary elements are required. ACI 318 provides two methods for this. The first approach, specified in ACI 318 Sec. 21.6.6.2 [21.7.6.2], uses a displacement based procedure. The second approach, described in ACI 318 Sec. 21.6.6.3 [21.7.6.3], is somewhat easier to implement but, due to its empirical nature, is generally more conservative. In the following presentation, only the displacement based method will be used for the design of the wall.

Using the displacement based approach, boundary elements are required if the length of the compression block, *c*, satisfies ACI 318 Eq. 21-8:

$$c \ge \frac{l_w}{600(\delta_u/h_w)}$$

where  $\delta_u$  is the total elastic plus inelastic deflection at the top of the wall. From Table 6-9b, the total elastic roof displacement is 4.36 in., and the inelastic drift is  $C_d$  times the elastic drift, or 6.5(4.36) = 28.4 in. or 2.37 feet. Recall that this drift is based on cracked section properties assuming  $I_{cracked} = 0.5 I_{gross}$  and assuming that flexure dominates. Using this value together with  $l_w = 22.5$  ft, and  $h_w = 155.5$  ft:

$$\frac{l_w}{600(\delta_u/h_w)} = \frac{22.5}{600(2.37/155.5)} = 2.46 \text{ ft} = 29.52 \text{ in}.$$

To determine if *c* is greater than this value, a strain compatibility analysis must be performed for the wall. In this analysis, it is assumed that the concrete reaches a maximum compressive strain of 0.003 and the wall reinforcement is elastic-perfectly plastic and yields at the nominal value. A rectangular stress block was used for concrete in compression, and concrete in tension was neglected. A straight line strain distribution was assumed (as allowed by ACI 318 Sec. 21.6.5.1 [21.7.5.1]). Using this straight line distribution, the extreme fiber compressive strain was held constant at 0.003, and the distance *c* was varied from 100,000 in. (pure compression) to 1 in. (virtually pure tension). For each value of *c*, a total cross sectional nominal axial force ( $P_n$ ) and nominal bending moment ( $M_n$ ) were computed. Using these values, a plot of the axial force ( $P_n$ ) versus neutral axis location (*c*) was produced. A design value axial force-bending moment interaction diagram was also produced.

The analysis was performed using an Excel spreadsheet. The concrete was divided into 270 layers, each with a thickness of 1 in. The exact location of the reinforcement was used. When the reinforcement was in compression, an adjustment was made to account for reinforcement and concrete sharing the same physical volume.

Two different sections were analyzed: one with  $f_c' = 4,000$  psi (LW concrete) and the other with  $f_c' = 6,000$  psi (NW concrete). In each case, the boundary elements were assumed to be 30 in. by 30 in. and the panel was assumed to be 12 in. thick. Each analysis also assumed that the reinforcement in the boundary element consisted of twelve #9 bars, producing a reinforcement ratio in the boundary element of 1.33 percent. Panel reinforcement consisted of two curtains of #4 bars spaced at approximately 12 in. on center. For this wall the main boundary reinforcement has a yield strength of 60 ksi, and the vertical panel steel yields at 40 ksi.

The results of the analysis are shown in Figures 6-34 and 6-35. The first of these figures is the nominal interaction diagram multiplied by  $\phi = 0.65$  for tied sections. Also plotted in the figure are the factored *P-M* combinations from Table 6-17. The section is clearly adequate for both 4,000 psi and 6,000 psi concrete because the interaction curve fully envelopes the design values.

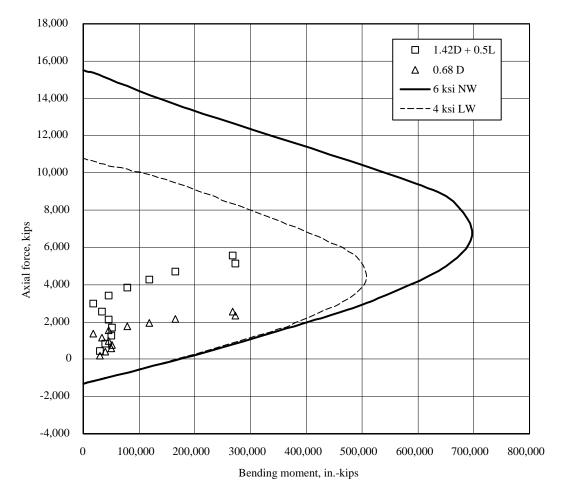


Figure 6-34 Interaction diagram for structural wall (1.0 kip = 4.45kN, 1.0 in.-kip = 0.113 kN-m).

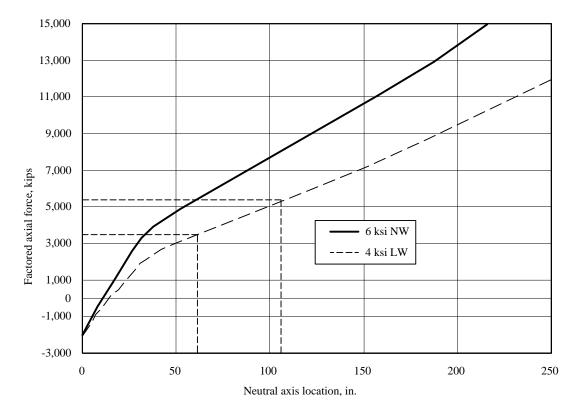


Figure 6-35 Variation of neutral axis depth with compressive force (1.0 in = 25.4 mm, 1.0 kip = 4.45 kN).

Figure 6-35 shows the variation in neutral axis depth with axial force. For a factored axial force of 5,550 kips, the distance c is approximately 58 in. for the 6,000 psi NW concrete and c is in excess of 110 in. for the 4,000 psi LW concrete. As both are greater than 29.52 in., special boundary elements are clearly required for the wall.

According to ACI 318 Sec. 21.6.6.4 [21.7.6.4], the special boundary elements must have a plan length of  $c - 0.1l_w$ , or 0.5c, whichever is greater. For the 4,000 psi concrete, the first of these values is 110 - 0.1(270) = 83 in., and the second is 0.5(110) = 55 in. Both of these are significantly greater than the 30 in. assumed in the analysis. Hence, the 30-in. boundary element is not adequate for the lower levels of the wall if  $f_c' = 4,000$  psi. For the 6,000 psi concrete, the required length of the boundary element is 58-0.1(270) = 31 in., or 0.5(58) = 29 in. The required value of 31 in. is only marginally greater than the 30 in. provided and will be deemed acceptable for the purpose of this example.

The vertical extent of the special boundary elements must not be less than the larger of  $l_w$  or  $M_u/4V_u$ . The wall length  $l_w = 22.5$  ft and, of the wall at Level 1,  $M_u/4V_u = 273,043/4(539) = 126.6$  in., or 10.6 ft. 22.5 ft controls and will be taken as the required length of the boundary element *above the first floor*. The special boundary elements will begin at the basement level, and continue up for the portion of the wall supporting Levels 2 and 3. Above that level, boundary elements will still be present, but they will not be reinforced as special boundary elements.

Another consideration for the boundary elements is at what elevation the concrete may change from 6,000 psi NW to 4,000 LW concrete. Using the requirement that boundary elements have a maximum plan dimension of 30 in., the neutral axis depth (*c*) must not exceed approximately 57 in. As may be seen from Figure 6-35, this will occur when the factored axial force in the wall falls below 3,000 kips. From Table 6-17, this will occur between Levels 6 and 7. Hence, 6,000 psi concrete will be continued up through Level 7. Above Level 7, 4,000 psi LW concrete may be used.

Where special boundary elements are required, transverse reinforcement must conform to ACI 318 Sec. 21.6.6.4(c) [21.7.6.4(c)], which refers to Sec. 21.4.4.1 through 21.4.4.3. If rectangular hoops are used, the transverse reinforcement must satisfy ACI 318 Eq. 21-4:

$$A_{sh} = 0.09 sh_c \frac{f_c'}{f_{yh}}$$

If #5 hoops are used in association with two crossties in each direction,  $A_{sh} = 4(0.31) = 1.24$  in.<sup>2</sup>, and  $h_c = 30 - 2(1.5) - 0.525 = 26.37$  in. With  $f_c' = 6$  ksi and  $f_{vh} = 60$  ksi:

$$s = \frac{1.24}{0.09(26.37)\frac{6}{60}} = 5.22$$

If 4,000 psi concrete is used, the required spacing increases to 7.83 in.

Maximum spacing is the lesser of h/4,  $6d_b$ , or  $s_x$  where  $s_x = 4 + (14-h_x)/3$ . With  $h_x = 8.83$  in., the third of these spacings controls at 5.72 in. The 5.22-in. spacing required by ACI 318 Eq. 21-4 is less than this, so a spacing of 5 in. on center will be used wherever the special boundary elements are required.

Details of the panel and boundary element reinforcement are shown in Figures 6-36 and 6-37, respectively. The vertical reinforcement in the boundary elements will be spliced as required using Type 2 mechanical splices at all locations. According to Table 6-13 (prepared for 4,000 psi LW concrete), there should be no difficulty in developing the horizontal panel steel into the 30-in.-by-30-in. boundary elements.

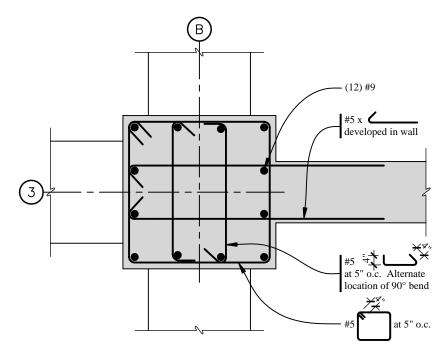


Figure 6-36 Details of structural wall boundary element (1.0 in = 25.4 mm).

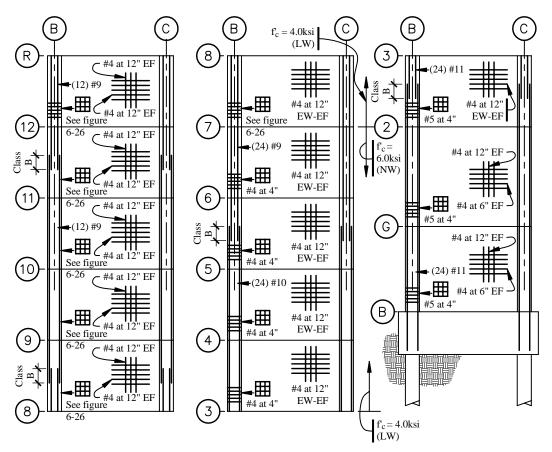


Figure 6-37 Overall details of structural wall (1.0 in = 25.4 mm).

ACI 318 Sec. 21.6.6.4(d) [21.7.6.4(d)] also requires that the boundary element transverse reinforcement be extended into the foundation tie beam a distance equal to the tension development length of the #9 bars used as longitudinal reinforcement in the boundary elements. Assuming the tie beam consists of 6,000 psi NW concrete, the development length for the #9 bar is 2.5 times the value given by ACI 318 Eq. 21-6:

$$l_d = 2.5 \left[ \frac{f_y d_b}{65 \sqrt{f_c'}} \right] = 2.5 \frac{60,000(1.128)}{65 \sqrt{6,000}} = 33.6$$
 in.

Hence, the transverse boundary element reinforcement consisting of #5 hoops with two crossties in each direction, spaced at 5 in. on center, will extend approximately 3 ft into the foundation tie beam.

# 6.5 STRUCTURAL DESIGN OF THE HONOLULU BUILDING

The structure illustrated in Figure 6-1 and 6-2 is now designed and detailed for the Honolulu building. Because of the relatively moderate level of seismicity, the lateral load resisting system will consist of a series of intermediate moment-resisting frames in both the E-W and N-S directions. This is permitted for Seismic Design Category C buildings under *Provisions* Sec. 9.6 [9.4]. Design guidelines for the reinforced concrete framing members are provided in ACI 318 Sec. 21.10 [21.12]. Preliminary design for the Honolulu building indicated that the size of the perimeter frame girders could be reduced to 30 in. deep by 20 in. wide (the Berkeley building has girders that are 32 in. deep by 22.5 in. wide) and that the columns could be decreased to 28 in. square (the Berkeley building uses 30-in.-by-30-in. columns). The haunched girders along Frames 2 through 7 have a maximum depth of 30 in. and a width of 20 in. in the Honolulu building (the Berkeley building had haunches with a maximum depth of 32 in. and a width of 22.5 in.). The Frame 2 through Frame 7 girders in Bays B-C have a constant depth of 30 in. Using these reduced properties, the computed drifts will be increased over those shown in Figure 6-6, but will clearly not exceed the drift limits.

# **6.5.1 Material Properties**

ACI 318 has no specific limitations for materials used in structures designed for moderate seismic risk. For the Honolulu building, 4,000 psi sand-LW concrete is used with ASTM A615 Grade 60 rebar for longitudinal reinforcement and Grade 60 or Grade 40 rebar for transverse reinforcement.

# 6.5.2 Combination of Load Effects

For the design of the Honolulu building, all masses and superimposed gravity loads generated for the Berkeley building are used. This is conservative because the members for the Honolulu building are slightly smaller than the corresponding members for the Berkeley building. Also, the Honolulu building does not have reinforced concrete walls on Gridlines 3, 4, 5, and 6 (these walls are replaced by infilled, nonstructural masonry designed with gaps to accommodate frame drifts in the Honolulu building).

*Provisions* Sec. 5.2.7 [4.2.2] and Eq. 5.2.7-1 and 5.2.7-2 [4.2-1 and 4.2-2] require a combination of load effects to be developed on the basis of ASCE 7, except that the earthquake load (E) is defined as:

 $E = \rho Q_E + 0.2S_{DS}D$ 

when gravity and seismic load effects are additive and as:

 $E = \rho Q_E - 0.2 S_{DS} D$ 

when the effects of seismic load counteract gravity.

For Seismic Design Category C buildings, *Provisions* Sec. 5.2.4.1 [4.3.3.1] permits the reliability factor  $(\rho)$  to be taken as 1.0. The special load combinations of *Provisions* Eq. 5.2.7-1 and 5.2.7-2 [4.2-3 and 4.2-4] do not apply to the Honolulu building because there are no discontinuous elements supporting stiffer elements above them. (See *Provisions* Sec. 9.6.2 [9.4.1].)

For the Honolulu structure, the basic ASCE 7 load combinations that must be considered are:

$$\begin{array}{l} 1.2D + 1.6L \\ 1.2D + 0.5L \pm 1.0E \\ 0.9D \pm 1.0E \end{array}$$

The ASCE 7 load combination including only 1.4 times dead load will not control for any condition in this building.

Substituting *E* from the *Provisions* and with  $\rho$  taken as 1.0, the following load combinations must be used for earthquake:

 $(1.2 + 0.2S_{DS})D + 0.5L + E$ (1.2 + 0.2S\_{DS})D + 0.5L - E (0.9 - 0.2S\_{DS})D + E (0.9 - 0.2S\_{DS})D - E

Finally, substituting 0.472 for  $S_{DS}$  (see Sec. 6.1.1), the following load combinations must be used for earthquake:

 $\begin{array}{l} 1.30D + 0.5L + E \\ 1.30D + 0.5L - E \\ 0.80D + E \\ 0.80D - E \end{array}$ 

Note that the coefficients on dead load have been slightly rounded to simplify subsequent calculations.

As E-W wind loads apparently govern the design at the lower levels of the building (see Sec. 6.2.6 and Figure 6-4), the following load combinations should also be considered:

 $\begin{array}{l} 1.2D + 0.5L + 1.6W \\ 1.2D + 0.5L - 1.6W \\ 0.9D - 1.6W \end{array}$ 

The wind load (W) from ASCE 7 includes a directionality factor of 0.85.

It is very important to note that use of the ASCE 7 load combinations in lieu of the combinations given in ACI 318 Chapter 9 requires use of the alternate strength reduction factors given in ACI 318 Appendix C:

Flexure without axial load  $\phi = 0.80$ Axial compression, using tied columns  $\phi = 0.65$  (transitions to 0.8 at low axial loads) Shear if shear strength is based on nominal axial-flexural capacity  $\phi = 0.75$ Shear if shear strength is <u>not</u> based on nominal axial-flexural capacity  $\phi = 0.55$ Shear in beam-column joints  $\phi = 0.80$ 

[The strength reduction factors in ACI 318-02 have been revised to be consistent with the ASCE 7 load combinations. Thus, the factors that were in Appendix C of ACI 318-99 are now in Chapter 9 of ACI 318-02, with some modification. The strength reduction factors relevant to this example as contained in ACI 318-02 Sec. 9.3 are:

Flexure without axial load  $\varphi = 0.9$  (tension-controlled sections) Axial compression, using tied columns  $\varphi = 0.65$  (transitions to 0.9 at low axial loads) Shear if shear strength is based o nominal axial-flexural capacity  $\varphi = 0.75$ Shear if shear strength is <u>not</u> based o nominal axial-flexural capacity  $\varphi = 0.60$ Shear in beam-column joints  $\varphi = 0.85$ ]

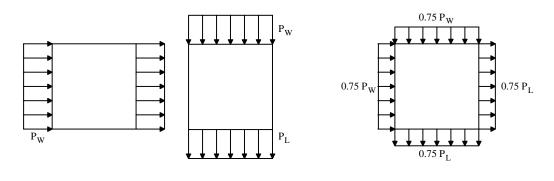
### 6.5.3 Accidental Torsion and Orthogonal Loading (Seismic Versus Wind)

As has been discussed and as illustrated in Figure 6-4, wind forces appear to govern the strength requirements of the structure at the lower floors, and seismic forces control at the upper floors. The seismic and wind shears, however, are so close at the midlevels of the structure that a careful evaluation

must be made to determine which load governs for strength. This determination is complicated by the differing (wind versus seismic) rules for applying accidental torsion and for considering orthogonal loading effects.

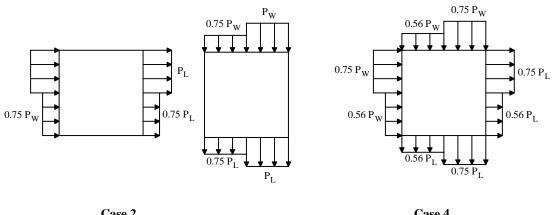
Because the Honolulu building is in Seismic Design Category C and has no plan irregularities of Type 5 in Provisions Table 5.2.3.2 [4.3-2], orthogonal loading effects need not be considered per Provisions Sec. 5.2.5.2.2 [4.4.2.2]. However, as required by *Provisions* Sec. 5.4.4.2 [5.2.4.2], seismic story forces must be applied at a 5 percent accidental eccentricity. Torsional amplification is not required per *Provisions* Sec. 5.4.4.3 [5.2.4.3] because the building does not have a Type 1a or 1b torsional irregularity. (See Sec. 6.3.2 and 6.3.4 for supporting calculations and discussion.)

For wind, ASCE 7 requires that buildings over 60 ft in height be checked for four loading cases. The required loads are shown in Figure 6-38, which is reproduced directly from Figure 6-9 of ASCE 7. In Cases 1 and 2, load is applied separately in the two orthogonal directions. Case 2 may be seen to produce torsional effects because 7/8 of the total force is applied at an eccentricity of 3.57% the building width. This is relatively less severe than required for seismic effects, where 100 percent of the story force is applied at a 5 percent eccentricity.





Case 3



Case 2

Case 4

Figure 6-38 Wind loading requirements from ASCE 7.

For wind, Load Cases 3 and 4 require that 75 percent of the wind pressures from the two orthogonal directions be applied simultaneously. Case 4 is similar to Case 2 because of the torsion inducing pressure unbalance. As mentioned earlier, the Honolulu building has no orthogonal seismic loading requirements.

In this example, only loading in the E-W direction is considered. Hence, the following lateral load conditions were applied to the ETABS model:

100% E-W Seismic applied at 5% eccentricity ASCE 7 Wind Case 1 applied in E-W direction only ASCE 7 Wind Case 2 applied in E-W direction only ASCE 7 Wind Case 3 ASCE 7 Wind Case 4

All cases with torsion are applied in such a manner as to maximize the shears in the elements of Frame 1.

# 6.5.4 Design and Detailing of Members of Frame 1

In this section, the girders and a typical interior column of Level 5 of Frame 1 are designed and detailed. For the five load cases indicated above, the girder shears produced from seismic effects control at the fifth level, with the next largest forces coming from direct E-W wind without torsion. This is shown graphically in Figure 6-39, where the shears in the exterior bay of Frame 1 are plotted vs. story height. Wind controls at the lower three stories and seismic controls for all other stories. This is somewhat different from that shown in Figure 6-4, wherein the total story shears are plotted and where wind controlled for the lower five stories. The basic difference between Figures 6-4 and 6-39 is that Figure 6-39 includes accidental torsion and, hence, Frame 1 sees a relatively larger seismic shear.

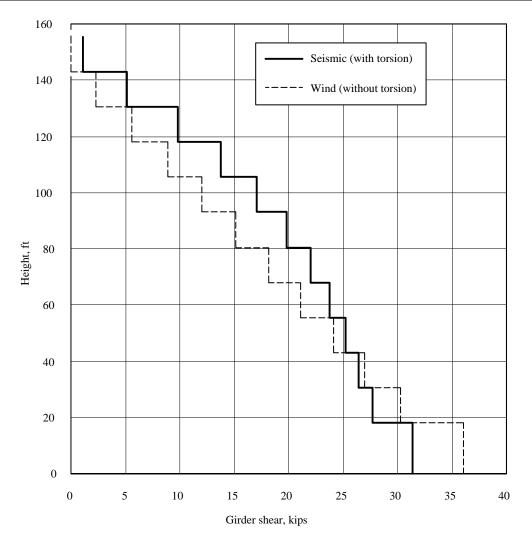


Figure 6-39 Wind vs. seismic shears in exterior bay of Frame 1 (1.0 ft = 0.3048 m, 1.0 kip = 4.45 kN).

### 6.5.4.1 Initial Calculations

The girders of Frame 1 are 30 in. deep and 20 in. wide. For positive moment bending, the effective width of the compression flange is taken as 20 + 20(12)/12 = 40.0 in. Assuming 1.5 in. cover, #3 stirrups and #8 longitudinal reinforcement, the effective depth for computing flexural and shear strength is 27.6 in.

#### 6.5.4.2 Design of Flexural Members

ACI 318 Sec. 21.10.4 [21.12.4] gives the minimum requirements for longitudinal and transverse reinforcement in the beams of intermediate moment frames. The requirements for longitudinal steel are as follows:

- 1. The positive moment strength at the face of a joint shall be at least one-third of the negative moment strength at the same joint.
- 2. Neither the positive nor the negative moment strength at any section along the length of the member shall be less than one-fifth of the maximum moment strength supplied at the face of either joint.

The second requirement has the effect of requiring top and bottom reinforcement along the full length of the member. The minimum reinforcement ratio at any section is taken from ACI 318 Sec. 10.5.1 as  $200/f_y$  or 0.0033 for  $f_y = 60$  ksi. However, according to ACI 318 Sec. 10.5.3, the minimum reinforcement provided need not exceed 1.3 times the amount of reinforcement required for strength.

The gravity loads and design moments for the first three spans of Frame 1 are shown in Figure 6-40. The seismic moments are taken directly from the ETABS analysis, and the gravity moments were computed by hand using the ACI coefficients. All moments are given at the face of the support. The gravity moments shown in Figures 6-40c and 6-40d are slightly larger than those shown for the Berkeley building (Figure 6-14) because the clear span for the Honolulu building increases due to the reduction in column size from 30 in. to 28 in.

Based on preliminary calculations, the reinforcement layout of Figure 6-41 will be checked. Note that the steel clearly satisfies the detailing requirements of ACI 318 Sec. 21.10.4 [21.12.4].

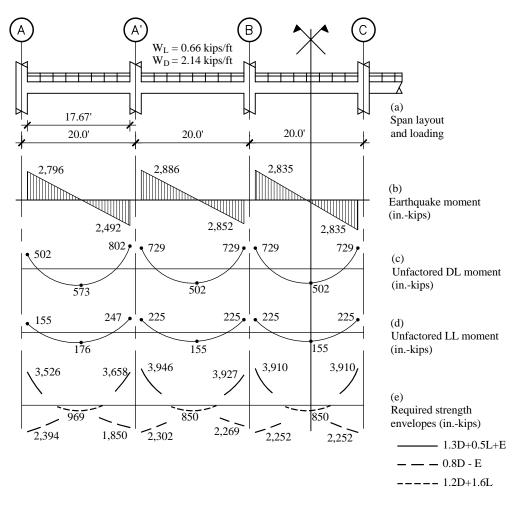


**Figure 6-40** Bending moment envelopes at Level 5 of Frame 1 (1.0 ft = 0.3048 m, 1.0 kip/ft = 14.6 kN/m, 1.0 in.-kip = 0.113 kN-m).

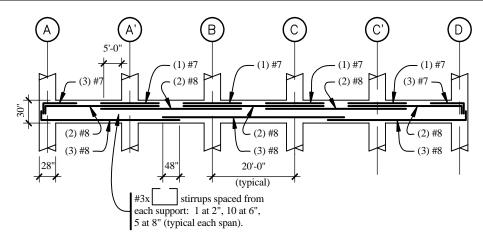


**Figure 6-41** Preliminary reinforcement layout for Level 5 of Frame 1 (1.0 in = 25.4 mm, 1.0 ft = 0.3048 m).

6.5.4.2.1 Design for Negative Moment at Face of Support A

 $M_{\mu}$  = -1.3 (502) - 0.5 (155) - 1.0 (2,796) = -3,526 in.-kips

Try three #7 short bars and two #8 long bars.

 $A_s = 3 (0.60) + 2 (0.79) = 3.38 \text{ in.}^2$   $\rho = 0.0061$ Depth of compression block, a = [3.38 (60)]/[0.85 (4) 20] = 2.98 in.Nominal moment capacity,  $M_n = A_s f_y (d - a/2) = [3.38 (60.0)] [27.6 - 2.98/2] = 5,295 \text{ in.-kips}$ Design capacity,  $\phi M_n = 0.8(5,295) = 4,236 \text{ in.-kips} > 3,526 \text{ in.-kips}$ 

6.5.4.2.2 Design for Positive Moment at Face of Support A

 $M_{\mu} = -0.8 (502) + 1.0 (2,796) = 2,394$  in.-kips

Try three #8 long bars.

 $A_s f_y = 3 (0.79) = 2.37 \text{ in.}^2$   $\rho = 0.0043$  a = 2.37 (60)/[0.85 (4) 40] = 1.05 in.  $M_n = A_s f_y (d - a/2) = [2.37 (60.0)][27.6 - 1.05/2] = 3,850 \text{ in.-kips}$  $\phi M_n = 0.8(3850) = 3,080 \text{ in.-kips} > 2,394 \text{ in.-kips}$ 

OK

OK

This reinforcement also will work for positive moment at all other supports.

6.5.4.2.3 Design for Negative Moment at Face of Support A'

 $M_{\mu} = -1.3 (729) - 0.5 (225) - 1.0 (2,886) = 3,946$  in.-kips

Try four #8 long bars and one #7 short bar:

 $A_s = 4 (0.79) + 1 (0.6) = 3.76 \text{ in.}^2$  $\rho = 0.0068$  a = [3.76 (60)]/[0.85 (4) 20] = 3.32 in.  $M_n = A_s f_y (d - a/2) = [3.76 (60.0)][27.6 - 3.32/2] = 5,852$  in.-kips  $\phi M_n = 0.8(5,852) = 4,681$  in.-kips > 3,946 in.-kips

This reinforcement will also work for negative moment at Supports B and C. Therefore, the flexural reinforcement layout shown in Figure 6-41 is adequate. The top short bars are cut off 5 ft-0 in. from the face of the support. The bottom bars are spliced in Spans A'-B and C-C' with a Class B lap length of 48 in. Unlike special moment frames, there are no requirements that the spliced region of the bars in intermediate moment frames be confined by hoops over the length of the splice.

6.5.4.2.4 Design for Shear Force in Span A'-B:

ACI 318 Sec. 21.10.3 [21.12.3] provides two choices for computing the shear strength demand in a member of an intermediate moment frame:

- 1. The first option requires that the design shear force for earthquake be based on the nominal moment strength at the ends of the members. Nominal moment strengths are computed with a flexural reinforcement tensile strength of  $1.0f_y$  and a flexural  $\phi$  factor of 1.0. The earthquake shears computed from the nominal flexural strength are added to the factored gravity shears to determine the total design shear.
- 2. The second option requires that the design earthquake shear force be 2.0 times the factored earthquake shear taken from the structural analysis. This shear is used in combination with the factored gravity shears.

For this example, the first option is used. The nominal strengths at the ends of the beam were computed earlier as 3850 in.-kips for positive moment at Support A' and 5,852 in.-kips for negative moment at Support B. Compute the design earthquake shear  $V_E$ :

$$V_E = \frac{5,852 + 3,850}{212} = 45.8 \text{ kips}$$

where 212 in. is the clear span of the member. For earthquake forces acting in the other direction, the earthquake shear is 43.1 kips.

The gravity load shears at the face of the supports are:

$$V_D = \frac{2.14(20 - 2.33)}{2} = 18.9$$
 kips  
 $V_L = \frac{0.66(20 - 2.33)}{2} = 5.83$  kips

The factored design shear  $V_u = 1.3(18.9) + 0.5(5.8) + 1.0(45.8) = 73.3$  kips. This shear force applies for earthquake forces coming from either direction as shown in the shear strength design envelope in Figure 6-42.

The design shear force is resisted by a concrete component  $(V_c)$  and a steel component  $(V_s)$ . Note that the concrete component may be used regardless of the ratio of earthquake shear to total shear. The required design strength is:

OK

$$V_{\mu} \leq \phi V_{c} + \phi V_{s}$$

where  $\phi = 0.75$  for shear.

$$V_c = \frac{(0.85) (2\sqrt{4,000})20(27.6)}{1,000} = 59.3$$
 kips

The factor of 0.85 above reflects the reduced shear capacity of sand-LW concrete.

The shear to be resisted by steel, assuming stirrups consist of two #3 legs ( $A_v = 0.22$ ) and  $f_v = 40$  ksi is:

$$V_s = \frac{V_u - \phi V_c}{\phi} = \frac{73.3 - 0.75(59.3)}{0.75} = 38.4$$
 kips

Using  $V_s = A_v f_v d/s$ :

$$s = \frac{(0.22)(40)(27.6)}{38.4} = 6.32$$
 in

Minimum transverse steel requirements are given in ACI 318 Sec. 21.10.4.2 [21.12.4.2]. The first stirrup should be placed 2 in. from the face of the support, and within a distance 2h from the face of the support, the spacing should be not greater than d/4, eight times the smallest longitudinal bar diameter, 24 times the stirrup diameter, or 12 in. For the beam under consideration d/4 controls minimum transverse steel, with the maximum spacing being 27.6/4 = 6.9 in. This is slightly greater, however, than the 6.32 in. required for strength. In the remainder of the span, stirrups should be placed at a maximum of d/2 (ACI 318 Sec. 21.10.4.3 [21.12.4.3]).

Because the earthquake shear (at midspan) is greater than 50 percent of the shear strength provided by concrete alone, the minimum requirements of ACI 318 Sec. 11.5.5.3 must be checked:

$$s_{max} = \frac{0.2(40,000)}{50(20)} = 8.0$$
 in.

This spacing controls over the d/2 requirement. The final spacing used for the beam is shown in Figure 6-41. This spacing is used for all other spans as well. The stirrups may be detailed according to ACI 318 Sec. 7.1.3, which requires a 90-degree hook with a  $6d_b$  extension. This is in contrast to the details of the Berkeley building where full hoops with 135-degree hooks are required in the critical region (within 2*d* from the face of the support) and stirrups with 135-degree hooks are required elsewhere.

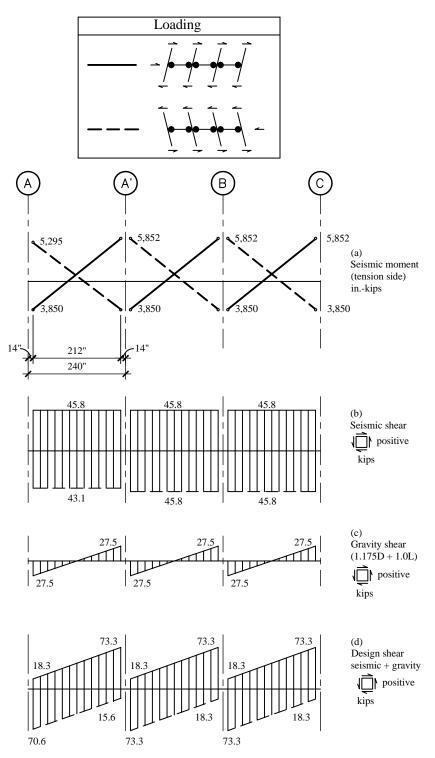


**Figure 6-42** Shear strength envelopes for Span A'-B of Frame 1 (1.0 in = 25.4 mm, 1.0 kip = 4.45 kN, 1.0 in.-kip = 0.113 kN-m).

## 6.5.4.3 Design of Typical Interior Column of Frame 1

This section illustrates the design of a typical interior column on Gridline A'. The column, which supports Level 5 of Frame 1, is 28 in. square and is constructed from 4,000 psi LW concrete, 60 ksi longitudinal reinforcement, and 40 ksi transverse reinforcement. An isolated view of the column is shown in Figure 6-43.

The column supports an unfactored axial dead load of 528 kips and an unfactored axial live load of 54 kips. The ETABS analysis indicates that the axial earthquake force is  $\pm 33.2$  kips, the earthquake shear force is  $\pm 41.9$  kips, and the earthquake moments at the top and the bottom of the column are  $\pm 2,137$  and  $\pm 2,708$  in.-kips, respectively. Moments and shears due to gravity loads are assumed to be negligible.

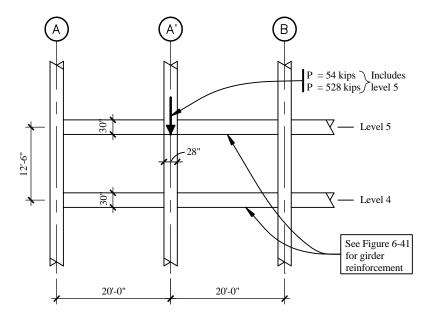


**Figure 6-43** Isolated view of column A' (1.0 ft = 0.3048 m, 1.0 kip = 4.45 kN).

## 6.5.4.3.1 Design of Longitudinal Reinforcement

The factored gravity force for maximum compression (without earthquake) is:

 $P_{\mu} = 1.2(528) + 1.6(54) = 720$  kips

This force acts with no significant gravity moment.

The factored gravity force for maximum compression (including earthquake) is:

 $P_{u} = 1.3(528) + 0.5(54) + 33.2 = 746.6$  kips

The factored gravity force for minimum compression (including earthquake) is:

 $P_u = 0.8(528) - 33.2 = 389.2$  kips

Since the frame being designed is unbraced in both the N-S and E-W directions, slenderness effects should be checked. For a 28-in.-by-28-in. column with a clear unbraced length.  $l_u = 120$  in., r = 0.3(28)= 8.4 in. (ACI 318 Sec. 10.11.3) and  $l_{\mu}/r = 120/8.4 = 14.3$ .

ACI 318 Sec. 10.11.4.2 states that the frame may be considered braced against sidesway if the story stability factor is less than 0.05. This factor is given as:

$$Q = \frac{\sum P_u \delta_0}{V_u l_c}$$

which is basically the same as *Provisions* Eq. 5.4.6.2-1 [5.2-16] except that in the ACI equation, the gravity forces are factored. [Note also that the equation to determine the stability coefficient has been changed in the 2003 Provisions. The importance factor, I, has been added to 2003 Provisions Eq. 5.2-16. However, this does not affect this example because I = 1.0.] ACI is silent on whether or not  $\delta_0$  should include  $C_d$ . In this example,  $\delta_0$  does not include  $C_d$ , and is therefore consistent with the *Provisions*. As can be seen from earlier calculations shown in Table 6-12b, the ACI story stability factor will be in excess of 0.05 for Level 5 of the building responding in the E-W direction. Hence, the structure must be considered unbraced.

Even though the frame is defined as unbraced, ACI 318 Sec. 10.13.2 allows slenderness effects to be neglected when  $kl_{\nu}/r < 22$ . This requires that the effective length factor k for this column be less than 1.54. For use with the nomograph for unbraced columns (ACI 318 Figure R10.12.1b):

$$\left(\frac{EI}{L}\right)_{Girder} = \frac{E(45,000)}{240} = 187.5E$$

According to ACI 318 Sec. 10.12.3:

$$\left(\frac{EI}{L}\right)_{Column} = \frac{\left(\frac{0.4EI_{Column}}{(1+\beta_d)}\right)}{150}$$

Using the 1.2 and 1.6 load factors on gravity load:

150

$$\beta_d = \frac{1.2(528)}{720} = 0.88$$

$$I_{Column} = \frac{28^3(28)}{12} = 51,221 \text{ in.}^4$$

$$\left(\frac{EI}{L}\right)_{Column} = \frac{\frac{0.4(51,221E)}{1+0.88}}{150} = 72.7E$$

Because there is a column above and below as well as a beam on either side:

$$\Psi_{Top} = \Psi_{Bottom} = \frac{72.7}{187.5} = 0.39$$

and the effective length factor k = 1.15 (ACI 318 Figure R10.12.1b). As the computed effective length factor is less than 1.54, slenderness effects need not be checked for this column.<sup>5</sup>

Continuing with the design, an axial-flexural interaction diagram for a 28-in.-by-28-in. column with 12 #8 bars ( $\rho = 0.0121$ ) is shown in Figure 6-44. The column clearly has the strength to support the applied loads (represented as solid dots in the figure).

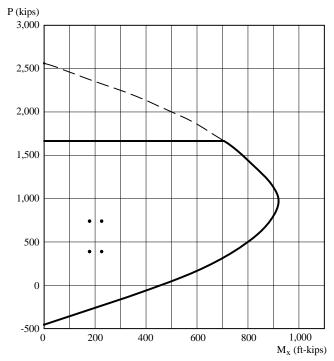


**Figure 6-44** Interaction diagram for column (1.0 kip = 4.45kN, 1.0 ft-kip = 1.36 kN-m).

## 6.5.4.3.2 Design and Detailing of Transverse Reinforcement

ACI 318 Sec. 21.10.3 [21.12.3] allows the column to be checked for 2.0 times the factored shear force as derived from the structural analysis. The ETABS analysis indicates that the shear force is 41.9 kips and the design shear is 2.0(41.9) = 83.8 kips.

The concrete supplies a capacity of:

$$V_c = 0.85(2)\sqrt{f_c'}b_w d = 0.85(2)\sqrt{4,000}(28)(25.6) = 77.1$$
 kips

<sup>&</sup>lt;sup>5</sup>For loading in the N-S direction, the column under consideration has no beam framing into it in the direction of loading. If the stiffness contributed by the joists and the spandrel beam acting in torsion is ignored, the effective length factor for the column in the N-S direction is effectively infinity. However, this column is only one of four in a story containing a total of 36 columns. Since each of the other 32 columns has a lateral stiffness well in excess of that required for story stability in the N-S direction, the columns on Lines A' and C' can be considered to be laterally supported by the other 32 columns and therefore can be designed using an effective length factor of 1.0. A P-delta analysis carried out per the ACI Commentary would be required to substantiate this.

The requirement for steel reinforcement is:

$$V_s = \frac{V_u - \phi V_c}{\phi} = \frac{83.8 - 0.75(77.1)}{0.75} = 34.6$$
 kips

Using ties with four #3 legs, s = [4(0.11)] [40.0 (25.6/34.6)] = 13.02 in.

ACI 318 Sec. 21.10.5 [21.12.5] specifies the minimum reinforcement required. Within a region  $l_o$  from the face of the support, the tie spacing should not exceed:

 $8.0d_b = 8.0 (1.008) = 8.00$  in. (using #8 longitudinal bars)  $24d_{tie} = 24 (3/8) = 9.0$  in. (using #3 ties) 1/2 the smallest dimension of the frame member = 28/2 = 14 in. 12 in.

The 8.0 in. maximum spacing controls. Ties at this spacing are required over a length  $l_o$  of:

1/6 clearspan of column = 120/6 = 20 in. maximum cross section dimension = 28 in. 18.0 in.

Given the above, a four-legged #3 tie spaced at 8 in. over a depth of 28 in. will be used. One tie will be provided at 4 in. below the beam soffit, the next tie is placed 4 in. above the floor slab, and the remaining ties are spaced at 8 in. on center. The final spacing is as shown in Figure 6-45. Note that the tie spacing is not varied beyond  $l_o$ .

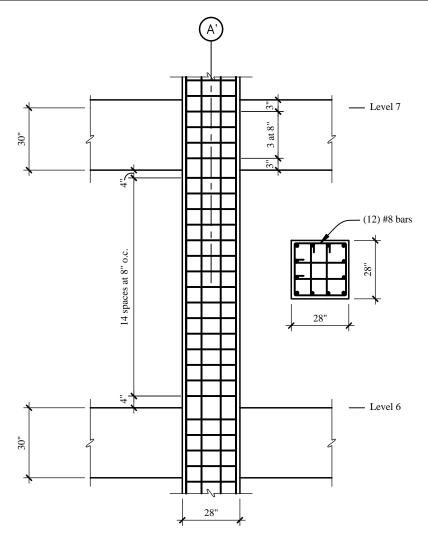


**Figure 6-45** Column reinforcement (1.0 in = 25.4 mm).

## 6.5.4.4 Design of Beam-Column Joint

Joint reinforcement for intermediate moment frames is addressed in ACI 318 Sec. 21.10.5.3 [21.12.5.5], which refers to Sec. 11.11.2. ACI 318 Sec. 11.11.2 requires that all beam-column connections have a minimum amount of transverse reinforcement through the beam-column joints. The only exception is in nonseismic frames where the column is confined on all four sides by beams framing into the column. The amount of reinforcement required is given by ACI 318 Eq. 11-13:

$$A_{v} = 50 \left( \frac{b_{w}s}{f_{y}} \right)$$

This is the same equation used to proportion minimum transverse reinforcement in beams. Assuming  $A_{\nu}$  is supplied by four #3 ties and  $f_{\nu} = 40$  ksi:

$$s = \frac{4(0.11)(40,000)}{50(28)} = 12.6$$
 in.

This effectively requires only two ties within the joint. However, the first tie will be placed 3 in. below the top of the beam and then three additional ties will be placed below this hoop at a spacing of 8 in. The final arrangement of ties within the beam-column joint is shown in Figure 6-45.

## 6.5.5 Design of Members of Frame 3

## 6.5.5.1 Design of Haunched Girder

A typical haunched girder supporting Level 5 of Frame 3 is now illustrated. This girder, located between Gridlines A and B, has a variable depth with a maximum depth of 30 in. at the support and a minimum depth of 20 in. for the middle half of the span. The length of the haunch at each end (as measured from the face of the support) is 106 in. The width of the girder is 20 in. throughout. The girder frames into 28-in.-by-28-in. columns on Gridlines A and B. As illustrated in Figure 6-46c, the reinforcement at Gridline B is extended into the adjacent span (Span B-C) instead of being hooked into the column.

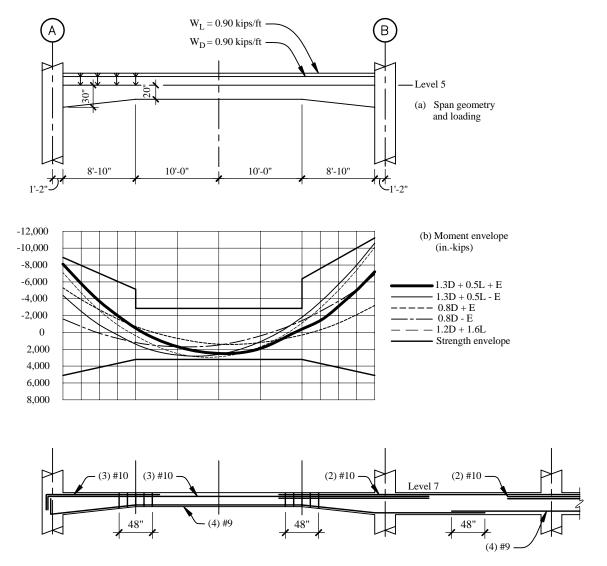


**Figure 6-46** Loads, moments, and reinforcement for haunched girder (1.0 in = 25.4 mm, 1.0 ft = 0.3048 m, 1.0 kip/ft = 14.6 kN/m, 1.0 in.-kip = 0.113 kN-m).

Based on a tributary gravity load analysis, this girder supports an average of 3.38 kips/ft of dead load and 0.90 kips/ft of reduced live load. A gravity load analysis of the girder was carried out in a similar manner similar to that described above for the Berkeley building.

For determining earthquake forces, the entire structure was analyzed using the ETABS program. This analysis included 100 percent of the earthquake forces in the E-W direction placed at a 5 percent eccentricity with the direction of the eccentricity set to produce the maximum seismic shear in the member.

## 6.5.5.2 Design of Longitudinal Reinforcement

The results of the analysis are shown in Figure 6-46b for five different load combinations. The envelopes of maximum positive and negative moment indicate that 1.2D + 1.6L and  $1.3D + 0.5L \pm E$  produce approximately equal negative end moments. Positive moment at the support is nearly zero under 0.8D - E, and gravity controls midspan positive moment. Since positive moment at the support is negligible, a positive moment capacity of at least one-third of the negative moment capacity will be supplied per ACI 318 Sec. 21.10.4.1 [21.12.4.1]. The minimum positive or negative moment strength at any section of the span will not be less than one-fifth of the maximum negative moment strength.

For a factored negative moment of 8,106 in.-kips on Gridline A, try six #10 bars. Three of the bars are short, extending just past the end of the haunch. The other three bars are long and extend into Span B-C.

 $\begin{aligned} A_s &= 6 \ (1.27) = 7.62 \ \text{in.}^2 \\ d &= 30 - 1.5 - 0.375 - 1.27/2 = 27.49 \ \text{in.} \\ \rho &= 7.62/[20 \ (27.49)] = 0.0139 \\ \text{Depth of compression block, } a &= [7.62 \ (60)]/[0.85 \ (4) \ 20.0] = 6.72 \ \text{in.} \\ \text{Nominal capacity, } M_n &= [7.62 \ (60)](27.49 - 6.72/2) = 11,031 \ \text{in-kips} \\ \text{Design capacity, } \phi M_n &= 0.8(11,031) = 8,824 \ \text{in.-kips} > 8,106 \ \text{in.-kips} \end{aligned}$ 

The three #10 bars that extend across the top of the span easily supply a minimum of one-fifth of the negative moment strength at the face of the support.

For a factored negative moment of 10,641 in.-kips on Gridline B, try eight #10 bars. Three of the bars extend from Span A-B, three extend from Span B-C, and the remaining two are short bars centered over Support B.

 $A_s = 8 (1.27) = 10.16 \text{ in.}^2$  d = 30 - 1.5 - 0.375 - 1.27/2 = 27.49 in.  $\rho = 10.16/[20 (27.49)] = 0.0185$  a = [10.16 (60)]/[0.85 (4) 20.0] = 8.96 in.  $M_n = [10.16 (60)](27.49 - 8.96/2) = 13,996 \text{ in.-kips}$  $\phi M_n = 0.8(13,996) = 11,221 \text{ in.-kips} > 10,641 \text{ in.-kips}$ 

For the maximum factored positive moment at midspan of 2,964 in-kips., try four #9 bars:

 $\begin{aligned} A_s &= 4 \ (1.0) = 4.00 \ \text{in.2} \\ d &= 20 - 1.5 - 0.375 - 1.128/2 = 17.56 \ \text{in.} \\ \rho &= 4.0/[20 \ (17.56)] = 0.0114 \\ a &= [4.00 \ (60)]/[0.85 \ (4) \ 84] = 0.84 \ \text{in.} \ (\text{effective flange width} = 84 \ \text{in.}) \\ M_n &= [4.00 \ (60)](17.56 - 0.84/2) = 4,113 \ \text{in.-kips} \\ \phi M_n &= 0.8(4,113) = 3,290 \ \text{in.-kips} > 2,964 \end{aligned}$ 

OK

OK

Even though they provide more than one-third of the negative moment strength at the support, the four #9 bars will be extended into the supports as shown in Figure 6-46. The design positive moment strength for the 30-in.-deep section with four #9 bars is computed as follows:

 $A_s = 4 (1.00) = 1.00 \text{ in.}^2$  d = 30 - 1.5 - 0.375 - 1.128/2 = 27.56 in.  $\rho = 4.00/[20 (27.56)] = 0.0073$  a = [4.0 (60)]/[0.85 (4) 20.0] = 0.84 in.  $M_n = [4.00 (60)] (27.56 - 0.84/2) = 6,514 \text{ in.-kips}$  $\phi M_n = 0.8(6,514) = 5,211 \text{ in.-kips}$ 

The final layout of longitudinal reinforcement used is shown in Figure 6-46. Note that the supplied design strengths at each location exceed the factored moment demands. The hooked #10 bars can easily be developed in the confined core of the columns. Splices shown are Class B and do not need to be confined within hoops.

## 6.5.5.3 Design of Transverse Reinforcement

For the design for shear, ACI 318 Sec. 21.10.3 [21.12.3] gives the two options discussed above. For the haunched girder, the approach based on the nominal flexural capacity ( $\phi = 1.0$ ) of the girder will be used as follows:

For negative moment and six #10 bars, the nominal moment strength = 11,031 in.-kips For negative moment and eight #10 bars, the nominal strength =13,996 in.-kips For positive moment and four #9 bars, the nominal moment strength = 6,514 in.-kips

Earthquake shear when Support A is under positive seismic moment is:

 $V_E = (13,996 + 6,514)/(480 - 28) = 45.4$  kips

Earthquake shear when Support B is under positive seismic moment is:

 $V_E = (11,031 + 6,514)/(480 - 28) = 38.8$  kips  $V_G = 1.3V_D + 0.5V_L = 1.3$  (63.6) + 0.5(16.9) = 91.1 kips

Maximum total shear occurs at Support B:

 $V_u = 45.4 + 91.1 = 136.5$  kips

The shear at Support A is 38.8 + 91.9 = 130.1 kips. The complete design shear (demand) strength envelope is shown in Figure 6-47a. Due to the small difference in end shears, use the larger shear for designing transverse reinforcement at each end.

Stirrup spacing required for strength is based on two #4 legs with  $f_v = 60$  ksi.

$$V_c = \frac{(0.85)(2)\sqrt{4,000})(20)(27.6)}{1,000} = 59.3$$
 kips

$$V_s = \frac{V_u - \phi V_c}{\phi} = \frac{136.5 - 0.75(59.3)}{0.75} = 122.7$$
 kips

Using  $V_s = A_v f_v d/s$ :

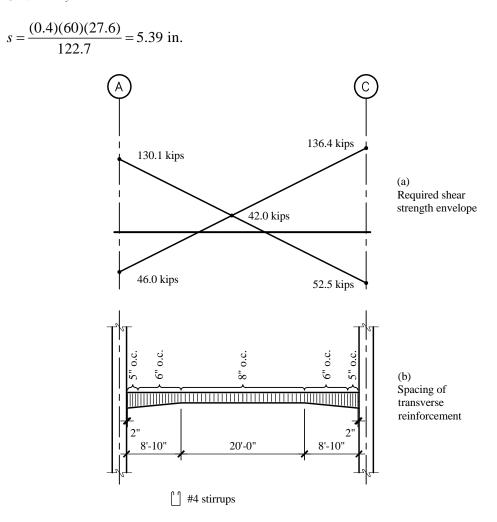


**Figure 6-47** Shear force envelope for haunched girder (1.0 ft = 0.3048m, 1.0 in = 25.4 mm, 1.0 kip = 4.45kN).

Following the same procedure as shown above, the spacing required for other stations is:

At support, $h = 30$ in., $V_U = 136.4$ kips	<i>s</i> = 5.39 in.
Middle of haunch, $h = 25$ in., $V_U = 114.9$ kips	<i>s</i> = 6.67 in.
End of haunch, $h = 20$ in., $V_U = 93.4$ kips	<i>s</i> = 7.61 in.
Quarter point of region of 20-in. depth, $V_U = 69.2$ kips	s = 12.1 in.
Midspan, $V_u = 45.1$ kips	<i>s</i> = 29.7 in.

Within a region 2h from the face of the support, the allowable maximum spacing is d/4 = 6.87 in. at the support and approximately 5.60 in. at midhaunch. Outside this region, the maximum spacing is d/2 = 11.2 in. at midhaunch and 8.75 in. at the end of the haunch and in the 20-in. depth region. At the haunched segments at either end of the beam, the first stirrup is placed 2 in. from the face of the support followed by four stirrups at a spacing of 5 in, and then 13 stirrups at 6 in. through the remainder of the haunch. For the constant 20-in.-deep segment of the beam, a constant spacing of 8 in. is used. The final spacing of stirrups used is shown in Figure 6-47b. Three additional stirrups should be placed at each bend or "kink" in the bottom bars. One should be located at the kink and the others approximately 2 in. on either side of the kink.

## 6.5.5.4 Design of Supporting Column

The column on Gridline A which supports Level 5 of the haunched girder is 28 in. by 28 in. and supports a total unfactored dead load of 803.6 kips and an unfactored reduced live load of 78.4 kips. The layout of the column is shown in Figure 6-48. Under gravity load alone, the unfactored dead load moment is 2,603 in.-kips and the corresponding live load moment is 693.0 in.-kips. The corresponding shears are 43.4 and 11.5 kips, respectively. The factored gravity load combinations for designing the column are as follows:

Bending moment, M = 1.2(2,603) + 1.6(693)= 4,232 in.-kips

This moment causes tension on the outside face of the top of the column and tension on the inside face of the bottom of the column.

Shear, V = 1.2(43.4) + 0.5(11.5) = 57.8 kips Axial compression, P = 1.2(803.6) + 1.6(78.4)= 1,090 kips

For equivalent static earthquake forces acting from west to east, the forces in the column are obtained from the ETABS analysis as follows:

Moment at top of column = 690 in.-kips (tension on inside face subtracts from gravity) Moment at bottom of column = 874 in.-kips (tension on outside face subtracts from gravity) Shear in column = 13.3 kips (opposite sign of gravity shear) Axial force = 63.1 kips tension

The factored forces involving earthquake from west to east are:

Moment at top 0.80(2603) - 690 = 1,392 in.-kips Moment at bottom = 0.80(2603) - 874 = 1,208 in.-kips Shear = 0.80(43.4) - 2(13.3) = 8.1 kips (using the second option for computing EQ shear) Axial force = 0.80(803.6) - 63.1 = 580 kips

For earthquake forces acting from east to west, the forces in the column are obtained from the ETABS analysis as follows:

Moment at top of column = 690 in.-kips (tension on outside face adds to gravity) Moment at bottom of column = 874 in.-kips (tension on inside face adds to gravity) Shear in column = 13.3 kips (same sign of gravity shear) Axial force = 63.1 kips compression

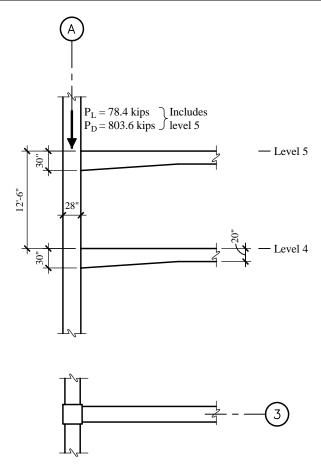


**Figure 6-48** Loading for Column A, Frame 3 (1.0 ft = 0.3048 m, 1.0 in = 25.4 mm, 1.0 kip = 4.45kN).

The factored forces involving earthquake from east to west are:

Moment at top 1.3(2,603) + 0.5(693) + 690 = 4,420 in.-kips Moment at bottom = 1.3(2,603) + 0.5(693) + 874 = 4,604 in.-kips Shear = 1.3(43.4) + 0.5(11.5) + 2(13.3) = 94.6 kips (using second option for computing EQ shear) Axial force = 1.3(803.6) + 0.5(78.4) + 63.1 = 1,147 kips

As may be observed from Figure 6-49, the column with 12 #8 bars is adequate for all loading combinations. Since the maximum design shear is less than that for the column previously designed for Frame 1 and since minimum transverse reinforcement controlled that column, the details for the column currently under consideration are similar to those shown in Figure 6-45. The actual details for the column supporting the haunched girder of Frame 3 are shown in Figure 6-50.

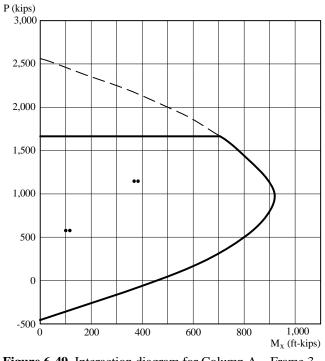


**Figure 6-49** Interaction diagram for Column A, Frame 3 (1.0 kip = 4.45 kN, 1.0 ft-kip = 1.36 kN-m).

## 6.5.5.5 Design of Beam-Column Joint

The detailing of the joint of the column supporting Level 5 of the haunched girder is the same as that for the column interior column of Frame A. The joint details are shown in Figure 6-50.

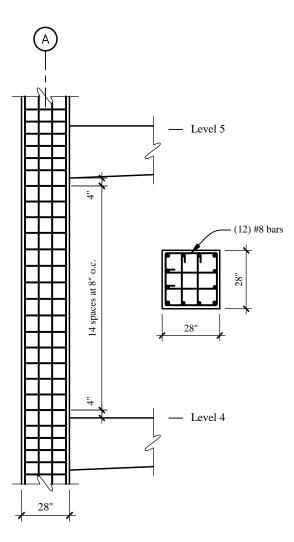


**Figure 6-50** Details for Column A, Frame 3 (1.0 in = 25.4 mm).

7

## PRECAST CONCRETE DESIGN

## Gene R. Stevens, P.E. and James Robert Harris, P.E., Ph.D.

This chapter illustrates the seismic design of precast concrete members using the *NEHRP Recommended Provisions* (referred to herein as the *Provisions*) for buildings in several different seismic design categories. Very briefly, for precast concrete structural systems, the *Provisions*:

- 1. Requires the system (even if the precast carries only gravity loads) to satisfy one of the following two sets of provisions:
  - a. Resist amplified chord forces in diaphragms and, if moment-resisting frames are used as the vertical system, provide a minimum degree of redundancy measured as a fraction of available bays, or
  - b. Provide a moment-resisting connection at all beam-to-column joints with positive lateral support for columns and with special considerations for bearing lengths.

(In the authors' opinion this does not apply to buildings in Seismic Design Category A.)

- 2. Requires assurance of ductility at connections that resist overturning for ordinary precast concrete shear walls. (Because ordinary shear walls are used in lower Seismic Design Categories, this requirement applies in Seismic Design Categories B and C.)
- 3. Allows special moment frames and special shear walls of precast concrete to either emulate the behavior of monolithic concrete or behave as jointed precast systems. Some detail is given for special moment frame designs that emulate monolithic concrete. To validate designs that do not emulate monolithic concrete, reference is made to a new ACI testing standard (ACI T1.1-01).
- 4. Defines that monolithic emulation may be achieved through the use of either:
  - a. Ductile connections, in which the nonlinear response occurs at a connection between a precast unit and another structural element, precast or not, or
  - b. Strong connections, in which the nonlinear response occurs in reinforced concrete sections (generally precast) away from connections that are strong enough to avoid yield even as the forces at the nonlinear response location increase with strain hardening.
- 5. Defines both ductile and strong connections can be either:
  - a. Wet connections where reinforcement is spliced with mechanical couplers, welds, or lap splices (observing the restrictions regarding the location of splices given for monolithic concrete) and the connection is completed with grout, or

- b. Dry connections, which are defined as any connection that is not a wet connection.
- 6. Requires that ductile connections be either:
  - a. Type Y, with a minimum ductility ratio of 4 and specific anchorage requirements, or
  - b. Type Z, with a minimum ductility ratio of 8 and stronger anchorage requirements.

Many of these requirements have been adopted into the 2002 edition of ACI 318, but some differences remain. Where those differences are pertinent to the examples illustrated here, they are explained.

The examples in Sec. 7.1 illustrate the design of untopped and topped precast concrete floor and roof diaphragms of the five-story masonry buildings described in Sec. 9.2 of this volume of design examples. The two untopped precast concrete diaphragms of Sec. 7.1.1 show the requirements for Seismic Design Categories B and C using 8-in.-thick hollow core precast, prestressed concrete planks. Sec. 7.1.2 shows the same precast plank with a 2 ½ in.-thick composite lightweight concrete topping for the five-story masonry building in Seismic Design Category D described in Sec. 9.2. Although untopped diaphragms are commonly used in regions of low seismic hazard, the only place they are addressed in the *Provisions* is the Appendix to Chapter 9. The reader should bear in mind that the appendices of the *Provisions* are prepared for trial use and comment, and future changes should be expected.

The example in Sec. 7.2 illustrates the design of an ordinary precast concrete shear wall building in a region of low or moderate seismicity, which is where most precast concrete seismic-force-resisting systems are constructed. The precast concrete walls in this example resist the seismic forces for a three-story office building, located in southern New England (Seismic Design Category B). There are very few seismic requirements for such walls in the *Provisions*. One such requirement qualifies is that overturning connections qualify as the newly defined Type Y or Z. ACI 318-02 identifies this system as an "intermediate precast concrete shear wall" and does not specifically define the Type Y or Z connections. Given the brief nature of the requirements in both the *Provisions* and ACI 318, the authors offer some interpretation. This example identifies points of yielding for the system and connection features that are required to maintain stable cyclic behavior for yielding.

The example in Sec. 7.3 illustrates the design of a special precast concrete shear wall for a single-story industrial warehouse building in the Los Angeles. For buildings in Seismic Design Category D, *Provisions* Sec. 9.1.1.12 [9.2.2.4] requires that the precast seismic-force-resisting system emulate the behavior of monolithic reinforced concrete construction or that the system's cyclic capacity be demonstrated by testing. The *Provisions* describes methods specifically intended to emulate the behavior of monolithic construction, and dry connections are permitted. Sec. 7.3 presents an interpretation of monolithic emulation of precast shear wall panels with ductile, dry connections. Whether this connection would qualify under ACI 318-02 is a matter of interpretation. The design is computed using the *Provisions* rules for monolithic emulation; however, the system probably would behave more like a jointed precast system. Additional clarity in the definition and application of design provisions of such precast systems is needed.

Tilt-up concrete wall buildings in all seismic zones have long been designed using the precast wall panels as shear walls in the seismic-force-resisting system. Such designs have usually been performed using design force coefficients and strength limits as if the precast walls emulated the performance of cast-in-place reinforced concrete shear walls, which they usually do not. In tilt-up buildings subject to strong ground shaking, the in-plane performance of the precast panels has rarely been a problem, primarily because there has been little demand for post-elastic performance in that direction. Conventional tilt-up buildings may deserve a unique treatment for seismic-resistant design, and they are not the subject of any of the examples in this chapter, although tilt-up panels with large height-to-width ratios could behave in the fashion described in design example 7.3.

In addition to the *Provisions*, the following documents are either referred to directly or are useful design aids for precast concrete construction:

ACI 318-99	American Concrete Institute. 1999. Building Code Requirements and Commentary for Structural Concrete.
ACI 318-02	American Concrete Institute. 2002. Building Code Requirements and Commentary for Structural Concrete.
AISC LRFD	American Institute of Steel Construction. 2002. <i>Manual of Steel Construction, Load &amp; Resistance Factor Design,</i> Third Edition.
ASCE 7	American Society of Civil Engineers. 1998 [2002]. Minimum Design Loads for Buildings and Other Structures.
Hawkins	Hawkins, Neil M., and S. K. Ghosh. 2000. "Proposed Revisions to 1997 NEHRP Recommended Provisions for Seismic Regulations for Precast Concrete Structures, Parts 1, 2, and 3." <i>PCI Journal</i> , Vol. 45, No. 3 (May-June), No. 5 (SeptOct.), and No. 6 (NovDec.).
Moustafa	Moustafa, Saad E. 1981 and 1982. "Effectiveness of Shear-Friction Reinforcement in Shear Diaphragm Capacity of Hollow-Core Slabs." <i>PCI</i> <i>Journal</i> , Vol. 26, No. 1 (JanFeb. 1981) and the discussion contained in <i>PCI</i> <i>Journal</i> , Vol. 27, No. 3 (May-June 1982).
PCI Handbook	Precast/Prestressed Concrete Institute. 1999. PCI Design Handbook, Fifth Edition.
PCI Details	Precast/Prestressed Concrete Institute. 1988. Design and Typical Details of Connections for Precast and Prestressed Concrete, Second Edition.
SEAA Hollow Core	Structural Engineers Association of Arizona, Central Chapter. Design and Detailing of Untopped Hollow-Core Slab Systems for Diaphragm Shear.

The following style is used when referring to a section of ACI 318 for which a change or insertion is proposed by the *Provisions*: *Provisions* Sec. xxx (ACI Sec. yyy) where "xxx" is the section in the *Provisions* and "yyy" is the section proposed for insertion into ACI 318-99.

Although this volume of design examples is based on the 2000 *Provisions*, it has been annotated to reflect changes made for the 2003 *Provisions*. Annotations within brackets, [], indicate both organizational changes (as a result of a reformatting of all chapters for the 2003 *Provisions*) and substantive technical changes to the *Provisions* and its primary reference documents. Although the general conepts of the changes are described, the design examples and calculations have not been revised to reflect the changes made for the 2003 *Provisions*.

The most significant change related to precast concrete in the 2003 *Provisions* is that precast shear wall systems are now recognized separately from cast-in-place systems. The 2003 *Provisions* recognizes ordinary and intermediate precast concrete shear walls. The design of ordinary precast shear walls is based on ACI 318-02 excluding Chapter 21 and the design of intermediate shear walls is based on ACI 318-02 Sec. 21.13 (with limited modifications in Chapter 9 of the 2003 *Provisions*). The 2003 *Provisions* does not distinguish between precast and cast-in-place concrete for special shear walls. Special precast shear walls either need to satisfy the design requirements for special cast-in-place concrete shear walls

(ACI 318-02 Sec. 21.7) or most be substantiated using experimental evidence and analysis (2003 *Provisions* Sec. 9.2.2.4 and 9.6). Many of the design provisions for precast shear walls in the 2000 *Provisions* have been removed, and the requirements in ACI 318-02 are in some ways less specific. Where this occurs, the 2000 *Provisions* references in this chapter are simply annotated as "[not applicable in the 2003 *Provisions*]." Commentary on how the specific design provision was incorporated into ACI 318-02 is included where appropriate.

Some general technical changes for the 2003 *Provisions* that relate to the calculations and/or designs in this chapter include updated seismic hazard maps, revisions to the redundancy requirements, and revisions to the minimum base shear equation. Where they affect the design examples in the chapter, other significant changes for the 2003 *Provisions* and primary reference documents are noted. However, some minor changes may not be noted.

## 7.1 HORIZONTAL DIAPHRAGMS

Structural diaphragms are horizontal or nearly horizontal elements, such as floors and roofs, that transfer seismic inertial forces to the vertical seismic-force-resisting members. Precast concrete diaphragms may be constructed using topped or untopped precast elements depending on the Seismic Design Category of the building. Reinforced concrete diaphragms constructed using untopped precast concrete elements are addressed in the Appendix to Chapter 9 of the *Provisions*. Topped precast concrete elements, which act compositely or noncompositely for gravity loads, are designed using the requirements of ACI 318-99 Sec. 21.7 [ACI 318-02 Sec. 21.9].

# 7.1.1 Untopped Precast Concrete Units for Five-Story Masonry Buildings Located in Birmingham, Alabama, and New York, New York

This example illustrates floor and roof diaphragm design for the five-story masonry buildings located in Birmingham, Alabama, on soft rock (Seismic Design Category B) and in New York, New York (Seismic Design Category C). The example in Sec. 9.2 provides design parameters used in this example. The floors and roofs of these buildings are to be untopped 8-in.-thick hollow core precast, prestressed concrete plank. Figure 9.2-1 shows the typical floor plan of the diaphragms.

## 7.1.1.1 General Design Requirements

In accordance with the *Provisions* and ACI 318, untopped precast diaphragms are permitted only in Seismic Design Categories A through C. The Appendix to Chapter 9 provides design provisions for untopped precast concrete diaphragms without limits as to the Seismic Design Category. Diaphragms with untopped precast elements are designed to remain elastic, and connections are designed for limited ductility. No out-of-plane offsets in vertical seismic-force-resisting members (Type 4 plan irregularities) are permitted with untopped diaphragms. Static rational models are used to determine shears and moments on joints as well as shear and tension/compression forces on connections. Dynamic modeling of seismic response is not required.

The design method used here is that proposed by Moustafa. This method makes use of the shear friction provisions of ACI 318 with the friction coefficient,  $\mu$ , being equal to 1.0. To use  $\mu = 1.0$ , ACI 318 requires grout or concrete placed against hardened concrete to have clean, laitance free, and intentionally roughened surfaces with a total amplitude of about 1/4 in. (peak to valley). Roughness for formed edges is provided either by sawtooth keys along the length of the plank or by hand roughening with chipping hammers. Details from the SEAA Hollow Core reference are used to develop the connection details.

The terminology used is defined in ACI 318 Chapter 21 and *Provisions* Chapter 9. These two sources occasionally conflict (such as the symbol  $\mu$  used above), but the source is clear from the context of the discussion. Other definitions (e.g., chord elements) are provided as needed for clarity in this example.

## 7.1.1.2 General In-Plane Seismic Design Forces for Untopped Diaphragms

The in-plane diaphragm seismic design force  $(F'_{px})$  for untopped precast concrete in *Provisions* Sec. 9A.3.3 [A9.2.2] "shall not be less than the force calculated from either of the following two criteria:"

- 1.  $\rho \Omega_0 F_{px}$  but not less than  $\rho \Omega_0 C_s w_{px}$  where
  - $F_{px}$  is calculated from *Provisions* Eq. 5.2.6.4.4<sup>1</sup> [4.6-3], which also bounds  $F_{px}$  to be not less than  $0.2S_{DS}Iw_{px}$  and not more than  $0.4S_{DS}Iw_{px}$ . This equation normally is specified for Seismic Design

<sup>&</sup>lt;sup>1</sup>Note that this equation is incorrectly numbered as 5.2.5.4 in the first printing of the 2000 *Provisions*.

Categories D and higher; it is intended in the *Provisions* Appendix to Chapter 9 that the same equation be used for untopped diaphragms in Seismic Design Categories B and C.

- $\rho$  is the reliability factor, which is 1.0 for Seismic Design Categories A through C per *Provisions* Sec. 5.2.4.1 [4.3.3.1].
- $\Omega_0$  is the overstrength factor (*Provisions* Table 5.2.2 [4.3-1])
- $C_s$  is the seismic response coefficient (*Provisions* Sec. 5.4.1.1 [5.2.1.1])
- $w_{px}$  is the weight tributary to the diaphragm at Level x

 $S_{DS}$  is the spectral response acceleration parameter at short periods (*Provisions* Sec. 4.1.2 [3.3.3])

I is the occupancy importance factor (Provisions Sec. 1.4 [1.3])

2. 1.25 times the shear force to cause yielding of the vertical seismic-force-resisting system.

For the five-story masonry buildings of this example, the shear force to cause yielding is first estimated to be that force associated with the development of the nominal bending strength of the shear walls at their base. This approach to yielding uses the first mode force distribution along the height of the building and basic pushover analysis concepts, which can be approximated as:

 $F'_{px} = 1.25 K F_{px}^{*}$  where

K is the ratio of the yield strength in bending to the demand,  $M_{\sqrt{M_u}}$ . (Note that  $\phi = 1.0$ )

 $F_{px}^{*}$  is the seismic force at each level for the diaphragm as defined above by *Provisions* Eq. 5.2.6.4.4 [4.6-2] and not limited by the minima and maxima for that equation.

This requirement is different from similar requirements elsewhere in the *Provisions*. For components thought likely to behave in a brittle fashion, the designer is required to apply the overstrength factor and then given an option to check the *maximum* force that can be delivered by the remainder of the structural system to the element in question. The maximum force would normally be computed from a plastic mechanism analysis. If the option is exercised, the designer can then use the smaller of the two forces. Here the *Provisions* requires the designer to compute both an overstrength level force and a yield level force and then use the larger. This appears to conflict with the *Commentary*.

For Seismic Design Categories B and C, *Provisions* Sec. 5.2.6.2.6 [4.6.1.9] defines a minimum diaphragm seismic design force that will always be less than the forces computed above.

For Seismic Design Category C, *Provisions* Sec. 5.2.6.3.1 [4.6.2.2] requires that collector elements, collector splices, and collector connections to the vertical seismic-force-resisting members be designed in accordance with *Provisions* Sec. 5.2.7.1 [4.2.2.2], which places the overstrength factor on horizontal seismic forces and combines the horizontal and vertical seismic forces with the effects of gravity forces. Because vertical forces do not normally affect diaphragm collector elements, splices, and connections, the authors believe that *Provisions* Sec. 5.2.7.1 [4.2.2.2] is satisfied by the requirements of *Provisions* Sec. 9A.3.3 [A9.2.2], which requires use of the overstrength factor.

Parameters from the example in Sec. 9.2 used to calculate in-plane seismic design forces for the diaphragms are provided in Table 7.1-1.

Table 7.1-1     Design Parameters from Example 9.2			
Design Parameter	Birmingham 1	New York City	
ρ	1.0	1.0	
$\Omega_{_{o}}$	2.5	2.5	
$C_s$	0.12	0.156	
$w_i$ (roof)	861 kips	869 kips	
$w_i$ (floor)	963 kips	978 kips	
$S_{DS}$	0.24	0.39	
Ι	1.0	1.0	

Table 7.1.1 Design Denometers from Example 0.2

1.0 kip = 4.45 kN, 1.0 ft-kip = 1.36 kN-m.

The *Provisions* Appendix to Chapter 9 does not give the option of using the overstrength factor  $\Omega_0$  to estimate the yield of the vertical system, so  $M_{\mu}$  for the wall is computed from the axial load moment interaction diagram data developed in Sec. 9.2. The shape of the interaction diagram between the balanced point and pure bending is far enough from a straight line (see Figure 9.2-6) in the region of interest that simply interpolating between the points for pure bending and balanced conditions is unacceptably unconservative for this particular check. An intermediate point on the interaction diagram was computed for each wall in Sec. 9.2, and that point is utilized here. Yielding begins before the nominal bending capacity is reached, particularly when the reinforcement is distributed uniformly along the wall rather than being concentrated at the ends of the wall. For lightly reinforced walls with distributed reinforcement and with axial loads about one-third of the balanced load, such as these, the yield moment is on the order of 90 to 95 percent of the nominal capacity. It is feasible to compute the moment at which the extreme bar yields, but that does not appear necessary for design. A simple factor of 0.95 was applied to the nominal capacity here. Thus, Table 7.1-2 shows the load information from Sec. 9.2 (the final numbers in this section may have changed, because this example was completed first).

The factor K is large primarily due to consideration of axial load. The strength for design is controlled by minimum axial load, whereas K is maximum for the maximum axial load, which includes some live load and a vertical acceleration on dead load.

	Birmingham 1	New York City
Pure Bending, $M_{n0}$	963 ft-kips	1,723 ft-kips
Intermediate Load, $M_{nB}$	5,355 ft-kips	6,229 ft-kips
Intermediate Load, $P_{nB}$	335 kips	363 kips
Maximum Design Load, $P_u$	315 kips	327 kips
Interpolated $M_n$	5,092 ft-kips	5,782 ft-kips
Approximate $M_y$	4,837 ft-kips	5,493 ft-kips
Design $M_u$	2,640 ft-kips	3,483 ft-kips
Factor $K = M_{y}/M_{u}$	1.83	1.58

 Table 7.1-2
 Shear Wall Overstrength

## 7.1.1.3 Diaphragm Forces for Birmingham Building 1

The weight tributary to the roof and floor diaphragms  $(w_{px})$  is the total story weight  $(w_i)$  at Level *i* minus the weight of the walls parallel to the direction of loading.

Compute diaphragm weight  $(w_{px})$  for the roof and floor as follows:

Roof

Total weight	= 861 kip	)S
Walls parallel to force = $(45 \text{ psf})(277 \text{ ft})(8.67 \text{ ft}/2)$	= <u>-54 kip</u>	)S
W <sub>px</sub>	= 807 kip	)S

Floors

Total weight	= 963 kips
Walls parallel to force = $(45 \text{ psf})(277 \text{ ft})(8.67 \text{ ft})$	= <u>-108 kips</u>
$W_{px}$	= 855 kips

Compute diaphragm demands in accordance with *Provisions* Eq. 5.2.6.4.4 [4.6.3.4]:

$$F_{px} = \frac{\sum_{i=x}^{n} F_i}{\sum_{i=x}^{n} w_i} w_{px}$$

Calculations for  $F_{px}$  are provided in Table 7.1-3.

		<b>Table 7.1-3</b>	Birminghan	n 1 $F_{px}$ Calculati	ions	
	W <sub>i</sub>	$\sum_{i=x}^{n} W_i$	$F_i$	$\sum_{i=x}^{n} F_i = V_i$	$W_{px}$	$F_{px}$
Level	(kips)	(kips)	(kips)	(kips)	(kips)	(kips)
Roof	861	861	175	175	807	164
4	963	1,820	156	331	855	155
3	963	2,790	117	448	855	137
2	963	3,750	78	527	855	120
1	963	4,710	39	566	855	103

<b>Table 7.1-3</b>	Birmingham 1 $F_{px}$ Calculations
--------------------	------------------------------------

1.0 kip = 4.45 kN.

The values for  $F_i$  and  $V_i$  used in Table 7.1-3 are listed in Table 9.2-2.

The minimum value of $F_{px} = 0.2S_{DS}Iw_{px}$	= 0.2(0.24)1.0(807 kips) = 0.2(0.24)1.0(855 kips)	= 38.7 kips (at the roof) = 41.0 kips (at floors)
The maximum value of $F_{px} = 0.4 S_{DS} I w_{px}$	= 2(38.7 kips) = 2(41.0 kips)	= 77.5 kips (at the roof) = 82.1 kips (at floors)

Note that  $F_{px}$  by Table 7.1-3 is substantially larger than the maximum  $F_{px}$ . This is generally true at upper levels if the R factor is less than 5. The value of  $F_{px}$  used for the roof diaphragm is 82.1 kips. Compare this value to  $C_{s}w_{px}$  to determine the minimum diaphragm force for untopped diaphragms as indicated previously.

 $C_{s}w_{px} = 0.12(807 \text{ kips}) = 96.8 \text{ kips}$  (at the roof)  $C_s w_{px} = 0.12(855 \text{ kips}) = 103 \text{ kips}$  (at the floors)

Since  $C_s w_{px}$  is larger than  $F_{px}$ , the controlling force is  $C_s w_{px}$ . Note that this will always be true when I =1.0 and *R* is less than or equal to 2.5. Therefore, the diaphragm seismic design forces are as follows:

 $F'_{px} = \rho \Omega_0 C_s w_{px} = 1.0(2.5)(96.8 \text{ kips}) = 242 \text{ kips}$  (at the roof)  $F'_{px} = \rho \Omega_0 C_s w_{px} = 1.0(2.5)(103 \text{ kips}) = 256 \text{ kips}$  (at the floors)

The second check on design force is based on yielding of the shear walls:

$$F'_{px} = 1.25 K F_{px}^* = 1.25 (1.85) 164 \text{ kips} = 379 \text{ kips}$$
 (at the roof)  
 $F'_{px} = 1.25 K F_{px}^* = 1.25 (1.85) 155 \text{ kips} = 358 \text{ kips}$  (at the floors)

For this example, the force to yield the walls clearly controls the design. To simplify the design, the diaphragm design force used for all levels will be the maximum force at any level, 379 kips.

## 7.1.1.4 Diaphragm Forces for New York Building

The weight tributary to the roof and floor diaphragms  $(w_{px})$  is the total story weight  $(w_i)$  at Level *i* minus the weight of the walls parallel to the force.

Compute diaphragm weight  $(w_{px})$  for the roof and floor as follows:

Roof

Total weight	= 870 kips
Walls parallel to force = $(48 \text{ psf})(277 \text{ ft})(8.67 \text{ ft}/2)$	= <u>-58 kips</u>
$W_{px}$	= 812 kips
Floors	

Total weight	= 978 kips
Walls parallel to force = $(48 \text{ psf})(277 \text{ ft})(8.67 \text{ ft})$	= <u>-115 kips</u>
W <sub>px</sub>	= 863 kips

Calculations for  $F_{px}$  using *Provisions* Eq. 5.2.6.4.4 [4.6.3.4] are not required for the first set of forces because  $C_s w_{px}$  will be greater than or equal to the maximum value of  $F_{px} = 0.4S_{DS}Iw_{px}$  when I = 1.0 and R is less than or equal to 2.5. Compute  $C_s w_{px}$  as:

 $C_s w_{px} = 0.156(812 \text{ kips}) = 127 \text{ kips}$  (at the roof)  $C_s w_{px} = 0.156(863 \text{ kips}) = 135 \text{ kips}$  (at the floors)

The diaphragm seismic design forces are:

 $F'_{px} = \rho \Omega_0 C_s w_{px} = 1.0(2.5)(127 \text{ kips}) = 318 \text{ kips}$  (at the roof)  $F'_{px} = \rho \Omega_0 C_s w_{px} = 1.0(2.5)(135 \text{ kips}) = 337 \text{ kips}$  (at the floors)

Calculations for  $F_{px}$  using *Provisions* Eq. 5.2.6.4.4 [4.6.3.4] are required for the second check  $F'_{px} = 1.25 K F_{px}$ . Following the same procedure as illustrated in the previous section, the maximum  $F_{px}$  is 214 kips at the roof. Thus,

 $1.25KF_{px}^* = 1.25(1.58)214$  kips = 423 kips (at the roof)

To simplify the design, the diaphragm design force used for all levels will be the maximum force at any level. The diaphragm seismic design force (423 kips) is controlled by yielding at the base of the walls, just as with the Birmingham 1 building.

## 7.1.1.5 Static Analysis of Diaphragms

The balance of this example will use the controlling diaphragm seismic design force of 423 kips for the New York building. In the transverse direction, the loads will be distributed as shown in Figure 7.1-1.

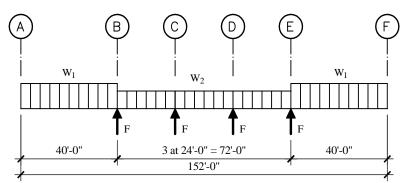


**Figure 7.1-1** Diaphragm force distribution and analytical model (1.0 ft = 0.3048 m).

Assuming the four shear walls have the same stiffness and ignoring torsion, the diaphragm reactions at the transverse shear walls (F as shown in Figure 7.1-1) are computed as follows:

F = 423 kips/4 = 105.8 kips

The uniform diaphragm demands are proportional to the distributed weights of the diaphragm in different areas (see Figure 7.1-1).

$W_1 = [67 \text{ psf}(72 \text{ ft}) + 48 \text{ psf}(8.67 \text{ ft})4](423 \text{ kips} / 863 \text{ kips})$	= 3,180 lb/ft
$W_2 = [67 \text{ psf}(72 \text{ ft})](423 \text{ kips} / 863 \text{ kips})$	= 2,364 lb/ft

Figure 7.1-2 identifies critical regions of the diaphragm to be considered in this design. These regions are:

Joint 1 – maximum transverse shear parallel to the panels at panel-to-panel joints

Joint 2 - maximum transverse shear parallel to the panels at the panel-to-wall joint

- Joint 3 maximum transverse moment and chord force
- Joint 4 maximum longitudinal shear perpendicular to the panels at the panel-to-wall connection (exterior longitudinal walls) and anchorage of exterior masonry wall to the diaphragm for out-of-plane forces

Joint 5 – collector element and shear for the interior longitudinal walls

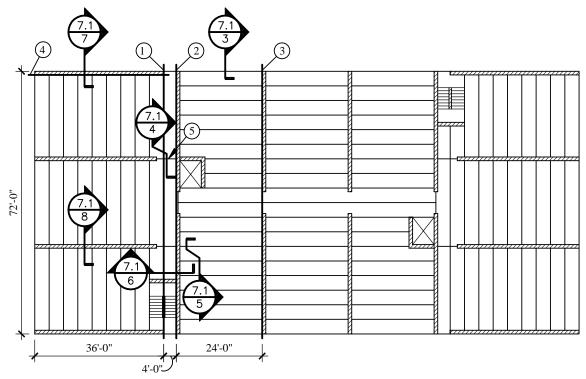


Figure 7.1-2 Diaphragm plan and critical design regions (1.0 ft = 0.3048 m).

*Provisions* Sec. 9.1.1.4 [not applicable in 2003 *Provisions*] defines a chord amplification factor for diaphragms in structures having precast gravity-load systems. [The chord amplification factor has been dropped in the 2003 *Provisions* and does not occur in ASC 318-02. See the initial section of this chapter for additional discussion on changes for the 2003 *Provisions*.] This amplification factor appears to apply to buildings with vertical seismic-force-resisting members constructed of precast or monolithic concrete. Because these masonry wall buildings are similar to buildings with concrete walls, this amplification factor has been included in calculating the chord forces. The amplification factor is:

$$b_d \frac{\left[1 + 0.4 \left(\frac{L_{eff}}{b_d}\right)^2\right]}{12h_s} \ge 1.0$$

where

 $L_{eff}$  = length of the diaphragm between inflection points. Since the diaphragms have no infection points, twice the length of the 40-ft-long cantilevers is used for  $L_{eff}$  = 80 ft  $h_s$  = story height = 8.67 ft  $h_s$  = diaphragm width = 72 ft

 $b_d$  = diaphragm width = 72 ft

The amplification factor = 
$$(72) \frac{\left[1+0.4\left(\frac{80}{72}\right)^2\right]}{12(8.67)} = 1.03$$

Joint forces are:

Joint 1 – Transverse forces	
Shear, $V_{u1} = 3.18$ kips/ft (36 ft) Moment, $M_{u1} = 114.5$ kips (36 ft/2) Chord tension force, $T_{u1} = M/d = 1.03(2,061$ ft-kips/71 ft)	= 114.5 kips = 2,061 ft-kips = 29.9 kips
Joint 2 – Transverse forces	
Shear, $V_{u2} = 3.18$ kips/ft (40 ft) Moment, $M_{u2} = 127$ kips (40 ft/2) Chord tension force, $T_{u2} = M/d = 1.03(2,540$ ft-kips/71 ft)	= 127 kips = 2,540 ft-kips = 36.9 kips
Joint 3 – Transverse forces	
Shear, $V_{u3} = 127$ kips + 2.36 kips/ft (24 ft) - 105.8 kips Moment, $M_{u3} = 127$ kips (44 ft) + 56.7 kips (12 ft) - 105.8 kips (24 ft) Chord tension force, $T_{u3} = M/d = 1.03(3,738 \text{ ft-kips}/71 \text{ ft})$	= 78.1 kips = 3,738 ft-kips = 54.2 kips
Joint 4 – Longitudinal forces	
Wall Force, $F = 423$ kips/8 Wall shear along wall length, $V_{u4} = 52.9$ kips (36 ft)/(152 ft /2) Collector force at wall end, $T_{u4} = C_{u4} = 52.9$ kips - 25.0 kips	= 52.9 kips = 25.0 kips = 27.9 kips
Joint 4 – Out-of-plane forces	

Joint 4 – Out-of-plane forces

The *Provisions* have several requirements for out-of-plane forces. None are unique to precast diaphragms and all are less than the requirements in ACI 318 for precast construction regardless of seismic considerations. Assuming the planks are similar to beams and comply with the minimum requirements of *Provisions* Sec. 5.2.6.1.1 [4.6.1.1] (Seismic Design Category A and greater) [In the 2003 *Provisions*, all requirements for Seismic Design Category A are in Sec. 1.5 but they generally are the same as those in the 2000 *Provisions*. The design and detailing requirements in 2003 *Provisions* Sec. 4.6 apply to Seismic Design Category B and greater], the required out-of-plane horizontal force is:

$$0.05(D + L)_{plank} = 0.05(67 \text{ psf} + 40 \text{ psf})(24 \text{ ft/2}) = 64.2 \text{ plf}$$

According to *Provisions* Sec. 5.2.6.1.2 [4.6.1.2] (Seismic Design Category A and greater), the minimum anchorage for masonry walls is:

$$F_p = 400(S_{DS})I = 400(0.39)1.0$$
 = 156 plf

According to *Provisions* Sec. 5.2.6.2.7 [4.6.1.3] (Seismic Design Category B and greater), bearing wall anchorage shall be designed for a force computed as:

$$0.4(S_{DS})W_{wall} = 0.4(0.39)(48 \text{ psf})(8.67 \text{ ft}) = 64.9 \text{ plf}$$

*Provisions* Sec. 5.2.6.3.2 [4.6.2.1] (Seismic Design Category C and greater) requires masonry wall anchorage to flexible diaphragms to be designed for a larger force. This diaphragm is

considered rigid with respect to the walls, and considering that it is designed to avoid yield under the loads that will yield the walls, this is a reasonable assumption.

$$F_p = 1.2(S_{DS})Iw_p = 1.2(0.39)1.0[(48 \text{ psf})(8.67 \text{ ft})] = 195 \text{ plf}$$

[In the 2003 *Provisions*, Eq. 4.6-1 in Sec. 4.6.2.1 has been changed to  $0.85S_{DS}IW_p$ .]

The force requirements in ACI 318 Sec. 16.5 will be described later.

Joint 5 – Longitudinal forces

Wall force, $F = 423$ kips/8	= 52.9 kips
Wall shear along each side of wall, $V_{\mu4} = 52.9$ kips $[2(36 \text{ ft})/152 \text{ ft}]/2$	= 12.5 kips
Collector force at wall end, $T_{u5} = C_{u5} = 52.9$ kips - 25.0 kips	= 27.9 kips

ACI 318 Sec. 16.5 also has minimum connection force requirements for structural integrity of precast concrete bearing wall building construction. For buildings over two stories there are force requirements for horizontal and vertical members. This building has no vertical precast members. However, ACI 318 Sec. 16.5.1 specifies that the strengths "... for structural integrity shall apply to all precast concrete structures." This is interpreted to apply to the precast elements of this masonry bearing wall structure. The horizontal tie force requirements are:

- 1. 1,500 lb/ft parallel and perpendicular to the span of the floor members. The maximum spacing of ties parallel to the span is 10 ft. The maximum spacing of ties perpendicular to the span is the distance between supporting walls or beams.
- 2. 16,000 lb parallel to the perimeter of a floor or roof located within 4 ft of the edge at all edges.

ACI's tie forces are far greater than the minimum tie forces given in the *Provisions* for beam supports and anchorage for of masonry walls. They do control some of the reinforcement provided, but most of the reinforcement is controlled by the computed connections for diaphragm action.

## 7.1.1.6 Diaphragm Design and Details

Before beginning the proportioning of reinforcement, a note about ACI's  $\phi$  factors is necessary. The *Provisions* cites ASCE 7 for combination of seismic load effects with the effects of other loads. Both ASCE 7 and the *Provisions* make it clear that the appropriate  $\phi$  factors within ACI 318 are those contained within Appendix C of ACI 318-99. These factors are about 10% less than the comparable factors within the main body of the standard. The 2002 edition of ACI 318 has placed the ASCE 7 load combinations within the main body of the standard and revised the  $\phi$  factors accordingly. This example uses the  $\phi$  factors given in the 2002 edition of ACI 318, which are the same as those given in Appendix C of the 1999 edition with one exception. Thus, the  $\phi$  factors used here are:

Tension control (bending and ties)  $\phi = 0.90$ Shear  $\phi = 0.75$ Compression control in tied members  $\phi = 0.65$ .

The minimum tie force requirements given in ACI 318 Sec. 16.5 are specified as nominal values, meaning that  $\phi = 1.00$  for those forces.

## 7.1.1.6.1 Design and Detailing at Joint 3

Joint 3 is designed first to check the requirements of *Provisions* Sec. 9A.3.9 [A9.2.4], which references ACI 318 Sec. 21.7.8.3 [21.9.8.3], which then refers to ACI 318 Sec. 21.7.5.3 [21.9.5.3]. This section provides requirements for transverse reinforcement in the chords of the diaphragm. The compressive stress in the chord is computed using the ultimate moment based on a linear elastic model and gross section properties. To determine the in-plane section modulus (*S*) of the diaphragm, an equivalent thickness (*t*) based on the cross sectional area is used for the hollow core precast units as follows.

t = area/width = 215/48 = 4.5 in. $S = td^2/6$ 

Chord compressive stress is computed as:

 $M_{\mu}/S = 6M_{\mu3}/td^2 = 6(3,738 \times 12)/(4.5)(72 \times 12)^2 = 80.1$  psi

The design 28-day compressive strength of the grout is 4,000 psi. Since the chord compressive stress is less than  $0.2 f_c' = 0.2(4,000) = 800$  psi, the transverse reinforcement indicated in ACI 318 Sec. 21.4.4.1 through 21.4.4.3 is not required.

Compute the required amount of chord reinforcement as:

Chord reinforcement,  $A_{s3} = T_{u3}/\phi f_v = (54.2 \text{ kips})/[0.9(60 \text{ ksi})] = 1.00 \text{ in.}^2$ 

Use two #7 bars,  $A_s = 2(0.60) = 1.20$  in.<sup>2</sup> along the exterior edges (top and bottom of the plan in Figure 7.1- 2). Require cover for chord bars and spacing between bars at splices and anchorage zones by ACI 318 Sec. 21.7.8.3 [21.9.8.3].

Minimum cover = 2.5(7/8) = 2.19 in., but not less than 2.0 in. Minimum spacing = 3(7/8) = 2.63 in., but not less than 1-1/2 in.

Figure 7.1-3 shows the chord element at the exterior edges of the diaphragm. The chord bars extend along the length of the exterior longitudinal walls and act as collectors for these walls in the longitudinal direction (see Joint 4 collector reinforcement and Figure 7.1-7).

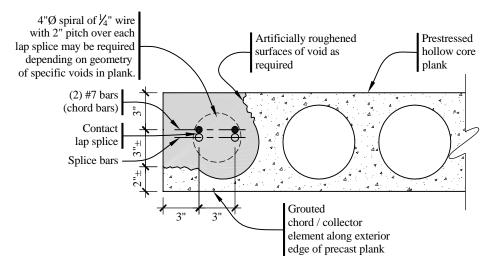


Figure 7.1-3 Joint 3 chord reinforcement at the exterior edge (1.0 in. = 25.4 mm).

Joint 3 must also be checked for the minimum ACI tie forces. The chord reinforcement obviously exceeds the 16 kip perimeter force requirement. The 1.5 kips per foot requirement requires a 6 kip tie at each joint between the planks, which is satisfied with a #3 bar in each joint (0.11 in.<sup>2</sup> at 60 ksi = 6.6 kips). This bar is required at all bearing walls and is shown in subsequent details.

## 7.1.1.6.2 Joint 1 Design and Detailing

The design must provide sufficient reinforcement for chord forces as well as shear friction connection forces as follows:

Chord reinforcement,  $A_{s1} = T_{ul}/\phi f_y = (29.9 \text{ kips})/[0.9(60 \text{ ksi})] = 0.55 \text{ in.}^2$  (collector force from Joint 4 calculations at 27.9 kips is not directly additive).

Shear friction reinforcement,  $A_{vf1} = V_{ul}/\phi\mu f_v = (114.5 \text{ kips})/[(0.75)(1.0)(60 \text{ ksi})] = 2.54 \text{ in.}^2$ 

Total reinforcement required =  $2(0.55 \text{ in.}^2) + 2.54 \text{ in.}^2 = 3.65 \text{ in.}^2$ 

ACI tie force = (3 kips/ft)(72 ft) = 216 kips; reinforcement =  $(216 \text{ kips})/(60 \text{ ksi}) = 3.60 \text{ in.}^2$ 

Provide four #7 bars (two at each of the outside edges) plus four #6 bars (two each at the interior joint at the ends of the plank) for a total area of reinforcement of  $4(0.60 \text{ in}^2) + 4(0.44 \text{ in.}^2) = 4.16 \text{ in.}^2$ 

Because the interior joint reinforcement acts as the collector reinforcement in the longitudinal direction for the interior longitudinal walls, the cover and spacing of the two # 6 bars in the interior joints will be provided to meet the requirements of ACI 318 Sec. 21.7.8.3 [21.9.8.3]:

Minimum cover = 2.5(6/8) = 1.88 in., but not less than 2.0 in. Minimum spacing = 3(6/8) = 2.25 in., but not less than 1-1/2 in.

Figure 7.1-4 shows the reinforcement in the interior joints at the ends of the plank, which is also the collector reinforcement for the interior longitudinal walls (Joint 5). The two #6 bars extend along the length of the interior longitudinal walls as shown in Figure 7.1-8.

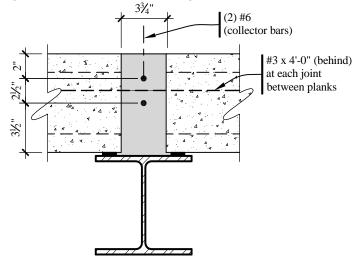


**Figure 7.1-4** Interior joint reinforcement at the ends of plank and the collector reinforcement at the end of the interior longitudinal walls - Joints 1 and 5 (1.0 in. = 25.4 mm).

Figure 7.1-5 shows the extension of the two #6 bars of Figure 7.1-4 into the region where the plank is parallel to the bars. The bars will need to be extended the full length of the diaphragm unless supplemental plank reinforcement is provided. This detail makes use of this supplement plank reinforcement (two #6 bars or an equal area of strand per ACI 318-99 Sec. 21.7.5.2 [21.9.5.2]) and shows the bars anchored at each end of the plank. The anchorage length of the #6 bars is calculated using ACI 318-99 Sec. 21.7.5.4 [21.9.5.4] which references ACI 318 Sec. 21.5.4:

$$l_d = 1.6(2.5) \left( \frac{f_y d_b}{65\sqrt{f_c'}} \right) = 1.6(2.5) \left[ \frac{60,000(d_b)}{65\sqrt{4,000}} \right] = 58.2d_b$$

The 2.5 factor is for the difference between straight and hooked bars, and the 1.6 factor applies when the development length is not within a confined core. Using #6 bars, the required  $l_d = 58.2(0.75 \text{ in.}) = 43.7$  in. Therefore, use  $l_d = 4$  ft, which is the width of the plank.

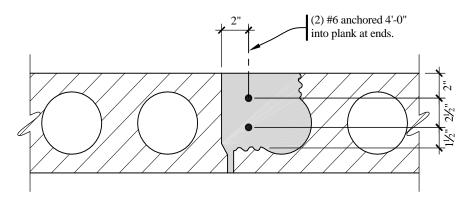


**Figure 7.1-5** Anchorage region of shear reinforcement for Joint 1 and collector reinforcement for Joint 5 (1.0 in. = 25.4 mm).

## 7.1.1.6.3 Joint 2 Design and Detailing

The chord design is similar to the previous calculations:

Chord reinforcement,  $A_{s2} = T_{u2}/\phi f_y = (36.9 \text{ kips})/[0.9(60 \text{ ksi})] = 0.68 \text{ in.}^2$ 

The shear force may be reduced along Joint 2 by the shear friction resistance provided by the supplemental chord reinforcement  $(2A_{chord} - A_{s2})$  and by the four #6 bars projecting from the interior longitudinal walls across this joint. The supplemental chord bars, which are located at the end of the walls, are conservatively excluded here. The shear force along the outer joint of the wall where the plank is parallel to the wall is modified as:

$$V_{u2}^{Mod} = V_{u2} - \left[\phi f_y \mu(A_{4\#6})\right] = 127 - \left[0.75(60)(1.0)(4 \times 0.44)\right] = 47.8 \text{ kips}$$

This force must be transferred from the planks to the wall. Using the arrangement shown in Figure 7.1-6, the required shear friction reinforcement  $(A_{\nu/2})$  is computed as:

$$A_{vf2} = \frac{V_{u2}^{Mod}}{\phi f_y \left(\mu \sin \alpha_f + \cos \alpha_f\right)} = \frac{47.8}{0.75(60)(1.0 \sin 26.6^\circ + \cos 26.6^\circ)} = 0.79 \text{ in.}^2$$

Use two #3 bars placed at 26.6 degrees (2-to-1 slope) across the joint at 4 ft from the ends of the plank and at 8 ft on center (three sets per plank). The angle ( $\alpha_f$ ) used above provides development of the #3 bars while limiting the grouting to the outside core of the plank. The total shear reinforcement provided is 9(0.11 in.<sup>2</sup>) = 0.99 in.<sup>2</sup>

The shear force between the other face of this wall and the diaphragm is:

 $V_{u2}$  - F = 127 - 106 = 21 kips

The shear friction resistance provided by #3 bars in the grout key between each plank (provided for the 1.5 klf requirement of the ACI) is computed as:

$$\phi A_{\nu} f_{\nu} \mu = (0.75)(10 \text{ bars})(0.11 \text{ in.}^2)(60 \text{ ksi})(1.0) = 49.5 \text{ kips}$$

The development length of the #3 and #4 bars will now be checked. For the 180 degree standard hook use ACI 318 Sec. 12.5,  $l_{dh} = l_{hb}$  times the factors of ACI 318 Sec. 12.5.3, but not less than  $8d_b$  or 6 in. Side cover exceeds 2-1/2 in. and cover on the bar extension beyond the hook is provided by the grout and the planks, which is close enough to 2 in. to apply the 0.7 factor of ACI 318 Sec. 12.5.3.2. The continuous #5 provides transverse reinforcement, but it is not arranged to take advantage of ACI 318's 0.8 factor. For the #3 hook:

$$l_{dh} = \frac{0.7(1,200)d_b}{\sqrt{f_c'}} = \frac{0.7(1,200)0.375}{\sqrt{4,000}} = 4.95 \text{ in.}$$
(6" minimum)

The available distance for the perpendicular hook is about 5-1/2 in. The bar will not be fully developed at the end of the plank because of the 6 in. minimum requirement. The full strength is not required for shear transfer. By inspection, the diagonal #3 hook will be developed in the wall as required for the computed diaphragm-to-shear-wall transfer. The straight end of the #3 will now be checked. The standard development length of ACI 318 Sec. 12.2 is used for  $l_d$ .

$$l_d = \frac{f_y d_b}{25\sqrt{f_c'}} = \frac{60,000(0.375)}{25\sqrt{4,000}} = 14.2$$
 in.

Figure 7.1-6 shows the reinforcement along each side of the wall on Joint 2.

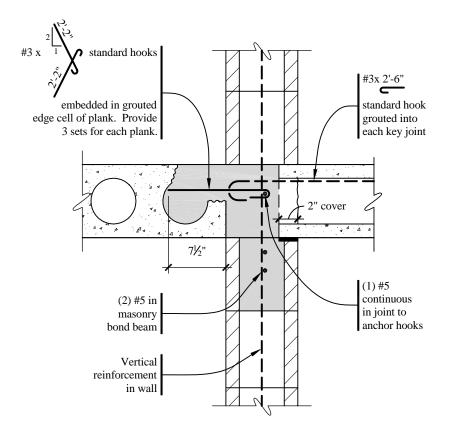


**Figure 7.1-6** Joint 2 transverse wall joint reinforcement (1.0 in. = 25.4 mm, 1.0 ft = 0.3048 m).

#### 7.1.1.6.4 Joint 4 Design and Detailing

The required shear friction reinforcement along the wall length is computed as:

$$A_{vf4} = V_{u4}/\phi\mu f_y = (25.0 \text{ kips})/[(0.75)(1.0)(60 \text{ ksi})] = 0.56 \text{ in.}^2$$

Based upon the ACI tie requirement, provide #3 bars at each plank-to-plank joint. For eight bars total, the area of reinforcement is 8(0.11) = 0.88 in.<sup>2</sup>, which is more than sufficient even considering the marginal development length, which is less favorable at Joint 2. The bars are extended 2 ft into the grout key, which is more than the development length and equal to half the width of the plank.

The required collector reinforcement is computed as:

$$A_{s4} = T_{u4}/\phi f_y = (27.9 \text{ kips})/[0.9(60 \text{ ksi})] = 0.52 \text{ in.}^2$$

The two #7 bars, which are an extension of the transverse chord reinforcement, provide an area of reinforcement of  $1.20 \text{ in.}^2$ 

The reinforcement required by the *Provisions* for out-of-plane force is (195 plf) is far less than the ACI 318 requirement.

Figure 7.1-7 shows this joint along the wall.

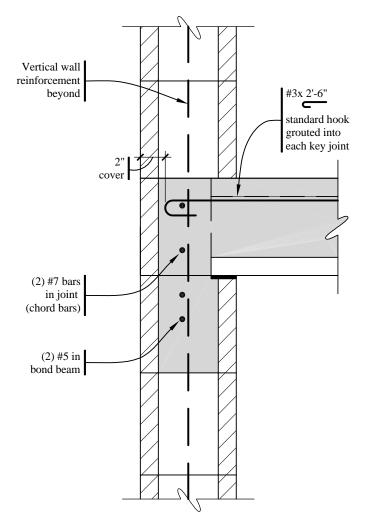


**Figure 7.1-7** Joint 4 exterior longitudinal walls to diaphragm reinforcement and out-of-plane anchorage (1.0 in. = 25.4 mm, 1.0 ft = 0.3048 m).

#### 7.1.1.6.5 Joint 5 Design and Detailing

The required shear friction reinforcement along the wall length is computed as:

 $A_{vt5} = V_{u5}/\phi\mu f_v = (12.5 \text{ kips})/[(0.75)(1.0)(60 \text{ ksi})] = 0.28 \text{ in.}^2$ 

Provide #3 bars at each plank-to-plank joint for a total of 8 bars.

The required collector reinforcement is computed as:

 $A_{s5} = T_{u5}/\phi f_y = (27.9 \text{ kips})/[0.9(60 \text{ ksi})] = 0.52 \text{ in.}^2$ 

Two #6 bars specified for the design of Joint 1 above provide an area of reinforcement of  $0.88 \text{ in.}^2$  Figure 7.1-8 shows this joint along the wall.

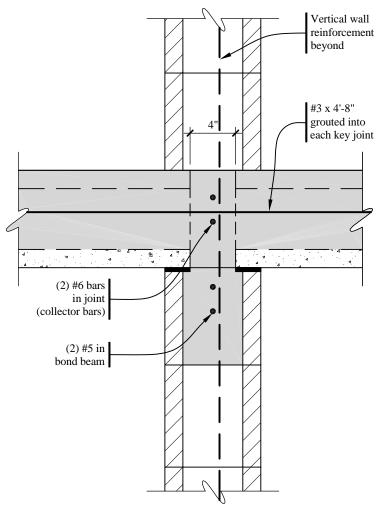


**Figure 7.1-8** Wall-to-diaphragm reinforcement along interior longitudinal walls - Joint 5 (1.0 in. = 25.4 mm, 1.0 ft = 0.3048 m).

# 7.1.2 Topped Precast Concrete Units for Five-Story Masonry Building, Los Angeles, California (see Sec. 9.2)

This design shows the floor and roof diaphragms using topped precast units in the five-story masonry building in Los Angeles, California. The topping thickness exceeds the minimum thickness of 2 in. as required for composite topping slabs by ACI 318 Sec. 21.7.4 [21.9.4]. The topping shall be lightweight concrete (weight = 115 pcf) with a 28-day compressive strength ( $f_c'$ ) of 4,000 psi and is to act compositely with the 8-in.-thick hollow-core precast, prestressed concrete plank. Design parameters are provided in Sec. 9.2. Figure 9.2-1 shows the typical floor and roof plan.

# 7.1.2.1 General Design Requirements

Topped diaphragms may be used in any Seismic Design Category. ACI 318 Sec. 21.7 [21.9]provides design provisions for topped precast concrete diaphragms. *Provisions* Sec. 5.2.6 [4.6] specifies the forces to be used in designing the diaphragms. The amplification factor of *Provisions* Sec. 9.1.1.4 [not applicable in the 2003 *Provisions*] is 1.03, the same as previously computed for the untopped diaphragm.

[As noted above, the chord amplification factor has been dropped for the 2003 Provisions and does not occur in ASC 318-02.]

#### 7.1.2.2 General In-Plane Seismic Design Forces for Topped Diaphragms

The in-plane diaphragm seismic design force  $(F_{px})$  is calculated using Provisions Eq. 5.2.6.4.4 [4.6-2] but must not be less than  $0.2S_{DS}Iw_{px}$  and need not be more than  $0.4S_{DS}Iw_{px}$ .  $V_x$  must be added to  $F_{px}$  calculated using Eq. 5.2.6.4.4 [4.6-2] where:

- the weight tributary to the diaphragm at Level x  $W_{nx} =$
- the spectral response acceleration parameter at short periods (Provisions Sec. 4.1.2 [3.3.5])  $S_{DS} =$
- I =occupancy importance factor (Provisions Sec. 1.4 [1.3])
- $V_r$  = the portion of the seismic shear force required to be transferred to the components of the vertical seismic-force-resisting system due to offsets or changes in stiffness of the vertical resisting member at the diaphragm being designed.

For Seismic Design Category C and higher, Provisions Sec. 5.2.6.3.1 [4.6.2.2] requires that collector elements, collector splices, and collector connections to the vertical seismic-force-resisting members be designed in accordance with Provisions Sec. 5.2.7.1 [4.2.2.2], which combines the diaphragm forces times the overstrength factor ( $\Omega_0$ ) and the effects of gravity forces. The parameters from example in Sec. 9.2 used to calculate in-plane seismic design forces for the diaphragms are provided in Table 7.1-4.

Table 7.1-4         Design Parameters from Sec. 9.2		
Design Parameter	Value	
$arOmega_{o}$	2.5	
$w_i$ (roof)	1,166 kips	
$w_i$ (floor)	1,302 kips	
$S_{DS}$	1.0	
Ι	1.0	
Seismic Design Category	D	

1.0 kip = 4.45 kN.

#### 7.1.2.3 Diaphragm Forces

As indicated previously, the weight tributary to the roof and floor diaphragms  $(w_{Dx})$  is the total story weight  $(w_i)$  at Level *i* minus the weight of the walls parallel to the force.

Compute diaphragm weight  $(w_{nx})$  for the roof and floor as:

Roof

Total weight	= 1,166 kips
Walls parallel to force = $(60 \text{ psf})(277 \text{ ft})(8.67 \text{ ft}/2)$	= <u>-72 kips</u>
$W_{px}$	= 1,094 kips

Floors

Total weight	= 1,302 kips
Walls parallel to force = $(60 \text{ psf})(277 \text{ ft})(8.67 \text{ ft})$	= <u>-144 kips</u>
W <sub>px</sub>	= 1,158 kips

Compute diaphragm demands in accordance with Provisions Eq. 5.2.6.4.4 [4.6-2]:

$$F_{px} = \frac{\sum_{i=x}^{n} F_i}{\sum_{i=x}^{n} w_i} w_{px}$$

Calculations for  $F_{px}$  are provided in Table 7.1-5. The values for  $F_i$  and  $V_i$  are listed in Table 9.2-17.

<b>Table 7.1-5</b> $F_{px}$ Calculations from Sec. 9.2						
Level	w <sub>i</sub> (kips)	$\sum_{i=x}^{n} w_i$ (kips)	F <sub>i</sub> (kips)	$\sum_{i=x}^{n} F_i = V_i$ (kips)	w <sub>px</sub> (kips)	$F_{px}$ (kips)
Roof	1,166	1,166	564	564	1,094	529
4	1,302	2,468	504	1,068	1,158	501
3	1,302	3,770	378	1,446	1,158	444
2	1,302	5,072	252	1,698	1,158	387
1	1,302	6,384	126	1,824	1,158	331

1.0 kip = 4.45 kN.

The minimum value of $F_{px} = 0.2S_{DS}Iw_{px}$	= 0.2(1.0)1.0(1,094 kips) = 0.2(1.0)1.0(1,158 kips)	= 219 kips (at the roof) = 232 kips (at floors)
The maximum value of $F_{px} = 0.4S_{DS}Iw_{px}$	= 2(219 kips) = 2(232 kips)	= 438 kips (at the roof) = 463 kips (at floors)

The value of  $F_{px}$  used for design of the diaphragms is 463 kips, except for collector elements where forces will be computed below.

#### 7.1.2.4 Static Analysis of Diaphragms

The seismic design force of 463 kips is distributed as in Sec. 7.1.1.6 (Figure 7.1-1 shows the distribution). The force is only 9.5 percent higher than that used to design the untopped diaphragm for the New York design due to the intent to prevent yielding in the untopped diaphragm. Figure 7.1-2 shows critical regions of the diaphragm to be considered in this design. Collector elements will be designed for 2.5 times the diaphragm force based on the overstrength factor ( $\Omega_0$ ).

Joint forces taken from Sec. 7.1.1.5 times 1.095 are as:

Joint 1 – Transverse forces

Shear, $V_{u1} = 114.5 \text{ kips} \times 1.095$ Moment, $M_{u1} = 2,061 \text{ ft-kips} \times 1.095$ Chord tension force, $T_u 1 = M/d = 1.03 \times 2,250 \text{ ft-kips} / 71 \text{ ft}$	= 125 kips = 2,250 ft-kips = 32.6 kips
Joint 2 – Transverse forces	
Shear, $V_{u2} = 127 \text{ kips} \times 1.095$ Moment, $M_{u2} = 2,540 \text{ ft-kips} \times 1.095$ Chord tension force, $T_{u2} = M/d = 1.03 \times 2,780 \text{ ft-kips} / 71 \text{ ft}$	= 139 kips = 2,780 ft-kips = 39.3 kips
Joint 3 – Transverse forces	
Shear, $V_{u3} = 78.1 \text{ kips} \times 1.095$ Moment, $M_{u2} = 3,738 \text{ ft-kips} \times 1.095$ Chord tension force, $T_{u3} = M/d = 1.03 \times 4,090 \text{ ft-kips}/71 \text{ ft}$	= 85.5 kips = 4,090 ft-kips = 59.3 kips
Joint 4 – Longitudinal forces	
Wall Force, $F = 52.9$ kips $\times 1.095$	= 57.9 kips

Wall Force, $F = 52.9$ kips $\times 1.095$	= 57.9  k1ps
Wall shear along wall length, $V_{u4} = 25 \text{ kips} \times 1.095$	= 27.4 kips
Collector force at wall end, $\Omega_0 T_{u4} = 2.5(27.9 \text{ kips})(1.095)$	= 76.4 kips

#### Out-of-Plane forces

Just as with the untopped diaphragm, the out-of-plane forces are controlled by ACI 318 Sec. 16.5, which requires horizontal ties of 1.5 kips per foot from floor to walls.

#### Joint 5 – Longitudinal forces

Wall Force, $F = 463$ kips / 8 walls	= 57.9 kips
Wall shear along each side of wall, $V_{\mu4} = 12.5$ kips $\times 1.095$	= 13.7 kips
Collector force at wall end, $\Omega_0 T_{u4} = 2.5(27.9 \text{ kips})(1.095)$	= 76.4 kips

#### 7.1.2.5 Diaphragm Design and Details

#### 7.1.2.5.1 Minimum Reinforcement for 2.5 in. Topping

ACI 318 Sec. 21.7.5.1 [21.9.5.1] references ACI 318 Sec. 7.12, which requires a minimum  $A_s = 0.0018bd$  for welded wire fabric. For a 2.5 in. topping, the required  $A_s = 0.054$  in.<sup>2</sup>/ft. WWF 10×10 - W4.5×W4.5 provides 0.054 in.<sup>2</sup>/ft. The minimum spacing of wires is 10 in. and the maximum spacing is 18 in. Note that the ACI 318 Sec. 7.12 limit on spacing of five times thickness is interpreted such that the topping thickness is not the pertinent thickness.

#### 7.1.2.5.2 Boundary Members

Joint 3 has the maximum bending moment and is used to determine the boundary member reinforcement of the chord along the exterior edge. The need for transverse boundary member reinforcement is reviewed using ACI 318 Sec. 21.7.5.3 [21.9.5.3]. Calculate the compressive stress in the chord with the ultimate moment using a linear elastic model and gross section properties of the topping. It is

conservative to ignore the precast units, but not necessary. As developed previously, the chord compressive stress is:

$$6M_{\mu3}/td^2 = 6(4,090 \times 12)/(2.5)(72 \times 12)^2 = 158 \text{ psi}$$

The chord compressive stress is less than  $0.2f_c' = 0.2(4,000) = 800$  psi. Transverse reinforcement in the boundary member is not required.

The required chord reinforcement is:

$$A_{s3} = T_{\mu3}/\phi f_{y} = (59.3 \text{ kips})/[0.9(60 \text{ ksi})] = 1.10 \text{ in.}^2$$

#### 7.1.2.5.3 Collectors

The design for Joint 4 collector reinforcement at the end of the exterior longitudinal walls and for Joint 5 at the interior longitudinal walls is the same.

$$A_{s4} = A_{s5} = \Omega_0 T_{u4} / \phi f_v = (76.4 \text{ kips}) / [0.9(60 \text{ ksi})] = 1.41 \text{ in.}^2$$

Use two #8 bars ( $A_s = 2 \times 0.79 = 1.58 \text{ in.}^2$ ) along the exterior edges, along the length of the exterior longitudinal walls, and along the length of the interior longitudinal walls. Provide cover for chord and collector bars and spacing between bars per ACI 318 Sec. 21.7.8.3 [21.9.8.3].

Minimum cover = 2.5(8/8) = 2.5 in., but not less than 2.0 in. Minimum spacing = 3(8/8) = 3.0 in., but not less than 1-1/2 in.

Figure 7.1-9 shows the diaphragm plan and section cuts of the details and Figure 7.1-10, the boundary member and chord/collector reinforcement along the edge. Given the close margin on cover, the transverse reinforcement at lap splices also is shown.

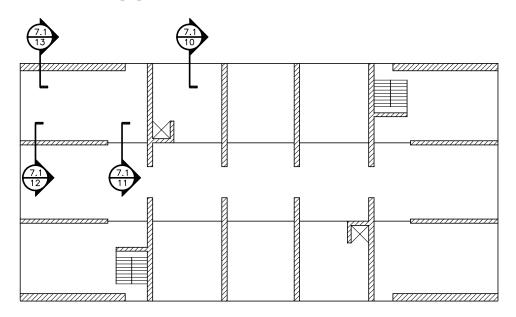
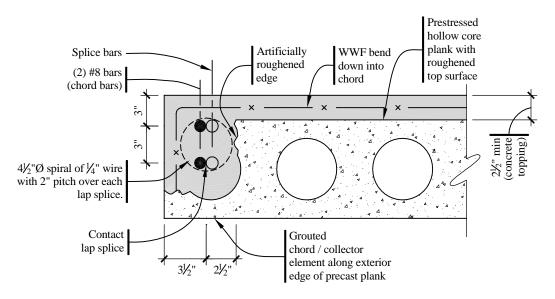
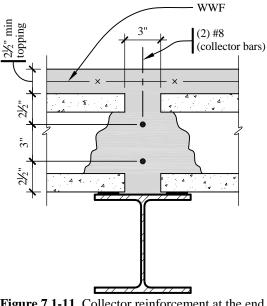


Figure 7.1-9 Diaphragm plan and section cuts.



**Figure 7.1-10** Boundary member, and chord and collector reinforcement (1.0 in. = 25.4 mm).

Figure 7.1-11 shows the collector reinforcement for the interior longitudinal walls. The side cover of 2-1/2 in. is provided by casting the topping into the cores and by the stems of the plank. A minimum space of 1 in. is provided between the plank stems and the sides of the bars.



**Figure 7.1-11** Collector reinforcement at the end of the interior longitudinal walls - Joint 5 (1.0 in. = 25.4 mm, 1.0 ft = 0.3048 m).

7.1.2.5.4 Shear Resistance

Thin composite and noncomposite topping slabs on precast floor and roof members may not have reliable shear strength provided by the concrete. In accordance with ACI 318 Sec. 21.7.7.2 [21.9.7.2], all of the shear resistance must be provided by the reinforcement (that is,  $V_c = 0$ ).

$$\phi V_n = \phi A_{cv} \rho_n f_v = 0.75(0.054 \text{ in.}^2/\text{ft}) 60 \text{ ksi} = 2.43 \text{ kips/ft}$$

The shear resistance in the transverse direction is:

2.43 kips/ft (72 ft) = 175 kips

which is greater than the Joint 2 shear (maximum transverse shear) of 139 kips. No. 3 dowels are used to make the welded wire fabric continuous across the masonry walls. The topping is to be cast into the masonry walls as shown in Figure 7.1-12, and the spacing of the No. 3 bars is set to be modular with the CMU.

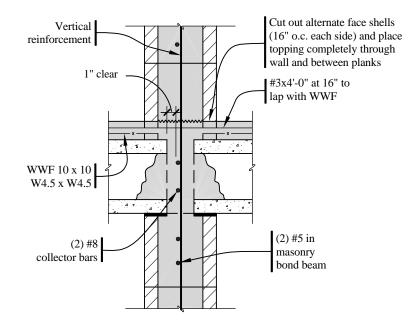


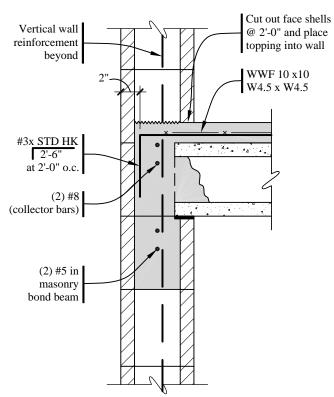
**Figure 7.1-12** Wall-to-diaphragm reinforcement along interior longitudinal walls - Joint 5 (1.0 in. = 25.4 mm, 1.0 ft = 0.3048 m).

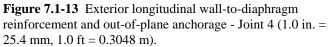
The required shear reinforcement along the exterior longitudinal wall (Joint 4) is:

 $A_{vf4} = V_{u4}/\phi\mu f_v = (27.4 \text{ kips})/[(0.75)(1.0)(60 \text{ ksi})] = 0.61 \text{ in.}^2$ 

#### 7.1.2.5.5 Check Out-of-Plane Forces

At Joint 4 with bars at 2 ft on center,  $F_p = 624$  plf = 2 ft(624 plf) = 1.25 kips. The required reinforcement,  $A_s = 1.25/(0.9)(60\text{ksi}) = 0.023 \text{ in.}^2$ . Provide #3 bars at 2 ft on center, which provides a nominal strength of 0.11 x 60 / 2 = 3.3 klf. The detail provides more than required by ACI 318 Sec. 16.5 for the 1.5 klf tie force. The development length was checked in the prior example. Using #3 bars at 2 ft on center will be adequate, and the detail is shown in Figure 7.1-13. The detail at joint 2 is similar.





# 7.2 THREE-STORY OFFICE BUILDING WITH PRECAST CONCRETE SHEAR WALLS

This example illustrates the seismic design of ordinary precast concrete shear walls that may be used in regions of low to moderate seismicity. The *Provisions* has one requirement for detailing such walls: connections that resist overturning shall be Type Y or Z. ACI 318-02 has incorporated a less specific requirement, renamed the system as intermediate precast structural walls, and removed some of the detail. This example shows an interpretation of the intent of the *Provisions* for precast shear wall systems in regions of moderate and low seismicity, which should also meet the cited ACI 318-02 requirements.

[As indicated at the beginning of this chapter, the requirements for precast shear wall systems in the 2003 *Provisions* have been revised – primarily to point to ACI 318-02 by reference. See also Sec. 7.2.2.1 for more discussion of system requirements.]

# 7.2.1 Building Description

This precast concrete building is a three-story office building (Seismic Use Group I) in southern New England on Site Class D soils. The structure utilizes 10-ft-wide by 18-in.-deep prestressed double tees (DTs) spanning 40 ft to prestressed inverted tee beams for the floors and the roof. The DTs are to be constructed using lightweight concrete. Each of the above-grade floors and the roof are covered with a 2-in.-thick (minimum), normal weight cast-in-place concrete topping. The vertical seismic-force-resisting system is to be constructed entirely of precast concrete walls located around the stairs and elevator/mechanical shafts. The only features illustrated in this example are the rational selection of the seismic design parameters and the design of the reinforcement and connections of the precast concrete shear walls. The diaphragm design is not illustrated.

As shown in Figure 7.2-1, the building has a regular plan. The precast shear walls are continuous from the ground level to 12 ft above the roof. Walls of the elevator/mechanical pits are cast-in-place below grade. The building has no vertical irregularities. The story-to-story height is 12 ft.

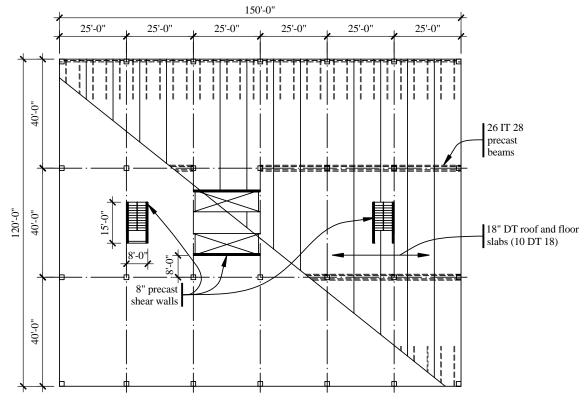


Figure 7.2-1 Three-story building plan (1.0 in. = 25.4 mm, 1.0 ft = 0.3048 m).

The precast walls are estimated to be 8 in. thick for building mass calculations. These walls are normal weight concrete with a 28-day compressive strength,  $f_c' = 5,000$  psi. Reinforcing bars used at the ends of the walls and in welded connectors are ASTM A706 (60 ksi yield strength). The concrete for the foundations and below-grade walls has a 28-day compressive strength,  $f_c' = 4,000$  psi.

# 7.2.2 Design Requirements

#### 7.2.2.1 Seismic Parameters of the *Provisions*

The basic parameters affecting the design and detailing of the building are shown in Table 7.2-1.

Table 7.2-1 Design Latanieters		
Design Parameter	Value	
Seismic Use Group I	<i>I</i> = 1.0	
<i>S<sub>s</sub></i> (Map 1 [Figure 3.3-1])	0.266	
<i>S</i> <sub>1</sub> (Map 2 [Figure 3.3-2])	0.08	
Site Class	D	
$F_a$	1.59	
$F_{v}$	2.4	
$S_{MS} = F_a S_S$	0.425	
$S_{MI} = F_{v}S_{I}$	0.192	
$S_{DS} = 2/3 S_{MS}$	0.283	
$S_{DI} = 2/3 S_{MI}$	0.128	
Seismic Design Category	В	
Basic Seismic-Force-Resisting System	Bearing Wall System	
Wall Type *	Ordinary Reinforced Concrete Shear Walls	
R	4	
$arOmega_{o}$	2.5	
$C_d$	4	

 Table 7.2-1
 Design Parameters

\* *Provisions* Sec. 9.1.1.3 [9.2.2.1.3] provides for the use of ordinary reinforced concrete shear walls in Seismic Design Category B, which does not require adherence to the special seismic design provisions of ACI 318 Chapter 21.

[The 2003 *Provisions* have adopted the 2002 U.S. Geological Survey probabilistic seismic hazard maps and the maps have been added to the body of the 2003 *Provisions* as figures in Chapter 3. These figures replace the previously used separate map package.]

[Ordinary precast concrete shear walls is recognized as a system in Table 4.3-1 of the 2003 *Provisions*. Consistent with the philosophy that precast systems are not expected to perform as well as cast-in-place systems, the design factors for the ordinary precast concrete shear walls per 2003 *Provisions* Table 4.3-1 are: R = 3,  $\Omega_0 = 2.5$ , and  $C_d = 3$ . Note that while this system is permitted in Seismic Design Category B, unline ordinary reinforced concrete shear walls, it is not permitted in Seismic Design Category C. Alternatively, as this example indicates conceptually, this building could be designed incorporating intermediate precast concrete shear walls with the following design values per 2003 *Provisions* Table 4.3-1: R = 4,  $\Omega_0 = 2.5$ , and  $C_d = 4$ .]

#### 7.2.2.2 Structural Design Considerations

#### 7.2.2.2.1 Precast Shear Wall System

This system is designed to yield in bending at the base of the precast shear walls without shear slippage at any of the joints. Although not a stated design requirement of the *Provisions* or ACI 318-02 for this Seismic Design Category, shear slip could kink the vertical rebar at the connection and sabotage the intended performance, which counts on an *R* factor of 4. The flexural connections at the ends of the

walls, which are highly stressed by seismic forces, are designed to be the Type Y connection specified in the *Provisions*. See *Provisions* Sec. 9.1.1.2 [9.2.2.1.1] (ACI Sec. 21.1 [21.1]) for the definitions of ordinary precast concrete structural walls and *Provisions* Sec. 9.1.1.12 [not applicable for the 2003 *Provisions*] (ACI Sec. 21.11.6) for the connections. The remainder of the connections (shear connectors) are then made strong enough to ensure that the inelastic straining is forced to the intended location.

[Per 2003 *Provisions* Sec. 9.2.2.1.1 (ACI 318-02 Sec. 21.1), ordinary precast concrete shear walls need only satisfy the requirements of ACI 318-02 Chapters 1-18 (with Chapter 16 superceding Chapter 14). Therefore, the connections are to be designed in accordance with ACI 318-02 Sec. 16.6.]

Although it would be desirable to force yielding to occur in a significant portion of the connections, it frequently is not possible to do so with common configurations of precast elements and connections. The connections are often unavoidable weak links. Careful attention to detail is required to assure adequate ductility in the location of first yield and that no other connections yield prematurely. For this particular example, the vertical bars at the ends of the shear walls act as flexural reinforcement for the walls and are selected as the location of first yield. The yielding will not propagate far into the wall vertically due to the unavoidable increase in flexural strength provided by unspliced reinforcement within the panel. The issue of most significant concern is the performance of the shear connections at the same joint. The connections are designed to provide the necessary shear resistance and avoid slip without unwittingly increasing the flexural capacity of the connection because such an increase would also increase the maximum shear force on the joint. At the base of the panel, welded steel angles are designed to be flexible for uplift but stiff for in-plane shear.

## 7.2.2.2.2 Building System

No height limitations are imposed (Provisions Table 5.2.2 [4.3-1]).

For structural design, the floors are assumed to act as rigid horizontal diaphragms to distribute seismic inertial forces to the walls parallel to the motion. The building is regular both in plan and elevation, for which, according to *Provisions* Table 5.2.5.1 [4.4-4], use of the ELF procedure (*Provisions* Sec. 5.4 [5.2]) is permitted.

Orthogonal load combinations are not required for this building (Provisions Sec. 5.2.5.2.1 [4.4.2.1]).

Ties, continuity, and anchorage (*Provisions* Sec. 5.2.6.1 and 5.2.6.2 [4.6.1.1 and 4.6.1.2]) must be explicitly considered when detailing connections between the floors and roof, and the walls and columns.

This example does not include consideration of nonstructural elements.

Collector elements are required due to the short length of shear walls as compared to the diaphragm dimensions, but are not designed in this example.

Diaphragms need to be designed for the required forces (*Provisions* Sec. 5.2.6.2.6 [4.6.1.9]), but that design is not illustrated here.

The bearing walls must be designed for a force perpendicular to their plane (*Provisions* Sec. 5.2.6.2.7 [4.6.1.3]), but this requirement is of no real consequence for this building.

The drift limit is 0.025*h*<sub>sx</sub> (*Provisions* Table 5.2.8 [4.5-1]), but drift is not computed here.

ACI 318 Sec. 16.5 requires minimum strengths for connections between elements of precast building structures. The horizontal forces were described in Sec. 7.1; the vertical forces will be described in this example.

# 7.2.3 Load Combinations

The basic load combinations (*Provisions* Sec. 5.2.7 [4.2.2]) require that seismic forces and gravity loads be combined in accordance with the factored load combinations presented in ASCE 7 except that the factors for seismic loads (*E*) are defined by *Provisions* Eq. 5.2.7-1 and 5.2.7-2 [4.2-1 and 4.2-2]:

 $E = \rho Q_E \pm 0.2S_{DS}D = (1.0)Q_E \pm (0.2)(0.283)D = Q_E \pm 0.0567D$ 

According to *Provisions* Sec. 5.2.4.1 [4.3.3.1],  $\rho = 1.0$  for structures in Seismic Design Categories A, B, and C, even though this seismic resisting system is not particularly redundant.

The relevant load combinations from ASCE 7 are:

 $1.2D \pm 1.0E + 0.5L$  $0.9D \pm 1.0E$ 

Into each of these load combinations, substitute E as determined above:

 $1.26D + Q_E + 0.5L$   $1.14D - Q_E + 0.5L \text{ (will not control)}$   $0.96D + Q_E \text{ (will not control)}$  $0.843D - Q_E$ 

These load combinations are for loading in the plane of the shear walls.

# 7.2.4 Seismic Force Analysis

#### 7.2.4.1 Weight Calculations

For the roof and two floors

= 5	6.0 psf
= 1	2.5 psf
=	4.5 psf
=	4.0 psf
=	5.0 psf
= 1	<u>0.0 psf</u>
= 9	2.0 psf
	= 1 = = = 1

The weight of each floor including the precast shear walls is:

(120 ft)(150 ft)(92 psf/1,000) + [15 ft(4) + 25 ft(2)](12 ft)(0.10 ksf) = 1,790 kips

Considering the roof to be the same weight as a floor, the total building weight is W = 3(1,790 kips) = 5,360 kips.

#### 7.2.4.2 Base Shear

The seismic response coefficient ( $C_s$ ) is computed using *Provisions* Eq. 5.4.1.1-1 [5.2-2]:

$$C_S = \frac{S_{DS}}{R/I} = \frac{0.283}{4/1} = 0.0708$$

except that it need not exceed the value from Provisions Eq. 5.4.1.1-2 [5.2-3] computed as:

$$C_{S} = \frac{S_{D1}}{T(R/I)} = \frac{0.128}{0.29(4/1)} = 0.110$$

where *T* is the fundamental period of the building computed using the approximate method of *Provisions* Eq. 5.4.2.1-1 [5.2-6]:

$$T_a = C_r h_n^x = (0.02)(36)^{0.75} = 0.29 \sec^{-1}{10}$$

Therefore, use  $C_s = 0.0708$ , which is larger than the minimum specified in *Provisions* Eq. 5.4.1.1-3 [not applicable in the 2003 *Provisions*]:

$$C_{\rm s} = 0.044IS_{DS} = (.044)(1.0)(0.283) = 0.0125$$

[The minimum  $C_s$  has been changed to 0.01 in the 2003 *Provisions*.]

The total seismic base shear is then calculated using Provisions Eq. 5.4-1 [5.2-1] as:

$$V = C_s W = (0.0708)(5,370) = 380$$
 kips

Note that this force is substantially larger than a design wind would be. If a nominal 20 psf were applied to the long face and then amplified by a load factor of 1.6, the result would be less than half this seismic force already reduced by an R factor of 4.

#### 7.2.4.3 Vertical Distribution of Seismic Forces

The seismic lateral force  $(F_x)$  at any level is determined in accordance with *Provisions* Sec. 5.4.3 [5.2.3]:

$$F_x = C_{vx}V$$

where

$$C_{vx} = \frac{w_x h_x^k}{\sum\limits_{i=1}^n w_i h_i^k}$$

Since the period, T < 0.5 sec, k = 1 in both building directions. With equal weights at each floor level, the resulting values of  $C_{vx}$  and  $F_x$  are as follows:

Roof	$C_{vr} = 0.50$	$F_r = 190 \text{ kips}$
Third Floor	$C_{v3} = 0.33$	$F_3 = 127 \text{ kips}$
Second Floor	$C_{v2} = 0.17$	$F_2 = 63.0$ kips

## 7.2.4.4 Horizontal Shear Distribution and Torsion

#### 7.2.4.4.1 Longitudinal Direction

Design each of the 25-ft-long walls at the elevator/mechanical shafts for half the total shear. Since the longitudinal walls are very close to the center of rigidity, assume that torsion will be resisted by the 15-ft-long stairwell walls in the transverse direction. The forces for each of the longitudinal walls are shown in Figure 7.2-2.

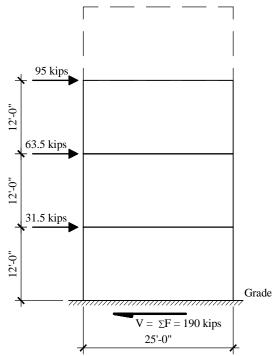


**Figure 7.2-2** Forces on the longitudinal walls (1.0 kip = 4.45 kN, 1.0 ft = 0.3048 m).

#### 7.2.4.4.2 Transverse Direction

Design the four 15-ft-long stairwell walls for the total shear including 5 percent accidental torsion (*Provisions* Sec. 5.4.4.2 [5.2.4.2]). A rough approximation is used in place of a more rigorous analysis considering all of the walls. The maximum force on the walls is computed as:

 $V = 380/4 + 380(0.05)(150)/[(100 \text{ ft moment arm}) \times (2 \text{ walls in each set})] = 109 \text{ kips}$ 

Thus

 $F_r = 109(0.50) = 54.5$  kips  $F_3 = 109(0.33) = 36.3$  kips  $F_2 = 109(0.167) = 18.2$  kips

Seismic forces on the transverse walls of the stairwells are shown in Figure 7.2-3.

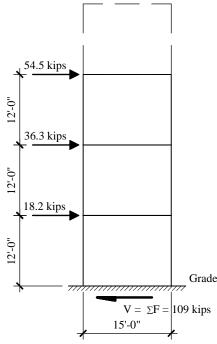


**Figure 7.2-3** Forces on the transverse walls (1.0 kip = 4.45 kN, 1.0 ft = 0.3048 m).

# 7.2.5 PROPORTIONING AND DETAILING

The strength of members and components is determined using the strengths permitted and required in ACI 318 excluding Chapter 21 (see *Provisions* Sec. 9.1.1.3 [9.2.2.1.3]).

# 7.2.5.1 Overturning Moment and End Reinforcement

Design shear panels to resist overturning by means of reinforcing bars at each end with a direct tension coupler at the joints. A commonly used alternative is a threaded post-tensioning bar inserted through the stack of panels, but the behavior is different, and the application of the rules for a Type Y connection to such a design is not clear.

#### 7.2.5.1.1 Longitudinal Direction

The free-body diagram for the longitudinal walls is shown in Figure 7.2-4. The tension connection at the base of the precast panel to the below grade wall is governed by the seismic overturning moment and the dead loads of the panel and supported floors and roof. In this example, the weights for an elevator penthouse, with a floor and equipment at 180 psf between the shafts and a roof at 20 psf, are included. The weight for the floors includes double tees, ceiling and partition (total of 70 psf), but not beams and columns. Floor live load is 50 psf, except 100 psf is used in the elevator lobby. Roof snow load is 30 psf. (The elevator penthouse is so small that it was ignored in computing the gross seismic forces on the building, but it is not ignored in the following calculations.)

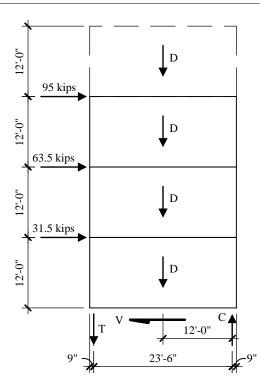


**Figure 7.2-4** Free-body diagram for longitudinal walls (1.0 kip = 4.45 kN, 1.0 ft = 0.3048 m).

At the base

 $M_E = (95 \text{ kips})(36 \text{ ft}) + (63.5 \text{ kips})(24 \text{ ft}) + (31.5 \text{ kips})(12 \text{ ft}) = 5,520 \text{ ft-kips}$ 

 $\sum D = \text{wall} + \text{exterior floors} (\& \text{ roof}) + \text{lobby floors} + \text{penthouse floor} + \text{penthouse roof}$ = (25 ft)(48 ft)(0.1 ksf) + (25 ft)(48 ft/2)(0.070 ksf)(3) + (25 ft)(8 ft/2)(0.070 ksf)(2) + (25 ft)(8 ft/2)(0.18 ksf) + (25 ft)(24 ft/2)(0.02 ksf) = 120 + 126 + 14 + 18 + 6 = 284 kips

 $\Sigma L = (25 \text{ ft})(48 \text{ ft/2})(0.05 \text{ ksf})(2) + (25 \text{ ft})(8 \text{ ft/2})(0.1 \text{ ksf}) = 60 + 10 = 70 \text{ kips}$ 

 $\sum S = (25 \text{ft})(48 \text{ ft} + 24 \text{ ft})(0.03 \text{ ksf})/2 = 27 \text{ kips}$ 

Using the load combinations described above, the vertical loads for combining with the overturning moment are computed as:

 $P_{max} = 1.26 D + 0.5 L + 0.2 S = 397$  kips  $P_{min} = 0.843 D = 239$  kips

The axial load is quite small for the wall panel. The average compression  $P_{max}/A_g = 0.165$  ksi (3.3 percent of  $f'_c$ ). Therefore, the tension reinforcement can easily be found from the simple couple shown on Figure 7.2-4.

The effective moment arm is:

jd = 25 - 1.5 = 23.5 ft

and the net tension on the uplift side is:

$$T_u = \frac{M}{jd} - \frac{P_{\min}}{2} = \frac{5320}{23.5} - \frac{239}{2} = 107$$
 kips

The required reinforcement is:

$$A_s = T_u/\phi f_v = (107 \text{ kips})/[0.9(60 \text{ ksi})] = 1.98 \text{ in.}^2$$

Use two #9 bars ( $A_s = 2.0 \text{ in.}^2$ ) at each end with direct tension couplers for each bar at each panel joint. Since the flexural reinforcement must extend a minimum distance d (the flexural depth)beyond where it is no longer required, use both #9 bars at each end of the panel at all three levels for simplicity.

At this point a check of ACI 318 Sec. 16.5 will be made. Bearing walls must have vertical ties with a nominal strength exceeding 3 kips/ft, and there must be at least two ties per panel. With one tie at each end of a 25 ft panel, the demand on the tie is:

 $T_n = (3 \text{ kip/ft})(25 \text{ ft})/2 = 37.5 \text{ kip}$ 

The two #9 bars are more than adequate for the ACI requirement.

Although no check for confinement of the compression boundary is required for ordinary precast concrete shear walls, it is shown here for interest. Using the check from ACI 318-99 Sec. 21.6.6.2 [21.7.6.2], the depth to the neutral axis is:

Total compression force  $= A_s f_y + P_{max} = (2.0)(60) + 397 = 517$  kips Compression block a = (517 kips)/[(0.85)(5 ksi)(8 in. width)] = 15.2 in. Neutral axis depth c = a/(0.80) = 19.0 in.

The maximum depth (c) with no boundary member per ACI 318-99 Eq. 21-8 [21-8] is:

$$c \leq \frac{l}{600(\delta_u / h_w)}$$

where the term  $(\delta_u/h_w)$  shall not be taken less than 0.007. Once the base joint yields, it is unlikely that there will be any flexural cracking in the wall more than a few feet above the base. An analysis of the wall for the design lateral forces using 50% of the gross moment of inertia, ignoring the effect of axial loads, and applying the  $C_d$  factor of 4 to the results gives a ratio  $(\delta_u/h_w)$  far less than 0.007. Therefore, applying the 0.007 in the equation results in a distance c of 71 in., far in excess of the 19 in. required. Thus, ACI 318-99 would not require transverse reinforcement of the boundary even if this wall were designed as a special reinforced concrete shear wall. For those used to checking the compression stress as an index:

$$\sigma = \frac{P}{A} + \frac{M}{S} = \frac{389}{8(25)12} + \frac{6(5,520)}{8(25)^2(12)} = 742 \text{ psi}$$

The limiting stress is  $0.2f_c'$ , which is 1000 psi, so no transverse reinforcement is required at the ends of the longitudinal walls.

#### 7.2.5.1.2 Transverse Direction

The free-body diagram of the transverse walls is shown in Figure 7.2-5. The weight of the precast concrete stairs is 100 psf and the roof over the stairs is 70 psf.

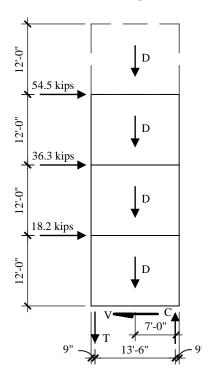


**Figure 7.2-5** Free-body diagram of the transverse walls (1.0 kip = 4.45 kN, 1.0 ft = 0.3048 m).

The transverse wall is similar to the longitudinal wall.

At the base

$$M_E = (54.5 \text{ kips})(36 \text{ ft}) + (36.3 \text{ kips})(24 \text{ ft}) + (18.2 \text{ kips})(12 \text{ ft}) = 3,052 \text{ ft-kips}$$

 $\sum D = (15 \text{ ft})(48 \text{ ft})(0.1 \text{ ksf}) + 2(12.5 \text{ ft}/2)(10 \text{ ft}/2)(0.07 \text{ ksf})(3) + (15 \text{ ft})(8 \text{ ft}/2)[(0.1 \text{ ksf})(3) + (0.07 \text{ ksf})] = 72 + 13 + 18 + 4 = 107 \text{ kips}$ 

 $\Sigma L = 2(12.5 \text{ ft/2})(10 \text{ ft/2})(0.05 \text{ ksf})(2) + (15 \text{ ft})(8 \text{ ft/2})(0.1 \text{ ksf})(3) = 6 + 18 = 24 \text{ kips}$ 

 $\sum S = [2(12.5 \text{ ft}/2)(10 \text{ ft}/2) + (15 \text{ ft})(8 \text{ ft}/2)](0.03 \text{ ksf}) = 3.7 \text{ kips}$ 

 $P_{max} = 1.26(107) + 0.5(24) + 0.2(4) = 148$  kips

 $P_{min} = 0.843(107) = 90.5$  kips

$$jd = 15 - 1.5 = 13.5$$
 ft

 $T_u = (M_{net}/jd) - P_{min}/2 = (3,052/13.5) - 90.5/2 = 181$  kips

 $A_s = T_u/\phi f_y = (181 \text{ kips})/[0.9(60 \text{ ksi})] = 3.35 \text{ in.}^2$ 

Use two #10 and one #9 bars ( $A_s = 3.54 \text{ in.}^2$ ) at each end of each wall with a direct tension coupler at each bar for each panel joint. All three bars at each end of the panel will also extend up through all three levels for simplicity. Following the same method for boundary member check as on the longitudinal walls:

Total compression force  $=A_s f_y + P_{max} = (3.54)(60) + 148 = 360$  kips Compression block a = (360 kips)/[(0.85)(5 ksi)(8 in. width)] = 10.6 in. Neutral axis depth c = a/(0.80) = 13.3 in.

Even though this wall is more flexible and the lateral loads will induce more flexural cracking, the computed deflections are still small and the minimum value of 0.007 is used for the ratio  $(\delta_u/h_w)$ . This yields a maximum value of c = 42.9 in., thus confinement of the boundary would not be required. The check of compression stress as an index gives:

$$\sigma = \frac{P}{A} + \frac{M}{S} = \frac{140}{8(15)12} + \frac{6(2,930)}{8(15)^2(12)} = 951 \text{ psi}$$

Since  $\sigma < 1,000$  psi, no transverse reinforcement is required at the ends of the transverse walls. Note how much closer to the criterion this transverse wall is by the compression stress check.

The overturning reinforcement and connection are shown in Figures 7.2-6. *Provisions* Sec. 9.1.1.12 [not applicable in the 2003 *Provisions*] (ACI 21.11.6.4) requires that this Type Y connection develop a probable strength of 125% of the nominal strength and that the anchorage on either side of the connection develop 130% of the defined probable strength. [As already noted, the connection requirements for ordianry precast concrete shear walls have been removed in the 2003 *Provisions* and the ACI 318-02 requirements are less specific.] The 125% requirement applies to the grouted mechanical splice, and the requirement that a mechanical coupler develop 125% of specified yield strength of the bar is identical to the Type 1 coupler defined by ACI 318 Sec. 21.2.6.1. Some of the grouted splices on the market can qualify as the Type 2 coupler defined by ACI, which must develop the specified tensile strength of the bar. The development length,  $l_d$ , for the spliced bars is multiplied by both the 1.25 and the 1.3 factors to satisfy the *Provisions* requirement. The bar in the panel. The dowel from the foundation will be hooked, otherwise the depth of the foundation would be more than required for structural reasons. The size of the foundation will provide adequate cover to allow the 0.7 factor on ACI's standard development length for hooked bars. For the # 9 bar:

$$1.3(1.25)l_{dh} = \frac{(1.6.25)0.7(1200)d_b}{\sqrt{f_c'}} = \frac{1365(1.128)}{\sqrt{4000}} = 24.3 \text{ in}.$$

Similarly, for the #10 bar, the length is 27.4 in.

Like many shear wall designs, this design does concentrate a demand for overturning resistance on the foundation. In this instance the resistance may be provided by a large footing (on the order of 20 ft by 28 ft by 3 ft thick) under the entire stairwell, or by deep piers or piles with an appropriate cap for load transfer. Refer to Chapter 4 for examples of design of each type of foundation, although not for this particular example.

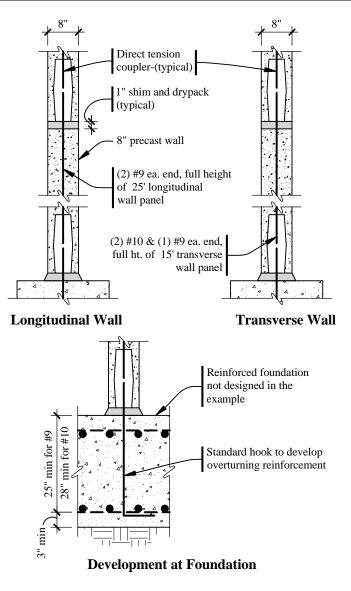


**Figure 7.2-6** Overturning connection detail at the base of the walls (1.0 in = 25.4 mm, 1.0 ft = 0.3048 m).

#### 7.2.5.2 Shear Connections and Reinforcement

Panel joints often are designed to resist the shear force by means of shear friction but that technique is not used for this example because the joint at the foundation will open due to flexural yielding. This opening would concentrate the shear stress on the small area of the dry-packed joint that remains in compression. This distribution can be affected by the shims used in construction. Tests have shown that this often leads to slip of the joint, which could lead to a kink in the principal tension reinforcement at or near its splice and destroy the integrity of the system. Therefore, the joint will be designed with direct shear connectors that will prevent slip along the joint. This is the authors' interpretation of the *Provisions* text indicating that "Type Y connections shall develop under flexural, shear, and axial load actions, as required, a probable strength. . . ." based upon 125 percent of the specified yield in the connection. It would not be required by the ACI 318-02 rules for intermediate precast walls.

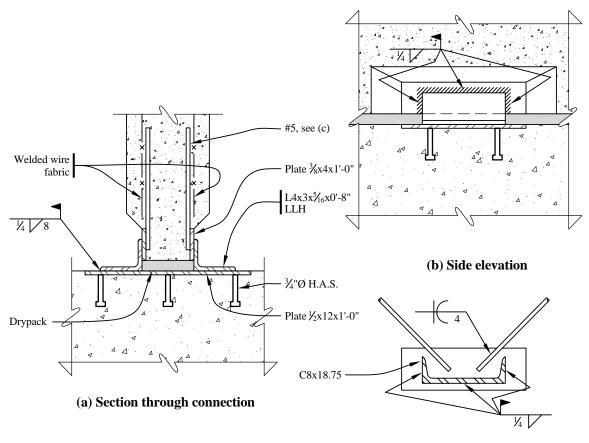
#### 7.2.5.2.1 Longitudinal Direction

The shear amplification factor is determined as:

$$\frac{M_{capacity}}{M_{demand}} = \frac{A_s(1.25)f_y jd + P_{\text{max}} jd/2}{M_u} = \frac{(2.0 \text{ in.}^2)(1.25)(60 \text{ ksi})(23.5 \text{ ft}) + (397 \text{ kip})(23.5 \text{ ft}/2)}{5320 \text{ ft-kip}}$$
  
=1.54

Therefore, the design shear  $(V_{\nu})$  at the base is 1.54(190 kips) = 292 kips

The base shear connection is shown in Figure 7.2-7 and is to be flexible vertically but stiff horizontally in the plane of the panel. The vertical flexibility is intended to minimize the contribution of these connections to overturning resistance, which would simply increase the shear demand.



(c) Section through embedded assembly

Figure 7.2-7 Shear connection at base (1.0 in = 25.4 mm, 1.0 ft = 0.3048 m).

In the panel, provide an assembly with two face plates 3/8 in.  $\times 4$  in.  $\times 12$  in. connected by a C8x18.75 and with diagonal #5 bars as shown in the figure. In the foundation provide an embedded plate  $1/2 \times 12 \times 1'$ -6" with six 3/4 in. diameter headed anchor studs. In the field, weld an L  $4 \times 3 \times 5/16 \times 0'$ -8", long leg horizontal, on each face. The shear capacity of this connection is checked:

Shear in the two loose angles

 $\phi V_n = \phi(0.6F_u)tl(2) = (0.75)(0.6)(58 \text{ ksi})(0.3125 \text{ in.})(8 \text{ in.})(2) = 130.5 \text{ kip}$ 

Weld at toe of loose angles

 $\phi V_n = \phi(0.6F_u)t_e l(2) = (0.75)(0.6)(70 \text{ ksi})(0.25 \text{ in.} / \sqrt{2})(8 \text{ in.})(2) = 89.1 \text{ kip}$ 

Weld at face plates, using Table 8-9 in AISC Manual (3rd edition; same table is 8-42 in 2rd edition)

 $\phi V_n = CC_1 Dl(2 \text{ sides})$   $C_1 = 1.0 \text{ for E70 electrodes}$  l = 8 in. D = 4 (sixteenths of an inch) k = 2 in. / 8 in. = 0.25  $a = \text{eccentricity, summed vectorially: horizontal component is 4 in.; vertical component is 2.67$ in.; thus, al = 4.80 in. and a = 4.8 in./8 in. = 0.6 from the table. By interpolation, C = 1.29 $\phi V_n = (1.29)(1.0)(4)(8)(2) = 82.6 \text{ kip}$ 

Weld from channel to plate has at least as much capacity, but less demand.

Bearing of concrete at steel channel

 $f_c = \phi(0.85f'_c) = 0.65(0.85)(5 \text{ ksi}) = 2.76 \text{ ksi}$ 

The C8 has the following properties:

 $t_w = 0.487$  in.  $b_f = 2.53$  in.  $t_f = 0.39$  in. (average)

The bearing will be controlled by bending in the web (because of the tapered flange, the critical flange thickness is greater than the web thickness). Conservatively ignoring the concrete's resistance to vertical deformation of the flange, compute the width (b) of flange loaded at 2.76 ksi that develops the plastic moment in the web:

 $M_p = \phi F_y t_w^2 / 4 = (0.9)(50 \text{ ksi})(0.487^2 \text{ in.}^2) / 4 = 2.67 \text{ in.-kip/in.}$  $M_u = f_c [(b - t_w)^2 / 2 - (t_w / 2)^2 / 2] = 2.76 [(b - 0.243 \text{ in.})^2 - (0.243 \text{ in.})^2] / 2$ setting the two equal results in b = 1.65 in.

Therefore bearing on the channel is

$$\phi V_c = f_c (2 - t_w)(l) = (2.76 \text{ ksi})[(2(1.65) - 0.487 \text{ in.}](6 \text{ in.}) = 46.6 \text{ kip}]$$

To the bearing capacity on the channel is added the 4 - #5 diagonal bars, which are effective in tension and compression;  $\phi = 0.75$  for shear is used here:

$$\phi V_s = \phi f_v A_s \cos \alpha = (0.75)(60 \text{ ksi})(4)(0.31 \text{ in.}^2)(\cos 45^\circ) = 39.5 \text{ kip}$$

Thus, the total capacity for transfer to concrete is:

 $\phi V_n = \phi V_c + \phi V_s = 46.6 + 39.6 = 86.1$  kip

The capacity of the plate in the foundation is governed by the headed anchor studs. The *Provisions* contain the new anchorage to concrete provisions that are in ACI 318-02 Appendix D. [In the 2003 *Provisions*, the anchorage to concrete provisions have been removed and replaced by the reference to ACI 318-02.] Capacity in shear for anchors located far from an edge of concrete, such as these, and with sufficient embedment to avoid the pryout failure mode is governed by the capacity of the steel:

 $\phi V_s = \phi n A_{se} f_{ut} = (0.65)(6 \text{ studs})(0.44 \text{ in.}^2 \text{ per stud})(60 \text{ ksi}) = 103 \text{ kip}$ 

*Provisions* Sec 9.2.3.3.2 (ACI 318-02 Sec. D.3.3.3) specifies an additional factor of 0.75 to derate anchors in structures assigned to Seismic Design Categories C and higher.

In summary the various shear capacities of the connection are:

Shear in the two loose angles:	130.5 kip
Weld at toe of loose angles:	89.1 kip
Weld at face plates:	82.6 kip
Transfer to concrete:	86.1 kip
Headed anchor studs at foundation:	103 kip

The number of embedded plates (*n*) required for a panel is:

n = 292/82.6 = 3.5

Use four connection assemblies, equally spaced along each side (5'-0" on center works well to avoid the end reinforcement). The plates are recessed to position the #5 bars within the thickness of the panel and within the reinforcement of the panel.

It is instructive to consider how much moment capacity is added by the resistance of these connections to vertical lift at the joint. The vertical force at the tip of the angle that will create the plastic moment in the leg of the angle is:

$$T = M_p / x = F_v lt^2/4 / (l-k) = (36 \text{ ksi})(8 \text{ in})(0.3125^2 \text{ in.}^2)/4]/(4 \text{ in.} - 0.69 \text{ in.}) = 2.12 \text{ kips}$$

There are four assemblies with two loose angles each, giving a total vertical force of 17 kips. The moment resistance is this force times half the length of the panel, which yields 212 ft-kips. The total demand moment, for which the entire system is proportioned, is 5320 ft - kips. Thus, these connections will add about 4% to the resistance and ignoring this contribution is reasonable. If a straight plate 1/4 in. x 8 in., which would be sufficient, were used and if the welds and foundation embedment did not fail first, the tensile capacity would be 72 kips each, a factor of 42 increase over the angles, and the shear connections would have the unintended effect of more than doubling the flexural resistance, which could easily cause failures in the system.

Using ACI 318 Sec. 11.10, check the shear strength of the precast panel at the first floor:

$$\phi V_c = \phi 2 A_{cv} \sqrt{f'_c} hd = 0.85(2) \sqrt{5,000} (8) (23.5) (12) = 271 \text{ kips}$$

Because  $\phi V_c \ge V_u = 190$  kips, the wall is adequate for shear without even considering the reinforcement. Note that the shear strength of wall itself is not governed by the overstrength required for the connection. However, since  $V_u \ge \phi V_c/2 = 136$  kips, ACI Sec. 11.10.8 requires minimum wall reinforcement in accordance with ACI 318 Sec. 11.10.9.4 rather than Chapter 14 or 16. For the minimum required  $\rho_h = 0.0025$ , the required reinforcement is:  $A_v = 0.0025(8)(12) = 0.24$  in.<sup>2</sup>/ft

As before, use two layers of welded wire fabric, WWF 4×4 - W4.0×W4.0, one on each face. Shear reinforcement provided,  $A_v = 0.12(2) = 0.24$  in.<sup>2</sup>/ft

Next, compute the shear strength at Level 2. Since the end reinforcement at the base extends to the top of the shear wall, bending is not a concern. Yield of the vertical bars will not occur, the second floor joint will not open (unlike at the base) and, therefore, shear friction could rationally be used to design the connections at this level and above. Shear keys in the surface of both panels would be advisable. Also, because of the lack of flexural yield at the joint, it is not necessary to make the shear connection be flexible with respect to vertical movement. To be consistent with the seismic force increase from yielding at the base, the shear at this level will be increased using the same amplification factor as calculated for the first story.

The design shear,  $V_{u2} = 1.54(95 + 63.5) = 244$  kips.

Using the same recessed embedded plate assemblies in the panel as at the base, but welded with a straight plate, the number of plates, n = 244/82.6 = 2.96. Use three plates, equally spaced along each side.

Figure 7.2-8 shows the shear connection at the second and third floors of the longitudinal precast concrete shear wall panels.

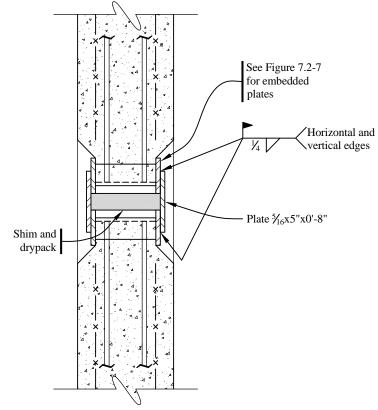


**Figure 7.2-8** Shear connections on each side of the wall at the second and third floors (1.0 in = 25.4 mm).

#### 7.2.5.2.2 Transverse Direction

Use the same procedure as for the longitudinal walls:

$$\frac{M_{capacity}}{M_{demand}} = \frac{A_s(1.25)f_y jd + P_{\text{max}} jd/2}{M_u} = \frac{(3.54 \text{ in.}^2)(1.25)(60 \text{ ksi})(13.5 \text{ ft}) + (148 \text{ kip})(23.5 \text{ ft}/2)}{3052 \text{ ft-kip}}$$
$$= 1.50$$

Design shear,  $V_u$  at base is 1.50(105 kips) = 157.5 kips.

Use the same shear connections as at the base of the longitudinal walls (Figure 7.2-7). The connection capacity is 82.6 kips and the number of connections required is n = 157.5/82.6 = 1.9. Provide two connections on each panel.

Check the shear strength of the first floor panel as described previously:

$$\phi V_c = \phi 2 \sqrt{f'_c} h d = 0.85(2) \sqrt{5,000} (8) (13.5) (12) = 156 \text{ kips}$$

Similar to the longitudinal direction,  $\phi V_c \ge V_u = 142$  kips, but  $V_u \ge \phi V_c/2$  so provide two layers of welded wire fabric, WWF 4×4 - W4.0×W4.0, one on each face as in the longitudinal walls.

Compute the shear demand at the second floor level joint as indicated below.

The design shear,  $V_u = 1.50(52.3 + 34.9) = 130.8$  kips.

Use the same plates as in the longitudinal walls. The number of plates, n = 130.8/82.6 = 1.6. Use two plates, equally spaced. Use the same shear connections for the transverse walls as for the longitudinal walls as shown in Figures 7.2-7 and 7.2-8.

# 7.3 ONE-STORY PRECAST SHEAR WALL BUILDING

This example illustrates precast shear wall seismic design using monolithic emulation as defined in the *Provisions* Sec. 9.1.1.12 [not applicable in the 2003 *Provisions*] (ACI Sec. 21.11.3) for a single-story building in a region of high seismicity. For buildings in Seismic Design Category D, *Provisions* Sec. 9.1.1.12 [not applicable in the 2003 *Provisions*] (ACI Sec. 21.11.2.1) requires that the precast seismic-force-resisting system emulate the behavior of monolithic reinforced concrete construction or that the system's cyclic capacity be demonstrated by testing. This example presents an interpretation of monolithic emulation design with ductile connections. Here the connections in tension at the base of the wall panels yield by bending steel angles out-of-plane. The same connections at the bottom of the panel are detailed and designed to be very strong in shear and to resist the nominal shear strength of the concrete panel.

[Many of the provisions for precast concrete shear walls in areas of high seismicity have been moved out of the 2003 *Provisions* and into ACI 318-02. For structures assigned to Seismic Design Category D, 2003 *Provisions* Sec. 9.2.2.1.3 (ACI 318-02 Sec. 21.21.1.4) permits special precast concrete shear walls (ACI 318-02 Sec. 21.8) or intermediate precast concrete shear walls (ACI 318-02 Sec. 21.13). The 2003 *Provisions* does not differentiate between precast or cast-in-place concrete for special shear walls. This is because ACI 318-02 Sec. 21.8 essentially requires special precast concrete shear walls to satisfy the same design requirements as special reinforced concrete shear walls (ACI 318-02 Sec. 21.7). Alternatively, special precast concrete shear walls are permitted if they satisfy experimental and analytical requirements contained in 2003 *Provisions* Sec. 9.2.2.4 and 9.6.]

# 7.3.1 Building Description

The precast concrete building is a single-story industrial warehouse building (Seismic Use Group I) located in the Los Angeles area on Site Class C soils. The structure has 8-ft-wide by 12-1/2-in.-deep prestressed double tee (DT) wall panels. The roof is light gage metal decking spanning to bar joists that are spaced at 4 ft on center to match the location of the DT legs. The center supports for the joists are joist girders spanning 40 ft to steel tube columns. The vertical seismic-force-resisting system is the precast/prestressed DT wall panels located around the perimeter of the building. The average roof height is 20 ft, and there is a 3 ft parapet. The building is located in the Los Angeles area on Site Class C soils. Figure 7.3-1 shows the plan of the building, which is regular.

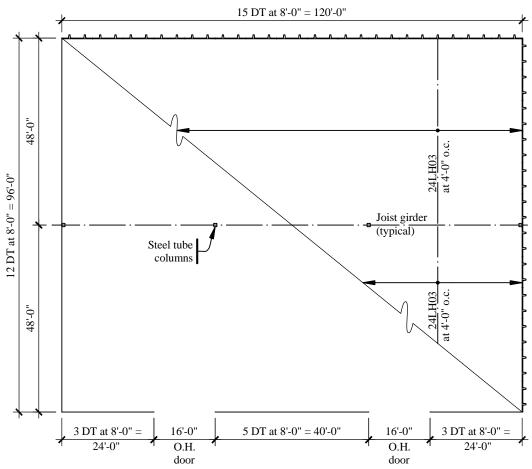


Figure 7.3-1 Single-story industrial warehouse building plan (1.0 ft = 0.3048 m).

The precast wall panels used in this building are typical DT wall panels commonly found in many locations but not normally used in Southern California. For these wall panels, an extra 1/2 in. has been added to the thickness of the deck (flange). This extra thickness is intended to reduce cracking of the flanges and provide cover for the bars used in the deck at the base. The use of thicker flanges is addressed later.

*Provisions* Sec. 9.1.1.5 [9.2.2.1.5.4] (ACI Sec. 21.2.5.1 [21.2.5.1]) limits the grade and type of reinforcement in boundary elements of shear walls and excludes the use of bonded prestressing tendons (strand) due to seismic loads. ACI 318-99 Sec. 21.7.5.2 [21.9.5.2] permits the use of strand in boundary elements of diaphragms provided the stress is limited to 60,000 psi. This design example uses the strand as the reinforcement based on that analogy. The rationale for this is that the primary reinforcement of the DT, the strand, is not working as the ductile element of the wall panel and is not expected to yield in an earthquake.

The wall panels are normal-weight concrete with a 28-day compressive strength,  $f_c' = 5,000$  psi. Reinforcing bars used in the welded connections of the panels and footings are ASTM A706 (60 ksi). The concrete for the foundations has a 28-day compressive strength,  $f_c' = 4,000$  psi.

# 7.3.2 Design Requirements

#### 7.3.2.1 Seismic Parameters of the Provisions

The basic parameters affecting the design and detailing of the building are shown in Table 7.3-1.

Design Parameter	Value			
Seismic Use Group I	I = 1.0			
$S_{s}$ (Map 1 [Figure 3.3-1])	1.5			
<i>S</i> <sub>1</sub> (Map 2 [Figure 3.3-2])	0.60			
Site Class	С			
$F_a$	1.0			
$F_{v}$	1.3			
$S_{MS} = F_a S_S$	1.5			
$S_{MI} = F_{v}S_{I}$	0.78			
$S_{DS}=2/3~S_{MS}$	1.0			
$S_{DI}=2/3~S_{MI}$	0.52			
Seismic Design Category	D			
Basic Seismic-Force-Resisting System	Bearing Walls System			
Wall Type *	Special Reinforced Concrete Shear Wall			
R	5			
$arOmega_{o}$	2.5			
$C_{d}$	5			

 Table 7.3-1
 Design Parameters

\* *Provisions* Sec. 9.7.1.2 [9.2.2.1.3] requires special reinforced concrete shear walls in Seismic Design Category D and requires adherence to the special seismic design provisions of ACI 318 Chapter 21.

[The 2003 *Provisions* have adopted the 2002 U.S. Geological Survey seismic hazard maps and the maps have been added to the body of the 2003 *Provisions* as figures in Chapter 3 (instead of the previously used separate map package).]

#### 7.3.2.2 Structural Design Considerations

#### 7.3.2.2.1 Precast Shear Wall System

The criteria for the design is to provide yielding in a dry connection for bending at the base of each precast shear wall panel while maintaining significant shear resistance in the connection. The flexural connection for a wall panel at the base is located in one DT leg while the connection at the other leg is used for compression. Per *Provisions* Sec. 9.1.1.12 (ACI Sec. 21.11.3.1) [not applicable in the 2003 *Provisions*], these connections resist the shear force equal to the nominal shear strength of the panel and have a nominal strength equal to twice the shear that exists when the actual moment is equal to  $M_{pr}$ 

(which ACI defines as  $\phi = 1.0$  and a steel stress equal to 125% of specified yield). Yielding will develop in the dry connection at the base by bending the horizontal leg of the steel angle welded between the embedded plates of the DT and footing. The horizontal leg of this angle is designed in a manner to resist the seismic tension of the shear wall due to overturning and then yield and deform inelastically. The connections on the two legs of the DT are each designed to resist 50 percent of the shear. The anchorage of the connection into the concrete is designed to satisfy the Type Z requirements in *Provisions* Sec. 9.1.1.12 (ACI Sec. 21.11.6.5) [not applicable in the 2003 *Provisions*.]. Careful attention to structural details of these connections is required to ensure tension ductility and resistance to large shear forces that are applied to the embedded plates in the DT and footing.

[Based on the 2003 *Provisions*, unless the design of special precast shear walls is substantiated by experimental evidence and analysis per 2003 *Provisions* Sec. 9.2.2.4 (ACI 318-02 Sec. 21.8.2), the design must satisfy ACI 318-02 Sec. 21.7 requirements for special structural walls as referenced by ACI 318-02 Sec. 21.8.1. The connection requirements are not as clearly defined as in the 2000 *Provisions*.]

## 7.3.2.2.2 Building System

Height limit is 160 ft (Provisions Table 5.2.2 [4.3-1]).

The metal deck roof acts as a flexible horizontal diaphragm to distribute seismic inertia forces to the walls parallel to the earthquake motion (*Provisions* Sec. 5.2.3.1 [4.3.2.1]).

The building is regular both in plan and elevation.

The reliability factor,  $\rho$  is computed in accordance with *Provisions* Sec. 5.2.4.2 [4.3.3]. The maximum  $\rho_x$  value is given when  $r_{max_x}$  is the largest value.  $r_{max_x}$  is the ratio of design story shear resisted by the single element carrying the most shear force to the total story shear. All shear wall elements (8-ft-wide panels) have the same stiffness. Therefore, the shear in each element is the total shear along a side divided by the number of elements (wall panels). The largest  $r_{max_x}$  value is along the side with the least

number of panels. Along the side with 11 panels,  $r_{max_{x}}$  is computed as:

$$r_{max_x} = \frac{\frac{1/2}{11}}{1.0} = 0.0455$$

$$A_{\rm x} = 96 \; {\rm ft} \times 120 \; {\rm ft} = 11,520 \; {\rm ft}^2$$

$$\rho_x = 2 - \frac{20}{r_{max_x}\sqrt{A_x}} = 2 - \frac{20}{0.0455\sqrt{11,520}} = -2.10$$

Therefore, use  $\rho = 1.0$ .

[The redundancy requirements have been substantially changed for the 2003 *Provisions*. For a shear wall building assigned to Seismic Design Category D,  $\rho = 1.0$  as long as it can be shown that failure of a single shear wall with an aspect ratio greater than 1.0 would not result in more than a 33 percent reduction in story strength or create an extreme torsional irregularity. Based on the design procedures for the walls, each individual panel should be considered a separate wall with an aspect ratio greater than 1.0. Alternatively, if the structure is regular in plan and there are at least two bays of perimeter framing on each side of the structure in each orthogonal direction, the exception in 2003 *Provisions* Sec. 4.3.3.2

permits the use of D,  $\rho = 1.0$ . This exception could be interpreted as applying to this example, which is regular and has more than two wall panels (bays) in both directions.]

The structural analysis to be used is the ELF procedure (*Provisions* Sec. 5.4 [5.2]) as permitted by *Provisions* Table 5.2.5 [4.4-1].

Orthogonal load combinations are not required for flexible diaphragms in Seismic Design Category D (*Provisions* Sec. 5.2.5.2.3 [4.4.2.3]).

This example does not include design of the foundation system, the metal deck diaphragm, or the nonstructural elements.

Ties, continuity, and anchorage (*Provisions* 5.2.6.1 through 5.2.6.4 [4.6]) must be explicitly considered when detailing connections between the roof and the wall panels. This example does not include the design of these connections, but sketches of details are provided to guide the design engineer.

There are no drift limitations for single-story buildings as long as they are designed to accommodate predicted lateral displacements (*Provisions* Table 5.2.8, footnote b [4.5-1, footnote c]).

# 7.3.3 Load Combinations

The basic load combinations (*Provisions* Sec. 5.2.7) require that seismic forces and gravity loads be combined in accordance with the factored load combinations as presented in ASCE 7, except that the load factor for earthquake effects (*E*) is defined by *Provisions* Eq. 5.2.7-1 and 5.2.7-2 [4.2-1 and 4.2-2]:

 $E = \rho Q_E \pm 0.2S_{DS}D = (1.0)Q_E \pm (0.2)(1.0)D = Q_E \pm 0.2D$ 

The relevant load combinations from ASCE 7 are:

 $\begin{array}{l} 1.2D \pm 1.0E + 0.5L \\ 0.9D \pm 1.0E \end{array}$ 

Note that roof live load need not be combined with seismic loads, so the live load term, *L*, can be omitted from the equation.

Into each of these load combinations, substitute E as determined above:

$1.4D + Q_E$	
$1.0D - Q_E$	(will not control)
$1.1D + Q_E$	(will not control)
$0.7D - Q_E$	

These load combinations are for the in-plane direction of the shear walls.

# 7.3.4 Seismic Force Analysis

#### 7.3.4.1 Weight Calculations

Compute the weight tributary to the roof diaphragm

Roofing	=	2.0 psf
Metal decking	=	1.8 psf
Insulation	=	1.5 psf
Lights, mechanical, sprinkler system etc.	=	3.2 psf
Bar joists	=	2.7 psf
Joist girder and columns	=	<u>0.8 psf</u>
Total	=	12.0 psf

The total weight of the roof is computed as:

(120 ft × 96 ft)(12 psf/1,000) = 138 kips

The exterior double tee wall weight tributary to the roof is:

$$(20 \text{ ft}/2 + 3 \text{ ft})[42 \text{ psf}/1,000](120 \text{ ft} + 96 \text{ ft})2 = 236 \text{ kips}$$

Total building weight for seismic lateral load, W = 138 + 236 = 374 kips

#### 7.3.4.2 Base Shear

The seismic response coefficient ( $C_s$ ) is computed using *Provisions* Eq. 5.4.1.1-1 [5.2-2] as:

$$C_s = \frac{S_{DS}}{R/I} = \frac{1.0}{5/1} = 0.20$$

except that it need not exceed the value from Provisions Eq. 5.4.1.1-2 [5.2-3] as follows:

$$C_s = \frac{S_{D1}}{T(R/I)} = \frac{0.52}{0.189(5/1)} = 0.55$$

where *T* is the fundamental period of the building computed using the approximate method of *Provisions* Eq. 5.4.2.1-1 [5.2-6]:

$$T_a = C_r h_n^x = (0.02) (20.0)^{0.75} = 0.189 \text{ sec}$$

Therefore, use  $C_s = 0.20$ , which is larger than the minimum specified in *Provisions* Eq. 5.4.1.1-3 [not applicable in the 2003 *Provisions*]:

$$C_{\rm s} = 0.044 I S_{\rm DS} = (0.044)(1.0)(1.0) = 0.044$$

[The minimum  $C_s$  value has been changed to 0.01 in. the 2003 *Provisions*.

The total seismic base shear is then calculated using Provisions Eq. 5.4-1 [5.2-1] as:

 $V = C_s W = (0.20)(374) = 74.8$  kips

#### 7.3.4.3 Horizontal Shear Distribution and Torsion

Torsion is not considered in the shear distribution in buildings with flexible diaphragms. The shear along each side of the building will be equal, based on a tributary area force distribution.

#### 7.3.4.3.1 Longitudinal Direction

The total shear along each side of the building is V/2 = 37.4 kips. The maximum shear on longitudinal panels (at the side with the openings) is:

 $V_{lu} = 37.4/11 = 3.4$  kips

On each side, each longitudinal wall panel resists the same shear force as shown in the free-body diagram of Figure 7.3-2, where  $D_1$  represents roof joist reactions and  $D_2$  is the panel weight.

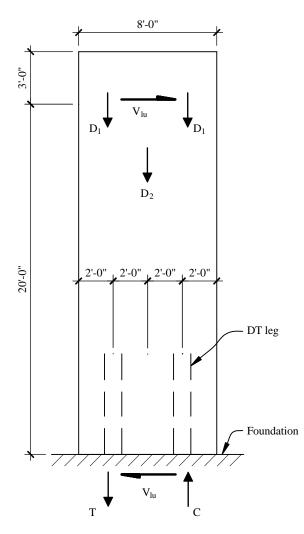


**Figure 7.3-2** Free-body diagram of a panel in the longitudinal direction (1.0 ft = 0.3048 m).

#### 7.3.4.3.2 Transverse Direction

Seismic forces on the transverse wall panels are all equal and are:

 $V_{tu} = 37.4/12 = 3.12$  kips

Figure 7.3-3 shows the transverse wall panel free-body diagram.

Note the assumption of uniform distribution to the wall panels in a line requires that the roof diaphragm be provided with a collector element along its edge. The chord designed for diaphragm action in the perpendicular direction will normally be capable of fulfilling this function, but an explicit check should be made in the design.

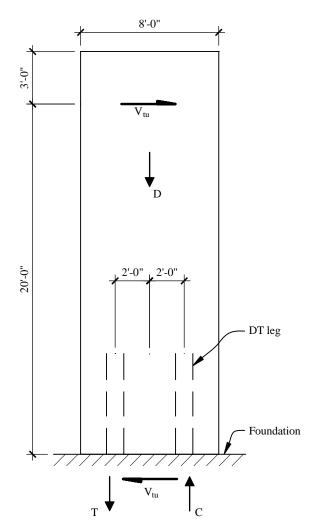


**Figure 7.3-3** Free-body diagram of a panel in the transverse direction (1.0 ft = 0.3048 m).

#### 7.3.5 Proportioning and Detailing

The strength of members and components is determined using the strengths permitted and required in ACI 318 including Chapter 21.

# 7.3.5.1 Tension and Shear Forces at the Panel Base

Design each precast shear panel to resist the seismic overturning moment by means of a ductile tension connector at the base of the panel. A steel angle connector will be provided at the connection of each leg of the DT panel to the concrete footing. The horizontal leg of the angle is designed to yield in bending as needed in an earthquake. *Provisions* Sec. 9.1.1.12 [not applicable in the 2003 *Provisions*] requires that dry connections at locations of nonlinear action comply with applicable requirements of monolithic concrete construction and satisfy the following:

- 1. Where the moment action on the connection is assumed equal to  $M_{pr}$ , the co-existing shear on the connection shall be no greater than  $0.5S_{nConnection}$  and
- 2. The nominal shear strength for the connection shall not be less than the shear strengths of the members immediately adjacent to that connection.

Precisely how ductile dry connections emulate monolithic construction is not clearly explained. The dry connections used here do meet the definition of a yielding steel element at a connection contained in ACI 318-02. For the purposes of this example, these two additional requirements are interpreted as:

- 1. When tension from the seismic overturning moment causes 1.25 times the yield moment in the angle, the horizontal shear on this connection shall not exceed one-half the nominal shear strength of the connection. For this design, one-half the total shear will be resisted by the angle at the DT leg in tension and the remainder by the angle at the DT leg in compression.
- 2. The nominal shear strength of the connections at the legs need to be designed to exceed the in-plane shear strength of the DT.

Determine the forces for design of the DT connection at the base.

# 7.3.5.1.1 Longitudinal Direction

Use the free-body diagram shown in Figure 7.3-2. The maximum tension for the connection at the base of the precast panel to the concrete footing is governed by the seismic overturning moment and the dead loads of the panel and the roof. The weight for the roof is 11.2 psf, which excludes the joist girders and columns.

At the base

 $M_E = (3.4 \text{ kips})(20 \text{ ft}) = 68.0 \text{ ft-kips}$ 

Dead loads

$$D_1 = (11.2/1,000) \left(\frac{48}{2}\right) 4 = 1.08$$
 kips

$$D_2 = 0.042(23)(8) = 7.73$$
 kips  
 $\Sigma D = 2(1.08) + 7.73 = 9.89$  kips  
 $1.4D = 13.8$  kips  
 $0.7 D = 6.92$  kips

Compute the tension force due to net overturning based on an effective moment arm, d = 4.0 ft (distance between the DT legs). The maximum is found when combined with 0.7D:

 $T_u = M_E/d - 0.7D/2 = 68.0/4 - 6.92/2 = 13.5$  kips

## 7.3.5.1.2 Transverse Direction

For the transverse direction, use the free-body diagram of Figure 7.3-3. The maximum tension for connection at the base of the precast panel to the concrete footing is governed by the seismic overturning moment and the dead loads of just the panel. No load from the roof is included, since it is negligible.

At the base

 $M_E = (3.12 \text{ kips})(20 \text{ ft}) = 62.4 \text{ ft-kips}$ 

The dead load of the panel (as computed above) is  $D_2 = 7.73$  kips, and 0.7D = 5.41.

The tension force is computed as above for d = 4.0 ft (distance between the DT legs):

 $T_u = 62.4/4 - 5.41/2 = 12.9$  kips

This tension force is less than that at the longitudinal wall panels. Use the tension force of the longitudinal wall panels for the design of the angle connections.

# 7.3.5.2 Panel Reinforcement

Check the maximum compressive stress in the DT leg for the requirement of transverse boundary element reinforcement per ACI 318 Sec. 21.6.6.3 [21.7.6.3]. Figure 7.3-4 shows the cross section used. The section is limited by the area of dry-pack under the DT at the footing.

The reason to limit the area of dry-pack at the footing is to locate the boundary elements in the legs of the DT, at least at the bottom of the panel. The flange between the legs of the DT is not as susceptible to cracking during transportation as are the corners of DT flanges outside the confines of the legs. The compressive stress due to the overturning moment at the top of the footing and dead load is:

$$A = 227 \text{ in.}^{2}$$
  

$$S = 3240 \text{ in.}^{3}$$
  

$$\sigma = \frac{P}{A} + \frac{M_{E}}{S} = \frac{13,800}{227} + \frac{12(68,000)}{3,240} = 313 \text{ psi}$$

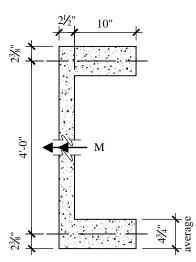


**Figure 7.3-4** Cross section of the DT dry-packed at the footing (1.0 in = 25.4 mm, 1.0 ft = 0.3048 m).

Roof live loads need not be included as a factored axial load in the compressive stress check, but the force from the prestress steel will be added to the compression stress above because the prestress force will be effective a few feet above the base and will add compression to the DT leg. Each leg of the DT will be reinforced with one 1/2-in. diameter and one 3/8-in. diameter strand. Figure 7.3-5 shows the location of these prestressed strands.

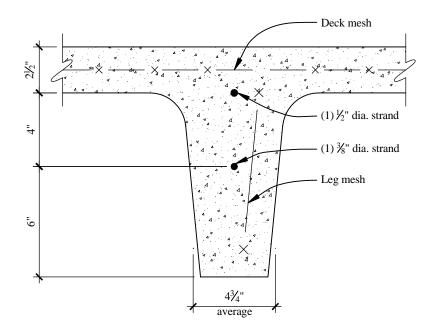


**Figure 7.3-5** Cross section of one DT leg showing the location of the bonded prestressing tendons or strand (1.0 in = 25.4 mm).

Next, compute the compressive stress resulting from these strands. Note the moment at the height of strand development above the footing, about 26 in. for the effective stress ( $f_{se}$ ), is less than at the top of footing. This reduces the compressive stress by:

$$\frac{(3.4)(26)}{3,240} \times 1000 = 27 \text{ psi}$$

In each leg, use

$$P = 0.58f_{pu}A_{ps} = 0.58(270 \text{ ksi})[0.153 + 0.085] = 37.3 \text{ kips}$$
  

$$A = 168 \text{ in.}^{2}$$
  

$$e = y_{b} - CG_{Strand} = 9.48 - 8.57 = 0.91 \text{ in.}$$
  

$$S_{b} = 189 \text{ in.}^{3}$$
  

$$\sigma = \frac{P}{A} + \frac{Pe}{S} = \frac{37,300}{168} + \frac{0.91(37,300)}{189} = 402 \text{ psi}$$

Therefore, the total compressive stress is approximately 313 + 402 - 27 = 688 psi.

The limiting stress is  $0.2 f_c'$ , which is 1000 psi, so no special boundary elements are required in the longitudinal wall panels.

Reinforcement in the DT for tension is checked at 26 in. above the footing. The strand reinforcement of the DT leg resisting tension is limited to 60,000 psi. The rationale for using this stress is discussed at the beginning of this example.

$$D_2 = (0.042)(20.83)(8) = 7.0$$
 kips

 $P_{min} = 0.7(7.0 + 2(1.08)) = 6.41$  kips  $M_E = (3.4)(17.83) = 60.6$  ft-kips  $T_u = M_{net}/d - P_{min}/2 = 12.0$  kips

The area of tension reinforcement required is:

$$A_s = T_{\mu}/\phi f_{\nu} = (12.0 \text{ kips})/[0.9(60 \text{ ksi})] = 0.22 \text{ in.}^2$$

The area of one  $\frac{1}{2}$  in. diameter and one  $\frac{3}{8}$  in. diameter strand is  $0.153 \text{ in.}^2 + 0.085 \text{ in.}^2 = 0.236 \text{ in.}^2$  The mesh in the legs is available for tension resistance, but not required in this check.

To determine the nominal shear strength of the concrete for the connection design, complete the shear calculation for the panel in accordance with ACI Sec. 21.6 [21.7]. The demand on each panel is:

$$V_u = V_{lu} = 3.4$$
 kips

Only the deck between the DT legs is used to resist the in-plane shear (the legs act like flanges, meaning that the area effective for shear is the deck between the legs). First, determine the minimum required shear reinforcement based on ACI Sec. 21.6.2.1 [21.7.2]. Since

$$A_{cv}\sqrt{f_c'} = 2.5(48)\sqrt{5,000} = 8.49$$
 kips

exceeds  $V_u = 3.4$  kips, the reinforcement of the deck is per ACI 318 Sec. 16.4.2. Using welded wire fabric, the required areas of reinforcement are:

$$A_{sh} = A_{sv} = (0.001)(2.5)(12) = 0.03 \text{ in.}^2/\text{ft}$$

Provide  $6 \times 6$  - W2.5 × W2.0 welded wire fabric.

$$A_{sh} = 0.05 \text{ in.}^2/\text{ft}$$
  
 $A_{sv} = 0.04 \text{ in.}^2/\text{ft}$ 

The nominal shear strength of the wall panel by ACI 318 Sec. 21.6.4.1 is:

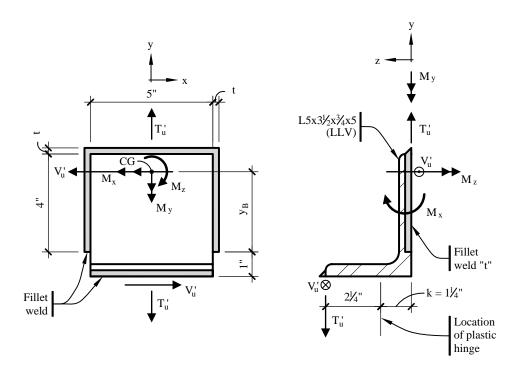
$$V_n = A_{cv} \left( \alpha_c \sqrt{f_c'} + \rho_n f_y \right) = (2.5) (48) \frac{2\sqrt{5,000}}{1,000} + 0.05 (4) (60) = 29.0 \text{ kips}$$

where  $\alpha_c$  is 2.0 for  $h_w/l_w = 23/4 = 5.75$ , which is greater than 2.0. Given that the connections will be designed for a shear of 29 kips, it is obvious that half the nominal shear strength will exceed the seismic shear demand, which is 3.4 kips.

The prestress force and the area of the DT legs are excluded from the calculation of the nominal shear strength of the DT wall panel. The prestress force is not effective at the base, where the connection is, and the legs are like the flanges of a channel, which are not effective in shear.

# 7.3.5.3 Size the Yielding Angle

The angle, which is the ductile element of the connection, is welded between the plates embedded in the DT leg and the footing. This angle is a  $L5 \times 3-1/2 \times 3/4 \times 0$  ft-5 in. with the long leg vertical. The steel for the angle and embedded plates will be ASTM A572, Grade 50. The horizontal leg of the angle needs to be long enough to provide significant displacement at the roof, although this is not stated as a



requirement in either the *Provisions* or ACI 318. This will be examined briefly here. The angle and its welds are shown in Figure 7.3-6.

**Figure 7.3-6** Free-body of the angle and the fillet weld connecting the embedded plates in the DT and the footing (elevation and section) (1.0 in = 25.4 mm).

The bending moment at a distance k from the heel of the angle (location of the plastic hinge in the angle) is:

$$M_{\mu} = T_{\mu}(3.5 - k) = 13.5(3.5 - 1.25) = 30.4$$
 in.-kips

$$\phi_b M_n = 0.9 F_y Z = 0.9 (50) \left[ \frac{5(0.75)^2}{4} \right] = 31.6$$
 in.-kips

Providing a stronger angle (e.g., a shorter horizontal leg) will simply increase the demands on the remainder of the assembly. Using *Provisions* Sec. 9.1.1.12 (ACI Sec. 21.11.6.5) [not applicable in the 2003 *Provisions*], the tension force for the remainder of this connection other than the angle is based upon a probable strength equal to 140% of the nominal strength. Thus

$$T'_{u} = \frac{M_{n}(1.4)}{3.5 - k} = \frac{(50)(5)(0.75)^{2}/4}{3.5 - 1.25} \times 1.4 = 21.9 \text{ kips}$$

Check the welds for the tension force of 21.9 kips and a shear force  $(V_u')$  of 29.0/2 = 14.5 kips, or the shear associated with  $T_u'$ , whichever is greater. The bearing panel, with its larger vertical load, will give a larger shear.

1.4D = 13.8 kips, and  $V = [T_u'(4) + 1.4D(2)]/20 = [21.9/4 + 13.8(2)]/20 = 5.76$  kips.  $V_n$  for the panel obviously controls.

But before checking the welds, consider the deformability of the system as controlled by the yielding angle. Ignore all sources of deformation except the angle. (This is not a bad assumption regarding the double tee itself, but other aspects of the connections, particularly the plate and reinforcement embedded in the DT, will contribute to the overall deformation. Also, the diaphragm deformation will overwhelm all other aspects of deformation, but this is not the place to address flexible diaphragm issues.) The angle deformation will be idealized as a cantilever with a length from the tip to the center of the corner, then upward to the level of the bottom of the DT, which amounts to:

L = 3.5 in. - t/2 + 1 in. - t/2 = 3.75 in.

Using an elastic-plastic idealization, the vertical deformation at the design moment in the leg is

 $\delta_v = TL^3/3EI = (13.5 \text{ kips})(3.75 \text{ in.})^3/[3(29000 \text{ ksi})(5 \text{ in.})(0.75 \text{ in.})^3/12] = 0.047 \text{ in.}$ 

This translates into a horizontal motion at the roof of 0.24 in. (20 ft to the roof, divided by the 4 ft from leg to leg at the base of the DT.) With  $C_d$  of 4, the predicted total displacement is 0.96 in. These displacements are not very large, but now compare with the expectations of the *Provisions*. The approximate period predicted for a 20-ft-tall shear wall building is 0.19 sec. Given a weight of 374 kips, as computed previously, this would imply a stiffness from the fundamental equation of dynamics:

$$T = 2\pi \sqrt{\frac{W/g}{K}} \Rightarrow K = 4\pi^2 W/(gT) = 4\pi^2 374/(386 \times 0.19) = 201 \text{ kip/in}.$$

Now, given the design seismic base shear of 74.8 kips, this would imply an elastic displacement of

$$\delta_h = 74.8 \text{ kip} / (201 \text{ kip/in.}) = 0.37 \text{ in.}$$

This is about 50% larger than the simplistic calculation considering only the angle. The bending of angle legs about their weak axis has a long history of providing ductility and, thus, it appears that this dry connection will provide enough deformability to be in the range of expectation of the *Provisions*.

## 7.3.5.4 Welds to Connection Angle

Welds will be fillet welds using E70 electrodes.

For the base metal,  $\phi R_n = \phi(F_v) A_{BM}$ .

For which the limiting stress is  $\phi F_{v} = 0.9(50) = 45.0$  ksi.

For the weld metal,  $\phi R_n = \phi(F_v)A_w = 0.75(0.6)70(0.707)A_w$ .

For which limiting stress is 22.3 ksi.

Size a fillet weld, 5 in. long at the angle to embedded plate in the footing:

Using an elastic approach

Resultant force =  $\sqrt{V^2 + T^2} = \sqrt{14.5^2 + 21.9^2} = 26.3$  kips

 $A_w = 26.3/22.3 = 1.18$  in.<sup>2</sup>

 $t = A_w/l = 1.18 \text{ in.}^2/5 \text{ in.} = 0.24 \text{ in.}$ 

For a 3/4 in. angle leg, use a 5/16 in. fillet weld. Given the importance of this weld, increasing the size to 3/8 in. would be a reasonable step. With ordinary quality control to avoid flaws, increasing the strength of this weld by such an amount should not have a detrimental effect elsewhere in the connection.

Now size the weld to the plate in the DT. Continue to use the conservative elastic method to calculate weld stresses. Try a fillet weld 5 in. long across the top and 4 in. long on each vertical leg of the angle. Using the free-body diagram of Figure 7.3-6 for tension and Figure 7.3-7 for shear, the weld moments and stresses are:

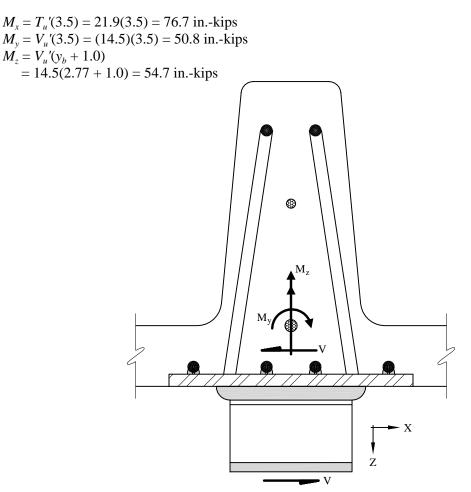


**Figure 7.3-7** Free-body of angle with welds, top view, showing only shear forces and resisting moments.

For the weld between the angle and the embedded plate in the DT as shown in Figure 7.3-7 the section properties for a weld leg (t) are:

 $A = 13t \text{ in.}^2$  $I_x = 23.0t \text{ in.}^4$  $I_y = 60.4t \text{ in.}^4$ 

$$I_p = I_x + I_y = 83.4t \text{ in.}^4$$
  
 $y_b = 2.77 \text{ in.}$   
 $x_L = 2.5 \text{ in.}$ 

To check the weld, stresses are computed at all four ends (and corners). The maximum stress is at the lower right end of the inverted U shown in Figure 7.3-6.

$$\sigma_x = \frac{V'_u}{A} + \frac{M_z y_b}{I_p} = \frac{14.5}{13t} + \frac{(54)(2.77)}{83.4t} = \left(\frac{2.93}{t}\right) \text{ksi}$$

$$\sigma_y = -\frac{T'_u}{A} + \frac{M_z x_L}{I_p} = -\frac{21.9}{13t} + \frac{(54.7)(2.5)}{83.4t} = \left(\frac{0.045}{t}\right) \text{ksi}$$

$$\sigma_z = -\frac{M_y x_L}{I_y} - \frac{M_x y_b}{I_x} = -\frac{(50.8)(2.5)}{60.4t} - \frac{(76.7)(2.77)}{23.0t} = \left(-\frac{11.3}{t}\right) \text{ksi}$$

$$\sigma_R = \sqrt{\sigma_x^2 + \sigma_y^2 + \sigma_z^2} = \frac{1}{t} \sqrt{(2.93)^2 + (0.045)^2 + (-11.3)^2} = \left(\frac{11.67}{t}\right) \text{ksi}$$

Thus, t = 11.67/22.3 = 0.52 in., say 9/16 in. Field welds are conservatively sized with the elastic method for simplicity and to minimize construction issues.

### 7.3.5.5 Tension and Shear at the Footing Embedment

Reinforcement to anchor the embedded plates is sized for the same tension and shear, and the development lengths are lengthened by an additional 30%, per *Provisions* Sec. 9.1.1.12 (ACI Sec. 21.11.6.5) [not applicable in the 2003 *Provisions*]. Reinforcement in the DT leg and in the footing will be welded to embedded plates as shown in Figure 7.3-8.

The welded reinforcement is sloped to provide concrete cover and to embed the bars in the central region of the DT leg and footing. The tension reinforcement area required in the footing is:

$$A_{s,Sloped} = \frac{T'_u}{\phi f_y \cos \theta} = \frac{21.9}{0.9(60)(\cos 26.5^\circ)} = 0.45 \text{ in.}^2$$

Use two #5 bars ( $A_s = 0.62 \text{ in.}^2$ ) at each embedded plate in the footing.

The shear bars in the footing will be two #4 placed on an angle of two (plus)-to-one. The resultant shear resistance is:

 $\phi V_n = 0.75(0.2)(2)(60)(\cos 26.5^\circ) = 16.1$  kips

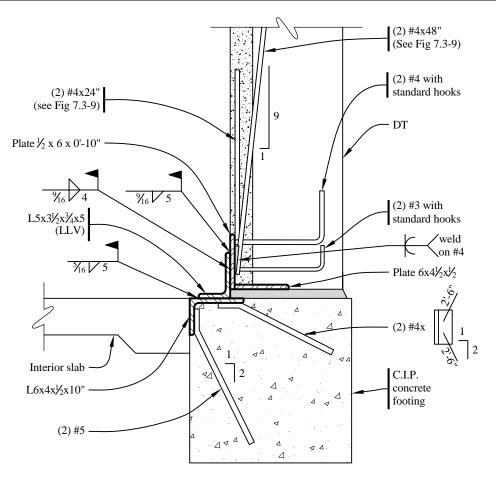


**Figure 7.3-8** Section at the connection of the precast/prestressed shear wall panel and the footing (1.0 in = 25.4 mm).

## 7.3.5.6 Tension and Shear at the DT Embedment

The area of reinforcement for the welded bars of the embedded plate in the DT, which develop tension as the angle bends through cycles is:

$$A_s = \frac{T'_u}{\phi f_v \cos \theta} = \frac{21.9}{0.9(60) \cos 6.3^\circ} = 0.408 \text{ in.}^2$$

Two #4 bars are adequate. Note that the bars in the DT leg are required to extend upward 1.3 times the development length, which would be 22 in. In this case they will be extended 22 in. past the point of development of the effective stress in the strand, which totals about 48 in.

The same embedded plate used for tension will also be used to resist one-half the nominal shear. This shear force is 14.5 kips. The transfer of direct shear to the concrete is easily accomplished with bearing on the sides of the reinforcing bars welded to the plate. Two #5 and two #4 bars (explained later) are welded to the plate. The available bearing area is approximately  $A_{br} = 4(0.5 \text{ in.})(5 \text{ in.}(\text{available})) = 10 \text{ in.}^2$  and the bearing capacity of the concrete is  $\phi V_n = (0.65)(0.85)(5 \text{ ksi})(10 \text{ in.}^2) = 27.6 \text{ kips} > 14.5 \text{ kip}$  demand.

The weld of these bars to the plate must develop both the tensile demand and this shear force. The weld is a flare bevel weld, with an effective throat of 0.2 times the bar diameter along each side of the bar. (Refer to the PCI Handbook.) For the #4 bar, the weld capacity is

 $\phi V_n = (0.75)(0.6)(70 \text{ ksi})(0.2)(0.5 \text{ in.})(2) = 6.3 \text{ kips/in.}$ 

The shear demand is prorated among the four bars as (14.5 kip)/4 = 3.5 kip. The tension demand is the larger of  $1.25 f_y$  on the bar (15 kip) or  $T_u/2$  (11.0 kip). The vectorial sum of shear and tension demand is 15.4 kip. Thus, the minimum length of weld is 15.4 / 6.3 = 2.4 in.

### 7.3.5.7 Resolution of Eccentricities at the DT Embedment

Check the twisting of the embedded plate in the DT for  $M_{z}$ .

Use  $M_{z} = 54.7$  in.-kips.

$$A_s = \frac{M_z}{\phi f_y(jd)} = \frac{54.7}{0.9(60)(9.0)} = 0.11 \text{ in.}^2$$

Use one #4 bar on each side of the vertical embedded plate in the DT as shown in Figure 7.3-9. This is the same bar used to transfer direct shear in bearing.

Check the DT embedded plate for  $M_y$  (50.8 in.-kips) and  $M_x$  (76.7 in.-kips) using the two #4 bars welded to the back side of the plate near the corners of the weld on the loose angle and the two #3 bars welded to the back side of the plate near the bottom of the DT leg (as shown in Figure 7.3-9). It is relatively straightforward to compute the resultant moment magnitude and direction, assume a triangular shaped compression block in the concrete, and then compute the resisting moment. It is quicker to make a reasonable assumption as to the bars that are effective and then compute resisting moments about the X and Y axes. This approximate method is demonstrated here. The #4 bars are effective in resisting  $M_x$ , and one each of the #3 and #4 bars are effective in resisting  $M_y$ . For  $M_y$  assume that the effective depth extends 1 in. beyond the edge of the angle (equal to twice the thickness of the plate). Begin by assigning one-half of the "corner" #4 to each component.

With 
$$A_{sx} = 0.20 + 0.20/2 = 0.30 \text{ in.}^2$$
,  
 $\phi M_{nx} = \phi A_s f_y j d = (0.9)(0.3 \text{ in.}^2)(60 \text{ ksi})(0.95)(5 \text{ in.}) = 77 \text{ in.-kips} (>76.7).$ 

With  $A_{sy} = 0.11 + 0.20/2 = 0.21$  in.<sup>2</sup>,  $\phi M_{ny} = \phi A_s f_y j d = (0.9)(0.21$  in.<sup>2</sup>)(60 ksi)(0.95)(5 in.) = 54 in.-kips (>50.8).

Each component is strong enough, so the proposed bars are satisfactory.

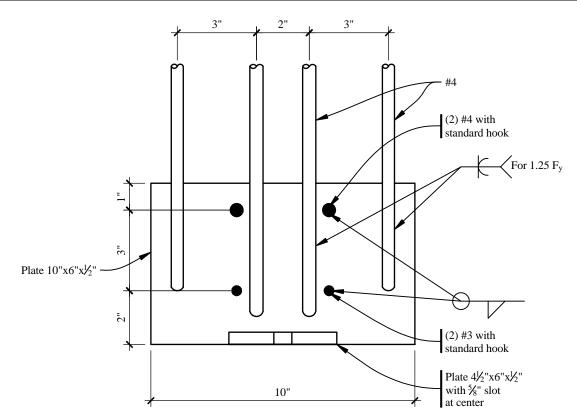
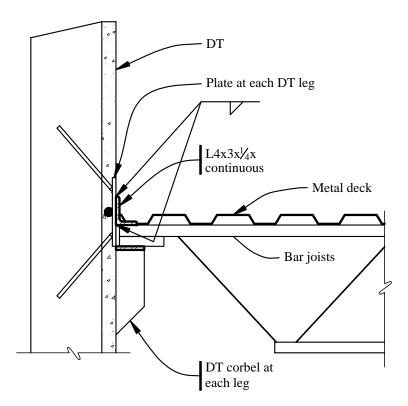


Figure 7.3-9 Details of the embedded plate in the DT at the base (1.0 in = 25.4 mm).



**Figure 7.3-11** Sketch of connection of load-bearing DT wall panel at the roof (1.0 in = 25.4 mm).

# 7.3.5.8 Other Connections

This design assumes that there is no in-plane shear transmitted from panel to panel. Therefore, if connections are installed along the vertical joints between DT panels to control the out-of-plane alignment, they should not constrain relative movement in-plane. In a practical sense, this means the chord for the roof diaphragm should not be a part of the panels. Figures 7.3-10 and 7.3-11 show the connections at the roof and DT wall panels. These connections are not designed here. Note that the continuous steel angle would be expected to undergo vertical deformations as the panels deform laterally.

Because the diaphragm supports concrete walls out of their plane, *Provisions* Sec. 5.2.6.3.2 [4.6.2.1] requires specific force minimums for the connection and requires continuous ties across the diaphragm. Also, it specifically prohibits use of the metal deck as the ties in the direction perpendicular to the deck span. In that direction, the designer may wish to use the top chord of the bar joists, with an appropriate connection at the joist girder, as the continuous cross ties. In the direction parallel to the deck span, the deck may be used but the laps should be detailed appropriately.

In precast double tee shear wall panels with flanges thicker than 2-1/2 in., consideration may be given to using vertical connections between the wall panels to transfer vertical forces resulting from overturning moments and thereby reduce the overturning moment demand. These types of connections are not considered here, since the uplift force is small relative to the shear force and cyclic loading of bars in thin concrete flanges is not always reliable in earthquakes.

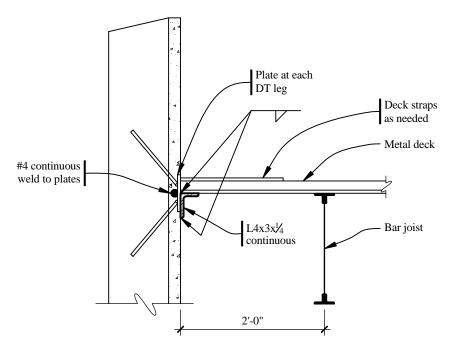


**Figure 7.3-10** Sketch of connection of non-load-bearing DT wall panel at the roof (1.0 in = 25.4 mm, 1.0 ft = 0.3048 m).

8

# **COMPOSITE STEEL AND CONCRETE**

# James Robert Harris, P.E., Ph.D. and Frederick R. Rutz, P.E., Ph.D.

This chapter illustrates application of the 2000 *NEHRP Recommended Provisions* to the design of composite steel and concrete framed buildings using partially restrained composite connections. This system is referred to as a "Composite Partially Restrained Moment Frame (C-PRMF)" in the *Provisions*. An example of a multistory medical office building in Denver, Colorado, is presented. The *Provisions* set forth a wealth of opportunities for designing composite steel and concrete systems, but this is the only one illustrated in this set of design examples.

The design of partially restrained composite (PRC) connections and their effect on the analysis of frame stiffness are the aspects that differ most significantly from a non-composite design. Some types of PRC connections have been studied in laboratory tests and a design method has been developed for one in particular, which is illustrated in this example. In addition, a method is presented by which a designer using readily available frame analysis programs can account for the effect of the connection stiffness on the overall frame.

The example covers only design for seismic forces in combination with gravity, although a check on drift from wind load is included.

The structure is analyzed using three-dimensional static methods. The RISA 3D analysis program, v.4.5 (Risa Technologies, Foothill Ranch, California) is used in the example.

Although this volume of design examples is based on the 2000 *Provisions*, it has been annotated to reflect changes made to the 2003 *Provisions*. Annotations within brackets, [], indicate both organizational changes (as a result of a reformat of all of the chapters of the 2003 *Provisions*) and substantive technical changes to the 2003 *Provisions* and its primary reference documents. While the general concepts of the changes are described, the design examples and calculations have not been revised to reflect the changes to the 2003 *Provisions*.

Chapter 10 in the 2003 *Provisions* has been expanded to include modifications to the basic reference document, AISC Seismic, Part II. These modifications are generally related to maintaining compatibility between the *Provisions* and the most recent editions of the ACI and AISC reference documents and to incorporate additional updated requirements. Updates to the reference documents, in particular AISC Seismic, have some affect on the calculations illustrated herein.

There are not any general technical changes to other chapters of the 2003 *Provisions* that have a significant effect on the calculations and/or design example in this chapter of the *Guide* with the possible exception of the updated seismic hazard maps.

Where they affect the design examples in this chapter, significant changes to the 2003 *Provisions* and primary reference documents are noted. However, some minor changes to the 2003 *Provisions* and the reference documents may not be noted.

In addition to the 2000 *NEHRP Recommended Provisions* (referred to herein as the *Provisions*), the following documents are referenced:

ACI 318	American Concrete Institute. 1999. <i>Building Code Requirements for Structural Concrete</i> , Standard ACI 318-99. Detroit: ACI.
AISC LRFD	American Institute of Steel Construction. 1999. Load and Resistance Factor Design Specification for Structural Steel Buildings. Chicago: AISC.
AISC Manual	American Institute of Steel Construction. 1998. <i>Manual of Steel Construction, Load and Resistance Factor Design</i> , Volumes 1 and 2, 2nd Edition. Chicago: AISC.
AISC Seismic	American Institute of Steel Construction. 1997. Seismic Provisions for Structural Steel Buildings, including Supplement No. 2 (2000). Chicago:
AISC SDGS-8	American Institute of Steel Construction. 1996. <i>Partially Restrained Composite Connections</i> , Steel Design Guide Series 8. Chicago: AISC.
ASCE TC	American Society of Civil Engineers Task Committee on Design Criteria for Composite Structures in Steel and Concrete. October 1998. "Design Guide for Partially Restrained Composite Connections," <i>Journal of Structural Engineering</i> 124(10)
ASCE 7	American Society of Civil Engineers. 1998. <i>Minimum Design Loads for Buildings and Other Structures</i> , ASCE 7-98. Reston: ASCE.

The short-form designations presented above for each citation are used throughout.

The symbols used in this chapter are from Chapter 2 of the *Provisions*, the above referenced documents, or are as defined in the text. Customary U.S. units are used.

# **8.1 BUILDING DESCRIPTION**

This four-story medical office building has a structural steel framework (see Figures 8-1 through 8-3). The floors and roof are supported by open web steel joists. The floor slab is composite with the floor girders and the spandrel beams and the composite action at the columns is used to create moment resisting connections. Figure 8-4 shows the typical connection. This connection has been studied in several research projects over the past 15 years and is the key to the building's performance under lateral loads. The structure is free of irregularities both in plan and elevation. This is considered a Composite Partially Restrained Moment Frame (C-PRMF) per *Provisions* Table 5.2.2 and in AISC Seismic, and it is an appropriate choice for buildings with low-to-moderate seismic demands, which depend on the building as well as the ground shaking hazard.

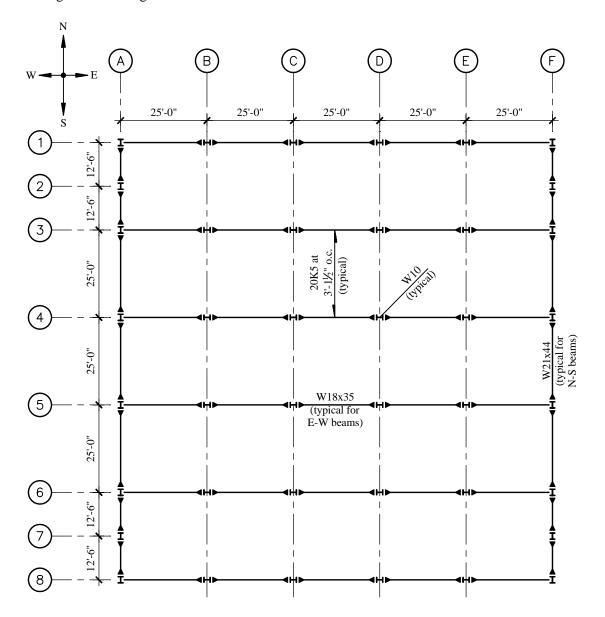


**Figure 8-1** Typical floor plan (1.0 ft = 0.3048 m).

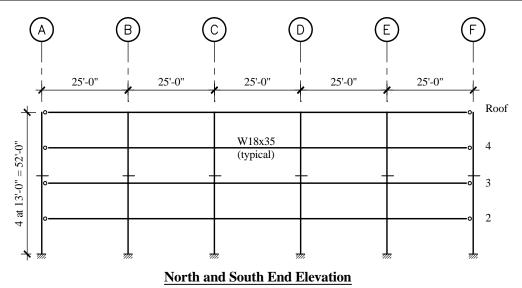


**Figure 8-2** Building end elevation (1.0 ft = 0.3048 m).

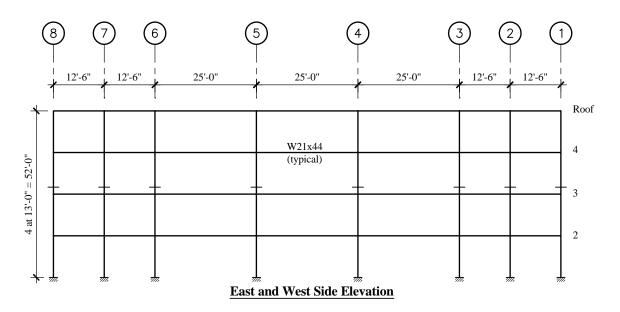


**Figure 8-3** Building side elevation (1.0 ft = 0.3048 m).

The building is located in a relatively low hazard region (Denver, Colorado), but some internal storage loading and Site Class E are used in this example to provide somewhat higher seismic design forces for purposes of illustration, and to push the example into Seismic Design Category C.

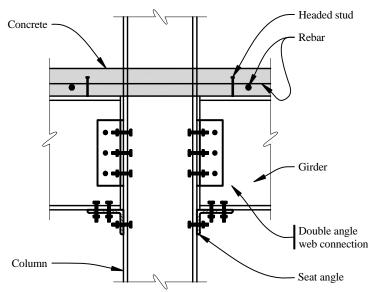


Figure 8-4 Typical composite connection.

There are no foundations designed in this example. For this location and system, the typical foundation would be a drilled pier and voided grade beam system, which would provide flexural restraint for the strong axis of the columns at their base (very similar to the foundation for a conventional steel moment frame). The main purpose here is to illustrate the procedures for the partially restrained composite connections. The floor slabs serve as horizontal diaphragms distributing the seismic forces, and by inspection they are stiff enough to be considered as rigid.

The typical bay spacing is 25 feet. Architectural considerations allowed an extra column at the end bay of each side in the north-south direction, which is useful in what is the naturally weaker direction. The exterior frames in the north-south direction have moment-resisting connections at all columns. The frames in each bay in the east-west direction have moment-resisting connections at all except the end columns. Composite connections to the weak axis of the column are feasible, but they are not required for this design. This arrangement is illustrated in the figures.

Material properties in this example are as follows:

1.	Structural steel beams and columns (ASTM A992):	$F_{\rm v} = 50 \text{ ksi}$
2.	Structural steel connection angles and plates (ASTM A36):	$\vec{F_v} = 36 \text{ ksi}$
3.	Concrete slab (4.5 inches thick on form deck, normal weight):	$f_c' = 3000 \text{ psi}$
4.	Steel reinforcing bars (ASTM A615):	$F_y = 60 \text{ ksi}$

The floor live load is 50 psf, except in 3 internal bays on each floor where medical records storage imposes 200 psf, and the roof snow load is taken as 30 psf. Wind loads per ASCE 7 are also checked, and the stiffness for serviceability in wind is a factor in the design. Dead loads are relatively high for a steel building due to the 4.5" normal weight concrete slab used to control footfall vibration response of the open web joist system and the precast concrete panels on the exterior walls.

This example covers the following aspects of seismic design that are influenced by partially restrained composite frame systems:

- 1. Load combinations for composite design
- 2. Assessing the flexibility of the connections
- 3. Incorporating the connection flexibility into the analytical model of the building

# 4. Design of the connections

# **8.2 SUMMARY OF DESIGN PROCEDURE FOR COMPOSITE PARTIALLY RESTRAINED MOMENT FRAME SYSTEM**

For buildings with low to moderate seismic demands, the partially restrained composite frame system affords an opportunity to create a seismic-force-resisting system in which many of the members are the same size as would already be provided for gravity loads. A reasonable preliminary design procedure to develop member sizes for a first analysis is as follows:

- 1. Proportion composite beams with heavy noncomposite loads based upon the demand for the unshored construction load condition. For this example, this resulted in W18x35 beams to support the open web steel joists.
- 2. Proportion other composite beams, such as the spandrel beams in this example, based upon judgment. For this example, the first trial was made using the same W18x35 beam.
- 3. Select a connection such that the negative moment strength is about 75 percent of the plastic moment capacity of the bare steel beam.
- 4. Proportion columns based upon a simple portal analogy for either stiffness or strength. If stiffness is selected, keep the column's contribution to story drift to no more than one-third of the target. If strength is selected, an approximate effective column length factor of K = 1.5 is suggested for preliminary design. Also check that the moment capacity of the column (after adjusting for axial loads) is at least as large as that for the beam.

Those final design checks that are peculiar to the system are explained in detail as the example is described. The key difference is that the flexibility of the connection must be taken into account in the analysis. There are multiple ways to accomplish this. Some analytical software allows the explicit inclusion of linear, or even nonlinear, springs at each end of the beams. Even for software that does not, a dummy member can be inserted at each end of each beam that mimics the connection behavior. For this example another method is illustrated, which is consistent with the overall requirements of the *Provisions* for linear analysis. The member properties of the composite beam are altered to become an equivalent prismatic beam that gives approximately the same flexural stiffness in the sway mode to the entire frame as the actual composite beams combined with the actual connections. Prudence in the use of this simplification does suggest checking the behavior of the connections under gravity loads to assure that significant yielding is confined to the seismic event.

Once an analytic model is constructed, the member and connection properties are adjusted to satisfy the overall drift limits and the individual strength limits. This is much like seismic design for any other frame system. Column stability does need to account for the flexibility of the connection, but the AISC LRFD and the *Provisions* approaches considering second order moments from the translation of gravity loads are essentially the same. The further checks on details, such as the strong column rule, are also generally familiar. Given the nature of the connection, it is also a good idea to examine behavior at service loads, but there are not truly standard criteria for this.

# **8.3 DESIGN REQUIREMENTS**

# 8.3.1 Provisions Parameters

The basic parameters affecting the design and detailing of the buildings are shown in Table 8.1 below.

Table 8-1	Design Parameters
Parameter	Value
<i>S</i> <sub>s</sub> (Map 1)	0.20
<i>S</i> <sub>1</sub> (Map 2)	0.06
Site Class	E
$F_a$	2.5
$F_{v}$	3.5
$S_{MS} = F_a S_s$	0.50
$S_{MI} = F_{\nu}S_{I}$	0.21
$S_{DS} = 2/3S_{MS}$	0.33
$S_{DI} = 2/3S_{MI}$	0.14
Seismic Design Category	С
Frame Type per	Composite Partially Restrained
Provisions Table 5.2.2	Moment Frame
R	6
$arOmega_0$	3
$C_d$	5.5

 Table 8-1
 Design Parameters

[The 2003 *Provisions* have adopted the 2002 USGS probabilistic seismic hazard maps, and the maps have been added to the body of the 2003 *Provisions* as figures in Chapter 3 (instead of the previously used separate map package).]

The frames are designed in accordance with AISC Seismic, Part II, Sec. 8 (*Provisions* Table 5.2.2). AISC SDGS-8 and ASCE TC describe this particular system in detail. Given the need to determine the flexibility of the connections, it would be difficult to design such structures without reference to at least one of these two documents.

# 8.3.2 Structural Design Considerations Per the Provisions

The building is regular both in plan and elevation. *Provisions* Table 5.2.5.1 indicates that use of the Equivalent Lateral Force procedure in accordance with *Provisions* Sec. 5.4 is permitted.

Nonstructural elements (Provisions Chapter 14) are not considered in this example.

Diaphragms must be designed for the required forces (*Provisions* Sec. 5.2.6.2.6), however this is not unique to this system and therefore is not explained in this example.

The story drift limit (*Provisions* Table 5.2.8) is 0.025 times the story height. Although the  $C_d$  factor is large, 5.5, the seismic forces are low enough that conventional stiffness rules for wind design actually control the stiffness.

Orthogonal effects need not be considered for Seismic Design Category C, provided the structure does not have a plan structural irregularity (*Provisions* Sec. 5.2.5.2.2).

# 8.3.3 Building Weight and Base Shear Summary

The unit weights are as follows:

Non-composite dead load:	
4.5 in. slab on 0.6 in. form deck, plus sag	58 psf
Joist and beam framing	6 psf
Columns	<u>2 psf</u>
	66 psf
Composite dead load:	
Fire insulation	4 psf
Mechanical and electrical	6 psf
Ceiling	2 psf
Partitions	<u>20 psf</u>
	32 psf
Exterior wall:	
Precast concrete panels:	0.80 klf

Records storage on 3 bays per floor 120 psf (50 percent is used for seismic weight; minimum per the *Provisions* is 25 percent)

The building weight, W, is found to be 8,080 kips. The treatment of the dead loads for analysis is described in more detail subsequently.

The Seismic Response Coefficient,  $C_s$ , is equal to 0.021:

$$C_s = \frac{S_{DI}}{T\frac{R}{I}} = \frac{0.14}{1.12\left(\frac{6}{1}\right)} = 0.021$$

The methods used to determine W and  $C_s$  are similar to those used elsewhere in this volume of design examples. The building is somewhat heavy and flexible. The computed periods of vibration in the first modes are 2.12 and 2.01 seconds in the north-south and east-west directions, respectively. These are much higher than the customary 0.1 second per story rule of thumb, but low-rise frames with small seismic force demands typically do have periods substantially in excess of the rule of thumb. The approximate period per the *Provisions* is 0.66 seconds, and the upper bound for this level of ground motion is 1.12 seconds.

The total seismic force or base shear is then calculated as follows:

 $V = C_s W = (0.021)(8,080) = 170$  kips

(Provisions Eq. 5.3.2)

The distribution of the base shear to each floor (again, by methods similar to those used elsewhere in this volume of design examples) is found to be:

Roof(Level 4):70 kipsStory 4(Level 3):57 kipsStory 3(Level 2):34 kipsStory 2(Level 1):8 kipsStory 1(Level 0):0 kipsΣ:169 kips (difference is rounding; total is 170)

Without illustrating the techniques, the gross service level wind force following ASCE 7 is 123 kips. When including the directionality effect and the strength load factor, the design wind force is somewhat less than the design seismic base shear. The wind force is not distributed in the same fashion as the

seismic force, thus the story shears and the overturning moments for wind are considerably less than for seismic.

# 8.4 DETAILS OF THE PRC CONNECTION AND SYSTEM

### 8.4.1 Connection *M*-*θ* Relationships

The composite connections must resist both a negative moment and a positive moment. The negative moment connection has the slab rebar in tension and the leg of the seat angle in compression. The positive moment connection has the slab concrete in compression (at least the "a" dimension down from the top of the slab) and the seat angle in tension (which results in flexing of the seat angle vertical leg). At larger rotations the web angles contribute a tension force that increases the resistance for both negative and positive bending.

Each of these conditions has a moment-rotation relationship available in AISC SDGS-8 and ASCE TC. (Unfortunately there are typographical errors in ASCE TC: A "+" should be replaced by "=" and the symbol for the area of the seat angle is used where the symbol should be that for the area of the web angle.) An M- $\theta$  curve can be developed from these equations:

Negative moment connection:

$$M_n^- = C_1(1 - e^{-C_2\theta}) + C_3\theta$$
 (AISC SDGS-8, Eq. 1)

where:

$$\begin{split} C_1 &= 0.18(4 \times A_s F_{yrb} + 0.857 A_L F_y)(d + Y_3) \\ C_2 &= 0.775 \\ C_3 &= 0.007(A_L + A_{wL})F_y (d + Y_3) \\ \theta &= \text{girder end rotation, milliradians (radians/1000)} \\ d &= \text{girder depth, in.} \\ Y_3 &= \text{distance from top flange of the girder to the centroid of the reinforcement, in.} \\ A_s &= \text{steel reinforcing area, in.}^2 \\ A_L &= \text{area of seat angle leg, in.}^2 \\ A_{wL} &= \text{gross area of double web angles for shear calculations, in.}^2 (For use in these equations A_{wL} is limited to 150 percent of A_I). \end{split}$$

 $F_{yrb}$  = yield stress of reinforcing, ksi

 $F_{v} =$  yield stress of seat and web angles, ksi

Positive moment connection:

$$M_n^+ = C_1(1 - e^{-C_2\theta}) + (C_3 + C_4)\theta$$
 (AISC SDGS-8, Eq. 2)

where:

$$\begin{split} &C_1 = 0.2400[(0.48A_{wL}) + A_L](d + Y_3)F_y\\ &C_2 = 0.0210(d + Y_3/2)\\ &C_3 = 0.0100(A_{wL} + A_L)(d + Y_3)F_y\\ &C_4 = 0.0065 \ A_{wL} \ (d + Y_3)F_y \end{split}$$

From these equations, curves for M- $\theta$  can be developed for a particular connection. Figures 8-5 and 8-6 are M- $\theta$  curves for the connections associated with the W18x35 girder and the W21x44 spandrel beam

respectively, which are used in this example. The selection of the reinforcing steel, connection angles, and bolts are described in the subsequent section, as are the bilinear approximations shown in the figures. Among the important features of the connections demonstrated by these curves are:

- 1. The substantial ductility in both negative and positive bending,
- 2. The differing stiffnesses for negative and positive bending, and
- 3. The substantial post-yield stiffness for both negative and positive bending.

It should be recognized that these curves, and the equations from which they were plotted, do not reproduce the line from a single test. They are averages fit to real test data by numerical methods. They smear out the slip of bolts into bearing. (There are several articles in the *AISC Engineering Journal* that describe actual test results. They are in Vol. 24, No.2; Vol. 24, No.4; Vol. 27, No.1; Vol. 27, No. 2; and Vol 31, No. 2. The typical tests clearly demonstrate the ability of the connection to meet the rotation capabilities of AISC Seismic, Section 8.4 - inelastic rotation of 0.015 radians and total rotation capacity of 0.030 radians.)

[Based on the modifications to AISC Seismic, Part II, Sec. 8.4 in 2003 *Provisions* Sec. 10.5.16, the required rotation capabilities are inelastic rotation of 0.025 radians and total rotation of 0.040 radians.]

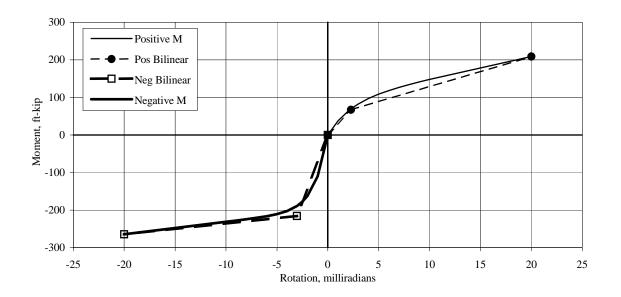


**Figure 8-5** *M*- $\theta$  Curve for W18x35 connection with 6-#5 (1.0 ft-kip = 1.36 kN-m)

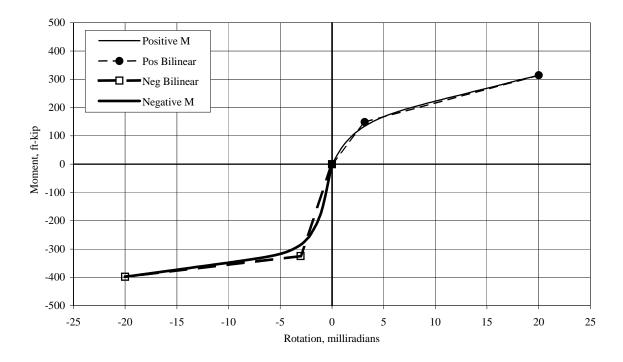


Figure 8-6  $M-\theta$  Curve for W21x44 connection with 8-#5 (1.0 ft-kip = 1.36 kN-m).

# 8.4.2 Connection Design and Connection Stiffness Analysis

Table 8-2 is taken from a spreadsheet used to compute various elements of the connections for this design example. It shows the typical W18x35 girder and the W21x44 spandrel beam with the connections used in the final analysis, as well as a W18x35 spandrel beam for the short exterior spans, where a W21x44 was used in the end. Each major step in the table is described in a line-by-line description following the table. [Based on the modifications to AISC Seismic, Part II, Sec. in 2003 *Provisions* Sec. 10.5.16, the nominal strength of the connection must be exceed  $R_yM_p$  for the bare steel beam, where  $R_y$  is the ratio of expected yield strength to nominal yield strength per AISC Seismic, Part I, Table I-6-1.]

	Table 8-2         Partially Restrained			
Line		Girder	Span	drels
	asic Data			
2	Beam size	W18x35	W21x44	W18x35
3	Span, ft	25	25	12.5
4	Area of beam, in. <sup>2</sup>	10.3	13	10.3
5	<i>I</i> , of beam alone, in. <sup>4</sup>	510	843	510
6	Z, plastic modulus of beam, in. <sup>3</sup>	66.5	95.4	66.5
7	Beam depth, in.	17.7	20.7	17.7
8	Slab thickness, in.	7.0	7.0	7.0
9	$Y_3$ to rebar, in.	5.5	5.5	5.5
10	Column	W10x77	W10x88	W10x77
11	Flange width, in.	10.2	10.3	10.2
12	Flange thickness, in.	0.87	0.99	0.87
13	Flange fillet, $k_i$ , in.	0.88	0.94	0.88
В	asic Negative Moment Capacity			
15	Reinforcing bars	6-#5	8-#5	6-#5
16	$A_s$ , rebar area, in. <sup>2</sup>	1.86	2.48	1.86
17	$T_r$ , rebar tension, kips	111.6	148.8	111.6
18	$M_n$ , nominal negative moment, ft-kips	215.8	324.9	215.8
19	$\% M_p (M_n) / \text{beam} M_p)$	78%	82%	78%
20	Check: $> 50\%$ ? (75% per ASCE TC)	OK	OK	OK
S	eat Demands for Negative Moment			
22	Seat angle	$L7x4x^{1/2}x8$	$L7x4x^{5}/_{8}x8.5$	$L7x4x^{1/2}x8$
23	Seat $F_{y}$ , ksi	36	36	36
24	Seat thickness, in.	0.5	0.625	0.5
25	Seat length, in.	8.0	8.5	8.0
26	Leg area, in. <sup>2</sup>	4.0	5.3125	4.0
27	Minimum area = 1.25 $T_r/F_v$ , in. <sup>2</sup>	3.875	5.167	3.875
28	Check	OK	OK	OK
29	Leg yield force, kips	144	191.25	144
30	Bolts to beam	(4) 1"-325X	(4) 1 <sup>1</sup> / <sub>8</sub> "-490X	(4) 1"-325X
31	Diameter, in.	1.0	0.875	1.0
32	Bolt design shear capacity, kips ( $\phi = 0.75$ )	141.2	223.6	141.2
33	Check	Close enough	OK	Close enough
	ominal Positive Moment Capacity	6		
35	Seat <i>k</i> , fillet length, in.	1.000	1.125	1.000
36	$M_p$ , vertical leg, inkips	18.0	29.9	18.0
37	b' (see Figure 8-7), in.	1.00	0.81	1.00
38	Seat tension from bending, kips	31.5	63.8	31.5
39	Seat tension from shear, kips	86.4	114.75	86.4
40	Tension to bottom flange, kips	31.5	63.8	31.5
41	Nominal Positive Moment, $M_n^+$ , ft-kips	67.4	149.9	67.4
42	Percent of Beam $M_n$	24%	38%	24%
	emand on Tension Bolts at Nominal Capacity	• •		
44	a' (see Figure 8-7), in.	2.0	2.1	2.0
45	Q (prying), kips	6.8	10.7	6.8
46	Bolt tension, kips	38.3	74.5	38.3
47	Bolts to column	(2) 1"-325X	(2) $1^{1}/_{8}$ "-490X	(2) 1"-325X
48	Bolt design tension, kips ( $\phi = 0.75$ )	106	168.4	106
49	Check	OK	OK	OK
		011	011	011

51 52 53 54	<b>Connection nominal</b> $M_n^- + M_n^+$ , ft-kips Minimum column $M_p$ (125% of sum) Average as percentage of beam	283	Span apacities 475	
51 52 53 54 Co	Connection nominal $M_n^+ + M_n^+$ , ft-kips Minimum column $M_p$ (125% of sum)	283	-	
53 54 Co	Minimum column $M_p$ (125% of sum)	1	475	283
53 54 Co		177	297	177
<u>54</u> Co		51%	60%	51%
Co	Check	OK	OK	OK
	oncrete Compression Transfer to Column			
50	Rebar $T_y$ + bottom seat $T_y$ , kips	143.10	212.62	143.10
57	$0.85 f'_c$ on two flanges, kips	364.14	367.71	364.14
58	Projection for flange $M_p$ , in.	2.72	3.10	2.72
59	Force from flange $M_p$ , kips	225.92	254.88	225.92
60	Ratio, demand / minimum capacity	0.63	0.83	0.63
	eb Shear Connection (needed for effective stif	fness)		
62	Seismic shear demand, kips	11.5	19.9	23.1
63	Web angles	$L4x4x^{1/4}x8.5$	$L4x4x^{1}/_{4}x11.5$	$L4x4x^{1}/_{4}x8.5$
64	$A_w$ , area of two legs, in. <sup>2</sup>	4.25	5.75	4.25
65	$A_w$ , limit based on area of rebar, in. <sup>2</sup>	2.79	3.72	2.79
66	$A_w$ , used in <i>M</i> - $\theta$ calculation, in. <sup>2</sup>	2.79	3.72	2.79
Μ	oment Rotation Values for Analysis of Effecti	ve Stiffness		
68	$M_{neg}$ at service level (0.0025 rad), ft-kip	-178.0	-267.8	-178.0
69	$M_{neg}^{neg}$ at maximum capacity(0.020 rad), ft-kip	-264.5	-397.7	-264.5
70	Secant stiffness for $M_{neg}$ at 0.0025 radian	71.2	107.1	71.2
71	$M_{pos}$ at service level (0.0025 rad), ft-kip	73.7	117.3	73.7
72	$M_{pos}$ at maximum capacity(0.020 rad), ft-kip	208.9	313.9	208.9
73	Secant stiffness for $M_{pos}$ at 0.0025 radian	29.5	46.9	29.5
74	Rotation at nominal $M_{neg}$	3.03	3.03	3.03
75	Rotation at nominal $M_{pos}$	2.29	3.70	2.29
-	eam Moments of Inertia			
77	Full composite action force, beam $AF_{y}$ , kips	515.0	650.0	515.0
78	$Y_2$ , to plastic centroid in concrete, in.	5.65	5.30	4.31
79	Composite beam inertia for pos. bending, in. <sup>4</sup>	1,593	2,435	1,402
80	Centroid of all steel for negative bending, in.	6.66	7.81	6.66
81	Composite beam inertia for neg. bending, in. <sup>4</sup>	834	1366	834
82	Equivalent beam for positive and negative, in. <sup>4</sup>	1,290	2,008	1,175
83	Weighted connection stiffness, ft-kips/radian	61,263	88,105	61,263
84	Eff. prismatic inertia, beam and PRCC, in. <sup>4</sup>	639	955	412
85	Ratio of eff. prismatic $I / I$ of beam alone	1.25	1.13	0.81
Cł	neck Bottom Bolt Tension at Maximum Defor	mation		
87	Rotation at $\phi \times$ (rotation at nominal $M_{pos}$ ) $\times C_d$	10.7	14.9	10.7
88	Moment at $\phi \times (\text{rot. at nom. } M_{pos}) \times C_d$ , ft-kips	152.3	268.2	152.3
89	Tension demand, kips	80.5	125.1	80.5
90	Nominal capacity of bolts, kips	141.3	224.5	141.3
	neck Positive Moment Capacity as a Percentag			
92	$M_{pos}$ (at 0.020 radians) / $M_p$ beam	75%	79%	75%

# **Detailed explanation of the computations in Table 8-2:**

*Step 1: Establish nominal negative moment capacity:* (This is a step created in this design example; is not actually an explicit step in the procedures recommended in the references. It appears to be necessary to satisfy the basic *Provisions* strength requirement. See *Provisions* Sec. 5.2.1, Sec. 5.2.7, and ASCE 7 Sec. 2.3.

Lines 15-18:  $M_n$  is taken as a simple couple of rebar in slab and force at connection of bottom flange of beam; the true maximum moment is larger due to strain hardening in rebar and the bottom connection and due to tension force in the web connection, so long as the bottom connection can handle the additional demand. The nominal capacity is plotted in Figures 8-5 and 8-6 as the break of the bilinear relation. The design capacity, using a resistance factor of 0.85, has two requirements:

- 1.  $\phi M_n$  exceeds demand from seismic load combination: basic *Provisions* requirement
- 2.  $\phi M_n$  exceeds demand from total service gravity loads simply a good idea to maintain reasonable initial stiffness for lateral loads; by "codes" the factored gravity demand can be checked using plastic analysis

Lines 19-20:  $M_n$  exceeds 50 percent (by AISC Seismic, Part II, 8.4) of  $M_p$  of the bare steel beam. In this example, the more stringent recommendation of 75 percent contained within the ASCE TC is followed. Note that this check is on nominal strength, not design strength. A larger  $M_n$  gives a larger stiffness, thus some drift problems can be addressed by increasing connection capacity.

## Step 2: Design bottom seat angle connection for negative moment:

Lines 22-28: Provide nominal yield of angle leg at least 125 percent of nominal yield of reinforcing steel. This allows for increased force due to web shear connection. Strain hardening in the rebar is a factor, but strain hardening the angle would probably be as large. AISC SDGS-8 recommends 120 percent. ASCE TC recommends 133 percent, but then uses 125 percent to check the bolts. This is a check in compression, and the authors elected to use 125 percent.

Lines 29-33: Provide high strength bolts in normal (not oversized) holes to transfer force between beam flange and angle by shear; conventional rules regarding threads in the shear plane apply. The references do apply a resistance factor to the bolts, which may be an inconsistent design methodology. A check based on overstrength might be more consistent. The capacity at bolt slip could be compared against service loads, which would be a good idea for designs subject to strong wind forces.

*Step 3: Establish nominal positive moment capacity:* This connection is less stiff and less linear for positive moment than for negative moment, and generally weaker. There is not a simple, clear mechanism for a nominal positive moment. The authors of this example suggest the following procedure which follows the normal methods of structural engineering and yields a point relevant to the results of connection tests, in so far as construction of a bilinear approximation is concerned. It significantly underestimates the ultimate capacity.

Lines 35-38: Compute the shear in the vertical leg associated with bending. Figure 8-7 shows the mechanics, which is based on methods in the AISC Manual, for computing prying in hanger-type connections. Compute the nominal plastic moment of the angle leg bending out of plane (line 36) and assume that the location of the maximum moments are at the end of the fillet on the vertical leg (line 35) and at the edge of the bolt shaft (line 37). The moment near the bolt is reduced for the material lost at the bolt hole.

Lines 39-40: Check the shear capacity, compare with the shear governed by moment, and use the smaller. Shear will control if the angle is thick.

Line 41: Compute the nominal positive moment as a couple with the force and the distance from the bottom of the beam to the center of the compression area of the slab on the column. The concrete compression area uses the idealized Whitney stress block (ACI 318). Note that the capacity to transfer

concrete compression force to the steel column flange is checked later. The nominal positive moment is also shown on Figures 8-5 and 8-6 at the break point in the bilinear relation.

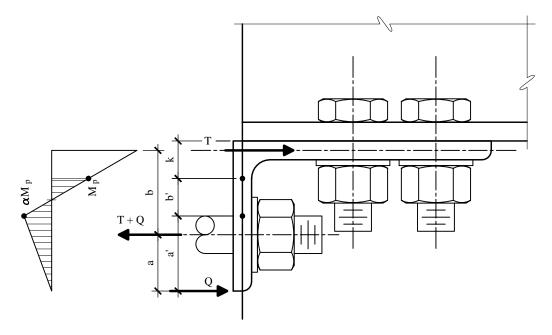


Figure 8-7 Analysis of seat angle for tension.

## Step 4: Design the bolts to transfer positive moment tension to the column:

Lines 44-45: Compute the prying force following AISC's recommended method. The moment in the vertical leg is computed as described above, and the moment arm extends from the edge of the bolt shaft (closest to the beam) to the bottom edge of the angle. Refer to Figure 8-7.

Lines 46-48: Add the basic tension to the prying force and compare to the factored design capacity of the bolts. Note that the resistance factor is used here to be consistent with step 2. It is common to use the same size and grade of bolt as used for the connection to the beam flange, which generally means that these bolts have excess capacity. Also, for seismic design, another check at maximum positive moment is recommended (see step 9).

*Step 5: Compute the flexural demand on the column:* AISC Seismic, Part II, 7 and 8, require that the flexural resistance of the column be greater than the demand from the connections, but it does not give any particular margin. ASCE TC recommends a ratio of 1.25.

Lines 51-52: The minimum nominal flexural strength of the column, summed above and below as well as adjusted for the presence of axial load, is set to be 125 percent of the demand from the sum of the nominal strengths of the connections.

Lines 53-54: AISC Seismic, Part II, 8.4 requires that the connection capacity exceed 50 percent of the plastic moment capacity of the beam. In this example, the negative moment connections are designed for 75 percent of the beam plastic moment, and this check shows that the average of negative and positive nominal moment capacities for the connection exceeds 50 percent of the plastic moment for the beam. A later check (step 10) will compare the maximum positive moment resistance to the 50 percent rule.

*Step 6: Check the transfer of force from concrete slab to steel column:* The tension in the reinforcing steel and the compression couple from positive bending must both transfer. Both flanges provide

resistance if concrete fills the space between the flanges, but full capacity of the second flange has probably not been exercised in tests.

Line 56: Add the yield force of the reinforcement and the tension yield force of the seat angle, both previously computed.

Line 57: Compute an upper bound concrete compression capacity as  $0.85f'_c$  times the area of concrete bearing on both flanges.

Lines 58-59: Compute the force that would yield the steel column flanges over the thickness of the slab by computing the projection beyond the web fillet that would yield at a load of 0.85f'c. This ignores the capacity of the flange beyond the slab thickness and is obviously conservative.

Line 60: Compare the demand with the smaller of the two capacities just computed.

Step 7: Select the web connection:

Line 62: The seismic shear is computed by assuming beam end moments equal to the nominal capacity of the connections, one in negative moment and one in positive.

Line 63: The gravity demand must be added, and straight gravity demand must also be checked before selecting the actual connection.

Lines 64-66: The web connection influences the overall stiffness and strength of the connection, especially at large rotation angles. The moment-rotation expression include the area of steel in the web angles, but also places a limitation based upon 150 percent of the area of the leg of the seat angle for use in the computation.

*Step 8: Determine the effective stiffness of the beam and connection system:* Determining the equivalent stiffness for a prismatic beam involves several considerations. Figure 8-8 shows how the moment along the beam varies for gravity and lateral loads as well as composite and non-composite conditions. The moment of inertia for the composite beam varies with the sense of the bending moment. The end connections can be modeled as regions with their own moments of inertia, as illustrated in the figure. Figure 8-9 shows the effective cross section for each of the four stiffnesses: positive and negative bending of the composite beam and positive and negative bending of the composite connection. Given a linear approximation of each connection stiffness expressed as moment per radian, flexural mechanics leads to a simple expression for a moment of an equivalent prismatic beam.

Lines 68-73: Compute the negative and positive moments at a rotation of 2.5 milliradians, which is the rotation angle that defines the effective stiffness for lateral analysis (per both AISC SDGS-8 and ASCE TC).

Lines 74-75: Using those moments, compute the rotations corresponding to the nominal strength, positive and negative. (This is useful when idealizing the behavior as bilinear, which is plotted in Figures 8-5 and 8-6.)

Lines 77-79: Compute the moment of inertia of the composite beam in positive bending. Note that the system is designed for full composite action, per the recommendations in AISC SDGS-8 and ASCE TC, using the criteria in the AISC manual. The positive bending moment of inertia here is computed using AISC's lower bound method, which uses an area of steel in the flange adequate to replace the Whitney stress block in the concrete flange. This moment of inertia is less than if one used the full concrete area in Figure 8-9.

Lines 80-81: Compute the moment of inertia of the composite beam in negative bending.

Line 82: Compute an equivalent moment of inertia for the beam recognizing that a portion of the span is in positive bending and the remainder is in negative bending. Following the recommendations in AISC SDGS-8 and ASCE TC, this is computed as 60 percent of  $I_{pos}$  and 40 percent of  $I_{neg}$ .

Lines 83-84: Compute the moment of inertia of a prismatic beam that will give the same total end rotation in a sway condition as the actual system. Gravity loads place both connections in negative moment, so one will be subject to increasing negative moment while the other will be subject to decreasing negative moment. Thus, initially, the negative moment stiffness is the appropriate stiffness, which is what is recommended in the AISC SDGS-8 and ASCE TC. For this example the positive and negative stiffnesses are combined, weighted by the nominal strengths in positive and negative bending, to yield a connection stiffness that is appropriate for analysis up to the nominal strengths defined earlier. Defining this weighted stiffness as  $K_{conn}$  and the equivalent composite beam moment of inertia as  $I_{comp}$ , the effective moment of inertia is found by:

$$I_{effective} = \frac{I_{comp}}{1 + \frac{6EI_{comp}}{LK_{conn}}}$$

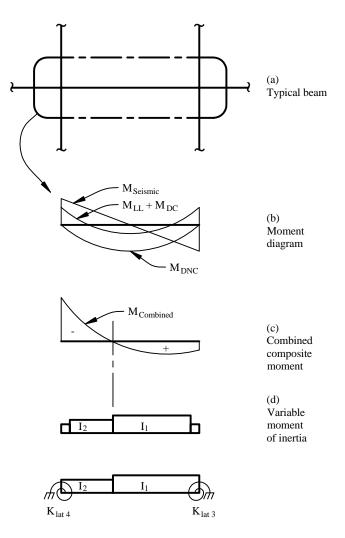


Figure 8-8 Moment diagram for typical beam.

Line 85: compute the ratio of the moment of inertia of the effective prismatic beam to that for the bare steel beam. When using standard computer programs for analysis that have a library of properties of steel cross sections, this ratio is a convenient way to adjust the modulus of elasticity and thus easily compute the lateral drift of a frame. This adjustment could invalidate routines in programs that automatically check various design criteria that depend on the modulus of elasticity.

# Step 9: Check the tension bolts at maximum rotation

Line 87: Compute the rotation at total drift as  $C_d$  times the drift at the design positive moment.

Line 88: Compute the positive moment corresponding to that drift.

Line 89: Compute the tension force at the bottom seat angle, ignoring any contribution of the web angles, from the moment and a moment arm between the center of the slab thickness and the inflection point in the vertical leg of the seat angle, then add the prying force already calculated for a maximum demand on the tension bolts.

Line 90: Compare with the nominal capacity of the bolts (set  $\phi = 1.0$ )

Step 10: Check the maximum positive moment capacity:

Line 92: The positive moment at 20 milliradians, already calculated, is compared to the plastic moment capacity of the steel beam. This is the point at which the 50 percent requirement of AISC Seismic, Part II, 8.4 is checked.

Figure 8-10 shows many of the details of the connection for the W18x35. The headed studs shown develop full composite action of the beam between the end and midspan. They do not develop full composite action between the column and the inflection point, but it may be easily demonstrated that they are more than capable of developing the full force in the reinforcing steel within that distance. The transverse reinforcement is an important element of the design, which will be discussed subsequently. Alternating the position above and below is simply a preference of the authors.

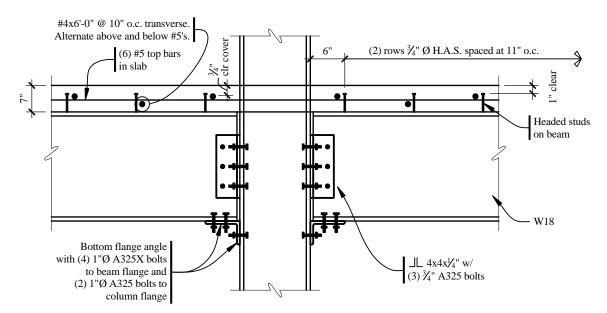


Figure 8-10 Elevation of typical connection (1.0 ft = 0.3048 m, 1.0 in. = 25.4 mm).

# 8.5 ANALYSIS

# 8.5.1 Load Combinations

A 3D model using Risa 3D was developed. Non-composite dead loads (steel beams, bar joists, form deck, and concrete) were input as concentrated loads at the columns on each level rather than uniformly distributed to the beams. This was because we want the model for the seismic load combinations to address the moments in the PRC connections. The loads subject to composite action are the composite dead loads, live loads, and seismic loads, not the non-composite dead loads. But the non-composite dead loads still contribute to mass, are subject to ground acceleration, and as such contribute to seismic loads. This gets confusing; so a detailed look at the load combinations is appropriate.

Let us consider four load cases (illustrated in Figures 8-11 and 8-12):

- 1.  $D_c$  Composite dead load, which is uniformly distributed and applied to beams (based on 32 psf)
- 2.  $D_{nc}$  Non-composite dead load, which is applied to the columns (based on 66 psf)
- 3. L Composite live load, which is uniformly distributed to beams, using live load reductions

4. E - Earthquake load, which is applied laterally to each level of the building and has a vertical component applied as a uniformly distributed load to the composite beams

We will investigate two load combinations. Recall that composite loads are applied to beams, while noncomposite loads are applied to columns. But there is an exception: the  $0.2S_{DS}D$  component, which represents vertical acceleration from the earthquake is applied to all the dead load on the beams whether it is composite or non-composite. This is because even non-composite dead load contributes to mass, and is subject to the ground acceleration. Because the non-composite dead load is not distributed on the beams in the computer model, an adjustment to the load factor is necessary. The assignment of loads gets a little complicated, so pay careful attention:

 $Q_E$  will be applied in both the north-south and the east-west directions, so this really represents two load combinations.

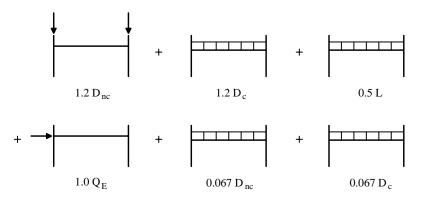


Figure 8-11 Illustration of input for load combination for  $1.2D + 0.5L + 1.0Q_E + 0.2S_{DS}D$ .

 $D_{nc}$  = non-composite dead load.  $D_c$  = composite dead load L = live load  $Q_E$  = horizontal seismic load

Now consider at the second load combination:

$$= 0.9D_{nc} + 0.9D_c + Q_E - 0.138D_c - 0.067D_c$$
  
= 0.9D<sub>nc</sub> + 0.9D<sub>c</sub> + Q<sub>E</sub> - 0.205D<sub>c</sub>  
= 0.9D<sub>nc</sub> + 0.695D<sub>c</sub> + Q<sub>E</sub>

Again,  $Q_E$  will be applied in both the north-south and the east-west directions, so this represents another two load combinations.

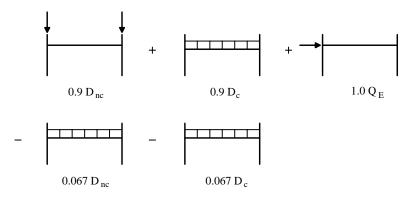


Figure 8-12 Illustration of input for load combination for  $0.9D + 1.0Q_E - 0.2S_{DS}D$ .

 $D_{nc}$  = non-composite dead load.  $D_c$  = composite dead load L = live load  $Q_E$  = horizontal seismic load

# 8.5.2 Drift and P-delta

As defined by the *Provisions*, torsional irregularity is considered to exist when the maximum displacement computed including accidental torsion at one end of the structure transverse to an axis is more than 1.2 times the average of the displacements at the two ends of the structure (*Provisions* Sec. 5.4.4.3). For this building the maximum displacement at the roof including accidental torsion, is 1.65 in. The displacement at the other end of the building in this direction is 1.43 in. The average is 1.54 in. Because 1.65 in. < 1.85 in. = (1.2)(1.54 in.), the structure is not torsionally irregular. Consequently, it is not necessary to amplify the accidental torsion nor to check the story drift at the corners. A simple check at the center of the building suffices. [In the 2003 *Provisions*, the maximum limit on the stability coefficient has been replaced by a requirement that the stability coefficient is permitted to exceed 0.10 if and only "if the resistance to lateral forces is determined to increase in a monotonic nonlinear static (pushover) analysis to the target displacement as determined in Sec. A5.2.3. P-delta effects shall be included in the analysis." Therefore, in this example, the stability coefficient should be evaluated directly using 2003 *Provisions* Eq. 5.2.-16.]

The elastic story drifts were computed by the RISA 3D analysis for the required load combinations. Like most modern computer programs for structural analysis, a P-delta amplification can be automatically computed, but to illustrate the effect of P-delta in this structure and to check the limit on the stability index, two computer runs have been performed, one without the P-delta amplifier and one with it. The allowable story drift is taken from *Provisions* Table 5.2.8. The allowable story drift is  $0.025 h_{sx} = (0.025)(13 \text{ ft} \times 12 \text{ in./ft}) = 3.9 \text{ in.}$  With a  $C_d$  of 5.5, this corresponds to a drift 0.71 in. under the equivalent elastic forces. At this point design for wind does influence the structure. A drift limit of h/400 (= 0.39 in.) was imposed, by office practice, to the service level wind load. In order to achieve the desired stiffness, the seismic story drift at elastic forces is determined thus:

Elastic story drift limit = (wind drift limit)(total seismic force)/(service level wind force) Elastic story drift limit = (0.39 in.)(170 kip)/123 kip = 0.54 in.

The structure complies with the story drift requirements, but it was necessary to increase the size of the spandrel beams from the preliminary W18x35 to W21x44 to meet the desired wind stiffness. This is summarized in Table 8-3. The structure also complies with the maximum limit on the stability index (Provisions 5.4.6.2-2):

$$\theta_{\max} = \frac{0.5}{\beta C_d} = \frac{0.5}{0.5*5.5} = 0.18 \le 0.25$$

 $\beta$  is the ratio of demand to capacity for the story shear, and has not yet been computed. Maximum demand and design capacity are tabulated in the following section; the average is about two-thirds. The preceding data show that the maximum resistance is higher, especially for positive moment, than the value suggested here for design capacity. The average ratio of demand to maximum capacity with a resistance factor is well below 0.5, so that value is arbitrarily used to show that the actual stability index is within the limits of the *Provisions*.

	North-south (X direction)			East-west (Z direction)				
Story	without	with	P-delta	Stability	without	with	P-delta	Stability
	P-delta	P-delta	amplifier	index	P-delta	P-delta	amplifier	index
1	0.358	0.422	1.179	0.152	0.312	0.360	1.154	0.133
2	0.443	0.517	1.167	0.143	0.410	0.471	1.149	0.130
3	0.449	0.513	1.143	0.125	0.402	0.453	1.127	0.113
4	0.278	0.304	1.094	0.086	0.239	0.259	1.084	0.077

Table 8-3 Story Drift (in.) and P-delta Analysis

# 8.5.3 Required and Provided Strengths

The maximum beam end moments from the frame analysis for the seismic load combinations are as follows:

Table 8-4         Maximum Connection Moments and Capacities (ft-kips)					
Quantity	W18 C	Birders	W21 Spandrels		
Quantity	Negative	Positive	Negative	Positive	
Demand (level 2), $M_{\mu}$	143	36.6	118	103	
Nominal, $M_n$	216	67.2	325	149	
Design capacity, $\phi M_n$	184	57.1	276	127	

The capacities, using a resistance factor of 0.85, are well in excess of the demands. The girder member sizes are controlled by gravity load in the construction condition. All other member and connection capacities are controlled by the design for drift. The negative moment demands are somewhat larger than would result from a more careful analysis, because the use of a prismatic member overestimates the end moments due to distributed load (composite gravity load) along the member. The higher stiffness of the portion of the beam in positive bending with respect to the connections would result in higher positive moments at midspan and lower negative moments at the supports. This conservatism has no real effect on this design example. (The above demands and capacities do not include the girders supporting the storage

bays, which are required to be W18x40 for the gravity load condition. The overall analysis does not take that larger member into account.)

Snow load is not included in the seismic load combinations. (According to the *Provisions*, snow load equal to or less than 30 psf does not have to be included in the mass.) Further, as a designer's judgment call, it was considered that the moments from 0.2S (= 6 psf) were so small, considering that the roof was designed with the same connections as the floors, that it would make no significant difference in the design analysis.

The maximum column forces are shown in Table 8-5; the particular column does support the storage load. The effective length of the columns about their weak axis will be taken as 1.0, because they are braced by perpendicular frames acting on the strong axes of the columns, and the P-delta analysis captures the secondary moments due to the "leaning" column effect. The effective length about their strong axis will exceed 1.0. The ratio of column stiffness to beam stiffness will use the same effective beam stiffness computed for the drift analysis, thus for the W10x77 framed into the W18x35 beams:

 $I_{col} / L_{col} = 455 / (13 \times 12) = 2.92$ 

 $I_{beam} / L_{beam} = 1.25 \times 510 / (25 \times 12) = 2.12$ 

and the ratio of stiffnesses, G = 2.92 / 2.12 = 1.37

Although the column in the lowest story has greater restraint at the foundation, and thus a lower K factor, it is illustrative to determine K for a column with the same restraint at the top and bottom. From the nomographs in the AISC Manual or from equivalent equations, K = 1.45. It turns out that the effective slenderness about the strong axis is less than that for the weak axis, so the K factor does not really control this design.

 Table 8-5
 Column Strength Check, for W10x77

Tuble 0 9 Column Strength Cheek, 101 W 10X77				
	Seismic Load Combination	Gravity Load Combination		
Axial force, $P_u$	391 kip	557 kip		
Moment, $M_u$	76.3 ft-kip	52.5 ft-kip		
Interaction equation	0.72	0.89		

# 8.6 DETAILS OF THE DESIGN

# 8.6.1 Overview

The requirements in AISC Seismic for C-PRMF systems are brief. Some of the requirements are references to Part I of AISC Seismic for the purely steel components of the system. A few of those detail checks are illustrated here. For this example, more attention is paid to the details of the joint.

# 8.6.2 Width-Thickness Ratios

The width-thickness ratio of the beam flanges,  $b_f/2t_f$  is compared to  $\lambda_p$  given in AISC Seismic, Part I, Table I-9-1. Both beam sizes, W18x35 and W21x44 are found to be acceptable. The W21x44 is illustrated below:

\_

$$\lambda_p = \frac{52}{\sqrt{F_y}} = \frac{52}{\sqrt{50}} = 7.35$$
 (AISC Seismic, Table I-9-1)  
 $\frac{b_f}{2t_f} = 7.22$  (AISC Manual)  
 $7.22 < 7.35$  OK

The limiting h/t ratios for columns is also given in AISC Seismic, Part I, Table I-9-1. A W10x77 column from the lower level of an interior bay with storage load is illustrated (the axial load from the seismic load combination is used):

$$\frac{P_u}{\phi_b P_y} = \frac{391 \text{ kips}}{(0.9)(22.6 \text{ in.}^2 \text{ x 50 ksi})} = 0.385 > 0.125$$
(AISC Seismic, Table I-9-1)

$$\lambda_{p} = \frac{191}{\sqrt{F_{y}}} \left[ 2.33 - \frac{P_{u}}{\phi_{b}P_{y}} \right] = \frac{191}{\sqrt{50}} \left[ 2.33 - 0.385 \right] = 52.5$$
 (AISC Seismic, Table I-9-1)

Check:

$$\lambda_p = 52.5 > 35.7 = \frac{253}{\sqrt{F_y}}$$
 OK

$$\frac{h}{t_w} = 13.0$$
(AISC Manual)

## 8.6.3 Column Axial Strength

AISC Seismic, Part I, 8.2 requires that when  $P_u/\phi P_n > 0.4$  (in a seismic load combination), additional requirements be met. Selecting the same column as above for our illustration:

$$\frac{P_u}{\phi P_n} = \frac{391 \text{ kips}}{(0.85)(22.6 \text{ in.}^2)(38.4 \text{ ksi})} = 0.53 > 0.4$$
(AISC Seismic, Part I, 8.2)

Therefore the requirements of AISC Seismic, Part I, 8.2a, 8.2b, and 8.2c apply. These necessitate the calculation of axial loads using the System Overstrength Factor,  $\Omega_0 = 3$ . Analysis needs to be run for two additional load combinations:

$$1.2D + 0.5L + 0.2S + \Omega_0 Q_E$$
 (AISC Seismic, Part I, Eq. 4.1)

and

$$0.9D - \Omega_0 Q_E$$
 (AISC Seismic, Part I, Eq. 4.2)

The axial seismic force in this column is only 7.5 kips, therefore  $P_u$  becomes 397 kips, obviously much less than  $\phi P_n$ . The low seismic axial load is common for a moment-resisting frame system. Given that this requirement is a check ignoring bending moment, it does not control the design.

[The special load combinations have been removed from the 2002 edition of AISC Seismic to eliminate inconsistencies with other building codes and standards. Therefore, 2003 *Provisions* Eq. 4.2-3 and 4.2-4 should be used in conjunction with the load combinations in ASCE 7.]

#### 8.6.4 Details of the Joint

Figure 8-13 shows a plan view at an edge column, concentrating on the arrangement of the steel elements. Figure 8-14 shows a section at the same location, showing the arrangement of the reinforcing steel. It is not required that the reinforcing bars be equally distributed on the two sides of the column, but it is necessary to place at least some of the bars on each side. This means that some overhang of the slab beyond the column flange is required. This example shows two of the six bars on the outside face. Figure 8-15 shows a plan view at a corner column. U shaped bent bars are used to implement the negative moment connection at such a location. Threaded bars directly attached to the column flange are also illustrated. Note the close spacing of the headed anchor studs for composite action. The reason for the close spacing at this location is that the beam span is half the normal span, yet full composite action is still provided.

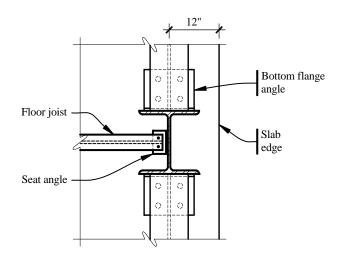


Figure 8-13 Detail at column.

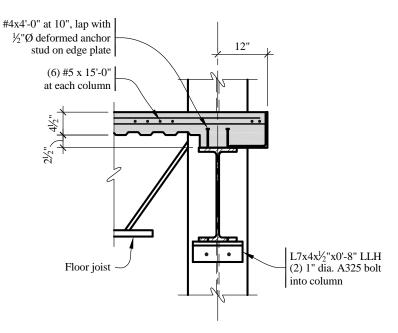


Figure 8-14 Detail at spandrel.

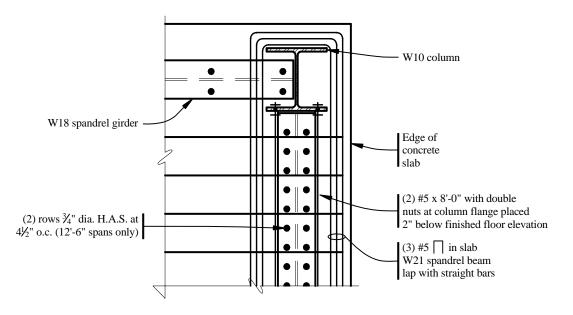


Figure 8-15 Detail at building corner.

The compressive force in the deck is transferred to both flanges of the column. This is shown in Figure 8-16. Note that both flanges can accept compressive forces from the concrete. Also note that the transverse reinforcement will carry tension as force is transferred from the principal tension reinforcement through the concrete to bearing on the column flange. Strut and tie models can be used to compute the appropriate tension.

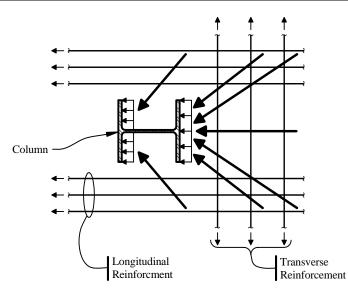


Figure 8-16 Force transfer from deck to column.

AISC SDGS-8 and ASCE TC include the following recommendations regarding the reinforcing steel:

- 1. Place the principal tension reinforcement within a strip of width equal to 7 times the width of the column flange (or less)
- 2. Use at least 6 bars for the principal reinforcement, extend it one quarter of the span from the column, but at least 24 bar diameters beyond the inflection point, and extend at least two of the bars over the full span
- 3. Do not use bars larger than number 6 (0.75 in. diameter)
- 4. Provide transverse reinforcement consistent with a strut and tie model to enable the transfer of forces (in the authors' observation such reinforcement is also necessary to preserve the capacity of the headed studs for shear transfer)

# 9

## MASONRY

### James Robert Harris, P.E., Ph.D., Frederick R. Rutz, P.E., Ph.D. and Teymour Manzouri, P.E., Ph.D.

This chapter illustrates application of the 2000 *NEHRP Recommended Provisions* (herein after the *Provisions*), to the design of a variety of reinforced masonry structures in regions with different levels of seismicity. Example 9.1 features a single-story masonry warehouse building with tall, slender walls; Example 9.2 presents a five-story masonry hotel building with a bearing wall system designed in areas with different seismicities; and Example 9.3 covers a twelve-story masonry building having the same plan as the hotel but located in a region of high seismicity. Selected portions of each building are designed to demonstrate specific aspects of the design provisions.

Masonry is a discontinuous and heterogeneous material. The design philosophy of reinforced grouted masonry approaches that of reinforced concrete; however, there are significant differences between masonry and concrete in terms of restrictions on the placement of reinforcement and the effects of the joints. These physical differences create significant differences in the design criteria.

All structures were analyzed using two-dimensional (2-D) static methods. Examples 9.2 and 9.3 use dynamic analyses to determine the structural periods. Example 9.2 employs the SAP 2000 program, V6.11 (Computers and Structures, Berkeley, California); Example 9.3 employs the RISA 2D program, V.5.5 (Risa Technologies, Foothill Ranch, California).

Although this volume of design examples is based on the 2000 *Provisions*, it has been annotated to reflect changes made to the 2003 *Provisions*. Annotations within brackets, [], indicate both organizational changes (as a result of a reformat of all of the chapters of the 2003 *Provisions*) and substantive technical changes to the 2003 *Provisions* and its primary reference documents. While the general concepts of the changes are described, the design examples and calculations have not been revised to reflect the changes to the 2003 *Provisions*.

The most significant change to the masonry chapter in the 2003 *Provisions* is the incorporation by reference of ACI 530-02 for strength design in masonry. A significant portion of 2003 *Provisions* Chapter 11 has been replaced by a reference to this standard as well as a limited number of modifications to the standard, similar to other materials chapters. This updated chapter, however, does not result in significant technical changes as ACI 530-02 is in substantial agreement with the strength design methodology contained in the 2000 *Provisions*.

Another change to the provisions for masonry structures is the addition of a new lateral system, prestressed masonry shear walls. This system is not covered in this volume of design examples.

Some general technical changes in the 2003 *Provisions* that relate to the calculations and/or design in this chapter include updated seismic hazard maps, changes to Seismic Design Category classification for short period structures, revisions to the redundancy requirements, revisions to the wall anchorage design requirement for flexible diaphragms, and a new "Simplified Design Procedure" that could be applicable to some of the examples in this chapter.

Where they affect the design examples in this chapter, other significant changes to the 2003 *Provisions* and primary reference documents are noted. However, some minor changes to the 2003 *Provisions* and the reference documents may not be noted.

In addition to the *Provisions*, the following documents are referenced in this chapter:

ACI 318	American Concrete Institute. 1999 [2002]. Building Code Requirements for Concrete Structures.
ACI 530	American Concrete Institute. 1999 [2002]. <i>Building Code Requirements for Masonry Structures</i> , ACI 530/ASCE 5/TMS 402.
ASCE 7	American Society of Civil Engineers. 1998 [2002]. <i>Minimum Design Loads for Buildings and Other Structures</i> .
Amrhein	Amrhein, J, and D. Lee. 1994. <i>Tall Slender Walls</i> , 2 <sup>nd</sup> Ed. Masonry Institute of America.
Drysdale	Drysdale R., A. Hamid, and L. Baker. 1999. <i>Masonry Structures, Behavior and Design</i> . Boulder Colorado: The Boulder Masonry Society.
IBC	International Code Council. 2000. International Building Code.
UBC	International Conference of Building Officials. 1997. Uniform Building Code.
NCMA	National Concrete Masonry Association. <i>A Manual of Facts on Concrete Masonry</i> , NCMA-TEK is an information series from the National Concrete Masonry Association, various dates.
SEAOC	Seismology Committee, Structural Engineers Association of California. 1999. Recommended Lateral Force Requirements and Commentary, 7 <sup>th</sup> Ed.

The short form designations for each citation are used throughout. The citation to the IBC exists for two reasons. One of the designs employees a tall, slender wall that is partially governed by wind loads and the IBC provisions are used for that design. Also, the R factors for masonry walls are significantly different in the IBC than in the *Provisions*; this is not true for other structural systems.

## 9.1 WAREHOUSE WITH MASONRY WALLS AND WOOD ROOF, LOS ANGELES, CALIFORNIA

This example features a one-story building with reinforced masonry bearing walls and shear walls.

#### 9.1.1 Building Description

This simple rectangular warehouse is 100 ft by 200 ft in plan (Figure 9.1-1). The masonry walls are 30 ft high on all sides, with the upper 2 ft being a parapet. The wood roof structure slopes slightly higher towards the center of the building for drainage. The walls are 8 in. thick on the long side of the building, for which the slender wall design method is adopted, and 12 in. thick on both ends. The masonry is grouted in the cells containing reinforcement, but it is not grouted solid. The assumed strength of masonry is 2,000 psi. Normal weight concrete masonry units (CMU) with type S mortar are assumed.

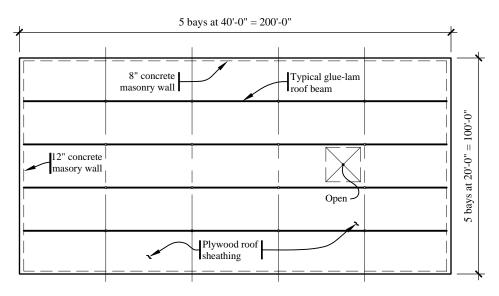


**Figure 9.1-1** Roof plan (1.0 in = 25.4 mm, 1.0 ft = 0.3048 m).

The long side walls are solid (no openings). The end walls are penetrated by several large doors, which results in more highly stressed piers between the doors (Figure 9.1-2); thus, the greater thickness for the end walls.

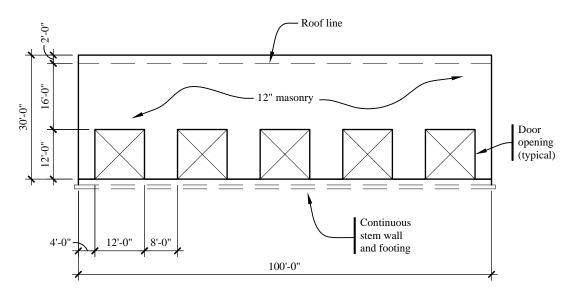


Figure 9.1-2 End wall elevation (1.0 in = 25.4 mm, 1.0 ft = 0.3048 m).

The floor is concrete slab-on-grade construction. Conventional spread footings are used to support the interior steel columns. The soil at the site is a dense, gravelly sand.

The roof structure is wood and acts as a diaphragm to carry lateral loads in its plane from and to the exterior walls. The roofing is ballasted, yielding a total roof dead load of 20 psf. There are no interior walls for seismic resistance. This design results in a highly stressed diaphragm with large calculated deflections. The design of the wood roof diaphragm and the masonry wall-to-diaphragm connections is illustrated in Sec. 10.2.

In this example, the following aspects of the structural design are considered:

- 1. Design of reinforced masonry walls for seismic loads and
- 2. Computation of P-delta effects.

#### 9.1.2 Design Requirements

[Note that the new "Simplified Design Procedure" contained in the 2003 *Provisions* Simplified Alternate Chapter 4 as referenced by the 2003 *Provisions* Sec. 4.1.1 is likely to be applicable to this example, subject to the limitations specified in 2003 *Provisions* Sec. Alt. 4.1.1.]

#### 9.1.2.1 Provisions Parameters

Site Class (Provisions Sec. 4.1.2.1 [Sec. 3.5])	= C
S <sub>s</sub> (Provisions Map 5 [Figure 3.3-3])	= 1.50
$S_1$ (Provisions Map 6 [Figure 3.3-4])	= 0.60
Seismic Use Group (Provisions Sec. 1.3[Sec. 1.2])	= I

[The 2003 *Provisions* have adopted the 2002 USGS probabilistic seismic hazard maps, and the maps have been added to the body of the 2003 *Provisions* as figures in Chapter 3 (instead of the previously used separate map package).]

The remaining basic parameters depend on the ground motion adjusted for site conditions.

#### 9.1.2.2 Response Parameter Determination

The mapped spectral response factors must be adjusted for site class in accordance with *Provisions* Sec. 4.1.2.4 [3.3.2]. The adjusted spectral response acceleration parameters are computed according to *Provisions* Eq. 4.1.2.4-1 [3.3-1] and 4.1.2.4-2 [3.3-2] for the short period and one-second period, respectively, as follows:

 $S_{MS} = F_a S_S = 1.0(1.50) = 1.50$  $S_{M1} = F_v S_1 = 1.3(0.60) = 0.78$ 

Where  $F_a$  and  $F_v$  are site coefficients defined in *Provisions* Tables 4.1.2.4a [3.3-1] and 4.1.2.4b [3.3-2], respectively. The design spectral response acceleration parameters (*Provisions* Sec. 4.1.2.5 [Sec. 3.3.3]) are determined in accordance with *Provisions* Eq. 4.1.2.5-1 [Eq. 3.3-3] and 4.1.2.5-2 [3.3-4] for the short-period and one-second period, respectively:

$$S_{DS} = \frac{2}{3}S_{MS} = \frac{2}{3}(1.50) = 1.00$$
$$S_{DI} = \frac{2}{3}S_{MI} = \frac{2}{3}(0.78) = 0.52$$

The Seismic Design Category may be determined by the design spectral acceleration parameters combined with the Seismic Use Group. For buildings assigned to Seismic Design Category D, masonry shear walls must satisfy the requirements for special reinforced masonry shear walls in accordance with *Provisions* Sec. 11.3.8.2 [ACI 530 Sec. 1.13.6.4]. A summary of the seismic design parameters follows:

Seismic Design Category ( <i>Provisions</i> Sec. 4.2.1 [1.4])	= D
Seismic Force Resisting System ( <i>Provisions</i> Table 5.2.2	
[4.3-1])	= Special Reinforced
	Masonry Shear Wall
Response Modification Factor, R (Provisions Table 5.2.2	
[4.3-1])	= 3.5
Deflection Amplification Factor, $C_d$ ( <i>Provisions</i> Table 5.2.2	
[4.3-1])	= 3.5
System Overstrength Factor, $\Omega_0$ ( <i>Provisions</i> Table 5.2.2	
[4.3-1])	= 2.5
Reliability Factor, $\rho$ ( <i>Provisions</i> Sec. 5.2.4.2 [Sec. 4.3.3])	= 1.0

(Determination of  $\rho$  is discussed in Sec. 9.1.3 below [see Sec. 9.1.3.1 for changes to the reliability factor in the 2003 *Provisions*].)

Note that the *R* factor for this system in the IBC and in ASCE 7 is 4.5. [5.0 in the 2003 IBC and ASCE 7-02] This difference would have a substantial effect on the seismic design; however, the vertical reinforcement in the tall 8-in. walls is controlled by wind loads so it would not change.

#### 9.1.2.3 Structural Design Considerations

With respect to the load path, the roof diaphragm supports the upper 16 ft of the masonry walls (half the clear span plus the parapet) in the out-of-plane direction, transferring the lateral force to in-plane masonry shear walls.

Soil structure interaction is not considered.

The building is of bearing wall construction.

Other than the opening in the roof, the building is symmetric about both principal axes, and the vertical elements of the seismic resisting system are arrayed entirely at the perimeter. The opening is not large enough to be considered an irregularity (per *Provisions* Table 5.2.3.2[Table 4.3-2]); thus, the building is regular, both horizontally and vertically. *Provisions* Table 5.2.5.1[Table 4.4-1], permits several analytical procedures to be used; the equivalent lateral force (ELF) procedure (*Provisions* Sec. 5.4) is selected for used in this example. The orthogonality requirements of *Provisions* Sec. 5.2.5.2 Sec. 4.4.2 are potentially significant for the piers between the door openings at the end walls. Thus, those walls will be designed for 100 percent of the forces in one direction plus 30 percent of the forces in the perpendicular direction.

There will be no inherent torsion because the building is symmetric. The effects of accidental torsion, and its potential amplification, need not be included because the roof diaphragm is flexible. This is the authors' interpretation of what amounts to a conflict between *Provisions* Table 5.2.3.2[Table 4.3-2], Item 1, and *Provisions* Sec. 5.4.4.2[Sec. 5.24.2] and Sec. 5.4.4.3[Sec. 5.2.4.3].

The masonry bearing walls also must be designed for forces perpendicular to their plane (*Provisions* Sec. 5.2.6.2.7)[Sec. 4.6.1.3].

For in-plane loading, the walls will be treated as cantilevered shear walls. For out-of-plane loading, the walls will be treated as pinned at the bottom and simply supported at the top. The assumption of a pinned connection at the base is deemed appropriate because the foundation is shallow and narrow which permits rotation near the base of the wall.

#### 9.1.3 Load Combinations

The basic load combinations (*Provisions* Sec. 5.2.7 [Sec. 4.2.2]) are the same as specified in ASCE 7 (and similar to the IBC). The seismic load effect, *E*, is defined by *Provisions* Eq. 5.2.7-1 [4.2-1] and Eq. 5.2.7-2 [4.2-2] as:

$$E = \rho Q_E \pm 0.2S_{DS} D = (1.0)Q_E \pm 0.2(1.00)D = Q_E \pm 0.2D$$

This assumes  $\rho = 1.0$  as will be confirmed in the following section.

#### 9.1.3.1 Reliability Factor

In accordance with *Provisions* Sec. 5.2.4.2[4.3.3], the reliability factor,  $\rho$ , applies to the in-plane load direction.

For the long direction of building:

$$r_{max_x} = \left(\frac{V_{wall}}{V_{story}}\right) \left(\frac{10}{l_w}\right)$$
$$r_{max_x} = (0.5) \left(\frac{10}{200}\right) = 0.025$$

$$\rho = 2 - \frac{20}{r_{max_x}\sqrt{20,000}} = 2 - \frac{20}{0.025\sqrt{20,000}} = -3.66$$

 $\rho = -3.66 < 1.0 = \rho_{min}$ , so use  $\rho = 1.0$ .

For the short direction of the building:

$$r_{max_{x}} = \left(\frac{V_{wall}}{V_{story}}\right) \left(\frac{10}{l_{w}}\right) = \left(\frac{(V_{wall})(0.23)}{V_{story}}\right) \left(\frac{10}{8}\right) = (0.5)(0.23)(1) = 0.115$$

Although the calculation is not shown here, note that a single 8-ft-long pier carries approximately 23 percent (determined by considering the relative rigidities of the piers) of the in-plane load for each end wall.

Also, 1.0 was used for the  $10/l_w$  term even though 10/8 ft > 1.0. According to *Provisions* 5.2.4.2, the  $10/l_w$  term need not exceed 1.0 *only* for walls of light frame construction. This example was created based on a draft version of the 2000 *Provisions*, which limited the value of the  $10/l_w$  term to 1.0 for all shear walls, a requirement that was later changed for the published edition. Thus, this calculation is not strictly correct. Using the correct value of  $r_{max}$ , would result in  $\rho = 1.02$  rather than the 0.77 computed below.

This would result in a slight change in the factor on  $Q_E$ , 1.02 vs. 1.00, which has not been carried through the remainder of this example.

(When the redundancy factor was developed by the Structural Engineers Association of California in the wake of the 1994 Northridge earthquake, the upper bound of 1.0 for  $10/l_w$  was simply not mentioned. The 1997 *Provisions*, the UBC, and the IBC were published with no upper bound on  $10/l_w$ . However, the original authors of the concept published their intent with the SEAOC document in 1999 with the upper bound of 1.0 on  $10/l_w$  for all types of shear walls. The same change was adopted within BSSC for the 2000 *Provisions*. A subsequent change to the 2000 *Provisions* limited the upper bound of 1.0 to apply only to light frame walls.)

Therefore,

$$r_{max_x} = 0.12$$

$$\rho = 2 - \frac{20}{0.115\sqrt{20,000}} = 0.77$$

$$\rho = 0.77 < 1.0 = \rho_{min}, \text{ so use } \rho = 1.0.$$

[The redundancy requirements have been substantially changed in the 2003 *Provisions*. For a shear wall building assigned to Seismic Design Category D,  $\rho = 1.0$  as long as it can be shown that failure of a shear wall with height-to-length-ratio greater than 1.0 would not result in more than a 33 percent reduction in story strength or create an extreme torsional irregularity. Therefore, the redundancy factor would have to be investigated only in the transverse direction where the aspect ratios of the piers between door openings are greater than 1.0. In the longitudinal direct, where the aspect ratio is (significantly) less than 1.0,  $\rho = 1.0$  by default.]

#### 9.1.3.2 Combination of Load Effects

Load combinations for the in-plane loading direction from ASCE 7 are:

1.2D + 1.0E + 0.5L + 0.2S

and

0.9D + 1.0E + 1.6H.

L, S, H do not apply for this example so the load combinations become:

1.2D + 1.0E

and

$$0.9D + 1.0E$$

When the effect of the earthquake determined above,  $1.2D + 1.0(Q_E \pm 0.2D)$ , is inserted in each of the load combinations:

$$1.4D + 1.0 Q_E$$
  
 $1.0D - 1.0 Q_E$ 

and

$$0.9D + 1.0(Q_E \pm 0.2D)$$

which results in:

$$1.1D + 1.0 Q_E$$

and

$$0.7D - 1.0 Q_E$$

Thus, the controlling cases from all of the above are:

$$1.4D + 1.0 Q_E$$

when gravity and seismic are additive and

$$0.7D - 1.0 Q_E$$

when gravity and seismic counteract.

These load combinations are for the in-plane direction of loading. Load combinations for the out-ofplane direction of loading are similar except that the reliability coefficient ( $\rho$ ) is not applicable. Thus, for this example (where  $\rho = 1.0$ ), the load combinations for both the in-plane and the out-of-plane directions are:

$$1.4D + 1.0 Q_E$$

and

#### $0.7D - 1.0 Q_E$ .

The combination of earthquake motion (and corresponding loading) in two orthogonal directions must be considered (*Provisions* Sec. 5.2.5.2.3) [Sec. 4.4.2.3].

#### 9.1.4 Seismic Forces

#### 9.1.4.1 Base Shear

Base shear is computed using the parameters determined previously. The *Provisions* does not recognize the effect of long, flexible diaphragms on the fundamental period of vibration. The approximate period equations, which limit the computed period, are based only on the height. Since the structure is relatively short and stiff, short-period response will govern the design equations. According to *Provisions* Sec. 5.4.1 [Sec. 5.2.1.1] and Eq. 5.4.1.1-1 [Eq. 5.2-3] (for short-period structures):

$$V = C_{S}W = \left[\frac{S_{DS}}{R/I}\right]W = \left[\frac{1.0}{3.5/1}\right]W = 0.286 W$$

The seismic weight for forces in the long direction is:

Roof = 20 psf (100)200	=	400 kips
End walls = 103 psf (2 walls)[(30 ft)(100 ft) - 5(12 ft)(12 ft)](17.8 ft/28 ft)	=	299 kips
Side walls = $65 \text{ psf} (30 \text{ft})(200 \text{ft})(2 \text{ walls})$	=	780 kips
Total	= 1	,479 kips

Note that the centroid of the end walls is determined to be 17.8 ft above the base, so the portion of the weight distributed to the roof is approximately the total weight multiplied by 17.8 ft/28 ft (weights and section properties of the walls are described subsequently).

Therefore, the base shear to each of the long walls is:

V = (0.286)(1,479 kips)/2 = 211 kips.

The seismic weight for forces in the short direction is:

Roof = 20 psf (100)200	=	400 kips
Side walls = 65 psf (2 walls)(30ft)(200ft)(15ft/28ft)	=	418 kips
End walls = $103 \text{ psf} (2 \text{ walls})[(30\text{ft})(100\text{ft})-5(12\text{ft})(12\text{ft})]$	<u> </u>	470 kips
Total	= 1	,288 kips

The base shear to each of the short walls is:

V = (0.286)(1,288 kips)/2 = 184 kips.

#### 9.1.4.2 Diaphragm Force

See Sec. 10.2 for diaphragm forces and design.

#### 9.1.4.3 Wall Forces

because the diaphragm is flexible with respect to the walls, shear is distributed to the walls on the basis of beam theory ignoring walls perpendicular to the motion (this is the "tributary" basis).

The building is symmetric. Given the previously explained assumption that accidental torsion need not be applied, the force to each wall becomes half the force on the diaphragm.

All exterior walls are bearing walls and, according to *Provisions* Sec. 5.2.6.2.7 [Sec. 4.6.1.3], must be designed for a normal (out-of-plane) force of  $0.4S_{DS}W_c$ . The out-of-plane design is shown in Sec. 9.1.5.3 below.

#### 9.1.5 Longitudinal Walls

The total base shear is the design force. *Provisions* Sec. 11.7 [Sec. 11.2] is the reference for design strengths. The compressive strength of the masonry  $(f_m')$  is 2,000 psi. *Provisions* Sec. 11.3.10.2 gives  $E_m = 750 f_m' = (750)(2 \text{ ksi}) = 1,500 \text{ ksi}.$ 

[2003 *Provisions* Sec. 11.2 adopts ACI 530 as a design basis for strength design masonry and provides some modifications to ACI 530. In general, the adoption of ACI 530 as a reference does not have a significant effect on this design example. Note that by adopting ACI 530 in the 2003 *Provisions*,  $E_m = 900f'_m$  per ACI 530 Sec. 1.8.2.2.1, eliminating the conflict discussed below.]

Be careful to use values consistent with the *Provisions*. Different standards call for different values. To illustrate this point, the values of  $E_m$  from different standards are shown in Table 9.1-1.

<b>Table 9.1-1</b> Comparison of $E_m$		
Standard	$E_m$	$E_m$ for this example
Provisions	$750 f_{m}'$	1,500 ksi
IBC	$900 f_{m'}$	1,800 ksi
ACI 530	$900 f_{m'}$	1,800 ksi

1.0 kip = 4.45 kN, 1.0 in. = 25.4 mm.

For 8-inch thick CMU with vertical cells grouted at 24 in. o.c. and horizontal bond beams at 48 inch o.c., the weight is conservatively taken as 65 psf (recall the CMU are normal weight) and the net bedded area is 51.3 in.<sup>2</sup>/ft based on tabulations in NCMA-TEK 141.

#### 9.1.5.1 Horizontal Reinforcement

As determined in Sec. 9.1.4.1, the design base shear tributary to each longitudinal wall is 211 kips. Based on Provisions Sec. 11.7.2.2 [ACI 530, Sec. 3.1.3], the design shear strength must exceed either the shear corresponding to the development of 1.25 times the nominal flexure strength of the wall, which is very unlikely in this example due to the length of wall, or 2.5 times  $V_{\mu} = 2.5(211) = 528$  kips.

From *Provisions* Eq. 11.7.3.2[ACI 530, Eq. 3-21], the masonry component of the shear strength capacity for reinforced masonry is:

$$V_m = \left[ 4.0 - 1.75 \left( \frac{M}{Vd} \right) \right] A_n \sqrt{f'_m} + 0.25 \ P \ .$$

Conservatively treating M/Vd as equal to 1.0 for the long walls and conservatively treating P as the weight of the wall only without considering the roof weight contribution:

$$V_m = [4.0 - 1.75(1.0)](51.3)(200)\sqrt{2000} + 0.25(390) = 1130$$
 kips

and

 $\phi V_m = 0.8(1,130) = 904$  kips > 528 kips

OK

where  $\phi = 0.8$  is the resistance factor for shear from *Provisions* Table11.5.3[ACI 530, sec. 3.1.4].

Horizontal reinforcement therefore is not required for shear but is required if the wall is to qualify as a "Special Reinforced Masonry Wall."

According to Provisions Sec. 11.3.8.3 [ACI 530, Sec. 1.13.6.3], minimum reinforcement is  $(0.0007)(7.625 \text{ in.})(8 \text{ in.}) = 0.043 \text{ in.}^2$  per course, but it may be wise to use more horizontal reinforcement for shrinkage in this very long wall and then use minimum reinforcement in the vertical direction (this concept applies even though this wall requires far more than the minimum reinforcement in the vertical direction due to its large height-to-thickness ratio). Two #5 bars at 48 in. on center provides 0.103 in.<sup>2</sup> per course. This amounts to 0.4 percent of the area of masonry plus the grout in the bond beams. The actual shrinkage properties of the masonry and the grout and local experience should be considered in deciding how much reinforcement to provide. For long walls that have no control joints, as in this example, providing more than minimum horizontal reinforcement is appropriate.

#### 9.1.5.2 Vertical Reinforcement

Steps for verifying a trial design are noted in the sections that follow.

#### 9.1.5.3 Out-of Plane Flexure

As indicated previously, the design demand for seismic out-of-plane flexure is  $0.4S_{DS}W_c$ . For a wall weight of 65 psf for the 8-in.-thick CMU side walls, this demand is 0.4(1.00)(65 psf) = 26 psf.

Calculations for out-of-plane flexure become somewhat involved and include the following:

- 1. Select a trial design.
- 2. Investigate to ensure ductility.
- 3. Make sure the trial design is suitable for wind (or other nonseismic) lateral loadings using the IBC.

Note that many section properties determined in accordance with the IBC are different from those indicated in the *Provisions* so section properties will have to be determined multiple times. The IBC portion of the calculation is not included in this example.

[2003 *Provisions* and the 2003 IBC both adopt ACI 530-02 by reference, so the section properties should be the same for both documents.]

- 4. Calculate midheight deflection due to wind by the IBC. (While the *Provisions* have story drift requirements, they do not impose a midheight deflection limit for walls).
- 5. Calculate seismic demand.
- 6. Determine seismic resistance and compare to demand determined in Step 5.

Proceed with these steps as follows:

#### 9.1.5.3.1 Trial design

A trial design of #7 bars at 24 in. on center is selected. See Figure 9.1-3.

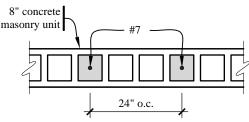


**Figure 9.1-3** Trial design for 8-in.-thick CMU wall (1.0 in = 25.4 mm).

#### 9.1.5.3.2 Investigate to ensure ductility

The critical strain condition corresponds to a strain in the extreme tension reinforcement (which is a single #7 centered in the wall in this example) equal to 1.3 times the strain at yield stress.

Based on Provisions Sec. 11.6.2.2 [ACI 530, Sec. 3.2.3.5.1] for this case:

$$t = 7.63 \text{ in.}$$
  

$$d = t/2 = 3.81 \text{ in.}$$
  

$$\varepsilon_m = 0.0025$$
  

$$\varepsilon_s = 1.3\varepsilon_y = 1.3(f_y/E_s) = 1.3(60 \text{ ksi }/29,000 \text{ ksi}) = 0.0027$$
  

$$c = \left[\frac{\varepsilon_m}{(\varepsilon_m + \varepsilon_s)}\right] d = 1.83 \text{ in.}$$

a = 0.8c = 1.46 in.

The Whitney compression stress block, a = 1.46 in. for this strain distribution, is greater than the 1.25 in. face shell width. Thus, the compression stress block is broken into two components: one for full compression against solid masonry (the face shell) and another for compression against the webs and grouted cells, but accounting for the open cells. These are shown as  $C_1$  and  $C_2$  in Figure 9.1-4:

$$\begin{array}{ll} C_1 &= 0.80 f_m' \ (1.25 \text{ in.}) b = (0.80)(2 \text{ ksi})(1.25)(24) = 48 \text{ kips (for a 24-in. length)} \\ C_2 &= 0.80 f_m' \ (a-1.25 \text{ in.})(8 \text{ in.}) = (0.80)(2 \text{ ksi})(1.46-1.25)(8) = 2.69 \text{ kips (for a 24-in. length)} \end{array}$$

The 8-in. dimension in the  $C_2$  calculation is for combined width of grouted cell and adjacent mortared webs over a 24-in. length of wall. The actual width of one cell plus the two adjacent webs will vary with various block manufacturers, and may be larger or smaller than 8 in. The 8-in. value has the benefit of simplicity and is correct when considering solidly grouted walls.

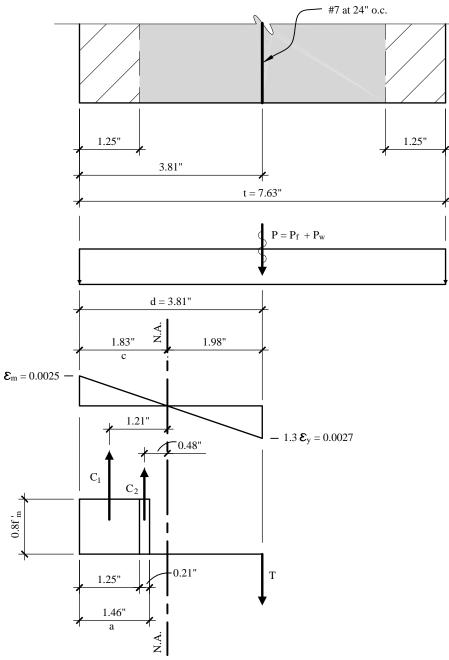


**Figure 9.1-4** Investigation of out-of-plane ductility for the 8-in.-thick CMU side walls (1.0 in = 25.4 mm).

*T* is based on 1.25  $F_v$  (*Provisions* Sec. 11.6.2.2)[ACI 530, Sec. 3.2.3.5.1]:

 $T = 1.25F_yA_s = (1.25)(60 \text{ ksi})(0.60 \text{ in.}^2) = 45 \text{ kips}$  (for a 24-in. length)

Use unfactored P (Provisions Sec. 11.6.2.2) [ACI 530, Sec. 3.2.3.5.1]:

$$P = (P_f + P_w) = (20 \text{ psf} (10 \text{ ft.}) + 65 \text{ psf} (16 \text{ ft.})) = 1.24 \text{ klf} = 2.48 \text{ kips} (\text{for a } 24\text{-in. length})$$

Check  $C_1 + C_2 > T + P$ :

$$T + P = 47.5$$
 kips  
 $C_1 + C_2 = 50.7$  kips > 47.5 kips.

OK

The compression capacity is greater than the tension capacity; therefore, the ductile failure mode criterion is satisfied.

[The ductility (maximum reinforcement) requirements in ACI 530 are similar to those in the 2000 *Provisions*. However, the 2003 *Provisions* also modify some of the ACI 530 requirements, including critical strain in extreme tensile reinforcement (1.5 times) and axial force to consider when performing the ductility check (factored loads).]

#### 9.1.5.3.3 Check for wind load using the IBC

Load factors and section properties are not the same in the IBC and the *Provisions* (The wind design check is beyond the scope of this seismic example so it is not presented here.) Both strength and deflection need to be ascertained in accordance with IBC.

Note that, for comparison, selected properties for the *Provisions* (and IBC) ductility check, IBC wind strength check, and *Provisions* seismic strength check are tabulated below. Keeping track of which version of a given parameter is used for each of the calculations can get confusing; be careful to apply the correct property for each analysis.

	_	_	-
Parameter	Provisions Ductility Calculation	Provisions Strength Calculation	<i>IBC</i> Wind Calculation
Р	1.24 klf	0.87 & 1.74 klf	1.12 klf
$E_m$	NA	1,500,000 psi	1,800,000 psi
$f_r$	NA	80 psi	112 psi
W	NA	26 psf	19 psf (service)
$\mathcal{E}_{s}$	0.0027	NA	NA
d	3.82 in.	3.82 in.	3.82 in.
С	1.83 in.	1.25 in.	1.25 in.
а	1.46 in.	1.00 in.	1.00 in.
$C_{res} = C_1 + C_2$	50.1 kips	52.1 kips	56.4 kips
$n = E_s/E_m$	NA	19.33	16.11
$I_g$	NA	355 in. <sup>4</sup>	355 in. <sup>4</sup>
$S_{g}$	NA	93.2 in. <sup>3</sup>	93.2 in. <sup>3</sup>
$A_{se}$	NA	0.32 in. <sup>2</sup> /ft	0.32 in. <sup>2</sup> /ft
$I_{cr}$	NA	48.4 in. <sup>4</sup> /ft	48.4 in. <sup>4</sup> /ft
$M_{cr} = f_r S$	NA	7.46 inkips	10.44 inkips
$\delta_{_{allow}}$	NA	NA	2.32 in.

 Table 9.1-2
 Comparison of Variables (explanations in the following text)

NA = not applicable, 1.0 kip = 4.45 kN, 1.0 ft = 0.3048 m, 1.0 in = 25.4 mm, 1.0 ksi = 6.98 MPa, 1.0 in.-kip = 0.113 kN-m.

#### 9.1.5.3.4 Calculate midheight deflection due to wind by the IBC

The actual calculation is not presented here. For this example the midheight deflection was calculated using IBC Eq. 21-41[ACI 530, Eq. 3-31] with  $I_{cr} = 47.3$  in.<sup>4</sup> per ft. Using IBC Eq. 21.41[ACI 530, Eq. 3-31], the calculated deflection is 2.32 in., which is less than 2.35 in. = 0.007*h* (IBC Eq. 21-39[ACI 530, Eq. 3-29]).

#### 9.1.5.3.5 Calculate seismic demand

For this case, the two load factors for dead load apply: 0.7D and 1.4D. Conventional wisdom holds that the lower dead load will result in lower moment-resisting capacity of the wall so the 0.7D load factor would be expected to govern. However, the lower dead load also results in lower P-delta so both cases should be checked. (As it turns out, the higher factor of 1.4D governs).

Check moment capacity for 0.7D:

$$P_u = 0.7(P_f + P_w)$$

For this example, the iterative procedure for addressing P-delta from Amrhein will be used, not *Provisions* Eq. 11.5.4.3[ACI 530, Commentary Sec. 3.1.5.3] which is intended for in-plane deflections:

Roof load,  $P_f = 0.7(0.2 \text{ klf}) = 0.14 \text{ klf}$ Eccentricity, e = 7.32 in. (distance from wall centerline to roof reaction centerline) Modulus of elasticity (*Provisions* Eq. 11.3.10.2 [ACI 530, 1.8.2.2]),  $E_m = 750 f_m' = 1,500,000$  psi

[Note that by adopting ACI 530 in the 2003 *Provisions*,  $E_m = 900f'_m$  per ACI 530 Sec. 1.8.2.2.1.]

Modular ratio, 
$$n = \frac{E_s}{E_m} = 19.3$$

The modulus of rupture  $(f_r)$  is found in *Provisions* Table 11.3.10.5.1[ACI 530, Sec. 3.1.7.2.1]. The values given in the table are for either hollow CMU or fully grouted CMU. Values for partially grouted CMU are not given; Footnote a indicates that interpolation between these values must be performed. As illustrated in Figure 9.1-6, the interpolated value for this example is 80 psi:

$$(f_r - 50 \text{ psi})/(103 \text{ in.}^2 - 60 \text{ in.}^2) = (136 \text{ psi} - 50 \text{ psi})/(183 \text{ in.}^2 - 60 \text{ in.}^2)$$
  
 $f_r = 80 \text{ psi}$   
 $I_g = 355 \text{ in.}^4/\text{ft}$   
 $S_g = 93.2 \text{ in.}^3/\text{ft}$   
 $M_{cr} = f_r S_g = 7460 \text{ in-lb/ft}$ 

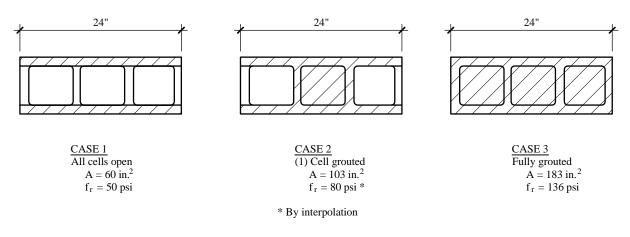
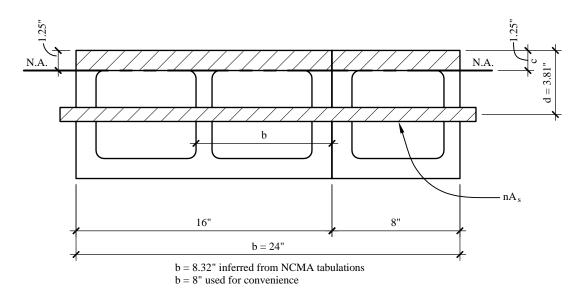


Figure 9.1-6 Basis for interpolation of modulus of rupture,  $f_r$  (1.0 in = 25.4 mm, 1.0 psi = 6.89 kPa).

Refer to Figure 9.1-7 for determining  $I_{cr}$ . The neutral axis shown on the figure is not the conventional neutral axis by linear analysis; instead it is the plastic centroid, which is simpler to locate, especially when the neutral axis position results in a T beam cross-section. (For this wall, the neutral axis does not produce a T section, but for the other wall in this building, a T section does result.) Cracked moments of inertia computed by this procedure are less than those computed by linear analysis but generally not so much less that the difference is significant. (This is the method used for computing the cracked section moment of inertia for slender walls in the standard for concrete structures, ACI 318.) Axial load does enter the computation of the plastic neutral axis and the effective area of reinforcement. Thus:

$$\begin{split} P &= 1.24 \text{ klf} \\ T &= ((0.60 \text{ in.}^2)/(2 \text{ ft.}))(60 \text{ ksi}) = 18.0 \text{ klf} \\ C &= T + P = 19.24 \text{ klf} \\ a &= C/(0.8 f'_m b) = (19.24 \text{ klf})/(0.8(2.0 \text{ ksi})(12 \text{ in./ft.})) = 1.002 \text{ in.} \\ c &= a/0.8 = 1.253 \text{ in.} \\ I_{cr} &= nA_{se}(d-c)^2 + bc^3/3 = 19.33(0.30 \text{ in.}^2 + (1.24 \text{ klf})/60 \text{ ksi})(3.81 \text{ in.} - 1.25 \text{ in.})^2 + (12 \text{ in./ft})(1.25 \text{ in.})^3/3 = 4.84 \text{ in.}^4/\text{ft} \end{split}$$



**Figure 9.1-7** Cracked moment of inertia  $(I_{cr})$  for 8-in.-thick CMU side walls (1.0 in = 25.4 mm).

Note that  $I_{cr}$  could be recomputed for P = 0.7D and P = 1.4D but that refinement is not pursued in this example.

The standard technique is to compute the secondary moment in an iterative fashion as shown below:

Axial load

$$P_{\mu} = 0.7(P_f + P_w) = 0.7(0.2 \text{ klf} + 1.04 \text{ klf}) = 0.868 \text{ klf}$$

First iteration

$$A_{se} = \frac{P_u + A_s f_y}{f_y} = \frac{0.868 + (0.60)(60)}{60} = 0.614 \text{ in.}^2 / 2 \text{ ft.} = 0.312 \text{ in.}^2 / \text{ft}$$
$$M_{u1} = w_u h^2 / 8 + P_0 e + (P_0 + P_w) \Delta$$
$$M_{u1} = \frac{(26 \text{ psf}/12)(336 \text{ in.})^2}{8} + (140 \text{ plf}) \left(\frac{7.32 \text{ in.}}{2}\right) + (140 \text{ plf} + 728 \text{ plf})(0)$$
$$M_{u1} = 31,088 \text{ in.-lb/lf} > M_{cr} = 7460$$
$$\Delta_{s1} = \frac{5(7460)(336)^2}{48(1,500,000)(355)} + \frac{5(31,088 - 7460)(336)^2}{48(1,500,000)(48.4)} = 0.165 + 3.827 = 3.99 \text{ in.}$$

Second iteration

$$M_{u2} = 30,576 + 512 + (140 + 728)(3.99) = 34,551 \text{ in.-lb}$$
  
$$\Delta_{s2} = 0.165 + \frac{5(34,551 - 7460)(336)^2}{48(1,500,000)(48.4)} = 0.165 + 4.388 = 4.55 \text{ in.}$$

Third iteration

$$M_{u3} = 30,576 + 512 + (140 + 728)(4.55) = 35,040 \text{ in.-lb/lf}$$
  
$$\Delta_{s3} = 0.165 + \frac{5(35,040 - 7460)(336)^2}{48(1,500,000)(48.4)} = 0.165 + 4.467 = 4.63 \text{ in.}$$

Convergence check

$$\frac{4.63 - 4.55}{4.55} = 1.8\% < 5\%$$

 $M_u = 35,040$  in.-lb (for the 0.7D load case)

Using the same procedure, find  $M_u$  for the 1.4D load case. The results are summarized below:

First iteration

$$P = 7360 \text{ plf}$$
  
 $M_{u1} = 31,601 \text{ in.-lb/ft}$ 

 $\Delta_{u1} = 4.08$  in.

Second iteration

 $M_{u2} = 38,684$  in.-lb/ft  $\Delta_{u2} = 5.22$  in.

Third iteration

 $M_{u3} = 40,667$  in.-lb/ft  $\Delta_3 = 5.54$  in.

Fourth iteration

 $M_{u4} = 41,225$  in.-lb/ft  $\Delta_{u4} = 5.63$  in.

Check convergence

$$\frac{5.63 - 5.54}{5.54} = 1.7\% < 5\%$$

 $M_u = 41,225$  in.-lb (for the 1.4D load case)

#### 9.1.5.3.6 Determine flexural strength of wall

Refer to Figure 9.1-8. As in the case for the ductility check, a strain diagram is drawn. Unlike the ductility check, the strain in the steel is not predetermined. Instead, as in conventional strength design of reinforced concrete, a rectangular stress block is computed first and then the flexural capacity is checked.

 $T = A_s f_v = (0.30 \text{ in.}^2/\text{ft.})60 \text{ ksi} = 18.0 \text{ klf}$ 

The results for the two axial load cases are tabulated below.

Load Case	0.7D + E	1.4D + E
Factored P, klf	0.87	1.74
T + P = C, klf	18.87	19.74
$a = C / (0.8f'_m b)$ , in.	0.981	1.028
$M_N = C (d - a/2)$ , inkip/ft.	62.6	65.1
$\varphi M_N = 0.85 M_N$ , inkip/ft.	53.2	55.3
$M_U$ , inkip/ft.	35.0	41.2
Acceptance	OK	OK

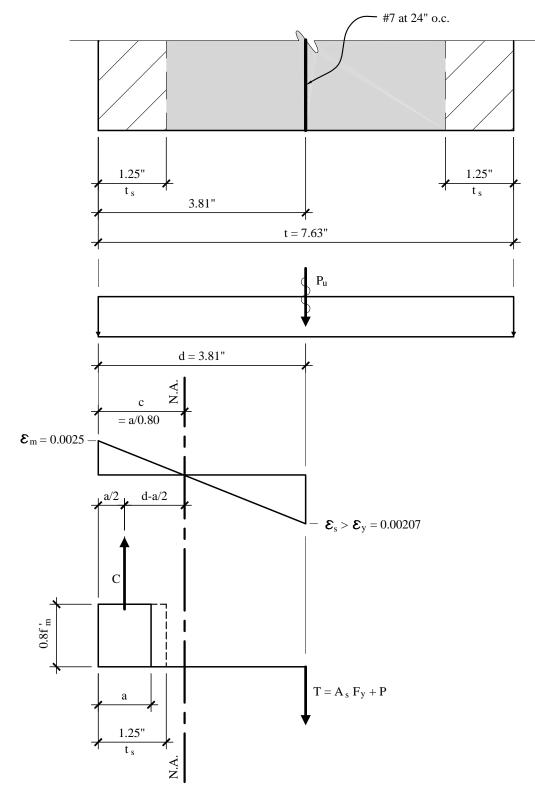


Figure 9.1-8 Out-of-plane strength for 8-in.-thick CMU walls (1.0 in = 25.4 mm).

Note that wind actually controls the stiffness and strength out-of-plane and that this is only a "tentative" acceptance for seismic. The *Provisions* requires a check of the combined orthogonal loads in accordance

with *Provisions* Sec. 5.2.5.2, Item a [Sec. 4.4.2.3]. However, as discussed below, a combined orthogonal load check was deemed unnecessary for this example.

#### 9.1.5.4 In-Plane Flexure

In-plane calculations for flexure in masonry walls include two items per the Provisions:

- 1. Ductility check and
- 2. Strength check.

It is recognized that this wall is very strong and stiff in the in-plane direction. In fact, most engineers would not even consider these checks necessary in ordinary design. The ductility check is illustrated here for two reasons: to show a method of implementing the requirement and to point out an unexpected result. (In the authors' opinion, the *Provisions* should reconsider the application of the ductility check where the  $M/Vd_v$  ratio is substantially less than 1.0.)

#### 9.1.5.4.1 Ductility check

*Provisions* Sec. 11.6.2.2 [ACI 530, 3.2.3.5.1] requires that the critical strain condition correspond to a strain in the extreme tension reinforcement equal to 5 times the strain associated with  $F_y$ . This calculation uses unfactored gravity loads. (See Figure 9.1-9.)

[The ductility (maximum reinforcement) requirements in ACI 530 are similar to those in the 2000 *Provisions*. However, the 2003 *Provisions* also modify some of the ACI 530 requirements, including critical strain in extreme tensile reinforcement (4 times yield) and axial force to consider when performing the ductility check (factored loads).]

$$P = P_w + P_f = (0.065 \text{ ksf} (30 \text{ ft.}) + 0.02 \text{ ksf} (10 \text{ ft.}))(200 \text{ ft.}) = 430 \text{ kips}$$

*P* is at the base of the wall rather than at the midheight.

$$c = \left(\frac{\varepsilon_m}{\varepsilon_m + \varepsilon_s}\right) d = \left(\frac{0.0025}{0.0025 + 0.0103}\right) 200 \text{ ft} = 38.94 \text{ ft}$$
  
$$a = 0.8c = 31.15 \text{ ft} = 373.8 \text{ in.}$$
  
$$C_m = 0.8f_m' a b_{avg} = 2,560 \text{ kips}$$

Where  $b_{avg}$  is taken from the average area used earlier, 51.3 in.<sup>2</sup>/ft.; see Figure 9.1-9 for locations of tension steel and compression steel (the rebar in the compression zone will act as compression steel). From this it can be seen that:

$$T_{sl} = (1.25f_y) \left( \frac{40.27}{(2)(2 \text{ ft o.c.})} \right) (0.60) = 453 \text{ kips}$$
$$T_{s2} = (1.25f_y) \left( \frac{120.79}{2} \right) (0.60) = 2,718 \text{ kips}$$
$$C_{sl} = f_y \left( \frac{6.73}{2 \text{ ft. o.c.}} \right) (0.60) = 121 \text{ kips}$$

$$C_{s2} = (f_y) \left(\frac{32.21}{(2)(2)}\right) (0.60) = 290$$
 kips

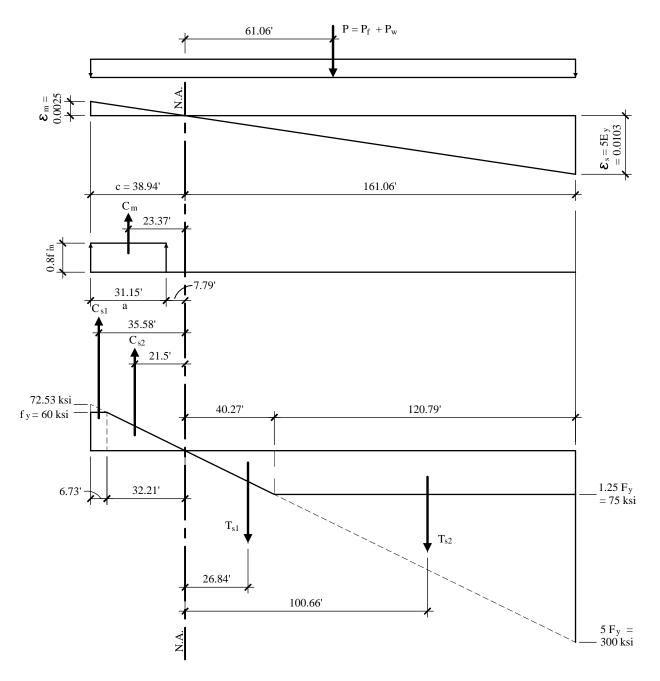


Figure 9.1-9 In-plane ductility check for side walls (1.0 in = 25.4 mm, 1.0 ksi = 6.89 MPa).

Note that some authorities would not consider the compression resistance of reinforcing steel that is not enclosed within ties. The *Provisions* clearly allows inclusion of compression in the reinforcement.

$$\Sigma C > \Sigma T$$

 $C_m + C_{s1} + C_{s2} > P + T_{s1} + T_{s2}$ 2.560 + 121 + 290 = 2.971 < 3.601 = 430 + 453 + 2.718

Therefore, there is not enough compression capacity to ensure ductile failure.

In order to ensure ductile failure with #7 bars at 24 in. on center, one of the following revisions must be made: either add (3,601 kips - 2,971 kips) = 630 kips to  $C_m$  or reduce T by reducing  $A_s$ . Since this amount of reinforcement is needed for out-of-plane flexure,  $A_s$  cannot be reduced.

Try filling all cells for 10 ft - 0 in. from each end of the wall. As shown in Figure 9.1-10, this results in 10 additional grouted cells.

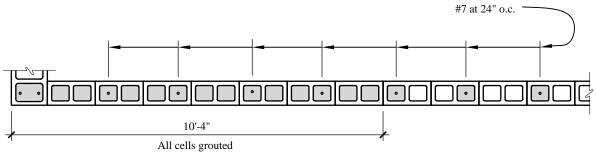


Figure 9.1-10 Grout cells solid within 10 ft of each end of side walls (1.0 in = 25.4 mm, 1.0 ft = 0.3048 m).

Area of one grouted cell:	$(8 \text{ in.})(5.13 \text{ in.}) = 41 \text{ in.}^2$	
Volume of grout for one cell:	$(6 \text{ in.})(5.13 \text{ in.})(30 \text{ ft.})/(144 \text{ in.}^2/\text{ft.}^2) = 6.41 \text{ ft.}^3$	
Weight of grout for one cell:	(0.140  kcf)(6.41) = 0.90  kips/cell	
Additional <i>P</i> :	(10  additional cells)(0.9) = 9.0  kips	
Additional $C_m$	$0.8 f_m'$ (41 in. <sup>2</sup> )(10 cells) = 656 kips	
Additional $C_m$ - additional P:	656 kips - 9 kips = 647 kips	
Net additional $C_m$ :	647 kips > 630 kips	OK

or, as expressed in terms of the above equation:

$$\Sigma C > \Sigma T$$
  
2,971 kips + 656 kips = 3,627 kips > 3,610 kips = 3,601 kips + 9 kips OK

Since C > T, the ductile criterion is satisfied.

This particular check is somewhat controversial. In the opinion of the authors, flexural yield is feasible for walls with M/Vd in excess of 1.0; this criterion limits the compressive strain in the masonry, which leads to good performance in strong ground shaking. For walls with M/Vd substantially less than 1.0, the wall will fail in shear before a flexural yield is possible. Therefore, the criterion does not affect performance. Well distributed and well developed reinforcement to control the shear cracks is the most important ductility attribute for such walls.

#### 9.1.5.4.2 Strength check

The wall is so long with respect to its height that in-plane strength for flexure is acceptable by inspection.

#### 9.1.5.5 Combined Loads

Combined loads are not calculated here because the in-plane strength is obviously very high. Out-ofplane resistance governs the flexural design.

#### 9.1.5.6 Shear in Longitudinal Walls (Side Walls)

Compute out-of-plane shear at base of wall in accordance with Provisions Sec. 5.2.6.2.7[Sec. 4.6.1.3]:

$$F_p = 0.4S_{DS}W_c = (0.4)(1.00)(65 \text{ psf})(28 \text{ ft/2}) = 364 \text{ plf.}$$

Information from the flexural design from Sec. 9.1.5.3 is needed to determine the required shear strength based upon development of the flexural capacity. The ratio of  $\varphi M_N$  to  $M_U$  is the largest for the load case 0.7D + E. The load that would develop the flexural capacity is approximated by ratio (a second P-delta analysis does not seem justified for this check):

w'= w × 
$$\frac{\phi M_N / \phi}{M_U}$$
 = 26 psf ×  $\frac{53.2 / 0.85}{35.0}$  = 46.5 psf

1.25 times this results in a load for shear design of 58 psf. Thus  $V_U = (58 \text{ psf})(28 \text{ ft. }/2) = 818 \text{ plf.}$  The capacity of computed per *Provisions* Eq.11.7.3.2[ACI 530, Eq. 3.2.1] :

$$V_m = \left[4.0 - 1.75 \left(\frac{M}{Vd}\right)\right] A_n \sqrt{f'_m} + 0.25 P$$

*M/Vd* need not be taken larger than 1.0.  $A_n$  is taken as  $b_w d = 8.32(3.81) = 31.7$  in.<sup>2</sup> per cell from Figure 9.17. Because this shear exists at both the bottom and the top of the wall, conservatively neglect the effect of *P*:

$$V_m = [4.0 - 1.75(1.0)](51.3 \text{ in.}^2 / 2 \text{ ft.})\sqrt{2,000} + 0 = 1.595 \text{ klf}$$
  
$$\phi V_m = (0.8)(1.595) = 1.28 \text{ klf} > 0.81 \text{ klf}$$

As indicated in Sec. 9.1.4.1 and Sec. 9.1.5.1, the in-plane demand at the base of the wall,  $V_u = 2.5(211 \text{ kips}) = 528 \text{ kips}$ , and the shear capacity,  $\phi V_m$  is larger than 904 kips.

For the purpose of understanding likely behavior of the building somewhat better,  $V_n$  is estimated more accurately for these long walls:

$$\begin{split} M/Vd &= h/l = 28/200 = 0.14 \\ P &= 0.7D = 0.7(430) = 301 \text{ kip} \\ V_m &= [4.0 - 1.75(0.14)][200(51.3) + 2(10)91.5-51.3)](0.045) + 0.25(301) = 1870 + 75 = 1945 \text{ kip} \\ V_s &= 0.5(A_s/s)f_sd = 0.5(0.62/4.0)(60)(200) = 930 \text{ kip} \\ V_n &= 1945 + 930 = 2875 \text{ kip} \\ \text{Maximum } V_n &= 6\sqrt{f_m}A = 6(0.045 \text{ ksi})(9234 \text{ in.}^2) = 2493 < 2875 \text{ kip} \\ \varphi V_n &= 0.8(2493) = 1994 \text{ kip} \\ V_E &= 211 \text{kip} \\ V_n/V_E &= 11.8 >> R \text{ used in design} \end{split}$$

In other words, it is unlikely that the long masonry walls will yield in either in-plane shear or flexure at the design seismic ground motion. The walls will likely yield in out-of-plane response and the roof diaphragm may also yield. The roof diaphragm for this building is illustrated in Sec. 10.2.

The combined loads for shear (orthogonal loading, per Provisions Sec. 5.2.5.2.2, Item a)[Sec. 4.4.2.3] are shown in Table 9.1-3.

	Out-of-Plane	In-Plane	Total
Case 1	1.00(810/1,280)+	0.30(528/1994)=	0.71 < 1.00 OK
Case 2	0.30(810/1,280)+	1.00(528/1994)=	0.45 < 1.00 OK

Values are in kips; 1.0 kip = 4.45 kN.

#### 9.1.6 Transverse Walls

The transverse walls will be designed in a manner similar to the longitudinal walls. Complicating the design of the transverse walls are the door openings, which leave a series of masonry piers between the doors.

#### 9.1.6.1 Horizontal Reinforcement

The minimum reinforcement, per *Provisions* Sec. 11.3.8.3[ACI 530, Sec.1.13.6.3], is (0.0007)(11.625) in.)(8 in.) =  $0.065 \text{ in.}^2$  per course. The maximum spacing of horizontal reinforcement is 48 in., for which the minimum reinforcement is 0.39 in.<sup>2</sup>. Two #4 in bond beams at 48 in. on center would satisfy the requirement. The large amount of vertical reinforcement would combine to satisfy the minimum total reinforcement requirement. However, given the 100-ft length of the wall, a larger amount is desired for control of restrained shrinkage as discussed in Sec. 9.1.5.1. Two #5 at 48 in. on center will be used.

#### 9.1.6.2 Vertical Reinforcement

The area for each bay subject to out-of-plane wind is 20 ft wide by 30 ft high because wind load applied to the doors is transferred to the masonry piers. However, the area per bay subject to both in-plane and out-of-plane seismic is reduced by the area of the doors. This is because the doors are relatively light compared to the masonry. See Figures 9.1-12 and 9.1-13.

#### 9.1.6.3 Out-of-Plane Flexure

Out-of-plane flexure will be considered in a manner similar to that illustrated in Sec. 9.1.5.3. The design of this wall must account for the effect of door openings between a row of piers. The steps are the same as identified previously and are summarized here for convenience:

- 1. Select a trial design,
- 2. Investigate to ensure ductility,
- 3. Make sure the trial design is suitable for wind (or other non-seismic) lateral loadings using IBC,
- 4. Calculate midheight deflection due to wind by IBC,
- 5. Calculate the seismic demand, and
- 6. Determine the seismic resistance and compare to the demand determined in Step 5.

#### 9.1.6.3.1 Trial design

A trial design of 12-in.-thick CMU reinforced with two #6 bars at 24 in. on center is selected. The selfweight of the wall, accounting for horizontal bond beams at 4ft on center, is conservatively taken as 103 psf. Adjacent to each door jamb, the vertical reinforcement will be placed into two cells. See Figure 9.1-11.

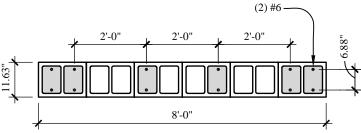


**Figure 9.1-11** Trial design for piers on end walls (1.0 in = 25.4 mm, 1.0 ft = 0.3048 m).

Next, determine the design loads. The centroid for seismic loads, accounting for the door openings, is determined to be 17.8 ft above the base. See Figures 9.1-12 and 9.1-13.

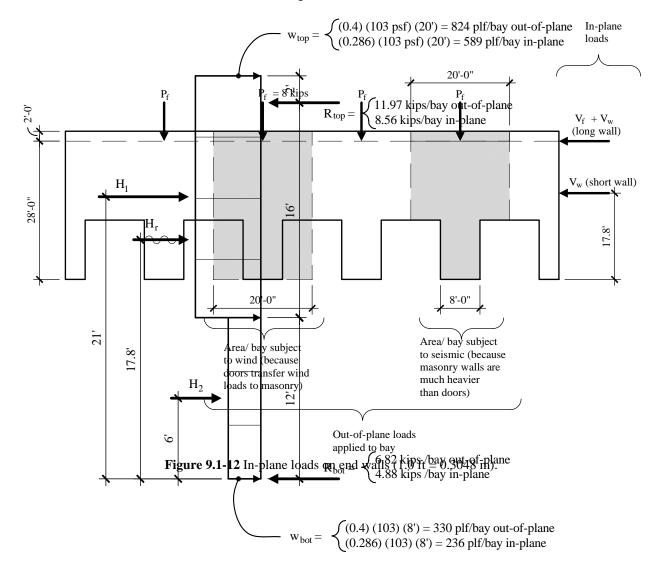


**Figure 9.1-13** Out-of-plane load diagram and resultant of lateral loads (1.0 ft = 0.3048 m, 1.0 lb = 4.45 N, 1.0 kip = 4.45 kN).

#### 9.1.6.3.2 Investigate to ensure ductility

The critical strain condition is corresponds to a strain in the extreme tension reinforcement (which is a pair of #6 bars in the end cell in this example) equal to 1.3 times the strain at yield stress. See Figures 9.1-11 and 9.1-14.

For this case:

t = 11.63 in. d = 11.63 - 2.38 = 9.25 in.  $\varepsilon_m = 0.0025$  (*Provisions* Sec. 11.6.2.1.b)[ACI 530, Sec. 3.2.2]  $\varepsilon_s = 1.3 \varepsilon_y = 1.3 (f_y/E_s) = 1.3 (60 \text{ ksi }/29,000 \text{ ksi}) = 0.0027$  (*Provisions* Sec. 11.6.2.2)[ACI 530, Sec. 3.2.3.5.1]

$$c = \left[\frac{\varepsilon_m}{(\varepsilon_m + \varepsilon_s)}\right] d = 4.45 \text{ in.}$$
  
$$a = 0.8c = 3.56 \text{ in.} (Provisions Sec. 11.6.2.2)$$

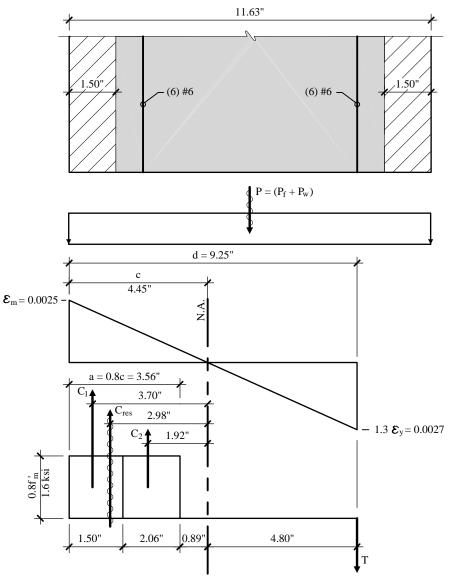


**Figure 9.1-14** Investigation of out-of-plane ductility for end wall (1.0 in = 25.4 mm, 1.0 ksi = 6.89 MPa).

Note that the Whitney compression stress block, a = 3.56 in. deep, is greater than the 1.50-in. face shell thickness. Thus, the compression stress block is broken into two components: one for full compression against solid masonry (the face shell) and another for compression against the webs and grouted cells but accounting for the open cells. These are shown as  $C_1$  and  $C_2$  on Figure 9.1-15. The values are computed using *Provisions* Sec. 11.6.2.1e:[ACI 530, 3.2.2.e];

 $C_1 = 0.80 f_m' (1.50 \text{ in.})b = (0.80)(2 \text{ ksi})(1.50)(96) = 230 \text{ kips}$  (for full length of pier)  $C_2 = 0.80 f_m' (a - 1.50 \text{ in.})(6(8 \text{ in.})) = (0.80)(2 \text{ ksi})(3.56 - 1.50)(48) = 158 \text{ kips}$ 

The 48 in. dimension in the  $C_2$  calculation is the combined width of grouted cell and adjacent mortared webs over the 96-in. length of the pier.

*T* is based on 1.25*F*<sub>v</sub> (*Provisions* Sec. 11.6.2.2)[ACI 530, Sec. 3.2.3.5.1]:

 $T = 1.25F_yA_s = (1.25)(60 \text{ ksi})(6 \times 0.44 \text{ in.}^2) = 198 \text{ kips/pier}$  $P = (P_f + P_w) = 8.0 \text{ k} + (0.103 \text{ ksf})(18 \text{ ft.})(20 \text{ ft.}) = 45.1 \text{ kips/pier}$ 

*P* is computed at the head of the doors:

 $C_1 + C_2 > P + T$ 388 kip > 243 kips

Since the compression capacity is greater than the tension capacity, the ductility criterion is satisfied.

[The ductility (maximum reinforcement) requirements in ACI 530 are similar to those in the 2000 *Provisions*. However, the 2003 *Provisions* also modify some of the ACI 530 requirements, including critical strain in extreme tensile reinforcement (1.5 times) and axial force to consider when performing the ductility check (factored loads).]

#### 9.1.6.3.3 Check for wind loading using IBC

Note that load factors and section properties are different in the IBC and the *Provisions*. Note also that wind per bay is over the full 20 ft wide by 30 ft high bay as discussed above. (The calculations are not presented here.)

#### 9.1.6.3.4 Calculate midheight deflection due to wind by IBC

Although the calculations are not presented here, note that in Figure 9.1-15 the neutral axis position and partial grouting results in a T beam cross section for the cracked moment of inertia. Use of the plastic neutral axis is a simplification for computation of the cracked moment of inertia. For this example, midheight out-of-plane deflection is 1.27 in. < 2.35 in. = 0.007h, which is acceptable.

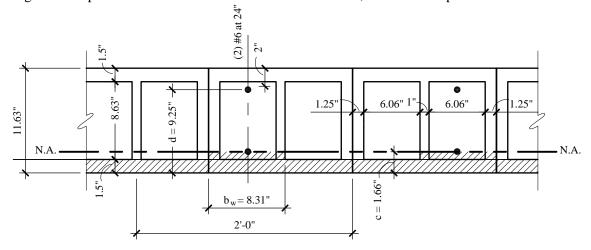


**Figure 9.1-15** Cracked moment of inertia ( $I_{cr}$ ) for end walls (1.0 in = 25.4 mm, 1.0 ft = 0.3048 m). Dimension "c" depends on calculations shown for Figure 9.1-16.

#### 9.1.6.3.5 Calculate Seismic Demand

For this example, the load combination with 0.7D has been used and, for this calculation, forces and moments over a single pier (width = 96 in.) are used. This does not violate the "b > 6t" rule (ACI 530 Sec. 7.3.3)[ACI 530, Sec. 3.2.4.3.3] because the pier is reinforced at 24 in. o.c. The use of the full width of the pier instead of a 24 in. width is simply for calculation convenience.

For this example, a P-delta analysis using RISA-2D was run. This resulted in:

Maximum moment,  $M_u = 66.22$  ft-kips/bay = 66.22/20 ft = 3.31 klf (does not govern) Moment at top of pier,  $M_u = 62.12$  ft-kips/pier = 62.12/8 ft = 7.77 klf (governs) Shear at bottom of pier,  $V_u = 6.72$  kips/pier Reaction at roof,  $V_u = 12.07$  kips/bay Axial force at base,  $R_u = 54.97$  kips/pier

The shears do not agree with the reactions shown in Figure 9.1-13; because the results in Figure 9.1-13 do not include the P-delta consideration.

#### 9.1.6.3.6 Determine moment resistance at the top of the pier

See Figure 9.1-16.

 $A_s = 6-\#6 = 2.64 \text{ in.}^2$  d = 9.25 in. T = 2.64(60) = 158.4 kip C = T + P = 203.5 kip $a = C / (0.8f'_mb) = 203.5 / [0.8(2)96] = 1.32 \text{ in.}$ 

Because a is less than the face shell thickness (1.50 in.), compute as for a rectangular beam. Moments are computed about the centerline of the wall.

$$\begin{split} M_N &= C \; (t/2 \; - \; a/2) + P \; (0) + T \; (d \; - \; t/2) \\ &= 203.5(5.81 \; - \; 1.32/2) + 158.4(9.25 \; - \; 1.32/2) = 1593 \; \text{in.-kip} = 132.7 \; \text{ft.-kip} \\ \varphi M_N &= 0.85(132.7) = 112.8 \; \text{ft.-kip} \end{split}$$

Because moment capacity at the top of the pier,  $\phi M_n = 112.8$  ft-kips, exceeds the maximum moment demand at top of pier,  $M_u = 62.1$  ft-kips, the condition is acceptable but note that this is only tentative acceptance.

The *Provisions* requires a check of the combined loads in accordance with *Provisions* 5.2.5.2, Item a [Sec. 4.4.2.3]. See Sec. 9.1.6.5 for the combined loads check.

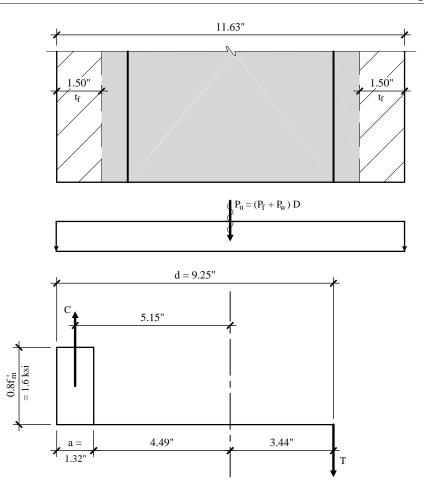


**Figure 9.1-16** Out-of-plane seismic strength of pier on end wall (1.0 in = 25.4 mm, 1.0 ksi = 6.89 MPa).

#### 9.1.6.4 In-Plane Flexure

There are several possible methods to compute the shears and moments in the individual piers of the end wall. For this example, the end wall was modeled using RISA-2D. The horizontal beam was modeled at the top of the opening, rather than at its midheight. The in-plane lateral loads (from Figure 9.1-12) were applied at the 12-ft elevation and combined with joint moments representing transfer of the horizontal forces from their point of action down to the 12-ft elevation. Vertical load due to roof beams and the self-weight of the end wall were included. The input loads are shown on Figure 9.1-17. For this example:

w = (18 ft.)(103 psf) + (20 ft.)(20 psf) = 2.254 klfH = (184 kip)/5 = 36.8 kipM = 0.286((400 + 418)(28 - 12) + 470(17.8 - 12)) = 452 ft-kip

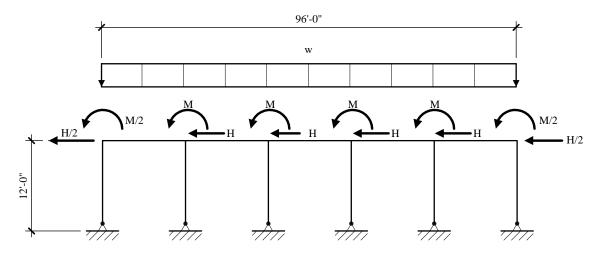
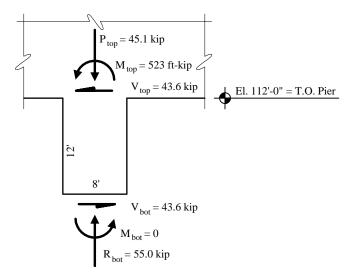


Figure 9.1-17 Input loads for in-plane end wall analysis (1.0 ft = 0.3048 m).

The input forces at the end wall are distributed over all the piers to simulate actual conditions. The RISA-2D frame analysis accounts for the relative stiffnesses of the 4-ft-and 8-ft-wide piers. The final distribution of forces, shears, and moments for an interior pier is shown on Figure 9.1-18.



**Figure 9.1-18** In-plane design condition for 8-ft-wide pier (1.0 ft = 0.3048 m).

As a trial design for in-plane pier design, use two #6 bars at 24 in. on center supplemented by adding two #6 bars in the cells adjacent to the door jambs (see Figure 9.1-19).

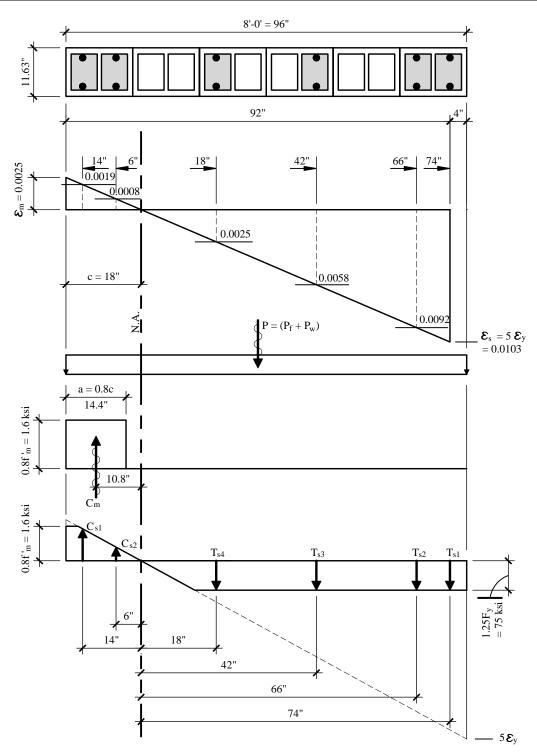


Figure 9.1-19 In-plane ductility check for 8-ft-wide pier (1.0 in = 25.4 mm, 1.0 ksi = 6.89 MPa).

The design values for in-plane design at the top of the pier are:

	<u>Unfactored</u>	0.7D + 1.0E	1.4D + 1.0E
Axia	P = 45.1  kips	$P_{u} = 31.6 \text{ kips}$	$P_{u} = 63.2 \text{ kips}$
Shea	V = 43.6 kips	$V_u = 43.6$ kips	$V_u = 43.6 \text{ kips}$
Mom	M = 523 ft-kips	$M_u = 523$ ft-kips	$M_u = 523$ ft-kips

The ductility check is illustrated in Figure 9.1-19:

 $\varepsilon_m = 0.0025$   $\varepsilon_s = 5\varepsilon_y = (5)(60/29,000) = 0.0103$ d = 92 in.

From the strain diagram, the strains at the rebar locations are:

 $\begin{array}{l} \varepsilon_{66} = 0.0092 \\ \varepsilon_{42} = 0.0058 \\ \varepsilon_{18} = 0.0025 \\ \varepsilon_{6} = 0.0008 \\ \varepsilon_{14} = 0.0019 \end{array}$ 

To check ductility, use unfactored loads:

 $P = P_f + P_w = (0.020 \text{ ksf})(20 \text{ ft})(20 \text{ ft}) + (0.103 \text{ ksf})(18 \text{ ft})(20 \text{ ft})$ P = 8 kips + 37.1 kips = 45.1 kips

 $\begin{array}{l} a=0.8c &= 14.4 \text{ in.} \\ C_m=(0.8f_m')ab=1.6 \text{ ksi})(14.4 \text{ in.})(11.63 \text{ in.})=268.0 \text{ kips} \\ T_{s1}=T_{s2}=T_{s3}=T_{s4}=(1.25F_y)(A_s)=(1.25)(60 \text{ ksi})(2\times0.44 \text{ in.}2)=66 \text{ kips} \\ C_{s1}=F_yA_s(\varepsilon_{14}/\varepsilon_y)=(60 \text{ ksi})(2\times0.44 \text{ in.}^2)(0.0019/0.00207)=48.5 \text{ kips} \\ C_{s2}=F_yA_s(\varepsilon_{6}/\varepsilon_y)=(60 \text{ ksi})(2\times0.44 \text{ in.}^2)(0.0008/0.00207)=20.4 \text{ kips} \end{array}$ 

$$\begin{split} \Sigma C > \Sigma \ T + P \\ C_m + C_{sl} + C_{s2} > T_{sl} + T_{s2} + T_{s3} + T_{s4} + P \\ 268 + 48.5 + 20.4 > 66 + +66 + 66 + 66 + 45.1 \\ 336.9 \ \text{kips} > 309.1 \ \text{kips} \end{split}$$

Since compression capacity exceeds tension capacity, ductile failure is ensured. Note that  $1.25F_y$  is used for tension calculations per *Provisions* Sec. 11.6.2.2 [ACI 530, Sec. 3.2.3.5-1].

[The ductility (maximum reinforcement) requirements in ACI 530 are similar to those in the 2000 *Provisions*. However, the 2003 *Provisions* also modify some of the ACI 530 requirements, including critical strain in extreme tensile reinforcement (4 times yield) and axial force to consider when performing the ductility check (factored loads).]

For the strength check, see Figure 9.1-20.

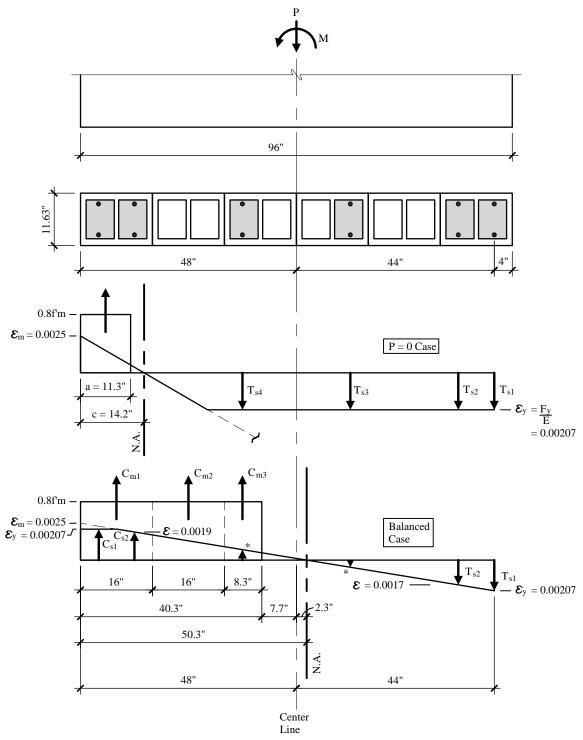


**Figure 9.1-20** In-plane seismic strength of pier (1.0 in = 25.4 mm). Strain diagram superimposed on strength diagram for both cases. Note that low force in reinforcement is neglected in calculations.

To ascertain the strength of the pier, a  $\phi P_n - \phi M_n$  curve will be developed. Only the portion below the "balance point" will be examined as that portion is sufficient for the purposes of this example. Ductile failures occur only at points on the curve that are below the balance point so this is consistent with the

overall approach).

For the P = 0 case, assume all bars in tension reach their yield stress and neglect compression steel (a conservative assumption):

$$T_{s1} = T_{s2} = T_{s3} = T_{s4} = (2)(0.44 \text{ in.} 2)(60 \text{ ksi}) = 52.8 \text{ kips}$$
  

$$C_m = \Sigma T_s = (4)(52.8) = 211.2 \text{ kips}$$
  

$$C_m = 0.8f_m^2 ab = (0.8)(2 \text{ ksi})a(11.63 \text{ in.}) = 18.6a$$

Thus, a = 11.3 in. and  $c = a/\phi = 11.3 / 0.8 = 14.2$  in.

$$\Sigma M_{cl} = 0:$$
  

$$M_n = 42.35 C_m + 44T_{sl} + 36T_{s2} + 12T_{s3} - 12T_{s4} = 13,168 \text{ in.-kips}$$
  

$$\phi M_n = (0.85)(13,168) = 11,193 \text{ in.-kips} = 933 \text{ ft-kips}$$

For the balanced case:

$$d = 92 \text{ in.}$$
  

$$\varepsilon = 0.0025$$
  

$$\varepsilon_y = 60/29,000 = 0.00207$$
  

$$c = \left(\frac{\varepsilon_m}{\varepsilon_m + \varepsilon_y}\right) d = 50.3 \text{ in}$$
  

$$a = 0.8c = 40.3 \text{ in.}$$

Compression values are determined from the Whitney compression block adjusted for fully grouted cells or nongrouted cells:

$$\begin{split} C_{ml} &= (1.6 \text{ ksi})(16 \text{ in.})(11.63 \text{ in.}) = 297.8 \text{ kips} \\ C_{m2} &= (1.6 \text{ ksi})(16 \text{ in.})(2 \times 1.50 \text{ in.}) = 76.8 \text{ kips} \\ C_{m3} &= (1.6 \text{ ksi})(8.3 \text{ in.})(11.63 \text{ in.}) = 154.4 \text{ kips} \\ C_{sl} &= (0.88 \text{ in.}2)(60 \text{ ksi}) = 52.8 \text{ kips} \\ C_{s2} &= (0.88 \text{ in.}2)(60 \text{ ksi})(0.0019 / 0.00207) = 48.5 \text{ kips} \\ T_{s2} &= (0.88 \text{ in.}2)(60 \text{ ksi})(0.0017 / 0/00207) = 43.4 \text{ kips} \\ \Sigma F_{s} &= (0.88 \text{ in.}2)(60 \text{ ksi})(0.0017 / 0/00207) = 43.4 \text{ kips} \\ \Sigma F_{n} &= \Sigma C - \Sigma T = 297.8 + 76.8 + 154.4 + 52.8 + 48.5 - 52.8 - 43.4 = 534 \text{ kips} \\ \phi P_{n} &= (0.85)(534) = 454 \text{ kips} \\ \Sigma M_{cl} &= 0; \\ M_{n} &= 40C_{ml} + 24C_{m2} + 11.85C_{m3} + 44C_{sl} + 36C_{s2} + 44T_{sl} + 36T_{s2} = 23,540 \text{ in.-kips} \\ \phi M_{n} &= (0.85)(23,540) = 20,009 \text{ in. - kips} = 1,667 \text{ ft-kips} \end{split}$$

The two cases are plotted in Figure 9.1-21 to develop the  $\phi P_n - \phi M_n$  curve on the pier. The demand  $(P_u, M_u)$  also is plotted. As can be seen, the pier design is acceptable because the demand is within the  $\phi P_n - \phi M_n$  curve. (See the Birmingham 1 example in Sec. 9.2 for additional discussion of  $\phi P_n - \phi M_n$  curves.) By linear interpolation,  $\phi M_n$  at the minimum axial load is 968 kip.

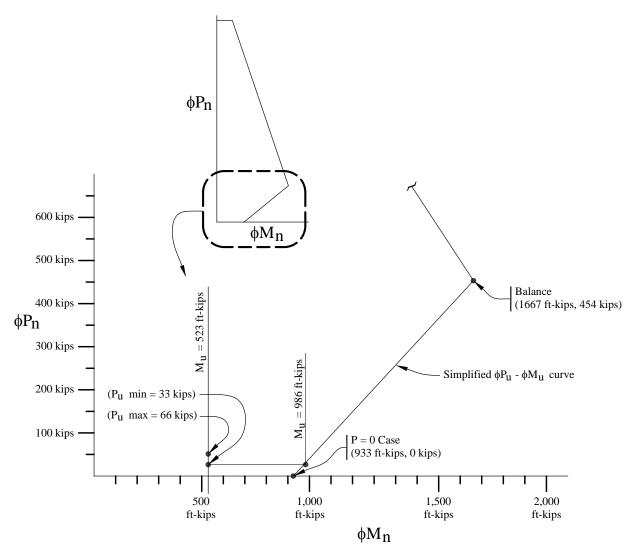


**Figure 9.1-21** In-plane  $\varphi P_{11} - \varphi M_{11}$  diagram for pier (1.0 kip = 4.45 kN, 1.0 ft-kip = 1.36 kN-m).

#### 9.1.6.5 Combined Loads

Combined loads for in-plane and out-of-plane moments in piers at end walls, per *Provisions* Sec. 5.2.5.2.2, Item a, are shown in Table 9.1-4.

	Out-of-Plane		In-Plane		Total	
0.7 <i>D</i>						
Case 1	1.0(62.12/112.8)	+	0.3(523/986)	=	0.71 < 1.00	OK
Case 2	0.3(62.12/112.8)	+	1.0(523/986)	=	0.70 < 1.00	OK

Table 9.1-4 Combined Loads for Flexure in End Pier

Values are in kips; 1.0 kip = 4.45 kN.

## 9.1.6.6 Shear at Transverse Walls (End Walls)

The shear at the base of the pier is 43.6 kips/bay. At the head of the opening where the moment demand is highest, the in-plane shear is slightly less (based on the weight of the pier). There, V = 43.6 kips - 0.286(8 ft)(12 ft)(0.103 ksf) = 40.8 kips. (This refinement in shear is not shown in Figure 9.1-18 although the difference in axial load at the two locations is shown.) The capacity for shear must exceed 2.5 times the demand or the shear associated with 125 percent of the flexural capacity. Using the results in Table 9.1-4, the 125 percent implies a factor on shear by analysis of:

$$1.25 \left(\frac{1}{\text{Demand to capacity ratio}}\right) \left(\frac{1}{\phi}\right) = 1.25 \left(\frac{1}{0.7}\right) \left(\frac{1}{0.85}\right) = 2.10$$

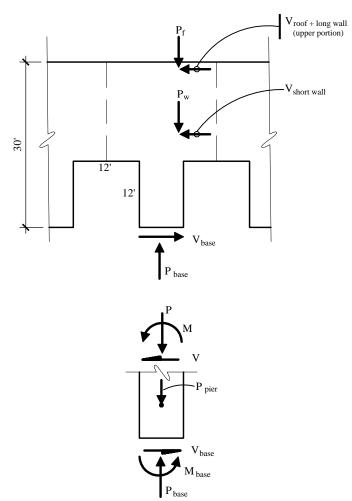


**Figure 9.1-22** In-plane shear on end wall and pier (1.0 ft = 0.3048 m).

Therefore, the required shear capacities at the head and base of the pier are 91.6 kips and 85.7 kips, respectively.

The in-plane shear capacity is computed as follows where the net area,  $A_n$ , of the pier is the area of face shells plus the area of grouted cells and adjacent webs:

$$V_m = \left[4.0 - 1.75 \left(\frac{M}{Vd}\right)\right] A_n \sqrt{f'_m} + 0.25P$$

 $A_n = (96 \text{ in.} \times 1.50 \text{ in.} \times 2) + (6 \text{ cells} \times 8 \text{ in.} \times 8.63 \text{ in.}) = 702 \text{ in.}^2$ 

$$V_{s} = 0.5 \left(\frac{A_{v}}{s}\right) f_{y} d_{v}$$
  
=  $0.5 \left(\frac{0.62 \text{ in.}^{2}}{48 \text{ in.}}\right) (60 \text{ ksi})(96 \text{ in.})$   
= 37.2 kips/bay

At the head of the opening:

 $V_m = [4.0 - 1.75(1.0)](702 \text{ in.}^2)(0.0447 \text{ ksi}) + (0.25)(0.7)(45.1 \text{ kips}) = 78.5 \text{ kips/bay}$ 

 $\phi V_N = (0.8)(78.5 + 37.2) = 92.6$  kips/bay

At the base:

$$V_m = [4.0 - 1.75(0)](702 \text{ in.}^2)(0.0447 \text{ ksi}) + (0.25)(0.7)(55.0 \text{ kips}) = 135.2 \text{ kips/bay}$$

 $\phi V_N = (0.8)(135.2 + 37.2) = 137.9$  kips/bay

As discussed previously, *M/Vd* need not exceed 1.0 in the above equation.

For out-of-plane shear, see Figure 9.1-13. Shear at the top of wall is 12.07 kips/bay and shear at the base of the pier is 6.72 kips/bay. From the values in the figure, the shear at the head of the opening is computed as 6.72 kips - (12 ft)(0.33 kip/ft) = 2.76 kips. The same multiplier of 2.10 for development of 125 percent of flexural capacity will be applied to out-of-plane shear resulting in 25.3 kips at the top of the wall, 5.80 kips at the head of the opening, and 14.11 kips at the base.

Out-of-plane shear capacity is computed using the same equation.  $\Sigma b_w d$  is taken as the net area  $A_n$ . Note that M/Vd is zero at the support because the moment is assumed to be zero; however, a few inches into the span, M/Vd will exceed 1.0 so the limiting value of 1.0 is used here. This is typically the case when considering out-of-plane loads on a wall.

For computing shear capacity at the top of the wall:

 $A_n = b_w d = ((8 \text{ in./2 ft.}) \times 20 \text{ ft})(9.25 \text{ in.}) = 740 \text{ in.}^2$   $V_m = [4.0 - 1.75(1)](740 \text{ in.}^2)(0.0447 \text{ ksi}) + (0.25)(8.0) = 76.9 \text{ kips/bay}$  $\phi V_m = (0.8)(76.9) = 61.5 \text{ kips/bay}$ 

For computing shear capacity in the pier:

 $\begin{array}{ll} A_n &= (8 \text{ in./cell})(6 \text{ cells})(9.25 \text{ in.}) = 444 \text{ in.}^2 \\ V_m &= [4.0 - 1.75(1)](444 \text{ in.}^2)(0.0447 \text{ ksi}) + (0.25)(41.67) = 55.4 \text{ kips/bay} \\ \phi V_m &= (0.8)(55.4) = 44.3 \text{ kips/bay} \end{array}$ 

The combined loads for shear at the end pier (per Provisions 5.2.5.2.2, Item a [Sec. 4.4-23]) are shown in

	Table 9.1-5 C	omome	cu Loaus foi Shear III E	ilu wa	.11
	In-Plane		Out-of-Plane		Total
Case 1 Pier base	1.0(91.6/137.9)	+	0.3(14.11/44.3)	=	0.76 < 1.00 OK
Case 2 Pier base	0.3(91.6/137.9)	+	1.0(14.11/44.3)	=	0.52<1.00 OK
Case 1 Pier head	1.0(85.7/92.6)	+	0.3(5.80/44.3)	=	0.96 > 1.00 OK
Case 2 Pier head	0.3(85.7/92.6)	+	1.0(5.80/44.3)	=	0.41 < 1.00 OK

**Table 9.1-5** Combined Loads for Shear in End Wall

Values are in kips; 1.0 kip = 4.45 kN.

## 9.1.7 Bond Beam

Table 9.1-5.

Reinforcement for the bond beam located at the elevation of the roof diaphragm can be used for the diaphragm chord. The uniform lateral load for the design of the chord is the lateral load from the long wall plus the lateral load from the roof and is equal to 0.87 klf. The maximum tension in rebar is equal the maximum moment divided by the diaphragm depth:

M/d = 4,350 ft-kips/100 ft = 43.5 kips

The seismic load factor is 1.0. The required reinforcement is:

 $A_{read} = T/\phi F_{v} = 43.5/(0.85)(60) = 0.85 \text{ in.}^{2}$ 

This will be satisfied by two #6 bars,  $A_s = (2 \times 0.44 \text{ in.}^2) = 0.88 \text{ in.}^2$ 

In Sec. 10.2, the diaphragm chord is designed as a wood member utilizing the wood ledger member. Using either the wood ledger or the bond beam is considered acceptable.

#### 9.1.8 In-Plane Deflection

Deflection of the end wall (short wall) has two components as illustrated in Figure 9.1-23.

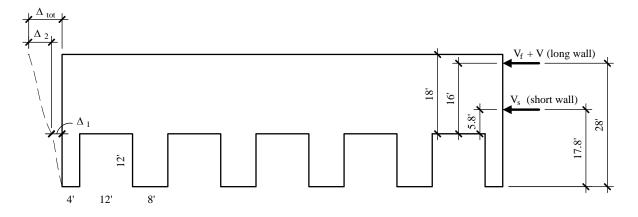


**Figure 9.1-23** In-plane deflection of end wall (1.0 ft = 0.3048 m).

As obtained from the RISA 2D analysis of the piers,  $\Delta_1 = 0.047$  in.:

$$\Delta_2 = \sum \frac{\alpha V L}{AG}$$

where  $\alpha$  is the form factor equal to 6/5 and

 $G = E_m/2(1 + \mu) = 1500 \text{ ksi } / 2(1 + 0.15) = 652 \text{ ksi}$   $A = A_n = \text{Area of face shells + area of grouted cells}$  $= (100 \text{ ft} \times 12 \text{ in./ft} \times 2 \times 1.50 \text{ in.}^2) + (50)(8 \text{ in.})(8.63 \text{ in.}) = 7,050 \text{ in.}^2$ 

Therefore:

$$\Delta_2 = \left(\frac{6}{5}\right) \frac{(67.15)(5.8 \times 12)}{(7,050)(652)} + \left(\frac{6}{5}\right) \frac{(116.9)(16 \times 12)}{(7,050)(652)} = 0.0013 + 0.0059 = 0.007 \text{ in.}$$

and,

$$\Delta_{total} = C_d(0.047 + 0.007) = 3.5(0.054 \text{ in.}) = 0.19 \text{ in.} < 3.36 \text{ in.}$$
  
(3.36 = 0.01 $h_n$  = 0.01 $h_{ss}$ ) (*Provisions* Sec. 11.5.4)

Note that the drift limits for masonry structures are smaller than for other types of structure. It is possible to interpret *Provisions* Table 5.2.8 [Table 4.5-1] to give a limit of  $0.007h_n$  for this structure but that limit also is easily satisfied. The real displacement in this structure is in the roof diaphragm; see Sec. 10.2.

# 9.2 FIVE-STORY MASONRY RESIDENTIAL BUILDINGS IN BIRMINGHAM, ALABAMA; NEW YORK, NEW YORK; AND LOS ANGELES, CALIFORNIA

# 9.2.1 Building Description

In plan, this five-story residential building has bearing walls at 24 ft on center (see Figures 9.2-1 and 9.2-2). All structural walls are of 8-in.-thick concrete masonry units (CMU). The floor is of 8-in.-thick hollow core precast, prestressed concrete planks. To demonstrate the incremental seismic requirements for masonry structures, the building is partially designed for four locations: two sites in Birmingham, Alabama; a site in New York, New York; and a site in Los Angeles, California. The two sites in Birmingham have been selected to illustrate the influence of different soil profiles at the same location. The building is designed for Site Classes C and E in Birmingham. The building falls in Seismic Design Categories B and D in these locations, respectively. For Site Class D soils, the building falls in Seismic Design Categories C and D for New York and Los Angeles, respectively.

[Note that the method for assigning seismic design category for short period buildings has been revised in the 2003 *Provisions*. If the fundamental period,  $T_a$ , is less than  $0.8T_s$ , the period used to determine drift is less than  $T_s$ , and the base shear is computed using 2003 *Provisions* Eq 5.2-2, then seismic design category is assigned using just 2003 *Provisions* Table 1.4-1 (rather than the greater of 2003 *Provisions* Tables 1.4-1 and 1.4-2). This change results in the Birmingham Site Class E building being assigned to Seismic Design Category C instead of D. The changes to this example based on the revised seismic design category are not noted in the remainder of the example. The New York building provides an example of what the Seismic Design Category C requirements would be for the Birmingham Site Class E building.]

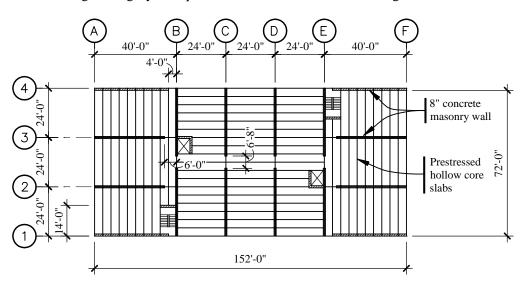


**Figure 9.2-1** Typical floor plan (1.0 in = 25.4 mm, 1.0 ft = 0.3048 m).

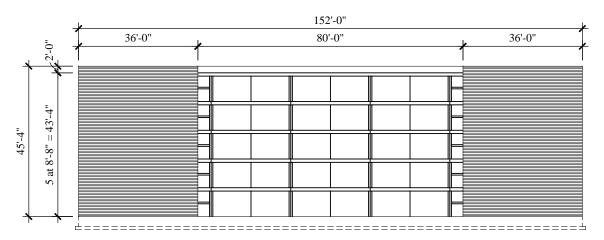


Figure 9.2-2 Building elevation (1.0 in = 25.4 mm, 1.0 ft = 0.3048 m).

For the New York and both Birmingham sites, it is assumed that shear friction reinforcement in the joints of the diaphragm planks is sufficient to resist seismic forces, so no topping is used. For the Los Angeles site, a cast-in-place 2 <sup>1</sup>/<sub>2</sub>-in.-thick reinforced lightweight concrete topping is applied to all floors. The structure is free of irregularities both in plan and elevation. The *Provisions*, by reference to ACI 318, requires reinforced cast-in-place toppings as diaphragms in Seismic Design Category D and higher. Thus, the Birmingham example in Site Class E would require a topping, although that is not included in this example.

*Provisions* Chapter 9 has an appendix (intended for trial use and feedback) for the design of untopped precast units as diaphragms. The design of an untopped diaphragm for Seismic Design Categories A, B, and C is not explicitly addressed in ACI 318. The designs of both untopped and topped diaphragms for these buildings are described in Chapter 7 of this volume using ACI 318 for the topped diaphragm in the Los Angeles building and using the appendix to *Provisions* Chapter 9 for untopped diaphragms in the New York building. It is assumed here that the diaphragm for the Birmingham 2 example would be similar to the New York example, and the extra weight of the Birmingham 2 topping is not included in the illustration here.

No foundations are designed in this example. However, for the purpose of determining the site class coefficient (*Provisions* Sec. 4.1.2.1 [Sec. 3.5]), a stiff soil profile with standard penetration test results of 15 < N < 50 is assumed for Los Angeles and New York sites resulting in a Site Class D for these two locations. For Birmingham, however, one site has soft rock with N > 50 and the other has soft clay with N < 15, which results in Site Classes C and E, respectively. The foundation systems are assumed to be able to carry the superstructure loads including the overturning moments.

The masonry walls in two perpendicular directions act as bearing and shear walls with different levels of axial loads. The geometry of the building in plan and elevation results in nearly equal lateral resistance in both directions. The walls are constructed of CMU and are typically minimally reinforced in all locations. The walls are assumed to act as columns in their planes. Figure 9.2-3 illustrates the wall layout.

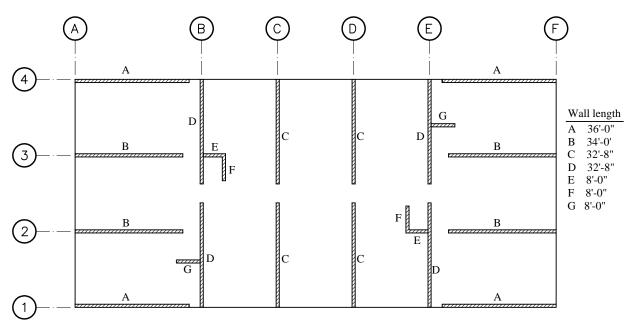


**Figure 9.2-3** Plan of walls (1.0 ft = 0.3048 m).

The floors serve as horizontal diaphragms distributing the seismic forces to the walls and are assumed to be stiff enough to be considered rigid. There is little information about the stiffness of untopped precast diaphragms. The design procedure in the appendix to *Provisions* Chapter 9 results in a diaphragm intended to remain below the elastic limit until the walls reach an upper bound estimate of strength, therefore it appears that the assumption is reasonable.

Material properties are as follows:

The compressive strength of masonry,  $f'_m$ , is taken as 2,000 psi and the steel reinforcement has a yield limit of 60 ksi.

The design snow load (on an exposed flat roof) is taken as 20 psf for New York; design for snow does not control the roof design in the other locations.

This example covers the following aspects of a seismic design:

- 1. Determining the equivalent lateral forces,
- 2. Design of selected masonry shear walls for their in-plane loads, and
- 3. Computation of drifts.

See Chapter 7 of this volume for the design and detailing of untopped and topped precast diaphragms.

# 9.2.2 Design Requirements

#### 9.2.2.1 Provisions Parameters

The basic parameters affecting the design and detailing of the buildings are shown in Table 9.2-1.

[The 2003 *Provisions* have adopted the 2002 USGS probabilistic seismic hazard maps, and the maps have been added to the body of the 2003 *Provisions* as figures in Chapter 3 (instead of the previously used separate map package).]

## 9.2.2.2 Structural Design Considerations

The floors act as horizontal diaphragms and the walls parallel to the motion act as shear walls for all four buildings

The system is categorized as a bearing wall system (*Provisions* Sec. 5.2.2[Sec. 4.3]). For Seismic Design Category D, the bearing wall system has a height limit of 160 ft and must comply with the requirements for special reinforced masonry shear walls (*Provisions* Sec. 11.11.5[Sec. 11.2.1.5]). Note that the structural system is one of uncoupled shear walls. Crossing beams over the interior doorways (their design is not included in this example) will need to continue to support the gravity loads from the deck slabs above during the earthquake, but are not designed to provide coupling between the shear walls.

The building is symmetric and appears to be regular both in plan and elevation. It will be shown, however, that the building is actually torsionally irregular. *Provisions* Table 5.2.5 [Table 4.4-1] permits use of the equivalent lateral force (ELF) procedure in accordance with *Provisions* Sec. 5.4 [Sec. 5.2] for Birmingham 1 and New York City (Seismic Design Categories B and C). By the same table, the Category D buildings must use a dynamic analysis for design. For this particular building arrangement, the modal response spectrum analysis does not identify any particular effect of the torsional irregularity, as will be illustrated.

	140	le 7.2 1 Design I ara		
Design Parameter	Value for Birmingham 1	Value for Birmingham 2	Value for New York	Value for Los Angeles
<i>S<sub>s</sub></i> (Map 1) [Figure 3.3-1]	0.3	0.3	0.4	1.5
<i>S</i> <sub>1</sub> (Map 2) [Figure 3.3-2]	0.12	0.12	0.09	0.6
Site Class	С	E	D	D
$F_a$	1.2	2.34	1.48	1
$F_{v}$	1.68	3.44	2.4	1.5
$S_{MS} = F_a S_s$	0.36	0.7	0.59	1.5
$S_{MI} = F_{\nu}S_{I}$	0.2	0.41	0.22	0.9
$S_{DS} = 2/3 S_{MS}$	0.24	0.47	0.39	1
$S_{DI} = 2/3 S_{MI}$	0.13	0.28	0.14	0.6
Seismic Design Category	В	D	С	D
Masonry Wall Type	Ordinary Reinforced	Special Reinforced	Intermediate Reinforced	Special Reinforced
	Provisions Des	sign Coefficients (Ta	ble 5.2.2 [4.3-1])	
R	2.0	3.5	2.5	3.5

 Table 9.2-1
 Design Parameters

Design Parameter	Value for Birmingham 1	Value for Birmingham 2	Value for New York	Value for Los Angeles
$arOmega_{0}$	2.5	2.5	2.5	2.5
$C_d$	1.75	3.5	2.25	3.5
IBC Desig	gn Coefficients (pre	esented for compariso	n with <i>Provisions</i> co	efficients)
R	2.5	5.0	3.5	5.0
$arOmega_{o}$	2.5	2.5	2.5	2.5
$C_d$	1.75	3.5	2.25	3.5

#### FEMA 451, NEHRP Recommended Provisions: Design Examples

The orthogonal effect (*Provisions* Sec. 5.2.5.2, Item a [Sec. 4.4.2]) applies to structures assigned to Seismic Design Categories C and D (all of the example buildings except for Birmingham 1). However, the arrangement of this building is not particularly susceptible to orthogonal effects. This is because the stresses developed under out-of-plane loading for short-height walls (story clear height is 8 ft) are low and, their contribution to orthogonal effects is minimal.

The walls are all solid and there are no significant discontinuities, as defined by *Provisions* Sec. 5.2.6.2.3 [Sec. 4.3.2.3], in the vertical elements of the seismic-force-resisting system.

Ignoring the short walls at stairs and elevators, there are eight shear walls in each direction, therefore, the system appears to have adequate redundancy (*Provisions* Sec. 5.2.6.2.4 [Sec. 4.3.3]). The reliability factor, however, will be computed. [See Sec. 9.2.3.1 for changes to the reliability factor.]

Tie and continuity requirements (*Provisions* Sec. 5.2.6.1.2 [Sec. 4.6]) must be addressed when detailing connections between floors and walls (see Chapter 7 of this volume).

Nonstructural elements (Provisions Chapter 14 [Chapter 6]) are not considered in this example.

Collector elements are required in the diaphragm for longitudinal response (*Provisions* Sec. 5.2.6.2.5 [Sec. 4.6]). Rebar in the longitudinal direction, spliced into bond beams, will be used for this purpose (see Chapter 7 of this volume).

Diaphragms must be designed for the required forces (Provisions Sec. 5.2.6.2.6 [Sec. 4.6]).

The bearing walls must be designed for the required force perpendicular to their plane (*Provisions* Sec. 5.2.6.2.7 [Sec. 4.6.1.3]).

Each wall is a vertical cantilever; there are no coupling beams. The walls are classified as masonry cantilever shear wall structures in *Provisions* Table 5.2.8 [Table 4.5-1], which limits interstory drift to 0.01 times the story height. *Provisions* Sec.11.5.4.1.1 also limits drift to 0.01 times the wall height for such a structure.

[The deflection limits have been removed from Chapter 11 of the 2003 *Provisions* because they were redundant with the general deflection limits. Based on ACI 530 Sec. 1.13.3.2, the maximum drift for all masonry structures is 0.007 times the story height. Thus, there appears to be a conflict between ACI 530 and 2003 *Provisions* Table 4.5-1.]

Vertical accelerations must be considered for the prestressed slabs in Seismic Design Category D (*Provisions* Sec. 5.2.6.4.3 [Sec. 4.6.3.1]); refer to Chapter 7 of this volume. The evaluation of such components involves the earthquake effect determined using *Provisions* Eq. 5.2.7-1 [4.2-1] and 5.2.7-2 [4.2-1]. The important load is the vertical effect (- $0.2S_{DS}D$ ), which reduces the effect of dead loads. Because the system is prestressed, application of this load might lead to tension where there would otherwise be no reinforcement. The reinforcement within the topping will control this effect. Refer to Sec. 7.1 of this volume for the design of precast, prestressed slabs and topping.

Design, detailing, and structural component effects are presented in the chapters of the *Provisions* that are relevant to the materials used.

# 9.2.3 Load Combinations

The basic load combinations (*Provisions* Sec. 5.2.7 [Sec. 4.2.2]) are the same as those in ASCE 7 (and are similar to those in the IBC). The seismic load effect, *E*, is defined by *Provisions* Eq. 5.2.7-1 [4.2-1] and 5.2.7-2 [4.2-2] as:

$$E = \rho Q_E \pm 0.2 S_{DS} D$$

## 9.2.3.1 Reliability Factor

Note that  $\rho$  is a multiplier on design force effects and applies only to the in-plane direction of the shear walls. For structures in Seismic Design Categories A, B and C,  $\rho = 1.0$  (*Provisions* Sec. 5.2.4.1 [Sec. 4.3.3.1]). For structures in Seismic Design Category D,  $\rho$  is determined per *Provisions* Sec. 5.2.4.2 [Sec. 4.3.3.2].

For the transverse direction, ignoring accidental torsion:

$$r_{max_x} = \left(\frac{V_{wall}}{V_{story}}\right) \left(\frac{10}{l_w}\right) \cong \left(\frac{1}{8}\right) \left(\frac{10}{33}\right) = 0.038$$

and,

$$\rho = 2 - \frac{20}{r_{max_x}\sqrt{A_x}} = 2 - \frac{20}{0.038\sqrt{10,944}} = -3.03$$

Since the computed  $\rho < 1.0$  use  $\rho = 1.0$  for the transverse direction. Accidental torsion does not change  $r_{max_{r}}$  enough to change this conclusion.

Based on similar calculations for the longitudinal direction,  $\rho$  is determined to be 1.0.

[The redundancy requirements have been substantially changed in the 2003 *Provisions*. For structures assigned to Seismic Design Categories B and C,  $\rho = 1.0$  in all cases. For a shear wall building assigned to Seismic Design Category D,  $\rho = 1.0$  as long as it can be shown that failure of a shear wall with height-to-length-ratio greater than 1.0 would not result in more than a 33 percent reduction in story strength or create an extreme torsional irregularity. The intent is that the aspect ratio is based on story height, not total height. Therefore, the redundancy factor would not have to be investigated ( $\rho = 1.0$ ) for the structure(s) assigned to Seismic Design Category D.]

## 9.2.3.2 Combination of Load Effects

The seismic load effect, *E*, determined for each of the buildings is:

Birmingham 1	$E = (1.0)Q_E \pm (0.2)(0.24)D = Q_E \pm 0.05D$
Birmingham 2	$E = (1.0)Q_E \pm (0.2)(0.47)D = Q_E \pm 0.09D$
New York	$E = (1.0)Q_E \pm (0.2)(0.39)D = Q_E \pm 0.08D$
Los Angeles	$E = (1.0)Q_E \pm (0.2)(1.00)D = Q_E \pm 0.20D$

The applicable load combinations from ASCE 7 are:

1.2D + 1.0E + 0.5L + 0.2S

when the effects of gravity and seismic loads are additive and

0.9D + 1.0E + 1.6H

when the effects of gravity and seismic loads are counteractive. (*H* is the effect of lateral pressures of soil and water in soil.)

Load effect *H* does not apply for this design, and the snow load effect, *S*, exceeds the minimum roof live load only at the building in New York. However, even for New York, the snow load effect is only used for combinations of gravity loading. Consideration of snow loads is not required in the effective seismic weight, *W*, of the structure when the design snow load does not exceed 30 psf (*Provisions* Sec. 5.3 [Sec. 5.2.1]).

The basic load combinations are combined with E as determined above, and the load combinations representing the extreme cases are:

Birmingham 1	$1.25D + Q_E + 0.5L$ $0.85D - Q_E$
Birmingham 2	$1.29D + Q_E + 0.5L$ $0.81D - Q_E$
New York	$\begin{array}{l} 1.28D + Q_E + 0.5L + 0.2S \\ 0.82D - Q_E \end{array}$
Los Angeles	$1.40D + Q_E + 0.5L$ $0.70D - Q_E$

These combinations are for the in-plane direction. Load combinations for the out-of-plane direction are similar except that the reliability coefficient (1.0 in all cases for in-plane loading) is not applicable.

It is worth noting that there is an inconsistency in the treatment of snow loads combined with seismic loads. IBC Sec. 1605.3 clearly deletes the snow term from the ASD combinations where the design snow load does not exceed 30 psf. There is no similar provision for the strength load combinations in the IBC for reference standard, ASCE 7.

[The strength design load combinations in the 2003 IBC do have a similar exemption for snow loads, but ASCE 7-02 load combinations do not.]

## 9.2.4 Seismic Design for Birmingham 1

## 9.2.4.1 Birmingham 1 Weights

Use 67 psf for 8-in.-thick, normal weight hollow core plank plus the nonmasonry partitions. This site is assigned to Seismic Design Category B, and the walls will be designed as ordinary reinforced masonry shear walls (*Provisions* Sec. 11.11.3 [Sec. 4.2.1.3]), which do not require prescriptive seismic reinforcement. However, both ACI 530 and IBC 2106.1.1.2 stipulate that ordinary reinforced masonry shear walls have a minimum of vertical #4 bars at 120 in. on center. [By reference to ACI 530, the 2003 *Provisions* (and 2003 IBC) do have prescriptive seismic reinforcement requirements for ordinary reinforced masonry shear walls. Refer to ACI 530 Sec. 1.13.2.2.3.] Given the length of the walls, vertical reinforcement of #4 bars at 8 ft on center works well for detailing reasons and will be used here. For this example, 45 psf will be assumed for the 8-in.-thick lightweight CMU walls. The 45 psf value includes grouted cells and bond beams in the course just below the floor planks.

Story weight,  $w_i$ , is computed as follows:

For the roof:

Roof slab (plus roofing) = (67 psf) (152 ft)(72 ft) = 733 kips Walls = (45 psf)(589 ft)(8.67 ft/2) + (45 psf)(4)(36 ft)(2 ft) =  $\underline{128 \text{ kips}}$ Total = 861 kips

Note that there is a 2-ft-high masonry parapet on four walls and the total length of masonry wall, including the short walls, is 589 ft.

For a typical floor:

Slab (plus partitions) = 733 kips Walls = (45 psf)(589 ft)(8.67 ft) = 230 kipsTotal = 963 kips

Total effective seismic weight, W = 861 + (4)(963) = 4,713 kips

This total excludes the lower half of the first story walls, which do not contribute to seismic loads that are imposed on CMU shear walls.

#### 9.2.4.2 Birmingham 1 Base Shear Calculation

The seismic response coefficient,  $C_s$ , is computed using *Provisions* Sec. 5.4.1.1 [Sec. 5.2.1.1]. Per *Provisions* Eq. 5.4.1.1-1 [Eq. 5.2-2]:

$$C_s = \frac{S_{DS}}{R/I} = \frac{0.24}{2/1} = 0.12$$

The value of  $C_s$  need not be greater than *Provisions* Eq. 5.4.1.1-2 [Eq. 5.2-3]:

$$C_s = \frac{S_{DI}}{T(R/I)} = \frac{0.13}{0.338(2/1)} = 0.192$$

T is the fundamental period of the building approximated per Provisions Eq. 5.4.2.1-1[Eq. 5.2-6] as:

$$T_a = C_r h_n^x = (0.02)(43.33^{0.75}) = 0.338$$
 sec

where  $C_r = 0.02$  and x = 0.75 are from *Provisions* Table 5.4.2.1 [Table 5.2-2].

The value for  $C_s$  is taken as 0.12 (the lesser of the two computed values). This value is still larger than the minimum specified in *Provisions* Eq. 5.4.1.1-3:

$$C_{\rm s} = 0.044IS_{\rm DS} = (0.044)(1.0)(0.24) = 0\ 0.0106$$

[This minimum Cs value has been removed in the 2003 *Provisions*. In its place is a minimum Cs value for long-period structures, which is not applicable to this example.]

The total seismic base shear is then calculated using Provisions Eq. 5.4.1 [Eq. 5.2-1]as:

$$V = C_s W = (0.12)(4,713) = 566$$
 kips

#### 9.2.4.3 Birmingham 1 Vertical Distribution of Seismic Forces

*Provisions* Sec. 5.4.4 [Sec. 5.2.3] stipulates the procedure for determining the portion of the total seismic load assigned to each floor level. The story force,  $F_x$ , is calculated using *Provisions* Eq. 5.4.3-1 [Eq. 5.2-10] and 5.4.3-2 [Eq. 5.2-11], respectively, as:

$$F_x = C_{vx}V$$

and

$$C_{vx} = \frac{w_x h_x^k}{\sum\limits_{i=1}^n w_i h_i^k}$$

For  $T = 0.338 \sec < 0.5 \sec, k = 1.0$ .

The seismic design shear in any story is determined from Provisions Eq. 5.4.4[Eq. 5.2-12]:

$$V_x = \sum_{i=x}^n F_i$$

The story overturning moment is computed from Provisions Eq. 5.4.5[Eq. 5.2-14]:

$$M_x = \sum_{i=x}^n F_i (h_i - h_x)$$

The application of these equations for this building is shown in Table 9.2-2.

Level (x)	$w_x$ (kips)	$h_x$ (ft)	$\frac{w_x h_x^k}{(\text{ft-kips})}$	$C_{vx}$	<i>F<sub>x</sub></i> (kips)	$V_x$ (kips)	$M_x$ (ft-kips)
5	861	43.34	37,310	0.3089	175	1.8e+14	1,515
4	963	34.67	33,384	0.2764	156		4,385
3	963	26.00	25,038	0.2073	117		8,272
2	963	17.33	16,692	0.1382	78		12,836
<u>1</u>	963	8.67	8,346	<u>0.0691</u>	<u>39</u>		17,739
Σ	4,715		120,770	1.0000	566		

1.0 kips = 4.45 kN, 1.0 ft = 0.3048 m.

A note regarding locations of *V* and *M*: the vertical weight at the roof (5<sup>th</sup> level), which includes the upper half of the wall above the 5<sup>th</sup> floor (4<sup>th</sup> level), produces the shear *V* applied at the 5<sup>th</sup> level. That shear in turn produces the moment applied at the top of the 4<sup>th</sup> level. Resisting this moment is the rebar in the wall combined with the wall weight above the 4<sup>th</sup> level. Note that the story overturning moment is applied to the level below the level thatreceives the story shear. This is illustrated in Figure 9.2-4.

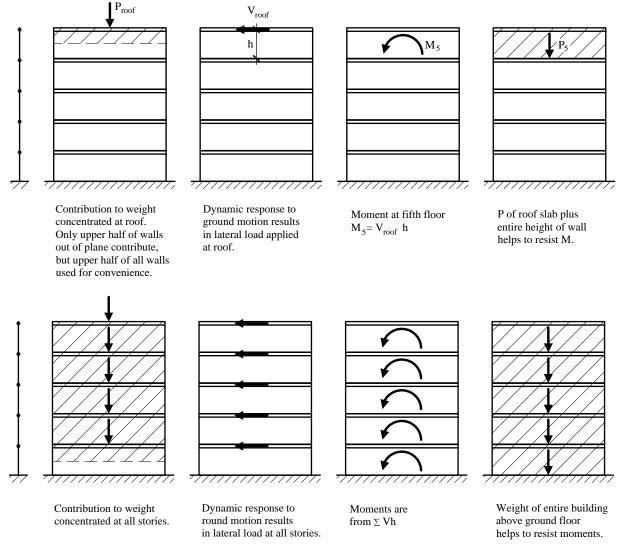


Figure 9.2-4 Location of moments due to story shears.

## 9.2.4.4 Birmingham 1 Horizontal Distribution of Forces

The wall lengths are shown in Figure 9.2-3. The initial grouting pattern is basically the same for walls A, B, and C. Because of a low relative stiffness, the effects Walls D, E, and F are ignored in this analysis. Walls A, B, and C are so nearly the same length that their stiffnesses will be assumed to be the same for this example.

Torsion is considered according to *Provisions* Sec. 5.4.4[Sec. 5.2.4]. For a symmetric plan, as in this example, the only torsion to be considered is the accidental torsion,  $M_{ta}$ , caused by an assumed eccentricity of the mass each way from its actual location by a distance equal to 5 percent of the dimension of the structure perpendicular to the direction of the applied loads.

Dynamic amplification of the torsion need not be considered for Seismic Design Category B per *Provisions* Sec. 5.4.4.3 [Sec. 5.2.4.3].

For this example, the building will be analyzed in the transverse direction only. The evaluation of Wall D is selected for this example. The rigid diaphragm distributes the lateral forces into walls in both directions. Two components of force must be considered: direct shear and shear induced by torsion.

The direct shear force carried by Wall D is one-eighth of the total story shear (eight equal walls). The torsional moment per *Provisions* Sec. 5.4.4.2 [Sec. 5.2.4.2] is:

$$M_{ta} = 0.05 b V_x = (0.05)(152 \text{ ft}) V_x = 7.6 V_x$$

The torsional force per wall,  $V_{t}$  is:

$$V_t = \frac{M_t K d}{\sum K d^2}$$

where *K* is the stiffness (rigidity) of each wall.

Because all the walls in this example are assumed to be equally stiff:

$$V_t = M_t \left[ \frac{d}{\sum d^2} \right]$$

where d is the distance from each wall to the center of twisting.

$$\sum d^2 = 4(36)^2 + 4(12)^2 + 4(36)^2 + 4(12)^2 = 11,520$$

The maximum torsional shear force in Wall D, therefore is:

 $V_t = 7.6 V(36/11,520) = 0.0238V$ 

Total shear in Wall D is:

$$V_{tot} = 0.125V + 0.0238V = 0.149V$$

The total story shear and overturning moment may now be distributed to Wall D and the wall proportions checked. The wall capacity will be checked before considering deflections.

## 9.2.4.5 Birmingham 1 Transverse Wall (Wall D)

The strength or limit state design concept is used in the *Provisions*. This method was introduced in the 2002 edition of ACI 530, the basic reference standard for masonry design. Because strength design was not in prior editions of ACI 530, strength design of masonry as defined in the *Provisions* is illustrated here.

[The 2003 *Provisions* adopts by reference the ACI 530-02 provisions for strength design in masonry, and the previous strength design section has been removed. This adoption does not result in significant technical changes, and the references to the corresponding sections in ACI 530 are noted in the following sections.]

## 9.2.4.5.1 Birmingham 1 Shear Strength

*Provisions* Sec. 11.7.2 [ACI 530, Sec. 3.1.3] states that the ultimate shear loads must be compared to the design shear strength per *Provisions* Eq. 11.7.2.1:

$$V_u \leq \phi V_n$$

The strength reduction factor,  $\phi$ , is 0.8 (*Provisions* Table 11.5.3, ACI 530 [See 3.1.4.3]). The design shear strength,  $\phi V_n$ , must exceed the shear corresponding to the development of 1.25 times the nominal flexural strength of the member but need not exceed 2.5 times  $V_u$  (*Provisions* Sec. 11.7.2.2 [ACI 530, Sec. 3.1.3]). The nominal shear strength,  $V_n$ , is (*Provisions* Eq. 11.7.3.1-1 [ACI 530, Eq. 3-18]):

$$V_n = V_m + V_s$$

The shear strength provided by masonry is (Provisions Eq. 11.7.3.2 [ACI 530, Eq. 3-21]):

$$V_m = \left[4.0 - 1.75 \left(\frac{M}{Vd}\right)\right] A_n \sqrt{f'_m} + 0.25 P$$

For grouted cells at 8 ft on center:

$$A_n = (2 \times 1.25 \text{ in.} \times 32.67 \text{ ft x } 12 \text{ in.}) + (8 \times 5.13 \text{ in.}^2 \times 5 \text{ cells}) = 1,185 \text{ in.}^2$$

The shear strength provided by reinforcement is given by *Provisions* Eq. 11.7.3.3 [ACI 530, Sec. 3.2.4.1.2.2] as:

$$V_s = 0.5 \left(\frac{A_v}{s}\right) F_y d_v$$

The wall will have a bond beam with two #4 bars at each story to bear the precast floor planks and wire joint reinforcement at alternating courses. Common joint reinforcement with 9 gauge wires at each face shell will be used; each wire has a cross-sectional area of 0.017 in.<sup>2</sup> With six courses of joint reinforcement and two #4 bars, the total area per story is 0.60 in.<sup>2</sup> or 0.07 in.<sup>2</sup>/ft.

$$V_s = 0.5(0.07 \text{ in.} 2/\text{ft.})(60 \text{ ksi})(32.67 \text{ ft.}) = 68.3 \text{ kips}$$

The maximum nominal shear strength of the member (Wall D in this case) for  $M/Vd_v > 1.00$  (the *Provisions* has a typographical error for the inequality sign) is given by *Provisions* Eq. 11.7.3.1-3 [ACI 530, Eq. 3-22]:

$$V_n(\max) = 4\sqrt{f'_m}A_n$$

The coefficient 4 becomes 6 for  $M/Vd_{\nu} < 0.25$ . Interpolation between yields the following:

$$V_N$$
 (max) = (6.67 - 2.67  $\left(\frac{M}{Vd_V}\right) \sqrt{f_m} A_n$ 

The shear strength of Wall D, based on the equations listed above, is summarized in Table 9.2-3. Note that  $V_x$  and  $M_x$  in this table are values from Table 9.2-2 multiplied by 0.149 (which represents the portion of direct and torsional shear assigned to Wall D). *P* is the dead load of the roof or floor times the tributary area for Wall D. (Note that there is a small load from the floor plank parallel to the wall.)

Story	$V_x$	$M_{x}$	$M_x/V_x d$	2.5 $V_x$	Р	$\varphi V_m$	$\varphi V_s$	$\varphi V_n$	$\varphi V_n max$
	(kips)	(ft-kips)		(kips)	(kips)	(kips)	(kips)	(kips)	(kips)
5	26	225	0.265	65.0	41	158.1	54.6	212.7	252.7
4	49.3	652	0.405	123.3	89	157.3	54.6	211.9	236.9
3	66.7	1230	0.564	166.8	137	155.1	54.6	209.7	218.8
2	78.4	1910	0.746	196.0	184	151.0	54.6	205.6	198.3
1	84.2	2640	0.960	210.5	232	144.8	54.6	199.4	174.1

 Table 9.2-3
 Shear Strength Calculations for Birmingham 1 Wall D

1.0 kip = 4.45 kN, 1.0 ft-kip = 1.36 kN-m.

 $V_U$  exceeds both  $\varphi V_n$  and  $\varphi V_n max$  at the first story. It would be feasible to add grouted cells in the first story to remedy the deficiency. However, it will be shown following the flexural design that the shear to develop 1.25 times the flexural capacity is 1.94(84.2 kips) = 163 kips, which is OK.

#### 9.2.4.5.2 Birmingham 1 Axial and Flexural Strength

All the walls in this example are bearing shear walls since they support vertical loads as well as lateral forces. In-plane calculations include:

- 1. Strength check and
- 2. Ductility check

## 9.2.4.5.2.1 Strength check

The wall demands, using the load combinations determined previously, are presented in Table 9.2-4 for Wall D. In the table, Load Combination 1 is  $1.25D + Q_E + 0.5L$  and Load Combination 2 is  $0.85D + Q_E$ .

		Table 9	.2-4 Demands for	Birmingham 1	Wall D	
			Load Comb	vination 1	Load Con	nbination 2
Level	$P_D$ (kips)	$P_L$ (kips)	$P_u$ (kips)	M <sub>u</sub> (ft-kips)	$P_u$ (kips)	<i>M<sub>u</sub></i> (ft-kips)
54321	4.2e+12	8172534	5.111518e+13	2.2565e+17	3.576116e+12	2.256521e+17

1.0 kip = 4.45 kN, 1.0 ft-kip = 1.36 kN-m.

Strength at the bottom story (where P, V, and M are the greatest) will be examined. (For a real design, all levels should be examined). The strength design will consider Load Combination 2 from Table 9.2-4 to be the governing case because it has the same lateral load as Load Combination 1 but with lower values of axial force.

For the base of the shear walls:

$$P_{u_{min}} = 197$$
 kips plus factored weight of lower ½ of 1<sup>st</sup> story wall = 197 + (0.85)(6.4) = 202 kips  
 $P_{u_{max}} = 307 + (1.25)(6.4) = 315$  kips  
 $M_{u} = 2,640$  ft-kips

Try one #4 bars in each end cell and a #4 bar at 8 ft on center for the interior cells. A  $\phi P_n - \phi M_n$  curve, representing the wall strength envelope, will be developed and used to evaluate  $P_u$  and  $M_u$  determined above. Three cases will be analyzed and their results will be used in plotting the  $\phi P_n - \phi M_n$  curve.

In accordance with *Provisions* Sec. 11.6.2.1 [ACI 530, Sec. 3.2.2], the strength of the section is reached as the compressive strains in masonry reach their maximum usable value of 0.0025 for CMU. The force equilibrium in the section is attained by assuming an equivalent rectangular stress block of  $0.8f'_m$  over an effective depth of 0.8c, where c is the distance of the neutral axis from the fibers of maximum compressive strain. Stress in all steel bars is taken into account. The strains in the bars are proportional to their distance from the neutral axis. For strains above yield, the stress is independent of strain and is taken as equal to the specified yield strength  $F_y$ . See to Figure 9.2-5 for strains and stresses for all three cases selected.

Case 1 (P = 0)

Assume all tension bars yield (which can be verified later):

 $T_{s1} = (0.20 \text{ in.}^2)(60 \text{ ksi}) = 12.0 \text{ kips}$  $T_{s2} = (0.20 \text{ in.}^2)(60 \text{ ksi}) = 12.0 \text{ kips each}$ 

Because the neutral axis is close to the compression end of the wall, compression steel,  $C_{sl}$ , will be neglected (it would make little difference anyway) for Case 1:

$$\Sigma F_y = 0:$$
  

$$C_m = \Sigma T$$
  

$$C_m = (4)(12.0) = 48.0 \text{ kips}$$

The compression block will be entirely within the first grouted cell:

 $C_m = 0.8 f'_m ab$  48.0 = (0.8)(2.0 ksi)a(7.625 in) a = 3.9 in. = 0.33 ftc = a/0.8 = 0.33/0.8 = 0.41 ft

Thus, the neutral axis is determined to be 0.41 ft from the compression end on the wall, which is within the first grouted cell:

 $\Sigma M_{cl} = 0$ : (The math will be a little easier if moments are taken about the wall centerline.)  $M_n = (16.33 - 0.33/2 \text{ ft})C_m + (16.00 \text{ ft}) T_{sl} + (0.00 \text{ ft})\Sigma T_{s2} + (0.00 \text{ ft})P_n$   $M_n = (16.17)(48.0) + (16.00)(12) + 0 + 0 = 968 \text{ ft-kips}$  $\phi M_n = (0.85)(968) = 823 \text{ ft-kips}$ 

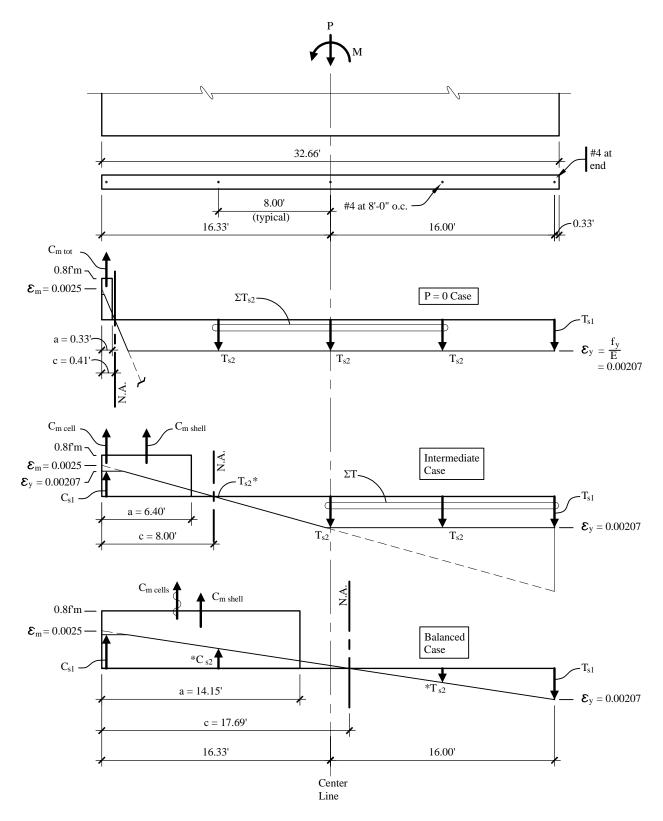


**Figure 9.2-5** Strength of Birmingham 1 Wall D (1.0 ft = 0.3048 m). Strain diagram superimposed on strength diagram for the three cases. The low force in the reinforcement is neglected in the calculations.

To summarize, Case 1:

 $\phi P_n = 0$  kips  $\phi M_n = 823$  ft-kips

<u>Case 2 (Intermediate case between P = 0 and  $P_{bal}$ )</u>

Let c = 8.00 ft.(this is an arbitrary selection). Thus, the neutral axis is defined at 8 ft from the compression end of the wall:

a = 0.8c = (0.8)(8.00) = 6.40 ft  $C_{m \ shells} = 0.8f'_m (2 \ shells)(1.25 \ in. \ / \ shell)(6.40 \ ft. \ (12 \ in.\/ft) = 307.2 \ kips$   $C_{m \ cells} = 0.8f'_m (41 \ in.^2) = 65.6 \ kips$   $C_{m \ tot} = C_{m \ shells} + C_{m \ cells} = 307.2 + 65.6 = 373 \ kips$   $C_{sl} = (0.20 \ in.^2)(60 \ ksi) = 12 \ kips \ (Compression \ steel \ is \ included \ in \ this \ case)$ 

 $T_{s1} = (0.20 \text{ in.}^2)(60 \text{ ksi}) = 12 \text{ kips}$  $T_{s2} = (0.20 \text{ in.}^2)(60 \text{ ksi}) = 12 \text{ kips each}$ 

Some authorities would not consider the compression resistance of reinforcing steel that is not enclosed within ties. The *Provisions* clearly allows inclusion of compression in the reinforcement.

$$\begin{split} \Sigma F_y &= 0: \\ C_{m \ tot} + C_{sl} &= P_n + T_{sl} + \Sigma T_{s2} \\ 373 + 12 &= P_n + (3)(12.0) \\ P_n &= 349 \text{ kips} \\ \phi P_n &= (0.85)(349) = 297 \text{ kips} \end{split}$$
 
$$\begin{split} \Sigma M_{cl} &= 0: \\ M_n &= (13.13 \ \text{ft}) C_{m \ shell} + (16.00 \ \text{ft}) (C_{m \ cell} + C_{sl}) + (16.00 \ \text{ft}) T_{sl} + (8.00 \ \text{ft}) T_{s2} \\ M_n &= (13.13)(307.2) + (16.00)(65.6 + 12) + (16.00)(12.0) + (8.00 \ \text{ft})(12.0) = 5,563 \ \text{ft-kips} \\ \phi M_n &= (0.85)(5,563) = 4,729 \ \text{ft-kips} \end{split}$$

To summarize Case 2:

 $\phi P_n = 297$  kips  $\phi M_n = 4,729$  ft-kips

Case 3 (Balanced case)

In this case,  $T_{sl}$  just reaches its yield stress:

$$c = \left[\frac{0.0025}{(0.0025 + 0.00207)}\right] (32.33 \text{ ft}) = 17.69 \text{ ft}$$
  

$$a = 0.8c = (0.8)(17.69) = 14.15 \text{ ft}$$
  

$$C_{m \ shells} = 0.8f'_m (2 \ shells)(1.25 \ in. \ / \ shell)(14.15 \ ft.) \ (12 \ in.\ /ft) = 679.2 \ kips$$
  

$$C_{m \ cells} = 0.8f'_m (2 \ cells)(41 \ in.^2/cell) = 131.2 \ kips$$
  

$$C_{m \ tot} = C_{m \ shells +} \ C_{m \ cells} = 810.4 \ kips$$

 $C_{sI} = (0.20 \text{ in.}^2)(60 \text{ ksi}) = 12.0 \text{ kips}$ 

 $T_{sl} = (0.20 \text{ in.}^2)(60 \text{ ksi}) = 12.0 \text{ kips}$ 

 $C_{s2}$  and  $T_{s2}$  are neglected because they are small, constituting less than 2 percent of the total  $P_n$ .

$$\Sigma F_y = 0:$$
  

$$P_n = \Sigma C - \Sigma T$$
  

$$P_n = C_{m \ tot} + C_{s1} - T_{s1} = 810.4 + 12.0 - 12.0 = 810.4 \text{ kips}$$
  

$$\phi P_n = (0.85)(810.4) = 689 \text{ kips}$$

 $\Sigma M_{cl} = 0:$   $M_n = 9.26 \ C_{m \ shells} + ((16 + 8)/2) \ C_{m \ cells} + 16 \ C_{sl} + 8 \ T_{s2} + 16 \ T_{sl}$   $M_n = (9.26)(679.2) + (12.0)(131.2) + (16.00)(12.0) + (\text{ignore small} \ T_{s2}) + (16.0)(12.0) = 8,248 \text{ kips}$  $\phi M_n = (0.85)(8,248) = 7,011 \text{ ft-kips}$ 

To summarize Case 3:

 $\phi P_n = 689 \text{ kips}$   $\phi M_n = 7,011 \text{ ft-kips}$ 

Using the results from the three cases above, the  $\phi P_n - \phi M_n$  curve shown in Figure 9.2-6 is plotted. Although the portion of the  $\phi P_n - \phi M_n$  curve above the balanced failure point could be determined, it is not necessary here. Thus, only the portion of the curve below the balance point will be examined. This is the region of high moment capacity.

Similar to reinforced concrete beam-columns, in-plane compression failure of the cantilevered shear wall will occur if  $P_u > P_{bal}$ , and tension failure will occur if  $P_u < P_{bal}$ . A ductile failure mode is essential to the design, so the portion of the curve above the "balance point" is not useable.

As can be seen, the points for  $P_{u \min}$ ,  $M_u$  and  $P_{u \max}$ , are within the  $\phi P_n - \phi M_n$  envelope; thus, the strength design is acceptable with the minimum reinforcement. Figure 9.2-6 shows two schemes for determining the design flexural resistance for a given axial load. One interpolates along the straight line between pure bending and the balanced load. The second makes use of intermediate points for interpolation. This particular example illustrates that there can be a significant difference in the interpolated moment capacity between the two schemes for axial loads midway between the balanced load and pure bending.

For the purpose of shear design, the value of  $\varphi M_N$  at the design axial load is necessary. Interpolating between the intermediate point and the P = 0 point for P = 202 kips yields  $\varphi M_N = 3,480$  ft-kip. Thus, the factor on shear to represent development of 125 percent of flexural capacity is:

$$1.25 \frac{\phi M_N / \phi}{M_U} = 1.25 \frac{3480 / 0.85}{2640} = 1.94$$

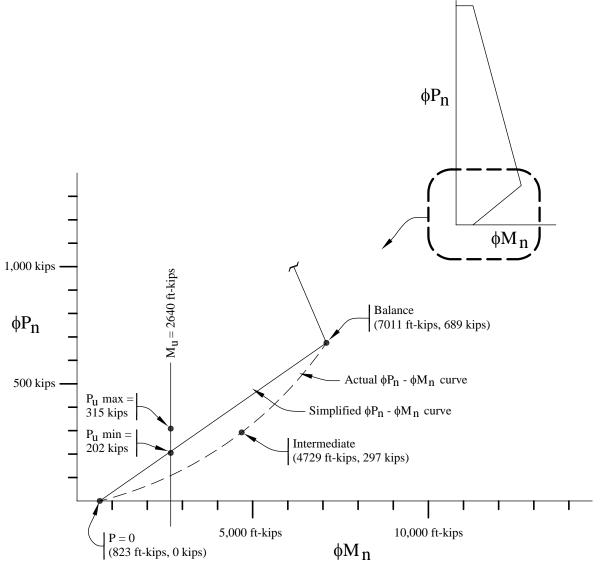


**Figure 9.2-6**  $\varphi P_{11} - \varphi M_{11}$  diagram for Birmingham 1 Wall D (1.0 kip = 4.45 kN, 1.0 ft-kip = 1.36 kN-m).

## 9.2.4.5.2.2 Ductility check

*Provisions* Sec.11.6.2.2 [ACI 530, Sec. 3.2.3.5] requires that the critical strain condition correspond to a strain in the extreme tension reinforcement equal to 5 times the strain associated with  $F_y$ . Note that this calculation uses unfactored gravity axial loads (*Provisions* Sec.11.6.2.2 [ACI 530, Sec. 3.2.3.5]). Refer to Figure 9.2-5 and the following calculations which illustrate this using loads at the bottom story (highest axial loads). Calculations for other stories are not presented in this example.

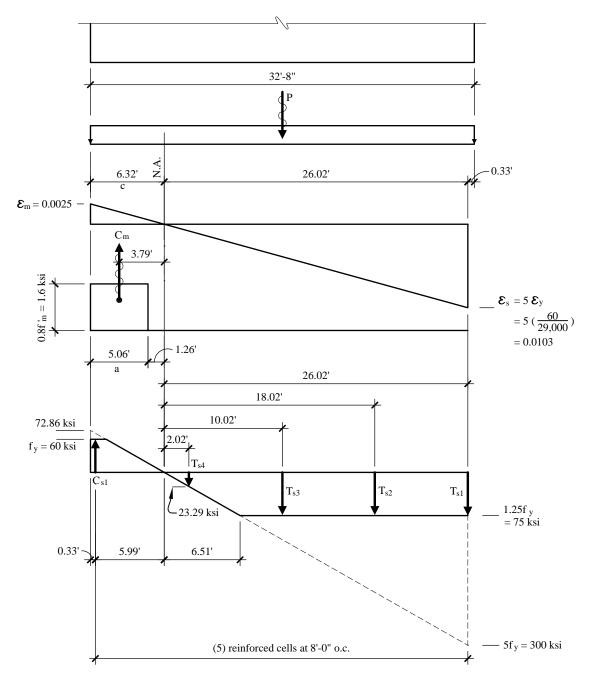


Figure 9.2-7 Ductility check for Birmingham 1 Wall D (1.0 ft = 0.3048 m, 1.0 ksi = 6.89 MPa).

For Level 1 (bottom story), the unfactored axial loads are:

P = 232 kips + weight of half of first story wall = 232 + 6.4 = 238.4 kips

Refer to Figure 9.2-7:

 $C_m = 0.8 f'_m (ab + A_{cell}) = (1.6 \text{ ksi})[(5.06 \text{ ft. x } 12 \text{ in./ft.})(2.5 \text{ in.}) + 41 \text{ in.}^2] = 308.5 \text{ kips}$  (same as above)  $C_{sl} = F_y A_s = (60 \text{ ksi})(0.20 \text{ in.}^2) = 12.0 \text{ kips}$  $T_{sl} = T_{s2} = T_{s3} = (1.25 \times 60 \text{ ksi})(0.20 \text{ in.}^2) = 15 \text{ kips}$   $T_{s4} = (23.29 \text{ ksi})(0.20 \text{ in.}^2) = 4.6 \text{ kips}$ 

 $\sum_{m} C > \sum_{m} P + T$   $C_{m} + C_{sl} > P + T_{sl} + T_{s2} + T_{s3} + T_{s4}$  308.5 + 12.0 > 238.4 + 15 + 15 + 15 + 4.6 320.5 kips > 288 kips

There is more compression capacity than required so ductile failure condition governs.

[The ductility (maximum reinforcement) requirements in ACI 530 are similar to those in the 2000 *Provisions*. However, the 2003 *Provisions* also modify some of the ACI 530 requirements, including critical strain in extreme tensile reinforcement (4 times yield) and axial force to consider when performing the ductility check (factored loads).]

### 9.2.4.6 Birmingham 1 Deflections

The calculations for deflection involve many variables and assumptions, and it must be recognized that any calculation of deflection is approximate at best.

Deflections are to be calculated and compared with the prescribed limits set forth by *Provisions* Table 5.2.8. Deformation requirements for masonry structures are given in *Provisions* Sec. 11.5.4 [Table 4.5-1].

The following procedure will be used for calculating deflections:

- 1. For each story, compare  $M_x$  (from Table 9.2-3) to  $M_{cr} = S(f_r + P_{u \min}/A)$  to determine if wall will crack.
- 2. If  $M_{cr} < M_x$ , then use cracked moment of inertia and *Provisions* Eq. 11.5.4.3.
- 3. If  $M_{cr} > M_x$ , then use  $I_n = I_g$  for moment of inertia of wall.
- 4. Compute deflection for each level.

Other approximations can be used such as the cubic interpolation formula given in *Provisions* 11.5.4.3, but that equation was derived for reinforced concrete members acting as single span beams, not cantilevers. In the authors' opinion, all these approximations pale in comparison to the approximation of nonlinear deformation using  $C_d$ .

For the Birmingham 1 building:

 $\begin{array}{l} b_e = \text{effective masonry wall width} \\ b_e = [(2 \times 1.25 \text{ in.})(32.67 \text{ ft} \times 12) + (5 \text{ cells})(41 \text{ in.}^2/\text{cell})]/(32.67 \text{ ft} \times 12) = 3.02 \text{ in.} \\ S = b_e \, l^2/6 \ = (3.02)(32.67 \times 12)^2/6 = 77,434 \text{ in.}^3 \\ f_r = 0.250 \text{ ksi} \\ A = b_e \, l = (3.02 \text{ in.})(32.67 \text{ ft} \times 12) = 1,185 \text{ in.}^2 \end{array}$ 

 $P_u$  is calculated using 1.00D (see Table 9.2-4). 1.00D is considered to be a reasonable value for axial load for this admittedly approximate analysis. If greater conservatism is desired,  $P_u$  could be calculated using 0.85D.

OK

The results are shown in Table 9.2-5.

Level	$P_{u_{min}}$ (kips)	<i>M<sub>cr</sub></i> (ft-kips)	M <sub>u</sub> (ft-kips)	Status
5	41	1836	225	uncracked
4	89	2098	652	uncracked
3	137	2359	1230	uncracked
2	185	2621	1910	uncracked
1	232	2877	2640	uncracked

 Table 9.2-5
 Birmingham 1 Cracked Wall Determination

1.0 kip = 4.45 kN, 1.0 ft-kip = 1.36 kN-m.

For uncracked walls:

 $I_n = I_g = bl^3/12 = (3.02 \text{ in.})(32.67 \times 12)^3/12 = 1.52 \text{ x } 10^7 \text{ in.}^4$ 

The calculation of  $\delta$  will consider flexural and shear deflections. For the final determination of deflection, a RISA-2D analysis was made. The result is summarized Table 9.2-6 below. Figure 9.2-8 illustrates the deflected shape of the wall.

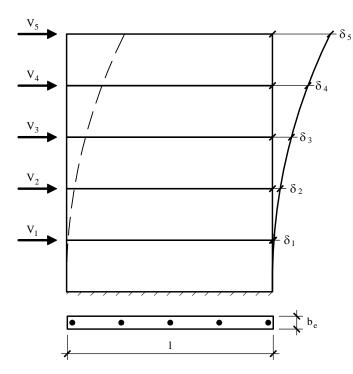


Figure 9.2-8 Shear wall deflections.

Level	F (kips)	$I_{eff}$ (in. <sup>4</sup> )	$\delta_{_{flexural}}$ (in.)	$\delta_{\scriptscriptstyle shear}$ (in.)	$\delta_{\scriptscriptstyle total}$ (in.)	$C_d \delta_{total}$ (in.)	⊿ (in.)
54321	26.0 23.2 17.4 11.7 5.8	$\begin{array}{c} 1.52 \times 10^{7} \\ 1.52 \times 10^{7} \\ 1.52 \times 10^{7} \\ 1.52 \times 10^{7} \\ 1.52 \times 10^{7} \end{array}$	0.108 0.078 0.049 0.024 0.007	0.054 0.049 0.041 0.028 0.015	0.162 0.128 0.090 0.052 0.021	0.284 0.223 0.157 0.091 0.037	0.061 0.066 0.066 0.054 0.037

Table 9.2-6 Deflections, Birmingham 1

1.0 kip = 4.45 kN, 1.0 in. = 25.4 mm.

The maximum story drift occurs at Level 4 (Provisions Table 5.2.8 [Table 4.5-1]):

[The specific procedures for computing deflection of shear walls have been removed from the 2003 Provisions. ACI 530 does not contain the corresponding provisions in the text, however, the commentary contains a discussion and equations that are similar to the procedures in the 2000 *Provisions*. However, as indicated previously, there is a potential conflict between the drift limits in 2003 *Provisions* Table 4.5-1 and ACI 530 Sec. 1.13.3.2.]

$$\Delta = 0.066 \text{ in.} < 1.04 \text{ in.} = 0.01h_n$$
 OK

#### 9.2.4.7 Birmingham 1 Out-of-Plane Forces

*Provisions* Sec 5.2.6.2.7 [Sec. 4-6.1.3] requires that the bearing walls be designed for out-of-plane loads determined as follows:

 $w = 0.40S_{DS}W_c \ge 0.1W_c$  $w = (0.40)(0.24)(45 \text{ psf}) = 4.3 \text{ psf} < 4.5 \text{ psf} = 0.1W_c$ 

The calculated seismic load, w = 4.5 psf, is much less than wind pressure for exterior walls and is also less than the 5 psf required by IBC Sec. 1607.13 for interior walls. Thus, seismic loads do not govern the design of any of the walls for loading in the out-of-plane direction.

#### 9.2.4.8 Birmingham 1 Orthogonal Effects

Orthogonal effects do not have to be considered for Seismic Design Category B (*Provisions* Sec. 5.2.5.2.1 [Sec. 4.4.2.1]).

This completes the design of Transverse Wall D.

#### 9.2.4.9 Summary of Design for Birmingham 1 Wall D

8 in. CMU  $f'_m = 2,000 \text{ psi}$ 

Reinforcement:

One vertical #4 bar at wall end cells Vertical #4 bars at 8 ft on center at intermediate cells throughout Bond beam with two - #4 bars at each story just below the floor and roof slabs Horizontal joint reinforcement at 16 inches

Grout at cells with reinforcement and at bond beams.

# 9.2.5 Seismic Design for New York City

This example focuses on differences from the design for the Birmingham 1 site.

# 9.2.5.1 New York City Weights

As before, use 67 psf for 8-in.-thick normal weight hollow core plank plus the nonmasonry partitions. This site is assigned to Seismic Design Category C, and the walls will be designed as intermediate reinforced masonry shear walls (*Provisions* Sec. 11.11.4 [Sec. 11.2.1.4] and Sec. 11.3.7 [Sec. 11.2.1.4]), which requires prescriptive seismic reinforcement (*Provisions* Sec. 11.3.7.3 [ACI 530, Sec. 1.13.2.2.4]). Intermediate reinforced masonry shear walls have a minimum of #4 bars at 4 ft on center. For this example, 48 psf will be assumed for the 8-in. CMU walls. The 48 psf value includes grouted cells and bond beams in the course just below the floor planks. In Seismic Design Category C, more of the regularity requirement must be checked. It will be shown that this symmetric building with a seemingly well distributed lateral force system is torsionally irregular by the *Provisions*.

Story weight, *w<sub>i</sub>*:

Roof

Roof slab (plus roofing) = 
$$(67 \text{ psf}) (152 \text{ ft})(72 \text{ ft}) = 733 \text{ kips}$$
  
Walls =  $(48 \text{ psf})(589 \text{ ft})(8.67 \text{ ft}/2) + (48 \text{ psf})(4)(36 \text{ ft})(2 \text{ ft}) = 136 \text{ kips}$   
Total = 869 kips

There is a 2-ft high masonry parapet on four walls and the total length of masonry wall is 589 ft.

Typical floor

Slab (plus partitions) = 733 kips Walls = (48 psf)(589 ft)(8.67 ft) = 245 kipsTotal = 978 kips

Total effective seismic weight, W = 869 + (4)(978) = 4781 kips

This total excludes the lower half of the first story walls, which do not contribute to seismic loads that are imposed on CMU shear walls.

## 9.2.5.2 New York City Base Shear Calculation

The seismic response coefficient,  $C_s$ , is computed from *Provisions* Sec. 5.4.1.1 [Sec. 5.2-1.1]:

$$C_s = \frac{S_{DS}}{R/I} = \frac{0.39}{2.5/1} = 0.156$$

The value of  $C_s$  need not be greater than:

$$C_{s} = \frac{S_{DI}}{T(R/I)} = \frac{0.14}{0.338(2.5/1)} = 0.166$$

where T is the same as found in Sec. 9.2.4.2.

The value for  $C_s$  is taken as 0.156 (the lesser of the two computed values). This value is still larger than the minimum specified in *Provisions* Eq. 5.3.2.1-3. Using *Provisions* Eq. 5.4.1.1-3:

$$C_s = 0.044 S_{DI}I = (0.044)(0.14)(1) = 0.00616$$

[This minimum Cs value has been removed in the 2003 *Provisions*. In its place is a minimum Cs value for long-period structures, which is not applicable to this example.]

The total seismic base shear is then calculated using *Provisions* Eq. 5.4.1 [Eq. 5.2-1]:

 $V = C_s W = (0.156)(4,781) = 746$  kips

#### 9.2.5.3 New York City Vertical Distribution of Seismic Forces

The vertical distribution of seismic forces is determined in accordance with *Provisions* Sec. 5.4.4 [Sec. 5.2.3], which was described in Sec. 9.2.4.3. Note that for *Provisions* Eq. 5.4.3-2 [Eq. 5.2-11], k = 1.0 since T = 0.338 sec (similar to the Birmingham 1 building).

The application of the *Provisions* equations for this building is shown in Table 9.2-7:

Level (x)	$w_x$ (kips)	$h_x$ (ft)	$w_x h_x^{\ k}$ (ft-kips)	$C_{vx}$	$F_x$ (kips)	$V_X$ (kips)	$M_x$ (ft-kips)
5	869	43.34	37,657	0.3076	229	2.3e+14	1,985
4	978	34.67	33,904	0.2770	207		5,765
3	978	26.00	25,428	0.2077	155		10,889
2	978	17.33	16,949	0.1385	103		16,907
<u>1</u>	978	8.67	8,476	0.0692	52		23,370
Σ	4,781		122,414	1.000	746		

 Table 9.2-7
 New York City Seismic Forces and Moments by Level

1.0 kip = 4.45 kN, 1.0 ft = 0.3048 m, 1.0 ft-kip = 1.36 kN-m.

#### 9.2.5.4 New York City Horizontal Distribution of Forces

The initial distribution is the same as Birmingham 1. See Sec. 9.2.4.4 and Figure 9.2-3 for wall designations.

Total shear in Wall Type D:

$$V_{tot} = 0.125V + 0.0238V = 0.149V$$

*Provisions* Sec.5.4.4.3 [Sec. 4.3.2.2] requires a check of torsional irregularity using the ratio of maximum displacement at the end of the structure, including accidental torsion, to the average displacement of the two ends of the building. For this simple and symmetric structure, the actual displacements do not have to be computed to find the ratio. Relying on symmetry and the assumption of rigid diaphragm behavior

used to distribute the forces, the ratio of the maximum displacement of Wall D to the average displacement of the floor will be the same as the ratio of the wall shears with and without accidental torsion:

$$\frac{F_{max}}{F_{ave}} = \frac{0.149V}{0.125V} = 1.190$$

This can be extrapolated to the end of the rigid diaphragm therefore:

$$\frac{\delta_{max}}{\delta_{ave}} = 1 + 0.190 \left(\frac{152/2}{36}\right) = 1.402$$

*Provisions* Table 5.2.3.2 [Table 4.3-2] defines a building as having a "Torsional Irregularity" if this ratio exceeds 1.2 and as having an "Extreme Torsional Irregularity" if this ratio exceeds 1.4. Thus, an important result of the Seismic Design Category C classification is that the total torsion must be amplified by the factor:

$$A_{x} = \left(\frac{\delta_{max}}{1.2\delta_{ave}}\right)^{2} = \left(\frac{1.402}{1.2}\right)^{2} = 1.365$$

Therefore, the portion of the base shear for design of Wall D is now:

$$V_{D} = 0.125V + 1.365(0.0238V) = 0.158V$$

which is a 5.8 percent increase from the fraction before considering torsional irregularity.

The total story shear and overturning moment may now be distributed to Wall D and the wall proportions checked. The wall capacity will be checked before considering deflections.

#### 9.2.5.5 New York City Transverse Wall D

The strength or limit state design concept is used in the *Provisions*.

#### 9.2.5.5.1 New York City Shear Strength

Similar to the design for Birmingham 1, the shear wall design is governed by:

$$V_{u} \leq \phi V_{n}$$

$$V_{n} = V_{m} + V_{s}$$

$$V_{n} \max = 4 \text{ to } 6\sqrt{f'_{m}}A_{n} \quad \text{depending on } M/Vd$$

$$V_{m} = \left[4 - 1.75\left(\frac{M}{Vd}\right)\right]A_{n}\sqrt{f'_{m}} + 0.25 P$$

$$V_{s} = 0.5\left(\frac{A_{v}}{s}\right)f_{y}d_{v}$$

where

$$A_n = (2 \times 1.25 \text{ in.} \times 32.67 \text{ ft} \times 12 \text{ in.}) + (41 \text{ in.}^2 \times 9 \text{ cells}) = 1,349 \text{ in.}^2$$

The shear strength of each Wall D, based on the aforementioned formulas and the strength reduction factor of  $\phi = 0.8$  for shear from *Provisions* Table 11.5.3 [ACI 530, Sec. 3.1.4.3], is summarized in Table 9.2-8. Note that  $V_x$  and  $M_x$  in this table are values from Table 9.2-7 multiplied by 0.158 (representing the portion of direct and indirect shear assigned to Wall D), and *P* is the dead load of the roof or floor times the tributary area for Wall D.

		<b>Table 9.2-</b>	<u>8 New Yor</u>	k City She	ar Strengtl	<u>n Calculati</u>	on for Wall	l D	
Story	$V_x$	$M_{x}$	$M_x/V_x d$	2.5 $V_x$	Р	$\varphi V_m$	$\varphi V_s$	$\varphi V_n$	$\varphi V_n max$
	(kips)	(ft-kips)		(kips)	(kips)	(kips)	(kips)	(kips)	(kips)
5	36.1	313	0.265	90.3	42	179.0	54.6	233.6	287.6
4	68.7	908	0.405	171.8	90	176.9	54.6	231.5	269.7
3	93.1	1715	0.564	232.8	139	173.2	54.6	227.8	249.2
2	109.3	2663	0.746	273.3	188	167.7	54.6	222.3	225.8
1	117.5	3680	0.959	293.8	236	159.3	54.6	213.9	198.4

1.0 kip = 4.45 kN, 1.0 ft-kip = 1.36 kN-m.

 $V_u$  exceeds  $\varphi V_n$  at the lower three stories. As will be shown at the conclusion of the design for flexure, the factor to achieve 125 percent of the nominal flexural capacity is 1.58. This results in  $V_u$  being less than  $\varphi V_n$  at all stories. If that were not the case, it would be necessary to grout more cells to increase  $A_n$  or to increase  $f_m^2$ .

## 9.2.5.5.2 New York City Axial and Flexural Strength

The walls in this example are all load-bearing shear walls because they support vertical loads as well as lateral forces. In-plane calculations include:

- 1. Strength check and
- 2. Ductility check.

### 9.2.5.5.2.1 Strength check

Wall demands, using load combinations determined previously, are presented in Table 9.2-9 for Wall D. In the table, Load Combination 1 is  $1.28D + Q_E + 0.5L$  and Load Combination 2 is  $0.82D + Q_E$ .

		P <sub>L</sub> (kips)	Load Com	bination 1	Load Combination 2		
Level	$P_D$ (kips)		$P_u$ (kips)	M <sub>u</sub> (ft-kips)	$P_u$ (kips)	$M_u$ (ft-kips)	
5	42	0	54	313	34	313	
4	90	8	119	908	74	908	
3	139	17	186	1715	114	1715	
2	188	25	253	2663	154	2663	
1	236	34	319	3680	194	3680	

<b>Table 9.2-9</b>	Demands for New	York City Wall D
--------------------	-----------------	------------------

1.0 kip = 4.45 kN, 1.0 ft-kip = 1.36 kN-m.

As in Sec. 9.2.4.5.2, strength at the bottom story (where P, V, and M are the greatest) will be examined. The strength design will consider Load Combination 2 from Table 9.2-9 to be the governing case because it has the same lateral load as Load Combination 1 but with lower values of axial force. Refer to Fig. 9.2-9 for notation and dimensions.

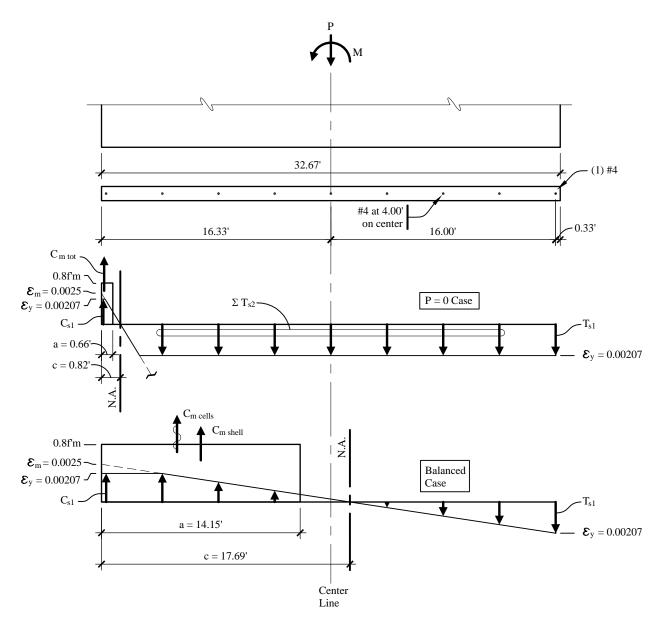


**Figure 9.2-9** Strength of New York City and Birmingham 2 Wall D. Strength diagrams are superimposed over the strain diagrams for the two cases (intermediate case is not shown) (1.0 ft = 0.3048 m).

Examine the strength of Wall D at Level 1:

$$P_{u_{min}} = 0.82 D = 0.82 (236 + \text{factored weight of lower half of first story wall)}$$
  
= 0.82(236 + 6.4) = 199 kips  
$$P_{u_{max}} = 1.28 D + 0.5 L 319 = 1.28(236 + 6.4) + 0.5(34) = 327 \text{ kips}$$
  
$$M_{u} = 3,680 \text{ ft-kips}$$

Because intermediate reinforced masonry shear walls are used (Seismic Design Category C), vertical reinforcement at is required at 4 ft on center in accordance with *Provisions* Sec. 11.3.7.3 [ACI 530, Sec. 1.13.2.2.4]. Therefore, try one #4 bar in each end cell and #4 bars at 4 ft on center at all intermediate cells.

The calculation procedure is similar to that for the Birmingham 1 building presented in Sec. 9.2.4.5.2. The results of the calculations (not shown) for the New York building are summarized below.

P = 0 case

 $\phi P_n = 0$  $\phi M_n = 1,475 \text{ ft-kips}$ 

Intermediate case

c = 8.0 ft  $\phi P_n = 330$  kips  $\phi M_n = 5,600$  ft-kips

Balanced case

$$\phi P_n = 807$$
  
$$\phi M_n = 8,214 \text{ ft-kips}$$

With the intermediate case, it is simple to use the three points to make two straight lines on the interaction diagram. Use the simplified  $\phi P_n - \phi M_n$  curve shown in Figure 9.2-10. The straight line from pure bending to the balanced point is conservative and can easily be used where the design is not as close to the criterion. It is the nature of lightly reinforced and lightly loaded masonry walls that the intermediate point is frequently useful.

Use one #4 bar in each end cell and one #4 bar at 4 ft on center throughout the remainder of the wall.

As shown in the design for Birmingham 1,for the purpose of shear design, the value of  $\varphi M_N$  at the design axial load is necessary. Interpolating between the intermediate point and the P = 0 point for P = 199 kips yields  $\varphi M_N = 3,960$  ft-kip. Thus, the factor on shear to represent development of 125 percent of flexural capacity is:

$$1.25 \frac{\phi M_N / \phi}{M_U} = 1.25 \frac{3960 / 0.85}{3680} = 1.58$$

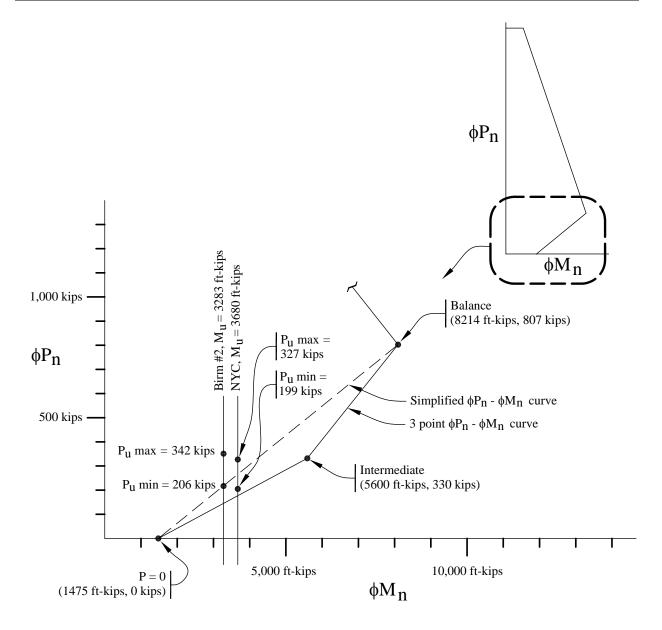


**Figure 9.2-10**  $\varphi P_{11} - \varphi M_{11}$  Diagram for New York City and Birmingham 2 Wall D (1.0 kip = 4.45 kN, 1.0 ft-kip = 1.36 kN-m).

#### 9.2.5.5.2.2 Ductility check

Refer to Sec. 9.2.4.5.2, Item 2, for explanation [see Sec. 9.2.4.5.2 for discussion of revisions to the ductility requirements in the 2003 *Provisions*.]. For Level 1 (bottom story), the unfactored loads are:

 $P = 236 + \text{weight of lower } \frac{1}{2} \text{ of first story wall} = 236 + 6.4 = 242.4 \text{ kips}$ M = 3,483 ft-kips

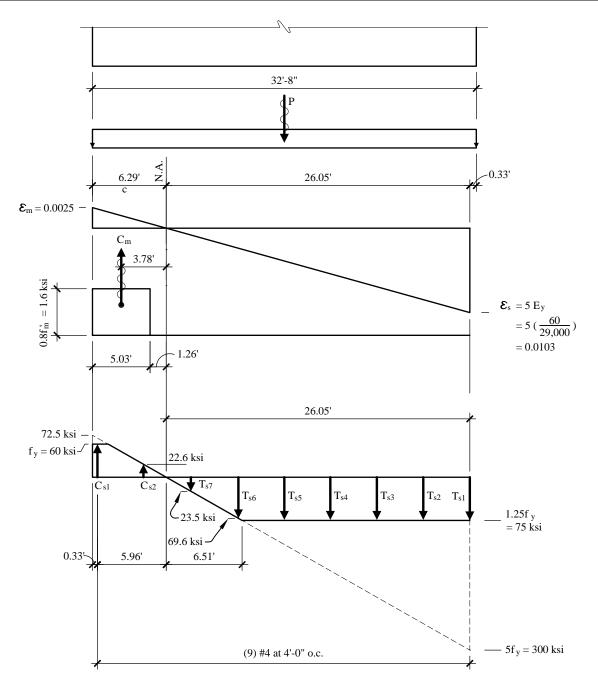
$$C_m = 0.8 f_m' [(a)(b) + A_{cells}]$$
  
where  $b = \text{face shells} = (2 \times 1.25 \text{ in.}) \text{ and } A_{cell} = 41 \text{ in.}^2$ 

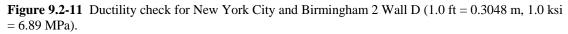
 $C_m = (1.6 \text{ ksi})[(5.03 \text{ ft} \times 12)(2.5 \text{ in.}) + (2)(41)] = 372.6 \text{ kips}$ 

 $C_{sI} = F_y A_s = (60 \text{ ksi})(0.20 \text{ in.}^2) = 12 \text{ kips}$   $C_{s2} = (22.6 \text{ ksi})(0.20 \text{ in.}^2) = 4.5 \text{ kips}$   $T_{sI} = T_{s2} = T_{s3} = T_{s4} = T_{s5} = (75 \text{ ksi})(0.20 \text{ in.}^2) = 15 \text{ kips}$   $T_{s6} = (69.6 \text{ ksi})(0.20 \text{ in.}^2) = 13.9 \text{ kips}$  $T_{s7} = (23.5 \text{ ksi})(0.20 \text{ sq. in.}) = 4.7 \text{ kips}$ 

 $\sum_{m} C > \sum_{m} P + T$   $C_{m} + C_{s1} + C_{s2} > P + T_{s1} + T_{s2} + T_{s3} + T_{s4} + T_{s5} + T_{s6} + T_{s7}$ 372.6 + 12.0 + 4.5 > 242.5 + 5(15) + 13.9 + 4.7 389 kips > 336 kips

OK





#### 9.2.5.6 New York Deflections

Refer to 9.2.4.6 for more explanation [see Sec. 9.2.4.6 for discussion of revisions to the deflection computations and requirements in the 2003 *Provisions*, as well as the potentially conflicting drift limits]. For the New York City building, the determination of whether the walls will be cracked is:

 $b_e$  = effective masonry wall width  $b_e = [(2 \times 1.25 \text{ in.})(32.67 \text{ ft} \times 12) + (9 \text{ cells})(41 \text{ in.}^2/\text{cell})]/(32.67 \text{ ft} \times 12) = 3.44 \text{ in.}$  $A = b_e l = (3.44 \text{ in.})(32.67 \times 12) = 1,349 \text{ in.}^2$ 

$$S = b_e l^2/6 = (3.44)(32.67 \times 12)^2/6 = 88,100 \text{ in.}^3$$
  
 $f_r = 0.250 \text{ ksi}$ 

 $P_u$  is calculated using 1.00D (see Table 9.2-8 for values and refer to Sec. 9.2.4.6 for discussion). Table 9.2-10 a summarizes of these calculations.

Status	$M_x$ (ft-kips)	M <sub>cr</sub> (ft-kips)	$P_u$ (kips)	Level
uncracked	313	2064	42	5
uncracked	908	2325	90	4
uncracked	1715	2592	139	3
uncracked	2663	2860	188	2
cracked	3680	3120	236	1

1.0 kip = 4.45 kN, 1.0 ft-kip = 1.36 kN-m.

For the uncracked walls:

$$I_n = I_g = bl^3/12 = (3.44 \text{ in.})(32.67 \times 12)^3/12 = 1.73 \times 10^7 \text{ in.}^4$$

For the cracked wall, observe that the intermediate point on the interaction diagram is relatively close to the design point. Therefore, as a different type of approximation, compute a cracked moment of inertia using the depth to the neutral axis of 8.0 ft:

$$I_{cr} = b_e c^3 / 3 + \sum n A_s d^2$$
  

$$I_{cr} = (3.44 \text{ in.})(8.0 \text{ ft} \times 12)^3 / 3 + 19.3(0.2)(4.33^2 + 8.33^2 + 12.33^2 + 16.33^2 + 20.33^2 + 24.33^2)144 = 1.01 \text{ x } 10^6 + 0.84 \text{ x } 10^6 = 1.85 \text{ x } 10^6 \text{ in.}^4$$

Per Provisions Eq. 11.5.4.3:

$$I_{eff} = I_n \left(\frac{M_{cr}}{M_a}\right)^3 + I_{cr} \left[1 - \left(\frac{M_{cr}}{M_a}\right)^3\right] \le I_n$$
$$I_{eff} = 1.13 \ge 10^7 \text{ in.}^4$$

*Provisions* 11.5.4.3 would imply that  $I_{eff}$  would be used for the full height. Another reasonable option is to use  $I_{cr}$  at the first story and  $I_g$  above that. The calculation of  $\delta$  should consider shear deflections in addition to the flexural deflections. For this example  $I_{eff}$  will be used over the full height for the final determination of deflection (a RISA 2D analysis was made). The result is summarized in Table 9.2-11.

Level	F (kips)	$I_{eff}$ (in. <sup>4</sup> )	$\delta_{flexural} \ ( ext{in.})$	$\delta_{\scriptscriptstyle shear} \ ( ext{in.})$	$\delta_{\scriptscriptstyle total} \ ( ext{in.})$	$C_d \delta_{total}$ (in.)	⊿ (in.)
54321	34.1 30.9 23.1 15.3 7.7	$\begin{array}{c} 1.13 \times 10^{7} \\ 1.13 \times 10^{6} \end{array}$	0.256 0.189 0.124 0.065 0.020	$\begin{array}{c} 0.080 \\ 0.075 \\ 0.064 \\ 0.050 \\ 0.033 \end{array}$	0.336 0.264 0.188 0.115 0.053	0.757 0.593 0.422 0.259 0.118	0.163 0.171 0.163 0.141 0.118

 Table 9.2-11
 New York City Deflections

1.0 kip = 4.45 kN, 1.0 in. = 25.4 mm

The maximum story drift occurs at Level 4:

$$\Delta_4 = 0.171$$
 in. < 1.04 in. = 0.01  $h_4$  (*Provisions* Table 5.2.8 [Table 4.5-1]) OK

The total displacement at the top of the wall is

$$\Delta = 0.757 \text{ in.} < 5.2 \text{ in.} = 0.01 h_n (Provisions 11.5.4.1.1)$$
 OK

#### 9.2.5.7 New York City Out-of-Plane Forces

*Provisions* Sec 5.2.6.2.7 [Sec. 4.4.2.2] requires that the bearing walls be designed for out-of-plane loads determined as

$$w = 0.40 S_{DS} W_c \ge 0.1 W_c$$

With  $S_{DS} = 0.39$ ,  $w = 0.156W_c > 0.1W_c$ , so w = (0.156)(48 psf) = 7.5 psf, which is much less than wind pressure for exterior walls. Even though Wall D is not an exterior wall, the lateral pressure is sufficiently low that it is considered acceptable by inspection, without further calculation. Seismic loads do not govern the design of Wall D for loading in the out-of-plane direction.

#### 9.2.5.8 New York City Orthogonal Effects

According to *Provisions* Sec. 5.2.5.2.2, orthogonal interaction effects have to be considered for Seismic Design Category C when the equivalent lateral force (ELF) procedure is used (as it is here). However, the out-of-plane component of only 30 percent of 7.5 psf on the wall will not produce a significant effect when combined with the in-plane direction of loads, so no further calculation will be made.

This completes the design of the transverse Wall D for the New York building.

#### 9.2.5.9 Summary of New York City Wall D Design

8 in. CMU  $f'_m = 2,000 \text{ psi}$  Reinforcement:

Vertical #4 bars at 4 ft on center throughout the wall Bond beam with two #4 at each story just below the floor or roof slabs Horizontal joint reinforcement at alternate courses

# 9.2.6 Birmingham 2 Seismic Design

The emphasis here is on differences from the previous two locations for the same building. Per *Provisions* Table 5.2.5.1 [Table 4.4-1], the torsional irregularity requires that the design of a Seismic Design Category D building be based on a dynamic analysis. Although not explicitly stated, the implication is that the analytical model should be three-dimensional in order to capture the torsional response. This example will compare both the equivalent lateral force procedure and the modal response spectrum analysis procedure and will demonstrate that, as long as the torsional effects are accounted for, the static analysis could be considered adequate for design.

# 9.2.6.1 Birmingham 2 Weights

The floor weight for this examples will use the same 67 psf for 8-in.-thick, normal weight hollow core plank plus roofing and the nonmasonry partitions as used in the prior examples (see Sec. 9.2.1). This site is assigned to Seismic Design Category D, and the walls will be designed as special reinforced masonry shear walls (*Provisions* Sec. 11.11.5 and Sec. 11.3.8[ACI 530, Sec. 1.13.2.2.5), which requires prescriptive seismic reinforcement (*Provisions* Sec. 11.3.7.3). Special reinforced masonry shear walls have a maximum spacing of rebar at 4 ft on center both horizontally and vertically. Also, the total area of horizontal and vertical reinforcement must exceed 0.0020 times the gross area of the wall, and neither direction may have a ratio of less than 0.0007. The vertical #4 bars at 48 in. used for the New York City design yields a ratio of 0.00055, so it must be increased. Two viable options are #5 bars at 48 in. (yielding 0.00085) and #4 bars at alternating spaces of 32 in. and 40 in. (12 bars in the wall), which yields 0.0080. The latter is chosen in order to avoid unnecessarily increasing the shear demand. Therefore, the horizontal reinforcement must be (0.0020 - 0.0008)(7.625 in.)(12 in./ft.) = 0.11 in.<sup>2</sup>/ft. or 0.95 in.<sup>2</sup> per story. Two #5 bars in bond beams at 48 in. on center will be adequate. For this example, 56 psf weight for the 8-in.-thick CMU walls will be assumed. The 56 psf value includes grouted cells and bond beams.

Story weight, *w<sub>i</sub>*:

Roof:

Roof slab (plus roofing) = $(67 \text{ psf}) (152 \text{ ft})(72 \text{ ft})$	= 733 kips
Walls = (56 psf)(589 ft)(8.67 ft/2) + (56 psf)(4)(36 ft)(2 ft)	= <u>159 kips</u>
Total	= 892 kips

There is a 2-ft-high masonry parapet on four walls and the total length of masonry wall is 589 ft.

Typical floor:

Slab (plus partitions)	= 733 kips
Walls = $(56 \text{ psf})(589 \text{ ft})(8.67 \text{ ft})$	= <u>286 kips</u>
Total	= 1,019 kips

Total effective seismic weight, W = 892 + (4)(1,019) = 4,968 kips

This total excludes the lower half of the first story walls which do not contribute to seismic loads that are imposed on CMU shear walls.

## 9.2.6.2 Birmingham 2 Base Shear Calculation

The ELF analysis proceeds as described for the other locations. The seismic response coefficient,  $C_s$ , is computed using *Provisions* Eq. 5.4.1.1-1 [Eq. 5.2-2] and 5.4.1.1-2 [Eq.5.2-3]:

$$C_{s} = \frac{S_{DS}}{R/I} = \frac{0.47}{3.5/1} = 0.134$$
(Controls)
$$C_{s} = \frac{S_{DI}}{T(R/I)} = \frac{0.28}{0.338(3.5/1)} = 0.237$$

This is somewhat less than the 746 kips computed for the New York City design due to the larger R factor.

The fundamental period of the building, based on *Provisions* Eq. 5.4.2.1-1 [Eq.5.2-6], is 0.338 sec as computed previously (the approximate period, based on building system and building height, will be the same for all locations). The value for  $C_s$  is taken as 0.134 (the lesser of the two values). This value is still larger than the minimum specified in *Provisions* Eq. 5.3.2.1-3 which is:

$$C_s = 0.044 S_{D1} I = (0.044)(0.28)(1) = 0.012$$

[This minimum  $C_s$  value has been removed in the 2003 *Provisions*. In its place is a minimum  $C_s$  value for long-period structures, which is not applicable to this example.]

The total seismic base shear is then calculated using Provisions Eq. 5.4.1 [Eq.5.2-1] as:

$$V = C_s W = (0.134)(4,968) = 666$$
 kips

A three-dimensional (3D) model was created in SAP 2000 for the modal response spectrum analysis. The masonry walls were modeled as shell bending elements and the floors were modeled as an assembly of beams and shell membrane elements. The beams have very little mass and a large flexural moment of inertia to avoid consideration of models of vertical vibration of the floors. The flexural stiffness of the beams was released at the bearing walls in order to avoid a wall slab frame that would inadvertently increase the torsional resistance. The mass of the floors was captured by the shell membrane elements. Table 9.2-12 shows data on the modes of vibration used in the analysis.

*Provisions* Sec. 4.1.2.6 [Sec. 3.3.4] was used to create the response spectrum for the modal analysis. The key points that define the spectrum are:

 $T_{s} = S_{DI}/S_{DS} = 0.28/0.47 = 0.60 \text{ sec}$   $T_{0} = 0.2 T_{s} = 0.12 \text{ sec}$ at  $T = 0, S_{a} = 0.4 S_{DS}/R = 0.0537 g$ from  $T = T_{0}$  to  $T_{s}, S_{a} = S_{DS}/R = 0.1343 g$ for  $T > T_{s}, S_{a} = S_{D}I/(RT) = 0.080/T$ 

The computed fundamental period is less than the approximate period. The transverse direction base shear from the SRSS combination of the modes is 457.6 kips, which is considerably less than that obtained using the ELF method.

*Provisions* Sec. 5.5.7 [Sec. 5.3.7] requires that the modal base shear be compared with the ELF base shear computed using a period somewhat larger than the approximate fundamental period  $(C_uT_a)$ . Per Sec. 9.2.4.2,  $T_a = 0.338$  sec. and per *Provisions* Table 5.4.2 [Table 5.2-1]  $C_u = 1.4$ . Thus,  $C_uT_a = 0.48$  sec., which is less that  $S_{DI}/S_{DS}$ . Therefore, the ELF base shear for comparison is 666 kips as just computed. Because 85 percent of 666 kips = 566 kips, *Provisions* Sec. 5.5.7 [Sec. 5.3.7] dictates that all the results of the modal analysis be factored by:

$$\frac{0.85V_{ELF}}{V_{Modal}} = \frac{566}{458} = 1.24$$

Both analyses will be carried forward as discussed in the subsequent sections.

		Trans	verse Direct	ion for Mo	des Used in	Analysis		
Mode	Period,	Individ	lual mode (p	ercent)	Cumul	ative sum (p	ercent)	Trans.
number	(seconds)	Long.	Trans.	Vert.	Long.	Trans.	Vert.	base shear
1	0.2467	0.00	0.00	0.00	0.00	0.00	0.00	0.0
2	0.1919	0.00	70.18	0.00	0.00	70.18	0.00	451.1
3	0.1915	70.55	0.00	0.00	70.55	70.18	0.00	0.0
4	0.0579	0.00	18.20	0.00	70.55	88.39	0.00	73.9
5	0.0574	17.86	0.00	0.00	88.41	88.39	0.00	0.0
6	0.0535	0.00	4.09	0.00	88.41	92.48	0.00	16.1
7	0.0532	4.17	0.00	0.00	92.58	92.48	0.00	0.0
8	0.0413	0.00	0.01	0.00	92.58	92.48	0.00	0.0
9	0.0332	1.50	0.24	0.00	94.08	92.72	0.00	0.8
10	0.0329	0.30	2.07	0.00	94.38	94.79	0.00	7.1
11	0.0310	1.28	0.22	0.00	95.66	95.01	0.00	0.8
12	0.0295	0.22	1.13	0.00	95.89	96.14	0.00	3.8
13	0.0253	1.97	0.53	0.00	97.86	96.67	0.00	1.7
14	0.0244	0.53	1.85	0.00	98.39	98.52	0.00	5.9
15	0.0190	1.05	0.36	0.00	99.44	98.89	0.00	1.1
16	0.0179	0.33	0.94	0.00	99.77	99.82	0.00	2.8
17	0.0128	0.19	0.07	0.00	99.95	99.90	0.00	0.2
18	0.0105	0.03	0.10	0.00	99.99	99.99	0.00	0.3

 
 Table 9.2-12
 Birmington 2 Periods, Mass Participation Factors, and Modal Base Shears in the Transverse Direction for Modes Used in Analysis

1 kip = 4.45 kN.

# 9.2.6.3 Birmingham 2 Vertical Distribution of Seismic Forces

The dynamic analysis will be revisited for the horizontal distribution of forces in the next section but as demonstrated there, the ELF procedure is considered adequate to account for the torsional behavior in this example. The dynamic analysis can certainly be used to deduce the vertical distribution of forces. This analysis was constructed to study amplification of accidental torsion. It would be necessary to integrate the shell forces to find specific story forces, and it is not necessary to complete the design. Therefore, the vertical distribution of seismic forces for the ELF analysis is determined in accordance with *Provisions* Sec. 5.4.4 [Sec. 5.2.3], which was described in Sec. 9.2.4.3. For *Provisions* Eq. 5.4.3-2 [Sec. 5.2-11], k = 1.0 since T = 0.338 sec (similar to the Birmingham 1 and New York City buildings). It should be noted that the response spectrum analysis may result in moments that are less than those calculated using the ELF method; however, because of its relative simplicity, the ELF is used in this example.

Application of the *Provisions* equations for this building is shown in Table 9.2-13:

Level (x)	$w_x$ (kips)	$h_x$ (ft)	$w_x h_x$ (ft-kips)	$C_{_{vx}}$	$F_x$ (kips)	$V_x$ (kips)	$M_x$ (ft-kips)
5	892	43.34	38,659	0.3045	203	203	1,760
4	1,019	34.67	35,329	0.2782	185	388	5,124
3	1,019	26.00	26,494	0.2086	139	527	9,693
2	1,019	17.33	17,659	0.1391	93	620	15,068
<u>1</u>	<u>1,019</u>	8.67	8,835	<u>0.0695</u>	46	666	20,843
Σ	4,968		126,976	1.000	666		

Table 9.2-13 B	Birmingham 2 Seismic	c Forces and Moments by Lev	el
----------------	----------------------	-----------------------------	----

1.0 kip = 4.45 kN, 1.0 ft = 0.3048 m, 1.0 ft-kip = 1.36 kN-m.

#### 9.2.6.4 Birmingham 2 Horizontal Distribution of Forces

For the ELF analysis, this is the same as that for New York City location; see Sec. 9.2.5.4.

Total shear in wall type D:

 $V_{tot} = 0.125V + 1.365(0.0238)V = 0.158V = 104.9$ kips

The dynamic analysis shows that the fundamental mode is a pure torsional mode. The fact that the fundamental mode is torsional does confirm, to an extent, that the structure is torsionally sensitive. This modal analysis does not show any significant effect of the torsion, however. The pure symmetry of this structure is somewhat idealistic. Real structures usually have some real eccentricity between mass and stiffness, and dynamic analysis then yields coupled modes, which contribute to computed forces.

The *Provisions* does not require that the accidental eccentricity be analyzed dynamically. For illustration, however, this was done by adjusting the mass of the floor elements to generate an eccentricity of 5 percent of the 152-ft length of the building. Table 9.2-14 shows the results of such an analysis. (Accidental torsion could also be considered using a linear combination of the dynamic results and a statically applied moment equal to the accidental torsional moment.)

The transverse direction base shear from the SRSS combination of the modes is 403.8 kips, significantly less than the 457.6 kips for the symmetric model. The amplification factor for this base shear is 566/404 = 1.4. This smaller base shear from modal analysis of a model with an artificially introduced eccentricity is normal. For two primary reasons. First, the mass participates in more modes. The participation in the largest mode is generally less, and the combined result is dominated by the largest single mode. Second, the period for the fundamental mode generally increases, which will reduce the spectral response except for structures with short periods (such as this one).

The base shear in Wall D was computed by adding the in-plane reactions. For the symmetric model the result was 57 kips, which is 12.5 percent of the total of 458 kips, as would be expected. Amplifying this by the 1.24 factor yields 71 kips The application of a static horizontal torsion equal to the 5 percent eccentricity times a base shear of 566 kips (the "floor") adds 13 kips, for a total of 84 kips. If the static horizontal torsion is amplified by 1.365, as found in the analysis for the New York location, the total becomes 89 kips, which is less than the 99 kips and 105 kips computed in the ELF analysis without and with, respectively, the amplification of accidental torsion. The Wall D base shear from the eccentric model was 66 kips; with the amplification of base shear = 1.4, this becomes 92 kips. Note that this value is less than the direct shear from the symmetric model plus the amplified static torsion. The obvious conclusion is that more careful consideration of torsional instability than actually required by the

*Provisions* does not indicate any more penalty than already given by the procedures for the ELF in the *Provisions*. Therefore the remainder of the example designs for this building are completed using the ELF.

Mode	Period	Individ	lual mode (p	ercent)	Cumula	ative sum (p	ercent)	Trans.
Number	(sec)	Long.	Trans.	Vert.	Long.	Trans.	Vert.	Base Shear
1	0.2507	0.0	8.8	0.0	0.0	8.8	0.0	56.3
2	0.1915	70.5	0.0	0.1	70.5	8.8	0.1	0.0
3	0.1867	0.0	61.4	0.0	70.5	70.2	0.1	394.9
4	0.0698	0.0	2.9	0.0	70.5	73.1	0.1	12.7
5	0.0613	1.1	0.0	23.0	71.6	73.1	23.1	0.0
6	0.0575	19.2	0.0	0.0	90.9	73.1	23.2	0.0
7	0.0570	0.0	13.7	0.0	90.9	86.8	23.2	55.5
8	0.0533	0.0	5.6	0.0	90.9	92.4	23.2	22.0
9	0.0480	1.2	0.0	12.8	92.0	92.4	35.9	0.0
10	0.0380	1.4	0.0	0.0	93.5	92.4	35.9	0.0
11	0.0374	0.0	0.4	0.0	93.5	92.8	35.9	1.3
12	0.0327	1.7	0.0	0.2	95.2	92.8	36.1	0.0
13	0.0322	0.0	3.1	0.0	95.2	95.9	36.1	10.4
14	0.0263	2.8	0.0	0.1	98.0	95.9	36.2	0.0
15	0.0243	0.0	3.0	0.0	98.0	98.8	36.2	9.5
16	0.0201	1.6	0.0	0.1	99.6	98.8	36.3	0.0
17	0.0164	0.0	1.1	0.0	99.6	100.0	36.3	3.4
18	0.0141	0.4	0.0	0.1	100.0	100.0	36.3	0

**Table 9.2-14** Birmingham periods, Mass Participation Factors, and Modal Base

 Shears in the Transverse Direction for Modes Used in Analysis

The total story shear and overturning moment (from the ELF analysis) may now be distributed to Wall D and the wall proportions checked. The wall capacity will be checked before considering deflections.

The "extreme torsional irregularity" has an additional consequence for Seismic Design Category D: *Provisions* 5.6.2.4.2 [Sec. 4.6.3.2] requires that the design forces for connections between diaphragms, collectors, and vertical elements (walls) be increased by 25 percent above the diaphragm forces given in *Provisions* 5.4.1 [Sec. 4.6.3.4]. For this example, the diaphragm of precast elements is designed using the different requirements of the appendix to *Provisions* Chapter 9 (see Chapter 7 of this volume).

# 9.2.6.5 Birmingham 2 Transverse Wall (Wall D)

The design demands are slightly smaller than for the New York City design, yet there is more reinforcement, both vertical and horizontal in the walls. This illustration will focus on those items where the additional reinforcement has special significance.

# 9.2.6.5.1 Birmingham 2 Shear Strength

Refer to Sec. 9.2.5.5.1 for most quantities. The additional horizontal reinforcement raises  $V_s$  and the additional grouted cells raises  $A_n$  and, therefore both  $V_m$  and  $V_n$  max.

 $A_v/s = (4)(0.31 \text{ in.}^2)/(8.67 \text{ ft.}) = 0.1431 \text{ in.}^2/\text{ft}$   $V_s = 0.5(0.1431)(60 \text{ ksi})(32.67 \text{ ft}) = 140.2 \text{ kips}$  $A_n = (2 \times 1.25 \text{ in.} \times 32.67 \text{ ft x } 12 \text{ in.}) + (41 \text{ in.}^2 \times 12 \text{ cells}) = 1,472 \text{ in.}^2$  The shear strength of Wall D is summarized in Table 9.2-15 below. (Note that  $V_x$  and  $M_x$  in this table are values from Table 9.2-13 multiplied by 0.158, the portion of direct and torsional shear assigned to the wall). Clearly, the dynamic analysis would make it possible to design this wall for smaller forces, but the minimum configuration suffices. The 1.96 multiplier on  $V_x$  to determine  $V_y$  is explained in the subsequent section on flexural design.

Level (x)	$V_x$ (kips)	$M_x$ (ft-kips)	$M_x/V_x d$	$\frac{1.98V_x}{\text{(kips)}}$	P (kips)	$\phi V_m$ (kips)	$\phi V_s$ (kips)	$\phi V_n$ (kips)	$\phi V_n max$ (kips)
5	32.0	277	0.265	63.4	42	194.6	112.2	306.8	313.9
4	61.1	907	0.454	121	90	186.8	112.2	299	287.3
3	83.0	1527	0.563	164.3	139	186.6	112.2	298.8	272.0
2	97.7	2373	0.743	193.4	188	179.7	112.2	291.9	246.7
1	104.9	3283	0.958	207.7	236	169.6	112.2	281.8	216.6

 Table 9.2-15
 Shear Strength Calculations for Wall D. Birmingham 2

1.0 kip = 4.45 kiN, 1.0 ft-kip = 1.36 kiN-m.

Note that  $V_n$  max is less than  $V_n$  at all levels except the top story. The capacity is greater than the demand at all stories, therefore, the design is satisfactory for shear.

## 9.2.6.5.2 Birmingham 2 Axial and Flexural Strength

Once again, the similarities to the design for the New York City location will be exploited. Normally, the in-plane calculations include:

1. Strength check

2. Ductility check

# 9.2.6.5.2.1 Strength check

The wall demands, using the load combinations determined previously, are presented in Table 9.2-16 for Wall D. In the table, Load Combination 1 is  $1.29D + Q_E + 0.5L$  and Load Combination 2 is  $0.81D + Q_E$ .

			Load Com	bination 1	Load Cor	nbination 2
Level	$P_D$ (kips)	$P_L$ (kips)	$P_u$ (kips)	M <sub>u</sub> (ft-kips)	$P_u$ (kips)	$M_u$ (ft-kips)
5	43	0	55	277	36	277
4	94	8	125	807	76	807
3	145	17	196	1527	117	1527
2	196	25	265	2373	159	2373
1	247	34	336	3283	200	3283

Table 9.2-16 Birmingham 2 Demands for Wall D

1.0 kip = 4.45 kN, 1.0 ft-kip = 1.36 kN-m

Strength at the bottom story (where P, V, and M are the greatest) are less than required for the New York City design. The demands are plotted on Figure 9.2-10, showing that the design for New York City has sufficient axial and flexural capacity for this Birmingham 2 location. For this design, the interaction capacity line will be shifted to the right, due to the presence of additional reinforcing bars. The only calculation here will be an estimate of the factor to develop the flexural capacity at the design axial load.

The flexural capacity for lightly load walls is approximately proportional to the sum of axial load plus the yield of the reinforcing steel:

$$\frac{\text{Birmingham #2 capacity}}{\text{NewYorkCapacity}} = \frac{200 \text{ kips } + 12 \times 0.20 \text{ in.}^2 \times 60 \text{ ksi}}{199 \text{ kips } + 9 \times 0.20 \text{ in.}^2 \times 60 \text{ ksi}} = \frac{344}{307} = 1.12$$

Therefore the factor by which the walls shears must be multiplied to represent 125 percent of flexural capacity, given that the factor was 1.58 for the New York design is:

$$1.58 \times 1.12 \frac{\text{New York base shear}}{\text{Birmingham #2 base shear}} = 1.77 \times \frac{746}{666} = 1.98$$

## 9.2.6.5.2.2 Ductility check

The *Provisions* requirements for ductility are described in Sec. 9.2.4.5.2 and 9.2.5.5.2. Since the wall reinforcement and loads are so similar to those for the New York City building, the computations are not repeated here.

[Refer to Sec. 9.2.4.5.2 for discussion of revisions to the ductility requirements in the 2003 Provisions.]

# 9.2.6.6 Birmingham 2 Deflections

The calculations for deflection would be very similar to that for the New York City location. Ironically, that procedure will indicate that the wall is not cracked at the design load. The  $C_d$  factor is larger, 3.5 vs. 2.25. However, the calculation is not repeated here; refer to Sec. 9.2.4.6 and Sec. 9.2.5.6.

[Refer to Sec. 9.2.4.6 for discussion of revisions to the deflection computations and requirements in the 2003 *Provisions*, as well as the potentially conflicting drift limits.]

# 9.2.6.7 Birmingham 2 Out-of-Plane Forces

*Provisions* Sec. 5.2.6.2.7 [Sec. 4.6.1.3] requires that the bearing walls be designed for out-of-plane loads determined:

 $w = 0.40 S_{DS} W_c \ge 0.1 W_c$ w = (0.40)(0.47)(56 psf) = 10.5 psf  $\ge 0.1 W_c$ 

The calculated seismic load, w = 10.5 psf, is less than wind pressure for exterior walls. Even though Wall D is not an exterior wall, the lateral pressure is sufficiently low that it is considered acceptable by inspection without further calculation. Seismic loads do not govern the design of Wall D for loading in the out-of-plane direction.

#### 9.2.6.8 Birmingham 2 Orthogonal Effects

According to *Provisions* Sec. 5.2.5.2.2 [Sec. 4.4.2.3], orthogonal interaction effects have to be considered for Seismic Design Category D when the ELF procedure is used (as it is here). However, the out-of-plane component of only 30 percent of 10.5 psf on the wall will not produce a significant effect when combined with the in-plane direction of loads so no further calculation will be made.

This completes the design of the Transverse Wall D.

# 9.2.6.9 Birmingham 2 Summary of Wall Design for Wall D

8-in. CMU  $f'_m = 2,000 \text{ psi}$ 

Reinforcement:

12 vertical #4 bars per wall (spaces alternate at 32 and 40 in. on center) Two bond beams with 2 - #5 at each story, at bearing for the planks, and at 4 ft above each floor. Horizontal joint reinforcement at alternate courses is recommended, but not required.

# 9.2.7 Seismic Design for Los Angeles

Once again, the differences from the designs for the other locations will be emphasized. As explained for the Birmingham 2 building, the *Provisions* would require a dynamic analysis for design of this building. For the reasons explained in Sec. 9.2.6.4, this design is illustrated using the ELF procedure.

## 9.2.7.1 Los Angeles Weights

Use 91 psf for 8-in.-thick, normal weight hollow core plank, 2.5 in. lightweight concrete topping (115 pcf), plus the nonmasonry partitions. This building is Seismic Design Category D, and the walls will be designed as special reinforced masonry shear walls (*Provisions* Sec. 11.11.5 and Sec. 11.3.8 [Sec.11.2.1.5]), which requires prescriptive seismic reinforcement (*Provisions* Sec. 11.3.8.3 [ACI 530, Sec. 1.13.2.2.5]). Special reinforced masonry shear walls have a minimum spacing of vertical reinforcement of 4 ft on center. For this example, 60 psf weight for the 8-in. CMU walls will be assumed. The 60 psf value includes grouted cells and bond beams in the course just below the floor planks and in the course 4 ft above the floors. A typical wall section is shown in Figure 9.2-12.

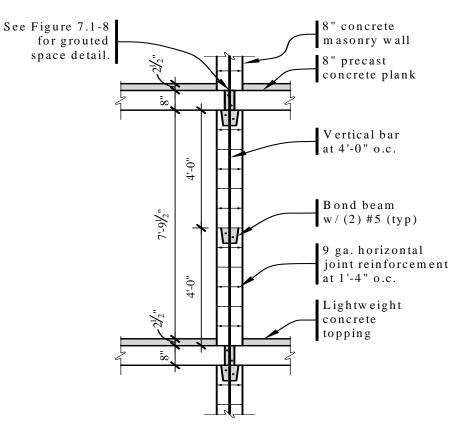


**Figure 9.2-12** Typical wall section for the Los Angeles location (1.0 in. = 25.4 mm, 1.0 ft = 0.3048 m)

Story weight ,  $w_i$ :

Roof weight:

Roof slab (plus roofing) = $(91 \text{ psf}) (152 \text{ ft})(72 \text{ ft})$	= 996 kips
Walls = $(60 \text{ psf})(589 \text{ ft})(8.67 \text{ ft/2}) + (60 \text{ psf})(4)(36 \text{ ft})(2 \text{ ft})$	= <u>170 kips</u>
Total	= 1,166 kips

There is a 2-ft-high masonry parapet on four walls and the total length of masonry wall is 589 ft.

Typical floor:

Slab (plus partitions)	= 996 kip	s
Walls = (60  psf)(589  ft)(8.67  ft)	= <u>306 kip</u>	9 <u>S</u>
Total	= 1,302 kip	S

Total effective seismic weight, W = 1,166 + (4)(1,302) = 6,374 kips

This total excludes the lower half of the first story walls, which do not contribute to seismic loads that are not imposed on the CMU shear walls.

## 9.2.7.2 Los Angeles Base Shear Calculation

The seismic response coefficient,  $C_s$ , is computed using *Provisions* Eq. 5.4.1.1-1 [Eq. 5.2-2] and 5.4.1.1-2 [Eq. 5.2-3]:

$$C_{s} = \frac{S_{DS}}{R/I} = \frac{1.00}{3.5/1} = 0.286$$
Controls
$$C_{s} = \frac{S_{DI}}{T(R/I)} = \frac{0.60}{0.338(3.5/1)} = 0.507$$

where *T* is the fundamental period of the building, which is 0.338 sec as computed previously (the approximate period, based on building system and building height, will be the same for all locations). The value for  $C_s$  is taken as 0.286 (the lesser of these two). This value is still larger than the minimum specified in *Provisions* Eq. 5.3.2.1-3 which is:

 $C_s = 0.044 S_{DI}I = (0.044)(0.60)(1) = 0.026$ 

[This minimum Cs value has been removed in the 2003 *Provisions*. In its place is a minimum Cs value for long-period structures, which is not applicable to this example.]

The total seismic base shear is then calculated *Provisions* Eq. 5.4.1 [Eq.5.2-1]:

 $V = C_s W = (0.286)(6,374) = 1,823$  kips

#### 9.2.7.3 Los Angeles Vertical Distribution of Seismic Forces

The vertical distribution of seismic forces is determined in accordance with *Provisions* Sec. 5.4.4 [Sec. 5.2.3], which as described in Sec. 9.2.4.3. Note that for *Provisions* Eq. 5.4.3-2 [Eq. 5.2-11], k = 1.0 since T = 0.338 sec (similar to the previous example buildings).

The application of the *Provisions* equations for this building is shown in Table 9.2-17:

Level ( <i>x</i> )	$w_x$ (kips)	$h_x$ (ft)	$w_x h_x^k$ (ft-kips)	$C_{vx}$	$F_x$ (kips)	$V_x$ (kips)	$M_x$ (ft-kips)
5	1,166	43.34	50,534	0.309	564	564	4,890
4	1,302	34.67	45,140	0.276	504	1,608	14,150
3	1,302	26.00	33,852	0.207	378	1,446	26,686
2	1,302	17.33	22,564	0.138	252	1,698	41,409
<u>1</u>	1,302	8.67	11,288	0.069	126	1,824	57,222
Σ	6,374		163,378	1.000	1,824		

 Table 9.2-17
 Los Angeles Seismic Forces and Moments by Level

1.0 kip = 4.45 kN, 1.0 ft = 0.3048 m, 1.0 ft-kip = 1.36 kN-m

#### 9.2.7.4 Los Angeles Horizontal Distribution of Forces

This is the same as for the Birmingham 2 design; see Sec. 9.2.6.4.

Total shear in Wall Type D:

 $V_{tot} = 0.125V + 1.365(0.0238)V = 0.158V$ 

The total story shear and overturning moment may now be distributed to each wall and the wall proportions checked. The wall capacity will be checked before considering deflections.

#### 9.2.7.5 Los Angeles Transverse Wall D

The strength or limit state design concept is used in the Provisions.

#### 9.2.7.5.1 Los Angeles Shear Strength

The equations are the same as for the prior locations for this example building. Looking forward to the design for flexural and axial load, the amplification factor on the shear is computed as:

$$1.25 \frac{M_n}{M_u} = 1.25 \frac{9156/0.85}{9012} = 1.49$$
 (which is less than the 2.5 upper bound)

Therefore, the demand shear is 1.49 times the value from analysis. (This design continues to illustrate the ELF analysis and; as explained for the Birmingham 2 design, smaller demands could be derived from the dynamic analysis.) All other parameters are similar to those for Birmingham 2 except that:

$$A_n = (2 \times 1.25 \text{ in.} \times 32.67 \text{ ft x } 12 \text{ in.}) + (41 \text{ in.}^2 \times 15 \text{ cells}) = 1,595 \text{ in.}^2$$

The shear strength of each Wall D, based on the aforementioned formulas and data, are summarized in Table 9.2-18.

Story	$V_x$ (kips)	$M_x$ (ft-kips)	$M_x/V_x d$	$\frac{1.49V_x}{\text{(kips)}}$	P (kips)	$\phi V_m$ (kips)	$\phi V_s$ (kips)	$\phi V_n$ (kips)	$\phi V_n max$ (kips)
5	88.8	770	0.265	132.3	42	210.1	112.2	322.3	340
4	168.2	2229	0.406	250.6	90	205.7	112.2	317.9	318.7
3	227.7	4203	0.565	339.3	139	199.6	112.2	311.8	294.5
2	267.4	6522	0.747	398.4	188	191.3	112.2	303.8	266.8
1	287.2	9012	0.960	427.9	236	179.5	112.2	291.7	234.3

 Table 9.2-18
 Los Angeles
 Shear Strength Calculations for Wall D

1.0 kip = 4.45 kN, 1.0 ft-kip = 1.36 kN-m

Just as for the Birmingham 2 design, the maximum on  $V_n$  controls over the sum of  $V_m$  and  $V_s$  at all stories except the top. Unlike the prior design, the shear capacity is inadequate in the lower three stories. The solution is to add grout. At the first story, solid grouting is necessary:

$$A_n = (7.625 \text{ in.})(32.67 \text{ ft.})(12 \text{ in./ft.}) = 2989 \text{ in.}^2$$
  
 $\varphi V_n max = 0.8(4.11)(0.0447 \text{ ksi})(2989 \text{ in.}2) = 439 \text{ kips} > 428 \text{ kips}$  OK

At the third story, six additional cells are necessary, and at the second story, approximately two out of three cells must be grouted. The additional weight adds somewhat to the demand but only about 2 percent. If the entire building were grouted solid (which would be common practice in the hypothetical location), the weight would increase enough that the shear strength criterion might be violated.

# 9.2.7.5.2 Los Angeles Axial and Flexural Strength

The basics of the flexural design have been demonstrated for the previous locations. The demand is much higher at this location, however, which introduces issues about the amount and distribution of reinforcement in excess of the minimum requirements. Therefore, the strength and ductility checks will both be examined.

# 9.2.7.5.2.1 Strength check

Load combinations, using factored loads, are presented in Table 9.2-19 for Wall D. In the table, Load Combination 1 is  $1.4D + Q_E + 0.5L$ , and Load Combination 2 is  $0.7D + Q_E$ .

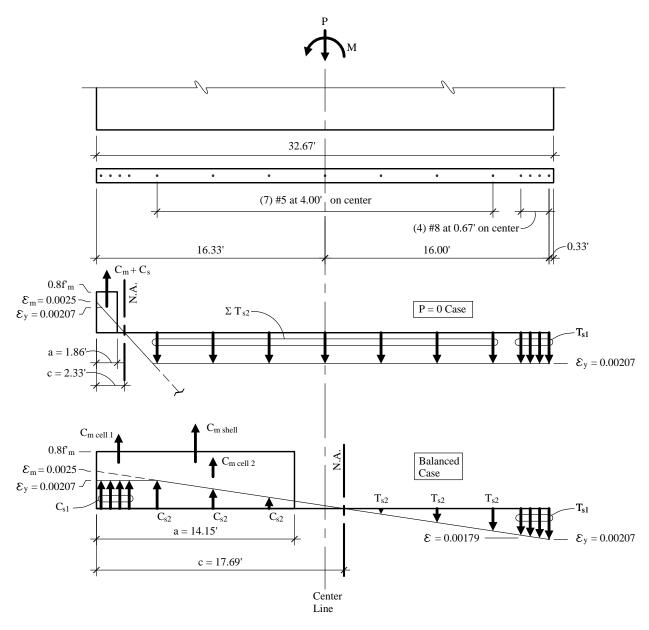
			Load Com	bination 1	Load Combination 2		
Level (x)	$P_D$ (kips)	$P_L$ (kips)	$P_u$ (kips)	M <sub>u</sub> (ft-kips)	$P_u$ (kips)	$M_u$ (ft-kips)	
5	63	0	88	770	44	770	
4	126	8	180	2229	88	2229	
3	189	17	273	4203	132	4203	
2	251	25	364	6522	176	6522	
1	314	34	456	9012	220	9012	

Table 9.2-19 Los Angeles Load Combinations for Wall D

1.0 kip = 4.45 kN, 1.0 ft-kip = 1.36 kN-m

Strength at the bottom story (where P, V, and M are the greatest) is examined. This example considers Load Combination 2 from Table 9.2.19 to be the governing case, because it has the same lateral load as Load Combination 1 but lower values of axial force.

Refer to Figure 9.2-13 for notation and dimensions.



**Figure 9.2-13** Los Angeles: Strength of wall D (1.0 ft = 0.3048 m). Strength diagrams superimposed on strain diagrams for the two cases.

Examine the strength of Wall D at Level 1:

 $P_{u_{min}} = 220$  kips  $P_{u_{max}} = 456$  kips  $M_u = 9,012$  ft-kips

Because special reinforced masonry shear walls are used (Seismic Design Category D), vertical reinforcement at 4 ft. on center and horizontal bond beams at 4 ft on center are prescribed (*Provisions* Sec. 11.3.7.3 [ACI 530, Sec. 1.13.2.2.5]). (Note that the wall is 43.33 ft high, not 8 ft high, for purposes of determining the maximum spacing of vertical and horizontal reinforcement.)

For this bending moment, the minimum vertical reinforcement will not suffice. For reinforcement uniformly distributed, a first approximation could be taken from a simple model using an effective internal moment arm of 80 percent of the overall length of the wall:

$$A_{s} = \frac{M - 0.8Pl/2}{60(\text{ksi})(0.8l/2)} = \frac{9012 - 0.8 \times 220 \times 32.67/2}{60 \times 0.8 \times 32.67/2} = 7.8 \text{ in}^{2} = 0.24 \text{ in}^{2}/\text{ft}.$$

The minimum vertical steel is 0.0007 times the gross area, which is 0.064 in.<sup>2</sup>/ft. At the maximum spacing of 4 ft, a #5 bar is slightly above the minimum. Experimental evidence indicates that uniformly distributed reinforcement will deliver good performance. This could be accomplished with a #9 bar at 48 in. or a #8 bar at 40 in. This design will work well in a wall that is solidly grouted; however, for walls that are grouted only at cells containing reinforcement, it will be found that this wall fails the ductility check (which can be remedied by placing several extra grouted cells near each end of the wall as was shown in Sec. 9.1.5.4). The flexural design was completed before the shear design (described in the previous section) discovered the need for solid grout in the first story. The remainder of this flexural design check is carried out without consideration of the added grout. (It is unlikely that the interaction line will be affected near the design points, but the balanced point will definitely change.)

It has long been common engineering practice to concentrate flexural reinforcement near the ends of the wall. (This a normal result of walls that intersect to form flanges with reinforcement in both web and flange.) For this design, if one uses the minimum #5 bar at 48 inches, then the extra steel at the ends of the walls is approximately:

$$A_{send} = (7.8 - 7 \times 0.31) / 2 = 2.8 \text{ in}^2$$

Try #8 bars in each of the first four end cells and #5 bars at 4 ft on center at all intermediate cells.

The calculation procedure is similar to that presented in Sec. 9.2.4.5.2. The strain and stress diagrams are shown in Figure 9.2-13 for the Birmingham 1 building and the results are as follows:

P = 0 case

 $\phi P_n = 0$  $\phi M_n = 6,636 \text{ ft-kips}$ 

Intermediate case, setting c = 4.0 ft

 $\phi P_n = 223 \text{ kips}$   $\phi M_n = 9,190 \text{ ft-kips}$ 

Balanced case

 $\phi P_n = 1049$  kips  $\phi M_n = 14,436$  ft-kips

The simplified  $\phi P_n - \phi M_n$  curve is shown in Figure 9.2-14 and indicates the design with #8 bars in the first four end cells and #5 bars at 4 ft on center throughout the remainder of the wall is satisfactory.

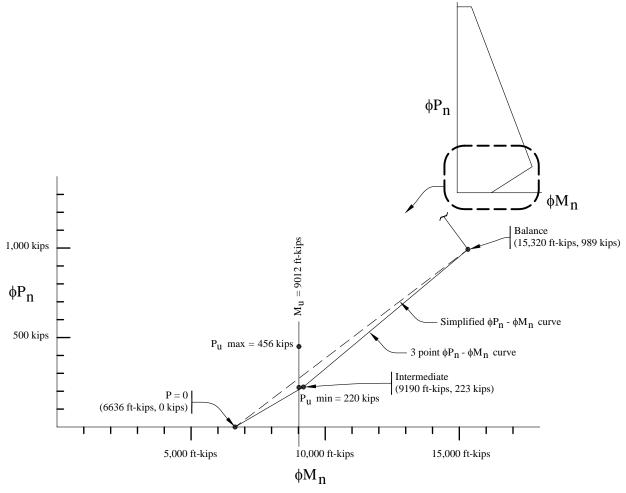


**Figure 9.2-14**  $\varphi P_{11} - \varphi M_{11}$  diagram for Los Angeles Wall D (1.0 kip = 4.45 kN, 1.0 kip-ft = 1.36 kN-m).

#### 9.2.7.5.2.2 Ductility check

*Provisions* Sec. 11.6.2.2 [ACI 530, Sec. 3.2.3.5] has been illustrated in the prior designs. Recall that this calculation uses unfactored gravity axial loads (*Provisions* Sec. 11.6.2.2 [ACI 530, Sec. 3.2.3.5]). Refer to Figure 9.2-15 and the following calculations which illustrate this using loads at the bottom story (highest axial loads). The extra grout required for shear is also ignored here. More grout gives higher compression capacity, which is conservative.

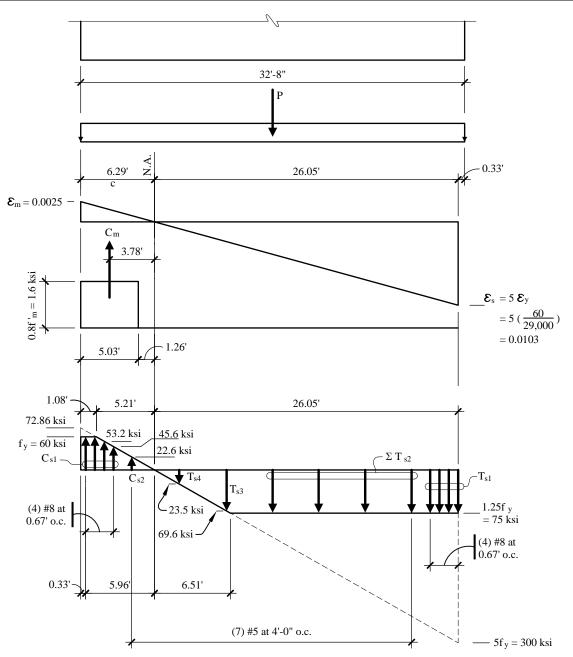


Figure 9.2-15 Ductility check for Los Angeles Wall D (1.0 ft = 0.3048 m, 1.0 ksi = 6.89 MPa)

For Level 1 (bottom story), the unfactored loads are:

P = 314 kips $C_m = 0.8f'_m[(a)(b) + A_{cells}]$ 

where b = flange width = (2 × 1.25 = 2.5 in.) and  $A_{cells} = 41$  in.<sup>2</sup>

 $C_m = (1.6 \text{ ksi})[(5.03 \text{ ft} \times 12)(2.5 \text{ in.}) + (5 \text{ cells})(41)] = 569.4 \text{ kips}$   $C_{s1} = 0.79(2 \text{ x} 60 + 53.2 + 45.6) = 172.9 \text{ kips}$  $C_{s2} = (22.6 \text{ ksi})(0.31 \text{ in.}^2) = 7.0 \text{ kips}$   $\sum C = 749 \text{ kips}$   $\sum T_{sl} = (4 \times 0.79 \text{ in.}^2)(75 \text{ ksi}) = 237 \text{ kips}$   $\sum T_{s2} = (4 \times 0.31 \text{ in.}^2)(75 \text{ ksi}) = 93.0 \text{ kips}$   $T_{s3} = (0.31 \text{ in.}^2)(69.6 \text{ ksi}) = 21.6 \text{ kips}$   $T_{s4} = (0.31 \text{ in.}^2)(23.5 \text{ ksi}) = 7.3 \text{ kips}$   $\sum T = 359 \text{ kips}$  $\sum C > \sum P + T$ 

749 kips > 673 kips

If a solution with fully distributed reinforcement were used, the tension from reinforcement would increase while the compression from grout at the end of the wall, as well as compression of steel at the compression would also decrease. The criterion would not be satisfied. Adding grout would be required.

[Refer to Sec. 9.2.4.5.2 for discussion of revisions to the ductility requirements in the 2003 Provisions.]

#### 9.2.7.6 Los Angeles Deflections

Recall the assertion that the calculations for deflection involve many variables and assumptions and that any calculation of deflection is approximate at best. The requirements and procedures for computing deflection are provided in Sec. 9.2.4.6. [Refer to Sec. 9.2.4.6 for discussion of revisions to the deflection computations and requirements in the 2003 *Provisions*, as well as the potentially conflicting drift limits.]

For the Los Angeles building, the determination of whether the walls will be cracked is as follows:

 $b_e$  = effective masonry wall width  $b_e = [(2 \times 1.25 \text{ in.})(32.67 \text{ ft} \times 12) + (15 \text{ cells})(41 \text{ in.}^2/\text{cell})]/32.67 \text{ ft} \times 12) = 4.07 \text{ in.}$   $A = b_e l = (4.07 \text{ in.})(32.67 \times 12) = 1595 \text{ in.}^2$   $S = b_e l^2/6 = (7.07)(32.67 \times 12)^2/6 = 104,207 \text{ in.}^3$  $f_r = 0.250 \text{ ksi}$ 

 $P_u$  is calculated using 1.00*D* (See Table 9.2-18 for values, and refer to Sec. 9.2.4.6 for discussion). Table 9.2-20 provides a summary of these calculations. (The extra grout required for shear strength is also not considered here; the revision would slightly reduce the computed deflections by raising the cracking moment.)

Level	$P_{u_{min}}$ (kips)	M <sub>cr</sub> (ft-kips)	$M_x$ (ft-kips)	Status
5	63	2514	770	uncracked
4	126	2857	2229	uncracked
3	189	3200	4203	cracked
2	251	3538	6522	cracked
1	314	3880	9012	cracked

Table 9.2-20 Los Angeles Cracked Wall Determination

1.0 kip = 4.45 kN, 1.0 ft-kip = 1.36 kN-m.

For the uncracked walls (Levels 4 and 5):

$$I_n = I_e = b_e l^3 / 12 = (4.07 \text{ in.})(32.67 \times 12)^3 / 12 = 2.04 \times 10^7 \text{ in.}^4$$

For the cracked walls, the transformed cross section will computed by classic methods. Assuming the neutral axis to be about 10 ft in from the compression face gives five #5 bars in tension. The tension reinforcement totals:

$$A_s = 4(0.79) + 5(0.31) = 3.16 + 1.55 = 4.71$$
 in.<sup>2</sup>

The axial compression stiffens the wall. The effect is approximated with an equivalent area of tension reinforcement equal to half the compression. Thus, the total reinforcement becomes:

$$A_{se} = 4.71 + 0.5(314)/60 = 4.71 + 2.62 = 7.33 \text{ in.}^2$$

The centroid of this equivalent reinforcement is 29.5 ft from the compression face. Following the classic method for transformed cracked cross sections and with n = 19.3:

 $\rho = 7.33/(4.04 \text{ x } 29.5 \text{ x } 12) = 0.0051$   $\rho n = 0.0051(19.3) = 0.099$   $k = \text{sqrt}(\rho n^2 + 2\rho n) - \rho n = 0.36$ kd = c = 10.5 feet (which is close enough to the assumed 10 feet)

$$I_{cr} = bc^{3}/3 + \sum nA_{s}d^{2} = 4.04(29.5 \text{ x } 12)^{3} + 19.3(7.33)(29.5 - 10.5)^{2}(144) = 1.01 \text{ x } 10^{7} \text{ in.}^{2}$$

The *Provisions* encourages the use of the cubic interpolation formula illustrated for the previous locations. For the values here, this yields  $I_{eff} = 1.09 \times 10^7$  in.<sup>4</sup>, which is about half the gross moment of inertia (which in itself is not a bad approximation for a cracked and well reinforced cross section). For this example, the deflection computation will instead use the cracked moment of inertia in the lower three stories and the gross moment of inertia in the upper two stories. The results from a RISA 2D analysis are shown in Table 9.2-21, and are about 5 percent higher than use of  $I_{eff}$  over the full height.

Level	F (kips)	$I_{eff}$ (in. <sup>4</sup> )	$\delta_{\scriptscriptstyle flexural} \ ( ext{in.})$	$\delta_{\scriptscriptstyle shear} \ ( ext{in.})$	$\delta_{\scriptscriptstyle total}$ (in.)	$C_d \delta_{total}$ (in.)	⊿ (in.)
5	84.0	$2.04  imes 10^7$	0.491	0.127	0.618	2.163	0.455
4	75.1	$2.04 \times 10^{7}$	0.370	0.118	0.488	1.708	0.543
3	56.3	1.01  imes 107	0.237	0.096	0.333	1.166	0.515
2	37.6	$1.01 \times 10^{7}$	0.118	0.068	0.186	0.651	0.413
1	18.8	$1.01  imes 10^7$	0.033	0.035	0.068	0.238	0.238

 Table 9.2-21
 Los Angeles Deflections

1.0 kip = 4.45 kN, 1.0 in. = 25.4 mm.

The maximum drift occurs at Level 4 per Provisions Table 5.2.8 is:

$$\Delta = 0.543$$
 in. < 1.04 in. = 0.01  $h_n$  (Provisions Table 5.2.8 [Table 4.5-1]) OK

#### 9.2.7.7 Los Angeles Out-of-Plane Forces

*Provisions* Sec 5.2.6.2.7 [Sec. 4.6.1.3] requires that the bearing walls be designed for out-of-plane loads determined as follows:

 $w = 0.40 S_{DS} W_c \ge 0.1 W_c$ w = (0.40)(1.00)(60 psf) = 24psf \ge 0.1 W\_c The out-of-plane bending moment, using the strength design method for masonry, for a pressure, w = 24psf and considering the P-delta effect, is computed to be 2,232 in.-lb/ft. This compares to a computed strength of the wall of 14,378 in.-lb/ft, considering only the #5 bars at 4 ft on center. Thus, the wall is loaded to about 16 percent of its capacity in flexure in the out-of-plane direction. (See Sec. 9.1 for a more detailed discussion of strength design of masonry walls, including the P-delta effect.)

# 9.2.7.8 Los Angeles Orthogonal Effects

According to Provisions Sec. 5.2.5.2.2 [Sec. 4.4.2.3], orthogonal interaction effects have to be considered for Seismic Design Category D when the ELF procedure is used (as it is here).

The out-of-plane effect is 16 percent of capacity, as discussed in Sec. 9.2.7.7 above. When considering the 0.3 combination factor, the out-of-plane action adds about 5 percent overall to the interaction effect. For the lowest story of the wall, this could conceivably require a slight increase in capacity for in-plane actions. In the authors' opinion, this is on the fringe of requiring real consideration (in contrast to the end walls of Example 9.1).

This completes the design of the transverse Wall D.

# 9.2.7.9 Los Angeles Summary of Wall Design for Wall D

8-in. CMU  $f'_{m} = 2,000 \text{ psi}$ 

**Reinforcement:** 

Four vertical #8 bars, one bar in each cell for the four end cells Vertical #5 bars at 4 ft on center at intermediate cells Two bond beams with two #5 bars at each story, at floor bearing and at 4 ft above each floor Horizontal joint reinforcement at alternate courses recommended, but not required

Grout:

All cells with reinforcement and bond beams, plus solid grout at first story, at two out of three cells in the second story, and at six extra cells in the third story

Table 9.2-22 compares the reinforcement and grout for Wall D designed for each of the four locations.

	Table 9.2-22         Variation in Reinforcement and Grout by Location							
	Birmingham 1	New York City	Birmingham 2	Los Angeles				
Vertical bars	5 - #4	9 - #4	12 - #4	8 - #8 + 7 - #5				
Horizontal bars	10#4 + jt. reinf	10 - #4 + jt. reinf	20 - #5	20 - #5				
Grout (cu. ft.)	91	122	189	295				

Table 0.2.22 Variation in Painforcement and Grout by Location

 $1 \text{ cu. ft.} = 0.0283 \text{ m}^3$ .

# 9.3 TWELVE-STORY RESIDENTIAL BUILDING IN LOS ANGELES, CALIFORNIA

# 9.3.1 Building Description

This 12-story residential building has a plan form similar to that of the five-story masonry building described in Sec. 9.2. The floor plan and building elevation are illustrated in Figures 9.3-1 and 9.3-2, respectively. The floors are composed of 14-in.-deep open web steel joists spaced at 30 in. that support a 3-in. concrete slab on steel form deck. A fire-rated ceiling is included at the bottom chord of the joists. Partitions, including the shaft openings, are gypsum board on metal studs, and the exterior nonstructural curtain walls are glass and aluminum.

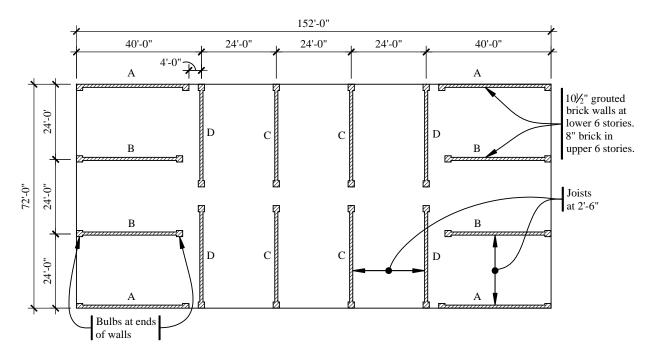


**Figure 9.3-1** Floor plan (1.0 ft = 0.3048 m, 1.0 in. = 25.4 mm)

All structural walls are of grouted brick. For purposes of illustration, two styles of wall are included. The lower six stories have 10-1/2in.-thick walls consisting of two wythes of 4-in. (nominal) brick and a 3-1/4-in. grout space. The upper six stories have 8-in. (nominal) brick, hollow unit style, with the vertical reinforcing in the cells and the horizontal reinforcing in bond beams. (In actual construction, however, a single style wall might be used throughout: either a two-wythe grouted wall or a through-the-wall unit of an appropriate thickness). The walls are subject to high overturning moments and have a reinforced masonry column at each end. The column concentrates the flexural reinforcement and increases resistance to overturning. (Similar concentration and strength could be obtained with transverse masonry walls serving as flanges for the shear walls had the architectural arrangement been conducive to this approach.) Although there is experimental evidence of improved performance of walls with all vertical reinforcement uniformly distributed, concentration at the ends is common in engineering practice and the flexural demands are such for this tall masonry building that the concentration of masonry and reinforcement at the ends is simply much more economical.

The compressive strength of masonry,  $f'_m$ , used in this design is 2,500 psi for Levels 1 through 6 and 3,000 psi for Levels 7 through 12.

This example illustrates the following aspects of the seismic design of the structure:

- 1. Development of equivalent lateral forces
- 2. Reinforced masonry shear wall design
- 3. Check for building deflection and story drift
- 4. Check of diaphragm strength.

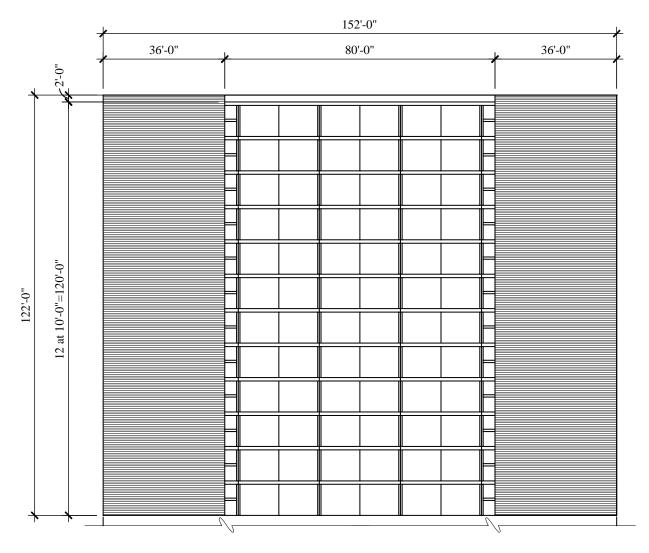


**Figure 9.3-2** Elevation (1.0 ft = 0.3048 m, 1.0 in. = 25.4 mm)

# **9.3.2 Design Requirements**

#### 9.3.2.1 *Provisions* Design Parameters

Table 9.3-1 shows the design parameters for building design.

Design Parameter	Value
<i>S<sub>s</sub></i> (Map 1 [Figure 3.3-3])	1.5
<i>S</i> <sub>1</sub> (Map 2 [Figure 3.3-4])	0.6
Site Class	С
$F_a$	1
$F_v$	1.3
$S_{MS} = F_a S_s$	1.5
$S_{MI} = F_{\nu}S_{I}$	0.78
$S_{DS} = 2/3 S_{MS}$	1
$S_{DI} = 2/3 S_{MI}$	0.52
Seismic Design Category	D
Masonry Wall Type	Special Reinforced
R	3.5
$arOmega_0$	2.5
$C_d$	3.5

 Table 9.3-1 Design Parameters

[The 2003 *Provisions* have adopted the 2002 USGS probabilistic seismic hazard maps, and the maps have been added to the body of the 2003 *Provisions* as figures in Chapter 3 (instead of the previously used separate map package).]

#### 9.3.2.2 Structural Design Requirements

The load path consists of the floors acting as horizontal diaphragms and the walls parallel to the motion acting as shear walls.

Soil-structure interaction is not considered.

The building is a bearing wall system (Provisions Table 5.2.2 [4.3-1]).

Deformational compatibility must be assured (*Provisions* Sec. 5.2.2.4.3 [Sec. 4.5.3]). The structural system is one of non-coupled shear walls. Crossing beams over the halls (their design is not included in this example) will need to continue to support the gravity loads from the floors and roof during an earthquake but will not provide coupling between the shear walls.

The building is symmetric in plan but has the same torsional irregularity described in Sec. 9.2.5.4. The vertical configuration is regular except for the change in wall type between the sixth and seventh stories, which produces a significant discontinuity in stiffness and strength, both for shear and flexure (*Provisions* Sec. 5.2.3.3 [Sec. 4.3.2.3] and 5.2.6.2.3 [Sec. 4.6.1.6]). There is no weak story because the strength does not increase as one goes upward. The stiffness discontinuity will be shown to qualify as regular.

*Provisions* Table 5.2.5.1 [Table 4.4-1] would not permit the use of the ELF procedure of *Provisions* Sec. 5.4 [Sec. 5.2]; instead a dynamic analysis of some type is required. As will be illustrated, this particular building does not really benefit from this requirement.

The design and detailing must comply with the requirements of Provisions Sec. 5.2.6 [Sec. 4.6].

The walls must resist forces normal to their plane (*Provisions* Sec. 5.2.6.2.7 [Sec. 4.6.1.3]). These forces will be used when addressing the orthogonal effects (*Provisions* Sec. 5.2.5.2.2 [Sec. 4.4.2.3]).

With eight walls in each direction, the system is expected to be redundant.

Tie and continuity requirements for anchorage of masonry walls must be considered when detailing the connections between floors and walls (*Provisions* Sec. 5.2.6.1.2 [Sec. 4.6.2.1] and 5.2.6.1.3).

Openings in walls and diaphragms need to be reinforced (Provisions Sec. 5.2.6.2.2 [Sec. 4.6.1.4]).

Diaphragms need to be designed to comply with Provisions Sec. 5.2.6.2.6 [Sec. 4.6.3.4].

The story drift limit is  $0.01h_{sx}$  (*Provisions* Sec. 5.2.8 [Sec. 4.5.1]) and the overall drift limit is  $0.01h_{sn}$  (*Provisions* Sec. 11.5.4.1). For this structure the difference between these two is significant, as will be shown.

[The deflection limits have been removed from Chapter 11 of the 2003 *Provisions* because they were redundant with the general deflection limits. Based on ACI 530 Sec. 1.13.3.2, the maximum drift for all masonry structures is 0.007 times the story height. Thus, there appears to be a conflict between ACI 530 and 2003 *Provisions* Table 4.5-1.]

# 9.3.2.3 Load Combinations

The basic load combinations (*Provisions* Sec. 5.2.7 [Sec. 4.2.2]) are the same as those in ASCE 7 except that the seismic load effect, *E*, is defined by *Provisions* Eq. 5.2.7-1 [Eq. 4.2-1] and 5.2.7-2 [Eq. 4.2-2] as:

$$E = \rho Q_E \pm 0.2 S_{DS} D$$

Based on the configuration of the shear walls and the results presented in Sec. 9.2, the reliability factor,  $\rho$ , is treated as equal to 1.0 for both directions of loading. Refer to Sec. 9.2.3.1 for additional information.

[The redundancy requirements have been substantially changed in the 2003 *Provisions*. For a shear wall building assigned to Seismic Design Category D,  $\rho = 1.0$  as long as it can be shown that failure of a shear wall with height-to-length-ratio greater than 1.0 would not result in more than a 33 percent reduction in story strength or create an extreme torsional irregularity. The intent is that the aspect ratio is based on story height, not total height. Therefore, the redundancy factor would not have to be investigated ( $\rho = 1.0$ ) for this building.]

The discussion on load combinations for the Los Angeles site in Sec.9.2 is equally applicable to this example. Refer to Sec. 9.2.3.2 for determination of load combinations.

The load combinations representing the extreme cases are:

$$1.4D + Q_E + 0.5L$$
$$0.7D + Q_E$$

# 9.3.3 Seismic Force Analysis

The analysis is performed using the ELF procedure of *Provisions* Sec. 5.4 [Sec. 5.2] and checked with a modal response spectrum (MRS) analysis in conformance with *Provisions* Sec. 5.5 [Sec. 5.3]. This

example illustrates an analysis for earthquake motions acting in the transverse direction only. Earthquake motions in all directions will need to be addressed for an actual project.

# 9.3.3.1 Building Weights

For the ELF analysis, the masses are considered to be concentrated at each floor level whereas, for the MRS analysis, it is distributed on both wall and floor elements. Note that the term "level" corresponds to the slab above each story. Thus Level 1 is the second floor; Level 12 is the roof.

Lower Levels:

Upper

Roof:

	Slab, joists, partitions, ceiling, mechanical/electrical (0.053 ksf)(152 ft)(72 ft) = $580$ kips/		
	Walls: 10.5 in. at 114 psf (brick at 73 psf + grout at (0.114 ksf)(10 ft)[(8)(29 ft) + (4)(30 ft) + (4)(32 ft)]		
	Bulbs at ends of walls: (24 in. $\times$ 24 in. bulb) Brick: 2.01 ft <sup>2</sup> /bulb; Grout: 1.99 ft <sup>2</sup> /bulb [(2.01 ft <sup>2</sup> )(0.120 kcf) + (1.99 ft <sup>2</sup> )(0.150 kcf)] (10 ft)(	32 bulbs) = 173 kips/story	
• ]	Levels:		
	Slab, joists, partitions, ceiling, M/E, curtain wall at 5 (0.053 ksf)(152 ft)(72 ft)	53 psf = 580 kips/story	
	Walls: 8 in. Partially grouted brick at 48 psf (0.048 ksf)(10 ft)[(8)(29.67 ft) + (4)(30.67 ft	32.67 ft)] = 236 kips/story	
	Bulbs at ends of walls (grouted 20 in. $\times$ 20 in. brick (0.315 klf/bulb)(10 ft)(32 bulbs)	bulb) = 101 kips/story	
	Slab, roofing, joists,, ceiling, M&E, curtain wall at 5 (0.053 ksf)(152 ft)(72 ft)	53 psf : = 580 kips	
	Walls (238 kips/story + 101 kips/story)/2 = 1	70 kips	
	Parapet		

(4 parapets)(2 ft)[(0.048 kips/lf)(33 ft) + (3.15 kips/bulb)(2 bulbs)/(10 ft)] = 18 kips

Preliminary design indicates a 10-1/2-in. wall with bulbs for the six lower stories and an 8-in. wall with bulbs for the six upper stories. Therefore, effective seismic weight, *W*, is computed as follows:

Levels 1-5	(5)(580 + 547 + 173)	= (5)(1,300  kips/level)	=	6,500 kips
Level 6	580 + (547 + 236)/2 + (173 + 101)/2	= 1,109 kips	=	1,109 kips
Levels 7-11	(5)(580 + 236 + 101)	= (5)(917  kips/level)	=	4,585 kips
Level 12 (roof)	(580 + 170 + 18)	= 768 kips	=_	<u>768 kips</u>
Total			=	12,962 kips

The weight of the lower half of walls for the first story are not included with the walls for Level 1 because the walls do not contribute to the seismic loads.

#### 9.3.3.2 Base Shear

The seismic coefficient,  $C_s$ , for the ELF analysis is computed as:

$$C_s = \frac{S_{DS}}{R/I} = \frac{1.00}{3.5/1.0} = 0.286$$

The value of  $C_s$  need not be greater than:

$$C_s = \frac{S_{DI}}{T(R/I)} = \frac{0.52}{(0.75)(3.5/1)} = 0.198$$

The value of the fundamental period, T, was determined from a dynamic analysis of the building modeled as a cantilevered shear wall. RISA 2D was used for this analysis, with cracked sections taken into account. From this analysis, a period of T = 0.75 sec was determined. See Sec. 9.3.4. This value is also obtained from the 3D dynamic analysis (described subsequently) for the first translational mode in the transverse direction when using a reduced modulus of elasticity to account for cracking in the masonry (approximately 60 percent of the nominal value for E). *Provisions* Sec. 5.4.2 [Sec. 5.2-2] requires that the fundamental period, T, established in a properly substantiated analysis be no larger than the approximate period,  $T_a$ , multiplied by  $C_u$ , determined from *Provisions* Table 5.4.2 [Table 5.2-1]. The approximate period of the building,  $T_a$ , is calculated based as:

$$T_a = C_r h_a^{3/4} = (0.02)(120)^{0.75} = 0.725 \text{ sec}$$

where  $C_r = 0.02$  from *Provisions* Table 5.4.2.1 [Table 5.2-2], and  $h_n = 120$  ft

$$T_a C_u = (0.725)(1.4) = 1.015 \text{ sec} > 0.75 \text{ sec} = T$$

(Note that T = 0.75 sec will be verified later when deflections are examined).

The value for  $C_s$  is taken to be 0.198 (the minimum of the two values computed above). This value is still larger than the minimum specified:

 $C_s = 0.044 IS_{DI} = (0.044)(1.0)(0.60) = 0.0264$ 

[This minimum Cs value has been removed in the 2003 *Provisions*. In its place is a minimum Cs value for long-period structures, which is not applicable to this example.]

The total seismic base shear is then calculated by Provisions Eq. 5.4.1 [Eq. 5.2-1]:

$$V = C_s W = (0.198)(12,962 \text{ kips}) = 2,568 \text{ kips}$$

A 3-D model was created in SAP 2000 for the MRS analysis. Just as for the five-story building described in Sec. 9.2, the masonry walls were modeled as shell bending elements and the floors were modeled as an assembly of beams and shell membrane elements. See Sec. 9.2.6.2 for further description. The difference in  $f'_m$  between upper and lower stories was not modeled; the value of  $E_m$  used was 1,100 ksi, which is 59 percent of the value from *Provisions* Eq. 11.3.10.2 for the lower stories. [Note that by adopting ACI 530 in the 2003 *Provisions*,  $E_m = 900f'_m$  per ACI 530 Sec. 1.8.2.2.1.] As mentioned, this value was selected as

an approximation of the effects of flexural cracking. Unlike the five-story building, the difference in length between the longitudinal and transverse walls was modeled. However, to simplify construction of the model, wall types A and B are the same length. Because this example illustrates design in the transverse direction, this liberty has little effect. Table 9.3-2 shows data on the modes of vibration used in the analysis.

	direction for modes used in analysis							
Mode	Period	Individu	ial mode (	percent)	Cumula	tive sum (	percent)	Trans.
number	(seconds)	Long.	Trans.	Vert.	Long.	Trans.	Vert.	base shear
1	0.9471	0.00	0.00	0.00	0.00	0.00	0.00	0.0
2	0.7469	0.00	59.12	0.00	0.00	59.12	0.00	1528.0
3	0.6941	59.16	0.00	0.00	59.16	59.12	0.00	0.0
4	0.2247	0.00	0.00	0.00	59.16	59.12	0.00	0.0
5	0.1763	0.00	24.38	0.00	59.16	83.50	0.00	896.2
6	0.1669	24.57	0.00	0.00	83.73	83.50	0.00	0.0
7	0.1070	0.00	0.01	0.00	83.73	83.51	0.00	0.5
8	0.1059	0.00	0.00	0.28	83.74	83.51	0.28	0.0
9	0.1050	0.00	0.00	29.48	83.74	83.51	29.76	0.0
10	0.0953	0.00	0.00	0.00	83.74	83.51	29.76	0.0
11	0.0900	0.00	0.00	1.51	83.74	83.51	31.27	0.0
12	0.0858	0.00	0.03	0.01	83.74	83.54	31.28	1.1
13	0.0832	0.00	7.25	0.00	83.74	90.79	31.28	234.4
14	0.0795	7.11	0.00	0.00	90.85	90.79	31.28	0.0
15	0.0778	0.04	0.00	0.19	90.88	90.79	31.48	0.0
16	0.0545	0.00	4.47	0.00	90.88	95.26	31.48	117.5
17	0.0526	4.44	0.00	0.00	95.32	95.26	31.48	0.0
18	0.0413	0.01	1.24	0.00	95.33	96.51	31.48	29.1
19	0.0392	1.66	0.05	0.00	96.99	96.55	31.48	1.1
20	0.0358	0.07	0.87	0.00	97.06	97.43	31.48	19.5
21	0.0288	1.59	0.33	0.01	98.66	97.76	31.49	7.0
22	0.0278	0.33	1.40	0.00	98.99	99.16	31.49	28.9
23	0.0191	0.76	0.23	0.01	99.75	99.39	31.50	4.3
24	0.0186	0.23	0.60	0.00	99.98	99.98	31.50	11.1

 Table 9.3-2
 Periods, mass participation ratios, and modal base shears in the transverse direction for modes used in analysis

1 kip = 4.45kN.

The combined modal base shear is 1,791 kips

The fundamental mode captures no translation of mass; it is a pure torsional response. This is a confirmation of the intent of the torsional irregularity provision. The first translational mode has a period of 0.75 sec, confirming the earlier statements. Also note that the base shear is only about 70 percent of the ELF base shear (2,568 kips) even though the fundamental period is the same. The ELF analysis assumes that all the mass participates in the fundamental mode whereas the dynamic analysis does not. The absolute sum of modal base shears is higher than the ELF but the statistical sum is not. *Provisions* Sec. 5.5.7 requires that the modal base shear be compared with 85 percent of the ELF base shear. The comparison value is 0.85(2,568 kips), which is 2,183 kips. Because this is greater than the value from the modal analysis, the modal analysis results would have to be factored upwards by the ratio 2,183/1,791 = 1.22. The period used for this comparison cannot exceed  $C_u T_a$ , which is 1.015 sec as described previously. Note that the period used is from Mode 2, because Mode 1 is a purely torsional mode. The 1.22 factor is very close to the factor for the five story building computed in Sec. 9.2.6.2; an additional comparison will follow.

# 9.3.3.3 Vertical Distribution of Seismic Forces

Carrying forward with the ELF analysis, *Provisions* Sec. 5.4.3 [Sec. 5.2.3] provides the procedure for determining the portion of the total seismic loads assigned to each floor level. The story force,  $F_x$ , is calculated as:

$$F_x = C_{vx}V$$

and

$$C_{vx} = \frac{w_x h_x^k}{\sum_{i=1}^n w_i h_i^k}$$

For T = 0.75 sec, which is between 0.5 sec and 2.5 sec, the value of k is determined to be 1.125 based on interpolation (*Provisions* Sec. 5.4.3 [Sec. 5.2.3]).

The seismic design shear in any story shall be determined from:

$$V_x = \sum_{i=x}^n F_i$$

The story overturning moment is computed from:

$$M_x = \sum_{i=x}^n F_i (h_i - h_x)$$

Table 9.3-3 shows the application of these equations for this building.

					•		
Level (x)	$w_x$ (kips)	$h_x$ (kips)	$w_x h_x^{1.125}$ (ft-kips)	$C_{vx}$	$F_x$ (kips)	$V_x$ (kips)	$M_x$ (kips)
12	768	120	167,700	0.128	329	329	3,300
11	917	110	181,500	0.139	357	686	10,200
10	917	100	163,100	0.125	320	1,006	20,200
9	917	90	144,800	0.111	284	1,291	33,100
8	917	80	126,900	0.097	249	1,540	48,500
7	917	70	109,200	0.084	214	1,754	66,000
6	1,109	60	111,000	0.085	218	1,972	85,800
5	1,300	50	106,000	0.081	208	2,181	107,600
4	1,300	40	82,500	0.063	162	2,342	131,000
3	1,300	30	59,700	0.046	117	2,460	155,600
2	1,300	20	37,800	0.029	74	2.534	181,000
1	1,300	10	17,300	0.013	34	2,568	206,600
			1,307,400	1.00	2,568		

Table 9.3-3 Seismic Forces and Moments by Level

1.0 kip = 4.45 kN, 1.0 ft = 0.3048 m, 1.0 ft-kip = 1.36 kN-m.

The dynamic modal analysis does give a direct output for the gross overturning moment, of about 66 percent of the moment from the ELF analysis. Because the model is built with shell elements, there is no direct value for the variation of moment with height.

#### 9.3.3.4 Horizontal Distribution

For the ELF analysis, the approach is essentially the same as used for the five-story masonry building described in Sec. 9.2.4.4:

Direct shear: All transverse walls have the same properties, except axial load. Axial load affects cracking but, each wall considered has the same stiffness. Therefore, each will resist an equivalent amount in direct shear:

$$V = V/8 = 0.125 V_x$$

Torsion: The center of mass corresponds with the center of resistance; therefore, the only torsion is due to the 5 percent accidental eccentricity in accordance with *Provisions* Sec. 5.4.4.2 [Sec. 5.2.4.2]:

$$M_{ta} = 0.05 \ bV = (0.05)(152 \ \text{ft})V = 7.6V$$

The longitudinal walls are slightly longer than the transverse walls. Unlike the example in Sec. 9.2, this difference will be illustrated here in a simple fashion. The diaphragm is assumed to be rigid. When the walls are not identical, a measure of the actual stiffness is necessary; for masonry walls, this involves both flexural and shear deformations. The conventional technique is an application of the following equation for deformation of a simple cantilever wall without bulbs or flanges at the ends:

$$\Delta_{wall} = \frac{Vh^3}{3E_mI} + \frac{6Vh}{5G_mA}$$

Considering  $G_m = 0.4 E_m$ , A = Lt, and  $I = L^3 t/12$ , this can be simplified to :

$$\Delta_{wall} = \frac{V}{Et} \left[ 4 \left( \frac{h}{L} \right)^3 + 3 \left( \frac{h}{L} \right) \right]$$

Rigidity, *K*, is inversely proportional to deflection. Considering *E* and *t* as equal for all walls:

$$K = \frac{1}{4\left(\frac{h}{L}\right)^3 + 3\left(\frac{h}{L}\right)}$$

Figure 9.3-3 identifies the walls.

For a multistory building, the quantity *h* is not easy to pin down. For this example, the authors suggest the following approach: use h = 10 ft (one story) to evaluate the shear in the wall at the base and also use h = 80 ft (two thirds of total height) to evaluate the moments in the walls. Table 9.3-4 shows some of the intermediate steps for these two assumptions.

(*d*, as used here, is the distance of the wall to the centroid of the building, not the length of the wall, as used elsewhere)

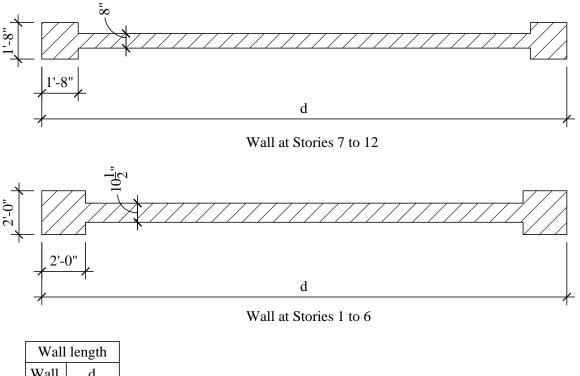
	Table 9.3-4         Relative Rigidities										
XX 7 11	T .1		for	shear, $h = 1$	10 ft	for	for moment, $h = 80$ ft				
Wall	Length (ft)	Arm, $d$ - (ft)	h/d	K	$Kd^2(\mathrm{ft}^2)$	h/d	K	$Kd^2(\mathrm{ft}^2)$			
А	36	36	0.278	1.088	1,410	2.22	0.01978	25.63			
В	34	12	0.294	1.017	146	2.35	0.01690	2.43			
С	33	12	0.303	0.980	141	2.42	0.01556	2.24			
D	33	36	0.303	0.980	1,270	2.42	0.01556	20.17			
					2,967			50.47			

1.0 ft = 03.048 m

The total torsional rigidity is four times the amount in Table 9.3-4, since there are four walls of each type. When considering torsion, Wall D is the critical member (shortest length, greatest d).

For shear due to accidental torsion:

$$V_{t} = \frac{MKd}{\Sigma Kd^{2}} = 7.6V \left[ \frac{(0.980)(36)}{4(2,967)} \right] = 0.0226V \text{ or } 7.6V \left[ \frac{0.01556(36)}{4(50.47)} \right] = 0.0211V$$



Wall length			
Wall	d		
А	36'-0"		
В	34'-0"		
С	33'-0"		
D	33'-0"		

Figure 9.3-3 Wall dimensions (1.0 in. = 25.4 mm, 1.0 ft = 0.0348 m).

When considering the approximations involved, the remainder of the ELF example will simply use 0.0226V for  $V_t$ . Because a 3D analytical model exists, a simplistic load case with a static horizontal torsion at each level was defined. The couple varied directly with height, so the variation of mass with height was ignored. Examining the base reactions for Wall D yields a torsional shear equal to 0.0221V and an overturning moment corresponding to 0.0191V. Therefore, the hand computations illustrated are somewhat conservative.

Total shear for Wall D is equal to the direct shear plus shear due to accidental torsion, which is computed as:

0.125V + 0.0226V = 0.148V

The resulting shears and overturning moments for Wall D are shown in Table 9.3-5.

x 1		ole 9.3-5 Shear		
Level	Story Shear	Wall Shear	Story Moment	Wall Moment
	(kips)	(kips)	(ft-kips)	(ft-kips)
12	329	49	3,300	500
11	686	102	10,200	1,500
10	1,006	149	20,200	3,000
9	1,291	191	33,100	4,900
8	1,540	228	48,500	7,200
7	1,754	260	66,000	9,800
6	1,972	292	85,800	12,700
5	2,181	323	107,600	15,900
4	2,342	347	131,000	19,400
3	2,460	364	155,600	23,000
2	2,534	375	181,000	26,800
1	2,568	380	206,600	30,60

Table 9.3-5 Shear for Wall D

1.0 kip = 4.45 kN, 1.0 ft-kip = 1.36 kN-m.

When considering accidental torsion, a check for torsional irregularity must be made. First consider the case used for design: a direct shear of 0.125V and a torsional shear of 0.0226V. The ratio of extreme displacement to average displacement can be found from these values and the dimensions, considering symmetry:

Average displacement is proportional to 0.125VTorsional displacement at Wall D is proportional to 0.0226VTorsional displacement at the corner is proportional to (0.0226V)((152 ft./2)/36 ft. = 0.0447VRatio of corner to average displacement = (0.125 + 0.0447)/(0.125 = 1.38)

If the lower value of torsional shear, 0.0191V, found from the 3D computer analysis for the static torsion is used, the ratio becomes 1.32. In either case, the result is a torsional irregularity (ratio exceeds 1.2) but not an extreme torsional irregularity (ratio does not exceed 1.4). The reason for the difference from the five-story building, in which the ratio exceeded 1.4, is that the longer walls in the longitudinal directions. For the ELF analysis, *Provisions* Sec. 5.4.4.3 [Sec. 5.2.4.3] requires the accidental torsion to be amplified:

$$A_x = \left(\frac{Max\ displacement}{1.2\ Ave\ displacement}\right)^2 \le 3.0$$

If one uses the ratio of 1.32 based on the 3D computer analysis, the amplifier is 1.21 and the torsional shear becomes 1.32(0.0191V) = 0.0231V. This is close enough to the unamplified 0.0226V that the ELF analysis will simply proceed with a torsional shear of 0.0226V.

As described in Sec. 9.2.6.4 for the five-story building, the 3D analytical model was altered to offset the center of mass from the center of rigidity. The modal periods, mass participation ratios, and base shears are given in Table 9.3-6. The total base shear is 1620 kips, down from the 1,791 kips found without the eccentricity. The 1,620 kips still slightly exceeds the minimum for design of 1,613 kips described earlier. Thus, MRS analysis can be used directly in the load combinations and can be considered to include the

amplified accidental torsion.

Direction for Modes Used in Analysis of Building with Deliberate Eccentricity								
Mode	Period	Individu	ial mode (j	percent)	Cumula	tive sum (j	percent)	Trans.
number	(seconds)	Long.	Trans.	Vert.	Long.	Trans.	Vert.	base shear
1	0.965	0.0	8.5	0.0	0.0	8.5	0.0	169.4
2	0.723	0.0	50.6	0.0	0.0	59.1	0.0	1352.7
3	0.694	59.2	0.0	0.0	59.2	59.1	0.0	0.0
4	0.229	0.0	3.3	0.0	59.2	62.5	0.0	122.7
5	0.171	0.0	21.0	0.0	59.2	83.5	0.0	772.7
6	0.167	24.6	0.0	0.0	83.7	83.5	0.0	0.0
7	0.120	0.0	0.0	20.3	83.7	83.5	20.3	0.0
8	0.108	0.0	1.0	0.0	83.7	84.4	20.3	35.3
9	0.105	0.0	0.0	0.0	83.7	84.4	20.3	0.1
10	0.097	0.0	0.0	0.0	83.7	84.4	20.3	0.1
11	0.090	0.0	0.0	11.4	83.8	84.4	31.7	0.0
12	0.081	0.0	6.2	0.0	83.8	90.7	31.7	198.6
13	0.079	7.1	0.0	0.1	90.9	90.7	31.8	0.0
14	0.074	0.0	0.0	3.1	90.9	90.7	34.8	0.1
15	0.072	0.0	0.6	0.1	90.9	91.3	34.9	17.5
16	0.061	0.0	0.5	0.1	90.9	91.7	34.9	12.8
17	0.053	4.3	0.0	0.0	95.2	91.7	34.9	0.0
18	0.052	0.0	4.1	0.0	95.2	95.8	34.9	104.8
19	0.043	0.7	0.0	0.0	95.9	95.8	34.9	0.0
20	0.037	1.5	0.0	0.0	97.4	95.8	35.0	0.1
21	0.035	0.0	2.5	0.0	97.4	98.3	35.0	54.7
22	0.027	1.8	0.0	0.0	99.2	98.3	35.0	0.0
23	0.022	0.0	1.7	0.0	99.2	100.0	35.0	32.8
24	0.018	0.8	0.0	0.0	100.0	100.0	35.0	0

**Table 9.3-6** Periods, Mass Participation Ratios, and Modal Base Shears in the Transverse

 Direction for Modes Used in Analysis of Building with Deliberate Eccentricity

1 kip = 4.45 kN

The combined modal base shear is 1620 kips.

Mode 1 now includes a translational component, and the comparison to an ELF base shear would be performed with its period. For T = 0.965 sec, the ELF base shear becomes 1,996 kips, and the comparison value is 0.85 (1996) = 1,696 kips. This is 78 percent of the value for the symmetric model and illustrates one of the problems in handling accidental torsion in a consistent fashion.

Without factoring the modal results up to achieve a base shear of 1,696 kips (a factor of 1.047), the reactions indicate that the base shear for wall D is 266.5 kips, or 0.1645 times the total base shear. If one takes the direct shear as one-eighth (0.125*V*), that leaves 0.0395*V* for the dynamically amplified shear due to accidental torsion, which could be interpreted to be an amplification of 1.79 over the shear of 0.0221V found for the static torsion. Thus, it is clear that the amplification value of 1.21 from the equation given for the ELF analysis underestimates the dynamic amplification of accidental torsion. The bottom line is that the Wall D shear of 266.5 kips from the dynamic analysis is significantly less than the shear of 380 kips found in the ELF analysis without amplification of accidental torsion. The example will proceed based upon the shear of 380 kips.

### 9.3.3.5 Transverse Wall (Wall D)

The strength or limit state design concept is used in the Provisions.

[The 2003 *Provisions* adopts by reference the ACI 530-02 provisions for strength design in masonry, and the previous strength design section has been removed. This adoption does not result in significant technical changes, and the references to the corresponding sections in ACI 530 are noted in the following sections.]

### 9.3.3.5.1 Axial and Flexural Strength General

The walls in this example are all bearing shear walls since they support vertical loads as well as lateral forces.

The demands for the representative design example, Wall D, are presented in this section. The design of the lower and upper portions of Wall D is presented in the next two sections. For both locations, in-plane calculations include:

- 1. Strength check and
- 2. Ductility check.

The axial and flexural demands for Wall D, using the load combinations identified in Sec. 9.3.2.3, are presented in Table 9.3-7. In the table, Load Combination 1 represents  $1.4D + 1.0 Q_E + 0.5L$ , and Load Combination 2 represents  $0.7D + 1.0 Q_E$ .

			Load Com	bination 1	Load Cor	nbination 2
Level	$P_D$ (kips)	$P_L$ (kips)	$P_u$ (kips)	M <sub>u</sub> (ft-kips)	$P_u$ (kips)	M <sub>u</sub> (ft-kips)
12	37	0	51	500	26	500
11	80	8	117	1,500	56	1,500
10	124	17	182	3,000	87	3,000
9	168	25	247	4,900	117	4,900
8	212	34	313	7,200	148	7,200
7	255	43	379	9,800	179	9,800
6	308	50	457	12,700	216	12,700
5	370	59	548	15,900	259	15,900
4	432	67	639	19,400	303	19,400
3	494	76	730	23,000	346	23,000
2	556	84	821	26,800	389	26,800
1	618	92	912	30,600	433	30,60

**Table 9.3-7** Load Combinations for Wall D

1.0 kip = 4.45 kN, 1.0 ft-kip = 1.36 kN-m.

Strength at the lowest story (where *P*, *V*, and *M* are the greatest) for both the lower wall (Level 1) and the upper wall (Level 7) constructions will be examined. The design for both locations is based on the values for Load Combination 2 in Table 9.3-7.

### 9.3.3.5.2 Axial and Flexural Strength Lower Levels

### Examine the strength of Wall D at Level 1:

### 9.3.3.5.2.1 Strength Check (Level 1)

 $P_{u_{min}} = 433$  kips + factored weight of half of 1<sup>st</sup> story wall = 433 + (0.7)(21.9) = 448 kips  $M_u = 30,600$  ft-kips

For this Seismic Design Category D building, the special reinforced masonry shear walls must have vertical and horizontal reinforcement spaced at no more than 4 ft on center. The minimum in either direction is  $0.0007(10.5 \text{ in.}) = 0.0074 \text{ in.}^2/\text{in.}$  (vertical #5 at 42 in. on center). That will be used as the vertical reinforcement (although some of the subsequent calculations of flexural resistance are based upon a spacing of 48 in. on center); the shear strength demands for horizontal reinforcement will be greater and will satisfy the total amount of  $0.0020(10.5 \text{ in.}) = 0.021 \text{ in.}^2/\text{in.}$ (horizontal #5 at 22 in. on center will suffice).

Try 16 #9 bars in each bulb. Refer to Figure 9.3-4 for the placement of the reinforcement in the bulb. In some of the strength calculations, the #5 bars in the wall will be neglected as a conservative simplification.

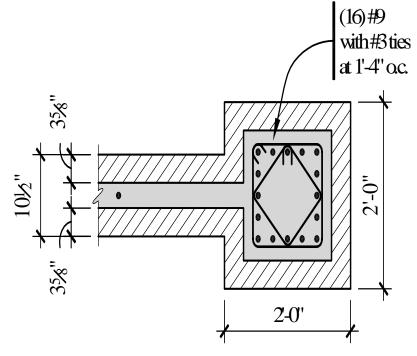
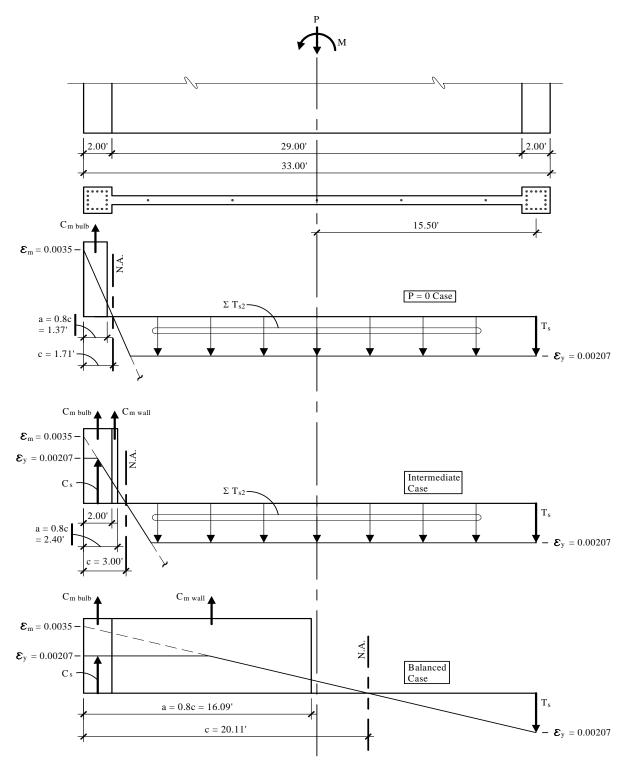


Figure 9.3-4 Bulb reinforcement at lower levels (1.0 in. = 25.4 mm, 1.0 ft = 0.3048 m).



**Figure 9.3-5** Strength of Wall D, Level 1 (1.0 ft = 0.3048 m)

For evaluating the capacity of the wall, a  $\phi P_n - \phi M_n$  curve will be developed to represent the wall strength envelope. The demands ( $P_u$  and  $M_u$  determined above) will then be compared to this curve. Several cases will be analyzed and their results used in plotting the  $\phi P_n - \phi M_n$  curve. Refer to Figure 9.3-5 for notation and dimensions.

### <u>Case 1 (P = 0)</u>

The neutral axis will be within the compression bulb, so assume that only the bars closest to the compression face are effective in compression. (Also recall that the *Provisions* clearly endorses the use of compression reinforcement in strength computations.)

$$T_{sl} = (16 \text{ bars})(1.00 \text{ in.}^2)(60 \text{ ksi}) = 960 \text{ kips}$$
  
 $T_{s2} = (7 \text{ bars})(0.31 \text{ in.}^2)(60 \text{ ksi}) = 130 \text{ kips}$   
 $C_s = (5 \text{ bars})(1.00 \text{ in.}^2)(60 \text{ ksi}) = 300 \text{ kips}$ 

 $\Sigma C = \Sigma T + P$   $C_m + C_s = T_{s1} + T_{s2} + P$  $C_m = 960 + 130 + 0 - 300 = 790 \text{ kips}$ 

 $C_m = 790 \text{ kips} = \phi f'_m (24 \text{ in.})a = (0.8)(2.5 \text{ ksi})(24 \text{ in.})a$ a = 16.46 in. = 1.37 ftc = a/0.8 = 1.37/0.8 = 1.71 ft = 20.7 in.

Check strain in compression steel

 $\varepsilon_s = 0.0035(20.7 \text{ in.} - 6 \text{ in.})/(20.7 \text{ in.}) = 0.0025 > \text{yield}; \text{ assumption OK}$ 

 $\Sigma M_{cl} = 0$   $M_n = (790 \text{ kips})(16.5 \text{ ft- } 1.37 \text{ ft/2}) + (300 + 960 \text{ kips})(15.5 \text{ ft}) + (130 \text{ kips})(0 \text{ ft.}) = 32,170 \text{ ft-kips}$  $\phi M_n = (0.85)(32,170) = 27,340 \text{ ft-kips}$ 

Case 2 (Intermediate case between P = 0 and balanced case):

Select an intermediate value of c. Let c = 3.0 ft, and determine  $P_n$  and  $M_n$  for this case.

a = 0.8c = 2.4 ft  $C_{m \ bulb} = (0.8)(2.5 \ \text{ksi})(24 \ \text{in.})^2 = 1152 \ \text{kips}$   $C_{m \ wall} = (0.8)(2.5 \ \text{ksi})(10.5 \ \text{in.})(0.4 \ \text{ft.} \times 12) = 101 \ \text{kips}$   $C_s = (16 \ \text{bars})(1.00 \ \text{in.}^2)(60 \ \text{ksi}) = 960 \ \text{kips} \ (\text{approximate; not all bars reach full yield})$   $\Sigma C = (1152 + 101 + 960) = 2213 \ \text{kips}$   $\Sigma T = 960 + 130 \ \text{kips} = 1090 \ \text{kips}$ 

 $\Sigma F_y = 0$   $P_n = \Sigma C - \Sigma T = 2213 - 1090 = 1123$  kips  $\phi P_n = (0.85)(1123) = 955$  kips

 $\Sigma M_{cl} = 0$   $M_u = (1152 + 960 \text{ kips})(15.5 \text{ ft}) + (101 \text{ kips})(14.1 \text{ ft}) + (960 \text{ kips})(15.5 \text{ ft}) = 49,040 \text{ ft-kips}$  $\phi M_n = (0.85)(49,040) = 41,680 \text{ ft-kips}$ 

Case 3 (Balanced case):

$$c = \left[\frac{0.0035}{0.0035 + 0.00207}\right] (32.00 \text{ ft}) = 20.11 \text{ ft}$$
  
$$a = (0.8)c = 16.09 \text{ ft}$$

Ignore the distributed #5 bars for this case.

$$\begin{split} C_{m \ bulb} &= 1152 \ \text{kips} \\ C_{m \ wall} &= (0.8)(2.5 \ \text{ksi})(10.5 \ \text{in.})(14.09 \ \text{ft.} \times 12) = 3,550 \ \text{kips} \\ C_s &= 960 \ \text{kips} \\ \Sigma C &= (1152 + 3550 + 960) = 5,662 \ \text{kips} \\ T_s &= 960 \ \text{kips} \\ \Sigma F_y &= 0 \\ P_n &= \Sigma C - \Sigma T = 5662 - 960 = 4,702 \ \text{kips} \\ \varphi P_n &= (0.85)(4,702) = 3,997 \ \text{kips} \\ \Sigma M_{cl} &= 0 \\ M_u &= (1152 + 960 \ \text{kips})(15.5 \ \text{ft}) + (3550 \ \text{kips})(7.46 \ \text{ft}) + (960 \ \text{kips})(15.5 \ \text{ft}) = 74,100 \ \text{ft-kips} \\ \varphi M_n &= (0.85)(74,100) = 62,980 \ \text{ft-kips} \end{split}$$

The actual design strength,  $\phi M_n$ , at the level of minimum axial load can be found by interpolation to be 33,840 ft.-kip.

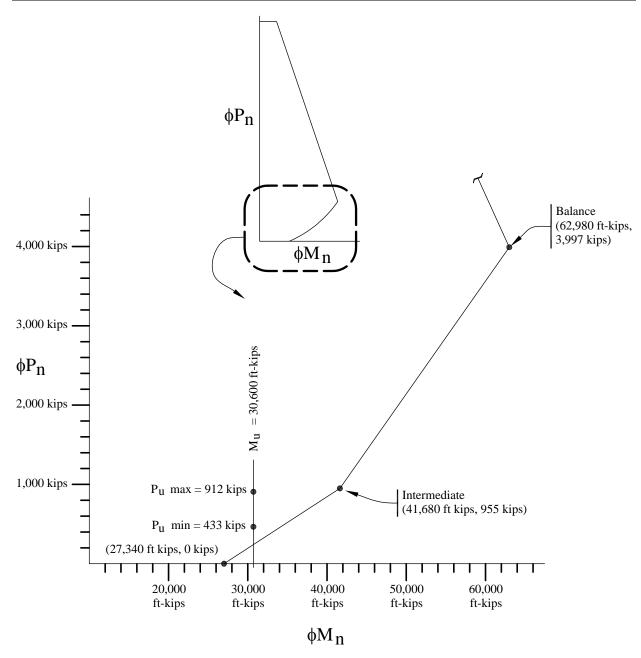


**Figure 9.3-6**  $\varphi P_{11} - \varphi M_{11}$  Diagram for Level 1 (1.0 kip = 4.45 kN, 1.0 ft-kip = 1.36 kN-m).

### 9.3.3.5.2.2 Ductility check (Level 1)

*Provisions* Sec. 11.6.2.2 [ACI 530, Sec. 3.2.3.5] requires that the critical strain condition correspond to a strain in the extreme tension reinforcement equal to 5 times the strain associated with  $F_y$ . Note that this calculation uses unfactored gravity axial loads (*Provisions* 11.6.2.2 [ACI 530, Sec. 3.2.3.5]). See Figure 9.3-7 and the following calculations.

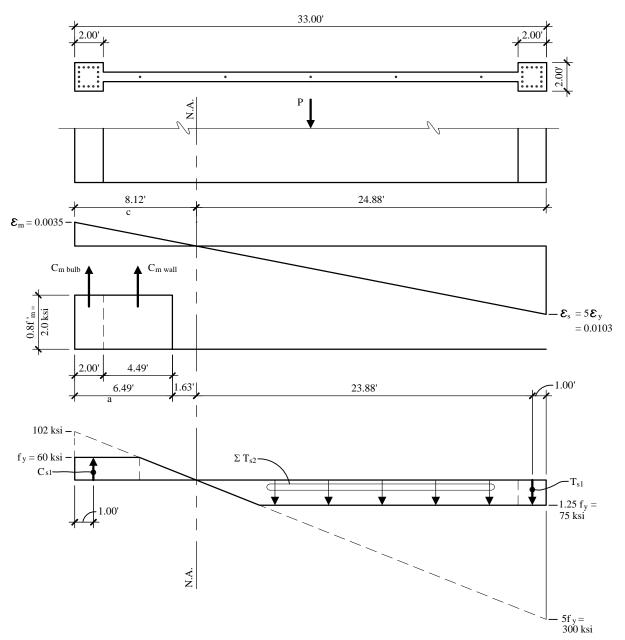


Figure 9.3-7 Ductility check for Wall D, Level 1 (1.0 ft = 0.3048 m, 1.0 ksi = 6.89 MPa).

$$c = \left[\frac{0.0035}{(0.0035+0.0103)}\right](32.00 \text{ ft}) = 8.12 \text{ ft}$$
  
$$a = 0.8 \ c = 6.49 \text{ ft}$$

For Level 1, the unfactored loads are:

$$P = 618 \text{ kips}$$
  

$$M = 30,600 \text{ ft-kips}$$
  

$$C_{m_{bulb}} = 0.8 f'_m A_{bulb} = 1,152 \text{ kips}$$
  

$$C_{m_{wall}} = 0.8 f'_m (10.5 \text{ in.})(4.49 \text{ ft} \times 12) = 1131 \text{ kips}$$

The distributed wall rebar that is near the neutral axis is divided between tension and compression, and therefore it will not have much effect on the result of this check, so it will be neglected.

 $C_{sI} = (60 \text{ ksi})(16 \times 1.00 \text{ in.}^2) = 960 \text{ kips}$  $T_{sI} = (16 \times 1.00 \text{ in.}^2)(75 \text{ ksi}) = 1,200 \text{ kips}$  $T_{s2} = (4 \times 0.31 \text{ in.}^2)(75 \text{ ksi}) = 93 \text{ kips}$ 

(unfactored dead load)

 $\sum C > \sum P + \sum T$ 1152 +1131 + 960 > 618 + 1200 + 93 3,243 kips > 1,818 kips

P = 618 kips

There is more compression capacity than tension capacity, so a ductile failure condition governs.

[The ductility (maximum reinforcement) requirements in ACI 530 are similar to those in the 2000 *Provisions*. However, the 2003 *Provisions* also modify some of the ACI 530 requirements, including critical strain in extreme tensile reinforcement (4 times yield) and axial force to consider when performing the ductility check (factored loads).]

### 9.3.3.5.3 Axial and Flexural Strength Upper Levels

Examine the strength of Wall D at Level 7.

 $P_{u_{min}} = 179$  kips + factored weight of ½ of 7<sup>th</sup> story wall = 179 + (0.7)(11.4) = 190 kips  $M_u = 9,800$  ft-kips

This is a point, however, where some of the reinforcement in the lower wall will be terminated. Although not required by the *Provisions*, most design standards require the longitudinal reinforcement to be extended a distance *d* beyond the point where it could theoretically be terminated. (The ASD chapter of ACI 530 has such a requirement.) Therefore, the reinforcement at level 6 (7<sup>th</sup> floor) should be capable of resisting the moment *d* below. *d* is approximately three stories for this wall, therefore, take  $M_u = 19,400$  ft-kip (and P = 303 kip) from Level 3.

Try eight #9 in each bulb and vertical #5 bars at 4 ft on center in the wall. Refer to Figure 9.3-8 for the placement of the bulb reinforcement.

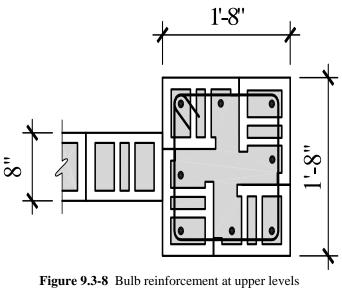
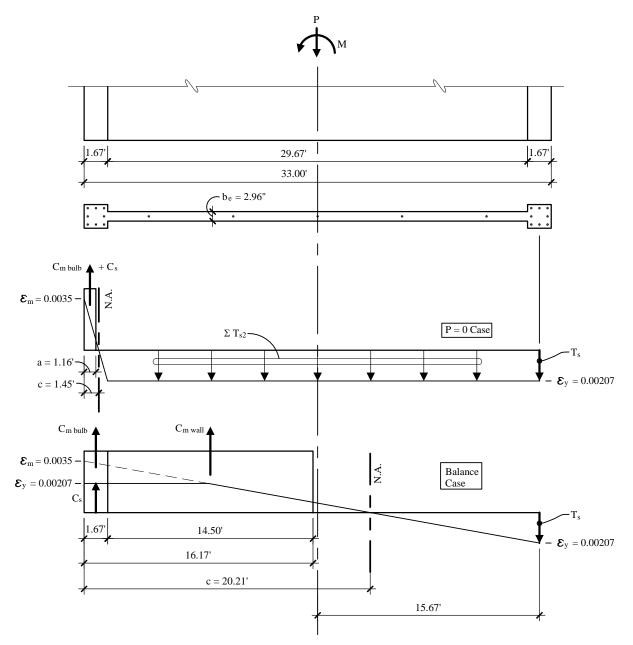


Figure 9.3-8 Bulb reinforcement at upper levels (1.0 ft = 0.3048 m, 1.0 in. = 25.4 mm).

For evaluating the capacity of the wall, a  $\phi P_n - \phi M_n$  curve will be developed to represent the wall strength envelope for Level 7. The demands ( $P_u$  and  $M_u$  determined above) will then be compared to this curve. Several cases will be analyzed and their results used in plotting the  $\phi P_n - \phi M_n$  curve. Refer to Figure. 9.3-9 for notation and dimensions.



**Figure 9.3-9** Strength of Wall D at Level 7 (1.0 ft = 0.3048 m)

### <u>Case 1 (P = 0)</u>

Tension forces:

$$T_{s1} = (8 \text{ bars})(1.00 \text{ in.}^2)(60 \text{ ksi}) = 480 \text{ kips}$$
  
 $T_{s2} = (7 \text{ bars})(0.31 \text{ in.}^2)(60 \text{ ksi}) = 130 \text{ kips}$ 

### Equilibrium:

$$\Sigma C = \Sigma T + P$$

 $\Sigma C = 480 + 130 + 0 = 610$  kips

Assume bars closest to compression face yield:

$$\Sigma C = C_s + C_m$$
  
 $C_s = (3 \text{ bars})(1.00 \text{ in.}^2)(60 \text{ ksi}) = 180 \text{ kips}$   
 $C_m = 610 - 180 = 430 \text{ kips}$ 

Locate equivalent stress block and neutral axis:

 $430 = \phi f'_m (20 \text{ in.})a = (0.8)(3 \text{ ksi})(20 \text{ in.})a$  a = 8.96 in. = 0.75 ftc = a/0.8 = 0.75/0.8 = 0.93 ft = 11.2 in.

Verify strain in compression steel:

At the outside layer,  $\varepsilon = (0.0035)(7.2 \text{ in.} / 11.2 \text{ in.}) = 0.0023 > \text{yield}$ , At the central layer,  $\varepsilon = (0.0035)(1.2 \text{ in.} / 11.2 \text{ in.}) = 0.0004 => f_s = 11 \text{ ksi}$ 

Resultant moment:

$$\begin{split} \Sigma M_{cl} &= 0; \\ M_n &= (430 \text{ kips})(16.5 \text{ ft} - 0.75 \text{ ft}/2) + (180 \text{ kips})(16.5 - 0.33 \text{ ft}) + (480 \text{ kips})(16.5 - 0.83 \text{ ft}) \\ &+ (130 \text{ kips})(0 \text{ ft}.) = 17,370 \text{ ft-kips} \\ \phi M_n &= (0.85)(17,280) = 14,760 \text{ ft-kips} \end{split}$$

Case 2 (Intermediate)

Assume the neutral axis at the face of the bulb, c = 1.67 ft

a = 0.8c = 1.33 ft. = 16 in.  $C_m = (2.4 \text{ ksi})(16 \text{ in.})(20 \text{ in.}) = 768 \text{ kip}$ 

For the compression steel, it is necessary to compute the strains:

At the outside layer,  $\varepsilon = (0.0035)(16 \text{ in.} / 20 \text{ in.}) = 0.0028 > \text{yield}$ At the central layer,  $\varepsilon = (0.0035)(10 \text{ in.} / 20 \text{ in.}) = 0.00175 => f_s = 50 \text{ ksi}$ At the inside layer,  $\varepsilon = (0.0035)(4 \text{ in.} / 20 \text{ in.}) = 0.0007 => f_s = 20 \text{ ksi}$  $C_s = (3.0 \text{ x } 60 \text{ ksi} + 2.0 \text{ x } 50 \text{ ksi} + 3.0 \text{ x } 20 \text{ ksi}) = 340 \text{ kips}$ 

 $T_{sl} = (8 \text{ bars})(1.00 \text{ in.}^2)(60 \text{ ksi}) = 480 \text{ kips}$  $T_{s2} = (7 \text{ bars})(0.31 \text{ in.}^2)(60 \text{ ksi}) = 130 \text{ kips}$ 

 $P_n = 768 + 340 - 480 - 130 = 498$  kips  $\phi P_n = (0.85)(498) = 423$  kips

 $M_n = (768 \text{ kips})(16.5 \text{ ft-} 1.33 \text{ ft/2}) + (340 + 480 \text{ kips})(16.5 - 1.67/2 \text{ ft}) + (130 \text{ kips})(0 \text{ ft})$ = 25,010 ft-kips  $\phi M_n = (0.85)(25,010) = 21,260 \text{ ft-kips}$ 

At P = 303 kips,  $\phi M_n = 19,990$  ft.-kips by interpolation (exceeds 19,400 ft.-kips, OK)

Case 3 (Balanced Case):

$$c = \left[\frac{0.0035}{0.0035 + 0.00207}\right](32.17 \text{ ft}) = 20.21 \text{ ft}$$

a = (0.8)c = 16.17 ft

 $\begin{array}{l} b_e = {\rm effective \ width \ of \ wall} \\ b_e = [(2)(1.3125 \ {\rm in.})(29.67 \ {\rm ft \ x \ 12}) + (8 \ {\rm cells})(15 \ {\rm in.}^2/{\rm cell})] = 2.96 \ {\rm in./ft} \\ C_{m \ bulb} = 960 \ {\rm kips} \\ C_{m \ wall} = (0.8)(3 \ {\rm ksi})(2.96 \ {\rm in.})(14.17 \ {\rm ft \ x \ 12}) = 101 \ {\rm kips} \\ C_s = 480 \ {\rm kips} \\ \Sigma C = (960 + 101 + 480) = 1,541 \ {\rm kips} \\ T_s = 480 \ {\rm kips, \ ignoring \ the \ distributed \ \#5 \ bars} \end{array}$ 

 $\Sigma F_y = 0$   $P_n = \Sigma C - \Sigma T = 1,541 - 480 = 1,061$  kips  $\phi P_n = (0.85)(1,061) = 902$  kips

 $\Sigma M_{cl} = 0$   $M_u = (480 + 960 \text{ kips})(15.67 \text{ ft}) + (101 \text{ kips})(7.42 \text{ ft}) + (480 \text{ kips})(15.67 \text{ ft}) = 30,830 \text{ ft-kips}$  $\phi M_u = (0.85)(30,830) = 26,210 \text{ ft-kips}$ 

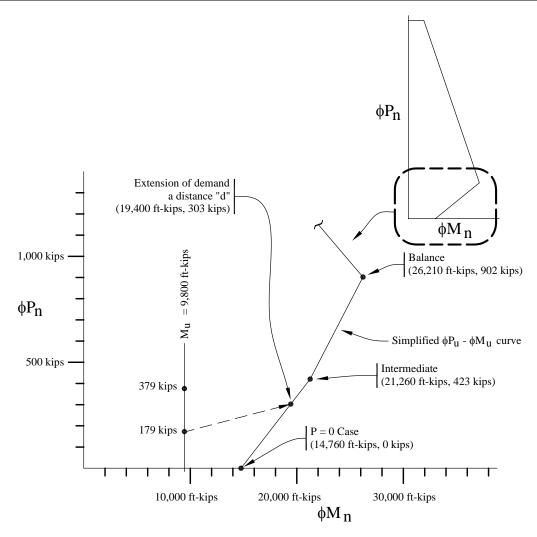


**Figure 9.3-10**  $\varphi P_{11} - \varphi M_{11}$  Diagram for Level 7 (1.0 kip = 4.45 kN, 1.0 ft-kip = 1.36 kN-m).

The ductility check is performed similar to that for the wall at Level 1. See Figure 9.3-11 and the following calculations.

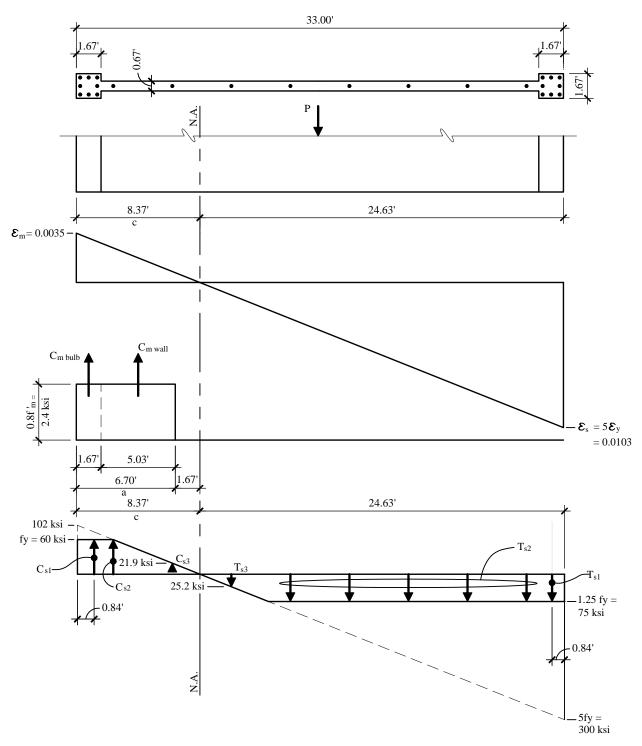


**Figure 9.3-11** Ductility check for Wall D, Level 7 (1.0 ft = 0.3048 m, 1.0 ksi = 6.89 MPa)

For Level 7, the unfactored loads are:

$$P = 255$$
 kips  
 $M = 11,600$  ft-kips

$$\begin{split} C_{mb} &= 0.8f^{\circ}_{m}A_{b} = 0.8(3.0 \text{ ksi})(400 \text{ in.}2) = 960 \text{ kips} \\ C_{mw} &= 0.8f^{\circ}_{m}A_{w} = 0.8(3.0 \text{ ksi})[2(1.3125 \text{ in.})(5.03 \text{ ft.})(12 \text{ in/ft}) + (1 \text{ cell})(25.6 \text{ in.}^{2}/\text{cell})] \\ &= 442 \text{ kips} \\ \\ C_{sl} &= (60 \text{ ksi})(8 \times 1.00 \text{ in.}^{2}) = 480 \text{ kips} \\ C_{s2} &= (60 \text{ ksi})(0.31 \text{ in.}^{2}) = 19 \text{ kips} \\ \\ T_{sl} &= (8 \times 1.00 \text{ in.}^{2})(75 \text{ ksi}) = 600 \text{ kips} \\ T_{s2} &= (4 \times 0.31 \text{ in.}^{2})(75 \text{ ksi}) = 116 \text{ kips} \\ \\ T_{s3} &= (0.31 \text{ in.}^{2})(25.2 \text{ ksi}) = 7 \text{ kips} \\ \\ P &= 255 \text{ kips} \text{ (unfactored dead load)} \\ \\ \\ \frac{\Sigma C > P + \Sigma T}{960 + 442 + 480 + 19 > 255 + 600 + 116 + 7} \\ 1901 \text{ kips} > 978 \text{ kips} \\ \\ \\ \text{There is more compression capacity than tension capacity, so a ductile failure condition governs.} \end{split}$$

9.3.3.5.4 Shear Strength

The first step is to determine the net area,  $A_n$ , for Wall D. The definition of  $A_n$  in the *Provisions*, however, does not explicitly address bulbs or flanges at the ends of walls. Following an analogy with reinforced concrete design, the area is taken as the thickness of the web of the wall times the overall length. In partially grouted walls this is not extended to the point of ignoring the grouted cores because the implication is that grouted cores are intended to be included. (However, if the spacing of bond beams greatly exceeds the spacing of grouted cores, even that assumption might be questionable.)

For Levels 1 through 6:

 $A_n = (10.5 \text{ in.} (33 \text{ ft} \times 12)) = 4,158 \text{ in.}^2$ 

For Levels 7 through 12 (using 8 x 8 x 12 clay brick units):

$$A_n = (2)(1.3125 \text{ in.})(12 \text{ in.})(33 \text{ ft}) + (7 + 2 \times 3 \text{ cells})(25.6 \text{ in.}^2/\text{cell with adjacent webs})$$
  
= 1,372 in.<sup>2</sup>

Shear strength is determined as described in Sec. 9.2 using *Provisions* Eq. 11.7.2.1 [ACI 520, Sec. 3.13] and *Provisions* Eq. 11.7.3.1-1 [ACI 530, Eq. 3-18], respectively:

$$V_u \le \phi V_n$$
$$V_n = V_m + V_s$$

For Levels 1 through 6 using *Provisions* Eq. 11.7.3.1-3 where  $\frac{M_x}{V_x d} > 1.0$ :

$$V_n(\max) = 4\sqrt{f'_m}A_n = (4)(\sqrt{2,500})(4,806) = 961$$
 kips (P3)

For Levels 7 through 12 where  $\frac{M_x}{V_x d}$  varies from 0.30 to 1.14:  $V_n$  (max) varies from  $5.87\sqrt{f'_m}A_n$  to  $4\sqrt{f'_m}A_n$ 

Therefore,  $V_n$  (max) varies from  $5.87\sqrt{3,000}(1836) = 590$  kips to  $4\sqrt{3,000}(1836) = 402$  kips

depending on the value of  $\frac{M_x}{V_x d}$ . The masonry shear strength is computed as:

$$V_m = \left[4 - 1.75 \left(\frac{M}{Vd}\right)\right] A_n \sqrt{f'_m} + 0.25P$$

The shear strength of Wall D, based on the aforementioned formulas and the strength reduction factor of  $\phi = 0.8$  for shear from *Provisions* Table 11.5.3 [ACI 530, Sec. 3.1.4.3], is summarized in Table 9.3-8.  $V_x$  and  $M_x$  in this table are values from Table 9.3-2 multiplied by 0.148 (the portion of direct and torsional shear assigned to Wall D). *P* is the dead load of the roof or floor multiplied by the tributary area for Wall D, and *d* is the wall length, not height (d = 32.67 ft for Wall D).

The demand shear, Vu, is found by amplifying the loads to a level that produces a moment of 125 percent of the nominal flexural strength at the base of the wall. Given the basic flexural demand of 30,600 ft-kips, a design resistance of 33,840 ft-kips,  $\varphi = 0.85$ , and the 1.25 factor, the overall amplification of design load is 1.63.

Level	V <sub>x</sub> /wall (kips)	<i>M<sub>x</sub></i> /wall (ft-kips)	$M_x/V_xd$	$1.63V_{x}$	$\phi V_n max$ (kips)	$\phi V_m$ (kips)	P (kips)	$\phi V_m$ (kips)	Req'd $\phi V_s$ (kips)
12	49	500	0.309	80	351.2	OK	37	215	-
11	102	1500	0.446	166	329.3	OK	80	210	-
10	149	3000	0.610	243	303.0	OK	124	201	42
9	191	4900	0.777	311	276.2	NG	168	192	119
8	228	7200	0.957	372	247.4	NG	212	182	190
7	260	9800	1.142	424	240.5	NG	255	186	238
6	292	12700	1.318	476	665.3	OK	308	436	40
5	323	15900	1.492	526	665.3	OK	370	448	78
4	347	19400	1.694	566	665.3	OK	432	461	106
3	364	23000	1.915	593	665.3	OK	494	473	120
2	375	26800	2.166	611	665.3	OK	556	485	126
1	380	30600	2.440	619	665.3	OK	618	498	121

Table 9.3-8 Shear Strength for Wall D

1.0 kip = 4.45 kN, 1.0 ft-kip = 1.36 kN-m.

Note that 1.63  $V_x$  exceeds  $V_{n max}$  at Levels 7, 8, and 9. The next most economical solution appears to be to add grout to increase  $A_n$  and, therefore, both  $V_m$  and  $V_{n max}$ . Check Level 7 using solid grout:

$$A_n = (7.5 \text{ in.})(33 \text{ ft})(12 \text{ in./ft}) = 2970 \text{ in.}^2$$
  

$$V_n(\max) = 4\sqrt{f'_m} A_n = (4)(\sqrt{2,500})(2,970) = 650 \text{ kips}$$
  

$$\varphi V_n \max = 0.8(650) = 520 \text{ kips} > 424 \text{ kips}$$

OK

$$\phi V_m = (0.80) \Big[ (4.0 - 1.75(1.0)) 2,970 \sqrt{3000} / 1000 + 0.25(255) \Big] = 344 \text{ kips}$$
  
 $\phi V_s = V_u - \phi V_m = 424 - 344 = 80 \text{ kips}$ 

Check minimum reinforcement for capacity. With vertical #5 at 48 in., a reinforcement ratio of 0.00086 is provided. Thus the horizontal reinforcement must exceed  $(0.0020 - 0.00086)(7.5 \text{ in.})(12 \text{ in.}) = 0.1025 \text{ in.}^2/\text{ft}$ . With story heights of 10 ft., bond beams at 40 in. on center are convenient, which would require 0.34 in.<sup>2</sup> Therefore, for 2 - #4 at 40 in. on center:

$$\varphi V_s = 0.80(0.5)(0.4 / 40) (60 \text{ ksi})(33 \text{ ft.})(12 \text{ in./ft.}) = 95 \text{ kips} > 80 \text{ kips}$$
 OK

The largest demand for  $\varphi V_x$  in the lower levels is 126 kips at level 2. As explained in the design of the lower level walls for flexural and axial loads (Sec. 9.3.3.5.1), horizontal #5 at 22 in. are required to satisfy minimum reinforcement. Given the story height, check for horizontal #5 at 20 in.:

$$\varphi V_s = 0.8(0.5)(0.31 / 20) (60 \text{ ksi})(33 \text{ ft.})(12 \text{ in./ft.}) = 147 \text{ kips} > 126 \text{ kips}$$
 OK

In summary, for shear it is necessary to grout the hollow units at story 7 solid, and to add some grout at stories 8 and 9. Horizontal reinforcement is 2 - #4 in bond beams at 40 in. on center in the upper stories and one #5 at 20 in. on center in the grouted cavity of the lower stories.

### 9.3.4 Deflections

The calculations for deflection involve many variables and assumptions, and it must be recognized that any calculation of deflection is approximate at best.

Deflections are to be calculated and compared with the prescribed limits set forth by *Provisions* Table 5.2.8 [Table 4.5-1]. Deformation requirements for masonry structures are discussed in *Provisions* Sec. 11.5.4.

The following procedure will be used for calculating deflections:

1. Determine if the wall at each story will crack by comparing  $M_x$  (see Table 9.3-6) to  $M_{cr}$  where  $M_{rr} = S(f_r + R_{rr} / A)$ 

$$M_{cr} = S\left(f_r + P_{u_{min}}/A\right)$$

- 2. If  $M_{cr} < M_x$ , then use cracked moment of inertia and *Provisions* Eq. 11.5.4.3.
- 3. If  $M_{cr} > M_x$ , then use  $I_n = I_g$  for moment of inertia of wall.
- 4. Compute deflection for each level.
- 5.  $\delta_{max} = \sum$  story drift

[The specific procedures for computing deflection of shear walls have been removed from the 2003 *Provisions*. ACI 530 does not contain the corresponding provisions in the text, however, the commentary contains a discussion and equations that are similar to the procedures in the 2000 *Provisions*. Based on ACI 530 Sec. 1.13.3.2, the maximum drift for all masonry structures is 0.007 times the story height. Thus, there appears to be a conflict between ACI 530 and 2003 *Provisions* Table 4.5-1.]

For the upper levels (the additional grout required for shear strength is not considered here):

 $b_e$  = effective masonry wall width  $b_e = [(2 \times 1.3125 \text{ in.})(356) + (7 \text{ cells})(15 \text{ in.}^2/\text{cell})]/(356) = 2.92 \text{ in.}$  $A = A_{wall} + 2A_{bulb} = (2.92 \text{ in.})(356 \text{ in.}) + (2)(400 \text{ in.}^2) = 1,840 \text{ in.}^2$  [Note that by adopting ACI 530 in the 2003 *Provisions*,  $E_m = 900f'_m$  per ACI 530 Sec. 1.8.2.2.1]

Per Provisions Eq. 11.3.10.2 [ACI 530, 1.8.2.2]:

$$E = 750 f'_{m} = 2,250 \text{ ksi } (n = 12.89)$$

$$I_{g} = I_{wall} + I_{bulb}$$

$$I_{g} = \frac{(2.96)(356)^{3}}{12} + (2 \text{ bulbs})(20 \times 20) \left(\frac{376}{2}\right)^{2} = 39.4 \times 10^{6} \text{ in.}^{4}$$

 $S = I_g/c = 39.4 \times 10^6 / (198) = 199,000 \text{ in.}^3$  $f_r = 0.250 \text{ ksi}$  $P_{u_{min}} = 1.00D$  (see Table 9.3-6.)

For the lower levels:

$$A = A_{wall} + 2A_{bulb} = (10.5 \text{ in.})(348 \text{ in.}) + (2)(576 \text{ in.}^2) = 4,806 \text{ in.}^2$$
  

$$E = 750 f''_m = 1,875 \text{ ksi} \quad (n = 15.47)$$
  

$$I = I_{wall} + I_{bulb}$$
  

$$I_g = \frac{(10.5)(348)^3}{12} + (2 \text{ bulbs})(24 \times 24) \left(\frac{372}{2}\right)^2 = 76.7 \times 10^6 \text{ in.}^4$$
  

$$S = I_g / c = 76.7 \times 10^6 / (198) = 387,000 \text{ in.}^3$$
  

$$f_r = 0.250 \text{ ksi}$$
  

$$P_{u_{min}} = 1.00D \text{ (see Table 9.3-6.)}$$

Table 9.3-9 provides a summary of these calculations.

Level	$P_{u_{min}}$ (kips)	<i>M<sub>cr</sub></i> (ft-kips)	$M_x$ (ft-kips)	Status
12	37	7,620	500	uncracked
11	80	8,820	1,500	uncracked
10	124	8,950	3,000	uncracked
9	168	9,620	4,900	uncracked
8	212	10,300	7,200	uncracked
7	255	11,000	9,800	uncracked
6	308	15,400	12,700	uncracked
5	370	16,000	15,900	uncracked
4	432	16,700	19,400	cracked
3	494	17,300	23,000	cracked
2	556	18,000	26,800	cracked
1	618	18,600	30,600	cracked

Table 9.3-9 Cracked Wall Determination

1.0 kip = 4.45 kN, 1.0 ft-kip = 1.36 kN-m.

For the uncracked walls at the upper levels:

$$I_n = I_g = 39.4 \times 10^6$$
 in.<sup>4</sup>

For the uncracked walls at the lower levels:

$$I_n = I_a = 76.7 \times 10^6$$
 in.<sup>4</sup>

For the cracked walls at the lower levels, the determination of  $I_{cr}$  will be for the load combination of 1.0D + 0.5L. The 0.5L represents an average condition of live load. Making reference to Figure 9.3-6, it can be observed that at this level of  $P_u$ , the point on the  $\phi P_n - \phi M_n$  curve is near the "intermediate point" previously determined. This is where c = 3.0 ft. (The actual *c* dimension will be very close to 3.0 ft). For this case, and referring to Figure 9.3-5, the cracked moment of inertia is:

$$I_{cr} = I_{bulb} + I_{wall} + I_{nAs}$$
  
= [24<sup>4</sup> + (24 × 24)(24)<sup>2</sup>] + [10.5 × 12<sup>3</sup>/3] + [(15.47 × 16 in.<sup>2</sup>)(29 ft × 12)<sup>2</sup>]  
= 30.3 × 10<sup>6</sup> in<sup>4</sup>.

Note that 98.9 percent of the value comes from one term: the reinforcement in the tension bulb. If the distributed #5 bars is added to this computation, the value becomes  $31.5 \times 10^6$  in.<sup>4</sup>

With the other masonry examples, the interpolation between gross and cracked section properties was used. The application of that is less clear here, where the properties step at midheight, so two analyses are performed. First, each story is considered to be cracked or uncracked. Second is the author's interpretation of the effective moment of inertia equation as:

For all the cracked walls (Provisions Eq. 11.5.4.3 [ACI 530, Commentary Sec. 3.1.5.3]):

$$I_{eff} = I_n \left(\frac{M_{cr}}{M_a}\right)^3 + I_{cr} \left[1 - \left(\frac{M_{cr}}{M_a}\right)^3\right] \le I_n$$
$$I_{eff} = \left(76.7 \times 10^6\right) \left(\frac{18,600}{30,600}\right)^3 + \left(30.6 \times 10^6\right) \left[1 - \left(\frac{18,600}{30,600}\right)^3\right] = 41.0 \times 10^6 \text{ in.}^4$$

The entire 12-story Wall D will be treated as a stepped, vertical masonry cantilever shear wall. For the lower step (Levels 1-6),  $I_{eff} = 41.0 \times 10^6$  in.<sup>4</sup> Even though the upper walls are uncracked,  $I_{eff}$  of the upper step (Levels 7-12), will be  $I_n$  reduced in the same proportion as the lower levels:

$$I_{eff} = (39.4 \times 10^6) \left( \frac{41.0 \times 10^6}{76.7 \times 10^6} \right) = 21.1 \times 10^6$$
 (upper levels)

Both the deflections and the fundamental period can now be found. Two RISA 2D analyses were run, and the deflections shown in Table 9.3-10 were obtained. The deflection from the RISA 2D analysis at each level is multiplied by  $C_d$  (= 3.5) to determine the inelastic deflection at each level. From these, the story drift,  $\Delta$ , at each level can be found.

The periods shown in the table validate the period of T = 0.75 sec previously used to determine the base shear in Sec. 9.3.3.2.

 Table 9.3-10
 Deflections for ELF Analysis (inches)

Using gross and cracked properties,	Using effective moment of inertia
-------------------------------------	-----------------------------------

FEMA 451, NEHRP Recommended Provisions: De	Design Examples
--	-----------------

	story by story ( $T = 0.798$ sec)					(T = 0.7)	755 sec)	
Level	Elastic	Total	Drift	Ratio	Elastic	Total	Drift	Ratio
12	3.40	11.90			3.14	10.99		
11	3.04	10.65	1.25		2.77	9.71	1.28	
10	2.68	9.38	1.27	1.01	2.40	8.41	1.30	1.01
9	2.32	8.10	1.27	1.00	2.04	7.13	1.28	0.99
8	1.95	6.84	1.26	0.99	1.68	5.87	1.26	0.98
7	1.60	5.60	1.24	0.98	1.34	4.68	1.19	0.95
6	1.26	4.41	1.19	0.96	1.02	3.58	1.10	0.92
5	0.95	3.34	1.07	0.90	0.76	2.65	0.93	0.85
4	0.66	2.31	1.03	0.96	0.52	1.82	0.83	0.90
3	0.40	1.40	0.91	0.88	0.32	1.11	0.71	0.85
2	0.20	0.68	0.71	0.78	0.16	0.55	0.56	0.79
1	0.06	0.20	0.48	0.67	0.05	0.17	0.38	0.68
0	0	0.00	0.20	0.42	0	0.00	0.17	0.44
101' 4	451NL 10.	25.4						

1.0 kip = 4.45 kN, 1.0 in. = 25.4 mm

The two methods give comparable results. The maximum building deflection is compared to the maximum deflection permitted by *Provisions* Sec. 11.5.4.1.1 as follows:

$$C_d \delta_{max} = 11.90 \text{ in.} < 14.4 \text{ in.} = 0.1 h_n$$
 OK

The maximum story drift occurs at Story 11 and is compared to the maximum story drift permitted by *Provisions* Table 5.2.8 [Table 4.5-1] as follows:

$$\Delta = 1.30 \text{ in.} > 1.20 \text{ in.} = 0.01 h_{sx}$$
 NG

Although this indicates a failure to satisfy the *Provisions*, in the author's opinion the drift is satisfactory for two reasons. First the MRS analysis shows smaller drifts (Table 9.3-11) that are within the criteria. On a more fundamental level, however, the authors believe the basic check for drift of a masonry wall is performed according to *Provisions* Sec. 11.5.4.1.1, which applies only to the total displacement at the top of the wall, and that the story drift for any particular story is more properly related to the values for non-masonry buildings. That limit is  $0.020 h_{sx}$ , or 2.4 in. per story. For a building with a torsional irregularity, *Provisions* Sec. 5.4.6.1 [Sec. 4.5.1] requires that the story drift be checked at the plan location with the largest drift, which would be a corner for this building. That limit is satisfied for this building, both by ELF and MRS analyses.

	maximum drift w	r of floor p displaceme ould be pe ugh not at	ents. Story rtinent,	At wall with maximum in-plane displacement. Roof limit for masonry would be pertinent.		
Level	Elastic	Total	Approx. Drift	Elastic	Total	Approx. Drift
12	2.48	8.67		1.91	6.70	
11	2.20	7.69	0.98	1.69	5.90	0.79
10	1.91	6.70	0.99	1.48	5.17	0.74
9	1.63	5.70	1.00	1.26	4.40	0.77
8	1.35	4.72	0.98	1.04	3.64	0.76
7	1.08	3.77	0.95	0.83	2.91	0.73
6	0.83	2.90	0.88	0.64	2.23	0.68
5	0.62	2.16	0.74	0.48	1.67	0.57
4	0.43	1.50	0.66	0.33	1.16	0.51
3	0.27	0.93	0.57	0.21	0.72	0.44
2	0.14	0.48	0.46	0.11	0.37	0.35
1	0.05	0.16	0.32	0.04	0.12	0.25
0	0.00	0.00	0.16	0.00	0.00	0.12
1.0 kip = 4.45 kN, 1.0 in. = 25.4 mm.						

 Table 9.3-11
 Displacements from Modal Analysis, inches

The drifts in Table 9.3-11 are not the true modal drifts. The values are computed from the modal sum maximum displacements, rather than being a modal sum of drifts in each mode. The values in the table are less than the true value.

Both tables also confirm that the change in stiffness at midheight does not produce a stiffness irregularity. *Provisions* Sec. 5.2.3.3, Exception 1 [Sec. 4.3.2.3, Exception 1], clarifies that if the drift in a story never exceeds 130 percent of the drift in the story above, then there is no vertical stiffness irregularity. Note that the inverse does not apply; even though the drift in Story 2 is more than double that in Story 1, it does not constitute a stiffness irregularity.

### 9.3.5 Out-of-Plane Forces

*Provisions* Sec 5.2.6.2.7 [Sec. 4.6.1.3] states that the bearing walls shall be designed for out-of-plane loads equal to:

$$w = 0.40 S_{DS} W_{c} \ge 0.1 W_{c}$$
  
w = (0.40)(1.00)(114 psf) = 45.6 psf \ge 0.1 W\_{c}

Therefore, w = 45.6 psf. Out-of-plane bending, using the strength design method for masonry, for a load of 45.6 psf acting on a 10 ft story height is approximated as 456 ft.-lb. per linear ft of wall. This compares to a computed strength of the wall of 1,600 in.-lb per linear foot of wall, considering only the #5 bars at 4 ft on center. Thus the wall is loaded to 28.5 percent of its capacity in flexure in the out-of-plane direction. The upper wall has the same reinforcement, about 42 percent of the load and about 71 percent of the thickness. Therefore, it will be loaded to a smaller fraction of its capacity. (Refer to Example 9.1 for a more detailed discussion of strength design of masonry walls, including the P-delta effect.)

### 9.3.6 Orthogonal Effects

In accordance with *Provisions* Sec. 5.2.5.2.2 [Sec. 4.4.2.3], orthogonal interaction effects must be considered for buildings in Seismic Design Category D when the ELF procedure is used. Any out-of-plane effect on the heavily reinforced bulbs is negligible compared to the in-plane effect, so orthogonal effects on the bulbs need not be considered further. Considering only the #5 bars and the load combination of 100 percent of in-plane load plus 30 percent of the out-of-plane load, yields a result that 0.3(0.285), or 8.6 percent of the capacity of the #5 bars is not available for in-plane resistance. Given that the #5 bars contribute about 12 percent to the tension resistance (130 kips, vs 960 kips for the bulb reinforcement), the overall effect is a change of about 1 percent in in-plane resistance, which is negligible.

This completes the design of the transverse Wall D.

### 9.3.7 Wall Anchorage

The anchorage for the bearing walls must be designed for the force,  $F_p$ , determined in accordance with *Provisions* Sec. 5.2.6.2.7 [Sec. 4.6.1.3] as:

 $F_p = 0.4S_{DS}W_c = (0.4)(1.00)(10 \text{ ft})(114 \text{ psf}) = 456 \text{ lb/ft}$ Minimum force =  $0.10W_c = (0.10)(10 \text{ ft})(114 \text{ psf}) = 114 \text{ lb/ft}$ 

*Provisions* Sec. 5.2.6.3.2 [Sec. 4.6.2.1] references *Provisions* Sec. 6.1.3 [Sec. 6.2.2] for anchorage of walls where diaphragms are not flexible. For the lower wall:

$$F_p = \frac{0.4a_p S_{DS} W_p}{R_p / I_p} (1 + 2z / h) = \frac{0.4(1.0)(1.0)(10 \,\text{ft.} \times 114 \,\text{psf})}{2.5 / 1.0} (1 + 2(0.5)) = 364 \,\text{lb./ft.}$$

Therefore, design for 456 lb/ft. For a 2 ft-6 in. joist spacing, the anchorage force at each joist is  $F_p = 1,140$  lb.

Refer to Figure 9.3-12 for the connection detail. A 3/16-in. fillet, weld 2 in. long on each side of the joist seat to its bearing plate will be more than sufficient. Two1/2 in.-diameter headed anchor studs on the bottom of the bearing plate also will be more than sufficient to transfer 4,560 lb into the wall.

### 9.3.8 Diaphragm Strength

See Example 7.1 for a more detailed discussion on the design of horizontal diaphragms.

To compute the story force associated with the diaphragm on each level, use *Provisions* Eq. 5.2.6.4-4 [Eq. 4.6-2]:

$$F_{px} = \frac{\sum_{i=x}^{n} F_i}{\sum_{i=x}^{n} w_i} w_{px}$$

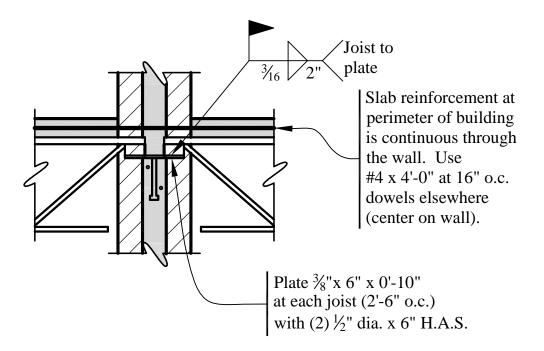


Figure 9.3-12 Floor anchorage to wall (1.0 in. = 25.4 mm, 1.0 ft = 0.3048 m).

The results are shown in Table 9.3-12. Note that  $w_i$  is approximately the same as  $w_{px}$  for this case, the only difference being the weight of the walls perpendicular to the force direction, so the  $w_i$  values were used for both.

Table	<b>9.3-12</b> Diaphr	agm Seismic	Forces
Level	w <sub>i</sub> (kips)	$F_i$ (kips)	$F_{px}$ (kips)
12	768	329	329
11	917	357	373
10	917	320	355
9	917	284	336
8	917	249	318
7	917	214	301
6	1109	218	338
5	1300	208	365
4	1300	162	336
3	1300	117	309
2	1300	74	282
1	1300	34	258

Table 9.3-12 Diaphragm Seismic Forces

1.0 kip = 4.45 kN

The maximum story force is 373 kips. Therefore, use 373 kips/152 ft = 2.45 kips/ft in the transverse direction. The shear in the diaphragm is shown in Figure 9.3-13b. The reaction, *R*, at each wall pair is 373/4 = 93.25 kips. The diaphragm force at each wall pair is 93.25 kips/(2 × 33 ft) = 1.41 kips/ft.

The maximum diaphragm shear stress is v = V/td = 1410 plf/(2.5 in.)(12 in.) = 47 psi. This compares to an allowable shear of

$$\phi v_c = (0.85)(2)\sqrt{f'_c} = (0.85)(2)\sqrt{3,000} = 93$$
 psi

for 3,000 psi concrete. Thus, no shear reinforcing is necessary. Provide  $\rho = 0.0018$  as minimum reinforcement, so  $A_s = 0.054$  in.<sup>2</sup>/ft. Use WWF 6 × 6-2.9/2.9, which has  $A_s = 0.058$  in.<sup>2</sup>/ft.

The moment in the diaphragm is shown in Figure 9.3-13c. The maximum moment is 2,460 ft-kips.

Perimeter reinforcement in the diaphragm is determined from:

$$T = M/d = (2,460 \text{ ft-kips})/(72 \text{ ft}) = 34.1 \text{ kips}$$

 $A_s = T/\phi F_y = 34.1$  kips / (0.85)(60 ksi) = 0.67 in.<sup>2</sup>

Boundary elements of diaphragms may also serve as collectors. The collector force is not usually the same as the chord force. *Provisions* Sec. 5.2.6.4.1 [Sec. 4.6.2.2] requires that collector forces be amplified by  $\Omega_0$ . Collector elements are required in this diaphragm for the longitudinal direction. A similar design problem is illustrated in Chapter 7 of this volume. Where reinforcing steel withing a topping slab is used for chords or collectors, ACI 318, Sec. 21.9.8 (2002 edition) imposes special spacing and cover requirements. Given the thin slab in this building, the chord reinforcement will have to be limited to bars with couplers at the splices or a thickened edge will be required.

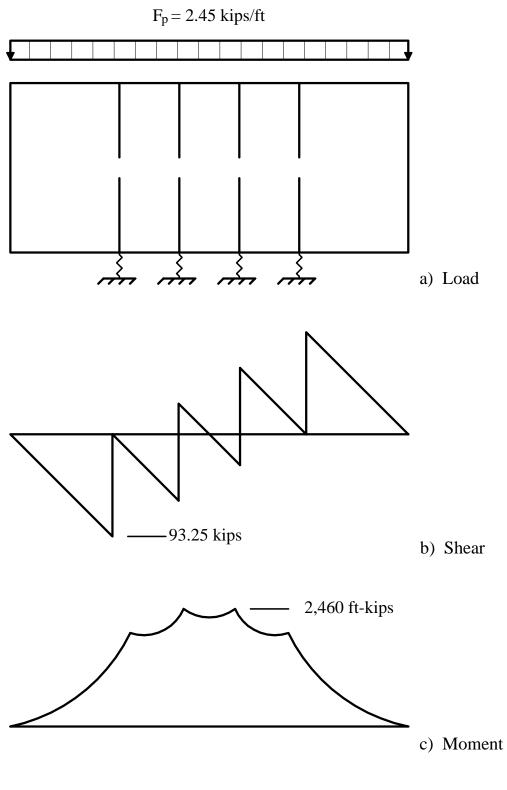




**Figure 9.3-13** Shears and moments for diaphragm (1.0 kip/ft = 14.6 kN/m, 1.0 kip = 4.45 kN, 1.0 kip-ft = 1.36kN-m)

# 10

## WOOD DESIGN

### Peter W. Somers, P.E. and Michael Valley, P.E.

This chapter examines the design of a variety of wood building elements. Section10.1 features a BSSC trial design prepared in the early 1980s as a starting point. Section 10.2 completes the roof diaphragm design for the building featured in Section 9.1. In both cases, only those portions of the designs necessary to illustrate specific points are included.

Typically, the weak links in wood systems are the connections, but the desired ductility must be developed by means of these connections. Wood members have some ductility in compression (particularly perpendicular to grain) but little in tension. Nailed plywood shear panels develop considerable ductility through yielding of nails and crushing of wood adjacent to nails. Because wood structures are composed of many elements that must act as a whole, the connections must be considered carefully to ensure that the load path is complete. "Tying the structure together," which is as much an art as a science, is essential to good earthquake-resistant construction.

Wood elements often are used in low-rise masonry and concrete buildings. The same basic principles apply to the design of wood elements, but certain aspects of the design (for example, wall-to-diaphragm anchorage) are more critical in mixed systems than in all-wood construction.

Wood structural panel sheathing is referred to as "plywood" in this chapter. As referenced in the 2000 *NEHRP Recommended Provisions*, wood structural panel sheathing includes plywood and other products, such as oriented-strand board (OSB), that conform to the materials standards of Chapter 12. According to *Provisions* Chapter 12, panel materials other than wood structural panel sheathing do not have a recognized capacity for seismic-force resistance in engineered construction.

In addition to the 2000 *NEHRP Recommended Provisions* and *Commentary* (hereafter, the *Provisions* and *Commentary*), the documents edited below are either referenced directly, or are useful design aids for wood construction.

AF&PA Manual	American Forest & Paper Association 1996. <i>Manual for Engineered Wood Construction (LRFD)</i> , including supplements, guidelines, and ASCE 16-95, AF&PA.
[AF&PA Wind & Seismic	American Forest and Paper Association. 2001. Special Design Provisions for Wind and Seismic, ADS/LRFD Supplement. AF&PA.]

ANSI/AITC A190.1	American National Standards Institute/American Institute of Timber Construction. 1992. American National Standard for Wood Products: Structural Glued-Laminated Timber, A190.1. AITC.
APA PDS	American Plywood Association. 1998. Plywood Design Specification, APA.
APA 138	American Plywood Association. 1998. <i>Plywood Diaphragms</i> , APA Research Report 138. APA.
ASCE 7	American Society of Civil Engineers. 1998 [2002]. <i>Minimum Design Loads for Buildings and Other Structures</i> . ASCE.
ASCE 16	American Society of Civil Engineers. 1995. Standard for Load and Resistance Factor Design (LRFD) for Engineered Wood Construction. ASCE.
UBC Std 23-2	International Conference of Building Officials. 1997. UBC Standard 23-2 Construction and Industrial Plywood, Uniform Building Code. ICBO.
Roark	Roark, Raymond. 1985. Formulas for Stress and Strain, 4th Ed. McGraw-Hill.
USGS CD-ROM	United States Geological Survey. 1996. Seismic Design Parameters, CD-ROM. USGS.
WWPA Rules	Western Wood Products Association. 1991. Western Lumber Grading Rules. WWPA.

Although this volume of design examples is based on the 2000 *Provisions*, it has been annotated to reflect changes made to the 2003 *Provisions*. Annotations within brackets,[], indicated both organizational changes (as a result of a reformat of all the chapters of the 2003 *Provisions*) and substantive technical changes to the 2003 *Provisions* and it's primary reference documents. While the general concepts of the changes are described, the design examples and calculations have not been revised to reflect the changes to the 2003 *Provisions*.

The most significant change to the wood chapter in the 2003 *Provisions* is the incorporation by reference of the AF&PA, ADS/LRFD Supplement, *Special Design Provisions for Wind and Seismic* for design of the engineered wood construction. A significant portion of the 2003 *Provisions* Chapter 12, including the diaphragm and shear wall tables, has been replaced by a reference to this document. This updated chapter, however, does not result in significant technical changes , as the Supplement, (referred to herein as AF&PA Wind&Seismic) is in substantial agreement with the 2000 *Provisions*. There are, however, some changes to the provisions for perforated shear walls, which are covered in Section 10.1

Some general technical changes in the 2003 *Provisions* that relate to the calculations and/or design in this chapter include updated seismic hazard maps, changes to the Seismic Design Category classification for short period structures, revisions to the redundancy requirements, revisions to the wall anchorage design requirement for flexible diaphragms, and a new "Simplified Design Procedure" that could be applicable to the examples in this chapter.

Where the affect the design examples in this chapter, other significant changes to the 2003 *Provisions* and primary reference documents are noted. However, some minor changes to the 2003 *Provisions* and the reference documents may not be noted.

### 10.1 THREE-STORY WOOD APARTMENT BUILDING; SEATTLE, WASHINGTON

This example features a wood frame building with plywood diaphragms and shear walls. It is based on a BSSC trial design by Bruce C. Olsen, Structural Engineer, Seattle, Washington.

### **10.1.1 BUILDING DESCRIPTION**

This three-story, wood frame apartment building has plywood floor diaphragms and shear walls. The building has a double-loaded central corridor. Figure 10.1-1 shows a typical floor plan, and Figure 10.1-2 shows a longitudinal section and elevation. The building is located in a neighborhood a few miles north of downtown Seattle. The site coordinates for determining the seismic design parameters are 47.69° N, 122.32° W.

The shear walls in the longitudinal direction are located on the exterior faces of the building and along the corridor. (In previous versions of this volume of design examples, the corridor walls were gypsum wallboard sheathed shear walls; however, gypsum wallboard sheathing, is no longer recognized for engineered design of shear walls per *Provisions* Sec. 12.3.5. Therefore, plywood shear walls are provided at the corridors.) The entire solid (non-glazed) area of exterior walls plywood sheathing, but only a portion of the corridor walls will require sheathing. For the purposes of this example, assume that each corridor wall will have a net of 55 ft of plywood (the reason for this is explained later). In the transverse direction, the end walls and one line of interior shear walls. The interior walls now are required for control of diaphragm deflections given the increased seismic ground motion design parameters for the Seattle area.)

The floor and roof systems consist of wood joists supported on bearing walls at the perimeter of the building, the corridor lines, plus one post-and-beam line running through each bank of apartments. Exterior walls are framed with  $2\times6$  studs for the full height of the building to accommodate insulation. Interior bearing walls require  $2\times6$  or  $3\times4$  studs on the corridor line up to the second floor and  $2\times4$  studs above the second floor. Apartment party walls are not load bearing; however, they are double walls and are constructed of staggered,  $2\times4$  studs at 16 in. on center. Surfaced, dry (seasoned) lumber, is used for all framing to minimize shrinkage. Floor framing members are assumed to be composed of Douglas Fir-Larch material, and wall framing is Hem-fir No. 2, as graded by the WWPA. The material and grading of other framing members associated with the lateral design is as indicated in the example. The lightweight concrete floor fill is for sound isolation, and is interrupted by the party walls, corridor walls, and bearing walls.

The building is founded on interior footing pads, continuous strip footings, and grade walls (Figure 10.1-3). The depth of the footings, and the height of the grade walls, are sufficient to provide crawl space clearance beneath the first floor.

The building is typical of apartment construction throughout the western United States, and has the weight necessary to balance potential overturning forces in the transverse direction. If the ground floor were a slab-on-grade, however, the resulting shallower grade wall might well require special attention, due to the possibility of overturning on some of the shear wall units.

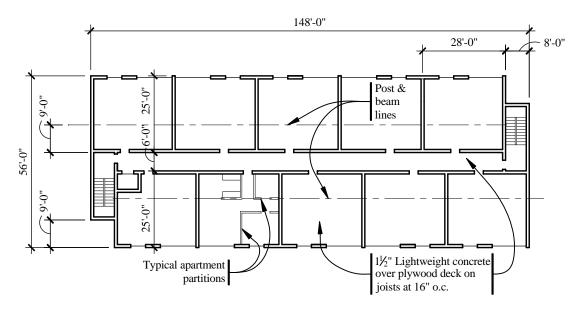


**Figure 10.1-1** Typical floor plan (1.0 ft = 0.3048 m).

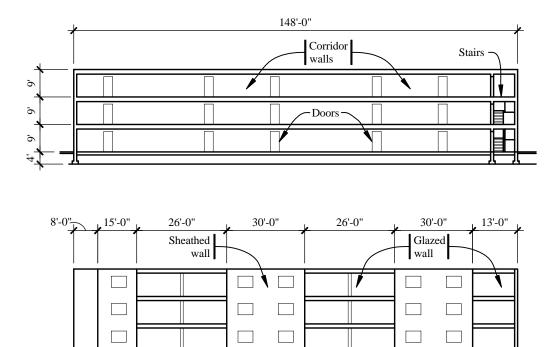


**Figure 10.1-2** Longitudinal section and elevation (1.0 ft = 0.3048 m).

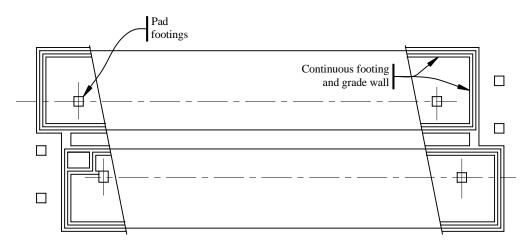


Figure 10.1-3 Foundation plan.

### 10.1.1.1 Scope

In this example, the structure is designed and detailed for forces acting in the transverse and longitudinal directions. However, greater attention is paid to the transverse direction, because of diaphragm flexibility. The example includes the following

- 1. Development of equivalent static loads, including torsional effects on plywood diaphragms,
- 2. Design and detailing of transverse plywood walls for shear and overturning moment,
- 3. Design and detailing of plywood floor and roof diaphragms,
- 4. Design and detailing of wall and diaphragm chord members,
- 5. Detailed deflection and P-delta calculations, and
- 6. Design and detailing of longitudinal plywood walls using the requirements for perforated shear walls.

[Note that the new "Simplified Design Procedure" contained in 2003 *Provisions* Simplified Alternate Chapter 4 as referenced by 2003 *Provisions* Sec. 4.1.1 is likely to be applicable to this example, subject to the limitations specified in 2003 *Provisions* Sec. Alt. 4.1.1.]

### **10.1.2 BASIC REQUIREMENTS**

### 10.1.2.1 Provisions Parameters

Seismic Use Group (Provisions Sec. 1.3 [1.2])	= I
Occupancy Importance Factor, I (Provisions Sec. 1.4 [1.3])	= 1.0
Site Coordinates	$= 47.69^{\circ} \text{ N}, 122.32^{\circ} \text{ W}$
Short Period Response, S <sub>s</sub> (USGS CD-ROM)	= 1.34
One Second Period Response, S <sub>1</sub> (USGS CD-ROM)	= 0.46
Site Class (Provisions Sec. 4.1.2.1 [3.5])	= D
Seismic Design Category (Provisions Sec. 4.2 [1.4])	= D
Seismic-Force-Resisting System (Provisions Table 5.2.2 [4.3-1])	= Wood panel shear wall
Response Modification Coefficient, <i>R</i> ( <i>Provisions</i> Table 5.2.2 [4.3-1)	= 6.5
System Overstrength Factor, $\Omega_0$ ( <i>Provisions</i> Table 5.2.2 [4.3-1)	= 3
Deflection Amplification Factor, $C_d$ ( <i>Provisions</i> Table 5.2.2 [4.3-1)	= 4

### 10.1.2.2 Structural Design Criteria

### 10.1.2.2.1 Ground Motion (Provisions Sec. 4.1.2 [3.3])

Based on the site location, the spectral response acceleration values can be obtained from either the seismic hazard maps accompanying the *Provisions* or from the USGS CD-ROM. For site coordinates 47.69° N, 122.32° W, the USGS CD-ROM returns short period response,  $S_s = 1.34$  and one second period response,  $S_1 = 0.46$ .

[The 2003 *Provisions* have adopted the 2002 USGS probabilistic seismic hazard maps, and the maps have been added to the body of the 2003 *Provisions* as figures in Chapter 3 (instead of the previously used separate map package). A CD-ROM containing the site response parameters based on the 2002 maps is also available.]

The spectral response factors are then adjusted for the site class (*Provisions* Sec. 4.1.2.4 [3.5]). For this example, it is assumed that a site class recommendation was not part of the soils investigation, which would not be uncommon for this type of construction. When soil properties are not known, *Provisions* Sec. 4.1.2.1 [3.5] defaults to Site Class D, provided that soft soils (Site Class E or F) are not expected to be present at the site (a reasonable assumption for soils sufficient to support a multistory building on shallow spread footings). The adjusted spectral response acceleration parameters are computed, according to *Provisions* Eq. 4.1.2.4-1 and 4.1.2.4-2 [3.3-1 and 3.3-4], for the short period and one second period, respectively, as:

 $S_{MS} = F_a S_s = 1.0(1.34) = 1.34$  $S_{M1} = F_v S_1 = 1.54(0.46) = 0.71$ 

where  $F_a$  and  $F_v$  are site coefficients defined in *Provisions* Tables 4.1.2.4a and 4.1.2.4b [3.3-1 and 3.3-2], respectively. Note that Straight line interpolation was used for  $F_v$ .

Finally, the design spectral response acceleration parameters (*Provisions* Sec. 4.1.2.5 [3.3.3]) are determined in accordance with *Provisions* Eq. 4.1.2.5-1 and 4.1.2.5-2 [3.3-3 and 3.3-4], for the short period and one second period, respectively, as:

$$S_{DS} = \frac{2}{3}S_{MS} = \frac{2}{3}(1.34) = 0.89$$
$$S_{DI} = \frac{2}{3}S_{MI} = \frac{2}{3}(0.71) = 0.47$$

10.1.2.2.3 Seismic Design Category (Provisions Sec. 4.2 [1.4])

Based on the Seismic Use Group and the design spectral response acceleration parameters, the Seismic Design Category is assigned to the building based on *Provisions* Tables 4.2.1a and 4.2.1b [1.4-1 and 1.4-2]. For this example, the building is assigned Seismic Design Category D.

[Note that the method for assigning seismic design category for short period buildings has been revised in the 2003 *Provisions*. If the fundamental period,  $T_{av}$  is less than  $0.8T_s$ , the period used to determine drift is less than  $T_s$ , and the base shear is computed using 2003 *Provisions* Eq 5.2-2, then seismic design category is assigned using just 2003 *Provisions* Table 1.4-1 (rather than the greater of 2003 *Provisions* Tables 1.4-1 and 1.4-2). The change does not affect this example.]

10.1.2.2.4 Load Path (Provisions Sec. 5.2.1 [14.2-1])

See Figure 10.1-4. For both directions, the load path for seismic loading consists of plywood floor and roof diaphragms and plywood shear walls. Because the lightweight concrete floor topping is discontinuous at each partition and wall, it is not considered to be a structural diaphragm.

10.1.2.2.5 Basic Seismic-Force-Resisting Systems (Provisions Sec. 5.2.2 [4.3])

Building Class (Provisions Table 5.2.2 [4.3-1]): Bearing Wall System

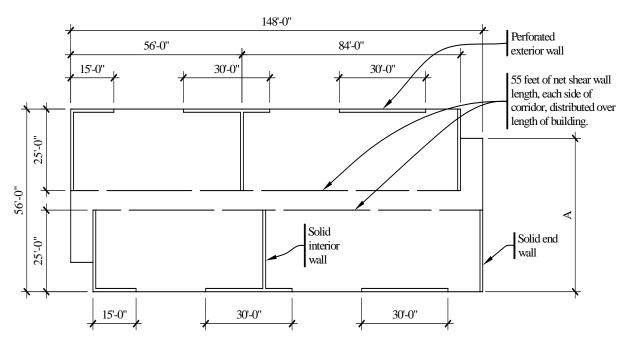
Seismic-Force-Resisting System (*Provisions* Table 5.2.2 [4.3-1]): Light frame walls with shear panels with R = 6.5,  $\Omega_0 = 3$ , and  $C_d = 4$  for both directions

10.1.2.2.6 Structure Configuration (Provisions Sec. 5.2.3 [5.3.2])

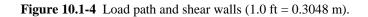
Diaphragm Flexibility (*Provisions* Sec. 5.2.3.1 [4.3.2.1]): Rigid (wood panel diaphragm in light frame structure with structural panels for shear resistance). *Provisions* Sec. 12.4.1.1 [4.3.2.1]defines a structural panel diaphragm as flexible, if the maximum diaphragm deformation is more than two times the average story drift. Due to the central shear wall, this is not expected to be the case in this building.

Plan Irregularity (*Provisions* Sec. 5.2.3.2 [4.3.2.2]): Since the shear walls are not balanced for loading in the transverse direction (see Figure 10.1-4), there will be some torsional response of the system. The potential for torsional response combined with the rigid diaphragm requires that the building be checked for a torsional irregularity (*Provisions* Table 5.2.3.2 [4.3-2]). This check will be performed following the initial determination of seismic forces, and the final seismic forces will be modified if required.

Vertical Irregularity (Provisions Sec. 5.2.3.3 [4.3.2.3]): Regular



A: Another solution would be to use the full end for the shear wall, not just 25 feet.



### 10.12.2.7 Redundancy (Provisions Sec. 5.2.4 [4.3.3])

For Seismic Design Category D, the reliability factor,  $\rho$ , is computed per *Provisions* Eq. 5.2.4.2 [4.3.3.2]. Since the computation requires more detailed information than is known prior to the design, assume  $\rho = 1.0$  for the initial analysis and verify later. If, in the engineer's judgement, the initial design appears to possess relatively few lateral elements, the designer may wish to use an initial  $\rho$  greater than 1.0 (but no greater than 1.5).

[The redundancy requirements have been substantially changed in the 2003 *Provisions*. For a shear wall building assigned to Seismic Design Category D,  $\rho = 1.0$  as long as it can be shown that failure of a shear wall with height-to-length-ratio greater than 1.0 would not result in more than a 33 percent reduction in story strength or create an extreme torsional irregularity. The intent is that the aspect ratio is based on story height, not total height. Therefore, the redundancy factor would have to be investigated only in the longitudinal direction where the aspect ratios of the perforated shear walls would be interpreted as having aspect ratios greater than 1.0 at individual piers. In the longitudinal direct, where the aspect ratio is less than 1.0,  $\rho = 1.0$  by default.]

### 10.1.2.2.8 Analysis Procedure (Provisions Sec. 5.2.5 [4.4.1])

Design in accordance with the equivalent lateral force (ELF) procedure (*Provisions* Sec. 5.4 [5.2]): No special requirements. In accordance with *Provisions* Sec. 5.2.5.2.3 [4.4.2], the structural analysis must consider the most critical load effect due to application of seismic forces in any direction for structures assigned to Seismic Design Category D. For the ELF procedure, this requirement is commonly satisfied by applying 100 percent of the seismic force in one direction, and 30 percent of the seismic force in the perpendicular direction; as specified in *Provisions* Sec. 5.2.5.2.2, Item a [4.4.2.2, Item 1]. For a light-framed shear wall building, with shear walls in two orthogonal directions, the only element affected by this directional combination would be the design of the shear wall end post and tie-down, located where the ends of two perpendicular walls intersect. In this example, the requirement only affects the shear wall intersections at the upper left and lower left corners of Figure 10.1-4. The directional requirement is satisfied using a two-dimensional analysis in the design of the remainder of the shear wall and diaphragm elements.

### 10.1.2.2.9 Design and Detailing Requirements (Provisions Sec. 5.2.6 [4.6])

See *Provisions* Chapters 7 and 12 for special foundation and wood requirements, respectively. As discussed in greater detail below, *Provisions* Sec. 12.2.1, now utilizes Load and Resistance Factor Design (LRFD) for the design of engineered wood structures. Therefore, the design capacities are consistent with the strength design demands of *Provisions* Chapter 5 [4 and 5].

### 10.1.2.2.10 Combination of Load Effects (Provisions Sec. 5.2.7 [4.2.2])

The basic design load combinations are as stipulated in ASCE 7 and modified by the *Provisions* Eq. 5.2.7-1 and 5.2.7-2 [4.2-1 and 4.2-1]. Seismic load effects according to the *Provisions* are:

$$E = \rho Q_E + 0.2 S_{DS} D$$

and

$$E = \rho Q_E - 0.2 S_{DS} D$$

when seismic and gravity are additive and counteractive, respectively.

For  $S_{DS} = 0.89$  and assuming  $\rho = 1.0$  (both discussed previously), the design load combinations are as stipulated in ASCE 7:

$$1.2D + 1.0E + 0.5L + 0.2S = 1.38D + 1.0Q_E + 0.5L + 0.2S$$

and

 $0.9D - 1.0E = 0.72D - 1.0Q_E$ 

10.1.2.2.11 Deflection and Drift Limits (Provisions Sec. 5.2.8 [4.5.1])

Assuming that interior and exterior finishes have not been designed to accommodate story drifts, then the allowable story drift is (*Provisions* Table 2.5.8 [4.5-1]):

 $\Delta_a = 0.020 \ h_{sx}$ 

where interstory drift is computed from story drift as (Provisions Eq. 5.4.6.1 [5.2-15]):

$$\Delta_{x} = \delta_{x} - \delta_{x-1} = \frac{C_{d} \left[ \delta_{xe} - \delta_{(x-1)e} \right]}{I}$$

where  $C_d$  is the deflection amplification factor, I is the occupancy importance factor, and  $\delta_{xe}$  is the total elastic deflection at Level x.

#### 10.1.2.3 Basic Gravity Loads

Roof:	
Live/Snow load (in Seattle, snow load governs over roof live load; in other areas this may not be the case)	= 25 psf
Dead load (including roofing, sheathing, joists, insulation, and gypsum ceiling)	= 15 psf
Floor:	
Live load	= 40 psf
Dead load (1 <sup>1</sup> / <sub>2</sub> in. lightweight concrete, sheathing, joists, and gypsum ceiling. At first floor, omit ceiling but add insulation.)	= 20 psf
Interior partitions, corridor walls (8 ft high at 11 psf) load	= 7 psf distributed floor
Exterior frame walls (wood siding, plywood sheathing, 2×6 studs, batt insulation, and 5/8-in. gypsum drywall)	= 15 psf of wall surface
Exterior double glazed window wall	= 9 psf of wall surface
Party walls (double-stud sound barrier)	= 15 psf of wall surface
Stairways	= 20 psf of horiz. projection

Perimeter footing (10 in. by 1 ft-4 in.) and grade beam (10 in. by 3 ft-2 in.)	= 562 plf
Corridor footing (10 in by 1 ft-4 in.) and grade wall (8 in. by 1 ft-3 in.); 18 in. minimum crawl space under first floor	= 292 plf
Applicable seismic weights at each level $W_{roof}$ = area (roof dead load + interior partitions + party walls) + end walls + longitudinal walls	= 182.8 kips
$W_3 = W_2$ = area (floor dead load + interior partitions + party walls) + end walls + longitudinal walls	= 284.2 kips
Effective total building weight, W	= 751 kips

For modeling the structure, the first floor is assumed to be the seismic base, because the short crawl space with concrete foundation walls is quite stiff compared to the superstructure.

# **10.1.3 SEISMIC FORCE ANALYSIS**

The analysis is performed manually following a step-by-step procedure for determining the base shear (*Provisions* Sec. 5.4.1 [5.2.1]), and the distribution of vertical (*Provisions* Sec. 5.4.3 [5.2.3]) and horizontal (*Provisions* Sec. 5.4.4 [5.2.4]) shear forces. Since there is no basic irregularity in the building mass, the horizontal distribution of forces to the individual shear walls is easily determined. These forces need only be increased to account for accidental torsion (see subsequent discussion).

No consideration is given to soil-structure interaction since there is no relevant soil information available; a common situation for a building of this size and type. The soil investigation ordinarily performed for this type of structure is important, but is not generally focused on this issue. Indeed, the cost of an investigation sufficiently detailed to permit soil-structure interaction effects to be considered, would probably exceed the benefits to be derived.

#### 10.1.3.1 Period Determination and Calculation of Seismic Coefficient (Provisions Sec. 5.4.1 [5.2.1])

Using the values for  $S_{DI}$ ,  $S_{DS}$ , R, and I from Sec. 10.1.2.1, the base shear is computed per *Provisions* Sec. 5.4.1 [5.2.1]. The building period is based on *Provisions* Eq. 5.4.2.1-1 [5.2-6]:

$$T_a = C_r h_n^x = 0.237$$

where  $C_r = 0.020$ ,  $h_n = 27$  ft, and x = 0.75.

According to Provisions Eq. 5.4.1.1-1 [5.2-2]:

$$C_s = \frac{S_{DS}}{R/I} = \frac{0.89}{6.5/1.0} = 0.137$$

but need not exceed Provisions Eq. 5.4.1.1-2 [5.2-3]:

$$C_s = \frac{S_{DI}}{T(R/I)} = \frac{0.47}{(0.237)(6.5/1.0)} = 0.305$$

Although it would probably never govern for this type of structure, also check minimum value according to *Provisions* Eq. 5.4.1.1-3:

 $C_s = 0.044IS_{DS} = (0.044)(1.0)(0.89) = 0.039$ 

[This minimum  $C_s$  value has been removed in the 2003 *Provisions*. In its place is a minimum  $C_s$  value for long-period structures, which is not applicable to this example.]

The calculation of actual *T* as based on the true dynamic characteristics of the structure would not affect  $C_s$ ; thus, there is no need to compute the actual period because the *Provisions* does not allow a calculated period that exceeds  $C_uT_a$  where  $C_u = 1.4$  (see *Provisions* Sec. 5.4.2 [5.2.2]). Computing the base shear coefficient, per *Provisions* Eq. 5.4.1.1-1 [5.2-2], using this maximum period, would give  $C_s = 0.218$ , which still exceeds 0.137. Therefore, short period response governs the seismic design of the structure, which is common for low-rise buildings.

#### 10.1.3.2 Base Shear Determination

According to *Provisions* Eq. 5.4.1 [5.2-1]:

 $V = C_s W = 0.137(751) = 103$  kips (both directions)

where effective total weight is W = 751 kips as computed previously.

#### **10.1.3.3 Vertical Distribution of Forces**

Forces are distributed as shown in Figure 10.1-5, where the story forces are calculated according to *Provisions* Eq. 5.4.3-1 and 5.4.3-2 [5.2-10 and 5.2-11]:

$$F_{x} = C_{vx}V = \left(\frac{w_{x}h_{x}^{k}}{\sum\limits_{i=1}^{n}w_{i}h_{i}^{k}}\right)V$$

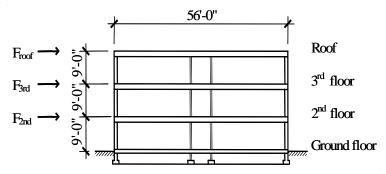


**Figure 10.1-5** Vertical shear distribution (1.0 ft = 0.3048 m).

For T < 0.5, k = 1.0 and  $\sum w_i h_i^k = 182.2(27) + 284.2(18) + 284.2(9) = 12,610$ 

$F_{roof} = [182.8(27)/12,608](103.2)$	= 40.4 kips
$F_{3rd} = [284.2(18)/12,608](103.2)$	= 41.9 kips
$F_{2nd} = [284.2(9)/12,608](103.2)$	= <u>20.9 kips</u>
Σ	= 103 kips

\_ \_ \_ \_ \_ \_ \_ \_ \_ \_ \_ \_ \_ \_ \_ \_ \_ \_

It is convenient and common practice, to perform this calculation along with the overturning moment calculation. Such a tabulation is given in Table 10.1-1.

	Ta	ble 10.1-1	Seismic Coeffi	cients, Force	s, and Mome	nts	
Level x	W <sub>x</sub> (kips)	$h_x$ (ft)	$w_{x}h_{x}^{k}$ $(k=1)$	$C_{vx}$	$F_x$ (kips)	$V_x$ (kips)	$M_x$ (ft-kips)
Roof	182.8	27	4,936	0.391	40.4		
						40.4	364
3	284.2	18	5,115	0.406	41.9		
						82.3	1,104
2	284.2	9	2,557	0.203	20.9		
						103.2	2,033
Σ	751.2		12,608				

1.0 ft = 0.3048 m, 1.0 kip = 4.45 kN, 1.0 ft-kip= 1.36 kN-m.

# 10.1.3.4 Horizontal Distribution of Shear Forces to Walls

Since the diaphragms are defined as "rigid" by the *Provisions* (Sec 5.2.3.1 [4.3.2.1] and 12.4.1.1), the horizontal distribution of forces must account for relative rigidity of the shear walls, and horizontal torsion must be included. As discussed below, for buildings with a Type 1a or 1b torsional irregularity (per *Provisions* Sec. 5.2.3.2 [4.3.2.2]) the torsional amplification factor (*Provisions* Sec. 5.4.4.3 [5.2.4.3]) must be calculated.

It has been common practice for engineers to consider wood diaphragms as flexible, regardless of the relative stiffness between the walls and the diaphragms. Under the flexible diaphragm assumption, loads are distributed to shear walls based on tributary area, without taking diaphragm continuity, or relative wall rigidity into account. Recognizing that diaphragm stiffness should not be ignored (even for wood structural panel sheathing), the *Provisions* provides limits on when the flexible diaphragm assumption may be used and when it may not be used.

The calculation of horizontal force distribution for rigid diaphragms, can be significantly more laborious than the relatively simple tributary area method. Therefore, this example illustrates some simplifications that can be used as relatively good approximations (as confirmed by using more detailed calculations). The design engineer is encouraged to verify all simplifying assumptions that are used to approximate rigid diaphragm force distribution.

For this example, forces are distributed as described below.

# 10.1.3.4.1 Longitudinal Direction

Based on the rigid diaphragm assumption, force is distributed based on the relative rigidity of the longitudinal walls, and the transverse walls are included for resisting torsion. By inspection, however, the center of mass coincides with the center of rigidity and , thus, the torsional demand is just the accidental torsional moment resulting from a 5 percent eccentricity of force from the center of mass (*Provisions* Sec. 5.4.4.2 [5.2.4.2]).

In this direction, there are four lines of resistance and the total torsional moment is relatively small. Although the walls are unequal in length, the horizontal distribution of the forces can be simplified by making two reasonable assumptions. First, for plywood shear walls, it is common to assume that stiffness is proportional to net in-plane length of sheathing (assuming sheathing thickness, nailing, and chord elements are roughly similar). Second, for this example, assume that all of the torsional moment is resisted by the end walls in the transverse directions. This is a reasonable assumption because the walls have a greater net length than the longitudinal exterior shear walls and are located much farther from the center of rigidity (and thus contribute more significantly to the rotational resistance).

Therefore, direct shear is distributed in proportion to wall length and torsional shear is neglected. Each exterior wall has 45 ft net length and each corridor wall has 55 ft net length for a total of 200 ft of net shear wall. The approximate load to each exterior wall is  $(45/200)F_x = 0.225F_x$ , and the load to each corridor wall is  $(55/200)F_x = 0.275F_x$ . (The force distribution was also computed using a complete rigidity model, including accidental torsion, with all transverse and longitudinal wall segments. The resulting distribution is  $0.231F_x$  to the exterior walls and  $0.276F_x$  to the corridor walls, for a difference of 2.7 percent and 0.4 percent, respectively).

# 10.1.3.4.2 Transverse Direction

Again, based on the rigid diaphragm assumption, force is to be distributed based on relative rigidity of the transverse walls, and the longitudinal walls are included for resisting torsion because the center of mass does not coincide with the center of rigidity. The torsional demand must be computed. Assuming that all six transverse wall segments have the same rigidity, the distance from the center of rigidity (*CR*) to the center of mass (*CM*) can be computed as:

$$CM - CR = 148/2 - \frac{4+60+144}{3} = 4.67$$
ft

The accidental torsional moment resulting from a 5 percent eccentricity of force from the center of mass (*Provisions* Sec. 5.4.4.2 [5.2.4.2]) must also be considered.

As in the longitudinal direction, the force distribution in the transverse direction can be computed with reasonable accuracy by utilizing a simplified model. This simplification is made possible largely because the transverse wall segments are all of the same length and, thus, the same rigidity (assuming nailing and chord members are also the same for all wall segments). First, although the two wall segments at each line of resistance are offset in plan (Figure 10.1-4), assume that the wall segments do align, and are located at the centroid of the two segments. Second, assume that the longitudinal walls do not resist the torsional moment. Third, since interior transverse wall segments are located close to the center of rigidity, assume that they do not contribute to the resistance of the torsional moment.

To determine the forces on each wall, split the seismic force into two parts: that due to direct shear and that due to the torsional moment. Because their rigidities are the same, the direct shear is resisted by all six wall segments equally and is computed as  $0.167F_x$ . The torsional moment is resisted by the four end wall segments. Including accidental torsion, the total torsional moment is computed as:

Total Torsional Moment,  $M_t + M_{ta} = F_x \times (4.67 \text{ ft} + 0.05 \times 148 \text{ ft}) = 12.07F_x$ Torsional Shear to End Walls =  $12.07F_x/140 \text{ ft} = 0.086F_x$ 

Therefore, the simplified assumption yields a total design force of  $0.167F_x + 0.086F_x/2 = 0.210F_x$ , at each of the end wall segments on the right side of Figure 10.4-1,  $0.167F_x - 0.086F_x/2 = 0.124F_x$  at each of the end wall segments on the left side of the figure, and  $0.167F_x$  at each interior wall segment.

Next, determine the relationship between the maximum and average story drifts, to determine if a torsional irregularity exists, as defined in *Provisions* Table 5.2.3.2 [4.3-2]. Assuming that all of the shear walls will have the same plywood and nailing, the deflection of each wall will be proportional to the force in that wall. Therefore, the maximum drift for any level, will be proportional to  $0.210F_x$ , and the average drift proportional to  $(0.210F_x + 0.124F_x)/2 = 0.167F_x$ . The ratio of maximum to average deflection is  $0.210F_x/0.167F_x = 1.26$ . Since the ratio is greater than 1.2, the structure is considered to have a torsional irregularity Type 1a, in accordance with *Provisions* Table 5.2.3.2 [4.3-2]. Therefore, the horizontal force distribution must be computed again using the torsional amplification factor,  $A_x$ , from *Provisions* Sec. 5.4.4.3 [5.2.4.3]. (Diaphragm connections and collectors, not considered in this example, must satisfy *Provisions* Sec. 5.2.6.4.2. [4.6.3.2])

In accordance with *Provisions* Eq 5.4.4.3-1 [5.2-13]:

$$A_{x} = \left[\frac{\delta_{max}}{1.2\delta_{avg}}\right]^{2} = \left[\frac{0.210F_{x}}{1.2(0.167F_{x})}\right]^{2} = 1.10$$

Therefore, recompute the torsional moment and forces as:

Total torsional moment,  $A_x(M_t + M_{ta}) = 1.10[F_x \times (4.67 \text{ ft} + 0.05 \times 148 \text{ ft})] = 13.28F_x$ Torsional shear to End walls =  $13.28F_x/140 \text{ ft} = 0.095F_x$ 

The revised simplified assumption yields a maximum total design force of  $0.167F_x + 0.095F_x/2 = 0.214F_x$  at the end walls (right side of Figure 10.4-1), which will be designed in the following sections.

(The force distribution was also computed using a complete rigidity model including all transverse and longitudinal wall segments. Relative rigidities were based on length of wall and the torsional moment was resisted based on polar moment of inertia. The resulting design forces to the shear wall segments were  $0.208F_x$ ,  $0.130F_x$ , and  $0.168F_x$  for the right end, left end, and interior segments, respectively. The structure is still torsionally irregular ( $\delta_{max} / \delta_{ave} = 1.23$ ), but the irregularity is less substantial and the resulting  $A_x = 1.05$ . This more rigorous analysis, has shown that the simplified approach provides reasonable results in this case. Since the simplified method is more likely to be used in design practice, the values from that approach will be used for the remainder of this example.)

#### 10.1.3.5 Verification of Redundancy Factor

Once the horizontal force distribution is determined, the assumed redundancy factor must be verified. *Provisions* Eq. 5.2.4.2, is used to compute the redundancy factor,  $\rho$ , for each story as:

$$\rho_x = 2 - \frac{20}{r_{max_x}\sqrt{A_x}}$$

where  $A_x$  is the floor area in square feet and  $r_{max_x}$  is the ratio of the design story shear resisted by the single element carrying the most shear force in the story to the total story shear. As defined for shear walls in *Provisions* Sec. 5.2.4.2,  $r_{max_x}$  shall be taken as the shear in the most heavily loaded wall, multiplied by  $10/l_w$ , where  $l_w$  is the wall length in feet.

The most heavily loaded wall is the end wall, farthest away from the interior shear wall. Since the force distribution is the same for all three levels, the redundancy factor need only be determined for one level, in this case, at the first floor. The redundancy factor is computed as:

Floor area =  $(140)(56) = 7,840 \text{ ft}^2$ Max load to wall = 0.214VWall length = 25 ft  $r_{max_a} = 0.214V(10/25)/V = 0.0856$ 

Therefore:

$$\rho_x = 2 - \frac{20}{0.0856\sqrt{7,840}} = -0.64$$

Because the calculated redundancy factor is less than the minimum permitted value of 1.0, the initial assumption of  $\rho = 1.0$  is correct, and the design can proceed using the previously computed lateral forces.

[See Sec. 10.1.2.2 for discussion of the changes to the redundancy requirements in the 2003 Provisions.]

# **10.1.3.6 Diaphragm Design Forces**

As specified in *Provisions* Sec. 5.2.6.4.4 [4.6.3.4], floor and roof diaphragms must be designed to resist a force,  $F_{pp}$  in accordance with *Provisions* Eq. 5.2.6.4.4 [4.6-2]:

$$F_{px} = \frac{\sum_{i=x}^{n} F_i}{\sum_{i=x}^{n} w_i} w_{px}$$

plus any force due to offset walls (not applicable for this example). The diaphragm force as computed above need not exceed  $0.4S_{DS}Iw_{px}$ , but shall not be less than  $0.2S_{DS}Iw_{px}$ . This latter value often governs at the lower levels of the building, as it does here. The maximum required diaphragm demand does not govern in this example.

The weight tributary to the diaphragm,  $w_{px}$ , need not include the weight of walls parallel to the force. For this example, however, since the shear walls in both directions are relatively light compared to the total tributary diaphragm weight, the diaphragm force is computed based on the total story weight, for convenience.

Transverse direction

Roof Level  $\Sigma F_i = 40.4$   $\Sigma w_i = 182.8$   $F_{P,roof} = (40.4/182.8)(182.8)$  $0.2S_{DS}Iw_{px} = (0.2)(0.89)(1.0)(182.8)$ 

= 40.4 kips (controls for roof) = 32.7 kips

Diaphragm forces in the longitudinal direction are computed in a similar manner. Since the weight of the exterior walls is more significant in the longitudinal direction, the designer may wish to subtract this weight from the story force in order to compute the diaphragm demands.

# **10.1.4 Basic Proportioning**

Designing a plywood diaphragm and plywood shear wall building, principally involves the determination of sheathing thicknesses and nailing patterns to accommodate the applied loads. In doing so, some successive iteration of steps may be needed to satisfy the deflection limits.

Nailing patterns in diaphragms and shear walls have been established on the basis of tabulated requirements included in the *Provisions*. It is important to consider the framing requirements for a given nailing pattern and capacity as indicated in the notes following the tables. In addition to strength requirements, *Provisions* Sec. 12.4.1.2 [12.4.1.1] places aspect ratio limits on plywood diaphragms (length/width shall not exceed 4/1 for blocked diaphragms), and *Provisions* Sec. 12.4.2.3 [12.4.2.3] places similar limits on shear walls (height/width shall not exceed 2/1 for full design capacities). However, it should be taken into consideration that compliance with these aspect ratios does not guarantee that the drift limits will be satisfied.

Therefore, diaphragms and shear walls have been analyzed for deflection as well as for shear capacity. A procedure for computing diaphragm and shear wall deflections is provided in *Commentary* Sec. 12.4.1. This procedure is illustrated below. The *Commentary* does not indicate how to compute the nail deformation (nail slip) factor, but there is a procedure contained in the commentary of ASCE16.

In the calculation of diaphragm deflections, the chord slip factor can result in large additions to the total deflection. This can be overcome by using "neat" holes for bolts, and proper shimming at butt joints. However, careful attention to detailing and field inspection are essential, to ensure that they are provided.

[AF&PA Wind & Seismic also contains procedures for computing diaphragm and shear wall deflections. The equations are slightly different from the more commonly used equations that appear in the *Commentary* and AF&PA LRFD *Manual*. In AF&PA Wind & Seismic, the shear and nail slip terms are combined using an "apparent shear stiffness" parameter. However, the apparent shear stiffness values are only provided for OSB. Therefore, the deflection equations in the *Commentary* or AF&PA LRFD *Manual* must be used in this example which has plywood diaphragms and shear walls. The apparent shear stiffness values for plywood will likely be available in future editions of AF&PA Wind & Seismic.]

# 10.1.4.1 Strength of Members and Connections

The 2000 *Provisions* has adopted Load and Resistance Factor Design (LRFD) for engineered wood structures. The *Provisions* includes the ASCE 16 standard by reference and uses it as the primary design procedure for engineered wood construction. Strength design of members and connections is based on the requirements of ASCE 16. The AF&PA Manual and supplements contain reference resistance values for use in design. For convenience, the *Provisions* contain design tables for diaphragms and shear walls that are identical to those contained in the AF&PA Structural-Use Panels Supplement. However, the modification of the tabulated design resistance for shear walls and diaphragms with framing other than Douglas Fir-Larch or Southern Pine is different between the two documents. This example illustrates the modification procedure contained in the *Provisions* tables, which is new to the 2000 edition.

Throughout this example, the resistance of members and connections subjected to seismic forces, acting alone, or in combination with other prescribed loads, is determined in accordance with ASCE 16 and the AF&PA Manual; with the exception of shear walls and diaphragms for which design resistance values are taken from the *Provisions*. The LRFD standard incorporates the notation D', T', Z', etc. to represent adjusted resistance values, which are then modified by a time effect factor,  $\lambda$ , and a capacity reduction factor,  $\phi$ , to compute a design resistance, which is defined as "factored resistance" in the *Provisions* and ASCE 16. Additional discussion on the use of LFRD is included in *Commentary* Sec. 12.2 and 12.3, and in the ASCE 16 commentary. It is important to note that ACSE 16 and the AF&PA Manual use the term, "resistance," to refer to the design capacities of members and connections while "strength" refers to material property values.

It is worth noting that the AF&PA Manual contains a Pre-engineered Metal Connections Guideline for converting allowable stress design values for cataloged metal connection hardware (for example, tie-down anchors) into ultimate capacities for use with strength design. This procedure is utilized in this example.

[The primary reference for design of wood diaphragms and shear walls in the 2003 *Provisions* is AF&PA Wind & Seismic. Much of the remaining text in the 2003 *Provisions* results from differences between AF&PA Wind & Seismic and Chapter 12 of the 2000 *Provisions* as well as areas not addressed by AF&PA Wind & Seismic. Because the AF&PA Wind & Seismic tabulated design values for diaphragms and shear walls do not completely replace the tables in the 2000 *Provisions*, portions of the tables remain in the 2003 *Provisions*. Therefore, some diaphragm and shear wall design values are in the 2003 *Provisions* and some are in AF&PA Wind & Seismic. The design values in the tables are different between the two documents. The values in the 2003 *Provisions* represent factored shear resistance ( $\lambda \varphi D'$ ), while the values in AF&PA Wind & Seismic represent nominal shear resistance that must then be multiplied by a resistance factor,  $\varphi$ , (0.65) and a time effect factor  $\lambda$ , (1.0 for seismic loads). Therefore, while the referenced tables may be different, the factored resistance values based on the 2003 *Provisions* should be the same as those in examples based on the 2000 *Provisions*. The calculations that follow are annotated to indicate from which table the design values are taken.]

# 10.1.4.2 Transverse Shear Wall Nailing

The design will focus on the more highly loaded end walls; interior walls are assumed to be similar.

#### 10.1.4.2.1 Load to Any One of Four 25-ft End Walls

$F_{roof} = 0.214(40.4)$	=	8.65 kips
$F_{3rd} = 0.214(41.9)$	=	8.97 kips
$F_{2nd} = 0.214(20.9)$	=	4.47 kips
Σ	= 2	22.09 kips

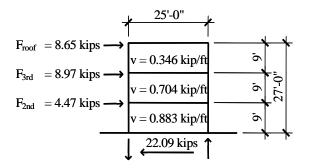


**Figure 10.1-6** Transverse section: end wall (1.0 ft = 0.3048 m, 1.0 kip = 4.45 kN, 1.0 kip/ft = 14.6 kN/m).

10.1.4.2.2 Roof to Third Floor Design

V = 8.65 kips v = 8.65/25 = 0.346 klf

Try a  $\frac{1}{2}$ -in. (15/32) plywood rated sheathing (not Structural I) on blocked 2-in. Douglas fir-Larch members at 16 in. on center with 10d common nails at six-in. on center at panel edges and 12 in. on center at intermediate framing members. According to Note b of *Provisions* Table 12.4.3-2a [12.4-3a], the design shear resistance must be adjusted for Hem-fir wall framing. The specific gravity adjustment factor equals 1-(0.5-SG) where SG is the specific gravity of the framing lumber. From Table 12A of the AF&PA Structural Connections Supplement, the SG = 0.43 for Hem-fir. Therefore, the adjustment factor is 1-(0.5-0.43) = 0.93.

From *Provisions* Table 12.4.3-2a [AF&PA Wind/Seismic Table 4.3A],  $\lambda \phi D' = 0.40$  klf Adjusted shear resistance = 0.93(0.40) = 0.37 klf > 0.346 klf OK

8d nails could be used at this level but, because 10d nails are required below, 10d nails are used here for consistency.

Deflection of plywood shear panels depends, in part, on the slip at the nails which, in turn, depends on the load per nail. See Sec. 10.1.4.3 for a detailed discussion of the appropriate slip for use with the *Provisions* and see Table 10.1-2 for fastener slip equations used here.

Load per nail = 0.346(6/12)(1000) = 173 lb Nail slip  $e_n = 1.2(173/769)^{3.276} = 0.00904$  in.

In the above equation, 1.2 = factor for plywood other than Structural I, and 769 and 3.276 are constants explained in Sec. 10.1.4.3.

[As indicated previously, AF&PA Wind & Seismic does not provide apparent shear stiffness values for plywood sheathing. Therefore, the deflection equations in the *Commentary* or AF&PA LRFD *Manual* must be used in this case.]

10.1.4.2.3 Third Floor to Second Floor

V = 8.65 + 8.97 = 17.62 kips

v = 17.62/25 = 0.704 klf

Try <sup>1</sup>/<sub>2</sub>-in. (15/32) plywood rated sheathing (not Structural I) on blocked 2-in. Douglas fir-Larch members at 16 in. on center with 10d nails at 3-in. on center at panel edges, and at 12 in. on center at intermediate framing members.

From *Provisions* Table 12.4.3-2a [AF&PA Wind&Seismic Table 4.3A],  $\lambda \phi D' = 0.78$  klf Adjusted shear resistance = 0.93(0.78) = 0.73 klf > 0.704 klf

Table Note e [AF&PA Wind&Seismic Sec. 4.3.7.1] requires 3-in. framing at adjoining panel edges.

Load per nail = 0.704(3/12)(1000) = 176 lb Nail slip  $e_n = 1.2(176/769)^{3.276} = 0.00960$  in.

#### 10.1.4.2 Second Floor to First Floor

V = 17.62 + 4.47 = 22.09 kips v = 22.09/25 = 0.883 klf

Try a <sup>1</sup>/<sub>2</sub>-in. (15/32) plywood rated sheathing (not Structural I) on blocked 2-in. Douglas fir-Larch members at 16 in. on center with 10d common nails at 2-in. on center at panel edges and 12 in. on center at intermediate framing members.

From *Provisions* Table 12.4.3-2a [AF&PA Wind&Seismic Table 4.3A],  $\lambda \phi D' = 1.00$  klf Adjusted shear resistance = 0.93(1.00) = 0.93 klf > 0.883 klf

OK

OK

Table Notes d and e [AF&PA Wind&Seismic Sec. 4.3.7.1]require 3-in. framing at adjoining panel edges.

Load per nail = 0.883(2/12)(1000) = 147 lb Nail slip  $e_n = 1.2(147/769)^{3.276} = 0.00534$  in.

#### 10.1.4.3 General Note on the Calculation of Deflections for Plywood Shear Panels

The commonly used expressions for deflection of diaphragms and shear walls, which are contained in *Commentary* Sec. 12.4.1, and the ASCE 16 commentary standard (see also UBC Std 23-2 or APA 138), include a term for nail slip. The ASCE 16 commentary includes a procedure for estimating nail slip that is based on LRFD design values.

The values for  $e_n$  used in this example (and in Sec. 10.2) are calculated according to Table 10.1-2, which is taken from Table C9.5-1 of ASCE 16.

Table 10.1-2         Fastener Slip Equations				
Fastanar	Minimum	For Maximum	Approxima	ate Slip, $e_n^*$
Fastener	Penetration (in.)	Loads Up to (lb.)	Green/Dry	Dry/Dry
6d common nail	1-1/4	180	$(V_n/434)^{2.314}$	$(V_n/456)^{3.144}$
8d common nail	1-7/16	220	$(V_n/857)^{1.869}$	$(V_n/616)^{3.018}$
10d common nail	1-5/8	260	$(V_n/977)^{1.894}$	$(V_n/769)^{3.276}$
14-ga staple	1 to 2	140	$(V_n/902)^{1.464}$	$(V_n/596)^{1.999}$
14-ga staple	2	170	$(V_n/674)^{1.873}$	$(V_n/361)^{2.887}$

\*Fabricated green/tested dry (seasoned); fabricated dry/tested dry.  $V_n$  = fastener load in pounds. Values based on Structural I plywood fastened to Group II lumber. Increase slip by 20 percent when plywood is not Structural I.

1.0 in. = 25.4 mm, 1.0 lb = 4.45 N.

This example is based on the use of surfaced dry lumber so the "dry/dry" values are used. The appearance of the equations for both shear wall and diaphragm deflection, implies greater accuracy than is justified. The reader should keep in mind that the deflections calculated are only rough estimates.

#### 10.1.4.4 Transverse Shear Wall Deflection

From Commentary Sec. 12.4, modified as described below, shear wall deflection is computed as:

$$\delta = \frac{8vh^3}{wEA} + \frac{vh}{Gt} + 0.75he_n + \frac{h}{w}d_a$$

The above equation produces displacements in inches and the individual variables must be entered in the force or length units as described below:

v = V/w where V is the total shear on the wall and v is in units of pounds/foot

8vh3/wEA = bending deflection, as derived from the formula  $\delta_b = Vh^3/3EI$ , where V is the total shear in pounds, acting on the wall and  $I = Aw^2/2$  (in.<sup>4</sup>)

vh/Gt = shear deflection, as derived from the formula  $\delta_v = Vh/GA'$ , where A' = wt (in.<sup>2</sup>)

 $0.75 he_n$  = nail slip, in inches. Note that with *h* being given in feet, the coefficient 0.75 carries units of 1/ft.

 $(h/w)d_a$  = deflection due to anchorage slip, in inches. Note that for use in the deflection equation contained in the *Commentary*, the term  $d_a$  represents the vertical deflection due to anchorage details. In the deflection equation contained in the commentary in the AF&PA Manual, there is no h/w factor, so it should be assumed that the term  $d_a$  represents the horizontal deflection at the top of the wall due to anchorage details.

For this example:

$$E = 1,600,000$$
 psi  
 $G = 75,000$  psi  
 $A \text{ (area)} = 2(2.5)5.5 = 27.5 \text{ in.}^2 \text{ for assumed double } 3 \times 6 \text{ end posts}$ 

w (shear wall length) = 25 ft h (story height) = 9 ft t (effective thickness) = 0.298 in. for  $\frac{1}{2}$ -in. unsanded plywood (not Structural I)  $e_n$  = nail deformation factor from prior calculations, inches.

This equation is designed for a one-story panel and some modifications are in order for a multistory panel. The components due to shear distortion and nail slip are easily separable (see Table 10.1-3).

Story	v	vh/Gt	$e_n$	$0.75e_{n}h$
	(plf)	(in.)	(in.)	(in.)
Roof	346	0.139	0.00904	0.061
3	704	0.284	0.00960	0.065
2	883	0.356	0.00534	0.036

101 2 W 11 D C

1.0 in. = 25.4 mm, 1.0 plf = 14.6 N/m.

Likewise, the component due to anchorage slip is easily separable; it is a rigid body rotation. If a 1/8-in. upward slip is assumed (on the tension side only), the deflection per story is (9/25)(1/8) = 0.045 in. (Table 10.1-4).

The component due to bending is more difficult to separate. For this example, a grossly simplified, distributed triangular load on a cantilever beam is used (Figure 10.1-7).



Figure 10.1-7 Force distribution for flexural deflections.

The total load V is taken as 21.3 kips, the sum of the story forces on the wall. The equation for the deflection, taken from Roark's Formulas for Stress and Strain, is:

$$\delta_x = \frac{2V}{5EAb^2h^2}(11h^5 - 15h^4x + 5hx^4 - x^5)$$

where x is the distance (ft) from the top of the building to the story in question, h is the total height (ft), b is the wall width (ft), A is the chord cross sectional area (in.<sup>2</sup>), E is the modulus of elasticity (psi), and the resulting displacement,  $\delta$ , is in inches.

This somewhat underestimates the deflections, but it is close enough for design. The results are shown in Table 10.1-4.

The total wall deflections, shown in Table 10.1-5, are combined with the diaphragm deflections (see Sec. 10.1.4.7, 10.1.4.8, and 10.1.4.9). Drift limits are checked after diaphragm deflections are computed.

Level	Effective	$(h/w)d_a$
	$8vh^3/wEA$ (in.)	(in.)
Roof	0.031	0.045
3	0.027	0.045
2	0.012	0.045

 Table 10.1-5
 Total Elastic Deflection and Drift of End Wall

Anchor

0.045

0.045

0.045

Drift  $\Delta_a$ 

(in.)

0.277

0.420

0.448

Total  $\delta_{a}$ 

(in.)

1.145

0.869

0.448

Bending

0.031

0.027

0.012

1.0 in. = 25.4 mm.

Level

Roof 3

2

#### (in.) (in.) (in.) Slip (in.) 0.061

Nail Slip

0.065

0.036

10.1.4.5 Transverse Shear Wall Anchorage

Shear

0.139

0.284

0.356

Provisions Sec. 12.4.2.4 [12.4.2.4.1] requires tie-down (hold-down) anchorage at the ends of shear walls where net uplift is induced. Net uplift is computed as the combination of the seismic overturning moment and the dead load counter-balancing moment using the load combination indicated in Provisions Eq. 5.2.7-2 [4.2-2].

Traditionally, tie-down devices were designed to resist this net overturning demand. However, Provisions Sec. 12.4.2.4 [12.4.2.4.1] requires that the nominal strength of tie-down devices exceeds the expected maximum vertical force that the shear panels can deliver to the tension-side end post. Specifically, the nominal strength ( $\phi = 1.0$ ) of the tie-down device must be equal to, or greater than the net uplift forces resulting from  $\Omega_0/1.3$  times the factored shear resistance of the shear panels, where  $\Omega_0$  is the system overstrength factor. These uplift forces are cumulative over the height of the building. Also, dead load forces are not used in these calculations to offset the uplift forces for the design of the tie-down anchorage.

[The requirements for uplift anchorage are slightly different in the 2003 Provisions. The tie down force is based on the "nominal strength of the shear wall" rather than the  $\Omega_0/1.3$  times the factored resistance as specified in the 2000 Provisions. This change is primarily intended to provide consistent terminology and should not result in a significant impact on the design of the tie down.]

An additional requirement of *Provisions* Sec. 12.4.2.4 [12.4.2.4.1], is that end posts must be sized such that failure across the net section does not control the capacity of the system. That is, the tensile strength of the net section must be greater than the tie-down strength. Note that the tie-downs designed in the following section are not located at wall intersections where the directional combination requirements of Provisions Sec. 5.2.5.2.3 [4.4.2.3] would apply (see also the "Analysis Procedure" in Sec. 10.1.2.2).

# 10.1.4.5.1 Tie-down Anchors at Third Floor

For the typical 25-ft end wall segment, the overturning moment at the third floor is:

 $M_0 = 9(8.65) = 77.8$  ft-kip =  $Q_F$ 

The counter-balancing moment,  $0.72 Q_D = 0.72D(25 \text{ ft/2})$ . The width of the floor contributing to this, is taken as half the span of the exterior window header equal to 6.5 feet (see Figures 10.1-1 and 10.1-2). For convenience, the same length is used for the longitudinal walls, the weight of which (interior and exterior glazed wall) is assumed to be 9 psf.

End wall self weight = 9 ft (25ft )15 psf/1000	= 3.4 kips
Tributary floor = $6.5$ ft (25 ft) (15) psf/1000	= 2.4 kips
Tributary longitudinal walls = 9 ft (6.5 ft) 9 psf $(2)/1000$	= <u>1.1 kips</u>
Σ	= 6.9 kips

 $0.72Q_D = 0.72(6.9)12.5 = 62.1$  ft-kip

 $M_0$  (net) = 77.8 - 62.1 = 15.7 ft-kip

Therefore, uplift anchorage is required. Using the procedure described above, nominal tie-down strength must be equal to or exceed the tension force, T, computed as:

T = 0.37 klf (3/1.3)(8ft) = 6.83 kips

where

0.37 klf = factored shear wall resistance at the third floor  $3/1.3 = \Omega_0/1.3$ 8 ft = net third floor wall height (9-ft story height minus approximately 1 ft of framing).

Use a double tie-down device to eliminate the eccentricity associated with a single tie-down. Also, use the same size end post over the full height of the wall to simplify the connections and alignments. As will be computed below, a  $6 \times 6$  (Douglas fir-Larch) post is required at the first floor. At the third floor, try two sets of double tie-down anchors connected through the floor with a 5/8-in. threaded rod to the end posts with two 5/8-in. bolts similar to Figure 10.1-8.

According to *Provisions* Sec. 12.4.2.4 [12.4.2.4.1], the nominal tie-down strength is defined as the "maximum test load the device can resist under cyclic testing without connection failure by either metal or wood failure." [Note that this definition for nominal tie down strength has been removed in the 2003 *Provisions*. This change is primarily intended to provide consistent terminology and should not result in a significant impact on the design of the tie down.] For a single tie-down device as described above, the cataloged allowable uplift capacity is 2.76 kips and the cataloged average ultimate load is 12.15 kips. However, according to the documentation in this particular supplier's product catalog, the ultimate values are based on static testing and the type of failure is not indicated. Therefore, for this example, the cataloged ultimate value is not considered to satisfy the requirements of the *Provisions*. As an alternate approach, this example will utilize the methodology contained in the AF&PA Manual for converting cataloged allowable stress values to strength values.

Based on the procedure in the AF&PA Manual, Pre-Engineered Metal Connectors Guide, the strength conversion factor for a connector for which the catalog provides an allowable stress value with a 1.33 factor for seismic is 2.88/1.33.

Since the typical product catalogs provide design capacities only for single tie-downs, the design of double tie-downs requires two checks. First, consider twice the capacity of one tie-down, and second, the capacity of the bolts in double shear.  $\phi = 1.0$  for both these calculations.

For the double tie-down, the nominal strength is computed as:

$$2\lambda\phi Z' = 2(1.0)(1.0)(2.76)(2.88/1.33) = 12.0$$
 kips > 6.83 kips OK

For the two bolts through the end post in double shear, the AF&PA Manual gives:

$$2\lambda\phi Z' = 2(1.0)(1.0)(4.90) = 9.80 \text{ kips} > 6.83 \text{ kips}$$
 OK

The factored capacity of the tie-downs must also be checked for the design loads, which in this case will not govern the design.

#### 10.1.4.5.2 Tie-down Anchors at Second Floor

Since tie-downs are required at the third floor, it would be common practice to provide tie-downs at the second and first floors, whether or not calculations indicate that they are required. Nevertheless, the overturning calculations are performed for illustrative purposes. The overturning moment at the second floor is:

 $M_0 = 18(8.65) + 9(8.97) = 236$  ft-kip.

The counter-balancing moment,  $0.72 Q_D = 0.72(DL)12.5$ .

End wall self weight = $18$ ft (25 ft) 15 psf/1000	= 6.75 kips
Tributary floor = $6.5$ ft (25 ft) (15 + 27) psf/1000	= 6.83 kips
Tributary longitudinal walls = $18 \text{ ft} (6.5 \text{ ft}) 9 \text{ psf} (2)/1000$	= <u>2.10 kips</u>
Σ	= 15.7 kips

 $0.72Q_D = 0.72(15.7)12.5 = 141$  ft-kips

 $M_0$  (net) = 236-141 = 95 ft-kips

As expected, uplift anchorage is required. The design uplift force is computed using an adjusted factored shear resistance of 0.73 klf at the second floor, and a net length of wall height equal to 8 ft. Note that 8 ft. is appropriate for this calculation given the detailing for this structure. As shown in Figure 10.1-10, the plywood sheathing is not detailed as continuous across the floor framing, which results in a net sheathing height of about 8ft. If the sheathing were detailed across the floor framing, then 9 ft would be the appropriate wall height for use in computing tie-down demands. Combined with the uplift force at the third floor, the total design uplift force at the second floor is:

T = 6.83 kips + 0.73 klf (3/1.3)(8ft) = 20.3 kips

Use two sets of double tie-down anchors to connect the  $6 \times 6$  end posts. Using the same procedure as for the third floor, tie-downs with a seven-eighths-in. threaded rod and three seven-eighths-in. bolts are computed to be adequate. See Figure 10.1-8.

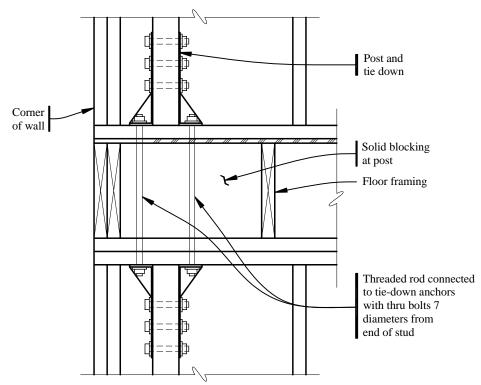


Figure 10.1-8 Shear wall tie down at suspended floor framing.

### 10.1.4.5.3 Tie-down Anchors at First Floor

The overturning moment at the first floor is:

$$M_0 = 27(8.65) + 18(8.97) + 9(4.47) = 435$$
 ft-kip =  $Q_{E_0}$ 

The counter-balancing moment, 0.72  $Q_D = 0.72D(25 \text{ ft/2})$ .

End wall self weight = $27 \text{ ft} (25 \text{ ft}) 15 \text{ psf}/1000$	= 10.1 kips
Tributary floor = 6.5 ft (25 ft) (15 + 27 + 27) psf/1000	= 11.2 kips
Tributary longitudinal walls = 27 ft (6.5 ft) 9 psf (2)/1000	= <u>3.2 kips</u>
Σ	= 24.5 kips

 $0.72Q_D = 0.72(24.5)12.5 = 221$  ft-kip

$$M_0$$
 (net) = 435 - 221 = 214 ft-kip

As expected, uplift anchorage is required. The design uplift force is computed using an adjusted factored shear resistance of 0.93 klf at the first floor, and a net wall height of 8ft. Combined with the uplift force at the floors above, the total design uplift force at the first floor is:

T = 20.3 kips + 0.93 klf (3/1.3)(8ft.) = 37.5 kips.

Use a double tie-down anchor that extends through the floor with an anchor bolt into the foundation. Tie-downs with a 7/8-in. threaded rod, and four 7/8-in. bolts are adequate.

The strength of the end post, based on failure across the net section, must also be checked (*Provisions* Sec. 12.4.2.4 [12.4.2.4.1]). For convenience, the same size post has been used over the height of the building, so the critical section is at the first floor. A reasonable approach to preclude net tension failure from being a limit state would be to provide an end post, whose factored resistance exceeds the nominal strength of the tie-down device. (Note that using the factored resistance rather than nominal strength of the end post provides an added margin of safety that is not explicitly required by the *Provisions*.) The nominal strength of the first floor double tie-down is 42.9 kips, as computed using the procedure described above. Therefore, the tension capacity at the net section must be greater than 42.9 kips.

Try a  $6 \times 6$  Douglas Fir-Larch No. 1 end post. In some locations, the shear wall end post also provides bearing for the window header, so this size is reasonable. Accounting for 1-in. bolt holes, the net area of the post is 24.75 in.<sup>2</sup> According to the AF&PA Manual, Structural Lumber Supplement:

$$\lambda \phi T' = (1.0)(0.8)(2.23 \text{ksi})(24.75 \text{in}^2) = 44.2 \text{ kips} > 42.9 \text{ kips}$$
 OK

For the maximum compressive load at the end post, combine maximum gravity load, plus the seismic overturning load. In the governing condition, the end post supports the header over the glazed portion of the exterior wall (end wall at right side of Figure 10.1-1). Assume that the end post at the exterior side of the wall supports all the gravity load from the header, and resists one-half of the seismic overturning load.

Compute gravity loads based on a 6.5-foot tributary length of the header:

Tributary $DL = ((27 \text{ ft})(9 \text{ psf}) + (8 \text{ ft})(15 + 27 + 27)\text{psf})(6.5\text{ft})/1000$	= 5.17 kips
Tributary LL = 8 ft (7 ft) $(40 + 40) \text{ psf}/1000$	= 4.48 kips
Tributary $SL = 8 \text{ ft} (6.5 \text{ ft}) (25 \text{ psf})/1000$	= 1.30 kips

The overturning force is based on the seismic demand (not wall capacity as used for tension anchorage) assuming a moment arm of 23 ft:

Overturning,  $Q_E = 435/23$  ft = 18.9 kips

Per load combination associated with *Provisions* Eq. 5.2.7.1-1 [4.2-1]:

Maximum compression = 1.38(5.17) + 1.0(18.9/2) + 0.5(4.48) + 0.2(1.30) = 19.1 kips.

Due to the relatively short clear height of the post, the governing condition is bearing perpendicular to the grain on the bottom plate. Check bearing of the  $6\times6$  end post on a  $3\times6$  Douglas fir-Larch No. 2 plate, per the AF&PA Manual, Structural Lumber Supplement:

$$\lambda \phi P' = (1.0)(0.8)(1.30 \text{ksi})(30.25 \text{ in.}^2) = 31.5 \text{ kips} > 19.1 \text{ kips}.$$
 OK

The  $6\times6$  end post is slightly larger than the double  $3\times6$  studs assumed above for the shear wall deflection calculations. Therefore, the computed shear wall deflection is slightly conservative, but the effect is minimal.

10.1.4.5.4 Check Overturning at the Soil Interface

A summary of the overturning forces is shown in Figure 10.1-9. To compute the overturning at the soil interface, the overturning moment must be increased for the 4-ft foundation height:

 $M_0 = 435 + 22.09(4.0) = 523$  ft-kip

However, it then may be reduced in accordance with Provisions Sec. 5.3.6:

 $M_0 = 0.75(523) = 392$  ft-kip

To determine the total resistance, combine the weight above with the dead load of the first floor and foundation.

Load from first floor = 25 ft (6.5 ft) (27 - 4 + 1)psf /1000 = 3.9 kips

where 4 psf is the weight reduction due to the absence of a ceiling, and 1 psf is the weight of insulation.

The length of the longitudinal foundation wall included, is a conservative approximation of the amount carried by minimum nominal reinforcement in the foundation.

Foundation weight = (562 plf (13 ft + 25 ft) + 292 plf (13 ft))/1000 = 25.1 kips First floor = 3.9 kips Structure above = 53.5 kips

Therefore,  $0.72D - 1.0Q_E = 0.72(53.5)12.5$  ft - 1.0(392) = 89.5 ft-kips, which is greater than zero, so the wall will not overturn.

10.1.4.5.5 Anchor Bolts for Shear

At the first floor:

v = 0.883 klf.

A common anchorage for non-engineered construction is a  $\frac{1}{2}$ -in. bolt at 4ft-0 in. For a  $\frac{1}{2}$ -in. bolt in a Douglas fir-Larch 3×6 plate, in single shear, parallel to the grain:

 $\lambda \phi Z'/4$ ft = (1.0)(0.65)(2.38 kips)/4 = 0.39 klf < 0.883 klf NG

Try a larger bolt and tighter spacing. For this example, use a 5/8-in. bolt at 32 in. on center:

 $\lambda \phi Z'/2.67 \text{ft} = (1.0)(0.65)(3.72 \text{ kips})/2.67 = 0.91 \text{ klf} > 0.883 \text{ klf}$  OK

*Provisions* Sec. 12.4.2.4 [12.4.2.4.2] requires plate washers at all shear wall anchor bolts. A summary of the transverse shear wall elements is shown in Figure 10.1-9.

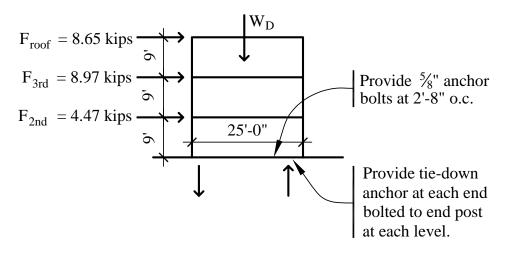


**Figure 10.1-9** Transverse wall: overturning (1.0 ft = 0.3048 m, 1.0 in. = 25.4 mm, 1.0 kip = 4.45 kN).

# 10.1.4.6 Remarks on Shear Wall Connection Details

In normal platform frame construction, details must be developed that will transfer the lateral loads through the floor system and, at the same time, accommodate normal material sizes and the cross-grain shrinkage in the floor system. The connections for wall overturning in Sec. 10.1.4.5 are an example of one of the necessary force transfers. The transfer of diaphragm shear to supporting shear walls is another important transfer as is the transfer from a shear wall on one level to the level below.

The floor-to-floor height is nine-ft with about one-ft occupied by the floor framing. Using standard 8-ftlong plywood sheets for the shear walls, a gap occurs over the depth of the floor framing. It is common to use the floor framing to transfer the lateral shear force. Figures 10.1-10 and 10.1-11 depict this accomplished by nailing the plywood to the bottom plate of the shear wall, which is nailed through the floor plywood to the double  $2\times12$  chord in the floor system.

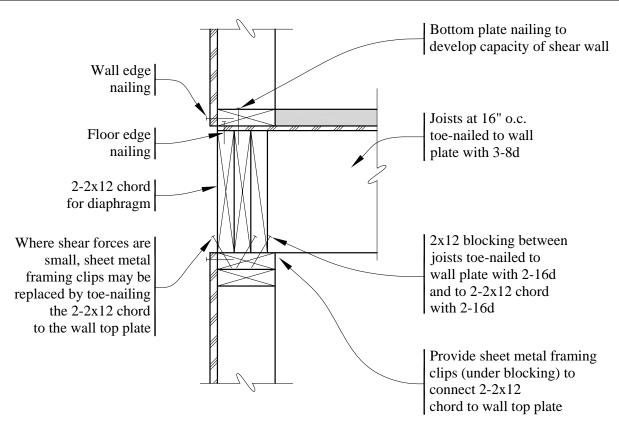


Figure 10.1-10 Bearing wall (1.0 in = 25.4 mm).

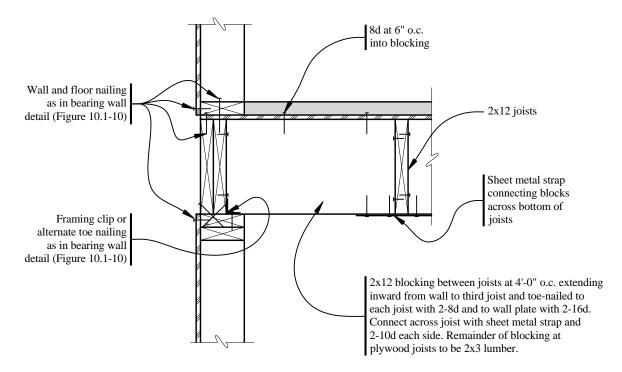
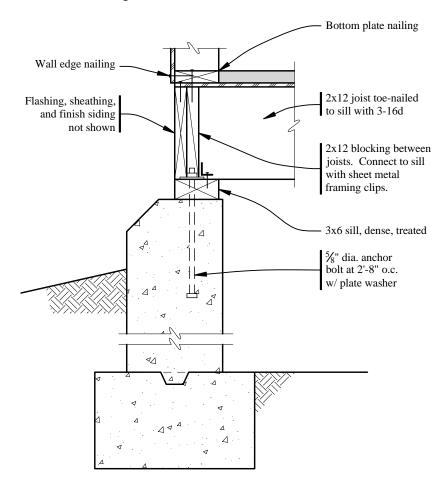


Figure 10.1-11 Nonbearing wall (1.0 in. = 25.4 mm).

The top plate of the lower shear wall also is connected to the double  $2 \times 12$  by means of sheet metal framing clips to the double  $2 \times 12$  to transfer the force back out to the lower plywood. (Where the forces are small, using toe nails between the double  $2 \times 12$  and the top plate may be used for this connection.) This technique leaves the floor framing free for cross-grain shrinkage. Although some designers in the past may have used a short tier of plywood nailed to the plates of the stud walls to accomplish the transfer, *Provisions* Sec. 12.4.2.6 prohibits this type of detailing.

The floor plywood is nailed directly to the framing at the edge of the floor, before the plate for the upper wall is placed. Also, the floor diaphragm is connected directly to framing that spans over the openings between shear walls. The axial strength, and the connections of the double  $2 \times 12$  chords, allow them to function as collectors to move the force from the full length of the diaphragm to the discrete shear walls. (According to *Provisions* Sec. 5.2.6.4.1 [4.6.2.2], the design of collector elements in wood shear wall buildings in Seismic Design Category D need not consider increased seismic demands due to overstrength.)

The floor joist is toe nailed to the wall below for forces normal to the wall. Likewise, full-depth blocking is provided adjacent to walls that are parallel to the floor joists, as shown in Figure 10.1-11. (Elsewhere the blocking for the floor diaphragm only need be small pieces, flat  $2\times4$ s, for example.) The connections at the foundation are similar (see Figure 10.1-12).



**Figure 10.1-12** Foundation wall detail (1.0 in. = 25.4 mm).

The particular combinations of nails and bent steel framing clips shown in Figures 10.1-10, 10.1-11, and 10.1-12, to accomplish the necessary force transfers, are not the only possible solutions. A great amount

of leeway exists for individual preference, as long as the load path has no gaps. Common carpentry practices often will provide most of the necessary transfers but, just as often, a critical few will be missed. As a result, careful attention to detailing and inspection is an absolute necessity.

# 10.1.4.7 Roof Diaphragm Design

While it has been common practice to design plywood diaphragms as simply supported beams spanning between shear walls, the diaphragm design for this example must consider the continuity associated with rigid diaphragms. The design will be based on the maximum shears and moments that occur over the entire diaphragm. From Sec. 10.1.3.5, the diaphragm design force at the roof is,  $F_{P,roof}$  = 40.4 kips.

As discussed previously, the design force computed in this example includes the internal force due to the weight of the walls parallel to the motion. Particularly for one-story buildings, it is common practice to remove that portion of the design force. It is conservative to include it, as is done here.

# 10.1.4.7.1 Diaphragm Nailing

The maximum diaphragm shear occurs at the end walls. From Sec. 10.1.3.4, each 25-ft end wall segment resists 21 percent of the total story (diaphragm, in this case) force. Distributing the diaphragm force at the same rate, the diaphragm shear over the entire diaphragm width at the end walls is:

V = (0.214)(2)(40.4)	= 17.3 kips
v = 17.3/56 ft.	= 0.308 klf

Try <sup>1</sup>/<sub>2</sub>-in. (15/32) plywood rated sheathing (not Structural I) on blocked 2-in. Douglas fir-Larch members at 16 in. on center, with 8d nails at 6 in. on center at panel edges and 12 in. on center at intermediate framing members.

From *Provisions* Table 12.4.3-1a [AF&PA Wind&Seismic Table 4.2A],  $\lambda \phi D' = 0.35$  klf > 0.308 klfOK

The determination of nail slip for diaphragms is included below.

# 10.1.4.7.2 Chord and Splice Connection

Diaphragm continuity is an important factor in the design of the chords. The design must consider the tension/compression forces, due to positive moment at the middle of the span, as well as negative moment at the interior shear wall. It is reasonable (and conservative) to design the chord for the positive moment assuming a simply supported beam and for the negative moment accounting for continuity. The positive moment is  $wl^2/8$ , where w is the unit diaphragm force, and l is the length of the governing diaphragm span. For a continuous beam of two unequal spans, under a uniform load, the maximum negative moment is:

 $M^{-} = \frac{wl_1^3 + wl_2^3}{8(l_1 + l_2)}$ 

where *w* is the unit diaphragm force, and  $l_1$  and  $l_2$  are the lengths of the two diaphragm spans. For w = 40.4 kips /140 ft = 0.289 klf, the maximum positive moment is:

 $0.289(84)^2 / 8 = 255$  ft-kip

and the maximum negative moment is:

 $\frac{0.289(84)^3 + 0.289(56)^3}{8(84+56)} = 198 \text{ ft-kip}$ 

The positive moment controls, and the design chord force is 255/56 = 4.55 kips. Try a double  $2 \times 12$  Douglas fir-Larch No. 2 chord. Due to staggered splices, compute the tension capacity based on a single  $2 \times 12$ , with a net area of  $A_n = 15.37$  in.<sup>2</sup> (accounting for 1-in. bolt holes). Per the AF&PA Manual, Structural Lumber Supplement:

$$\lambda \phi T' = (1.0)(0.8)(1.55\text{psi})(15.37\text{in}^2) = 19.1 \text{ kips} > 4.55 \text{ kips}$$
 OK

For chord splices, use 4 in. diameter split-ring connectors with 3/4-in. bolts. For split rings is single shear, the capacity of one connector is:

$$\lambda \phi T' = (1.0)(0.65)(17.1) = 11.1 \text{ kips} > 4.55 \text{ kips}.$$
 OK

This type of chord splice connection, shown in Figure 10.1-13, is generally used only for heavily loaded chords and is shown here for illustrative purposes. A typical chord splice connection for less heavily loaded chords can be accomplished more easily by using 16d nails to splice the staggered chord members.

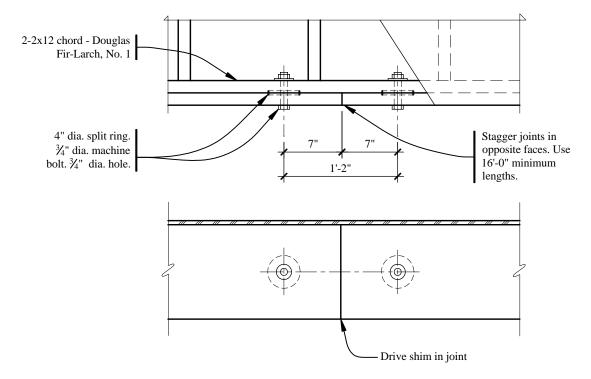


Figure 10.1-13 Diaphragm chord splice (1.0 ft = 0.3048 m, 1.0 in. = 25.4 mm).

#### 10.1.4.7.3 Diaphragm Deflection

The procedure for computing diaphragm deflections, contained in *Commentary* Sec. 12.4 (similar to the commentary of ASCE 16), is intended for the single span, "flexible" diaphragm model that has been used in common practice. The actual deflections of multiple span "rigid" diaphragms may, in general, be similar to those of single-span diaphragms because shear deflection and nail slip (both based on shear demand) tend to dominate the behavior. As multiple span deflection computations tend to be cumbersome, it is suggested that the design engineer compute diaphragm deflections based on the single

span model. This will result with a reasonable (and conservative), estimation of overall displacements. If these displacements satisfy the drift criteria, then the design is assumed to be adequate; if not, then a more rigorous computation of displacements could be performed.

It is the authors' opinion that for diaphragm displacement computations, the diaphragm loading should be according to *Provisions* Eq. 5.2.6.4.4 [5.2-11]; the minimum design demand  $(0.2S_{DS}Iw_{px})$  need not be considered. Although the *Provisions* does not provide a specific requirement either way, this interpretation is consistent with *Provisions* Sec. 5.4.6.1 [5.2.6.1], which indicates that the minimum base shear equation (*Provisions* Eq. 5.4.1.1-3) need not be used for calculation of story drift.

[See Sec. 10.1.3.1 for a discussion of diaphragm deflection computation using the 2003 Provisions and AF&PA Wind & Seismic reference.]

From Commentary Sec. 12.4, the diaphragm deflection is computed as:

$$\delta = \frac{5vL^3}{8wEA} + \frac{vL}{4Gt} + 0.188Le_n + \frac{\sum(\Delta_c X)}{2w}.$$

The equation produces the midspan diaphragm displacement in inches, and the individual variables *must* be entered in the force or length units as described below. For the single span approximation, consider the longer, 84 ft long span so that:

$$v = \frac{F_{px}(84/140)}{2w}$$

where  $F_{px}$  is the story diaphragm force at Level *x*, *w* is the diaphragm width, and *v* is in pounds/ft. For this calculation, the unit shear will be the same at both ends of the diaphragm. Therefore, it underestimates the actual unit shear at the end wall but overestimates the actual unit shear at the interior wall. These inaccuracies are assumed to be roughly offsetting. The individual terms of the above equation represent the following:

 $5vL^3/8wEA$  = bending deflection, as derived from the formula  $\delta_b = 5vL^4/384EI$ , where v is the diaphragm unit force in pounds per ft and  $I = Aw^2/2$  (in<sup>2</sup>)

vL/4Gt = shear deflection as derived from the formula  $\delta_v = vL^2/8GA$ , where v is the diaphragm unit force in pounds per ft and A = wt (in<sup>2</sup>)

 $0.188Le_n =$ nail slip deflection in inches

 $\Sigma(\Delta_c X)/2w$  = deflection due to chord slip in inches

For this example:

v = 40.4(84/140)/[(2(56))(1000)] = 216 plf (ignoring torsion) L = 84 ft and w = 56 ft, diaphragm length and width  $A = 2(1.5) \ 11.25 = 33.75$  in.<sup>2</sup> (double 2×12) t = 0.298 in. for ½-in. unsanded plywood E = 1,600,000 psi G = 75,000 psi

Nail slip is computed using the same procedure as for shear walls (Sec. 10.1.4.3), with the load per nail based on the diaphragm shear from this section. The diaphragm nailing is 8d at 6 in. on center.

Load per nail = 216(6/12) = 108 lb Nail slip  $e_n = 1.2(108/616)^{3.018} = 0.0063$  in.

In the above equation, 1.2 is the factor for plywood other than Structural I and 616 and 3.018 are coefficients for seasoned lumber.

Although a tight chord splice has been specified, the chord slip is computed for illustrative purposes. Assume chord slip occurs only at the side tension since the compression splices are tightly shimmed as shown in Figure 10.1-13. For this example:

 $\Delta_c$  = chord splice slip (1/16 in. used for this example)

X = distance from chord splice to nearest support

Assuming splices at 20 ft on center, along the 84-ft diaphragm length (ignore diaphragm continuity for this term), the sum of the chord splice slip is:

$$\Sigma(\Delta_c X) = (1/16)(20 + 40 + 24 + 4) = 5.5$$

Thus:

$$\delta = \frac{5(216)(84^3)}{8(1,600,000)(33.75)(56)} + \frac{216(84)}{4(75,000)(0.298)} + 0.188(84)(0.0063) + \frac{5.5}{2(56)}$$

= 0.027 + 0.203 + 0.100 + 0.055 = 0.385 in.

Wall and floor drifts are added, and checked in Sec. 10.1.4.9.

# 10.1.4.8 Second and Third Floor Diaphragm Design

The design of the second and third floor diaphragms follows the same procedure as the roof diaphragm. From Sec. 10.1.3.6, the diaphragm design force for both floors is  $F_{p,3rd} = F_{p,2nd} = 50.8$  kips.

# 10.1.4.8.1 Diaphragm Nailing

The maximum diaphragm shear occurs at the end walls. From Sec. 10.1.3.4, each end wall segment resists 21 percent of the total story (diaphragm, in this case) force. Distributing the diaphragm design force at the same rate, the diaphragm shear at the end walls is:

V = (0.214)(2)(50.8)	= 21.7 kips
v = 21.7/56 ft	= 0.388 klf

Try <sup>1</sup>/<sub>2</sub>-in. (15/32) plywood rated sheathing (not Structural I) on blocked 2-in. Douglas fir-Larch members at 16 in. on center, with 8d nails at 4 in. on center at boundaries and continuous panel edges, at 6 in. on center at other panel edges, and 12 in. on center at intermediate framing members.

From *Provisions* Table 12.4.3-1a [AF&PA Wind&Seismic Table 4.2A],  $\lambda \varphi D' = 0.47$  klf > 0.388 klf OK

# 10.1.4.8.2 Chord and Splice Connection

Computed as described above for the roof diaphragm, the maximum positive moment is 320 kips and the design chord force is 5.71 kips.

By inspection, a double  $2 \times 12$  chord spliced with 4-in. diameter split ring connectors, as at to the roof level, is adequate. A typical chord splice connection is shown in Figure 10.1-13.

10.1.4.8.3 Diaphragm Deflection

Using the same procedure as before:

*L* = 84 ft and *w* = 56 ft, diaphragm length and width *A* = 2(1.5) 11.25 = 33.75 in.<sup>2</sup> (double 2×12) *t* = 0.298 in. for ½-in. unsanded plywood *E* = 1,600,000 psi *G* = 75,000 psi

As discussed previously, diaphragm deflection computations need not consider the minimum diaphragm design forces.

Therefore, at the third floor:

v = 50.1(84/140)/[(2(56))(1000)] = 268 plf Load per nail = 268(4/12) = 89 lb Nail slip  $e_n = 1.2(89/616)^{3.018} = 0.0035$  in.

 $\delta = \frac{5(268)(84^3)}{8(1,600,000)(33.75)(56)} + \frac{268(84)}{4(75,000)(0.298)} + 0.188(84)(0.0035) + \frac{5.5}{2(56)}$ 

= 0.033 + 0.252 + 0.056 + 0.055 = 0.396 in.

At the second floor:

v = 39.1(84/140)/(2(56))(1000) = 209 plf Load per nail = 209(4/12) = 70 lb Nail slip  $e_n = 1.2(70/616)^{3.018} = 0.0017$  in.

 $\delta = \frac{5(209)(84^3)}{8(1,600,000)(33.75)(56)} + \frac{209(84)}{4(75,000)(0.298)} + 0.188(84)(0.0017) + \frac{5.5}{2(56)}$ 

= 0.026 + 0.197 + 0.026 + 0.055 = 0.304 in.

# 10.1.4.9 Transverse Deflections, Drift, and P-delta Effects

Transverse deflections for walls and diaphragms were calculated above. The diaphragm deflections for the second and third floors are based on the seismic force analysis and not the minimum diaphragm design forces (*Provisions* Sec. 5.2.6.4.4 [5.2.3]).

To determine the maximum story deflections and drifts (see Section 10.1.2.2), the midspan diaphragm deflection is combined with the wall deflection. This is summarized in Table 10.1-6, which shows the drift below the level considered.

Table 10.1-6         Total Deflection and Drift					
Level	Wall (in.)	Diaphragm (in.)	Total $\delta_e$ (in.)	$\delta = C_d \delta_e / I$ (in.)	Δ,drift (in.)

<sup>2</sup> Kecommendea Pr	ovisions: Design E.	xamples		
1.14	0.38	1.52	6.08	1.00
0.87	0.40	1.27	5.08	2.08
0.45	0.30	0.75	3.00	3.00
	1.14 0.87	1.14     0.38       0.87     0.40	0.87 0.40 1.27	1.14       0.38       1.52       6.08         0.87       0.40       1.27       5.08

. . . . . .

1.0 in. = 25.4 mm.

The maximum permissible drift is 0.020  $h_s = 2.16$  in. Therefore, the drift limitations are satisfied at the third floor and roof. The drift in the first story is about 38 percent too large so the design must be revised.

One beneficial aspect of the design that has been ignored in these calculations is the lightweight concrete floor fill. Although it is discontinuous at the stud walls, it will certainly stiffen the diaphragm. No studies that would support a quantitative estimate of the effect have been found. Because the shear deformation of the <sup>1</sup>/<sub>2</sub>-in. plywood diaphragm represents a significant portion of the total drift at the first and second levels, any significant increase in shear stiffness that might be provided by the concrete would further reduce the expected drifts. In this case, about 60 percent of the drift is contributed by the shear walls. The diaphragm stiffness would need to be tripled to meet the drift criteria, so the shear walls will be revised.

If Structural I plywood is used for the shear walls in this direction, the drift criteria are satisfied at all levels. In Sec. 10.1.4.4, G becomes 90,000 ksi, and t (effective thickness) becomes 0.535 in. The deflections due to shear and nail slip (the 1.2 factor no longer applies) are reduced. The resulting total elastic deflection of the shear walls at Levels 2, 3, and Roof are, 0.242 in., 0.488 in., and 0.669 in., respectively. Table 10.1-6b shows the revised results, which satisfy the drift criteria.

Та	Table 10.1-6b         Total Deflection and Drift (Structural I Plywood Shear Walls)					
Level	Wall (in.)	Diaphragm (in.)	Total $\delta_e$ (in.)	$\delta = C_d \delta_e / I$ (in.)	$\Delta$ , drift (in.)	
Roof	0.67	0.38	1.05	4.20	0.64	
3	0.49	0.40	0.89	3.56	1.40	
2	0.24	0.30	0.54	2.16	2.16	

1.0 in. = 25.4 mm.

Because the tie-down calculations (Sec. 10.1.4.5) depend on the tabulated capacities of the shear wall panels and Structural I panels have slightly higher capacities, the connection designs must be verified. Additional calculations (not shown here) confirm that the hardware that was previously selected still works. It is also worth noting that although many designers fail to perform deflection calculations for wood construction, the drift criteria control the selection of sheathing grade in this example.

The P-delta provision also must be examined. Following *Provisions* Sec. 5.4.6.2 [5.2.6.2] and assuming the total mass deflects two-thirds of the maximum diaphragm deflection, the P-delta coefficient is as shown in Table 10.1-7.

[Note that the equation to determine the stability coefficient has been changed in the 2003 Provisions. The importance factor, I, has been added to 2003 Provisions Eq. 5.2-16. However, this does not affect this example because I = 1.0.]

		<b>Table 10.1</b>	-7 P-delta Stal	bility Coefficie	ent	
Level	$P_D$ (kips)	$P_L$ (kips)	ΣP (kips)	Δ (in.)	V (kips)	$\theta = P\Delta/VhC_d$

					Chapte	er 10, Wood Design
Roof	183	204	387	0.67	40.4	0.015
3	284	130	801	1.27	82.3	0.029
2	284	130	1,215	1.76	103.2	0.048

1.0 in. = 25.4 mm, 1.0 kip = 4.45 kN.

For example, to compute the effective P-delta drift at the roof:

$$\begin{split} &\delta_{roof} = C_d [\delta_{wall} + 2/3(\delta_{diaphragm})] = 4[0.67 + 2/3(0.38)] = 3.693 \text{ in.} \\ &\delta_3 = 4[0.49 + 2/3(0.40)] = 3.027 \text{ in.} \\ &\delta = 3.693 - 3.027 = 0.67 \text{ in.} \end{split}$$

The story dead load is the same as shown in Table 10.1-1, and the story live load is based on 25 psf snow load for the roof and 16 psf reduced live load ( $0.4 \times 40$  psf) acting over the entire area of Levels 2 and 3. For  $\theta < 0.10$ , no deflection amplification due to P-delta effects is necessary.

# **10.1.4.10** Longitudinal Direction

Only one exterior shear wall section will be designed here. The design of the corridor shear walls would be similar to the transverse walls. (This example has assumed a greater length of corridor wall than would likely be required to resist the design forces. This increased length is intended to reduce the demand to the exterior walls, assuming rigid diaphragm distribution, to a level below the maximum permitted in-plane shear for the perforated shear wall design procedure as discussed below.) For loads in the longitudinal direction, diaphragm stresses and deflections are negligible.

The design of the exterior wall will utilize the guidelines for perforated shear walls (*Provisions* Sec. 12.4.3 [AF&PA Wind&Seismic Sec. 4.3]), which are new to the 2000 *Provisions*. [The provisions for perforated shear walls are contained in AF&PA Wind & Seismic and therefore have been removed from the 2003 *Provisions*. The design provisions are spread throughout AF&PA Wind & Seismic Sec. 4.3.3, but are not substantially different for the provisions contained in the 2000 *Provisions* except for the revisions to the tie down requirements as noted below.] The procedure for perforated shear walls applies to walls with openings that have not been specifically designed and detailed for forces around the openings. Essentially, a perforated wall is treated in its entirety, rather than as a series of discrete wall piers. The use of this design procedure is limited by several conditions (*Provisions* Sec. 12.4.3.2 [AF&PA Wind&Seismic Sec. 4.3.5.2]), the most relevant to this example is that the factored design shear resistance shall not exceed 0.64 klf. This requirement essentially limits the demand on perforated shear walls such that the required factored design shear resistance is less than 0.64 klf. If the configuration required higher design values, then walls must be added in order to reduce the demand.

The main aspects of the perforated shear wall design procedure are as follows. The design shear capacity of the shear wall is the sum of the capacities of each segment (all segments shall have the same sheathing and nailing) reduced by an adjustment factor that accounts for the geometry of the openings. Uplift anchorage (tie-down) is required only at the ends of the wall (not at the ends of all wall segments), but all wall segments must resist a specified tension force (using anchor bolts at the foundation and with strapping or other means at upper floors). Requirements for shear anchorage and collectors (drag struts) across the openings are also specified. It should be taken into account that the design capacity of a perforated shear wall, is less than a standard segmented wall with all segments restrained against overturning. However, the procedure is useful in eliminating interior hold downs for specific conditions and, thus, is illustrated in this example.

The portion of the story force resisted by each exterior wall was computed previously as  $0.225F_x$ . The exterior shear walls are composed of three separate perforated shear wall segments (two at 30 ft long and one at 15 ft long, all with the same relative length of full height sheathing), as shown in Figure 10.1-2. This section will focus on the design of a 30-ft section. Assuming that load is distributed to the wall sections based on relative length of shear panel, then the total story force to the 30-ft section is  $(30/75)0.225F_x = 0.090F_x$  per floor. The load per floor is

$F_{roof} = 0.090(40.4)$	= 3.64 kips
$F_{3rd} = 0.090(41.9)$	= 3.77 kips
$F_{2nd} = 0.090(20.9)$	= <u>1.88 kips</u>
Σ	= 9.29 kips

#### 10.1.4.10.1 Perforated Shear Wall Resistance

The design shear capacity (*Provisions* Sec. 12.4.3.3 [AF&PA Wind&Seismic Table 4.3.3.4]) is computed as the factored shear resistance for the sum of the wall segments, multiplied by an adjustment factor that accounts for the percentage of full height (solid) sheathing and the ratio of the maximum opening to the story height. At each level, the design shear capacity,  $V_{wall}$ , is:

 $V_{wall} = (vC_0)\Sigma L_i$ 

where

- v = unadjusted factored shear resistance (*Provisions* Table 12.4.3-2a [Table 12.4.3a or AF&PA Wind&Seismic Table 4.3A).
- $C_0$  = shear capacity adjustment factor (*Provisions* Table 12.4.3-1 [AF&PA Wind&Seismic Table 4.3.3.4]) = 0.83

The percent of full height sheathing is (4 + 10 + 4)/30 = 0.60, and the maximum opening height ratio is 4 ft /8 ft = 0.5. Per *Provisions* Table 12.4.3-1 [AF&PA Wind&Seismic Table 4.3.3.4],  $C_0 = 0.83$ .

 $\Sigma L_i$  = sum of widths of perforated shear wall segments = 4 + 10 + 4 = 18 ft

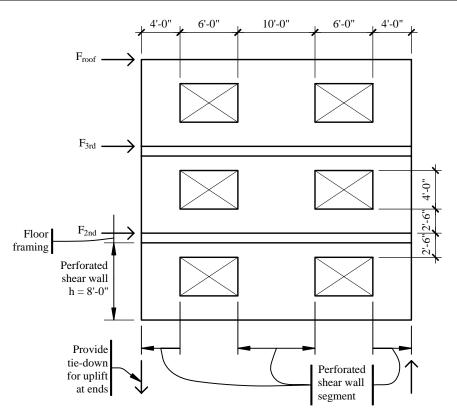


Figure 10.1-14 Perforated shear wall at exterior (1.0 ft = 0.3048 m, 1.0 in. = 25.4 mm)

The wall geometry (and thus the adjustment factor and total length of wall segments) is the same at all three levels, as shown in Figure 10.1-14. Perforated shear wall plywood and nailing are determined below.

Roof to third floor:

V = 3.64 kips Required v = 3.64/0.83/18 = 0.244 klf

Try <sup>1</sup>/<sub>2</sub>-in. (15/32) Structural I plywood rated sheathing on blocked 2-in. Douglas fir-Larch members at 16 in. on center with 10d common nails at 6 in. on center at panel edges and 12 in. on center at intermediate framing members. (Structural I plywood would not be required to satisfy the strength requirements. However, to minimize the possibility for construction errors, the same grade of sheathing is used on walls in both directions.)

From *Provisions* Table 12.4.3-2a [AF&PA Wind&Seismic Table 4.3A],  $\lambda \varphi D' = 0.44$  klf > 0.244 klf OK

Third floor to second floor:

V = 3.64 + 3.77 = 7.41 kips Required v = 7.41/0.83/18 = 0.496 klf Try <sup>1</sup>/<sub>2</sub>-in. (15/32) Structural I plywood rated sheathing on blocked 2 in. Douglas fir-larch members at 16 in. on center with 10d common nails at four in. on center at panel edges and 12 in. on center at intermediate framing members.

From *Provisions* Table 12.4.3-2a [AF&PA Wind&Seismic Table 4.3A]:

 $\lambda \varphi D' = 0.66$  klf (0.64 klf max) > 0.496 klf

As discussed above, *Provisions* Sec. 12.4.3.2, Item b [12.4.3], limits the factored shear resistance in *Provisions* Table 12.4.3-2a [AF&PA Wind&Seismic Table 4.3A] to 0.64 klf, which still exceeds the demand at this level, so the limitation is satisfied.

Second floor to first floor:

V = 7.41 + 1.88 = 9.29 kips Required v = 9.29/0.83/18 = 0.622 klf

By inspection, the same plywood and nailing from above will work.

# 10.1.4.10.2 Perforated Shear Wall Uplift Anchorage

According to *Provisions* Sec. 12.4.3.4.1 [AF&PA Wind&Seismic Table 4.3A], the requirements for uplift anchorage must be evaluated at the ends of the wall only. Uplift at each wall segment is treated separately as described later. Uplift forces, based on the strength of the shear panels (per *Provisions* Sec. 12.4.2.4 [12.4.2.4.1]), are to be computed as discussed in Sec. 10.1.4.5. For this example, calculations involving seismic overturning and counter-balancing moments are assumed not to be applicable for perforated shear walls, as they are not expected to act as rigid bodies in resisting global overturning.

The tie-down design force is determined as  $\Omega_0/1.3$  times the factored shear resistance of the shear panels, as discussed previously. For this example, the tie-down will be designed at the first floor only; the other floors would be computed similarly, and tie-down devices, as shown in Figure 10.1-8, would be used.

[The requirements for uplift anchorage are slightly different in the 2003 *Provisions*. The tie down force is based on the "nominal strength of the shear wall" rather than the  $\Omega_0/1.3$  times the factored resistance as specified in the 2000 *Provisions*. This change is primarily intended to provide consistent terminology and should not result in a significant impact on the design of the tie down.]

The uplift forces are computed as:

Roof: $T = 0.44$ klf (3.0/1.3) (8 ft)	= 8.12 kips
Third floor: $T = 0.66$ klf (3.0/1.3) (8 ft)	= 12.18 kips
Second floor: $T = 0.66 \text{ klf} (3.0/1.3) (8 \text{ ft})$	= <u>12.18 kips</u>
$\Sigma = 32.48 \text{ kips}$	

Since the chord member supports the window header as well, use a  $6 \times 6$  Douglas fir-Larch No. 1 similar to the transverse walls. Try a double tie-down device with a 7/8-in. anchor bolt and three 7/8-in. stud bolts. Using the method described above for computing the strength of a double tie-down, the nominal design strength is 34.3 kips, which is greater than the demand of 32.48 kips.

The design of the tie-downs at the second and third floors is similar.

10.1.4.10.3 Perforated Shear Wall Compression Chords

OK

*Provisions* Sec. 12.4.3.4.4 [AF&PA Wind&Seismic Sec. 4.3.6.1], requires each end of a perforated shear wall to have a chord member designed for the following compression force from each story:

$$C = \frac{Vh}{C_0 \Sigma L_i}$$

where

V = design shear force in the shear wall (not wall capacity as used for uplift)

h = shear wall height (per floor)

 $C_0$  = shear capacity adjustment factor

 $\Sigma L_i$  = sum of widths of perforated shear wall segments

For h = 8 ft,  $C_0 = 0.83$  and  $\Sigma L_i = 18$  ft, the compression force is computed as:

Third floor: $C = 3.64(8)/0.83/18$	=	1.95 kips
Second floor: $C = (3.64 + 3.77)(8)/0.83/18$	=	3.96 kips
First floor: $C = (3.64 + 3.77 + 1.88)(8)/0.83/18$	=	4.98 kips
Σ	=	10.89 kips

Again, just the chord at the first floor will be designed here; the design at the upper floors would be similar. Although not explicitly required by *Provisions* Sec. 12.4.3.4.4 [AF&PA Wind&Seismic Sec. 4.3.6.1], it is rational to combine the chord compression with gravity loading (using the load combination  $1.38D + 1.0Q_E + 0.5L + 0.2S$  in accordance with *Provisions* Eq. 5.2.7.1-1 [4.2-1]), in order to design the chord member. The end post of the longitudinal shear wall supports the same tributary weight at the end post of the transverse shear walls. Using the weights computed previously in Sec. 10.1.4.5, the design compression force is:

$$1.38(5.17) + 1.0(10.89) + 0.5(4.48) + 0.2(1.30) = 20.5$$
 kips.

The bearing capacity on the bottom plate was computed previously as 31.5 kips, which is greater than 20.5 kips. Where end posts are loaded in both directions, orthogonal effects must be considered in accordance with *Provisions* Sec. 5.2.5.2 [4.4.2.3].

# 10.1.4.10.4 Anchorage at Shear Wall Segments

The anchorage at the base of a shear wall segment (bottom plate to floor framing or foundation wall), is designed per *Provisions* Sec. 12.4.3.4.2 [AF&PA Wind&Seismic Sec. 4.3.6.4]. While this anchorage need only be provided at the full height sheathing, it is usually extended over the entire length of the perforated shear wall to simplify the detailing and reduce the possibility of construction errors.

$$v = \frac{V}{C_0 \sum L_i}$$

where

V = design shear force in the shear wall  $C_0 =$  shear capacity adjustment factor  $\Sigma L_i =$  sum of widths of perforated shear wall segments This equation is the same as was previously used to compute unit shear demand on the wall segments. Therefore, the in-plane anchorage will be designed to meet the following unit, in-plane shear forces:

Third floor: v = 0.244 klf Second floor: v = 0.496 klf First floor: v = 0.622 klf.

In addition to resisting the in-plane shear force, *Provisions* Sec. 12.4.3.4.3 [AF&PA Wind&Seismic Sec. 4.3.6.4] requires that the shear wall bottom plates be designed to resist a uniform uplift force, *t*, equal to the unit in-plane shear force. Per *Provisions* Sec. 12.4.3.4.5 [AF&PA Wind&Seismic Sec. 4.3.6.4], this uplift force must be provided with a complete load path to the foundation. That is, the uplift force at each level must be combined with the uplift forces at the levels above (similar to the way overturning moments are accumulated down the building).

At the foundation level, the unit in-plane shear force, v, and the unit uplift force, t, are combined for the design of the bottom plate anchorage to the foundation wall. The design unit forces are:

Shear: v = 0.622 klf Tension: t = 0.244 + 0.496 + 0.622 = 1.36 klf

Assuming that stresses on the wood bottom plate govern the design of the anchor bolts, the anchorage is designed for shear (single shear, wood-to-concrete connection) and tension (plate washer bearing on bottom plate). The interaction between shear and tension need not be considered in the wood design for this configuration of loading. As for the transverse shear walls, try a 5/8-in. bolt at 32 in. on center with a 3-in. square plate washer (*Provisions* Sec. 12.4.2.4 [12.4.2.4.2] requires  $1/4 \times 3 \times 3$  in. plate washer for 5/8-in. anchor bolts). As computed previously, the shear capacity is 0.91 klf so the bolts are adequate.

For anchor bolts at 32 in. on center, the tension demand per bolt is 1.36 klf (32/12) = 3.63 kips. Bearing capacity of the plate washer (using a Douglas fir No. 2 bottom plate) is computed per the AF&PA Manual, Structural Connections Supplement, as:

$$\lambda \phi P' = (1.0)(0.8)(1.30 \text{ ksi})(9 \text{ in.}^2) = 9.36 \text{ kips} > 3.63 \text{ kips}$$
 OK

The anchor bolts themselves must be designed for combined shear, and tension in accordance with *Provisions* Sec. 9.2 [11.2].

In addition to designing the anchor bolts for uplift, a positive load path must be provided to transfer the uplift forces into the bottom plate. One method for providing this load path continuity, is to use metal straps nailed to the studs and lapped around the bottom plate, as shown in Figure 10.1-15. Attaching the studs directly to the foundation wall (using embedded metal straps) for uplift and using the anchor bolts for shear only is an alternative approach.

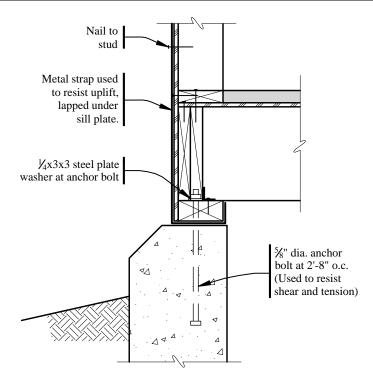


Figure 10.1-15 Perforated shear wall detail at foundation (1.0 ft = 0.3048 m, 1.0 in. = 25.4 mm).

At the upper floors, the load transfer for in-plane shear is accomplished by using nailing or framing clips between the bottom plates, rim joists, and top plates in a manner similar to that for standard shear walls. The uniform uplift force can be resisted either by using the nails in withdrawal (for small uplift demand) or by providing vertical metal strapping between studs above and below the level considered. This type of connection is shown in Figure 10.1-16. For this type of connection (and the one shown in Figure 10.1-15) to be effective, shrinkage of the floor framing must be minimized using dry or manufactured lumber.

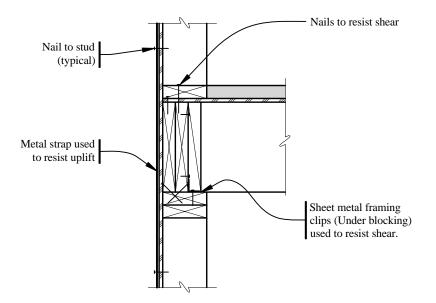


Figure 10.1-16 Perforated shear wall detail at floor framing.

For example, consider the second floor. The required uniform uplift force, t = 0.244 + 0.496 = 0.740 klf. Place straps at every other stud, so the required strap force is 0.740 (32/12) = 1.97 kips. Provide an 18-gauge strap with 1210d nails at each end.

# 10.2 WAREHOUSE WITH MASONRY WALLS AND WOOD ROOF, LOS ANGELES, CALIFORNIA

This example features the design of the wood roof diaphragm, and wall-to-diaphragm anchorage for the one-story masonry building, described in Sec. 9.1 of this volume of design examples. Refer to that example for more detailed building information and the design of the masonry walls.

# **10.2.1 Building Description**

This is a very simple rectangular warehouse, 100 ft by 200 ft in plan (Figure 10.2-1), with a roof height of 28 ft. The wood roof structure slopes slightly, but it is nominally flat. The long walls (side walls) are 8 in. thick and solid, and the shorter end walls are 12 in. thick and penetrated by several large openings.

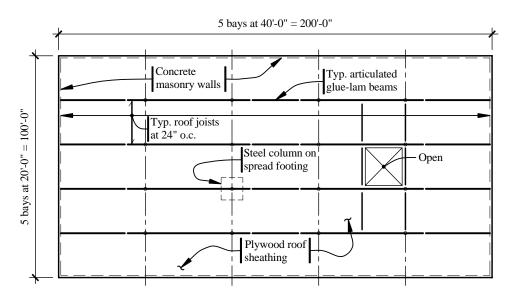


**Figure 10.2-1** Building plan (1.0 ft = 0.3048 m, 1.0 in. = 25.4 mm).

Based on gravity loading requirements, the roof structure consists of wood joists, supported by 8<sup>3</sup>/<sub>4</sub>-in. wide, by 24-in. deep, glued-laminated beams, on steel columns. The joists span 20 ft and the beams span 40 ft, as an articulated system. Typical roof framing is assumed to be Douglas fir-Larch No.1 as graded by the WWPA. The glued-laminated beams meet the requirements of combination 24F-V4 per ANSI/AITC A190.1.

The plywood roof deck acts as a diaphragm to carry lateral loads to the exterior walls. There are no interior walls for seismic resistance. The roof contains a large opening that interrupts the diaphragm continuity.

The diaphragm contains continuous cross ties in both principal directions. The details of these cross ties and the masonry wall-to-diaphragm anchorage are substantially different from those shown in previous versions of this example. This is primarily due to significant revisions to the *Provisions* requirements for anchorage of masonry (and concrete) walls to flexible wood diaphragms.

The following aspects of the structural design are considered in this example:

- 1. Development of diaphragm forces based on the equivalent lateral force procedure used for the masonry wall design (Sec. 9.1)
- 2. Design and detailing of a plywood roof diaphragm with a significant opening
- 3. Computation of drift and P-delta effects
- 4. Anchorage of diaphragm and roof joists to masonry walls and
- 5. Design of cross ties and subdiaphragms

[Note that as noted in Sec. 9.1, the new "Simplified Design Procedure" contained in 2003 *Provisions* Simplified Alternate Chapter 4 as referenced by 2003 *Provisions* Sec. 4.1.1 is likely to be applicable to this example, subject to the limitations specified in 2003 *Provisions* Sec. Alt. 4.1.1.]

### **10.2.2 Basic Requirements**

### **10.2.2.1** *Provisions* Parameters

S <sub>s</sub> (Provisions Maps [Figure 3.3.3])	= 1.50
S <sub>1</sub> (Provisions Maps [Figure 3.3.4])	= 0.60
Site Class (Provisions Sec. 4.1.2.1 [3.5])	= C
Seismic Use Group (Provisions Sec. 1.3 [1.2])	= I
Seismic Design Category (Provisions Sec. 4.2 [1.4])	= D
Seismic Force Resisting System ( <i>Provisions</i> Table 5.2.2 [4.3-1])	= Special reinforced
	masonry shear wall
Response Modification Factor, <i>R</i> ( <i>Provisions</i> Table 5.2.2 [4.3-1])	= 3.5
System Overstrength Factor, $\Omega_0$ ( <i>Provisions</i> Table 5.2.2 [4.3-1])	= 2.5
Deflection Amplification Factor, $C_d$ ( <i>Provisions</i> Table 5.2.2 4.3-1])	= 3.5

[The 2003 *Provisions* have adopted the 2002 USGS probabilistic seismic hazard maps, and the maps have been added to the body of the 2003 *Provisions* as figures in Chapter 3 (instead of the previously used separate map package).]

### 10.2.2.2 Structural Design Criteria

A complete discussion on the criteria for ground motion, seismic design category, load path, structural configuration, redundancy, analysis procedure, and shear wall design, is included in Sec. 9.1 of this volume of design examples.

### 10.2.2.2.1 Design and Detailing Requirements (Provisions Sec. 5.2.6 [4.6])

See *Provisions* Chapter 12, for wood design requirements. As discussed in greater detail in Sec. 10.1, *Provisions* Sec. 12.2.1 utilizes load and resistance factor design (LRFD) for the design of engineered wood structures. The design capacities are therefore, consistent with the strength design demands of *Provisions* Chapter 5.

The large opening in the diaphragm must be fitted with edge reinforcement (*Provisions* Sec. 5.2.6.2.2 [4.6.1.4]). However, the diaphragm does not require any collector elements that would have to be designed for the special load combinations (*Provisions* Sec. 5.2.6.4.1 [4.6.2.2]).

The requirements for anchoring of masonry walls to flexible diaphragms (*Provisions* Sec. 5.2.6.3.2 [4.6.2.1]) are of great significance in this example.

10.2.2.2.2 Combination of Load Effects (Provisions Sec. 5.2.7 [4.2.2])

The basic design load combinations for the lateral design, as stipulated in ASCE 7, and modified by the *Provisions* Eq. 5.2.7-1 and 5.2.7-2 [4.2-1 and 4.2-2], were computed in Sec. 9.1 of this volume of design examples as:

 $1.4D + 1.0Q_E$ 

and

 $0.7D - 1.0Q_{E}$ 

The roof live load,  $L_r$ , is not combined with seismic loads, and the design snow load is zero for this Los Angeles location.

10.2.2.2.3 Deflection and Drift Limits (Provisions Sec. 5.2.8 [4.5.1])

In-plane deflection and drift limits for the masonry shear walls are considered in Sec. 9.1.

As illustrated below, the diaphragm deflection is much greater than the shear wall deflection. According to *Provisions* Sec. 5.2.6.2.6 [4.5.2], in-plane diaphragm deflection shall not exceed the permissible deflection of the attached elements. Because the walls are essentially pinned at the base, and simply supported at the roof, they are capable of accommodating large deflections at the roof diaphragm.

For illustrative purposes, story drift is determined and compared to the requirements of *Provisions* Table 5.2.8 [4.5-1]. However, according to this table, there is essentially no drift limit for a single story structure as long as the architectural elements can accommodate the drift (assumed to be likely in a warehouse structure with no interior partitions). As a further check on the deflection, P-delta effects (*Provisions* Sec. 5.4.6.2 [5.2.6.2]) are evaluated.

### 10.2.3 Seismic Force Analysis

Building weights and base shears are as computed in Sec. 9.1 of this volume of design examples. (The building weights used in this example are based on a preliminary version of Example 9.1 and, thus, minor numerical differences may exist between the two examples). *Provisions* Sec. 5.2.6.4.4 [4.6.3.4]specifies that floor and roof diaphragms be designed to resist a force,  $F_{px}$ , in accordance with *Provisions* Eq. 5.2.6.4.4 [4.6-2]as follows:

$$F_{px} = \frac{\sum_{i=x}^{n} F_i}{\sum_{i=x}^{n} w_i} w_{px}$$

plus any force due to offset walls (not applicable for this example). For one-story buildings, the first term of this equation will be equal to the seismic response coefficient,  $C_s$ , which is 0.286. The effective diaphragm weight,  $w_{px}$ , is equal to the weight of the roof, plus the tributary weight of the walls perpendicular to the direction of the motion. The tributary weights are:

Roof = 20(100)(200)	= 400 kips
Side walls = $2(65)(28/2+2)(200)$	= 416 kips
End walls = $2(103)(28/2+2)(100)$	= 330 kips

The diaphragm design force is computed as:

Transverse	$F_{p,roof} = 0.286(400 + 416)$	= 233 kips
Longitudinal	$F_{p,roof} = 0.286(400 + 330)$	= 209 kips

These forces exceed the minimum diaphragm design forces given in *Provisions* Sec. 5.2.6.4.4 [4.6.3.4], because  $C_s$  exceeds the minimum factor of  $0.2S_{DS}$ .

### 10.2.4 Basic Proportioning of Diaphragm Elements

The design of plywood diaphragms primarily involves the determination of sheathing sizes and nailing patterns to accommodate the applied loads. Large openings in the diaphragm and wall anchorage requirements, however, can place special requirements on the diaphragm capacity. Diaphragm deflection is also a consideration.

Nailing patterns for diaphragms are established on the basis of tabulated requirements included in the *Provisions*. It is important to consider the framing requirements for a given nailing pattern and capacity as indicated in the notes following the tables. In addition to strength requirements, *Provisions* Sec. 12.4.1.2 places aspect ratio limits on plywood diaphragms (length-to-width shall not exceed 4/1 for blocked diaphragms). However, it should be taken into consideration that compliance with this aspect ratio does not guarantee that drift limits will be satisfied.

While there is no specific limitation on deflection for this example, the diaphragm has been analyzed for deflection as well as for shear capacity. A procedure for computing diaphragm deflections is illustrated in detail, in Sec. 10.1.4.7.

In the calculation of diaphragm deflections, the chord splice slip factor can result in large additions to the total deflection. This chord splice slip, however, is often negligible where the diaphragm is continuously anchored to a bond beam in a masonry wall. Therefore, chord splice slip is assumed to be zero in this example.

### 10.2.4.1 Strength of Members and Connections

The 2000 *Provisions* have adopted Load and Resistance Factor Design (LRFD) for engineered wood structures. The *Provisions* includes the ASCE 16 standard by reference and uses it as the primary design procedure for engineered wood construction. Strength design of members and connections is based on the requirements of ASCE 16. The AF&PA Manual and supplements contain reference resistance values for use in design. For convenience, the *Provisions* contains design tables for diaphragms that are identical to those contained in the AF&PA Structural-Use Panels Supplement. Refer to Sec. 10.1.4.1 for a more complete discussion of the design criteria.

[The primary reference for design of wood diaphragms in the 2003 *Provisions* is AF&PA Wind & Seismic. Much of the remaining text in the 2003 *Provisions* results from differences between AF&PA Wind & Seismic and Chapter 12 of the 2000 *Provisions* as well as areas not addressed by AF&PA Wind & Seismic. Because the AF&PA Wind & Seismic tabulated design values for diaphragms do not completely replace the tables in the 2000 *Provisions*, portions of the tables remain in the 2003 *Provisions*. Therefore, some diaphragm design values are in the 2003 *Provisions* and some are in AF&PA Wind & Seismic. The design values in the tables are different between the two documents. The values in the 2003 *Provisions* represent factored shear resistance ( $\lambda \varphi D'$ ), while the values in AF&PA Wind & Seismic represent nominal shear resistance that must then be multiplied by a resistance factor,  $\varphi$ , (0.65) and a time effect factor  $\lambda$ , (1.0 for seismic loads). Therefore, while the referenced tables may be different, the factored resistance values based on the 2003 *Provisions* should be the same as those in examples based on

the 2000 Provisions. The calculations that follow are annotated to indicate from which table the design values are taken.]

### 10.2.4.2 Roof Diaphragm Design for Transverse Direction

### 10.2.4.2.1 Plywood and Nailing

The diaphragm design force,  $F_{p,roof} = 233$  kips. Accounting for accidental torsion (*Provisions* Sec. 5.4.4.2 [5.2.4.2]), the maximum end shear =  $0.55F_{p,roof}$  = 128 kips. This corresponds to a unit shear force v = (128/100) = 1.28 klf. Although there is not a specific requirement in the *Provisions*, it is the authors' opinion that accidental torsion should be considered, even for "flexible" diaphragms, to account for the possibility of a non-uniform mass distribution in the building.

Because the diaphragm shear demand is relatively high, the plywood sheathing and roof framing at the ends of the building, must be increased in size over the standard roof construction for this type of building. Assuming 3-in. nominal framing, try blocked 3/4-in. (23/32) Structural I plywood rated sheathing with two lines of 10d common nails at 2-1/2 in. on center at diaphragm boundaries, continuous panel edges, and two lines at 3 in. on center at other panel edges.

From *Provisions* Table 12.4.3-1a [12.4-1a],  $\lambda \phi D' = 1.60$  klf > 1.28 klf OK

Because the diaphragm shear decreases towards the midspan of the diaphragm, the diaphragm capacity may be reduced towards the center of the building. Framing size and plywood thickness are likely to have a more significant impact on cost than nail spacing, determine a reasonable location to transition to 2 in. nominal roof joists and  $\frac{1}{2}$  in. (15/32) plywood. A reasonable configuration for the interior of the building utilizes <sup>1</sup>/<sub>2</sub> -in. (15/32) Structural I plywood rated sheathing with a single line of 10d at 2 <sup>1</sup>/<sub>2</sub> in. on center nailing at diaphragm boundaries, continuous panels edges, and 4 in. on center nailing at other panel edges. Using 2×4 flat blocking at continuous panel edges, the requirements found in Notes f, and g of Provisions Table 12.4.3-1a [AF&PA Wind&Seismic Sec. 4.2.7.1] are met. Determine the distance, X, from the end wall where the transition can be made as:

 $\lambda \phi D' = 0.83$  klf (*Provisions* Table 12.4.3-1a [AF&PA Wind&Seismic Table 4.2A]), Shear Capacity = 0.83(100) = 83.0 kips Uniform Diaphragm Demand = 233/200 = 1.165 klf X = (128 - 83)/1.165 = 38.6 ft, say 40 ft from the diaphragm edge

[Here is an example where both the *Provisions* tables and the AF&PA Wind & Seismic tables are required to complete the design. The design value for this plywood thickness and nailing pattern is contained in AF&PA Wind & Seismic, but the design value for the higher-capacity diaphragm at the ends is contained in the *Provisions*.]

In a building of this size, it may be beneficial to further reduce the diaphragm nailing towards the middle of the roof. However, due to the requirements for subdiaphragms, (see below) and diaphragm capacity, in the longitudinal direction and for simplicity of design, no additional nailing pattern is used.

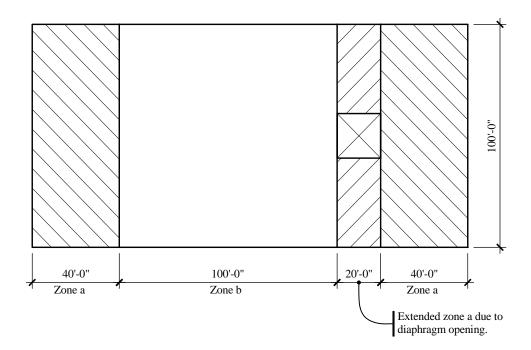
Table 10.2-1 contains a summary of the diaphragm framing and nailing requirements (All nails are 10d common). See Figure 10.2-2 for designation of framing and nailing zones, and Figure 10.2-3 for typical plywood layout.

	Table 1	10.2-1 ROOT D1	aphragm Framing and Nailing Requirements	
Zone <sup>*</sup>	Framing	Plywood	Nail Spacing (in.)	Capacity
				(kip/ft)

			Boundaries and Cont. Panel Edges	Other Panel Edges	Intermediate Framing Members	
а	3×12	<sup>3</sup> ⁄4 in.	21/2 (2 lines)	3 (2 lines)	12 (1 line)	1.60
b	2×12	1⁄2 in.	21/2 (1 line)	4 (1 line)	12 (1 line)	0.83

1.0 in. = 25.4 mm, 1.0 kip/ft = 14.6 kN/m.

\* Refer to Figure 10.2-2 for zone designation.



**Figure 10.2-2** Diaphragm framing and nailing layout (1.0 ft = 0.3048 m).

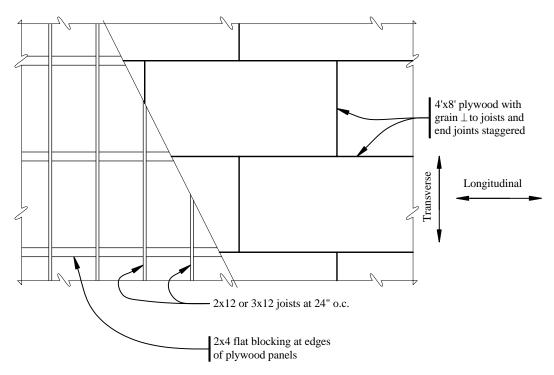


**Figure 10.2-3** Plywood layout (1.0 ft = 0.3048 m, 1.0 in. = 25.4 mm).

### 10.2.4.2.2 Chord Design

Although the bond beam at the masonry wall could be used as a diaphragm chord, this example illustrates the design of the wood ledger member as a chord. Chord forces are computed using a simply supported beam analogy, where the design force is the maximum moment divided by the diaphragm depth.

Diaphragm moment,  $M = wL^2/8 = F_{p,roof}L/8 = 233(200/8) = 5,825$  ft-kips Chord force, T = C = 5,825/(100 - 16/12) = 59.0 kips

Try a select structural Douglas fir-larch  $4 \times 12$ , for the chord. Assuming two 1/16 in. bolt holes (for 1-in. bolts) at splice locations, the net chord area is 31.9 in.<sup>2</sup> Tension strength (parallel to wood grain), per the AF&PA Manual, Structural Lumber Supplement:

 $\lambda \phi T'(1.0)(0.8)(2.70)(31.9) = 68.9 \text{ kips} > 59.0 \text{ kips}$ 

Design the splice for the maximum chord force of 59.0 kips. Try bolts with steel side plates using 1 in. A307 bolts, with a  $3\frac{1}{2}$  in. length in the main member. The capacity, according to the AF&PA Manual, Structural Connections Supplement, is:

 $\lambda \phi Z' = (1.0)(0.65)(16.29) = 10.6$  kips per bolt.

Number of bolts required = 59.0/10.6 = 5.6

Use two rows of three bolts. The reduction (group action factor) for multiple bolts is negligible. Net area of the  $4\times12$  chord with two rows of 1-1/16 in. holes is 31.9 in.<sup>2</sup> as assumed above. Therefore, use six 1 in. A307 bolts on each side of the chord splice (Figure 10.2-4). Although it is shown for illustration, this type of chord splice may not be the preferred splice against a masonry wall since the bolts, and side plate, would have to be recessed into the wall.

OK

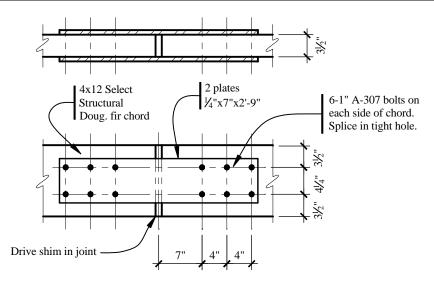


Figure 10.2-4 Chord splice detail (1.0 ft = 0.3048 m, 1.0 in. = 25.4 mm).

## 10.2.4.2.3 Diaphragm Deflection and P-delta Check

The procedure for computing diaphragm deflection is described in Sec. 10.1.4.7.

[AF&PA Wind & Seismic also contains procedures for computing diaphragm deflections. The equations are slightly different from the more commonly used equations that appear in the *Commentary* and AF&PA LRFD *Manual*. In AF&PA Wind & Seismic, the shear and nail slip terms are combined using an "apparent shear stiffness" parameter. However, the apparent shear stiffness values are only provided for OSB. Therefore, the deflection equations in the *Commentary* or AF&PA LRFD *Manual* must be used in this example which has plywood diaphragms. The apparent shear stiffness values for plywood will likely be available in future editions of AF&PA Wind & Seismic.]

As stated in *Commentary* Sec. 12.4, the diaphragm deflection is computed as:

$$\delta = \frac{5\nu L^3}{8wEA} + \frac{\nu L}{4Gt} + 0.188Le_n + \frac{\sum(\Delta_c X)}{2w}$$

The equation produces the midspan diaphragm displacement in inches, and the individual variables *must* be entered in the force or length units as described below. A small increase in diaphragm deflection due to the large opening is neglected. An adjustment factor, F, for non-uniform nailing is applied to the third term of the above equation for this example.

Bending deflection = $5vL^3/8wEA$	= 0.580 in.
Shear deflection = $vL/4Gt$	= 1.210 in.
Effective nails slip deflection = $0.188 Le_n F$	= 0.265 in.
Deflection due to chord slip at splices = $\Sigma(\Delta_c X)/2w$	= 0.000 in.

(The chord slip deflection is assumed to be zero because the chord is connected to the continuous bond beam at the top of the masonry wall.)

The variables above and associated units used for computations are:

v = (233/2)/100 = 1,165 plf (shear per foot at boundary, ignoring torsion)

L = 200 ft and w = 100 ft (diaphragm length and depth)

A = effective area of 4×12 chord and two-#6 rebars assumed to be in the bond beam

 $= 39.38 \text{ in.}^2 + 2(0.44)(29,000,000/1,900,000) = 52.81 \text{ in.}^2$ 

t = 0.535 in. (effective, for  $\frac{1}{2}$  in. Structural I plywood, unsanded; neglect  $\frac{3}{4}$  in. plywood at edge)

- E = 1,900,000 psi (for Douglas fir-larch select structural chord)
- G = 90,000 psi (Structural I plywood)
- $e_n$  = nail slip for 10d nail at end of diaphragm (use one and one-half-in. nail spacing, two lines at 3 in., not the 1-1/4 in. perimeter spacing)

Design nail load = 1,165/(12/1.5) = 146 lb/nail

Using the procedure in Sec. 10.1.4.3 and the value for dry/dry lumber from Table 10.1-2,  $e_n = (146/769)^{3.276} = 0.00433$  in.

F = adjustment for non-uniform nail spacing

The 0.188 coefficient assumes a uniform nail spacing, which implies an average load per nail of one-half the maximum. One common practice for calculating deformation is simply to use the load per nail that would result from the larger spacing should that spacing be used throughout. However, this gives a large estimate for deformation due to nail slip. Figure 10.2-5 shows the graphic basis for computing a more accurate nail slip term. The basic amount is taken as that for the smaller nail spacing (1-1/2 in.), which gives 146 lbs per nail.

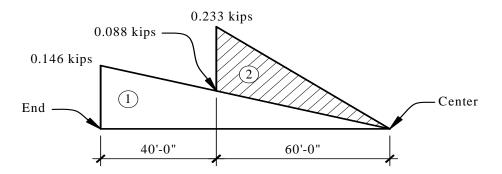


**Figure 10.2-5** Adjustment for nonuniform nail spacing (1.0 ft = 0.3048 m, 1.0 kip = 4.45 kN)

Using a larger nail spacing at the interior increases the deformation. The necessary increase may be determined as the ratio of the areas of the triangles in Figure 10.2-5, which represents the load per nail along the length of the diaphragm. The ratio is for Triangle 2 representing zone b compared to Triangle 1 representing zone a, where zones a and b are as shown Figure 10.2-2.

Ratio = (233 - 88)60 / 146(100) = 0.63

thus, F = 1 + 0.63 = 1.63.

Total for diaphragm:

 $\delta = 0.580 + 1.210 + 0.265 + 0.00 = 2.055$  in.

End wall deflection = 0.037 in. (see Sec. 9.1 of this volume of design examples)

Therefore, the total elastic deflection  $\delta_{xe} = 2.055 + 0.037 = 2.092$  in.

Total deflection,  $\delta_x = C_d \, \delta_{xe} / I = 3.5(2.092) / 1.0 = 7.32$  in. =  $\Delta$ 

P-delta effects are computed according to *Provisions* Sec. 5.4.6.2 [5.2.6.2]using the stability coefficient computed per *Provisions* Eq. 5.4.6.2-1 [5.2-16]:

$$\theta = \frac{P_x \Delta}{V_x h_{sx} C_d}$$

Because the midspan diaphragm deflection is substantially greater than the deflection at the top of the masonry end walls, it would be overly conservative to consider the entire design load at the maximum deflection. Therefore, the stability coefficient is computed by splitting the P-delta product into two terms one for the diaphragm and one for the end walls.

For the diaphragm, consider the weight of the roof and side walls at the maximum displacement. (This overestimates the P-delta effect. The computation could consider the average displacement of the total weight, which would lead to a reduced effective delta. Also, the roof live load need not be included.)

P = 400 + 416 = 816 kips  $\Delta = 7.32$  in. V = 233 kips (diaphragm force)

For the end walls, consider the weight of the end walls at the wall displacement:

P = 330 kips  $\Delta = (3.5)(0.037) = 0.13$  in. V = 264 kips (additional base shear for wall design)

For story height, h = 28 feet, the stability coefficient is:

$$\theta = \left(\frac{P\Delta}{V} + \frac{P\Delta}{V}\right) / hC_d = \left(\frac{816(7.32)}{233} + \frac{330(0.13)}{264}\right) / (28)(12)(3.5) = 0.022$$

For  $\theta < 0.10$ , no deflection amplification due to P-delta effects is necessary.

[Note that the equation to determine the stability coefficient has been changed in the 2003 *Provisions*. The importance factor, *I*, has been added to 2003 *Provisions* Eq. 5.2-16. However, this does not affect this example because I = 1.0.]

Drift index  $=\Delta/h_{sx} = 7.32/[28(12)] = 0.022$ .

This is slightly less than the limiting drift ratio of 0.025 applied for most low-rise buildings in Seismic Use Group I (*Provisions* Sec. 5.2.8 [4.5.1] and Table 5.2.8 [4.5-1]). However, for one-story buildings, Table 5.2.8, Note b [4.5-1, Note c], and *Provisions* Sec. 5.2.6.2.6 [4.5.2], permit unlimited drift provided that the structural elements and finishes can accommodate the drift. The limit for masonry cantilever shear wall structures (0.007) should only be applied to the in-plane movement of the end walls ( $0.13/h = 0.0004 \ll 0.007$ ). The construction of the out-of-plane walls allows them to accommodate very large drifts. It is further expected that the building does not contain interior elements that are sensitive to drift.

Given the above conditions, and the fact that P-delta effects are not significant for this structure, the computed diaphragm deflections appear acceptable.

### 10.2.4.2.4 Detail at Opening

Consider diaphragm strength at the roof opening (Figure 10.2-6), as required by *Provisions* Sec. 5.2.6.2.2 [4.6.1.4].

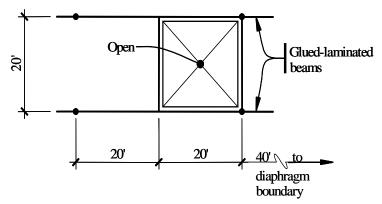


Figure 10.2-6 Diaphragm at roof opening (1.0 ft = 0.3048 m).

Check diaphragm nailing for required shear area (shear in diaphragm at edge of opening):

Shear = 128 - [40(1.165)] = 81.4 kips v = 81.4/(100 - 20) = 1.02 klf

Because the opening is centered in the width of the diaphragm, half the force to the diaphragm must be distributed on each side of the opening.

Diaphragm capacity in this area = 0.830 klf as computed previously (see Table 10.2-1 and Figure 10.2-2). Because the diaphragm demand at the reduced section exceeds the capacity, the extent of the Zone a nailing and framing should be increased. For simplicity, extend the Zone a nailing to the interior edge of the opening (60 ft from the end wall). The diaphragm strength is now adequate for the reduced overall width at the opening.

### 10.2.4.2.5 Framing around Opening

The opening is located 40 ft from one end of the building and is centered in the other direction (Figure 10.2-6). This does not create any panels with very high aspect ratios.

In order to develop the chord forces, continuity will be required across the glued-laminated beams in one direction and across the roof joists in the other direction.

## 10.2.4.2.6 Chord Forces at Opening

To determine the chord forces on the edge joists, model the diaphragm opening as a Vierendeel truss and assume the inflection points will be at the midpoint of the elements (Figure 10.2-7). Compute forces at the opening using a uniformly distributed diaphragm demand of 233/200 = 1.165 klf.

For Element 1 (shown in Figure 10.2-7):

 $w_I = 1.165/2 = 0.582$  kips/ft  $V_{IB} = 0.5[128-(40)(1.165)] = 40.7$  kips  $V_{IA} = 40.7 - 20(0.582) = 29.1$  kips  $M_I$  due to Vierendeel action = ( $\frac{1}{2}$ )[40.7(10) + 29.1(10)] = 349 ft-kips

Chord force due to  $M_1 = 349/40 = 8.72$  kips. This is only 41 psi on the glued-laminated beam on the edge of the opening. This member is adequate by inspection. On the other side of this diaphragm element, the chord force is much less than the maximum global chord force (59.0 kips), so the ledger and ledger splice are adequate.

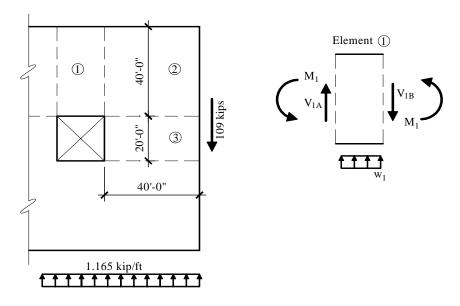


Figure 10.2-7 Chord forces and Element 1 free-body diagram (1.0 ft = 0.3048 m, 1.0 kip = 4.45 kN, 1.0 kip/ft = 14.6 kN/m).

For Element 3, analyze Element 2 (shown in Figure 10.2-8):

 $w_2 = 1.165(40/100) = 0.466$  kips/ft  $V_3 = 128(40/100) = 51.2$  kips  $V_{IB} = 40.7$  kips  $M_I = 349$  ft-kips.

 $T_{IB}$  is the chord force due to moment on the total diaphragm:

 $M = 128(40) - 1.165(40^2/2) = 4,188$  ft-kips  $T_{IB} = 4,188/100 = 41.9$  kips  $\Sigma M_0$ :  $M_3 = M_1 + 40V_3 - 40T_{IB} - w_2 40^2/2 = 348$  ft-kips

Therefore, the chord force on the roof joist = 348/40 = 8.7 kips

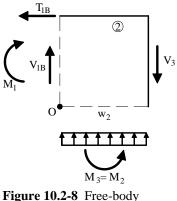


Figure 10.2-8 Free-body diagram for Element 2.

Alternatively, the chord design should consider the wall anchorage force interrupted by the opening. As described in Sec. 10.2.4.3, the edge members on each side of the opening are used as continuous cross-ties, with maximum cross-tie force of 25.0 kips. Therefore, the cross-tie will adequately serve as a chord at the opening.

## 10.2.4.3 Roof Diaphragm Design for Longitudinal Direction

Force = 209 kips Maximum end shear = 0.55(209) = 115 kips Diaphragm unit shear v = 115/200 = 0.58 klf

For this direction, the plywood layout is Case 3 in *Provisions* Table 12.4.3-1a [AF&PA Wind&Seismic Table 4.2A]. Using ½ in. Structural I plywood rated sheathing, blocked, with 10d common nails at 2 ½ in. on center at diaphragm boundaries and continuous panel edges parallel to the load (ignoring the capacity of the extra nails in the outer zones):

 $\lambda \varphi D' = 0.83 \text{ plf} > 0.58 \text{ plf}, Provisions Table 12.4.3-1a [AF&PA Wind&Seismic Table 4.2A] OK$ 

Therefore, use the same nailing designed for the transverse direction. Compared with the transverse direction, the diaphragm deflection and P-delta effects will be satisfactory.

### 10.2.4.4 Masonry Wall Anchorage to Roof Diaphragm

As stipulated in *Provisions* Sec. 5.2.6.3.2 [4.6.2.1], masonry walls must be anchored to flexible diaphragms to resist out-of-plane forces computed per *Provisions* Eq. 5.2.6.3.2 [4.6-1]as:

 $F_P = 1.2S_{DS}IW_p = 1.2(1.0)(1.0)W_p = 1.2 W_p$ Side walls,  $F_P = 1.2(65\text{psf})(2+28/2)/1000 = 1.25$  klf End walls,  $F_P = 1.2(103\text{psf})(2+28/2)/1000 = 1.98$  klf

[In the 2003 *Provisions* the anchorage force for masonry walls connected to a flexible diaphragm has been reduced to  $0.8S_{DS}IW_{p}$ .]

10.2.4.3.1 Anchoring Joists Perpendicular to Walls (Side Walls)

Because the roof joists are spaced at 2 ft on center, provide a connection at each joist that will develop 2(1.25) = 2.50 kip/joist.

A common connection for this application is metal tension tie or hold-down device that is anchored to the masonry wall with an embedded bolt and is either nailed or bolted to the roof joist. Other types of anchors include metal straps that are embedded in the wall and nailed to the top of the joist. The ledger is not used for this force transfer because the eccentricity between the anchor bolt and the plywood creates tension perpendicular to the grain in the ledger (cross-grain bending), which is prohibited. Also, using the edge nails to resist tension perpendicular to the edge of the plywood, is not permitted.

Try a tension tie with a 3/4 in. headed anchor bolt, embedded in the bond beam and 18 10d nails into the side of the joist (Figure 10.2-10). Modifying the allowable values using the procedure in Sec. 10.1.4.5 results in a design strength of:

$$\lambda \phi Z' = (1.0)(0.65)(4.73) = 3.07$$
 kips per anchor > 2.50 kips OK

The joists anchored to the masonry wall must also be adequately connected to the diaphragm sheathing. Determine the adequacy of the typical nailing for intermediate framing members. The nail spacing is 12 in. and the joist length is 20 ft, so there are 20 nails per joist. From the AF&PA Manual, Structural Connections Supplement, the strength of a single 10d common nail is:

 $\lambda \phi Z' = (1.0)(0.65)(0.298) = 0.194$  kips per nail 20(0.194) = 3.88 kips > 2.50 kips

The embedded bolt also serves as the ledger connection, for both gravity loading, and in-plane shear transfer at the diaphragm. Therefore, the strength of the anchorage to masonry, and the strength of the bolt in the wood ledger, must be checked.

For the anchorage to masonry, check the combined tension and shear, resulting from the out-of-plane seismic loading (2.50 kips/bolt), and the vertical gravity loading. Assuming 20 psf dead load (roof live load is not included), and a 10-foot tributary roof width, the vertical load per bolt = (20 psf)(10 ft)(2 ft)/1000 = 0.40 kip. Using the load combination described previously, the design horizontal tension and vertical shear on the bolt are:

 $b_a = 1.0Q_E = 2.50$  kips  $b_v = 1.4$ D = 1.4(0.40) = 0.56 kip

The anchor bolts in masonry, are designed according to *Provisions* Sec. 11.3.12. Using 3/4 in. headed anchor bolts, both axial strength,  $B_a$ , and shear strength,  $B_v$ , will be governed by masonry breakout. Per *Provisions* Eq. 11.3.12.3-1, and 11.3.12.1-1, respectively, the design strengths are:

$$B_a = 4\phi A_p \sqrt{f'_m}$$
$$B_v = 1750\phi \sqrt[4]{f'_m A_b}$$

where  $\varphi = 0.5$ ,  $f'_m = 2,000$  psi,  $A_b =$  tensile area of bolt = 0.44 in.<sup>2</sup>, and  $A_p =$  projected area on the masonry surface of a right circular cone = 113 in.<sup>2</sup> (assuming 6 in. effective embedment). Therefore,  $B_a = 10.1$  kips and  $B_v = 4.8$  kips. Shear and tension are combined per *Provisions* Eq. 11.3.12.4 as:

$$\frac{b_a}{B_a} + \frac{b_v}{B_v} = \frac{2.50}{10.1} + \frac{0.56}{4.8} = 0.36 < 1.0$$
 OK

OK

[The 2003 *Provisions* refers to ACI 530, Sec. 3.1.6 for strength design of anchorage to masonry, as modified by 2003 Provisions Sec. 11.2. In general, the methodology for anchorage design using ACI 530 should be comparable to the 2000 *Provisions*, though some of the equations and reduction factors may be different. In addition, the 2003 *Provisions* require that anchors are either controlled by a ductile failure mode or are designed for 2.5 times the anchorage force.]

Figure 10.2-9 summarizes the details of the connection. In-plane seismic shear transfer (combined with gravity) and orthogonal effects are considered in a subsequent section.

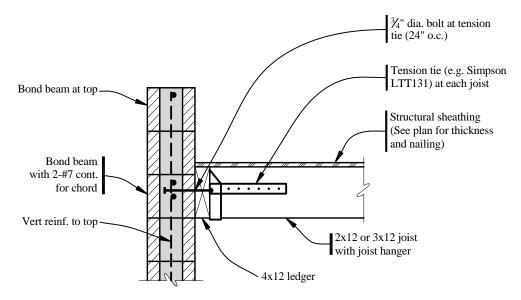


Figure 10.2-9 Anchorage of masonry wall perpendicular to joists (1.0 in. = 25.4 mm).

According to *Provisions* Sec. 5.2.6.3.2 [4.6.2.1, diaphragms must have continuous cross-ties to distribute the anchorage forces into the diaphragms. Although the *Provisions* do not specify a maximum spacing, 20 ft is common practice for this type of construction and Seismic Design Category.

For cross-ties at 20 ft on center, the wall anchorage force per cross-tie is:

(1.25 klf)(20 ft) = 25.0 kips

Try a  $3 \times 12$  (Douglas fir-Larch No. 1) as a cross-tie. Assuming one row of 15/16 in. bolt holes, the net area of the section is 25.8 in.<sup>2</sup> Tension strength (parallel to wood grain) per the AF&PA Structural Lumber Supplement, is:

$$\lambda \phi T' = (1.0)(0.8)(1.82)(25.8) = 37.5 \text{ kips} > 25.0 \text{ kips}$$
 OK

At the splices, try a double tie-down device with four 7/8 in. bolts in double shear through the  $3 \times 12$  (Figure 10.2-10). Product catalogs provide design capacities for single tie-downs only; the design of double hold downs requires two checks. First, consider twice the capacity of one tie-down and, second, consider the capacity of the bolts in double shear.

For the double tie-down, use the procedure in Sec. 10.1.4.5 to modify the allowable values:

$$2\lambda\phi Z' = 2(1.0)(0.65)(20.66) = 26.9$$
 kips > 25.0 kips

OK

The reduction (group action) factor for multiple bolts,  $C_g = 0.97$ .

For the four bolts, the AF&PA Manual, Structural Connections Supplement, gives:

$$4\lambda\phi C_g Z' = 4(1.0)(0.65)(0.97)(10.17) = 25.6$$
 kips > 25.0 kips

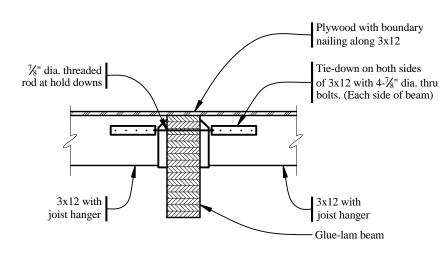


**Figure 10.2-10** Chord tie at roof opening (1.0 in. = 25.4 mm).

In order to transfer the wall anchorage forces into the cross-ties, the subdiaphragms between these ties must be checked per *Provisions* Sec. 5.2.6.3.2 [4.6.2.1]. There are several ways to perform these subdiaphragm calculations. One method is illustrated in Figure 10.2-11. The subdiaphragm spans between cross-ties and utilizes the glued-laminated beam and ledger as it's chords. The 1-to-1 aspect ratio meets the requirement of  $2\frac{1}{2}$  to 1 for subdiaphragms per *Provisions* Sec. 5.2.6.3.2 [4.2.6.1].

For the typical subdiaphragm (Figure 10.2-11):

 $F_p = 1.25$  klf v = (1.25)(20/2)/20 = 0.625 klf.

The subdiaphragm demand is less than the minimum diaphragm capacity (0.83 klf along the center of the side walls). In order to develop the subdiaphragm strength, and boundary nailing must be provided along the cross-tie beams.

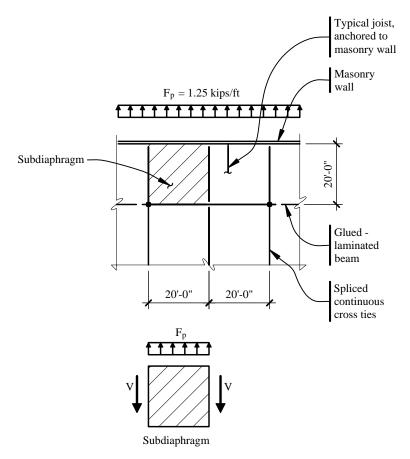


**Figure 10.2-11** Cross tie plan layout and subdiaphragm free-body diagram for side walls (1.0 ft = 0.3048 m, 1.0 kip/ft = 14.6 kN/m).

### 10.2.4.3.2 Anchorage at Joists Parallel to Walls (End Walls)

Where the joists are parallel to the walls, tied elements must transfer the forces into the main body of the diaphragm, which can be accomplished by using either metal strapping and blocking or metal rods and blocking. This example uses threaded rods that are inserted through the joists and coupled to the anchor bolt (Figure 10.2-12). Blocking is added on both sides of the rod to transfer the force into the plywood sheathing. The tension force in the rod causes a compression force on the blocking through the nut, and bearing plate at the innermost joist.

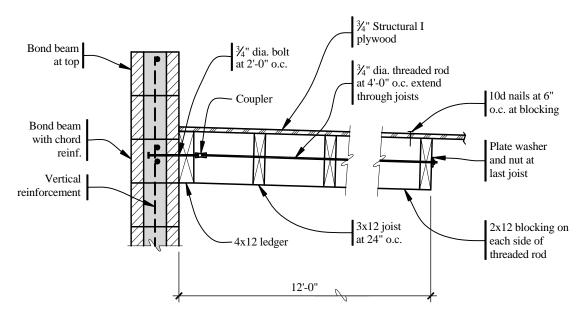


Figure 10.2-12 Anchorage of masonry wall parallel to joists (1.0 ft = 0.3048 m, 1.0 in. = 25.4 mm)

The anchorage force at the end walls is 1.98 klf. Space the connections at 4 ft on center so that the wall need not be designed for flexure (*Provisions* Sec. 5.2.6.1.2 [4.6.1.2]). Thus, the anchorage force is 7.92 kips per anchor.

Try a 3/4 in. headed anchor bolt, embedded into the masonry. In this case, gravity loading on the ledger is negligible and can be ignored, and the anchor can be designed for tension only. (In-plane shear transfer and orthogonal effects are considered later.)

As computed for 3/4 in. headed anchor bolts (with 6 in. embedment), the design axial strength  $B_a = 10.1$  kips > 7.92 kips. Therefore, the bolt is acceptable.

Using couplers rated for 125 percent of the strength of the rod material, the threaded rods are then coupled to the anchor bolts and extend six joist spaces (12 ft) into the roof framing. (The 12 ft are required for the subdiaphragm force transfer as discussed below.)

Nailing the blocking to the plywood sheathing is determined, using the AF&PA Structural Connections Supplement. As computed previously, the capacity of a single 10d common nail,  $\lambda \varphi Z' = 0.194$  kips. Thus, 7.92/0.194 = 41 nails are required. This corresponds to a nail spacing of about 7 in. for two 12-ft rows of blocking. Space nails at 6 in. for convenience.

Use the glued-laminated beams (at 20 ft on center) to provide continuous cross-ties, and check the subdiaphragms between the beams to provide adequate load transfer to the beams per Provisions Sec. 5.2.6.3.2 [4.6.2.1].

Design tension force on beam = (1.98 klf)(20 ft) = 39.6 kips

The stress on the beam is  $f_t = 39.600/[8.75(24)] = 189$  psi, which is small. The beam is adequate for combined moment due to gravity loading and axial tension.

At the beam splices, try one-in. bolts with steel side plates. Per the AF&PA Manual, Structural Connections Supplement:

lfZ' = (1.0)(0.65)(18.35) = 11.93 kips per bolt.

The number of bolts required = 39.6/11.93 = 3.3.

Use four bolts in a single row at midheight of the beam, with 1/4-in. by 4-in. steel side plates. The reduction (group action factor) for multiple bolts is negligible. Though not included in this example, the steel side plates should be checked for tension capacity on the gross and net sections. There are pre-engineered hinged connectors for glued-laminated beams that could provide sufficient tension capacity for the splices.

In order to transfer the wall anchorage forces into the cross-ties, the subdiaphragms between these ties must be checked per *Provisions* Sec. 5.2.6.3.2 [4.6.2.1]. The procedure is similar to that used for the side walls as described previously. The end wall condition is illustrated in Figure 10.2-13. The subdiaphragm spans between beams and utilizes a roof joist as its chord. In order to adequately engage the subdiaphragm, the wall anchorage ties must extend back to this chord. The maximum aspect ratio for subdiaphragms is  $2\frac{1}{2}$  to 1 per *Provisions* Sec. 5.2.6.3.2 [4.6.2.1]. Therefore, the minimum depth is 20/2.5 = 8 ft.

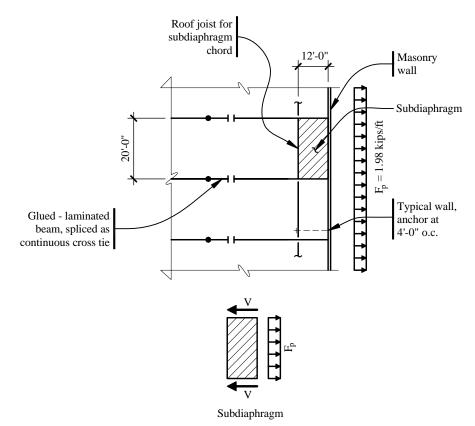


**Figure 10.2-13** Cross tie plan layout and subdiaphragm free-body diagram for end walls (1.0 ft = 0.3048 m, 1.0 kip/ft = 14.6 kN/m).

For the typical subdiaphragm (Figure 10.2-13):

OK

 $F_p = 1.98$  klf v = (1.98)(20/2)/8 = 2.48 klf

As computed previously (see Table 10.2-1 and Figure 10.2.2), the diaphragm strength in this area is 1.60 klf < 2.48 klf. Therefore, increase the subdiaphragm depth to 12 ft (six joist spaces):

v = (1.98)(20/2)/12 = 1.65 klf  $\approx 1.60$  klf

In order to develop the subdiaphragm strength, boundary nailing must be provided along the cross-tie beams. There are methods of refining this analysis using multiple subdiaphragms so that all of the tension anchors need not extend 12 ft into the building.

### 10.2.4.3.3 Transfer of Shear Wall Forces

The in-plane diaphragm shear must be transferred to the masonry wall by the ledger, parallel to the wood grain. The connection must have sufficient capacity for the diaphragm demands as:

Side walls = 0.575 klf End walls = 1.282 klf

For each case, the capacity of the bolted wood ledger and the capacity of the anchor bolts embedded into masonry must be checked. Because the wall connections provide a load path for both in-plane shear transfer and out-of-plane wall forces, the bolts must be checked for orthogonal load effects in accordance with *Provisions* Sec. 5.2.5.2.3 [4.4.2.3]. That is, the combined demand must be checked for 100 percent of the lateral load effect in one direction (e.g., shear) and 30 percent of the lateral load effect in the other direction (e.g., tension).

At the side walls, the wood ledger with 3/4-in. bolts (Figure 10.2-9) must be designed for gravity loading (0.56 kip per bolt as computed above) as well as seismic shear transfer. The seismic load per bolt (at 2 ft on center) is 0.575(2) = 1.15 kips.

Combining gravity shear and seismic shear, produces a resultant force of 1.38 kips at an angle of 26 degrees from the axis of the wood grain. Using the formulas for bolts at an angle to the grain per the AF&PA Structural Connections Supplement gives

$$lfZ' = (1.0)(0.65)(3.47) = 2.26 \text{ kips} > 1.38.$$
 OK

This bolt spacing satisfies the load combination for gravity loading only.

For the check of the embedded anchor bolts, the factored demand on a single bolt is 1.15 kips in horizontal shear (in-plane shear transfer), 2.50 kips in tension (out-of-plane wall anchorage), 0.56 kip in vertical shear (gravity). Orthogonal effects are checked, using the following two equations:

$$\frac{(0.3)(2.5)}{19.1} + \frac{\sqrt{1.15^2 + 0.56^2}}{4.8} = 0.34$$

and

$$\frac{(2.5)}{10.1} + \frac{\sqrt{[0.3(1.15)]^2 + 0.56^2}}{4.8} = 0.38 \text{ (controls)} < 1.0 \text{ OK}$$

At the end walls, the ledger with 3/4-in. bolts (Figure 10.2-12) need only be checked for in-plane seismic shear because gravity loading is negligible. For bolts spaced at 4 ft on center, the demand per bolt is 1.282(4) = 5.13 kips parallel to the grain of the wood. Per the AF&PA Structural Manual, Connections Supplement:

$$Z' = (1.0)(0.65)(5.37) = 3.49 \text{ kips} < 5.13 \text{ kips}$$
 NG

Therefore, add 3/4-in. headed bolts evenly spaced between the tension ties such that the bolt spacing is 2 ft on center and the demand per bolt is 1.282(2) = 2.56 kips. These added bolts are used for in-plane shear only and do not have coupled tension tie rods.

For the check of the embedded bolts, the factored demand on a single bolt is 2.56 kips in horizontal shear (in-plane shear transfer), 7.92 kips in tension (out-of-plane wall anchorage), 0 kip in vertical shear (gravity is negligible). Orthogonal effects are checked using the following two equations:

$$\frac{(0.3)(7.92)}{10.1} + \frac{2.56}{4.8} = 0.77$$

and

$$\frac{7.92}{10.1} + \frac{0.3(2.56)}{4.8} = 0.94 \text{ (controls)} < 1.0 \text{ OK}$$

Therefore, the wall connections satisfy the requirements for combined gravity, and seismic loading, including orthogonal effects.

11

# SEISMICALLY ISOLATED STRUCTURES Charles A. Kircher, P.E., Ph.D.

Chapter 13 of the 2000 *NEHRP Recommended Provisions* addresses the design of buildings that incorporate a seismic isolation system. The *Provisions* provides essentially a stand alone set of design and analysis criteria for an isolation system. Chapter 13 defines load, design, and testing requirements specific to the isolation system and interfaces with the appropriate materials chapters for design of the structure above the isolation system and of the foundation and structural elements below.

A discussion of background, basic concepts, and analysis methods is followed by an example that illustrates the application of the *Provisions* to the structural design of a building with an isolation system. In this example, the building is a three-story emergency operations center (EOC) with a steel concentrically braced frame above the isolation system. Although the facility is hypothetical, it is of comparable size and configuration to actual base-isolated EOCs, and is generally representative of base-isolated buildings.

The EOC is located in San Francisco and has an isolation system that utilizes elastomeric bearings, a type of bearing commonly used for seismic isolation of buildings. The example comprehensively describes the EOC's configuration, defines appropriate criteria and design parameters, and develops a preliminary design using the equivalent lateral force (ELF) procedure of Chapter 13. It also includes a check of the preliminary design using dynamic analysis as required by the *Provisions* and specifies isolation system design and testing criteria.

Located in a region of very high seismicity, the building is subject to particularly strong ground motions. Large seismic demands pose a challenge for the design of base-isolated structures in terms of the capacity of the isolation system and the configuration of the structure above the isolation system. The isolation system must accommodate large lateral displacements (e.g., in excess of 2 ft). The structure above the isolation system should be configured to produce the smallest practical overturning loads (and uplift displacements) on the isolators. The example addresses these issues and illustrates that isolation systems can be designed to meet the requirements of the *Provisions*, even in regions of very high seismicity. Designing an isolated structure in a region of lower seismicity would follow the same approach. The isolation system displacement, overturning forces, and so forth would all be reduced, and therefore, easier to accommodate using available isolation system devices.

The isolation system for the building in the example is composed of high-damping rubber (HDR) elastomeric bearings. HDR bearings are constructed with alternating layers of rubber and steel plates all sheathed in rubber. The first base-isolated building in the United States employed this type of isolation system. Other types of isolation systems used to base isolate buildings employed lead-core elastomeric bearings (LR) and sliding isolators, such as the friction pendulum system (FPS). In regions of very high seismicity, viscous dampers have been used to supplement isolation system damping (and reduce displacement demand). Using HDR bearings in this example should not be taken as an endorsement of this particular type of isolator to the exclusion of others. The concepts of the *Provisions* apply to all types

of isolations systems, and other types of isolators (and possible supplementary dampers) could have been used equally well in the example.

In addition to the 2000 *NEHRP Recommended Provisions* and *Commentary* (hereafter, the *Provisions* and *Commentary*), the following documents are either referenced directly or are useful aids for the analysis and design of seismically isolated structures.

ATC 1996	Applied Technology Council. 1996. Seismic Evaluation and Retrofit of Buildings, ATC40.
Constantinou	Constantinou, M. C., P. Tsopelas, A. Kasalanati, and E. D. Wolff. 1999. <i>Property Modification Factors for Seismic Isolation Bearings</i> , Technical Report MCEER-99-0012. State University of New York.
CSI	Computers and Structures, Inc. (CSI). 1999. ETABS Linear and Nonlinear Static and Dynamic Analysis and Design of Building Systems.
FEMA 273	Federal Emergency Management Agency. 1997. NEHRP Guidelines for the Seismic Rehabilitation of Buildings, FEMA 273.
FEMA 222A	Federal Emergency Management Agency. 1995. NEHRP Recommended Provisions for Seismic Regulations for New Buildings, FEMA 222A.
91 UBC	International Conference of Building Officials. 1991. Uniform Building Code.
94 UBC	International Conference of Building Officials. 1994. Uniform Building Code.
Kircher	Kircher, C. A., G. C. Hart, and K. M. Romstad. 1989. "Development of Design Requirements for Seismically Isolated Structures" in <i>Seismic Engineering and Practice</i> , Proceedings of the ASCE Structures Congress, American Society of Civil Engineers, May 1989.
SEAOC 1999	Seismology Committee, Structural Engineers Association of California. 1999. Recommended Lateral Force Requirements and Commentary, 7 <sup>th</sup> Ed.
SEAOC 1990	Seismology Committee, Structural Engineers Association of California. 1990. Recommended Lateral Force Requirements and Commentary, 5th Ed.
SEAONC Isolation	Structural Engineers Association of Northern California. 1986. <i>Tentative Seismic Isolation Design Requirements</i> .

Although the guide is based on the 2000 *Provisions*, it has been annotated to reflect changes made to the 2003 *Provisions*. Annotations within brackets, [], indicate both organizational changes (as a result of a reformat of all of the chapters of the 2003 *Provisions*) and substantiative technical changes to the 2003 *Provisions* and its primary reference documents. While the general changes to the document are described, the deign examples and calculations have not been revised to reflect the changes to the 2003 *Provisions*.

In the 2003 edition of the *Provisions*, Chapter 13 has been restructured so that it is better integrated into the *Provisions* as a whole and is less of a stand alone set of requirements. Where they affect the design examples in this chapter, other significant changes to the 2003 *Provisions* and primary reference documents may be noted.

# 11.1 BACKGROUND AND BASIC CONCEPTS

Seismic isolation, commonly referred to as base isolation, is a design concept that presumes a structure can be substantially decoupled from potentially damaging earthquake ground motions. By decoupling the structure from ground shaking, isolation reduces the level of response in the structure that would otherwise occur in a conventional, fixed-base building. Conversely, base-isolated buildings may be designed with a reduced level of earthquake load to produce the same degree of seismic protection. That decoupling is achieved when the isolation scheme makes the fundamental period of the isolated structure several times greater than the period of the structure above the isolation system.

The potential advantages of seismic isolation and the advancements in isolation system products led to the design and construction of a number of isolated buildings and bridges in the early 1980s. This activity, in turn, identified a need to supplement existing seismic codes with design requirements developed specifically for such structures. These requirements assure the public that isolated buildings are safe and provide engineers with a basis for preparing designs and building officials with minimum standards for regulating construction.

Initial efforts developing design requirements for base-isolated buildings began with ad hoc groups of the Structural Engineers Association of California (SEAOC), whose Seismology Committee has a long history of contributing to codes. The northern section of SEAOC was the first to develop guidelines for the use of elastomeric bearings in hospitals. These guidelines were adopted in the late 1980s by the California Office of Statewide Health Planning and Development (OSHPD) and were used to regulate the first base-isolated hospital in California. At about the same time, the northern section of SEAOC published SEAONC Isolation, first set of general requirements to govern the design of base-isolated buildings. Most of the basic concepts for the design of seismically isolated structures found in the *Provisions* can be traced back to the initial work by the northern section of SEAOC.

By the end of the 1980s, the Seismology Committee of SEAOC recognized the need to have a more broadly based document and formed a statewide committee to develop design requirements for isolated structures Kircher. The "isolation" recommendations became an appendix to the 1990 SEAOC Blue Book. The isolation appendix was adopted with minor changes as a new appendix in the 1991 Uniform Building Code and has been updated every three years, although it remains largely the same as the original 91 UBC appendix. (SEAOC 1990 and 1999 are editions of SEAOC's *Recommended Lateral Force Requirements and Commentary*, which is also known as the *Blue Book*.)

In the mid-1990s, the Provisions Update Committee of the Building Seismic Safety Council incorporated the isolation appendix of the 94 UBC into the 1994 *Provisions* (FEMA 222A). Differences between the *Uniform Building Code* (UBC) and the *Provisions* were intentionally minimized and subsequent editions of the *UBC* and the *Provisions* are nearly identical. Additional background may be found in the commentary to the 1999 SEAOC *Blue Book*.

The *Provisions* for designing the isolation system of a new building were used as the starting point for the isolation system requirements of the *NEHRP Guidelines for Seismic Rehabilitation of Buildings* (FEMA 273). FEMA 273 follows the philosophy that the isolation system for a rehabilitated building should be comparable to that for a new building (for comparable ground shaking criteria, etc.). The superstructure, however, could be quite different, and FEMA 273 provides more suitable design requirements for rehabilitating existing buildings using an isolation system.

# **11.1.1 Types of Isolation Systems**

The *Provisions* requirements are intentionally broad, accommodating all types of acceptable isolation systems. To be acceptable, the *Provisions* requires the isolation system to:

- 1. Remain stable for maximum earthquake displacements,
- 2. Provide increasing resistance with increasing displacement,
- 3. Have limited degradation under repeated cycles of earthquake load, and
- 4. Have well-established and repeatable engineering properties (effective stiffness and damping).

The *Provisions* recognizes that the engineering properties of an isolation system, such as effective stiffness and damping, can change during repeated cycles of earthquake response (or otherwise have a range of values). Such changes or variability of design parameters are acceptable provided that the design is based on analyses that conservatively bound (limit) the range of possible values of design parameters.

The first seismic isolation systems used in buildings in the United States were composed of elastomeric bearings that had either a high-damping rubber compound or a lead core to provide damping to isolated modes of vibration. Other types of isolation systems now include sliding systems, such as the friction pendulum system (FPS), or some combination of elastomeric and sliding isolators. Some applications at sites with very strong ground shaking use supplementary fluid-viscous dampers in parallel with either sliding or elastomeric isolators to control displacement. While generally applicable to all types of systems, certain requirements of the *Provisions* (in particular, prototype testing criteria) were developed primarily for isolation systems with elastomeric bearings.

Isolation systems typically provide only horizontal isolation and are rigid or semi-rigid in the vertical direction. A rare exception to this rule is the full isolation (horizontal and vertical) of a building in southern California isolated by large helical coil springs and viscous dampers. While the basic concepts of the *Provisions* can be extended to full isolation systems, the requirements are only for horizontal isolation systems. The design of a full isolation system requires special analyses that explicitly include vertical ground shaking and the potential for rocking response.

Seismic isolation is commonly referred to as base isolation because the most common location of the isolation system is at or near the base of the structure. The *Provisions* does not restrict the plane of isolation to the base of the structure but does require the foundation and other structural elements below the isolation system to be designed for unreduced ( $R_I = 1.0$ ) earthquake forces.

## 11.1.2 Definition of Elements of an Isolated Structure

The design requirements of the *Provisions* distinguish between structural elements that are either components of the isolation system or part of the structure below the isolation system (e.g., foundation) and elements of the structure above the isolation system. The isolation system is defined by the *Provisions* as:

The collection of structural elements that includes all individual isolator units, all structural elements that transfer force between elements of the isolation system, and all connections to other structural elements. The isolation system also includes the wind-restraint system, energy-dissipation devices, and/or the displacement restraint system if such systems and devices are used to meet the design requirements of Chapter 13.

Figure 11.1-1 illustrates this definition and shows that the isolation system consists not only of the isolator units but also of the entire collection of structural elements required for the system to function properly. The isolation system typically includes segments of columns and connecting girders just above the isolator units because such elements resist moments (due to isolation system displacement) and their yielding or failure could adversely affect the stability of isolator units.

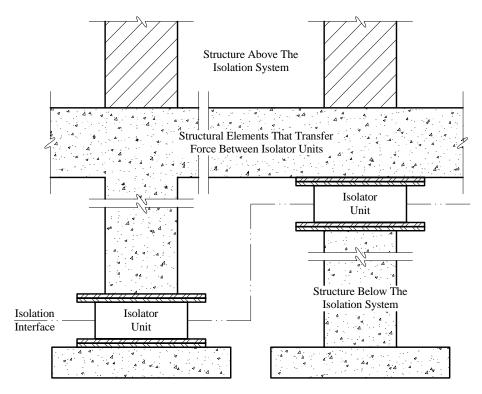


Figure 11.1-1 Isolation system terminology.

The isolation interface is an imaginary boundary between the upper portion of the structure, which is isolated, and the lower portion of the structure, which is assumed to move rigidly with the ground. Typically, the isolation interface is a horizontal plane, but it may be staggered in elevation in certain applications. The isolation interface is important for design of nonstructural components, including components of electrical and mechanical systems that cross the interface and must accommodate large relative displacements.

The wind-restraint system is typically an integral part of isolator units. Elastomeric isolator units are very stiff at very low strains and usually satisfy drift criteria for wind loads, and the static (breakaway) friction force of sliding isolator units is usually greater than the wind force.

# 11.1.3 Design Approach

The design of isolated structures using the *Provisions* (like the *UBC* and SEAOC's *Blue Book*) has two objectives: achieving life safety in a major earthquake and limiting damage due to ground shaking. To meet the first performance objective, the isolation system must be stable and capable of sustaining forces and displacements associated with the maximum considered earthquake and the structure above the isolation system must remain essentially elastic when subjected to the design earthquake. Limited ductility demand is considered necessary for proper functioning of the isolation system. If significant inelastic response was permitted in the structure above the isolation system, unacceptably large drifts could result due to the nature of long-period vibration. Limiting ductility demand on the superstructure has the additional benefit of meeting the second performance objective of damage control.

The Provisions addresses the performance objectives by requiring:

- 1. Design of the superstructure for forces associated with the design earthquake, reduced by only a fraction of the factor permitted for design of conventional, fixed-base buildings (i.e.,  $R_I = 3/8 R \le 2.0$ ).
- 2. Design of the isolation system and elements of the structure below the isolation system (e.g., foundation) for unreduced design earthquake forces.
- 3. Design and prototype testing of isolator units for forces (including effects of overturning) and displacements associated with the maximum considered earthquake.
- 4. Provision of sufficient separation between the isolated structure and surrounding retaining walls and other fixed obstructions to allow unrestricted movement during the maximum considered earthquake.

## 11.1.4 Effective Stiffness and Effective Damping

The *Provisions* utilizes the concepts of effective stiffness and damping to define key parameters of inherently nonlinear, inelastic isolation systems in terms of amplitude-dependent linear properties. Effective stiffness is the secant stiffness of the isolation system at the amplitude of interest. Effective damping is the amount of equivalent viscous damping described by the hysteresis loop at the amplitude of interest. Figure 11.1-2 shows the application of these concepts to both hysteretic isolator units (e.g., friction or yielding devices) and viscous isolator units and shows the *Provisions* equations used to determine effective stiffness and damping from tests of prototypes. Ideally, the effective damping of velocity-dependent devices (including viscous isolator units) should be based on the area of hysteresis loops measured during cyclic testing of the isolation system at full-scale earthquake velocities. Tests of prototypes are usually performed at lower velocities (due to test facility limitations), resulting in hysteresis loops with less area, which produce lower (conservative) estimates of effective damping.

## **11.2 CRITERIA SELECTION**

As specified in the *Provisions* the design of isolated structures must be based on the results of the equivalent lateral force (ELF) procedure, response spectrum analysis, or (nonlinear) time history analysis. Because isolation systems are typically nonlinear, linear methods (ELF procedure and response spectrum analysis) use effective stiffness and damping properties to model nonlinear isolation system components.

The ELF procedure is intended primarily to prescribe minimum design criteria and may be used for design of a very limited class of isolated structures (without confirmatory dynamic analyses). The simple equations of the ELF procedure are useful tools for preliminary design and provide a means of expeditious review and checking of more complex calculations. The *Provisions* also uses these equations to establish lower-bound limits on results of dynamic analysis that may be used for design. Table 11.2-1 summarizes site conditions and structure configuration criteria that influence the selection of an acceptable method of analysis for designing of isolated structures. Where none of the conditions in Table 11.2-1 applies, all three methods are permitted.

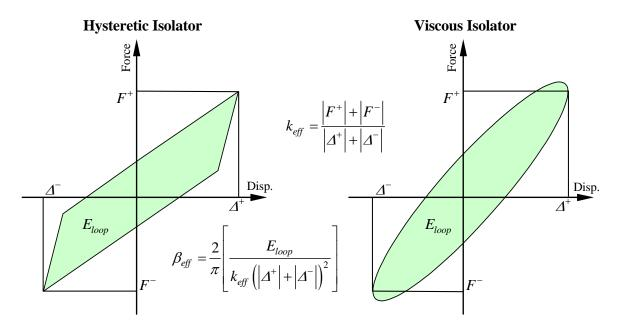


Figure 11.1-2 Effective stiffness and effective damping.

Site condition or Structure Configuration Criteria	ELF Procedure	Response Spectrum Analysis	Time History Analysis
Site C	onditions		
Near-source ( $S_1 > 0.6$ )	NP	Р	Р
Soft soil (Site Class E or F)	NP	NP	Р
Superstructu	re Configuratior	1	
Flexible or irregular superstructure (height > 4 stories, height > 65 ft, or $T_M > 3.0$ sec., or $T_D \le 3T$ )	NP	Р	Р
Nonlinear superstructure (requiring explicit modeling of nonlinear elements; <i>Provisions</i> Sec. 13.2.5.3.1) [13.4.1.2]	NP	NP	Р
Isolation System Configuration			
Highly nonlinear isolation system or system that otherwise does not meet the criteria of <i>Provisions</i> Sec. 13.2.5.2, Item 7 [13.2.4.1, Item 7]	NP	NP	Р

Table 11.2-1	Acceptable Methods of Analysis*

\* P indicates permitted and NP indicates not permitted by the Provisions.

Seismic criteria are based on the same site and seismic coefficients as conventional, fixed-base structures (e.g., mapped value of  $S_1$  as defined in *Provisions* Chapter 4 [3]). Additionally, site-specific design criteria are required for isolated structures located on soft soil (Site Class E of F) or near an active source such that  $S_1$  is greater than 0.6, or when nonlinear time history analysis is used for design.

## **11.3 EQUIVALENT LATERAL FORCE PROCEDURE**

The equivalent lateral force (ELF) procedure is a displacement-based method that uses simple equations to determine isolated structure response. The equations are based on ground shaking defined by 1 second spectral acceleration and the assumption that the shape of the design response spectrum at long periods is inversely proportional to period as shown in *Provisions* Figure 4.1.2.6 [3.3-15]. [In the 2003 edition of the *Provisions*, there is also a  $1/T^2$  portion of the spectrum at periods greater than  $T_L$ . However, in most parts of the Unites States  $T_L$  is longer than the period of typical isolated structures.] Although the ELF procedure is considered a linear method of analysis, the equations incorporate amplitude-dependent values of effective stiffness and damping to implicitly account for the nonlinear properties of the isolation system. The equations are consistent with the nonlinear static procedure of FEMA 273 assuming the superstructure is rigid and lateral displacements to occur primarily in the isolation system.

### 11.3.1 Isolation System Displacement

The isolation system displacement for the design earthquake is determined by using *Provisions* Eq. 13.3.3.1 [13.3-1]:

$$D_D = \left(\frac{g}{4\pi^2}\right) \frac{S_{DI}T_D}{B_D}$$

where the damping factor  $B_D$ , is based on effective damping,  $\beta_D$ , using *Provisions* Table 13.3.3.1 [13.3-1]. This equation describes the peak (spectral) displacement of a single-degree-of-freedom (SDOF) system with period,  $T_D$ , and damping,  $\beta_D$ , for the design earthquake spectrum defined by the seismic coefficient,  $S_{D1}$ .  $S_{D1}$  corresponds to 5 percent damped spectral response at a period of 1 second.  $B_D$ , converts 5 percent damped response to the level of damping of the isolation system.  $B_D$  is 1.0 when effective damping,  $\beta_D$ , is 5 percent of critical. Figure 11.3-1 illustrates the underlying concepts of *Provisions* Eq. 13.3.3.1 [13.3-1] and the amplitude-dependent equations of the *Provisions* for effective period,  $T_D$ , and effective damping,  $\beta_D$ .

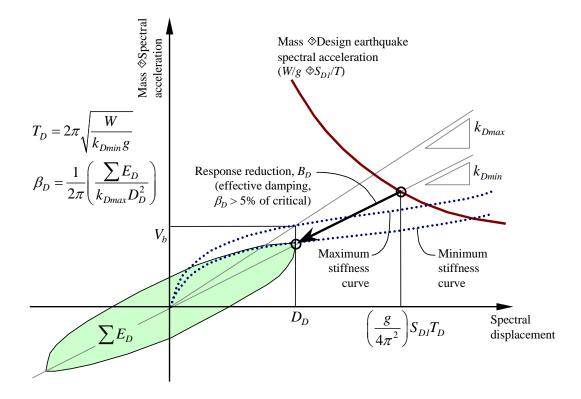


Figure 11.3-1 Isolation system capacity and earthquake demand.

The equations for maximum displacement,  $D_M$ , and design displacement,  $D_D$ , reflect differences due to the corresponding levels of ground shaking. The maximum displacement is associated with the maximum considered earthquake (characterized by  $S_{MI}$ ) whereas the design displacement corresponds to the design earthquake (characterized by  $S_{DI}$ ). In general, the effective period and the damping factor ( $T_M$  and  $B_M$ , respectively) used to calculate the maximum displacement are different from those used to calculate the design displacement ( $T_D$  and  $B_D$ ) because the effective period tends to shift and effective damping may change with the increase in the level of ground shaking.

As shown in Figure 11.3-1, the calculation of effective period,  $T_D$ , is based on the minimum effective stiffness of the isolation system,  $k_{Dmin}$ , as determined by prototype testing of individual isolator units. Similarly, the calculation of effective damping is based on the minimum loop area,  $E_D$ , as determined by prototype testing. Use of minimum effective stiffness and damping produces larger estimates of effective period and peak displacement of the isolation system.

The design displacement,  $D_D$ , and maximum displacement,  $D_M$ , represent peak earthquake displacements at the center of mass of the building without the additional displacement, that can occur at other locations due to actual or accidental mass eccentricity. Equations for determining total displacement, including the effects of mass eccentricity as an increase in the displacement at the center of mass, are based on the plan dimensions of the building and the underlying assumption that building mass and isolation stiffness have a similar distribution in plan. The increase in displacement at corners for 5 percent mass eccentricity is about 15 percent if the building is square in plan, and as much as 30 percent if the building is long in plan. Figure 11.3-2 illustrates design displacement,  $D_D$ , and maximum displacement,  $D_M$ , at the center of mass of the building and total maximum displacement,  $D_{TM}$ , at the corners of an isolated building.

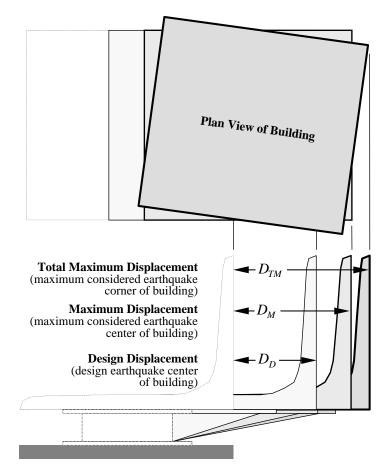


Figure 11.3-2 Design, maximum, and total maximum displacement.

# 11.3.2 Design Forces

Forces required by the *Provisions* for design of isolated structures are different for design of the superstructure and design of the isolation system and other elements of the structure below the isolation system (e.g., foundation). In both cases, however, use of the maximum effective stiffness of the isolation system is required to determine a conservative value of design force.

In order to provide appropriate overstrength, peak design earthquake response (without reduction) is used directly for design of the isolation system and the structure below. Design for unreduced design earthquake forces is considered sufficient to avoid inelastic response or failure of connections and other elements for ground shaking as strong as that associated with the maximum considered earthquake (i.e., shaking as much as 1.5 times that of the design earthquake). The design earthquake base shear,  $V_b$ , is given by *Provisions* Eq. 13.3.4.1 [13.3-7]:

$$V_b = k_{Dmax} D_{D_a}$$

where  $k_{Dmax}$  is the maximum effective stiffness of the isolation system at the design displacement,  $D_D$ . Because the design displacement is conservatively based on minimum effective stiffness, *Provisions* Eq. 13.3.4.1 implicitly induces an additional conservatism of a worst case combination mixing maximum and minimum effective stiffness in the same equation. Rigorous modeling of the isolation system for dynamic analyses precludes mixing of maximum and minimum stiffness in the same analysis (although separate analyses are typically required to determine bounding values of both displacement and force).

Design earthquake response is reduced by a modest factor for design of the superstructure above the isolation interface, as given by *Provisions* Eq. 13.3.4.2 [13.3-8]:

$$V_s = \frac{V_b}{R_I} = \frac{k_{Dmax}D_D}{R_I}$$

The reduction factor,  $R_I$ , is defined as three-eighths of the *R* factor for the seismic-force-resisting system of the superstructure, as specified in *Provisions* Table 5.2.2 [4.3-1], with an upper-bound value of 2.0. A relatively small  $R_I$  factor is intended to keep the superstructure essentially elastic for the design earthquake (i.e., keep earthquake forces at or below the true strength of the seismic-force-resisting system). The *Provisions* also impose three limits on design forces that require the value of  $V_s$  to be at least as large as each of:

- 1. The shear force required for design of a conventional, fixed-base structure of period  $T_D$ .
- 2. The shear force required for wind design, and/or
- 3. A factor of 1.5 times the shear force required for activation of the isolation system.

These limits seldom govern design but reflect principles of good design. In particular, the third limit is included in the *Provisions* to ensure that isolation system displaces significantly before lateral forces reach the strength of the seismic-force-resisting system.

For designs using the ELF procedure, the lateral forces,  $F_{x}$ , must be distributed to each story over the height of the structure, assuming an inverted triangular pattern of lateral load (*Provisions* Eq.13.3.5 [13.3-9]):

$$F_x = \frac{V_s w_x h_x}{\sum\limits_{i=1}^n w_i h_i}$$

Because the lateral displacement of the isolated structure is dominated by isolation system displacement, the actual pattern of lateral force in the isolated mode of response is distributed almost uniformly over height. The *Provisions* require an inverted triangular pattern of lateral load to capture possible higher-mode effects that might be missed by not modeling superstructure flexibility. Rigorous modeling of superstructure flexibility for dynamic analysis would directly incorporate higher-mode effects in the results.

Example plots of the design displacement,  $D_D$ , total maximum displacement,  $D_{TM}$ , and design forces for the isolation system,  $V_b$ , and the superstructure,  $V_s$  ( $R_I = 2$ ), are shown in Figure 11.3-3 as functions of the effective period of the isolation system. The figure also shows the design base shear required for a conventional building, V(R/I = 5). The example plots are for a building assigned to Seismic Design Category D with a one-second spectral acceleration parameter,  $S_{DI}$ , equal to 0.6, representing a stiff soil site (Site Class D) located in a region of high seismicity but not close to an active fault. In this example, the isolation system is assumed to have 20 percent effective damping (at all amplitudes of interest) and building geometry is assumed to require 25 percent additional displacement (at corners/edges) due to the requisite 5 percent accidental eccentricity.

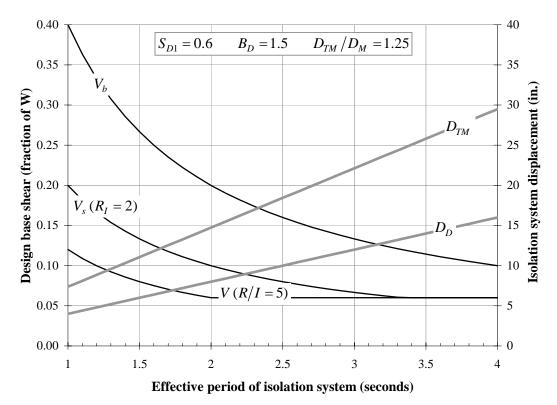


Figure 11.3-3 Isolation system displacement and shear force as function of period (1.0 in. = 25.4 mm).

The plots in Figure 11.3-3 illustrate the fundamental trade off between displacement and force as a function of isolation system displacement. As the period is increased, design forces decrease and design displacements increase linearly. Plots like those shown in Figure 11.3-3 can be constructed during conceptual design once site seismicity and soil conditions are known (or are assumed) to investigate trial values of effective stiffness and damping of the isolation system. In this particular example, an isolation system with an effective period falling between 2.5 and 3.0 seconds would not require more than 22 in. of total maximum displacement capacity (assuming  $T_M \leq 3.0$  seconds). Design force on the superstructure would be less than about eight percent of the building weight (assuming  $T_D \geq 2.5$  seconds and  $R_I \geq 2.0$ ).

## 11.4 DYNAMIC LATERAL RESPONSE PROCEDURE

While the ELF procedure equations are useful tools for preliminary design of the isolations system, the *Provisions* requires a dynamic analysis for most isolated structures. Even where not strictly required by the *Provisions*, the use of dynamic analysis (usually time history analysis) to verify the design is common.

## 11.4.1 Minimum Design Criteria

The *Provisions* encourages the use of dynamic analysis but recognize that along with the benefits of more complex models and analyses also comes an increased chance of design error. To avoid possible under design, the *Provisions* establishes lower-bound limits on results of dynamic analysis used for design. The limits distinguish between response spectrum analysis (a linear, dynamic method) and time history analysis (a nonlinear, dynamic method). In all cases, the lower-bound limit on dynamic analysis is established as a percentage of the corresponding design parameter calculated using the ELF procedure equations. Table 11.4-1 summarizes the percentages that define lower-bound limits on dynamic analysis.

5	0	5
Design Parameter	Response Spectrum Analysis	Time History Analysis
Total design displacement, $D_{TD}$	90% D <sub>TD</sub>	90% D <sub>TD</sub>
Total maximum displacement, $D_{TM}$	$80\% D_{TM}$	$80\% D_{\rm TM}$
Design force on isolation system, $V_b$	90% V <sub>b</sub>	90% V <sub>b</sub>
Design force on irregular superstructure, $V_s$	$100\% V_s$	80% V <sub>s</sub>
Design force on regular superstructure, $V_s$	80% V <sub>s</sub>	60% V <sub>s</sub>

 Table 11.4-1
 Summary of Minimum Design Criteria for Dynamic Analysis

The *Provisions* permits more liberal drift limits when the design of the superstructure is based on dynamic analysis. The ELF procedure drift limits of  $0.010h_{sx}$  are increased to  $0.015h_{sx}$  for response spectrum analysis and to  $0.020h_{sx}$  for time history analysis (where  $h_{sx}$  is the story height at level *x*). Usually a stiff system (e.g., braced frames) is selected for the superstructure and drift demand is typically less than about  $0.005h_{sx}$ . *Provisions* Sec. 13.4.7.4 [13.4.4] requires an explicit check of superstructure stability at the maximum considered earthquake displacement if the design earthquake story drift ratio exceeds  $0.010/R_I$ .

## **11.4.2 Modeling Requirements**

As for the ELF procedure, the *Provisions* requires the isolation system to be modeled for dynamic analysis using stiffness and damping properties that are based on tests of prototype isolator units. Additionally, dynamic analysis models are required to account for:

- 1. Spatial distribution of individual isolator units,
- 2. Effects of actual and accidental mass eccentricity,
- 3. Overturning forces and uplift of individual isolator units, and
- 4. Variability of isolation system properties (due to rate of loading, etc.).

The *Provisions* requires explicit nonlinear modeling of elements if time history analysis is used to justify design loads less than those permitted for ELF or response spectrum analysis. This option is seldom exercised and the superstructure is typically modeled using linear elements and conventional methods. Special modeling concerns for isolated structures include two important and related issues: the uplift of isolator units, and the P-delta effects on the isolated structure. Isolator units tend to have little or no ability to resist tension forces and can uplift when earthquake overturning (upward) loads exceed factored gravity (downward) loads. Local uplift of individual elements is permitted (*Provisions* Sec. 13.6.2.7 [13.2.5.7]) provided the resulting deflections do not cause overstress or instability. To calculate uplift effects, gap elements may be used in nonlinear models or tension may be released manually in linear models.

The effects of P-delta loads on the isolation system and adjacent elements of the structure can be quite significant. The compression load, *P*, can be large due to earthquake overturning (and factored gravity loads) at the same time that large displacements occur in the isolation system. Computer analysis programs (most of which are based on small-deflection theory) may not correctly calculate P-delta moments at the isolator level in the structure above or in the foundation below. Figure 11.4-1 illustrates moments due to P-delta effects (and horizontal shear loads) for an elastomeric bearing isolation system and a sliding isolation system. For the elastomeric system, the P-delta moment is split one-half up and one-half down. For the sliding system, the full P-delta moment is applied to the foundation below (due to the orientation of the sliding surface). A reverse (upside down) orientation would apply the full P-delta moment on the structure above.

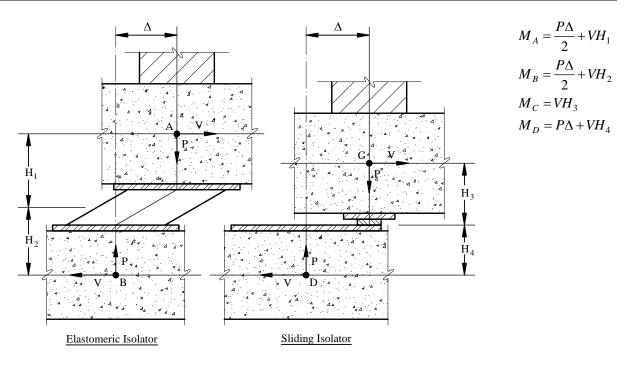


Figure 11.4-1 Moments due to horizontal shear and P-delta effects.

For time history analysis, nonlinear force-deflection characteristics of isolator units are explicitly modeled (rather than using effective stiffness and damping). Force-deflection properties of isolator units are typically approximated by a bilinear, hysteretic curve whose properties can be accommodated by commercially available nonlinear structural analysis programs. Such bilinear hysteretic curves should have approximately the same effective stiffness and damping at amplitudes of interest as the true force-deflection characteristics of isolator units (as determined by prototype testing).

Figure 11.4-2 shows a bilinear idealization of the response of a typical nonlinear isolator unit. Figure 11.4-2 also includes simple equations defining the yield point  $(D_y, F_y)$  and end point (D, F) of a bilinear approximation that has the same effective stiffness and damping as the true curve (at a displacement, D).

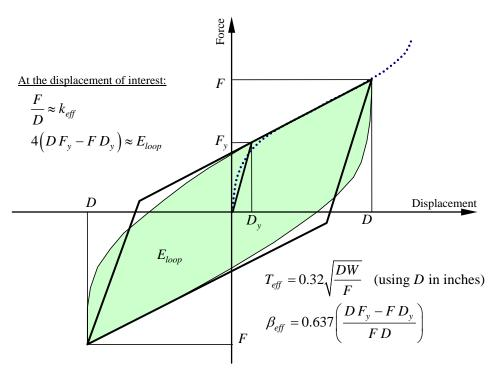


Figure 11.4-2 Bilinear idealization of isolator unit behavior.

# 11.4.3 Response Spectrum Analysis

Response spectrum analysis requires that isolator units be modeled using amplitude-dependent values of effective stiffness and damping that are the same as those for the ELF procedure. The effective damping of the isolated modes of response is limited to 30 percent of critical. Higher modes of response are usually assumed to have five percent damping—a value of damping appropriate for the superstructure, which remains essentially elastic. As previously noted, maximum and minimum values of effective stiffness are typically used to individually capture maximum displacement of the isolation system and maximum forces in the superstructure. Horizontal loads are applied in the two orthogonal directions, and peak response of the isolation system and other structural elements is determined using the 100 percent plus 30 percent combination method.

# 11.4.4 Time History Analysis

Time history analysis with explicit modeling of nonlinear isolator units is commonly used for the evaluation of isolated structures. Where at least seven pairs of time history components are employed, the values used in design for each response parameter of interest may be the average of the corresponding analysis maxima. Where fewer pairs are used (with three pairs of time history components being the minimum number permitted), the maximum value of each parameter of interest must be used for design.

The time history method is not a particularly useful design tool due to the complexity of results, the number of analyses required (e.g., to account for different locations of eccentric mass), the need to combine different types of response at each point in time, etc. It should be noted that while *Provisions* Chapter 5 does not require consideration of accidental torsion for either the linear or nonlinear response history procedures, Chapter 13 does require explicit consideration of accidental torsion, regardless of the analysis method employed. Time history analysis is most useful when used to verify a design by

checking a few key design parameters, such as: isolation displacement, overturning loads and uplift, and story shear force.

# 11.5 EMERGENCY OPERATIONS CENTER USING ELASTOMERIC BEARINGS, SAN FRANCISCO, CALIFORNIA

This example features the seismic isolation of a hypothetical emergency operations center (EOC), located in the center of San Francisco, California, an area of very high seismicity. Using high-damping rubber bearings, other types of isolators could be designed to have comparable response properties. Isolation is an appropriate design strategy for EOCs and other buildings where the goal is to limit earthquake damage and protect facility function. The example illustrates the following design topics:

- 1. Determination of seismic design parameters,
- 2. Preliminary design of superstructure and isolation systems (using the ELF procedure),
- 3. Dynamic analysis of seismically isolated structures, and
- 4. Specification of isolation system design and testing criteria.

While the example includes development of the entire structural system, the primary focus is on the design and analysis of the isolation system. Examples in other chapters may be referred to for more in-depth descriptions of the provisions governing detailed design of the superstructure (i.e., the structure above the isolation system) and the foundation.

# 11.5.1 System Description

This EOC is a three-story, steel-braced frame structure with a large, centrally located mechanical penthouse. Story heights of 15 ft at all floors accommodate computer access floors and other architectural and mechanical systems. The roof and penthouse roof decks are designed for significant live load to accommodate a helicopter-landing pad and meet other functional requirements of the EOC. Figure 11.5-1 shows the three-dimensional model of the structural system.

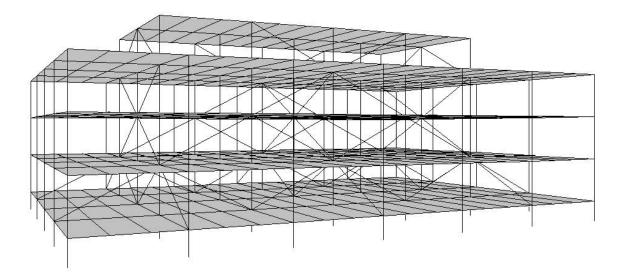
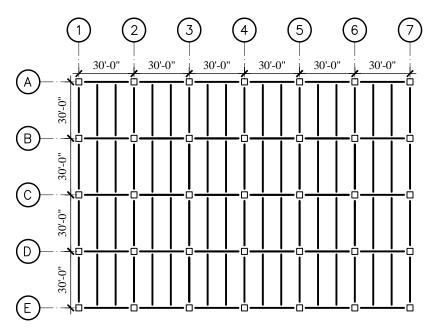
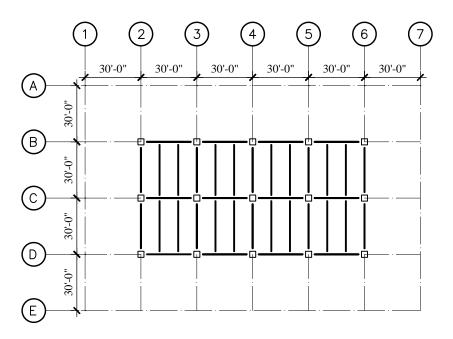


Figure 11.5-1 Three-dimensional model of the structural system.

The structure (which is regular in configuration) has plan dimensions of 120 ft. by 180 ft. at all floors except for the penthouse, which is approximately 60 ft by 120 ft in plan. Columns are spaced at 30 ft in both directions. This EOC's relatively large column spacing (bay size) is used to reduce the number of isolator units for design economy and to increase gravity loads on isolator units for improved earthquake performance. Figures 11.5-2 and 11.5-3, are framing plans for the typical floor levels (1, 2, 3, and roof) and the penthouse roof.



**Figure 11.5-2** Typical floor framing plan (1.0 ft = 0.3048 m).



**Figure 11.5-3** Penthouse roof framing plan (1.0 ft = 0.3048 m).

The vertical load carrying system consists of concrete fill on steel deck floors, roofs supported by steel beams at 10 ft on center, and steel girders at column lines. Isolator units support the columns below the first floor. The foundation is a heavy mat (although the spread footings or piles could be used depending on the soil type, depth to the water table, and other site conditions).

The lateral system consists of a symmetrical pattern of concentrically braced frames. These frames are located on Column Lines B and D in the longitudinal direction, and on Column Lines 2, 4 and 6 in the transverse direction. Figures 11.5-4 and 11.5-5, respectively, show the longitudinal and transverse elevations. Braces are specifically configured to reduce the concentration of earthquake overturning, and uplift loads on isolator units by:

- 1. Increasing the continuous length of (number of) braced bays at lower stories,
- 2. Locating braces at interior (rather than perimeter) column lines (more hold-down weight), and
- 3. Avoiding common end columns for transverse and longitudinal bays with braces.

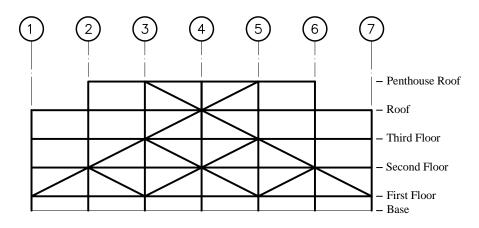


Figure 11.5-4 Longitudinal bracing elevation (Column Lines B and D).

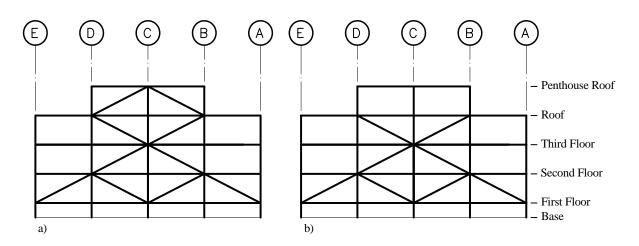


Figure 11.5-5 Transverse bracing elevations: (a) on Column Lines 2 and 6 and (b) on Column Line 4.

The isolation system is composed of 35 identical elastomeric isolator units, located below columns. The first floor is just above grade, and the isolator units are approximately 3 ft below grade to provide

clearance below the first floor, for construction and maintenance personnel. A short retaining wall borders the perimeter of the facility and provides 30 in. of "moat" clearance for lateral displacement of the isolated structure. Access to the EOC is provided at the entrances by segments of the first floor slab, which cantilever over the moat.

Girders at the first-floor column lines are much heavier than the girders at other floor levels, and have moment-resisting connections to columns. These girders stabilize the isolator units by resisting moments due to vertical (P-delta effect) and horizontal (shear) loads. Column extensions from the first floor to the top plates of the isolator units are stiffened in both horizontal directions, to resist these moments and to serve as stabilizing haunches for the beam-column moment connections.

# **11.5.2 Basic Requirements**

# 11.5.2.1 Specifications

General: 1997 Uniform Building Code (UBC)

Seismic: NEHRP Recommended Provisions

# 11.5.2.2 Materials

Concrete:

Strength	$f_c' = 3$ ksi
Weight (normal)	$\gamma = 150 \text{ pcf}$

Steel:

$F_y = 50$ ksi
$F_{y} = 50 \text{ ksi}$
$F_y = 36 \text{ ksi}$
$F_y = 46 \text{ ksi}$

Steel deck:

Seismic isolator units (high-damping rubber):

Maximum long-term-load $(1.2D + 1.6L)$ face pressure, $\sigma_{LT}$	1,400 psi
Maximum short-term-load $(1.5D + 1.0L + Q_{MCE})$ face pressure, $\sigma_{sT}$	2,800 psi
Minimum bearing diameter (excluding protective cover)	$1.25D_{TM}$
Minimum rubber shear strain capacity (isolator unit), $\gamma_{max}$	300 percent
Minimum effective horizontal shear modulus, $G_{min}$	65 - 110 psi
Third cycle at $\gamma = 150$ percent (after scragging/recovery)	
Maximum effective horizontal shear modulus, $G_{max}$	$1.3 \times G_{min}$
First cycle at $\gamma = 150$ percent (after scragging/recovery)	
Minimum effective damping at 150 percent rubber shear strain, $\beta_{eff}$	15 percent

# 11.5.2.3 Gravity Loads

Dead loads:

Main structural elements (slab, deck, and framing)

self weight

3-in.-deep, 20-gauge deck

Miscellaneous structural elements (and slab allowance) Architectural facades (all exterior walls) Roof parapets Partitions (all enclosed areas) Suspended MEP/ceiling systems and supported flooring Mechanical equipment (penthouse floor) Roofing Reducible live loads:	10 psf 750 plf 150 plf 20 psf 15 psf 50 psf 10 psf
Floors (1-3)	100 psf
Roof decks and penthouse floor	50 psf

#### Live load reduction:

The 1997 *UBC* permits area-based live load reduction, of not more than 40 percent for elements with live loads from a single story (e.g., girders), and not more than 60 percent for elements with live loads from multiple stories (e.g., axial component of live load on columns at lower levels and isolator units).

EOC weight (dead load) and live load:

Penthouse roof	$W_{PR}$	= 965 kips
Roof (penthouse)	$W_R$	= 3,500 kips
Third floor	$W_3$	= 3,400 kips
Second floor	$W_2$	= 3,425 kips
First floor	$\underline{W}_{I}$	<u>= 3,425 kips</u>
Total EOC weight	W	= 14,715 kips

(See Chapter 1 for a discussion of live load contributions to the seismic weight.)

Live load (L) above isolation system	L	=	7,954 kips
Reduced live load (RL) above isolation system	RL	=	3,977 kips

	Dead/live loads (kips)			
Column line	1	2	3	4
А	182/73	349/175	303/153	345/173
В	336/166	570/329	606/346	539/309
С	295/149	520/307	621/356	639/358

Table 11.5-1 Gravity Loads on Isolator Un	its
---	-----

1.0 kip = 4.45 kN.

\* Loads at Column Lines 5, 6 and 7 (not shown) are the same as those at Column Lines 3, 2, and 1, respectively; loads at Column Lines D and E (not shown) are the same as those at Column Lines B and A, respectively.

# **11.5.2.4** *Provisions* Parameters

11.5.2.4.1 Performance Criteria (Provisions Sec. 1.3 [1.2 and 1.3])	
Designated Emergency Operation Center	Seismic Use Group III
Occupancy Importance Factor	I = 1.5 (conventional)
Occupancy Importance Factor ( <i>Provisions</i> Chapter 13)	I = 1.0 (isolated)

Chapter 13 does not require use of the occupancy importance factor to determine the design loads on the structural system of an isolated building (that is, I = 1.0), but the component importance factor is required by Chapter 6, to determine seismic forces on components ( $I_p = 1.5$  for some facilities).

11.5.2.4.2 Ground Motion (Provisions Chapter 4 [3])

Site soil type (assumed)	Site Class D
Maximum considered earthquake (MCE) spectral acceleration at short periods ( <i>Provisions</i> Map 7)	$S_{s} = 1.50$

[The 2003 Provisions have adopted the 2002 USGS probabilistic seismic hazard maps, and the maps have been added to the body of the 2003 Provisions as figures in Chapter 3 (instead of the previously used separate map package.]

Site coefficient ( <i>Provisions</i> Table 4.1.2.4b [3.3-1])	$F_{a} = 1.0$
MCE spectral acceleration adjusted for site class $(F_a S_S)$	$S_{MS} = 1.50$
Design earthquake (DE) spectral acceleration $(2/3S_{MS})$	$S_{DS} = 1.0$
MCE spectral acceleration at a period of 1 second ( <i>Provisions</i> Map 8)	$S_1 = 0.9$

On Map 8, the contour line of  $S_1 = 0.9$  runs approximately through the center of the San Francisco peninsula, with other San Francisco peninsula contour lines ranging from 0.6 (greatest distance from San Andreas Fault), to about 1.6 (directly on top of the San Andreas Fault).

Site coefficient (Provisions Table 4.1.2.4b [3.3-2])	$F_{v} = 1.5$
MCE spectral acceleration adjusted for site class $(F_v S_I)$	$S_{MI} = 1.35$
Design earthquake (DE) spectral acceleration $(2/3S_{MI})$	$S_{D1} = 0.9$
Seismic Design Category (Provisions Table 4.2.1b [1.4-2])	Seismic Design Category F

[In the 2003 edition of the Provisions, the ground motion trigger for Seismic Design Categories E and F have been changed to  $S_1 \ge 0.60$ . No change would result for this example.]

# 11.5.2.4.3 Design Spectra (Provisions Sec. 13.4.4.1)

Figure 11.5-6 plots design earthquake and maximum considered earthquake response spectra as constructed in accordance with the procedure of *Provisions* Sec. 13.4.4.1 [3.4] using the spectrum shape defined by *Provisions* Figure 4.1.2.6 [3.3-15]. [In the 2003 edition of *Provisions*, the shape of the design spectrum changes at period beyond  $T_L$ , but no change would result for this example.] *Provisions* Sec. 13.4.4.1[13.2.3.1] requires site-specific design spectra to be calculated for sites with  $S_1$  greater than 0.6 (e.g., sites near active sources). Site-specific design spectra may be taken as less than 100 percent but not less than 80 percent of the default design spectra of *Provisions* Figure 4.1.2.6 [3.3-15].

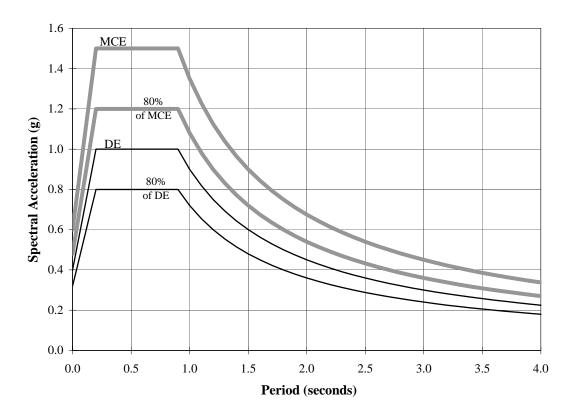


Figure 11.5-6 Example design spectra (5 percent damping).

For this example, site-specific spectra for the design earthquake and the maximum considered earthquake, were assumed to be 80 percent (at long periods) and 100 percent (at short periods) of the respective spectra shown in Figure 11.5-6. The 80 percent factor reflects a reduction in demand that could be achieved through a detailed geotechnical investigation of site soil conditions. In general, site-specific spectra for regions of high seismicity, with well defined fault systems (like those of the San Francisco Bay Area), would be expected to be similar to the default design spectra of *Provisions* Figure 4.1.2.6 [3.3-15].

# 11.5.2.4.4 Design Time Histories (Provisions Sec. 13.4.4.2 [13.2.3.2])

For time history analysis, *Provisions* Sec. 13.4.4.7 [13.4.2.3] requires no less than three pairs of horizontal ground motion time history components to be selected from actual earthquake records, and scaled to match either the design earthquake (DE) or the maximum considered earthquake (MCE) spectrum. The selection and scaling of appropriate time histories is usually done by an earth scientist, or a geotechnical engineer experienced in the seismology of the region; and takes the earthquake

magnitudes, fault distances, and source mechanisms that influence hazards at the building site into consideration.

For this example, records from the El Centro Array Station No. 6, the Newhall Fire Station, and the Sylmar Hospital are selected from those recommended by *ATC-40* [ATC, 1996], for analysis of buildings at stiff soil sites with ground shaking of 0.2g or greater. These records, and the scaling factors required to match the design spectra are summarized in Table 11.5-2. These three records represent strong ground shaking recorded relatively close to fault rupture; and contain long-period pulses in the direction of strongest shaking, which can cause large displacement of the isolated structures. MCE scaling factors for the El Centro No. 6 and Sylmar records are 1.0, indicating that these records are used without modification for MCE time history analysis of the EOC.

*Provisions* Sec. 13.4.4.2 [13.2.3.2] provides criteria for scaling earthquake records to match a target spectrum over the period range of interest, defined as  $0.5T_D$  to  $1.25T_M$ . In this example,  $T_D$  and  $T_M$  are both assumed to be 2.5 seconds, so the period range of interest is from 1.25 seconds to 3.125 seconds. For each period in this range, the average of the square-root-of-the-squares (SRSS) combination of each pair of horizontal components of scaled ground motion, may not fall below the target spectrum by more 10 percent. The target spectrum is defined as 1.3 times the design spectrum of interest (either the DE or the MCE spectrum).

Figure 11.5-7 compares the spectra of scaled time history components with the spectrum for the design earthquake. Rather than comparing the average of the SRSS spectra with 1.3 times the design spectrum, as indicated in the *Provisions*, Figure 11.5-7 shows the (unmodified) design spectrum and the average of the SRSS spectra divided by 1.3. The effect is the same, but the method employed eliminates one level of obscurity and permits direct comparison of the calculated spectra without additional manipulation. A comparison of maximum, considered earthquake spectra would look similar (with values that were 1.5 times larger). The fit is very good at long periods - the period range of interest for isolated structures. At 2.5 seconds, the spectrum of the scaled time histories has the same value as the target spectrum. Between 1.25 seconds and 3.125 seconds, the spectrum of the scaled time histories is never less than the target spectrum by more than 10 percent. At short periods, the spectrum of scaled time histories to match the long-period portion of the design spectrum.

Figure 11.5-7 also includes plots of upper-bound (maximum demand) and lower-bound (minimum demand) envelopes of the spectra of the six individual components of scaled time histories. The maximum demand envelope illustrates that the strongest direction (component) of shaking of at least one of the three scaled time histories is typically about twice the site-specific spectrum in the period range of the isolated structure - consistent with strong ground shaking recorded near sources in the fault normal direction.

Record	Earthquake Source and Recording Station				Scaling factor	
No.	Year	Earthquake	Station (owner)	DE	MCE	
1	1979	Imperial Valley, CA	El Centro Array Station 6 (USGS)	0.67	1.0	
2	1994	Northridge, CA	Newhall Fire Station (CDMG)	1.0	1.5	
3	1994	Northridge, CA	Sylmar Hospital (CDMG)	0.67	1.0	

 Table 11.5-2
 Earthquake Time History Records and Scaling Factors

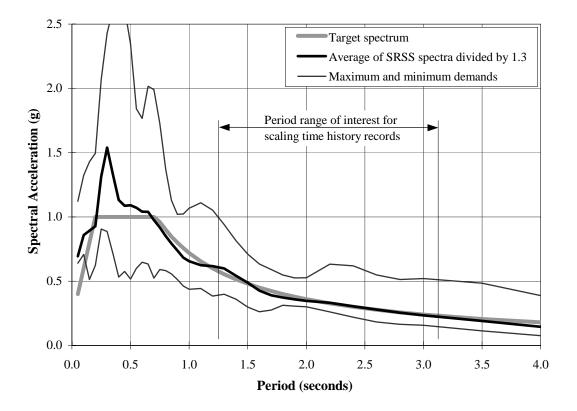


Figure 11.5-7 Comparison of design earthquake spectra.

#### 11.5.2.5 Structural Design Criteria

11.5.2.5.1 Design Basis (Provisions Sec. 5.2 and 13.2 [4.3 and 13.2])

Seismic-force-resisting system.	Special steel concentrically braced frames (height < 100 ft)
Response modification factor, R (Provisions Table 5.2.2 [4.3-1]	6 (conventional)
Response modification factor for design of the superstructure, $R_I$ ( <i>Provisions</i> Sec. 13.3.4.2 [13.3.3.2], $3/8R \le 2$ )	2 (isolated)
Plan irregularity (of superstructure) - (Provisions Table 5.2.3.2)	None
Vertical irregularity (of superstructure) - from Table 5.2.3.3	None
Lateral response procedure (Provisions Sec. 13.2.5.2 [13.2.4.1], $S_1 > 0.6$	) Dynamic analysis
Redundancy/reliability factor - (Provisions Sec. 5.2.4.2 [4.3.3])	$\rho > 1.0$ (conventional) $\rho = 1.0$ (isolated)

*Provisions* Sec. 5.2.4.2 [4.3.3] requires the use of a calculated  $\rho$  value, which would be greater than 1.0 for a conventional structure with a brace configuration similar to the superstructure of the base-isolated EOC. However, in the author's opinion, the use of  $R_I$  equal to 2.0 (rather than R equal

to 6) as required by *Provisions* Sec. 13.3.4.2 precludes the need to further increase superstructure design forces for redundancy/reliability. Future editions of the *Provisions* should address this issue.

[The redundancy factor is changed substantially in the 2003 Provisions. However, the rationale set forth above by the author still holds; use of  $\rho = 1.0$  is reasonable since  $R_I = 2.0$ .] 11.5.2.5.2 Horizontal Earthquake Loads and Effects (Provisions Chapters 5 and 13)

Design earthquake (acting in either the X or Y direction)	DE (site specific)
Maximum considered earthquake (acting in either the X or Y direction)	MCE (site specific)
Mass eccentricity - actual plus accidental	$0.05b = 6 \text{ ft} (\perp \text{ to X axis})$ $0.05d = 9 \text{ ft} (\perp \text{ to Y axis})$

The superstructure is symmetric about both principal axes, however, the placement of the braced frames results in a ratio of maximum corner displacement to average displacement of 1.25, exceeding the threshold of 1.2 per the definition of the *Provisions*. If the building were not on isolators, the accidental torsional moment would need to be increased from 5 percent to 5.4 percent of the building dimension. The input to the superstructure is controlled by the isolation system, and it is the author's opinion that the amplification of accidental torsion is not necessary for such otherwise regular structures. Future editions of the *Provisions* should address this issue. Also refer to the discussion of analytical modeling of accidental eccentricities in *Guide* Chapter 1.

Superstructure design (reduced DE response)	$Q_E = Q_{\rm DE/2} = \rm DE/2.0$
Isolation system and foundation design (unreduced DE response)	$Q_E = Q_{\rm DE} = {\rm DE}/1.0$
Check of isolation system stability (unreduced MCE response)	$Q_E = Q_{\rm MCE} = { m MCE}/1.0$

11.5.2.5.3 Combination of Horizontal Earthquake Load Effects (Provisions Sec. 5.25.2.3 [4.4.2.3] and 13.4.6.3 [13.4.2.2])

Response due earthquake loading in the X and Y directions  $Q_E = Max (1.0Q_{EX}+0.3Q_{EY}, 0.3Q_{EX}+1.0Q_{EY})$ 

In general, the horizontal earthquake load effect,  $Q_E$ , on the response parameter of interest is influenced by only one direction of horizontal earthquake load, and  $Q_E = Q_{EX}$  or  $Q_E = Q_{EY}$ . Exceptions include vertical load on isolator units due to earthquake overturning forces.

11.5.2.5.4 Combination of Horizontal and Vertical Earthquake Load Effects (Provisions Sec. 5.2.7 [4.2.2.1])

Design earthquake ( $\rho Q_E \pm 0.2 S_{DS} D$ )	$E = Q_E \pm 0.2D$
Maximum considered earthquake ( $\rho Q_E \pm 0.2 S_{MS} D$ )	$E = Q_E \pm 0.3D$
11.5.2.5.5 Superstructure Design Load Combinations (UBC Sec. 1612.2	$2, using R_I = 2)$
Gravity loads (dead load and reduced live load)	1.2D + 1.6L
Gravity and earthquake loads $(1.2D + 0.5L + 1.0E)$	$1.4D + 0.5L + Q_{\text{DE/2}}$

 $0.7D - Q_{DE/2}$ 

Gravity and earthquake loads (0.9D - 1.0E)

11.5.2.5.6 Isolation System and Foundation Design Load Combinations (UBC Sec. 1612.2)

Gravity loads (for example, long term load on isolator units)	1.2D + 1.6L			
Gravity and earthquake loads $(1.2D + 0.5L + 1.0E)$	$1.4D + 0.5L + Q_{\rm DE}$			
Gravity and earthquake loads $(0.9D - 1.0E)$	$0.7D$ - $Q_{\rm DE}$			
11.5.2.5.7 Isolation System Stability Load Combinations (Provisions Sec. 13.6.2.6 [13.2.5.6])				

Maximum short term load on isolator units (1.2D + 1.0L + |E|)  $1.5D + 1.0L + Q_{MCE}$ 

Minimum short term load on isolator units (0.8D - |E|) 0.8D -  $Q_{MCE}$ 

Note that in the above combinations, the vertical earthquake load  $(0.2S_{MS}D)$  component of |E| is included in the maximum (downward) load combination, but excluded from the minimum (uplift) load combination. It is the author's opinion that vertical earthquake ground shaking is of a dynamic nature, changing direction too rapidly to affect appreciably uplift of isolator units and need not be used with the load combinations of *Provisions* Sec. 13.6.2.6 [13.2.5.6] for determining minimum (uplift) vertical loads on isolator units due to the MCE. Future editions of the *Provisions* should explicitly address this issue.

# **11.5.3 Seismic Force Analysis**

# 11.5.3.1 Basic Approach to Modeling

To expedite calculation of loads on isolator units, and other elements of the seismic-force-resisting system, a 3-dimensional model of the EOC is developed and analyzed using the ETABS computer program (CSI, 1999). While there are a number of programs to choose from, ETABS (version 7.0) is selected for this example since it permits the automated release of tension in isolator units subject to uplift and has built-in elements for modeling other nonlinear properties of isolator units. Arguably, all of the analyses performed by the ETABS program could be done by hand, or by spreadsheet calculation (except for confirmatory time history analyses).

The ETABS model is used to perform the following types of analyses and calculations:

- 1. Dead load weight and live loads for the building--calculate maximum long-term load on isolator units (*Guide* Table 11.5-1)
- 2. ELF procedure for gravity and reduced design earthquake loads--design superstructure (ignoring uplift of isolator units)
- 3. Nonlinear static analysis with ELF loads for gravity and unreduced design earthquake loads--design isolation system and foundation (considering uplift of isolator units)
- 4. Nonlinear static analysis with ELF loads gravity and unreduced design earthquake loads--calculate maximum short-term load (downward force) on isolator units (*Guide* Table 11.5-5) and calculate minimum short-term load (downward force) of isolator units (*Guide* Table 11.5-6)

- 5. Nonlinear static analysis with ELF loads for gravity and unreduced MCE loads--calculate maximum short-term load (downward force) on isolator units (*Guide* Table 11.5-7) and calculate minimum short-term load (uplift displacement) of isolator units (*Guide* Table 11.5-8)
- 6. Nonlinear time history analysis gravity and scaled DE or MCE time histories--verify DE displacement of isolator units and design story shear (*Guide* Table 11.5-10), verify MCE displacement of isolator units (*Guide* Table 11.5-11), verify MCE short-term load (downward force) on isolator units (*Guide* Table 11.5-12), and verify MCE short-term load (uplift displacement) of isolator units (*Guide* Table 11.5-13).

The *Provisions* requires a response spectrum analysis for the EOC (see *Guide* Table 11.2-1). In general, the response spectrum method of dynamic analysis is considered sufficient for facilities that are located at a stiff soil site, which have an isolation system meeting the criteria of *Provisions* Sec. 13.2.5.2.7, Item 7 [13.2.4.1, Item 7]. However, nonlinear static analysis is used for the design of the EOC, in lieu of response spectrum analysis, to permit explicit modeling of uplift of isolator units. For similar reasons, nonlinear time history analysis is used to verify design parameters.

# 11.5.3.2 Detailed Modeling Considerations

Although a complete description of the ETABS model is not possible, key assumptions and methods used to model elements of the isolation system and superstructure are described below.

# 11.5.3.2.1 Mass Eccentricity

*Provisions* Sec. 13.4.5.2 [13.4.1.1] requires consideration of mass eccentricity. Because the building in the example is doubly symmetric, there is no actual eccentricity of building mass (but such would be modeled if the building were not symmetric). Modeling of accidental mass eccentricity would require several analyses, each with the building mass located at different eccentric locations (for example, four quadrant locations in plan). This is problematic, particularly for dynamic analysis using multiple time history inputs. In this example, only a single (actual) location of mass eccentricity is considered, and calculated demands are increased moderately for the design of the seismic-force-resisting system, and isolation system (for example, peak displacements calculated by dynamic analysis are increased by 10 percent for design of the isolation system).

# 11.5.3.2.2 P-delta Effects

P-delta moments in the foundation and the first floor girders just above isolator units due to the large lateral displacement of the superstructure are explicitly modeled. The model distributes half of the P-delta moment to the structure above, and half of the *P*-delta moment to the foundation below the isolator units. ETABS (version 7.0) permits explicit modeling of the P-delta moment, but most computer programs (including older versions of ETABS) do not. Therefore, the designer must separately calculate these moments and add them to other forces for the design of affected elements. The P-delta moments are quite significant, particularly at isolator units that resist large earthquake overturning loads along lines of lateral bracing.

# 11.5.3.2.5 Isolator Unit Uplift

*Provisions* Sec. 13.6.2.7 [13.2.5.7] permits local uplift of isolator units provided the resulting deflections do not cause overstress of isolator units or other structural elements. Uplift of some isolator units is likely (for unreduced earthquake loads) due to the high seismic demand associated with the site. Accordingly, isolator units are modeled with gap elements that permit uplift when the tension load exceeds the tensile capacity of an isolator unit. Although most elastomeric bearings can resist some tension stress before

yielding (typically about 150 psi), isolator units are assumed to yield as soon as they are loaded in tension, producing larger estimates of uplift displacement and overturning loads on isolator units that are in compression.

The assumption that isolator units have no tension capacity is not conservative, however, for design of the connections of isolator units to the structure above and the foundation below. The design of anchor bolts and other connection elements, must include the effects of tension in isolator units (typically based on a maximum stress of 150 psi).

# 11.5.3.2.4 Bounding Values of Bilinear Stiffness of Isolator Units

The design of elements of the seismic-force-resisting system is usually based on a linear, elastic model of the superstructure. When such models are used, *Provisions* Sec. 13.4.5.3.2 [13.4.1.2] requires that the stiffness properties of nonlinear isolation system components be based on the maximum effective stiffness of the isolation system (since this assumption produces larger earthquake forces in the superstructure). In contrast, the *Provisions* require that calculation of isolation system displacements be based on the minimum effective stiffness of the isolation system (since this assumption produces larger isolation system displacements).

The concept of bounding values, as discussed above, applies to all of the available analysis methods. For the ELF procedure, the *Provisions* equations are based directly on maximum effective stiffness,  $k_{Dmax}$  and  $k_{Mmax}$ , are used for calculating design forces; and on minimum effective stiffness,  $k_{Dmin}$  and  $k_{Dmax}$ , are used for calculating design displacements. Where (nonlinear) time history analysis is used, isolators are explicitly modeled as bilinear hysteretic elements with upper or lower-bound stiffness curves. Upper-bound stiffness curves are used to verify the forces used for the design of the superstructure and lower-bound stiffness curves are used to verify design displacements of the isolation system.

# 11.5.4 Preliminary Design Based on the ELF Procedure

# 11.5.4.1 Calculation of Design Values

#### 11.5.4.1.1 Design Displacements

Preliminary design begins with the engineer's selection of the effective period (and damping) of the isolated structure, and the calculation of the design displacement,  $D_D$ . In this example, the effective period of the EOC facility (at the design earthquake displacement) is  $T_D = 2.5$  seconds; and the design displacement is calculated as follows, using *Provisions* Eq. 13.3.3.1:

$$D_D = \left(\frac{g}{4\pi^2}\right) \frac{S_{DI}T_D}{B_D} = (9.8) \frac{0.9(2.5)}{1.35} = 16.3$$
 in.

The 1.35 value of the damping coefficient,  $B_D$ , is given in *Provisions* Table 13.3.3.1 [13.3-1] assuming 15 percent effective damping at 16.3 in. of isolation system displacement. Effective periods of 2 to 3 seconds and effective damping values of 10 to 15 percent are typical of high-damping rubber (and other types of) bearings.

Stability of the isolation system must be checked for the maximum displacement,  $D_M$ , which is calculated using *Provisions* Eq. 13.3.3 as follows:

$$D_M = \left(\frac{g}{4\pi^2}\right) \frac{S_{MI}T_M}{B_M} = (9.8) \frac{1.35(2.5)}{1.35} = 24.5 \text{ in.}$$

For preliminary design, the effective period and effective damping at maximum displacement are assumed to be the same as the values at the design displacement. While both the effective period and damping values may reduce slightly at larger rubber strains, the ratio of the two parameters tend to be relatively consistent.

The total displacement of specific isolator units (considering the effects of torsion) is calculated based on the plan dimensions of the building, the total torsion (due to actual, plus accidental eccentricity), and the distance from the center of resistance of the building to the isolator unit of interest. Using *Provisions* Eq. 13.3.3.5-1 and 13.3.3.5-2 [13.3-5 and 13.3-6], the total design displacement,  $D_{TD}$ , and the total maximum displacement,  $D_{TM}$ , of isolator units located on Column Lines 1 and 7 are calculated for the critical (transverse) direction of earthquake load as follows:

$$D_{TD} = D_D \left[ 1 + y \left( \frac{12e}{b^2 + d^2} \right) \right] = 16.3 \left[ 1 + 90 \left( \frac{12(0.05)(180)}{120^2 + 180^2} \right) \right] = 16.3(1.21) = 19.7 \text{ in}$$

$$D_{TM} = D_M \left[ 1 + y \left( \frac{12e}{b^2 + d^2} \right) \right] = 24.5 \left[ 1 + 90 \left( \frac{12(0.05)(180)}{120^2 + 180^2} \right) \right] = 24.5(1.21) = 29.6 \text{ in.}$$

The equations above assume that mass is distributed in plan in proportion to isolation system stiffness and shifted by 5percent, providing no special resistance to rotation of the building on the isolation system. In fact, building mass is considerably greater toward the center of the building, as shown by the schedule of gravity loads in Table 11.5-1. The stiffness of the isolation system is uniform in plan (since all isolators are of the same size) providing significant resistance to dynamic earthquake rotation of the building. While the *Provisions* permit a reduction in the total displacements calculated using the ELF procedure (with proper substantiation of resistance to torsion), in this example the 21 percent increase is considered to be conservative for use in preliminary design and for establishing lower-bound limits on dynamic analysis results.

#### 11.5.4.1.2 Minimum and Maximum Effective Stiffness

*Provisions* Eq. 13.3.3.2 [13.3-2] expresses the effective period at the design displacement in terms of building weight (dead load) and the minimum effective stiffness of the isolation system,  $k_{Dmin}$ . Rearranging terms and solving for minimum effective stiffness:

$$k_{Dmin} = \left(\frac{4\pi^2}{g}\right) \frac{W}{T_D^2} = \left(\frac{1}{9.8}\right) \frac{14,715}{2.5^2} = 240 \text{ kips/in.}$$

This stiffness is about 6.9 kips/in. for each of 35 identical isolator units. The effective stiffness can vary substantially from one isolator unit to another and from one cycle of prototype test to another. Typically, an isolator unit's effective stiffness is defined by a range of values for judging acceptability of prototype (and production) bearings. The minimum value of the stiffness range,  $k_{Dmin}$ , is used to calculate isolation system design displacements; the maximum value of the stiffness,  $k_{Dmax}$ , is used to define design forces.

The variation in effective stiffness depends on the specific type of isolator, elastomeric compound, loading history, etc., but must, in all cases, be broad enough to comply with the *Provisions* Sec. 13.9.5.1 [13.6.4.1]requirements that define maximum and minimum values of effective stiffness based on testing of isolator unit prototypes. Over the three required cycles of test at  $D_D$ , the maximum value of effective stiffness (for example, at the first cycle) should not be more than about 30 percent greater than the minimum value of effective stiffness (for example, at the third cycle) to comply with *Provisions* Sec.

13.9.4 [13.6.3]. On this basis, the maximum effective stiffness,  $k_{Dmax}$ , of the isolation system in this example, is limited to 312 kips/in. (that is,  $1.3 \times 240$  kips/in.).

The range of effective stiffness defined by  $k_{Dmin}$  and  $k_{Dmax}$  (as based on cyclic tests of prototype isolator units) does not necessarily bound all the possible variations in the effective stiffness of elastomeric bearings. Other possible sources of variation include: stiffness reduction, due to post-fabrication "scragging" of bearings (by the manufacturer), and partial recovery of this stiffness over time. Temperature and aging effects of the rubber material, and other changes in properties that can also occur over the design life of isolator units. (Elastomeric bearings are typically "scragged" immediately following molding and curing to loosen up the rubber molecules by application of vertical load.) Provisions Sec. 13.6.2.1 [13.2.5.1] requires that such variations in isolator unit properties be considered in design, but does not provide specific criteria. A report - Property Modification Factors for Seismic Isolation Bearings (Constantinou, 1999) - provides guidance for establishing a range of effective stiffness (and effective damping) properties that captures all sources of variation over the design life of the isolator units. The full range of effective stiffness has a corresponding range of effective periods (with different levels of spectral demand). The longest effective period (corresponding to the minimum effective stiffness) of the range would be used to define isolation system design displacements; and the shortest effective period (corresponding to the maximum effective stiffness) of the range would be used to define the design forces on the superstructure.

#### 11.5.4.1.3 Lateral Design Forces

The lateral force required for the design of the isolation system, foundation, and other structural elements below the isolation system, is given by *Provisions* Eq. 13.3.4.1 [13.3-7]:

$$V_b = k_{Dmax} D_D = 312(16.3) = 5,100$$
 kips

The lateral force required for checking stability and ultimate capacity of elements of the isolation system, may be calculated as follows:

$$V_{MCE} = k_{Dmax} D_M = 312(24.5) = 7,650$$
 kips

The (unreduced) base shear of the design earthquake is about 35 percent of the weight of the EOC, and the (unreduced) base shear of the MCE is just over 50 percent of the weight. In order to design the structure above the isolation system, the design earthquake base shear is reduced by the  $R_1$  factor in *Provisions* Eq. 13.3.4.2 [13.3-8]:

$$V_s = \frac{k_{Dmax}D_D}{R_1} = \frac{312(16.3)}{2.0} = 2,550$$
 kips

This force is about 17 percent of the dead load weight of the EOC, which is somewhat less than, but comparable to, the force that would be required for the design of a conventional, fixed-base building of the same size and height, seismic-force-resisting system, and site seismic conditions. Story shear forces on the superstructure are distributed vertically over the height of the structure in accordance with *Provisions* Eq. 13.3.5 [13.3-9], as shown in Table 11.5-3.

#### Table 11.5-3 Vertical Distribution of Reduced Design Earthquake Forces (DE/2)

Story level, <i>x</i>	Weight, w <sub>x</sub> (kips)	Height above isolation system, $h_x$ (ft)	Force, $F_{x} = \frac{w_{x}h_{x}V_{s}}{\sum_{i}w_{i}h_{i}}$ (kips)	Cumulative force (kips)	Force divided by weight, $\frac{F_x}{w_x}$
Penthouse roof	965	64	370	370	0.38
Roof	3,500	49	1,020	1,390	0.29
Third floor	3,400	34	690	2,080	0.20
Second floor	3,425	19	390	2,470	0.11
First floor	3,425	4	80	2,550	0.023

1.0 ft = 0.3048 m, 1.0 kip = 4.45 kN.

*Provisions* Eq. 13.3.5 distributes lateral seismic design forces (DE/2) over the height of the building in an inverted, triangular, pattern as indicated by the ratio of  $F_x/w_x$ , shown in Table 11.5-3. Because the superstructure is much stiffer laterally, than the isolation system, it tends to move as a rigid body in the first mode with a pattern of lateral seismic forces that is more uniformly distributed over the height of the building. The use of a triangular load pattern for design is intended to account for higher-mode response that may be excited due to flexibility of the superstructure. *Provisions* Eq. 13.3.5 [13.3-9] is also used to distribute forces over the height of the building for unreduced DE and MCE forces, as summarized in Table 11.5-4.

	Design earthquake (DE)			Maximum considered earthquake (MCE)		
Story level, <i>x</i>	Force (kips)	Cumulative force (kips)	Force divided by weight	Force (kips)	Cumulative force (kips)	Force divided by weight
Penthouse roof	740	740	0.76	1,110	1,110	1.14
Roof	2,040	2,780	0.59	3,060	4,170	0.88
Third floor	1,380	4,160	0.41	2,070	6,240	0.61
Second floor	780	4,940	0.23	1,170	7,410	0.34
First floor	160	5,100	0.047	240	7,650	0.071

 Table 11.5-4
 Vertical Distribution of Unreduced DE and MCE Forces

1.0 kip = 4.45 kN.

# 11.5.4.1.4 Design Earthquake Forces for Isolator Units

Tables 11.5-5 and 11.5-6 show the maximum and minimum downward forces for design of the isolator units. These forces are a result from the simultaneous application of unreduced design earthquake story forces, summarized in Table 11.5-4 and appropriate gravity loads to the model of the EOC. (See *Guide* Sec. 11.5.2.5 for the design load combinations.) As described in *Guide* Sec. 11.5.2.5, loads are applied simultaneously in two horizontal directions. The tables report the results for both of the orientations: 100 percent in the X direction, plus 30 percent in the Y direction, and 30 percent in the X direction, plus 100 percent in the Y direction. Where the analyses indicate that certain isolator units could uplift during peak DE response (as indicated by zero downward force), the amount of uplift is small and would not appreciably affect the distribution of earthquake forces in the superstructure.

			e .	≈DL/	
	Maximum downward force (kips) 100%(X) ± 30%(Y) / 30%(X) ± 100%(Y)				
Column line	1	2	3	4	
А	347/ <u>348</u>	661/ <u>892</u>	522/ <u>557</u>	652/ <u>856</u>	
В	833/634	1,335/ <u>1,<b>519</b></u>	<u>1,418</u> /1,278	984/ <u>1,186</u>	
С	<u>537</u> /502	<u>939</u> /890	<u>1,053</u> /1,046	<u>1,074</u> /1,070	

**Table 11.5-5** Maximum Downward Force (kips) for Isolator Design  $(1.4D + 0.5L + Q_{DE})^*$ 

1.0 kip = 4.45 kN

.\*Forces at column lines 5, 6 and 7 (not shown) are the same as those at column lines 3, 2, and 1, respectively; loads at column lines D and E (not shown) are the same as those at column lines B and A, respectively.

		Downward I blee (kip	is) for isofator Design	(one goe)	
	Maximum downward force (kips) $100\%(X) \pm 30\%(Y) / 30\%(X) \pm 100\%(Y)$				
Column line	1	2	3	4	
А	87/ <u>84</u>	165/ <u>0</u>	200/ <u>169</u>	163/ <u>0</u>	
В	<u>0</u> /123	11/ <u>0</u>	<u>23</u> /69	280/ <u>59</u>	
С	<u>169</u> /196	299/ <u>243</u>	428/ <u>427</u>	447/ <u>442</u>	

**Table 11.5-6** Minimum Downward Force (kips) for Isolator Design  $(0.7D - Q_{DE})^*$ 

1.0 kip = 4.45 kN

\* Forces at column lines 5, 6 and 7 (not shown) are the same as those at column lines 3, 2, and 1, respectively; loads at column lines D and E (not shown) are the same as those at column lines B and A, respectively.

#### 11.5.4.1.5 Maximum Considered Earthquake Forces and Displacements for Isolator Units

Simultaneous application of the unreduced MCE story forces, as summarized in Table 11.5-4 and appropriate gravity loads to the model of the EOC, result in the maximum downward forces on isolator units shown in *Guide* Table 11.5-7, and the maximum uplift displacements shown in Table 11.5-8. The load orientations and MCE load combinations, are described in *Guide* Sec. 11.5.2.5. The tables report the results for both of the load orientations: 100 percent in the X direction, plus 30 percent in the Y direction, and 30 percent in the X direction, plus 100 percent in the Y direction. Since the nonlinear model assumes that the isolators have no tension capacity, the values given in *Guide* Table 11.5-8 are upper bounds on uplift displacements.

		-			
	Maximum downward force (kips) 100%(X) ± 30%(Y) / 30%(X) ± 100%(Y)				
Column line	1	2	3	4	
А	444/ <u>445</u>	829/ <u>1,202</u>	645/ <u>710</u>	819/ <u>1,146</u>	
В	<u>1,112</u> /794	1,739/ <u>2,006</u>	<u>1,848</u> /1,635	1,219/ <u>1,521</u>	
С	<u>680</u> /618	<u>1,171</u> /1,091	<u>1,298</u> /1,282	<u>1,316</u> /1,307	

**Table 11.5-7** Maximum Downward Force (kips) on Isolator Units  $(1.5D + 1.0L + Q_{MCE})^*$ 

1.0 kip = 4.45 kN.

\* Forces at column lines 5, 6 and 7 (not shown) are the same as those at column lines 3, 2, and 1, respectively; loads at column lines D and E (not shown) are the same as those at column lines B and A, respectively.

14	Table 11.3-6 Maximum Opint Displacement (in.) of Isolator Omits (0.0D - Q <sub>MCE</sub> )						
Maximum uplift displacement (in.) 100%(X) ± 30%(Y) / 30%(X) ± 100%(Y)							
Column line	1	2	3	4			
А	No uplift	0.00/ <u><b>0.94</b></u>	No uplift	0.00/ <u>0.50</u>			
В	<u>0.54</u> /0.00	0.19/ <u>0.45</u>	<u>0.13</u> /0.00	0.00/ <u>0.14</u>			
С	No uplift	No uplift	No uplift	No uplift			

**Table 11.5-8** Maximum Uplift Displacement (in.) of Isolator Units  $(0.8D - Q_{MCE})^*$ 

1.0 in. = 25.4 mm.

\* Displacements at column lines 5, 6 and 7 (not shown) are the same as those at column lines 3, 2, and 1, respectively; displacements at column lines D and E (not shown) are the same as those at column lines B and A, respectively.

#### 11.5.4.1.6 Limits on Dynamic Analysis

The displacements and forces determined by the ELF procedure provide a basis for expeditious assessment of size and capacity of isolator units and the required strength of the superstructure. The results of the ELF procedure also establish limits on design parameters when dynamic analysis is used as the basis for design. Specifically, the total design displacement,  $D_{TD}$ , and the total maximum displacement of the isolation system,  $D_{TM}$ , determined by dynamic analysis cannot be less than 90 percent and 80 percent, respectively, of the corresponding ELF procedure values:

 $D_{TD, dynamic} \ge 0.9 D_{TD, ELF} = 0.9(19.7) = 17.7$  in.

$$D_{TM, dynamic} \ge 0.8 D_{TM, ELF} = 0.8(29.6) = 23.7$$
 in.

The superstructure, if regular, can also be designed for less base shear, but not less than 80 percent of the base shear from the ELF procedure:

 $V_{s, dynamic} \ge 0.8 V_{s, ELF} = 0.8(2,550) = 2,040 \text{ kips} (= 0.14W)$ 

As an exception to the above, design forces less than 80 percent of the ELF results are permitted if justified by time history analysis (which is seldom, if ever, the case).

# 11.5.4.2 Design of the Superstructure

The lateral forces, developed in the previous section, in combination with gravity loads, provide a basis for the design of the superstructure, using methods similar to those used for a conventional building. In this example, selection of member sizes were made based on the results of ETABS model calculations. Detailed descriptions of the design calculations are omitted, since the focus of this section is on design aspects unique to isolated structures (i.e., design of the isolation system, which is described in the next section).

Figures 11.5-8 and 11.5-9 are elevation views at Column Lines 2 and B, respectively. Figure 11.5-10 is a plan view of the building that shows the framing at the first floor level.

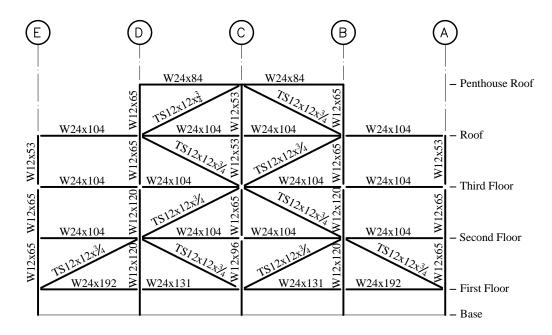


Figure 11.5-8 Elevation of framing on Column Line 2 (Column Line 6 is similar).

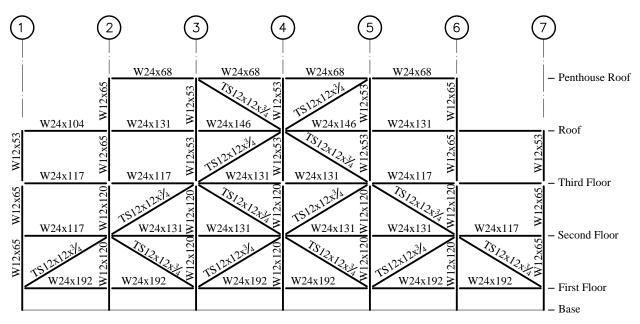


Figure 11.5-9 Elevation of framing on Column Line B (Column Line D is similar).

		$\mathbf{D}$						$\mathbf{D}$		4	Ð		(5	$\mathbf{b}$		(6	$\mathbf{D}$		Ċ	$\mathcal{O}$
(A)	 		24 x14	6		24 x13	1	)W	24 x11	7		24 x11	7	W	24 x13	<u>31</u>	W	24 x14	. <u>6</u>	
$\bigcirc$	W24 x131	W18x40	W18x40	W24 x192	W18x40	W18x40	W24 x146	W18x40	W18x40	W24 x176	W18x40	W18x40	W24 x146	W18x40	W18x40	W24 x192	W18x40	W18x40	W24 x131	
(B)-	·C		W24	<u>x192</u>	][	W24	x192	)——	W24	<u>x192</u>	]	W24	x192	)	W24	<u>x192</u>	][	W24	<u>x192</u>	-
)	W24 x104	W18x40	W18x40	W24 x131	W18x40	W18x40	W24 x117	W18x40	W18x40	W24 x131	W18x40	W18x40	W24 x117	W18x40	W18x40	W24 x131	W18x40	W18x40	W24 x104	
(C)-	·	][	W24	<u>x162</u>		W24	x146	]	W24	x146	]	W24	x146	]	W24	<u>x146</u>		W24	<u>x162</u>	]
U	W24 x104	W18x40	W18x40	W24 x131	W18x40	W18x40	W24 x117	W18x40	W18x40	W24 x131	W18x40	W18x40	W24 x117	W18x40	W18x40	W24 x131	W18x40	W18x40	W24 x104	
(D)-	·	]	W24	x192	]	W24	x192	]	W24	x192	]	W24	x192	]	W24	x192	]	W24	x192	  -
$\bigcirc$	W24 x131	W18x40	W18x40	W24 x192	W18x40	W18x40	W24 x146	W18x40	W18x40	W24 x176	W18x40	W18x40	W24 x146	W18x40	W18x40	W24 x192	W18x40	W18x40	W24 x131	
E-	·C	]	W24	x146	][	W24	x131	]	W24	x131	]	W24	x131	]	W24	x131	][	W24	x146	]

Figure 11.5-10 First floor framing plan.

As shown in the elevations (Figures 11.5-8 and 11.5-9), fairly large  $(12 \times 12 \times 34 \text{ in.})$  tubes are consistently used throughout the structure for diagonal bracing. A quick check of these braces indicates that stresses will be at, or below yield for design earthquake loads. The six braces at the third floor, on lines 2, 4, and 6 (critical floor and direction of bracing) carry a reduced design earthquake force of about 400 kips each (= 2,080 kips/6 braces × cos(30°)). The corresponding stress is about 12.5 ksi for reduced design earthquake forces, or about 25 ksi for unreduced design earthquake forces; indicating that the structure is expected to remain elastic during the design earthquake.

As shown in Figure 11.5-10, the first floor framing has heavy, W24 girders along lines of bracing (lines B, D, 2, 4, and 6). These girders resist P-delta moments, as well as other forces. A quick check of these girders indicates that only limited yielding is likely, even for the MCE loads (up to about 2 ft of MCE displacement). Girders on Line 2 that frame into the column at Line B (critical columns and direction of framing), resist a P-delta moment due to the MCE of about 1,000 kip-ft (2,000 kips/2 girders  $\times 2$  ft/2). Moment in these girders due to MCE shear force in isolators is about 450 kip-ft (8.9 kips/in.  $\times 24$  in.  $\times 4$  ft/2 girders). Considering additional moment due to gravity loads, the plastic capacity of the first floor girders (1,680 kip-ft) would not be reached until isolation system displacements exceed about 2 ft. Even beyond this displacement, post-yield deformation would be limited (due to the limited extent and duration of MCE displacements beyond 2 ft), and the first floor girders would remain capable of stabilizing the isolator units.

# 11.5.4.3 Design of the Isolation System

The displacements and forces calculated in *Guide* Sec. 11.5.4.1 provide a basis to either:

- 1. Develop a detailed design of the isolator units or
- 2. Include appropriate design properties in performance-based specifications.

Developing a detailed design of an elastomeric bearing, requires a familiarity with rubber bearing technology, that is usually beyond the expertise of most structural designers; and often varies based on the materials used by different manufacturers. This example, like most recent isolation projects, will define design properties for isolator units that are appropriate for incorporation into a performance specification (and can be bid by more than one bearing manufacturer). Even though the specifications will place the responsibility for meeting performance standards with the supplier, the designer must still be knowledgeable of available products and potential suppliers, to ensure success of the design.

# 11.5.4.3.1 Size of Isolator Units

The design properties of the seismic isolator units are established based on the calculations of ELF demand, recognizing that dynamic analysis is required to verify these properties (and will likely justify slightly more lenient properties). The key parameters influencing size are:

- 1. Peak displacement of isolator units,
- 2. Average long-term (gravity) load on all isolator units,
- 3. Maximum long-term (gravity) load on individual isolator units, and
- 4. Maximum short-term load on individual isolator units (gravity plus MCE loads) including maximum uplift displacement.

These parameters are summarized in *Guide* Table 11.5-9. Loads or displacements on individual isolator units are taken as the maximum load or displacement on all isolator units (since the design is based on only one size of isolator unit). Reduced live load is used for determining long-term loads on isolators.

Key Design Parameter	ELF Procedure or Gravity Analysis	Dynamic Analysis Limit
DE displacement at corner of building $(D_{TD})$	19.7 in. [A1]	> 17.7 in. [A1]
MCE displacement at corner of building $(D_{TM})$	29.6 in. [A1]	> 23.7 in. [A1]
Average long-term load $(1.0D + 0.5L)$	477 kips [ALL]	N/A
Maximum long-term load $(1.2D + 1.6L)$	1,053 kips [C4]	N/A
DE max short-term load $(1.4D + 0.5L + Q_{DE})$	1,519 kips [B2]	N/A
DE minimum short-term load (0.7D - $Q_{DE}$ )	150 kips uplift [A2]	N/A
MCE max short-term load $(1.5D + 1.0L + Q_{MCE})$	2,006 kips [B2]	N/A
MCE minimum short-term load ( $0.8D - Q_{MCE}$ )	0.94 in. uplift [A2]	N/A

 Table 11.5-9
 Summary of Key Design Parameters [isolator unit location]

1.0 in. = 25.4 mm, 1.0 kip = 4.45 kN.

As rule of thumb, elastomeric isolators should have a diameter, excluding the protective layer of cover, of no less than 1.25 times maximum earthquake displacement demand. In this case, the full displacement determined by the ELF procedure would require an isolator diameter of:

 $\emptyset_{ISO} \ge 1.25(29.6) = 37$  in. (0.95 m)

If justified by dynamic analysis, then 80 percent of the ELF procedure displacement would require an isolator diameter of:

$$\emptyset_{ISO} \ge 1.25(23.7) = 30$$
 in. (0.75 m)

For this example, a single size of isolator unit is selected with a nominal diameter of no less than 35.4 in. (0.90 m). Although the maximum vertical loads vary enough to suggest smaller diameter of isolator units at certain locations (such as at building corners), all of the isolator units must be large enough to sustain MCE displacements; which are largest at building corners, due to torsion. An isolator unit with a diameter of 35.4 in., has a corresponding bearing area of about  $A_b = 950$  square in. The maximum long-term face pressure is about 1,100 psi (i.e., 1,053 kips/950 in.<sup>2</sup>), which is less than the limit for most elastomeric bearing compounds. Average long-term face pressure is about 500 psi (i.e., 477 kips/950 in.<sup>2</sup>) indicating the reasonably good distribution of loads among all isolator units.

The minimum effective stiffness is 6.9 kips/in. per isolator unit at the design displacement (i.e., about 16 in.). The height of the isolator unit is primarily a function of the height of the rubber,  $h_r$ , required to achieve this stiffness, given the bearing area,  $A_b$ , and the effective stiffness of the rubber compound. The EOC design accommodates rubber compounds with minimum effective shear modulus (at 150 percent shear strain) ranging from  $G_{150\%}$  = 65 psi to 110 psi. Numerous elastomeric bearing manufacturers have rubber compounds with a shear modulus that falls within this range. Since rubber compounds (and in particular, high-damping rubber compounds) are nonlinear, the effective stiffness used for design must be associated with a shear strain that is close to the strain level for the design earthquake (e.g., 150 percent shear strain). For a minimum effective shear modulus of 65 psi, the total height of the rubber,  $h_r$ , would be:

$$h_r = \frac{G_{150\%} A_b}{k_{eff}} = \frac{65 \text{ lb/in.}^2 \times 950 \text{ in.}^2}{6,900 \text{ lb/in.}} = 8.9 \text{ in.} \cong 9 \text{ in.}$$

The overall height of the isolator unit, H, including steel shim and flange plates, would be about 15 in. For compounds with an effective minimum shear modulus of 110 psi, the rubber height would be proportionally taller (about 15 in.), and the total height of the isolator unit would be about 24 in.

# 11.5.4.3.2 Typical Isolation System Detail

For the EOC design, the isolation system has a similar detail at each column, as shown in Figure 11.5-11. The column has an extra large base plate that bears directly on the top of the isolator unit. The column base plate is circular, with a diameter comparable to that of the top plate of the isolator unit. Heavy, first floor girders frame into, and are moment connected to the columns (moment connections are required at this floor only). The columns and base plates are strengthened by plates that run in both horizontal directions, from the bottom flange of the girder to the base. Girders are stiffened above the seat plates, and at temporary jacking locations. The top plate of the isolator unit is bolted to the column base plate, and the bottom plate of the isolator unit is bolted to the foundation.

The foundation connection accommodates the removal and replacement of isolator units, as required by *Provisions* Sec. 13.6.2.8 [13.2.5.8]. The bottom plate of the isolator unit bears on a steel plate, that has a shear lug at the center grouted to the reinforced concrete foundation. Anchor bolts pass through holes in this plate and connect to threaded couplers that are attached to deeply embedded rods.

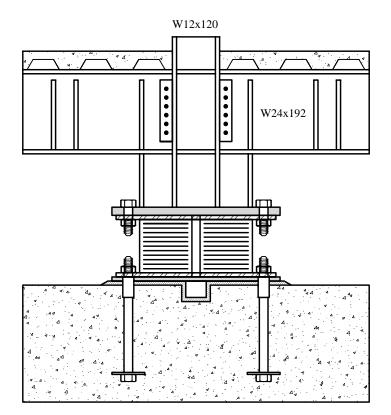


Figure 11.5-11 Typical detail of the isolation system at columns (for clarity, some elements not shown).

With the exception of the portion of the column above the first floor slab, each element shown in Figure 11.5-11 is an integral part of the isolation system (or foundation), and is designed for the gravity and

unreduced design earthquake loads. In particular, the first floor girder, the connection of the girder to the column, and the connection of the column to the base plate, are designed for gravity loads and forces caused by horizontal shear and P-delta effects due to the unreduced design earthquake load (as shown earlier in Figure 11.4-1).

#### 11.5.4.3.3 Design of Connections of Isolator Units

Connection of the top plate of the isolator unit, to the column base plate; and the connection of the bottom plate to the foundation, are designed for load combinations that include maximum downward forces  $(1.4D + 0.5L + Q_{DE})$ , and minimum downward (uplift) forces  $(0.7D - Q_{DE})$ . The reactions to bolts at the top and bottom plates of isolator units (ignoring shear friction and shear capacity of the lug at the base) are approximately equal, and include shear, axial load, and moment, in the most critical direction of response for individual bolts. Moments include the effects of P-delta and horizontal shear across the isolator unit, as described by the equations shown in Figure 11.4-1:

$$M = \frac{P\Delta}{2} + \frac{VH}{2}$$

In this case,  $H_1 = H_2 = H/2$ , where *H* is the height of the isolator unit (assumed to be 24 in., the maximum permissible height of isolator units). For maximum downward acting loads, maximum tension on any one of *N* (12) uniformly spaced bolts located in a circular pattern of diameter,  $D_b$ , must be equal to 43 in. and is estimated as follows:

$$F = \left(\frac{M}{S} - \frac{P}{A_b}\right) \frac{A_b}{N} = \left(\frac{4M}{A_b \cdot D_b} - \frac{P}{A_b}\right) \frac{A_b}{N} = \frac{1}{N} \left(\frac{4M}{D_b} - P\right) = \frac{1}{N} \left(\frac{2(P\Delta + VH)}{D_b} - P\right)$$
$$= \frac{1}{12} \left(\frac{2(1,519 \text{ kips})(19.7 \text{ in.}) + 175 \text{ kips}(24 \text{ in.})}{43 \text{ in.}} - 1,519 \text{ kips}\right) = \frac{1,587 - 1,519}{12} \approx 6 \text{ kips}$$

In this calculation, the vertical load, P = 1,519 kips, is the maximum force occurring at Column B2, the deflection is based on  $D_{TD} = 19.7$  in., and the shear force is calculated as V = 8.9 kips/in. × 19.7 in. The calculation indicates only a modest amount of tension force in anchor bolts, due to the maximum downward loads on the isolator units. However, the underlying assumption of the plane section's remaining plane is not conservative if top and bottom flange plates yield during a large lateral displacement of the isolator units. Rather than fabricate bearings with overly thick flange plates, manufacturers usually recommend anchor bolts that can carry substantial amounts of shear and tension, which can arise due to local bending of flanges.

Tension forces in anchor bolts can occur due to local uplift of isolator units. The ETABS model did not calculate uplift forces, since it was assumed that the isolator units would yield in tension. An estimate of the uplift load may be based on a maximum tension yield stress of about 150 psi, which produces a tension force,  $F_t$ , of no more than 150 kips for isolator units with a bearing area of 950 in.<sup>2</sup> Applying uplift and shear loads to the isolator unit, the maximum tension force in each bolt is estimated at:

$$F_{t} = \left(\frac{M}{S} + \frac{P}{A_{b}}\right) \frac{A_{b}}{N} = \frac{1}{N} \left(\frac{2(P\Delta + VH)}{D_{b}} + P\right)$$
$$= \frac{1}{12} \left(\frac{2(150 \text{ kips}(19.7 \text{ in.}) + 175 \text{ kips}(24 \text{ in.})}{43 \text{ in.}} + 150 \text{ kips}\right) = \frac{333 + 150}{12} \approx 40 \text{ kips}$$

The maximum shear load per bolt is:

$$F_v = \frac{V}{N} = \frac{175}{12} \cong 15 \text{ kips}$$

Twelve 1<sup>1</sup>/<sub>4</sub>-in. diameter anchor bolts of A325 material are used for these connections. Alternatively, eight 1<sup>1</sup>/<sub>2</sub>-in. diameter bolts are permitted for isolator units manufactured with eight, rather than twelve, bolt holes. Bolts are tightened as required for a slip-critical connection (to avoid slip in the unlikely event of uplift).

Design of stiffeners and other components of the isolation system detail are not included in this example, but would follow conventional procedures for design loads. Design of the isolator unit including top and bottom flange plates is the responsibility of the manufacturer. *Guide* Sec. 11.5.6 includes example performance requirements of specifications that govern isolator design (and testing) by the manufacturer.

# 11.5.5 Design Verification Using Nonlinear Time History Analysis

The design is verified (and in some cases isolation system design properties are improved) using time history analysis of models that explicitly incorporate isolation system nonlinearity, including lateral force-deflection properties and uplift of isolator units, which are subject to net tension loads. Using three sets of horizontal earthquake components the EOC is analyzed separately for design earthquake (DE) and MCE ground shaking,. All analyses are repeated for two models of the EOC, one with upper-bound (UB) stiffness properties and the other with lower-bound (LB) stiffness properties of isolator units.

# 11.5.5.1 Ground Motion

Each pair of horizontal earthquake components is applied to the model in three different orientations relative to the principal axes of the building. Time histories are first applied to produce the maximum response along the X axis of the EOC model. The analyses are then repeated with the time histories, they are rotated 90° to produce the maximum response along the Y axis of the EOC model. Additionally, the time histories are rotated 45° to produce the maximum response along an X-Y line (to check if this orientation would produce greater response in certain elements than the two principal axis orientations). A total of 18 analyses (2 models × 3 component orientations × 3 sets of earthquake components) are performed separately for both DE and the MCE loads. Results are based on the maximum response of the parameter of interest calculated by each DE or MCE analysis, respectively. Parameters of interest include:

Design earthquake

- 1. Peak isolation system displacement
- 2. Maximum story shear forces (envelope over building height)

Maximum considered earthquake

- 1. Peak isolation system displacement
- 2. Maximum downward load on any isolator unit  $(1.5D + 1.0L + Q_{MCE})$
- 3. Maximum uplift displacement of any isolator unit (0.8L  $Q_{\text{MCE}}$ ).

# 11.5.5.2 Bilinear Stiffness Modeling of Isolator Units

Nonlinear force-deflection properties of the isolator units are modeled using a bilinear curve; whose hysteretic behavior is a parallelogram, which is supplemented by a small amount of viscous damping. A bilinear curve is commonly used to model the nonlinear properties of elastomeric bearings; although other approaches are sometimes used, including a trilinear curve that captures stiffening effects of some rubber compounds at very high strains.

Using engineering judgement, the initial stiffness, the yield force, the ratio of post-yield to pre-yield stiffness for the bilinear curves, and the amount of supplementary viscous damping,  $\beta_v$ , are selected. The effective stiffness and effective damping values are used for preliminary design. The lower-bound bilinear stiffness curve is based on  $k_{Dmin} = 6.9$  kips/in. (rounded to 7 kips/in.). The upper-bound bilinear stiffness curve is based on an effective stiffness of  $k_{Dmax} = 8.9$  kips/in. times 1.2 (which the result is rounded to 11 kips/in.). The 1.2 factor is taken into account for the effects of aging over the design life of the isolators. Both upper-bound and lower-bound stiffness curves are based on effective damping (combined hysteretic and supplementary viscous) of  $\beta_D \cong 15$  percent. Figure 11.5-12 illustrates upper-bound and lower-bound bilinear stiffness curves, and summarizes the values of the parameters that define these curves.

For isolators with known properties, parameters defining bilinear stiffness may be based on test data provided by the manufacturer. For example, the bilinear properties shown in Figure 11.5-12, are compared with effective stiffness and effective damping test data that are representative of a HK090H6 high-damping rubber bearing manufactured by Bridgestone Engineered Products Company, Inc. Bridgestone is one of several manufacturers of high-damping rubber bearings and provides catalog data on design properties of standard isolators. The HK090H6 bearing has a rubber height of about 10 in., a diameter of 0.9 m, without the cover, and a rubber compound with a relatively low shear modulus (less than 100 psi at high strains).

Plots of the effective stiffness and damping of the HK090H6 bearing, are shown in Figure 11.5-13 (solid symbols), and are compared with plots of the calculated effective stiffness and damping (using the equations from Figure 11.4-2 and the bilinear stiffness curves shown in Figure 11.5-12). The effective stiffness curve of the HK090H6 bearing, is based on data from the third cycle of testing; and therefore, best represents the minimum effective (or lower-bound) stiffness. The plots indicate the common trend in effective stiffness of high-damping elastomeric bearings– significant softening up to 100 percent shear strain, fairly stable stiffness from 100 percent to 300 percent shear strain, and significant stiffening beyond 300 percent shear strain. The trend in effective damping is a steady decrease in damping with amplitude beyond about 150 percent shear strain.

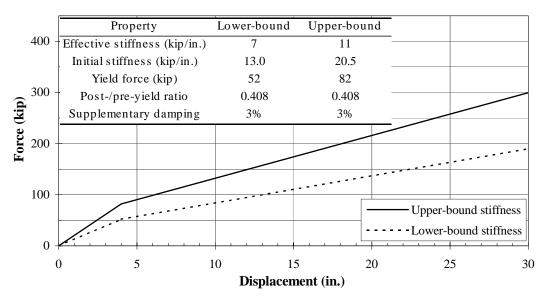


**Figure 11.5-12** Stiffness and damping properties of EOC isolator units (1.0 in. = 25.4 mm, 1.0 kip = 4.45 kN).

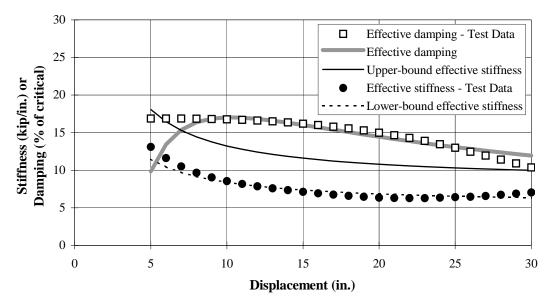


Figure 11.5-13 Comparison of modeled isolator properties to test data (1.0 in. = 25.4 mm, 1.0 kip/in. = 0.175 kN/mm).

The effective stiffness and damping of the bilinear stiffness curves capture the trends of the HK090H6 bearing reasonably well, as shown in Figure 11.5-13. Lower-bound effective stiffness fits the HK090H6 data well for response amplitudes of interest (i.e., the displacements in the range of about 15 in. through 25 in.). Likewise, the effective damping of the bilinear stiffness curves, is conservatively less than the effective damping based on test data for the same displacement range. These comparisons confirm that the bilinear stiffness properties of isolator units used for nonlinear analysis, are valid characterizations of the force-deflection properties of the Bridgestone HK090H6 bearing, also presumably, the bearings of other manufacturers that have comparable values of effective stiffness and damping.

#### 11.5.5.3 Summary of Results for Time History Analyses

Tables 11.5-10 and 11.5-11, compare the results of the design earthquake and maximum considered earthquake time history analyses, respectively, with the corresponding values calculated using the ELF procedure. The peak response values noted for the time history analyses are, the maxima of X-axis and Y-axis directions of response. Because torsional effects were neglected in the time history analyses for this example, the displacement at the corner of the EOC was assumed to be 1.1 times the center displacement; this assumption may not be conservative. The reported shears occur below the indicated level.

Response parameter	ELF	Tim	Time history analysis		
	procedure	Peak response	Model	Record	
Isola	tion system disp	lacement (in.)			
Displacement at center of EOC, $D_D$	16.3 in.	14.3 in.	LB	Sulmor	
Displacement at corner of EOC, $D_{TD}$	19.7 in.	15.7 in.*	stiffness	Sylmar	
Superstr	ructure forces –	story shear (kips)			
Penthouse roof	740 kips	400 kips			
Roof (penthouse)	2,780 kips	1,815 kips			
Third floor	4,160 kips	3,023 kips	UB stiffness	Newhall	
Second floor	4,940 kips	4,180 kips			
First floor	5,100 kips	5,438 kips			

Table 11.5-10         Design Earthquake Response Parameters - Results of ELF Procedure and Nonlinear
Time History Analysis

1.0 in. = 25.4 mm, 1.0 kip = 4.45 kN.

\* Displacement includes an arbitrary 10 percent increase for possible torsional response.

Table 11.5-11         Maximum Considered Earthquake Response Parameters – Results of ELF Procedure
and Nonlinear Time History Analysis

Response parameter	ELF procedure	Time	history analys	is
		Peak response	Model	Record
Displacement at center of EOC, $D_M$	24.5 in.	26.4 in.	LB	El Centro
Displacement at corner of EOC, $D_{TM}$	29.7 in.	29.0 in. <sup>1</sup>	stiffness	No. 6

1.0 in. = 25.4 mm.

\* Displacement includes an arbitrary 10 percent increase for possible torsional response.

The results of the design earthquake time history analyses, verify that the results of the ELF procedure are generally conservative. A design displacement of 16 in., and total design displacement of 20 in., are conservative bounds on calculated displacements, even if significant torsion should occur. The story shears calculated using the ELF procedure, are larger than those from the dynamic analyses at all superstructure elevations. The higher the elevation, the larger the margin between the story shears, which is an indication that the inverted triangular pattern (the results from *Provisions* Eq. 13.3.5 [13.3-9]), produces conservative results. At the second story (below the third floor), the critical level for the brace design the story shear from the dynamic analyses (3,023 kips) is only about three-quarters of the story shear from the ELF procedure (4,160 kips). The results of the MCE time history analyses show that the ELF procedure can underestimate the maximum displacement. Accordingly, a maximum displacement of 27 in., and total maximum displacement of 30 in., are used for the design specifications.

Tables 11.5-12 and 11.5-13, respectively, report the maximum downward forces on isolator units and the maximum uplift displacements determined from the maximum considered earthquake time history analyses.

These tables report two values for each isolator location representing both the X-axis and Y-axis orientations of the strongest direction of shaking of the time history record.

140	<b>Tuble 11.3-12</b> Maximum Downward Force (Rips) on isolator Onits ( $1.5D + 1.0L + Q_{MCE}$ )				
	Upper-bound s	tiffness model – Newha	all record – X-axis/Y-a	axis orientations	
Column line	1	2	3	4	
А	<u>417</u> /411	930/ <u>1,076</u>	651/ <u>683</u>	889/ <u>1,027</u>	
В	<u>1,048</u> /881	1,612/ <u>1,766</u>	<u>1,696</u> /1,588	1,308/ <u>1,429</u>	
С	<u>656</u> /628	<u>1,145</u> /1,127	<u>1,301</u> /1,300	<u>1,319</u> /1,318	

**Table 11.5-12** Maximum Downward Force (kips) on Isolator Units  $(1.5D + 1.0L + Q_{MCE})^*$ 

1.0 kip = 4.45 kN.

\* Forces on Column Lines 5, 6 and 7 (not shown) are enveloped by those on Column Lines 3, 2, and 1, respectively; forces on Column Lines D and E (not shown) are enveloped by those on Column Lines B and A, respectively.

	Upper-bound sti	ffness model – Newha	ll record – X-axis/Y-a	axis orientations
Column line	1	2	3	4
А	No uplift	0.00/ <u>0.39</u>	No uplift	0.00/ <u>0.17</u>
В	<u>0.26</u> /0.00	0.19/ <u>0.12</u>	No uplift	No uplift
С	No uplift	No uplift	No uplift	No uplift

**Table 11.5-13** Maximum Uplift Displacement (in.) Of Isolator Units  $(0.8D - Q_{MCE})^1$ 

1.0 in. = 25.4 mm.

\* Displacement on Column Lines 5, 6 and 7 (not shown) enveloped by those on Column Lines 3, 2, and 1, respectively; displacement on Column Lines D and E (not shown) are enveloped by those on Column Lines B and A, respectively.

Table 11.5-12 indicates a maximum downward force of 1,766 kips (at column B2), which is somewhat less than the value predicted using the ELF procedure (2,006 kips in Table 11.5-7). Table 11.5-13 includes the results from the controlling analysis, and indicates a maximum uplift displacement of 0.39 in. (at column A2), which is significantly less than the value predicted using the ELF procedure (0.94 in. as noted in Table 11.5-8). Based on these results, the design specification (*Guide* Sec. 11.5.2.10) uses values of 2,000 kips maximum downward force and  $\frac{1}{2}$  in. of maximum uplift displacement.

# 11.5.6 Design and Testing Criteria for Isolator Units

Detailed design of the isolator units for the EOC facility, is the responsibility of the bearing manufacturer subject to the design and testing (performance) of the criteria included in the construction documents (drawings and/or specifications). Performance criteria typically includes a basic description, and requirements for isolator unit sizes, the design life and durability, the environmental loads and fire-resistance criteria, Quality Assurance and Quality Control (including QC testing of production units), the design forces and displacements, and prototype testing requirements. This section summarizes key data and performance criteria for the EOC, including the criteria for prototype testing of isolator units, as required by *Provisions* Sec. 13.9.2 [13.6.1].

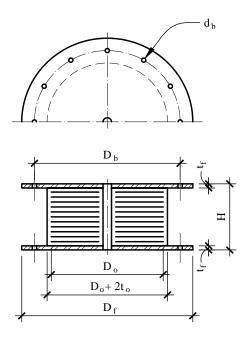


Figure 11.5-14 Isolator dimensions.

#### 11.5.6.1 Dimensions and Configuration

Steel shim plate diameter,  $D_o \ge 35.4$  in.

Rubber cover thickness,  $t_o \ge 0.5$  in.

Rubber layer thickness,  $t_r \leq 0.375$  in.

Gross rubber diameter,  $D_o + 2t_o \le 38$  in.

Bolt pattern diameter,  $D_b = 43$  in.

Bolt hole diameter,  $d_b = 1.5$  in.

Steel flange plate diameter,  $D_f = 48$  in.

Steel flange plate thickness,  $t_f \ge 1.5$  in.

Total height,  $H \leq 24$  in.

#### 11.5.6.2 Prototype Stiffness and Damping Criteria

Minimum effective stiffness (third cycle of test, typical vertical load)	$k_{Dmin}, k_{Mmin} \ge 7.0$ kips/in.
Maximum effective stiffness (first cycle test, typical vertical load)	$k_{Dmax}$ , $k_{Mmax} \leq 9.0$ kips/in.

The  $k_{Dmin}$ ,  $k_{Dmax}$ ,  $k_{Mmin}$ , and  $k_{Mmax}$ , are properties of the isolation system as a whole (calculated from the properties of individual isolator units using Provisions Eq. 13.9.5.1-1 through 13.9.5.1-4 [13.6-3 through 13.6-6]). Individual isolator units may have stiffness properties that fall outside the limits (by, perhaps, 10 percent), provided the average stiffness of all isolator units complies with the limits.

Effective damping (minimum of three cycles of test, typical vertical load) (minimum of three cycles of test, typical vertical load)	$\beta_D \ge 15$ percent $\beta_M \ge 12$ percent
Vertical Stiffness (average of three cycles of test, typical vertical load ± 50 percent)	$k_{\nu} \ge$ 5,000 kips/in.
11.5.6.3 Design Forces (Vertical Loads)	
Maximum long-term load (individual isolator)	1.2D + 1.6L = 1,200 kips
Typical load - cyclic load tests (average of all isolators)	1.0D + 0.5L = 500 kips
Upper-bound load - cyclic load tests (all isolators)	1.2D + 0.5L +  E  = 750 kips
Lower-bound load - cyclic load tests (all isolators)	0.8D -  E  = 250 kips
Maximum short-term load (individual isolator)	1.2D + 1.0L +  E  = 2,000 kips
Minimum short-term load (individual isolator)	0.8D -  E  = tension force due to $\frac{1}{2}$ in. of uplift
11.5.6.4 Design Displacements	
Design earthquake displacement	$D_D = 16$ in.
Total design earthquake displacement	$D_{TD} = 20$ in.
Maximum considered earthquake displacement	$D_M = 27$ in.
Total maximum considered earthquake displacement	$D_{TM} = 30$ in.

# 11.5.6.5 Prototype Testing Criteria

Table 11.5-14 summarizes the prototype test criteria found in *Provisions* Sec. 13.9.2 [13.6.1] as well as the corresponding loads on isolator units of the EOC.

	<b>Table 11.5-</b>	14 Prototype Test F	Requirements	
	Provision	es criteria	EOC c	riteria
No. of cycles	Vertical load	Lateral load	Vertical load	Lateral load
		Vertical stiffness tes	st	
3 cycles	Typical $\pm$ 50%	None	$500 \pm 250$ kips	None
Cyclic	load tests to check w	vind effects (Provisi	ons Sec. 13.9.2.3 [13.6	.1.2])
20 cycles	Typical	Design force	500 kips	$\pm 20 \ kips$
Cyclic load tests	to establish effective	stiffness and damping	ng (Provisions Sec. 13.	9.2.3 [13.6.1.2])
3 cycles	Typical	$0.25D_{D}$	500 kips	$\pm 4$ in.
3 cycles	Upper-bound*	$0.25D_{D}$	750 kips	± 4 in.
3 cycles	Lower-bound*	$0.25D_{D}$	250 kips	± 4 in.
3 cycles	Typical	$0.5D_D$	500 kips	$\pm$ 8 in.
3 cycles	Upper-bound*	$0.5D_D$	750 kips	$\pm$ 8 in.
3 cycles	Lower-bound*	$0.5D_D$	250 kips	$\pm$ 8 in.
3 cycles	Typical	$1.0D_D$	500 kips	± 16 in.
3 cycles	Upper-bound*	$1.0D_D$	750 kips	± 16 in.
3 cycles	Lower-bound*	$1.0D_D$	250 kips	± 16 in.
3 cycles	Typical	$1.0D_M$	500 kips	$\pm 27$ in.
3 cycles	Upper-bound*	$1.0D_M$	750 kips	$\pm 27$ in.
3 cycles	Lower-bound*	$1.0D_M$	250 kips	± 27 in.
3 cycles	Typical	$1.0D_{TM}$	500 kips	± 30 in.
Cycl	ic load tests to check	durability (Provisio	ns Sec. 13.9.2.3 [13.6.1	.2])
$30S_{Dl}/S_{DS}B_{D}(=20)^{**}$	Typical load	$1.0D_{TD}$	500 kips	$\pm 20$ in.
Stat	ic load test of isolator	stability (Provision	es Sec. 13.9.2.6 [13.6.1.	.5])
N/A	Maximum	$1.0D_{TM}$	2,000 kips	30 in.
N/A	Minimum	$1.0D_{TM}$	<sup>1</sup> ∕₂-in. of uplift	30 in.

1.0 in. = 25.4 mm, 1.0 kip = 4.45 kN.

\* Tests with upper-bound and lower-bound vertical loads are required by *Provisions* Sec. 13.9.2.3 [13.6.1.2] for isolator units that are vertical-load-carrying elements.

\*\* The *Provisions* contains a typographical error where presenting this expression. The errata to the *Provisions* correct the error.

12

# NONBUILDING STRUCTURE DESIGN

# Harold O. Sprague Jr., P.E.

Chapter 14 of the 2000 *NEHRP Recommended Provisions* and *Commentary* (hereafter, the *Provisions* and *Commentary*) is devoted to nonbuilding structures. Nonbuilding structures comprise a myriad of structures constructed of all types of materials with markedly different dynamic characteristics and a wide range of performance requirements.

Nonbuilding structures are a general category of structure distinct from buildings. Key features that differentiate nonbuilding structures from buildings include human occupancy, function, dynamic response, and risk to society. Human occupancy, which is incidental to most nonbuilding structures, is the primary purpose of most buildings. The primary purpose and function of nonbuilding structures can be incidental to society or the purpose and function can be critical for society.

In the past, many nonbuilding structures were designed for seismic resistance using building code provisions developed specifically for buildings. These code provisions were not adequate to address the performance requirements and expectations that are unique to nonbuilding structures. For example consider secondary containment for a vertical vessel containing hazardous materials. Nonlinear performance and collapse prevention, which are performance expectations for buildings, are inappropriate for a secondary containment structure, which must not leak.

Traditionally, the seismic design of nonbuilding structures depended on the various trade organizations and standards development organizations that were disconnected from the building codes. The *Provisions* have always been based upon strength design and multiple maps for seismic ground motion definition, whereas most of the industry standards were based on allowable stress design and a single zone map. The advent of the 1997 *Provisions* exacerbated the problems of the disconnect for nonbuilding structures with direct use of seismic spectral ordinates, and with the change to a longer recurrence interval for the seismic ground motion. It became clear that a more coordinated effort was required to develop appropriate seismic design provisions for nonbuilding structures.

This chapter develops examples specifically to help clarify Chapter 14 of the *Provisions*. The solutions developed are not intended to be comprehensive but instead focus on interpretation of *Provisions* Chapter 14 (Nonbuilding Structure Design Requirements). Complete solutions to the examples cited are beyond the scope of this chapter.

Although this volume of design examples is based on the 2000 *Provisions*, it has been annotated to reflect changes made to the 2003 *Provisions*. Annotations within brackets, [], indicate both organizational changes (as a result of a reformat of all of the chapters of the 2003 *Provisions*) and substantive technical changes to the 2003 *Provisions* and its primary reference documents. While the general concepts of the changes are described, the design examples and calculations have not been revised to reflect the changes to the 2003 *Provisions*.

Several noteworthy changes were made to the nonbuilding structures requirements of the 2003 *Provisions*. These include clearer definition of the scopes of Chapters 6 and 14, expanded, direct definition of structural systems (along with design parameters and detailing requirements) in Chapter 14, and a few specific changes for particular nonbuilding structural systems.

In addition to changes *Provisions* Chapter 14, the basic earthquake hazard maps were updated, the redundancy factor calculation was completely revised, and the minimum base shear equation for areas without near-source effects was eliminated.

Where they affect the design examples in this chapter, significant changes to the 2003 *Provisions* and primary reference documents are noted. However, some minor changes to the 2003 *Provisions* and the reference documents may not be noted.

In addition to the Provisions and Commentary, the following publications are referenced in this chapter:

United States Geological Survey, 1996. Seismic Design Parameters (CD-ROM) USGS.

[The 2003 *Provisions* have adopted the 2002 USGS probabilistic seismic hazard maps, and the maps have been added to the body of the 2003 *Provisions* as figures in Chapter 3 (instead of the previously used separate map package). The CD-ROM also has been updated.]

American Water Works Association. 1996. Welded Steel Tanks for Water Storage. AWWA.

American Petroleum Institute (API), Welded steel tanks for oil storage. API 650, 10<sup>th</sup> Edition, November 1998.

# 12.1 NONBUILDING STRUCTURES VERSUS NONSTRUCTURAL COMPONENTS

Many industrial structures are classified as either nonbuilding structures or nonstructural components. This distinction is necessary to determine how the practicing engineer designs the structure. The intent of the *Provisions* is to provide a clear and consistent design methodology for engineers to follow regardless of whether the structure is a nonbuilding structure or a nonstructural component. Central to the methodology is how to determine which classification is appropriate.

The design methodology contained in *Provisions* Chapter 6, Architectural, Mechanical, and Electrical Components Design Requirements, focuses on nonstructural component design. As such, the amplification by the supporting structure of the earthquake-induced accelerations is critical to the design of the component and its supports and attachments. The design methodology contained in *Provisions* Chapter 14 focuses on the direct effects of earthquake ground motion on the nonbuilding structure.

Supporting	Supported Item					
Structure	Nonstructural Component	Nonbuilding Structure				
Building	Chapter 5 [4 and 5]for supporting structure	Chapter 5 [4 and 5]for supporting structure				
C C	Chapter 6 for supported item	Chapter 14 for supported item				
Nonbuilding	Chapter 14 for supporting structure Chapter 6 for supported item	Chapter 14 for both supporting structure and supported item				

 Table 12-1
 Applicability of the Chapters of the Provisions

The example shown in Figure 12-1 is a combustion turbine, electric-power-generating facility with four bays. Each bay contains a combustion turbine and supports an inlet filter on the roof. The uniform seismic dead load of the supporting roof structure is 30 psf. Each filter weighs 34 kips.

The following two examples illustrate the difference between nonbuilding structures that are treated as nonstructural components, using *Provisions* Chapter 6, and those which are designed in accordance with *Provisions* Chapter 14. There is a subtle difference between the two chapters:

6.1: "... if the combined weight of the supported *components* and *nonbuilding structures* with flexible dynamic characteristics exceeds 25 percent of the weight of the *structure*, the *structure* shall be designed considering interaction effects between the *structure* and the supported items."

14.4: "If the weight of a *nonbuilding structure* is 25 percent or more of the combined weight of the *nonbuilding structure* and the supporting *structure*, the design seismic forces of the *nonbuilding structure* shall be determined based on the combined *nonbuilding structure* and supporting structural system...."

The difference is the plural *components* and the singular *nonbuilding structure*, and that difference is explored in this example.

[The text has been cleaned up considerably in the 2003 edition but some inconsistencies persist. Sec. 14.1.5 indicates the scopes of Chapters 6 and 14. Both chapters consider the weight of an individual supported component or nonbuilding structure in comparison to the total seismic weight. Where the weight of such an individual item does not exceed 25 percent of the seismic weight, forces are determined in accordance with Chapter 6. Where a nonbuilding structure's weight exceeds 25 percent of the seismic weight, Sec. 14.1.5 requires a combined system analysis and the rigidity or flexibility of the supported nonbuilding structure is used in determining the R factor. In contrast, Sec. 6.1.1 requires consideration of interaction effects only where the weight exceeds 25 percent of the seismic weight and the supported item has flexible dynamic characteristics.]

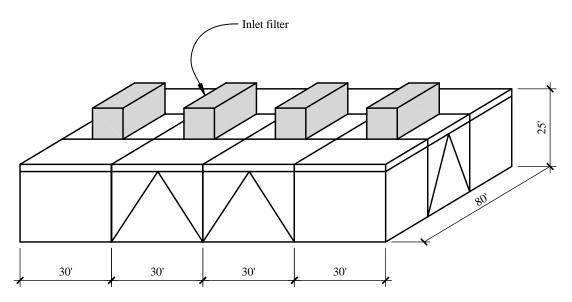


**Figure 12-1** Combustion turbine building (1.0 ft = 0.3048 m).

#### 12.1.1 Nonbuilding Structure

For the purpose of illustration assume that the four filter units are connected in a fashion that couples their dynamic response. Therefore, the plural components used in *Provisions* Sec. 6.1 is apparently the most meaningful provision.

[The text no longer contains a plural, but conceptually the frame could be considered a single item in this instance (just as the separate items within a single roof-top unit would be lumped together).]

# 12.1.1.1 Calculation of Seismic Weights

All four inlet filters =  $W_{IF}$  = 4(34 kips) = 136 kips

Support structure =  $W_{SS}$  = 4 (30 ft)(80 ft)(30 psf) = 288 kips

The combined weight of the nonbuilding structure (inlet filters) and the supporting structural system is

 $W_{combined} = 136 \text{ kips} + 288 \text{ kips} = 424 \text{ kips}$ 

# 12.1.1.2 Selection of Design Method

The ratio of the supported weight to the total weight is:

$$\frac{W_{IF}}{W_{Combined}} = \frac{136}{424} = 0.321 > 25\%$$

Because the weight of the inlet filters is 25 percent or more of the combined weight of the nonbuilding structure and the supporting structure (*Provisions* Sec. 14.4 [14.1.5]), the inlet filters are classified as "nonbuilding structures" and the seismic design forces must be determined from analysis of the combined seismic-resistant structural systems. This would require modeling the filters, the structural components of the filters, and the structural components of the combustion turbine supporting structure to determine accurately the seismic forces on the structural elements as opposed to modeling the filters as lumped masses. [See the discussion added to Sec. 12.1.]

# **12.1.2 NONSTRUCTURAL COMPONENT**

For the purpose of illustration assume that the inlet filters are independent structures, although each is supported on the same basic structure. In this instance, one filter is the nonbuilding structure. The question is whether it is heavy enough to significantly change the response of the combined system.

# 12.1.2.1 Calculation of Seismic Weights

One inlet filter =  $W_{IF}$  = 34 kips

Support structure =  $W_{SS}$  = 4 (30 ft)(80 ft)(30 psf) = 288 kips

The combined weight of the nonbuilding structures (all four inlet filters) and the supporting structural system is

 $W_{combined} = 4 (34 \text{ kips}) + 288 \text{ kips} = 424 \text{ kips}$ 

# 12.1.2.2 Selection of Design Method

The ratio of the supported weight to the total weight is:

$$\frac{W_{IF}}{W_{Combined}} = \frac{34}{424} = 0.08 < 25\%$$

Because the weight of an inlet filter is less than 25 percent of the combined weight of the nonbuilding structures and the supporting structure (*Provisions* Sec. 14.4 [14.1.5]), the inlet filters are classified as "nonstructural components" and the seismic design forces must be determined in accordance with *Provisions* Chapter 6. In this example, the filters could be modeled as lumped masses. The filters and the filter supports could then be designed as nonstructural components.

# 12.2 PIPE RACK, OXFORD, MISSISSIPPI

This example illustrates the calculation of design base shears and maximum inelastic displacements for a pipe rack using the equivalent lateral force (ELF) procedure.

# 12.2.1 Description

A two-tier, 12-bay pipe rack in a petrochemical facility has concentrically braced frames in the longitudinal direction and ordinary moment frames in the transverse direction. The pipe rack supports four runs of 12-in.-diameter pipe carrying naphtha on the top tier and four runs of 8-in.-diameter pipe carrying water for fire suppression on the bottom tier. The minimum seismic dead load for piping is 35 psf on each tier to allow for future piping loads. The seismic dead load for the steel support structure is 10 psf on each tier.

Pipe supports connect the pipe to the structural steel frame and are designed to support the gravity load and resist the seismic and wind forces perpendicular to the pipe. The typical pipe support allows the pipe to move in the longitudinal direction of the pipe to avoid restraining thermal movement. The pipe support near the center of the run is designed to resist longitudinal and transverse pipe movement as well as provide gravity support; such supports are generally referred to as fixed supports.

Pipes themselves must be designed to resist gravity, wind, seismic, and thermally induced forces, spanning from support to support.

If the pipe run is continuous for hundreds of feet, thermal/seismic loops are provided to avoid a cumulative thermal growth effect. The longitudinal runs of pipe are broken up into sections by providing thermal/seismic loops at spaced intervals. In Figure 12-2, it is assumed thermal/seismic loops are provided at each end of the pipe run.

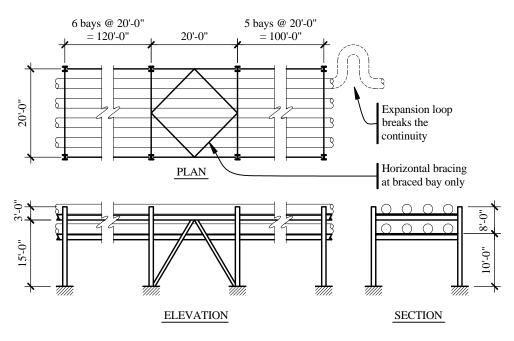


**Figure 12-2** Pipe rack (1.0 ft = 0.3048 m).

# 12.2.2 Provisions Parameters

# 12.2.2.1 Ground Motion

The spectral response acceleration coefficients at the site are

$$S_{DS} = 0.40$$
  
 $S_{DI} = 0.18.$ 

[The 2003 *Provisions* have adopted the 2002 USGS probabilistic seismic hazard maps, and the maps have been added to the body of the 2003 *Provisions* as figures in Chapter 3 (instead of the previously used separate map package).]

# 12.2.2.2 Seismic Use Group and Importance Factor

The upper piping carries a hazardous material (naphtha) and the lower piping is required for fire suppression. The naphtha piping is included in *Provisions* Sec. 1.3.1, Item 11 [Sec. 1.2.1, Item 11], therefore, the pipe rack is assigned to Seismic Use Group III.

According to *Provisions* Sec. 14.5.1.2 [14.2.1], the importance factor, *I*, is 1.5 based on Seismic Use Group, Hazard, and Function. If these three measures yield different importance factors, the largest factor applies.

# 12.2.2.3 Seismic Design Category

For this structure assigned to Seismic Use Group III with  $S_{DS} = 0.40$  and  $S_{DI} = 0.18$ , the Seismic Design Category is D according to *Provisions* Sec. 4.2.1 [1.4].

# 12.2.3 Design in the Transverse Direction

[Chapter 14 has been revised so that it no longer refers to Table 4.3-1. Instead values for design coefficients and detailing requirements are provided with the chapter.]

#### 12.2.3.1 Design Coefficients

Using *Provisions* Table 14.5.1.1 [14.4-2] (which refers to *Provisions* Table 5.2.2 [4.3-1]), the parameters for this ordinary steel moment frame are

$$R = 4$$
$$\Omega_0 = 3$$
$$C_d = 3^{1/2}$$

[In the 2003 *Provisions*, *R* factor options are presented that correspond to required levels of detailing. R = 3.5,  $\Omega = 3$ ;  $C_d = 3$ .]

Ordinary steel moment frames are retained for use in nonbuilding structures such as pipe racks because they allow greater flexibility for accommodating process piping and are easier to design and construct than special steel moment frames.

#### 12.2.3.2 Seismic Response Coefficient

Using Provisions Eq. 5.4.1.1-1 [5.2-2]:

$$C_s = \frac{S_{DS}}{R/I} = \frac{0.4}{4/1.5} = 0.15$$

From analysis, T = 0.42 sec. For nonbuilding structures, the fundamental period is generally approximated for the first iteration and must be verified with final calculations. For many nonbuilding structures the maximum period limit contained in the first paragraph of *Provisions* Sec. 5.4.2 [5.2.2] is not appropriate. As a result, the examples in this chapter neglect that limit. Future editions of the *Provisions* will clarify that this limit does not apply to nonbuilding structures. [In the 2003 *Provisions*, Sec. 14.2.9 makes clear that the approximate period equations do not apply to nonbuilding structures.]

Using Provisions Eq. 5.4.1.1-2 [5.2-3],  $C_s$  does not need to exceed

$$C_s = \frac{S_{DI}}{T(R/I)} = \frac{0.18}{0.42(4/1.5)} = 0.161$$

Using Provisions Eq. 5.4.1.1-3,  $C_s$  shall not be less than

$$C_s = 0.044IS_{DS} = 0.044(1.5)(0.4) = 0.0264$$

[This minimum  $C_s$  value has been removed in the 2003 *Provisions*. In its place is a minimum  $C_s$  value for long-period structures, which is not applicable to this example.]

*Provisions* Eq. 5.4.1.1-1 [5.2-2] controls;  $C_s = 0.15$ .

#### 12.2.3.3 Seismic Weight

W = 2(20 ft)(20 ft)(35 psf + 10 psf) = 36 kips

12.2.3.4 Base Shear (Provisions Sec. 5.3.2 [5.2.1])

 $V = C_s W = 0.15(36 \text{ kips}) = 5.4 \text{ kips}$ 

#### 12.2.3.5 Drift

Although not shown here, drift of the pipe rack in the transverse direction was calculated by elastic analysis using the design forces calculated above. The calculated lateral drift,  $\delta_{xe} = 0.328$  in. Using *Provisions* Eq. 14.3.2.1 [5.2-15],

$$\delta_x = \frac{C_d \delta_{xe}}{I} = \frac{3.5(0.328 \text{ in.})}{1.5} = 0.765 \text{ in.}$$

The lateral drift must be checked with regard to acceptable limits. The acceptable limits for nonbuilding structures are not found in codes. Rather, the limits are what is acceptable for the performance of the piping. In general, piping can safely accommodate the amount of lateral drift calculated in this example. P-delta effects must also be considered and checked as required in *Provisions* Sec. 5.4.6.2 [5.2.6.2].

#### 12.2.3.6 Redundancy Factor

Some nonbuilding structures are designed with parameters from *Provisions* Table 5.2.2 [4.3-1]; if they are termed "nonbuilding structures similar to buildings". For such structures the redundancy factor applies, if the structure is in Seismic Design Category D, E, or F. Pipe racks, being fairly simple moment frames or braced frames, are in the category similar to buildings. Because this structure is assigned to Seismic Design Category D, *Provisions* Sec. 5.2.4.2 [4.3.3.2] applies. The redundancy factor is calculated as

$$\rho = 2 - \frac{20}{r_{max_x}\sqrt{A_x}}$$

where  $r_{\max_x}$  is the fraction of the seismic force at a given level resisted by one component of the vertical seismic-force-resisting system at that level, and  $A_x$  is defined as the area of the diaphragm immediately above the story in question. Some interpretation is necessary for the pipe rack. Considering the transverse direction, the seismic-force-resisting system is an ordinary moment resisting frame with only two columns in a single frame. The frames repeat in an identical pattern. The "diaphragm" is the pipes themselves, which are not rigid enough to make one consider the 240 ft length between expansion joints as a diaphragm. Therefore, for the computation of  $\rho$  in the transverse direction, each 20-by-20 ft bay will be considered independently.

The maximum of the sum of the shears in the two columns equals the story shear, so the ratio  $r_{max}$  is 1.0. The diaphragm area is simply the bay area:

$$A_{\rm r} = 20 \, {\rm ft} \times 20 \, {\rm ft} = 400 \, {\rm ft}^{2}$$

therefore,

$$\rho = 2 - \frac{20}{1.0\sqrt{400}} = 1.0$$

[The redundancy requirements have been changed substantially in the 2003 Provisions.]

#### 12.2.3.7 Determining E

*E* is defined to include the effects of horizontal and vertical ground motions as follows:

$$E = \rho Q_E \pm 0.2 \ S_{DS} D$$

where  $Q_E$  is the effect of the horizontal earthquake ground motions, which is determined primarily by the base shear just computed, and *D* is the effect of dead load. By putting a simple multiplier on the effect of dead load, the last term is an approximation of the effect of vertical ground motion. For the moment frame, the joint moment is influenced by both terms. *E* with the "+" on the second term when combined with dead and live loads will generally produce the largest negative moment at the joints, while *E* with the "-"on the second term when combined with the minimum dead load (0.9*D*) will produce the largest positive joint moments.

The *Provisions* also requires the consideration of an overstrength factor,  $\Omega_0$ , on the effect of horizontal motions in defining *E* for components susceptible to brittle failure.

$$E = \rho \ \Omega_0 \ Q_E \pm 0.2 \ S_{DS}$$

The pipe rack does not appear to have components that require such consideration.

# 12.2.4 Design in the Longitudinal Direction

[In the 2003 *Provisions*, Chapter 14 no longer refers to Table 4.3-1. Instead, Tables 14.2-2 and 14.2-3 have design coefficient values and corresponding detailing requirements for each system.]

#### 12.2.4.1 Design Coefficients

Using *Provisions* Table 14.5.1.1 [14.2-2] (which refers to *Provisions* Table 5.2.2 [4.3-1]), the parameters for this ordinary steel concentrically braced frame are:

$$R = 4$$
$$\Omega_0 = 2$$
$$C_d = 4^{1/2}$$

[The 2003 *Provisions* allow selection of appropriate design coefficients and corresponding detailing for several systems. In the case of this example, *R* would equal 5, but the calculations that follow are not updated.]

Where *Provisions* Table 5.2.2 [4.3-1] is used to determine the values for design coefficients, the detailing reference sections noted in the table also apply. A concentric braced frame has an assigned R of 5, but an R of 4 is used to comply with *Provisions* Sec. 5.2.2.2.1 [4.3.1.2.1].

[In the 2003 *Provisions*, Chapter 14 no longer refers to Table 4.3-1. Instead, Tables 14.2-2 and 14.2-3 have design coefficient values and corresponding detailing requirements for each system. Chapter 14 contains no requirements corresponding to that found in Sec. 4.3.1.2.1 (related to *R* factors for systems in orthogonal directions).]

#### 12.2.4.2 Seismic Response Coefficient

Using Provisions Eq. 5.4.1.1-1 [5.2-2]:

$$C_s = \frac{S_{DS}}{R/I} = \frac{0.4}{4/1.5} = 0.15$$

From analysis, T = 0.24 seconds. The fundamental period for nonbuilding structures, is generally approximated for the first iteration and must be verified with final calculations. For many nonbuilding structures the maximum period limit contained in the first paragraph of *Provisions* Sec. 5.4.2 [5.2.2] is not appropriate. As a result, the examples in this chapter neglect that limit. Future editions of the *Provisions* are expected to clarify that this limit does not apply to nonbuilding structures. [In the 2003 *Provisions*, Sec. 14.2.9 makes clear that the approximate period equations do not apply to nonbuilding structures.]

Using Provisions Eq. 5.4.1.1-2 [5.2-3],  $C_s$  does not need to exceed:

$$C_s = \frac{S_{D1}}{T(R/I)} = \frac{0.18}{0.24(4/1.5)} = 0.281$$

*Provisions* Sec. 14.5.1 [14.2.8] provides equations for minimum values of  $C_s$  that replace corresponding equations in *Provisions* Sec. 5.4.1.1 [5.2.1.1]. However, according to Item 2 of Sec. 14.5.1 [14.2.8, replacement of Chapter 5 equations for minima occurs only "for nonbuilding systems that have an *R* value provided in Table 14.5.1.1" [14.4-2]. In the present example the *R* values are taken from Table 5.2.2 so the minima defined in Sec. 5.4.1.1 apply. [In the 2003 *Provisions* this is no longer the case as reference to Table 4.3-1 has been eliminated. Since the example structure would satisfy exception 1 of Sec. 14.2.8 and the minimum base shear equation in Chapter 5 was removed, no additional minimum base shear must be considered.]

Using *Provisions* Eq. 5.4.1.1-3,  $C_s$  shall not be less than:

 $C_s = 0.044IS_{DS} = 0.044(1.5)(0.4) = 0.0264$ 

*Provisions* Eq. 5.4.1.1-1 [5.2-2] controls;  $C_s = 0.12$ .

# 12.2.4.3 Seismic Weight

W = 2(240 ft)(20 ft)(35 psf + 10 psf) = 432 kips

# 12.2.4.4 Base Shear

Using Provisions Eq. 5.3.2 [5.2-1]:

 $V = C_s W = 0.15(432 \text{ kips}) = 64.8 \text{ kips}$ 

#### 12.2.4.5 Redundancy Factor

For the longitudinal direction, the diaphragm is the horizontal bracing in the bay with the braced frames. However, given the basis for the redundancy factor, it appears that a more appropriate definition of  $A_x$  would be the area contributing to horizontal forces in the diagonal braces. Thus  $A_x = 20(240) = 4800$  ft<sup>2</sup>. The ratio  $r_x$  is 0.25; each of the four braces has the same stiffness, and each is capable of tension and compression. Therefore:

$$\rho = 2 - \frac{20}{0.25\sqrt{4800}} = 0.85 < 1.0$$
, use 1.0

[The redundancy requirements have been changed substantially in the 2003 Provisions.]

# 12.3 STEEL STORAGE RACK, OXFORD, MISSISSIPPI

This example uses the equivalent lateral force (ELF) procedure to calculate the seismic base shear in the east-west direction for a steel storage rack.

# 12.3.1 Description

A four-tier, five-bay steel storage rack is located in a retail discount warehouse. There are concentrically braced frames in the north-south and east-west directions. The general public has direct access to the aisles and merchandise is stored on the upper racks. The rack is supported on a slab on grade. The design operating load for the rack contents is 125 psf on each tier. The weight of the steel support structure is assumed to be 5 psf on each tier.

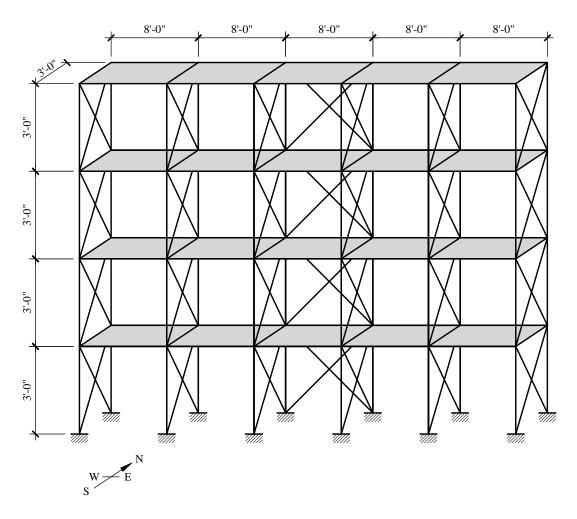


Figure 12-3 Steel storage rack (1.0 ft = 0.3048 m).

# 12.3.2 Provisions Parameters

# 12.3.2.1 Ground Motion

The spectral response acceleration coefficients at the site are as follows:

$$S_{DS} = 0.40$$
  
 $S_{DI} = 0.18$ 

[The 2003 *Provisions* have adopted the 2002 USGS probabilistic seismic hazard maps, and the maps have been added to the body of the 2003 *Provisions* as figures in Chapter 3 (instead of the previously used separate map package).]

#### 12.3.2.2 Seismic Use Group and Importance Factor

Use *Provisions* Sec. 1.3 [1.2]. The storage rack is in a retail facility. Therefore the storage rack is assigned to Seismic Use Group I. According to *Provisions* Sec. 14.6.3.1 and 6.1.5 [14.3.5.2],  $I = I_p = 1.5$  because the rack is in an area open to the general public.

#### 12.3.2.3 Seismic Design Category

Use *Provisions* Tables 4.2.1a and 4.2.1b [1.4-1 and 1.4-2]. Given Seismic Use Group I,  $S_{DS} = 0.40$ , and  $S_{DI} = 0.18$ , the Seismic Design Category is C.

# 12.3.2.4 Design Coefficients

According to Provisions Table 14.5.1.1 [14.2-3], the design coefficients for this steel storage rack are

$$R = 4$$
$$\Omega_0 = 2$$
$$C_d = 3\frac{1}{2}$$

# 12.3.3 Design of the System

#### 12.3.3.1 Seismic Response Coefficient

*Provisions* Sec. 14.6.3 [14.3.5]allows designers some latitude in selecting the seismic design methodology. Designers may use the Rack Manufacturer's Institute specification if they modify the equations to incorporate the seismic spectral ordinates contained in the *Provisions*; or they may use an *R* of 4 and use *Provisions* Chapter 5 according to the exception in *Provisions* Sec. 14.6.3.1. The exception is used in this example. [In the 2003 *Provisions* these requirements have been restructured so that the primary method is use of Chapter 5 with the design coefficients of Chapter 14; racks designed using the RMI method of Sec. 14.3.5.6 are deemed to comply.]

Using Provisions Eq. 5.4.1.1-1 [5.2-3]:

$$C_s = \frac{S_{DS}}{R/I} = \frac{0.4}{4/1.5} = 0.15$$

From analysis, T = 0.24 seconds. For this particular example the short period spectral value controls the design. The period, for taller racks, however, may be significant and will be a function of the operating weight. Using *Provisions* Eq. 5.4.1.1-2 [5.2-3],  $C_s$  does not need to exceed

$$C_s = \frac{S_{DI}}{T(R/I)} = \frac{0.18}{0.24(4/1.5)} = 0.281$$

*Provisions* Sec. 14.5.1 [14.2.8] provides equations for minimum values of  $C_s$  that replace corresponding equations in Sec. 5.4.1.1 [5.2.1.1]. The equations in Sec. 14.5.1 [14.2.8] are more conservative than those in Sec. 5.4.1.1 [5.2.1.1] because nonbuilding structures generally lack redundancy and are not as highly damped as building structures. These equations generally govern the design of systems with long periods. According to Item 2 of Sec. 14.5.1 [14.2.8], replacement of the Chapter 5 equations for minima occurs only "for nonbuilding systems that have an *R* value provided in Table 14.5.1.1" [14.2-2]. In the present example the *R* value is taken from Table 14.5.1.1 [14.2-2] and the Seismic Design Category is C so Eq. 14.5.1-1 [14.2-2] applies. Using that equation,  $C_s$  shall not be less than the following:

 $C_s = 0.14 S_{DS} I = 0.14(0.4)(1.5) = 0.084$ 

*Provisions* Eq. 5.4.1.1-1[5.2-2] controls;  $C_s = 0.15$ .

# 12.3.3.2 Condition "a" (each rack loaded)

#### 12.3.3.2.1 Seismic Weight

In accordance with *Provisions* Sec. 14.6.3.2 [14.3.5.3], Item a:

 $W_a = 4(5)(8 \text{ ft})(3 \text{ ft})[0.67(125 \text{ psf})+5 \text{ psf}] = 42.6 \text{ kips}$ 

12.3.3.2.2 Design Forces and Moments

Using Provisions Eq. 5.4.1 [5.2-1], the design base shear for condition "a" is calculated

 $V_a = C_s W = 0.15(42.6 \text{ kips}) = 6.39 \text{ kips}$ 

In order to calculate the design forces, shears, and overturning moments at each level, seismic forces must be distributed vertically in accordance with *Provisions* Sec. 14.6.3.3 [14.3.5.4]. The calculations are shown in Table 12.3-1.

Table 12.3-1         Seismic Forces, Shears, and Overturning Moments							
Level x	$W_x$ (kips)	$h_x$ (ft)	$w_{x}h_{x}^{k}$ $(k=1)$	$C_{vx}$	$F_x$ (kips)	$V_x$ (kips)	$M_x$ (ft-kips)
5	10.65	12	127.80	0.40	2.56		
						2.56	7.68
4	10.65	9	95.85	0.30	1.92	4.40	01.1
2	10.65	6	(2.00	0.20	1 29	4.48	21.1
3	10.65	6	63.90	0.20	1.28	5.76	38.4
2	10.65	3	31.95	0.10	0.63	5.70	50.4
-	10.00	5	01190	0.10	0.00	6.39	57.6
Σ	42.6		319.5				

1.0 ft = 0.3048 m, 1.0 kip = 4.45 kN, 1.0 ft-kip = 1.36 kN-m.

12.3.3.2.3 Resisting Moment at the Base

 $M_{OT, resisting} = W_a (1.5 \text{ ft}) = 42.6(1.5 \text{ ft}) = 63.9 \text{ ft-kips}$ 

#### 12.3.3.3 Condition "b" (only top rack loaded)

#### 12.3.3.3.1 Seismic Weight

In accordance with *Provisions* Sec. 14.6.3.2 [14.3.5.3], Item b:

 $W_b = 1(5)(8 \text{ ft})(3 \text{ ft})(125 \text{ psf}) + 4(5)(8 \text{ ft})(3 \text{ ft})(5 \text{ psf}) = 17.4 \text{ kips}$ 

#### 12.3.3.3.2 Base Shear

Using Provisions Eq. 5.4.1 [5.2-1], the design base shear for condition "b" is calculated as follows:

 $V_b = C_s W = 0.15(17.4 \text{ kips}) = 2.61 \text{ kips}$ 

12.3.3.3.3 Overturning Moment at the Base

Although the forces could be distributed as shown above for condition "a", a simpler, conservative approach for condition "b" is to assume that a seismic force equal to the entire base shear is applied at the top level. Using that simplifying assumption,

 $M_{OT} = V_b$  (12 ft) = 2.61 kip (12 ft) = 31.3 ft-kips

12.3.3.3.4 Resisting Moment at the Base

 $M_{OT, resisting} = W_b (1.5 \text{ ft}) = 17.4(1.5 \text{ ft}) = 26.1 \text{ ft-kips}$ 

#### 12.3.3.4 Controlling Conditions

Condition "a" controls shear demands at all but the top level.

Although the overturning moment is larger under condition "a ," the resisting moment is larger than the overturning moment. Under condition "b" the resistance to overturning is less than the applied

overturning moment. Therefore, the rack anchors must be designed to resist the uplift induced by the base shear for condition "b".

# 12.3.3.5 Torsion

It should be noted that the distribution of east-west seismic shear will induce torsion in the rack system because the east-west brace is only on the back of the storage rack. The torsion should be resisted by the north-south braces at each end of the bay where the east-west braces are placed. If the torsion were to be distributed to each end of the storage rack, the engineer would be required to calculate the transfer of torsional forces in diaphragm action in the shelving, which may be impractical.

# 12.4 ELECTRIC GENERATING POWER PLANT, MERNA, WYOMING

This example highlights some of the differences between the design of nonbuilding structures and the design of building structures. The boiler building in this example illustrates a solution using the equivalent lateral force (ELF) procedure. Due to mass irregularities, the boiler building would probably also require a modal analysis. For brevity, the modal analysis is not illustrated.

# 12.4.1 Description

Large boilers in coal-fired electric power plants are generally suspended from support steel near the roof level. Additional lateral supports (called buck stays) are provided near the bottom of the boiler. The buck stays resist lateral forces but allow the boiler to move vertically. Lateral seismic forces are resisted at the roof and at the buck stay level. Close coordination with the boiler manufacturer is required in order to determine the proper distribution of seismic forces.

In this example, a boiler building for a 950 mW coal-fired electric power generating plant is braced laterally with ordinary concentrically braced frames in both the north-south and the east-west directions. The facility is part of a grid and is not for emergency back up of a Seismic Use Group III facility.

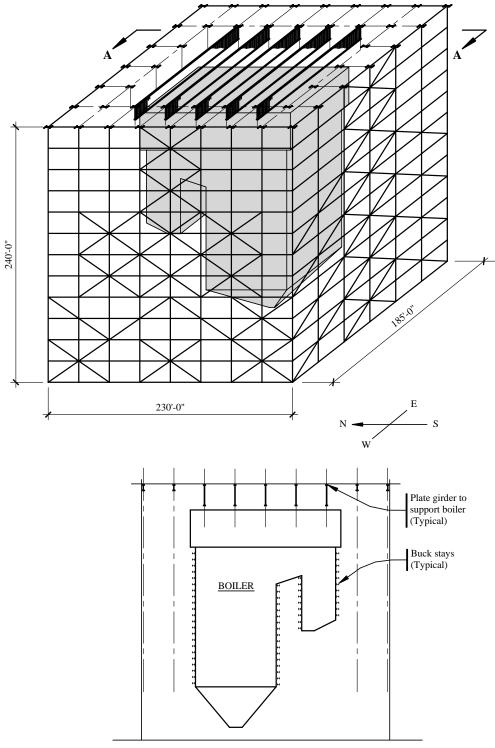
The dead load of the structure, equipment, and piping,  $W_{DL}$ , is 16,700 kips.

The weight of the boiler in service,  $W_{Boiler}$ , is 31,600 kips.

The natural period of the structure (determined from analysis) is as follows:

North-South,  $T_{NS} = 1.90$  seconds

East-West,  $T_{EW} = 2.60$  seconds



Section A-A

# **12.4.2** *Provisions* Parameters

Seismic Use Group ( <i>Provisions</i> Sec. 1.3 [1.2]) (for continuous operation, but not for emergency back up of a Seismic Use Group III facility)	=	Π
Occupancy Importance Factor, I (Provisions Sec. 1.4 [14.2.1])	=	1.25
Site Coordinates	=	42.800° N, 110.500° W
Short Period Response, S <sub>s</sub> (Seismic Design Parameters)	=	0.966
One Second Period Response, S <sub>1</sub> (Seismic Design Parameters)	=	0.278
Site Class (Provisions Sec. 4.1.2.1 [3.5])	=	D (default)
Acceleration-based site coefficient, $F_a$ ( <i>Provisions</i> Table 4.1.2.4a [3.3-1])	=	1.11
Velocity-based site coefficient, $F_{\nu}$ ( <i>Provisions</i> Table 4.1.2.4b [3.3-2])	=	1.84
Design spectral acceleration response parameters $S_{DS} = (2/3)S_{MS} = (2/3)F_aS_s = (2/3)(1.11)(0.966)$ $S_{DI} = (2/3)S_{MI} = (2/3)F_vS_I = (2/3)(1.84)(0.278)$	=	0.715 0.341
Seismic Design Category (Provisions Sec. 4.2 [1.4])	=	D
Seismic-Force-Resisting System ( <i>Provisions</i> Table 14.5.1.1 [14.2-2])	=	Steel concentrically braced frame (Ordinary)
Response Modification Coefficient, <i>R</i> ( <i>Provisions</i> Table 5.2.2)	=	5
System Overstrength Factor, $\Omega_0$ ( <i>Provisions</i> Table 5.2.2)		2
Deflection Amplification Factor, $C_d$ ( <i>Provisions</i> Table 5.2.2)	=	41/2
Height limit (Provisions Table 14.5.1.1)		None

Note: If the structure were classified as a "building," its height would be limited to 35 ft for a Seismic Design Category D ordinary steel concentrically braced frame, according to the *Provisions* Table 5.2.2. The structure is, however, defined as a nonbuilding structure according to *Provisions* Sec. 14.6.3.4. *Provisions* Table 14.5.1.1 does not restrict the height of a nonbuilding structure using an ordinary steel concentrically braced frame.

[Changes in the 2003 *Provisions* would affect this example significantly. Table 14.2-2 would be used to determine design coefficients and corresponding levels of detailing. For structures of this height using an ordinary concentrically braced frame system, R = 1.5,  $\Omega_0 = 1$ , and  $C_d = 1.5$ . Alternatively, a special concentrically braced frame system could be employed.]

# 12.4.3 Design in the North-South Direction

#### 12.4.3.1 Seismic Response Coefficient

Using Provisions Eq. 5.4.1.1-1[5.2-2]:

$$C_s = \frac{S_{DS}}{R/I} = \frac{0.715}{5/1.25} = 0.179$$

From analysis, T = 1.90 seconds. Using *Provisions* Eq. 5.4.1.1-2 [5.2-3],  $C_s$  does not need to exceed

$$C_s = \frac{S_{DI}}{T(R/I)} = \frac{0.341}{1.90(5/1.25)} = 0.045$$

but using *Provisions* Eq. 5.4.1.1-3,  $C_s$  shall not be less than:

 $C_s = 0.044IS_{DS} = 0.044(1.25)(0.715) = 0.0393$ 

[Under the 2003 *Provisions* no additional minimum base shear must be considered since the example structure would satisfy exception 1 of Sec. 14.2.8 and the minimum base shear equation in Chapter 5 was removed.]

*Provisions* Eq. 5.4.1.1-2 [5.2-3] controls;  $C_s = 0.045$ .

#### 12.4.3.2 Seismic Weight

Calculate the total seismic weight, *W*, as:

 $W = W_{DL} + W_{Boiler} = 16,700 \text{ kips} + 31,600 \text{ kips} = 48,300 \text{ kips}$ 

# 12.4.3.3 Base Shear

Using Provisions Eq. 5.4.1 [5.2-1]:

 $V = C_s W = 0.045(48,300 \text{ kips}) = 2170 \text{ kips}$ 

# 12.4.3.4 Redundancy Factor

Refer to Sec. 12.2.3.6 for an explanation of the application of this factor to nonbuilding structures similar to buildings. The seismic force resisting system is an ordinary concentric braced frame with five columns in a single line of framing. The number of bays of bracing diminishes near the top, and the overall plan area is large. For the purposes of this example, it will be assumed that the structure lacks redundancy and  $\rho = 1.5$ .

[The redundancy requirements have been substantially changed in the 2003 *Provisions*. If it is assumed that the structure would fail the redundancy criteria,  $\rho = 1.3$ .]

# 12.4.3.5 Determining E

See Sec. 12.2.3.7.

# 12.4.4 Design in the East-West Direction

# 12.4.4.1 Seismic Response Coefficient

Using Provisions Eq. 5.4.1.1-1 [5.2-2]:

$$C_s = \frac{S_{DS}}{R/I} = \frac{0.715}{5/1.25} = 0.179$$

From analysis, T = 2.60 seconds. Using *Provisions* Eq. 5.4.1.1-2 [5.2-3],  $C_s$  does not need to exceed:

$$C_s = \frac{S_{DI}}{T(R/I)} = \frac{0.341}{2.60(5/1.25)} = 0.0328$$

Using *Provisions* Eq. 5.4.1.1-3,  $C_s$  shall not be less than:

 $C_s = 0.044IS_{DS} = 0.044(1.25)(0.715) = 0.0393$ 

[Under the 2003 *Provisions* no additional minimum base shear must be considered since the example structure would satisfy exception 1 of Sec. 14.2.8 and the minimum base shear equation in Chapter 5 was removed.]

*Provisions* Eq. 5.4.1.1-3 controls;  $C_s = 0.0393$ . [Under the 2003 *Provisions*, Eq. 5.2-3 would control the base shear coefficient for this example.]

#### 12.4.4.2 Seismic Weight

Calculate the total seismic weight, W, as

 $W = W_{DL} + W_{Boiler} = 16,700 \text{ kips} + 31,600 \text{ kips} = 48,300 \text{ kips}$ 

# 12.4.4.3 Base Shear

Using Provisions Eq. 5.4.1 [5.2-1]:

 $V = C_s W = 0.0393(48,300 \text{ kips}) = 1900 \text{ kips}$ 

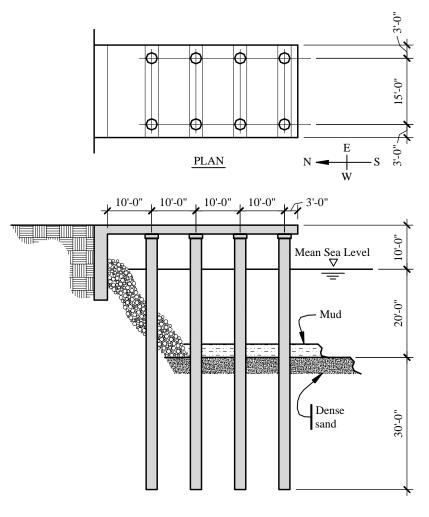
# 12.5 PIER/WHARF DESIGN, LONG BEACH, CALIFORNIA

This example illustrates the calculation of the seismic base shear in the east-west direction for the pier using the ELF procedure.

# 12.5.1 Description

A private shipping company is developing a pier in Long Beach, California, to service container vessels. In the north-south direction, the pier is tied directly to an abutment structure supported on grade. In the east-west direction, the pier resists seismic forces using moment frames.

The design live load for container storage is 1000 psf.



ELEVATION

**Figure 12-5** Pier plan and elevation (1.0 ft = 0.3048 m).

# 12.5.2 Provisions Parameters

Seismic Use Group ( <i>Provisions</i> Sec. 1.3 [1.2]) (The pier serves container vessels that carry no hazardous materials.)	=	Ι
Importance Factor, I (Provisions Sec. 14.5.1.2 [14.2.1])	=	1.0
Short Period Response, $S_s$	=	1.75
One Second Period Response, $S_1$	=	0.60
Site Class (Provisions Sec. 4.1.2.1 [3.5])	=	D (dense sand)
Acceleration-based Site Coefficient, $F_a$ ( <i>Provisions</i> Table 4.1.2.4a [3.3-1])	=	1.0

Velocity-based Site Coefficient, $F_v$ ( <i>Provisions</i> Table 4.1.2.4b [3.3-2])	=	1.5
Design spectral acceleration response parameters		
$S_{DS} = (2/3)S_{MS} = (2/3)F_aS_s = (2/3)(1.0)(1.75)$ $S_{DI} = (2/3)S_{MI} = (2/3)F_vS_I = (2/3)(1.5)(0.60)$	=	1.167 0.60
Seismic Design Category (Provisions Sec. 4.2)	=	D
Seismic-Force-Resisting System ( <i>Provisions</i> Table 14.5.1.1 [14.2-2])	=	Intermediate concrete moment frame
Response Modification Coefficient, <i>R</i> ( <i>Provisions</i> Table 5.2.2)	=	5
(The <i>International Building Code</i> and the 2002 edition of ASCE 7 would require an <i>R</i> value of 3.)		
System Overstrength Factor, $\Omega_0$ ( <i>Provisions</i> Table 5.2.2)	=	3
Deflection Amplification Factor, $C_d$ (Provisions Table 5.2.2)		41/2
Height limit (Provisions Table 14.5.1.1)	=	50 ft

If the structure was classified as a building, an intermediate reinforced concrete moment frame would not be permitted in Seismic Design Category D.

[Changes in the 2003 *Provisions* would affect this example significantly. Table 14.2-2 would be used to determine design coefficients and corresponding levels of detailing. For structures of this height using an intermediate concrete moment frame system, R = 3,  $\Omega_0 = 2$ , and  $C_d = 2.5$ .]

# 12.5.3 Design of the System

# 12.5.3.1 Seismic Response Coefficient

Using Provisions Eq. 5.4.1.1-1 [5.2-2]:

$$C_s = \frac{S_{DS}}{R/I} = \frac{1.167}{5/1.0} = 0.233$$

From analysis, T = 0.596 seconds. Using *Provisions* Eq. 5.4.1.1-2 [5.2-3],  $C_s$  does not need to exceed:

$$C_s = \frac{S_{DI}}{T(R/I)} = \frac{0.60}{0.596(5/1.0)} = 0.201$$

Using *Provisions* Eq. 5.4.1.1-3,  $C_s$  shall not be less than:

$$C_s = 0.044IS_{DS} = 0.044(1.0)(1.167) = 0.0513$$

[Under the 2003 *Provisions* no additional minimum base shear must be considered since the example structure would satisfy exception 1 of Sec. 14.2.8 and the minimum base shear equation in Chapter 5 was removed.]

*Provisions* Eq. 5.4.1.1-2 [5.2-3] controls;  $C_s = 0.201$ .

# 12.5.3.2 Seismic Weight

In accordance with Provisions Sec. 5.3 [5.2.1] and 14.6.6 [14.2.6], calculate the dead load due to the deck, beams, and support piers, as follows:

 $W_{Deck} = 1.0 \text{ ft}(43 \text{ ft})(21 \text{ ft})(0.150 \text{ kip/ft}^3) = 135.5 \text{ kips}$ 

 $W_{Beam} = 4(2 \text{ ft})(2 \text{ ft})(21 \text{ ft})(0.150 \text{ kip/ft}^3) = 50.4 \text{ kips}$ 

 $W_{Pier} = 8[\pi(1.25 \text{ ft})^2][(10 \text{ ft} - 3 \text{ ft}) + (20 \text{ ft})/2](0.150 \text{ kip/ft}^3) = 100.1 \text{ kips}$ 

 $W_{DL} = W_{Deck} + W_{Beams} + W_{Piers} = 135.5 + 50.4 + 100.1 = 286.0$  kips

Calculate 25 percent of the storage live load

 $W_{1/4LL} = 0.25(1000 \text{ psf})(43 \text{ ft})(21 \text{ ft}) = 225.8 \text{ kips}$ 

Calculate the weight of the displaced water (Provisions Sec. 14.6.6 [14.3.3.1])

 $W_{Disp. water} = 8[\pi (1.25 \text{ ft})^2](20 \text{ ft})(64 \text{ pcf}) = 50.27 \text{ kips}$ 

Therefore, the total seismic weight is

 $W = W_{DL} + W_{1/4LL} + W_{Disp. water} = 286.0 + 225.8 + 50.27 = 562.1$  kips

# 12.5.3.3 Base Shear

Using Provisions Eq. 5.3.2 [5.2-1]:

 $V = C_s W = 0.201(562.1 \text{ kips}) = 113.0 \text{ kips}$ 

# 12.5.3.4 Redundancy Factor

This structure is small in area and has a large number of piles. Following the method described in Sec. 12.2.3.6, yields  $\rho = 1.0$ .

# 12.6 TANKS AND VESSELS, EVERETT, WASHINGTON

The seismic response of tanks and vessels can be significantly different from that of buildings. For a structure composed of interconnected solid elements, it is not difficult to recognize how ground motions accelerate the structure and cause inert forces within the structure. Tanks and vessels, when empty, respond in a similar manner.

When there is liquid in the tank, the response is much more complicated. As earthquake ground motions accelerate the tank shell, the shell applies lateral forces to the liquid. The liquid, which responds to those lateral forces. The liquid response may be amplified significantly if the period content of the earthquake ground motion is similar to the natural sloshing period of the liquid.

Earthquake-induced impulsive fluid forces are those calculated assuming that the liquid is a solid mass. The convective fluid forces are those that result from sloshing in the tank. It is important to account for the convective forces on columns and appurtenances inside the tank, because they are affected by sloshing in the same way that waves affect a pier in the ocean.

The freeboard considerations are critical. Often times, the roof acts as a structural diaphragm. If a tank does not have sufficient freeboard, the sloshing wave can rip the roof from the wall of the tank. This could result in the failure of the wall and loss of the liquid within.

The nature of seismic design for liquid containing tanks and vessels is complicated. The fluid mass that is effective for impulsive and convective seismic forces is discussed in the literature referenced in the NEHRP *Provisions* and *Commentary*.

# **12.6.1 Flat-Bottom Water Storage Tank**

#### 12.6.1.1 Description

This example illustrates the calculation of the design base shear using the equivalent lateral force (ELF) procedure for a steel water storage tank used to store potable water for a process within a chemical plant (Figure 12-6).

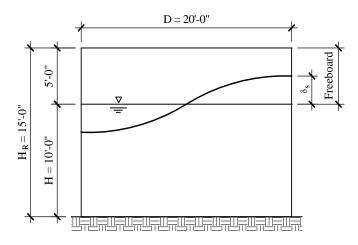


**Figure 12-6** Storage tank section (1.0 ft = 0.3048 m).

The tank is located away from personnel working within the facility.

The weight of the tank shell, roof, and equipment is 15,400 lb.

#### 12.6.1.2 Provisions Parameters

Seismic Use Group (Provisions Sec. 1.3 [1.2])	=	Ι
Importance Factor, I (Provisions Sec. 14.5.1.2 [14.2.1])	=	1.0
Site Coordinates	=	48.000° N, 122.250° W
Short Period Response, $S_s$	=	1.236

FEMA 451, NEHRP Recommended Provisions: Design Examples

One Second Period Response, $S_1$		0.406
Site Class (Provisions Sec. 4.1.2.1 [3.5])		C (per geotech)
Acceleration-based Site Coefficient, $F_a$ ( <i>Provisions</i> Table 4.1.2.4a [3.3-1])	=	1.0
Velocity-based Site Coefficient, $F_{\nu}$ ( <i>Provisions</i> Table 4.1.2.4b [3.3-2])	=	1.39
Design spectral acceleration response parameters		
$S_{DS} = (2/3)S_{MS} = (2/3)F_aS_s = (2/3)(1.0)(1.236)$ $S_{DI} = (2/3)S_{MI} = (2/3)F_vS_I = (2/3)(1.39)(0.406)$	=	0.824 0.376
Seismic-Force-Resisting System ( <i>Provisions</i> Table 14.5.1.1 [14.2-3])	=	Flat-bottom, ground- supported, anchored, bolted steel tank
Response Modification Coefficient, <i>R</i> ( <i>Provisions</i> Table 14.5.1.1 [14.2-3])	=	3
System Overstrength Factor, $\Omega_0$ ( <i>Provisions</i> Table 5.2.2 [14.2-3])	=	2
Deflection Amplification Factor, $C_d$ ( <i>Provisions</i> Table 5.2.2 [14.2-3])	=	21/2

[The 2003 *Provisions* have adopted the 2002 USGS probabilistic seismic hazard maps, and the maps have been added to the body of the 2003 *Provisions* as figures in Chapter 3 (instead of the previously used separate map package). The CD-ROM also has been updated.]

# 12.6.1.3 Calculations for Impulsive Response

12.6.1.3.1 Natural Period for the First Mode of Vibration

Based on analysis, the period for impulsive response of the tank and its contents is  $T_i = 0.14$  sec.

12.6.1.3.2 Spectral Acceleration

Based on Provisions Figure 14.7.3.6-1 [14.4-1]:

$$T_s = \frac{S_{DI}}{S_{DS}} = \frac{0.376}{0.824} = 0.456$$
 seconds

Using *Provisions* Sec. 14.7.3.6.1 [114.4.7.5.1] with  $T_i < T_s$ ;

 $S_{ai} = S_{DS} = 0.824$ 

12.6.1.3.3 Seismic (Impulsive) Weight

 $W_{tank} = 15.4$  kips

 $W_{lwater} = \pi (10 \text{ ft})^2 (10 \text{ ft}) (0.0624 \text{ kip/ft}^3) (W_l/W_T) = 196.0 (0.75) \text{ kips} = 147 \text{ kips}$ 

The ratio  $W_l/W_T$  (= 0.75) was determined from AWWA D100 (it depends on the ratio of height to diameter)

 $W_i = W_{tank} + W_{lwater} = 15.4 + 147 = 162.4$  kips

12.6.1.3.4 Base Shear

According to Provisions Sec. 14.7.3.6.1 [14.4.7.5.1]:

$$V_i = \frac{S_{ai}W_i}{R} = \frac{0.824(162.4 \text{ kips})}{3} = 44.6 \text{ kips}$$

#### 12.6.1.4 Calculations for Convective Response Natural Period for the First Mode of Sloshing

12.6.1.4.1 Natural Period for the First Mode of Sloshing

Using Provisions Section 14.7.3.6.1 [14.4.7.5.1]:

$$T_c = 2\pi \sqrt{\frac{D}{3.68g \tanh\left(\frac{3.68H}{D}\right)}} = 2\pi \sqrt{\frac{20 \text{ ft}}{3.68(32.174 \frac{\text{ft}}{\text{s}^2}) \tanh\left(\frac{3.68(10 \text{ ft})}{10 \text{ ft}}\right)}} = 2.58 \text{ s}$$

12.6.1.4.2 Spectral Acceleration

Using *Provisions* Sec. 14.7.3.6.1 [14.4.7.5.1] with  $T_c < 4$  seconds:

$$S_{ac} = \frac{1.5S_{DI}}{T_c} = \frac{1.5(0.376)}{2.58} = 0.219$$

12.6.1.4.3 Seismic (Convective) Weight

 $W_c = W_{water} (W_2/W_T) = 196 (0.30) = 58.8 \text{ kips}$ 

The ratio  $W_2/W_T$  (= 0.30) was determined from AWWA D100.

#### 12.6.1.4.4 Base Shear

According to Provisions Sec. 14.7.3.6.1 [14.4.7.5.1]:

$$V_c = \frac{S_{ac}W_c}{R} = \frac{0.219(58.8 \text{ kips})}{3} = 4.29 \text{ kips}$$

# 12.6.1.5 Design Base Shear

Although Item b of *Provisions* Sec. 14.7.3.2 [14.4.7.1] indicates that impulsive and convective components may, in general, be combined using the SRSS method, *Provisions* Sec. 14.7.3.6.1 [14.4.7.5.1] requires that the direct sum be used for ground-supported storage tanks for liquids. Using *Provisions* Eq. 14.7.3.6.1 [14.4-1]:

 $V = V_i + V_c = 44.6 + 4.29 = 48.9$  kips

[In the 2003 *Provisions*, use of the SRSS method is also permitted for ground-supported storage tanks for liquids.]

# **12.6.2 FLAT-BOTTOM GASOLINE TANK**

# 12.6.2.1 Description

This example illustrates the calculation of the base shear and the required freeboard using the ELF procedure for a petro-chemical storage tank in a refinery tank farm near a populated city neighborhood. An impoundment dike is not provided to control liquid spills.

The tank is a flat-bottom, ground-supported, anchored, bolted steel tank constructed in accordance with API 650. The weight of the tank shell, roof, and equipment is 15,400 lb.

#### 12.6.2.2 Provisions Parameters

Seismic Use Group (Provisions Sec. 1.3 [1.2])	=	III
(The tank is used for storage of hazardous material.)		
Importance Factor, I (Provisions Sec. 14.5.1.2 [14.2.1])	=	1.5
Site Coordinates	=	48.000° N, 122.250° W
Short Period Response, $S_S$	=	1.236
One Second Period Response, $S_1$	=	0.406
Site Class (Provisions Sec. 4.1.2.1 [3.5])	=	C (per geotech)
Acceleration-based Site Coefficient, $F_a$ ( <i>Provisions</i> Table 4.1.2.4a [3.3-1])	=	1.0
Velocity-based Site Coefficient, $F_v$ ( <i>Provisions</i> Table 4.1.2.4b [3.3-2])	=	1.39
Design spectral acceleration response parameters		
$S_{DS} = (2/3)S_{MS} = (2/3)F_aS_s = (2/3)(1.0)(1.236)$ $S_{DI} = (2/3)S_{MI} = (2/3)F_vS_I = (2/3)(1.39)(0.406)$	=	0.824 0.376

Seismic-Force-Resisting System ( <i>Provisions</i> Table 14.5.1.1 [14.2-3])	=	Flat-bottom, ground- supported, anchored, bolted steel tank
Response Modification Coefficient, <i>R</i> ( <i>Provisions</i> Table 14.5.1.1 [14.2-3])	=	3
System Overstrength Factor, $\Omega_0$ ( <i>Provisions</i> Table 5.2.2 [14.2-3])	=	2
Deflection Amplification Factor, $C_d$ ( <i>Provisions</i> Table 5.2.2 [14.2-3])	=	21/2

[The 2003 *Provisions* have adopted the 2002 USGS probabilistic seismic hazard maps, and the maps have been added to the body of the 2003 *Provisions* as figures in Chapter 3 (instead of the previously used separate map package). The CD-ROM also has been updated.]

# 12.6.2.3 Calculations for Impulsive Response

# 12.6.2.3.1 Natural Period for the First Mode of Vibration

Based on analysis, the period for impulsive response of the tank and its contents is  $T_i = 0.14$  sec.

#### 12.6.2.3.2 Spectral Acceleration

Based on Provisions Figure 14.7.3.6-1 [14.4-1]:

$$T_s = \frac{S_{DI}}{S_{DS}} = \frac{0.376}{0.824} = 0.456$$
 seconds

Using *Provisions* Sec. 14.7.3.6.1 [14.4.7.5.1] with  $T_i < T_s$ ;

$$S_{ai} = S_{DS} = 0.824$$

12.6.2.3.3 Seismic (Impulsive) Weight

$$W_{tank} = 15.4$$
 kips

 $W_{Gas} = \pi (10 \text{ ft})^2 (10 \text{ ft}) (0.046 \text{ kip/ft}^3) (W_I/W_T) = 144.5 \text{ kips} (0.75) = 108.4 \text{ kips}$ 

Note: The ratio  $W_l/W_T$  was determined from AWWA D100, but API 650 should be used.

 $W_i = W_{tank} + W_{Gas} = 15.4 + 108.4 = 123.8$  kips

12.6.2.3.4 Base Shear

According to Provisions Sec. 14.7.3.6.1 [14.4.7.5.1]:

$$V_i = \frac{S_{ai}IW_i}{R} = \frac{0.824(1.5)(123.8 \text{ kips})}{3} = 51.0 \text{ kips}$$

#### 12.6.2.4 Calculations for Convective Response

12.6.2.4.1 Natural Period for the First Mode of Sloshing

The dimensions are the same as those used for the water tank in Sec. 12.6.1; therefore,  $T_c = 2.58$  sec.

12.6.2.4.2 Spectral Acceleration

Likewise,  $S_{ac} = 0.219$ .

12.6.2.4.3 Seismic (Convective) Weight

 $W_c = W_{LNG} (W_2/W_T) = 144.5 (0.30) = 43.4 \text{ kips}$ 

The ratio  $W_2/W_T$  was determined from AWWA D100.

12.6.2.4.4 Base shear

According to Provisions Sec. 14.7.3.6.1 [14.4.7.5.1]:

$$V_c = \frac{S_{ac}IW_c}{R} = \frac{0.824(1.5)(43.5 \text{ kips})}{3} = 17.9 \text{ kips}$$

#### 12.6.2.5 Design Base Shear

Using Provisions Eq. 14.7.3.6.1 [14.4-1]:

 $V = V_i + V_c = 51.0 + 17.9 = 68.9$  kips

#### 12.6.2.6 Minimum Freeboard

*Provisions* Table 14.7.3.6.1.2 [14.4-2] indicates that a minimum freeboard equal to  $\delta_s$  is required for this tank. Using *Provisions* Eq. 14.7.3.6.1.2 [14.4-9]:

 $\delta_s = 0.5 DIS_{ac} = 0.5(20 \text{ ft})(1.5)(0.219) = 3.29 \text{ ft}$ 

The 5 ft freeboard provided is adequate.

# **12.7 EMERGENCY ELECTRIC POWER SUBSTATION STRUCTURE, ASHPORT, TENNESSEE**

The main section addressing electrical transmission, substation, and distribution structures is in the appendix to Chapter 14 of the *Provisions*. The information is in an appendix so that designers can take time to evaluate and comment on the seismic design procedures before they are included in the main text of the *Provisions*.

[In the 2003 *Provisions* Sections A14.2.1 and A14.2.2 were removed because the appropriate industry standards had been updated to include seismic design criteria and earthquake ground motions consistent with the *Provisions*. Therefore, all references to the *Provisions* in Sec. 12.7 of this chapter are obsolete.]

# 12.7.1 Description

This example illustrates the calculation of the base shear using the ELF procedure for a braced frame that supports a large transformer (Figure 12-7). The substation is intended to provide emergency electric power to the emergency control center for the fire and police departments of a community. There is only one center designed for this purpose.

The weight of the transformer equipment is 17,300 lb.

The weight of the support structure is 12,400 lb.

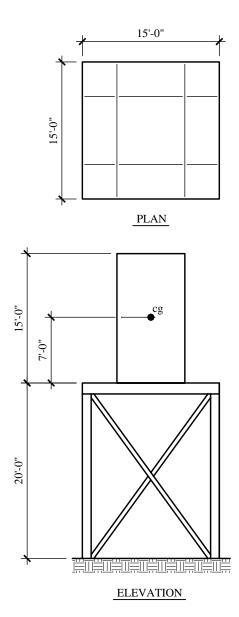


Figure 12-7 Platform for elevated transformer (1.0 ft = 0.3048 m).

The period of the structure is T = 0.240 sec.

Although the ratio of the supported structure over the total weight is greater than 25 percent, experience indicates that the transformer will behave as a lumped rigid mass.

# 12.7.2 Provisions Parameters

# 12.7.2.1 Ground Motion

The design response spectral accelerations are defined as

$$S_{DS} = 1.86$$
  
 $S_{DI} = 0.79$ 

# 12.7.2.2 Seismic Use Group and Importance Factor

The structure is for emergency electric power for a Seismic Use Group III facility. Therefore, the platform is assigned to Seismic Use Group III, as required by *Provisions* Sec. 1.3 [1.2]. Using *Provisions* Table 14.5.1.2 [14.2-1], the Importance Factor, *I*, is equal to 1.5.

# 12.7.2.3 Response Modification Coefficient

From *Provisions* Table 14A.2.1, *R* is 3.

# 12.7.3 Design of the System

# 12.7.3.1 Seismic Response Coefficient

*Provisions* Sec. 14A.2.2 defines  $C_s$  in a manner that is not consistent with the rest of the *Provisions*. This inconsistency will be eliminated in future editions of the *Provisions*. In this example, the equations are applied in a manner that is consistent with Chapters 5 [4 and 5] and 14 – that is, *R* is applied in the calculation of  $C_s$  rather than in the calculation of *V*.

Using Provisions Section 14A.2.2:

$$C_s = \frac{S_{DS}}{R/I} = \frac{1.86}{3/1.5} = 0.93$$

but  $C_s$  need not be larger than:

$$C_s = \frac{S_{DI}}{T(R/I)} = \frac{0.79}{0.24(3/1.5)} = 1.646$$

Therefore,  $C_s = 0.93$ .

# 12.7.3.2 Seismic Weight

$$W = W_{Transformer} + W_{Support structure} = 17.3 + 12.4 = 29.7$$
 kips

# 12.7.3.3 Base Shear

Using Provisions Section 14A.2.2:  $V = C_s W = 0.93(29.7 \text{ kips}) = 27.6 \text{ kips}$ 

# 13

# DESIGN FOR NONSTRUCTURAL COMPONENTS

# Robert Bachman, P.E. and Richard Drake, P.E.

Chapter 6 of the 2000 *NEHRP Recommended Provisions* and *Commentary* (hereinafter, the *Provisions* and *Commentary*) addresses architectural, mechanical, and electrical components of buildings. Two examples are presented here to illustrate many of the requirements and procedures. Design and anchorage are illustrated for exterior precast concrete cladding, and for a roof-mounted HVAC unit. The rooftop unit is examined in two common installations: directly attached, and isolated with snubbers. This chapter also contains an explanation of the fundamental aspects of the *Provisions*, and an explanation of how piping, designed according to the ASME Power Piping code, is checked for the force and displacement requirements of the *Provisions*.

A large variety of materials and industries are involved with nonstructural components is large, and numerous documents define and describe methods of design, construction, manufacture, installation, attachment, etc. Some of the documents address seismic issues but many do not. *Provisions* Sec. 6.1.1 [6.1.2] contains a listing of approved standards for various nonstructural components.

Although the *Guide* is based on the 2000 *Provisions*, it has been annotated to reflect changes made to the 2003 *Provisions*. Annotations within brackets, [], indicate both organizational changes (as a result of a reformat of all of the chapters of the 2003 *Provisions*) and substantive technical changes to the 2003 *Provisions* and its primary reference documents. While the general concepts of the changes are described, the design examples and calculations have not been revised to reflect the changes to the 2003 *Provisions*.

A few noteworthy changes were made to the nonstructural components requirements of the 2003 *Provisions*. These include explicit definition of load effects (including vertical seismic forces) within the chapter and revised classification of nonductile anchors (based on demonstrated ductility or prequalification rather than embedment-length-to-diameter ratio).

In addition to changes *Provisions* Chapter 6, the basic earthquake hazard maps were updated and the concrete design reference was updated to ACI 318-02 (with a significant resulting changes to the calculations for anchors in concrete).

Where they affect the design examples in this chapter of the *Guide*, significant changes to the 2003 *Provisions* and primary reference documents are noted. However, some minor changes to the 2003 *Provisions* and the reference documents may not be noted.

In addition to the *Provisions*, the following are referenced in this chapter:

ACI 318	American Concrete Institute. 1999 [2002]. Building Code Requirements and Commentary for Reinforced Concrete.
ASCE 7	American Society of Civil Engineers. 1998 [2002]. Minimum Design Loads for Buildings and Other Structures.
ASHRAE APP IP	American Society of Heating, Refrigeration, and Air-Conditioning Engineers (ASHRAE). 1999. Seismic and Wind Restraint Design, Chapter 53.
ASME B31.1	American Society of Mechanical Engineers. Power Piping Code.
IBC	International Code Council. 2000. International Building Code.

The symbols used in this chapter are drawn from Chapter 2 of the *Provisions* or reflect common engineering usage. The examples are presented in U.S. customary units.

[In the 2003 *Provisions*, definitions and symbols specific to nonstructural components appear in Sec. 6.1.3 and 6.1.4, respectively.]

# 13.1 DEVELOPMENT AND BACKGROUND OF THE PROVISIONS FOR NONSTRUCTURAL COMPONENTS

# 13.1.1 Approach to Nonstructural Components

The *Provisions* requires that nonstructural components be checked for two fundamentally different demands placed upon them by the response of the structure to earthquake ground motion: resistance to inertial forces and accommodation of imposed displacements. Building codes have long had requirements for resistance to inertial forces. Most such requirements apply to the component mass an acceleration that vary with the basic ground motion parameter and a few broad categories of components. The broad categories are intended distinguish between components whose dynamic response couples with that of the supporting structure in such a fashion as to cause the component response accelerations to be amplified above the accelerations of the structure and those components that are rigid enough with respect to the structure so that the component response is not amplified over the structural response. In recent years, a coefficient based on the function of the building or of the component have been introduced as another multiplier for components important to life safety or essential facilities.

The *Provisions* includes an equation to compute the inertial force that involves two additional concepts: variation of the acceleration with relative height within the structure, and reduction in design force based upon available ductility in the component, or its attachment. The *Provisions* also includes a quantitative measure for the deformation imposed upon nonstructural components. The inertial force demands tend to control the seismic design for isolated or heavy components, whereas, the imposed deformations are important for the seismic design for elements that are continuous through multiple levels of a structure, or across expansion joints between adjacent structures, such as cladding or piping.

The remaining portions of this section describe the sequence of steps and decisions prescribed by the *Provisions* to check these two seismic demands on nonstructural components.

# 13.1.2 Force Equations

The following seismic force equations are prescribed for nonstructural components:(*Provisions* Eq. 6.1.3-1 [6.2-1], 6.1.3-2 [6.2-3], and 6.1.3-3 [6.2-4]):

$$F_{p} = \frac{0.4a_{p}S_{DS}W_{p}}{R_{p}/I_{p}} \left(1 + 2\frac{z}{h}\right)$$
$$F_{p_{max}} = 1.6S_{DS}I_{p}W_{p}$$
$$F_{p_{min}} = 0.3S_{DS}I_{p}W_{p}$$

where:

- $F_p$  = horizontal equivalent static seismic design force centered at the component's center of gravity and distributed relative to the component's mass distribution.
- $a_p$  = component amplification factor (either 1.0 or 2.5) as tabulated in *Provisions* Table 6.2.2 [6.3-1] for architectural components and *Provisions* Table 6.3.2 [6.4-1] for mechanical and electrical components (Alternatively, may be computed by dynamic analysis)
- $S_{DS}$  = five percent damped spectral response acceleration parameter at short period as defined in *Provisions* Sec. 4.1.2 [3.3.3]
- $W_p$  = component operating weight
- $R_p$  = component response modification factor (varies from 1.0 to 5.0) as tabulated in *Provisions* Table 6.2.2 [6.3-1]for architectural components and *Provisions* Table 6.3.2 [6.4-1] for mechanical and electrical components
- $I_p$  = component importance factor (either 1.0 or 1.5) as indicated in *Provisions* Sec. 6.1.5 [6.2-2]
- z = elevation in structure of component point of attachment relative to the base
- h = roof elevation of the structure or elevation of highest point of the seismic-force-resisting system of the structure relative to the base

The seismic design force,  $F_p$ , is to be applied independently in the longitudinal, and transverse directions. The effects of these loads on the component are combined with the effects of static loads. *Provisions* Eq. 6.1.3-2 [6.2-3 and 6.2-4] and 6.1.3-3, provide maximum and minimum limits for the seismic design force.

For each point of attachment, a force,  $F_p$ , should be determined based on *Provisions* Eq. 6.1.3-1 [6.2-1]. The minima and maxima determined from *Provisions* Eq. 6.1.3-2 and 6.1.3-3 [6.2-1] must be considered in determining each  $F_p$ . The weight,  $W_p$ , used to determine each  $F_p$  should be based on the tributary weight of the component associated with the point of attachment. For designing the component, the attachment force,  $F_p$ , should be distributed relative to the component's mass distribution over the area used to establish the tributary weight. With the exception of the bearing walls, which are covered by *Provisions* Sec. 5.2.6.2.7 [4.6.1.3], and out-of-plane wall anchorage to flexible diaphragms, which is covered by *Provisions* Sec. 5.2.6.3.2 [4.6.2.1], each anchorage force should be based on simple statics determined by using all the distributed loads applied to the complete component. Cantilever parapets that are part of a continuous element, should be separately checked for parapet forces.

# 13.1.3 Load Combinations and Acceptance Criteria

# 13.1.3.1 Seismic Load Effects

When the effects of vertical gravity loads and horizontal earthquake loads are additive, *Provisions* Eq. 5.2.7.1-1 [4.2-1] is used:

 $E = \rho Q_E + 0.2 S_{DS} D$ 

When the effects of vertical gravity load counteract those of horizontal earthquake loads, *Provisions* Eq. 5.2.7.1-2 [4.2-2] is used:

 $E = \rho Q_E - 0.2 S_{DS} D$ 

where:

E = effect of horizontal and vertical earthquake-induced forces

 $\rho$  = redundancy factor (= 1.0 for nonstructural components)

 $Q_E$  = effect of horizontal seismic forces (due to application of  $F_p$  for nonstructural components)

D = effect of dead load

 $0.2S_{DS}D =$  effect of vertical seismic forces

#### 13.1.3.2 Strength Load Combinations

*Provisions* Sec. 5.2.7 [4.2.2] requires the use of ASCE 7 factored load combinations. The combinations from ASCE 7 Sec. 2.3.2 that include earthquake effects are:

U = 1.2D + 1.0E + 0.5L + 0.2S

U = 0.9D + 1.0E + 1.6H

# 13.1.4 Component Amplification Factor

The component amplification factor,  $a_p$ , found in *Provisions* Eq. 6.1.3-1 [6.2-1] represents the dynamic amplification of the component relative to the maximum acceleration of the component support point(s). Typically, this amplification is a function of the fundamental period of the component,  $T_{p}$ , and the fundamental period of the support structure, T. It is recognized that at the time the components are designed or selected, the effective fundamental period of the structure, T, is not always available. It is also recognized that for a majority of nonstructural components, the component fundamental period,  $T_{n}$ , can be accurately obtained only by expensive shake-table or pullback tests. As a result, the determination of a component's fundamental period by dynamic analysis, considering  $T/T_p$  ratios, is not always practicable. For this reason, acceptable values of  $a_p$  have been provided in the *Provisions* tables. Therefore, component amplification factors from either these tables or a dynamic analysis may be used. Values for  $a_p$  are tabulated for each component based on the expectation that the component will behave in either a rigid or a flexible manner. For simplicity, a step function increase based on input motion amplifications is provided to help distinguish between rigid and flexible behavior. If the fundamental period of the component is less than 0.06 seconds, no dynamic amplification is expected and  $a_n$  may be taken to equal 1.00. If the fundamental period of the component is greater than 0.06 seconds, dynamic amplification is expected, and  $a_p$  is taken to equal 2.50. In addition, a rational analysis determination of

 $a_p$  is permitted if reasonable values of both *T* and  $T_p$  are available. Acceptable procedures for determining  $a_p$  are provided in *Commentary* Chapter 6.

# 13.1.5 Seismic Coefficient at Grade

The short period design spectral acceleration,  $S_{DS}$ , considers the site seismicity and local soil conditions. The site seismicity is obtained from the design value maps (or CD-ROM), and  $S_{DS}$  is determined in accordance with *Provisions* Sec. 4.1.2.5 [3.3.3]. The coefficient  $S_{DS}$  is the used to design the structure. The *Provisions* approximates the effective peak ground acceleration as  $0.4S_{DS}$ , which is why 0.4 appears in *Provisions* Eq. 6.1.3-1 [6.2-1].

[The 2003 *Provisions* have adopted the 2002 USGS probabilistic seismic hazard maps, and the maps have been added to the body of the 2003 *Provisions* as figures in Chapter 3 (instead of the previously used separate map package). The CD-ROM also has been updated.]

# 13.1.6 Relative Location Factor

The relative location factor,  $\left(1+2\frac{z}{h}\right)$ , scales the seismic coefficient at grade, resulting in values linearly

varying from 1.0 at grade to 3.0 at roof level. This factor approximates the dynamic amplification of ground acceleration by the supporting structure.

# 13.1.7 Component Response Modification Factor

The component response modification factor,  $R_p$ , represents the energy absorption capability of the component's construction and attachments. In the absence of applicable research, these factors are based on judgment with respect to the following benchmark values:

- 1.  $R_p = 1.0$  or 1.5, brittle or buckling failure mode is expected
- 2.  $\vec{R_p} = 2.5$ , some minimal level of energy dissipation capacity
- 3.  $R_p^P = 3.5$  or 5.0, highly ductile materials and detailing

# 13.1.8 Component Importance Factor

The component importance factor,  $I_p$ , represents the greater of the life safety importance and/or the hazard exposure importance of the component. The factor indirectly accounts for the functionality of the component or structure by requiring design for a lesser amount of inelastic behavior (or higher force level). It is assumed that a lesser amount of inelastic behavior will result in a component that will have a higher likelihood of functioning after a major earthquake.

# 13.1.9 Accommodation of Seismic Relative Displacements

The *Provisions* requires that seismic relative displacements,  $D_p$ , be determined in accordance with several equations. For two connection points on Structure A (or on the same structural system), one at Level x and the other at Level y,  $D_p$  is determined from *Provisions* Eq. 6.1.4-1 [6.2-5] as:

$$D_p = \delta_{xA} - \delta_{yA}$$

Because the computed displacements are frequently not available to the designer of nonstructural components, one may use the maximum permissible structural displacements per *Provisions* Eq. 6.1.4-2 [6.2-6]:

$$D_{p_{max}} = (X - Y) \frac{\Delta_{aA}}{h_{sx}}$$

For two connection points on Structures A and B (or on two separate structural systems), one at Level *x*, and the other at Level *y*,  $D_P$  and  $D_{Pmax}$  are determined from *Provisions* Eq. 6.1.4-3 [6.2-7] and 6.1.4-4 [6.2-8], respectively, as:

$$D_{p} = \left| \delta_{xA} \right| + \left| \delta_{yB} \right|$$
$$D_{p_{max}} = \frac{X \Delta_{aA}}{h_{sx}} + \frac{Y \Delta_{aB}}{h_{sx}}$$

where:

- $D_p$  = seismic relative displacement that the component must be designed to accommodate
- $\delta_{xA}$  = deflection of building Level x of Structure A, determined by an elastic analysis as defined in *Provisions* Sec. 5.4.6.1 or 5.5.5 [5.2.6, 5.3.5, or 5.4.3] and multiplied by the  $C_d$  factor
- $\delta_{vA}$  = deflection of building Level y of Structure A, determined in the same fashion as  $\delta_{xA}$
- X = height of upper support attachment at Level *x* as measured from the base
- Y = height of lower support attachment at Level y as measured from the base
- $\Delta_{aA}$  = allowable story drift for Structure A as defined in *Provisions* Table 5.2.8 [4.5-1]
- $h_{sx} =$ story height used in the definition of the allowable drift,  $\Delta_a$ , in *Provisions* Table 5.2.8 [4.5-1]
- $\delta_{yB}$  = deflection of building Level y of Structure B, determined in the same fashion as  $\delta_{xA}$
- $\Delta_{aB}$  = allowable story drift for Structure B as defined in *Provisions* Table 5.2.8 [4.5-1]

The effects of seismic relative displacements must be considered in combination with displacements caused by other loads as appropriate. Specific methods for evaluating seismic relative displacement effects of components and associated acceptance criteria are not specified in the *Provisions*. However, the intention is to satisfy the purpose of the *Provisions*. Therefore, for nonessential facilities, nonstructural components can experience serious damage during the design level earthquake provided they do not constitute a serious life safety hazard. For essential facilities, nonstructural components can experience some damage or inelastic deformation during the design level earthquake provided they do not significantly impair the function of the facility.

# 13.1.10 Component Anchorage Factors and Acceptance Criteria

Design seismic forces in the connected parts,  $F_p$ , are prescribed in *Provisions* Sec. 6.1.3 [6.2.6].

When component anchorage is provided by expansion anchors or shallow anchors, a value of  $R_p = 1.5$  is used. Shallow anchors are defined as those with embedment length-to-diameter ratios of less than 8. Anchors embedded in concrete or masonry are proportioned to carry the least of the following:

1. The design strength of the connected part

- 2. 1.3 times the prescribed seismic design force or
- 3. The maximum force that can be transferred to the connected part by the component structural system

Determination of design seismic forces in anchors must consider installation eccentricities, prying effects, multiple anchor effects, and the stiffness of the connected system.

Use of powder-driven fasteners is not permitted for seismic design tension forces in Seismic Design Categories D, E, and F unless approved for such loading.

[In the 2003 *Provisions* reference is made to "power-actuated" fasteners so as to cover a broader range of fastener types than is implied by "powder-driven."]

The design strength of anchors in concrete is determined in accordance with, *Provisions* Chapter 9, which is basically the same as IBC Sec. 1913, and has been updated somewhat in Appendix D of ACI 318-2002. (These rules for anchors in concrete will probably be deleted from the next edition of the *Provisions* in favor of a reference to ACI 318.)

[The 2003 *Provisions* refer to Appendix D of ACI 318-02 rather than providing specific, detailed requirements.]

# **13.1.11** Construction Documents

Construction documents must be prepared by a registered design professional and must include sufficient detail for use by the owner, building officials, contractors, and special inspectors; *Provisions* Table 6.1.7 [6.2-1] includes specific requirements.

# **13.2 ARCHITECTURAL CONCRETE WALL PANEL**

# **13.2.1 Example Description**

In this example, the architectural components are a 4.5-in.-thick precast normal weight concrete spandrel panel and a column cover supported by the structural steel frame of a five-story building as shown in Figures 13.2-1 and 13.2-2.

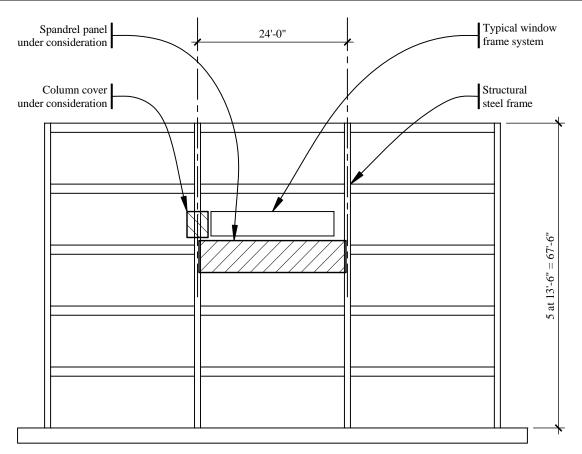


**Figure 13.2-1** Five-story building elevation showing panel location (1.0 ft = 0.3048 m)

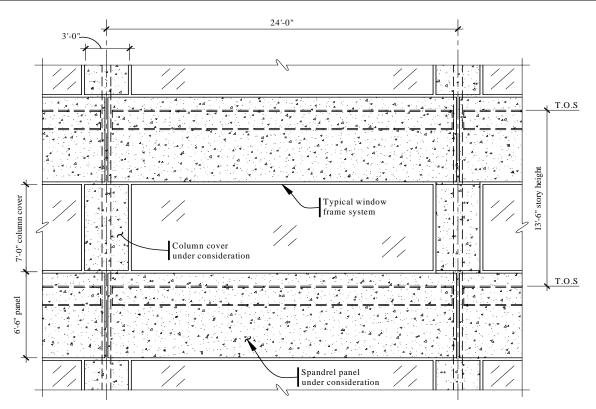


**Figure 13.2-2** Detailed building elevation (1.0 ft = 0.3048 m).

The columns, at the third level of the five-story office building, support the spandrel panel under consideration. The columns between the third and fourth levels of the building support the column cover under consideration. The building, located near a significant active fault in Los Angeles, California, is assigned to Seismic Use Group I. Wind pressures normal to the building are 17 psf determined in accordance with ASCE 7. The spandrel panel supports glass windows weighing 10 psf.

This example develops prescribed seismic forces for the selected spandrel panel and prescribed seismic displacements for the selected column cover.

It should be noted that details of precast connections vary according to the preferences and local practices of the precast panel supplier. In addition, some connections may involve patented designs. As a result, this example will concentrate on quantifying the prescribed seismic forces and displacements. After the prescribed seismic forces and displacements are determined, the connections can be detailed and designed according to the appropriate AISC and ACI codes and PCI (Precast/Prestressed Concrete Institute) recommendations.

# 13.2.2 Design Requirements

# 13.2.2.1 Provisions Parameters and Coefficients

$a_p = 1.0$ for wall panels	(Provisions Table 6.2.2 [6.3-1])
$a_p = 1.25$ for connection fasteners	(Provisions Table 6.2.2 [6.3-1])

 $S_{DS} = 1.487$  (Design Values CD-ROM for the selected location and site class)

[The 2003 *Provisions* have adopted the 2002 USGS probabilistic seismic hazard maps, and the maps have been added to the body of the 2003 *Provisions* as figures in Chapter 3 (instead of the previously used separate map package). The CD-ROM also has been updated.]

[In the footnote to 2003 *Provisions* Table 1.4-1, the value of  $S_1$  used to trigger assignment to Seismic Design Category E or F was changed from 0.75 to 0.6.]

 Spandrel Panel  $W_p = (150 \text{ lb/ft}^3)(24 \text{ ft})(6.5 \text{ ft})(0.375 \text{ ft}) = 8775 \text{ lb}$  

 Glass  $W_p = (10 \text{ lb/ft}^2)(21 \text{ ft})(7 \text{ ft}) = 1470 \text{ lb}$  (supported by spandrel panel)

 Column Cover  $W_p = (150 \text{ lb/ft}^3)(3 \text{ ft})(7 \text{ ft})(0.375 \text{ ft}) = 1181 \text{ lb}$  (Provisions Table 6.3.2 [6.3-1])

  $R_p = 1.0$  for connection fasteners
 ((Provisions Sec. 6.1.6.1 [6.2.8.1])

[In the 2003 *Provisions* component anchorage is designed using  $R_p = 1.5$  unless specific ductility or prequalification requirements are satisfied.]

$$I_{p} = 1.0$$
 (Provisions Sec. 6.1.5 [6.2.2])  
$$\frac{z}{h} = \frac{40.5 \text{ ft}}{67.5 \text{ ft}} = 0.6$$
 (at third floor)

$$\rho = 1.0$$
 (Provisions Sec. 6.1.3)

[The 2003 *Provisions* indicate that the redundancy factor does not apply to the design of nonstructural components. Although the effect is similar to stating that  $\rho = 1$ , there is a real difference since load effects for such components and their supports and attachments are now defined in Chapter 6 rather than by reference to Chapter 4.]

# 13.2.2.2 Performance Criteria

Component failure should not cause failure of an essential architectural, mechanical, or electrical component (*Provisions* Sec. 6.1 [6.2.3]).

Component seismic attachments must be bolted, welded, or otherwise positively fastened without considering the frictional resistance produced by the effects of gravity (*Provisions* Sec. 6.1.2 [6.2.5]).

The effects of seismic relative displacements must be considered in combination with displacements caused by other loads as appropriate (*Provisions* Sec. 6.1.4 [6.2.7]).

Exterior nonstructural wall panels that are attached to or enclose the structure shall be designed to resist the forces in accordance with *Provisions* Eq. 6.1.3-1 or 6.1.3-2 [6.2.6] and must be able to accommodate movements of the structure resulting from response to the design basis ground motion,  $D_p$ , or temperature changes (*Provisions* Sec. 6.2.4 [6.3.2]).

# 13.2.3 Spandrel Panel

# 13.2.3.1 Connection Details

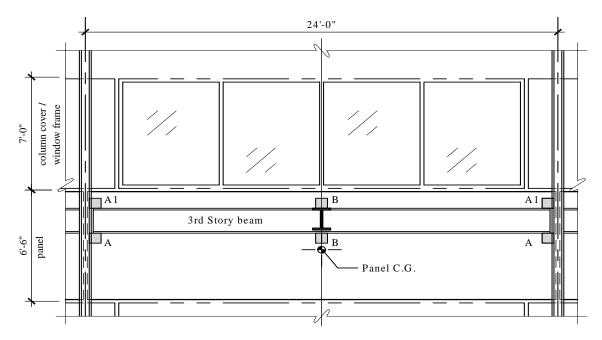


Figure 13.2-3 shows the types and locations of connections that support one spandrel panel.

Figure 13.2-3 Spandrel panel connection layout from interior (1.0 ft = 0.3048 m).

The connection system must resist the weight of the panel and supported construction including the eccentricity between that load and the supports as well as inertial forces generated by response to the seismic motions in all three dimensions. Furthermore, the connection system must not create undue interaction between the structural frame and the panel, such as restraint of the natural shrinkage of the panel or the transfer of floor live load from the beam to the panel. The panels are usually very stiff compared to the frame, and this requires careful release of potential constraints at connections. PCI's *Architectural Precast Concrete* (2<sup>nd</sup> Ed. 1989), provides an extended discussion of important design concepts for such panels.

For this example, the basic gravity load, and vertical accelerations are resisted at Points A, which provides the recommended simple and statically determinant system for the main gravity weight. The eccentricity of vertical loads is resisted by a force couple at the two pairs of A1 and A connections. Horizontal loads parallel to the panel are resisted by the A connections. Horizontal loads perpendicular to the panel are resisted by all six connections. The A connections, therefore, restrain movement in three dimensions while the A1 and B connections restrain movement in only one dimension, perpendicular to the panel. Connection components can be designed to resolve some eccentricities by bending of the element; for example, the eccentricity of the horizontal in-plane force with the structural frame can be resisted by bending the A connection.

The practice of resisting the horizontal in-plane force at two points varies with seismic demand and local industry practice. The option is to resist all of the in-plane horizontal force at one connection in order to avoid restraint of panel shrinkage. The choice made here depends on local experience indicating that precast panels of this length have been restrained at the two ends without undue shrinkage restraint problems.

The A and A1 connections are often designed to take the loads directly to the columns, particularly on steel moment frames where attachments to the flexural hinging regions of beams are difficult to accomplish. The lower B connection often require an intersecting beam to provide sufficient stiffness and strength to resist the loads.

The column cover is supported both vertically and horizontally by the column, transfers no loads to the spandrel panel, and provides no support for the window frame.

The window frame is supported both vertically and horizontally along the length of the spandrel panel and transfers no loads to the column covers.

# 13.2.3.2 Prescribed Seismic Forces

Lateral forces on the wall panels and connection fasteners include seismic loads in accordance with the *Provisions* and wind loads in accordance with ASCE 7 as indicated in the problem statement. Wind forces are not illustrated here.

13.2.3.2.1 Panels

 $D = W_p = 8775 \text{ lb} + 1470 \text{ lb} = 10245 \text{ lb}$  (vertical gravity effect)

$$F_{p} = \frac{0.4(1.0)(1.487)(10245 \text{ lb})}{(2.5/1.0)}(1+2(0.6)) = 5362 \text{ lb}$$
(Provisions Eq. 6.1.3-1 [6.2-1])  

$$F_{p_{max}} = 1.6(1.487)(1.0)(10245 \text{ lb}) = 24375 \text{ lb}$$
(Provisions Eq. 6.1.3-2 [6.2-3])  

$$F_{p_{min}} = 0.3(1.487)(1.0)(10245 \text{ lb}) = 4570 \text{ lb}$$
(Provisions Eq. 6.1.3-3 [6.2-4])

[2003 *Provisions* Sec. 6.2.6 now treats load effects differently. The vertical forces that must be considered in design are indicated directly and the redundancy factor does not apply, so the following five steps would be cast differently; the result is the same.]

$Q_E$ (due to application of $F_p$ ) = 5362 lb	(Provisions Sec. 6.1.3)
$\rho Q_E = (1.0)(5362 \text{ lb}) = 5362 \text{ lb}$	(horizontal earthquake effect)
$0.2S_{DS}D = (0.2)(1.487)(10245 \text{ lb}) = 3047 \text{ lb}$	(vertical earthquake effect)
$E = \rho Q_E + 0.2 S_{DS} D$	(Provisions Eq. 5.2.7.1-1 [4.2-1])
$E = \rho Q_E - 0.2 S_{DS} D$	(Provisions Eq. 5.2.7.1-2 [4.2-2])

# 13.2.3.2.2 Connection Fasteners

The *Provisions* specifies a reduced  $R_P$  and an increased  $a_P$  for "Fasteners," which is intended to prevent premature failure in those elements of connections that are inherently brittle, such as embedments that depend on concrete breakout strength, or are simply too small to adequately dissipate energy inelastically, such as welds or bolts. The net effect more than triples the design seismic force.

$$F_{p} = \frac{0.4(1.25)(1.487)(10245 \text{ lb})}{\binom{1.0}{1.0}} (1+2(0.6)) = 16757 \text{ lb}$$
(Provisions Eq. 6.1.3-1 [6.2-1])

$F_{p_{max}} = 1.6(1.487)(1.0)(10245 \text{ lb}) = 24375 \text{ lb}$	(Provisions Eq. 6.1.3-2 [6.2-3])
$F_{p_{min}} = 0.3(1.487)(1.0)(10245 \text{ lb}) = 4570 \text{ lb}$	(Provisions Eq. 6.1.3-3 [6.2-4])

[2003 *Provisions* Sec. 6.2.6 now treats load effects differently. The vertical forces that must be considered in design are indicated directly and the redundancy factor does not apply, so the following five steps would be cast differently; the result is the same.]

$Q_E$ (due to application of $F_p$ ) = 16757 lb	(Provisions Sec. 6.1.3)
$\rho Q_E = (1.0)(16757 \text{ lb}) = 16757 \text{ lb}$	(horizontal earthquake effect)
$0.2S_{DS}D = (0.2)(1.487)(10245 \text{ lb}) = 3047 \text{ lb}$	(vertical earthquake effect)
$E = \rho Q_E + 0.2 \mathrm{S}_{DS} D$	(Provisions Eq. 5.2.7.1-1 [4.2-1])
$E = \rho Q_E - 0.2 \mathrm{S}_{DS} D$	(Provisions Eq. 5.2.7.1-2 [4.2-2])

## **13.2.3.3** Proportioning and Design

#### 13.2.3.3.1 Panels

The wall panels should be designed for the following loads in accordance with ACI 318. The design of the reinforced concrete panel is standard and is not illustrated in this example. Spandrel panel moments are shown in Figure 13.2-4. Reaction shears  $(V_u)$ , forces  $(H_u)$ , and moments  $(M_u)$  are calculated for applicable strength load combinations.

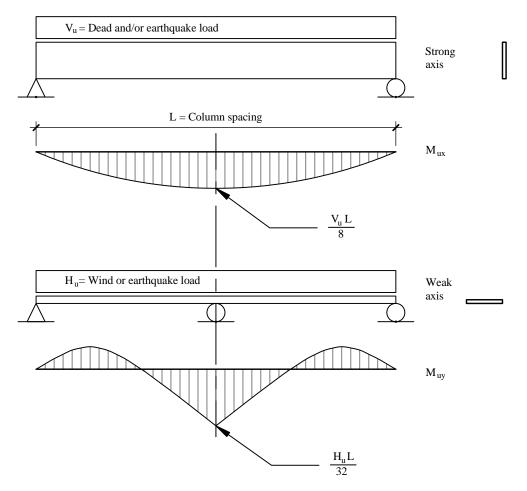


Figure 13.2-4 Spandrel panel moments.

U = 1.4D

$$V_{u} = 1.4(10245 \text{ lb}) = 14343 \text{ lb} \qquad (\text{vertical load downward})$$

$$M_{ux} = \frac{(14343 \text{ lb})(24 \text{ ft})}{8} = 43029 \text{ ft-lb} \qquad (\text{strong axis moment})$$

$$U = 1.2D + 1.0E$$

$$V_{u_{max}} = 1.2(10245 \text{ lb}) + 1.0(3047 \text{ lb}) = 15341 \text{ lb} \qquad (\text{vertical load downward})$$

$$\Leftrightarrow H_{u} = 1.0(5362 \text{ lb}) = 5362 \text{ lb} \qquad (\text{horizontal load parallel to panel})$$

$$\perp H_{u} = 1.0(5362 \text{ lb}) = 5362 \text{ lb} \qquad (\text{horizontal load perpendicular to panel})$$

$$M_{ux_{max}} = \frac{(15341 \text{ lb})(24 \text{ ft})}{8} = 46023 \text{ ft-lb} \qquad (\text{vertical load downward})$$

$$W = 0.9D + 1.0E$$

$$V_{u_{max}} = 0.9(10245 \text{ lb}) - 1.0(3047 \text{ lb}) = 6174 \text{ lb} \qquad (\text{vertical load downward})$$

$$\Leftrightarrow H_{u} = 1.0(5362 \text{ lb}) = 5362 \text{ lb} \qquad (\text{horizontal load perpendicular to panel})$$

$$U = 0.9D + 1.0E$$

$$V_{u_{max}} = 0.9(10245 \text{ lb}) - 1.0(3047 \text{ lb}) = 6174 \text{ lb} \qquad (\text{vertical load downward})$$

$$\Leftrightarrow H_{u} = 1.0(5362 \text{ lb}) = 5362 \text{ lb} \qquad (\text{horizontal load perpendicular to panel})$$

$$\perp H_{u} = 1.0(5362 \text{ lb}) = 5362 \text{ lb} \qquad (\text{horizontal load perpendicular to panel})$$

$$\downarrow H_{u} = 1.0(5362 \text{ lb}) = 5362 \text{ lb} \qquad (\text{horizontal load perpendicular to panel})$$

$$\downarrow H_{u} = 1.0(5362 \text{ lb}) = 5362 \text{ lb} \qquad (\text{horizontal load perpendicular to panel})$$

$$\downarrow H_{u} = 1.0(5362 \text{ lb}) = 5362 \text{ lb} \qquad (\text{horizontal load perpendicular to panel})$$

$$\downarrow H_{u} = 1.0(5362 \text{ lb}) = 5362 \text{ lb} \qquad (\text{horizontal load perpendicular to panel})$$

$$\downarrow H_{u} = 1.0(5362 \text{ lb}) = 5362 \text{ lb} \qquad (\text{horizontal load perpendicular to panel})$$

$$\downarrow H_{u} = 1.0(5362 \text{ lb}) = 5362 \text{ lb} \qquad (\text{horizontal load perpendicular to panel})$$

$$\downarrow H_{u} = 1.0(5362 \text{ lb}) = 5362 \text{ lb} \qquad (\text{horizontal load perpendicular to panel})$$

$$\downarrow H_{u} = 1.0(5362 \text{ lb}) = 5362 \text{ lb} \qquad (\text{horizontal load perpendicular to panel})$$

$$\downarrow H_{u} = 1.0(5362 \text{ lb}) = 5362 \text{ lb} \qquad (\text{horizontal load perpendicular to panel})$$

$$M_{uy} = \frac{(5362 \text{ lb})(24 \text{ ft})}{32} = 4022 \text{ ft-lb}$$
 (weak axis moment)

#### 13.2.3.3.2 Connection Fasteners

The connection fasteners should be designed for the following loads in accordance with ACI 318-2002 (Appendix D) and the AISC specification. There are special reduction factors for anchorage in high seismic demand locations, and the parameters for this project would invoke those reduction factors. The design of the connection fasteners is not illustrated in this example. Spandrel panel connection forces are shown in Figure 13.2-5. Reaction shears  $(V_u)$ , forces  $(H_u)$ , and moments  $(M_u)$  are calculated for applicable strength load combinations.

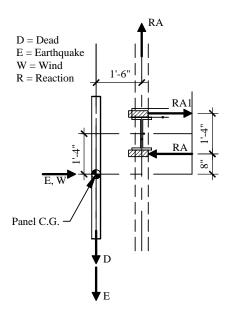


Figure 13.2-5 Spandrel panel connection forces.

# <u>U = 1.4D</u>

 $V_{uA} = \frac{1.4(10245 \text{ lb})}{2} = 7172 \text{ lb}$  (vertical load downward at Point A and A1)  $M_{uA} = (7172 \text{ lb})(1.5 \text{ ft}) = 10758 \text{ ft-lb}$  (moment resisted by paired Points A and A1)

Horizontal couple from moment at A and A1 = 10758 / 1.33 = 8071 lb

# U = 1.2D + 1.0E

$$V_{uA_{max}} = \frac{1.2(10245 \text{ lb}) + 1.0(3047 \text{ lb})}{2} = 7671 \text{ lb} \qquad (\text{vertical load downward at Point A})$$

$$\perp H_{uA} = 1.0(16757 \text{ lb})\frac{3}{16} = 3142 \text{ lb} \qquad (\text{horizontal load perpendicular to panel at Points A and A1})$$

$$H_{Ain} = (7671 \text{ lb})(1.5 \text{ ft}) / (1.33 \text{ ft}) + (3142 \text{ lb})(2.0 \text{ ft}) / (1.33 \text{ ft}) = 13366 \text{ lb} \qquad (\text{inward force at Point A})$$

$$H_{Alout} = (7671 \text{ lb})(1.5 \text{ ft}) / (1.33 \text{ ft}) + (3142 \text{ lb})(0.67) / (1.33 \text{ ft}) = 10222 \text{ lb}(\text{outward force at Point A})$$

$$H_{alout} = (7671 \text{ lb})(1.5 \text{ ft}) / (1.33 \text{ ft}) + (3142 \text{ lb})(0.67) / (1.33 \text{ ft}) = 10222 \text{ lb}(\text{outward force at Point A})$$

$$H_{uA} = \frac{1.0(16757 \text{ lb})}{2} = 8378 \text{ lb} \qquad (\text{horizontal load parallel to panel at Point A})$$

$$M_{u2A} = (8378 \text{ lb})(1.5 \text{ ft}) = 12568 \text{ ft-lb} \qquad (\text{flexural moment at Point A})$$

$$\perp H_{uB} = 1.0(16757 \text{ lb})\frac{5}{8} = 10473 \text{ lb} \qquad (\text{horizontal load perpendicular to panel at Points B and B1})$$

Chapter 13, Nonstructural Components

U = 0.9D + 1.0E

$$V_{uA_{min}} = \frac{0.9(10245 \text{ lb}) - 1.0(3047 \text{ lb})}{2} = 3086 \text{ lb}$$
 (vertical load downward at Point A)

Horizontal forces are the same as combination 1.2 D + 1.0 E. No uplift occurs; the net reaction at A is downward. Maximum forces are controlled by prior combination. It is important to realize that inward and outward acting horizontal forces generate different demands when the connections are eccentric to the center of mass as it is in this example. Only the maximum reactions are computed above.

# 13.2.3.4 Prescribed Seismic Displacements

Prescribed seismic displacements are not applicable to the building panel because all connections are essentially at the same elevation.

# 13.2.4 Column Cover

# 13.2.4.1 Connection Details

Figure 13.2-6 shows the key to the types of forces resisted at each column cover connection.

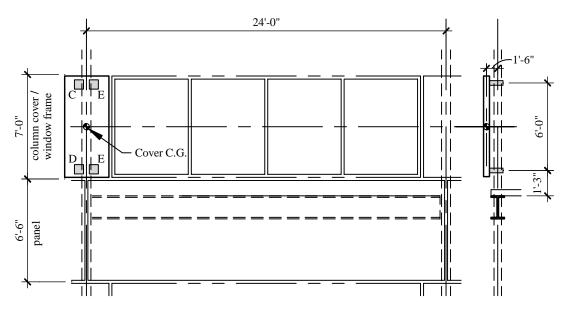


**Figure 13.2-6** Column cover connection layout (1.0 ft = 0.3048 m).

Vertical loads, horizontal loads parallel to the panel, and horizontal loads perpendicular to the panel are resisted at Point C. The eccentricity of vertical loads is resisted by a force couple at Points C and D. The horizontal load parallel to the panel eccentricity between the panel and the support is resisted in flexure of the connection. The connection is designed to take the loads directly to the columns.

Horizontal loads parallel to the panel and horizontal loads perpendicular to the panel are resisted at Point D. The vertical load eccentricity between the panel and the support is resisted by a force couple of Points

C and D. The eccentricity of horizontal loads parallel to the panel is resisted by flexure at the connection. The connection must not restrict vertical movement of the panel due to thermal effects or seismic input. The connection is designed to take the loads directly to the columns.

Horizontal loads perpendicular to the panel are resisted at Points E. The connection is designed to take the loads directly to the columns.

There is no load eccentricity associated with the horizontal loads perpendicular to the panel.

In this example, all connections are made to the sides of the column because there usually is not enough room between the outside face of the column and the inside face of the cover to allow a feasible load-carrying connection.

# 13.2.4.2 Prescribed Seismic Forces

Calculation of prescribed seismic forces for the column cover are not shown in this example. They should be determined in the same manner as illustrated for the spandrel panels.

# 13.2.4.3 Prescribed Seismic Displacements

The results of an elastic analysis of the building structure are not usually available in time for use in the design of the precast cladding system. As a result, prescribed seismic displacements are usually calculated based on allowable story drift requirements:

 $h_{sx} = \text{story height} = 13 \text{ ft } 6 \text{ in}$ 

X = height of upper support attachment = 47 ft 9 in

Y = height of lower support attachment = 41 ft 9 in

$$\Delta_{a} = 0.020h_{sx}$$
(Provisions Table 5.2.8 [4.5-1])  
$$D_{p_{max}} = (X - Y)\frac{\Delta_{a}}{h_{sx}} = (72 \text{ in.})\frac{0.020h_{sx}}{h_{sx}} = 1.44 \text{ in.}$$
(Provisions Eq. 6.1.4-2 [6.2-6])

The joints at the top and bottom of the column cover must be designed to accommodate an in-plane relative displacement of 1.44 inches. The column cover will rotate somewhat as these displacements occur, depending on the nature of the connections to the column. If the supports at one level are "fixed" to the columns while the other level is designed to "float," then the rotation will be that of the column at the point of attachment.

# 13.2.5 Additional Design Considerations

# 13.2.5.1 Window Frame System

The window frame system is supported by the spandrel panels above and below. Assuming that the spandrel panels move rigidly in-plane with each floor level, the window frame system must accommodate a prescribed seismic displacement based on the full story height.

$$D_{p_{max}} = (X - Y)\frac{\Delta_a}{h_{sx}} = (162 \text{ in.})\frac{0.020h_{sx}}{h_{sx}} = 3.24 \text{ in.}$$
(Provisions Eq. 6.1.4-2 [6.2-6])

The window frame system must be designed to accommodate an in-plane relative displacement of 3.24 in. between the supports. This is normally accommodated by a clearance between the glass and the frame. *Provisions* Sec. 6.2.10.1 [6.3.7], prescribes a method of checking such a clearance. It requires that the clearance be large enough so that the glass panel will not fall out of the frame unless the relative seismic displacement at the top and bottom of the panel exceeds 125 percent of the value predicted amplified by the building importance factor. If  $h_p$  and  $b_p$  are the respective height and width of individual panes and if the horizontal and vertical clearances are designated  $c_1$  and  $c_2$ , respectively, then the following expression applies:

$$D_{clear} = 2c_1 \left( 1 + \frac{h_p c_2}{b_p c_1} \right) \ge 1.25 D_p$$

For  $h_p = 7$  ft,  $b_p = 5$  ft, and  $D_p = 3.24$  in., and setting  $c_1 = c_2$ , the required clearance is 0.84 in.

# 13.2.5.2 Building Corners

Some thought needs to be given to seismic behavior at external building corners. The preferred approach is to detail the corners with two separate panel pieces, mitered at a 45 degree angle, with high grade sealant between the sections. An alternative choice of detailing L-shaped corner pieces, would introduce more seismic mass and load eccentricity into connections on both sides of the corner column.

# 13.2.5.3 Dimensional Coordination

It is important to coordinate dimensions with the architect and structural engineer. Precast concrete panels must be located a sufficient distance from the building structural frame to allow room for the design of efficient load transfer connection pieces. However, distances must not be so large as to unnecessarily increase the load eccentricities between the panels and the frame.

# 13.3 HVAC FAN UNIT SUPPORT

# **13.3.1 Example Description**

In this example, the mechanical component is a 4-ft-high, 5-ft-wide, 8-ft-long, 3000-lb HVAC fan unit that is supported on the two long sides near each corner (Figure 13.3-1). The component is located at the roof level of a five-story office building, near a significant active fault in Los Angeles, California. The building is assigned to Seismic Use Group I. Two methods of attaching the component to the 4,000 psi, normal-weight roof slab, are considered as follows:

- 1. Direct attachment to the structure with 36 ksi, carbon steel, cast-in-place anchors and
- 2. Support on vibration isolation springs, that are attached to the slab with 36 ksi carbon steel post-installed expansion anchors.

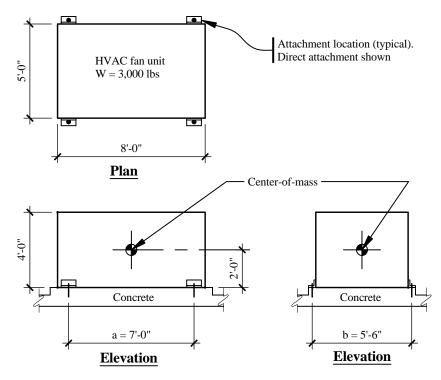


**Figure 13.3-1** Air handling fan unit (1.0 ft = 0.3048 m, 1.0 lb = 4.45 N).

# 13.3.2 Design Requirements

## 13.3.2.1 Provisions Parameters and Coefficients

$a_p = 1.0$ for direct attachment	(Provisions Table 6.3.2 [6.4-1])
$a_p = 2.5$ for vibration isolated	(Provisions Table 6.3.2 [6.4-1])
$S_{DS} = 1.487$	(Design Values CD-ROM)

[The 2003 *Provisions* have adopted the 2002 USGS probabilistic seismic hazard maps, and the maps have been added to the body of the 2003 *Provisions* as figures in Chapter 3 (instead of the previously used separate map package).]

Seismic Design Category = D	(Provisions Table 4.2.1a [14.4-1])
$W_p = 3000 \text{ lb}$	(given)
$R_p = 2.5$ for HVAC system equipment	(Provisions Table 6.3.2 [6.4-1])
$R_p = 1.5$ for expansion anchors and shallow, cast-in-place anchors*	((Provisions Sec. 6.1.6.1 [6.2.8.1])

Shallow anchors are defined by *Provisions* Sec. 2.1 as anchors having embedment-to-diameter ratios of less than 8.

[In the 2003 *Provisions* component anchorage is treated differently. Rather than making distinctions based on an anchor being "shallow," component anchorage is designed using  $R_p = 1.5$  unless specific ductility or prequalification requirements are satisfied.]

$I_p = 1.0$	(Provisions Sec. 6.1.5 [6.2.2])
z/h = 1.0	(for roof mounted equipment)
ho = 1.0	(Provisions Sec. 6.1.3 [6.2.6])

[The 2003 *Provisions* indicate that the redundancy factor does not apply to the design of nonstructural components. Although the effect is similar to stating that  $\rho = 1$ , there is a real difference since load effects for such components and their supports and attachments are now defined in Chapter 6 rather than by reference to Chapter 4.]

# 13.3.2.2 Performance Criteria

Component failure should not cause failure of an essential architectural, mechanical, or electrical component (*Provisions* Sec. 6.1 [6.2.3]).

Component seismic attachments must be bolted, welded, or otherwise positively fastened without consideration of frictional resistance produced by the effects of gravity (*Provisions* Sec. 6.1.2 [6.2.5]).

Anchors embedded in concrete or masonry must be proportioned to carry the least of: (a) the design strength of the connected part, (b) 1.3 times the force in the connected part due to the prescribed forces, or (c) the maximum force that can be transferred to the connected part by the component structural system (*Provisions* Sec. 6.1.6.2 [6.2.8.2]).

Attachments and supports transferring seismic loads must be constructed of materials suitable for the application and must be designed and constructed in accordance with a nationally recognized structural standard (*Provisions* Sec. 6.3.13.2.a [6.4.4, item 6]).

Components mounted on vibration isolation systems must have a bumper restraint or snubber in each horizontal direction. Vertical restraints must be provided where required to resist overturning. Isolator housings and restraints must also be constructed of ductile materials. A viscoelastic pad, or similar material of appropriate thickness, must be used between the bumper and equipment item to limit the impact load (*Provisions* Sec. 6.3.13.2.e). Such components must also resist an amplified design force.

# 13.3.3 Direct Attachment to Structure

This section illustrates design for cast-in-place concrete anchors with embedment-length-to-diameters ratios of 8 or greater; thus, the use of  $R_p = 2.5$  is permitted. [In 2003 *Provisions* Sec. 6.2.8.1, the value of  $R_p$  used in designing component anchorage is no longer based on the embedment depth-to-diameter ratio. Instead  $R_p = 1.5$  unless specific ductility or prequalification requirements are satisfied.]

# 13.3.3.1 Prescribed Seismic Forces

See Figure 13.3-2 for freebody diagram for seismic force analysis.

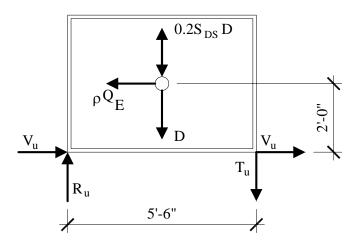


Figure 13.3-2 Free-body diagram for seismic force analysis (1.0 ft = 0.348 m).

$$F_{p} = \frac{0.4(1.0)(1.487)(3000 \text{ lb})}{(2.5/1.0)}(1+2(1)) = 2141 \text{ lb}$$
(Provisions Eq. 6.1.3-1 [6.2-1])  

$$F_{p_{max}} = 1.6(1.487)(1.0)(3000 \text{ lb}) = 7138 \text{ lb}$$
(Provisions Eq. 6.1.3-2 [6.2-3])  

$$F_{p_{min}} = 0.3(1.487)(1.0)(3000 \text{ lb}) = 1338 \text{ lb}$$
(Provisions Eq. 6.1.3-3 [6.2-4])

[2003 *Provisions* Sec. 6.2.6 now treats load effects differently. The vertical forces that must be considered in design are indicated directly and the redundancy factor does not apply, so the following six steps would be cast differently; the result is the same.]

$Q_E$ (due to application of $F_p$ ) = 2141 lb	(Provisions Sec. 6.1.3)
$\rho Q_E = (1.0)(2141 \text{ lb}) = 2141 \text{ lb}$	(horizontal earthquake effect)
$0.2S_{DS}D = (0.2)(1.487)(3000 \text{ lb}) = 892 \text{ lb}$	(vertical earthquake effect)
$D = W_p = 3000 \text{ lb}$	(vertical gravity effect)
$E = \rho Q_E + 0.2 S_{DS} D$	(Provisions Eq. 5.2.7.1-1 [4.2-1])
$E = \rho Q_E - 0.2 S_{DS} D$	(Provisions Eq. 5.2.7.1-2 [4.2-2])
$\underline{U} = 1.2D + 1.0E + 0.5L + 0.2S$	

$$V_{u} = \frac{1.0(2141 \text{ lb})}{4 \text{ bolts}} = 535 \text{ lb/bolt}$$

$$T_{u} = \frac{-1.2(3000 \text{ lb})(2.75 \text{ ft}) + 1.0(2141 \text{ lb})(2 \text{ ft}) + 1.0(892 \text{ lb})(2.75 \text{ ft})}{(5.5 \text{ ft})(2 \text{ bolts})} = -288 \text{ lb/bolt}$$

$$\underline{\text{no tension}}$$

$$U = 0.9\text{D} - (1.3\text{W or } 1.0\text{E})$$

$$V_{u} = \frac{1.0(2141 \text{ lb})}{4 \text{ bolts}} = 535 \text{ lb/bolt}$$
  
$$T_{u} = \frac{-0.9(3000 \text{ lb})(2.75 \text{ ft}) + 1.0(2141 \text{ lb})(2 \text{ ft}) + 1.0(892 \text{ lb})(2.75 \text{ ft})}{(5.5 \text{ ft})(2 \text{ bolts})} = -63 \text{ lb/bolt}$$
no tension

## 13.3.3.2 Proportioning and Design

See Figure 13.3-3 for anchor for direct attachment to structure.

Check one <sup>1</sup>/<sub>4</sub>-in.-diameter cast-in-place anchor embedded 2 in. into the concrete slab with no transverse reinforcing engaging the anchor and extending through the failure surface. Although there is no required tension strength on these anchors, design strengths and tension/shear interaction acceptance relationships are calculated to demonstrate the use of the *Provisions* equations.

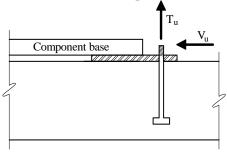


Figure 13.3-3 Anchor for direct attachment to structure.

## 5.3.3.2.1 Design Tension Strength on Isolated Anchor in Slab, Away from Edge, Loaded Concentrically

[The 2003 *Provisions* refer to Appendix D of ACI 318-02 rather than providing specific, detailed requirements. Note also that some of the resistance factors,  $\phi$ , are different.]

Following *Provisions* Sec. 9.2, for a headed bolt or a rod with a nut at the bottom:

$$\frac{L}{d} = \frac{2 \text{ in.}}{0.25 \text{ in.}} = 8.0$$
 (not shallow,  $R_p = 2.5$  is permitted)

[In 2003 *Provisions* selection of  $R_p$  is no longer based on the L/d ratio; see Sec. 6.2.8.1.]

Tension capacity of steel,  $\phi = 0.80$ :

$$N_s = A_{se}F_v = (0.049 \text{ in.}^2)(36000 \text{ psi}) = 1764 \text{ lb}$$
 (*Provisions* Sec. 9.2.5.1.2 [ACI 318-02 Eq. D-3])

[In Appendix D of ACI 318-02 this capacity calculation is based on  $f_{ut}$  rather than  $F_y$ , since "the large majority of anchor materials do not exhibit a well-defined yield point."]

Tension capacity of concrete,  $\phi = 0.70$ , with no eccentricity, no pullthrough, and no edge or group effect:

$$N_c = k \sqrt{f'_c} h_{ef}^{1.5} = 24 \sqrt{4000 \text{ psi}(8^{1.5})} = 4293 \text{ lb} Provisions Eq. 9.2.5.2.2-1 [ACI 318-02 Eq. D-7])$$

[In Appendix D of ACI 318-02 this item is defined as  $N_b$  rather than  $N_{c}$ .]

The steel controls but, with no tension demand, the point is moot.

# 5.3.3.2.2 Design Shear Strength on Isolated Anchor, Away from Edge

Shear capacity of steel,  $\phi = 0.80$ :

 $V_s = A_{se}F_v = (0.049 \text{ in.}^2)(36000 \text{ psi}) = 1764 \text{ lb}$  (*Provisions* Eq. 9.2.6.1.2-1 [ACI 318-02 Eq. D-17)

[In Appendix D of ACI 318-02 this capacity calculation is based on  $f_{ut}$  rather than  $F_v$ , since "the large majority of anchor materials do not exhibit a well-defined yield point."]

Shear capacity of concrete, far from edge, limited to pryout,  $\phi = 0.70$ :

$$V_{cp} = 2N_c = 2(4293) = 8493$$
 lb (*Provisions* Eq. 9.2.6.3.1 [ACI 318-02 Eq. D-28)

The steel controls, with  $\phi V_N = 0.8(1764) = 1411$  lb

Per Provisions Sec. 6.1.6.2 [6.2.8.2], anchors embedded in concrete or masonry are to be proportioned to carry at least 1.3 times the force in the connected part due to the prescribed forces. Thus,  $V_u = 1.3(535) =$ 696 lb and the anchor is clearly adequate.

## 5.3.3.2.3 Combined Tension and Shear

The Provisions gives a new equation (Eq. 9.2.7.3 [ACI 318-02 Eq. D-29]) for the interaction of tension and shear on an anchor or a group of anchors:

$$\frac{N_u}{\phi N_N} + \frac{V_u}{\phi V_N} \le 1.2$$
, which applies when either term exceeds 0.2

# 5.3.3.2.3 Summary

At each corner of the component, provide one 1/4-in.-diameter cast-in-place anchor embedded 2 in. into the concrete slab. Transverse reinforcement engaging the anchor and extending through the failure surface is not necessary.

# **13.3.4 Support on Vibration Isolation Springs**

# 13.3.4.1 Prescribed Seismic Forces

Design forces for vibration isolation springs are determined by an analysis of earthquake forces applied in a diagonal horizontal direction as shown in Figure 13.3-4. Terminology and concept are taken from ASHRAE APP IP.

Angle of diagonal loading:

$$\theta = \tan^{-1}\left(\frac{b}{a}\right)$$
 (ASHRAE APP IP. Eq. 17)

Tension per isolator:

(ASHRAE APP IP. Eq. 18)

(ASHRAE APP IP. Eq. 19)

$$T_u = \frac{W_p - F_{pv}}{4} - \frac{F_p h}{2} \left( \frac{\cos \theta}{b} + \frac{\sin \theta}{a} \right)$$

Compression per isolator:

<i>C</i> –	$W_p + F_{pv}$	$F_ph$	$\cos\theta$	$\sin\theta$	
$C_u$ –	4	2	$\overline{b}$	$\left(\frac{a}{a}\right)$	

Shear per isolator:

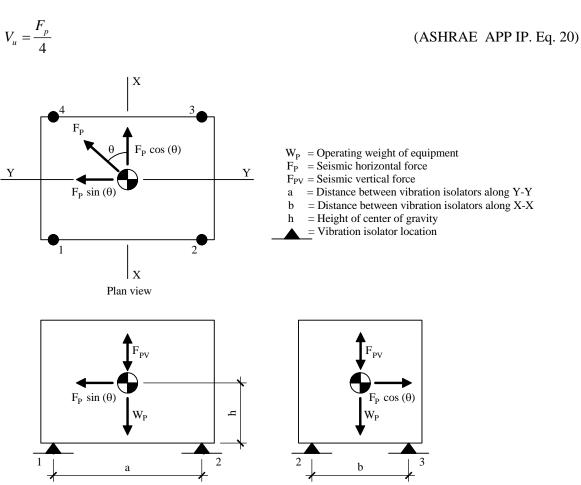


Figure 13.3-4 ASHRAE diagonal seismic force analysis for vibration isolation springs.

Select worst case assumption: Design for post-installed expansion anchors, requiring the use of  $R_p = 1.5$ .

$$F_{p} = \frac{0.4(2.5)(1.487)(3000 \text{ lb})}{(1.5/1.0)}(1+2(1)) = 8922 \text{ lb}$$
(Provisions Eq. 6.1.3-1 [6.2-1])  

$$F_{p_{max}} = 1.6(1.487)(1.0)(3000 \text{ lb}) = 7138 \text{ lb}$$
(Provisions Eq. 6.1.3-2 [6.2-3])  

$$F_{p_{min}} = 0.3(1.487)(1.0)(3000 \text{ lb}) = 1338 \text{ lb}$$
(Provisions Eq. 6.1.3-3 [6.2-4])

Components mounted on vibration isolation systems shall have a bumper restraint or snubber in each horizontal direction. Per Provisions Table 6.3.2 [6.4-1], Footnote B, the design force shall be taken as  $2F_p$ .

[2003 *Provisions* Sec. 6.2.6 now treats load effects differently. The vertical forces that must be considered in design are indicated directly and the redundancy factor does not apply, so the following steps would be cast differently; the result is the same.]

$$Q_E = F_p = 2(7138 \text{ lb}) = 14276 \text{ lb}$$
 (Provisions Sec. 6.1.3)

  $\rho Q_E = (1.0)(14276 \text{ lb}) = 14276 \text{ lb}$ 
 (horizontal earthquake effect)

  $F_{pv(ASHRAE)} = 0.2S_{DS}D = (0.2)(1.487)(3000 \text{ lb}) = 892 \text{ lb}$ 
 (vertical earthquake effect)

  $D = W_p = 3000 \text{ lb}$ 
 (vertical gravity effect)

  $E = \rho Q_E + 0.2S_{DS}D$ 
 (Eq. 5.2.7.1-1 [4.2-1])

  $E = \rho Q_E - 0.2S_{DS}D$ 
 (Eq. 5.2.7.1-2 [4.2-2])

U = 1.2D + 1.0E + 0.5L + 0.2S

$$\theta = \tan^{-1} \left( \frac{7 \text{ ft}}{5.5 \text{ ft}} \right) = 51.8^{\circ}$$

$$T_{u} = \frac{1.2(3000 \text{ lb}) - (892 \text{ lb})}{4} - \frac{(14276 \text{ lb})(2 \text{ ft})}{2} \left( \frac{\cos(51.8^{\circ})}{7 \text{ ft}} + \frac{\sin(51.8^{\circ})}{5.5 \text{ ft}} \right) = -2624 \text{ lb}$$

$$C_{u} = \frac{1.2(3000 \text{ lb}) + (892 \text{ lb})}{4} + \frac{(14276 \text{ lb})(2 \text{ ft})}{2} \left( \frac{\cos(51.8^{\circ})}{7 \text{ ft}} + \frac{\sin(51.8^{\circ})}{5.5 \text{ ft}} \right) = 4424 \text{ lb}$$

$$V_{u} = \frac{14276 \text{ lb}}{4} = 3569 \text{ lb}$$

U = 0.9D + 1.0E

$$\theta = \tan^{-1} \left( \frac{7 \text{ ft}}{5.5 \text{ ft}} \right) = 51.8^{\circ}$$

$$T_{u} = \frac{0.9(3000 \text{ lb}) - (892 \text{ lb})}{4} - \frac{(14276 \text{ lb})(2 \text{ ft})}{2} \left( \frac{\cos(51.8^{\circ})}{7 \text{ ft}} + \frac{\sin(51.8^{\circ})}{5.5 \text{ ft}} \right) = -2849 \text{ lb}$$

$$C_{u} = \frac{0.9(3000 \text{ lb}) + (892 \text{ lb})}{4} + \frac{(14276 \text{ lb})(2 \text{ ft})}{2} \left( \frac{\cos(51.8^{\circ})}{7 \text{ ft}} + \frac{\sin(51.8^{\circ})}{5.5 \text{ ft}} \right) = 4199 \text{ lb}$$

$$V_{u} = \frac{14276 \text{ lb}}{4} = 3569 \text{ lb}$$

13.3.4.2 Proportioning and Details

Anchor and snubber loads for support on vibration isolation springs are shown in Figure 13.3-5.

Check vibration isolation system within housing anchored with two 1-in.-diameter post-installed expansion anchors embedded 9 inches into the concrete.

The *Provisions* does not provide a basis for determining the design strength of post-installed expansion anchors. Although manufacturers provide ultimate strength shear and tension loads for their products, the *Provisions* does not provide resistance or quality values,  $\phi$ , to allow determination of design shear and tension strengths. The 2002 edition of ACI 318 contains provisions for post-installed anchors which depend on anchor testing per the ACI 355.2-01 testing standard. Prior to the adoption of this method, the best course available was to use allowable stress loads published in evaluation reports prepared by model building code agencies. These allowable stress loads were then multiplied by 1.4 to convert to design strengths. This technique will be illustrated in the following.

[The 2003 Provisions refer to Appendix D of ACI 318-02.]

Allowable stress combinations are included in the 2000 *IBC*. The 1.4 strength conversion factor is unnecessary when using allowable stress loads published in evaluation reports prepared by model building code agencies.

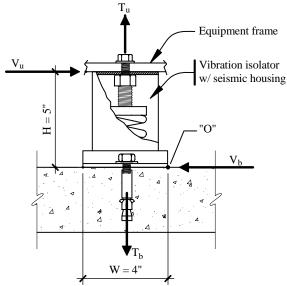


**Figure 13.3-5** Anchor and snubber loads for support on vibration isolation springs (1.0 in. = 25.4 mm).

# 13.3.4.2.1 Design Tension Strength on Isolated Anchor in Slab, Away from Edge

Allowable stress tension values are obtained from ICBO Evaluation Services, Inc., ER-4627 for Hilti Kwik Bolt II concrete anchors. Similar certified allowable values are expected with anchors from other manufacturers.

anchor diameter = 1 in. anchor depth = 9 in.  $f_c' = 4000$  psi with special inspection

 $T_{allow} = 8800 \text{ lb}$  $P_s = \phi P_c = 1.4(8800 \text{ lb}) = 12320 \text{ lb}$ 

13.3.4.2.2 Design Shear Strength on Isolated Anchor in Slab, Away from Edge

Allowable stress shear values are obtained from ICBO Evaluation Services, Inc., ER-4627 for Hilti Kwik Bolt II concrete anchors. Similar certified allowable values are expected with anchors from other manufacturers.

anchor diameter = 1 in. anchor depth = 9 in.  $f_c' = 4000$  psi  $V_{allow} = 8055$  lb  $V_s = \phi V_c = 1.4(8055$  lb) = 11277 lb

13.3.4.2.3 Combined Tension and Shear

Per *Provisions* Sec. 6.1.6.2 [6.2.8.2], anchors embedded in concrete or masonry shall be proportioned to carry at least 1.3 times the force in the connected part due to the prescribed forces.

In the *Provisions* and in the 2000 *IBC*, the factor of 2.0 is reduced to 1.3. This will greatly reduce the prescribed seismic forces.

Interaction relationships for combined shear and tension loads are obtained from ICBO Evaluation Services, Inc. ER-4627 for Hilti Kwik Bolt II concrete anchors. Similar results are expected using other anchors.

As stated in ICBO ES evaluation report:

$$\left(\frac{P_s}{P_t}\right)^{5/3} + \left(\frac{V_s}{V_t}\right)^{5/3} \le 1$$

Using Provisions terminology:

$$\left(\frac{T_b}{\phi P_c}\right)^{\frac{5}{3}} + \left(\frac{V_b}{\phi V_c}\right)^{\frac{5}{3}} \le 1$$

$$\left(\frac{2 \times 4462 \text{ lb}}{11277 \text{ lb}}\right)^{\frac{5}{3}} + \left(\frac{2 \times 1785 \text{ lb}}{12075 \text{ lb}}\right)^{\frac{5}{3}} = 0.68 + 0.13 = 0.81 < 1$$
OK

13.3.4.2.4 Summary

At each corner of the HVAC fan unit, provide a vibration isolation system within a housing anchored with two 1-in.-diameter post-installed expansion anchors embedded 9 in. into the concrete slab. <u>Special inspection is required</u>. A raised concrete pad is probably required to allow proper embedment of the post-installed expansion anchors.

Other post-installed anchors, such as chemical (adhesive) or undercut post-installed anchors also could be investigated. These anchors may require more involved installation procedures, but they may allow the use of  $R_p = 2.5$  if they have an embedment depth-to-diameter ratio of at least 8 (i.e., are not shallow anchors). The higher  $R_p$  value will result in much smaller prescribed seismic forces and, therefore, a much reduced embedment depth.

[Again note that in 2003 *Provisions* selection of  $R_p$  is no longer based on the L/d ratio; see Sec. 6.2.8.1.]

# 13.3.5 Additional Considerations for Support on Vibration Isolators

Vibration isolation springs are provided for equipment to prevent vibration from being transmitted to the building structure. However, they provide virtually no resistance to horizontal seismic forces. In such cases, some type of restraint is required to resist the seismic forces. Figure 13.3-6 illustrates one concept where a bolt attached to the equipment base is allowed to slide a controlled distance (gap) in either direction along its longitudinal axis before it contacts resilient impact material.

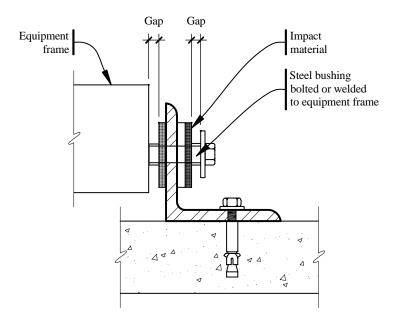


Figure 13.3-6 Lateral restraint required to resist seismic forces.

Design of restraints for vibration-isolated equipment varies for different applications and for different manufacturers. In most cases, restraint design incorporates all directional capability with an air gap, a soft impact material, and a ductile restraint or housing.

Restraints should have all-directional restraint capability to resist both horizontal and vertical motion. Vibration isolators have little or no resistance to overturning forces. Therefore, if there is a difference in height between the equipment center of gravity and the support points of the springs, rocking is inevitable and vertical restraint is required.

An air gap between the restraint device and the equipment prevents vibration from transmitting to the structure during normal operation of the equipment. Air gaps are generally no greater than  $\frac{1}{4}$  in. Dynamic tests indicate a significant increase in acceleration for air gaps larger than  $\frac{1}{4}$  in.

A soft impact material often an elastomer such as bridge bearing neoprene reduces accelerations and impact loads by preventing steel-to-steel contact. The thickness of the elastomer can significantly reduce accelerations to both the equipment and the restraint device and should be specifically addressed for life safety applications.

A ductile restraint or housing is critical to prevent catastrophic failure. Unfortunately, housed isolators made of brittle materials such as cast iron often are assumed to be capable of resisting seismic loads and continue to be installed in seismic zones.

Overturning calculations for vibration- isolated equipment must consider a worst case scenario as illustrated in *Guide* Sec. 13.3.4.1. However, important variations in calculation procedures merit further discussion. For equipment that is usually directly attached to the structure, or mounted on housed vibration isolators, the weight can be used as a restoring force since the equipment will not transfer a tension load to the anchors until the entire equipment weight is overcome at any corner. For equipment installed on any other vibration isolated system (such as the separate spring and snubber arrangement shown in Figure 13.3-5), the weight cannot be used as a restoring force in the overturning calculations.

As the foregoing illustrates, design of restraints for resiliently mounted equipment is a specialized topic. The *Provisions* sets out only a few of the governing criteria. Some suppliers of vibration isolators in the highest seismic zones are familiar with the appropriate criteria and procedures. Consultation with these suppliers may be beneficial.

# **13.4 ANALYSIS OF PIPING SYSTEMS**

# 13.4.1 ASME Code Allowable Stress Approach

Piping systems are typically designed to satisfy national standards such as ASME B31.1. Piping required to be designed to other ASME piping codes use similar approaches with similar definition of terms.

# 13.4.1.1 Earthquake Design Requirements

ASME B31.1 Sec. 101.5.3 requires that the effects of earthquakes, where applicable, be considered in the design of piping, piping supports, and restraints using data for the site as a guide in assessing the forces involved. However, earthquakes need not be considered as acting concurrently with wind.

# 13.4.1.2 Stresses Due to Sustained Loads

The effects of pressure, weight, and other sustained loads must meet the requirements of ASME B31.1 Eq. 11A:

$$S_{L} = \frac{PD_{o}}{4t_{n}} + \frac{0.75iM_{A}}{Z} \le 1.0S_{h}$$

where:

 $S_L$  = sum of the longitudinal stresses due to pressure, weight, and other sustained loads

P = internal design pressure, psig

 $D_o$  = outside diameter of pipe, in.

 $t_n$  = nominal pipe wall thickness, in.

- *i* = stress intensification factor from ASME Piping Code Appendix D, unitless
- = 1.0 for straight pipe
- $\geq 1.0$  for fittings and connections

 $M_A$  = resultant moment loading on cross section due to weight and other sustained loads, in.-lb

Z = section modulus, in.<sup>3</sup>

 $S_h$  = basic material allowable stress at maximum (hot) temperature from ASME Piping Code Appendix A

For example, ASTM A53 seamless pipe and tube, Grade B:  $S_h = 15.0$  ksi for -20 to 650 degrees F.

## 13.4.1.3 Stresses Due to Occasional Loads

The effects of pressure, weight, and other sustained loads, and occasional loads including earthquake must meet the requirements of ASME B31.1 Eq. 12A:

$$\frac{PD_o}{4t_n} + \frac{0.75iM_A}{Z} + \frac{0.75iM_B}{Z} \le kS_h$$

where:

- $M_B$  = resultant moment loading on cross-section due to occasional loads, such as from thrust loads, pressure and flow transients, and earthquake. Use one-half the earthquake moment range. Effects of earthquake anchor displacements may be excluded if they are considered in Eq. 13A, in.-lb
  - k = duration factor, unitless
    - = 1.15 for occasional loads acting less than 10% of any 24 hour operating period
    - = 1.20 for occasional loads acting less than 1% of any 24 hour operating period
    - = 2.00 for rarely occurring earthquake loads resulting from both inertial forces and anchor movements (per ASME interpretation)

## 13.4.1.4 Thermal Expansion Stress Range

The effects of thermal expansion must meet the requirements of ASME B31.1 Eq. 13A:

$$S_E = \frac{iM_C}{Z} \le S_A + f\left(S_h - S_L\right)$$

where:

 $S_E$  = sum of the longitudinal stresses due to thermal expansion, ksi

- $M_c$  = range of resultant moments due to thermal expansion. Also includes the effects of earthquake anchor displacements if not considered in Eq. 12A, in.-lb
- $S_A$  = allowable stress range, ksi (per ASME B31.1 Eq. 1,  $S_A = f(1.25S_c + 0.25S_h)$ f = stress range reduction factor for cyclic conditions from the ASME Piping Code Table 102.3.2.
- $S_c$  = basic material allowable stress at minimum (cold) temperature from the ASME Piping Code Appendix A

## 13.4.1.5 Summary

In the ASME B31.1 allowable stress approach, the earthquake's effects only appear in the  $M_B$  and  $M_C$ terms.

Earthquake inertial effects  $\Rightarrow M_B$  term

Earthquake displacement effects  $\Rightarrow M_C$  term

## 13.4.2 Allowable Stress Load Combinations

ASME B31.1 utilizes an allowable stress approach; therefore, allowable stress force levels and allowable stress load combinations should be used. While the Provisions are based on strength design, the IBC provides the following two sets of allowable stress loads and load combinations. The IBC load combinations are appropriate for use for piping systems when considering earthquake effects. When earthquake effects are not considered, load combinations should be taken from the appropriate piping system design code.

## 13.4.2.1 IBC Basic Allowable Stress Load Combinations

No increases in allowable stress are permitted for the following set of load combinations:

D	(IBC Eq. 16-7)
$D + L + (L_r \text{ or } S \text{ or } R)$	(IBC Eq. 16-9)
D + (W  or  0.7 E)	(IBC Eq. 16-10)
0.6 <i>D</i> - 0.7 <i>E</i>	(IBC Eq. 16-12)

## 13.4.2.2 IBC Alternate Basic Allowable Stress Load Combinations

Increases in allowable stress (typically 1/3) are permitted for the following alternate set of load combinations that include *W* or *E*:

$D + L + (L_r \text{ or } S \text{ or } R)$	(IBC Eq. 16-13)
D + L + S + E/1.4	(IBC Eq. 16-17)
0.9D + E/1.4	(IBC Eq. 16-18)

## 13.4.2.3 Modified IBC Allowable Stress Load Combinations

It is convenient to define separate earthquake load terms to represent the separate inertial and displacement effects.

 $E_I$  = Earthquake inertial effects  $\Rightarrow M_B$  term

 $E_{\Delta}$  = Earthquake displacement effects  $\Rightarrow M_C$  term

It is also convenient to use the IBC Alternate Basic Allowable Stress Load Combinations modified to use ASME Piping Code terminology, deleting roof load effects ( $L_r$  or S or R) and multiplying by 0.75 to account for the 1.33 allowable stress increase when W or E is included. Only modified IBC Eq. 16-17 and 16-18 will be considered in the discussion that follows.

 $0.75[D + L + S + (E_I + E_A)/1.4]$  (modified IBC Eq. 16-17) 0.75[0.9D + (E\_I + E\_A)/1.4] (modified IBC Eq. 16-18)

# 13.4.3 Application of the Provisions

## 13.4.3.1 Overview

*Provisions* Sec. 6.3.11 [6.4.2, item 4] requires that, in addition to their attachments and supports, piping systems assigned an  $I_p$  greater than 1.0 must themselves be designed to meet the force and displacement requirements of *Provisions* Sec. 6.1.3 and 6.1.4 [6.2.6 and 6.2.7] and the additional requirements of this section.

## 13.4.3.1 Forces

*Provisions* Sec. 6.1.3 [6.2.6] provides specific guidance regarding the equivalent static forces that must be considered. In computing the earthquake forces for piping systems, the inertial portion of the forces (noted as  $E_t$  in this example) are computed using *Provisions* Eq. 6.1.3-1, 6.1.3-2, and 6.1.3-3 [6.2-1, 6.2-3, and 6.2-4] for  $F_p$  with  $a_p = 1$  and  $R_p = 3.5$ . For anchor points with different elevations, the average value of the  $F_p$  may be used with minimum and maximums observed. In addition, when computing the inertial forces, the vertical seismic effects ( $\pm 0.2S_{DS}W_p$ ) should be considered.

The term  $E_I$  can be expressed in terms of the forces defined in the *Provisions* converted to an allowable stress basis by the 1.4 factor:

$$E_{I} = \left(\frac{F_{p}}{1.4}\right)_{horizontal} \pm \left(\frac{0.2S_{DS}W_{p}}{1.4}\right)_{vertic}$$

It is convenient to designate the term  $\left(1 \pm \frac{0.2S_{DS}}{1.4}\right)$  by the variable  $\beta$ .

The vertical component of  $E_I$  can now be defined as  $\beta M_a$  and applied to all load combinations that include  $E_I$ .

 $M_B$  can now be defined as the resultant moment induced by the design force  $F_p/1.4$  where  $F_p$  is as defined by *Provisions* Eq. 6.1.3-1, 6.1.3-2, or 6.1.3-3.

## **13.4.3.3 Displacements**

*Provisions* Sec. 6.1.4 [6.2.7] provides specific guidance regarding the relative displacements that must be considered. Typically piping systems are designed considering forces and displacements using elastic analysis and allowable stresses for code prescribed wind and seismic equivalent static forces in combination with operational loads.

However, no specific guidance is provided in the *Provisions* except to say that the relative displacements should be accommodated. The intent of the word "accommodate" was not to require that a piping system remain elastic. Indeed, many types of piping systems typically are very ductile and can accommodate large amounts of inelastic strain while still functioning quite satisfactorily. What was intended was that the relative displacements between anchor and constraining points that displace significantly relative to one another be demonstrated to be accommodated by some rational means. This accommodation can be made by demonstrating that the pipe has enough flexibility and/or inelastic strain capacity to accommodate the displacement by providing loops in the pipeline to permit the displacement or by adding flex lines or articulating couplings which provide free movement to accommodate the displacement. Sufficient flexibility may not exist where branch lines, may be forced to move with a ceiling or other structural system are connected to main lines. Often this "accommodation" is done by using engineering judgment, without calculations. However, if relative displacement calculations were required for a piping system, a flexibility analysis would be required. A flexibility analysis is one in which a pipe is modeled as a finite element system with commercial pipe stress analysis programs (such as Autopipe or CAESAR II) and the points of attachment are displaced by the prescribed relative displacements. The allowable stress for such a condition may be significantly greater than the normal allowable stress for the pipe.

The internal moments resulting from support displacement may be computed by means of elastic analysis programs using the maximum computed relative displacements as described earlier and then adjusted. As with elastic inertial forces, the internal moments caused by relative displacement can be divided by  $R_p$  to account for reserve capacity. A reduction factor of 1.4 may be used to convert them for use with allowable stress equations. Therefore,  $M_c$  can now be defined as the resultant moment induced by the design relative seismic displacement  $D_p/1.4R_p$  where  $D_p$  is defined by *Provisions* Eq. 6.1.4-1, 6.1.4-2, 6.1.4-3, or 6.1.4-4 [6.2-5, 6.2-6, 6.2-7, or 6.2-8].

# 13.4.3.4 Load Combinations

Combining ASME B31.1 Eq. 12A and 13A with modified IBC Eq. 1605.3.2.5 and 1605.3.2.6 yields the following:

For modified IBC Eq. 16-17

$$\begin{split} & \frac{PD_{o}}{4t_{n}} + \beta \bigg( \frac{0.75iM_{A}}{Z} \bigg) \pm \frac{0.75iM_{B}}{Z} \leq kS_{h} \\ & \frac{iM_{C}}{Z} \leq S_{A} + f\left(S_{h} - S_{L}\right) \end{split}$$

and for modified IBC Eq. 16-18

$$\begin{split} & \frac{PD_o}{4t_n} + 0.9\,\beta \bigg(\frac{0.75iM_A}{Z}\bigg) - \frac{0.75iM_B}{Z} \le kS_f \\ & \frac{iM_C}{Z} \le S_A + f\left(S_h - S_L\right) \end{split}$$

where:

$$\beta = \left(1 \pm \frac{0.2S_{DS}}{1.4}\right)$$

 $M_A$  = the resultant moment due to weight

- $M_B$  = the resultant moment induced by the design force  $F_p/1.4$  where  $F_p$  is as defined by *Provisions* Eq. 6.1.3-1, 6.1.3-2, or 6.1.3-3 [6.2-1, 6.2-3, or 6.2-4].
- $M_C$  = the resultant moment induced by the design relative seismic displacement  $D_p/1.4R_p$  where  $D_p$  is as defined by *Provisions* Eq. 6.1.4-1, 6.1.4-2, 6.1.4-3, or 6.1.4-4 [6.2-5, 6.2-6, 6.2-7, or 6.2-8].
- $S_{DS}$ ,  $W_p$ , and  $R_p$  are as defined in the *Provisions*.
- $P, D_o, t_n, I, Z, k, S_h, S_A, f$ , and  $S_L$  are as defined in ASME B31.1.

# Appendix A

# THE BUILDING SEISMIC SAFETY COUNCIL

The purpose of the Building Seismic Safety Council is to enhance the public's safety by providing a national forum to foster improved seismic safety provisions for use by the building community. For the purposes of the Council, the building community is taken to include all those involved in the planning, design, construction, regulation, and utilization of buildings.

To achieve its purposes, the Council shall conduct activities and provide the leadership needed to:

- 1. Promote development of seismic safety provisions suitable for use throughout the United States;
  - 2. Recommend, encourage, and promote adoption of appropriate seismic safety provisions in voluntary standards and model codes;
  - 3. Assess implementation progress by federal, state, and local regulatory and construction agencies;
  - 4. Identify opportunities for the improvement of seismic regulations and practices and encourage public and private organizations to effect such improvements;
  - 5. Promote the development of training and educational courses and materials for use by design professionals, builders, building regulatory officials, elected officials, industry representatives, other members of the building community and the public.
  - 6. Provide advice to governmental bodies on their programs of research, development, and implementation; and
  - 7. Periodically review and evaluate research findings, practice, and experience and make recommendations for incorporation into seismic design practices.

The scope of the Council's activities encompasses seismic safety of structures with explicit consideration and assessment of the social, technical, administrative, political, legal, and economic implications of its deliberations and recommendations.

Achievement of the Council's purpose is important to all in the public and private sectors. Council activities will provide an opportunity for participation by those at interest, including local, State, and Federal Government, voluntary organizations, business, industry, the design professions, the construction industry, the research community and the public. Regional and local differences in the nature and magnitude of potentially hazardous earthquake events require a flexible approach adaptable to the relative risk, resources and capabilities of each community. The Council recognizes that appropriate earthquake hazard reduction measures and initiatives should be adopted by existing organizations and institutions and incorporated into their legislation, regulations, practices, rules, codes, relief procedures and loan

requirements, whenever possible, so that these measures and initiatives become part of established activities rather than being superposed as separate and additional.

The Council is established as a voluntary advisory, facilitative council of the National Institute of Building Sciences, a nonprofit corporation incorporated in the District of Columbia, under the authority given the Institute by the Housing and Community Development Act of 1974, (Public Law 93-383), Title VIII, in furtherance of the objectives of the Earthquake Hazards Reduction Act of 1977 (Public Law 95-124) and in support of the President's National Earthquake Hazards Reduction Program, June 22, 1978.

## 2005-2006 BSSC BOARD OF DIRECTION

Chair -- Jim W. Sealy, FAIA, Architect/Consultant, Dallas, TX

Vice Chair -- David Bonneville, Degenkolb Engineers, San Francisco, California

Secretary -- Jim Rinner, Project Manager II, Kitchell CEM, Sacramento, California

**Ex-Officio Member --** Charles Thornton, Chairman/Principal, Thornton-Tomasetti Group, Inc., New York, New York

## Members

Edwin Dean, Nishkian Dean, Portland, Oregon

Bradford K. Douglas, Director of Engineering, American Forest and Paper Association, Washington, D.C.

Cynthia J. Duncan, Director of Specifications, American Institute of Steel Construction, Chicago, Illinois Henry Green, Executive Director, Bureau of Construction Codes and Fire Safety, State of Michigan, Department of Labor and Economic Growth, Lansing, Michigan (representing the National Institute of Building Sciences)

Jay W. Larson, American Iron and Steel Institute, Betlehem, Pennsylvania

Joseph Messersmith, Coordinating Manager, Regional Code Services, Portland Cement Association, Rockville, Virginia (representing the Portland Cement Association)

Ronald E. Piester, Assistant Director for Code Development, New York State, Department of State, Kinderhook, New York

James Rossberg, Manager, Technical Activities for the Structural Engineering Institute, American Society of Civil Engineers, Reston Virginia

W. Lee Shoemaker, Director, Engineering and Research, Metal Building Manufacturers Association, Cleveland, Ohio

Howard Simpson, Simpson Gumpertz and Heger, Arlington, Massachusetts (representing National Council of Structural Engineers Associations)

Shyam Sunder, Deputy Director, Building Fire Research Laboratory, National Institute of Standards and Technology, Gaithersburg, Maryland (representing Interagency Committee on Seismic Safety in Construction)

Charles A. Spitz, Architect/Planner/Code Consultant, Wall New Jersey (representing the American Institute of Architects)

Robert D. Thomas, Vice President Engineering, National Concrete Masonry Association, Herndon, Virginia

# **BSSC Staff**

Claret M. Heider, Vice President for BSSC Programs

Bernard F. Murphy, PE, Director, Special Projects Carita Tanner, Communications Manager

#### **BSSC MEMBER ORGANIZATIONS**

#### **Voting Members**

AFL-CIO Building and Construction Trades Department American Concrete Institute American Consulting Engineers Council American Forest and Paper Association American Institute of Architects American Institute of Steel Construction American Iron and Steel Institute American Society of Civil Engineers ASCE, Kansas City Chapter American Society of Heating, Refrigeration, and Air-Conditioning Engineers American Society of Mechanical Engineers American Welding Society APA - The Engineered Wood Association Applied Technology Council Associated General Contractors of America Association of Engineering Geologists Association of Major City Building Officials Brick Industry Association California Geotechnical Engineers Association California Division of the State Architect, Office of Regulation Services Canadian National Committee on Earthquake Engineering Concrete Masonry Association of California and Nevada Concrete Reinforcing Steel Institute Earthquake Engineering Research Institute General Services Administration Seismic Program Hawaii State Earthquake Advisory Board Institute for Business and Home Safety Interagency Committee on Seismic Safety in Construction International Code Council International Masonry Institute Masonry Institute of America Metal Building Manufacturers Association Mid-America Earthquake Center National Association of Home Builders National Concrete Masonry Association National Conference of States on Building Codes and Standards National Council of Structural Engineers Associations National Elevator Industry, Inc. National Fire Sprinkler Association National Institute of Building Sciences National Ready Mixed Concrete Association

Portland Cement Association Precast/Prestressed Concrete Institute Rack Manufacturers Institute Santa Clara University Seismic Safety Commission (California) Steel Deck Institute, Inc. Structural Engineers Association of California Structural Engineers Association of Central California Structural Engineers Association of Colorado Structural Engineers Association of Illinois Structural Engineers Association of Kentucky Structural Engineers Association of Northern California Structural Engineers Association of Oregon Structural Engineers Association of San Diego Structural Engineers Association of Southern California Structural Engineers Association of Texas Structural Engineers Association of Utah Structural Engineers Association of Washington The Masonry Society U.S. Army CERL Western States Clay Products Association Wire Reinforcement Institute

## Affiliate Members

Bay Area Structural, Inc. Building Technology, Incorporated City of Hayward, California Felten Engineering Group, Inc. H&H Group HLM Design LaPay Consulting, Inc. Niehoff, Dennis, PE Square D Company Steel Joist Institute Vibration Mountings and Controls York, a Johnson Controls Company

# **BSSC PUBLICATIONS**

Available free from the Federal Emergency Management Agency at 1-800-480-2520 (by FEMA Publication Number). For detailed information about the BSSC and its projects, contact: BSSC, 1090 Vermont Avenue, N.W., Suite 700, Washington, D.C. 20005 Phone 202-289-7800; Fax 202-289-1092; e-mail ctanner@nibs.org

## NEW BUILDINGS PUBLICATIONS

NEHRP (National Earthquake Hazards Reduction Program) Recommended Provisions for Seismic Regulations for New Buildings, 2003 Edition, 2 volumes and maps, FEMA 450 (issued as a CD with only limited print copies available)

NEHRP (National Earthquake Hazards Reduction Program) Recommended Provisions for Seismic Regulations for New Buildings, 2000 Edition, 2 volumes and maps, FEMA 368 and 369

NEHRP Recommended Provisions: Design Examples, 2006, FEMA 451 (issued as a CD) A Nontechnical Explanation of the NEHRP Recommended Provisions, Revised Edition, 1995, FEMA 99

Homebuilders' Guide to Earthquake-Resistant Design and Construction, 2006, FEMA 232 Seismic Considerations for Steel Storage Racks Located in Areas Accessible to the Public. 2005, FEMA 460

Seismic Considerations for Communities at Risk, Revised Edition, 1995, FEMA 83

Seismic Considerations: Apartment Buildings, Revised Edition, 1996, FEMA 152

Seismic Considerations: Elementary and Secondary Schools, Revised Edition, 1990, FEMA 149

Seismic Considerations: Health Care Facilities, Revised Edition, 1990, FEMA 150

Seismic Considerations: Hotels and Motels, Revised Edition, 1990, FEMA 151

Seismic Considerations: Office Buildings, Revised Edition, 1996, FEMA 153

Societal Implications: Selected Readings, 1985, FEMA 84

## **EXISTING BUILDINGS**

NEHRP Guidelines for the Seismic Rehabilitation of Buildings, 1997, FEMA 273

NEHRP Guidelines for the Seismic Rehabilitation of Buildings: Commentary, 1997, FEMA 274 Case Studies: An Assessment of the NEHRP Guidelines for the Seismic Rehabilitation of Buildings, 1999, FEMA 343

Planning for Seismic Rehabilitation: Societal Issues, 1998, FEMA 275

Example Applications of the NEHRP Guidelines for the Seismic Rehabilitation of Buildings, 1999, FEMA 276

NEHRP Handbook of Techniques for the Seismic Rehabilitation of Existing Buildings, 1992, FEMA 172

NEHRP Handbook for the Seismic Evaluation of Existing Buildings, 1992, FEMA 178

An Action Plan for Reducing Earthquake Hazards of Existing Buildings, 1985, FEMA 90

# MULTIHAZARD

An Integrated Approach to Natural Hazard Risk Mitigation, 1995, FEMA 261/2-95

# LIFELINES

Abatement of Seismic Hazards to Lifelines: An Action Plan, 1987, FEMA 142

Abatement of Seismic Hazards to Lifelines: Proceedings of a Workshop on Development of An Action Plan, 6 volumes:

Papers on Water and Sewer Lifelines, 1987, FEMA 135 Papers on Transportation Lifelines, 1987, FEMA 136 Papers on Communication Lifelines, 1987, FEMA 137 Papers on Power Lifelines, 1987, FEMA 138 Papers on Gas and Liquid Fuel Lifelines, 1987, FEMA 139 Papers on Political, Economic, Social, Legal, and Regulatory Issues and General Workshop Presentations, 1987, FEMA 143

(August 2006)